Regional Geology Reviews

Cecilio Quesada
José Tomás Oliveira
Editors

The Geology of Iberia: A Geodynamic Approach

Volume 2: The Variscan Cycle

José Fernando Simancas
Volume Coordinator

Springer

Regional Geology Reviews

The Geology of series seeks to systematically present the geology of each country, region and continent on Earth. Each book aims to provide the reader with the state-of-the-art understanding of a regions geology with subsequent updated editions appearing every 5 to 10 years and accompanied by an online "must read" reference list, which will be updated each year. The books should form the basis of understanding that students, researchers and professional geologists require when beginning investigations in a particular area and are encouraged to include as much information as possible such as: Maps and Cross-sections, Past and current models, Geophysical investigations, Geochemical Datasets, Economic Geology, Geotourism (Geoparks etc.), Geo-environmental/ecological concerns, etc.

More information about this series at http://www.springer.com/series/8643

Cecilio Quesada · José Tomás Oliveira
Editors

The Geology of Iberia: A Geodynamic Approach

Volume 2: The Variscan Cycle

Springer

Editors
Cecilio Quesada
Instituto Geológico y Minero de España (IGME)
and Faculty of Geological Sciences
Universidad Complutense de Madrid
Madrid, Spain

José Tomás Oliveira
LNEG
Amadora, Portugal

ISSN 2364-6438 ISSN 2364-6446 (electronic)
Regional Geology Reviews
ISBN 978-3-030-10518-1 ISBN 978-3-030-10519-8 (eBook)
https://doi.org/10.1007/978-3-030-10519-8

Library of Congress Control Number: 2019932835

Cover illustration: Ending and Dawn of Wilson cycles: Moscovian folded turbidites unconformably overlain by Late Triassic red beds, Telheiro beach, SW Portugal.
Photographed with a drone by JC Kullberg

This Springer imprint is published by the registered company Springer Nature Switzerland AG
The registered company address is: Gewerbestrasse 11, 6330 Cham, Switzerland

Editors and Volume Coordinator

About the Editors

Cecilio Quesada has developed his entire professional career at Instituto Geológico y Minero de España (Spanish Geological Survey), from where he retired in 2013. He is currently Honor Professor at the Faculty of Geological Sciences, Universidad Complutense, Madrid, where he also served temporarily as Associate Professor. As a "*survey person*," his research interests, past and present, include geological mapping, regional geology, tectonics, and geochronology, mainly focused on the Variscan orogen in its global context. He has participated in ten IGCP projects since 1979, being currently involved in Project 648: Supercontinent cycles & Global Geodynamics.

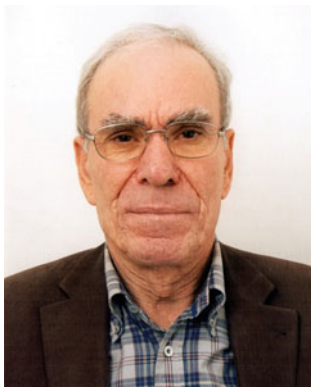

José Tomás Oliveira Ph.D. and Aggregation by Portuguese universities, geologist and presently collaborator at Laboratorio Nacional de Energia e Geologia, former Geological Survey of Portugal, where he acted also as head of the departments of Geology and Mineral Resources. As a *survey geologist*, his main activity has been concentrated in regional geological mapping in Portugal and Mozambique, with particular interest in stratigraphy, clastic sedimentology, and basin analysis. Professor at universities of Portugal and Angola, author and editor of several geological maps, the last one as co-editor of the recently published Geological Map of Portugal and Spain, 2015, scale 1:1,000,000.

About the Volume Coordinator

Prof. Dr. José Fernando Simancas teaches at the University of Granada (Spain). His main research interest is in the structural geology (including seismic crustal structure) and tectonics of the Variscan Orogen, focusing his fieldwork on southern Iberia and Morocco. He is also actively interested in the Alpine evolution of the westernmost Mediterranean.

Contributors

J. Abati Departamento de Petrología y Geoquímica, Instituto de Geociencias (UCM, CSIC), Universidad Complutense, Madrid, Spain

C. Aguilar Centre for Lithospheric Research, Czech Geological Survey, Metamorphic Petrology and Geochronology, Prague, Czech Republic

L. Albardeiro Laboratório Nacional de Energia e Geologia (LNEG), Aljustrel, Portugal

A. Almeida Departamento de Ciências do Ambiente e Ordenamento do Território, Instituto de Ciências da Terra, FCUP, Porto, Portugal

Juan Luis Alonso Departamento de Geología, Universidad de Oviedo, Oviedo, Spain

J. J. Álvaro Instituto de Geociencias IGEO (CSIC-UCM), Madrid, Spain

Maider Armendáriz Instituto Geológico y Minero de España, Madrid, Spain

P. Andonaegui Departamento de Petrología y Geoquímica, Instituto de Geociencias (UCM, CSIC), Universidad Complutense, Madrid, Spain

A. Azor Departamento de Geodinámica, Facultad de Ciencias, Universidad de Granada, Granada, Spain

Juan Ramón Bahamonde Departamento de Geología, Universidad de Oviedo, Oviedo, Spain

F. Bellido Instituto Geológico y Minero de España (IGME), Madrid, Spain

J. M. Benítez-Pérez Department of Geology, University of Salamanca, Salamanca, Spain

T. Bento dos Santos Departamento de Geologia, Faculdade de Ciências, Instituto Dom Luiz (IDL), Universidade de Lisboa, Lisboa, Portugal

E. Bernárdez Vicerrectoría de Investigación y Posgrado, Universidad de Atacama, Copiapó, Atacama, Chile

James A. Braid Department of Earth Sciences, Saint Francis Xavier University, Antigonish, NS, Canada

J. Carrilho Lopes Departamento de Geociências, Universidade de Évora, Évora, Portugal

J. M. Casas Departamento de Dinàmica de la Terra i de l'Oceà, Institut de Recerca Geomodels, Universitat de Barcelona, Barcelona, Spain

P. Castiñeiras Departamento de Petrología y Geoquímica, Instituto de Geociencias (UCM, CSIC), Universidad Complutense, Madrid, Spain

A. Castro Institute of Geosciences (IGEO), CSIC-UCM, Ciudad Universitaria, Madrid, Spain

M. Chichorro GeoBioTec, Department of Earth Sciences, Faculty of Science and Technology, New University of Lisbon, Lisbon, Portugal

P. Clariana Instituto Geológico y Minero de España, Zaragoza, Spain

S. Clausen UMR 8198 EEP CNRS, Université de Lille 1, Villeneuve d'Ascq, France

J. Colmenar Departamento de Geologia and Faculdade de Ciências, Instituto Dom Luiz, Universidade de Lisboa, Lisbon, Portugal

Juan Ramón Colmenero Departamento de Geología, Universidad de Salamanca, Salamanca, Spain

I. Coronado Institute of Paleobiology, Warsaw, Poland

P. Cózar Departamento de Paleontología, Facultad de Ciencias Geológicas, Instituto de Geociencias (CSIC, UCM), Madrid, Spain

R. Dias Earth Sciences Institute (ICT), Pole of the Évora University and Departamento de Geociências ECTUE, Évora, Portugal
Laboratório de Investigação de Rochas Industriais e Ornamentais da Escola de Ciências e Tecnologia, Universidade de Évora (LIRIO-ECTUE), Estremoz, Portugal

A. Díez-Montes Instituto Geológico y Minero de España (IGME), Oficina de Salamanca, Plaza de la Constitución, Salamanca, Spain

J. Esteve Departamento de Geociencias, Universidad de Los Andes, Bogotá, Colombia

I. Expósito Departamento de Ciencias Ambientales, Universidad Pablo de Olavide, Seville, Spain

Paulo Fernandes CIMA - Centro de Investigação Marinha e Ambiental, Universidade do Algarve, Faro, Portugal

Luis Pedro Fernández Departamento de Geología, Universidad de Oviedo, Oviedo, Spain

J. Fernández-Suárez Departamento de Petrología y Geoquímica, Instituto de Geociencias (UCM, CSIC), Universidad Complutense, Madrid, Spain

P. Ferreira LNEG-Laboratorio Nacional de Energia e Geologia, Amadora, Portugal

Vicente Gabaldón Instituto Geológico y Minero de España, Madrid, Spain

D. C. García-Bellido School of Biological Sciences, University of Adelaide, South Australia, Australia

Antonio García-Casco Departamento de Mineralogía y Petrología, Instituto Andaluz de Ciencias de la Tierra (IACT), Universidad de Granada (UGR)-Consejo Superior de Investigaciones Científicas (CSIC), Armilla, Granada, Spain

J. García-Sansegundo Departamento de Geología, Universidad de Oviedo, Oviedo, Spain

J. Gómez Barreiro Departamento de Geología, Universidad de Salamanca, Salamanca, Spain

María Teresa Gómez-Pugnaire Departamento de Mineralogía y Petrología, Instituto Andaluz de Ciencias de la Tierra (IACT), Universidad de Granada (UGR)-Consejo Superior de Investigaciones Científicas (CSIC), Armilla, Granada, Spain

E. González-Clavijo Instituto Geológico y Minero de España (IGME), Oficina de Salamanca, Plaza de la Constitución, Salamanca, Spain

P. González Cuadra Instituto Geológico y Minero de España, Madrid, Spain

F. González Lodeiro Facultad de Ciencias, Departamento de Geodinámica, Universidad de Granada, Granada, Spain

L. González Menéndez Instituto Geológico y Minero de España Parque Científico de León, León, Spain

G. Gutiérrez-Alonso Facultad de Ciencias, Área de Geodinámica Interna, Departamento de Geologia, Universidad de Salamanca, Salamanca, Spain

J. C. Gutiérrez-Marco Departamento de Paleontología, Facultad de Ciencias Geológicas, Instituto de Geociencias (CSIC, UCM), Madrid, Spain

C. Inverno Laboratório Nacional de Energia e Geologia (LNEG), Amadora, Portugal

Antonio Jabaloy-Sánchez Departamento de Geodinámica, Universidad de Granada, Granada, Spain

A. Jesus Departamento de Geologia, Faculdade de Ciências, Universidade de Lisboa, Lisbon, Portugal

S. T. Johnston Earth and Atmospheric Sciences, University of Alberta, Edmonton, AB, Canada

R. S. Jorge Faculdade de Ciências, IDL - Instituto Dom Luiz, Universidade de Lisboa, Lisbon, Portugal

Casto Laborda-López Instituto Andaluz de Ciencias de la Tierra (IACT), Universidad de Granada (UGR)-Consejo Superior de Investigaciones Científicas (CSIC), Armilla, Granada, Spain

J. A. Lains Departamento de Geologia, Faculdade de Ciências, Instituto Dom Luiz (IDL), Universidade de Lisboa, Lisbon, Portugal

N. Leal GeoBioTec and Departamento de Ciências da Terra, Faculdade de Ciências e Tecnologia, Universidade Nova de Lisboa, Costa da Caparica, Portugal

M. Liesa Departament de Mineralogia, Petrologia i Geologia Aplicada, Facultat de Ciències de la Terra, Universitat de Barcelona, Barcelona, Spain

G. Lopes Department of Earth Science, University of Bergen, Bergen, Norway

J. C. Lopes Departamento de Geociências, Universidade de Évora, Évora, Portugal

A. López-Carmona Facultad de Ciencias, Área de Geodinámica Interna, Departamento de Geologia, Universidad de Salamanca, Salamanca, Spain

Vicente López Sánchez-Vizcaíno Instituto Andaluz de Ciencias de la Tierra (IACT), Universidad de Granada (UGR)-Consejo Superior de Investigaciones Científicas (CSIC), Armilla, Granada, Spain
Departamento de Geología, Escuela Politécnica Superior, Universidad de Jaén, Linares, Spain

S. Lorenzo Departamento de Ingeniería Geológica y Minera, Escuela de Ingeniería Minera e Industrial, Instituto de Geología Aplicada (IGEA, UCLM), Universidad de Castilla-La Mancha, Almadén, Ciudad Real, Spain

Gil Machado Galp Exploração e Produção, R. Tomás da Fonseca, Lisbon, Portugal

Alberto Marcos Departamento de Geología, Universidad de Oviedo, Oviedo, Spain

A. Margalef Centre d'Estudis de la Neu i de la Muntanya d'Andorra, Institut d'Estudis Andorrans, Sant Julià de Lòria, Andorra

Agustín Martín-Algarra Departamento de Estratigrafía y Paleontología, Facultad de Ciencias, Instituto Andaluz de Ciencias de la Tierra (IACT), Universidad de Granada (UGR)-Consejo Superior de Investigaciones Científicas (CSIC), Armilla, Granada, Spain

F. J. Martínez Departament de Geologia, Facultat de Ciències, Universitat Autònoma de Barcelona, Bellaterra (Barcelona), Spain

J. R. Martínez Catalán Department of Geology, Faculty of Science, University of Salamanca, Salamanca, Spain

D. Martínez Poyatos Departamento de Geodinámica, Facultad de Ciencias, Universidad de Granada, Granada, Spain

H. C. B. Martins Departamento de Ciências do Ambiente e Ordenamento do Território, Instituto de Ciências da Terra, FCUP, Porto, Portugal

J. Mata Departamento de Geologia, Faculdade de Ciências, Instituto Dom Luiz (IDL), Universidade de Lisboa, Lisbon, Portugal

A. Mateus Departamento de Geologia, Faculdade de Ciências, Instituto Dom Luiz (IDL), Universidade de Lisboa, Lisboa, Portugal

J. X. Matos Laboratório Nacional de Energia e Geologia (LNEG), Centro de Estudos Geológicos e Mineiros do Alentejo, Aljustrel, Portugal

Stefano Mazzoli Dipartimento di Scienze della Terra, dell'Ambiente e delle Risorse (DiSTAR), Università di Napoli Federico II, Naples, Italy

C. A. Meireles Laboratório Nacional de Energia e Geologia, São Mamede de Infesta, Portugal

M. H. Mendes Geobiotec, Departamento de Geociências da Universidade de Aveiro, Aveiro, Portugal

Óscar Merino-Tomé Departamento de Geología, Universidad de Oviedo, Oviedo, Spain

P. Moita HERCULES, Departamento de Geociências, Universidade de Évora, Évora, Portugal

I. Morais Laboratório Nacional de Energia e Geologia (LNEG), Aljustrel, Portugal

Noel Moreira Laboratório de Investigação de Rochas Industriais e Ornamentais (LIRIO), University of Évora, Estremoz Pole, Convento das Maltezas, Estremoz, Portugal
Earth Sciences Institute (ICT), Pole of the University of Évora, Évora, Portugal

J. Brendan Murphy Department of Earth Sciences, Saint Francis Xavier University, Antigonish, NS, Canada

Pilar Navas-Parejo Departamento de Estratigrafía y Paleontología, Facultad de Ciencias, Universidad de Granada, Granada, Spain
Estación Regional del Noroeste, Instituto de Geología, UNAM, Hermosillo, Mexico

M. Navidad Departamento de Petrología y Geoquímica, Universidad Complutense de Madrid, Madrid, Spain

A. M. R. Neiva Departamento de Ciências da Terra, Universidade de Coimbra, Coimbra, Portugal
Geobiotec, Departamento de Geociências, Universidade de Aveiro, Aveiro, Portugal

José Tomás Oliveira Laboratorio Nacional de Energia e Geologia (LNEG), Amadora, Portugal

M. Padel BRGM, Orléans, France

D. Pastor-Galán Center for Northeast Asian Studies, Tohoku University, Sendai, Japan

J. Pedro Instituto de Ciências da Terra, Departamento de Geociências da Universidade de Évora, Évora, Portugal
Earth Sciences Institute (ICT), Pole of the Évora University and Departamento de Geociências ECTUE, Évora, Portugal

S. Pereira Departamento de Ciências da Terra, Faculdade de Ciências e Tecnologia, Universidade Nova de Lisboa, Caparica, Portugal

Zélia Pereira Laboratório Nacional de Energia e Geologia (LNEG), São Mamede de Infesta, Portugal

I. Pérez-Cáceres Departamento de Geodinámica, Facultad de Ciencias, Universidad de Granada, Granada, Spain

Vincenzo Perrone Dipto di Scienze Geologiche e Tecnologie Chimiche e Ambientali, Università di Urbino, Urbino, Italy

J. M. Piçarra Laboratório Nacional de Energia e Geologia, Centro de Estudos Geológicos e Mineiros de Aljustrel (CEGMA), Aljustrel, Portugal

Ary Pinto de Jesus Departamento de Geociências, Ambiente e Ordenamento do Território, University of Porto, Porto, Portugal

C. Puddu Departamento de Ciencias de la Tierra, Universidad de Zaragoza, Zaragoza, Spain

Cecilio Quesada Instituto Geológico y Minero de España, Madrid, Spain

J. Reche Departament de Geologia, Facultat de Ciències, Universitat Autònoma de Barcelona, Bellaterra (Barcelona), Spain

J. Relvas Faculdade de Ciências, Universidade de Lisboa, Lisbon, Portugal

A. Ribeiro Museu Nacional de História Natural e da Ciência, Departamento de Geologia, Faculdade de Ciências, Instituto Dom Luiz (IDL), Universidade de Lisboa, Lisboa, Portugal

M. A. Ribeiro Departamento de Ciências do Ambiente e Ordenamento do Território, Instituto de Ciências da Terra, FCUP, Porto, Portugal

M. L. Ribeiro Serviços Geológicos de Portugal, Laboratório Nacional de Energia e Geologia (LNEG), Amadora, Portugal

B. Rodrigues CIMA, Universidade do Algarve, Faro, Portugal

Rosario Rodríguez-Cañero Departamento de Estratigrafía y Paleontología, Facultad de Ciencias, Universidad de Granada, Granada, Spain

J. Romão Laboratório Nacional de Energia e Geologia, UGCG, Alfragide, Portugal

C. Rosa CRosa Geology Consulting, Famões, Portugal

D. Rosa Geological Survey of Denmark and Greenland, Copenhagen, Denmark

Idoia Rosales Instituto Geológico y Minero de España, Madrid, Spain

A. A. Sá Departamento de Geologia, Universidade de Trás-os-Montes e Alto Douro, Vila Real, Portugal
Centro de Geociências, Universidade de Coimbra–Pólo II, Coimbra, Portugal

T. Sánchez-García Departamento de Investigación Recursos Geológicos, Área Recursos Minerales y Geoquímica, Instituto Geológico y Minero de España, Madrid, Spain

Antonio Sánchez-Navas Departamento de Mineralogía y Petrología, Instituto Andaluz de Ciencias de la Tierra (IACT), Universidad de Granada (UGR)-Consejo Superior de Investigaciones Científicas (CSIC), Armilla, Granada, Spain

J. F. Santos Geobiotec, Departamento de Geociências da Universidade de Aveiro, Aveiro, Portugal

J. Sanz-López Departamento de Geología, Universidad de Oviedo, Oviedo, Spain

J. F. Simancas Departamento de Geodinámica, Facultad de Ciencias, Universidad de Granada, Granada, Spain

A. R. Solá Laboratório Nacional de Energia e Geologia (LNEG), Estrada da Portela, Bairro do Zambujal, Amadora, Portugal

Ángela Súarez Instituto Geológico y Minero de España-Unidad de León, León, Spain

P. Valverde-Vaquero Instituto Geológico y Minero de España (IGME), Madrid, Spain

N. Vaz Departamento de Geologia, Universidade de Trás-os-Montes e Alto Douro, Vila Real, Portugal
Centro de Geociências, Universidade de Coimbra–Pólo II, Coimbra, Portugal

Elisa Villa Departamento de Geología, Universidad de Oviedo, Oviedo, Spain

Arlo Weil Department of Geology, Bryn Mawr College, Bryn Mawr, PA, USA

S. Zamora Instituto Geológico y Minero de España, Delegación en Aragón, Zaragoza, Spain

Preface

The geology of the Iberian Peninsula and its continental shelves is complex and varied despite its relatively small size. With some 590,000 km^2 inland (Iberian Peninsula, the Balearic and other small Atlantic and Mediterranean islands) and some additional 200,000 km^2 making up the continental shelves, the record exposed spans for nearly the last 600 Ma of Earth's history. The geological record is not only long but also deep: from surficial to upper mantle, segments are exposed both inland and under the sea. At the surface, three main divisions are evident after a quick glance at any large-scale geological map: (1) several, rather large Cenozoic to Quaternary basins; which overlie, (2) a vast area in the western part of the Iberian Peninsula where Paleozoic and Precambrian rocks crop out (Iberian Massif, making the southwestern end of the European Variscan orogen); and (3) the eastern half of the peninsula and the Balearic islands (westernmost extent of the Alpine–Carpathian–Himalayan orogenic system) where mostly Mesozoic rocks are exposed although some Precambrian and Paleozoic basement inliers also exist.

Several reviews of the geology of Iberia have been published in the last decades, which collectively provide a reasonably good and complete description of all the stratigraphic and structural elements of Iberian Geology. However, the advances produced in almost every geological discipline since the last of those books was published are outstanding and it is worthwhile to try and synthesize them and their implications to a better understanding of the global evolution. Previous reviews were organized following either a purely stratigraphic arrangement or one related to a time-ordered description of the various tectono-stratigraphic units cropping out in Iberia. For the present case, a geodynamic approach is preferred. The term "geodynamic" is herein used in its widest significance, i.e., pertaining to every kind of time-evolving process taking place in the Earth that has an expression in the geological record. It is thus not restricted to its current use as synonymous of "tectonic" and also refers to sub-lithospheric processes (e.g., mantle plumes and lithospheric delamination), lithospheric processes (e.g., isostasy, plate tectonics, magmatism and metamorphism) as well as outer processes (e.g., climate, eustacy, erosion–transport–sedimentation). Obviously, most of these are interrelated and have mutual feedback effects. Nevertheless and despite the previous statement, we acknowledge that the most readily recognizable first-order geodynamic events are those related to the tectonic evolution, and we use them to establish a first-order division of the Iberian geological record. From a geodynamic (plate tectonics) point of view, several events are recorded in Iberia, the most significant of which relate to the following global scale processes:

- Amalgamation of Gondwana in the Neoproterozoic (Cadomian arc and orogeny),
- Cambrian rifting that led to opening the Rheic Ocean in the Lower Ordovician,
- Drift of Gondwana from Lower Ordovician to Devonian times,
- Subduction and collision with the Laurussian plate to form Pangea (Variscan orogeny) in the Lower Devonian–Lower Permian interval,
- Various rifting events that led to Pangea's breakup by sequential opening of the Neotethys, North Atlantic and Biscay oceans (Upper Permian–Lower Cretaceous)

- Individualization and drift of an Iberian microplate during most of the Cretaceous,
- Collision with the Eurasian plate in the north and with the African plate in the south (Alpine orogeny) from the latest Cretaceous to the present.

Collectively, these events characterize two complete Wilson cycles (Variscan and Alpine) and an older, incompletely exposed, Neoproterozoic cycle (Cadomian). These are affected and are recorded in a relatively small continental area that was always located in peripheral positions relative to the major continents to which it successively belonged: Gondwana in the Neoproterozoic–Devonian timespan, Pangea between the Devonian and the Lower Jurassic, Laurasia from then up to the Lower Cretaceous when Iberia became an independent microplate, and finally returning to the southwestern tip of Eurasia since the Paleogene to the present.

All these events marked an imprint in the history of deformation, magmatism, and metamorphism at all lithospheric levels, as well as in the formation of basins and their subsequent evolution. According to the prevailing tectonic regime at the time of their formation, sedimentary basins of each cycle include: (i) terrestrial to marine rift-related types; (ii) platform, slope, and continental rise basins during passive margin stages; (iii) syn-orogenic forearc and foreland basins; and (iv) late-to-post-orogenic intermontane basins. Apart from paleotectonic influences, the sedimentary basins and the surface were obviously subjected to variable paleoclimatic, isostatic, and eustatic conditions, which also imparted their imprint on sedimentation.

The main purpose of this book is to produce an updated review of all the aforementioned events and processes as expressed in the geological record in Iberia, and their contribution to understanding the global evolution of the Earth in the last 600 million years. The response to the editors' call for contributions among various specialists has been overwhelming: nearly 300 contributors and many hundred manuscript pages. As a result, we have been forced to change the originally intended single book into a five-volume publication but trying to keep its overall entity as an integral piece of work. Under the general title *The Geology of Iberia: A Geodynamic Approach*, we have split the publication into the following volumes and subtitles:

Volume 1: General Introduction and Cadomian Cycle
Volume 2: The Variscan Cycle
Volume 3: The Alpine Cycle
Volume 4: Cenozoic Basins
Volume 5: Active Processes: Seismicity, Active Faulting and Relief

The present *Preface* appears in all five volumes, but the *General Introduction to the Geology of Iberia* is only published as Chap. 1 in Part 1 of Volume 1, to which the potential interested readers are referred to.

Finally, we wish to express our warmest acknowledgment to all the contributors, and very especially to the book and chapter coordinators, for their enthusiastic collaboration and good work, which has made possible the completion of this exciting challenge. Every possible success is theirs, and every failure is ours. Last but not least, we acknowledge Springer and especially Dr. Alexis Vizcaino, *Earth Sciences, Geography and Environment* editor, for bringing the idea, inviting us to edit the book and for providing continuous support and encouragement.

This work is dedicated to our friends and colleagues Prof. Jorge Civis and Prof. João Pais, who passed away unexpectedly during the development of this contribution.

Acknowledgements

Co-editor José Tomás Oliveira would like to thank the Directorate of Laboratório Nacional de Energia e Geologia-LNEG for all the facilities provided during the course of this book preparation, including financial support to study the Mafic Rocks of the Pulo do Lobo Domain.

Madrid, Spain — Cecilio Quesada
Amadora, Portugal — José Tomás Oliveira
December 2018

Contents

Variscan Cycle

1

J. F. Simancas

Abstract

This chapter summarizes the classical and recent ideas together with the geodynamic hypotheses regarding the Variscan Cycle in Iberia, as an introduction to the more extensive presentations developed in the following chapters. Thus, the review focuses on the following issues: (i) uncertainties about the onset and end of the Variscan cycle; (ii) putative continents and terranes involved in the Variscan puzzle; (iii) main stages of the Variscan evolution in Iberia; (iv) deep crustal features of the Iberian Variscides; and (v) arc-shaped geometry. A brief reference to the particular problems of the Variscan basement in the Iberian Alpine orogens is also made. The attempt has been made to display a broad and rather eclectic state-of-the-art, though the author's preferences have not been totally avoided.

1.1 Introduction

An overview of the time frame, geological features and geodynamic interpretations of the Variscan Orogeny in Iberia will be given here as an introduction to the specific sections of this chapter. A good deal of significant data have been obtained in the last years on topics such as the characterization of the Iberian Orocline through paleomagnetic data, the age of tectonometamorphic and magmatic events through new U-Pb geochronology, the isotopic signature of mafic rocks, the identification of cratonic sources and basements by inherited zircon age populations and Sm–Nd and Hf isotopic systematics, the geochemistry of sediments, and the seismic imaging of the crust. These studies have promoted new geodynamic hypotheses that will be briefly exposed in the following overview.

1.2 Place of Iberia in the Variscan Orogen

The end of Paleozoic times was a period of collision between two major continents, namely Laurussia (Laurentia/Baltica) and Gondwana (Fig. 1.1a), giving way to a great orogenic belt that has been subdivided into three main segments: Appalachians (Alleghanian belt), Variscides and Urals (e.g. Matte 1991, 2002a). We refer to the Variscan Orogen or Variscides as the late-Paleozoic belt extending from Morocco to Iberia and Central Europe (Fig. 1.1a): the SW end of the Variscides may be located at the Anti-Atlas region of Morocco (Michard et al. 2010), while to the NE the Variscan belt is bounded by the Tornquist zone or Trans-European Fault extending from the Baltic coast of Poland to the Carpathians (Berthelsen 1992; Pharaoh et al. 2006). The northern front of the Variscides (the Laurussia foreland) is well defined from England to Germany, where the passage to the Caledonian crust has been seismically imaged under a post-orogenic cover (Cazes et al. 1985; BIRPS and ECORS 1986; Franke et al. 1990; Pharaoh et al. 2006); also, the northern Variscan foreland has been identified against the East European craton in SE Poland (Krzywiec et al. 2017) and the Black Sea region (Okay and Topuz 2017). By contrast, the southern front of the Variscides (the Gondwana foreland) is poorly defined due to Alpine reworking, a difficulty that is at the heart of some paleogeographic and paleotectonic discussions (Corsini and Rolland 2009; Guillot and Ménot 2009; von Raumer et al. 2009; Dörr et al. 2015; Plissart et al. 2017).

The Variscides crop out largely in the Iberian Peninsula (Fig. 1.1b). The largest outcrop is called Iberian Massif and has been divided into a number of zones of variable significance. The classical zoning (Fig. 1.1c) comprises the Cantabrian (CZ), Western Asturian-Leonese (WALZ),

J. F. Simancas (✉)
Facultad de Ciencias, Departamento de Geodinámica, Universidad de Granada, Campus de Fuentenueva S/N, 18071 Granada, Spain
e-mail: simancas@ugr.es

C. Quesada and J. T. Oliveira (eds.), *The Geology of Iberia: A Geodynamic Approach*, Regional Geology Reviews,
https://doi.org/10.1007/978-3-030-10519-8_1

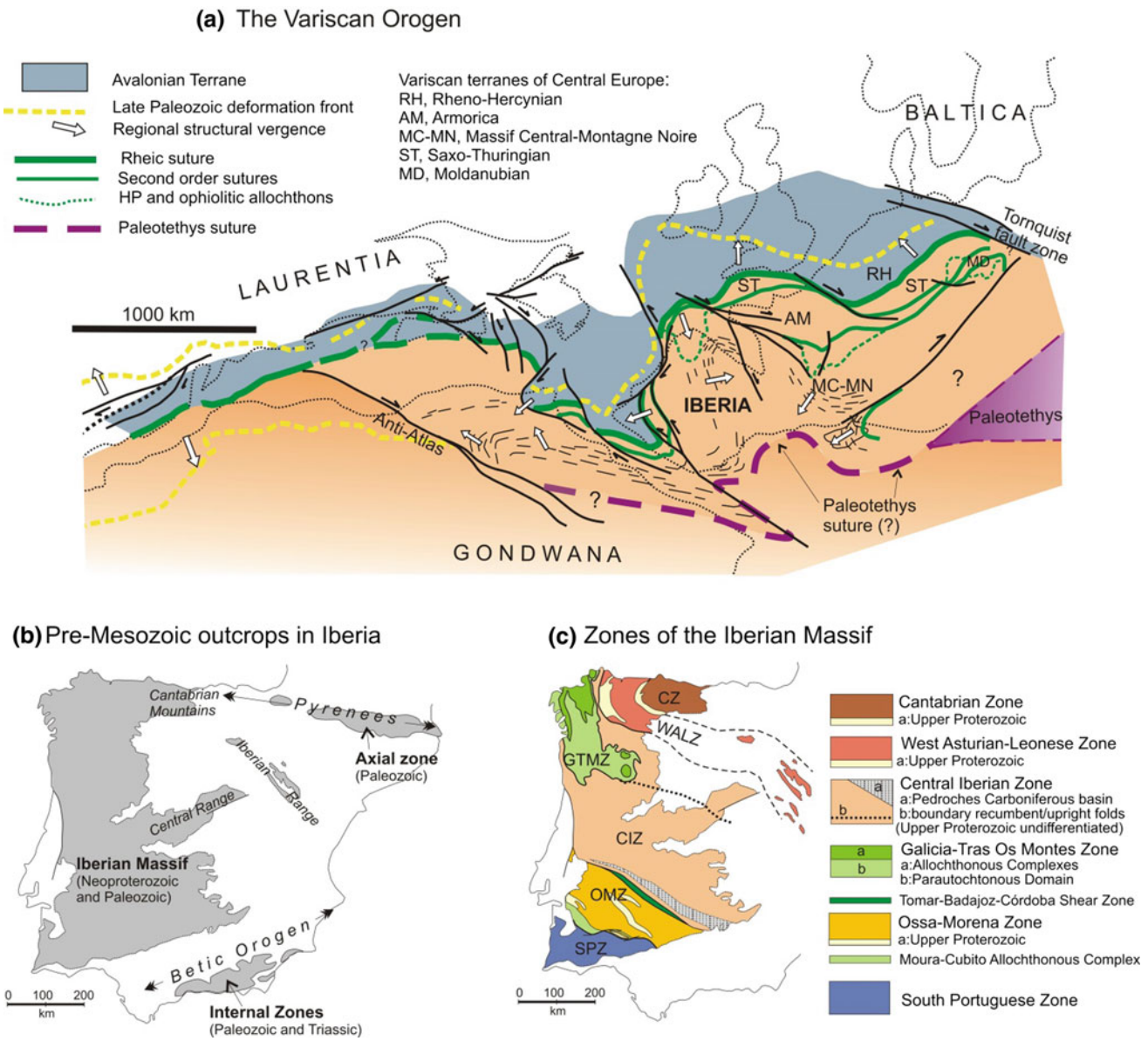

Fig. 1.1 **a**. The location of Iberia in the Variscan Orogen at Permian time. **b** Pre-Mesozoic outcrops (gray) in Iberia. The largest outcrop is called Iberian Massif; other outcrops are the basement of Alpine Mountain Ranges, i.e. the Iberian Range, the Pyrenees and the Betic Orogen. The relationships between the Iberian Massif and the basements of the Pyrenees and the Betic Orogen are uncertain (see text for discussion). **c** Classical zoning of the Iberian Massif, modified from Pérez-Estaún and Bea (2004)

Central Iberian (CIZ), Galicia—Tras-Os-Montes (GTMZ), Ossa-Morena (OMZ) and South Portuguese (SPZ) zones, referred hereafter by their abbreviations. Some authors have proposed the division of the CIZ into two (Ballèvre et al. 1992, 2009), while Arenas et al. (2016b) have grouped the GTMZ and the OMZ in a single zone; these and other deviations from the zonal scheme of Fig. 1.1c will emerge from discussions in the following pages. The insertion of the Iberian Variscides in the Paleozoic broad-scale tectonic plate context usually places the CZ facing the Gondwanan foreland and the SPZ facing the Laurussian one (Fig. 1.1a; Matte 1991; Quesada 1991; Ribeiro et al. 1995, 2007; Franke 2000; Simancas et al. 2005; Murphy et al. 2016).

1.3 The Cadomian and Avalonian Basement of the Variscides

The Late Proterozoic paleogeography depicts a major continent (Gondwana) bounded to the north by a subduction zone (e.g. Murphy et al. 2004). Since most of the Variscan Orogeny recycled crust from the border of Gondwana, the

basement of the Variscides exhibits calc-alkaline magmatic bodies and siliciclastic—volcanoclastic greywacke deposits of late Neoproterozoic (Ediacaran) age, which are thought to belong to a Cadomian Orogen or Cadomian magmatic arc (Linnemann et al. 2014). Furthermore, inherited zircons of late Neoproterozoic age are always present as a significant population in clastic Variscan Paleozoic rocks (Fernández-Suarez et al. 2002, 2014; Linnemann and Romer 2002; Neubauer 2002; Linnemann et al. 2004, 2014; Pérez-Cáceres et al. 2017). In Iberia, the Cadomian magmatism is widespread (Fernández-Suárez et al. 1998; Valladares et al. 2002; Rodríguez-Alonso et al. 2004b; Fuenlabrada et al. 2016), though it is best represented in SW Iberia north and south of the CIZ/OMZ boundary (Sánchez Carretero et al. 1990; Pin et al. 2002; Bandrés et al. 2002, 2004; Sánchez Lorda et al. 2014, 2016; Henriques et al. 2015). Inside the OMZ there are also late Ediacaran mafic-ultramafic rocks (Calzadilla de los Barros serpentinites; Fernández Carrasco et al. 1983; Sánchez Carretero et al. 1990; Ordóñez-Casado 1998) of ophiolitic supra-subduction signature, which may correspond to a Cadomian intra-arc setting (Lunar et al. 2011; Merinero et al. 2014; Arenas et al. 2018). On the other hand, Cadomian deformation and metamorphism in Iberia have been well documented locally (Blatrix and Burg 1981; Ortega Gironés and González Lodeiro 1986; Dallmeyer and Quesada 1992; Abalos 2001; Díaz García 2006; Henriques et al. 2015), with deformation being considered as generally mild by some authors (Simancas et al. 2004) though the disputed Cadomian/Variscan attribution of deformation and metamorphism at some localities introduces caution on that appraisal (Abalos et al. 1991; Quesada 1991, 1997; Eguiluz et al. 2000; Mateus et al. 2016 vs. Azor et al. 1993; Martínez Catalán et al. 1997; Simancas et al. 2001; Expósito et al. 2002; Arenas et al. 2014a). The Cadomian-Gondwanan terranes of the Variscan Orogen match Sm–Nd isotopic characteristics that point to recycling of a ≈ 2Ga West or North African crust (Murphy et al. 2006).

Avalonia is a former composed microcontinent (Avalonian terranes: Carolinia, Avalonia) that was amalgamated to Laurentia and Baltica during the Caledonian Orogeny. Later on, the collision of Laurussia with Gondwana brought an Avalonian crust to the dominant Cadomian-African crust of the Variscides (Fig. 1.1a). A particular feature of the Avalonian terranes is that they have Sm–Nd isotopic characteristics of recycling of a juvenile ≈1 Ga crust (Grenvillian, possibly Baltican), which makes a difference with respect to the Cadomian-African terranes (Murphy et al. 2006; Henderson et al. 2016). In Iberia, the SPZ is considered Avalonian on the basis that it lies outboard of the putative main Variscan (Rheic) suture (see below).

1.4 Time Frame of the Variscan Cycle in Iberia

The useful concept of Orogenic Cycle (Wilson 1969) has to be adapted to real orogenies. Its application to the Variscan Orogeny in Iberia is not free from ambiguities regarding the beginning and end of the cycle.

1.4.1 The Beginning of the Variscan Cycle

The end of the Cadomian Orogeny in Iberia has to be defined first. Unfortunately, the cessation of the widespread mostly calc-alkaline magmatism that characterizes the Cadomian Orogeny is not a sharp line (Salman 2004; Simancas et al. 2004; Andonaegui et al. 2016; Sánchez Lorda et al. 2016). However, the Cadomian deformation and metamorphism can apparently provide with better constraints: (i) at the southern border of the CIZ the first low-grade foliation observed in Ediacaran rocks (Serie Negra formation) has been dated at 560–550 Ma (Blatrix and Burg 1981; Dallmeyer and Quesada 1992), while an amphibolite facies metamorphic event dated at 540 Ma has also been described (Henriques et al. 2015); (ii) in the interior of the CIZ, the Cadomian deformation is manifested as a simple unconformity (Ortega Gironés and González Lodeiro 1986; Palero 1993) formed between 575 and 555 Ma (Talavera et al. 2015); (iii) in the Iberian Range of northeastern Iberia, a poorly deformed conglomerate of Lower Cambrian age, probably older than 520 Ma, contains pebbles with microstructures denoting low-grade deformation (Abalos 2001); (iv) in the Cantabrian region of northern Iberia, asymmetric folds with axial plane cleavage are thought to develop between 560 and 540 Ma (Díaz García 2006). Therefore, the Cadomian deformation seems to have ended at the Ediacaran-Cambrian boundary.

The stratigraphic record agrees with the deformational evidence. The Cambrian starts everywhere in Iberia with siliciclastic deposits, passing upwards to carbonate or mixed terrigenous and carbonate platform deposits (Liñán et al. 2002). This Lower Cambrian platform is indeed a feature common to a very large domain, from Morocco (Piqué 1981) to the Saxothuringian Zone in central Europe (Falk et al. 1995); accordingly, a general stage of tectonic quiescence seems to have prevailed at Early Cambrian time in extended domains of the Variscides. Moreover, the geochemistry of Ediacaran and Cambrian sediments (Fuenlabrada et al. 2016) supports that the Ediacaran greywackes were associated with a mature active margin (volcanic arc), while the Cambrian shales fit better with a more stable

context with a higher contribution from cratonic sources; therefore, the geochemistry of the Ediacaran–Cambrian transition in Central Iberia documents a tectonic switch in the periphery of Gondwana, from an active margin to a more stable context related to the onset of a passive margin (Fuenlabrada et al. 2016). Subsequently, some signs of tectonic instability started to appear in the form of terrigenous sediments and associated tholeiitic-alkaline volcanics, which have been interpreted as the beginning of the rifting affecting the border of Gondwana during Cambrian-Ordovician time (Liñán and Quesada 1990; Mata and Munhá 1990; Crowley et al. 2000; Sánchez-García et al. 2003). The Furongian-Early Ordovician unconformity recognized in Iberia (Gutiérrez-Marco et al. 2002) lacks clear geodynamic interpretation, though the prevailing view relates this unconformity to extensional tilting of blocks (e.g. González-Clavijo et al. 2017a).

Despite the above evidence, the tectonic significance of the Cambrian-Ordovician magmatism has been raised as an issue to divide up into Cadomian and Variscan Cycle. This early Paleozoic magmatism is interpreted either as related to a tectonically distinctive rifting stage or a protracted subduction continuous since late Proterozoic time. Thus, the calc-alkaline signature of part of this magmatism has been related to active subduction (Díaz-Alvarado et al. 2016; Villaseca et al. 2016; Andonaegui et al. 2017) though oxygen and hafnium isotopic data indicate that the most voluminous of these magmatic bodies resulted from anatexis of immature sediments mostly derived from Ediacaran igneous rocks (Ollo de Sapo Formation; Montero et al. 2017). On the other hand, a remarkable volume of tholeiitic and alkaline rocks of Cambrian-Ordovician age also exists, particularly in SW Iberia (Mata and Munhá 1990; Giese and Bühn 1993; Sánchez-García et al. 2003; Galindo and Casquet 2004; Montero and Floor 2004).

Altogether, the stratigraphy, sedimentary geochemistry, extensional context and partly the nature of magmatism lead most authors to support a distinctive rifting scenario at Cambrian-Ordovician time (Liñán and Quesada 1990; Crowley et al. 2000; Montero and Floor 2004; Etxebarría et al. 2006; Bea et al. 2007; Chichorro et al. 2008; Díez Montes et al. 2010; Sarrionandía et al. 2012; Diez Fernández et al. 2014; Sánchez-García et al. 2014; Montero et al. 2017; Orejana et al. 2017). Thus, to conclude, the more suitable choice for the beginning of the Variscan Cycle in Iberia seems to be the early-middle Cambrian. Uncertainty about the timing and geodynamics of the transition from Cadomian subduction-arc to passive continental margin also exists in other regions of the Variscides (Linnemann and Romer 2002; Sláma et al. 2008; Linnemann et al. 2014; Hajná et al. 2017; Chelle-Michou et al. 2017).

1.4.2 The End of the Variscan Cycle

Regarding the end of the Variscan Cycle, it must be noticed that: (i) molasse undeformed basins with Stephanian B, C-Autunian sediments mark an upper boundary for the age of penetrative shortening deformation, which is thus found to have finished at the beginning of Permian time (Wagner et al. 1983; Wallis 1983; Arche and López-Gómez 1996; Fernández et al. 2004; Sierra and Moreno 2004; Dinis et al. 2012); (ii) paleomagnetic data indicate that the arched shape of the northern Iberian Variscides would have developed at latest Carboniferous-earliest Permian times, which imply a late along-strike shortening of the whole orogenic belt (Weil et al. 2001, 2013; Gutiérrez-Alonso et al. 2004; Pastor-Galán et al. 2015a, 2016, 2017a; Fernández-Lozano et al. 2016); (iii) Permian extensional tectonics would be excluded from the Variscan Cycle if extension related to mechanisms exceeding the realm of the orogen (Arche and López-Gómez 1996; Doblas et al. 1998; Henk 1999; Wilson et al. 2004; McCann et al. 2006); nevertheless, Stampfli et al. (2013) have associated the collapse of the Variscan Orogen to Permian slab roll-back at the Paleotethys oceanic domain (Fig. 1.1a).

Besides deformational evidence, metamorphism is older than Permian in the Iberian Massif, though early Permian high-grade metamorphism has been accredited in the Paleozoic basement of the Betics (Fig. 1.1b; Acosta-Vigil et al. 2014). Regarding orogenic magmatism, late- to post-collisional calc-alkaline granitic and volcanic magmatism extends continuously from late Carboniferous to early Permian times (Bea 2004; Gutiérrez-Alonso et al. 2011a; Gómez-Pugnaire et al. 2012; Pereira et al. 2015); afterward a significant change is observed between early Permian calc-alkaline magmatism and late Permian-Triassic alkaline volcanism (Lago et al. 2004a, b; Denèle et al. 2011).

1.5 Continents and Terranes Involved in the Variscan Orogeny. The Terranes of the Iberian Variscides

1.5.1 Paleobiological, Paleomagnetic and Paleotectonic Constraints

Paleobiological data constitute an important constraint on paleogeography, suggesting the existence of barriers for free communication of fauna and flora (Cocks and Fortey 1982; Robardet and Gutiérrez-Marco 2002; McKerrow et al. 2000; Nysaether et al. 2002; Fortey and Cocks 2003; Robardet 2003; González et al. 2011); nevertheless, some ambiguities may exist in the paleogeographic interpretation of

paleontological data (Fortey and Cocks 2003). Paleomagnetism yields primary information on continental displacements, though the information is frequently undermined by data shortage and methodological difficulties (Van der Voo 1993; Tait et al. 2000; Edel 2001; Nysaether et al. 2002; Cocks and Torsvik 2006; Derder et al. 2006; Domeier et al. 2012; Torsvik and Cocks 2013; Domeier and Torsvik 2014). Regarding the Variscan evolution, paleomagnetic and paleontological data basically agree on: (i) the Paleozoic paleogeography up to early Ordovician times, with three major continental blocks (Laurentia, Baltica and Gondwana); (ii) the subsequent fragmentation of the border of Gondwana giving way to Avalonia with the Rheic Ocean in-between (I refer here to Avalonia in a broad sense, i.e. including Carolinia; Nance et al. 2012); (iii) the amalgamation of Avalonia with Laurentia (early Appalachian orogenic events) and Baltica (Caledonian Orogeny); (iv) the final assembly of Laurentia-Baltica-Avalonia with Gondwana at Late Carboniferous time (Fig. 1.1a; e.g. Matte 2002a; Nance et al. 2012). However, consensual paleogeographies have not been reached yet for the Late Ordovician-Early Carboniferous time span, with major discrepancies concerning the characterization of peri-Gondwanan terranes and the paleolatitude of Gondwana. For that period, most paleomagnetic models show a wide separation between Africa (Gondwana) and the Variscan terranes of central Europe-central Iberia (Cocks and Torsvik 2006; Derder et al. 2006; Torsvik and Cocks 2013; Domeier and Torsvik 2014), while a good number of paleobiological data suggest continental proximity at Devonian time (McKerrow et al. 2000; Robardet and Gutiérrez-Marco 2002; Robardet 2003). Nevertheless, some paleobiological data permit several interpretations: dissimilarities between Middle Mississippian miospore assemblages of Western Europe and North Africa have been variably interpreted as evidence of: (i) a large ocean separating two continents (Clayton et al. 2002), (ii) an extensive seaway to the east (the Paleotethys) but close proximity to the west (González et al. 2011), or (iii) continents already assembled at that time with floral dissimilarities being caused by climatic belts (McKerrow et al. 2000). Therefore additional data are needed before considering that the paleogeographic scenarios during the critical Late Ordovician-Early Carboniferous time span are well founded.

The recognition and correlation of high-pressure metamorphic and ophiolitic belts along the Variscan orogen constitute another major constraint on paleotectonic and paleogeographic reconstructions. These geological data apparently indicate where subduction events took place and oceanic-like crust existed in the past, but the width of the putative oceanic domains is unknown and the correlation of the disparate high-pressure/ophiolitic belts is far from obvious. The whole currently available paleobiological, paleomagnetic and geological evidence suggests that the Variscan Orogen must exhibit the major suture of the Rheic Ocean as well as some second-order sutures related to the amalgamation of terranes of arguable significance (Matte 1991, 2001; Dias and Ribeiro 1995; Franke 2000, 2014; Simancas et al. 2005; Winchester et al. 2006; Ballèvre et al. 2009, 2014; Franke et al. 2017). Moreover, if current paleomagnetic reconstructions (Torsvik and Cocks 2013; Domeier and Torsvik 2014) are essentially correct, another suture would exist, corresponding to the Paleotethys Ocean envisaged by Stampfli et al. (2013). The Paleotethys suture would be masked in the Alpine orogens of southern Europe.

1.5.2 The Elusive Rheic Suture

The Rheic Ocean is the major oceanic domain that existed at early Paleozoic time between the Avalonia (Avalonia-Carolinia) composite terrane and the border of Gondwana (e.g. Matte 1991, 2001); its inception, fast spreading and closure have been reviewed by Nance et al. (2012). The rift that gave way to the Rheic Ocean nucleated at or very near to the previous Neoproterozoic sutures of accretion/dispersal along the northern Gondwanan margin, in a clear case of inheritance of lithospheric structures (Murphy et al. 2006).

The suture of the Rheic Ocean in the Appalachian-Variscan orogenic belt (Fig. 1.1a) can be labeled as elusive drawing on a number of reasons. In the southern Appalachians, the Rheic suture is probably located southeast of the Carolina terrane, hidden underneath the Coastal Plane sediments (Cook and Vasudevan 2006; Duff and Kellog 2017). In the northern Appalachians, the location of this suture depends on the relationships between Avalonia and Meguma (Murphy et al. 2004; Linnemann et al. 2012; Nance et al. 2015). Furthermore, the Rheic suture does not crop out in the adjacent Moroccan Variscides (Simancas et al. 2005); actually, this region shows strong similarities in Paleozoic faunas with the Montagne Noire-Barrandian regions of central Europe (Piqué 1994; Robardet 2003). Regarding the European Variscides, a number of ophiolitic units in southernmost England, central Germany and Iberia have been sometime attributed to the Rheic Ocean suture, though their interpretation is rather complex. Thus, the Lizard ophiolite in southern England is thought to not derive from the Rheic Ocean but from a nearby small oceanic domain (Shail and Leveridge 2009), the Rheic suture itself being unexposed and/or obliterated. In the same way, the Devonian MORB-featured metabasalts of the Giessen Nappe at the boundary between the Rheno-Hercynian and Saxothuringian zones (Germany) do not represent the Rheic Ocean; instead, they are a young element of a protracted evolution that involved closure of the Rheic Ocean (late Silurian-earliest Devonian), opening of a new Rheno-Hercynian Ocean

(early-middle Devonian) and final closure of this new oceanic domain at late Devonian-Carboniferous times (Berthelsen 1992; Franke 2000, 2006; Franke and Dulce 2017). On the other hand, there is no evidence of a Rheic subduction-related magmatic arc, with the exception of subordinate Silurian-early Devonian magmatism at the Mid-German Crystalline High and the Northern Phyllite Zone (Rheno-Hercynian—SaxoThuringian boundary). This fact has been attributed to intraoceanic subduction coupled with arc removal by subduction erosion (Nance et al. 2012), though detrital zircons in Late Devonian and Carboniferous rocks indirectly provide with some evidence for that missing magmatic arc (Pereira et al. 2012a, 2017; Pérez-Cáceres et al. 2017).

In NW Iberia, the ophiolitic units of the allochthonous complexes (Fig. 1.1c) are embedded between the Upper and Basal continental units, representing a rootless suture that has been classically interpreted as corresponding to the Rheic Ocean (Martínez Catalán et al. 1997, 2009; Díaz García et al. 1999; Ribeiro et al. 2006; Arenas et al. 2007). Unlike that interpretation, they have also been correlated with the second-order suture of the Massif Central (Matte 1991; Roger and Matte 2005; Ribeiro et al. 2007). Recently, the view of the NW Iberia allochthonous ophiolites as a second-order Variscan suture has gained momentum with new data: (i) clastic zircon populations favor a West African Craton provenance for both the upper allochthons overlying the ophiolites (Fernández-Suárez et al. 2003; Albert et al. 2015) and the lower allochthons underlying them (Díez Fernández et al. 2010); (ii) the Lu–Hf isotope signature of zircons from the ophiolites suggests some contribution of an old continental source, and the presence in the ophiolites of Mesoproterozoic zircon xenocrysts suggest that mafic magmas intruded a late Mesoproterozoic-early Paleoproterozoic crust (Arenas et al. 2014b). Actually, there are two groups of ophiolites in the allochthonous complexes (Arenas et al. 2016a and references therein): (i) a Cambrian-Ordovician group perhaps related to the closure of a minor oceanic domain at the border of Gondwana, coeval with the birth of the Rheic Ocean, and (ii) a Lower-Middle Devonian group whose tectonic setting might be a small (pull-apart?) oceanic basin opened between two high-P events (Arenas et al. 2014a, b). The attribution of the NW Iberia ophiolites is not resolved, however, since the hafnium isotopic array of the upper allochthonous units has been found rather similar to the one of Avalonia, thus favoring the existence of the Rheic suture in between the upper and lower allochthonous units (Henderson et al. 2016).

In SW Iberia, the presence of three appealing units at the OMZ/SPZ boundary (Fig. 1.1c) has led to consider it as the location of the Rheic suture. These units are: (i) the Beja-Acebuches Amphibolites, a strip of metamorphosed MORB-like mafic and ultramafic rocks that crop out all along this major contact (Bard 1977; Bard and Moine 1979; Crespo-Blanc and Orozco 1991; Fonseca and Ribeiro 1993; Quesada et al. 1994; Castro et al. 1996); (ii) the Pulo do Lobo unit, a polydeformed low-grade metasedimentary unit of lower Frasnian age with minor MORB-featured metabasalts (Eden and Andrews 1990; Silva et al. 1990; Eden 1991; Giese and Bühn 1993; Pereira et al. 2008; Braid et al. 2010; Martínez Poza et al. 2012; Dahn et al. 2014; Pérez-Cáceres et al. 2015); and (iii) the Moura-Cubito unit, an allochthonous complex tectonically emplaced onto the OMZ border, which contains high-pressure and MORB-like rocks (Fonseca et al. 1999; Araújo et al. 2005; Booth-Rea et al. 2006; Ponce et al. 2012; Rubio Pascual et al. 2013b). However, these key units are becoming reassessed drawing on new data, particularly geochronological. Thus, the mafic rocks of Beja-Acebuches have revealed to be younger (≈340 Ma; Azor et al. 2008, 2009) than envisaged for a Rheic Ocean ophiolite. In a similar way, the interpretation of the Pulo do Lobo unit as an accretionary prism with shavings of the Rheic oceanic floor has become weakened by the early Carboniferous age of the mafic rocks, which are thus intrusive in the Devonian schists (Braid et al. 2010; Dahn et al. 2014; Murphy et al. 2015; Pérez-Cáceres et al. 2015). Since these magmatic ages are coeval with basin development in SW Iberia, a Carboniferous transtensional intraorogenic event has been suggested (Simancas et al. 2001, 2006; Azor et al. 2008; Pereira et al. 2009, 2012b). However, there is also the alternative explanation that the OMZ/SPZ boundary was a protected tract of Rheic oceanic lithosphere that did not close until Carboniferous time, postdating the main collisional event (Braid et al. 2018). To conclude, the uncertainties about the Beja-Acebuches Amphibolites and the Pulo do Lobo units leave the location of the Rheic Ocean suture ultimately relying on the Moura-Cubito allochthonous complex (Fonseca et al. 1999; Araújo et al. 2005; Ponce et al. 2012; Rubio Pascual et al. 2013b), which exhibits HP metamorphism at ≈370 Ma (Sm/Nd whole rock-garnet isochron from an eclogite; Moita et al. 2005) and MORB-featured mafic rocks of 480 Ma (U-Pb SHRIMP analyses; Pedro et al. 2010).

1.5.3 Second-Order Variscan Sutures

In addition to the Rheic suture at the OMZ/SPZ boundary and its classically accepted continuation towards the Lizard region (not necessarily the Lizard ophiolite itself) and the Rheno-Hercynian/Saxothuringian boundary, the Variscan Orogen displays other along-strike suture-like tectonic belts. Thus, south of the putative Rheic Ocean suture there must be the cryptic Saxothuringian/Armorican boundary (northernmost France), correlative to the east with the Saxothuringian/Moldanubian boundary (Münchberg-Teplá

suture); further south, there is the Armorican/Massif Central boundary, which continues to the east at the southern part of the Bohemian Massif and may come back to northern Corsica through a belt curvature and a Stephanian dextral shear displacement (Fig. 1.1a; Matte 1991, 2002a; Franke 2000, 2014; Simancas et al. 2005; Rossi et al. 2009).

In the Iberian Variscides, the CIZ/OMZ boundary at SW Iberia is usually located at a crustal-scale shear zone (Tomar-Badajoz-Córdoba shear zone, hereafter TBCSZ), whose signification is debated as a Variscan or Cadomian suture boundary (Fig. 1.1c). The TBCSZ contains relics of eclogites, MORB-like mafic rocks, high-to-medium grade gneisses and aluminous schists, exhibiting a prominent S-L tectonic fabric with subhorizontal stretching lineation and left-lateral kinematics (Burg et al. 1981; Abalos et al. 1991; Azor et al. 1994). Some authors view the CIZ/OMZ boundary as a mega-shear zone representing a Variscan suture (Burg et al. 1981; Matte 1991; Azor et al. 1994; Simancas et al. 2001, 2003; Gómez Pugnaire et al. 2003; López Sánchez-Vizcaíno et al. 2003) based on the Late Devonian to Carboniferous Ar/Ar ages (Quesada and Dallmeyer 1994), the late Cambrian to early Ordovician ages of migmatitic and orthogneissic bodies (Oschner 1993; Azor et al. 1995; Ordóñez-Casado 1998; Pereira et al. 2012b), and the early Ordovician age obtained for eclogitized protoliths (Ordóñez-Casado 1998). Thus, the OMZ would be a peri-Gondwanan terrane that, in view of paleontological (Robardet and Gutiérrez-Marco 2002) and Sm–Nd isotopic (López-Guijarro et al. 2008) similarities, remained proximal to the CIZ. Other authors hold, despite no geochronological support, that the TBCSZ is a Cadomian suture reworked by a Variscan shear zone (Quesada 1991; Abalos et al. 1991, 2002; Ribeiro et al. 2007, 2010; Henriques et al. 2015), claiming that most reported geochronological ages could have been reset by a thermal imprint related to the Cambrian-Ordovician rifting and the Variscan activity. The second-order rank of this suture zone is evident in any case because Ediacaran rocks are the same across the TBCSZ; actually, it is north of the TBCSZ where a change of the Ediacaran series occurs (San José et al. 2004), coincident with variations in clastic zircon populations (Fernández-Suárez et al. 2000, 2002; Bea et al. 2010; Pereira et al. 2011). Accordingly, Pérez-Cáceres et al. (2017) have suggested that a main Cadomian fault exists north of the TBCSZ, hidden under the Pedroches Carboniferous basin (Fig. 1.1c), the Cadomian subduction itself being located south of the OMZ (Sánchez Lorda et al. 2014).

A radically different tectonic interpretation of the TBCSZ boundary and the Iberian Variscides in general has been presented by Díez Fernández and Arenas (2015), Arenas et al. (2016b) and Díez Fernández et al. (2016, 2017), who consider that most of the OMZ plus the rocks of the TBCSZ and the southernmost CIZ constitute an allochthonous complex in continuity with the allochthonous complex (GTMZ) of NW Iberia (Fig. 1.1c). This hypothesis has been criticized on structural and kinematic grounds, as well as drawing on crustal seismic imaging (Simancas et al. 2016).

Another Variscan tectonic boundary of arguable significance has been suggested to exist (vaguely located) at the northern part of the CIZ, mostly based on paleofaunistic correlations (Ballèvre et al. 1992; Franke et al. 2017). In this region it must be noticed the presence of some HP metabasites in the Central Range, with Early Ordovician protolith ages and continental tholeiitic signature. This HP metamorphism has been explained as due to intracontinental crustal subduction (Barbero and Villaseca 2000; Villaseca et al. 2015). This hypothetical boundary inside the CIZ approximately coincides with the passage between Variscan recumbent folds (to the north) and upright folds (Fig. 1.1c; Díez Balda et al. 1990), as well as with contrasting geochemical signatures of Neoproterozoic sediments (Villaseca et al. 2014). However, detailed mapping (González-Clavijo and Martínez Catalán 2002; Díez Fernández et al. (2016); González-Clavijo et al. 2016) does not support a Variscan suture-like boundary in this region.

If the allochthonous ophiolites in NW Iberia do not represent the Rheic suture and the CIZ/OMZ boundary (TBCSZ) is a Variscan suture (see discussions above), they could mutually correlate (Fig. 1.1a; Matte and Burg 1981; Roger and Matte 2005; Simancas et al. 2009), though such a view is far from consensual (Ribeiro et al. 2007). Independently of the disputed intra-Iberian correlations, the NW Iberian ophiolites have been also correlated with the Armorican/Massif Central suture boundary (Fig. 1.1a; Matte and Burg 1981; Matte 1986, 1991; Franke 2006, 2014; Días et al. 2016), a linkage that has been criticized by Robardet (2002, 2003) because that suture would cut across regions (Armorica and Central Iberia) with faunal and stratigraphic similarities in the Ordovician. Actually, despite proposals of one to one suture correlation between Iberia and Central Europe (Franke 2014; Franke et al. 2017; Paquette et al. 2017), the Iberian transect probably contains only two Variscan sutures (OMZ/SPZ and CIZ/OMZ; but see discussion above), while the French and German transects apparently contain three: the Rhenohercynian/Saxothuringian boundary, the Saxothuringian/Armorican (cryptic) or Saxothuringian/Moldanubian boundary, and the Armorican/Massif Central boundary (Fig. 1.1a; Matte 1986, 1991; Franke 2000, 2006, 2014; Simancas et al. 2005; Ballèvre et al. 2009). This difference would prevent a simple connection between the sutures of Iberia and Central Europe; however, transform faults interrupting to the west the Massif Central oceanic domain might solve both the paleontological continuity between Armorica and Central Iberia as well as the different number of suture belts at each side of the transform zone (Simancas et al. 2002, 2005).

1.5.4 The Paleotethys Suture

Besides the orogenic sutures visible at outcrop, a suture could exist at the southern side of the Variscan Orogen, hidden in the Alpine orogens of the western Mediterranean. The name Paleotethys is given here to the oceanic domain represented in this hypothetical suture (Fig. 1.1a; Stampfli et al. 2013), though the usage is not fully consistent; thus, for instance, Ribeiro et al. (2007) use the name Paleotethys for the oceanic domain represented in the Armorican/Massif Central suture boundary, i.e. the Massif Central or Southern Brittany Ocean of other authors (Matte 1991, 2002a; Franke 2014).

The Paleotethys is depicted in all the late Permian paleogeographies as an ocean that widens southeast of the Variscides (Fig. 1.1a), though its extent and location at early Permian and pre-Permian times would vary according to different authors. Concerning Permian paleogeography, some models favor different positions of the Variscan terranes in early (abutting South America) and late (abutting Africa) Permian time, thus needing a major Permian dextral megashear entering an eastern Paleotethys Ocean (Muttoni et al. 2003). New paleomagnetic assessment has apparently led to abandon that paleogeographic picture, in favor of a Pangea with Iberia already contiguous to northern Africa at early Permian time (Weil et al. 2001; Domeier et al. 2012), though the debate has been recently revived (Gallo et al. 2017). Regarding pre-Permian time, there are models in which the Paleotethys is simply an eastern ocean residual to the closing of the Rheic Ocean (Matte 2001; Scotese 2004). However, paleomagnetic data suggest that a Paleotethys oceanic domain could have separated all the Variscan outcrops of Iberia-central Europe from the Gondwana (Africa) continent, extending along the southern boundary of the Variscan belt before Permian time (Torsvik and Cocks 2013; Stampfli et al. 2013; Domeier and Torsvik 2014).

Which were the geological effects related to the birth and closing of that southern oceanic domain? First, it seems that a southeastern Paleotethys bounding a ribbon-like continental Variscides is a necessary scenario for the late Variscan orocline buckling (Johnston et al. 2013). Moreover, it has been proposed that mantle activity related to the Paleotethyan rifting/subduction south of the Variscides might have been the ultimate reason for the lithospheric thinning and heating that characterizes the early Carboniferous evolution of the Variscides (Franke 2014). Also, it has been suggested that the late Carboniferous-early Permian magmatism of the Variscides (e.g. the granitoids dominating central and NW Iberia) formed by subduction of this southern oceanic domain, once the Rheic ocean get closed (Finger and Steyrer 1990; Pereira et al. 2015). Alternatively, the influence of the Paleotethys could have been restricted to deformation, metamorphism and magmatism in the Variscan basement of the Alps, Betics and (Wernert et al. 2016) some regions of the Morocan Variscides. In this respect, it must be noted that paleontological (Robardet 2003) and inherited zircons evidence (Drost et al. 2011; Pastor-Galán et al. 2013) are hardly compatible with a major Paleotethys ocean south of the Variscan belt; accordingly, a minor oceanic domain or an oceanic wedge restricted to the eastern Variscides could be solutions of compromise (Nance et al. 2012). At late Carboniferous time free crossing of floras and faunas from Africa to Europe was definitely achieved (McKerrow et al. 2000; González et al. 2011), with only the easternmost regions of the Variscides around the Black Sea never reaching collision (Fig. 1.1a; Stampfli et al. 2013; Okay and Topuz 2017).

1.5.5 Inherited Zircon Populations

The age of inherited zircon populations, sometimes coupled with the Hf isotopic fingerprint of zircons and Sm–Nd whole-rock isotopic systematics, yield information either on sedimentary sources (clastic zircons) or the nature of the underlying basement (restitic and xenolithic zircons in magmatic rocks). Despite plagued with inherent ambiguities, these studies have become a support for paleogeographic reconstructions (Linnemann et al. 2004, 2012, 2014; Nance and Linnemann 2008; López-Guijarro et al. 2008; Bea et al. 2010; Henderson et al. 2016; Chelle-Michou et al. 2017). Since the Neoproterozoic location of Avalonian terranes is thought to have been at the Gondwana margin westwards of the so-called Gondwanan (i.e. African) terranes (Scotese 2004; Pollock et al. 2009; Nance et al. 2012; Stampfli et al. 2013), the former should include Mesoproterozoic Grenvillian components (Amazonian or more probably Baltican; Henderson et al. 2016), while Gondwanan terranes must be dominated by ≈2.0 Ga West African Craton-Saharan Metacraton components, without excluding Mesoproterozoic components of northeast Africa (Murphy et al. 2000, 2006; Fernández-Suárez et al. 2003; Bea et al. 2010; Dörr et al. 2015; Cambeses et al. 2017). The existence of several sources for Mesoproterozoic zircons introduces some ambiguity in the interpretation; furthermore, the affinity of some terranes remains unclear when their basement is suspected to be of Avalonian type but their exposed cover contains abundant Paleoproterozoic (African) zircons. This seems to be the case of the Meguma terrane in Northern America and the SPZ in SW Iberia, where felsic igneous rocks probing the basement are isotopically more juvenile than their host Paleozoic rocks (Nance et al. 2015). Notwithstanding that, the SPZ is considered Avalonian on the basis that it lies outboard of the putative Rheic suture,

while the Upper Allochthonous Units of northwest Iberia have disputed Avalonian or Gondwanan affinity (Albert et al. 2015; Henderson et al. 2016; Pérez-Cáceres et al. 2017). The remaining Variscan outcrops of Iberia have Gondwanan (African) affinity according to inherited zircons (López-Guijarro et al. 2008; Bea et al. 2010; Pastor-Galán et al. 2013; Cambeses et al. 2017) and other geological and paleontological data (Quesada 1991; Robardet 2003).

As a result of studies on inherited zircon populations, the location of the Variscan terranes of Iberia along the border of Gondwana at Neoproterozoic times is starting to be constrained, not without discussion (Bea et al. 2010; Murphy et al. 2011; Pastor-Galán et al. 2013; Gutiérrez Alonso et al. 2015; Pérez-Cáceres et al. 2017; Cambeses et al. 2017). Additionally, clastic zircon populations have contributed to demonstrate the huge volume of the Cadomian magmatic arc, and to hypothesize the existence of Cadomian boundaries (Pérez-Cáceres et al. 2017), cryptic (rift-related?) Cambrian magmatism in Central Iberia (Chichorro et al. 2017) and Devonian (arc?) magmatism not found at outcrop (Pereira et al. 2012a, 2017; Pérez-Cáceres et al. 2017).

1.5.6 Armorican Superterrane versus Galatian Superterrane

Besides the consensual drift of Avalonia since early Ordovician time (e.g. Matte 2001; Linnemann et al. 2012; Stampfli et al. 2013; Franke et al. 2017), many authors envisage that the evolution of the northern border of Gondwana involved the formation of another microplate or superterrane, namely Armorica, conceived as the collection of terranes (the OMZ in Iberia; the Saxothuringian, Armorican and Moldanubian regions in Central Europe) between the second-order sutures defined above (Fig. 1.1a; Matte 1991, 2001, 2002a; Franke 2000, 2006; Nysaether et al. 2002; Fortey and Cocks 2003; Simancas et al. 2005; Ballèvre et al. 2009; Ribeiro et al. 2010). Geological and paleontological evidence suggests that these terranes split up from Gondwana at Ordovician time, like Avalonia, but they always remained very near the Gondwana continent (e.g. Nysaether et al. 2002; Robardet 2003).

At odds with this scenario, the paleogeographic reconstruction of Stampfli et al. (2013) is characterized by the so-called Galatian superterrane, which started to drift away from Gondwana in Devonian time giving way to a broad Paleotethys ocean in-between (see also Domeier and Torsvik 2014). However, a Devonian drift is hardly compatible with the geological record in the Iberian Massif, which points instead to rifting-drifting at Cambrian-Silurian time and collision since early Devonian (Liñán and Quesada 1990; Ribeiro et al. 1990; Martínez Catalán et al. 1997; Expósito et al. 2002).

Despite the differences, the Armorican and Galatian notions are not mutually exclusive, because it is possible to envisage a first split up of terranes (Armorica) at Ordovician time while a diminished Galatian terrane may have come apart later. Whatever the case of the peri-Gondwanan terranes, they constitute the greatest part of the Variscan belt and can be taken as the orogenic parautochthon, while the comparatively minor Avalonian and Rheic parts (the SPZ, the MORB-featured mafic rocks of the Moura-Cubito allochthonous Complex of SW Iberia, the upper allochthons and ophiolitic units of NW Iberia (?) and the Rhenohercynian zone) can be considered as "exotic" (Quesada 1991).

1.6 Deep Crustal Features of the Iberian Variscides

The Variscan crust of the Iberian Massif has been imaged in a number of seismic studies: ESCIN-N1 and N3 (Gutiérrez-Alonso 1995; Martínez Catalán et al. 1995; Pérez-Estaún et al. 1995; Ayarza et al. 1998), IBERSEIS (Simancas et al. 2003; Carbonell et al. 2004; Palomeras et al. 2009, 2011a) and ALCUDIA (Martínez-Poyatos et al. 2012; Ehsan et al. 2014). I summarize below the most important crustal features revealed by these experiments (Fig. 1.2; Simancas et al. 2013).

The flat Moho observed in the Iberian Massif seismic profiles indicates that, as in the majority of old orogens, crustal and lithospheric orogenic roots have been erased by poorly known late- or post-orogenic processes (Cook 2002; Seyferth and Henk 2004). Wedge structures have been imaged in the lower crust, but the mantle is nearly transparent from a seismic point of view (Fig. 1.2).

In the northern Iberian Massif, the detachment level of deformation deepens suddenly at the passage from the CZ to the WALZ, the entire crust thus becoming involved in deformation westwards. This feature is in agreement with the east orogenic vergence and the appearance of collisional granites at the interior of the WALZ, which become very abundant at the northern part of the CIZ. Furthermore, some HP metabasites crop out at the northern CIZ, perhaps indicative of intracontinental crustal subduction (Barbero and Villaseca 2000; Villaseca et al. 2015). Unfortunately, the crustal structure of this region of the CIZ has not been seismically imaged (Fig. 1.2).

In the southern Iberian Massif, a rather constant detachment level at the middle crust of the SPZ and the OMZ is revealed, with a strongly deformed upper crust decoupled from the lower crust. This structural pattern seems to reflect the ability of the lower crust to subduct at the OMZ/SPZ and CIZ/OMZ boundaries. Since only the upper crust was strongly deformed, crustal thickening was rather moderate,

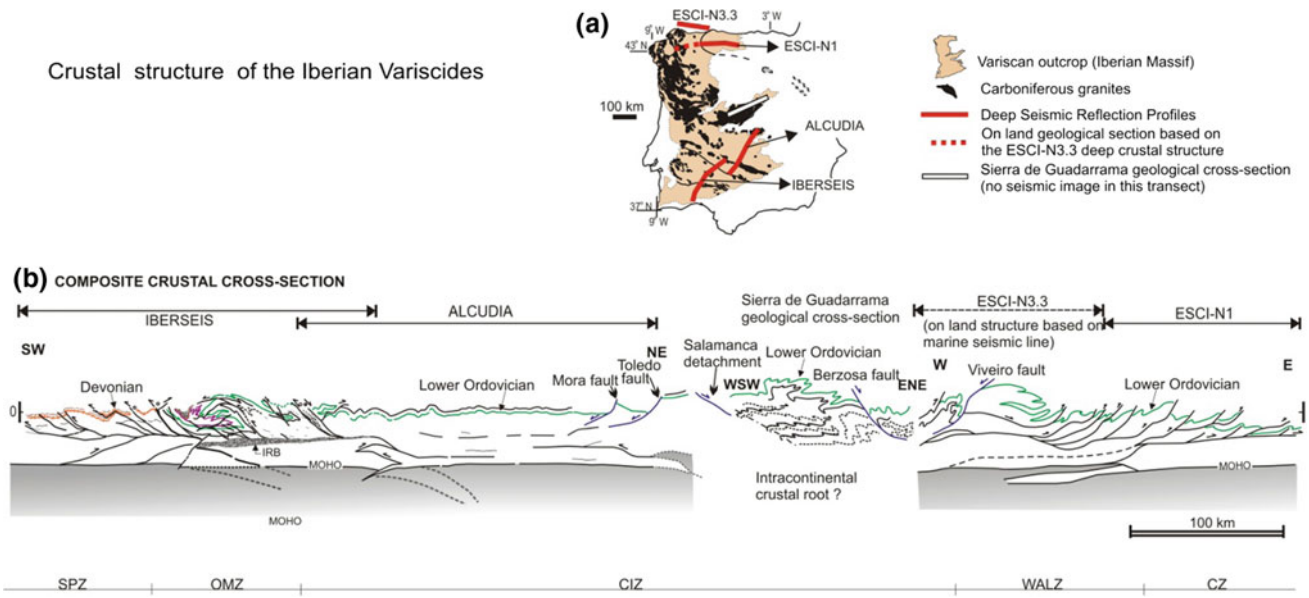

Fig. 1.2 Crustal structure of the Iberian Variscides based on surface geology and deep seismic profiling. IRB: Iberseis Reflective Body. The correspondence with zones of the Iberian Massif is indicated at the bottom (modified from Simancas et al. 2013)

in agreement with the few and small outcrops of collisional (late Carboniferous-earliest Permian) granites in SW Iberia (Fig. 1.2). North of the CIZ/OMZ boundary, the southern part of the CIZ is characterized by a moderate deformation of the upper crust which, in turn, can be balanced with a few discrete structural wedges imaged in the lower crust.

A 1–2 s band of high amplitude interfingering reflection packages has been imaged at the middle crust of the OMZ and the southern CIZ (Iberseis Reflective Body, IRB; Fig. 1.2; Simancas et al. 2003). This singular feature has been interpreted as a sill-like complex of mafic-ultramafic rocks and interlayered metasediments (Flecha et al. 2009; Palomeras et al. 2011b; Brown et al. 2012). The most probable age of the mafic intrusions is early Carboniferous, a time plentiful of mafic rocks in SW Iberia (Simancas et al. 2006; Pérez-Cáceres et al. 2015). The Cambrian-Ordovician was another period of abundant magmatism (rifting on the Gondwana margin) that could account for the formation of the IRB (Sarrionandía et al. 2012), though the existence of Devonian structures reaching the middle crust (e.g., Monesterio thrust) fossilized by the IRB reflectors undermines that interpretation.

Regarding gravimetry, the Bouguer anomaly map of the Iberian Peninsula (Mezcua et al. 1976) shows regional anomalies that can be explained in terms of crustal thickness, Neogene basins and crustal composition. Crustal thickness and Neogene basins are related to the Alpine evolution and will not be treated here. However, the positive anomaly that characterizes the SW part of the Iberian Massif suggests a denser crust as compared to central Iberia. By integrating the crustal geometry and velocity models derived from seismic experiments together with other observables such as geoid, gravity and topography, Palomeras et al. (2011b) have tested the consistency of models with high density bodies in the mid-crust of SW Iberia. Accordingly, significant volumes of dense (mafic) rocks seem to characterize the crust of SW Iberia, as a result of a particular evolution that will be summarized below.

1.7 Stages of the Iberian Variscan Evolution

After the latest records of Cadomian compressional deformation at around 550 Ma, an early Cambrian platform stage is defined by clastic and carbonate sediments, such as the Torreárboles sandstones and Alconera limestones, or the Complexo detritico-carbonatado de Assumar, in SW Iberia, the Azorejo-Tamames sandstones and Navalucillos-Tamames limestones, in central Iberia, and the Herrerías-Cándana sandstones and Láncara-Vegadeo limestones, in northern Iberia (Liñán and Quesada 1990; Liñán et al. 2002; Aramburu et al. 2004; Rodríguez-Alonso et al. 2004a; Pereira et al. 2015).

A Middle Cambrian-Ordovician rifting event broke the sedimentary platform (Mata and Munhá 1990; Crowley et al. 2000; Sánchez-García et al. 2003, 2010, 2014; Montero and Floor 2004; Etxebarría et al. 2006; Chichorro et al. 2008; Nance et al. 2012; Sarrionandía et al. 2012; Fuenlabrada et al. 2016; Días da Silva et al. 2017; Montero et al. 2017; Orejana et al. 2017; Paquette et al. 2017). The geodynamic scenario of this event is uncertain: a back-arc setting over an active subduction zone at the border of Gondwana (Martínez

Catalán et al. 2009; Díaz-Alvarado et al. 2016; Villaseca et al. 2016), the oblique arrival of a mid-ocean ridge in the subduction trench (Quesada 2017) or another type of rifting geodynamics. The earliest and best magmatic expression of the rift is found at the OMZ (Quesada 2017), but Ordovician magmatism is also found elsewhere in the Iberian Variscides. Actually, the exceptionally long Ollo de Sapo formation at the CIZ/WALZ boundary (≈490–470 Ma; Bea et al. 2007; Díez Montes et al. 2010; Díaz-Alvarado et al. 2016) and the ash-fall tuff beds reported in the CZ (477 Ma; Gutiérrez-Alonso et al. 2016) represent great igneous events outside the OMZ. The subsequent drift stage is recorded on passive-margin sedimentation during the late Ordovician-earliest Devonian time-span (Gutiérrez-Marco et al. 2002; Robardet 2002). The collisional stage developed along the Devonian and Carboniferous time, extending perhaps to the earliest Permian. Synorogenic flysch deposits at the external zones (SPZ, CZ) mark the climax of collisional deformation, which corresponds to Visean-Bashkirian time (Oliveira 1990; Fernández et al. 2004).

In NW Iberia, the final continental collision started at around 375 Ma, but older (early Variscan) tectonometamorphic events of debatable tectonic meaning are recorded in the allochthonous units of the GTMZ (Dallmeyer et al. 1997; Gómez Barreiro et al. 2006; Martínez Catalán et al. 2009; López-Carmona et al. 2014); the collision originated a thick orogenic wedge progressively propagating to the Cantabrian foreland (Pérez-Estaún et al. 1991; Díez Fernández et al. 2012a; Martínez Catalán et al. 2016). Three main questions about the allochthonous units of NW Iberia (GTMZ; Fig. 1.1c) remain controversial: (i) the paleogeographic and tectonic significance of the different units, including whether or not the intermediate ophiolitic units represent the Rheic Ocean suture (Ribeiro et al. 1990; Martínez Catalán et al. 1997, 2009; Arenas et al. 2007 vs. Matte 1991; Ribeiro et al. 2007; Arenas et al. 2014a, b); (ii) the existence or not of a significant Cadomian tectonothermal evolution in the upper allochthonous units (Ribeiro et al. 1990, 2006; Marques et al. 1996; Mateus et al. 2016 vs. Martínez Catalán et al. 1997; Ordóñez-Casado et al. 2001; Roger and Matte 2005); (iii) the amount of displacement. Concerning this latter issue, there are three different views (Fig. 1.3a): (a) the maximum extent of the GTM allochthons in Iberia corresponds approximately with their current outcrops; (b) the allochthons completely covered central Iberia (Rubio Pascual et al. 2013a); (c) the allochthons spread even longer, not only over central Iberia but also including the OMZ as part of the allochthonous package, thus having covered most of the Iberian Massif (Díez Fernández and Arenas 2015; Rubio Pascual et al. 2016; see discussion by Simancas et al. 2016). The reason behind spreading so much the allochthons is to justify the load needed for the early Variscan metamorphic evolution of the Central Range (Alcock et al. 2015); however, the age and location of the synorogenic frontal sedimentation (González-Clavijo et al. 2016; Martínez Catalán et al. 2016) apparently puts shorter limits on the advance of the allochthonous wedge.

In SW Iberia, collision started in early Devonian, as accredited by the flysch deposits of Terena (Piçarra et al. 1998; Pereira et al. 1999), the southward-vergent recumbent folds of the OMZ (Expósito et al. 2002) and the emplacement of the Moura-Cubito allochthonous complex at the OMZ/SPZ boundary (Fig. 1.1c; Araújo and Ribeiro 1997; Araújo et al. 2005; Ponce et al. 2012). The collisional deformation of SW Iberia is characterized by two particular features: (i) the left-lateral component of the whole collisional evolution (e.g. Matte and Ribeiro 1975), and (ii) a conspicuous transtensional and magmatic (mafic dominated) intraorogenic Carboniferous stage at early Carboniferous time (e.g. Simancas et al. 2006). The oblique collisional convergence is partitioned into thin bands dominated by left-lateral strike-slip kinematics, namely the northern and southern boundaries of the OMZ, and broader regions combining frontal shortening and left-lateral displacements, namely the OMZ and the SPZ interiors (Burg et al. 1981; Crespo-Blanc and Orozco 1988; Quesada 1991, 1997; Crespo-Blanc 1992; Azor et al. 1994; Quesada et al. 1994; Expósito et al. 2002; Silva and Pereira 2004; Díaz Azpiroz and Fernández 2005; Ponce et al. 2012; Pérez-Cáceres et al. 2015, 2016). The transient transtensional and magmatic intraorogenic episode is attested at upper crustal levels by the development of early Carboniferous basins and mafic magmatism (Munhá 1983; Oliveira 1990; Simancas et al. 2006; Armendáriz et al. 2008; Azor et al. 2008; Pereira et al. 2009; Rosas et al. 2008; Valenzuela et al. 2011; Cambeses et al. 2014; Cambeses 2015; Jesús et al. 2016), while mid-crustal rocks exhibit medium-to high-grade, low-pressure metamorphism (Bard 1977; Díaz Azpiroz and Fernández 2008; Rosas et al. 2008; Pereira et al. 2009); the collisional convergence resumed at middle-late Carboniferous time, after the transtensional event. A number of tectonic scenarios have been suggested for the intraorogenic trantensional stage of SW Iberia, such as: deflection of the oblique convergence (Simancas, 1993), transtension at releasing bends (Silva and Pereira 2004), mantle upwelling interfering with the oblique collisional process (Simancas et al. 2006), and slab break-off (Pin et al. 2008). Early Carboniferous extensional and magmatic events have been also reported in other regions of the Variscides (Floyd 1995; Dessureau et al. 2000; Franke 2006; Faryad et al. 2016; Laurent et al. 2017; Chelle-Michou et al. 2017), where lithospheric thinning and heating has been tentatively related to the Paleotethys rift propagation (Franke et al. 2011; Franke 2014).

The late Carboniferous-early Permian "post-kinematic" granitoids of the Variscides are a main orogenic feature that

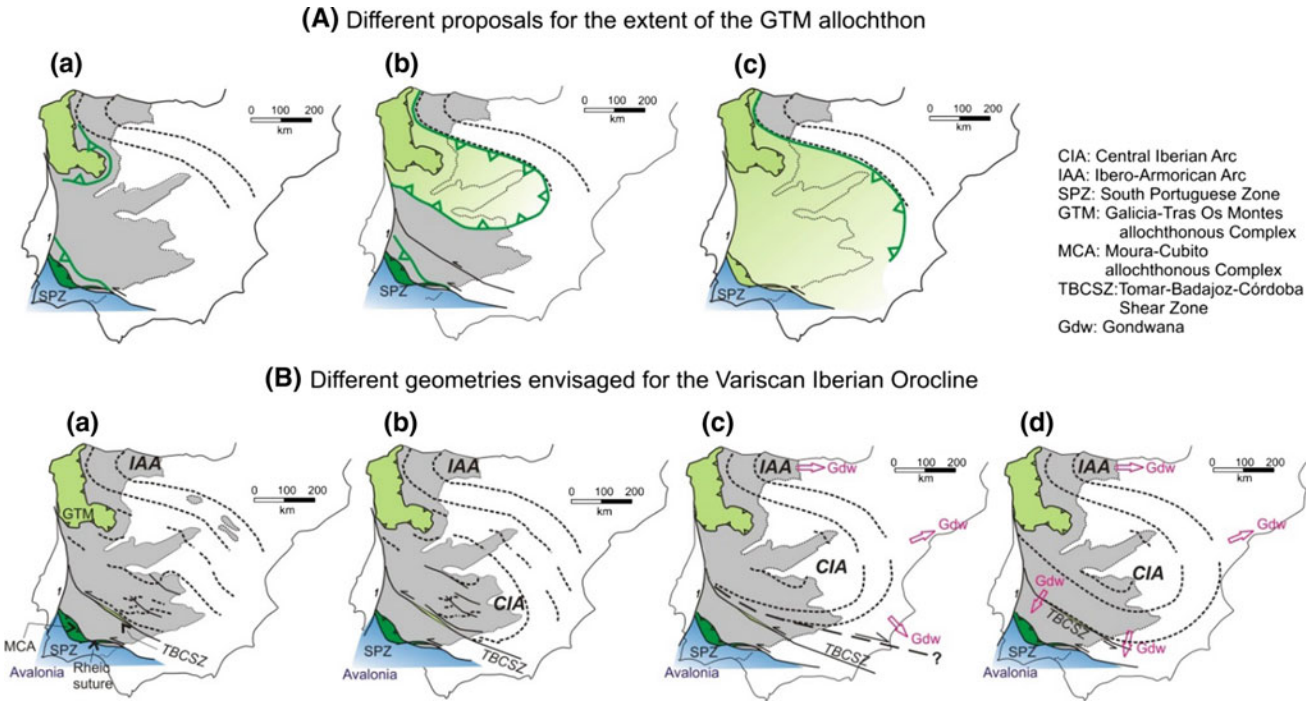

Fig. 1.3 **A** Different extents proposed for the GTM allochthon. **a** The current outcrop (classical view up to recent years. **b** The allochthon would have extended from Galicia to cover central Iberia (Rubio Pascual et al. 2013a). **c** The allochthon would have covered nearly all the Iberian Massif (Díez Fernández and Arenas 2015; Rubio Pascual et al. 2016). **B** Sketches of different geometries proposed for the Variscan Iberian Orocline. Differences only concern the CIA, the IAA being not geometrically disputed. **a** The CIA does not exist (Pérez-Estaún and Bea 2004; Pastor-Galán et al. 2015a; Dias et al. 2016). **b** The CIA is a rather open orogenic curvature, tightened in its southern part by superposed folding (Aerden 2004; Simancas et al. 2013; González-Clavijo et al. 2017b). **c** The CIA is an isoclinal arc bounded to the south by a hypothetical dextral megashear zone located north of the TBCSZ (Martínez Catalán 2011). **d** The CIA is an isoclinal arc bounded to the south by the TBCSZ (Shaw et al. 2012) or including the OMZ in the arc structure (Shaw and Johnston 2016). Note that the latter hypothesis is irreconcilable with the geological differences between the CZ and the OMZ, as well as with the suspected polarities towards the Gondwanan and Avalonian forelands

has received different geodynamic interpretations. The calc-alkaline signature of part of this magmatism has been interpreted by some authors as due to the Paleotethys subduction south of the Variscan belt (Finger and Steyrer 1990; Pereira et al. 2015). However, calc-alkaline features may be explained also as a consequence of a previously enriched mantle source and/or variable degrees of crustal contamination (Rottura et al. 1998; Henk et al. 2000). Moreover, the isotopic signatures of most of the Iberian granitoids support derivation from different sources in the continental crust, with some involvement of mantle-derived melts (Villaseca et al. 1998, 2012; Fernández Suárez et al. 2000a, 2011; Castro et al. 2002; Bea et al. 2003; Orejana et al. 2012). Thus, instead of Paleotethys subduction, the origin of the post-kinematic Iberian granitoids might have been dominated by collisional crustal thickening (Bea et al. 2003, 2004; Azevedo and Valle Aguado 2006; Simancas et al. 2013; Alcock et al. 2015). A further important hypothesis considers that the main orogenic process triggering post-kinematic magmatism is lithospheric delamination caused by orocline buckling (Gutiérrez-Alonso et al. 2011a, b).

1.8 The Iberian Orocline

The Iberian Variscides depict a curved trend, with a clear northern curvature, namely Cantabrian Arc or Cantabrian Orocline (Pérez-Estaún et al. 1988; Pastor-Galán et al. 2015a), and a poorly defined (arguable) southern opposite curvature that has been named Central Iberian Arc or Central Iberian Orocline (Aerden 2004; Martínez Catalán 2011, 2012). The Cantabrian Arc is part of a broader structure known as Ibero-Armorican Arc (Matte 1991). Altogether, the Cantabrian and the Central Iberian curvatures would define an S-shaped orogenic belt (Fig. 1.3b).

The Ibero-Armorican Arc is a major and well-studied feature of the Variscan belt (Matte 1986; Hirt et al. 1992; Ribeiro et al. 1995; Weil et al. 2000, 2001; Pastor-Galán et al. 2015a,b), which was originally explained by indentation of an Iberian block (Matte and Ribeiro 1975; Matte 1986; Ribeiro et al. 1995). However, paleomagnetic data lend support to a late growth of the curvature at latest Carboniferous to earliest Permian time, thus suggesting buckling of a Carboniferous

linear belt (Weil et al. 2001, 2013; Pastor-Galán et al. 2015b, 2017). Indentation and buckling models are hard to reconcile but attempts have been made by Murphy et al. (2016) and Dias et al. (2016). As a buckling-related arc, the Ibero-Armorican orocline brings important questions regarding its mechanical development: (i) how the vertically folded crustal/lithospheric orogenic belt decoupled from the undeformed forelands, and (ii) whether this folding affected the whole lithosphere (Gutiérrez-Alonso et al. 2004; Weil et al. 2013) or significant intracrustal and crustal-mantle decoupling existed (Pérez-Estaún et al. 1988; Simancas et al. 2013). If lithospheric folding would have taken place, subsequent lithospheric delamination can be predicted, which, in turn, could have triggered Permian magmatism (Gutiérrez-Alonso et al. 2011a). The easternmost Variscan Orogen (Bohemian Massif) depicts another, opposite sense, latest Carboniferous to earliest Permian tight curvature, somehow coupled with the Ibero-Armorican Arc (Fig. 1.1a; Matte 2002a; Guillot and Ménot 2009).

The existence of another arc shaping central Iberia (Central Iberian Arc) has been proposed based mainly on discontinuous structural alignments and magnetic anomalies under the post-Paleozoic cover (Fig. 1.3b; Aerden 2004; Martínez Catalán 2011, 2012; Shaw et al. 2012; Martínez Catalán et al. 2015; González-Clavijo et al. 2017b); it is in agreement with the NE-SW trend of a poorly-defined first set of folds in superposed folding at southern Central Iberia (Julivert et al. 1983). However, paleomagnetic studies do not support large-scale folding around a vertical axis here, at least as a late Carboniferous event (Pastor-Galán et al. 2016, 2017), thus making the Central Iberian Arc a dubious feature (Fig. 1.3b; Pérez-Estaún and Bea 2004; Dias et al. 2016). If it were real it would have formed before the Ibero-Armorican Arc, so that mechanisms envisaging both orogenic curvatures as approximately coeval (Aerden 2004; Martínez Catalán 2011, 2012; Carreras and Druguet 2014; Martínez Catalán et al. 2015; Shaw and Johnston 2016a) are not satisfactory. Mechanisms compatible with the above time constraint have been suggested, such as buckling diachroneity in a continued orogen-parallel shortening (Johnston et al. 2013) or dragging around the Galicia-Trás-os-Montes allochthonous wedge (Días da Silva et al. this volume), but the issue of the Central Iberian Arc is currently plagued by uncertainties.

1.9 The Variscan Basement of the Alpine Orogens

Besides the vast continuous Variscan outcrop that shapes the western half of Iberia, the basement of the Alpine orogens also shows a Variscan imprint. The Cantabrian Mountains and the Central Range (Fig. 1.1b) are the mere consequence of crustal uplift by discrete Alpine faults, thus forming part of the Iberian Massif. As for the Iberian Range (Fig. 1.1b), it constitutes a tectonically inverted but not intensely deformed Mesozoic basin whose basement is easily correlated with the WALZ of the Iberian Massif (Fig. 1.1c; Julivert et al. 1974; Liñán et al. 2002).

The Alpine mountain belts developed at the margins of the Iberian plate (Betics and Pyrenees; Fig. 1.1b) are more intensely deformed and have undergone large displacements relative to the Iberian Massif, hence the much greater difficulties to correlate their Variscan basements. Aeromagnetic anomalies indicate that the crust of the Iberian Massif has continuity under the Mesozoic-Cenozoic cover of the External Zones of the Betics (Ardizone et al. 1989). However, the tectonic complexes of the Internal Zones (Maláguide, Alpujárride and Nevado-Filábride) have moved westwards relative to the Iberian autochthon (e.g. Martín-Algarra and Vera 2004), and the Iberian crust underthrusts these complexes with variable detachment/sinking into the mantle (Mancilla et al. 2015). Stratigraphically, the Maláguide complex (Rodríguez-Cañero and Martín-Algarra 2014; Martín Algarra et al. this volume) bears some resemblance with the CZ and Minorca (Herbig 1985), and a Variscan imprint is not disputed since Paleozoic deformed rocks are covered by undeformed Permian rocks (Chalouan and Michard 1990; Martín-Algarra et al. 2009). As for the Nevado-Filábride complex, its stratigraphy is poorly known (Tendero et al. 1993; Laborda-López et al. 2015; Martín-Algarra et al. this chapter), though Bashkirian conodont associations very similar to those in the Cantabrian Zone have been recently reported (Rodríguez-Cañero et al. 2017); largely because of the stratigraphic uncertainties, the extent of the Variscan imprint in the Nevado-Filábride rocks is particularly controversial (Puga and Díaz de Federico 1976; Gómez-Pugnaire et al. 2000; Puga et al. 2002). Finally, in the Alpujárride complex the major significance of the Variscan tectonothermal imprint has been recently demonstrated but still awaits a neat separation from the Alpine imprint (Montel et al. 2000; Zeck and Whitehouse 2002; Acosta-Vigil et al. 2014; Sanchez-Navas et al. 2014). Small granitic bodies (currently orthogneisses) of early Permian age intrude the Paleozoic rocks of the Nevado-Filábride and Alpujárride complexes (Zeck and Whitehouse 1999; Gómez-Pugnaire et al. 2000; Sanchez-Navas et al. 2014). On the whole, the Variscan basement of the Betics presents particular stratigraphic features and younger metamorphic and granitic ages compared to the Iberian Massif. The basement of the Betics is a window into the southernmost (Paleotethyan) border of the Variscan Orogen, so that a deeper understanding of their pre-Alpine evolution would help to clarify the Paleotethys Ocean issue.

Unlike the Betics basement, the Paleozoic basement of the Pyrenees forms unquestionably part of the northern

branch of the Ibero-Armorican Arc, the nearest connections of the Variscan Pyrenees being the Montagne Noire and Sardinia (Martínez et al. 2015; Margalef et al. 2016). Anyway, the unfolding of the Ibero-Armorican Arc roughly aligns the Pyrenees with the WALZ of the Iberian Massif (Matte 1991, 2002b).

1.10 Concluding Remarks

The above overview of the Iberian Variscides shows that, despite intense research, the paleogeography and the geodynamic processes building the Iberian Variscides are far from being well determined. I hope that the current broad orogenic picture is robust, though there are significant issues under discussion and, presumably, others not yet glimpsed. The last years have seen a particular emergence of new ideas and, despite the fact that some of them will not resist future coming data, an updated presentation of geological research is a fascinating and necessary task. This introduction has been intended as a broad and (as far as possible) eclectic outline, with specific accounts given in the following chapters of this volume.

References

Abalos B (2001) Nuevos datos microestructurales sobre la existencia de deformaciones precámbricas en la Sierra de la Demanda (Cordillera Ibérica). Geogaceta 30:3–6

Abalos, B., Gil Ibarguchi, J.I., Eguiluz, L. (1991) Cadomian subduction/collision and Variscan transpression in the Badajoz-Córdoba shear belt, southwest Spain. Tectonophysics 199, 51–72

Abalos B, Carreras J, Druguet E, Escuder Viruete J, Gómez Pugnaire MT, Álvarez SL, Quesada C, Rodríguez Fernández LR, Gil Ibarguchi JI (2002) Variscan and Pre-Variscan Tectonics. In: Gibbons W, Moreno MT (eds) The Geology of Spain. Geological Society, London, 155–183

Acosta-Vigil A, Rubatto D, Bartoli O, Cesare B, Meli S, Pedrera A, Azor A, Tajcmanová (2014) Age of anatexis in the crustal footwall of the Ronda peridotites, S Spain. Lithos 210–211:147–167. https://doi.org/10.1016/j.lithos.2014.08.018

Aerden DG (2004) Correlating deformation in Variscan NW-Iberia using porphyroblasts; implications for the Ibero-Armorican Arc. Journal of Structural Geology 26:177–196. https://doi.org/10.1016/s0191-8141(03)00070-1

Albert R, Arenas R, Gerdes A, Sánchez Martínez S, Fernández-Suárez J, Fuenlabrada JM (2015) Provenance of the Variscan Upper Allochthon (Cabo Ortegal Complex, NW Iberian Massif). Gondwana Research 34:129–148. https://doi.org/10.1016/j.gr.2014.10.016

Alcock JE, Martínez Catalán JR, Rubio Pascual J, Díez Montes A, Díez Fernández R, Gómez Barreiro J, Arenas R, Dias da Silva I, González Clavijo E (2015) 2-D thermal modeling of HT-LP metamorphism in NW and Central Iberia: Implications for Variscan magmatism, rheology of the lithosphere and orogenic evolution. Tectonophysics 657:21–37. https://doi.org/10.1016/j.tecto.2015.05.022

Andonaegui P, Arenas R, Albert R, Sánchez Martínez S, Díez Fernández R, Gerdes A (2016) The last stages of the Avalonian-Cadomian arc in NW Iberian Massif: isotopic and igneous record for a long-lived peri-Gondwanan magmatic arc. Tectonophysics 681:6–14. https://doi.org/10.1016/j.tecto.2016.02.032

Andonaegui P, Abati J, Díez Fernández R (2017) Late Cambrian magmatic activity in peri-Gondwana: geochemical evidence from metagranitoid rocks of the Basal Allochthonous Units of NW Iberia. Geologica Acta 15:3015–321. https://doi.org/10.1344/geologicaacta2017.15.4.4

Aramburu C, Méndez-Bedia I, Arbizu M, García-López S (2004) Zona Cantábrica. Estratigrafía. La secuencia preorogénica. In: Vera, J.A. (ed) Geología de España, SGE-IGME, Madrid, 27–34

Araújo A, Ribeiro A (1997) Estrutura dos dominios meridionais da Zona de Ossa-Morena. In: Araújo, A.A., Pereira, M.F. (eds), Estudo sobre a Geologia da Zona de Ossa-Morena (Maciço Ibérico), Univ. Évora, 169–182

Araújo A, Fonseca P, Munhá, J, Moita P, Pedro J, Ribeiro A (2005) The Moura Phyllonitic Complex: an Accretionary Complex related with obduction in the Southern Iberia Variscan Suture. Geodinamica Acta, 18:375–388

Arche A, López-Gómez J (1996) Origin of the Permian-Triassic Iberian Basin, central-eastern Spain. Tectonophysics 266:443–464

Ardizone J, Mezcua J, Socías I (1989) Mapa aeromagnético de España Peninsular, Escala 1:1.000.000. Instituto Geográfico Nacional, Madrid

Arenas R, Martínez Catalán JR, Sánchez Martínez S, Díaz García F, Abati J, Fernández-Suárez J, Andonaegui P, Gómez-Barreiro J (2007) Paleozoic ophiolites in the Variscan suture of Galicia (northwest Spain): Distribution, characteristics and meaning. In: Hatcher, R.D., Carlson, M.P., McBride, J.H., Martínez Catalán, J.R. (eds), 4-D Framework of Continental Crust. Geological Society of America Memoir 200:425–444. https://doi.org/10.1130/2007.1200(22)

Arenas R, Díez Fernández R, Sánchez Martínez S, Gerdes A, Fernández-Suárez J, Albert R (2014a) Two-stage collision: Exploring the birth of Pangea in the Variscan terranes. Gondwana Research 25:756–763

Arenas R, Sánchez Martínez S, Gerdes A, Albert R, Díez Fernández R, Andonaegui P (2014b) *Re*-interpreting the Devonian ophiolites involved in the Variscan suture: U-Pb and Lu-Hf zircon data of the Moeche Ophiolite (Cabo Ortegal Complex, NW Iberia). International Journal of Earth Sciences 103:1385–1402. https://doi.org/10.1007/s00531-013-0880-x

Arenas R, Sánchez Martínez S, Díez Fernández R, Gerdes A, Abati J, Fernández-Suárez J, Andonaegui, P., González Cuadra, P, López Carmona A, Albert R, Fuenlabrada JM, Rubio Pascual FJ (2016a) Allochthonous terranes involved in the Variscan suture of NW Iberia: A review of their origin and tectonothermal evolution. Earth-Science Reviews 161:140–178. https://doi.org/10.1016/j.earscirev.2016.08.010

Arenas R, Díez Fernández R, Rubio Pascual FJ, Sánchez Martínez S, Martín Parra LM, Matas J, González del Tánago J, Jiménez-Díaz A, Fuenlabrada JM, Andonaegui P, Garcia-Casco A (2016b) The Galicia–Ossa-Morena Zone: Proposal for a new zone of the Iberian Massif. Variscan implications.Tectonophysics 681:135–143. https://doi.org/10.1016/j.tecto.2016.02.030

Arenas R, Fernández-Suárez J, Montero P, Díez Fernández R, Andonaegui P, Sánchez Martínez S, Albert R, Fuenlabrada JM, Matas J, Martín Parra LM, Rubio Pascual FJ, Jiménez-Díaz A, Pereira MF (2018) The Calzadilla Ophiolite (SW Iberia) and the Ediacaran fore-arc evolution of the African Margin of Gondwana. Gondwana Research 58:71–86. https://doi.org/10.1016/j.gr.2018.01.015

Armendáriz M, López-Guijarro R, Quesada C, Pin C, Bellido F (2008) Genesis and evolution of a syn-orogenic basin in transpression: Insights from petrography, geochemistry and Sm–Nd systematics in the Variscan Pedroches basin (Mississippian, SW Iberia). Tectonophysics 461:395–413. https://doi.org/10.1016/j.tecto.2008.02.007

Palomeras I, Carbonell R, Flecha I, Simancas F, Ayarza, P, Matas J, Martínez Poyatos D, Azor A, González Lodeiro F, Pérez-Estaún A (2009) Nature of the lithosphere across the Variscan orogen of SW Iberia: Dense wide-angle seismic reflection data. Journal of Geophysical Research 114:Bo2302. https://doi.org/10.1029/2007jb005050

Ayarza P, Martínez Catalán JR, Gallart J, Pulgar J, Dañobeitia JJ (1998) Estudio Sísmico de la Corteza Ibérica Norte 3.3: A seismic image of the Variscan crust in the hinterland of the NW Iberian Massif. Tectonics 17:171–186

Azevedo MR, Valle Aguado B (2006) Origem e instalaçao de granitoides variscos na Zona Centro-Ibérica. In: Dias, R., Araújo, A., Terrinha, P., Kullberg, J.C. (eds), Geologia de Portugal no contexto da Ibéria, Univ. Évora, 107–121

Azor A, González Lodeiro F, Simancas JF (1993) Cadomian subduction/collision and Variscan transpression in the Badajoz-C6rdoba Shear Belt, southwest Spain: a discussion on the age of the main tectonometamorphic events. Tectonophysics 217:343–346

Azor A, González Lodeiro F, Simancas JF (1994) Tectonic evolution of the boundary between the Central Iberian and Ossa-Morena zones (Variscan belt, southwest Spain). Tectonics 13:45–61

Azor A, Bea F, González Lodeiro F, Simancas JF (1995) Geochronological constraints on the evolution of a suture: the Ossa-Morena/Central Iberian contact. Geologische Rundschau 84:375–383

Azor A, Rubatto D, Simancas JF, González Lodeiro F, Martínez Poyatos D, Martín Parra LM, Matas J (2008) Rheic Ocean ophiolitic remnants in southern Iberia questioned by SHRIMP U-Pb zircon ages on the Beja-Acebuches amphibolites. Tectonics 27, TC5006, https://doi.org/10.1029/2008TC002306

Azor A, Rubatto D, Marchesi C, Simancas JF, González Lodeiro F, Martínez Poyatos D, Martín Parra LM, Matas J (2009) Reply to comment by C. Pin and J. Rodríguez on "Rheic Ocean ophiolitic remnants in southern Iberia questioned by SHRIMP U-Pb zircon ages on the Beja-Acebuches amphibolites". Tectonics 28. https://doi.org/10.1029/2009tc002527

Ballèvre M, Paris F, Robardet M (1992) Corrélations ibéro-armoricaines au Paléozoïque: une confrontation des données paléobiogéographiques et tectonometamorphiques. Comptes Rendus Académie des Sciences, Paris, 315, Série II, 1783–1789

Ballèvre M, Bosse V, Ducassou C, Pitra P (2009) Palaeozoic history of the Armorican Massif: Models for the tectonic evolution of the suture zones. Comptes Rendus Geoscience 341:174–201. https://doi.org/10.1016/j.crte.2008.11.009

Ballèvre M, Martínez Catalán JR, López Carmona A, Pitra P, Abati J, Díez Fernández R, Ducassou C, Arenas R, Bosse V, Castiñeiras P, Fernández-Suárez J, Gómez Barreiro J, Paquette JL, Peucat JJ, Poujol M, Ruffet G, Sánchez Martínez S (2014) Correlation of the nappe stack in the Ibero-Armorican arc across the Bay of Biscay: a joint French-Spanish project. Geological Society, London, Special Publications:77–113. https://doi.org/10.1144/sp405.13

Bandrés A, Eguíluz L, Gil Ibarguchi JI, Palacios T (2002) Geodynamic evolution of a Cadomian arc region: the northern Ossa-Morena Zone, Iberian Massif. Tectonophysics 352, 105–120. https://doi.org/10.1016/s0040-1951(02)00191-9

Bandrés A, Eguíluz L, Pin C, Paquette JL, Ordóñez B, Le Fèvre B, Ortega LA, Gil Ibarguchi JI (2004) The northern Ossa-Morena Cadomian batholith (Iberian Massif): magmatic arc origin and early evolution. International Journal of Earth Sciences 93:860–885. https://doi.org/10.1007/s00531-004-0423-6

Barbero L, Villaseca, C (2000) Eclogite facies relics in metabasites from the Sierra de Guadarrama (Spanish Central System): P-T estimations and implications for the Hercynian evolution. Mineralogical Magazine 64:816–836

Bard JP (1977) Signification tectonique des metatholeites d'affinité abyssale de la ceinture de basse pression d'Aracena (Huelva, Espagne), Bulletin de la Société Géologique de France 19: 385–393

Bard JP, Moine B (1979) Acebuches amphibolites in the Aracena hercynian metamorphic belt (southwest Spain): Geochemical variations and basaltic affinities. Lithos 12:271–282

Bea F (2004) La naturaleza del magmatismo de la Zona Centroibérica: consideraciones generales y ensayo de correlación. In: Vera, JA (ed) Geología de España. SGE-IGME, Madrid, 128–133

Bea F, Montero P, Zinger T (2003) The Nature and Origin of the Granite Source Layer of Central Iberia: Evidence from Trace Element, Sr and Nd Isotopes, and Zircon Age Patterns. The Journal of Geology 111:579–595

Bea F, Montero P, González-Lodeiro F, Talavera C (2007) Zircon Inheritance Reveals Exceptionally Fast Crustal Magma Generation Processes in Central Iberia during the Cambro-Ordovician. Journal of Petrology 48:2327–2339. https://doi.org/10.1093/petrology/egm061

Bea F, Montero P, Talavera C, Anbar MA, Scarrow JH, Molina JF, Moreno JA (2010) The palaeogeographic position of Central Iberia in Gondwana during the Ordovician: evidence from zircon chronology and Nd isotopes. Terra Nova 22:341–346. https://doi.org/10.1111/j.1365-3121.2010.00957.x

Berthelsen A (1992) Mobile Europe. In: Blundell, D., Freeman, R., Mueller, S. (eds), A continent revealed. The European Geotraverse. Cambridge University Press, 11–32

BIRPS and ECORS (1986) Deep seismic reflection profiling between England, France and Ireland. Journal of the Geological Society, London, 143:45–52

Blatrix P, Burg JP (1981) $^{40}Ar/^{39}Ar$ dates from Sierra Morena (Southern Spain). Variscan metamorphism and Cadomian Orogeny. Neues Jharbuch für Mineralogie-Monatshefte 10:470–478

Booth-Rea G, Simancas JF, Azor A, Azañón JM, González Lodeiro F, Fonseca P (2006) HP-LT Variscan metamorphism in the Cubito-Moura schists (Ossa-Morena Zone, southern Iberia). Comptes Rendus Geoscience 338:1260–1267. https://doi.org/10.1016/j.crte.2006.08.001

Braid JA, Murphy JB, Quesada C (2010) Structural analysis of an accretionary prism in a continental collision setting, the Late Paleozoic Pulo do Lobo Zone, Southern Iberia. Gondwana Research 17:422–439. https://doi.org/10.1016/j.gr.2009.09.003

Braid JA, Murphy JB, Quesada C, Gladney ER, Dupuis N (2018) Progressive magmatism and evolution of the Variscan suture in souther Iberia. International Journal of Earth Sciences. https://doi.org/10.1007/s00531-017-1540-3

Brown D, Zhang X, Palomeras I, Simancas JF, Carbonell R, Juhlin C, Salibury M (2012) Petrophysical analysis of a mid-crustal reflector in the IBERSEIS profile, SW Spain. Tectonophysics 550–553:35–46. https://doi.org/10.1016/j.tecto.2012.05.004

Burg JP, Iglesias M, Laurent Ph, Matte Ph, Ribeiro A (1981) Variscan intracontinental deformation: the Coimbra-Córdoba Shear Zone (SW Iberian Peninsula). Tectonophysics 78:161–177

Cambeses A (2015) Ossa-Morena Zone Variscan "calc-alkaline" hybrid rocks: interaction of mantle- and crustal-derived magmas as a result of intra-orogenic extension-related intraplating. PhD, University of Granada, Spain

Cambeses A, Scarrow SH, Montero P, Molina JF, Moreno JA (2014) SHRIMP U–Pb zircon dating of the Valencia del Ventoso plutonic complex, Ossa-Morena Zone, SW Iberia: Early Carboniferous

intra-orogenic extension-related calc-alkaline magmatism. Gondwana Research 28:735–756. https://doi.org/10.1016/j.gr.2014.05.013

Cambeses A, Scarrow J.H, Montero P, Lázaro C, Bea F (2017) Palaeogeography and crustal evolution of the Ossa-Morena Zone, southwest Iberia, and the North Gondwana margin during the Cambro-Ordovician: a review of isotopic evidence. International Geoloy Review 59:94–130. https://doi.org/10.1080/00206814.2016.1219279

Carbonell R, Simancas F, Juhlin C, Pous J, Pérez-Estaún A, González Lodeiro F, Muñoz G, Heise W, Ayarza P (2004) Geophysical evidence of a mantle derived intrusion in SW Iberia. Geophysical Research Letters 31:L11601. https://doi.org/10.1029/2004gl019684

Carreras J, Druguet E (2014) Framing the tectonic regime of the NE Iberian segment. In: Schulmann, K., Martínez Catalán, J.R., Lardeaux, J.M., Janousek, V., Oggiano, G. (eds), The Variscan Orogeny: Extent, Timescale and the Formation of the European Crust. London, Geological Society Special Publication 405:249–264

Castro A, Fernández C, De la Rosa J, Moreno-Ventas I, Rogers G (1996) Significance of MORB-derived Amphibolites from the Aracena Metamorphic Belt, Southwest Spain. Journal of Petrology 37:235–260. https://doi.org/10.1093/petrology/37.2.235

Castro A, Corretgé LG, De La Rosa J, Enrique P, Martínez FJ, Pascual E, Lago M, Arranz E, Galé C, Fernández C, Donaire T, López S (2002) Palaeozoic Magmatism. In: Gibbons, W., Moreno, T. (eds), The Geology of Spain. Geological Society, London, 117–153

Cazes M, Torreilles G, Bois C, Damotte B, Galdeano A, Mascle A, Matte P, Pham VN, Raoult JF (1985) Structure de la croute hercynienne du Nord de la France: premiers résultats du profil ECORS. Bulletin de la Societé Géologique de France 8:925–941

Chalouan A, Michard A (1990) The Ghomarides nappes, Rif Coastal Range, Morocco: a Variscan chip in the Alpine Belt. Tectonics 9:1565–1583

Chelle-Michou C, Laurent O, Moyen JF, Block S, Paquette JL, Couzinié S, Gardien V, Vanderhaeghe O, Villaros A, Zeh A (2017) Pre-Cadomian to late-Variscan odyssey of the eastern Massif Central, France: Formation of the West European crust in a nutshell. Gondwana Research 46:170–190. https://doi.org/10.1016/j.gr.2017.02.010

Chichorro M, Pereira MF, Díaz-Azpiroz M, Williams IS, Fernández C, Pin C, Silva JB (2008) Cambrian ensialic rift-related magmatism in the Ossa-Morena Zone (Évora–Aracena metamorphic belt, SW Iberian Massif): Sm–Nd isotopes and SHRIMP zircon U–Th–Pb geochronology. Tectonophysics 461:91–113. https://doi.org/10.1016/j.tecto.2008.01.008

Chichorro M, Rita Solá A, Quesada C, Álvaro JJ, Sánchez-García T, Díez Montes A (2017) Cryptic Early-to-Main rift-related Cambrian magmatism in Central Iberian and Galicia-Trás-os-Montes zones (Iberian Massif) revealed by U-Pb dating of inherited zircon. In: Álvaro JJ, Casas JM, Clausen S (eds) Géologie de la France 1(4): 13–14

Clayton G, Wicander R, Pereira Z (2002) Palynological evidence concerning the relative positions of northern Gondwana and southern Laurussia in latest Devonian and Mississippian times. Studies in Palaeozoic palaeontology and biostratigraphy in honour of Charles Hepworth Holland. Special Papers in Palaeontology 67:45–56

Cocks LRM, Fortey R (1982) Faunal evidences for oceanic separations in the Palaeozoic of Britain. Journal of the Geological Society of London 139:465–478

Cocks LRM, Torsvik TH (2006) European geography in a global context from the Vendian to the end of Palaeozoic. In: Gee, DG, Stephenson, RA (eds), European Lithosphere Dynamics. Geological Society of London Memoir 32:83–95

Cook FA (2002) Fine structure of the continental reflection Moho. GSA Bulletin 114:64–79

Cook FA, Vasudevan K (2006) Reprocessing and enhanced interpretation of the initial COCORP Southern Appalachian traverse. Tectonophysics 420:161–174

Corsini M, Rolland Y (2009) Late evolution of the southern European Variscan belt: Exhumation of the lower crust in a context of oblique convergence. Comptes Rendus Geoscience 341:214–223. https://doi.org/10.1016/j.crte.2008.12.002

Crespo-Blanc A (1992) Structure and kinematics of a sinistraltranspressive suture between the Ossa-Morena and the South Portuguese Zones, South Iberian Massif. Journal of the Geological Society, London, 149:401–411

Crespo-Blanc A, Orozco M (1988) The Southern Iberian Shear Zone: a major boundary in the Hercynian folded belt. Tectonophysics 148:221–227

Crespo-Blanc A, Orozco M (1991) The boundary between the Ossa-Morena and the South-portuguese Zones (southern Iberian Massif): a major suture in the european Hercynian chain. Geologische Rundschau 80:691–702

Crowley QG, Floyd PA, Winchester JA, Franke W, Holland JG. (2000) Early Palaeozoic rift-related magmatism in Variscan Europe: fragmentation of the Armorican Terrane Assemblage. Terra Nova 12:171–180

Dahn DRL, Braid JA, Murphy JB, Quesada C, Dupuis N, McFarlane CRM (2014) Geochemistry of the Peramora Mélange and Pulo do Lobo schist: geochemical investigation and tectonic interpretation of mafic mélange in the Pangean suture zone, Southern Iberia. International Journal of Earth Sciences (Geol Rundsch) 103:1415–1431. https://doi.org/10.1007/s00531-014-1024-7

Dallmeyer RD, Quesada C (1992) Cadomian versus Variscan evolution of the Ossa-Morena Zone (SW Iberia): field and $^{40}Ar/^{39}Ar$ mineral age constraints. Tectonophysics 216:339–364

Dallmeyer RD, Martínez Catalán JR, Arenas R, Gil Ibarguchi JI, Gutiérrez-Alonso G, Farias P, Aller J, Bastida F (1997) Diachronous Variscan tectonothermal activity in the NW Iberian Massif: Evidence from $^{40}Ar/^{39}Ar$ dating of regional fabrics. Tectonophysics 277:307–337. https://doi.org/10.1016/s0040-1951(97)00035-8

Denèle Y, Paquette JL, Olivier Ph, Barbey P (2011) Permian granites in the Pyrenees: the Aya pluton (Basque country). Terra Nova 24:105–113. https://doi.org/10.1111/j.1365-3121.2011.01043.x

Derder MEM, Henry B, Bayou B, Ouabadi A, Bellon H, Djellit H, Khaldi A, Amenna M, Baziz K, Hemmi A, Guemache MA (2006) New African Lower Carbonferous paleomagnetic pole from intrusive rocks of the Tin Serririne basin (Southern border of the Hoggar, Algeria). Tectonophysics 418:189–203. https://doi.org/10.1016/j.tecto.2006.02.002

Dessureau G, Piper DJW, Pe-Piper G (2000) Geochemical evolution of earliest Carboniferous continental tholeiitic basalts along a crustal-scale shear zone, southwestern Maritimes basin, eastern Canada. Lithos 50: 27–50

Días da Silva I, González Clavijo E, Díez Montes A, Martínez Catalán JR, Gómez Barreiro J, Hoffman M, Gärtner A (2017) Furongian-Late Ordovician volcanism in the Upper Parautochthon of the Galicia-Tràs-os-Montes Zone (NE Portugal): Paleogeographic meaning and geodynamic setting. Géologie de la France 1:19–21

Dias R, Ribeiro A (1995) The Ibero-Armorican Arc: A collision effect against an irregular continent? Tectonophisics 246:113–128. https://doi.org/10.1016/0040-1951(94)00253-6

Dias R, Ribeiro A, Romao J, Coke C, Moreira N (2016) Reviewing the arcuate structures in the Iberian Variscides; constraints and genetical

models. Tectonophysics 681:170–194. https://doi.org/10.1016/j.tecto.2016.04.011

Díaz Azpiroz M, Fernández C (2005) Kinematic analysis of the southern Iberian shear zone and tectonic evolution of the Acebuches metabasites (SW Variscan Iberian Massif). Tectonics 24:TC3010. https://doi.org/10.1029/2004tc001682

Díaz Azpiroz M, Fernández C (2008) Quartz *c*-axis fabrics of poly-deformed leucocratic gneisses from the Aracena metamorphic belt (SW Variscan Chain). Comptes Rendus Geoscience 340:315–323. 10.1016/j.crte.2007.12.010

Díaz García F (2006) Geometry and regional significance of Neoproterozoic (Cadomian) structures of the Narcea Antiform, NW Spain. Journal of the Geological Society, London, 163:499–508

Díaz García F, Martínez Catalán JR, Arenas R, González Cuadra P (1999) Early Ordovician orogenic event in Galicia (NW Spain): evidence from U–Pb ages in the uppermost unit of the Ordenes Complex. International Journal of Earth Sciences 88:337–351. https://doi.org/10.1007/s005310050269

Díaz-Alvarado JD, Fernández C, Chichorro M, Castro A, Pereira MF (2016) Tracing the Cambro-Ordovician ferrosilicic to calc-alkaline magmatic association in Iberia by in situ U-Pb SHRIMP zircon geochronology (Gredos massif, Spanish Central System batholith). Tectonophysics 681:95–110. https://doi.org/10.1016/j.tecto.2016.02.031

Díez Balda MA, Vegas R, González Lodeiro F (1990) Structure. In: Dallmeyer RD, Martínez García E (eds) Pre-Mesozoic Geology of Iberia. Springer, Berlin, 172–188

Díez Fernández R, Arenas R (2015) The Late Devonian Variscan suture of the Iberian Massif: A correlation of high-pressure belts in NW and SW Iberia. Tectonophysics 654:96–100. https://doi.org/10.1016/j.tecto.2015.05.001

Díez Fernández R, Martínez Catalán JR, Gerdes A, Abati J, Arenas R, Fernández-Suárez J (2010) U-Pb ages of detrital zircons from the basal allochthonous units of NW Iberia: Provenance and paleoposition on the northern margin of Gondwana during the Neoproterozoic and Paleozoic. Gondwana Research 18:385–399

Díez Fernández R, Martínez Catalán JR, Arenas R, Abati J (2012) The onset of the assembly of Pangea in NW Iberia: Constraints on the kinematics of continental subduction. Gondwana Research 22:20–25. https://doi.org/10.1016/j.gr.2011.08.004

Díez Fernández R, Arenas R, Pereira FM, Sánchez Martínez S, Albert R, Martín Parra LM, Rubio Pascual FJ, Matas J (2016) Tectonic evolution of Variscan Iberia: Gondwana-Laurussia collision revisited. Earth-Science Reviews 162:269–292. https://doi.org/10.1016/j.earscirev.2016.08.002

Díez Fernández R, Fuenlabrada JM, Chichorro M, Pereira MF, Sánchez-Martínez S, Silva JB, Arenas R (2017) Geochemistry and tectonostratigraphy of the basal allochthonous units of SW Iberia (Évora Massif, Portugal): keys to the reconstruction of pre-Pangean paleogeography in southern Europe. Lithos 268–271:285-301. https://doi.org/10.1016/j.lithos.2016.10.031

Díez Montes A, Martínez Catalán JR, Bellido Mulas F (2010) Role of the Ollo de Sapo massive felsic volcanism of NW Iberia in the Early Ordovician dynamics of northern Gondwana. Gondwana Research 17:363–376.https://doi.org/10.1016/j.gr.2009.09.001

Dinis P, Andersen T, Machado G, Guimaraes F (2012) Detrital zircon U-Pb ages of a late-Variscan Carboniferous succession associated with the Porto-Tomar shear zone (West Portugal): Provenance implications. Sedimentary Geology 273–274:19-29. https://doi.org/10.1016/j.sedgeo.2012.06.007

Doblas M, Oyarzun R, López-Ruiz JL, Cebriá JM, Youbi N, Mahecha V, Lago M, Pocoví A, Cabanis B (1998) Permo-Carboniferous volcanism in Europe and northwest Africa: a superplume exhaust valve in the centre of Pangea? Journal of African Earth Sciences 26:89–99

Domeier M, Torsvik TH (2014) Plate tectonics in the late Paleozoic. Geoscience Frontiers 5:303–350. https://doi.org/10.1016/j.gsf.2014.01.002

Domeier M, Van der Voo R, Torsvik TH (2012) Paleomagnetism and Pangea: The road to reconciliation. Tectonophysics 514–517:14-43. https://doi.org/10.1016/j.tecto.2011.10.021

Dörr W, Zulauf G, Gerdes A, Lahaye Y, Kowalczyk G (2015) A hidden Tonian basement in the eastern Mediterranean: Age constraints from U-Pb data of magmatic and detrital zircons of the External Hellenides (Crete and Peloponnesus). Precambrian Research 258:83–108. https://doi.org/10.1016/j.precamres.2014.12.015

Drost K, Gerdes A, Jeffries T, Linnemann U, Storey C (2011) Provenance of Neoproterozoic and early Paleozoic siliciclastic rocks of the Teplá-Barrandian unit (Bohemian Massif): Evidence from U-Pb detrital zircon ages. Gondwana Research 19:213–231. https://doi.org/10.1016/j.gr.2010.05.003

Duff PD, Kellog JN (2017) Reinterpretation of adcoh and cocorp seismic reflection datawith constraints from detailed forward modelling of potential field data. Implications for Laurentia-Peri-Gonwana suture. Tectonophysics 712–713:426-437. https://doi.org/10.1016/j.tecto.2017.06.002

Edel JB (2001) The rotations of the Variscides during the Carboniferous collision: paleomagnetic constraints from the Vosges and the Massif Central (France). Tectonophysics 332:69–92

Eden CP (1991) Tectonostratigraphic analysis of the northern extent of the oceanic exotic terrane, Northwestern Huelva Province, Spain. PhD thesis, University of Southampton, England, 293 p.

Eden CP, Andrews JR (1990) Middle to Upper Devonian melanges in SW Spain and their relationship to the Meneage Formation in south Cornwall. Proceedings of the Ussher Society 7:217–222

Eguiluz L, Gil Ibarguchi JI, Ábalos B, Apraiz A (2000) Superposed Hercynian and Cadomian orogenic cycles in the Ossa-Morena zone and related areas of the Iberian Massif. GSA Bulletin 112:1398–1413

Ehsan SA, Carbonell R, Ayarza P, Martí D, Pérez-Estaún A, Martínez Poyatos D, Simancas JF, Azor A, Mansilla L (2014) Crustal deformation styles along the reprocessed deep seismic reflection transect of the Central Iberian Zone (Iberian Peninsula). Tectonophysics 621:159–174. https://doi.org/10.1016/j.tecto.2014.02.014

Etxebarría M, Chalot-Prat F, Apraiz A, Eguiluz L (2006) Birth of a volcanic passive margin in Cambrian time: Rift paleogeography of the Ossa-Morena Zone, SW Spain. Precambrian Research 147:366–386. https://doi.org/10.1016/j.precamres.2006.01.022

Expósito I, Simancas JF, González Lodeiro F, Azor A, Martínez Poyatos D (2002) Estructura de la mitad septentrional de la Zona de Ossa-Morena: deformación en el bloque inferior de un cabalgamiento cortical de evolución compleja. Revista de la Sociedad Geológica de España 15:3–14

Falk F, Franke W, Kurze M (1995) Saxothuringian Basin. Stratigraphy. In: Dallmeyer, R.D., Franke, W., Weber, K. (eds), Pre-Permian Geology of Central and Eastern Europe. Springer, Berlin, 221–234

Faryad SW, Kachlík V, Sláma J, Jedlicka R (2016) Coincidence of gabbro and granulite formation and their implication for Variscan HT metamorphism in the Moldanubian Zone (Bohemian Massif), example from the Kutná Hora Complex. Lithos 264:56–69

Fernández Carrasco J, Garrote A, Arriola A, Eguiluz L, Sánchez Carretero R (1983) Mapa Geológico de España escala 1:50 000, Fuente de Cantos. IGME, Madrid

Fernández LP, Bahamonde JR, Barba P, Colmenero JR, Heredia N, Rodríguez-Fernández LR, Salvador C, Sánchez de Posada LC, Villa E, Merino-Tomé O, Motis K (2004) Zona Cantábrica. Estratigrafía. Secuencia sinorogénica. In: Vera, J.A. (ed), Geología de España, SGE-IGME, Madrid, 34–42

Fernández-Lozano J, Pastor-Galán D, Gutiérrez-Alonso G, Franco P (2016) New kinematic constraints on the Cantabrian orocline: A

paleomagnetic study from the Peñalba and Truchas synclines, NW Spain. Tectonophysics 681:195–208. https://doi.org/10.1016/j.tecto.2016.02.019

Fernández-Suarez J, Gutiérrez-Alonso G, Jeffries TE (2002) The importance of along-margin terrane transport in northern Gondwana: insights from detrital zircon parentage in Neoproterozoic rocks from Iberia and Brittany. Earth and Planetary Science Letters 204:75–88

Fernández-Suárez J, Gutiérrez-Alonso G, Jenner GA., Jackson SE (1998) Geochronology and geochemistry of the Pola de Allande granitoids (northern Spain): their bearing on the Cadomian-Avalonian evolution of northwest Iberia. Canadian Journal of Earth Sciences 35:1–15

Fernández-Suárez J, Dunning, GR, Jenner GA, Gutiérrez-Alonso G (2000) Variscan collisional magmatism and deformation in NW Iberia: constraints from U-Pb geochronology of granitoids. Journal of the Geological Society, London, 157:565–576

Fernández-Suárez J, Díaz-García F, Jeffries TE, Arenas R, Abati J (2003) Constraints on the provenance of the uppermost allochthonous terrane of the NW Iberian Massif: inferences from detrital zircon U–Pb ages. Terra Nova 15:138–144. https://doi.org/10.1046/j.1365-121.2003.00479.x

Finger F, Steyrer HP (1990) I-type granitoids as indicators of a late Paleozoic convergent ocean-continent margin along the southern flank of the central European Variscan orogen. Geology 18:1207–1210

Flecha I, Palomeras I, Carbonell R, Simancas JF, Ayarza P, Matas J, González Lodeiro F, Pérez-Estaún A (2009) Seismic imaging and modelling of the lithosphere of SW Iberia. Tectonophysics 472:148–157

Floyd PA (1995) Rhenohercynian foldbelt: autochthon and non metamorphic nappe units—igneous activity. In: Dallmeyer RD, Franke W, Weber K (eds), Pre-permian geology of central and eastern Europe. Springer, Berlin, 59–81

Fonseca P, Ribeiro A (1993) Tectonics of the Beja-Acebuches Ophiolite: a major suture in the Iberian Variscan Fold-belt. Geologische Rundschau 82:440–447

Fonseca P, Munhá J, Pedro J, Rosas F, Moita P, Araújo A, Leal N (1999) Variscan Ophiolites and High-Pressure Metamorphism in Southern Iberia. Ophiolioti 24:259–268

Fortey RA, Cocks LRM (2003) Palaeontological evidence bearing on global Ordoviacian-Silurian continental reconstructions. Earth-Science Reviews 61:245–307. https://doi.org/10.1016/s0012-8252(02)00115-0

Franke W (2000) The mid-European segment of the Variscides: tectonostratigraphic units, terrane boundaries and plate tectonic evolution. In: Franke W, Haak V, Oncken O, Tanner D (eds), Orogenic Processes: Quantification and Modelling in the Variscan Belt. Geological Society, London, Special Publications 179:35–61. https://doi.org/10.1144/gsl.sp.2000.179.01.05

Franke W (2006) The Variscan orogen in Central Europe: construction and collapse. In: Gee DG, Stephenson RA (eds), European Lithosphere Dynamics. Geological Society, London, Memoirs, 32:333–343

Franke W (2014) Topography of the Variscan orogen in Europe: failed-not collapsed. International Journal of Earth Sciences 103:1471–1499. https://doi.org/10.1007/s00531-014-1014-9

Franke W, Dulce JC (2017) Back to sender: tectonic accretion and recycling of Baltica-derived Devonian clastic sediments in the Rheno-Hercynian Variscides. International Journal of Earth Sciences 106:377–386. https://doi.org/10.1007/s00531-016-1408-y

Franke W, Bortfeld RK, Brix M, Drozdzewski G, Dürbaum HJ, Giese P, Janoth W, Jödicke H, Reichert C, Scherp A, Schmoll J, Thomas R, Thünker M, Weber K, Wiesner MG, Wong HK (1990) Crustal structure of the Rhenish Massif: results of deep seismic reflection lines DEKORP 2-North and 2-North-Q. Geologische Rundschau 79:523–566

Franke W, Doublier MP, Klama K, Potel S, Wemmer K (2011) Hot metamorphic core complex in a cold foreland. International Journal of Earth Sciences 100:753–758. https://doi.org/10.1007/s00531-010-0512-7

Franke W, Cocks RM, Torsvik TH (2017) The Paleozoic Variscan oceans revisited. Gondwana Research 48:257–284. https://doi.org/10.1016/j.gr.2017.03.005

Fuenlabrada JM, Pieren AP, Díez Fernández R, Sánchez Martínez S, Arenas R (2016) Geochemistry of the Ediacaran-Early Cambrian transition in Central Iberia: Tectonic setting and isotopic sources. Tectonophysics 681:15–30. https://doi.org/10.1016/j.tecto.2015.11.013

Galindo C, Casquet C (2004) El magmatismo prevarisco de la Zona de Ossa-Morena. In: Vera JA (ed), Geología de España. SGE-IGME, Madrid, 190–194

Gallo LC, Tomezzoli RN, Cristallini EO (2017) A pure dipole analysis of the Gondwana apparent polar wander path: Paleogeographic implications in the evolution of Pangea, Geochemistry, Geophysics, Geosystems 18:1499–1519. https://doi.org/10.1002/2016gc006692

Giese U, Bühn B (1993) Early Paleozoic rifting and bimodal volcanism in the Ossa-Morena Zone of south-west Spain. Geologische Rundschau 83:143–160

Gómez Barreiro J, Wijbrans JR, Castiñeiras P, Martínez Catalán JR, Arenas R, Díaz García F, Abati J (2006) 40Ar/39Ar laser probe dating of mylonitic fabrics in a polyorogenic terrane of NW Iberia. Journal of the Geological Society 163:61–73. https://doi.org/10.1144/0016-764905-012

Gómez Pugnaire MT, Azor A, Fernández-Soler JM, López Sánchez--Vizcaíno, V (2003) The amphibolites from the Ossa-Morena/Central Iberian Variscan suture (Southwestern Iberian Massif): geochemistry and tectonic interpretation. Lithos 68:23–42. https://doi.org/10.1016/s0024-4937(03)00018-5

Gómez-Pugnaire MT, Braga JC, Martín JM, Sassi FP, del Moro A (2000) Regional implication of a Palaeozoic age for the Nevado-Filábride cover of the Betic Cordillera, Spain. Schweiz. Mineral. Petrogr. Mitt. 80:45–52

Gómez-Pugnaire MT, Rubatto D, Fernández-Soler JM, Jabaloy A, López Sánchez- Vizcaíno V, González-Lodeiro F, Galindo-Zaldívar J, Padrón-Navarta JA (2012) U–Pb geochronology of Nevado–Filábride gneisses: evidence for the Variscan nature of the deepest Betic complex (SE Spain). Lithos 146–147:93-111

González-Clavijo E, Martínez Catalán JR (2002) Stratigraphic record of preorogenic to synorogenic sedimentation, and tectonic evolution of imbricate units in the Alcañices synform (northwestern Iberian Massif). In: Martínez Catalán JR, Hatcher RD Jr, Arenas R, Díaz García F (eds), Variscan-Appalachian dynamics: The building of the late Paleozoic basement: Boulder, Colorado, Geological Society of America Special Paper 364:17–35

González-Clavijo E, Dias da Silva Í, Gutiérrez-Alonso G, Díez Montes A (2016) U/Pb age of a large dacitic block locked in an early carboniferous synorogenic mélange in the parautochthon of NW Iberia: New insights on the structure/sedimentation variscan interplay. Tectonophysics first online (TECTO-126895):11. https://doi.org/10.1016/j.tecto.2016.01.001

González-Clavijo E, Díez Montes A, Días da Silva IF, Sánchez-García T (2017a) An overview of the Ordovician volcanic rocks and unconformities in the Central Iberian and Galicia-Trás-os-Montes Zones of the Iberian Variscan Massif. In: Álvaro JJ, Casas JM, Clausen S (eds) Géologie de la France 1(4): 22–24

González-Clavijo E, Martín García G, Martínez Catalán JR, Gómez Barreiro J (2017b) Aportaciones estructurales al conocimiento del sinclinal de Tamames: Dominio del Esquisto Grauváquico de la Zona Centro Ibérica (Macizo Ibérico). Geogaceta 62:3–6

González F, Moreno C, Playford G (2011) The Gondwana-Laurussia convergence process: evidence from the Middle Mississippian (Visean) palynostratigraphic record. Geological Magazine 148:317–328. https://doi.org/10.1017/s0016756810000713

Guillot S, Ménot RP (2009) Paleozoic evolution of the External Crystalline Massifs of the Western Alps. Comptes Rendus Geoscience 341:253–265. https://doi.org/10.1016/j.crte.2008.12.010

Gutiérrez-Alonso G (1995) Structure of the Internal-External Transition Zone in the northern Iberian Massif: implications for the interpretation of deep crustal seismic profiles. Revista de la Sociedad Geológica de España 8:322–330

Gutiérrez-Alonso G, Fernández-Suárez J, Weil AB (2004) Orocline triggered lithospheric delamination. Geological Society of America, Special Paper 383:121–130

Gutiérrez-Alonso G, Fernández-Suárez J, Jeffries TE, Johnston ST, Pastor-Galán D, Murphy BJ, Franco MP, Gonzalo JC (2011a) Diachronous post-orogenic magmatism within a developing orocline in Iberia, European Variscides. Tectonics 30:TC5008. https://doi.org/10.1029/2010tc002845

Gutiérrez-Alonso G, Murphy JB, Fernández-Suárez J, Weil AB, Franco MP, Gonzalo JC (2011b) Lithospheric delamination in the core of Pangea: Sm-Nd insights from the Iberian mantle. Geology 39:155–158.

Gutiérrez-Alonso G, Fernández-Suárez J, Pastor-Galán D, Johnston ST, Linnemann U, Hofmann M, Shaw J, Colmenero JR, Hernández P (2015) Significance of detrital zircons in Siluro-Devonian rocks from Iberia. Journal of the Geological Society, London, 172:309–332. https://doi.org/10.1144/jgs2014-118

Gutiérrez-Alonso G, Gutiérrez-Marco JC, Fernández-Suárez J, Bernárdez E, Corfu F (2016) Was there a super-eruption on the Gondwanan coast 477 Ma ago? Tectonophysics 681:85–94. https://doi.org/10.1016/j.tecto.2015.12.012

Gutiérrez-Marco JC, Robardet M, Rábano I, Sarmiento G, San José Lancha MA, Herranz Araújo P, Pieren Pidal E (2002) Ordovician. In: Gibbons W, Moreno MT. (eds), The Geology of Spain. Geological Society, London, 31–49

Hajná J, Zák J, Dörr W (2017) Time scales and mechanisms of growth of active margins of Gondwana: A model based on detrital zircon ages from the Neoproterozoic to Cambrian Blovice accretionary complex, Bohemian Massif. Gondwana Research 42:63–83. https://doi.org/10.1016/j.gr.2016.10.004

Henderson BJ, Collins WJ, Murphy JB, Gutiérrez-Alonso G, Hand M (2016) Gondwanan basement terranes of the Variscan-Appalachian orogen: Baltica, Saharan and West African hafnium isotopic fingerprints in Avalonia, Iberia and the Armorican Terranes. Tectonophysics 681:278–304. https://doi.org/10.1016/j.tect.2015.11.020

Henk A (1999) Did the Variscides collapse or were they torn apart?: A quantitative evaluation of the driving forces for postconvergent extension in central Europe. Tectonics 18:774–792

Henk A, Blanckenburg F von, Finger F, Schaltegger U, Zulauf G (2000) Syn-convergent high-temperature metamorphism and magmatism in the Variscides: a discussion of potential heat sources. In: Franke W, Haak W, Oncken O, Tanner D (eds), Orogenic Processes: Quantification and Modelling in the Variscan Belt. Geological Society, London, Special Publications, 179:387–399

Henriques SBA, Neiva AMR, Ribeiro ML, Dunning GR, Tagcmanová L (2015) Evolution of a Neoproterozoic suture in the Iberian Massif, Central Portugal: New U-Pb ages of igneous and metamorphic events at the contact between the Ossa Morena Zone and Central Iberian Zone. Lithos 220–223:43-59. https://doi.org/10.1016/j.lithos.2015.02.001

Herbig HG (1985) An upper Devonian limestone slide block near Marbella (Betic Cordillera, southern Spain) and the palaeogeographic relations between Malaguides and Menorca. Acta Geológica Hispánica 20:155–178

Hirt AM, Lowrie W, Julivert M, Arboleya ML (1992) Paleomagnetic results in support of a model for the origin of the Asturian Arc. Tectonophysics 213:321–339

Jesús AP, Mateus A, Munhá JM, Tassinari CCG, Bento dos Santos TM, Benoit M (2016) Evidence for underplating in the genesis of the Variscan synorogenic Beja Layered Gabbroic Sequence (Portugal) and related mesocratic rocks. Tectonophysics 683:148–171. https://doi.org/10.1016/j.tecto.2016.06.001

Johnston ST, Weil AB, Gutiérrez-Alonso G (2013) Oroclines: thick and thin. Geological Society of America Bulletin 125:643–663. https://doi.org/10.1130/b30765.1

Julivert M, Fontboté JM, Ribeiro A, Nabais-Conde LE (1974) Mapa Tectónico de la Península Ibérica y Baleares a escala 1:1.000.000. IGME, Memoria explicativa

Julivert M, Vegas R, Roiz JM, Martínez Ríus A (1983) La estructura de la extensión sureste de la Zona Centro-Ibérica con metamorfismo de bajo grado. In: Comba, J.A. (Ed.) Geología de España, V-1, IGME, Madrid, 477–490

Krzywiec P, Mazur S, Gagala L, Kufrasa M, Lewandowski M, Malinowski M, Buffenmyer V (2017) Late Carboniferous thin-skinned compressional deformation above the SW edge of the East European craton as revealed by seismic reflection and potential field data-Correlations with the Variscides and the Appalachians. The Geological Society of America Memoir 213. https://doi.org/10.1130/2017.1213(14)

Laborda-López C, Aguirre J, Donovan SK (2015) Surviving metamorphism: taphonomy of fossil assemblages in marble and calc-silicate schist. Palaios 30:668–679

Lago M, Arranz E, Pocoví A, Galé C, Gil-Imaz A (2004a) Permian magmatism and basin dynamics in the southern Pyrenees: a record of the transition from Late Variscan transtension to early Alpine extension. Geological Society, London, Special Publications 223:439–464. https://doi.org/10.1144/gsl.sp.2004.223.01.19

Lago M, Galé A, Arranz E, Gil-Imaz A (2004b) El magmatismo pérmico. In: Vera, J.A. (ed), Geología de España, SGE-IGME, Madrid, 271–272

Laurent O, Couzinié S, Zeh A, Vanderhaeghe O, Moyen JF, Villaros A, Gardien V, Chelle-Michou C (2017) Protracted, coeval crust and mantle melting during Variscan late-orogenic evolution: U-Pb dating in the eastern French Massif Central. International Journal of Earth Sciences (Geol Rundsch) 106:421–451. https://doi.org/10.1007/s00531-016-1434-9

Liñán E, Quesada C (1990) Ossa Morena Zone. Stratigraphy. Rift Phase (Cambrian). In: Dallmeyer RD, Martínez García E (eds), Pre-Mesozoic Geology of Iberia. Springer, Berlin, 259–266

Liñán E, Gozalo R, Palacios T, Gámez Vintaned JA, Ugidos JM, Mayoral E (2002) Cambrian. In: Gibbons W, Moreno MT (eds), The Geology of Spain. Geological Society, London, 17–29

Linnemann U, Romer LR (2002) The Cadomian Orogeny in Saxo-Thuringia, Germany: geochemical and Nd–Sr–Pb isotopic characterization of marginal basins with constraints to geotectonic setting and provenance. Tectonophysics 352:33–64

Linnemann U, McNaughton NJ, Romer RL, Gehmlich M, Drost K, Tonk C, (2004) West African provenance for Saxo-Thuringian (Bohemian Massif): did Armorica ever leave pre-Pangean Gondwana?- U/Pb-SHRIMP zircon evidence and the Nd-isotopic record. International Journal of Earth Sciences 93:683–705

Linnemann U, Hersboch A, Liégeois J, Pin C, Gärtner A, Hofmann M (2012) The Cambrian to Devonian odyssey of the Brabant Massif within Avalonia: A review with new zircon ages, geochemistry, Sm-Nd isotopes, stratigraphy and palaeogeography. Earth-Science Reviews 112:126–154. https://doi.org/10.1016/j.earscirev.2012.02.007

Linnemann U, Gerdes A, Hofmann M, Marko L (2014) The Cadomian Orogen: Neoproterozoic to Early Cambrian crustal growth and orogenic zoning along the periphery of the West African Craton—constraints from U-Pb zircon ages and Hf isotopes (Schwarxburg Antiform, Germany). Precambrian Research 244:236–278. https://doi.org/10.1016/j.precamres.2013.08.007

López-Carmona A, Abati J, Pitra P, Lee JW (2014) Retrogressed lawsonite blueschists from the NW Iberian Massif: P–T–t constraints from thermodynamic modelling and 40Ar/39Ar geochronology. Contributions to Mineralogy and Petrology 167:1–20. https://doi.org/10.1007/s00410-014-0987-5

López-Guijarro R, Armendáriz M, Quesada C, Fernández-Suárez J, Murphy JB, Pin C, Bellido F (2008) Ediacaran-Palaeozoic tectonic evolution of the Ossa Morena and Central Iberian zones (SW Iberia) as revealed by Sm-Nd isotope systematics. Tectonophysics 461:202–214. https://doi.org/10.1016/j.tecto.2008.06.006

Lunar R, Ortega L, Piña R, Gervilla F, Monterrubio S, Merinero R (2011) Podiform chromitites from the Calzadilla de los Barros serpentinite, Iberian Massif, SW Spain. 11th SGA Biennal Meeting, Let's Talk Ore Deposits, Antofagasta, Chile, 636–638

Mancilla FL, Booth-Rea G, Stich D, Pérez-Peña JV, Morales J, Azañón JM, Martín R, Giaconia F (2015) Slab rupture and delamination under the Betics and Rif constrained from receiver functions. Tectonophysics 663:225–237. https://doi.org/10.1016/j.tecto.2015.06.028

Margalef A, Castiñeiras P, Casas JM, Navidad M, Liesa M, Linnemann U, Hofmann M, Gärtner A (2016) Detrital zircons from the Ordovician rocks of the Pyrenees: Geochronological constraints and provenance. Tectonophysics 681:124–134. https://doi.org/10.1016/j.tecto.2016.03.015

Marques FO, Ribeiro A, Munhá J (1996) Geodynamic evolution of the Continental Allochthonous Terrane (CAT) of the Bragança Nappe Complex, NE Portugal. Tectonics 15:747–762

Martín-Algarra A, Vera JA (2004) La Cordillera Bética y las Baleares en el contexto del Mediterráneo Occidental. In: Vera JA (ed), Geología de España. SGE-IGME, 352–354

Martín-Algarra A, Mazzoli S, Perrone V, Rodríguez-Cañero R, Navas-Parejo P (2009) Variscan tectonics in the Malaguide Complex (Betic Cordillera, Southern Spain): stratigraphic and structural Alpine versus Pre-Alpine constraints from the Ardales Area (Province of Málaga). I. Stratigraphy. Journal of Geology 117:241–262

Martínez Catalán JR (2011) Are the oroclines of the Variscan belt related to late Variscan strike-slip tectonics? Terra Nova 23:241–247. https://doi.org/10.1111/j.1365-3121.2011.01005.x

Martínez Catalán JR (2012) The Central Iberian arc, an orocline centered in the Iberian Massif and some implications for the Variscan belt. International Journal of Earth Sciences 101:1299–1314. https://doi.org/10.1007/s00531-011-0715-6

Martínez Catalán JR, Ayarza P, Pulgar JA, Pérez Estaún A, Gallart J, Marcos A, Bastida F, Álvarez-Marrón J, González Lodeiro F, Aller J, Dañobeitia JJ, Banda E, Córdoba D, Comas MC (1995) Results from the ESCI-N3.3 marine deep seismic profile along the Cantabrian continental margin. Revista de la Sociedad Geológica de España 8:341–354

Martínez Catalán JR, Arenas R, Díaz García F, Abati J (1997) Variscan accretionary complex of northwest Iberia: Terrane correlation and succession of tectonothermal events. Geology 25:1103–1106

Martínez Catalán JR, Arenas R, Abati J, Sánchez Martínez S, Díaz García F, Fernández-Suárez J, González Cuadra P, Castiñeiras P, Gómez Barreiro J, Díez Montes A, González Clavijo E, Rubio Pascual FJ, Andonaegui P, Jeffries TE, Alcock JE, Díez Fernández R, López Carmona A (2009) A rootless suture and the loss of the roots of a mountain chain: The Variscan belt of NW Iberia. Comptes Rendus Geoscience 341:114–126. https://doi.org/10.1016/j.crte.2008.11.004

Martínez Catalán JR, Aerden DGAM, Carreras J (2015) The "Castillian bend" of Rudolf Staub (1926): historical perspective of a forgotten orocline in Central Iberia. Swiss Journal Geoscience 108:289–303, https://doi.org/10.1007/s00015-015-0202-3

Martínez Catalán JR, González Clavijo E, Meireles C, Díez Fernández R, Bevis J (2016) Relationships between syn-orogenic sedimentation and nappe emplacement in the hinterland of the Variscan belt in NW Iberia deduced from detrital zircons. Geological Magazine 153:38–60, https://doi.org/10.1017/s001675681500028x

Martínez Poza I, Martínez Poyatos D, Simancas JF, Azor A (2012) La estructura varisca de la Unidad del Pulo o Lobo (SO del Macizo Ibérico) en las transversales de Aroche y Rosal de la Frontera (Huelva). Geogaceta 52:21–24

Martínez FJ, Dietsch C, Aleinikoff J, Cirés J, Arboleya ML, Reche J, Gómez-Gras D (2015) Provenance, age, and tectonic evolution of Variscan flysch, southeastern France and northeastern Spain, based on zircon geochronology. Geological Society of America Bulletin 128:842–859. https://doi.org/10.1130/b31316.1

Martínez-Poyatos D, Carbonell R, Palomeras I, Simancas JF, Ayarza P, Martí D, Azor A, Jabaloy A, González Cuadra P, Tejero R, Martín Parra LM, Matas J, González Lodeiro F, Pérez-Estaún A, García Lobón JL, Mansilla L (2012) Imaging the crustal structure of the Central Iberian Zone (Variscan Belt): The ALCUDIA deep seismic reflection transect. Tectonics 31:TC3017. https://doi.org/10.1029/2011tc002995

Mata J, Munhá J (1990) Magmatogénese de Metavulcanito Cambricos do Nordeste Alentejano: os stadios iniciais de rifting continental. Comunicaçoes dos Serviços Geológicos de Portugal 76:61–89

Mateus A, Munhá J, Ribeiro A, Tassinari CCG, Sato K, Pereira E, Santos JF (2016) U-Pb SHRIMP zircon dating of high-grade rocks from the Upper Allochthonous Terrane of Bragança and Morais Massifs (NE Portugal); geodynamic consequences. Tectonophysics 675:23–49. https://doi.org/10.1016/j.tecto.2016.02.048

Matte Ph (1986) Tectonics and plate tectonics model for the Variscan belt of Europe. Tectonophysics 126:329–374

Matte Ph (1991) Accretionary history and crustal evolution of the Variscan belt in Western Europe. Tectonophysics 196:309–337

Matte Ph (2001) The Variscan collage and orogeny (480–290 Ma) and the tectonic definition of the Armorica microplate: a review. Terra Nova 13:122-128

Matte Ph, Burg JP (1981) Sutures, thrusts and nappes in the Variscan Arc of western Europe: plate tectonic implications. Thrust and Nappe Tectonics, Geological Society of London, Special Publications, 353–358

Matte Ph (2002a) Variscides between the Appalachians and the Urals: Similarities and differences between Paleozoic subduction and collision belts. In: Martínez Catalán JR, Hatcher RD Jr, Arenas R, Díaz García F (eds), Variscan-Appalachian dynamics: The building of the late Paleozoic basement: Boulder, Colorado, Geological Society of America Special Paper 364:239–251.

Matte Ph (2002b) Les plis hercyniens kilométriques couchés vers l'ouest-sud-ouest dans la région du pic du Midi d'Ossau-col du Somport (zone axiale des Pyrénées occidentales) Comptes Rendus Geoscience 334:773–779

Matte Ph, Ribeiro A (1975) Forme et orientation de la virgation hercynienne de Galice. Relations avec le plissement et hypothèses sur la genèse de l'arc Ibero-Armoricaine. Comptes Rendus Académie des Sciences Paris, 280D:2825–2828

McCann T, Pascal C, Timmerman MJ, Krzywiec P, López-Gómez J, Wetzel A, Krawczyk CM, Rieke H, Lamarche J (2006) Post-Variscan (end Carboniferous-Early Permian) basin evolution in Western and Central Europe. In: Gee, DG, Stephenson, RA (eds),

European Lithosphere Dynamics. Geological Society of London Memoir 32:355–388

McKerrow WS, Mac Niocaill C, Ahlberg PE, Clayton G, Cleal CJ, Eagar RMC (2000) The late Palaeozoic relations between Gondwana and Laurussia. In: Franke W, Haak V, Oncken O, Tanner D (eds), Orogenic Processes: Quantification and Modelling in the Variscan Belt. Geological Society, London, Special Publication 179:9–20

Merinero R, Lunar R, Ortega L, Piña R, Monterrubio S, Gervilla F (2014) Zoned chromite records multiple metamorphic episodes in the Calzadilla de los Barros ultramafic bodies (SW Iberian peninsula). European Journal of Mineralogy 26:757–770. https://doi.org/10.1127/ejm/2014/0026-2406

Mezcua J, Gil A, Benarroch R (1976) Estudio gravimétrico de la Península Ibérica y Baleares. Instituto Geográfico Nacional, Madrid

Michard A, Soulaimani A, Hoepffner C, Baidder L, Rjimati EC, Saddiqi O (2010) The South-Western Branch of the Variscan Belt: Evidence from Morocco. Tectonophysics 492:1–24. https://doi.org/10.1016/j.tecto.2010.05.021

Moita P, Munhá J, Fonseca P, Pedro J, Tassinari CCG, Araújo A, Palacios T (2005) Phase equilibria and geochronology of Ossa-Morena eclogites. Actas XIV Semana de Geoquímica/ VIII Congresso do Geoquímica dos Países de Língua Portuguesa, 2:471–474

Montel JM, Kornprobst J, Vielzeuf D (2000) Preservation of old U-Th-Pb ages in shielded monazite: example from the Beni Bousera Hercynian kinzigites (Morocco). Journal of Metamorphic Geology 18:335–342. https://doi.org/10.1046/j.1525-1314.2000.00261.x

Montero P, Floor P (2004) Los complejos alcalinos prevariscos (magmatismo del Paleozoico inferior en las unidades basales). In: Vera JA (ed), Geología de España. SGE-IGME, Madrid, 149–150

Montero P, Talavera C, Bea F (2017) Geochemical, isotopic, and zircon (U-Pb, O, Hf isotopes) evidence for the magmatic sources of the volcano-plutonic Ollo de Sapo Formation, Central Iberia. Geologica Acta 15:245–260. https://doi.org/10.1344/geologicaacta2017.15.4.1

Munhá J (1983) Hercynian magmatism in the Iberian Pyrite Belt. In: Sousa MJL, Oliveira JT (eds), The Carbonferous of Portugal. Memórias dos Serviços Geológicos de Portugal 29:39–81

Murphy JB, Strachan RA, Nance RD, Parker KD, Fowler MB (2000) Proto-Avalonia: A 1.2–1.0 Ga tectonothermal event and constraints for the evolution of Rodinia. Geology 28:1071-1074

Murphy JB, Fernández-Suárez J, Keppie JD, Jeffries TE (2004) Contiguous rather than discrete Paleozoic histories forthe Avalon and Meguma terranes based on detrital zircon data. Geology 32:585–588. https://doi.org/10.1130/g20351.1

Murphy JB, Gutiérrez-Alonso G, Nance D, Fernández-Suárez J, Duncan Keppie J, Quesada C, Strachan RA, Dostal J (2006) Origin of the Rheic Ocean: Rifting along a Neoproterozoic suture? Geology 34:325–328. https://doi.org/10.1130/g22068.1

Murphy JB, Cousens BL, Braid JA, Strachan RA, Dostal J, Keppie JD, Nance RD (2011) Highly depleted oceanic lithosphere in the Rheic Ocean: implications for Paleozoic plate reconstructions. Lithos 123:165–175

Murphy JB, Braid JA, Quesada C, Dahn D, Gladney E, Dupuis NE (2015) An eastern Mediterranean analogue for the Late Paleozoic evolution of the Pangean suture zone. In: Li, Z.X., Evans, D.A.D., Murphy, J.B. (ed), Supercontinent Cycles Through Earth History. Geological Society of London Special Publication 424. https://doi.org/10.1144/sp424.9

Murphy JB, Quesada C, Gutiérrez-Alonso G, Johnston, ST, Weil A (2016) Reconciling competing models for the tectono-stratigraphic zonation of the Variscan orogen in western Europe. Tectonophysics 681:209–219. https://doi.org/10.1016/j.tecto.2016.01.006

Muttoni G, Kent DV, Garzanti E, Brack P, Abrahamsen N, Gaetani M (2003) Early Permian Pangea "B" to Late Permian Pangea "A". Earth and Planetary Science Letters 215:379–394. https://doi.org/10.1016/s0012-821x(03)00452-7

Nance RD, Linnemann U (2008) The Rheic Ocean: origin, evolution, and significance. GSA Today 18:4–12.

Nance RD, Gutiérrez-Alonso G, Keppie JD, Linnemann U, Murphy JB, Quesada C, Strachan RA, Woodcock NH (2012) A brief history of the Rheic Ocean. Geoscience Frontiers 3:125–135. https://doi.org/10.1016/j.gsf.2011.11.008

Nance RD, Neace ER, Braid JA, Murphy JB, Dupuis N, Shail RK (2015) Does the Meguma Terrane extend into SW England? Geoscience Canada 42:61–76. https://doi.org/10.12789/geocanj.2014.41.056

Neubauer F (2002) Evolution of late Neoproterozoic to early Paleozoic tectonic elements in Central and Southeast European Alpine mountain belts: review and synthesis. Tectonophysics 352:87–103

Nysaether E, Torsvik TH, Feist R, Walderhaug HJ, Eide EA (2002) Ordovician paleogeography with new paleomagnetic data from the Montagne Noire (Southern France). Earth and Planetary Science Letters 203:329–341

Okay AI, Topuz G (2017) Variscan orogeny in the Black Sea region. International Journal of Earth Sciences (Geol Rundsch) 106:569–592. https://doi.org/10.1007/s00531-016-1395-z

Oliveira JT (1990) The South Portuguese Zone. Stratigraphy and Synsedimentary Tectonism. In: Dallmeyer RD, Martínez García E (eds), Pre-Mesozoic Geology of Iberia. Springer, Berlin, 334–347

Ordóñez-Casado B (1998) Geochronological studies of Pre-Mesozoic basement of the Iberian Massif: the Ossa-Morena Zone and the Allochthonous Complexes within the Central Iberian Zone. PhD Thesis, University of Zürich

Ordóñez-Casado B, Gebauer D, Schäfer HJ, Gil Ibarguchi JI, Peucat JJ (2001) A single Devonian subduction event for the HP/HT metamorphism of the Cabo Ortegal complex within the Iberian Massif. Tectonophysics 332:359–385. https://doi.org/10.1016/s0040-1951(00)00210-9

Orejana D, Villaseca C, Valverde-Vaquero P, Belousova EA, Armstrong RA (2012) U-Pb geochronology and zircon composition of late Variscan S- and I-type granitoids from the Spanish Central System batholith. International Journal of Earth Sciences 101:1789–1815. doi:10.1007/ s00531-012-0750-y

Orejana D, Villaseca C, Merino Martínez E, (2017) Basic Ordovician magmatism of the Spanish Central System: Constraints on the source and geodynamic setting. Lithos 284-285:608–624

Ortega Gironés E, González Lodeiro F (1986) La discordancia intra-Alcudiense en el dominio meridional de la Zona Centroibérica. Breviora Geológica Astúrica 27:27–32

Oschner A (1993) U-Pb geochronology of the Upper Proterozoic lower Paleozoic geodynamic evolution in the Ossa-Morena Zone (SW Iberia): Constraints on the Timing of the Cadomian Orogeny. PhD Thesis University of Zürich

Palero FJ (1993) Tectónica pre-hercínica de las series infraordovícicas del anticlinal de Alcudia y la discordancia intraprecámbrica en su parte oriental (sector meridional de la Zona Centroibérica). Boletín Geológio y Minero 104:227–242

Palomeras I, Carbonell R, Ayarza P, Fernández M, Simancas JF, Martínez Poyatos D, González Lodeiro F, Pérez-Estaún A (2011b) Geophysical model of the lithosphere across the Variscan Belt of SW-Iberia: Multidisciplinary assessment. Tectonophysics 508:42–51. https://doi.org/10.1016/j.tecto.2010.07.010

Palomeras I, Carbonell R, Ayarza P, Martí D, Brown D, Simancas JF (2011a) Shear wave modelling and Poisson's ratio in the Variscan Belt of SW Iberia. Geochemistry Geophysics Geosystems 12: Q07008. https://doi.org/10.1029/2011gc003577

Paquette JL, Ballèvre M, Peucat JL, Cornen G (2017) From opening to subduction of an oceanic domain constrained by LA-ICP-MS U-Pb zircon dating (Variscan belt, Southern Armorican Massif, France).

Lithos 294–295:418-437. https://doi.org/10.1016/j.lithos.2017.10.005

Pastor-Galán D, Gutiérrez-Alonso G, Murphy JB, Fernández-Suárez J, Hofmann M, Linnemann U (2013) Provenance analysis of the Paleozoic sequences of the northern Gondwana margin in NW Iberia: Passive margin to Variscan collision and orocline development. Gondwana Research 23:1089–1103. https://doi.org/10.1016/j.gr.2012.06.015

Pastor-Galán D, Ursem B, Meere PA, Langereis C (2015b) Extending the Cantabrian Orocline to two continents (from Gondwana to Laurussia). Paleomagnetism from South Ireland. Earth and Planetary Science Letters 432:223–231. https://doi.org/10.1016/j.epsi.2015.10.019.

Pastor-Galán D, Dekkers MJ, Gutiérrez-Alonso G, Brouwer D, Groenewegen Th, Krigsman W, Fernández-Lozano J, Yenes M, Álvarez-Lobato F (2016) Paleomagnetism of the Central Iberian curve's putative hinge: too many oroclines in the Iberian Variscides. Gondwana Research 39:96–113. https://doi.org/10.1016/j.gr.2016.06.016

Pastor-Galán D, Groenewegen T, Brouwer D, Krijgsman W, Dekkers MJ (2015a) One or two oroclines in the Variscan orogen of Iberia? Implications for Pangea amalgamation. Geology 43:527–530. https://doi.org/10.1130/g36701.1

Pastor-Galán D, Mulchrone, KF, Koymans MR, van Hinsbergen DJJ, Langereis CG (2017) Bootstrapped total least squares orocline test: A robust method to quantify vertical axis rotation patterns in orogens, with examples from the Cantabrian and Aegean oroclines. Lithosphere GSA Data Repository Item 2017085. https://doi.org/10.1130/l547.1

Pedro J, Araújo A, Fonseca P, Tassinari C, Ribeiro A (2010) Geochemistry and U-Pb zircon age of the internal Ossa-Morena Zone Ophiolite Sequences: a remnant of Rheic Ocean in SW Iberia. Ofioliti 35:117–130. https://doi.org/10.4454/ofioliti.v35i2.390

Pereira Z, Piçarra JM, Oliveira JT (1999) Lower Devonian Palynomorphs from the Barrancos region, Ossa-Morena Zone, Portugal. Bolletino della Società Paleontologica Italiana 38:239–245

Pereira Z, Matos J, Fernandez P, Oliveira JT (2008) Palynostratigraphy and systematic palynology of the Devonian and Carboniferous successions of the South Portuguese Zone, PORTUGAL. Memórias Geológicas do Instituto Nacional de Engenharia, Tecnologia e Innovaçao 34

Pereira MF, Chichorro M, Williams IS, Silva JB, Fernández C, Díaz-Azpiroz M, Aparaiz A, Castro C (2009) Variscan intra-orogenic extensional tectonics in the Ossa-Morena Zone (Évora-Aracena-Lora del Río metamorphic belt, SW Iberian Massif): SHRIMP zircon U-Th-Pb geochronology. In: Murphy JB, Keppie JD, Hynes AJ (eds), Ancient Orogens and Modern Analogues. Geological Society, London, Special Publications 327:215–237. https://doi.org/10.1144/sp327.11

Pereira MF, Chichorro M, Solá AR, Silva JB, Sánchez-García T, Bellido F (2011) Tracing the Cadomian magmatism with detrital/inherited zircon ages by *in-situ* U-Pb SHRIMP geochronology (Ossa-Morena Zone, SW Iberian Massif). Lithos 123:204–217. https://doi.org/10.1016/j.lithos.2010.11.008

Pereira MF, Chichorro M, Johnston ST, Gutiérrez-Alonso G, Silva JB, Linnemann U, Hofmann M, Drost K (2012a) The missing Rheic Ocean magmatic arcs: Provenance analysis of Late Paleozoic sedimentary clastic rocks of SW Iberia. Gondwana Research 22:882–891. https://doi.org/10.1016/j.gr.2012.03.010

Pereira MF, Chichorro M, Silva JB, Ordóñez-Casado B, Lee JKW, Williams IS (2012b) Early Carboniferous wrenching, exhumation of high-grade metamorphic rocks and basin instability in SW iberia: Constraints derived from structural geology and U-Pb and $^{40}Ar/^{39}Ar$ geochronology. Tectonophysics 558–559:28-44. https://doi.org/10.1016/j.tecto.2012.06.020

Pereira MF, Castro A, Fernández C (2015) The inception of a Paleotethyan magmatic arc in Iberia. Geoscience Frontiers 6:297–306. https://doi.org/10.1016/j.gsf.2014.02.006

Pereira MF, Gutiérrez-Alonso, G, Murphy JB, Drost K, Gama, Silva JB (2017) Birth and demise of the Rheic Ocean magmatic arc(s): Combined U-Pb and Hf isotope analyses in detrital zircon from SW Iberia siliciclastic strata. Lithos 278–281:383-399. https://doi.org/10.1016/j.lithos.2017.02.009

Pérez-Cáceres I, Martínez Poyatos D, Simancas JF, Azor A (2015) The elusive nature of the Rheic Ocean suture in SW Iberia. Tectonics 34:2429–2450. https://doi.org/10.1002/2015tc003947

Pérez-Cáceres I, Martínez Poyatos D, Simancas JF, Azor A (2017) Testing the Avalonian affinity of the South Portuguese Zone and the Neoproterozoic evolution of SW Iberia through detrital zircon populations. Gondwana Research 42:177–192. https://doi.org/10.1016/j.gr.2016.10.010

Pérez-Cáceres I, Simancas JF, Martínez Poyatos D, Azor A, González Lodeiro, F (2016) Oblique collision and deformation partitioning in the SW Iberian Variscides. Solid Earth 7:857–872. https://doi.org/10.5194/se-7-857-2016

Pérez-Estaún A, Pulgar J, Álvarez-Marrón J, ESCI-N Group (1995) Crustal structure of the Cantabrian Zone: seismic image of a Variscan foreland thrust and fold belt (NW Spain). Revista de la Sociedad Geológica de España 8:307–319

Pérez-Estaún A, Bea F (eds) (2004) Macizo Ibérico. In: Vera JA (ed), Geología de España. SGE-IGME, Madrid, 19–230

Pérez-Estaún A, Bastida F, Alonso JL, Marquínez J, Aller J, Álvarez-Marrón J, Marcos A, Pulgar JA. (1988) A thin-skinned tectonic model for an arcuate fold and thrust belt: The Cantabrian Zone (Variscan Ibero-Armorican Arc). Tectonics 7:517–537. https://doi.org/10.1029/tc007i003p00517

Pérez-Estaún A, Martínez Catalán JR, Bastida F (1991) Crustal thickening and deformation sequence in the footwall to the suture of the Variscan belt of northwest Spain. Tectonophysics191:243–253

Pharaoh TC, Winchester JA, Verniers J, Lassen A, Seghedi A (2006) The Western Accretionary Margin of the East European Craton: an overview. In: Gee, DG, Stephenson, RA (eds), European Lithosphere Dynamics. Geological Society of London Memoir 32:291–311

Piçarra JM (1998) First Devonian graptolites from Portugal.In: Gutiérrez-Marco JC, RábanoI (eds) Proceedings 6th International GraptoliteConference (GWG-IPA) & 1998 Field Meeting, IUGS Subcomission on Silurian Stratigraphy. Temas Geológico-Mineros ITGE, 23: 242–243

Pin C, Liñán E, Pascual E, Donaire T, Valenzuela A (2002) Late Neoproterozoic crustal growth in the European variscides: Nd isotope and geochemical evidence from the Sierra de Córdoba Andesites (Ossa-Morena Zone, Southern Spain). Tectonophysics 352:133–151

Pin C, Fonseca P, Paquette JL, Castro P, Matte Ph (2008) The ca. 350 Ma Beja Igneous Complex: A record of transcurrent slab break-off in the southern Iberia Variscan Belt? Tectonophysics 461:356–377. https://doi.org/10.1016/j.tecto.2008.06.001

Piqué A (1981) Northwestern Africa and the Avalonian plate. Relations during late Precambrian and late Paleozoic time. Geology 9:319–322

Piqué A (1994) Géologie du Maroc. Editions PUMAG, Marrakech, 284 p.

Plissart G, Monnier C, Diot H, Maruntiu M, Berger J, Triantafyllou A (2017) Petrology, geochemistry and Sm-Nd analyses on the Balkan-Carpathian Ophiolite (BCO-Romania, Serbia, Bulgaria): Remnants of a Devonian back-arc basin in the easternmost part of the Variscan domain. Journal of Geodynamics 105:27–50. https://doi.org/10.1016/j.jog.2017.01.001

Pollock JC, Hibbard JP, Sylvester PJ (2009) Early Ordovician rifting of Avalonia and birth of the Rheic Ocean: U-Pb detrital zircon constraints from Newfoundland. Journal of the Geological Society, London 166:501–515. https://doi.org/10.1144/0016-76492008-088

Ponce C, Simancas JF, Azor A, Martínez Poyatos D, Booth-Rea G, Expósito I (2012) Metamorphism and kinematics of the eary deformation in the Variscan suture of SW Iberia. Journal of Metamorphic Geology 30:625–638. https://doi.org/10.1111/j.1525-1314.2012.00988.x

Puga E, Díaz de Federico A (1976) Metamorfismo polifásico y deformaciones alpinas en el Complejo de Sierra Nevada (Cordilleras Béticas). Implicaciones geodinámicas. In: Reunión sobre la Geodinámica de la Cordillera Bética y del Mar de Alborán, Secretariado de Publicaciones Universidad de Granada 79–114

Puga E, Díaz de Federico A, Nieto JM (2002) Tectonostratigraphic subdivision and petrological characterization of the deepest complexes of the Betic Zone: a review. Geodinamica Acta 15:23–43

Quesada C (1991) Geological constraints on the Paleozoic tectonic evolution of tectonostratigraphic terranes in the Iberian Massif. Tectonophysics 185:225–245

Quesada C (1997) Evolución geodinámica de la Zona Ossa Morena durante el ciclo Cadomiense. In: Araújo AA, Pereira MF (eds.), Estudo sobre a geología da zona de Ossa Morena (Maciço Ibérico). Livro homenagem Prof. Francisco Gonçalves, University of Évora, 205–230

Quesada C (2017) Early Paleozoic evolution of Gondwanan units in the Iberian Massif: from subduction through rifting and drift on the southern passive margin of the Rheic Ocean. In: Álvaro JJ, Casas JM, Clausen S (eds) Géologie de la France 1:29–30

Quesada C, Dallmeyer RD (1994) Tectonothermal evolution of the Badajoz-Córdoba shear zone (SW Iberia): characteristics and 40Ar/39Ar mineral age constrains. Tectonophysics 231:195–213

Quesada C, Fonseca PE, Munhá J, Oliveira JT, Ribeiro A (1994) The Beja-Acebuches Ophiolite (Southern Iberia Variscan fold belt): geological characterization and geodynamic significance. Boletín Geológio y Minero 105:3–49

Ribeiro A, Quesada C, Dallmeyer RD (1990) Geodynamic evolution of the Iberian Massif. In: Dallmeyer RD, Martínez García E (eds), Pre-Mesozoic Geology of Iberia. Springer, Berlin, 399–410.

Ribeiro A, Dias R, Silva B (1995) Genesis of the Ibero-Armorican arc. Geodinamica Acta 8:173–184

Ribeiro A, Pereira E, Ribeiro ML, Castro P (2006) Unidades Alóctones da regiao de Morais (Trás-Os-Montes oriental). In: Dias R, Araújo A, Terrinha P, Kullberg JC (eds), Geologia de Portugal no contexto da Ibéria, Univ. Évora, 85–105

Ribeiro A, Munhá J, Dias R, Mateus A, Pereira E, Ribeiro L, Fonseca P, Araújo A, Oliveira T, Romao J, Chaminé H, Coke C, Pedro J (2007) Geodynamic evolution of the SW Europe Variscides. Tectonics 26:TC6009. https://doi.org/10.1029/2006tc002058

Ribeiro A, Munhá J, Fonseca P, Araújo A, Pedro JC, Mateus A, Tassinari C, Machado G, Jesus A (2010) Variscan ophiolite belts in the Ossa-Morena Zone (Southwest Iberia): Geological characterization and geodynamic significance. Gondwana Research 17:408–421. https://doi.org/10.1016/j.gr.2009.09.005

Robardet M (2002) Alternative approach to the Variscan Belt in southwestern Europe: Preorogenic paleobiogeographical constraints. In: Martínez Catalán JR, Hatcher RD Jr, Arenas R, Díaz García F (eds), Variscan-Appalachian dynamics: The building of the late Paleozoic basement: Boulder, Colorado, Geological Society of America Special Paper 364:1–15

Robardet M (2003) The Armorica "microplate": fact or fiction? Critical review of the concept and contradictory palaeobiogeographical data. Palaeogeography, Palaeoclimatology, Palaeoecology 195:125–148

Robardet M, Gutiérrez-Marco JC (2002) Silurian. In: Gibbons W, Moreno MT (eds), The Geology of Spain. Geological Society, London, 51–66

Rodríguez-Alonso MD, Díez Balda MA, Perejón A, Pieren A, Liñán E, López Díaz F, Moreno F, Gámez Vintaned JA, González Lodeiro F, Martínez Poyatos D, Vegas R (2004a). Zona Centroibérica. Estratigrafía. In: Vera, JA (ed), Geología de España, SGE-IGME, Madrid, 78–81

Rodríguez-Alonso MD, Peinado M, López-Plaza M, Franco P, Carnicero A, Gonzalo JC (2004b) Neoproterozoic-Cambrian synsedimentary magmatism in the Central Iberian Zone (Spain): geology, petrology and geodynamic significance. International Journal of Earth Sciences (Geol Rundsch) 93:897–920. https://doi.org/10.1007/s00531-004-0425-4

Rodríguez-Cañero R, Martín-Algarra A (2014) Frasnian–Famennian crisis in the Malaguide Complex (Betic Cordillera, Spain). Terra Nova 26:38–54. https://doi.org/10.1111/ter.12068

Rodríguez-Cañero R, Jabaloy A, Navas-Parejo P, Martín Algarra A (2017) Lower Bashkirian conodonts from the Nevado-Filábride complex (Betic Cordilleras, Spain): tectonic and palaeogeographic implications. Geophysical Research Abstracts 19, EGU2017–13925

Roger F, Matte Ph (2005) Early Variscan HP metamorphism in the western Iberian Allochthon—A 390 Ma U-Pb age for the Bragança eclogite (NW Portugal). International Journal of Earth Sciences (Geol Rundsch) 94:173–179. https://doi.org/10.1007/s00531-005-0466-3

Rosas FM, Marques FO, Ballèvre M, Tassinari C (2008) Geodynamic evolution of the SW Variscides: Orogenic collapse shown by new tectonometamorphic and isotopic data from western Ossa-Morena Zone, SW Iberia. Tectonics 27:TC6008. https://doi.org/10.1029/2008tc002333

Rossi Ph, Oggiano G, Cocherie A (2009) A restored section of the "southern Variscan realm" across the Corsica-Sardinia microcontinent. Comptes Rendus Geoscience 341:224–238. https://doi.org/10.1016/j.crte.2008.12.005

Rottura A, Bargossi GM, Caggianelli A, Del Moro A, Visona D, Tranne CA (1998) Origin and significance of the Permian high-K calc-alkaline magmatism in the central-eastern Southern Alps, Italy. Lithos 45:329–348

Rubio Pascual FJ, Arenas R, Martínez Catalán JR, Rodríguez Fernández LR, Wijbrans JR (2013a) Thickening and exhumation of the Variscan roots in the Iberian Central System: Tectonothermal processes and $^{40}Ar/^{39}Ar$ ages. Tectonophysics 587:207–221. https://doi.org/10.1016/j.tecto.2012.10.005

Rubio Pascual FJ, Mata J, Martín Parra LM (2013b) High-pressure metamorphism in the Early Variscan subduction complex of the SW Iberian Massif. Tectonophysics 592:187–199. https://doi.org/10.1016/j.tecto.2013.02.022

Rubio Pascual FJ, López-Carmona A, Arenas R (2016) Thickening versus extension in the Variscan belt: P–T modelling in the Central Iberian autochthon. Tectonophysics 681:144–158. https://doi.org/10.1016/j.tecto.2016.02.033

Salman K (2004) The timing of the Cadomian and Variscan cycles in the Ossa-Morena Zone, SW Iberia: granitic magmatism from subduction to extension. Journal of Iberian Geology 30:119–132

San José MA, Herranz P, Pieren AP (2004) A review of the Ossa-Morena Zone and its limits. Implications for the definition of the Lusitan-Marianic Zone. Journal of Iberian Geology 30:7–22

Sánchez Carretero R, Eguiluz L, Pascual E, Carracedo M (1990) Igneous Rocks. In: Dallmeyer RD, Martínez García E (eds), Pre-Mesozoic Geology of Iberia. Springer, Berlin, 292–312

Sánchez Lorda ME, Sarrionandia F, Ábalos B, Carracedo M, Eguíluz L, Gil Ibarguchi JL (2014) Geochemistry and paleotectonic setting of Ediacaran metabasites from the Ossa-Morena Zone (SW Iberia).

International Journal of Earth Sciences 103:1263–1286. https://doi.org/10.1007/s00531-013-0937-x

Sánchez Lorda ME, Ábalos B, García de Madinabeitia S, Eguíluz L, Gil Ibarguchi JI, Paquette JL (2016) Radiometric discrimination of pre-Variscan amphibolites in the Ediacaran Serie Negra (Ossa-Morena Zone, SW Iberia). Tectonophysics 681:31–45. https://doi.org/10.1016/j.tecto.2015.09.020

Sánchez-García MT, Bellido F, Quesada C (2003) Geodynamic setting and geochemical signatures of Cambrian-Ordovician rift-related igneous rocks (Ossa-Morena Zone, SW Iberia). Tectonophysics 365:233–255

Sánchez-García T, Bellido F, Pereira MF, Chichorro M, Quesada C, Pin Ch, Silva JB. (2010) Rift-related volcanism predating the birth of the Rheic Ocean (Ossa-Morena zone, SW Iberia). Gondwana Research 17:392–407

Sánchez-García MT, Pereira MF, Bellido F, Chichorro M, Silva JB, Valverde-Vaquero P, Pin Ch, Solá AR (2014) Early Cambrian granitoids of North Gondwana margin in the transition from a convergent setting to intra-continental rifting (Ossa-Morena Zone, SW Iberia). International journal of Earth Sciences (Geol Rundsch) 103:1203.1218. https://doi.org/10.1007/s00531-013-0939-8

Sanchez-Navas A, García-Casco A, Martín-Algarra A (2014) Pre-Alpine discordant granitic dikes in the metamorphic core of the Betic Cordillera: tectonic implications. Terra Nova 26:477–486. https://doi.org/10.1111/ter.12123

Sarrionandía F, Carracedo Sánchez M, Eguiluz L, Ábalos B, Rodriguez J, Pin C, Gil Ibarguchi JI (2012) Cambrian rift-related magmatism in the Ossa-Morena Zone (Iberian Massif): Geochemical and geophysical evidence of Gondwana break-up. Tectonophysics 570–571:135-150. https://doi.org/10.1016/j.tecto.2012.07.023

Scotese CR (2004) A continental drift flipbook. Journal of Geology 112:729–741

Seyferth M, Henk A (2004) Syn-convergent exhumation and lateral extrusion in continental collision zones—insights from three-dimensional numerical models. Tectonophysics 382:1–29. https://doi.org/10.1016/j.tecto.2003.12.004

Shail RK, Leveridge BE (2009) The Rhenohercynian passive margin of SW England: Development, inversion and extensional reactivation. Comptes Rendus Geoscience 341:140–155. https://doi.org/10.1016/j.crte.2008.11.002

Shaw J, Johnston ST (2016) Oroclinal buckling of the Armorican ribbon continent: An alternative tectonic model for Pangean amalgamation and Variscan orogenesis. Lithosphere 8:769–777. https://doi.org/10.1130/L559.1

Shaw J, Johnston ST, Gutiérrez-Alonso G, Weil AB (2012) Oroclines of the Variscan orogen of Iberia: Paleocurrent analysis and paleogeographic implications. Earth and Planetary Science Letters 329–330:60-70. https://doi.org/10.1016/j.epsl.2012.02.014

Sierra S, Moreno C (2004) Cuenca Pérmica del Viar. In: Vera JA (ed), Geología de España. SGE-IGME, Madrid, 214–215

Silva JB, Pereira MF (2004) Transcurrent continental tectonics model for the Ossa-Morena Zone Neoproterozoic-Paleozoic evolution, SW Iberian Massif, Portugal. International Journal of Earth Sciences (Geol Rundsch) 93:886–896. https://doi.org/10.1007/s00531-004-0424-5

Silva JB, Oliveira JT, Ribeiro A (1990) The South Portuguese Zone. Structural Outline. In: Dallmeyer RD, Martínez E (eds), Pre-Mesozoic Geology of Iberia. Springer, Berlin, 334–362

Simancas JF (1993) Extension related to slight changes in plate kinematics: the tectonic evolution of the SW corner of the Hercynian orogen in the Iberian Peninsula. In: Late Orogenic Extension in Mountain Belts, Document du BRGM 219:180–181

Simancas JF, Martínez Poyatos DJ, Expósito I, Azor A, González Lodeiro F (2001) The structure of a major suture zone in the SW Iberian Massif: the Ossa Morena/Central Iberian contact. Tectonophysics 332:295–308

Simancas JF, González Lodeiro F, Expósito I, Azor A, Martínez Poyatos D (2002) Opposite subduction polarities connected by transform faults in the Iberian Massif and western European Variscides. In: Martínez Catalán JR, Hatcher RD Jr, Arenas R, Díaz García F (eds), Variscan-Appalachian dynamics: The building of the late Paleozoic basement: Boulder, Colorado, Geological Society of America Special Paper 364:253–262

Simancas JF, Carbonell R, González Lodeiro F, Pérez-Estaún A, Juhlin C, Ayarza P, Kashubin A, Azor A, Martínez Poyatos D, Almodóvar GR, Pascual E, Sáez R, Expósito I (2003) The crustal structure of the transpressionalVariscan Orogen of SW Iberia: The IBERSEIS deep seismic reflection profile. Tectonics 22(6), 1062. https://doi.org/10.1029/2002tc001479

Simancas JF, Expósito I, Azor A, Martínez Poyatos D, González Lodeiro F (2004) From the Cadomian orogenesis to the Early Palaeozoic Variscan rifting in Southwest Iberia. Journal of Iberian Geology 30:53–71.

Simancas JF, Tahiri A, Azor A, González Lodeiro F, Martínez Poyatos D, El Hadi H (2005) The tectonic frame of the Variscan-Alleghanian Orogen in Southern Europe and Northern Africa. Tectonophysics 398:181–198. https://doi.org/10.1016/j.tecto.2005.02.006

Simancas JF, Carbonell R, González Lodeiro F, Pérez Estaún A, Juhlin C, Ayarza P, Kashubin A, Azor A, Martínez Poyatos D, Sáez R, Almodóvar GR, Pascual E, Flecha I, Martí D (2006) Transpressional collision tectonics and mantle plume dynamics: the Variscides of southwestern Iberia. In: Gee DG, Stephenson RA (eds), European Lithosphere Dynamics. Geological Society, London, Memoirs, 32:345–354

Simancas JF, Azor A, Martínez Poyatos D, Tahiri A, El Hadi H, González Lodeiro F, Pérez-Estaún A, Carbonell R (2009) Tectonic relationships of Southwest Iberia with the allochthons of Northwest Iberia and the Moroccan Variscides. Comptes Rendus Geoscience 341:103–113. https://doi.org/10.1016/j.crte.2008.11.003

Simancas JF, Ayarza P, Azor A, Carbonell R, Martínez Poyatos D, Pérez-Estaún A, González Lodeiro F (2013) A seismic geotraverse across the Iberian Variscides: Orogenic shortening, collisional magmatism and orocline development. Tectonics 32:1–16. https://doi.org/10.1002/tect.20035

Simancas JF, Azor A, Martínez Poyatos D, Expósito I, Pérez-Cáceres I, González Lodeiro F (2016) Comment on "The Late Devonian Variscan suture of the Iberian Massif: A correlation of high-pressure belts in NW and SW Iberia. Tectonophysics 654:96–100 by R. Fernández and R. Arenas. Tectonophysics 666:281-284. https://doi.org/10.1016/j.tecto.2015.07.040.

Sláma J, Dunkley DJ, Kachlík V, Kusiak Ma (2008) Transition from island-artc to passive setting on the continental margin of Gondwana: U-Pb zircon dating of Neoproterozoicmetaconglomerates from the SE margin of the Tepla-Barrandian Unit, Bohemian Massif. Tectonophysics 461:44–59. https://doi.org/10.1016/j.tecto.2008.03.005

Stampfli GM, Hochard C, Vérard C, Wilhem C, vonRaumer J (2013) The formation of Pangea. Tectonophysics 593:1–19. https://doi.org/10.1016/j.tecto.2013.02.037

Tait J, Schätz M, Bachtadse V, Soffel H (2000) Palaeomagnetism and Palaeozoic palaeogeography of Gondwana and European terranes. In: Franke W, Haak V, Oncken O, Tanner D (eds), Orogenic Processes: Quantification and Modelling in the Variscan Belt. Geological Society, London, Special Publication 179:21–30

Talavera C, Martínez Poyatos D, González Lodeiro F (2015) SHRIMP U-Pb geochronological constraints on the timing of the intra-Alcudian (Cadomian) angular unconformity in the Central Iberian Zone (Iberian Massif, Spain). International Journal of Earth

Sciences (Geol Rundsch) 104:1575–1739. https://doi.org/10.1007/s00531-015-1171-5

Tendero JA, Martín-Algarra A, Puga E, Díaz de Federico A (1993) Lithostragraphy des métasediments de l'association ophiolitique Nevado-Filabride (SE Espagne) et mise en evidence d'objects ankéritiques évocant des foraminifères planctoniques du Crétacé: consequènces paléogeographiques. Comptes Rendus Académie des Sciences Paris 316:1115–1122

Torsvik TH, Cocks LRM (2013) Gondwana from top to base in space and time. Gondwana Research 24:999–1030. https://doi.org/10.1016/j.gr.2013.06.012

Valenzuela A, Donaire, T, Pin C, Toscano M, Hamilton MA, Pascual E (2011) Geochemistry and U-Pb dating of felsic volcanic rocks in the Riotinto-Nerva unit, Iberian Pyrite Belt, Spain: crustal thinning, progressive melting and massive sulphide genesis. Journal of the Geological Society, London, 168:717–731. https://doi.org/10.1144/0016-76492010-081

Valladares MI, Barba P, Ugidos JM (2002) Precambrian. In: Gibbons W, Moreno MT (eds), The Geology of Spain. Geological Society, London, 7–16

Van der Voo R (1993) Paleomagnetism of the Atlantic, Tethys and Iapetus Oceans. Cambridge University Press, Cambridge, 411 p.

Van der Voo R, Stamatakos JA, Parés JM (1997) Kinematic constraints on thrust- belt curvature from syndeformational magnetizations in the Lagos del Valle Syncline in the Cantabrian arc, Spain. Journal of Geophysical Research 102:10105–10120

Villaseca C, Barbero, L, Rogers G (1998) Crustal origin of Hercynian peraluminous granitic batholiths of Central Spain: petrological, geochemical and isotopic (Sr, Nd) constraints. Lithos, 43:55–79

Villaseca C, Orejana D, Belousova EA (2012) Recycled metaigneous crustal sources for S- and I-type Variscan granitoids from the Spanish Central System batholith: Constraints from Hf isotope zircon composition. Lithos 153:84–93. https://doi.org/10.1016/j.lithos.2012.03.024

Villaseca C, Merino E, Oyarzun R, Orejana D, Pérez-Soba C, Chicharro E (2014) Contrasting chemical and isotopic signatures from Neoproterozoic metasedimentary rocks in the Central Iberian Zone (Spain) of pre-Variscan Europe: Implications for terrane analysis and Early Ordovician magmatic belts. Precambrian Research 245:131–145

Villaseca C, Castiñeiras P, Orejana D (2015) Early Ordovician metabasites from the Spanish Central System: A remnant of intraplate HP rocks in the Central Iberian Zone. Gondwana Research 27:392–409. https://doi.org/10.1016/j.gr.2013.10.007

Villaseca C, Merino Martínez E, Orejana D, Andersen T, Belousova EA (2016) Zircon Hf signatures from granitic orthogneisses of the Spanish Central System: Significance and sources of the Cambro-Ordovician magmatism in the Iberian Variscan Belt. Gondwana Research 34:60–83. https://doi.org/10.1016/j.gr.2016.03.004

von Raumer JF, Bussy F, Stampfli GM (2009) The Variscan evolutionin the External massifs of the Alps and place in their Variscan framework. Comptes Rendus Geoscience 341:239–252. https://doi.org/10.1016/j.crte.2008.11.007

Wagner RH, Lemos de Sousa MJ, Gomes da Silva S (1983) Stratigraphy and fossil flora of the Upper Stepahnian C of Buçaco, north of Coimbra (Portugal). In: Lemos de Sousa M.J (ed.) Contributions to the Carboniferous Geology and Palaeontology of the Iberian Peninsula. Universidade do Porto-Faculdade de Ciencias, 1983, 127–156

Wallis R.J (1983) A lacustrine/deltaic/fluvial/swamp succession from the Stepahanian B of Puertollano, Spain. In: Lemos de Sousa M.J (ed.) Contributions to the Carboniferous Geology and Palaeontology of the Iberian Peninsula. Universidade do Porto-Faculdade de Ciencias, 1983, 51–67

Weil AB, Van der Voo, R, van der Pluijm BA, Parés JM (2000) The formation of an orocline by multiphase deformation: a paleomagnetic investigation of the Cantabria-Asturias Arc (northern Spain). Journal of Structural Geology 22:735–756. https://doi.org/10.1016/s0191-8141(99)00188-1

Weil AB, Van der Voo R, van der Pluijm BA (2001) Oroclinal bending and evidence against the Pangea megashear: The Cantabria-Asturias arc (northern Spain). Geology 29:991–994.

Weil AB, Gutiérrez-Alonso G, Johnston ST, Pastor-Galán D (2013) Kinematic constraints on buckling a lithospheric-scale orocline along the northern margin of Gondwana: A geologic synthesis. Tectonophysics 582:25–49. https://doi.org/10.1016/j.tecto.2012.10.006

Wernert P, Schulmann K, Chopin F, Stípská P, Bosch D, El Houicha M (2016) Tectonometamorphic evolution of an intracontinental orogeny inferred from P-T-t-d paths of the metapelites from the Rehamna massif (Morocco). Journal of metamorphic Geology 34:917–940. https://doi.org/10.1111/jmg.12214

Wilson JT (1969) Static or Mobile Earth: the current scientific revolution. Amer. Philos. Soc. Proc. 112:309–320

Wilson M, Neumann ER, Davies GR, Timmerman MJ, Heeremans M, Larsen BT (2004) Permo-Carboniferous magmatism and rifting in Europe: introduction. Geological Society, London, Special Publications 223:1–10. https://doi.org/10.1144/gsl.sp.2004.223.01.01

Winchester JA, Pharaoh TC, Verniers J, Ioane D, Seghedi A (2006) Palaeozoic accretion of Gondwana-derived terranes to the East European Craton: recognition of detached terrane fragments dispersed after collision with promontories. In: Gee, DG, Stephenson, RA (eds), European Lithosphere Dynamics. Geological Society of London Memoir 32:323–332

Zeck HP, Whitehouse MJ (1999) Hercynian, Pan-African, Proterozoic and Archean ion-microprobe zircon ages for a Betic-Rif core complex, Alpine belt, W Mediterranean—consequences for its *P-T-t* path. Contributions to Mineralogy and Petrology 134:134–149

Zeck HP, Whitehouse MJ (2002) Repeated age resetting in zircons from Hercynian-Alpine polymetamorphic schists (Betic-Rif tectonic belt, S. Spain)—a U-Th-Pb ion microprobe study. Chemical

The Cambrian-Early Ordovician Rift Stage in the Gondwanan Units of the Iberian Massif

2

T. Sánchez-García, M. Chichorro, A. R. Solá, J. J. Álvaro, A. Díez-Montes, F. Bellido, M. L. Ribeiro, C. Quesada, J. C. Lopes, Í. Dias da Silva, E. González-Clavijo, J. Gómez Barreiro, and A. López-Carmona

Abstract

A rifting stage initiated the Variscan cycle in NW Gondwana, lasted from Terreneuvian to Early Ordovician times and culminated in opening of the Rheic Ocean. The result of lithospheric stretching was the development of a horst-and-graben structure in the upper crust and formation of basins with sharp variations in thickness and facies of the sedimentary infill. Emplacement of large volumes of igneous rocks, both plutonic and volcanic, accompanied this stage in three different intervals: (i) Early Igneous Event (Terreneuvian), exclusively composed of felsic peraluminous rocks associated with the formation of core complexes in the mid-upper crust; (ii) Main Igneous Event (Cambrian Series 2 to Furongian), displaying bimodal character; and iii) Late Event (Tremadocian-Floian), with mixed characteristics of the other two events and abundant peralkaline rocks. The rifting axis was initially located close to the Cadomian suture that fringed the Ossa Morena Zone. For about 60 m.y. the rifting processes initially propagated "zip-like" along the axis and then widened cratonward to affect inner parts of Gondwana, such as the Central Iberian Zone. The rift/drift transition was diachronous, starting in Iberia (Ossa Morena Zone) in the Furongian.

Coordinator: T. Sánchez-García.

T. Sánchez-García (✉) · F. Bellido · C. Quesada
Instituto Geológico y Minero de España (IGME), Ríos Rosas 23, 28003 Madrid, Spain
e-mail: t.sanchez@igme.es

F. Bellido
e-mail: ffbbmm50@gmail.com

C. Quesada
e-mail: quesada.cecilio@gmail.com

M. Chichorro
Department of Earth Sciences, Faculty of Science and Technology, New University of Lisbon, Campus de Caparica, Quinta da Torre, 2829-516 Caparica, Portugal
e-mail: ma.chichorro@fct.unl.pt

A. R. Solá · M. L. Ribeiro
Laboratório Nacional de Energia e Geologia (LNEG), Estrada da Portela, Bairro do Zambujal, Apartado 7586-Alfragide, 2610-999 Amadora, Portugal
e-mail: rita.sola@lneg.pt

M. L. Ribeiro
e-mail: luisacarvalhoduarte@gmail.com

J. J. Álvaro
Instituto de Geociencias (IGEO-CSIC), Dr. Severo Ochoa 7, 28040 Madrid, Spain
e-mail: jj.alvaro@csic.es

A. Díez-Montes · E. González-Clavijo
Instituto Geológico y Minero de España (IGME), C/Azafranal 48, 37001 Salamanca, Spain
e-mail: al.diez@igme.es

E. González-Clavijo
e-mail: e.clavijo@igme.es

C. Quesada
Facultad de Ciencias Geológicas, Universidad Complutense, 28040 Madrid, Spain

J. C. Lopes
Departamento de Geociências, Universidade de Évora, Largo dos Colegiais 2, 7000 Évora, Portugal
e-mail: carrilho@uevora.pt

Í. Dias da Siva
Faculty of Science, Instituto Dom Luiz, University of Lisbon, Campo Grande, Edifício C8, Piso 3, 1749-016 Lisbon, Portugal
e-mail: ipicaparopo@gmail.com

J. Gómez Barreiro · A. López-Carmona
Department of Geology, University of Salamanca, Plaza de la Merced s/n, 37008 Salamanca, Spain
e-mail: jugb@usal.es

A. López-Carmona
e-mail: alioli@usal.es

C. Quesada and J. T. Oliveira (eds.), *The Geology of Iberia: A Geodynamic Approach*, Regional Geology Reviews,
https://doi.org/10.1007/978-3-030-10519-8_2

2.1 Introduction

The initial rifting stage of the Variscan cycle recorded in the Iberian margin of Gondwana started in the Terreneuvian, immediately after cessation of the Cadomian orogeny. Its effects are variably recorded in the Iberian Massif as well as in other peri-Gondwanan units exposed in the Iberian Peninsula (e.g. see in this volume Chap. 8. *Paleozoic Basement of the Pyrenees*). In tectonic terms, this stage was characterized by a significant lithospheric stretching, which resulted in the development of a horst-and-graben structure in the upper crust and consequent sharp variations in thickness and facies of the coeval sedimentary fill. Graben and half-graben structures were the site of tectonically enhanced subsidence and accumulation space availability (reaching sedimentary thicknesses of several thousands of metres) associated with the record of thick volcano sedimentary units neighbouring the fault-boundaries of horst structures.

Differentiation of Variscan tectonostratigraphic zones in the Iberian Massif is largely reminiscent of this rifting framework. The rifting axis was located close to the Cadomian suture (Murphy et al. 2006), as indicated by enhanced compartmentalization and massive rift-type volcanic activity recorded in the Iberian Massif during Cambrian and Early Ordovician times. Throughout this time span (about 60 m.y.) the area affected by stretching processes widened from the initially axial, Ossa-Morena Zone (Quesada 1991; Sánchez-García et al. 2003, 2008a, 2010) to innermost parts of West Gondwana (collectively called Cantabro-Iberian Basin; Pérez-Estaún et al. 1990; Martínez Catalán et al. 1992; Díaz-García 2002; Valverde-Vaquero et al. 2005; Díez-Montes 2006; Murphy et al. 2008; Álvaro et al. 2013a), and progressively affected the Central-Iberian, West Asturian-Leonese and Cantabrian zones and laterally equivalent inliers (e.g. the Sierra de la Demanda and the Iberian and Hesperian Chains, NE Spain; Fig. 2.1). This "inward" migration of rifting towards progressively

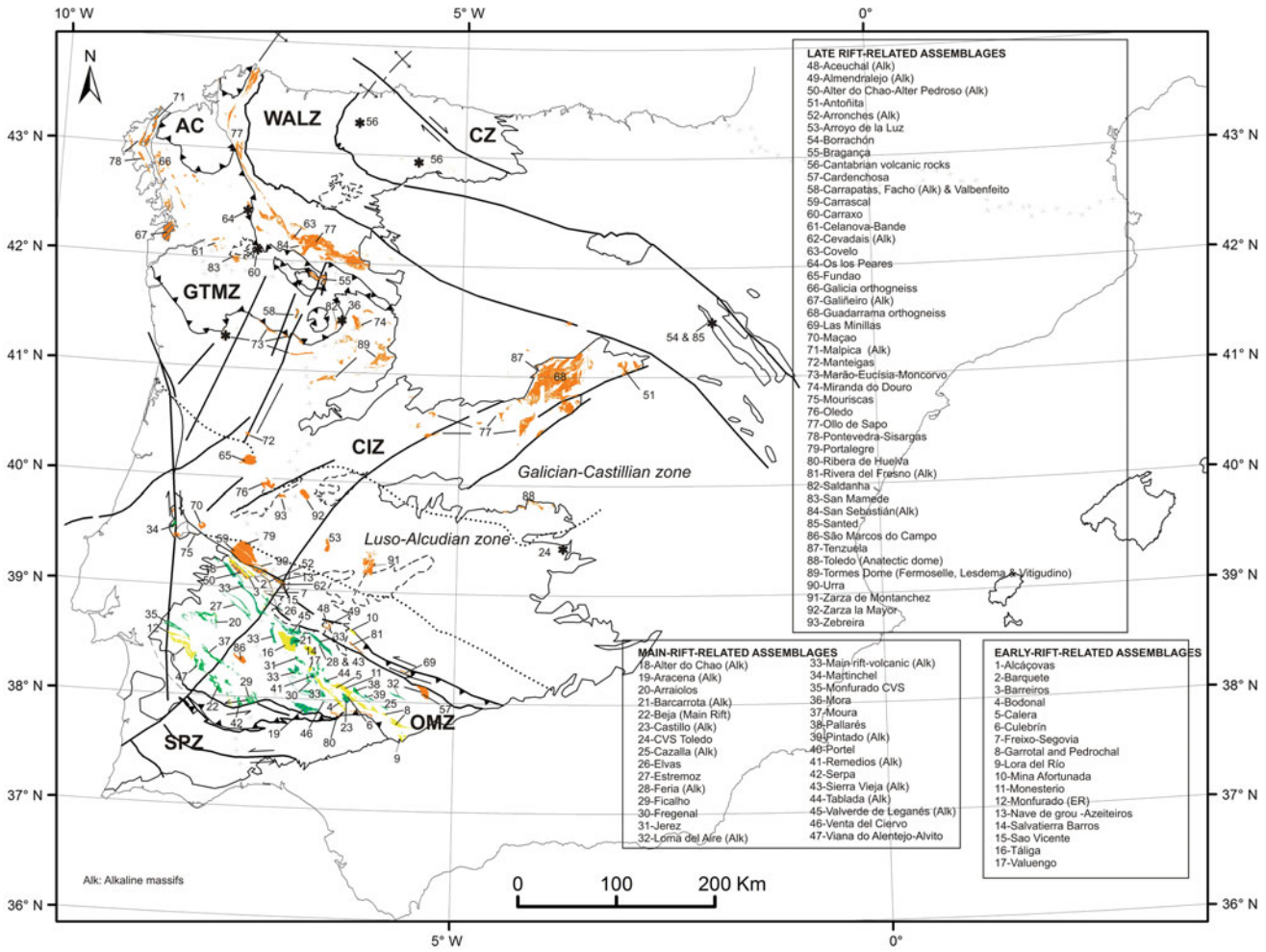

Fig. 2.1 Rift-related outcrops in the Iberian Massif. Zone boundaries modified after Julivert et al. (1974), Quesada (1991) and Martínez-Catalán et al. (2014). Dotted lines mark the boundaries of the previous division of the Central Iberian Zone by Lotze (1945)

innermost parts of the Gondwanan continent was preceded by an initial stage of "zip-style" along-margin propagation, as recently proposed by Álvaro et al. (2014) to account for the south-to-north migration of rifting from the Moroccan Anti-Atlas to the Ossa-Morena Zone and later to the Armorican and Bohemian massifs.

Lithospheric stretching culminated in continental breakup and opening of a new oceanic tract, pertaining to the Rheic Ocean in the Early Ordovician (Murphy et al. 2006; Pereira et al. 2007, 2012b; Chichorro et al. 2008; Sánchez-García et al. 2003, 2008a, 2010; Linnemann et al. 2008; Nance et al. 2010, 2012; Díez Montes et al. 2010; among others). Relics of the Rheic and some probable remains of marginal oceanic basins are interpreted to occur as exotic ophiolitic units sensu lato in the intermediate allochthons of the Galicia-Trás-os-Montes Zone (see Chap. 5 in this volume), the Ossa-Morena Zone and the Pulo do Lobo Domain of the South-Portuguese Zone (see Chap. 6 in this volume).

In the Iberian Massif, the base of the rifting succession is marked by angular discordances and erosive unconformities capping variably deformed Neoproterozoic-lowermost Terreneuvian rocks of the Cadomian orogen. In contrast, its top is not so clearly established everywhere. In marginal units (i.e. Ossa-Morena and southern Central-Iberian zones) it is marked by a distinct angular discordance, currently named Toledanian unconformity (Gutiérrez-Marco et al. 2002; Aramburu et al. 2004; Quesada 2006; Álvaro et al. 2007, 2018, among other references), previously misinterpreted (Lotze 1956, 1961; Ribeiro et al. 1990a; Quesada 1991) as correlative to the Sardian unconformity in Sardinia, Pyrenees, Montagne Noire or the Alps (Álvaro et al. 2018 and references therein). The Toledanian unconformity separates variably tilted Cambrian-lowermost Ordovician rift-related successions (locally resting directly over Neoproterozoic basement) from an overlying passive-margin succession (see Chap. 3 in this volume). In these units, the rift/drift contact is associated with a variable stratigraphic gap, which at least includes most of the Furongian and the basal Ordovician, although it may locally reach parts of (or even the entire) Cambrian, as is the case in most of the southern Central-Iberian Zone (Liñán et al. 2002; Gutiérrez-Marco et al. 2002 and references therein). This contact has been interpreted as a breakup unconformity recording the onset of spreading in the newly formed Rheic Ocean and drift of the intervening continents (Quesada 1991, 2006).

In the northeastern (paleogeographically proximal) Iberian Massif's units (i.e. northern Central-Iberian, West Asturian-Leonese and Cantabrian zones), the passage from the rifting stage to the passive margin stage is apparently transitional and, despite some local gaps in the Cantabrian Zone (Aramburu et al. 1992; Albani et al. 2006; Palacios 2015), no significant stratigraphic hiatuses exist (Martínez-Poyatos et al. 2004; Álvaro et al. 2007; Shorttle 2008). Irrespective of the interpretation of the geodynamic significance of the Toledanian unconformity, the ubiquity of a prominent Lower Ordovician conglomerate-quartzarenite succession (Armorican Quartzite Formation and lateral equivalents) overstepping across all the peri-Gondwanan units of the Iberian Massif is envisaged as evidence for the establishment of stable platform conditions fringing the newly formed passive Gondwanan margin facing the Rheic Ocean. Noteworthy, similar Lower Ordovician quartzarenite formations occur in other parts of the Variscan Belt in Europe and Northwest Africa (Álvaro et al. 2007; Gasquet et al. 2005; Gutiérrez-Marco et al. 2011 and references therein). In the northern zones of the Iberian Massif, where no gap or angular discordance exist, the rift/drift transition is generally agreed to be located at the base of this distinct overstep succession. As stated for the rift-related processes, propagation of this transition also proceeded from the Ossa-Morena Zone, where the equivalent of this forced transgression related to thermal subsidence after continental breakup is late Furongian (Stage 10) in age (Venta del Ciervo/S. Romão quartzites and conglomerate; Oliveira 1984; López-Guijarro et al. 2007), whereas in the northernmost Iberian Massif's zones the geodynamic equivalent Armorican Quartzite is Floian (former Arenig) in age (Paris et al. 2007; Gutiérrez-Marco et al. 2011 and references therein).

The relatively abrupt change recorded in West Gondwana from Cadomian subduction (latest evidence in Iberia at ca. 533 Ma ago; Murphy et al. 2006; Linnemann et al. 2008; Nance et al. 2008, 2010; Sánchez-García et al. 2003, 2008a, b; Pereira et al. 2006, 2008a, 2011, 2012b) to Cambrian rifting (oldest evidence at ca. 530 Ma ago; Schäfer 1990; Ochsner 1993; Ordóñez-Casado 1998; Bandrés et al. 2002, 2004; Salman 2004; Romeo et al. 2006; Sánchez-García et al. 2008a) remains controversial. Some authors (Nance et al. 2002, 2008, 2010, 2012; Keppie et al. 2003; Murphy et al. 2004) claim that the oblique collision of a mid-ocean ridge with the trench located at the outer margin of West Gondwana (Fig. 2.2) would have progressively transformed the former subduction margin into a transcurrent one. A similar process has been reported in the Cenozoic of western North America that led to transformation of a previous active margin into the San Andreas transcurrent margin, whereas the opening of the Gulf of California and separation of Baja California from mainland Mexico may probably represents an analogue to the opening of the Rheic Ocean (Umhoefer 2011; Nance et al. 2012).

Other authors add to the previous model a component of subduction of the mid-ocean ridge beneath the continental upper plate (Sánchez-García et al. 2003, 2008a, 2010) (Fig. 2.3), analogue to the presently ongoing case of subduction of the East Pacific Rise beneath North America, which is causing the rifting of Baja California (Lizarralde et al. 2007 and references therein). Others, finally, claim that

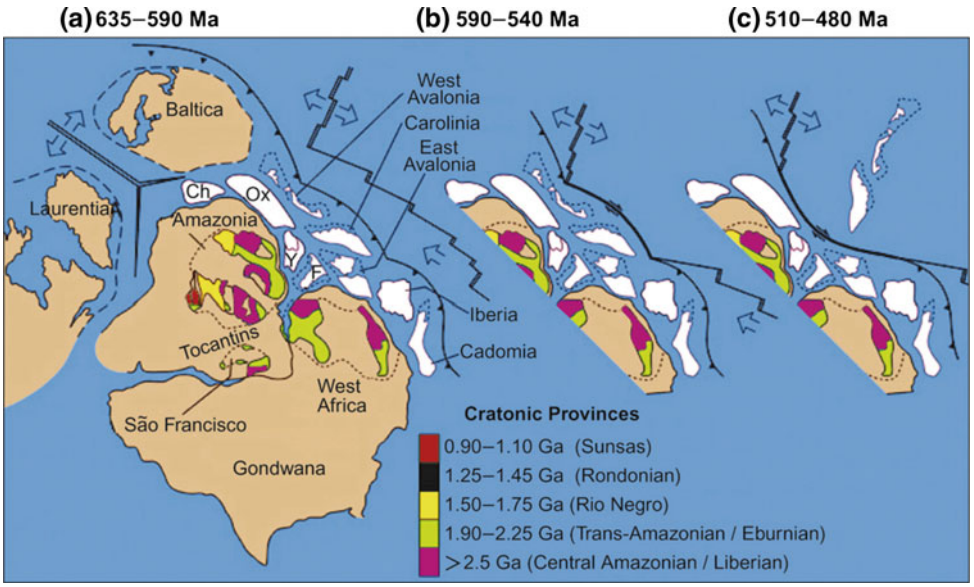

Fig. 2.2 Restoration of Avalonia and related peri-Gondwana terranes relative to the northern margin of Gondwana (from Nance et al. 2002, 2008). **a** Late Neoproterozoic (ca. 635–590 Ma) subduction along the periphery of Gondwana (Ch—Chortis Block, Ox—Oaxaquia, Y—Yucatan Block, F—Florida); **b** latest Neoproterozoic (ca. 590–540 Ma) ridge-trench collision with diachronous termination of subduction and generation of continental transform margin; **c** early Paleozoic (ca. 510–480 Ma) continental rifting and separation of Avalonia and Carolinia from Gondwana with the opening of the Rheic Ocean

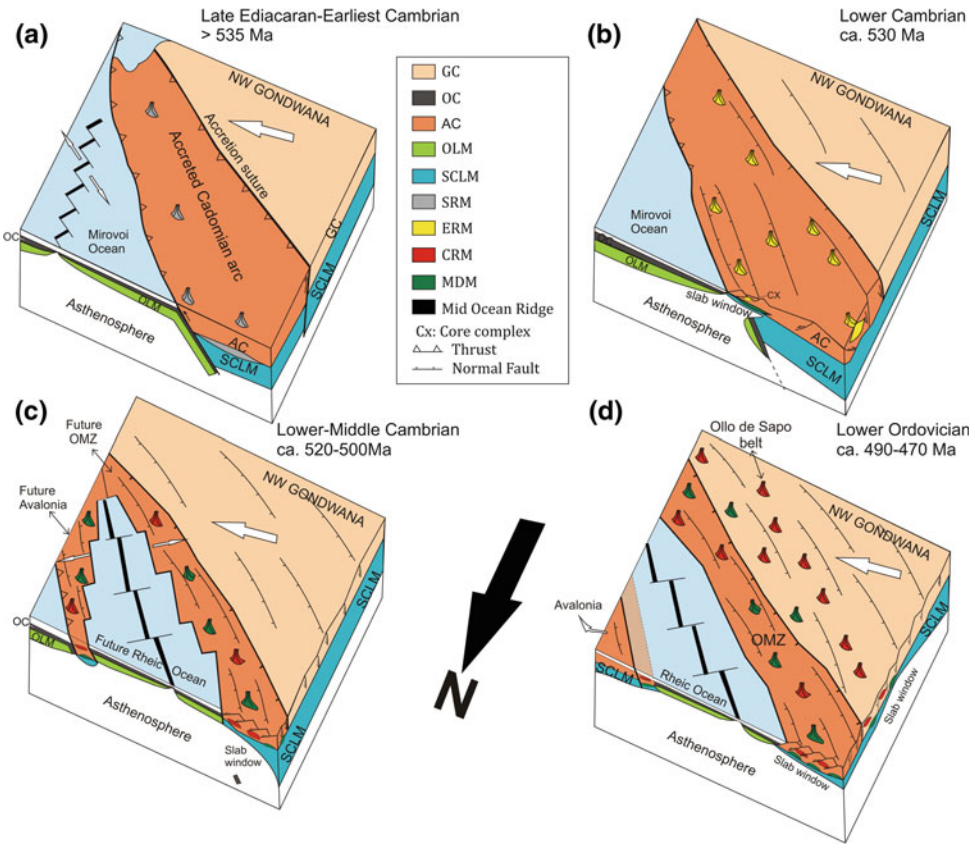

Fig. 2.3 Schematic model to explain the sudden transition from subduction to rifting by a process of ridge-trench collision culminating in ocean opening and terrane capture. **a** Subduction stage; **b** ridge-trench collision/early rifting stage; **c** main rifting stage; **d** late rifting stage. GC: Gondwana crust; OC: Oceanic crust; AC: Arc crust; OLM: Oceanic lithospheric mantle; SCLM: Subcontinental lithospheric mantle; SRM: Subduction-related magmas; ERM: Early-rift-related magmas; CRM: Crustal-derived magmas; MDM: Mantle-derived magmas

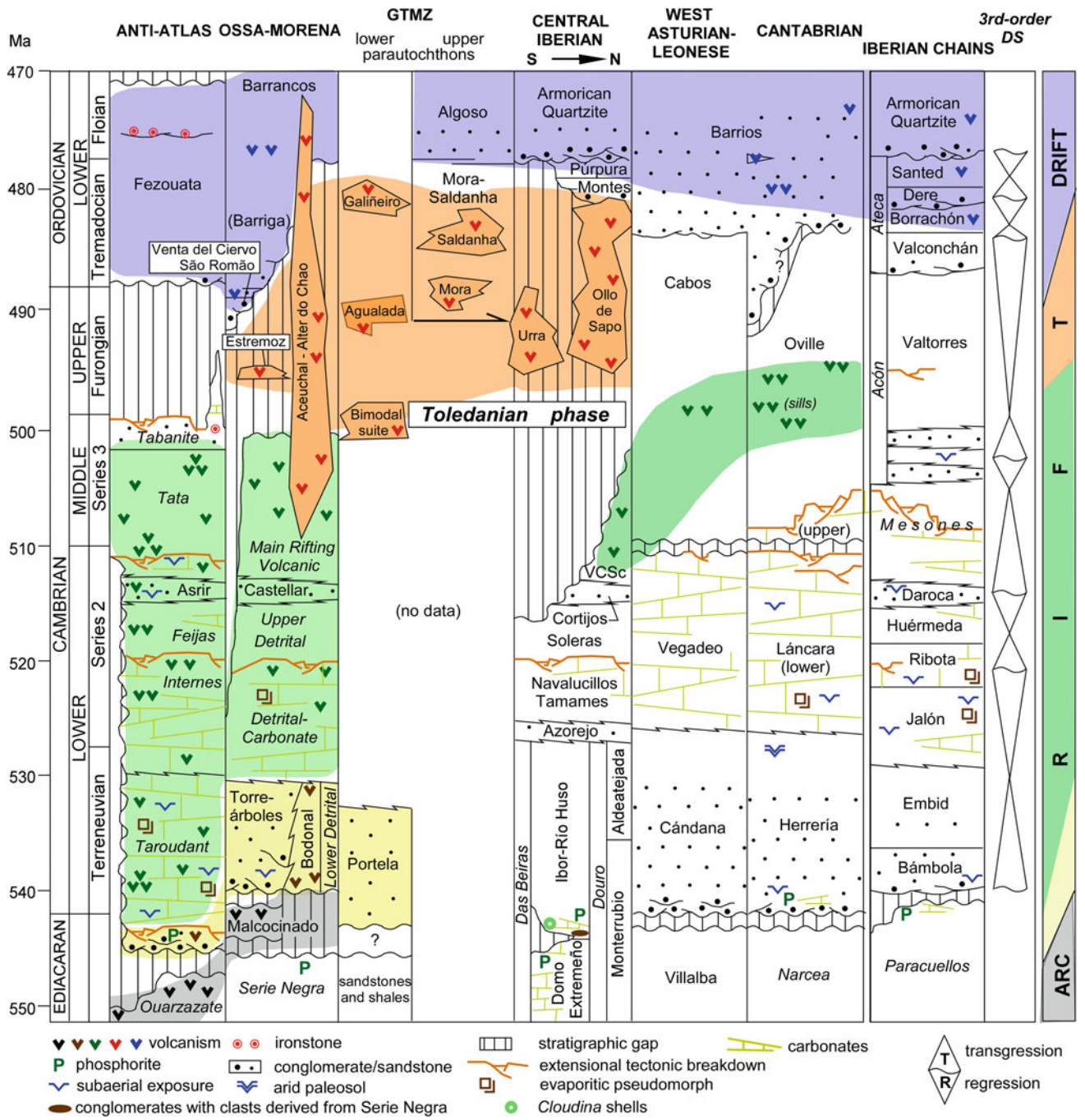

Fig. 2.4 Tectonostratigraphic correlation chart of the rift-related successions in the various zones of the Iberian Massif

a process of slab-pull related to the onset of subduction in the Iapetus and Prototethys oceans may have triggered slab roll-back and back-arc rifting along the previous active margin around West Gondwana (von Raumer et al. 2003; Stampfli et al. 2002; Stampfli and Borel 2004).

Obviously, none of those models are mutually exclusive, and we believe they may have added their effects on one another. Both the onset of extensive or transtensive tectonics and its culmination in opening new oceanic tracts must have been diachronous, as recently documented by Álvaro et al. (2014) for the stepwise propagation of rifting conditions from the (Moroccan) Anti-Atlas Rift to the (Iberian Massif) Ossa-Morena Rift, later propagated to the Pyrenees and the Montagne Noire in southern France (see Fig. 2.4) and eventually into the Bohemian Massif (Murphy et al. 2004, 2006, 2016; Pereira et al. 2006; Martínez Catalán et al. 2007; Álvaro et al. 2007, 2013a, 2014, 2018; Linnemann et al. 2008; Chichorro et al. 2008; Nance et al. 2012; among other

references). Concerning the Iberian margin of West Gondwana, the rifting started in Fortunian times, the transition from subduction therefore being bracketed between a narrow ca. 533–530 Ma gap according to the available age dating (Schäfer 1990; Ochsner 1993; Ordóñez-Casado 1998; Bandrés et al. 2002, 2004; Salman 2004; Romeo et al. 2006; Sánchez-García et al. 2008a, b, 2016).

The first stages of rifting were accompanied by lower crustal anatexis and emplacement of peraluminous calc-alkaline magmas (*Early rift-related igneous event* of Sánchez-García et al. 2003, 2008a, b, 2010) in localized grabens. By late lower Cambrian times, the area submitted to extension widened significantly and covered the entire Ossa Morena Zone coeval to a change in the characteristics of the associated magmatism, then represented by a bimodal association comprising very depleted basaltic melts of tholeiitic affinity and a complex suite of felsic rocks (*Main rift-related igneous event* of Sánchez-García et al. 2003, 2008a, 2010; see also Sarrioanandía et al. 2012, among others). According to the available age data (Sánchez-García et al. 2008a, 2016) this stage lasted up to nearly the Cambrian-Ordovician boundary. The oldest evidence of initiation of breakup and formation of oceanic crust is recorded in the Ossa-Morena at ca. 489 Ma, age of Venta del Ciervo K-bentonite interbedded close to the base of the quartzarenite overstep sequence above the unconformity (López-Guijarro et al. 2007). This important unconformity has been interpreted as evidence for tilting and thermal expansion after the main rifting event, leading to emersion and unroofing of the middle Cambrian sequences and even the Neoproterozoic basement locally (Quesada 1991, 2006). Later on, as it has been stated above, extension started to propagate inward, towards innermore domains of the Gondwanan margin, reaching the Central Iberian, West Asturian-Leonese and even the Cantabrian zones during the Early Ordovician. This propagation was also accompanied by magmatic activity (*Late rift-related igneous event*; Chichorro et al. 2017a, b) with contrasting characteristics depending on the zone. In the Central Iberian Zone it is largely characterized by felsic peraluminous rocks resembling those of the *Early rift-related igneous event* in the Ossa Morena Zone (Ollo de Sapo volcanics, see below) and some alkaline mafic rocks and peralkaline felsic rocks, which are also present in the latter zone although interbedded within the passive margin succession or intruded in basement sequences (Díez-Fernández et al. 2014; and references therein). This temporal and space evolution from tholeiitic to alkaline mafic compositions and related felsic peralkaline rocks points to a decrease of the extension rate and consequently an evidence that rifting was waning (Ribeiro and Mata 1994).

In addition to the active extensive (or transtensive) regime, in overall geodynamic terms the evolution recorded in the Iberian margin during this initial rifting stage of the Variscan cycle was the result of the combined effects of many other processes pertaining to both external (e.g. atmospheric and hydrospheric) and internal (lithospheric and asthenospheric) causes, among which those related to isostasy, eustasy, climate, deformation and igneous activity had a major influence. In order to analyse the respective role of these processes in building the preserved geological record, many of which have mutual feedback effects, special attention is focused below on three main aspects of the geological record, including the structure and the succession of magmatic and paleogeographic events, the latter influenced by the Cambrian poleward migration of West Gondwana crossing subtropical-to-temperate latitudes (Álvaro et al. 2000b, 2007, 2013a). The distribution of rift-related sequences in the Iberian Massif is depicted in Fig. 2.1, and a tectonostratigraphic correlation cartoon of the various zones in the Iberian Massif is shown in Fig. 2.4.

2.2 Rifting Structure in the Iberian Margin of West Gondwana

The Iberian margin of Gondwana was severely affected by deformation under a convergent tectonic regime during the Late Paleozoic Variscan orogeny and its aftermath. These protracted deformation events produced important modifications of the original relationships among Cambrian-Ordovician paleogeographic units and strong overprinting on preexisting structural elements. This fact makes the recognition and analysis of the structures formed during the Cambrian-Early Ordovician rifting stage a very difficult task. In a vast majority, the presumed original normal or oblique faults are now inverted as thrusts, many of which were subsequently even folded and faulted. Only in few exceptional cases, the original normal faults are preserved in pressure shadows of the Variscan orogenic system, generally at a small scale. At a larger scale, it is also possible to identify locally some structural features reminiscent of the rifting stage despite the subsequent Variscan orogenic inversion.

(i) In the Ossa-Morena Zone, where lied the Cambrian rifting axis, several fault-controlled troughs are recognized. The so-called Alconera and Córdoba units (Liñán and Quesada 1990) show remarkable lateral thickening of their Cambrian stratigraphic successions approaching syn-sedimentary listric faults, currently reactivated as thrusts (Odriozola et al. 1983). Their associated thickness changes suggest preservation of half- or asymmetric graben structures during most of the Terreneuvian to Cambrian Epoch 3 (Pereira and Quesada 2006).

(ii) Complementarily, an indirect means to figure out the characteristics of the structure developed during this stage is provided by a thorough analysis of the

Cambrian-Lower Ordovician stratigraphic record, within and across the Iberian Massif's Gondwanan zones (Liñán and Quesada 1990; Quesada 1991, 2006; Martínez Catalán et al. 2007; Gutiérrez-Marco et al. 2002, 2011; Simancas et al. 2004; Pereira et al. 2006, 2008a, 2012a, b; Chichorro et al. 2008; Linnemann et al. 2008; Sánchez-García et al. 2003, 2008a, b, 2010; Nance et al. 2012; Álvaro et al. 2016; Murphy et al. 2016, among others). This allows recognition of significant facies and thickness changes across many units' boundary faults at all scales, which can be readily interpreted as evidence of reactivation as thrusts and/or strike-slip faults of previously existing normal faults delimiting domains with contrasting subsidence patterns at those times. A syn-rift horst and graben structure is thus indicated, although it is impossible to prove in most cases if the present boundary faults are exactly the inverted expression of those active during the rift stage and even if the now adjacent units originally had the same paleogeographical relationships. An example of such a stratigraphic analysis was performed on the main structural units making up the Ossa Morena Zone by Liñán and Quesada (1990) and Oliveira et al. (1991), later on refined by Sánchez-García et al. (2003), the latter being graphically depicted in Fig. 2.5. At a larger scale, a comparison of stratigraphic columns representative of the syn-rift successions (Fig. 2.4) in the four Gondwanan zones of the Iberian Massif allows defining the Ossa Morena and West Asturian-Leonese zones as overall graben domains while the Central Iberian and Cantabrian zones largely behaved as horst domains at that time.

(iii) The inner Gondwanan zones that were progressively affected by the widening of the area subjected to extension from the rifting axis, collectively behaved as a passive margin basin (the so-called Cantabro-Iberian Basin; Aramburu et al. 1992; Álvaro et al. 2000a, b). There, three Cambrian episodes of enhanced tectonic activity are broadly recognized based on associated gravity-induced deformation structures, the overall facies and thickness changes

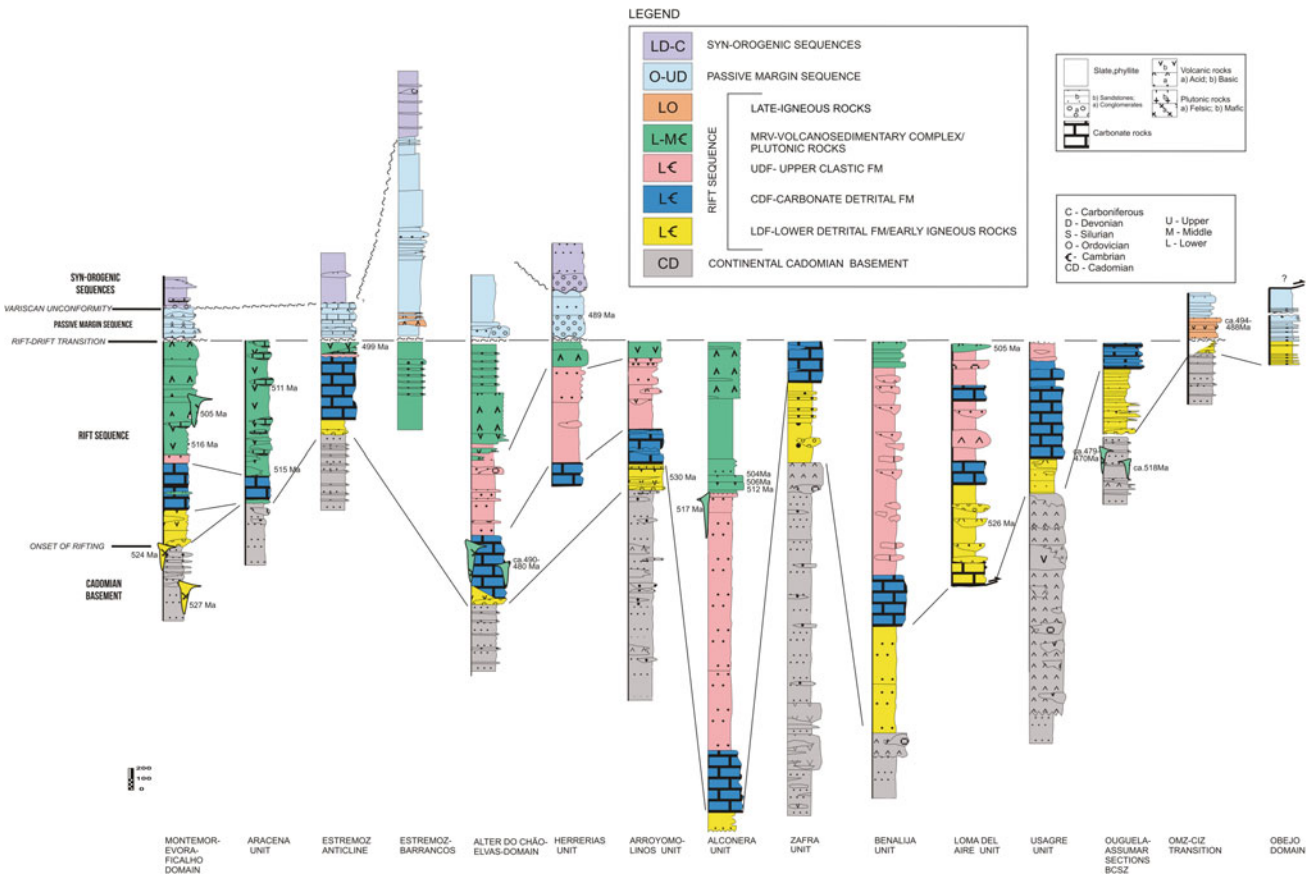

Fig. 2.5 Schematic correlation cartoon of representative sedimentary successions of the main tectonic units in the OMZ. Note the extreme facies and thickness differences within the Cambrian-Ordovician rift sequences and the strong diachronic nature of the volcanic rocks, reminiscent of the development of a horst and graben structure and the sequential propagation of rifting, respectively (modified after Sánchez-García et al. 2003)

along linear trends in isopach maps, and the estimation of the intra-platform relative subsidence rates (Liñán et al. 2002; Aramburu et al. 2004 and references therein). The earlier episode took place during a Cambrian-Age-2 widespread drowning of carbonate platforms leading to their flooding and establishment of offshore-dominated clayey substrates. This marks the top of the Detrital-Carbonate Group in Ossa-Morena, the Navalucillos/Soleras contact in the Central-Iberian Zone and a member contact of the Ribota Formation in the Iberian Chains (Álvaro and Vennin 1996; Álvaro et al. 2013c, 2014). A second episode of block-faulting development of a major paleotopography, which differentiated into assemblages of relative horsts and grabens, took place across the Cambrian Epoch 2/3 transition. Carbonate production in topographic highs gave rise to the so-called "griotte" facies (upper Láncara Member and Valdemiedes and Mansilla formations in the Cantabrian Zone), whereas intervening grabens recorded a monotonous offshore clayey sedimentation (Zamarreño 1972; Sdzuy and Liñán 1993; Álvaro and Vennin 1996; Álvaro et al. 2000a). This tectonic episode has also been traced along the faulted contact that marks the western boundary of the West Asturian-Leonese Zone. According to Martínez Catalán et al. (1992) and Russo and Bechstädt (1994) to the west of the Vivero Fault, basinal deposition probably represents the lateral equivalent of the carbonate Vegadeo and Láncara formations. A later episode of widespread tectonic breakdown is represented by common development of olistostromic beds in the Furongian Valtorres Formation of the Iberian Chains, one of the scarce platforms that did not record the Toledanian uplift (Álvaro and Vennin 1996; Álvaro et al. 2007).

(iv) The compartmentalization outlined in the previous paragraphs attests for the upper crustal expression of the structures formed during the initial rifting stage of the Variscan cycle. However, the existence of igneous rocks (both plutonic and volcanic) at this stage, including lithospheric and asthenospheric components (Mata and Munhá 1990; Ochsner 1993; Sánchez-García et al. 2003, 2008a, 2010, 2016; Etxebarría et al. 2006; Chichorro et al. 2008; Sarrioanandía et al. 2012; Dias da Silva et al. 2014) imply that some of these faults may have reached the subcontinental lithospheric mantle and even the asthenosphere at some stage.

We are dealing thus with a thick-skinned extensional process at least during the mature stages of rifting. Two of those lithosphere-through faults probably were those bounding the Central Iberian Zone, as suggested by two impressive Lower Ordovician igneous belts developed in the vicinity of such boundaries: the volcanic and volcaniclastic Urra Formation near the southern boundary with the Ossa Morena Zone and the famous Ollo de Sapo Formation near the northern boundary with the West Asturian-Leonese Zone (see Fig. 2.1 for location and under Sect. 2.4: *Magmatic Events During the Rifting Stage* for a description).

To the south of both Urra and Ollo de Sapo formations and in close association, contemporaneous peralkaline plutonic and volcanic rocks define parallel lineaments at the northern boundaries of OMZ and GTMZ, respectively. In addition, inside the Central Iberian Zone and Galicia-Trás os Montes other aligned occurrences can be also recognized. They include middle-to upper crustal plutonic bodies exhumed during the Variscan orogeny in the Spanish Central System and Beira Baixa-Estremadura belt (see Fig. 2.1). The former belt includes the gneisses of Galicia and Castilian, Guadarrama, Salamanca, Zamora and Toledo (hereafter called Galicia and Castilian lineament respectively (Fig. 2.1; Ribeiro 1987a, b; Pin et al. 1992; Montero and Bea 1998; Montero et al. 2007, 2009b; Castro et al. 2002; Bea et al. 2006; Antunes et al. 2008; Rubio-Ordóñez et al. 2012; Talavera et al. 2013; Villaseca et al. 2015). The Beira Baixa-Estremadura belt, recently documented is located in the southern part of the CIZ and comprises the plutons of Gouveia, Fundão, Oledo and Zarza la Mayor (Antunes et al. 2008, 2012; Neiva et al. 2009; González-García et al. 2011; Rubio-Ordóñez et al. 2012). Rocks in these two igneous belts are largely felsic in composition but connections with the mantle of their respective feeding systems are indicated by the local presence of volumetrically minor mafic rocks.

(v) Little can be said about the structures formed at deeper crustal levels. Exceptions to this statement are provided by several migmatitic domes occurring at the core of the Monesterio antiform, a Variscan antiformal stack in the central Ossa-Morena Zone. There, the mid-crustal Valuengo, Monesterio and Lora del Río migmatitic complexes, developed after Neoproterozoic Serie Negra protoliths were exhumed in the hangingwall of a major, high-angle Variscan thrust (e.g. Monesterio thrust; Eguiluz 1987). All three show domal structures surrounded by much lower grade (biotite or less) Neoproterozoic and/or Terreneuvian and Cambrian Series 2 rocks. The contact zone is defined by either a narrow (hectometre to metre scale) band of anastomosing ductile to brittle shear zones or by discrete flat-lying brittle faults. On the basis of the age of the migmatites (ca. 530 Ma, Ochsner 1993; Expósito et al. 2003; Sánchez-García et al. 2008a, b), these domes have been interpreted as

variably overprinted relics of core-complexes developed in the middle crust of the Ossa-Morena Zone during early rifting stages (Sánchez-García et al. 2003, 2008a, 2010). A somewhat similar situation may be suggested for the relationships between the middle crustal segments exposed in the Sierra de Guadarrama (see Fig. 2.1) overlain to the east, through the so-called Berzosa detachment, by the upper crustal section exposed in the Somosierra sector, although the Variscan overprint is much more important here (Navidad and Castiñeiras 2011; Villaseca et al. 2015; Orejana et al. 2017). If true, it would attest for a similar core-complex development in this part of the Central-Iberian Zone during the Early Ordovician (Talavera et al. 2013).

2.3 Paleogeographic and Sequence Events During the Rifting Stage

The stratigraphic record of the syn-rift deposits in the Gondwanan units of the Iberian Massif is very complex and includes important facies and thickness changes in response to the coeval development of the aforementioned horst-and-graben structure. It starts with a transgressive sequence and generally consists of a basal terrigenous succession, an intermediate carbonate-terrigenous succession and an upper terrigenous succession. Many formations have been defined in the various units, formally and informally, but reference to them is reduced to a minimum herein for the sake of clarity. Interestingly, the syn-rift succession was episodically flooded by volcanic rocks, which have been adscribed to three main magmatic events (see below under Sect. 2.4; Sánchez-García et al. 2003; Chichorro et al. 2017b). In what follows we review the main common events that have been identified within the syn-rift stratigraphic record and their paleogeographic and paleotectonic implications.

Although their boundaries (sequence boundaries and/or maximum flooding surfaces) are not isochronous, due to the interplay of eustatism, sedimentation rate and subsidence/uplift frequencies, several transgressive/regressive third-order depositional sequences (ranging 3–50 m.y.) are broadly recognized throughout the Cambrian of the Iberian Massif (see Fig. 2.4):

(i) Terreneuvian transgression under extensional (post-Cadomian) conditions

Besides uplift and erosion, thermal expansion would have induced gravitational instabilities triggering processes of extensional collapse. In the Iberian Massif rift and neighbouring extended basins, both rifting branches (in the former) and tilted fault blocks (in the latter) recorded sharp differences in accommodation space and facies. Coarse-grained sediments were deposited as accommodation space was sharply generated during extensional pulses, controlling rapid thickness changes and onlapping of inherited (Cadomian) paleoreliefs. Subsequently, graben and half-graben structures were flooded and onlapped by distinct Terreneuvian alluvial-to-fluvial strata; e.g. lower breccias and conglomerates of the upper-Terreneuvian Torreárboles Formation (Liñán 1978) in the Córdoba and Alconera troughs (Ossa-Morena Zone) or the lower part of the ca. 530 Ma old *Early rift-related volcanic sequence* (Sánchez-García et al. 2003, 2008a, b, 2010, 2016; Romeo et al. 2006) in the Arroyomolinos and Loma del Aire troughs (Liñán and Quesada 1990); and the lower alluvial-fluvial-deltaic parts of the Cándana (West Asturian-Leonese Zone), Herrería (Cantabrian Zone) and Bámbola formations (Iberian Ranges) (Fig. 2.4; Álvaro et al. 2003, 2008 and references therein).

In addition to passive gravitationally-driven collapse, which could by itself provide an explanation to the formation of the aforementioned troughs, active extension also started to operate soon after, as suggested by the rapid flooding of the entire area and the generalization of the horst and graben structures beyond the limits of the entire Iberian Massif. By late Terreneuvian times, the entire Ossa Morena Zone was flooded, the transgression rapidly progressing northward (in present coordinates) toward more internal parts of the Gondwanan margin and covering the whole margin by the end of Cambrian Epoch 2. Active extension may well have been promoted by the process of slab-pull referred to above but, alone, this model cannot explain the sequence of events recorded in the Iberian margin, especially in Ossa Morena. The fact that uplift, localized collapse, important magmatism (*Early rift-related volcanic sequence*) and strong modification of the geothermal regime preceded the onset of significant extension and marine transgression rather supports that the initial motor of the abrupt change was related to the development of a slab window as proposed by Sánchez-García et al. (2003, 2008a, b, 2010). Indeed, we believe that it was the locking of subduction beneath Gondwana, after collision of a mid-ocean ridge with the trench, what caused the mechanical coupling of the two plates and the initiation of subduction of the Iapetus and Prototethys oceans beneath Laurentia and Baltica, respectively. Once these latter processes started, slab pull forces would have become operative on the opposite Gondwanan margin.

(ii) Cambrian-Epoch-2 arid carbonate platforms punctuated with microbial-archaeocyathan reefal complexes, and final tilting and drowning

Although Terreneuvian tilted blocks were originally sites of coarse-grained siliciclastic sedimentation, microbial and shelly carbonate production subsequently sited on footwall crests. This led to nucleation and development of giant

archaeocyathan-microbial reef complexes (Detrital-Carbonate Group in Ossa-Morena; Moreno-Eiris 1987) separating ramps with ooidal shoals and stromatolitic buildups. In the adjacent Cantabro-Iberian Basin, a similar episode of carbonate productivity led to the record of distinct carbonate facies rich in birdseyes, microbial and microbial-archaeocyathan reefs and ooidal grainstones (Tamames and Navalucillos and Vegadeo formations, lower Láncara Member, Jalón and Ribota formations; Fig. 2.4) containing dolomite rhombs, evaporitic pseudomorphs, and scattered idiomorphic quartz interpreted as being characteristic of hypersaline conditions (Zamarreño 1972, 1975; Aramburu et al. 1992, 2004; Aramburu and García-Ramos 1993; Russo and Bechstädt 1994; Álvaro et al. 1995, 2000b).

As stated above, the end of this episode of carbonate productivity was marked in the Iberian Massif by sharp drowning and collapse of platforms, locally associated with hydrothermal influence. This generalized drowning event probably marks the time when passive extensional processes started to predominate over active thermal expansion and associated gravitational collapse.

(iii) Latest Cambrian-Epoch-2 Daroca Regression

After a general drowning and flooding of some rifting troughs and extensive platforms, a late Cambrian-Epoch2 regression (the so-called Daroca Regression; Álvaro and Vennin 1998) is recorded in the Iberian Massif. The regression culminated close to the Cambrian Epoch 2/3 boundary, led to progradation of shallow-marine sandstone formations and eventually emergence (Fig. 2.4). This worldwide eustatic fall has been correlated with the Hawke Bay event in Laurentia and the Toyonian Regression in the Siberian Platform (Palmer and James 1980; Rowland and Gangloff 1988; Liñán et al. 2002). Initial eruption of volcanic rocks of the so-called *Main rift-related volcanic event* (Sánchez-García et al. 2003, 2008a, 2010, 2016) took place during this event.

(iv) Cambrian-Epoch-3 transgressive-regressive composite trend

The Daroca Regression led to aggradational and transgressive trends, locally punctuated by the above-reported episode of enhanced tectonic activity (Fig. 2.4). A general drowning took place across the Cantabrian Zone and the Iberian Chains, although in a diachronous way, as a result of lateral migration of the tectonic activity responsible for the related paleohorst carbonate productivity (Zamarreño 1972; Sdzuy and Liñán 1993; Álvaro et al. 2000b).

The late Cambrian-Epoch-3 sedimentary evolution recorded final drowning and flooding of the previous paleorelief, followed by a regression. The latter is manifested by development of alluvial sand bars (also interpreted as foreshore and sand ridges of a delta complex), and unsorted, coarse-grained sandstones displaying channels that represent migration of sheet (fluvial) braid-plain and delta deposits (Aramburu et al. 1992, 2004; Aramburu and García-Ramos 1993; Álvaro et al. 2008).

This transgressive-regressive composite trend, spanning for most of the Cambrian Epoch 3, was coeval to a phase of enhanced active extension during which most of the *Main rift-related volcanic sequence* (Sánchez-García et al. 2003, 2008a, 2010, 2016) was erupted in the Ossa-Morena Zone.

(v) Toledanian uplift (forced regression) coeval with Furongian transgression

The above-reported Cambrian Epoch 3 regression culminated in the emergence and erosion of the entire Ossa-Morena and southern Central-Iberian zones, where a gap covering at least the Furongian stage but locally involving even the entire Cambrian is recorded (Fig. 2.4). This regression may have been forced by enhanced thermal expansion associated to the *Main rift-related igneous event* (Sánchez-García et al. 2003, 2008a, b, 2010, 2016), during which several kilometre-thick successions of volcanic rocks were erupted and many plutons, both felsic and mafic, were emplaced in the Ossa Morena crust. The extension of the uplift into the adjacent Central-Iberian Zone may reflect the propagation and growth of a speculated slab window beneath this zone at this time (see below under Sects. 2.4.4 and 2.7).

In contrast, away from the area subjected to thermal uplift, the Furongian was characterized by transgressive, offshore-dominated clayey successions (e.g. Valtorres Formation in the Iberian Chains; Álvaro et al. 2007, 2013b) or mudstone-sandstone alternating substrates (e.g. Los Cabos Series in the West Asturian-Leonese Zone or the Oville Formation in the Cantabrian Zone; Liñán et al. 2002 and references therein); the latter two formations extending into early Tremadocian times.

This event was followed by a new transgression, starting in the late Furongian in the Ossa Morena rift axis, which flooded this zone and somewhat later the also uplifted Central Iberian Zone inaugurating the new passive margin stage on the newly formed margin of Gondwana. This transgressive event is interpreted in connection to thermal contraction following opening of the Rheic Ocean, thence the interpretation of the Toledanian event as a breakup unconformity (Quesada 1991, 2006; Pereira and Quesada 2006 and references therein). In the zones that had not been affected by the Toledanian forced regression, this transgression added to the already existing transgressive regime.

2.4 Magmatic Events During the Rifting Stage

A voluminous igneous activity was recorded in the reputed axial zone of the rift (e.g. the Ossa-Morena Zone) throughout this stage, starting from its very beginning and extending

into the Early Ordovician, even well after opening of the Rheic Ocean by ca. 489 Ma ago (López-Guijarro et al. 2007). Away from this zone, and with the exception of the two occurrences situated close to the boundaries of the Central-Iberian Zone, igneous activity was less important and discontinuous, becoming progressively minor with increasing distance from the rift axis (i.e. toward the Cantabrian Zone, Fig. 2.1). In what follows we use the Ossa-Morena Zone as a reference to establish a frame of events that may serve for comparison with igneous events in other zones of the Iberian Massif.

Rift-related igneous activity in the Iberian Massif is subdivided into three main events with contrasting characteristics and separated by relatively quiescent periods. The first two events *Early and Main igneous events* were described in detail in the Ossa-Morena Zone by Sánchez-García et al. (2003, 2008a, b, 2010, 2016) and their terminology is followed herein. We will refer to the third event as *Late rift-related igneous event*. It occurs mainly in the Central Iberian Zone, within which the well-known in the scientific literature *Ollo de Sapo Formation* and associated plutons are the most widely exposed representatives. The terms *Early, Main and Late* rift-related magmatism should be read as space-time diachronic events (Figs. 2.4 and 2.5; see also Fig. 2.20). They are merely descriptive of the progressive variation of the nature of the rift-related magmatism with time and in space.

In the Iberian Massif, the geochemical evolution of magmas with time reflects the gradual opening of the system to the mantle. In general, it is possible to assume that there is a diachronic and transient evolution from felsic S-I type magmatism (*Early*), progressively more influenced by the underplating and emplacement of mantle-derived magmas (*Main*) and culminating with alkaline/peralkaline magmatism. In the Ossa Morena Zone a time-space migration of the late alkaline/peralkaline magmatism from south to north is evident. The ages of the southern outcorps are ~500–505 Ma old (e.g. Barcarrota-Castillo-Feria-Sierra Vieja-Remedios plutons; Ochsner 1993; Montero et al. 2000; Salman 2002; Sánchez-García et al. 2008a, b) whereas in the north they are 490–470 Ma old (e.g. Elvas-Cevadais-Arronches plutons; Díez-Fernández et al. 2014), see Fig. 2.1 for location.

The migration of rift processes from OMZ to CIZ domains is also noticeable. In fact, the *Early, Main* and *Late* rift-related magmatic events are repeated in the CIZ but delayed in time (Díez Montes et al. 2015, see Fig. 2.4). The late alkaline/peralkaline magmatism in northern Ossa Morena Zone coincides with triggering of the first steps of rifting in Central Iberian Zone, evidenced by predominantly peraluminous magmatism in four main belts (e.g. Ollo de Sapo, Castilian-Galician, Gouveia-Oledo Zarza and Urra–Portalegre–Carrascal belts; Talavera et al. 2013 and references therein; see Fig. 2.1 for location).

Taken as a whole, Cambrian-Ordovician rift-related magmatism in the Iberian Massif spanned for a long period, from ~530 to 470 Ma (Fig. 2.4). However, magmatic events in the Central Iberian Zone were shorter: started at 500–495 Ma, reached a maximum activity between 495–480 Ma, and ceased at ~470 Ma (Talavera 2009). Recent ages of 453 and 452–456 Ma obtained respectively in metabasites intrusive into pre-Floian metasedimentary rocks in Guadarrama sector (Orejana et al. 2016) and in a biotite orthogneiss in the Porto-Tomar shear zone (Sousa et al. 2014) could extend the duration of the rifting event there. Nevertheless, the authors did not provide exhaustive description of the samples and the analysed zircons, reason why these ages should be taken with caution.

In the Galicia-Trás-os-Montes Zone the rift related sequences are exposed exclusively in the parauthoctonous and the basal allochtonous units. They are represented by Cambrian-Lower Ordovician terrigenous metasedimentary rocks intruded by Furongian to Ordovician granitoids (calcalkaline to peralkaline) and mafic igneous rocks. The oldest ages cluster around 500–495 Ma (Abati et al. 1999; Montero et al. 2009b; Dias da Silva et al. 2014) and the youngest around 470 Ma (Valverde-Vaquero et al. 2005) as in the Central Iberian Zone (Talavera 2009). Structural complexity in the Galicia-Trás-os-Montes Zone prevents detailed characterization of the pre-orogenic history of these rocks, reason why it is dealt with in a separate section (see below under Sect. 2.5).

The study of magmatic events must be done considering their spacial localization, stratigraphy and geochemical features. The geochemical features of the *Early, Main* and *Late* rift-related magmatism are described below, considering available published data, and plotted in Figs. 2.6, 2.7, 2.8, 2.9, 2.10, 2.11, 2.12, 2.13, 2.14, 2.15, 2.16, 2.17 and 2.18. The geochemical classification used herein is based on immobile elements, such as the Nb/Y versus Zr/Ti diagram of Pearce (1996) that groups the compositions into sub-alkaline, alkaline and ultra-alcaline affinities. However, this classification is more appropriated for volcanic than for plutonic rocks. In fact, volcanic rocks cool rapidly, reducing the occurrence of accumulation, assimilation and reequilibrium/mixing processes with other liquids and therefore are most reliable to characterize the geotectonic evolution of igneous rocks.

2.4.1 Early Rift-Related Igneous Event

In the Iberian Massif, the first manifestation of rifting occurs in the Ossa-Morena Zone. The associated igneous rocks include volcanic, hypabyssal, plutonic types with local migmatitic manifestations that formed during Terreneuvian times (late Fortunian to Early Age 2; ca 531–525 Ma). This

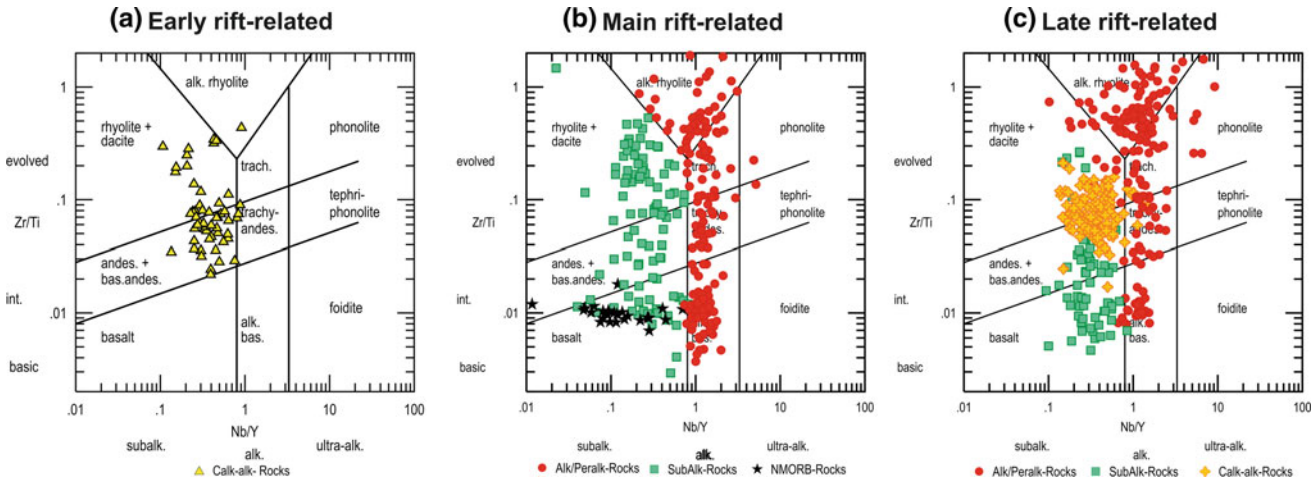

Fig. 2.6 Geochemical features of the different rift-related groups in the Zr/Ti versus Nb/Y diagram (Pearce 1996). **a** Early rift-related group; **b** main rift-related group; **c** late rift-related group (Analytical data tables can be obtained from the corresponding author of this chapter)

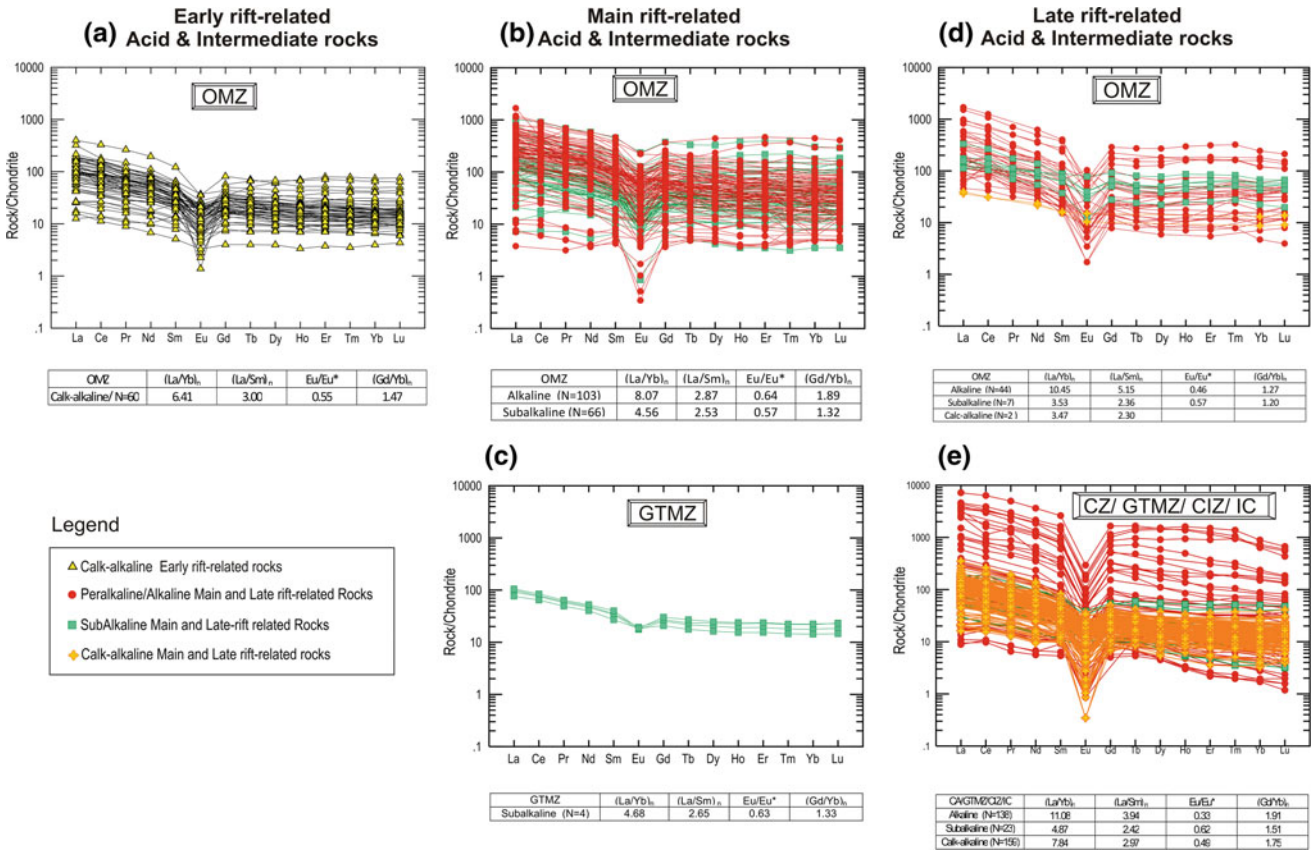

OMZ	$(La/Yb)_n$	$(La/Sm)_n$	Eu/Eu*	$(Gd/Yb)_n$
Calk-alkaline/ N=60	6.41	3.00	0.55	1.47

OMZ	$(La/Yb)_n$	$(La/Sm)_n$	Eu/Eu*	$(Gd/Yb)_n$
Alkaline (N=103)	8.07	2.87	0.64	1.89
Subalkaline (N=66)	4.56	2.53	0.57	1.32

OMZ	$(La/Yb)_n$	$(La/Sm)_n$	Eu/Eu*	$(Gd/Yb)_n$
Alkaline (N=44)	10.45	5.15	0.46	1.27
Subalkaline (N=7)	3.53	2.36	0.57	1.20
Calc-alkaline (N=2)	3.47	2.30		

GTMZ	$(La/Yb)_n$	$(La/Sm)_n$	Eu/Eu*	$(Gd/Yb)_n$
Subalkaline (N=4)	4.68	2.65	0.63	1.33

CVGTMZ/CIZ/IC	$(La/Yb)_n$	$(La/Sm)_n$	Eu/Eu*	$(Gd/Yb)_n$
Alkaline (N=138)	11.08	3.94	0.33	1.91
Subalkaline (N=23)	4.87	2.42	0.62	1.51
Calc-alkaline (N=156)	7.84	2.97	0.46	1.75

Fig. 2.7 Geochemical comparison of different rift-related acid and intermediate rocks on the basis of their chondrite-normalized REE patterns (Sun and McDonough 1989). **a** early rift-related group in Ossa-Morena Zone (OMZ); **b** main rift-related group in OMZ; **c** main rift-related group in Galicia-Trás-os-Montes Zone (GTMZ); **d** late rift-related group in OMZ; **e** late rift-related group in GTMZ and the Central Iberian Zone. Main mean values are included for the different groups (Analytical data tables can be obtained from the corresponding author of this chapter)

magmatism occurred coevally with the siliciclastic sedimentation of the Lower Detrital Formation, which unconformably overlies previously deformed Upper Ediacaran strata of the Serie Negra Group (Alía 1963). The lower Cambrian Lower Detrital Group consists of conglomerates, sandstones and mudstones associated with felsic volcanic,

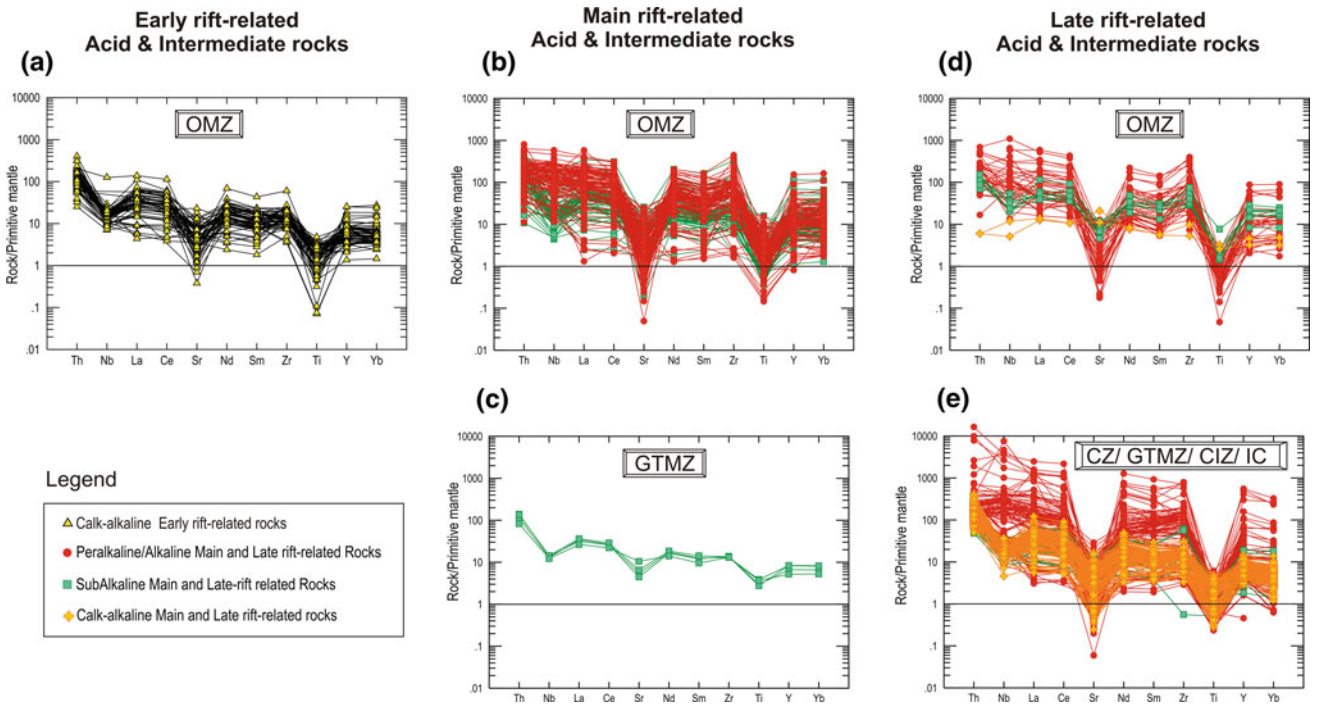

Fig. 2.8 Geochemical comparison of different rift-related acid and intermediate rocks. Primitive mantle-normalized spider diagrams (Palme and O'Neill 2004). **a** early rift-related group in Ossa-Morena Zone (OMZ); **b** main rift-related group in OMZ; **c** main rift-related group in Galicia-Trás-os-Montes Zone (GTMZ); **d** late rift-related group in OMZ; **e** late rift-related group in GTMZ and the Central Iberian Zone (Analytical data tables can be obtained from the corresponding author of this chapter)

volcanosedimentary and subvolcanic rocks, which belong to the following stratigraphic units (see Fig. 2.1 for location): Bodonal-Cala beds (Hernández Enrile 1971) and minor volcanic intercalations in the Torreárboles Formation (Liñán 1978) in Spain, and Freixo-Segovia, Nave de Grou-Azeiteiros, São Vicente, and the lower part of Monfurado volcanic-sedimentary complexes in Portugal (Pereira and Silva 2002, 2006; Chichorro et al. 2008, Sánchez-García et al. 2010). In addition to those eruptive types, the following plutons are thought to belong to this early event: Barquete, Barreiros, Calera, Culebrin, Garrotal, Monesterio, Salvatierra de los Barros, Táliga (Salman and Montero 1999; Salman 2002; Sánchez-García et al. 2010, 2013) and the Alcáçovas orthogneiss (Chichorro et al. 2008).

The volcano-sedimentary rocks of this group show considerable variations in both facies and thickness. They comprise mainly rhyolitic lavas, breccias, tuffs, quartz- and feldspar-rich crystal tuffs and ignimbrites. Lavas are massive or porphyritic, aphanitic to fine-grained in texture and light colored (white, green to pinkish). Available geochronological data (ID-TIMS, LA-ICPMS, KOBER and SHRIMP U-Pb on zircon and Rb-Sr on minerals and whole-rock) show a spread of early Cambrian ages bracketed between 516–532 Ma (Galindo et al. 1990; Schäfer 1990; Ochsner 1993; Ordóñez-Casado 1998; Salman and Montero 1999; Montero et al. 2000; Salman 2004; Díez-Montes 2006; Romeo et al. 2006; Chichorro et al. 2006, 2008; Sánchez-García et al. 2008a, 2013, 2016; Pereira et al. 2011; Navidad and Castiñeiras 2011; López-Sánchez et al. 2012; Díez Fernández et al. 2012a).

The plutonic types comprise leucogranites, biotite and muscovite granites to monzogranites and granodiorites. Metamorphic contact aureoles are rarely observed (Ochsner 1993) with few exceptions (e.g. Salvatierra de los Barros pluton; Galindo and Casquet 2004; Carracedo et al. 2007). Most of the plutonic rocks contain mafic microgranular enclaves and also metre-scale xenoliths of previously deformed metasedimentary Serie Negra host rocks (e.g. Barquete, Barreiros, Salvatierra, Garrotal and Táliga plutons; Galindo et al. 1990; Ochsner1993; Salman 2004; Carracedo et al. 2007; Pereira et al. 2011; Sánchez-García et al. 2013).

The geochemical study of the Early Rift Event took into account the results obtained from 60 samples (28 volcanic, 32 plutonic). They are represented by silica oversaturated felsic rocks, with SiO_2 contents ranging from 59 to 81 wt% (Schäfer 1990; Mata and Munhá 1990; Ochsner 1993; Apraiz 1998; Sánchez-García et al. 2003, 2008a, b, 2010, 2013, 2016; Chichorro 2006; Pereira et al. 2006, 2010, 2011; López-Guijarro et al. 2008). In the Nb/Y versus Zr/Ti diagram of Pearce (1996), these rocks plot in the fields of sub-alkaline andesites, basaltic andesites and rhyolites (Fig. 2.6a). All plutonic samples plot in the calc-alkaline

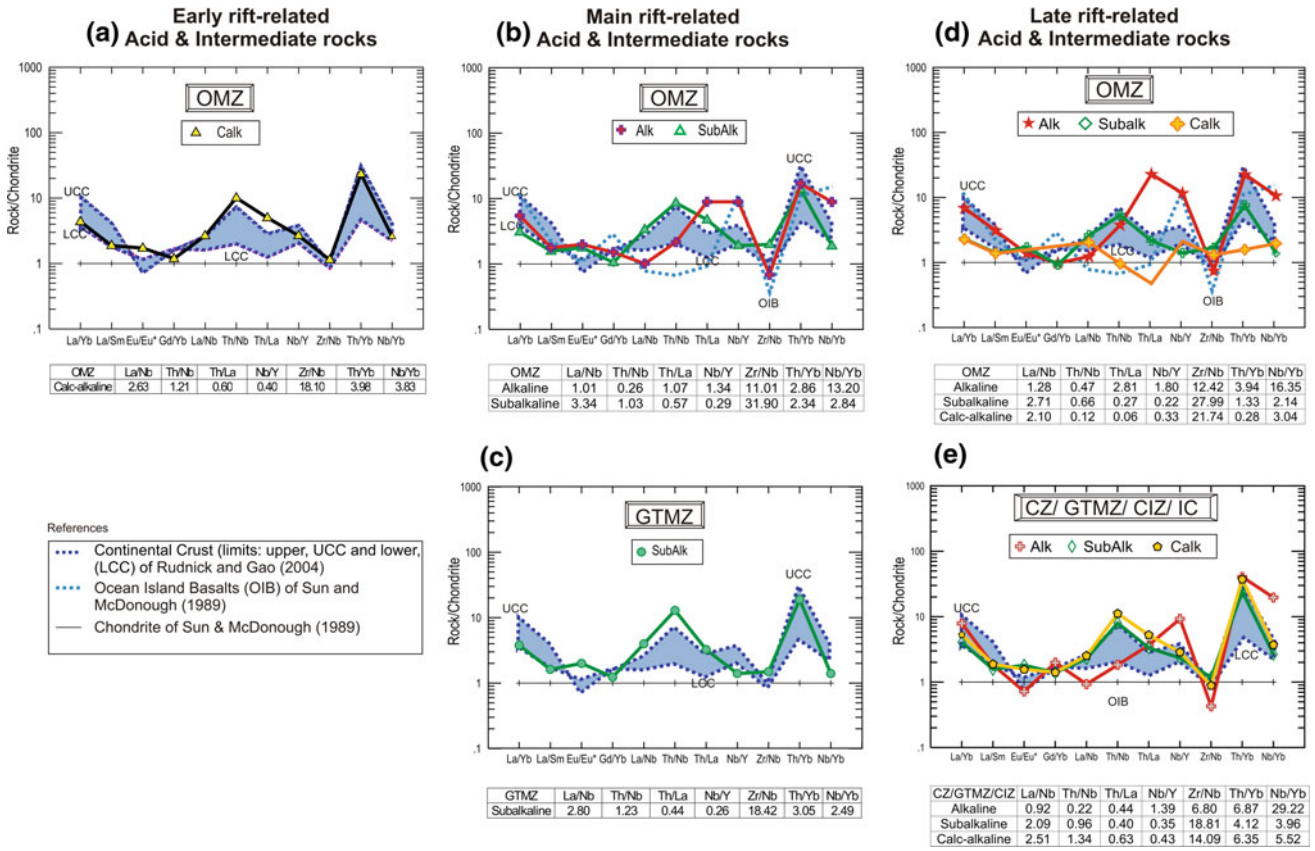

OMZ	La/Nb	Th/Nb	Th/La	Nb/Y	Zr/Nb	Th/Yb	Nb/Yb
Calc-alkaline	2.63	1.21	0.60	0.40	18.10	3.98	3.83

OMZ	La/Nb	Th/Nb	Th/La	Nb/Y	Zr/Nb	Th/Yb	Nb/Yb
Alkaline	1.01	0.26	1.07	1.34	11.01	2.86	13.20
Subalkaline	3.34	1.03	0.57	0.29	31.90	2.34	2.84

OMZ	La/Nb	Th/Nb	Th/La	Nb/Y	Zr/Nb	Th/Yb	Nb/Yb
Alkaline	1.28	0.47	2.81	1.80	12.42	3.94	16.35
Subalkaline	2.71	0.66	0.27	0.22	27.99	1.33	2.14
Calc-alkaline	2.10	0.12	0.06	0.33	21.74	0.28	3.04

GTMZ	La/Nb	Th/Nb	Th/La	Nb/Y	Zr/Nb	Th/Yb	Nb/Yb
Subalkaline	2.80	1.23	0.44	0.26	18.42	3.05	2.49

CZ/GTMZ/CIZ	La/Nb	Th/Nb	Th/La	Nb/Y	Zr/Nb	Th/Yb	Nb/Yb
Alkaline	0.92	0.22	0.44	1.39	6.80	6.87	29.22
Subalkaline	2.09	0.96	0.40	0.35	18.81	4.12	3.96
Calc-alkaline	2.51	1.34	0.63	0.43	14.09	6.35	5.52

Fig. 2.9 Chondrite-normalized isotope ratios patterns (Sun and McDonough 1989) for acid and intermediate rocks. **a** early rift-related group in Ossa-Morena Zone (OMZ); **b** main rift-related group in OMZ; **c** main rift-related group in Galicia-Trás-os-Montes Zone (GTMZ); **d** late rift-related group in OMZ; **e** late rift-related group in GTMZ and the Central Iberian Zone. Main mean values are included for the different groups (Analytical data tables can be obtained from the corresponding author of this chapter)

differentiated field in the AFM diagram (Irvine and Baragar 1971) and have peraluminous to metaluminous compositions (A/CNK = 0.6–1.2). Chondrite normalized REE patterns (Fig. 2.7a) show fractionation of LREE relative to the HREE. The Eu anomalies vary from moderate negative to weakly positive values. These results suggest crustal sources of their parental magmas.

Primitive mantle-normalized spider diagrams (Fig. 2.8b) show no significant negative Nb anomalies, being closer to upper continental crust values (Rudnick and Gao 2003). Element ratios as La/Nb, Th/Nb and Th/La, which are little affected by petrogenetic processes can help to understand the source of these magmas. The average Th/Nb ratio (1.07) is closer to continental crust value (0.9), whereas the average Th/La ratio (0.66) is higher (Fig. 2.9a). The geochemical characterization of the tectonic setting of these rocks is not straightforward as they overlap both anorogenic and orogenic fields in Pearce et al. (1984) diagram (Fig. 2.10a), although most of them plot into the orogenic field. All the geochemical characteristics outlined above suggest that these rocks mainly derived from a continental crust source, although they have some features that indicate an important subcrustal participation (Sánchez-García et al. 2010). Average Zr content is 133 ppm but some samples from Barreiros pluton and Monfurado Complex reach values greater than 650 ppm. This could indicate a mixed nature in the magmas of this group between felsic crustal melts and (differentiated) basic mantle-derived melts.

Sm/Nd isotopic data of the volcanic rocks show ε_{Nd} values at the age considered (532–514 Ma, see above) ranging from +2.2 and −11.0 (Fig. 2.11; Ordóñez-Casado 1998; Montero et al. 1999; Salman 2004; Chichorro et al. 2008; López-Guijarro et al. 2008; Sánchez-García et al. 2008a, 2010, 2013, 2016). Depleted mantle model ages (Depleted mantle model) calculated according to the model of DePaolo (1981) vary between 1.03 and 1.84 Ga, which would indicate crustal sources and high residence times. In turn, plutonic rocks of this early event show ε_{Nd} values ranging from +0.8 to −4.3 (Fig. 2.11) and $^{147}Sm/^{144}Nd$ ratios varying from 0.158 to 0.115, except the Calera granite which yielded a value (0.178) above the upper limit ($^{147}Sm/^{144}Nd = 0.15$) proposed by Stern (2002) as suitable to perform Nd T_{DM} calculations. Depleted mantle model ages (T_{DM}) calculated following the model of DePaolo

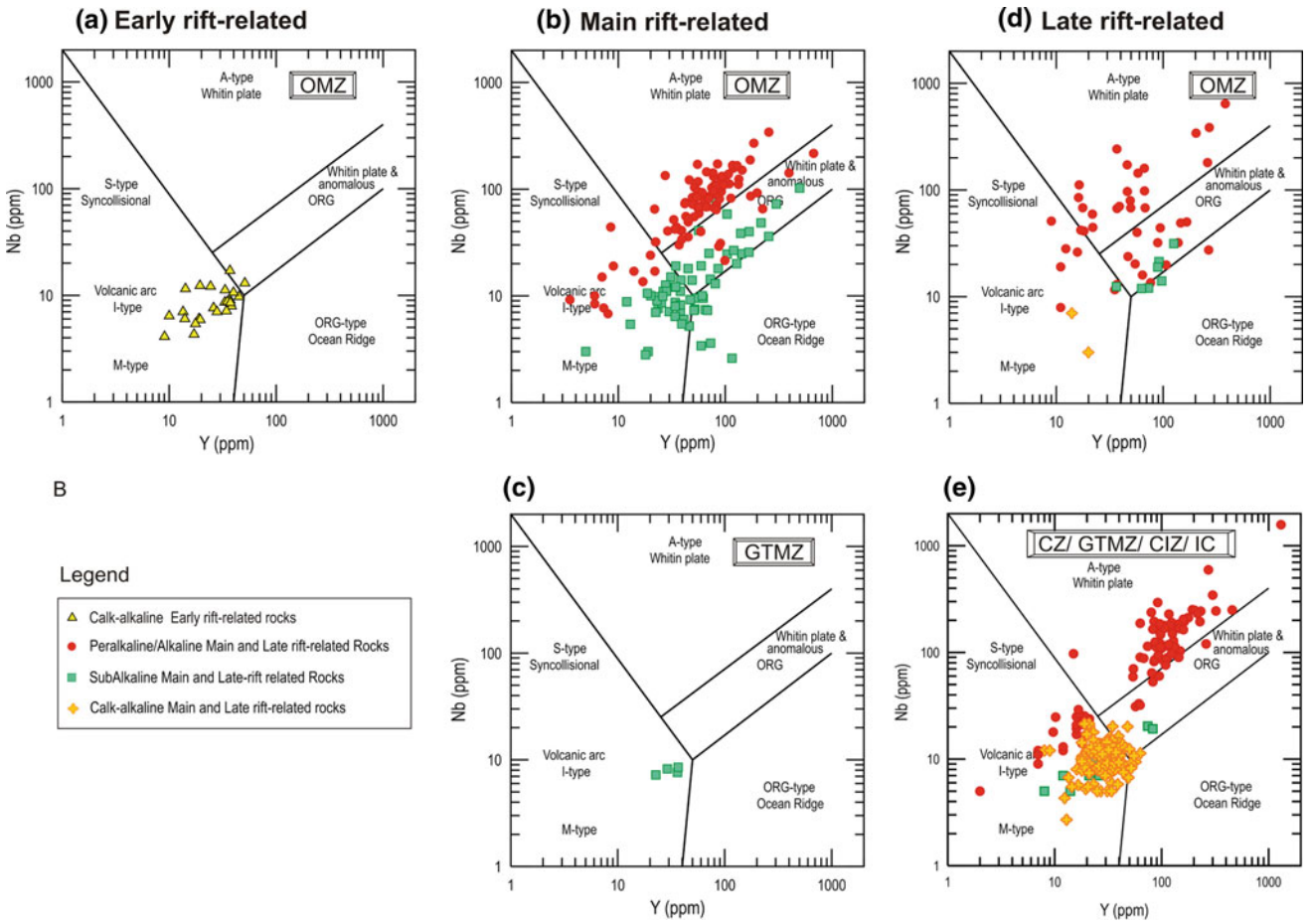

Fig. 2.10 Nb versus Y tectonic discrimination diagram (Pearce et al. 1984). **a** early rift-related group in the Ossa-Morena Zone; **b** main rift-related group in OMZ; **c** main rift-related group in the Galicia-Trás-os-Montes Zone; **d** late rift related in the OMZ; **e** late rift related in the GTMZ and the CIZ (Analytical data tables can be obtained from the corresponding author of this chapter)

(1981) vary between 1.30 and 2.04 Ga, which would indicate crustal sources and higher residence times in the crust that their volcanic equivalents.

All the geochemical characteristics outlined above suggest that these rocks mainly derived from a continental crust source, though they have some features that point to relatively important subcrustal (lithospheric mantle-derived) contributions. Their calk-alkaline affinity, resembling typical arc-related igneous rocks could be inherited from the source and explained by considering an origin by melting of crustal of rocks with similar composition to mature continental arcs (Sánchez-García et al. 2003, 2008a, 2010, 2016). This is in fact very likely as the basement underlying the Iberian Massif represents a segment of the Cadomian arc/back-arc system that surrounded West Gondwana in the Neoproterozoic (Murphy et al. 2006; Linnemann et al. 2008; Nance et al. 2008, 2010; Sánchez-García et al. 2003, 2016, and references therein).

The generation of these rocks was associated with the formation of migmatites during the development of core-complex structures (e.g. Monesterio and Valuengo migmatite domes) in middle to upper crust environments, promoting diachronic and transient ascent of felsic, I and S-type magmas to the upper crust and surface exploiting coeval extensional faults. A complete rock series of this Early igneous event ranges from in situ migmatitic complexes (e.g. Alcácovas, lower part of Monfurado volcano-sedimentary complex, Mina Afortunada, Monesterio, Valuengo, Lora del Río, etc.) in the middle crust, through allochthonous unrooted plutons in the upper crust (Barquete, Barreiros, Calera, Salvatierra de los Barros, Táliga, etc.) to erupted volcanic complexes (Bodonal-Cala beds, Nave de Grou-Azeiteiros, São Vicente, etc.).

These rocks had been previously interpreted as belonging to late evolutionary phases (late extensional collapse) of the Cadomian orogeny (Eguiluz 1987; Quesada and Munhá 1990; Bandrés et al. 2002, 2004). However, available ages for both volcanic and plutonic rocks (Schäfer 1990; Ochsner 1993; Ordóñez-Casado 1998; Romeo et al. 2006; Sánchez-García et al. 2008a) are younger than the basal metasediments of the unconformably overlying rift sequence. These data, along with their association with extensional tectonic processes, are interpreted to suggest that

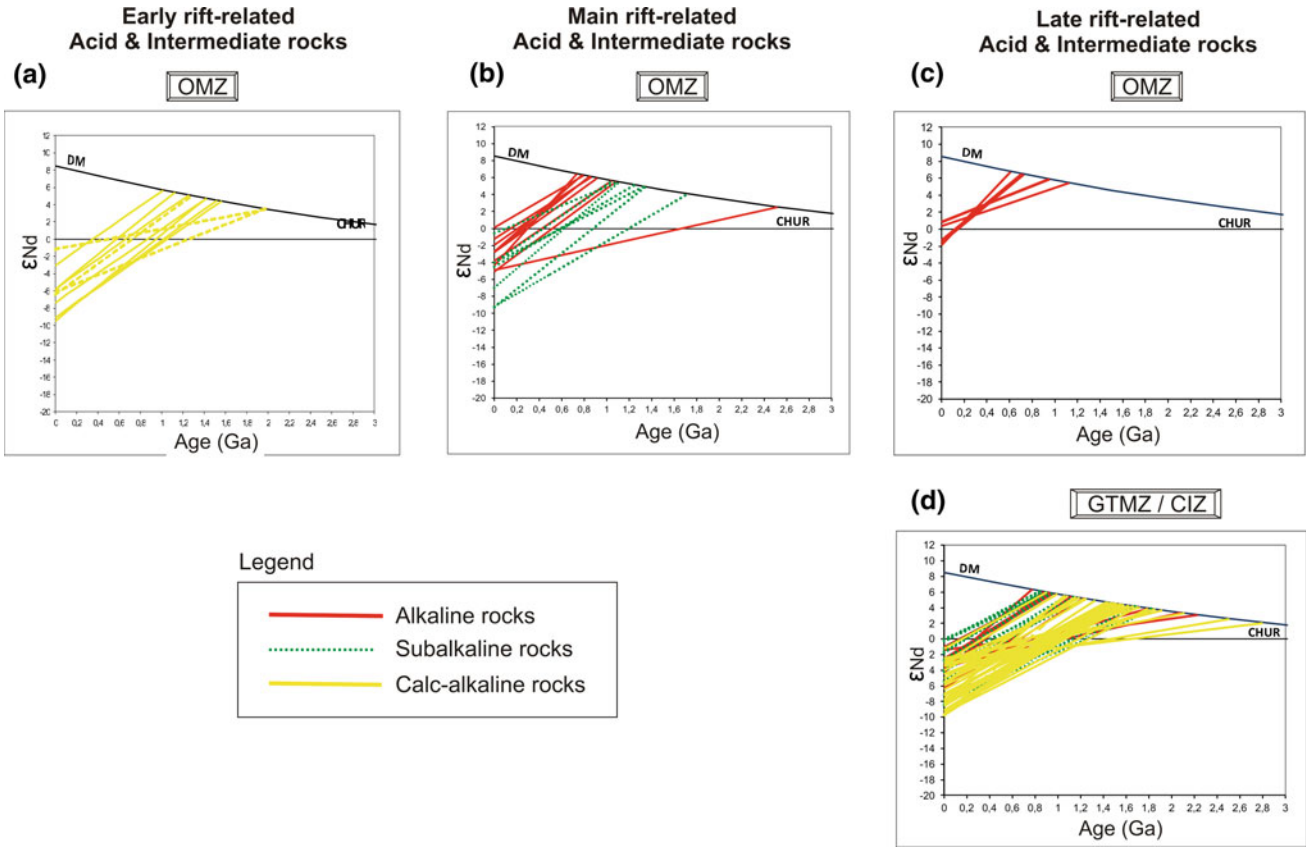

Fig. 2.11 $\varepsilon_{Nd(t)}$ versus age diagram (DePaolo and Wasserburg 1976; DePaolo 1981) for acid and intermediate rocks. **a** early rift-related group in the OMZ; **b** main rift-related group in OMZ; **c** late rift related in the OMZ; **d** late rift related in the GTMZ and the CIZ (Analytical data tables can be obtained from the corresponding author of this chapter)

they represent the onset of rifting and the initial stages of a severe thermal modification of the lithosphere, probably caused by an underlying thermal anomaly in the mantle (Sánchez-García et al. 2003, 2008a, 2010; Pereira et al. 2008a; Chichorro et al. 2008).

2.4.2 Main Rift-Related Igneous Event

This is by far the most important event of igneous activity of this stage in the Ossa-Morena Zone and also includes volcanic and plutonic rocks. Volcanic rocks may reach thicknesses in excess of 2–3 km in some graben units, where they occur interbedded with shallow-marine siliciclastic sediments. This event started by mid-Age 3 (Cambrian Epoch 2) and spanned up to the Guzhangian (late Epoch 3). Available radiometric ages constrain this event to ca. 518–489 Ma (Lancelot and Allegret 1982; Galindo et al. 1990; Schäfer 1990; Ochsner 1993; Ordóñez-Casado 1998; Montero et al. 2000; Salman 2004; Cordani et al. 2006; López-Guijarro et al. 2007; Solá 2007; Zeck et al. 2007; Chichorro et al. 2008; Pereira et al. 2010, 2012b; Coke et al. 2011; Sánchez-García et al. 2008a, 2016; Talavera et al. 2013; Dias da Silva 2013; Díez-Fernández et al. 2014; Farias et al. 2014; Villaseca et al. 2016). Some volcanic activity is also registered at this stage in the Galicia-Trás-Os-Montes and Central Iberian zones, but it is minor there.

Compositionally this group is typically bimodal with respect to SiO_2 and contain predominant basaltic and rhyolitic types and minor proportions of intermediate compositions (Fig. 2.6b). Volcanic rocks are represented by lava-flows, breccias, ignimbrites, hyaloclastites, tuffs and epiclastic sediments that appear interbedded mainly within marine shale, sandstone and greywacke successions of the so-called Upper Detrital Group (Liñán and Quesada 1990) and in minor proportion within carbonates towards the top of the underlying Detrital-Carbonate Group. It should be noted here that all these rocks show a widespread secondary alteration as a result of Variscan penetrative deformation and metamorphism and late-to-post magmatic hydrothermal alteration. In addition, seafloor spilitisation could be high in most volcanic rocks (Sánchez-García et al. 2003, 2008a, 2010; Sarrioanandía et al. 2012). Despite these problems, the geochemical diagrams remain interpretable and may reflect the primary magmatic distribution of at least the most immobile elements (Sánchez-García et al. 2003).

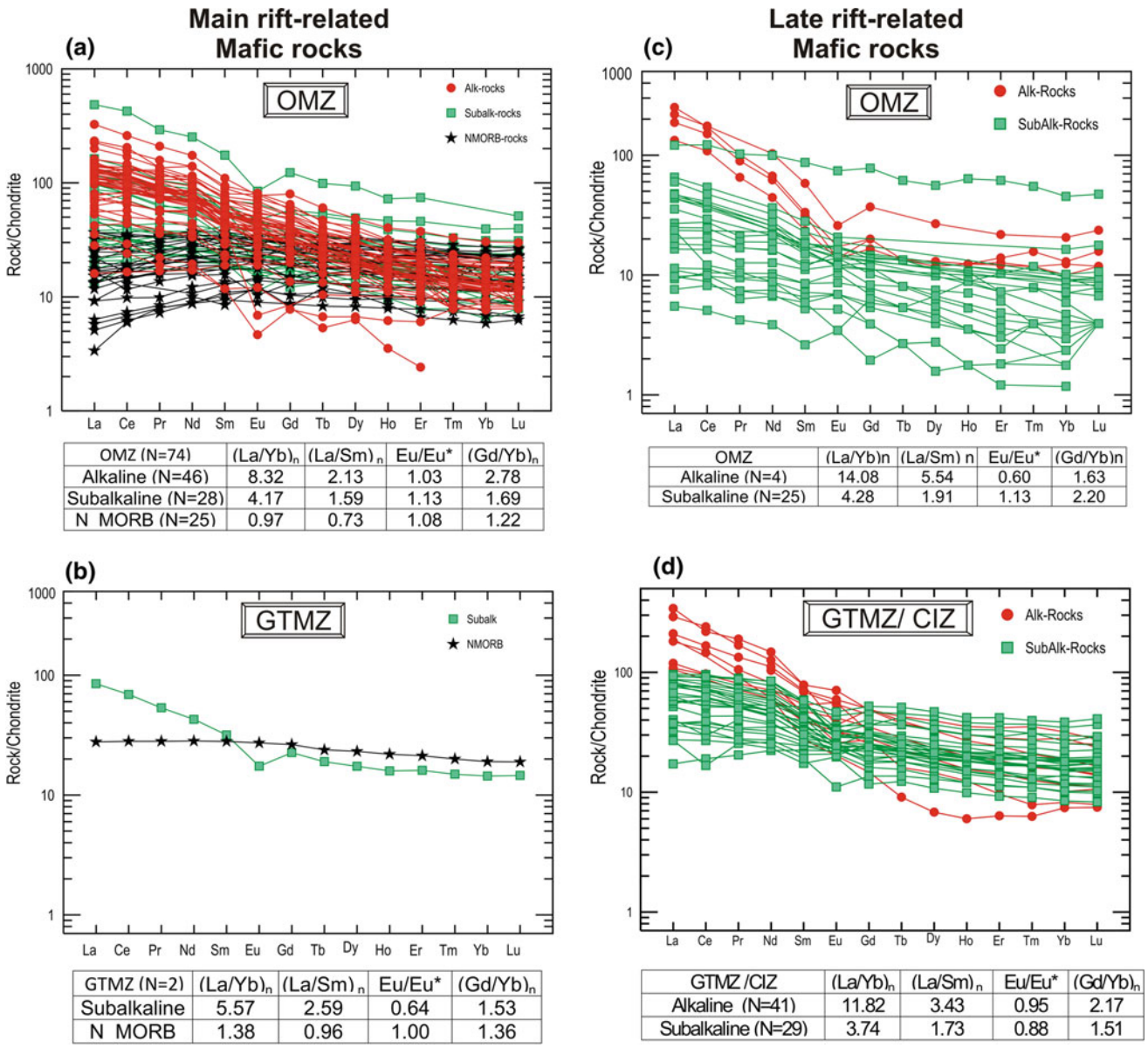

OMZ (N=74)	$(La/Yb)_n$	$(La/Sm)_n$	Eu/Eu*	$(Gd/Yb)_n$
Alkaline (N=46)	8.32	2.13	1.03	2.78
Subalkaline (N=28)	4.17	1.59	1.13	1.69
N MORB (N=25)	0.97	0.73	1.08	1.22

OMZ	(La/Yb)n	(La/Sm) n	Eu/Eu*	(Gd/Yb)n
Alkaline (N=4)	14.08	5.54	0.60	1.63
Subalkaline (N=25)	4.28	1.91	1.13	2.20

GTMZ (N=2)	$(La/Yb)_n$	$(La/Sm)_n$	Eu/Eu*	$(Gd/Yb)_n$
Subalkaline	5.57	2.59	0.64	1.53
N MORB	1.38	0.96	1.00	1.36

GTMZ /CIZ	$(La/Yb)_n$	$(La/Sm)_n$	Eu/Eu*	$(Gd/Yb)_n$
Alkaline (N=41)	11.82	3.43	0.95	2.17
Subalkaline (N=29)	3.74	1.73	0.88	1.51

Fig. 2.12 Chondrite-normalized REE geochemical comparison of different Main and Late rift-related mafic rocks. **a** main rift-related group in the Ossa-Morena Zone; **b** main group in the Galicia-Trás-os-Montes Zone (GTMZ); **c** late group in the OMZ; **d** late group in the GTMZ and CIZ. Normalizing values from Sun and McDonough (1989). Main mean values are included for the different groups (Analytical data tables can be obtained from the corresponding author of this chapter)

In our study 267 samples were taken into account (Bellido et al. 2010; Carrilho Lopes 2004; Castro et al. 1996; Chichorro 2006; Chichorro et al. 2008; Dias da Silva 2013; Galindo 1989; López-Guijarro et al. 2008; Mata and Munhá 1990; Pereira et al. 2006; Ribeiro et al. 1992; Sánchez-García et al. 2003, 2008a, 2010, 2013, 2016; Sarrioanandía et al. 2012). Two major groups are distinguished: (i) mafic rocks, with $SiO_2 < 52\%$, and (ii) acid and intermediate rocks, with $SiO_2 > 52\%$.

2.4.2.1 Mafic Rocks

The mafic rocks vary between plagioclase and amphibole-rich basalts and their respective plutonic equivalents. The mafic rocks show plagioclase albitization accompanied by formation of chlorite, calcite, epidote, prehnite and other low-temperature hydrous minerals typical of the greenschist facies (Sánchez-García et al. 2010). Within this group of rocks ($SiO_2 < 52\%$) three different subgroups are differentiated according to their geochemical

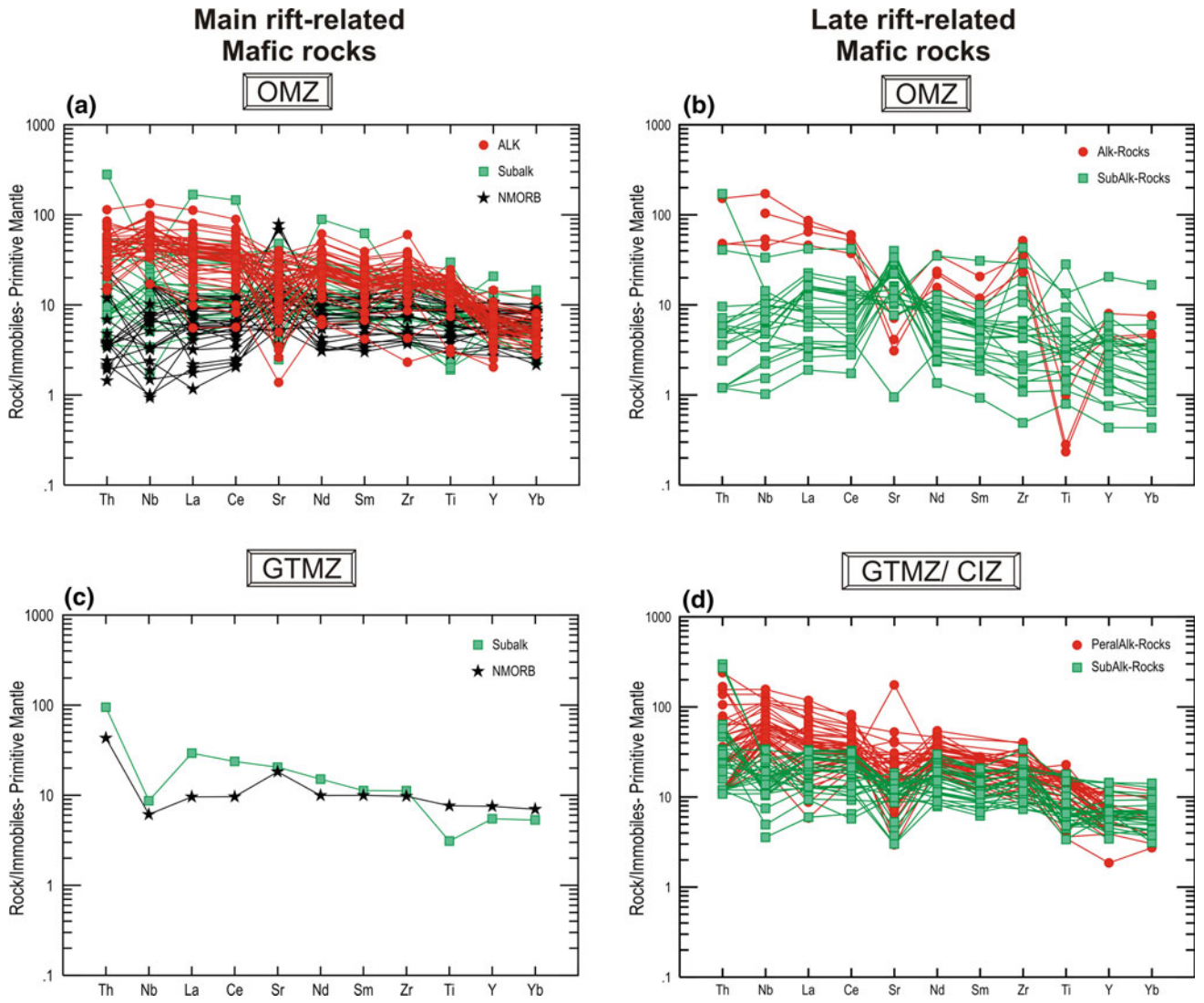

Fig. 2.13 Primitive mantle-normalized spider diagrams (Palme and O'Neill 2004) geochemical comparison of different rift-related mafic rocks. **a** main rift-related group in OMZ; **b** late group in OMZ; **c** main group in GTMZ; **d** late group in GTMZ and CIZ (Analytical data tables can be obtained from the corresponding author of this chapter)

characteristics (Fig. 2.6b): alkaline, sub-alkaline and N-MORB-types. These three subgroups are indistinguishable in the field and petrographycally, and occur intimately associated to each other within the same outcrops.

The **Alkaline group** (OIB affinity) exhibits a wide range (39.13% < SiO_2 < 51.45%) of metaluminous to peraluminous (A/CNK = 0.43–1.34) compositions and includes plutonic, subvolcanic and volcanic rock types. In the Nb/Y versus Zr/Ti diagram of Pearce (1996) the studied samples plot in the alkaline basalt field (Fig. 2.6b), showing characteristics similar to those of oceanic island basalt as indicated by the flat patterns when normalized to average OIB (Sun and McDonough 1989). They present less fractionated values for LREE relative to HREE and a smaller Eu anomaly (Eu/Eu* = 1.03) than sub-alkaline types (Fig. 2.12a). In the spider-diagram normalized to the primitive mantle (Palme and O'Neill 2004; Fig. 2.13a) most of the computed samples show a slight negative Nb anomaly, but some samples show a positive anomaly. The La/Nb, Nb/Y, Th/Yb and Nb/Yb ratios are close to OIB values of Sun and McDonough (1989), although Th/La average ratio is closer to lower continental crust values and Zr/Nb is closer to EMORB (Fig. 2.14a). In the tectonic discrimination diagram of Pearce and Cann (1973) the studied samples plot in the intraplate field (Fig. 2.15a). Geochemical isotopic data of the mafic alkaline types show ε_{Nd} values ranging from +0.8 to +3.8 (Sánchez-García et al. 2010; Sarrioanandía et al. 2012; Fig. 2.11b) indicating a mainly mantle-derived source for these rocks. The Nd T_{DM} values range from 0.83 to 1.58 Ga indicating intermediate residence times in the crust

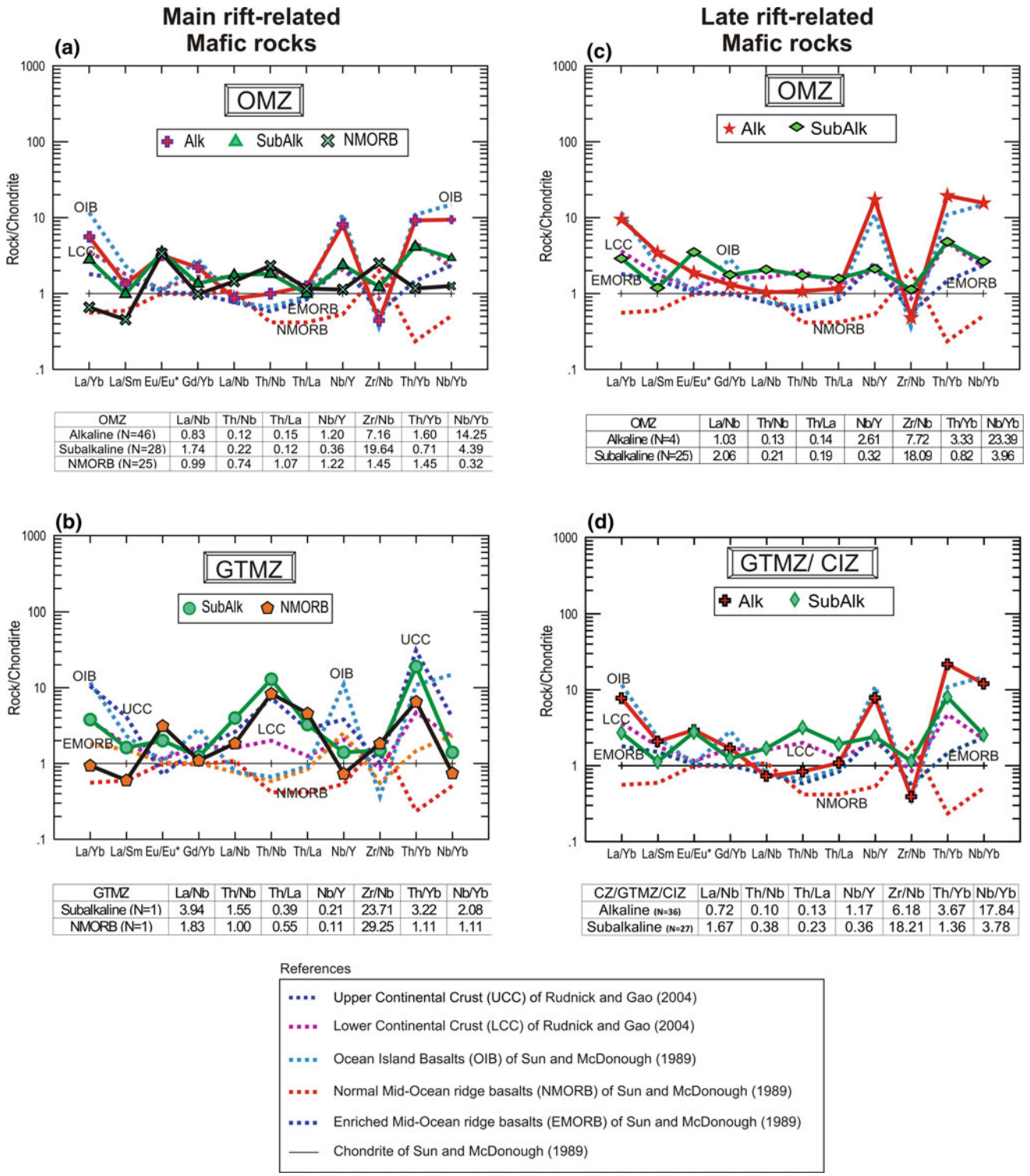

OMZ	La/Nb	Th/Nb	Th/La	Nb/Y	Zr/Nb	Th/Yb	Nb/Yb
Alkaline (N=46)	0.83	0.12	0.15	1.20	7.16	1.60	14.25
Subalkaline (N=28)	1.74	0.22	0.12	0.36	19.64	0.71	4.39
NMORB (N=25)	0.99	0.74	1.07	1.22	1.45	1.45	0.32

OMZ	La/Nb	Th/Nb	Th/La	Nb/Y	Zr/Nb	Th/Yb	Nb/Yb
Alkaline (N=4)	1.03	0.13	0.14	2.61	7.72	3.33	23.39
Subalkaline (N=25)	2.06	0.21	0.19	0.32	18.09	0.82	3.96

GTMZ	La/Nb	Th/Nb	Th/La	Nb/Y	Zr/Nb	Th/Yb	Nb/Yb
Subalkaline (N=1)	3.94	1.55	0.39	0.21	23.71	3.22	2.08
NMORB (N=1)	1.83	1.00	0.55	0.11	29.25	1.11	1.11

CZ/GTMZ/CIZ	La/Nb	Th/Nb	Th/La	Nb/Y	Zr/Nb	Th/Yb	Nb/Yb
Alkaline (N=36)	0.72	0.10	0.13	1.17	6.18	3.67	17.84
Subalkaline (N=27)	1.67	0.38	0.23	0.36	18.21	1.36	3.78

Fig. 2.14 Chondrite-normalized isotope ratios patterns (Sun and McDonough 1989) for mafic rocks. **a** main rift-related group in the Ossa-Morena Zone; **b** main rift-related group in the Galicia-Trás-os-Montes Zone; **c** late rift-related in the OMZ; **d** late rift related in the GTMZ and CIZ. Main mean values are included for the different groups (Analytical data tables can be obtained from the corresponding author of this chapter)

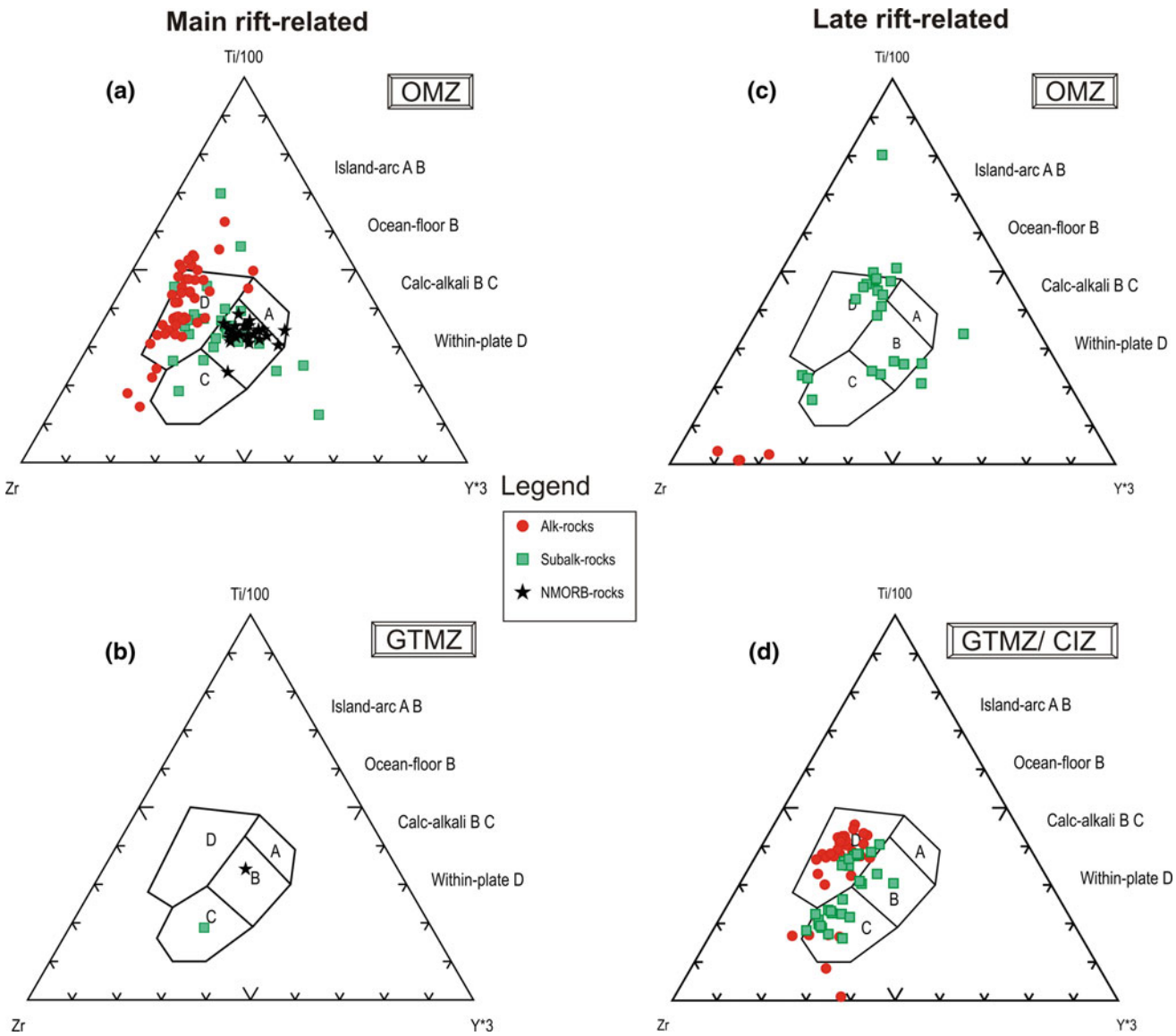

Fig. 2.15 Tectonic discrimination diagrams of Pearce and Cann (1973) for mafic rocks of the different groups. **a** main group in OMZ; **b** main group in GTMZ; **c** late group in OMZ; **d** late group in GTMZ and CIZ (Analytical data tables can be obtained from the corresponding author of this chapter)

(Salman 2004; Sánchez-García et al. (2010, 2013, 2016; Sarrioanandía et al. 2012).

The **Sub-alkaline group** (E-MORB affinity) also presents a wide range of compositions (37.42% < SiO_2 < 51.40%; Fig. 2.6) and have metaluminous to peraluminous characteristics (A/CNK = 0.27–1.27). The REE-chondrite normalized diagram shows a typical E-MORB pattern with lesser fractionation for the LREE and HREE (Fig. 2.12b). A variable Europium anomaly is observed, with an average value of Eu/Eu* = 1.13, as well as light Nb, Sr and Ti anomalies in the spider-diagram (Fig. 2.13a). Negative Sr anomalies could result from plagioclase fractionation or from Sr mobility during metamorphism (Pin et al. 1992). Negative Ti anomalies occur as a result of earlier fractionation of oxide minerals (Pin et al. 1992). Concerning Nd isotopes, the samples show a general pattern similar to that of the lower continental crust in their chondrite–normalized isotope ratios (Fig. 2.14a) and plot in the tholeiitic field in Pearce and Cann (1973) diagram (Fig. 2.15b). Sub-alkaline types display moderate to high ε_{Nd} values ranging from +2.4 to +7.3 (Casquet et al. 2001; Chichorro et al. 2008; Bellido et al. 2010; Sánchez-García et al. 2010, 2016; Fig. 2.11b). The corresponding T_{DM} ages for all samples range from 0.45 to 1.36 Ga. These values point to a mantle source for these rocks. Despite this, the only sample of the Galicia Trás-os Montes Zone (Fig. 2.13c) shows a negative Nb anomaly that

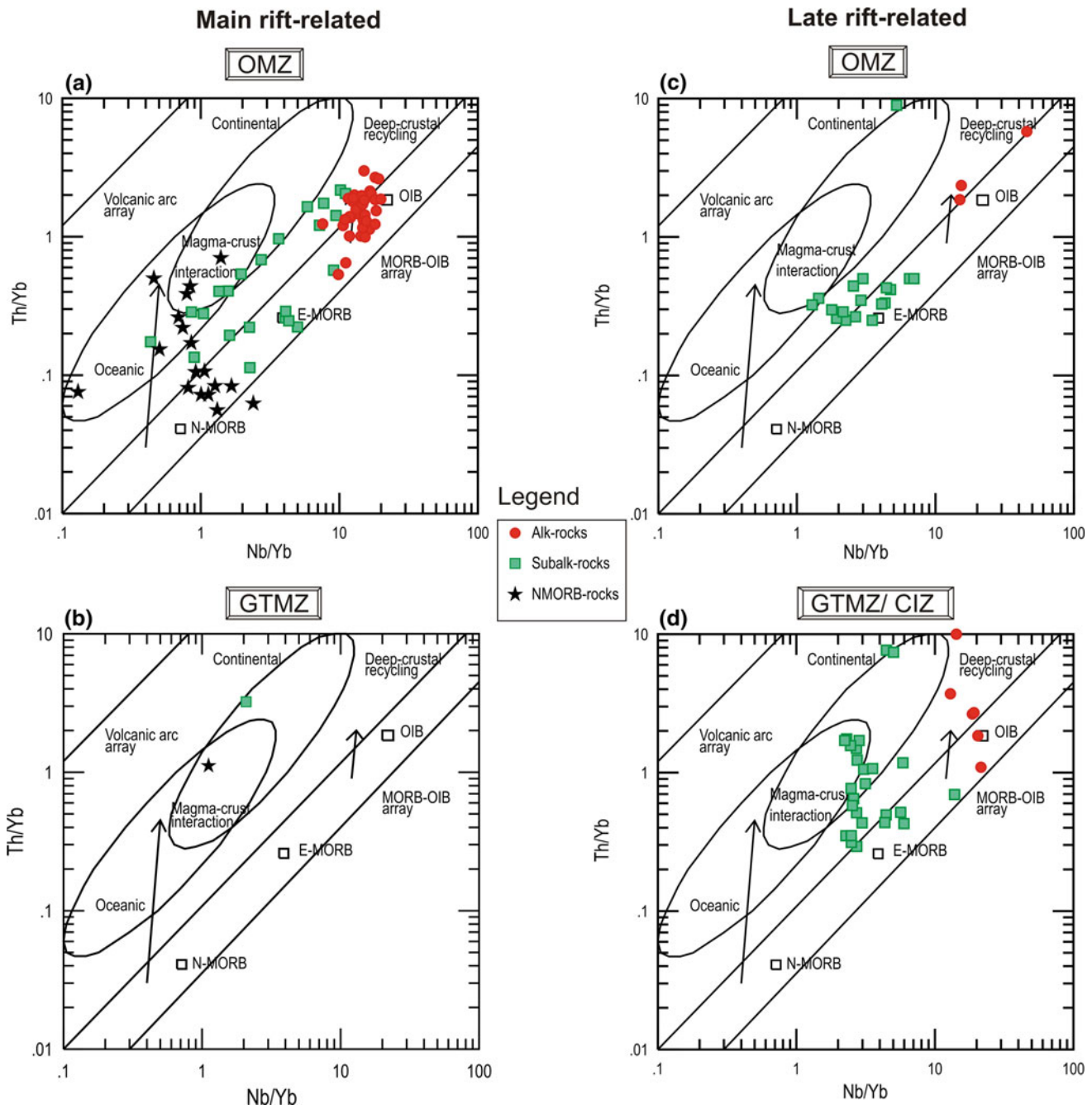

Fig. 2.16 Th/Yb versus Nb/Yb tectonic discriminating diagrams (Pearce 2008) for mafic rocks of the different groups. **a** main group in OMZ; **b** main group in GTMZ; **c** late group in OMZ. **d** Late group in GTMZ and CIZ (Analytical data tables can be obtained from the corresponding author of this chapter)

indicates a crustal component, which is characteristic of basalts in volcanic rifted margins due to processes of magma-crust interaction (Díez Montes et al. 2015).

Finally, the **N-MORB group** is represented by basalts interbedded within the Upper Detrital Group in the Ossa-Morena Zone and by the Mora Volcanic Complex in the Galicia-Trás-Os-Montes Zone (Fig. 2.4). This group shows a smaller range in silica content (43.06% < SiO_2 < 51.77%; Fig. 2.6b), a chondrite-normalized flat to negative slope REE pattern and no Europium anomalies (Eu/Eu* = 1.08; Fig. 2.12a). In the spider diagram, Nb exhibits a slightly negative to flat pattern, which is also almost flat for the rest of elements (Fig. 2.13a). Together, these data suggest some degree of crustal contamination, opposite to most alkaline (OIB) types which do not show negative Nb anomalies. In turn, the sub-alkaline types

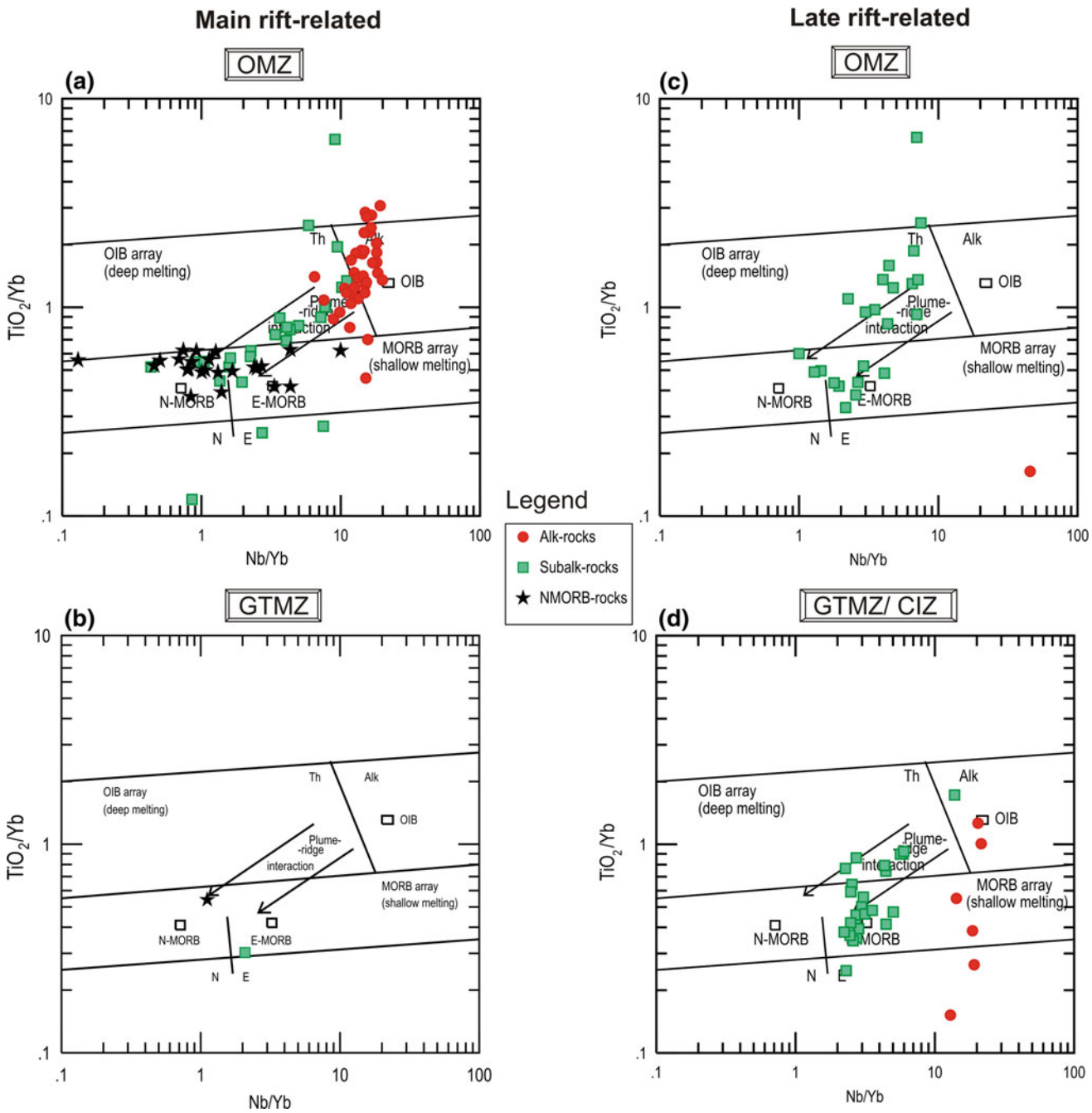

Fig. 2.17 TiO_2/Yb versus Nb/Yb tectonic discrimination diagrams (Pearce 2008) for mafic rocks of the different groups. **a** main group in OMZ; **b** main group in GTMZ; **c** late group in OMZ. **d** late group in GTMZ and CIZ (Analytical data tables can be obtained from the corresponding author of this chapter)

(E-MORB) have intermediate values between the OIB and N-MORB groups. Chondrite–normalized isotope ratios of the N-MORB group samples show a general pattern similar to average N-MORB but with enrichment in Th/Nb, Th/La, Nb/Y, Th/Yb and Nb/Yb (Fig. 2.14a), also suggesting some crustal contamination in their source. They show tholeiitic/MORB characteristics in the Pearce and Cann (1973) tectonic discrimination diagram (Fig. 2.15a). The difference between the three types of basalt is well reflected in the Th/Yb versus Nb/Yb diagrams (Pearce 2008; Fig. 2.16a). All of them display some samples displaced to higher Th/Yb values (Fig. 2.17c), which is distinctive of a recycled crustal component according to Pearce's criteria (2008). This N-MORB group yields the highest ε_{Nd} values of the *Main rift-related event* rocks, from +5.2 to +9.2, and the lowest T_{DM} values (0.54–1.06 Ga) (Casquet et al. 2001;

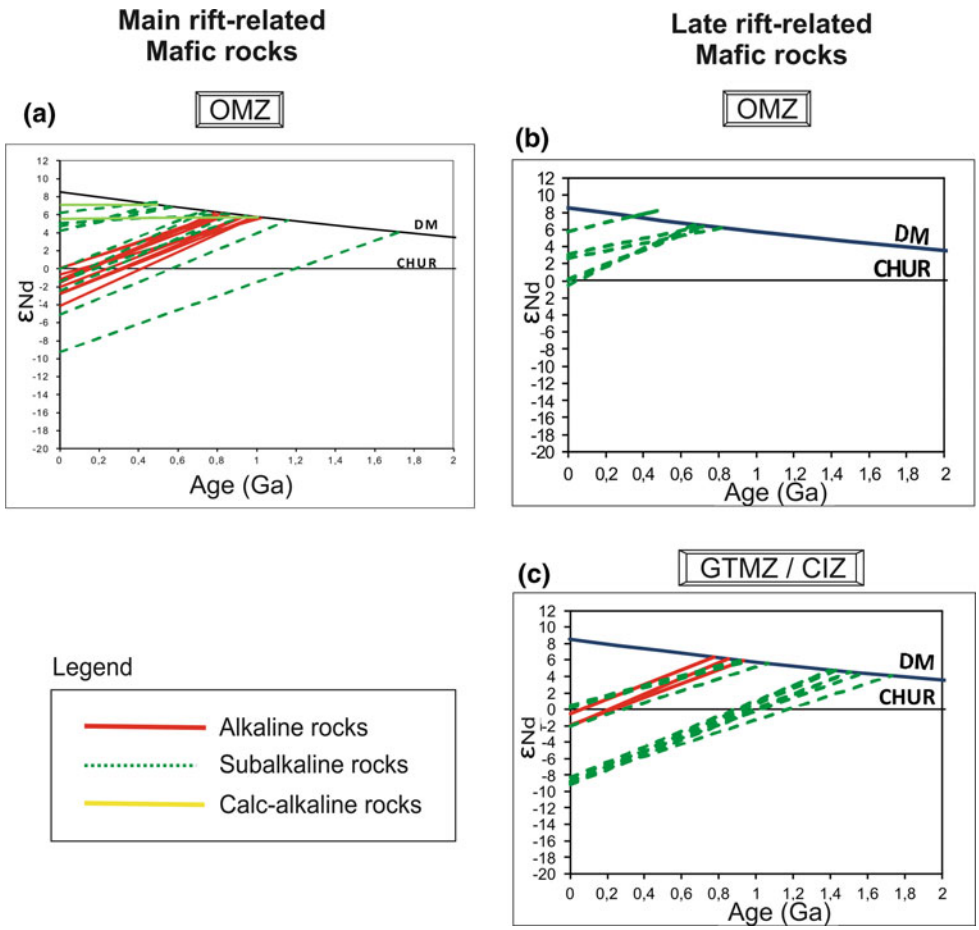

Fig. 2.18 $\varepsilon_{Nd(t)}$ versus age diagram (DePaolo and Wasserburg 1976; DePaolo 1981) for mafic rocks of different rift-related groups. **a** main group in OMZ; **b** late group in OMZ; **c** late group in GTMZ and CIZ (Analytical data tables can be obtained from the corresponding author of this chapter)

Bellido et al. 2010; Chichorro et al. 2008; Sánchez-García et al. 2010, 2013, 2016; Sarrioanandía et al. 2012; Fig. 2.18a). These values are indicative of a main mantle source and very low crustal residence times, and suggest that the aforementioned crustal contamination component must have been minor.

2.4.2.2 Acid and Intermediate Rocks

This group constitutes a very heterogeneous set ranging in composition from andesites to rhyolites and their respective plutonic equivalents (52% < SiO_2 < 82%). The felsic rocks have high alkali contents, varying between potassic and sodic end-members and include, among the volcanics, lavas (locally with peperitic contacts), autobreccias, tuffs and some ignimbrites with glass shards, K-feldspar and quartz crystals and lithic fragments in a devitrified fine-grained groundmass (Sánchez-García et al. 2003, 2008a, 2010). The most acid types predominate by far. Felsic volcanic rocks also show evidence of the same sort of alteration than the mafic rocks, related to a combination of sea-water interaction, syn-to-post eruption hydrothermalism and low-grade metamorphism during the Variscan orogeny. The result is the retrogradation of the original igneous minerals to parageneses with albite or albite-oligoclase, epidote, chlorite and calcite (Sánchez-García et al. 2010). We distinguish two different subgroups, according to their geochemical characteristics (Fig. 2.6b): alkaline (OIB-affinity) and sub-alkaline-tholeiitic (E-MORB affinity). These two subgroups are indistinguishable in the field and petrographically, and they occur intimately associated to each other within the same outcrops. In some cases there is evidence for simultaneous emplacement of felsic and mafic rocks, both in the volcanic as in the plutonic/subvolcanic environments (Sánchez-García et al. 2010).

The **alkaline and peralkaline types** (OIB affinity) are only found in the Ossa Morena Zone. Most are alkaline but some peralkaline rocks also exist. The alkaline types exhibit a wider range (52% < SiO_2 < 82.40%) of compositions and present a wide variation in the A/CNK content (A/CNK = 0.20–12.34). In the Nb/Y versus Zr/Ti diagram (Pearce 1996) they plot in the alkaline and peralkaline field (Fig. 2.6b) being classified as trachyandesites, trachytes and alkaline rhyolites. REE patterns present more fractionated values for LREE than HREE and Eu anomalies vary from moderate to strongly negative values (see Fig. 2.7b). In the spider-diagram (Fig. 2.8b) they show a slightly negative Nb

anomaly and strongly negative Sr and Ti anomalies. Nb/Y, Th/Yb and Nb/Yb average ratios are close to OIB values of Sun and McDonough (1989), although the Th/Nb and Zr/Nb average ratios are closer to lower continental crust values and the Th/Yb average ratio is closer to bulk continental crust values (Fig. 2.9b). These results could indicate a certain degree of crustal contamination. In the tectonic discrimination diagram of Pearce et al. (1984), most samples plot in the within-plate field (Fig. 2.10b) but some plot in the volcanic arc and anomalous within-plate fields. The acid and intermediate alkaline samples display negative to positive ε_{Nd} values, ranging from −3.5 to +4.0 (Salman 2004; Sánchez-García et al. 2010, 2016; Sarrioanandía et al. 2012; Fig. 2.11b). The corresponding T_{DM} ages vary between 0.74 and 2.59 Ga. These characteristics indicate a possible mantle source for the primitive magmas, but with variable degrees of contamination with continental crust components (Sánchez-García et al. 2010).

The **sub-alkaline-tholeiitic types** (E-MORB affinity) include samples from the Ossa-Morena and Galicia-Trás-Os-Montes zones. They also show a wide range (53.27% < SiO_2 < 78.5%) of compositions and correspond to metaluminous to peraluminous types (A/CNK = 0.52–2.91). According to the Nb/Y versus Zr/Ti diagram (Pearce 1996) they are classified as andesites, basaltic andesites, rhyolites and dacites (Fig. 2.6b, c). REE patterns show more fractionation of LREE than HREE and typical Eu anomaly (Eu/Eu* = 0.57–063; Fig. 2.7b, c). In the spider-diagram (Fig. 2.8b, c) they show a slight negative anomaly of Nb and strong negative anomaly of Sr and Ti, which could indicate crustal participation in the source. The sub-alkaline rocks present an overall pattern close to the values of the upper continental crust (Rudnick and Gao 2003), although they have Nb/Y and Nb/Yb average ratios somewhat lower than the LCC values (Fig. 2.9b, c). This could indicate a certain degree of crustal contamination and recycling of materials. In the tectonic discrimination diagram of Pearce et al. (1984), most samples plot in the volcanic arc field (Fig. 2.10b) but some OMZ samples plot in the anomalous within-plate or ocean-ridge fields. The rocks of this subgroup display ε_{Nd} values ranging from −5.4 to +2.2 (Chichorro et al. 2008; López-Guijarro et al. 2008; Sánchez-García et al. 2010, 2016; Fig. 2.11b), indicating crustal and mantle participation in their genesis and high times of residence in the crust. All these features suggest heterogeneous sources with different proportions of crustal and mantle contributions. Inconsistencies in the geodynamic characterization are interpreted as a reflection of the complexity of their genesis, which involved mantle and crustal components and, on the other hand, as due to the possibility that some geochemical parameters may be partly inherited from the rocks at the sources (Bellido et al. 2010).

In conclusion, the rocks formed during the *Main rift-related igneous event* show a wide spread in composition and geochemical characteristics, including alkaline and sub-alkaline types, which suggests contribution of magmas derived from various sources. Magmas generated in the crust add to those derived from depleted and OIB mantle sources, the latter eventually contaminated during ascent by mixing/assimilation with/of crustal magmas or rocks (Ribeiro et al. 1997; Sánchez-García et al. 2003, 2008a, b, 2010; Pereira and Quesada 2006; Chichorro et al. 2008; Sarrioanandía et al. 2012; Dias da Silva 2013; Díez Montes et al. 2015).

2.4.3 Late Igneous Event

This third rift-related igneous event is for the first time well represented in Iberian Massif's zones away from the Ossa-Morena rift axis (CIZ, GTMZ, WALZ and CZ). In fact, its main representative, the Ollo de Sapo Formation, occurs in the northern Central-Iberian Zone, close to its contact with the West Asturian-Leonese Zone (Fig. 2.1). Stratigraphically this event spanned from the late Furongian through the Floian (ca. 490–470 Ma) and includes volcanic, subvolcanic and plutonic rocks. Geochronological data show Furongian-Early Ordovician ages between 495 and 460 Ma (Lancelot and Allegret 1982; Ribeiro et al. 1995; Vialette et al. 1986; Ochsner 1993; Valverde-Vaquero 1997; Valverde-Vaquero and Dunning 2000; Expósito et al. 2003; Valverde-Vaquero et al. 2005; Bea et al. 2006; Díez-Montes 2006; Solá 2007; Zeck et al. 2007; Montero et al. 2007, 2009a, b; Solá et al. 2008; Preto-Gomes et al. 2008; Antunes et al. 2008, 2012; Talavera et al. 2008, 2013; Gomes et al. 2009; Neiva et al. 2009; Romão et al. 2010; Coke et al. 2011; Navidad and Castiñeiras 2011; Pereira et al. 2012b; Rubio-Ordóñez et al. 2012; López-Sánchez et al. 2012; Díez Fernández et al. 2012a, 2014; Dias da Silva 2013; Farias et al. 2014; Henriques et al. 2015; Teixeira et al. 2015; Urbano et al. 2015; Orejana et al. 2016; Villaseca et al. 2016; Azor et al. 2016).

In the Ossa-Morena Zone this late rift-stage event occurs mainly in northern sectors (Alter do Chão-Elvas-Cumbres Mayores and Tomar-Badajoz–Córdoba shear zone, including the Cevadais, Aceuchal, Almendralejo and Ribera del Fresno massifs (alkaline belt of northern ZOM, see Figs. 2.1 and 2.5). Here, peralkaline and alkaline granitoids are found in close relation with alkaline mafic rocks, such as amphibolites, gabbros, and ultramafic rocks (Assunção 1956; Assunção and Gonçalves 1970; Carrilho Lopes 2004).

In the Central Iberian Zone the late magmatism has greater expression and mainly developed along two main belts: near its northern boundary with the WALZ (Ollo de

Sapo Formation and correlative plutons; 470–495 Ma in age; Bea et al. 2006; Montero et al. 2007, 2009a, b; Díez Montes et al. 2010) and near its southern boundary with the OMZ (Urra Formation, similar but less voluminous and more ephemeral than the Ollo de Sapo; 488–495 Ma in age; Solá et al. 2008). Also within the CIZ, middle-to upper crustal plutonic bodies exhumed during the Variscan orogeny also occur in the Spanish Central System and along the Beira-Baixa Estremadura belt (see Fig. 2.1). This latter lineament includes unmetamorphosed and almost undeformed tonalite-granodiorite igneous bodies, previously believed to be Variscan: plutons of Gouveia (Neiva et al. 2009), Oledo (Antunes et al. 2008) and Zarza la Mayor (Rubio-Ordóñez et al. 2012). Rocks in these two lineaments are largely felsic in composition but connections with the mantle of their respective feeding systems are indicated by the local presence of volumetrically minor mafic rocks.

In the Galicia Trás-os Montes Zone this event is represented by calc-alkaline, alkaline and peralkaline rocks (Floor 1966; Ribeiro 1987a; Pin et al. 1992; Montero and Bea 1998; Montero et al. 2009a, b; Abati et al. 2010; Díez Fernández et al. 2012a; Dias da Silva 2013).

For this study, published results from 322 samples were taken into account (Antunes et al. 2008; Carrilho Lopes 2004; Cordani et al. 2006; Dias da Silva 2013; Díez-Montes 2006; ENRESA, unpublished data; González-García et al. 2011; Mata et al. 1999; Montero and Bea 1998; Montero et al. 2007, 2009b; Ochsner 1993; Pin et al. 1992; Ribeiro 1987a, b; Solá 2007; Solá et al. 2008; Villaseca et al. 2015, 2016). Although acid and intermediate rocks largely predominate, mafic rocks are also present.

2.4.3.1 Mafic Rocks

Within this group we have found two different subgroups according to their geochemical characteristics: alkaline and sub-alkaline/tholeiitic (Fig. 2.6c).

The **alkaline group** (OIB affinity) is represented in the OMZ (Carrilho Lopes 2004) and in the GTMZ (Floor 1966; Ribeiro 1987a; Pin et al. 1992; Montero and Bea 1998; Montero et al. 2009a; Dias da Silva 2013). Metaluminous (A/CNK = 0.78–0.99) alkaline basalts of this group (Fig. 2.6c) present more fractionated values for LREE than HREE and a smaller Europium anomaly (Eu/Eu* = 0.95; Fig. 2.12c, d) than the sub-alkaline types. In the spider diagram they show slight negative anomalies of Sr and Ti but not in Nb (Fig. 2.13b, d). Chondrite-normalized isotope ratios patterns are close to the values of OIB basalts of Sun and McDonough (1989) with some enrichment in La/Nb, Th/Nb and Th/Yb (Fig. 2.14c, d). In the tectonic discrimination diagram of Pearce and Cann (1973) most samples from the GTMZ plot in the within-plate field (Fig. 2.15d), while in the Th/Yb versus Nb/Yb diagrams of Pearce (2008), a small contamination by deep-crustal recycling can be ascertained (Figs. 2.16c, d and 2.17c, d). Concerning Nd isotope data, this group yields moderate positive to negative ε_{Nd} values, from +3.8 to −3.8, and low to moderate T_{DM} values (0.78–0.93 Ga) (Pin et al. 1992; Carrilho Lopes et al. 2008; Fig. 2.18b, c). This is compatible with a lithospheric mantle source and small times of residence in the crust. According to Pin et al. (1992) some crustal assimilation may have accompanied the differentiation of the basaltic magmas. Carrilho Lopes et al. (2008) found that the mafic and felsic igneous rocks of this group spatially associated in the Elvas region (OMZ) do not represent a comagmatic suite. The felsic facies ($+2.5 < \varepsilon_{Nd480} < +3.4$) reflect petrogenesis associated with time integrated depleted mantle sources, whereas surprisingly the mafic ones ($-3.8 < \varepsilon_{Nd480} < -1.1$) derived from time-integrated enriched sources, which may have a mantle origin but probably affected by strong crustal contamination.

The **sub-alkaline/tholeiitic group** (E-MORB affinity) is exposed along all the aforementioned belts in the OMZ, GTMZ and CIZ (Mata et al. 1999; Carrilho Lopes 2004; Solá 2007; Antunes et al. 2008; Talavera et al. 2013; Villaseca et al. 2015; Henriques et al. 2015; Orejana et al. 2016. It consists of metaluminous to peraluminous (A/CNK = 0.34–1.73) rocks that plot in the sub-alkaline field (Fig. 2.6c). However, according to Carrilho Lopes 2004, the presence of kaersutite and the chemistry of diopsidic pyroxenes in some of these rocks reveal the alkaline character of the parental magmas, despite plotting in the subalkaline field, and they are related and coeval with peralkaline felsic rocks (see below). Rocks in this group present less fractionated values for LREE than HREE and no Europium anomaly (Eu/Eu* = 1.13) (Fig. 2.12c, d). Also, no Nb anomaly is detected (Fig. 2.13b, d). They exhibit an overall pattern close to values of the lower continental crust, with slight enrichment in the Th/Nb, Th/La, Nb/Y and Th/Yb (Fig. 2.14c, d). In the tectonic discrimination diagram of Pearce and Cann (1973) two subgroups exist, one with within-plate affinity and other with ocean-floor affinity (Fig. 2.15c, d). Slight evidence of magma-crust interaction (Fig. 2.16c, d) as well as association with plume-ridge interaction processes (Fig. 2.17c, d) can be detected. Isotopic compositions vary depending on the location, and refect contrasting petrogenetic processes in each case. On one end, rocks in the northern OMZ show a narrow range of isotopic composition: $^{87}Sr/^{86}Sr$ = 0.7030–0.7045 and high ε_{Nd} (+8.2 to +4.7), compatible with a source in the lithospheric mantle (Carrilho Lopes 2004; Henriques et al. 2015), also indicated by short residence times in the crust (T_{DM} = 0.34–0.83 Ga; Fig. 2.18b). On the other end, rocks in the Spanish Central System (CIZ) yielded ε_{Nd} negative values (−5.1 to −3.8) and higher T_{DM} = 1.40–1.71, suggesting important crustal contamination (Talavera et al. 2013; Fig. 2.18c). Intermediate values were reported from the

Carrascal pluton, also in the CIZ, with ε_{Nd} positive values (+3.3 to +1.3) and T_{DM} = 0.91–1.07 (Solá 2007).

2.4.3.2 Acid and Intermediate Rocks

This group constitutes a very heterogeneous set ranging in composition from rhyolites to andesites, and their respective plutonic/subvolcanic equivalents. Volcanic types are represented by various kinds of tuffs, ignimbrites and lavas. In areas subjected to penetrative deformation and metamorphism, both plutonic and volcanic types were transformed to various kinds of orthogneisses and felsic amphibolites. Within this group we have considered published results from samples with 57 < SiO_2 < 79%, in which three subgroups: alkaline, sub-alkaline and calk-alkaline may be distinguished.

Within the **alkaline group** (OIB affinity) peralkaline rocks are also present. Rocks in this group are metaluminous to peraluminous with a wide variation in the A/CNK contents (A/CNK = 0.59–1.31). In the Nb/Y versus Zr/Ti diagram they plot in the alkaline and peralkaline field (Fig. 2.6c), being classified as trachyandesites, trachytes and alkaline rhyolites. REE patterns present more fractionated values for LREE than HREE, average Eu anomalies vary from moderate to strongly negative values (Fig. 2.7d) and average REE compositions are close to the upper continental crust of Rudnick and Gao 2003 (Fig. 2.9d). Some samples are extremely rich in REE, which is typical of peralkaline provinces (Pin et al. 1992). They also show a slightly negative Nb anomaly and strongly negative anomaly of Sr and Ti (Fig. 2.8d, e). These characteristics could indicate a certain degree of crustal contamination and strong fractionation of plagioclase. In the Nb versus Y tectonic discrimination diagram most samples plot in the within-plate field (Fig. 2.10d, e), but some plot in the volcanic arc and anomalous within-plate fields. As in the previous group, Nd isotope results in the acid and intermediate rocks group display varying results depending on their location. Positive ε_{Nd} values (+4.8 to +2.6) and T_{DM} = 0.61–1.13 were obtained by Carrilho Lopes (2004) in OMZ samples (Fig. 2.18b). These data were interpreted as due to a petrogenesis associated with time integrated depleted mantle sources (Carrilho Lopes et al. 2008). Opposite to this area, Antunes et al. (2008) and Talavera et al. (2013) reported ε_{Nd} values ranging from +5.3 to −5.1 (Fig. 2.18c) and T_{DM} values between 0.78 and 2.23 Ga in different areas of the CIZ. The authors considered that magmas from various distinct sources might have been involved, from more primitive mantle magmas to more evolved crustal magmas, with very different times of residence in the crust, complicated by interaction among the magmas from the various sources. Partial melting of Ediacaran-lower Cambrian igneous rocks was envisaged by Talavera et al. (2013) as a suitable source for the metagranites and metavolcanic rocks of this group in Central and NW Iberia.

Within the *Late magmatic event*, the **sub-alkaline group** (E-MORB affinity) is the least represented and consists of metaluminous trachyandesites, trachytes and alkaline rhyolites that plot in the sub-alkaline field in the Nb/Y versus Zr/Ti diagram of Pearce (1996) (Fig. 2.6c). REE patterns present more fractionated values for LREE than HREE and average Eu anomalies vary from moderate to strongly negative values (see Fig. 2.7d, e). In the spider-diagram of Palme and O'Neill (2004) they show negative anomalies of Nb, Sr and Ti (Fig. 2.8d, e). LREE, Nb/Y, La/Nb, Th/Nb and Th/La average ratios are generally close to lower continental crust values (Fig. 2.9d, e). In the tectonic discrimination diagram of Pearce et al. (1984), most OMZ samples plot in the anomalous within-plate field (Fig. 2.10d), whereas those from the CIZ plot in the volcanic arc, I type field (Fig. 2.10e). This group presents a large dispersion in the ε_{Nd} values (+3.5 to −5.2) (Fig. 2.11d) that might indicate involvement of different sources of magmas (López-Guijarro et al. 2007; Antunes et al. 2008; Orejana et al. 2016). ε_{Nd} values between +4.4 and +6 in the Tenzuela massif (CIZ) are exceptional and Villaseca et al. (2015) interpreted that they imply melting of an isotopically depleted mantle.

The **calk-alkaline group** is by far the most represented, as it includes the most extensive volume of igneous rocks along the Ollo de Sapo belt, which extends along the southern limb of the Cantabrian arc for more than 500 km, from the Cantabrian coastline to the eastern end of the Spanish Central System (see Fig. 2.1). Most of what follows comes from Ollo de Sapo rock samples but other samples from the OMZ, GTMZ and CIZ are also taken into account. All rocks in this group are peraluminous (Fig. 2.6c) and vary in composition from andesites to high-silica rhyolites. REE patterns present more fractionated values for LREE than HREE and average Eu anomalies vary from moderate to strongly negative values, reflecting significant plagioclase crystallization (Fig. 2.7d). They also show negative anomalies of Nb, Sr and Ti (Fig. 2.8d, e). Overall chondrite-normalized patterns are close to the values of the upper continental crust, with slight enrichment in the Th/Nb, Th/La and Th/Yb ratios (Fig. 2.9d, e). In the tectonic discrimination diagram of Pearce et al. (1984) they plot in the volcanic arc, I-type field (Fig. 2.10d, e). ε_{Nd} values range from +2.6 to −5.9 and T_{DM} vary between 0.12 and 2.6 Ga.

All the above geochemical features suggest crustal sources for their parental magmas despite their volcanic arc affinity, which can be also attributed to partial melting of crustal protoliths with volcanic arc signature due to the rise of mafic magmas in extensional environments (Ribeiro 1987a, b, 1991; Díez-Montes 2006; Solá 2007; Solá et al. 2008; Díez Montes et al. 2015). The almost exclusively

felsic, peraluminous, calc-alkaline arc affinity compositions of the rocks in this group resemble very much those described in the Ossa-Morena Zone (e.g. the Bodonal Formation) during the *Early rift-related igneous event* (see above under Sect. 2.4.1). Alike in the latter case and following Sánchez-García et al. (2003), the arc-like signature may be inherited from the crustal source (Ribeiro 1987a; Ribeiro and Floor 1987; Santos Zalduegui et al. 1995; Montero et al. 2009a, b; Montero and Floor 2004; Díez Montes et al. 2010; Orejana et al. 2017). However some authors have interpreted these rocks as truly formed in a subduction environment (Valverde-Vaquero and Dunning 2000; von Raumer et al. 2003; Navidad and Bea 2004; Villaseca et al. 2015) but this interpretation is difficult to reconcile with their location (several hundred km) away from the continental margin and their transitional relationships with the interbedded sediments, the Armorican Quartzite Formation in particular, which extends both inboard and outboard throughout the Iberian Massif at the beginning of the passive margin phase. Also, the presence of space-related and contemporaneous plutonic and volcanic peralkaline rocks coeval with the crustal anatexis favours an anorogenic setting. Most of the igneous activity of this event took place in fact after continental breakup and opening of the Rheic Ocean, dated at ca. 489 Ma ago (Díez-Montes 2006; López-Guijarro et al. 2007). We include it in this section as, according to the characteristics of its constituent rocks, the processes involved in their genesis probably represent late waning stages of those taking place before breakup. In fact, a continuation of the *Main rift-related igneous event* may be inferred in the Ossa-Morena Zone if attention is paid to the plutonic rocks. Also the sources of the magmas (mantellic and crustal) mimic those described in the other two previous events.

In the Ossa-Morena Zone this event exhibits rather different characteristics. It is represented by a bimodal association that contains both felsic and mafic compositions that appears as volcanic and plutonic types. Noteworthy, peralkaline rocks, though present within the *Main rift-related igneous event* (Sánchez-García et al. 2003, 2008a, b), are much more common during this *Late event*, and coeval with the triggering of the first steps of rifting in the Central Iberian Zone, evidenced by the predominantly peraluminous magmatism that has just been reviewed in the previous paragraphs.

This *Late igneous event* was also recorded during Early Ordovician times in the eastern Pyrenees and northern Montagne Noire and also constitutes the first and main event there, therefore reinforcing the interpretation of rift propagation in this direction (see above under Sect. 2.1; Álvaro et al. 2007, 2013a, 2014). Finally, the Cambrian-Early Ordovician magmatism of the Iberian massif, together with that of many other areas in the Variscan belt (Pyrenees, Armorican massif, Montagne Noire, Sardinia, Saxo–Thuringian Zone), may define a large igneous province (LIP) similar to those described by Bryan et al. (2002), heralding continental breakup and terrane dispersion along the northern Gondwanan margin during the Furongian–Early Ordovician (Díez Montes et al. 2010).

2.4.4 Geodynamic Context of the Rift-Related Magmatism

The Cadomian subduction process that was active during the Ediacaran in West Gondwana had an abrupt end across the Ediacaran-Cambrian transition (Murphy et al. 2006; Linnemann et al. 2008; Nance et al. 2008, 2010; Sánchez-García et al. 2003, 2008a, 2010; Pereira et al. 2006, 2008b, 2011, 2012b). In Iberia, the first evidence of the new conditions is provided by the ca. 533–530 Ma gap recorded in the Ossa-Morena Zone, promoted by ongoing uplift and erosion, which resulted in variable exhumation of previously deformed Ediacaran-Fortunian successions making up the Cadomian basement (see Fig. 2.3a). This uplift event, which initiated passive, gravitationally-driven extensional processes, has been interpreted as a response to thermal expansion of the upper plate triggered by the previous subduction of a mid-ocean ridge and opening of a slab window after locking of subduction of the hot and buoyant lithosphere along the ridge (Sánchez-García et al. 2003, 2008a, 2010). If the slab window scenario is correct, it would have triggered the onset of thermal erosion of the lithospheric root and lithospheric thinning as a consequence of it, ponding of asthenospheric magmas at the base of the upper plate lithosphere and a strong modification of the regional geothermal gradient. Evidence supporting this interpretation is provided by the so-called *Early rift-related igneous event* . This is characterized by felsic igneous rocks of broadly calk-alkaline arc affinity, probably inherited from their crustal source, the Cadomian arc rocks of the Ossa-Morena Zone (Sánchez-García et al. 2003, 2008a, 2016). This was coeval and partly sourced in middle crustal migmatitic rocks, such as those occurring at the core of inferred metamorphic core complexes along the Monesterio antiform that have been referred to in the previous section (see Fig. 2.3b). The absence of significant mantle-derived lavas at this stage may be due to softening of the lower crust by massive partial melting that prevented propagation of fissures and dikes (Sánchez-García et al. 2003, 2008a).

As indicated above, passive extension added to the above scenario soon after, probably related to slab-pull forces created by the initiation of subduction of the Iapetus and Proto-Tethys oceans beneath Laurentia and Baltica, respectively (von Raumer et al. 2003; Stampfli et al. 2002; Keppie

et al. 2003; Stampfli and Borel 2004; Keppie 2015). As a result the area was affected by passive extension. It was then when a large volume of magma was emplaced into upper crustal environments. Underplating and temporal storage of mantle-derived magmas would have resulted in strong differentiation through crystal fractionation and assimilation and mixing of lithospheric and crustal rocks and melts, which in turn enhanced partial melting in the lower crust. Renewed injection of more primitive melts into these chambers is suggested by the alternating nature of the magmas erupted at the surface. The eruptive/intrusive rocks emplaced in the upper crust of the Ossa Morena Zone from magmas derived from mantle and crustal sources constitutes the *Main rift-related igneous event* of Sánchez-García et al. (2003, 2008a, 2010). Magmatic ascent was probably facilitated by coeval normal faulting that was also responsible for the collapse of the pre-existing platforms recorded during deposition of the Upper Detrital Group (Fig. 2.3c). Massive emplacement of mafic magma into the crust at this stage would have caused renewed thermal expansion, uplift and erosion leading to formation of the Toledanian gap. Subsequent thermal collapse was responsible for the rapid inundation of the Ossa-Morena Zone recorded by the Early Ordovician transgression (see above under Sect. 2.3; Sánchez-García et al. 2003, 2008a). This marks the onset of passive margin conditions in most of the area and is taken as evidence for the existence of a significant tract of new oceanic lithosphere, consistent with its interpretation as a breakup unconformity (Quesada 1991, 1992).

Subsequent to the opening of the new oceanic domain, thought to belong to the Rheic Ocean (Murphy et al. 2006; Pereira et al. 2007, 2012a; Chichorro et al. 2008; Sánchez-García et al. 2003, 2008a, 2010; Linnemann et al. 2008; Nance et al. 2010; Díez-Montes et al. 2008, among others), extension and magmatism progressively migrated and affected innermost parts of Gondwana, giving rise to the formation of the Cantabro-Iberian Basin (Pérez-Estaún et al. 1990; Martínez Catalán et al. 1992; Díaz-García 2002; Valverde-Vaquero et al. 2005; Díez-Montes 2006; Murphy et al. 2008; see Fig. 2.3d). This propagation can be explained as a result of the widening of the underlying slab window towards inner parts of the upper plate (Gondwana) that was probably drifting westwards. The associated magmatism (*Late rift-related igneous event*) only reached the initial evolutionary stages, similar to the *Early* event in the Ossa Morena Zone but with an additional component of alkaline/peralkaline rocks, compatible with its post-breakup nature. The diachronous character of the three rift-related magmatic events is schematically depicted in Fig. 2.19.

2.5 Characterization of Sedimentary and Igneous Sources Through Zircon Geochronology

Detrital and xenocrystic-inherited zircon grains from some Cambrian-Lower Ordovician stratigraphic successions of the OMZ, CIZ, WALZ, CZ and GTMZ contribute to understand some tectono-magmatic features related to the rifting and rift-drift stages.

2.5.1 Detrital Zircon

The distribution of zircon ages in siliciclastic rocks of OMZ from the Lower and Upper Detrital groups and from Cambrian Series 3-Furongian metasediments (Linnemann et al. 2008; Pereira et al. 2011; Fig. 2.20A) shows a remarkable similarity with the zircon age records found in the underlying Ediacaran Serie Negra succession (Chichorro et al. 2014), indicating the proximity of the same source areas or recycling of the latter into the former. The contribution of several stages of Paleoproterozoic crustal growth events (Eburnian orogeny) is noticeable. However, the lack of Stenian-Tonian (1.2 Ga to ~720 Ma) zircon-forming events (Grenvillian orogeny) is referred to as a typical feature of the Ossa-Morena Zone (Fernández-Suárez et al. 2002). The scarcity of Mesoproterozoic grains in OMZ indicates that the Cambrian to Early Ordovician basins did not receive (as occurred also with the Ediacaran basins) debris from sources located close to the Amazonian craton or from the Arabian–Nubian shield (Keppie et al. 1998; Avigad et al. 2003; Goodge et al. 2004; Linnemann et al. 2004). This means that a peri-West African craton paleoposition persisted during the Cambrian as it is advocated for Neoproterozoic times (Fernández-Suárez et al. 2002; Gutiérrez-Alonso et al. 2003; Pereira et al. 2008a; Linnemann et al. 2008; Pereira 2014).

In Cambrian times, over at least 40–70 m.y., the erosional and depositional system did not record substantial changes. The data suggest an intracontinental rift system (Chichorro et al. 2008) with no significant variations in paleogeography. The Cambrian clastic rocks derived predominantly, directly and by recycling, from sources dominated by Cadomian/Pan-African tectonothermal events (Ediacaran grains with main peaks at ca. 615 Ma and ca. 558 Ma, but also Cryogenian grains, Fig. 2.20A). This implies that the Neoproterozoic Serie Negra was partly emerged after the Cadomian magmatic arc activity and collision (Pereira and Quesada 2006; Pereira et al. 2006). In addition to Serie Negra sediments, an evident potential source for the detrital zircons is

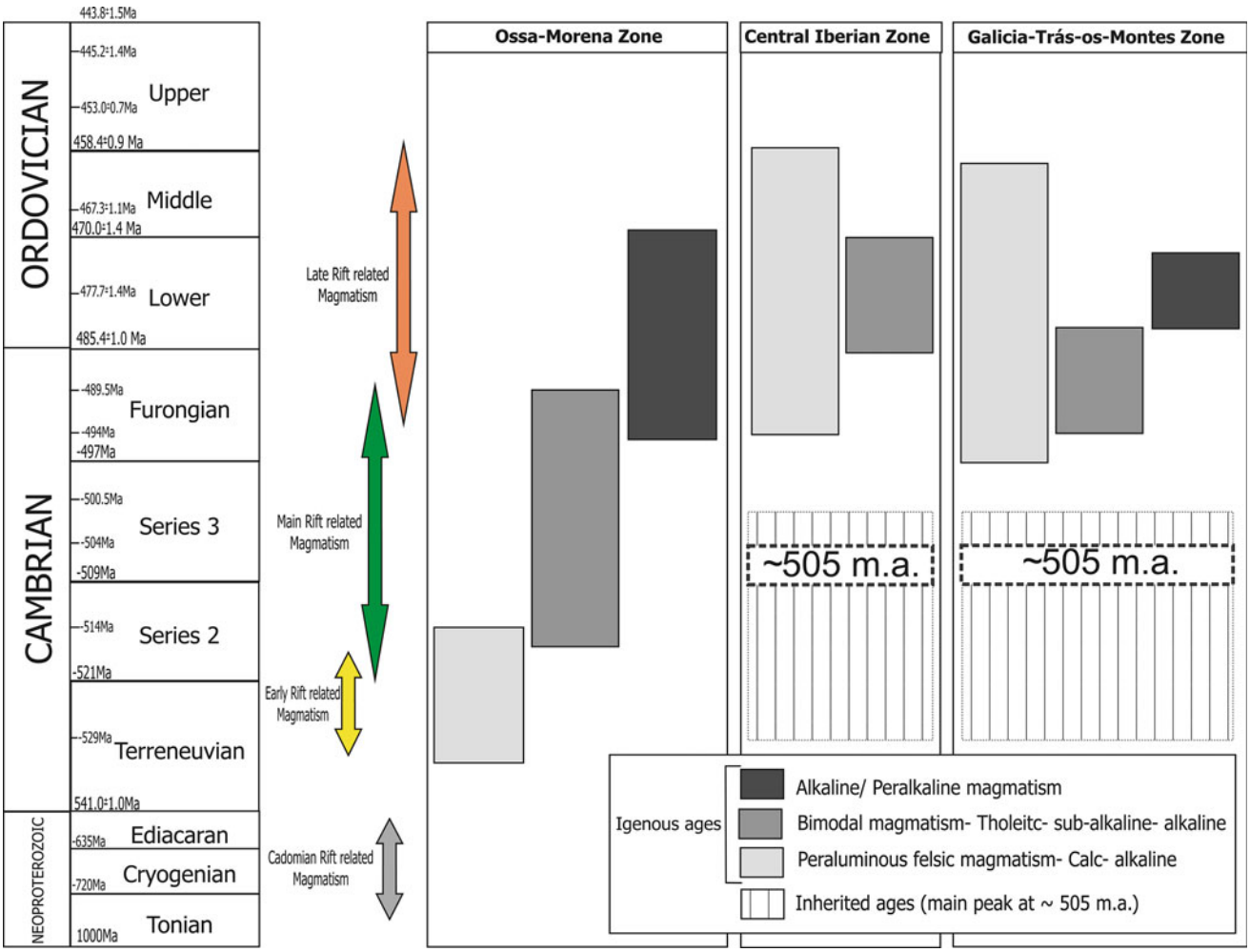

Fig. 2.19 Diachronism of the rift-related magmatism in the Cambrian-Ordovician rifting event

represented by Neoproterozoic igneous rocks, including some remnants of the Cadomian magmatic arc, exposed mainly in the northern OMZ (Eguiluz et al. 2000; Bandrés et al. 2002, 2004; Henriques et al. 2015; Sánchez-Lorda et al. 2016).

The syn-rift Terreneuvian-Cambrian Series 3 siliciclastic rocks of OMZ show an absence or a very limited contribution of coeval magmatic rocks (only 1.9%; Fig. 2.20A). The scarcity of syn-rift Cambrian igneous zircons in the Cambrian sediments suggests that the Cambrian volcanism was essentially submarine and associated with hypabyssal intrusive complexes. The data agree with a rift system partitioned into fault-bounded grabens or half-grabens (Oliveira et al. 1992), some close to volcanic centers while other without Cambrian volcanic contributions, received sediments essentially sourced in the Cadomian igneous representatives and from recycled Ediacaran metasediments.

The same low representation of Cambrian zircon persists in the equivalent syn-rift detrital rocks of the CIZ (Azorejo-Tamames sandstones and Aldeatejada end Monterrubio formations-0.6%; Fig. 2.20B) and WALZ-CZ (Cándana and Herrería formations—2.3%; Fig. 2.20C). This means that the main magmatic complexes prevalent at the time in the OMZ were neither exposed nor supplying OMZ or CIZ basins. The zircon age distributions in CIZ and OMZ are similar, although in CIZ there is a slight increase in the percentage of Stenian-Tonian zircons (Martínez Catalán et al. 2004). On this basis, it is concluded that there were no significant palaeogeographic differences in both zones concerning sediment supply. Based on the Neoproterozoic curves and considering the scarce to low presence of Stenian-Tonian zircons, the sources basically remained the same. However, it should be noted that in the WALZ and CZ, the age distribution clearly reveals a closer influence of Eburnian and Liberian sources (Fig. 2.20C), probably indicating their closer proximity to emerged parts of the West African craton (Reguibat Shield and Western and Eastern Moroccan Meseta). In conclusion, the OMZ, CIZ and WACZ-CZ sectors of the Gondwanan margin were paleogeographically close during the syn-rift stage, although the

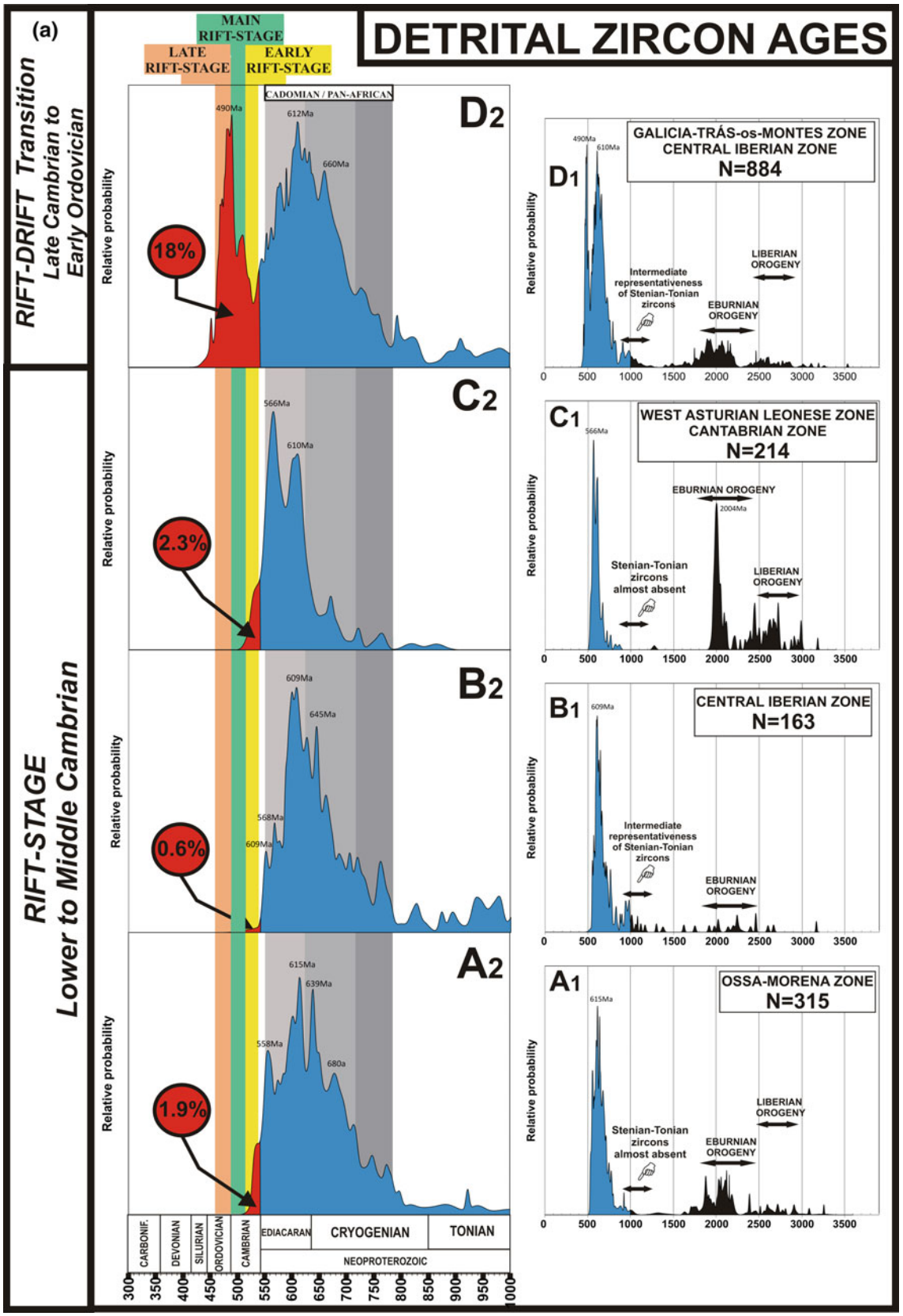
(a)
RIFT-DRIFT Transition
Late Cambrian to
Early Ordovician
RIFT-STAGE
Lower to Middle Cambrian
DETRITAL ZIRCON AGES
MAIN
RIFT-STAGE
LATE
RIFT-STAGE
EARLY
RIFT-STAGE
CADOMIAN / PAN-AFRICAN
D2
C2
B2
A2
490Ma
612Ma
660Ma
18%
566Ma
610Ma
2.3%
609Ma
645Ma
568Ma
609Ma
0.6%
615Ma
639Ma
558Ma
680a
1.9%
Relative probability
CARBONIF.
DEVONIAN
SILURIAN
ORDOVICIAN
CAMBRIAN
EDIACARAN
CRYOGENIAN
TONIAN
NEOPROTEROZOIC
300 350 400 450 500 550 600 650 700 750 800 850 900 950 1000
D1
GALICIA-TRÁS-os-MONTES ZONE
CENTRAL IBERIAN ZONE
N=884
490Ma
610Ma
Intermediate
representativeness
of Stenian-Tonian
zircons
LIBERIAN
OROGENY
EBURNIAN
OROGENY
C1
WEST ASTURIAN LEONESE ZONE
CANTABRIAN ZONE
N=214
566Ma
EBURNIAN OROGENY
2004Ma
Stenian-Tonian
zircons
almost absent
LIBERIAN
OROGENY
B1
CENTRAL IBERIAN ZONE
N=163
609Ma
Intermediate
representativeness
of Stenian-Tonian
zircons
EBURNIAN
OROGENY
A1
OSSA-MORENA ZONE
N=315
615Ma
Stenian-Tonian
zircons
almost absent
LIBERIAN
OROGENY
EBURNIAN
OROGENY
0 500 1000 1500 2000 2500 3000 3500

◀ **Fig. 2.20** Combined probability density plots of U-Pb detrital and inherited zircon ages for rift and rift-drift transition stages in clastic (**A**, **B**, **C** and **D**) and igneous rocks (**G**, **F** and **E**). The left diagrams represent a magnification of the right graphs. **a** Detrital zircon ages. **A**—Zircon data from Ossa-Morena Zone: Lower to Upper Detrital groups and from middle Cambrian-Furongian metasediments. *Sources* Linnemann et al. (2008), Pereira et al. (2011, 2012b), Chichorro (Unpublished data). **B**—Zircon data from Central Iberian Zone: lower Cambrian metasandstones from Douro Group (Azorejo-Tamanes metasandstones; Aldeatejada and Monterrubio formations). *Sources* Gutiérrez-Alonso et al. (2003), Fernández-Suárez et al. (2014). **C**—Zircon data from West Asturian-Leonese and Cantabrian zones lower Cambrian Cándana (eastern WALZ) metaarkoses and Cándana-Herrería metasandstones (CZ). *Sources* Fernández-Suárez et al. (2000, 2014). **D**—Zircon data from rift-drift Furongian to Lower Ordovician metasediments. The data cover several Furongian to Lower Ordovician (Tremadocian) metasediments overlain by the Armorican Quartzite. Sources: Sarnelhas arkosic metasandstones (SW-CIZ, Pereira et al. 2012a, b), Malpica do Tejo Shales (central CIZ, Talavera et al. 2012), Villalcampo schists (Talavera et al. 2012), the arkosic metasandstones from the Mora-Saldanha volcano-sedimentary complex (Upper Para-utochthon, GTMZ, Dias da Silva et al. 2015) and the Upper sequence of GTMZ (Díez Fernández et al. 2010). **b** Inherited zircon ages. **E**—Zircon ages from lower to middle Cambrian felsic volcanic rocks and cogenetic shallow plutonic rocks from the OMZ. *Sources* Alcaçovas Orthogneiss (Chichorro et al. 2008); Barquete granite (Pereira et al. 2011); Bodonal-Cala, Pallares granite and other felsic orthogneisses (Ordóñez-Casado 1998). **F** and **G**—Zircon data from Furongian to Lower Ordovician peraluminous and calc-alkaline and alkaline suites. **F**—Central Iberian Zone. *Sources* Urra Formation (Solá et al. 2008), Carrascal gabbro and Portalegre granites (Solá 2007), Ollo de Sapo Formation (Bea et al. 2007) and Castilian region (Bea et al. 2006; Talavera et al. 2013; Villaseca et al. 2016). **G**—Galicia-Trás-os-Montes Zone. *Sources* Schistose Domain (Talavera et al. 2008, 2013; Díez-Fernández et al. 2012a) and Malpica-Tuy Basal Allochthonous Units (Díez-Fernández et al. 2012a)

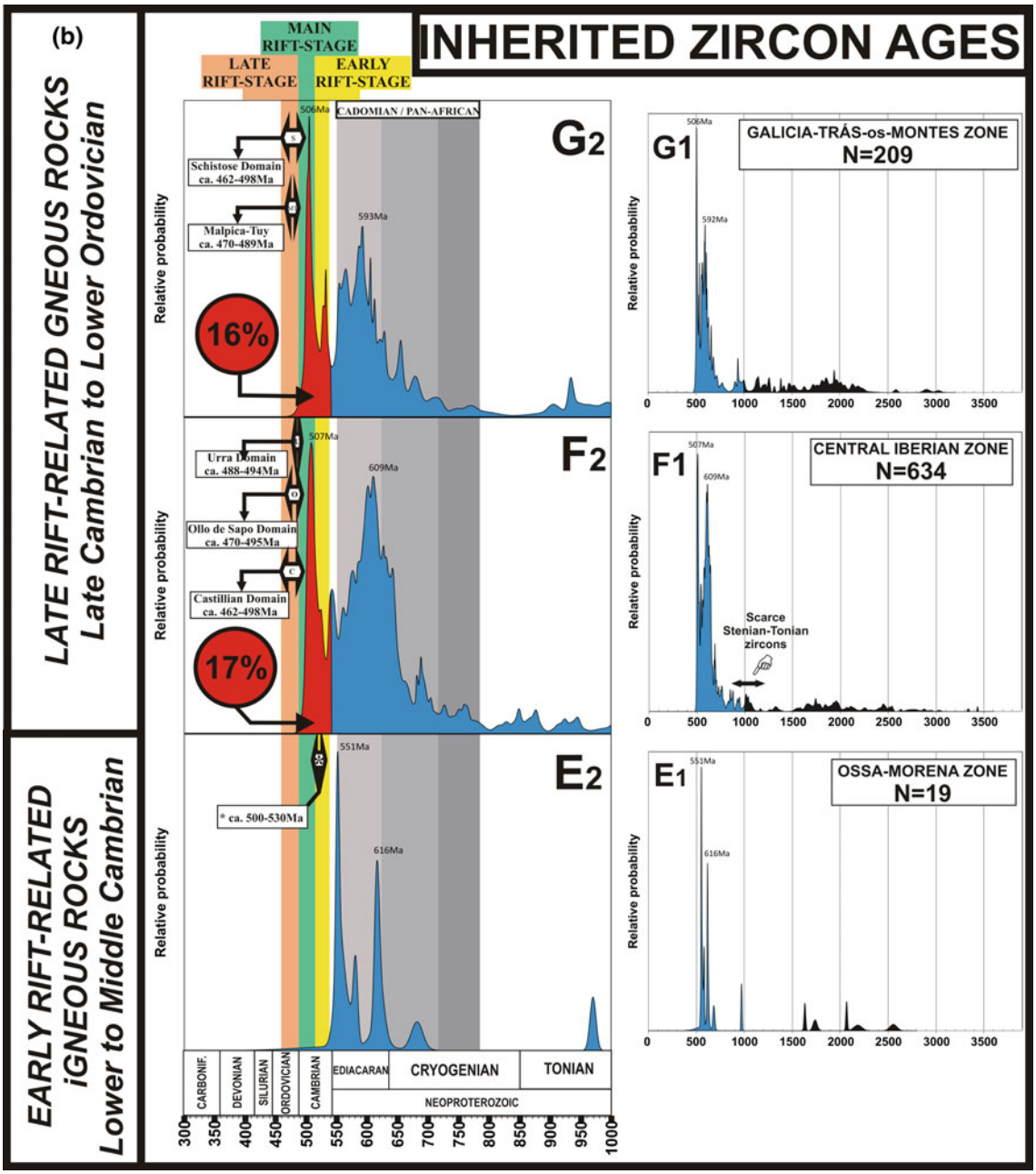

Fig. 2.20 (continued)

WALZ-CZ depocenters appear to have been in more internal positions of the West African craton realm than the OMZ and CIZ.

The age distribution of detrital zircon from the Furongian to the Lower Ordovician arkoses and pelites overlain by the Armorican Quartzite (Fig. 2.20D) reveals a substantial difference by comparison with Terreneuvian-Cambrian Series 3 samples. In fact, these sediments incorporated a much higher percentage of syn-rift zircon grains and the probability density diagram reflects the three above-reported rift-related igneous events, which only coexist in the OMZ (see Fig. 2.4). With the exception of the Cambrian-Lower Ordovician sediments from the Basal Allochthonous units of the GTMZ (Díez Fernández et al. 2010), which mainly recorded the *Early* and *Main* rift-related events (typical of OMZ), the most prominent aspect in the other zones is the simultaneity between the sedimentary processes in this interval and the *Late* rift-related igneous processes. The presence of Furongian–Lower Ordovician zircon in the sediments indicates partial erosion of the coeval *Late* rift-related igneous rocks represented in the Schistose Domain (GTMZ—Mora-Saldanha Volcanosedimentary Complex), in the Castilian (Guadarrama, Tormes dome, Gredos, Miranda do Douro) and Ollo de Sapo domains of the CIZ (Dias da Silva et al. 2015). However, both the high percentage of zircon grains of this age and its significant decrease in the overlying Armorican Quartzite (Linnemann et al. 2008; Pereira et al. 2012a; Shaw et al. 2014) suggest that this component in the pre-Armorican Quartzite metasediments resulted not only from erosion, but also incorporates a syn-volcanic component suggesting that part of these units may be considered as essentially epiclastic, sometimes pointing for a strongly proximal character.

The zircon age distribution (prevalence of Ediacaran relative to Cryogenian peaks, almost absence of Stenian-Tonian zircon and subordinate Eburnian-Liberian record) resembles the distribution of detrital zircon ages in the OMZ, typical of the West African craton, reason why the main source of detritus were probably derived from the OMZ Cadomian basement (Pereira et al. 2012a) but also from the coeval Terreneuvian-Cambrian Epoch 3 *Late* rift-related volcanic rocks. This apparently contradictory situation, in which areas located in the outer continental margin (OMZ) supply detritus to innermore parts of the margin, can be explained by considering that prior to the post-Toledanian event, the OMZ and part of the southern CIZ were thermally uplifted and subjected to erosion, whereas the remaining zones (Cantabro-Iberian Basin) were undergoing a transgressive event (see Sect. 2.3). During this period significant parts of the syn-rift and basement sequences of the OMZ were eroded and could eventually supply the adjacent basinal areas, prior to the post-Toledanian transgression in latest Furongian times that brought the OMZ to outer shelf conditions during the entire passive margin stage.

2.5.2 Xenocrystic/Inherited Zircon in the Rift-Related Igneous Rocks

The xenocrystic/inherited component recorded in the *Early* and *Main* rift-related felsic igneous rocks, mostly represented in the Ossa-Morena Zone, is scarce in most samples studied so far (Fig. 2.20E). The scarcity of inherited cores or older zircons in Cambrian leptinites/orthogneisses of the Évora massif was explained by melting of zircon undersaturated source rocks leading to production of zircon-undersaturated magmas (Chichorro et al. 2008). This hypothesis implies a limited participation of sedimentary protoliths at least in some sectors of OMZ (Chichorro et al. 2008). This apparently contradicts the presence at Monesterio and other high grade metamorphic domes of migmatites and related products of crustal melting, derived from metasedimentary protoliths (Ediacaran Serie Negra). However, the evidence at Monesterio (mid-upper crustal level) does not preclude the participation on Cambrian magmas of mafic zircon undersaturated source rocks (representative of lower crustal sections). Melting at the highest grade of metamorphism ($T > 837$ °C; granulite facies) can also explain the scarcity of zircon inheritance, as at such high temperatures the U-Pb isotopic system would have been opened in most zircon grains. However, this scenario implies melting of a substantial portion of crustal material.

This fact contrasts with much higher zircon inheritance observed in the Furongian-Lower Ordovician *Late rift-related igneous* units (ca. 490–460 Ma) in CIZ and GTMZ (Fig. 2.20F, G) (Bea et al. 2007). Zircon inheritance in these rocks, which seems to emulate the first stages of rifting in the OMZ (*Early rift-related igneous event*), reveals a protracted history of zircon-growth events recorded in a Neoproterozoic cluster with higher percentage of Ediacaran and relative scarcity of Mesoproterozoic ages. The combined probability density plots of Fig. 2.20F, G show an additional and significant contribution of Cambrian, *Early* and *Main* rift-related igneous zircon in these rocks: 17% and 16%, respectively (Fig. 2.20F, G), This is somewhat surprising since the *Early* and *Main* igneous events are apparently not represented in CIZ and GTMZ. To account for this presence, in addition to some Ediacaran (Schist-Greywacke Complex) and Terreneuvian to Cambrian Series 3 siliciclastics (Fig. 2.20B, C), the contemporaneous Furongian to Lower Ordovician detrital formations from CIZ (Beiras and Douro

Group) and GTMZ (Fig. 2.20D) should be also involved in melting as source layer of those anatectic *Late* stage magmas in high upper crust levels. However, high-grade melting at high crustal levels, even admitting wet melting conditions seems unlikely, given the large volume of magmas produced (e.g. Ollo de Sapo rocks and correlatives). Alternatively, the existence of *Early* and *Main* events magmas underplated/entrapped in the crust-mantle transition zone may be envisaged. The presence of such syn-rift Terreneuvian-Cambrian Series 3 zircon grains, incorporated into the *Late* magmas ascending through the crust, provides undirect evidence of the existence at depth of representatives of the early stages of rift-related magmatism also in CIZ, probably heralding for the propagation of rifting into this zone. This scenario of magma underplating is compatible with the proposed scenario of stepwise progressive stretching and thinning of the continental lithosphere towards inner zones of Gondwana.

2.6 The Rifting Stage in the Galicia-Trás-os-Montes Zone

The complex structure and pervasive deformation that affected the hiterland areas during the Variscan orogeny, which involved subduction beneath Laurussia of the leading hyperextended margin of Gondwana, unable a detailed characterization of the pre-orogenic evolution of such units; e.g. Lower Allochthon (Basal units) and Parautochthon of the Galicia-Trás-os-Montes Zone. For this reason, these units deserve being dealt with separately in the following independent sections.

2.6.1 The Rift Sequence in the Upper Parautochthon

Í. Dias da Silva, E. González-Clavijo, A. Díez-Montes, J. Gómez Barreiro

The Upper Parauthochthon (UP) is a tectonic unit composed of sedimentary and igneous sequences bounded by Variscan structures (see Figs. 4.1 and 4.2 in Chap. 4 of this volume). The lower boundary is the Main Trás-os-Montes Thrust (MTMT; Dias da Silva 2014). This fault inhibits the observation of the lowermost part of the sedimentary sequence and is responsible for its mechanical contact with the Devono-Carboniferous synorogenic basins of the Lower Parautochthon (see Sect. 11.1.1 in Chap. 11 of this volume). Moreover, the strong development of a pervasive tectonic foliation during the Variscan orogeny, almost completely concealed the stratigraphic evidences and the fossil record. This difficulty led to an earlier proposal of an anomalously thick Silurian sequence for the GTMZ, due to findings of graptolite faunas (Ribeiro 1974; Iglesias Ponce de León and Robardet 1980; Farias et al. 1987). Later works provided data supporting a thinner Silurian sequence (Díaz García 1991; Marcos and Llana Fúnez 2002; Dias da Silva 2014) and the existence of a Furongian to Late Ordovician continuous succession based on U-Pb crystallization ages of rhyolitic and dacitic rocks (Valverde-Vaquero et al. 2005, 2007; Dias da Silva et al. 2014, 2016, 2017) and the fossiliferous record (Rodríguez et al. 2004).

The upper limit of the UP is formed by a complex array of Variscan thrusts and out-of-sequence thrusts partially reactivated by extensional detachments (e.g. Martínez Catalán et al. 2007; Díez Fernández et al. 2012c, 2013; Gómez Barreiro et al. 2010, 2015) that separates the low metamorphic grade rocks of the UP from the structurally overlying Lower and Middle Allochthons, which display a complex metamorphic history involving higher grades (e.g. Munhá et al. 1984; Ribeiro 1987a, b; Gil Ibarguchi and Dallmeyer 1991; Ballèvre et al. 2014; González Clavijo et al. 2016). Recent research around the Morais Allochthonous Complex revealed that the UP occupies most of the extent of Centro-Transmontano Group (or Lower Allochthonous Thrust Complex, Ribeiro et al. 1990b, 2013), producing a major change in the previous subdivision of the allochthonous and parautochthonous units in NE-Portugal (see Ribeiro 1974; Pereira et al. 2006; Ribeiro et al. 2013; Rodrigues et al. 2013).

The UP is presently considered a structural slice of Gondwanan affinity with a sedimentary record encompassing Furongian to Silurian rocks (Dias da Silva 2014; Dias da Silva et al. 2014, 2016, 2017). During pre-Variscan times, this unit is envisaged as occupying an intermediate position on the central part of West Gondwana between the more continental Central Iberian Zone (CIZ) and the more distal Lower Allochthon of the GTMZ. Although no unconformities were identified to date in the UP we will consider that, according to what is described in this book for the CIZ, its lithostratigraphy can also be formed by "rift-related" (described below) and "drift-related" sequences (see Sect. 3.7 in Chap. 3 of this volume), with the Armorican-type quartzite marking the geodynamic shift between them (Fig. 2.21, see also Fig. 2.4).

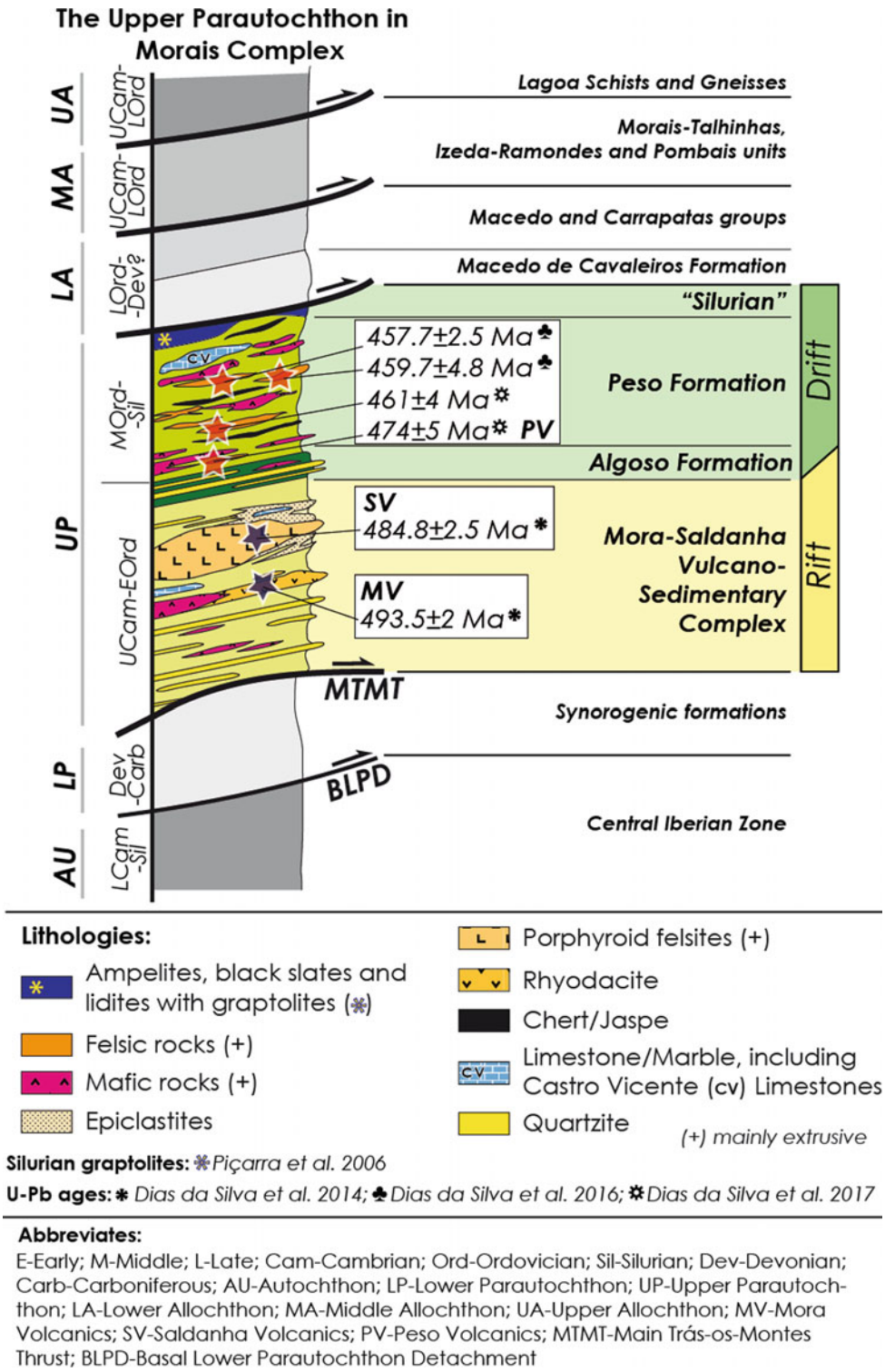

Fig. 2.21 Synthetic lithostratigraphic column of the Upper Parautochthon in the Morais Complex, NE Portugal

Rift-related sequence

The syn-rift sedimentary succession is represented by the **Mora-Saldanha Volcano-Sedimentary Complex** (MSVSC, Fig. 2.21; Dias da Silva 2014; Dias da Silva et al. 2014), which is formed by a thick metasedimentary sequence (over 1000 m) consisting of alternations of green to dark-grey pelites and sandy interbeds, with frequent volcanic layers or lenses, some of them of kilometric scale, and locally presenting centimeter to meter-thick beds of carbonates. The lower major volcanic episode, **Mora Volcanics** (MV), is a bimodal event of Furongian age (493.5 ± 2 Ma, U-Pb age) with calc-alkaline felsic and intermediate rocks

and tholeiitic E-MORB basalts, probably correlative to the *Main rift-related igneous event* in the OMZ (see above Figs. 2.6b, 2.7c, 2.8c, 2.9c, 2.10c, 2.12b, 2.13c, 2.14b, 2.15b, 2.16b and 2.17b). Some rhyolitic tuffs present sulfide ores disposed in deformed stockworks and in centimeter-thick lenses. Rhyodacites with magnetite crystals also occur. The upper **Saldanha Volcanics** (SV) form a calc-alkaline rhyolitic dome that yielded an Early Ordovician age (484.8 ± 2.5 Ma, U-Pb zircon). The SV are geochemically and petrographically identical to the Ollo de Sapo Formation in the CIZ (e.g. Díez Montes et al. 2010) and do not present any kind of ore mineralization (Dias da Silva 2014). The SV are adscribed to the *Late rift-related igneous event* and their geochemical characteristics have been included in the review presented in Sect. 2.4.3 (see Figs. 2.6c, 2.7e, 2.8e, 2.9e, 2.10e, 2.11d, 2.12d, 2.13d, 2.14d, 2.15d, 2.16d, 2.17d and 2.18c). Over this unit, the MSVSC presents a regressive stratigraphic sequence, with increasing amount and thickness of quartzite and arkose/volcanoclastic beds towards the top.

The apparent stratigraphic continuity with the overlying Armorican Quartzite, known here as the **Algoso Formation** (Dias da Silva 2014; Dias da Silva et al. 2014) raises some questions on the stratigraphic position of the Toledanian unconformity and the beginning of the "drift" sequence in the UP (see *Discussion* in Sect. 3.7, Chap. 3 of this volume). As for now, two possibilities arise: (1) the unconformity is located below the MV or the SV, in a similar stratigraphic position like, for instance, the Lower Ordovician Eucísia volcanic suite in the nearby CIZ (Sá et al. 2005; Coke et al. 2011). This means that the "Ollo de Sapo" rift-related magmatism in the UP is positioned over the unconformity and the passage to the "drift" sequence is rather continuous; (2) the unconformity is absent, and the stratigraphic record is somewhat like that described in the West Asturian-Leonese Zone (Cabos Series, Pérez-Estaún et al. 1990).

Either way, it is assumed that the Mora and Saldanha volcanic suites were produced in an extensional geodynamic setting, as proposed for the "Ollo de Sapo" case (e.g. Bea et al. 2007). The calc-alkaline geochemical signature of the more acid end members (rhyolites and dacites) is related to the Furongian-Tremadocian fast thinning of the crust and the production of anatectic melts with geochemical and zircon inheritance from the Cadomian (arc) basement of N Gondwana (Díez Montes et al. 2010; Dias da Silva et al. 2014). The presence of tholeiitic basaltic magmas in the MV suite, which reveals the contribution of E-MORB magmatic sources, attests for the possibility of an extensional, (continental) rift-related, geodynamic setting for the MSVSC.

2.6.2 The Lower Allochthon: The Stretched Continental Margin of Northwest Gondwana

Í. Dias da Silva, M. Chichorro, J. Gómez Barreiro, A. López-Carmona

The Lower Allochthon (LA, see Figs. 4.1 and 4.2 in Chap. 4 of this volume; Table 2.1; Ballèvre et al. 2014) is exposed below the Middle and Upper Allochthons of the GTMZ and tectonically overlies the lower grade domain known as Parautochthon or Schistose Domain (see previous section; Farias et al. 1987; Ribeiro et al. 1990b). The LA records early Variscan high-pressure (HP) metamorphism, interpreted as the product of continental subduction at 370–365 Ma (Rodríguez et al. 2003; Abati et al. 2010; López-Carmona et al. 2014). It represents the outermost W-Gondwana continental margin, hyperextended during the opening of the Rheic Ocean and the drifting of the peri-Gondwanan Upper Allochthon Cambro-Ordovician magmatic arc (see Chap. 4 in this volume; e.g. Martínez Catalán et al. 2009).

The LA is currently exposed in all the allochthonous complexes of the GTMZ (Table 2.1) and, according to the metamorphic peak, can be grouped in high- to middle-temperature (HT-MT) units and low-temperature (LT) units, all affected by HP metamorphism. The HT-MT units are represented by the Malpica-Tui unit in the Malpica-Tui Complex, the Agualada, Santiago, Lalín and Forcarei units in the Órdenes Complex, and the Espasante unit, in the Cabo Ortegal Complex. The LT units surround

Table 2.1 Lower Allochthon units of the NW Iberian Massif

		NW Iberian Massif			
Allochthonous complexes		Malpica-Tui	Órdenes	Cabo Ortegal	Bragança and Morais
Lower Allochthon	High-P units	Malpica-Tui	Agualada, Santiago, Lalín, Forcarei	Espasante	Lower Allochthonous Thrust Complex, Macedo de Cavaleiros Symplex[a]
	Temperature	High to middle-temperature			Law-temperature
	Ages	Neoproterozoic—Lower Ordovician			Ordovician-Devonian

[a]With transitional character, can be incorporated in the Middle Allochthon, as proposed in Sect. 4.3

the Morais and Bragança complexes in NE Portugal and are represented by the Centro-Transmontano Group (or Lower Allochthonous Thrust Complex), which includes the Macedo de Cavaleiros Formation (Pereira et al. 2006) and the Culminating Green-schists and Quartz-phyllites Formation (Ribeiro 1974; Ribeiro et al. 2013). Stratigraphic ages proposed for these units, point to Neoproterozoic/early Cambrian—Early Ordovician for both groups (Díez Fernández et al. 2010).

2.6.2.1 The Lower Allochthon in Galicia

The Lower Allochthon can be separated in two tectonically juxtaposed sequences with different affinity, metamorphism and tectonostratigraphy: "the lower sequence" and the "upper sequence" (Díez Fernández et al. 2010; López-Carmona et al. 2010). The upper HT-MT sequence (including the Ceán Unit; López-Carmona et al. 2010, 2013) is represented by a monotonous pile of glaucophane-chloritoid-bearing metapelites and mafic rocks with pseudomorphs after lawsonite and minor graphitic schists, metacherts, calc-silicate lenses, greywackes and quartzites (López-Carmona et al. 2013, 2014), and has been recently included in the Middle Allochthon as an "ocean-continent transitional domain" (Ballèvre et al. 2014).

The lower sequence occurs at the base of the nappe stack and comprises a thick metasedimentary sequence intruded by Furongian-Lower Ordovician igneous rocks (e.g. Díez Fernández et al. 2010). The metasedimentary rocks include immature sandstones (greywackes), pelites, graphitic shales, impure carbonates, quartzites and sandstones; in some instances, Bouma-type sequences can be recognized. This thick pile of sediments is unconformably overlain by the Portela quartzites. The lower sequence rocks were transformed into paragneisses, schists, phyllites, carbonaceous schists, calc-silicate rocks, and meta-quartzites of the high-to mid-temperature group. One characteristic feature is the presence of albite, oligoclase and garnet porphyroblasts.

The igneous rocks are (i) mafic dikes (alkali basalts; Marquínez García 1984; Rodríguez 2005); (ii) a calc-alkaline suite formed by high-K granites, granodiorites and tonalites; and (iii) an alkaline to peralkaline suite including metaluminous alkali-feldspar quartz-syenites and granites, peraluminous alkali-feldspar granites, and peralkaline granites (Floor 1966; Rodríguez 2005). During the Variscan Orogeny both magmatic series were metamorphosed into eclogite facies conditions (Rodríguez 2005; López-Carmona et al. 2014).

Knowing the westward-directed component of subduction and the characteristics of each allochthonous unit of the GTMZ, it is suggested that the Middle Allochthon would occupy an oceanward position compared to the Lower Allochthon before the Variscan collision (Martínez Catalán et al. 1996, 2009; Díez Fernández et al. 2012a, b). Thus, the Lower Allochthon is interpreted as a slice of continental crust, whereas the Middle Allochthon is interpreted to represent a volcano-sedimentary sequence viewed as a more distal part of the same continental margin transitional to an oceanic domain (cf. Rodríguez et al. 2003; Díez Fernández et al. 2010; López-Carmona et al. 2010). The Lower Allochthon represents the outermost sections of the NW Gondwana continental margin subducted beneath Laurussia during the Late Devonian (Martínez Catalán et al. 1996, 2009; Rodríguez et al. 2003; Abati et al. 2010; López-Carmona et al. 2014).

The youngest zircon age population for the greywackes of the lower sequence is 566 Ma, similar to the youngest population found in the Portela quartzites (557 Ma; Díez Fernández et al. 2010). The maximum depositional ages and the Precambrian zircon age spectra, especially the relative low proportion of Mesoproterozoic zircons in both assemblages, suggest proximity to the West African craton, with a paleogeographic location estimated in the central part of the northwestern Gondwana margin (Díez Fernández et al. 2010). The turbiditic, then regressive character of the LA sequence, together with sedimentary geochemical data (Fuenlabrada et al. 2012), point to a geodynamic setting in a back-arc or retro-arc environment, close to the stretched continental margin and at some distance from a magmatic (Cadomian?) arc. The geochemistry also reflects the transition to a passive margin setting, reflecting the geodynamic changes in the Gondwana margin from back-arc to rifting/drifting during the late Ediacaran–mid Cambrian periods (Fuenlabrada et al. 2012). On the other hand, the maximum depositional ages estimated from detrital zircon are quite similar to those observed in late Neoproterozoic and lower Cambrian sediments of the Ossa Morena Zone (OMZ) and the zircon age spectra strongly supports the OMZ resemblance (Pereira et al. 2012a; see also above under Sect. 2.5). Therefore, the greywackes and the Portela quartzites may represent the transition from syn-orogenic Avalonian-Cadomian active margin sedimentation to the initial syn-rift sediments, apparently reflecting what is also observed in OMZ (Fuenlabrada et al. 2012; Díez Fernández et al. 2017).

The age of the metasediments is also constrained by the Furongian granitoids (~495 Ma) which intruded them, so that they must have been deposited between the late Ediacaran and the Furongian. The igneous intrusions include granitic orthogneisses and amphibolites which are highly flattened, folded and arranged parallel to the Variscan tectonic banding, thus marking the regional deformation associated to the HP-HT subductive event (Díez Fernández et al. 2011, 2012b).

The large variety of rift-related granitoids define two compositional suites (Floor 1966; Rodríguez 2005; Montero et al. 2009a; Abati et al. 2010; Díez Fernández et al. 2012a):

(i) an older and dominant calc-alkaline bimodal meta to peraluminous suite, represented by tonalites, granodiorites and granites (ca. 495–500 Ma), which includes the Agualada felsic gneisses (ca. 493 Ma); and (ii) a younger suite of alkaline and peralkaline granitoids (ca. 475–470 Ma for Malpica-Tui and ca. 482 Ma for the Galiñeiro peralkaline complex). A dike swarm of mafic rocks intruded mainly the calc-alkaline granitic series. Most of them are tholeiitic, but some are alkali basalts, probably related to the formation of the A-type granitoids with alkaline and peralkaline signatures (Montero et al. 2009a and references therein), which reflect mantle contribution to the LA magmatism, possibly triggered by back-arc extension which ultimately led to the formation of the part of the Rheic Ocean adjacent to these units (Díez Fernández et al. 2012a). It is remarkable that the oldest evidence for continental breakup in Iberia dates back to the late Furongian in the OMZ (see the previous Sects. 2.1, 2.3 and 2.4). Contrary to what is observed in the OMZ, only the *Late rift-related* magmatism is recorded in the LA, being roughly coeval to the Cambro-Ordovician suites in the CIZ and the stage of the peralkaline magmatism observed in the northwestern OMZ (see Fig. 2.19).

Summing up, the mainly greywacke and pelite "lower sequence" (albite-bearing paragneisses and schists) of the LA represents an Ediacaran sedimentary pile submitted to extension across the Cambrian-Ordovician transition, while the Rheic oceanic lithosphere was being created. Considering the geochemical and tectonostratigraphic similarities between the LA in northwest Iberia and the southwestern OMZ (i.e. Évora Massif; Díez Fernández et al. 2017) it cannot be ruled out that they represent relatively neighbouring parts of a same sedimentary basin, sharing a roughly similar stratigraphic evolution in the outermost shelf of W-Gondwana. This margin was later dismembered by the Devonian subduction and exhumation and by the Devonian-Carboniferous transcurrence during the Variscan orogeny. However, the dissimilar magmatic evolution and the age differences of magmatism suggest that they may represent different crustal portions positioned in slightly different paleogeographic contexts, as is also suggested by differences in Nd T_{DM} model ages (Fuenlabrada et al. 2012; Díez Fernández et al. 2017).

2.6.2.2 Lower Allochthon in NE Portugal

Recent investigations around the allochthonous complexes of NE Portugal have revealed that the magnitude of the originally proposed extension of the Lower Allochthon (Lower Allochthonous Thrust Complex, according to Ribeiro et al. 1990b; Centro-Transmontano Group after Ribeiro et al. 2013) is much smaller than expected, being most of it presently incorporated into the lower grade rocks of the Upper Parautochthon (Pereira et al. 2006; Rodrigues et al. 2013; Dias da Silva et al. 2014, 2015). In this way, we will consider as part of the LA only the units that are located between the Upper Parautochthon (structurally below) and the Middle Allochthon ophiolitic units (above) in the Bragança and Morais complexes (see Figs. 4.1 and 4.22 in Chap. 4 of this volume; González Clavijo et al. 2016).

The LA lithostratigraphic sequence in NE Portugal includes a mainly pelitic metasedimentary succession showing an assorted suite of igneous rocks (sub-plutonic and volcanic; Ribeiro 1986, 1991; Ribeiro et al. 2013). According to Ribeiro et al. (2013 and references therein), the ages of the LA in Portugal could range from the Lower Ordovician to the Devonian (without further precision or chronological data), based on stratigraphic resemblances with sequences of other Variscan domains, such as the OMZ (Ribeiro et al. 1990a). This age range prevents a direct correlation with the LA sequence of the Galician allochthonous complexes. However, the lack of age constraints of the LA in Portugal enables us to view it as representing a Neoproterozoic-Ordovician stratigraphic sequence, thus facilitating regional correlations along northwest Iberia and north-central Europe (e.g. Ballèvre et al. 2014).

The LA of NE Portugal shows relicts of blueschist facies metamorphism related to Variscan continental subduction, which were retrogressed into amphibolite (W of Morais) and greenschist (E of Morais) facies metamorphism during adiabatic exhumation associated with Variscan extensional detachments and out-of-sequence thrusting. The only available radiometric age (~330 Ma; $^{40}Ar/^{39}Ar$ on white mica) was obtained by Gil Ibarguchi and Dallmeyer (1991) who interpreted it as dating the HP metamorphic peak in the LA of Morais. This interpretation has been considered not reliable due to regional geological constrains (e.g. Navarro et al. 2003; see also discussion in Sect. 12.3.1.3 in Chap. 12 of this volume). Consequently, it is assumed a 375–365 Ma age for the HP metamorphism in the LA of NE-Portugal, as profusely supported by radiometric dating in Galicia (Rodríguez et al. 2003; Abati et al. 2010).

As in Galicia, albite-oligoclase and garnet-bearing schists are common in the LA as well as schists bearing glaucophane, crossite and/or lawsonite porphyroblasts (Schermerhorn and Kotsch 1984; Munhá et al. 1984; Ribeiro 1987a, 1991; see also Sect. 12.3.1.3 in Chap. 12 of this volume).

Two LA laterally equivalent units are distinguished in NE Portugal:

- Surrounding the Morais and Bragança allochthonous complexes, the **Culminating greenschist and quartz-phyllite Formation** (Ribeiro 1974; Ribeiro et al. 2013), also known as **Macedo de Cavaleiros Formation** by Pereira et al. (2006), is composed, from bottom-to-top, of dark-grey to dark-purple phyllites with black slates and siltite beds, greenish tuffs, felsic and

mafic volcanic rocks, laminated phyllites and quartz-phyllites with immature quartzite lenses. This sequence is locally cut by felsic and metagabbro dykes. The mafic metavolcanic rocks show metamorphic albite-oligoclase, green amphibole (actinolite-tremolite), epidote, zoisite, clinozoisite and chlorite. Other minerals such as iron and titanium oxides, carbonates, titanite, muscovite, biotite, (hydro)grossular and apatite occur as accessory minerals (Ribeiro et al. 2013).

- To the W of the Morais Complex, the **Macedo de Cavaleiros Simplex** (Ribeiro 1974, 1986, 1991; Ribeiro et al. 1990b, 2013) encompasses two volcano-sedimentary sequences. The tectonically lower is the **Carrapatas Group**, which includes alkaline volcanics and peralkaline sub-volcanic rocks. It is overlain by the more tholeiitic rocks of the **Macedo Group**.

The **Carrapatas Group** is composed of four formations (Ribeiro 1987a). At the base, the **Alto de Sequeira Formation** is formed by albite-bearing phyllites and quartz (+feldspathic) phyllites with minor volcanoclastic contribution. The stratigraphically overlying **Facho Formation** includes massive peralkaline rhyolites at the base, gradually passing to banded rhyolites and basalt beds, which occur sporadically at the top of this unit. Minor sedimentary contribution is associated with the felsic tuffs (i.e. banded rhyolites). The rhyolites of the Facho Formation contain riebeckite, Mg-riebeckite and aegirine-augite, attesting for their paralkaline character, also confirmed by their whole-rock geochemical signatures (Ribeiro 1987a; Ribeiro et al. 2013). Local presence of crossite and garnet (andradite) are indicative of the HP event of Variscan metamorphism. This unit is overlain by the **Carrapatas Formation**, which is mainly formed by metabasaltic rocks (greenschists) with two metric layers of peralkaline rhyolites at the base and top, scarce intermediate (andesitic) volcanics and purple chert and pelite beds. The uppermost unit of the Carrapatas Group is the **Alto de Casais Formation** being composed by felsic tuffs, with centimetric pelitic layers towards the top and associated metacherts. Geochemically, the rocks from the Carrapatas and the Facho formations match those from the Peso Formation of the Upper Parautochthon (see the previous section; Díez Montes et al. 2015; Dias da Silva et al. 2016, 2017), pointing to the same geodynamic setting and suggesting a Mid-Upper Ordovician age.

The **Macedo Group** presents at its base the **Madorra Formation** and the intrusive igneous rocks of the **Valbenfeito Complex**. The first is composed of greenish-grey to purple quartz and feldspar-rich phyllites. They include some beds of greenschists (metabasaltic rocks) and dark-purple cherts. Garnet porphyroblasts with andradite, grossular and almandine components have been described (Ribeiro 1987a; Ribeiro et al. 2013). The **Valbenfeito Complex**, intrusive in the quartz-feldspathic rocks, is mainly formed by blasto-mylonitic metagabbro dikes and thin and laterally discontinuous rhyolitic to andesitic dikes, where albite is the main component (Ribeiro 1987b). These units are overlain by the **Macedo de Cavaleiros Formation** (s.s. after Ribeiro 1987a and Ribeiro et al. 2013), which is a monotonous unit composed of amphibolites and greenschists (metabasalts and basaltic tuffs) with local intercalations of phyllites and quartz-feldspathic rocks like those of the Madorra Formation.

The lithostratigraphy of the Macedo de Cavaleiros Simplex shows a transitional character between the typical, mainly sedimentary LA sequence and the ophiolites of the Middle Allochthon (MA), as pointed out by its geochemical patterns (Ribeiro 1987a). The evolution from alkaline-transitional to tholeiitic affinity can be viewed as an indication of the breakup of a highly stretched continental margin leading to formation a true rift. In this way, the attribution to a specific unit (LA or MA) depends on the assumed criteria—hyperextended continental crust versus continental rift. Therefore, if a Furongian-Upper Ordovician age is assumed for the Macedo de Cavaleiros Simplex, it is correct to consider it as an equivalent to the "upper sequence" (or Ceán unit) in the Malpica-Tui Complex (Díez Fernández et al. 2010; López-Carmona et al. 2014) and view it as a Cambro-Ordovician ophiolitic unit of the MA, as proposed in Sect. 4.1, Chap. 4 of this volume.

2.7 Discussion: Overall Geodynamic Evolution During Rifting

According to the geological evidence in the Iberian Massif and neighbouring areas discussed above, the West Gondwana continental margin underwent a dramatic change in the prevailing tectonic conditions near the Ediacaran Cambrian boundary. The convergent, subduction-related regime lasting for most of the Ediacaran was rapidly replaced by one dominated by extension (Quesada et al. 1991; Murphy et al. 2004, 2006, 2016; Sánchez-García et al. 2003, 2008a, 2010, 2016; Pereira et al. 2006; Martínez Catalán et al. 2007; Linnemann et al. 2008; Chichorro et al. 2008; Nance et al. 2012; among others). This sudden change was largely diachronous. It started in the Moroccan Anti-Atlas in late-Ediacaran times, from where it propagated "zip-like" northwards along the margin (Álvaro et al. 2014 and references therein), reaching the Ossa-Morena Zone by ca. 530 Ma ago (near the Fortunian-Stage 2 boundary) and the Montagne Noire-Pyrenean area and the Bohemian Massif in Early Ordovician times (Murphy et al. 2004, 2006, 2016; Pereira et al. 2006; Martínez Catalán et al. 2007; Álvaro

et al. 2007, 2013a, 2014; Linnemann et al. 2008; Chichorro et al. 2008; Nance et al. 2012). The causes of this change remain controversial. A process of slab roll-back and back-arc rifting along the previous active margin could account for it (von Raumer et al. 2003; Stampfli et al. 2002; Stampfli and Borel 2004) and this model has been also applied for NW Iberia (Díez Fernández et al. 2012a and references therein). However, such a model alone does not provide an explanation for the along-margin propagation, which can be better accounted for by a scenario of oblique collision of a mid-ocean ridge with the trench (see Figs. 2.2 and 2.3a). This would have progressively transformed the former subduction margin into a transcurrent one, in a way similar to the Cenozoic evolution of western North America that led to transformation of a previous active margin into the San Andreas transcurrent margin (Nance et al. 2002, 2008, 2010; Keppie et al. 2003; Murphy et al. 2004).

Cessation of subduction-related arc growth (by ca. 533 Ma) was accompanied by a short period of uplift and erosion of the former arc zone (Quesada 1990a, b, 1991, 2006). Zircon geochronological data reinforce this statement, and indicate that Ediacaran metasediments were already partly emerged after the Cadomian collision (Pereira and Quesada 2006; Pereira et al. 2006). Formation of terrestrial troughs and, most important, the onset of igneous activity by ca. 530 Ma ago (*Early rift-related igneous event*) require however an additional explanation. This can be provided if a component of subduction of the mid-ocean ridge beneath the continental upper plate (Gondwana) is added to the oblique collision model referred to above (Sánchez-García et al. 2003, 2008a, 2010) (Fig. 2.3a). This model would be analogue to the presently ongoing case of subduction of the East Pacific Rise, which is causing the rifting of Baja California and, as a consequence, the development of a slab-window beneath this part of the North American plate (Lizarralde et al. 2007; Umhoefer 2011, and references therein).

The initial evolution, dominated by horst-and-graben basin formation and emplacement of the *Early rift-related igneous event* rocks could be accounted for by processes of thermal expansion connected to the development of the mentioned slab-window and associated gravitational collapse processes in the upper crust. However, the widening of the area subjected to stretching and the rapid propagation across it of a transgressive succession during the late Terreneuvian, which implies that subsidence must have overcome thermal uplift, requires additional processes. The fact that subduction of the Iapetus and Prototethys ocean started to operate roughly at that time (Murphy et al. 2006; Martínez Catalán et al. 2007; Nance et al. 2010, among others), makes it possible that slab-pull processes may have added to the passively extending margin of Gondwana, which would thence be also variably affected by active extension processes since then.

Culmination of the Terreneuvian transgression was suceeded by development of carbonate factories (Fig. 2.4) under prevailing sub-tropical paleogeographic conditions in lower Epoch 2 times (see above under Sect. 2.3). The overall poleward drift of Gondwana during the Cambrian (Álvaro et al. 2013a and references therein) is also well-documented in Iberia and adjacent areas, where the progressive passage from sub-tropical to temperate latitudes is indicated by the termination of carbonate sedimentation by mid-Epoch 2 times in the Ossa-Morena Zone, by the Cambrian Epoch 2–3 in the northernmost Iberian Massif zones and by Cambrian Epoch 3 in the Montagne Noire (see Fig. 2.4; Álvaro et al. 2000a, b, 2016). Existence of several events of enhanced extensional deformation, separated by intervening relatively quiescent periods, controlled the prevailing paleogeographic conditions and the sequential evolution of the various zones as well as the emplacement of igneous rocks (*Early* and *Main rift-related igneous events*). The cumulative result of all these processes was the opening of a new oceanic tract (part of the Rheic Ocean) immediately before 489 Ma ago, age of a K-bentonite layer interbedded near the base of the overlying passive margin succession in the Ossa Morena Zone (López-Guijarro et al. 2007). As interpreted for the propagation of rifting, ocean opening also propagated northwards and culminated in separation and drift of a ribbon continent (Avalonia sensu lato) in the Lower Ordovician (Murphy et al. 2006; Pereira et al. 2007, 2012a, b; Chichorro et al. 2008; Sánchez-García et al. 2003, 2008a, b, 2010; Linnemann et al. 2008; Nance et al. 2010, 2012; Díez-Montes et al. 2008; among others). This inaugurated a new passive margin stage of the Variscan cycle in the newly formed margin of Gondwana facing the Rheic Ocean, which is dealt with in some detail in Chap. 3 of this volume.

Notwithstanding, magmatic activity and presumably some punctuated extension, continued on the Iberian Gondwanan margin after ocean opening and extended well away from the previous rift axis (Ossa-Morena Zone) towards inner domains of Gondwana (e.g. Galicia-Trás-os-Montes, Central Iberian, West Asturian-Leonese and Cantabrian zones). This is materialized by the Furongian-Early Ordovician *Late igneous event*. However, due to the similarities of the igneous rocks of this event in the Central Iberian and Galicia-Trás-os-Montes zones with those of the *Early rift-related igneous event* in the Ossa-Morena Zone, and the sparse representation of any igneous activity prior to this *Late event* outside Ossa Morena, we prefer linking this event to the rifting stage by assuming growth and propagation of the speculated slab window towards inner parts of the margin; i.e. a return to active, gravitationally driven extension caused by thermal uplift, once the coupling with the

oceanic part of the Iapetus plate was broken by the onset of spreading in the Rheic Ocean (Fig. 2.3d).

Finally, scattered and volumetrically minor Middle Ordovician rocks (mainly dikes and sills), generally earlier than 470 Ma but locally reaching up to ca. 450 Ma, have been reported throughout the Iberian Massif (Talavera et al. 2013; Orejana et al. 2016, 2017; Pereira et al. 2012b). They may represent either residual activity related to the previous rifting event or, alternatively, a remote expression of events taken place somewhere else. In this respect, it is worthwhile noticing that important igneous activity existed at that time further to the east along the Gondwanan margin (Alps, Occitan Domain, Corsica, Sardinia; Álvaro et al. 2007, 2013a, 2014, 2018, and references therein), in the future location of, and probably heralding for, the opening of the Paleotethys Ocean (Stampfli 2000; Stampfli et al. 2002; Stampfli and Borel 2004; Cocks and Torsvik 2006; Torsvik and Cocks 2013; Domeier and Torsvik 2014; among others).

References

Abati J, Dunning GR, Arenas R, Díaz García F, González Cuadra P, Martínez Catalán JR, Andonaegui P (1999) Early Ordovician orogenic event in Galicia (NW Spain): Evidence from U-Pb ages in the uppermost unit of the Ordenes complex. Earth Planet Sci Lett 165: 213–228

Abati J, Gerdes A, Fernández Suárez J, Arenas R, Whitehouse MJ, Díez Fernández R (2010) Magmatism and early-Variscan continental subduction in the northern Gondwana margin recorded in zircons from the basal units of Galicia, NW Spain. Geol Soc Am Bull 122 (1–2):219–235. https://doi.org/10.1130/b26572.1

Albani R, Bagnoli G, Bernárdez E, Ribecai C (2006) Late Cambrian acritarchs from the "Túnel Ordovícico del Fabar", Cantabrian Zone, N Spain. Rev Paleobot Palynol 139: 41–52

Alía M (1963) Rasgos estructurales de la Baja Extremadura. Bol R Soc Esp Hist Nat (Geol) 20: 247–262

Álvaro JJ, Vennin E (1996) Tectonic control on Cambrian sedimentation in south-western Europe. Eclog Geol Helv 89: 935–948

Álvaro JJ, Vennin E (1998) Stratigraphic signature of a terminal Early Cambrian regressive event in the Iberian Peninsula. Can J Earth Sci 35: 402–411

Álvaro JJ, Liñán E, Vennin E, Gozalo R (1995) Palaeogeographical evolution within a passive margin with syndepositional faulting: The Marianian deposits (Lower Cambrian) of the Iberian Cahins (NE Spain). N Jb Geol Paläont Mh H9:521–540

Álvaro JJ, Vennin E, Moreno-Eiris E, Perejón A, Bechstädt T (2000a) Sedimentary patterns across the Lower-Middle Cambrian transition in the Esla nappe (Cantabrian Mountains, northern Spain). Sediment Geol 137: 43–61

Álvaro JJ, Rouchy JM, Bechstädt T, Boucot A, Boyer F, Debrenne F, Moreno-Eiris E, Perejón A, Vennin E (2000b) Evaporitic constraints on the southward drifting of the western Gondwana margin during Early Cambrian times. Paleogeogr. Paleoclimat. Paleoecol. 160: 105–122

Álvaro JJ, Van Vliet-Lanoë B, Vennin E, Blanc-Valleron MM (2003) Lower Cambrian paleosols from the Cantabrian Mountains (northern Spain): a comparison with Neogene-Quaternary analogues. Sediment Geol 163: 67–84

Álvaro JJ, Ferretti F, González-Gómez C, Serpagli E, Tortello MF, Vecoli M Vizcaïno D (2007) A review of the Late Cambrian (Furongian) paleogeography in the western Mediterranean region, NW Gondwana. Earth-Sci Revi 85: 47–81

Álvaro JJ, Bauluz B, Gil Imaz A Simón JL (2008) Multidisciplinary constraints about Cadomian compression and early Cambrian extension in the Iberian Chains, NE Spain. Tectonophysics 461: 215–227

Álvaro JJ, Ahlberg P, Babcock LE, Bordonaro OL, Choi DK, Cooper RA, Ergaliev GKH, Gapp IW, Pour MG, Hughes NC, Jago JB, Korovnikov I, Laurie JR, Lieberman BS, Paterson JR, Pegel TV, Popov LE, Rushton AWA, Sukhov SS, Tortello MF, Zhou Z, Zylinska A (2013a) Global Cambrian trilobite paleobiogeography assessed using parsimony analysis of endemicity. In Harper DAT, Servais T (eds), Early Paleozoic Biogeography and Paleogeography. Geol Soc London Mem 38: 273–296

Álvaro JJ, Zamora S, Clausen S, Vizcaïno D, Smith AB (2013b) The role of abiotic factors in the Cambrian Substrate Revolution: A review from the benthic community replacements of West Gondwana. Earth-Sci Revi 118: 69–82

Álvaro JJ, Zamora S, Vizcaïno D, Ahlberg P (2013c) Guzhangian (mid Cambrian) trilobites from siliceous concretions of the Valtorres Formation, Iberian Chains, NE Spain. Geol Mag 150: 123–142

Álvaro JJ, Bellido F, Gasquet D, Pereira F, Quesada C Sánchez-García T (2014) Diachronism of late Neoproterozoic-Cambrian arc-rift transition of North Gondwana: a comparison of Morocco and the Iberian Ossa-Morena Zone. J African Earth Sci 98: 113–132

Álvaro JJ, Shields GA, Ahlberg P, Jensen S, Palacios T (2016) Ediacaran-Cambrian phosphorites from the western margins of Gondwana and Baltica. Sedimentology 63: 350–377

Álvaro JJ, Casas JM, Clausen S, Quesada C (2018) Early Palaeozoic geodynamics in NW Gondwana. J Ib Geol 44 (4): 551–565

Antunes IMHR, Neiva AMR, Silva MMVG, Corfu F (2008) The genesis of I- and S-type granitoid rocks of the Early Ordovician Oledo pluton, Central Iberian Zone (central Portugal). Lithos 111:168–185

Antunes IMHR, Neiva AMR, Corfu F (2012) U-Pb Early Ordovician emplacement ages and K-Ar Variscan recrystallization ages of the Fundão granitic pluton, central Portugal. European Mineralogical Conference. Vol 1, EMC2012-747

Apraiz A (1998) Geología de los macizos de Lora del Río y Valuengo (Zona de Ossa-Morena). Evolución tectonometamórfica y evolucion geodinámica. PhD Univ Pais Vasco, 575 p

Aramburu C, García-Ramos C (1993) La sedimentación cambro–ordovícica en la Zona Cantábrica (NO de España). Trab Geol, Univ Oviedo 19: 45–73

Aramburu C, Truyols J, Arbizu M, Méndez-Bedia I, Zamarreño I, García-Ramos J, Suárez de Centi C, Valenzuela M (1992) El Paleozoico Inferior de la Zona Cantábrica. In: Gutiérrez-Marco JC, Saavedra JC, Rábano I (Eds.) Paleozoico Inferior de Ibero-América. UNEX Press, Mérida 397–422

Aramburu C, Méndez-Bedia I, Arbizu M, García López S (2004) Zona Cantábrica. Estratigrafía. La secuencia preorogénica. In: Vera, J.A. (ed.), Geología de España. SGE and IGME Madrid, 27–34

Assunção CFT (1956) Notas de mineralogia e petrografia portuguesas: um anortosito (bytownitito) do Alto Alentejo (Campo Maior). Bol Mus Lab Min Geol Fac Ciênc Univ Lisboa 24 (7ªs): 141–145

Assunção CFT, Gonçalves F (1970) Contribuição para o conhecimento das rochas hiperalcalinas e alcalinas (gnaisses hastingsíticos) do Alto Alentejo (Portugal). Bol Soc Geol Portugal 17: 187–228

Avigad D, Kolodner K, Mcwilliams M, Persing H, Weissbrod T (2003) Origin of northern Gondwana Cambrian sandstone revealed by detrital zircon SHRIMP dating. Geology 331:227–230

Azor A, Simancas JF, Martínez Poyatos DJ, Montero P, González Lodeiro F, Pérez-Cáceres I (2016) U-Pb zircon age and tectonic

meaning of the Cardenchosa pluton (Ossa-Morena Zone). Geo-Temas 2:23–26
Ballèvre M, Martínez Catalán JR, López Carmona A, Pitra P, Abati J, Díez Fernández R, Ducassou C, Arenas R, Bosse V, Castiñeiras P, Fernández-Suárez J, Gómez Barreiro J, Paquette JL, Peucat JJ, Poujol M, Ruffet G, Sánchez Martínez S (2014) Correlation of the nappe stack in the Ibero-Armorican arc across the Bay of Biscay: a joint French-Spanish project. Geol Soci London Spec Publ:77–113. https://doi.org/10.1144/sp405.13
Bandrés A, Eguiluz, Gil-Ibarguchi J, Palacios T (2002) Geodynamic evolution of a Cadomian arc region: the northern Ossa-Morena Zone, Iberian Massif. Tectonophysics 352:105–120
Bandrés A, Eguíluz L, Pin C, Paquette JL, Ordóñez B, Le Fèvre B, Ortega LA, Gil- Ibarguchi JI (2004) The northern Ossa-Morena Cadomian batholith magmatic arc origin and early evolution. Int J Earth Sci (Geol Runds) 93:860–885
Bea F, Montero P, Talavera C, Zinger T(2006) A revised Ordovician age for the Miranda do Douro orthogneiss, Portugal. Zircon U-Pb ion-microprobe and LA-ICPMS dating. Geol Acta 4:395–401
Bea F, Montero P, González-Lodeiro F, Talavera C (2007) Zircon inheritance reveals exceptionally fast crustal magma generation processes in central Iberia during the Cambro-Ordovician. J Petrol 48:2327–2339. https://doi.org/10.1093/petrology/egm061
Bellido F, Díez Montes A, Sánchez-García T (2010) Caracterización geoquímica y estudio comparativo de plagiogranitos de las Zonas Surportuguesa y Ossa-Morena (SO del Macizo Ibérico, España). Est Geol 66(1):13–23
Bryan SE, Riley TR, Jerram DA, Stephens ChJ, Leat PhT (2002) Silicic volcanism: An undervalued component of large igneous provinces and volcanic rifted margins. Geol Soci Am Spec Pap 362: 99–120
Carracedo M, Sarrionandía F, Eguiluz L, Apalategui O (2007) Petrography, geochemistry and possible origin of the Salvatierra de los Barros pluton (Ossa Morena Zone, Badajoz). Geogaceta 41: 43–46
Carrilho Lopes JM (2004) Petrologia e geoquimica dos Complexos básicos e ultrabásicos do Nordeste Alentejo e das rocas hiperal-calinasassociadas. PhD University Évora
Carrilho Lopes J, Munhá J, Pin C, Mata J (2008) Contrasting isotopic (Sm-Nd) signatures in an equivocal bimodal igneous complex (Ossa-Morena Zone, SW Iberia). Goldsmidt Conf abst A139
Casquet C, Galindo C, Tornos F, Velasco F, Canales A (2001) The Aguablanca Cu-Ni ore deposit (Extremadura, Spain), a case of synorogenic orthomagmatic mineralization: age and isotope composition of magmas (Sr, Nd) and ore (S). Ore Geol Revi 18: 237–250
Castro A, Fernández C, De la Rosa J, Moreno-Ventas I, Rogers G (1996) Significance of MORB-derived Amphibolites from the Aracena Metamorphic Belt, Southwest Spain. J Petrol 37 (2): 235–260
Castro A, Corretgé LG, De la Rosa J, Enrique P, Martínez FJ, Pascual E, Lago M, Arranz E, Galé C, Fernández C, Donaire T, López S (2002) Palaeozoic magmatism. In Gibbons W and Moreno T (eds), The geology of Spain, The Geological Society, London 117–153
Chichorro M (2006) Estrutura do Sudoeste da Zona de Ossa-Morena: Área de Santiago de Escoural — Cabrela (Zona de Cisalhamento de Montemor-o-Novo, Maciço de Évora). PhD Universidade Évora.
Chichorro M, Pereira MF, Díaz-Azpíroz M, Williams IS, Fernández C, Pin Ch, Silva JB (2008) Cambrian ensialic rift-related magmatism in the Ossa-Morena Zone (Évora–Aracena metamorphic belt, SW Iberian Massif): Sm–Nd isotopes and SHRIMP zircon U–Th–Pb geochronology. Tectonophysics 461:91–113
Chichorro M, Solá AR, Pereira MF, Hofmann M, Linnemann U, Gerdes A, Medina J, Lopes L, Silva JB (2014) Provenance analysis of the Late Ediacaran basins from SW Iberia (Serie Negra Succession and Beiras Group): Evidence for a common Neoproterozoic evolution. First International Congress on Stratigraphy: At the cutting edge of Stratigraphy. Rocha R, Pais J, Finney S, Kullberg JC (Eds) Springer Geology, XXVII, ISBN 978-3-319-04363-0. 711–716. https://doi.org/10.1007/978-3-319-04364-7_134
Chichorro M, Solá R, Álvaro JJ, Sánchez-García T, Quesada C, Díez Montes A (2017a) The Cantabro-Iberian Basin: Insights of the rift-stage revealed by detrital zircon age distributions. In: Álvaro JJ, Casas JM, Clausen S (eds), Ordovician Geodynamics: the Sardic Phase in the Pyrenees, Mouthoumet and Montagne Noire massifs. Géol France 1 (4): 14–15
Chichorro M, Solá R, Díez Montes A, Álvaro JJ, Sánchez-García T, Quesada C (2017b) The evolution of the rift-drift transition in the Central Iberian and Galicia-Trás-os-Montes zones, Iberian Massif. In: Álvaro JJ, Casas JM, Clausen S (eds), Ordovician Geodynamics: the Sardic Phase in the Pyrenees, Mouthoumet and Montagne Noire massifs. Géol France 1 (4): 15
Cocks LRM, Torsvik TH (2006) European geography in a global context from the Vendian to the end of the Palaeozoic. In: Gee DG, Stephenson RA (eds), European Lithosphere Dynamics. Geol Soc London Mem 32:83–95
Coke C, Teixeira RJS, Gomes MEP, Corfu F, Rubio Ordóñez A (2011) Early Ordovician volcanism in Eucísia and Mateus areas, Central Iberian Zone, northern Portugal. Mineral Mag 75 (3):685
Cordani UG, Nutman AP, Andrade AS, Santos JF, Azevedo MR, Mendes MH, Pinto MS (2006) New U-Pb SHRIMP zircon ages for pre-Variscan orthogneisses from Portugal and their bearing on the evolution of the Ossa-Morena tectonic zone. An Acad Brasil Ciências, 78(1):133–149
DePaolo DJ (1981) Neodymiun isotopes in the Colorado Front Range and crust-mantle evolution in the Proterozoic. Nature 291:193–196
DePaolo DJ, Wasserburg GJ (1976) Nd isotopic variations and petrogenetic models. Geophys Res Lett 3 (5):249–252
Dias da Silva I (2013) Geología de las Zonas Centro Ibérica y Galicia – Trás-os-Montes en la parte oriental del Complejo de Morais, Portugal/España. PhD Univ Salamanca.
Dias da Silva Í (2014) Geología de las Zonas Centro Ibérica y Galicia – Trás-os-Montes en la parte oriental del Complejo de Morais, Portugal/España, Serie Nova Terra, vol 45. Instituto Universitario de Geología "Isidro Parga Pondal" - Área de Xeoloxía e Minería do Seminario de Estudos Galegos, Coruña
Dias da Silva I, Valverde-Vaquero P, González Clavijo E, Díez-Montes A, Martínez Catalán JR (2014) Structural and stratigraphical significance of U–Pb ages from the Mora and Saldanha volcanic complexes (NE Portugal, Iberian Variscides). In: Schulmann K, Martínez Catalán JR, Lardeaux JM, Janousek V, Oggiano G (eds), The Variscan Orogeny: Extent, Timescale and the Formation of the European Crust. Geol Soci London Spec Publ 405:115–135. https://doi.org/10.1144/sp405.3
Dias da Silva Í, Linnemann U, Hofmann M, González-Clavijo E, Díez-Montes A, Martínez Catalán JR (2015) Detrital zircon and tectonostratigraphy of the Parautochthon under the Morais Complex (NE Portugal): implications for the Variscan accretionary history of the Iberian Massif. J Geol Soc 172 (1):45–61. https://doi.org/10.1144/jgs2014-005
Dias da Silva Í, Díez Fernández R, Díez Montes A, González Clavijo E, Foster DA (2016) Magmatic evolution in the N-Gondwana margin related to the opening of the Rheic Ocean—evidence from the Upper Parautochthon of the Galicia-Trás-os-Montes Zone and from the Central Iberian Zone (NW Iberian Massif). Int J Earth Sci 105 (4):1127–1151. https://doi.org/10.1007/s00531-015-1232-9
Dias da Silva Í, González Clavijo E, Díez Montes A, Martínez Catalán JR, Gómez Barreiro J, Hoffmann M, Gärtner (2017) A Furongian-Late Ordovician volcanism in the Upper Parautochthon

of the Galicia-Trás-os-Montes Zone (NE Portugal): Paleogeographic meaning and geodynamic setting. In: Alvaro JJ, Casas JM, Clausen S (eds) Ordovician Geodynamics: The Sardic Phase in the Pyrenees, Mouthoumet and Montagne Noire massifs, BRGM/SGF, Géol France 4:19–21

Díaz García, F (1991) La estructura y la evolución metamórfica en un corte comprendido entre Carballiño y Forcarei. Área Esquistosa de Galicia Central, NW de España. Cuad Lab Xeol Laxe 16:273–299

Díaz-García F (2002) Tectónica y magmatismo Ordovícicos en el área de Sanabria, Macizo Ibérico. Geogaceta 32:119–122

Díez Fernández R, Martínez Catalán JR, Gerdes A, Abati J, Arenas R, Fernández-Suárez J (2010) U-Pb ages of detrital zircons from the Basal allochthonous units of NW Iberia: Provenance and paleoposition on the northern margin of Gondwana during the Neoproterozoic and Paleozoic. Gondwana Res 18 (2–3):385–399. doi:https://doi.org/10.1016/j.gr.2009.12.006

Díez Fernández R, Martínez Catalán JR, Arenas R, Abati J (2011) Tectonic evolution of a continental subduction-exhumation channel: Variscan structure of the basal allochthonous units in NW Spain. Tectonics 30 (3):1–22. https://doi.org/10.1029/2010tc002850

Díez Fernández R, Castiñeiras P, Gómez Barreiro J (2012a) Age constraints on Lower Paleozoic convection system: Magmatic events in the NW Iberian Gondwana margin. Gondwana Res 21 (4):1066–1079. doi:https://doi.org/10.1016/j.gr.2011.07.028

Díez Fernández R, Martínez Catalán JR, Arenas R, Abati J (2012b) The onset of the assembly of Pangaea in NW Iberia: Constraints on the kinematics of continental subduction. Gondwana Res 22 (1):20–25. https://doi.org/10.1016/j.gr.2011.08.004

Díez Fernández R, Martínez Catalán JR, Arenas R, Abati J, Gerdes A, Fernández-Suárez J (2012c) U–Pb detrital zircon analysis of the lower allochthon of NW Iberia: Age constraints, provenance and links with the Variscan mobile belt and Gondwanan cratons. J Geol Soc 169: 655–665

Díez Fernández R, Foster D, Gómez Barreiro J, Alonso-García M (2013) Rheological control on the tectonic evolution of a continental suture zone: the Variscan example from NW Iberia (Spain). Int J Earth Sci 102 (5): 1305–1319 https://doi.org/10.1007/s00531-013-0885-5

Díez-Fernández R, Pereira MF, Foster DA (2014) Peralkaline and alkaline magmatism of the Ossa-Morena zone (SW Iberia): Age, source, and implications for the Paleozoic evolution of Gondwanan. Lithosphere 7(1):79–90

Díez Fernández R, Fuenlabrada JM, Chichorro M, Pereira MF, Sánchez-Martínez S, Silva JB, Arenas R (2017) Geochemistry and tectonostratigraphy of the basal allochthonous units of SW Iberia (Évora Massif, Portugal): Keys to the reconstruction of pre-Pangean paleogeography in southern Europe. Lithos 268–271 (Supplement C):285–301. https://doi.org/10.1016/j.lithos.2016.10.031

Díez-Montes A (2006) La geologia del Dominio "Ollo de Sapo" en las comarcas de Sanabria y Terra do Bolo. PhD Univ Salamanca

Díez Montes A, Martínez Catalán JR, Bellido Mulas F (2010) Role of Ollo de Sapo massive felsic volcanism of NW Iberia in the Early Ordovician dynamics of northern Gondwana. Gondwana Res 17 (2–3):363–376. https://doi.org/10.1016/j.gr.2009.09.001

Díez Montes A, González Clavijo E, Dias da Silva Í, Gómez Barreiro J, Martínez Catalán JR, Castiñeiras P (2015) Geochemical Evolution of Volcanism during the Upper Cambrian-Ordovician Extension of the North Gondwana Margin. In: X Congresso Ibérico de Geoquímica/XVIII Semana de Geoquímica, Alfragide. Laboratório Nacional de Geologia e Energia, 54–57

Domeier M, Torsvik TH (2014) Plate tectonics in the Late Paleozoic. Geosci Front 5:303–350; https://doi.org/10.1016/j.gsf.2014.01.002

Eguiluz L (1987) Petrogénesis de rocas ígneas y metamórficas en el antiforme de Burguillos-Monesterio. Macizo Ibérico Meridional. PhD Univ Pais Vasco

Eguiluz L, Gil Ibarguchi JI, Abalos B, Apraiz A (2000). Superposed Hercynian and Cadomian orogenic cycles in the Ossa-Morena zone and related areas of the Iberian Massif. Geol Soc Am Bull 112:1398–1413

Expósito I, Simancas JF, González Lodeiro F, Bea, F, Montero P, Salman K (2003) Metamorphic and deformational imprint of Cambrian–Lower Ordovician rifting in the Ossa-Morena Zone (Iberian Massif, Spain). J Struct Geol 25:2077–2087

Etxebarria M, Chalot-Prat F, Apraiz A, Eguiluz E (2006) Birth of a volcanic passive margin in Cambrian time: Rift paleogeography of the Ossa-Morena Zone, SW Spain. Precambrian Res 147:366–386

Farias P, Gallastegui G, González-Lodeiro F, Marquínez J, Martín Parra LM, Martínez Catalán JR, de Pablo Maciá JG, Rodríguez Fernández LR (1987) Aportaciones al conocimiento de la litoestratigrafía y estructura de Galicia Central. Mem Fac Ciênc Univ Porto 1:411–431

Farias P, Ordoñez-Casado B, Marcos A, Rubio-Ordoñez A, Fanning CM (2014) U–Pb zircon SHRIMP evidence for Cambrian volcanism in the Schistose Domain within the Galicia-Trás-os-Montes Zone (Variscan Orogen, NW Iberian Peninsula). Geolo Acta 12 (3):209–218

Fernández-Suárez J, Gutiérrez-Alonso G, Jenner GA, Tubrett MN (2000) New ideas on the Proterozoic–Early Paleozoic evolution of NW Iberia: Insights from U–Pb detrital zircon ages. Precambrian Res 102:185–206

Fernández-Suárez J, Corfu F, Arenas R, Marcos A, Martínez Catalán JR, Díaz García F, Abati J, Fernández FJ (2002) U-Pb evidence for a polyorogenic evolution of the granulitic eclogitic units of the NW Iberian Massif. Contr Mineral Petrol 143:236–253

Fernández-Suárez J, Gutiérrez-Alonso G, Pastor-Galán D, Hoffman M, Murphy JB, Linnemann U (2014) The Ediacaran–Early Cambrian detrital zircon record of NW Iberia: Possible sources and paleogeographic constraints. Int J Earth Sci 103(5):1335–1357, https://doi.org/10.1007/s00531-013-0923-3

Floor P (1966) Petrology of an aegirine-riebeckite gneiss-bearing part of the Hesperian Massif: the Galiñeiro and surrounding areas, Vigo, Spain. Leid Geol Meded 36 (1):1–201

Fuenlabrada JM, Arenas R, Díez Fernández R, Sánchez Martínez S, Abati J, López Carmona A (2012) Sm–Nd isotope geochemistry and tectonic setting of the metasedimentary rocks from the basal allochthonous units of NW Iberia (Variscan suture, Galicia). Lithos 148 (Supplement C):196–208. https://doi.org/10.1016/j.lithos.2012.06.002

Galindo C (1989) Petrología y geocronología del Complejo Plutónico Táliga-Barcarrota (Badajoz). PhD Univ Complutense Madrid

Galindo C, Casquet C (2004) El magmatismo prevarisco de la zona de Ossa-Morena. In: Vera JA (ed), Geología de España. SGE-IGME, Madrid, 190–194

Galindo C, Portugal Ferreira MR, Casquet C, Priem HHA (1990) Dataciones Rb/Sr en el complejo plutónico Táliga- Barcarrota. Geogaceta 8:7–10

Gasquet D, Levresse G, Cheilletz A, Rachid Azizi-Samiz M, Mouttaqi A (2005) Contribution to a geodynamic reconstruction of the Anti-Atlas (Morocco) during Pan-African times with the emphasis on inversion tectonics and metallogenic activity at the Precambrian-Cambrian transition. Precambrian Res 140:157–182

Gil Ibarguchi JI, Dallmeyer RD (1991) Hercynian blueschist metamorphism in North Portugal: tectonothermal implications. Journal of Metamorphic Geology 9 (5):539–549. https://doi.org/10.1111/j.1525-1314.1991.tb00547.x

Gomes M, Coke C, Teixeira R, Azevedo M, Corfu F (2009) New insights in the Early Ordovician magmatism from the Marão anticline, Northern Portugal. Goldschmidt Conf Abstr, A450

Gómez Barreiro J, Martínez Catalán JR, Díez Fernández R, Arenas R, Díaz García F (2010) Upper crust reworking during gravitational

collapse: the Bembibre-Pico Sacro detachment system (NW Iberia). J Geol Soc 167:769–784
Gómez Barreiro J, Durán Oreja M, Martínez Catalán JR, González Clavijo E, Díez Montes A (2015) The sole thrust of the Lower Allochthon to the west of the Morais Complex (Portugal): Correlation with the Lalín-Forcalei thrust in the Órdenes Complex (Spain). In: Pitra P, Ballèvre M, Martínez Catalán JR (eds), Variscan 15 - The Variscan belt: Correlations and plate dynamics, Rennes, BRGM/SGF, p 73
González Clavijo E, Dias da Silva ÍF, Gutiérrez-Alonso G, Díez Montes A (2016) U/Pb age of a large dacitic block locked in an Early Carboniferous synorogenic mélange in the Parautochthon of NW Iberia: New insights on the structure/sedimentation Variscan interplay. Tectonophysics 681:159–169. https://doi.org/10.1016/j.tecto.2016.01.001
González-García D, Rubio-Ordóñez A, Cuesta A, Corretgé LG (2011) Geoquímica de las ortoanfibolitas y rocas metabásicas de Zarza la Mayor-Ceclavín (Cáceres, España) Geogaceta 50 (1):63–66
Goodge JW, Williams IS, Myrow PM (2004) Provenance of Neoproterozoic and lower Paleozoic siliciclastic rocks of the central Ross orogen, Antarctica: Detrital record of rift- to active-margin sedimentation. Geol Soci Am Bull 116: 1253–1279
Gutiérrez-Alonso G, Fernández-Suárez J, Jeffries TE, Jenner GA, Tubrett MN, Cox R, Jackson SE (2003) Terrane accretion and dispersal in the northern Gondwana margin. An Early Paleozoic analogue of a long-lived active margin. Tectonophysics 365: 221–232
Gutiérrez-Marco JC, Robardet M. Rábano I, Sarmiento GN, San José-Lancha MA, Herranz Araujo P, Pieren Pidal AP (2002) Ordovician. In Gibbons W and Moreno T (eds), The geology of Spain, The Geological Society, London, 31–49
Gutiérrez-Marco JC, Piçarra JM, García-Bellido DC, Vaz N, Aceñolaza GF (2011) Ordovician vs. "Cambrian" ichnofossils in the armorican Quartzite of central Portugal. In Gutiérrez-Marco JC, Rábano I, García-Bellido DC (eds), Ordovician of the World. Cuad Mus Geomin 14. IGME, Madrid
Henriques SBA, Neiva SBA, Ribeiro ML, Dunning GR, Tajčmanová L (2015) Evolution of a Neoproterozoic suture in the Iberian Massif, Central Portugal: New U-Pb ages of igneous and metamorphic events at the contact between the Ossa Morena Zone and Central Iberian Zone. Lithos 220–223:43–49
Hernández Enrile JL (1971) Las rocas porfiroides del límite Cámbrico-Precámbrico del flanco meridional del anticlinorio Olivenza-Monesterio (Badajoz). Bol Geol Min 82: 143–154
Iglesias Ponce de León M, Robardet M (1980) El Silúrico de Galicia Media (central) su importancia en la paleografía varisca. Cuad Lab Xeol Laxe 1:99–115
Irvine I, Baragar WR (1971) A guide to the chemical classification of the common volcanic rocks. Can J Earth Sci 8: 523–548
Julivert M, Fonboté JM, Ribeiro A, Conde LA (1974) Mapa Tectónico de la Península Ibérica y Baleares E: 1:1.000.000 y memoria explicativa. Publ IGME, 113 p
Keppie DF (2015) How the closure of paleo-Tethys and Tethys oceans controlled the early breakup of Pangaea. Geology 43 (4):335–338
Keppie JD, Davis DW, Krogh TE (1998) U-Pb geochronological constraints on Precambrian stratified units in the Avalon Composite Terrane of Nova Scotia, Canada: tectonic implications. Can J Earth Sci 35:222–236
Keppie JD, Nance RD, Murphy JB, Dostal J (2003) Tethyan, Mediterranean, and Pacific analogues for the Neoproterozoic–Paleozoic birth and development of peri-Gondwanan terranes and their transfer to Laurentia and Laurussia. Tectonophysics 365:195–220
Lancelot R, Allegret A (1982) Radiochronologie U/Pb de l'orthogneiss alcalin de Pedroso (Alto Alentejo, Portugal) et évolution antéhercynienne de l'Europe occidentale. N Jb Miner Abh 9: 385–394
Liñán E (1978) Bioestratigrafía de la Sierra de Córdoba. PhD Univ Granada 191: 1–212
Liñán E, Quesada C (1990) Rift Phase (Cambrian) stratigraphy of the Ossa-Morena zone. In: Dallmeyer RD, Martínez García E (eds), Pre-Mesozoic Geology of Iberia. Springer-Verlag, Berlin, 259–266
Liñán E, Gozalo R, Palacios T, Gámez Vintanez JA, Ugidos JM, Mayoral E (2002) Cambrian. In Gibbons W and Moreno T (eds), The geology of Spain, The Geological Society, London, 17–29
Linnemann U, McNaughton NJ, Romer RL, Gehmlich M, Drost K, Tonk C (2004) West African provenance for Saxo-Thuringia (Bohemian Massif): Did Armorica ever leave pre-Pangean Gondwana?—U/Pb-SHRIMP zircon evidence and the Nd isotopic record. Int J Earth Sci 93 (5):683–705
Linnemann U, Pereira FC, Jeffries TE, Drost K, Gerdes A (2008) The Cadomian Orogeny and the opening of the Rheic Ocean: The diachrony of geotectonic processes constrained by LA-ICP-MS U–Pb zircon dating (Ossa-Morena and Saxo-Thuringian Zones, Iberian and Bohemian Massifs). Tectonophysics 461:21–43
Lizarralde D, Axen GJ, Brown HE, Fletcher JM, González-Fernández A, Harding AJ, Holbrook WS, Kent GM, Páramo P, Sutherland F, Umhoefer PJ (2007) Variation in styles of rifting in the Gulf of California. Nature 448:466–469
López-Carmona A, Abati J, Reche J (2010) Petrologic modelling of chloritoid-glaucophane schists from the NW Iberian Massif. Gondwana Res 17(2): 377–391. https://doi.org/10.1016/j.gr.2009.10.003
López-Carmona A, Pitra P, Abati J (2013) Blueschist-facies pelites from the Malpica-Tui Unit (NW Iberian Massif): phase equilibria modeling and H_2O and Fe_2O_3 influence in high-pressure assemblages. J Metamorphic Geol 31(3), 263–280. https://doi.org/10.1111/jmg.12018
López-Carmona A, Abati J, Pitra P, Lee JW (2014) Retrogressed lawsonite blueschists from the NW Iberian Massif: P–T–t constraints from thermodynamic modelling and 40Ar/39Ar geochronology. Contr Miner Petrol 167 (3):1–20. https://doi.org/10.1007/s00410-014-0987-5
López-Guijarro R, Quesada C, Fernández-Suárez J, Jeffries T, Pin C (2007) Age of the Early Ordovician rift–drift transition of the Rheic Ocean in the Ossa Morena Zone: K-bentonite in the succession at "Venta del Ciervo". In: The Rootless Variscan Suture of NW Iberia (Galicia, Spain). IGCP-497 Meeting, Abstracts and Programme. Publ IGME, 142–143
López-Guijarro R, Armendáriz M, Quesada C, Fernández-Suárez J, Murphy JB, Pin Ch, Bellido F (2008) Ediacaran-Paleozoic tectonic evolution of the Ossa Morena and Central Iberian zones (SW Iberia) as revealed by Sm-Nd isotope systematics. Tectonophysics 461: 202–214
López-Sánchez MA, Iriondo A, Marcos A, Martínez FJ (2012) Una edad de 478,7 Ma (U-Pb Shrimp-RG) en la Formación Ollo de Sapo: implicaciones para el volcanismo Cambro-Ordovícico de la Península Ibérica. Geotemas, 07-285
Lotze F (1945) Zur Gliederung der Varisziden der Iberischen Meseta. Geotekt Forsch 6:78–92
Lotze F (1956) Über Sardischen Bewegungen in Spanien und ihre Beziehungen zur Assyntischen Faltung. Geotekt Symp Hans Stille, 129–139
Lotze F (1961) Das Kambrium Spaniens. Teil 1: Stratigraphie. Akad Wiss Literat, Abh Math-Natuwiss KI 6:216 p
Marcos A, Llana Fúnez S (2002) Estratigrafía y estructura de la lámina tectónica del Para-autóctono y de su autóctono en el área de Chantada (Galicia, NO de España). Trab Geol, Univ Oviedo, 23:53–72
Marquínez García JL (1984) La geología del área esquistosa de Galicia Central (Cordillera Herciniana, NW de España). Mem IGME 100

Martínez Catalán JR, Hacar Rodríguez MP, Villar Alonso P, Pérez-Estaún A, González Lodeiro F (1992) Lower Paleozoic extensional tectonics in the limit between the West Asturian-Leonese and the Central Iberian Zones of the Variscan Fold-Belt in NW Spain. Geolog Runds 81:545–560

Martínez Catalán JR, Arenas R, Díaz García F, Rubio Pascual FJ, Abati J, Marquínez J (1996) Variscan exhumation of a subducted Paleozoic continental margin: The basal units of the Ordenes Complex, Galicia, NW Spain. Tectonics 15: 106–121

Martínez Catalán JR, Fernández Suárez J, Jenner GA, Belousova E, Díez-Montes A (2004) Provenance constraints from detrital zircon UePb ages in the northwestern Iberian Massif: implications for Paleozoic plate configuration and Variscan evolution. J Geol Soci London 161:461–473

Martínez Catalán JR, Arenas R, Díaz García F, González Cuadra P, Gómez Barreiro J, Abati J, Castiñeiras P, Fernández-Suárez J, Sánchez Martínez S, Andonaegui P, González Clavijo E, Díez Montes A, Rubio Pascual F, Valle Aguado B (2007) Space and time in the tectonic evolution of the northwestern Iberian Massif: Implications for the Variscan belt. In: Hatcher Jr. RD, Carlson MP, McBride JH, Martínez Catalán JR (eds) 4-D Framework of Continental Crust. Geol Soc Am, Boulder, pp 403–423. https://doi.org/10.1130/2007.1200(21)

Martínez Catalán JR, Arenas R, Abati J, Sánchez Martínez S, Díaz García F, Fernández-Suárez J, González Cuadra P, Castiñeiras P, Gómez Barreiro J, Díez Montes A, González Clavijo E, Rubio Pascual F, Andonaegui P, Jeffries TE, Alcock JE, Díez Fernández R, López Carmona A (2009) A rootless suture and the loss of the roots of a mountain chain: The Variscan Belt of NW Iberia. CR Geosci 341 (2–3):114–126. https://doi.org/10.1016/j.crte.2008.11.004

Martínez Catalán JR, Rubio Pascual, FJ, Díez-Montes A, Díez-Fernández R, Gómez Bareiro J, Días da Silva I, González-Clavijo E, Ayarza P, Alcook JE (2014) The late Variscan HT/LP metamorphic event in NW and Central Iberia: relationships to crustal thickening, extension, orocline development and crustal evolution. Geol Soci London Spec Publ 405:225–247

Martínez-Poyatos D, Gutíerrez-Marco JC, Pardo Alonso MV, Rábano I, Sarmiento G (2004) Dominio del Complejo Esquisto-Grauváquico: La secuencia Paleozoica postcámbrica. In Vera JA (ed), Geología de España, SGE-IGME, Madrid, p 81–83

Mata J, Munhá J (1990) Magmatogénese de metavulcanitos câmbricos do Nordeste Alentejano nos estadios iniciais de "rifting" continental. Com Ser Geol Portugal 76:61–89

Mata J, Ribeiro ML, Piçarra JM (1999) Geochemical characteristic of the S. Marcos do Campo Volcanic Complex (Ossa-Morena Zone): evidence for subduction-related magmatism. Com Inst Geol Min 86:3–14

Montero P, Bea F (1998) Accurate determination of 87Rb/86Sr and 147Sm/144Nd ratios by inductively-coupled-plasma mass spectrometry in isotope geoscience: an alternative to isotope dilution analysis. Anal Chim Acta 358: 227–233

Montero P, Salman K, Zinger T, Bea F (1999) Rb-Sr and single - zircon grain ^{207}Pbf/^{206}Pb chronology of the Monesterio granodiorite and related migmatites. Evidence of a late Cambrian melting event in the Ossa-Morena Zone, Iberian massif. Est Geol 55:3–8

Montero P, Salman K, Bea F, Azor A, Expósito I, González-Lodeiro F, Martínez-Poyatos D, Simancas F (2000) New data on the geochronology of the Ossa-Morena Zone, Iberian Massif. In: Variscan-Appalachian dynamics: the building of the Upper Paleozoic basement. Tectonics 15, A Coruña Abstracts 136–138

Montero P, Bea F, González Lodeiro F, Talavera C, Whitehouse MJ (2007) Zircon ages of the metavolcanic rocks and metagranites of the Ollo de Sapo Domain in central Spain: implications for the Neoproterozoic to Early Paleozoic evolution of Iberia. Geol Mag 144: 963–976

Montero P, Bea F, Corretgé LG, Floor P, Whitehouse MJ (2009a) U-Pb ion microprobe dating and Sr and Nd isotope geology of the Galiñeiro Igneous Complex: A model for the peraluminous/peralkaline duality of the Cambro-Ordovician magmatism of Iberia. Lithos 107 (3):227–238. https://doi.org/10.1016/j.lithos.2008.10.009

Montero P, Talavera C, Bea F, Gonzalez Lodeiro F, Whitehouse MJ (2009b) Zircon Geochronology of the Ollo de Sapo Formation and the Age of the Cambrian-Ordovician Rifting in Iberia. J Geol 117:174–191

Moreno-Eiris E (1987) Los montículos arrecifales de algas y arqueociatos del Cámbrico Inferior de Sierra Morena. Publ Esp Bol Geol Min 98:1–127

Munhá J, Ribeiro A, Ribeiro ML (1984) Blueschists in the Iberian Variscan Chain (Trás-os-Montes, NE Portugal). Comun Serv Geol Portugal 70 (1):31–53

Murphy JB, Pisaresvsky SA, Nance RD, Keppie D (2004) Neoproterozoic-Early Paleozoic evolution of peri-Gondwanan terranes: implications for Laurentia-Gondwana connections. Int J Earth Sci 93:659–682

Murphy JB, Gutiérrez-Alonso G, Nance RD, Fernández-Suárez J, Keppie JD, Quesada C, Strachan RA, Dostal J (2006) Origin of the Rheic Ocean: Rifting along a Neoproterozoic suture? Geology 34: 325–328

Murphy JB, Gutiérrez-Alonso G, Fernández-Suárez J, Braid JA (2008) Probing crustal and mantle lithosphere origin through Ordovician volcanic rocks along the Iberian passive margin of Gondwana. Tectonophisics 461:166–180

Murphy JB, Quesada C, Gutiérrez-Alonso G, Johnston ST, Weil A (2016) Reconciling competing models for the tectono-stratigraphic zonation of the Variscan orogen in Western Europe. Tectonophysics 681:209–219

Nance RD, Murphy JB, Keppie JD (2002) Cordilleran model for the evolution of Avalonia. Tectonophysics 352:11–31

Nance RD, Murphy JB, Strachan RA, Keppie JD, Gutiérrez-Alonso G, Fernández-Suarez J, Quesada C, Linnemann U, D'lemos R, Pisarevsky SA (2008) Neoproterozic-early Paleozoic tectonostratigraphy and paleogeography of the peri-Gondwanan terranes: Amazonian vs. West African connections. Geol Soc London Spec Publ 297:345–383

Nance RD, Gutiérrez-Alonso G, Keppie JD, Linnemann U, Murphy JB, Quesada C, Strachan RA, Woodcock NH (2010) Evolution of the Rheic Ocean. Gondwana Res 17:194–222

Nance RD, Gutiérrez-Alonso G, Keppie JD, Linnemann U, Murphy JB, Quesada C, Strachan RA, Woodcock NH (2012) A brief history of the Rheic Ocean. Geosci Front 3:125–135

Navarro NB, Maresch WV, Schertl H, Baumann A, Krebs M (2003) Petrology of the high-pressure "Basal Unit", Morais Complex, Northeast Portugal. Indian J Geol 75 (1–4):9–37

Navidad M, Bea F (2004) El magmatismo prevarisco de la Zona Centroibérica. In Vera JA (ed), Geología de España. Madrid, SGE-IGME, 92–96

Navidad M., Castiñeiras P (2011) Early Ordovician magmatism in the northern Central Iberian Zone (Iberian Massif): new U–Pb (SHRIMP) ages and isotopic Sr–Nd data. In: Gutiérrez-Marco JC,, Rábano I, García-Bellido D (Eds.), Ordovician of the World. IGME, Madrid, pp 391–398

Neiva AMR, Williams IS, Ramos JM, Gomes MEP, Silva MMVG, Antunes IMHR (2009) Geochemical and isotopic constraints on the petrogenesis of Early Ordovician granodiorite and Variscan two-mica granites from the Gouveia area, central Portugal. Lithos 111:168–185

Ochsner A (1993) U-Pb Geochronology of the Upper Proterozoic-Lower Paleozoic geodynamic evolution in the Ossa Morena Zone (SW Iberia): Constraints on the timing of the Cadomian Orogeny. PhD ETH Zurich

Odriozola JM, Peón A, Vargas I, Quesada C, Cueto LA (1983) Memoria de la Hoja nº 854 (Zafra), Segunda Serie (MAGNA), IGME. Depósito legal: M-35.070-1983, 1–57

Oliveira VM (1984) Contribuiçao para o conhecimento geológico-mineiro da região de Alandroal-Juromenha (Alto Alentejo). Est Not Trab Serv Fom Min 26 (1–4): 103–126

Oliveira JT, Oliveira V, Piçarra JM (1991) Traços gerais da evolução tectono-estratigráfica da Zona de Ossa Morena, em Portugal: síntese crítica do estado actual dos conhecimentos. Comun Serv Geol Portugal 77:3–26

Oliveira JT, Pereira E, Piçarra JM, Young T, Romano M (1992) O Paleozóico Inferior de Portugal: Síntese da estratigrafia e da evolução paleogeografica. In: Gutiérrez Marco JG, Saavedra J, Rábano I (Eds), Paleozoico inferior de Ibero-América. Univ Extremadura, Spain, 359–375

Ordóñez Casado B (1998) Geochronological studies of the Pre-Mesozoic basement of the Iberian Massif: The Ossa Morena Zone and the Allochthonous Complexes within the Central Iberian Zone. PhD ETH Zurich

Orejana D, Villaseca C, Merino Martínez E (2016) Age and geological setting of the basic Ordovician magmatism from the Spanish Central System. IX Congreso Geológico de España. Geo-Temas 16 (1):415–418

Orejana D, Villaseca C, Merino Martínez E (2017) Basic Ordovician magmatism of the Spanish Central System: Constraints on the source and geodynamic setting. Lithos 284–285:608–624

Palacios T (2015) Acritarch assemblages from the Oville and Barrios Formations, northern Spain: A pilot proposal of a middle Cambrian (Series 3) acritarch biozonation in northwestern Gondwana. Rev of Paleobot Palynol 219:71–105

Palme H, O'Neill HSC (2004) Cosmochemical estimates of mantle composition. In: RW Carlson (ed) The mantle and core. Treatise on Geochemistry (Holland HD, Turekian KK, eds), Elsevier-Pergamon Oxford, v 2: 1–38

Palmer AR, James NP (1980) The Hawke Bay event: a circum- Iapetus regression near the Lower–Middle Cambrian boundary. In: Wones DR (Ed), The Caledonides in USA. Virginia Polytech Inst State Univ Mem 2:15–18

Paris F, Boumendel K, Dabrard MP, Ghienne JF, Loi A, Tang P, Videt B, Achab A (2007) Chitinozoan-based calibration of Early-Mid Ordovician transgressive events on northern Gondwana. Acta Palaeontol Sin 46:370–375

Pearce, JA, Cann JR (1973) Tectonic setting of basic volcanic rocks determined using trace element analyses. Earth Planet Sci Lett 19 (2):290–300

Pearce JA (1996) Sources and settings of granitic rocks. Episodes 19:120–125

Pearce JA (2008) Geochemical fingerprinting of oceanic basalts with applications to ophiolite classification and the search for Archean oceanic crust. Lithos 100:14–48

Pearce JA, Harris NBW, Tindle AG (1984) Trace element discrimination diagrams for the tectonic interpretation of granitic rocks. J Petrol 25:956–983

Pereira MF (2014) Potential sources of Ediacaran strata of Iberia: a review. Geodin Acta 27 (1): 1–14. http://dx.doi.org/10.1080/09853111.2014.957505

Pereira MF, Quesada C (2006) Ediacaran to Visean crustal growth processes in the Ossa-Morena zone (SW Iberia). IGCP 497 Evora Meeting 2006: Conference abstracts and Field trip guide. Publ IGME 1–115

Pereira MF, Silva JB (2002) Neoproterozoic-Paleozoic tectonic evolution of the Coimbra-Cordoba shear zone and related areas of the Ossa-Morena and Central-Iberian zones (Northeast Alentejo, Portugal). Comun Insti Geol Min 89:47–62

Pereira MF, Silva JB (2006) Nordeste Alentejano. In: Dias R, Araújo A, Terrinha P, Kullberg JC (eds), Geología de Portugal no Contexto da Ibéria, Univ Évora, 145–150

Pereira MF, Chichorro M, Linnemann U, Eguiluz L, Silva JB (2006) Inherited arc signature in Ediacaran and Early Cambrian basin of the Ossa-Morena Zone (Iberian Massif Portugal): plaleogeographic link with European and North African Cadomian correlatives Precambrian Res 144:297–315

Pereira MF, Silva JB, Chichorro M, Moita P, Santos JF, Apraiz A, Ribeiro C (2007) Crustal growth and deformational processes in the northern Gondwana margin: constraints from the Évora Massif (Ossa Morena Zone, southwest Iberia, Portugal) Geol Soc Am Spec Pap 42:333–358

Pereira MF, Chichorro M, Williams IS, Silva JB (2008a) Zircon U-Pb geochronology of paragneisses and biotite granites from the SW Iberian Massif (Portugal): evidence for a paleogeographic link between the Ossa-Morena Ediacaran basins and the West African craton. In: Ennih N, Liégeois JP (eds), The Boundaries of the West African Craton. Geol Soc London Spec publ 297:385–404

Pereira MF, Apraiz A, Silva JB, Chichorro M (2008b) Tectonothermal analysis of high-temperature mylonitization in the Coimbra–Córdoba shear zone (SW Iberian Massif, Ouguela tectonic unit, Portugal): Evidence of intra-continental transcurrent transport during the amalgamation of Pangea. Tectonophysics 461:378–394

Pereira MF, Silva JB, Drost K, Chichorro M, Apraiz A (2010) Relative timing of transcurrent displacements in northern Gondwana: U–Pb laser ablation ICP-MS zircon and monazite geochronology of gneisses and sheared granites from the western Iberian Massif (Portugal). Gondwana Res 17:461–481

Pereira MF, Chichorro M, Solá AR, Silva JB, Sánchez-García T, Bellido F (2011) Tracing the Cadomian magmatism with detrital/inheritedzirconagesby in-situ U–Pb SHRIMP geochronology (Ossa-Morena Zone, SW IberianMassif). Lithos 123 (1–4):204–217

Pereira MF, Linnemann U, Hofmann M, Chichorro M, Solá AR, Medina J, Silva JB (2012a) The provenance of late Ediacaran and early Ordovician siliciclastic rocks in the Southwest Central Iberian Zone: constraints from detrital zircon data on northern Gondwana margin evolution during the late Neoproterozoic. Precambrian Res 192–195:166–189, https://doi.org/10.1016/j.precamres.2011.10.019

Pereira MF, Solá AR, Chichorro M, Lopes L, Gerdes A, Silva JB (2012b) North-Gondwana assembly, break-up and paleogeography: U–Pb isotope evidence from detrital and igneous zircons of Ediacaran and Cambrian rocks of SW Iberia. Gondwana Res 22:866–881

Pérez-Estaún A, Bastida F, Martínez Catalán JR, Gutiérrez Marco JC, Marcos A, Pulgar JA (1990) West Asturian-Leonese Zone: Stratigraphy. In: Dallmeyer RD, Martínez García E (eds), Pre-Mesozoic Geology of Iberia. Springer-Verlag, Berlin, 92–102

Pin C, Ortega Cuesta LA, Gil Ibarguchi JI (1992) Mantle-derived, early Paleozoic A-type metagranitoids from the NW Iberian massif: Nd isotope and trace-element constraints. Bull Soc géol France 163 (4): 483–494

Quesada C (1990a) Precambrian terranes in the Iberian Variscan Foldbelt. In: Strachan RA, Taylor GK (Eds), Avalonian and Cadomian geology of the North Atlantic. Blackie, New York, 109–133

Quesada C (1990b) Precambrian successions in SW Iberia: their relationship to "Cadomian" orogenic events. In: D'Lemos RS, Strachan RA, Topley CG (eds), The Cadomian Orogeny. Geol Soc Spec Publ 51:353–362

Quesada C (1991) Geological constraints on the Paleozoic tectonic evolution of tectonostratigraphic terranes in the Iberian Massif. Tectonophysics 185:225–245

Quesada C (1992) Evolución tectónica del Macizo Ibérico: una historia de crecimiento por acrecencia sucesiva de terrenos durante el Proterozoico y el Paleozoico. In: Gutierrez Marco JG, Saavedra J, Rábano I (eds), Paleozoico Inferior de Ibero-América, Universidad de Extremadura, 173–190

Quesada C (2006) The Ossa-Morena zone of the Iberian Massif: a tectonostratigraphic approach to its evolution. Z Deuts Gesell Geowiss 157:585–595

Quesada C, Munhá J (1990) Metamorphism in the Ossa-Morena Zone. In Dallmeyer RD, Martínez García E (eds), Pre-Mesozoic Geology of Iberia. Springer-Verlag, Berlin, 314–320

Quesada C, Bellido F, Dallmeyer RD, Gil Ibarguchi I, Oliveira JT, Pérez Estaun A, Ribeiro A, Robardet M, Silva JB (1991) Terranes within the Iberian Massif: correlations with West African sequences. In: Dallmeyer RD, Lecorché JP (eds), The West African Orogens and Circum-Atlantic Correlations. Springer, Berlin, 251– 277

Ribeiro A (1974) Contribution à l'étude téctonique de Trás-os-Montes Oriental Mem Serviços Geol Portugal 24:1–174

Ribeiro ML (1986) Geologia e petrologia da região a SW de Macedo de Cavaleiros. PhD Unive Lisboa

Ribeiro ML (1987a) Petrogenesis of early Paleozoic peralkaline ryolites from the Macedo de Cavaleiros region (NW Portugal). Geol Runds 76: 147–168

Ribeiro ML (1987b) The significance of Valbenfeito Felsic Dikes on the definition of the Regional Tectonic Setting. Com Ser Geol Portugal 73: (1–2):3–10

Ribeiro ML (1991) Contribuição para o conhecimento estratigráfico e petrológico da região a SW de Macedo de Cavaleiros (Trás-os--Montes oriental). Mem Serv Geol Portugal 30:1–85

Ribeiro ML, Floor P (1987) Magmatismo peralcalino no Macizo Hespérico: sua distribuiçao e significado geodinamico. In: Bea F (ed), Geología de los granitoides y rocas asociadas del Macizo Hespérico. Rueda, Madrid, 211–221

Ribeiro ML, Mata J (1994) Early Paleozoic evolution in NW Gondwana. Abstract, Inter. Meeting Proj 351, Abstracts, 100–102. Fac.Sci. Mohammed V University, Rabat, Morocco

Ribeiro A, Quesada C, Dallmeyer RD (1990a) Geodynamic evolution of the Iberian Massif. In: Dallmeyer RD, Martínez García E (eds), Pre-Mesozoic Geology of Iberia, Springer, Berlin, 399–410

Ribeiro A, Pereira E, Dias R (1990b) Allochthonous sequences – Structure in the Northwest of the Iberian Peninsula. In: Dallmeyer RD, Martínez García E (eds), Pre-Mesozoic Geology of Iberia. Springer Berlin-Heidelberg, 222–236

Ribeiro ML, Mata J, Munhá J (1992) Magmatismo do Paleozóico Inferior em Portugal. In: Gutiérrez Marco JC, Saavedra J, Rábano I (eds), Paleozoico inferior de Ibero-América. Univ Extremadura, 378–394

Ribeiro ML, Priem HNA, Boelrjik AIM, Schermerhorn LJG (1995) Rb-Sr Whole-rock age of peralkaline acidic volvacins in the Macedo de Cavaleiros area, Trás-os-montes (NE Portugal). Comun Serv Geol Portugal, 71(2):171–174

Ribeiro ML, Munhá J, Mata J, Palácios T (1997) Vulcanismo na Zona de Ossa Morena e seu enquadramento geodinâmico. In: Araújo A, Pereira MF (eds), Estudo sobre a geologia de Ossa-Morena (Maciço Ibérico). Homenagem Prof Francisco Gonçalves. Univ Évora, 37–55

Ribeiro A, Pereira E, Ribeiro ML, Castro P (2013) Unidades Alóctones da região de Morais (Trás-os-Montes oriental). In: Dias R, Araújo A, Terrinha P, Kullberg JC (eds), Geologia de Portugal, vol I - Geologia Pré-mesozoica de Portugal, 333–376

Rodrigues JF, Ribeiro A, Pereira E (2013) Complexo de Mantos Parautóctones do NE de Portugal: estructura interna e tectonoestratigrafia. In: Dias R, Araújo A, Terrinha P, Kullberg JC (eds), Geologia de Portugal, vol I - Geologia Pré-mesozoica de Portugal, 275–331

Rodríguez J (2005) Recristalización y deformación de litologías supracorticales sometidas a metamorfismo de alta presión (Complejo de Malpica-Tuy, NO del Macizo Ibérico), vol 29. Nova Terra 29, Instituto Universitario de Geología "Isidro Parga Pondal" - Área de Xeoloxía e Minería do Seminario de Estudos Galegos, A Coruña

Rodríguez J, Cosca MA, Gil Ibarguchi JI, Dallmeyer RD (2003) Strain partitioning and preservation of 40Ar/39Ar ages during Variscan exhumation of a subducted crust (Malpica–Tui complex, NW Spain). Lithos 70 (3–4):111–139. https://doi.org/10.1016/s0024-4937(03)00095-1

Rodríguez R, Marcos A, Farias P (2004) Palynological data on the age of the meta-sediments of the "Schistose Domain" in the Cabo Ortegal area (Galicia-Tras-os-Montes Zone, NW Spain). N Jb Geol Paläont 4:214–232

Romão J, Dunning G, Marcos A, Dias R, Ribeiro A (2010) Mação-Penhascoso laccolith granite: age and its implications (SWCentral-Iberia Zone). Geosci On-line J 16 (13)

Romeo I, Lunar R, Capote R, Quesada C, Piña R, Dunning GR, Ortega L (2006) U/Pb age constraints on Variscan magmatism and Ni-Cu-PGE metallogeny in the Ossa-Morena zone (SW Iberia). J Geol Soc London 163:1–9

Rowland SM, Gangloff RA (1988) Structure and paleoecology of Lower Cambrian reefs. Palaios 3:111–135

Rubio-Ordóñez A, Valverde-Vaquero P, Corretgé LG, Cuesta-Fernández A, Gallastegui G, Fernández-González M, Gerdes A (2012) An Early Ordovician tonalitic–granodioritic belt along the Schistose-Greywacke Domain of the Central Iberian Zone (Iberian Massif, Variscan Belt). Geol Mag 149 (5):927–939

Rudnick RL, Gao S (2003) Composition of the Continental Crust. In Rudnick RL (ed), The Crust. Treatise on Geochemistry (Holland HD, Turekian KK, eds), First Edicion, Elsevier-Pergamon Oxford, Vol 3: 1–64

Russo A, Bechstädt T (1994) Evolución sedimentológica y paleogeográfica de la formación Vegadeo (Cámbrico Inferior-Medio) en la zona entre Visuña y Piedrahita do Laurel (Lugo, NO de España). Rev Soc Geol Es 7:299–310

Sá AA, Meireles C, Coke C, Gutiérrez-Marco JC (2005) Unidades litoestratigráficas do Ordovícico da região de Trás-os-Montes (Zona Centro Ibérica). Comun Geol 92:31–74

Salman K (2002) Estudio petrológico, geoquímico y geocronológico de los granitoides del área Monesterio-Cala, Zona de Ossa Morena (Macizo Ibérico). PhD Univ Granada

Salman K (2004) The timing of the Cadomian and Variscan cycles in the Ossa Morena Zone, SW Iberia: granitic magmatism from subduction to extension. J Ib Geol 30:119–132

Salman K, Montero P (1999) Geochronological, Geochemical and Petrological Studies in two areas of the Ossa-Morena Zone: the Monesterio Complex and the Calera de León Granite. XV Reunión de Geología del Oeste Peninsular – International Meeting on Cadomian Orogens, Badajoz. J Conf Abstr 4/3:1020

Sánchez-García T, Bellido F, Quesada C (2003) Geodynamic setting and geochemical signatures of Cambrian-Ordovician rift-related igneous rocks (Ossa-Morena Zone, SW Iberia). Tectonophysics 365:233–255

Sánchez-García T, Quesada C, Bellido F, Dunning G, González de Tánago J (2008a) Two-step magma flooding of the upper crust during rifting: The Early Paleozoic of the Ossa-Morena Zone (SW Iberia). Tectonophysics 461:72–90

Sánchez-García T, Bellido F, Pereira MF, López-Guijarro R, Quesada C, Chichorro, M, Silva JB, Pin Ch (2008b) Expresión magmática temprana de un rift intracontinental en el margen de Gondwana durante el Cámbrico Inferior: Zona de Ossa-Morena (SW Macizo Ibérico, Portugal., España). Geo-Temas 10: 1567–1572

Sánchez-García T, Bellido F, Pereira MF, Chichorro M, Quesada C, Pin Ch, Silva JB (2010) Rift-related volcanism predating the birth of the Rheic Ocean (Ossa-Morena zone, SW Iberia).Gondwana Res 17:392–407

Sánchez-García T, Pereira MF, Bellido F, Chichorro M, Silva JB, Valverde-Vaquero P, Pin Ch, Solá AR (2013) Early Cambrian granitoids of the Ossa-Morena Zone (SW Iberia) in the transition from a convergent setting to intra-continental rifting in the Northern margin of Gondwana. Int J Earth Sci (Geol Rundsch) 103:1203–1218

Sánchez-García T, Quesada C, Bellido F, Dunning GR, Pin Ch, Moreno-Eiris E, Perejón A (2016) Age and characteristics of the Loma del Aire unit (SW Iberia): Implications for the regional correlation of the Ossa-Morena Zone. Tectonophysics 681:58–72

Sánchez-Lorda ME, Ábalos B, García de Madinabeitia S, Eguíluz L, Gil Ibarguchi JI, Paquette JL (2016) Radiometric discrimination of pre-Variscan amphibolites in the Ediacaran Serie Negra (Ossa-Morena Zone, SW Iberia). Tectonophysics 681:31–46

Santos Zalduegui JF, Schärer U, Gil Ibarguchi JI (1995) Isotope constraints on the age and origin of magmatism and metamorphism in the Malpica-Tuy allochton, Galicia, NW Spain. Chem Geol 121:91–103

Sarrioanandía F, Carracedo Sánchez M, Eguiluz L, Ábalos B, Rodríguez J, Pin Ch, Gil Ibarguchi JL (2012) Cambrian Rift-related magmatism in the Ossa-Morena Zone (Iberian massif): Geochemical and geophysical evidence of Gondwana break-up. Tectonophysics 570–571:135–150

Schäfer HJ (1990) Geochronological investigations in the Ossa Morena Zone, SW Spain. PhD ETH Zurich

Schermerhorn LJG, Kotsch S (1984) First occurrence of lawsonite in Portugal and tectonic implications. Comun Inst Geol Min 70 (1):23–29

Sdzuy K, Liñán E (1993) Rasgos paleogeográficos del Cámbrico Inferior y Medio del norte de España. Cuad Lab Xeol Laxe 18:189–215

Shaw J, Gutiérrez-Alonso G, Johnston ST, Pastor Galán D (2014) Provenance variability along the Early Ordovician north Gondwana margin: paleogeographic and tectonic implications of U–Pb detrital zircon ages from the Armorican Quartzite of the Iberian Variscan belt. Geol Soc Am Bull 125 (5–6):702–719, http://dx.doi.org/10.1130/b30935.1

Shorttle O (2008) The Geology of the Cantabrians around Crémenes, North Western Spain. Part II Mapping Project, Queens' College University of Cambridge, 1–45

Simancas JF, Expósito I, Azor A, Martínez Poyatos D, González Lodeiro F (2004) From the Cadomian orogenesis to the early Paleozoic Variscan rifting in Southwest Iberia. J Ib Geol 30: 53–71

Solá AR (2007) Relações Petrogeoquímicas dos Maciços Graníticos do NE Alentejano. PhD Univ Coimbra

Solá AR, Pereira MF, Williams IS, Ribeiro ML, Neiva AMR, Montero P, Bea F, Zinger T (2008) New insights from U–Pb zircon dating of Early Ordovician magmatism on the northern Gondwana margin: the Urra Formation (SW Iberian Massif, Portugal). Tectonophysics 461:114–129

Sousa M, Sant'Ovaia H, Tassinari C, Noronha F (2014) Geocronologia U-Pb (SHRIMP) e Sm-Nd do ortognaisse biotítico do Complexo Metamórfico da Foz do Douro (NW de Portugal). Comun Geol 101:225–228

Stampfli GM (2000) Tethyan oceans. In: Bozkurt E, Winchester JA, Piper JDA (eds) Tectonics and magmatism in Turkey and surrounding area. Geol Soc London Spec Publ 173:1–23

Stampfli GM, Borel GD (2004) The TRANSMED transects in space and time: Constraints on the paleotectonic evolution of the Mediterranean domain. In; Cavazza W, Roure F, Spakman W, Stampfli G M, Ziegler P (eds), The TRANSMED Atlas: The Mediterranean Region from Crust to Mantle. Springer Verlag, Heidelberg, 53–80

Stampfli GM, von Raumer JF, Borel GD (2002) Paleozoic evolution of pre-Variscan terranes: From Gondwana to the Variscan collision. In: Martínez Catalán JR, Hatcher RD, Arenas R, Díaz García F (eds), Variscan-Appalachian Dynamics: the Building of the Late Paleozoic Basement. Geol Soc Am Spec Pap 364:263–280

Stern RJ (2002) Crustal evolution in the East African Orogen: a neodymium isotopic perspective. J African Earth Sci 34:109–117

Sun SS, McDonough WF (1989) Chemical and isotopic systematics of oceanic basalts: implications for mantle composition and processes. In: Saunders AD, Norry MJ (Eds), Magmatism in the Ocean Basins. Geol Soc Spec Publ 42:313–345

Syme EC (1998) Ore-Associated and Barren Rhyolites in the central Flin Flon Belt: Case Study of the Flin Flon Mine Sequence. Manitoba Energy and Mines, Open File Report OF98-9: 1–32

Talavera C (2009) Pre-Variscan magmatism of the Central Iberian Zone: chemical and isotope composition, geochronology and geodynamic significance. PhD Univ Granada

Talavera C, Bea F, Montero PG, Whitehouse M (2008) A revised Ordovician age for the Sisargas orthogneiss, Galicia(Spain). Zircon U-Pb ion-microprobe and LA-ICPMS dating. Geol Acta 6 (4):313–317

Talavera C, Montero P, Martínez Poyatos D, Williams IS (2012) Ediacaran to Lower Ordovician age for rocks ascribed to the Schist–Graywacke Complex (Iberian Massif, Spain): Evidence from detrital zircon SHRIMP U–Pb geochronology. Gondwana Res 22: 928–942

Talavera C, Montero P, Bea F, González-Lodeiro F, Whitehouse M (2013) U–Pb Zircon geochronology of the Cambrian-Ordovician metagranites and metavolcanic rocks of central and NW Iberia. Int J Earth Sci (Geol Rundsch) 102:1–23

Teixeira RJS, Urbano EEMC, Gomes MEP, Meireles CA, Corfu F, Santos JF, Azevedo MR, Sá AA (2015) Geochemistry and isotopic characterization of Lower Ordovician volcanogenic sedimentary deposits of Moncorvo Sinclinal, ortheast Portugal. In: X Congresso Ibérico de Geoquímica/XVIII Semana de Geoquímica, Alfragide. Laboratório Nacional de Geologia e Energia, 426–429

Torsvik TH, Cocks IRM (2013) Gondwana from top to base in space and time. Gondwana Res 24:999–1030

Umhoefer PJ (2011) Why did the southern Gulf of California rupture so rapidly? Oblique divergence across hot, weak lithosphere along a tectonically active margin. GSA Today 21 (11):1–10

Urbano E, Gomez M, Meireles C, Teixeira R, Sá A, Corfu F (2015) Geochemistry and U-Pb age of Early Ordovician ash-fall tuff beds from Moncorvo, Northern Portugal. Goldschmidt Abstr, 3213

Valverde Vaquero P (1997) An integrated field, geochemical and U-pb geochronological study of the southwest Hermitage Flexure (Newfoundland Appalachians, Canada) and the Sierra De Guadarrama (Iberian Massif, Central Spain): a contribution to the understanding of the geological evolution of circum-Atlantic Peri-Gondwana. PhD Memorial Univ Newfoundland

Valverde Vaquero P, Dunning GR (2000) New U-Pb ages for Early Ordovician magmatism in Central Spain. J Geol Soc London 157: 15–26

Valverde Vaquero P, Marcos A, Farias P, Gallastegui G (2005) U-Pb dating of Ordovician felsic volcanism in the schistose Domain of the Galicia-Trás-os-Montes Zone near Cabo Ortegal (NW Spain) Geol Acta 3 (1):27–37, https://doi.org/10.1344/105.000001412

Valverde-Vaquero P, Farias P, Marcos A, Gallastegui G (2007) U-Pb dating of Siluro-Ordovician volcanism in the Verín Synform (Ourense; Schistose Domain, Galicia-Trás-os-Montes Zone). Geogaceta 41:247–250

Vialette Y, Casquet C, Fúster JM, Ibarrola E, Navidad M, Peinado M, Villaseca C (1986) Orogenic granitic magmatism of pre-Hercinian age in the Spanish Central System (S.C.S.). Terra Cognita 6:2–143

Villaseca C, Castiñeiras P, Orejana D (2015) Early Ordovician metabasites from the Spanish Central System: A remnant of intraplate HP rocks in the Central Iberian Zone. Gondwana Res 27:392–409

Villaseca C, Merino Martínez E, Orejana D, Andersen T, Belousova E (2016) Zircon Hf signatures from granitic orthogneisses of the Spanish Central System: Significance and sources of the Cambrian-Ordovician magmatism in the Iberian Variscan Belt. Gondwana Res 34:60–83

von Raumer J F, Stampfli G M, Bussy F (2003) Gondwana-derived microcontinents: the constituents of the Variscan and Alpine collisional orogens. Tectonophysics 365:7–22

Zamarreño I (1972) Las litofacies carbonatadas del Cámbrico de la Zona Cantábrica (NW España) y su distribución paleogeográfica. Trab Geología Univ Oviedo 5:1–118

Zamarreño l (1975) Peritidal ongin of Cambrian carbonates in Northwest Spain. In: Guínsburg RN (ed), Tidal Deposits: a Casebook of Recent Examples and Fossil Counterparts. Springer, Berlin, 289–298

Zeck HP, Whitehouse MJ, Ugidos JM (2007) 496 ± 3 Ma zircon ion microprobe age for pre-Hercynian granite, Central Iberian Zone, NE Portugal (earlier claimed 618 ± 9 Ma). Geol Mag 144:21–21

3 Early Ordovician–Devonian Passive Margin Stage in the Gondwanan Units of the Iberian Massif

J. C. Gutiérrez-Marco, J. M. Piçarra, C. A. Meireles, P. Cózar, D. C. García-Bellido, Z. Pereira, N. Vaz, S. Pereira, G. Lopes, J. T. Oliveira, C. Quesada, S. Zamora, J. Esteve, J. Colmenar, E. Bernárdez, I. Coronado, S. Lorenzo, A. A. Sá, Í. Dias da Silva, E. González-Clavijo, A. Díez-Montes, and J. Gómez-Barreiro

Abstract

Progressive opening of the Rheic Ocean led to the drifting away of one or several ribbon terranes, generally ascribed to Avalonia, and inaugurated a passive margin stage on the newly formed margin of NW Gondwana. In Iberia, which remained on the Gondwanan side of the ocean, the rift to drift transition is recorded in the Ossa Morena Zone in latest Furongian times and migrated towards more internal parts of the margin during the Lower Ordovician. The passive margin stage is characterized by development of open marine platform sedimentation locally punctuated by eruption/intrusion of mainly basaltic, alkaline volcanic rocks, during transient periods of tectonic extension. A progression from outer (Ossa Morena Zone), through intermediate (Central Iberian and West Asturian-Leonese Zone, to inner (Cantabrian Zone) shelf environments can be generally established, although with significant variations related to local tectonic development. The end of the passive margin stage is marked by the formation of

Coordinator: J. C. Gutierrez-Marco.

J. C. Gutiérrez-Marco (✉) · P. Cózar
Instituto de Geociencias (CSIC, UCM), Severo Ochoa 7, 28040 Madrid, Spain
e-mail: jcgrapto@ucm.es

P. Cózar
e-mail: pcozar@ucm.es

J. C. Gutiérrez-Marco · P. Cózar
Departamento de Paleontología, Facultad de Ciencias Ge, José Antonio Novais 12, 28040 Madrid, Spain

J. M. Piçarra
Laboratório Nacional de Energia e Geologia, Centro de Estudos Geológicos e Mineiros de Aljustrel (CEGMA), Bairro da Vale d´ Oca, Ap. 14, 7601-909 Aljustrel, Portugal
e-mail: jose.picarra@lneg.pt

C. A. Meireles · Z. Pereira
Laboratório Nacional de Energia e Geologia, I.P., Ap. 1089 4466-901, São Mamede de Infesta, Portugal
e-mail: carlos.meireles@lneg.pt

Z. Pereira
e-mail: zelia.pereira@lneg.pt

D. C. García-Bellido
School of Biological Sciences, University of Adelaide, 5005 South Australia, Australia
e-mail: Diego.Garcia-Bellido@adelaide.edu.au

N. Vaz · A. A. Sá
Departamento de Geologia, Universidade de Trás-os-Montes e Alto Douro, 5000-801 Vila Real, Portugal
e-mail: nunovaz@utad.pt

A. A. Sá
e-mail: asa@utad.pt

N. Vaz · A. A. Sá
Centro de Geociências, Universidade de Coimbra–Pólo II, 3030-790 Coimbra, Portugal

S. Pereira
Departamento de Ciências da Terra, Faculdade de Ciências e Tecnologia, Universidade Nova de Lisboa, Quinta da Torre, 2829-516 Caparica, Portugal
e-mail: ardi_eu@hotmail.com

J. Colmenar · Í. Dias da Silva
Departamento de Geologia and Faculdade de Ciências, Instituto Dom Luiz, Universidade de Lisboa, 1749-016 Lisbon, Portugal
e-mail: jorgecolmenarlallena@gmail.com

Í. Dias da Silva
e-mail: ipicaparopo@gmail.com

G. Lopes
Department of Earth Science, University of Bergen, PO box 7803 N-5020 Bergen, Norway
e-mail: gildalopes83@gmail.com

J. T. Oliveira
Laboratorio Nacional de Energia e Geologia (LNEG), Estrada da Portela, Bairro do Zambujal, Apartado 7586-Alfragide, 2610-999 Amadora, Portugal
e-mail: josetomas.oliveira@gmail.com

C. Quesada
Instituto Geológico y Minero de España, Ríos Rosas 23 Madrid, Spain
e-mail: quesada.cecilio@gmail.com

C. Quesada and J. T. Oliveira (eds.), *The Geology of Iberia: A Geodynamic Approach*, Regional Geology Reviews,
https://doi.org/10.1007/978-3-030-10519-8_3

syn-orogenic basins, which roughly migrate in the same direction, i.e. from external to internal parts of the margin, as a response to the propagation towards the foreland of the Variscan orogenic wedge.

3.1 Introduction

After the attenuation of the rifting event started in the early Cambrian, and which culminated with the progressive opening of the Rheic Ocean by the Early Ordovician—and the subsequent drifting away from Gondwana of the Avalonia microcontinent—, a long period (ca. 100 Ma) of relative tectonic stability was established in the Iberian marine shelf before the onset of the convergent events leading to the Variscan orogenic cycle. This passive margin stage extends from the late Early Ordovician to—at least—the Middle Devonian and is well documented in the sedimentary record, showing the influx of several paleoclimatic, depositional and tectono-sedimentary major events of regional and global significance.

S. Zamora
Instituto Geológico y Minero de España, Delegación en Aragón, Manuel Lasala 44-9ºB, 500006 Zaragoza, Spain
e-mail: s.zamora@igme.es

J. Esteve
Departamento de Geociencias, Universidad de Los Andes, Cra 1 No 18ª-10, AA 4976, Bogotá, Colombia
e-mail: Jv.esteve@uniandes.edu.co

E. Bernárdez
Vicerrectoría de Investigación y Posgrado, Universidad de Atacama, Avda. Copayapu 485, Copiapó, Atacama, Chile
e-mail: enrique.bernardez@uda.cl

I. Coronado
Institute of Paleobiology, ul. Twarda 51/55, PL-00-818 Warsaw, Poland
e-mail: icoronad@twarda.pan.pl

S. Lorenzo
Departamento de Ingeniería Geológica y Minera, Escuela de Ingeniería Minera e Industrial, Instituto de Geología Aplicada (IGEA, UCLM), Universidad de Castilla-La Mancha, Plaza Manuel Meca 1, 13400 Almadén, Ciudad Real, Spain
e-mail: saturnino.lorenzo@uclm.es

E. González-Clavijo · A. Díez-Montes
Instituto Geológico y Minero de España, Delegación de Salamanca, Azafranal 48, 37001 Salamanca, Spain
e-mail: e.clavijo@igme.es

A. Díez-Montes
e-mail: al.diez@igme.es

J. Gómez-Barreiro
Departamento de Geología, Universidad de Salamanca, Plaza de la Merced s/n, 37008 Salamanca, Spain
e-mail: jugb@usal.es

The Paleozoic rocks corresponding to this phase outcrop extensively in the different areas of the Hesperian Massif (=the Iberian Massif plus its subsurface extension to the eastern border outcrops in the Demanda and Iberian Range: San José 2006), with the exception of the South Portuguese Zone, that belongs to the Avalonian paleogeographic realm. The pre-Variscan basement of the Alpine Pyrenean and Betic orogens show clear resemblance to certain Upper Ordovician to Devonian sequences of the Hesperian Massif, but is treated in a separate chapter of the volume (see Chaps. 8 and 9). Terrigenous sedimentation clearly dominated in the Ordovician and during most of the Silurian periods, whereas limestone units started to occur from the upper Silurian, became widespread in the Lower to Middle Devonian and continued in the upper Mississippian. This is a consequence of the slow movement of the Gondwana continent towards the southern hemisphere, inducing a northward drift of the entire Ibero-North African shelf, which changes from a position near the South Pole at the end of the Ordovician to more temperate and even tropical paleolatitudes, before docking with Laurussia in Variscan times.

The transition from the rift to a drift stage related with the opening of the Rheic Ocean, occurred in a complex tectonic framework that led to a long-lived magmatism (the 'Ollo de Sapo' plutonic and volcanic event), as well to graben-like subsiding zones active during the Cambrian-Ordovician transition. In the West Asturian-Leonese Zone, as well as in its southeastern extension into the Sierra de la Demanda and the Iberian Range, the Cambrian/Ordovician boundary beds are in clear stratigraphic continuity. However, both in the Cantabrian Zone and in the Ossa-Morena Zone (Estremoz-Barrancos-Hinojales sector), the oldest Ordovician sediments bearing Tremadocian fossils, paraconformably to disconformably overlie uncomplete middle to upper Cambrian successions, involving stratigraphic gaps of variable amplitude but without the development of angular unconformities. Finally, the situation in the Central Iberian Zone is even more complex, with the genesis of one or more breakup unconformities (Fig. 3.1), above which the marine shelf sedimentation typical of the passive margin setting was established. The main unconformity was alternatively interpreted as related with a crustal thickening of the Gondwana margin during a period of flat subduction, in a stage which also evolved towards the passive margin setting described below (Villaseca et al. 2016).

3.2 The Ordovician Sequence

The Lower Ordovician sequence in the Hesperian Massif is mainly represented by the ubiquitous Armorican Quartzite Formation (5–500 m thick), which gets its name from the Armorican Massif of western France (Grès Armoricain) and

Fig. 3.1 Field view of the Toledanian unconformity in the norwestern bank of the Estena River near Navas de Estena (Ciudad Real Province, Cabañeros National Park). The sandstones and shales of the early Cambrian Azorejo Formation (left, vertical bedding) are onlapped in angular erosive discordance (of ~45º) by the early Ordovician 'Intermediate Beds', the unit that underlies the Armorican Quartzite (inclined to the right in this picture). The tectonic and erosive contact is interpreted as the breakup unconformity revealing the rift-to-drift transition to the shelf sedimentation belonging to the passive margin stage. The encircled person serves as scale

typically occurs in the Central Iberian Zone and the Iberian Range, but also is known—under some local equivalent names—in the Cantabrian and West Asturian-Leonese zones. Despite a large diachroneity has been suggested in Portugal for the sedimentation of these light-colored and thick-bedded mature sandstones (references in Sá et al. 2011), the entire Armorican Quartzite of southwestern Europe is presently correlated with the single *Eremochitina brevis* chitinozoan Biozone (Paris 1990), which is broadly equivalent to a late Floian (='middle' Arenigian) age (Videt et al. 2010). However, the recent dating (Gutiérrez-Alonso et al. 2016) of a widespread K-bentonite bed occurring in the Barrios Fm, whose Tanes (=upper) member has been correlated with the Armorican Quartzite, places the Tremadocian-Floian boundary relatively close to the top of the formation in the Cantabrian Zone. This fact, and the previous paleontological dating reviewed by Sá et al. (2011), makes improbable a migration of the basal breakup discontinuity of the passive margin stage from south to north at least in inner platform zones (from the southern Central Iberian Zone to the Cantabrian Zone). Some authors (Quesada 2006; López Guijarro et al. 2007; Álvaro et al. 2014, 2018) have interpreted the unconformity at Venta del Ciervo locality in the Ossa-Morena Zone as representing the same breakup discontinuity but, there, U–Pb zircon dating of K-bentonites interbedded in quartzites yielded a ca. 489 Ma age, suggesting that the rift-to drift transition may have started earlier in the Ossa-Morena Zone (during the late Furongian).

Besides the Ollo de Sapo magmatic belt, and its coeval large volcanic event recorded in other northern Iberia localities (Gutiérrez-Alonso et al. 2016), alignments of Furongian and/or Tremadocian igneous rocks are known: (a) near the boundary with the Ossa-Morena Zone (Urra Fm., Portalegre and Carrascal granitoids); (b) in the south-central part of the Central Iberian Zone (the Beira Baixa-Central Extremadura tonalite-granodiorite belt of Rubio-Ordóñez et al. 2012), and (c) in the eastern Mounts of Toledo region

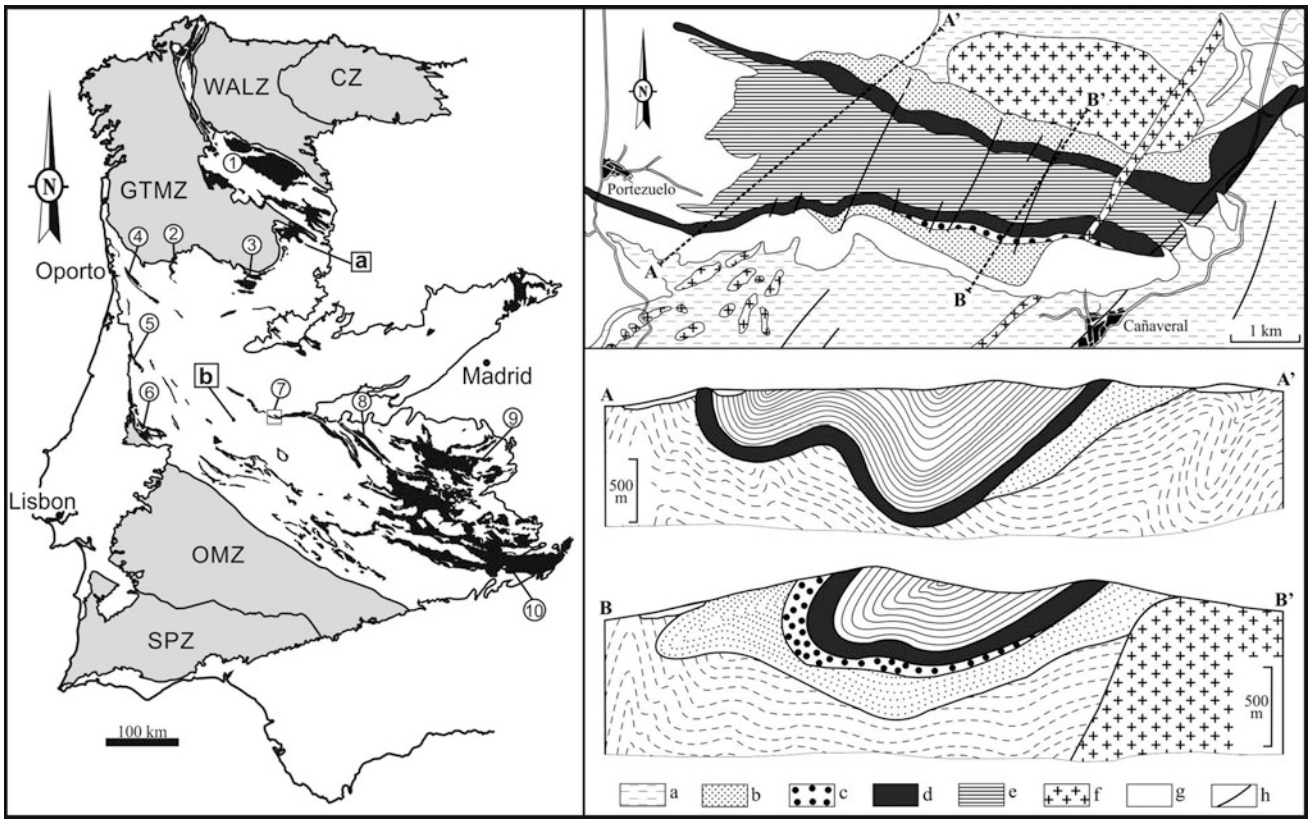

Fig. 3.2 Left: Schematic map of the Iberian Massif (left) with position of reference areas for Lower Ordovician sedimentary rocks (in black) within the Central Iberian Zone. CZ, Cantabrian Zone; WALZ, West Asturian-Leonese Zone; GTMZ, Galicia—Trás-os-Montes Zone; OMZ, Ossa-Morena Zone; SPZ, South Portuguese Zone. Localities: 1. Ollo de Sapo antiform; 2. Marão; 3. Moncorvo; 4. Valongo; 5. Buçaco; 6. Mação; 7. Cañaveral; 8. Guadarranque; 9. eastern Mounts of Toledo; 10. Despeñaperros pass (eastern Sierra Morena). a–b, outcrops of Lower Ordovician shales previously assigned to the pre-Ordovician Schist-Graywacke Complex: a, Pino del Oro schist; b, Malpica do Tejo shale (after Talavera et al. 2013). Right: detail of the Paleozoic structure in the framed area (number 7), showing part of the Cañaveral syncline just east of the Plasencia Fault. A-A′ and B-B′, underneath, correspond to the cross sections illustrating several angular unconformities between the Schist-Graywacke Complex (a. Neoproterozoic to middle Cambrian), an unnamed shale and sandstone unit (b. Tremadocian), the Serra Gorda conglomeratic beds underlying the Armorican Quartzite (c. lower Floian) and the Armorican Quartzite (d. upper Floian). Remaining symbols: e. Middle to Upper Ordovician shale and sandstone units; f. Variscan igneous rocks (Cancho García granite and Alentejo-Plasencia toleitic dyke); g. post-Paleozoic cover; h. faults. Geological map and cross sections adapted from Martín Herrero et al. (1987). Figure reproduced from (Sá et al. 2014, Fig. 1, ©Springer)

(the 'Volcano-Sedimentary Complex' of Martín Escorza 1976). As a result of the thermal subsidence and the extensional tectonics active in the Central Iberian Zone at the beginning of the Ordovician, sedimentation of unfossiliferous units of conglomerates, sandstones and shales tentatively assigned to the lower Floian and uppermost Tremadocian generally occurred in several grabens and half-grabens mostly showing Cadomian orientations. They correspond to diverse formations preceding the Armorican Quartzite (Fig. 3.2), which show great variations in thicknesses (0–450 m) and sedimentary facies, so that in short distances the sedimentation could rapidly have changed from almost continental conglomerates to fan deltas and storm-dominated shallow-marine deposits (e.g., McDougall et al. 1987). The active tectonism and the considerable paleotopography influenced the formation in the Central Iberian Zone of at least two angular unconformities (Figs. 3.2 and 3.3) and various sedimentary gaps. The main and more widespread of these is the Toledanian Unconformity, originally placed by Lotze (1956) below the Cambrian/Ordovician boundary, which has a more important structural significance and puts the Lower Ordovician sequence directly over Neoproterozoic or lower Cambrian rocks.

In the 'Ollo de Sapo' Domain, local outcrops of grey shales erroneously attributed to the Schist-Graywacke Complex by Talavera et al. 2012: (localities a–b in Fig. 3.3) were dated as late Tremadocian or even as Floian based on detrital zircons. However, in agreement with González-Clavijo (2006), these rocks clearly occur as an intercalation in the Villadepera/'Ollo de Sapo' gneisses, which are laterally correlatable with the basal Constantim member of the Angueira Fm of the Portuguese part (Meireles 2013).

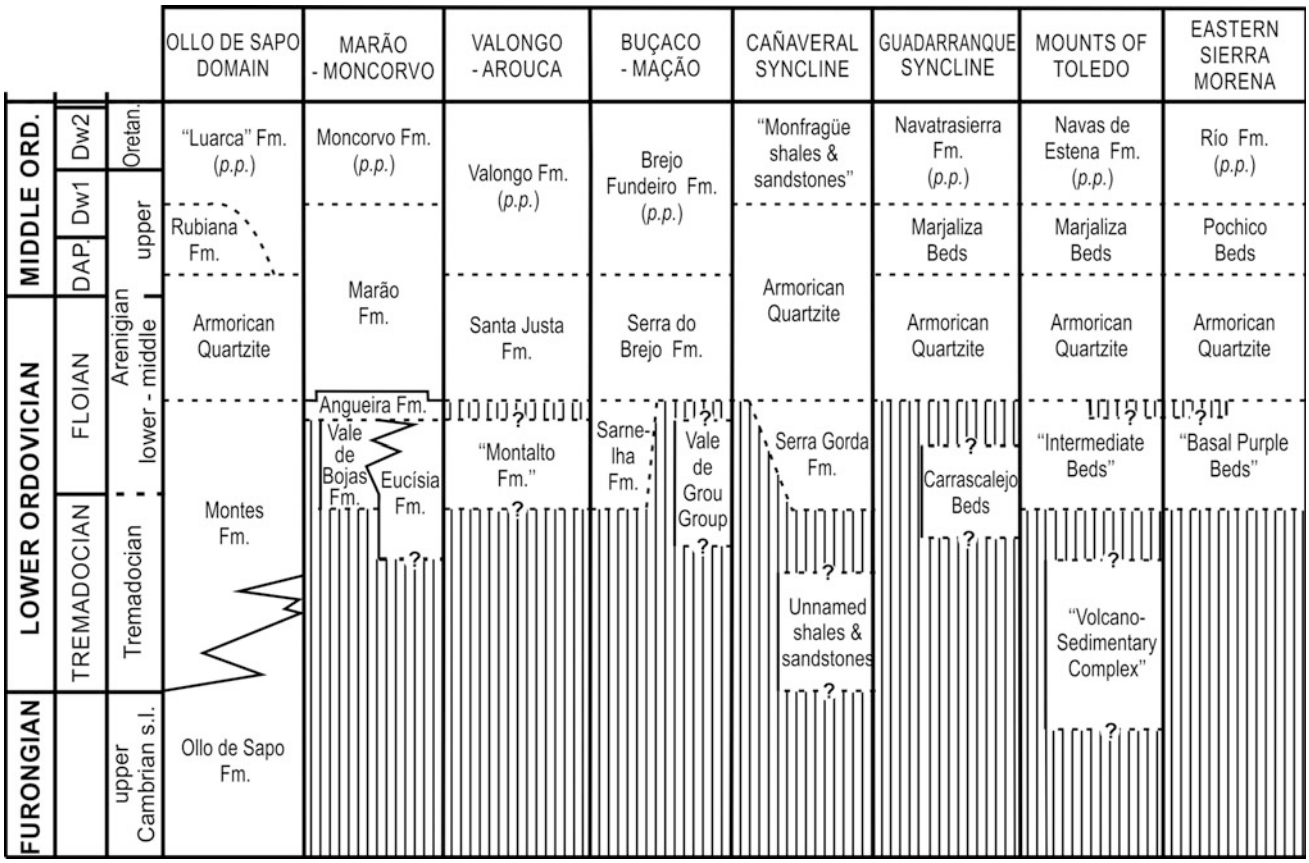

Fig. 3.3 Correlation chart of the main stratigraphic units around the Cambrian/Ordovician and Lower/Middle Ordovician boundaries in the 'Ollo de Sapo' Domain (left) and the southern Central Iberian Zone (Portugal and Spain), showing the sedimentary gaps (vertical stripes). For localization of the columns, see Fig. 3.2

The late Floian marine transgression leading to the deposition of the Armorican Quartzite operated over a huge area of SW Europe, and the unit usually ends with a variably developed succession (20–250 m) of alternating quartzites and shales, which make the transition into the Middle Ordovician shales. In some places, this alternation was incorporated as an upper member of the Armorican Quartzite sensu lato (e.g., the Fragas da Ermida Mb of the Marão Fm: Sá et al. 2005), but most frequently it was differentiated as an independent unit (e.g., Rubiana Fm, Marjaliza or Pochico 'beds'), which may extend regionally up to the lower Darriwilian. However, in some places, such as in the Portuguese inliers of Buçaco and Valongo, the top of the Armorican Quartzite grades up abruptly into dark shales already bearing Dapingian graptolites, implicating that the chronostratigraphic frame for the end of the widespread sand sedimentation is also quite complex (Gutiérrez-Marco et al. 2014a).

In the West Asturian-Leonese Zone, Lower Ordovician strata conformably succeed Cambrian formations, the bases of which discordantly overlie the Neoproterozoic. The lower limit of the Ordovician lies within the upper part of the very thick Los Cabos Group (up to 4,400 m in the Navia-Alto Sil Domain) that consists of alternating shallow marine sandstones and shales (Marcos 1973 Pérez-Estaún et al. 1990). This group extends from the Miaolingian up into the Floian in its uppermost part where sandstones closely similar to those of the Armorican Quartzite predominate.

The Lower Ordovician sequence of the Iberian Range conformably overlies a thick Cambrian succession and is subdivided into distinct formations (Wolf 1980). The base of the Ordovician, traditionally placed at the upper part of the Valconchán Formation (thick-bedded quartzites with some grey to green shaly intercalations), has been recently moved up to the upper-middle part of the succeeding Borrachón Formation (320–900 m of green to grey laminated siltstones and shales with some sandy intercalations). Above it, the sandstones and quartzites of the Deré Fm (420–850 m) are followed by green to brown siltstones and shales of the Santed Fm (200–950 m), where the Tremadocian-Floian boundary can be traced and is, in turn, overlain by the Armorican Quartzite (450–650 m).

In most regions of the Iberian Massif, the remaining Ordovician strata can be grouped into two other major sequences. The first is composed predominantly of dark

mudstones and siltstones with more or less important sandstone intercalations, being roughly representative of the Middle Ordovician. The upper sequence is much less uniform and is incomplete in many areas, where it can also show internal unconformities. These Upper Ordovician strata consist of alternating mudstones, siltstones and sandstones overlain by limestone, glaciomarine diamictites and massive quartzites.

After the complete erosion of the rift shoulders flanking the Rheic Ocean opening, the compartmentalisation of the Gondwanan segment of the Iberian Massif was considerably attenuated, so that monotonous units of dark mudstones, richly fossiliferous and with a mean thickness of about 300 m (but ranging from 150 up to 1,000 m) were deposited over the areas previously reached by the Armorican Quartzite. This Middle Ordovician transgression was diachronical from the Dapingian to the late Darriwilian, starting at the base with few meters of relatively condensed strata and a widely distributed ooidal ironstone bed. The latter represents the initial deposit above a disconformity, associated with a rapid eustatic rise and showing a good development in the shallower parts of the shelf. The main ooidal ironstone bed is recorded at the base of the middle Darriwilian sequence and occurred almost synchronously over a wide area of the Central Iberian Zone, indicating uniform sedimentary conditions across large areas of a shallow, low gradient shelf (Young 1992). However, the eustatic control of the deposition of this first ooidal ironstone is not so evident in the Cantabrian Zone and in the Iberian Range, where the bed directly ovelies the Armorican Quartzite and is of a late middle Darriwilian age. This may reflect uplifting of the area by faults and generation of the corresponding paraconformity, involving an extensive sedimentary gap from the Dapingian to the lower middle Darriwilian strata.

The sedimentation of dark mudstones by the middle and early late Darriwilian is generalised in Iberia, but a regressive tendency predominates in the late Darriwilian with the record of new sandstone units. They are well-developed in the southeastern Central Iberian Zone within and above the fossiliferous mudstones discussed above, known as the so-called 'Los Rasos' or 'Monte da Sombadeira Sandstone' and 'Quartzites inférieurs' or 'Botella Quartzite', respectively. The former unit is especially interesting because this sandstone, 25–200 m thick and covering an area of approximately 75,000 km^2 in the southern Central Iberian Zone, corresponds —according to the sedimentological study of Brenchley et al. (1986)—to a single storm-generated body deposited more than 100 km from the shore. This allowed to estimate an average seaward-dip of the Ordovician Central Iberian shelf of less than 0.1º, taking into account the maximal depth known (ca. 50–80 m) in which a sediment surface above storm wave base is capable of forming hummocky cross-stratification. The thickness and the distribution of these sandstone facies, decreasing to zero northward, also indicates that the shoreline should have been positioned towards the present south and southeast, in the actual place of the Obejo-Valsequillo Domain. The latter was juxtaposed to the Central Iberian Zone in Variscan times by the Puente Génave-Castelo de Vide shear zone (Martín Parra et al. 2006). This has recently been reinterpreted as a huge rootless nappe related with an eo-Variscan continental subduction, previous to the Rheic Ocean closure, and stacked by the Late Devonian the Ossa-Morena Zone onto the Central Iberian shelf (Díez Fernández and Arenas 2015, 2016; Arenas et al. 2016).

The general deepening towards the north of the Central Iberian shelf was also confirmed by other stratigraphic evidences and by the distribution of trilobite biofacies (Hammann and Henry 1978, Rábano 1989, Robardet and Gutiérrez-Marco 1990). However, this shelf gradient is exactly inverse to the model proposed by Rubio-Ordóñez et al. (2012), which postulates an ocean over the emerged, source area for the siliciclastics, being the Beira-Extremadura belt tentatively interpreted as a continental volcanic arc in their tectonic model.

By the late middle Darriwilian (global chronostratigraphic nomenclature after Bergström et al. 2009) the whole Iberia was almost uniformly blanketed by shelf muds (e.g., Luarca, Navas de Estena, Castillejo, Sueve, Brejo Fundeiro, Moncorvo and Valongo formations). The predominantly shallow siliciclastic sedimentation without any trace of limestones, and the abundant fossil record consisting of low diversity benthic assemblages of invertebrates regarded as cold-water faunas, indicate a high paleolatitudinal position for the Iberian shelf in Gondwana. The 'polar gigantism' observed in some groups of Darriwilian trilobites (Gutiérrez-Marco et al. 2009) also supports the general placement of Iberia near the South Pole, as represented in most paleogeographic reconstructions for the Ordovician (e.g. Cocks and Fortey 1990, Robardet 2002, Torsvik and Cocks 2013, 2017). Also the close similarities of certain Darriwilian faunas from Ibero-Armorica to those recorded from northeast Algeria, Libya and Saudi Arabia, led Gutiérrez-Marco et al. (2002) to propose that, during Ordovician times, central Iberia was probably north of present-day Libya or Egypt instead of in the vicinity of Morocco/NW Africa. The new location, closer to the Arabian-Nubian shield and the Sahara metacraton, was later supported by isotopic and provenance studies of magmatic rocks (Bea et al. 2010, Fernández-Suárez et al. 2014), information not taken into account by Franke et al. (2017).

Paleoecological data derived from Middle Ordovician fossils confirm the general dipping of the Central Iberian shelf towards the north, with a maximal depth reached in its extension in the Navia-Alto Sil domain of the West Asturian-Leonese Zone and the Iberian Range, where some mesopelagic graptolites have been recorded (Gutiérrez-Marco et al. 1999). The Cantabrian Zone, by the way,

remain emerged during much of the Middle and Late Ordovician times, with the sporadic record of some units bound by stratigraphic discontinuities in certain corridors limited by faults, within the wide uplifted area. This is the case of the Sueve Fm, yielding inshore trilobites but with some rare elements derived from offshore settings (e.g., raphiophorids: Gutiérrez-Marco and Bernárdez 2003).

The general gradient in the Ordovician shelf documented in the Central Iberian Zone would require a shoreline and an emerged area in the region presently occupied by the Obejo-Valsequillo Domain and the Ossa-Morena Zone, previous to the Variscan Orogeny. The first is a complex area of mixed paleogeographic affinities for the Lower Paleozoic, especially along the Ordovician (Gutiérrez-Marco et al. 2014b, 2016). On the other hand, the Ossa-Morena Zone clearly represents the outer and distal-shelf counterpart of the Iberian platform which was tectonically (laterally) juxtaposed to its present position during the Variscan Orogeny (Quesada 1991). The Lower Ordovician sequence starts here with offshore sediments bearing late Tremadocian mesopelagic graptolites and trilobites, followed by Floian to early Darriwilian green shales and slates, which rarely show the discontinuous ooidal ironstone bed correlatable with the widespread bed of basal middle Darriwilian age. In the Valle syncline of northern Seville, the middle Darriwilian shales yielded a fossil assemblage of Bohemian affinities, unique for Iberia and representative of deeper environments than the typical '*Neseuretus* fauna' (Gutiérrez-Marco et al. 2002, Robardet and Gutiérrez-Marco 2004). Above this unit, sedimentation proceeded with micaceous and calcareous sands continuing until the Late Ordovician.

The upper part of the Ordovician sequence generally begins with argillaceous units that, at its base or within their lower third, intercalate an ooidal ironstone bed with common phosphatic pebbles and remanié fossils. This is the so-called Favaçal or Chôsa Velha bed in Portugal, which is also widely recognized in the Cantera Shale of the Central Spain, the base of the Fombuena Fm of the Iberian Range and in the Manto de Mondoñedo Domain of the West Asturian-Leonese Zone. The age of this bed and the starting of sedimentation above it has been established as middle Berounian, by using the high-resolution biochronological scheme and the regional chronostratigraphic scale for the Mediterranean Ordovician (Gutiérrez-Marco et al. 2015, 2016, 2017). This dating is roughly equivalent to the late Sandbian–earliest Katian of the global scale and, in regional terms, is correlatable with the age of formation of the Sardic Uncorformity in SW Sardinia, that in its type area seals a sedimentary gap equivalent to the entire Middle Ordovician and part of the Early and earliest Late Ordovician (Leone et al. 1991, Pillola et al. 2008). Due to the great continuity of this 'early Caradoc' ironstone, extending even to Armorica and other places of the Mediterranean area, it has been interpreted as associated with an eustatically controlled episode of sea-level rise (Young 1989, 1992). But their coincidence in time with the Sardic movements also favoured a complementary interpretation associated to the discrete uplift of part of western Iberia as reflecting the distal echoes of the Sardic phase (Gutiérrez-Marco et al. 2002 with references). In this scenario, the minimal sedimentary gap sealed by the ooidal ironstone in Iberia varies from a partly Sandbian (late early Berounian to earliest middle Berounian) interval in the southern Central Iberian and the Iberian Range, to include part of the Middle Ordovician in north Portugal (Sá et al. 2006). The ironstone's petrographic features—more phosphatic and conglomeratic towards the south of the Central Iberian Zone—also fits with the general paleoslope of the shelf. The existence of a variable paleotopography previous to the interval or non deposition—and erosion—is demonstrated by minor uplifting areas such as the 'Dornes/Amêndoa rise' of central Portugal (Young 1989) and also by the Valongo 'rise' that emerged in the latest Darriwilian. The absence of latest Darriwilian-early Sandbian sedimentation over a large area of NW Spain (Gutiérrez-Marco et al. 1999) may also be due to the same tectonic rise, with some sin-sedimentary rifting later developed in the Truchas area (Martínez Catalán et al. 1992) and the important subsiding trough of the Navia-Alto Sil Domain of the West Asturian-Leonese Zone. Here, deep-sedimentation with up to 1,500 m-thick turbidites of the Agüeira Fm. (Pérez-Estaún and Marcos 1981) was recorded mainly along the Katian. The interpretation of the Sardic phase as a general episode of uplift (the 'Sardinian-Taurian rise' of Hammann 1992) may include also the Cantabrian Zone, that remains uplifted until the end of the Ordovician with the exception of two small fault-controlled troughs where Middle–Late Ordovician sedimentation and rare rifting-associated volcanism (in the Peñas Cape) took place. According to some authors, the Sardic Phase can be better interpreted as linked to orogenic subduction or alternatively to transtensive-transpressive modification of the Rheic Ocean opening patterns leading to the Paleotethys (Stampfli et al. 2002, Álvaro et al. 2016 and references therein).

The post-Sardic Ordovician sedimentation in Sardinia displays many facies and faunas in common with other Mediterranean settings including Iberia. Most deposits developed during the early and middle Katian (=middle–late Berounian) are thick units of alternating shales, siltstones and sandstones, with some intercalations of quartzites and dark shales, or micaceous shales with minor proportion of intercalated sandstones, within shallow shelf environments with storm influence. By the late Katian (=Kralodvorian regional stage), the global warming climatic event that preceded the Latest Ordovician glaciation (Boda Event of Fortey and Cocks 2005) favoured the arrival of warm-water taxa to south Polar Gondwana, as well as limestone

deposition in several places of Iberia. The base of the limestone seems to rest conformably on middle Katian beds, but sometimes the contact is clearly disconformable (the Urbana Limestone of the southern Central Iberian Zone), or develop a ferruginous bed at the base (of the Cystoid Limestone of the Iberian Range). In the Ossa Morena Zone, a true ooidal ironstone bed marks the basal contact of the limestone which directly rests on Middle Ordovician shales (Gutiérrez-Marco et al. 2002, Robardet and Gutiérrez-Marco 2004). The basal sedimentary gap is greater in NW Iberia, where the Aquiana Limestone may even be transgressive over the Cambrian, reaching a maximum thickness of 250 m. The enormous variations of thickness observed in the late Katian limestone unit in relatively short distances (0–250 m), has been associated with the erosive processes linked to the global lowering of the sea-level induced by the Late Ordovician glaciation, perhaps combined with synsedimentary tectonics (Martínez Catalán et al. 1992, Gutiérrez-Marco et al. 2002). A Katian ooidal ironstone bed is also recorded at the base of some volcano-sedimentary units (e.g. Porto de Santa Anna Fm) that partly replaced or precluded carbonate deposition in some places of central Portugal (Buçaco).

The uppermost part of the Ordovician sequence is under the direct influx of the Hirnantian Glaciation centered in African Gondwana (Ghienne et al. 2007). This, again, demonstrates the general location of Iberia at high latitudes in the southern hemisphere during the Late Ordovician. Evidence that the main ice-sheet must have also extended to the Cantabrian Zone was presented by Gutiérrez-Marco et al. (2010), who found subglacial tunnel valleys incised on the upper part of the Barrios Fm (Armorican Quartzite). Nevertheless, the ubiquitous sediments associated with the Hirnantian Glaciation are the widespread glaciomarine diamictite formations that, under several local names, occur all over the Hesperian Massif. These deposits may be preceded by shallow sandstone-dominated sediments or, more rarely, they can show some quartzitic intercalations at its middle part (Las Majuelas Quartzite of the Gualija Fm). A terminal, overlying quartzite is rather common at the top of the Ordovician sequence (the Criadero Quartzite and equivalents such as the Luna Quartzite/La Serrona Fm of the Barrios de Luna Reservoir, previously mistaken for the Armorican Quartzite: Gutiérrez-Marco et al. 2010, Toyos and Aramburu 2014), which may extend to the Silurian. A majority of the dropstones contained in the diamictites seem to be of close provenance, but some other pebbles are striated and of clear exotic origin, having suffered a long transport by icebergs. The opportunistic *Hirnantia* Fauna, coeval with the glaciation, has been recorded so far in the Cantabrian and Central Iberian zones, as well as in the Iberian Range, associated to coarse sandstones and fine volcanoclastic sediments (Bernárdez et al. 2014). Acritarchs, trilobites and brachiopods of Hirnantian age were also recovered from central Portugal (Lopes et al. 2011, Lopes 2013, Colmenar et al. 2019).

3.3 The Silurian Sequence

The platformal sedimentation on a drifting passive margin setting prevails in the Silurian Period during spreading of the Rheic Ocean. The latitudinal position of the Iberian Massif can be estimated roughly as intermediate between the south-polar paleolatitudes of the latest Ordovician (Hirnantian glaciomarine sediments and tunnel valleys) and the warm temperate to subtropical latitudes of the Early Devonian (limestones with local reefs), with a latitudinal displacement to about 40–35º S in the latest Silurian (Robardet and Gutiérrez-Marco 2002).

The onset of the Silurian sedimentation is somewhat diachronic in the different areas of the Hesperian Massif, where strata of this system can be adscribed to two basic types of succession (Fig. 3.4). However, by the Telychian (late Llandovery) the sedimentation of graptolitic black shales constitutes an uniform event, shared with the remaining part of the Mediterranean area. This early Silurian sea-level rise was likely caused by a combination of global eustatic rise and local increased rates of tectonic subsidence.

The regional analyses show that both types of basic Silurian successions in Iberia, also associated with different faunas, probably correspond to distinct paleoenvironmental conditions and paleogeographical positions.

The first type of succession is widespread and occurs in most of the Central Iberian Zone, the Iberian Cordillera, in some units of the West Asturian-Leonese Zone (Mondoñedo) and in the Cantabrian Zone. Except in the latter, it begins with sandstone units at the Ordovician-Silurian transition. Euxinic black-shale sedimentation started generally during the late Aeronian and Telychian and persisted during the Wenlock and, in some regions, until the early Ludlow. This black-shale sequence, which received local lithostratigraphic names (e.g., Formigoso, Bádenas, Llagarinos, Guadarranquejo or 'Xistos Carbonosos' formations) was overlain by thick units of alternating sandstones, siltstones and shales of Ludlow and Pridoli age (e.g., Furada-San Pedro, Alcolea, Luesma or Sobrado formations), which are in turn overlain by other sandstone and quartzite units of the earliest Devonian. Within these sand-dominated sequences forming the upper part of the Silurian succession, the fossil record is scarce and consists mainly of shallow-water shelly faunas. The abundance of terrestrial palynomorphs and thin ooidal ironstone beds in the Furada-San Pedro Fm of the Cantabrian Zone would indicate a close proximity to the emerged source areas.

The shallow character of sedimentation of this first type of the Silurian succession is also recognised in the euxinic

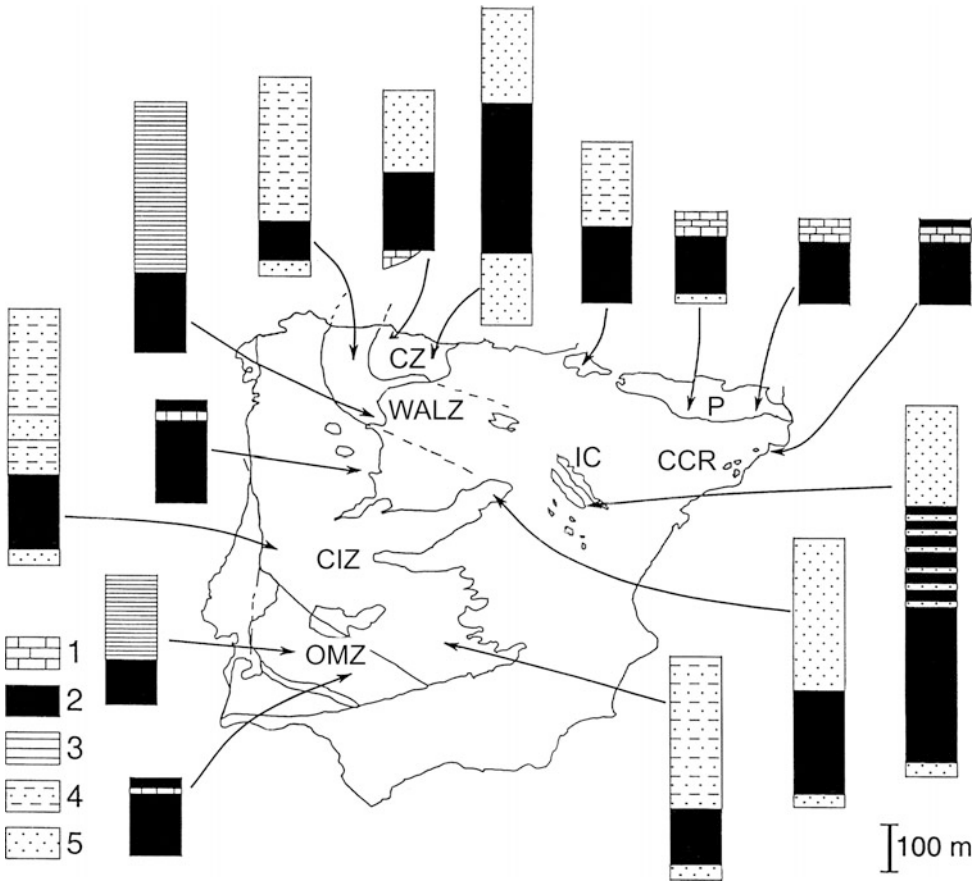

Fig. 3.4 The different types of Silurian successions in the Iberian Peninsula, reproduced from Gutiérrez-Marco et al. (1998) with permission from IGME, the copyright holder. Dominant lithofacies: 1. limestones; 2. black shales; 3. shales and siltstones; 4. alternating sandstones, siltstones and shales; 5. sandstones. Abbreviations: CZ, Cantabrian Zone; WALZ, West Asturian-Leonese Zone; CIZ, Central Iberian Zone; OMZ, Ossa-Morena Zone; IC, Iberian Range; CCR, Catalonian Coastal Ranges; P, Pyrenees. The three columns from Portugal are, from North to South, Moncorvo, Dornes-Mação and Barrancos

graptolitic facies, probably generated in areas with a stable stratification on the water masses instead of involving deep environments. This could be inferred by the presence of some Telychian graptolites listed by Robardet and Gutiérrez-Marco (2002) which are shared with those inshore environments of the pericratonic and intracratonic basins of Algeria and Libya, but that have never been found in the Ossa-Morena Zone, the northern Central Iberian Zone, the Pyrenees or the Catalonian Coastal Ranges.

In the West Asturian-Leonese Zone and the transitional area to the Central Iberian Zone, the Late Silurian sandstone-dominated sedimentation is replaced by massive chloritoid slates, extending into the Devonian, which have yielded Ludlow and Pridoli benthic and planktic elements of Bohemian type (Gutiérrez-Marco et al. 2001). The Palentian Region of the southeastern Cantabrian Zone, which probably originated in the West Asturian-Leonese Zone, also displays a lithological succession slightly different from the general scheme of the first type of Silurian succession. It starts with thick, white sandstones (Robledo Fm, Wenlock), then follows with siltstones and black shales (Las Arroyacas Fm, Wenlock to Pridoli age) and ends with sansdtones and some carbonate beds (Carazo Fm, Pridoli to Lochkovian), as indicated by García Alcalde et al. (2002). The Silurian sequences in both areas are hence representative of slightly deeper environments than those in the southern Central Iberian, Cantabrian or Iberian Range successions, as indicated also by the record of Bohemian (=Hercynian) faunas and scyphocrinoids around the Silurian/Devonian boundary beds.

The second main type of Silurian succession recorded in the Hesperian Massif is characterized by a continuous euxinic black shale or black shale-black limestone sedimentation, rather condensed (up to 200 m thick) that ranges from the basal Llandovery to the Lochkovian. It is characteristically represented in the Ossa-Morena Zone, but a similar sequence, also intercalating thin beds of black chert, occurs in the Moncorvo syncline and in the nearby autochthonous units of the northernmost part of the Central Iberian Zone in Portugal (Sarmiento et al. 1999, Meireles 2013). Because of the absence of important clastic influx of coarser terrigenous particles, it can be assumed that all these regions were situated at a distance from the terrestrial emerged land source areas, in the outer distal part of the Gondwanan marine shelf.

The Silurian-Lochkovian succession of northern Seville consists of 130–150 m of black argillaceous graptolitic shales with intercalations of siliceous slates and cherts, it is stratigraphically almost complete and fossiliferous (Jaeger and Robardet 1979, Robardet and Gutiérrez-Marco 2004, Loydell et al. 2015 with earlier references). A thin (0.5–1 m) black limestone level with orthoceratids and bivalves occurs

in the Ludlow, and a thicker alternation of limestones and shales with benthic faunas of Bohemian type (the '*Scyphocrinites* Limestone', 10–15 m) was intercalated on the Pridoli black shales.

Silurian limestones have never been observed in other areas of the western Ossa-Morena Zone, neither in Spain nor Portugal. In Villanueva del Fresno and Estremoz, unfossiliferous sandstones and quartzites occur in the lowermost part of the Silurian, below the graptolitic shales. The most complete succession of this system is known from the Barrancos area (Portugal), starting from the base of the Silurian according to the graptolites recognized in the uppermost levels of the Colorada Fm (Piçarra et al. 1995). This is overlain by the 'Xistos com Nódulos' Fm (30–50 m of black shales and thin intercalations of chert) where most of the biozones ranging from Llandovery to Ludlow strata were characterized, and by the suceeding 'Xistos Raiados' Fm (100 m of banded chloritoid shales and siltstones), which include successive graptolite biozones of upper Ludlow, Pridoli and Lochkovian ages (Piçarra et al. 1998, 1999, Araújo et al. 2013). The general succession of graptolite faunas from Barrancos displays a close identity with those of the Valle syncline, especially around the Homerian Lundgreni Event, with similar lithologies and non-graptolitic faunas present in both areas (Gutiérrez-Marco et al. 1996, Rigby et al. 1997, Lopes 2013).

According to Robardet and Gutiérrez-Marco (2002), there is a general trend within the Hesperian Massif, from shallow deposits in the south of the Central Iberian Zone to deeper and more distal sediments in the northern Central Iberian Zone and in the southern part of the West Asturian-Leonese Zone. To this regard, Pridolian '*Scyphocrinites* limestones' occur in the Moncorvo area and at Guadramil (Portugal), in the north of the Central Iberian Zone, and Silurian successions of the Peñalba and Sil synclines are more shaly and silty, while Ludlow limestones bear trilobites of Bohemian affinities, in some way reminiscent of the Silurian of Pyrenees and Catalonia. These Hercynian magnafacies were also recognized in the Palentian Domain of the Cantabrian Zone. A different distal area of the Gondwanan platform is represented by the Ossa-Morena Zone, where the terrigenous influx was permanently weak in the Silurian and where the faunas were almost exclusively pelagic. Quesada (1991) considers these deposits as sedimented in the thinned, distalmost parts of the Gondwanan margin, before being juxtaposed tectonically to other Iberian zones that have occupied more internal parts of it. However, there is no consensus on the timing of the juxtaposition, with some authors that favoured the late Paleozoic Variscan orogeny (Simancas et al., 2001, 2003, 2005, 2006) and others who proposed a much earlier accretion during the Neoproterozoic Cadomian orogeny (Ábalos 1990, Quesada 1990a, b, 1997, 2006). The latter would require an important combination of Variscan tectonism to move the Ossa-Morena Zone to its actual position, displacing the emerged Ordovician land to the present southeast. The latter would have acted as the source area of the Central Iberian shelf during the Ordovician and Silurian, as has been repeatedly demonstrated by its general gradient indicated in both sediments and faunas (Gutiérrez-Marco et al. 2014b).

3.4 Silurian-Devonian Within-Plate Magmatism

Locally and discontinuous in time, mostly alkaline mafic intraplate volcanic and volcaniclastic rocks occur interbedded/intruded into the passive margin succession in the Iberian Massif. The most important activity was located in the southern Central Iberian Zone; e.g. Almadén area with its gigantic Hg ore deposits in Silurian and Lower Devonian times (Higueras et al. 2013 and references therein), La Codosera syncline close to the Badajoz-Córdoba shear zone (López-Moro et al. 2007) or El Castillo volcanics at the Tamames syncline.

The Almadén syncline is by far the area with more abundant and varied magmatic rocks, spanning in age from Early Silurian to Late Devonian times (Saupé 1990; Higueras 1995; Hall et al. 1997; Hernández et al. 1999; Higueras et al. 1995, 2013). Volcanic types mainly include porphyritic metabasalts but minor outcrops of differentiated rocks, such as trachyte, trachyandesite and rhyolite lavas also occur. Pyroclastic rocks are also abundant throughout the succession, among which the so-called Frailesca rock, a lapilli tuff with basaltic, sedimentary and ocassional ultramafic fragments that generally infills diatreme-like structures, has deserved special attention due to its presence in most mercury deposits in the region and its interpretation as genetically linked to their formation (Hernández et al. 1999; Jébrak et al. 1997; Higueras et al. 2011, 2013). In addition to lavas and pyroclastic rocks, mafic dolerite sills intrude the passive margin succession in this area.

In terms of composition, a spread from basanites and nephelinites, through olivine-basalts, pyroxenitic-basalts (interpreted as pyroxene cumulates), trachybasalts, trachytes, to very rare rhyolites is found. Phenocrysts comprise olivine, diopsidic pyroxene, analcite and plagioclase in the mafic rocks, biotite and plagioclase in intermediate rocks, and K-feldspar and quartz in the rare rhyolites. Late magmatic kaersutitic amphibole and Ti-rich biotite are also conspicuous in the mafic types. Textures are porphyritic, with a crystalline matrix, and often vesicular (Higueras et al. 2013). In addition to their presence as clasts in the Frailesca rock, ultramafic fragments also occur as xenoliths in the least differentiated basalts. They contain 50–80% olivine, pyroxene, and minor spinel, usually unaltered, which allows their classification as spinel lherzolites.

A peculiar characteristic of the Almadén mafic rocks is their high content in CO_2, with concentrations ranging from 8 to 15%; 20 to 30% in basalts and ultramafic xenoliths, respectively, in and around the mercury deposits (Higueras, 1995). The isotopic composition of these carbonates suggests a primary character and a probable mantle origin. Helo et al. (2011) interpreted that given its low solubility, CO_2 is the only magmatic volatile phase that may be significantly exsolved as the magmas ascend to the surface, resulting in explosive eruptions. This model could explain the explosive nature of the volcanism at Almadén as shown by the numerous Frailesca rock units and pyroclastic rocks along the stratigraphic succession (Higueras et al. 2013).

All the geochemical characteristics indicate (Higueras et al. 2013): (i) most rocks show alkaline affinities with some transitional to a tholeiite affinity; (ii) derivation from primitive mantle-derived magmas, with most rocks plotting in the alkali basalt and basanite/nephelinite fields typical of within-plate settings; and (iii) enriched nature of the mantle source, with eventual contribution from asthenospheric sources.

In the southwestern corner of the Central Iberian Zone, close to the Badajoz-Córdoba shear zone, mostly mafic magmatic rocks occur at La Codosera syncline as meter to decameter-thick sills (ocassionally reaching ca. 300 m in thickness and up to 3 km in length; López-Moro et al. 2001, 2007). The sills intrude at various levels into a metasedimentary succession which includes Lower and Upper Devonian rocks (Santos et al. 2003; López Díaz et al. 2007). López-Moro et al. (2007) published a 436 ± 17 Ma Sm–Nd isochron age (early Silurian) obtained from samples collected in four different sills. However, intrusion of these sills produced thermal metamorphic aureoles in the fossiliferous Devonian country rocks that postdate development of a first deformation fabric (Santos et al. 2003; López Díaz et al. 2007). This fact contradicts the early Silurian radiometric age obtained by López-Moro et al. (2007), casting doubts on their emplacement during the passive margin stage, and shows the need for further geochronological work. Compositionally the mafic rocks correspond to high-Mg tholeiites and tholeiitic andesites but their source is hard to characterize (López-Moro et al. 2007). On one hand, a εNd value of +6 indicates a significant mantle component; on the other hand, a moderate LREE enrichment relative to HREE and a Nb negative anomaly suggest contribution of a crustal component. To account for this apparent contradiction (López-Moro et al. 2007), inferred a hybrid mantle source with contribution of a metasomatised component and a major, depleted component.

SW of Salamanca, the El Castillo volcanics crop out in the Tamames syncline. They mainly consist of basaltic sills intruded in fossiliferous Silurian shales and minor pyroclastic rocks. Initially considered as Silurian in age (Díez Balda 1986), recent dating of a basaltic sample as Middle Devonian (394.7 ± 1.4 Ma, U–Pb zircon age, Gutiérrez Alonso et al. 2008) suggests that magmatism may have extended in this area from the Silurian, to account for the interbedded pyroclastics, into at least the Middle Devonian. According to Díez Balda (1986) both lavas and pyroclastic rocks exhibit alkaline basaltic compositions (basanites).

In addition to the above areas, Silurian and/or Devonian alkaline mafic rocks are known in many other localities across the Iberian passive margin of Gondwana; e.g. Alcañices syncline in the northern Central Iberian Zone (González-Clavijo 2006), eastern Central Iberian Zone (Ancochea et al. 1988), Ossa-Morena Zone (Piçarra 2000), and even the Cantabrian Zone, where volcanic rocks belonging to the Huergas Fm where dated at ca. 395 Ma (whole-rock Rb–Sr method; Loeschke 1983). All these volcanic manifestations attest for punctuated extensional tectonic events affecting the Iberian Gondwanan shelf during the duration of the passive margin stage.

3.5 The Devonian Sequence

The Devonian sedimentation is continuous with the Silurian in different areas of the Hesperian Massif, where the boundary between both systems is placed within certain successions dominated by sandstones or alternation of shales and sandstones, with some ooidal ironstone beds and, in the upper part, impure fossiliferous limestones that are already of Lochkovian age. These units are the Furada-San Pedro and Carazo formations of the Cantabrian Zone, the Luesma Fm of the Iberian Range, and the Seceda and Alcolea formations of the 'Ollo de Sapo' Domain (northern Central Iberian Zone). Above them, Devonian rocks are mostly calcareous in northern Spain with some remarkable reefal developments, especially during the late Emsian and Givetian. The greatest thicknesses of Devonian rocks recorded in the Hesperian Massif, to the north of the South-Portuguese Zone, are located in the Iberian Range (>4,000 m) and in the Cantabrian Zone (>2,000 m), essentially developed in shallow-water marine facies bearing abundant fossils. Outside these areas, Devonian outcrops are more scarce and discontinuous, with scattered occurrences in the southern Central Iberian Zone and in the Ossa-Morena Zone, which also included frequent volcanic intercalations.

In the Cantabrian Zone, Devonian rocks can be typified by two distinct marine domains: the so-called Asturo-Leonian facies, mainly representing nearshore to shallow shelf environments, and the Palentian facies, representing the offshore settings and deeper environments of the same platform. The first facies is widely distributed across the Cantabrian Zone, showing a general deepening trend towards the west and southwest, in a general regressive

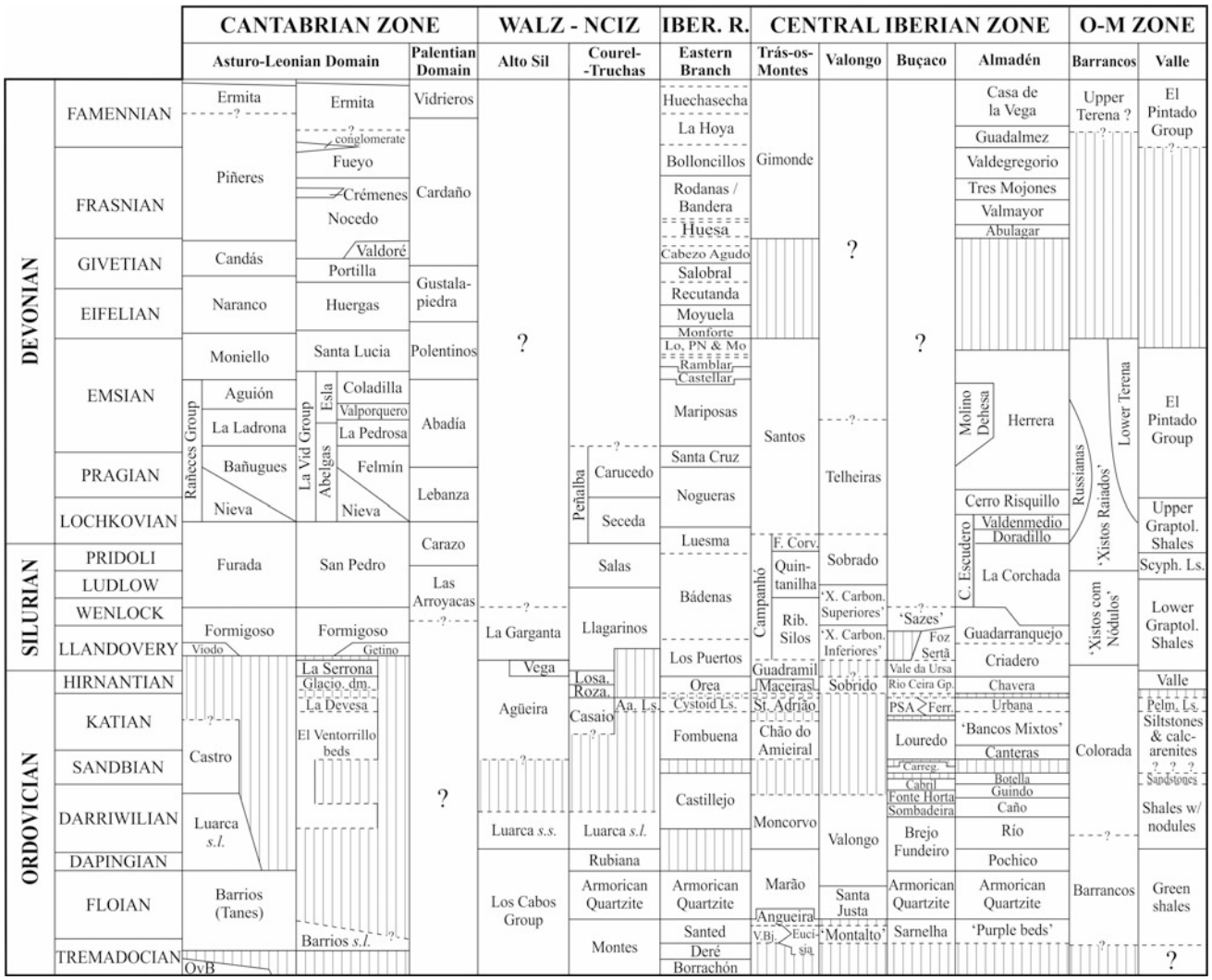

Fig. 3.5 General correlation chart of the most complete and continuous Ordovician to Devonian sedimentary units occurring in the Hesperian Massif. Devonian data mainly adapted from García Alcalde et al. (2002), Robardet and Gutiérrez-Marco (2004) and Meireles (2013). Lithostratigraphic abbreviations for formation names: Aa. Ls., La Aquiana limestone; F. Corv., Fraga dos Corvos; Ferr., Ferradosa; Glacio. Dm., unnamed glaciomarine diamictites; Losa, Losadilla; 'Lo, PN and Mo', Loscos, Peña Negra and Molino (in ascending order); OvB, Oville or lower Barrios (La Matosa Member); Pelm. Ls., Pelmatozoan limestone; PSA, Porto de Santa Anna; Rib. Silos, Ribeira de Silos; Roza, Rozadais; Sombadeira; Monte da Sombadeira; V. Bj., Vale de Bojas; 'X. Carbon.', Xistos Carbonosos; Other abbreviations: CA., Cerro; Graptol., Graptolitic; Gp., Group; Ls., limestone; O-M, Ossa-Morena; Rib., Ribeira; *s.l.*, sensu lato; *s.s.*, sensu stricto; St., Santo; WALZ—NCIZ, West Asturian-Leonese Zone

context due to regional vertical movements (García Alcalde et al. 2002). The second is restricted to an area of nappes which is thrusted over the SE of the Cantabrian Zone, probably originating in southern areas of the West Asturian-Leonese Zone (Henn and Jahnke 1984).

The Devonian succession in the Asturo-Leonian Domain is formed by an alternation of formations of either siliciclastic or carbonatic predominance, whose lithostratigraphic nomenclature shows obvious equivalences among the northern and southern slopes of the Cantabrian Ranges (Fig. 3.5). Details of the different formations have been summarized by García-Alcalde et al. (2002) and Aramburu et al. (2004), who described the continuous character of the sedimentation from the Lochkovian to the Frasnian, and the appearance of paraconformities and disconformities in the Famennian within the most complete Devonian sequences. Over an extense part of the Cantabrian Zone and towards the Asturian arc core, an important pre-upper Famennian sedimentation gap was developped, also affecting Silurian and some Ordovician strata.

The Devonian sequence of the Palentian Domain starts with shallow-water sandstones, limestones and shales that predominated in ascending order during the deposition of the early Lochkovian Carazo Fm, the late Lochkovian to Pragian

Lebanza Fm, and the Pragian to late Emsian Abadía Fm. Above the latter, the incoming of pelagic faunas of ammonoids, dacryoconarids and certain conodonts in the next four Devonian formations suggest quieter water to relatively deep conditions starting from the latest Emsian to the Famennian. To this regard, the quartz sandstones of the Murcia Fm (early Famennian) were interpreted as posible turbidites, and the reddish nodular limestones and shales of the overlying Vidrieros Fm (early Famennian to earliest Tournaisian) are representative of offshore deposits close to the slope. As in the previous case, a summary description of the formations of the Palentian Domain, including the location of the Devonian global events, was presented by García Alcalde et al. (2002), Aramburu et al. (2004).

The thick Devonian succession of the Iberian Range was deposited in an active subsiding trough presently outcropping to the west of the Datos fault, being the sedimentation continuous from the Silurian at least up to middle Famennian times. Devonian strata mostly represent shallow-water marine environments dominated by clastic sediments, richly fossiliferous, also with common thin intercalations of shelly limestones and marls. Rhythmothems due to variations in subsidence and water depth are also frequent, some of them containing pelagic faunas on black shales and limestones in alternation with neritic faunas. These pelagic faunas of dacryoconarids, ammonoids, ostracods, conodonts and epiplanktonic bivalves became relatively more abundant in the succession of the Late Devonian, where a background sedimentation of fine shale predominates. A basic study of the Devonian formations in the Iberian Range, including general aspects of correlation and paleogeographical problems, was presented by Carls (in García Alcalde et al. 2002) and Carls et al. (2004).

Scattered outcrops with Lower Devonian sedimentary rocks known from the West Asturian-Leonese Zone, other than the nappes of the Palentian Domain displaced onto the Cantabrian Zone, are only preserved in the transitional area with the 'Ollo de Sapo' Domain of the northern Central Iberian Zone. The main areas lie in the core of the Courel-Peñalba syncline, as well as in the eastern Guadarrama Sierra (García Alcalde et al. 2002). Other Devonian outcrops occurring in the autochthonous part of the Trás-os-Montes region and the Alcañices syncline are still very poorly known because of a complex tectonic overprint (González-Clavijo 2006; Meireles 2013).

The main Devonian successions of the southern Central Iberian Zone occur in the Portuguese inliers of Valongo, Marão, Dornes, Mação and Portalegre, as well as in the Spanish outcrops of the Sierra de San Pedro, Cáceres syncline, Almadén region and the eastern Sierra Morena area, each one with slightly different stratigraphical features. Nevertheless, a 'mid-Devonian stratigraphical gap' is a common feature even in the most complete successions of the domain. This involves a paraconformably contact, only detectable by biostratigraphic criteria, between successive deposits of Emsian and Frasnian (sometimes latest Givetian) ages, all developed in very similar marine facies. The 'mid-Devonian stratigraphical gap' has been interpreted as produced by an 'eo-Variscan' tectonic phase that in some parts of the southern 'Obejo-Valsequillo' Domain generates an angular unconformity of the Frasnian sandstones upon Early Devonian or earlier Paleozoic formations (Herranz Araújo 1985), being in the latter folded by a compressive/transpressive event. Oliveira et al. (1991) were the first authors who linked such tectonic episode to the initial subduction of oceanic lithosphere ('Pulo do Lobo Ocean') in the south of the Iberian Peninsula, now related with the starting of the Variscan collision and its 'echoes' in some of the apparently stable shelf areas at a wider scale.

The more complete and better-known Devonian sequences of the southern Central Iberian Zone are located in the Almadén area, lying in the core of the Herrera del Duque, Almadén and Guadalmez synclines, as well as in the Sierra de San Pedro. They are mainly composed of thick alternations of sandstones and shales, separated by metric to decametric packages of massive sandstones and quartzites. The shale-dominated formations are more frequent in the Late Devonian, whereas limestones are only recorded in the Herrera Fm (the Molino de la Dehesa Mb, Emsian) but also occur—as limestone lenses and nodules—within the Casa de la Vega Fm (early Famennian to late Tournaisian). In the Almadén syncline, a thick development of volcanic rocks (the 'Chillón Volcano-Sedimentary Complex') locally ranges along the entire Frasnian (see previous section). Details of the different Devonian formations and faunas of the southern Iberian Zone have been summarized by García Alcalde et al. (2002). In the same work the main Devonian sequences recognized in the 'Obejo-Valsequillo' Domain are also envisaged, being different from the southern Central Iberian Zone successions by a larger presence of shales and more abundant intercalations of Lower Devonian limestones (e.g. Rodríguez et al. 2010), but with some Frasnian faunas in common. Recent papers on the Devonian strata of south-central Portugal are by Gourvennec et al. (2008), Vaz (2010), Lopes (2013) and Schemm-Gregory and Piçarra (2013).

Devonian rocks have a relatively low number of well-characterised occurrences in the Ossa-Morena Zone. The better sections are located in the Zafra-Alanís and in the Barrancos-Hinojales sectors, and have been summarized by Robardet and Gutiérrez-Marco (2004). The first Unit includes the Devonian outcrops of the Valle and Cerrón del Hornillo synclines of northern Seville, where the Lochkovian graptolitic black shales, continuous with the Silurian, are conformably overlain by green to brown shales and siltst-ones of the lower part of the El Pintado Group. They

have yielded brachiopods, trilobites and ostracods of the whole Pragian and the early Emsian. The upper part of the El Pintado Group concordantly overlies these Lower Devonian strata, and started with limestones and calcareous sandstones with Famennian brachiopods and conodonts, followed by black shales and black argillaceous limestones with other Famennian bivalves and conodonts. These datings demonstrate the existence of an enlarged 'mid-Devonian stratigraphical gap' within the El Pintado Group and its extension to this part of the Ossa-Morena Zone.

The Devonian sequences of the Barrancos-Hinojales sector are quite different and sparsely fossiliferous, regarding the diverse Portuguese and Spanish sections. The most complete is represented in the Barrancos area, where the 'Xistos Raiados' Fm, continuous with the Silurian, yielded Lochkovian graptolites and palynomorphs, as well as some Praguian spores at the upper beds. A lateral defined formation (Russianas Fm) composed of grey-green shales with crinoidal limestone, yielded some Pragian trilobites, brachiopods, tabulate corals, bryozoans and crinoid columnals. Above the 'Xistos Raiados' Fm and in apparent gradual to concordant basal stratigraphic contact, the Lower Terena Formation consists of greywackes and shales with conglomeratic levels. The unit yielded Lochkovian graptolites and spores from their lowermost part, and Pragian and Emsian spore assemblages from higher levels. The biostratigraphic data raise paleogeographical or structural problems because three partly coeval Early Devonian lithosomes ('Xistos Raiados', Russianas and Lower Terena) seem to occur in different parts of the Barrancos region, perhaps involving various tectonic slices (Piçarra 2000, vol. 2, p. 143).

Other interesting Lower Devonian successions in the Ossa-Morena Zone are located in the Venta del Ciervo area, where fossiliferous shales of the Verdugo Fm having yielded brachiopods, trilobites, ostracods, rugose corals and a single graptolite of Pragian-early Emsian age. Also scattered occurrences of Upper Devonian rocks considered as syn-orogenic deposits (see Chap. 11 in this volume), located in the western Beja Massif, occur in the Cabrela and Toca da Moura complexes interbedded with terrigenous sediments dated as early Carboniferous (Pereira et al. 2006a, b; Oliveira et al. 2013). The Engenharia quarry (near Montemor-o-Novo) contains calciturbidites with late Eifelian conodonts, and the limestone lenses of the Cabrela Fm yielded late Frasnian conodonts, besides some poorly preserved macrofauna of possible Late Devonian age. Mid and Late Devonian limestones are now interpreted as olistholiths dislocated from a Devonian carbonate platform, situated south of the region in present day coordinates (Pereira et al. 2006a, b). In the upper part of the Odivelas Basic Complex in the Beja Massif, the Odivelas Limestone bears Emsian-Eifelian conodonts and reefal faunas, occurring in a sequence of calciturbidites and debris-flow deposits, which include hemipelagic tufites related to a reefal system resting on top of volcanic buildings within a large volcanic complex (Machado et al. 2009, 2010).

Finally, the recent finding of Early Devonian free-living tentaculitoids and crinoid columnals, occurring in marbles belonging to the 'Volcanic-Sedimentary Complex of Estremoz', opens the possibility of a complete reconsideration of the age of one of the most distinctive units in the Paleozoic basement of soutwestern Iberia (Piçarra et al. 2014).

3.6 The Latest Devonian-Early Carboniferous Sequences

The onset of the Variscan collision between Laurussia and Gondwana in late Lower Devonian times (see Chaps. 10 and 11 in this volume) brought to an end the tectonically quiescent passive margin stage. This was specially rapid in the outer margin Gondwanan domains such as the Middle and Lower allochthons and the Parautochthon of the Galicia-Trás-os-Montes Zone, which were subducted beneath Laurussia. The associated deformation of those domains renders very difficult the identification of the passive margin record in them, reason why they are dealt with separately in the next section. Away from the orogenic hinterland, the initial expression of the collisional event is varied and diachronous. In the Ossa-Morena, Central Iberian and probably the West Asturian-Leonese zones it is expressed by the sedimentary gaps, with or without associated tilting described in the previous section (see also Fig. 3.5), but platformal sedimentary conditions resumed until the propagation of deformation towards the foreland progressively reached them during the Carboniferous.

Owing to the southeasterly escape the Ossa-Morena Zone, accommodated by sinistral displacement along the Badajoz-Córdoba shear zone since Lower Devonian times (see Chaps. 10 and 11 in this volume), a process of transpressional uflift and transtensional basin formation affected most of the Ossa-Morena and the southernmost Central Iberian Zone. Denudation of part or all the passive margin succession took place in the uplifted blocks, whereas sedimentary continuity or paraconformity happened in the subsiding basins.

The transition from the Devonian into the Carboniferous sedimentation is marked by an unconformity in the Cantabrian Zone located at the base of the Ermita Fm in the late Famennian. No true unconformity (only a disconformity or paraconformity) is recognized in the Ossa-Morena Zone, where it seems to be younger from SW to NE from the Late Devonian into the Mississippian (Oliveira et al. 1991 and references therein), nor in the southern Central Iberian Zone or Obejo-Valsequillo Domain (Fig. 3.6). Lithological

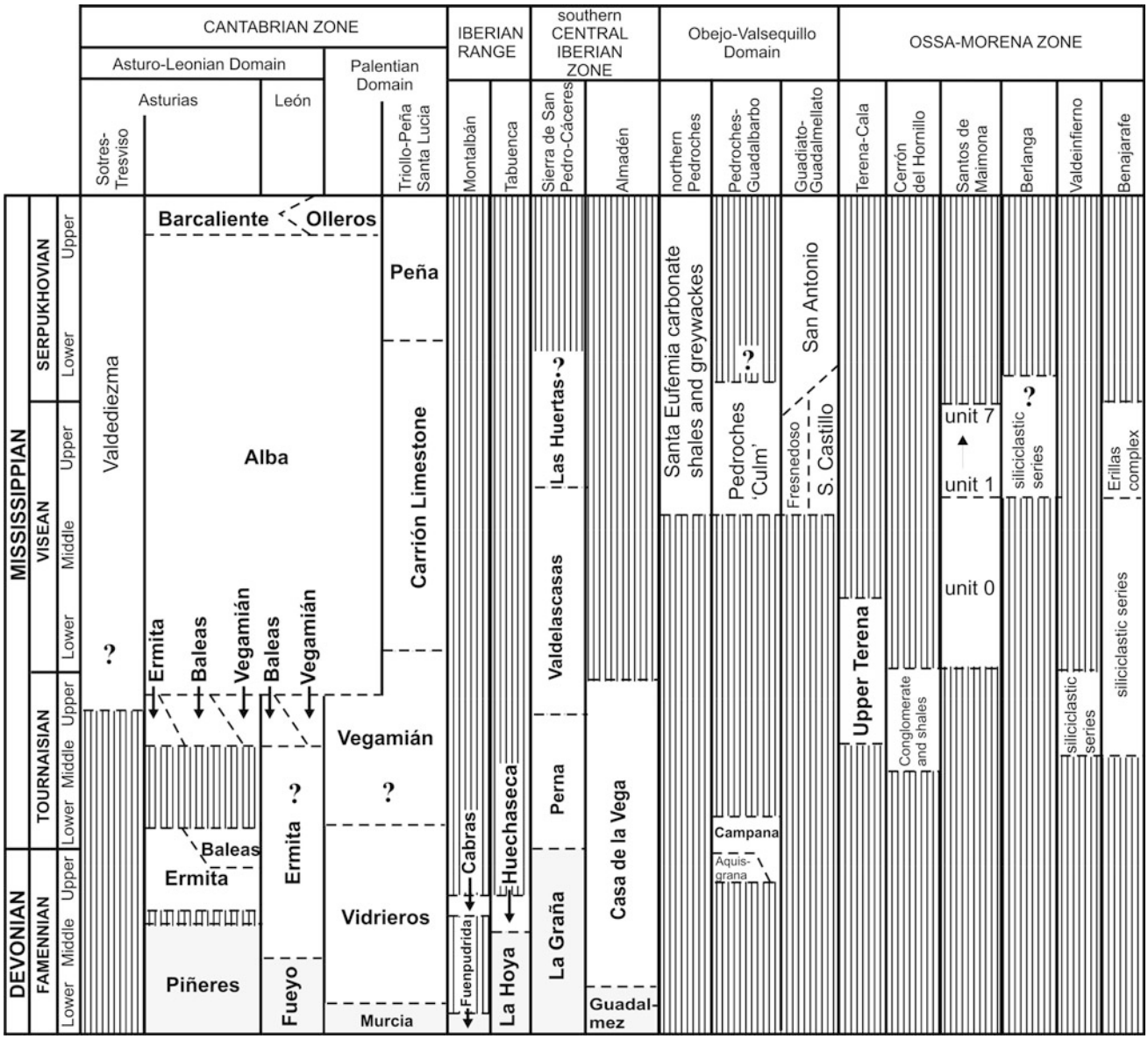

Fig. 3.6 Correlation chart of the main late Famennian and Mississippian rocks. Note that formal formations are not defined in many areas of the southern Central Iberian and Ossa-Morena zones (formal units are highlighted in bold font). Formations with grey filling are considered as pre-orogenic

descriptions are mostly based on García Alcalde et al. (2002), Colmenero et al. (2002), Fernández et al. (2004) and references therein.

In the Cantabrian Zone, the Ermita Fm is 5–75 m thick and composed of cross-bedded sandstones, siltstones, shales, and sandy limestone lenses with microconglomeratic sandstone layers. Above and laterally, it passes into sandy bioclastic packstone and grainstone limestone (mostly encrinitic) of the Baleas Fm (1–15 m thick). The overlying Vegamián Fm contains 2–5 m of black siltstones with phosphatic nodules and lydite bands with an erosive base over the Ermita Fm in some localities (Sanz-López and Blanco-Ferrera 2012). The synorogenic rocks seem to be apparently in continuity in the Palentian Domain, where the Vidrieros Fm, an ammonoid-bearing reddish nodular limestones interbedded with shales in a condensed sedimentation, and is deposited over the Murcia Fm. Laterally the Palentian Domain, Nemyrovska et al. (2011) named this formation as the Montó Fm, where it contains 30–40 m of shales and siltstones, with yellowish to pale grey nodular limestones.

There are no detailed sedimentological studies in those formations, and the Ermita Fm and lateral equivalents were interpreted as deposited in intertidal to supratidal

environments, whereas the Baleas limestone was considered as submarine shoals separated by slightly deeper channels with coarser grain than the Ermita and Vegamián formations, although the presence of black shales and lydites suggest deeper water settings, and possibly anoxica. The Vidrieros Fm was interpreted as offshore deposits close to the slope. The sedimentation was continuous through the Devonian/Carboniferous boundary in the Ermita, Baleas and Vidrieros formations, although their bases and tops are not synchronous (Fig. 3.6). Another gap occurs within these formations in the Cantabrian Zone, from the lowermost Tournaisian to the upper Tournaisian (Fig. 3.6). However, it has not been demonstrated yet if it extends into the Palentian and León domains (Sanz-López and Blanco-Ferrera 2012).

The latest Devonian in the Iberian Range is limited to the Tabuenca outcrops, where a composite succession of 1,300 m was described for the Frasnian-Famennian. The succession probably ends at the late Famennian, although the area is poorly known biostratigraphically, due to it being mostly composed of pelagic shales with rather sparse fauna.

The latest Devonian is absent in most of the Central Iberian Zone, where it only occurs in the southern outcrops (Fig. 3.6). In the Almadén area, the late Famennian is represented by limestones of the Casa de Vegas Fm (early Famennian to late Tournaisian) overlying pelagic black shales and carbonate nodules of the Guadalmez Fm. In the Sierra de San Pedro, the Famennian is recognized in the La Graña Fm, mostly composed of shales with greywackes, shales and microconglomerates in its upper part. The formation passes into the Perna Fm, composed of brecciated volcanic rocks and shales, attributed to the early Tournaisian. In the Obejo-Valsequillo Domain, east of Pedroches and close to La Carolina, the 'Aquisgrana shales' are regarded as the base of the Campana Fm, which contains siltstones, shales and quartzites, with ostracods of late Famennian age.

From the late Tournaisian upwards, the succession in the Cantabrian Mountains contains the Alba Fm (late Tournaisian–late Serpukhovian) and Barcaliente Fm (latest Serpukhovian–early Baskhirian; Sanz-López et al. 2013). The Alba Fm, 20–30 m thick, is a predominantly ammonoid-bearing reddish to grey nodular limestone composed of up to 6 members (Sanz-López and Blanco-Ferrera 2012), and interpreted as a pelagic platform. However, in the Palentian Domain, Nemyrovska et al. (2005, 2011) described the Carrión Limestone and Peña formations. The former is composed of grey to yellowish nodular to well-bedded limestone (ca. 15 m thick) and it ranges from the early Visean up to the lower part of the early Serpukhovian. The Peña Fm is composed of well-bedded partly bioclastic limestones, ca. 250 m thick, and it ranges up to the earliest Bashkirian. The Carrión Limestone Fm is interpreted as a pelagic platform, whereas the Peña Fm was considered as shallow-water platform. In the core of the Picos de Europa province, the informal Valdediezma Limestone (latest Tournaisian to early Bashkirian) has been recently described (Sanz-López et al. 2018). This limestone is the result of a highly subsiding agradational platform which accumulated more than 1,200 m of massive to well-bedded limestones, mostly corresponding to microbial carbonate mounds developed in shallow-water platform, surrounded by bioclastic and oncoidal beds in the lower and upper parts of the succession. Lateral facies changes with the typical Alba and Barcaliente formations are observed in the southeastern outcrops (Sanz-López et al. 2018). The Barcaliente Fm is mostly composed of black, laminated micrites with disperse organic matter and levels with quartz grains of silt size and scattered bioclasts, interpreted as distal turbidites and deep-water background sedimentation, mostly in its lower half. This formation passes laterally to the turbiditic shales of the Olleros Fm.

The Mississippian succession is sparsely distributed in the southern Central Iberian and Ossa-Morena zones, and the Obejo-Valsequillo Domain, whereas it is absent in northern Central Iberian Zone and Iberian Range (Fig. 3.6). It is also noteworthy, that Mississippian lithostratigraphical units are rarely formally defined.

In the southwestern part of the Central Iberian Zone, in the Sierra de San Pedro, the Mississipian contains the Perna, Valedelascasas and Huertas formations (Soldevila Bartolí 1992) with a total thickness of ca. 600 m. The Perna (Tournaisian) is a volcano-sedimentary unit composed of tuffs, limrstones, shales and lydites with numerous lateral facies changes. The Valedelascasas limestones (latestTournaisian-middle Visen) are pale grey to dark limestones, very recrystallized and dolomitized. Above, extend outcrops of the shales and Huertas Fm occur, up to 400 m. The shales were compared to those of the Cáceres syncline, and assigned to the Mississipian.

In La Codosera—Puebla de Obando syncline, the Mississippian is represented by the Gévora Fm (early to late Visean), which is mostly composed of shales with interbedded sandstones, local volcanic rocks and limestone olistoliths, and may reach up to 5,000 m in thickness (Rodriguez Gonzalez et al. 2007. In the Portuguese part of the syncline, early Carboniferous palynostratigraphic data (Z. Pereira, unpublished data; Lopes 2013) have been recently recorded in the so-called Rabaça Fm (Geological Map of Portugal, sheet 6, 1: 200,000 scale, in prep.).

In the north of the Obejo-Valsequillo Domain, close to Santa Eufemia, two successions are recognized: one with massive to well-bedded limestones and shales (ca. 100 m thick) and the other composed of shales and greywackes (ca. 4,000 m thick) (Rodríguez Pevida et al. 1990). The limestone lenses were considered as olistoliths, and the alternating shales and greywackes as part of the 'culm' facies fill

of the Pedroches basin. Limestone lenses were attributed to the late Visean, although the siliciclastic complex can be assigned to late Visean–earliest Bashkirian on the basis of conodonts. The Pedroches 'Culm' forms the most extensive outcrops in the Obejo-Valsequillo Domain (with a similar succession than that in the Guadalbarbo 'Culm'), where numerous folds and faults were recognized and its general thickness was estimated to be ca. 1,500 m. The base of the succession is composed of pyroclastic rocks (tuffs and volcanic ashes) interbedded with shales and carbonate breccias. Higher up in the succession, thick shale, siltstone and greywacke alternations are observed. A slope environment was proposed by Pérez-Lorente (1979). Foraminifers in the basal limestone boulders allow an assignation of the base of Pedroches "culm" to the late Visean. The upper part has not been dated as yet, but compared with neighbouring 'culm' facies in the Guadiato or Santa Eufemia, it might range into the Serpukhovian. More diverse rocks are recorded in the Guadiato and Guadalmellato areas (see Chap. 11 in this volume). Three tectonostratigraphic units were defined to characterize the Mississippian in the Guadiato area: the Fresnedoso, Sierra del Castillo and San Antonio-La Juliana units (Cózar and Rodríguez 1999). In the Fresnedoso Unit, a basal conglomerate is recorded in the so-called Alhondiguilla 'Culm' where abundant olistoliths are recorded, mostly carbonates but also fragments of nearshore sandstones and shales. The Sierra del Castillo Unit preserves fragments of the carbonate shallow-water platform. Both units were dated as late Visean. The succession during the late Visean corresponds to a deepening sequence with black shales at the top. The youngest unit, San Antonio-La Juliana Unit is composed of shales with common olistoliths and calciturbidites in a shallowing sequence reaching intertidal to supratidal carbonates interbedded with shales, veneered by deltaic conglomerates, and ranging from the early Serpukhovian to the lower part of the late Serpukhovian. The succession in the Guadalmellato area is rather similar (Cózar et al. 2006).

In the Ossa-Morena Zone some sparse marine outcrops occur (Fig. 3.6), which represent preserved parts of the infill of the syn-orogenic basins referred to above (see Chap. 11 in this volume). In the Terena-Cala area, represented by the Upper Terena Fm, the succession is composed of turbiditic shales interbedded with sandstones and conglomerates, ca. 1,000 m thick, interpreted to be deposited in a subsiding trough. In the upper part of the succession, calcareous sandstone lenses yield late Tournaisian-early Visean conodonts. The lenses were interpreted as shallow-water buildups redeposited in a toe-of-slope due to storm events. The succession in Los Santos de Maimona is composed of green shales and greywackes (rare coal) with common volcanic rocks in the lower part, followed by ca. 220 m of predominantly bioclastic and reefal limestones, and un upper part, ca. 500 m thick of siltstones, black shales, sandstones, conglomerates and some limestone olistoliths (Rodríguez 1992). The lower and upper parts of the succession were interpreted as 'culm' facies and slope deposits, whereas the limestones correspond to tidal-controlled sediments in middle and inner platform settings. The succession was assigned to the late Visean. In the area of Benajarafe, a 200–300 m thick succession is recorded, composed of conglomerates passing into marine siltstones and sandstones (with thin volcanic rocks and coal) and, in the younger part, a volcanic sequence (several hundred metres thick). In Berlanga, three units were recognized, a predominantly conglomeratic unit in the lower part (with interbedded shales and greywackes), a second shaly interval with thin sandstone beds, and the upper greywackes, interbedded with thin shales. A late Tournaisian-early Visean age was proposed for the lower part of the succession, which might range up to the late Visean. The sedimentation in Benajarafe and Berlanda were interpreted as deltaic and lagoonal (Gabaldón et al. 1985). The Cerrón del Hornillo is a poorly-known sequence, composed of a basal conglomerate, ca. 200 m of shales and rare sandy-encrinitic limestone lenses in its upper part. The lower part of the shales was assigned to the mid-late Tournaisian (Robardet et al. 1986, 1988).

3.6.1 The Drift Stage in the Upper Parautochthon of the Galicia Trás-Os-Montes Zone

Í. Dias da Silva, E. González-Clavijo, A. Díez-Montes, J. Gómez Barreiro

The drifting stage in the Upper Parautochthon (see definition in Chap. 4 of this volume) of the Galicia Trás-os-Montes Zone starts with a relatively thin (100 m) orthoquartzite unit, the Algoso Formation (Fig. 3.7; Dias da Silva 2014; Dias da Silva et al. 2014, 2016), which constitutes a reference bed suitable to unravel the Variscan structure in the Upper Parautochthon, and can be correlated to the widespread Armorican-type quartzite in Western Europe and the tectonically underlying Autochthon (Central Iberian Zone). The sedimentation of this sandy shoreline facies stratigraphic unit represents the establishment of a stable platform that culminates the regressive sequence of the stratigraphically underlying Mora-Saldanha Volcano-Sedimentary Complex (Fig. 3.7). Although no stratigraphic unconformity has been identified to date at the base of the Algoso Formation, we assume that it represents the rift-drift transition in the Upper Parautochthon stratigraphic sequence as it marks the maximum regression of the platform in the Lower Ordovician period.

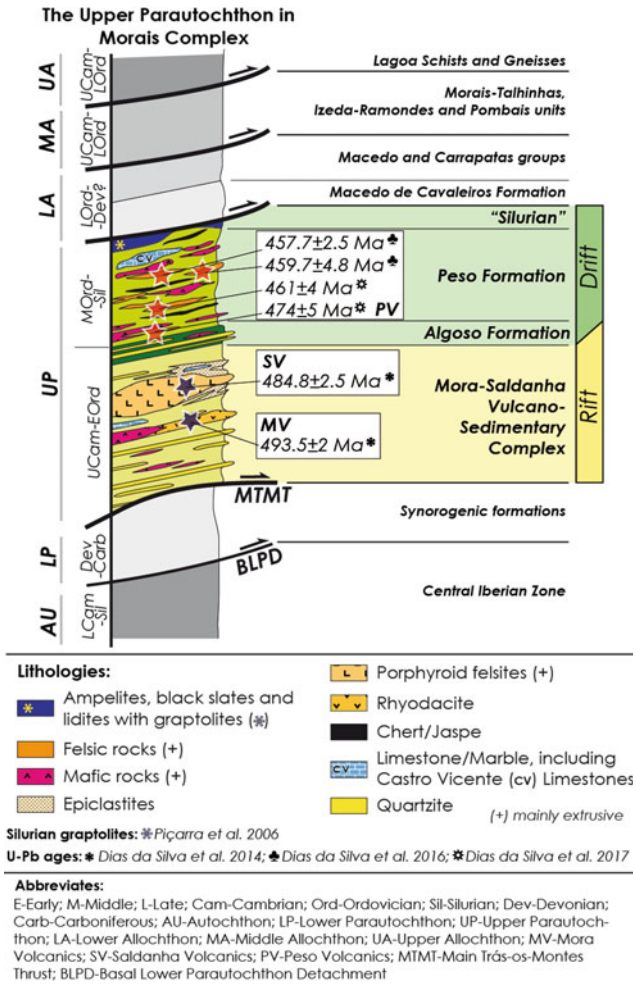

Fig. 3.7 Synthetic lithostratigraphic column of the Upper Parautochthon, in the Morais Complex, NE Portugal

The Algoso Formation is overlain by a relatively thick volcano-sedimentary unit named Peso Formation (Fig. 3.7; Dias da Silva 2014; Dias da Silva et al. 2016). It is made of black slates, locally purple probably in relation with volcanic exhalations, and includes a voluminous bimodal volcanism with abundant pyroclastic and epiclastic rocks, as well as some thin chert levels. Towards the upper part of the Peso Formation, a carbonate sedimentary unit, the Castro Vicente limestones (Pereira et al. 2006a, b), has an ambiguous stratigraphic position, pending for a better understanding of the geological structure. Meanwhile, it can be correlated to the Upper Ordovician limestones locally described at several localities of the nearby autochthonous Central Iberian Zone (Santo Adrião in Trás-os-Montes, Sá et al. 2005; and La Aquiana in the Truchas Syncline, Martínez Catalán et al. 1992). The Peso Formation volcanics include calc-alkaline rhyolites and rhyodacites, tholeiitic E-MORB basalts, and alkaline OIB basalts with locally associated plagiogranite dykes (Dias da Silva et al. 2016). Two ages of ~455 Ma were obtained in calc-alkaline rhyolites lying above the Algoso Formation (Dias da Silva et al. 2016). Together with new preliminary magmatic ages of 461 and 474 Ma found in similar rocks to the W of the Morais Complex (Dias da Silva et al. 2017), U–Pb dating confirms a Middle-Upper Ordovician age for the Peso Formation.

The volcanism of this unit shows an alkaline increase of the basaltic end-members in comparison with the Furongian Mora Volcanics. This may be an evidence of a second lithospheric stretching event as response of the extensional geodynamic setting of the N-Gondwana margin at this stage (Middle-Upper Ordovician), which ultimately led to the formation of different magmatic reservoirs/sources with a wide range of geochemical compositions (calc-alkaline, tholeiitic and alkaline) that evidence mantellic and crustal origins.

Finally, a thin unit of black ampelite and lydite beds is observed. It is gently deformed and yielded fauna with a paleogeographic affinity with the autochthonous realm, the Central Iberian Zone (Piçarra et al. 2006). This Silurian black layer is overlain by the Variscan shear zones at the top of the Upper Parautochthon, and then, by the higher metamorphic grade realm of the Lower Allochthon (Maçedo de Cavaleiros Formation, Pereira et al. 2006a, b; González-Clavijo et al. 2016).

3.6.2 Discussion of the Geodynamic Significance of the Upper Parautochthon Stratigraphic Sequence

Inside the Upper Parautochthon, no evidences of unconformities have been found. Two possibilities arise, the existence of a continuous sedimentary record from the middle Cambrian to the Silurian, as in the West Asturian-Leonese Zone (Cabos Series, Pérez-Estaún et al. 1990), or the unconformities are not recognized due to the superimposed pervasive deformation. In the second option, and comparing to what is known from the autochthonous Central Iberian Zone, two major discontinuities might be hidden. The lower one is the Toledanian unconformity (in the sense of Gutiérrez-Marco et al. 2002), that should be expected at the base of the Mora or Saldanha Volcanics, as described in the nearby CIZ in Serra do Marão, São Gabriel, Eucísia and Poiares zones, according to Sá et al. (2005), Coke et al. (2001, 2011), Gomes et al. (2009), Teixeira et al. (2013) and Dias da Silva (2014). In a higher stratigraphic position, the Sardic unconformity, would be located at the base of the Castro Vicente limestone, by correlation with the Santo Adrião Upper Ordovician limestones (Sá et al. 2005), occurring in the Autochthon, close to the Morais Complex, where this unconformity has been recently mapped (Dias da Silva 2014; Dias da Silva et al. 2010, 2011).

Assuming the simplest option, that of a continuous sedimentary sequence, the Furongian-Silurian sequence of the Upper Parautochthon correlates better to the West Asturian-Leonese Zone, starting with the Cabos Series in the middle Cambrian, than with the nearer Central Iberian Zone sequence, where the bottom of the Montes Beds is located at the Cambrian-Ordovician boundary. However, the very thick stratigraphic sequence that characterizes an Ordovician trough in the former (Marcos et al. 2004) is not identified at the Upper Parautochthon. Moreover, it is difficult to explain how, during the Variscan orogeny, a slice of a more proximal continental upper crust (West Asturian-Leonese Zone) was thrust on top of the more distal crust (Central Iberian Zone). For these reasons, it looks more realistic to envisage a wide continental shelf, with the Central Iberian Zone in an inner position and the Upper Parautochthon in a contiguous more external situation.

Thus, the Upper Parautochthon sedimentary facies could be considered similar to the nearby Central Iberian Zone and, therefore, we propose that during the Ordovician both areas were parts of a shallow shelf in the Gondwana margin, evolving to a tidal or littoral environment at the Floian (Robardet 2002). During the Middle Ordovician, sedimentation has characteristics of an anoxic distal shelf (Gutiérrez-Marco et al. 2002). The Castro Vicente limestones may have formed on top of a non-identified unconformity, occupying the upthrown block of a normal fault, as proposed by Martínez Catalán et al. (1992) for the La Aquiana limestones at the Truchas region, and by Dias da Silva (2014) for the Santo Adrião Formation in NE-Portugal. Finally, the uppermost thin Silurian black unit would indicate a starved basin in a distal shelf environment.

This paleogeographic history fits that of a passive continental margin reflecting transgressions and regressions. But the abundant and long-lasting, though episodic, volcanism suggests a more complex evolution, involving extensional deformation suitable to provide channels for the outpouring of igneous rocks, some of them of mantellic derivation. Syn-sedimentary tectonic activity during the Ordovician has been proposed also in the nearby autochthonous Central Iberian Zone (Martínez Catalán et al. 1992). The calc-alkaline affinity of the volcanism in both areas is considered inherited from the melting of Cadomian arc-related basement during rifting of the N-Gondwana margin (Bea et al. 2007; Díez-Montes et al. 2010), and is not related to an island-arc setting (Dias da Silva et al. 2014, 2015).

The Upper Parautochthon tectonic slice was part of a large N Gondwana continental shelf that underwent extension during the Furongian-Silurian period allowing profuse and long term (about 50 Ma) volcanic activity. The current structural position, on top of the autochthonous and forming part of a piggy-back nappe stack (Schermerhorn and Kotsch 1984; Dallmeyer et al. 1997), suggests that it was previously placed in a relatively distal position of the margin relative to the Central Iberian Zone. This extensional process is being related to the rifting/drifting of Gondwana resulting in the detachment of a ribbon continent including a magmatic arc, the Upper Allochthon (see Chap. 4 in this volume), produced by back-arc (hyper) extension, preserved in the Lower Allochthon (see Chaps. 2 and 4) and resulting in the formation of an intermediate ocean, partially preserved in the Middle Allochthon (Chap. 4 in this volume; Dias da Silva et al. 2014, 2016).

References

Abalos B (1990) Cinemática y mecanismos de la deformación en régimen de transpresión. Evolución estructural y metamórfica de la Zona de Cizalla Dúctil de Badajoz-Córdoba. PhD Thesis, University of the Vasque Country.

Álvaro JJ, Bellido F, Gasquet D, Pereira F, Quesada C Sánchez-García T (2014) Diachronism of late Neoproterozoic-Cambrian arc-rift transition of North Gondwana: a comparison of Morocco and the Iberian Ossa-Morena Zone. Journal of African Earth Sciences 98:113–132.

Álvaro JJ, Casas JM, Clausen S, Quesada C (2018) Early Palaeozoic geodynamics in NW Gondwana. Jour Iberian Geol 44 (4): 551–565.

Álvaro JJ, Colmenar J, Monceret E, Pouclet A, Vizcaïno D (2016) Late Ordovician (post-Sardic) rifting branches in the North Gondwanan Montagne Noire and Mouthoumet massifs of southern France, Tectonophysics 681, 111–123.

Ancochea E, Arenas R, Brandle JL, Peinado M, Sagredo J (1988) Caracterización de las rocas metavolcánicas silúricas del NO del Macizo Ibérico. Geociências, Aveiro, 3: 23–34.

Aramburu C, Méndez-Bedia I, Arbizu M, García-López S (2004) Zona Cantábrica. La secuencia preorogénica, in Geología de España (Vera JA, ed), IGME-Sociedad Geológica de España, 27–34, Madrid.

Araújo A, Piçarra Almeida J, Borrego J, Pedro J, Oliveira JT (2013) As regiões central e sul da Zona de Ossa-Morena, in Geologia de Portugal—volume I (Dias, R, Araújo A, Terrinha, P, Kullberg JC, eds), Escolar Editora, 509–549, Lisboa.

Arenas R, Díez Fernández R, Rubio Pascual FJ, Sánchez Martínez S, Martín Parra LM, Matas J, González del Tánago J, Jiménez-Díaz A, Fuenlabrada JM, Andonaegui P, García-Casco A (2016) The Galicia-Ossa-Morena Zone: Proposal for a new zone of the Iberian Massif. Variscan implications, Tectonophysics 681, 135–145.

Bea F, Montero P, González-Lodeiro F, Talavera C (2007) Zircon Inheritance Reveals Exceptionally Fast Crustal Magma Generation Processes in Central Iberia during the Cambro-Ordovician. Journal of Petrology 48:2327–2339. https://doi.org/10.1093/petrology/egm061.

Bea F, Montero P, Talavera C, Abu Anbar M, Scarrow JH, Molina JF, Moreno JA (2010) The palaeogeographic position of Central Iberia in Gondwana during the Ordovician: evidence from zircon chronology and Nd isotopes, Terra Nova 22, 341–346.

Bernárdez E, Colmenar J, Gutiérrez-Marco JC, Rábano I, Zamora S (2014) New peri-Gondwanan records of the Hirnantia Fauna in the latest Ordovician of Spain, in Gondwana 15 North meets South, Abstracts Book (Pankhurst RJ, Castiñeiras P, Sánchez Martínez S, eds), Instituto Geológico y Minero de España, 15, Madrid.

Bergström SM, Chen X, Gutiérrez-Marco JC, Dronov AV (2009) The new chronostratigraphic classification of the Ordovician System and

its relations to major regional series and stages and $\delta^{13}C$ chemostratigraphy, Lethaia 42, 97–107.

Brenchley PJ, Romano M, Gutiérrez-Marco JC (1986) Proximal and distal Hummocky cross-stratified facies on a wide Ordovician Shelf in Iberia, in Shelf Sands and Sandstones (Knight RJ, McLean JR, eds), Canadian Society of Petroleum Geologists Memoir 11, 241–255, Calgary.

Carls P, Gozalo R, Valenzuela-Ríos J.I., Truyols-Massoni, M (2004) La sedimentación marina devónico-carbonífera, Cordilleras Ibérica y Costero-Catalana, in Geología de España (Vera JA, ed), Sociedad Geológica de España, Instituto Geológico y Minero de España, 475–479, Madrid.

Cocks LRM, Fortey RA (1990) Biogeography of Ordovician and Silurian faunas, in Palaeozoic Palaeogeography and Biogeography (McKerrow WS, Scotese CR, eds), Geological Society Memoir 12, 97–104, London.

Coke C, Pires CAC, Sá A, Ribeiro A (2001) O Vulcanismo na transição Câmbrico/Ordovícico da Zona Centro-Ibérica na região de Trás-os-Montes (NE Portugal) como elemento de referência estratigráfica. Cuadernos Xeolóxicos de Laxe 26:121–136.

Coke C, Teixeira RJS, Gomes MEP, Corfú F, Rubio Ordoñéz A (2011) Early Ordovician volcanism in Eucísia and Mateus areas, Central Iberian Zone, northern Portugal. Mineralogical Magazine 75 (3):685.

Colmenar J, Pereira S, Young TP, da Silva CM, Sa AA (2019) First report of Hirnantian (Upper Ordovician) high-latitude peri-gondwanan macrofossil assemblages from Portugal. Journal of Paleontology, in press, https://doi.org/10.1017/jpa.2018.88.

Colmenero JR, Fernández LP, Moreno C, Bahamonde JR, Barba P, Heredia N, González F (2002) Carboniferous, Chapter 7 in The Geology of Spain (Gibbons W, Moreno MT, eds), The Geological Society, 93–116, London.

Cózar P, Rodríguez S (1999) Propuesta de nueva nomenclatura para las unidades del Carbonífero Inferior del sector Norte del área del Guadiato (Córdoba). Boletín Geológico y Minero 110:237–254.

Cózar P, Somerville ID, Rodríguez S, Mas R, Medina-Varea P (2006) Development of a late Viséan (Mississippian) mixed carbonate/siliciclastic platform in the Guadalmellato Valley (south-western Spain), Sedimentary Geology 183, 269–295.

Dallmeyer RD, Martínez Catalán JR, Arenas R, Gil Ibarguchi JI, Gutiérrez-Alonso G, Farias P, Aller J, Bastida F (1997) Diachronous Variscan tectonothermal activity in the NW Iberian Massif: Evidence from $^{40}Ar/^{39}Ar$ dating of regional fabrics. Tectonophysics 277:307–337. https://doi.org/10.1016/s0040-1951(97)00035-8.

Dias da Silva Í (2014) Geología de las Zonas Centro Ibérica y Galicia—Trás-os-Montes en la parte oriental del Complejo de Morais, Portugal/España, vol 45. Serie Nova Terra, vol 45. Instituto Universitario de Geología "Isidro Parga Pondal"—Área de Xeoloxía e Minería do Seminario de Estudos Galegos, Coruña.

Dias da Silva Í, González Clavijo E, Barba P, Valladares MI, Ugidos JM (2011) Geochemistry of Lower Palaeozoic shales. A case study in a sector of the Iberian Variscides. In: Gutiérrez Marco JC, Rábano I, García-Bellido D (eds), 11th International Symposium on the Ordovician System, Alcalá de Henares, 2011. Instituto Geológico y Minero de España, pp 121–125.

Dias da Silva Í, González Clavijo E, Martínez Catalán JR Evolução tectono-térmica de um sector da Zona Centro Ibérica na região do Palaçoulo (leste do Maciço de Morais, NE Portugal). In: Brilha J, Pamplona J, Valente T (eds) VIII Congresso Nacional de Geología, Braga, 2010. vol 14. e-Terra, pp 1–4.

Dias da Silva Í, Valverde-Vaquero P, González-Clavijo E, Díez-Montes A, Martínez Catalán JR (2014) Structural and stratigraphical significance of U–Pb ages from the Mora and Saldanha volcanic complexes (NE Portugal, Iberian Variscides). Geological Society, London, Special Publications 405:115–135. https://doi.org/10.1144/sp405.3.

Dias da Silva Í, Linnemann U, Hofmann M, González-Clavijo E, Díez-Montes A, Martínez Catalán JR (2015b) Detrital zircon and tectonostratigraphy of the Parautochthon under the Morais Complex (NE Portugal): implications for the Variscan accretionary history of the Iberian Massif. Journal of the Geological Society 172 (1):45–61. https://doi.org/10.1144/jgs2014-005.

Dias da Silva Í, Díez Fernández R, Díez-Montes A, González Clavijo E, Foster DA (2016) Magmatic evolution in the N-Gondwana margin related to the opening of the Rheic Ocean—evidence from the Upper Parautochthon of the Galicia-Trás-os-Montes Zone and from the Central Iberian Zone (NW Iberian Massif). International Journal of Earth Sciences 105 (4):1127–1151. https://doi.org/10.1007/s00531-015-1232-9.

Días da Silva I, González Clavijo E, Díez Montes A, Martínez Catalán JR, Gómez Barreiro J, Hoffman M, Gärtner A (2017) Furongian-Late Ordovician volcanism in the Upper Parautochthon of the Galicia-Tràs-os-Montes Zone (NE Portugal): Paleogeographic meaning and geodynamic setting. Géologie de la France 1:19–21.

Díez Balda MA (1986) El Complejo Esquisto-Grauváquico, las series paleozoicas y la estructura hercínica al Sur de Salamanca. Acta Salmanticensia 52: 1–162.

Díez Fernández R, Arenas R (2015) The Late Devonian Variscan suture of the Iberian Massif: A correlation of high-pressure belts in NW and SW Iberia, Tectonophysics 654, 96–100.

Díez Fernández R, Arenas R (2016) Reply to Comment on "The Late Devonian Variscan suture of the Iberian Massif: A correlation of high-pressure belts in NWand SW Iberia". Tectonophysics 670: 155–160. https://doi.org/10.1016/j.tecto.2015.11.033.

Díez-Montes A, Martínez Catalán JR, Bellido Mulas F (2010) Role of the Ollo de Sapo massive felsic volcanism of NW Iberia in the Early Ordovician dynamics of northern Gondwana. Gondwana Research 17:363–376. https://doi.org/10.1016/j.gr.2009.09.001.

Fernández LP, Bahamonde JR, Barba P, Colmenero JR, Heredia N, Rodríguez-Fernández LR, Salvador C, Sánchez de Posada LC, Villa E, Merino-Tomé O, Motis K (2004) Secuencia sinorogénica, in Geología de España (Vera JA, ed), Sociedad Geológica de España-Instituto Geológico y Minero de España, 34–41. Madrid.

Fernández-Suárez J, Gutiérrez-Alonso G, Pastor-Galán D, Hoffman M, Murphy JB, Linnemann U (2014) The Ediacaran–Early Cambrian detrital zircon record of NW Iberia: Possible sources and paleogeographic constraints: International Journal of Earth Sciences, https://doi.org/10.1007/s00531.

Fortey RA, Cocks RLM (2005) Late Ordovician global warming—The Boda event, Geology 33, 405–408.

Franke W, Cocks LRM, Torsvik TH, 2017, The Palaeozoic Variscan oceans revisited, Gondwana Research 48, 257–284.

Gabaldón V, Garrote A, Quesada C (1985) El Carbonífero Inferior del Norte de la Zona de Ossa-Morena (SW de España. CR 10th Int Carboniferous Congr, Madrid, 3:173–186.

García Alcalde JL, Carls P, Pardo Alonso MV, Sanz López J, Soto F, Truyols-Massoni M, Valenzuela-Ríos JL (2002) Devonian, Chapter 6 in The Geology of Spain (Gibbons W, Moreno T, eds), The Geological Society, 67–91, London.

Ghienne J-F, Le Heron DP, Moreau J, Denis M, Deynoux M (2007) The Late Ordovician glacial sedimentary system of the North Gondwana platform, in Glacial sedimentary processes and products (Hambrey MJ, Christoffersen P, Glasser NF, Hubbard B, eds), International Association of Sedimentologists, Special Publication 39, 295–319, Blackwell Publising, Oxford.

Gomes M, Coke C, Teixeira R, Azevedo M, Corfu F (2009) New insights in the Early Ordovician magmatism from the Marão anticline, Northern Portugal. Goldschmidt Conference Abstracts 2009, A450.

González-Clavijo EJ (2006) La geología del sinforme de Alcañices, Oeste de Zamora, Ediciós do Castro, Serie Nova Terra 31, 238 pp, A Coruña.

González-Clavijo E, Dias da Silva ÍF, Gutiérrez-Alonso G, Díez Montes A (2016) U/Pb age of a large dacitic block locked in an Early Carboniferous synorogenic mélange in the Parautochthon of NW Iberia: New insights on the structure/sedimentation Variscan interplay. Tectonophysics 681:159–169. https://doi.org/10.1016/j.tecto.2016.01.001.

Gourvennec R, Plusquellec Y, Pereiza Z, Piçarra JM, Le Menn, J, Robardet M, Oliveira JT (2008) A reassessment of the Lochkovian (Lower Devonian) benthic faunas and palynomorphs from the Dornes region (Southern Central Iberian Zone, Portugal). Comunicaçoes do Instituto Geológico e Mineiro 95, 5–25.

Gutiérrez-Alonso G, Murphy JB, Fernández-Suárez J, Hamilton MA (2008) Geocronología de las rocas volcánicas de El Castillo (Salamanca, Zona Centroibérica). Geogaceta 44: 3–6.

Gutiérrez-Alonso G, Gutiérrez-Marco JC, Fernández-Suárez J, Bernárdez E, Corfu F (2016) Was there a super-eruption on the Gondwanan coast 477 My ago? Tectonophysics 681, 85–94.

Gutiérrez-Marco JC, Bernárdez E (2003) Un tesoro geológico en la Autovía del Cantábrico. El Túnel Ordovícico del Fabar, Ribadesella (Asturias), Libro-catálogo de la Exposición, Ministerio de Fomento, 398 pp, Madrid.

Gutiérrez-Marco JC, Lenz AC, Robardet M, Piçarra JM (1996) Wenlock-Ludlow graptolite biostratigraphy and extinction: a reassessment from the southwestern Iberian Peninsula (Spain and Portugal), Canadian Journal of Earth Sciences 33, 656–663.

Gutiérrez-Marco JC, Robardet M, Piçarra JM (1998) Silurian Stratigraphy and Paleogeography of the Iberian Peninsula (Spain and Portugal), Temas Geológico-Mineros ITGE 23, 13–44.

Gutiérrez-Marco JC, Aramburu C, Arbizu M, Bernárdez E, Hacar Rodríguez MP, Méndez-Bedia I, Montesinos López R, Rábano I, Truyols J, Villas E (1999) Revisión bioestratigráfica de las pizarras del Ordovícico Medio en el noroeste de España (Zonas Cantábrica, Asturoccidental-leonesa y Centroibérica septentrional), Acta Geologica Hispanica 34, 3–87.

Gutiérrez-Marco JC, Sarmiento GN, Robardet M, Rábano I, Vanek J (2001) Upper Silurian fossils of Bohemian type from NW Spain and their palaeogeographical interest, Journal of the Czech Geological Society 46, 247–258.

Gutiérrez-Marco JC, Robardet M, Rábano I, Sarmiento GN, San José Lancha MA, Herranz Araújo P, Pieren Pidal AP (2002) Ordovician. Chapter 4 in The Geology of Spain (Gibbons W, Moreno T, eds), The Geological Society, 31–49, London.

Gutiérrez-Marco JC, Sá AA, García-Bellido DC, Rábano I, Valério M (2009) Giant trilobites and trilobite clusters from the Ordovician of Portugal, Geology 37, 443–446.

Gutiérrez-Marco JC, Ghienne J-F, Bernárdez E, Hacar MP (2010) Did the Late Ordovician African ice sheet reach Europe?, Geology 38, 279–282.

Gutiérrez-Marco JC, Sá AA, García-Bellido DC, Rábano I (2014a) The extent of the Middle Ordovician Dapingian Stage in peri-Gondwanan Europe and North Africa. Stratigraphic record, biostratigraphic tools, and regional chronostratigraphy, GFF 136, 90–94.

Gutiérrez-Marco JC, Sarmiento GN, Rábano I (2014b) Un olistostroma con cantos y bloques del Paleozoico Inferior en la cuenca carbonífera del Guadalmellato (Córdoba). Parte 2: Bioestratigrafía y afinidades paleogeográficas, Revista de la Sociedad Geológica de España 27, 25–43.

Gutiérrez-Marco JC, Sá AA, Rábano I, Sarmiento GN, García-Bellido DC, Bernárdez E, Lorenzo S, Villas E, Jiménez-Sánchez A, Colmenar J, Zamora S (2015) Iberian Ordovician and its international correlation, Stratigraphy 12, 257–263.

Gutiérrez-Marco JC, Lorenzo S, Rábano I, Sarmiento GN, Carlorosi J (2016) Fósiles ordovícicos del Dominio de Obejo-Valsequillo (Complejo de Ossa Morena, Zona Galicia-Ossa Morena), suroeste de España, Geotemas 16, 211–214.

Gutiérrez-Marco JC, Sá AA, García-Bellido DC, Rábano I (2017) The Bohemo-Iberian regional chronostratigraphic scale for the Ordovician System and palaeontological correlations within South Gondwana, Lethaia 50, 258–295.

Hall, C.M., Higueras, P., Kesler, S., Lunar, R., Dong, H., Halliday, A.N., 1997. Dating of alteration episodes related to mercury mineralization in the Almadén district, Spain. Earth Planet Sci Lett 148: 287–298.

Hammann W (1992) The Ordovician trilobites from the Iberian Chains in the province of Aragón, NE-Spain. I. The trilobites of the Cystoid Limestone (Ashgill Series), Beringeria 6, 3–219.

Hammann W, Henry J-L (1978) Quelques espèces de *Calymenella*, *Eohomalonotus* et *Kerfornella* (Trilobita, Ptychopariida) de l'Ordovicien du Massif Armoricain et de la Péninsule Ibérique, Senckenbergiana lethaea 59, 401–429.

Helo C, Longpré MA, Shimuzi N, Clague DA, Stix J (2011) Explosive eruptions at mid-ocean ridges driven by CO2-rich magmas. Nature Geosci 4: 260–263.

Henn A, Jahnke H (1984) Die palentinische Faziesentwicklung im Devon des Kantabrischen Gebirges, Zeitschrift der Deutschen Geologischen Gesellschaft 135, 131–147.

Hernández A, Jébrak M, Higueras P, Oyarzun R, Morata D, Munhá J (1999) The Almadén mercury mining district. Mineral Deposita 34: 539–548.

Herranz Araújo P (1985) El Precámbrico y su cobertera paleozoica en la región centro-oriental de la provincia de Badajoz, Seminarios de Estratigrafía, serie Monografías 10, 1342 pp.

Higueras P (1995) Procesos petrogenéticos y de alteración de las rocas magmáticas asociadas a las mineralizaciones de mercurio del distrito de Almadén. Ediciones de la Universidad de Castilla-La Mancha, Cuenca (Spain), 270 pp.

Higueras P, Mansilla L, Lorenzo S, Esbrí JM (2011) The Almadén mercury mining district. In: Ortiz JE, Puche O, Rábano I, Mazadiego LF (eds), History of Research in Mineral Resources. Cuadernos del Museo Geominero 13: 75–88.

Higueras P, Oyarzún R, Lillo J, Morata D (2013) Intraplate mafic magmatism, degasification, and deposition of mercury: The giant Almadén mercury deposit (Spain) revisited. Ore Geol Rev 51: 93–102.

Jaeger H, Robardet M (1979) Le Silurien et le Dévonien basal dans le Nord de la province de Séville (Espagne), Géobios 12, 687–714.

Jébrak M, Higueras P, Hernández A, Marcoux E (1997) Datos geoquímicos e isotópicos sobre el yacimiento de Nuevo Entredicho, Almadén, España. Bol Soc Esp Mineral 20ª: 87–88.

Leone F, Hammann W, Laske R, Serpagli E, Villas E (1991) Lithostratigraphic units and biostratigraphy of the post-sardic Ordovician sequence in south-west Sardinia. Bollettino della Società Paleontologica Italiana 30, 201–235.

Loeschke J (1983) Igneous and pyroclastic rocks in Devonian and Lower Carboniferous strata of the Cantabrian Mountains (NW Spain) Neues Jahrbuch für Geologie und Palaeontologie, Mh 8: 495–504.

Lopes G (2013) Investigação em palinologia e isótopos estáveis do Paleozoico da Zona Centro-Ibérica (Buçaco, Dornes, Mação e Portalegre) e Zona de Ossa-Morena (Toca da Moura e Barrancos), Portugal. Implicações paleogeográficas e paleoambientais, Ph.D. Thesis Universidade do Algarve, Faro, 678 pp.

Lopes G, Vaz N, Sequeira AJD, Piçarra J, Fernandes P, Pereira Z (2011) New insights on the palynostratigraphy of the Hirnantian of the Rio Ceira section, Buçaco, Portugal, Cuadernos del Museo Geominero 14, 313-319.

López Díaz F, Monteserín V, Pineda A et al. (2007) Mapa Geológico de España, escala 1:50000, sheet no. 728: Puebla de Obando. Instituto Geológico y Minero de España.

López-Guijarro, R., Quesada, C., Fernández-Suárez, J., Jeffries, T., Pin, C. (2007) Age of the rift–drift transition of the Rheic Ocean in the Ossa

Morena Zone: K-bentonite in the Early Ordovician succession at "Venta del Ciervo". The Rootless Variscan Suture of NW Iberia (Galicia, Spain). IGCP-497 Meeting. Abstracts and Programme. Publicaciones del Instituto Geológico y Minero de España, pp. 142–143.

López-Moro FJ, Murciego A, Rodríguez MA (2001) Aspectos estructurales, petrográficos y geoquímicos de los sills de rocas básicas e intermedias del área de Alburquerque-Villar del Rey-La Roca de la Sierra (Badajoz). Bol Soc Esp Mineral 24-A: 135–136.

López-Moro FJ, Murciego A, López-Plaza M (2007) Silurian/Ordovician asymmetrical sill-like bodies from La Codosera syncline, W Spain: A case of tholeiitic partial melts emplaced in a single magma pulse and derived from a metasomatized mantle source.

Lotze F (1956) Über sardischen Bewegungen im Spanien und ihre Beziehungen zur assynthischen Faltung, in Geotektonische Symposium zu Ehren von Hans Stille, 128–139, Stuttgart.

Loydell DK, Frýda J, Gutiérrez-Marco JC (2015) The Aeronian/Telychian (Llandovery, Silurian) boundary, with particular reference to sections around the El Pintado reservoir, Seville Province, Spain, Bulletin of Geosciences 90, 743–794.

Machado G, Hladil J, Koptíková L, Fonseca P, Rocha F, Galle A (2009) The Odivelas Limestone: evidence for a Middle Devonian reef system in western Ossa-Morena Zone (Portugal), Geologica Carpathica 60, 121–137.

Machado G, Hladil J, Slavik L, Koptikova L, Moreira N, Fonseca M, Fonseca P (2010) An Emsian-Eifelian carbonate-volcaniclastic sequence and the possible correlatable pattern of the Basal Chotec event in Western Ossa-Morena Zone, Portugal (Odivelas Limestone), Geologica Belgica 13, 431–446.

Marcos A (1973) Las series del Paleozoico inferior y la estructura herciniana del occidente de Asturias (NW de España), Trabajos de Geología Oviedo 6, 1–113.

Marcos A, Martínez Catalán JR, Gutiérrez Marco JC, Pérez Estaún A (2004). Zona Asturoccidental-Leonesa: Estratigrafía y paleogeografía. In: Vera JA (ed), Geología de España. IGME-SGE, Madrid, 49–52.

Martín Herrero D, Bascones Alvira L, Corretgé Castañón LG (1987) Mapa y Memoria Explicativa de la Hoja nº 650 (Cañaveral) del Mapa Geológico de España E. 1:50.000, IGME, 63 pp, Madrid.

Martín Escorza C (1976) Las "Capas de Transición", Cámbrico inferior y otras series preordovícicas (¿Cámbrico superior?) en los Montes de Toledo surorientales: sus implicaciones geotectónicas, Estudios Geológicos 32, 591–613.

Martín Parra LM, González Lodeiro F, Martínez Poyatos D, Matas J (2006) The Puente Génave-Castelo de Vide Shear Zone (southern Central Iberian Zone, Iberian Massif): geometry, kinematics and regional implications, Bulletin de la Société Géologique de France 177, 191–202.

Martínez Catalán JR, Hacar Rodríguez MP, Villar Alonso P, Pérez-Estaún A, González Lodeiro F (1992) Lower Paleozoic extensional tectonics in the limit between the West Asturian-Leonese and Central Iberian Zones of the Variscan Fold-Belt in NW Spain, Geologische Rundschau 81, 545–560.

McDougall N, Brenchley PJ, Rebelo JA, Romano M (1987) Fans and fan deltas—precursors to the Armorican Quartzite (Ordovician) in western Iberia. Geological Magazine 124, 347–359.

Meireles CAP (2013) Litoestratigrafia do Paleozóico do sector a nordeste de Bragança (Trás-os-Montes), Instituto Universitario de Geología Isidro Parga Pondal, Serie Nova Terra 42, 471 pp, A Coruña.

Nemyrovska TI (2005) Late Viséan/early Serpukhovian conodont succession from the Triollo section, Palencia (Cantabrian Mountains, Spain), Scripta Geologica 129, 13–89.

Nemyrovska TI, Wagner RH, Winkler Prins CF, Montañez I (2011) Conodont faunas across the mid-Carboniferous boundary from the Barcaliente Formation at La Lastra (Palentian Zone, Cantabrian Mountians, northwest Spain); geological setting, sedimentological characters and faunal descriptions, Scripta Geologica 143, 127–183.

Oliveira JT, Oliveira V, Piçarra JM (1991) Traços gerais da evolução tectono–estratigráfica da Zona de Ossa Morena, em Portugal: síntese crítica do estado actual dos conhecimentos, Comunicações dos Serviços Geológicos de Portugal 77, 3–26.

Oliveira JT, Relvas J, Pereira Z, Munhá J, Matos J, Barriga F, Rosa C (2013) O complexo vulcano-sedimentar de Toca da Moura—Cabrela (Zona de Ossa-Morena); evolução tectono-estratigráfica e mineralizações associadas, in Geologia de Portugal, vol. 1 (Dias R, Araújo A, Terrinha P, Kullberg J, eds), Escolar Editora, 621–645, Lisboa.

Paris F (1990) The Ordovician chitinozoan biozones of the Northern Gondwana Domain, Review of Palaeobotany and Palynology 66, 181–209.

Pereira E, Pereira DÍ, Rodrigues JF, Ribeiro A, Noronha F, Ferreira N, Sá CMd, Farinha Ramos J, Moreira A, Oliveira AF (2006a) Notícia Explicativa da Folha 2 da Carta Geológica de Portugal à Escala 1:200.000. 1 edn. Instituto Nacional de Engenharia, Tecnologia e Inovação, Lisboa.

Pereira Z, Oliveira V, Oliveira, JT (2006b) Palynostratigraphy of the Toca da Moura and Cabrela Complexes, Ossa Morena Zone, Portugal. Geodynamic implications, Review of Palaeobotany and Palynology 139, 227–240.

Pérez-Estaún A, Marcos A (1981) La Formación Agüeira en el sinclinorio de Vega de Espinareda: aproximación al modelo de sedimentación durante el Ordovícico superior en la zona Asturoccidental-leonesa (NW de España), Trabajos de Geología Oviedo 11, 135-145.

Pérez-Estaún A, Bastida F, Martínez Catalán JR, Gutiérrez-Marco JC, Marcos A, Pulgar JA (1990) West Asturian-Leonese Zone: Stratigraphy, in Pre-Mesozoic Geology of Iberia (Dallmeyer RD, Martínez García E, eds), Springer-Verlag, 92–102, Berlin-Heidelberg.

Pérez-Lorente F (1979) Geología de la Zona de Ossa-Morena al norte de Córdoba (Pozoblanco-Belmez-Villaviciosa de Córdoba), Tesis Doctorales de la Universidad de Granada 281, 1–340.

Piçarra JM (2000) Estudo estratigráfico do sector de Estremoz-Barrancos, Zona de Ossa Morena, Portugal, PhD Thesis Universidade de Évora, 2 vols, 95+173 pp.

Piçarra JM, Štorch P, Gutiérrez-Marco JC, Oliveira JT (1995) Characterization of the *Parakidograptus acuminatus* graptolite Biozone in the Silurian of the Barrancos region (Ossa Morena Zone, South Portugal), Comunicações do Instituto Geológico e Mineiro 81, 3–8.

Piçarra JM, Gutiérrez-Marco JC, Lenz AC, Robardet M (1998) Pridoli graptolites from the Iberian Peninsula: a review of previous data and new records, Canadian Journal of Earth Sciences 35, 65–75.

Piçarra JM, Le Menn J, Pereira Z, Gourvennec R, Oliveira JT, Robardet M (1999) Novos dados sobre o Devónico inferior de Barrancos (Zona de Ossa Morena, Portugal), Temas Geológico--Mineros ITGE 26, 628–631.

Piçarra JM, Gutiérrez-Marco JC, Sá AA, Meireles C, González-Clavijo E (2006) Silurian graptolite biostratigraphy of the Galicia-Tras-os-Montes Zone (Spain and Portugal). GFF/The Geological Society of Sweden Geologiske Föreningen/The Geological Society of Sweden, vol. 128, pp. 185–188.

Piçarra JM, Sarmiento GN, Gutiérrez-Marco JC (2014) Geochronological vs. Paleontological dating of the Estremoz Marbles (Ossa Morena Zone, Portugal)—new data and reappraisal, in Gondwana 15 North meets South, Abstracts Book (Pankhurst RJ, Castiñeiras P, Sánchez Martínez S, eds), Instituto Geológico y Minero de España, 140, Madrid.

Pillola GL, Piras S, Serpagli E (2008) Tremadoc–Lower Arenig? Anisograptid-Dichograptid fauna from the Cabitza Formation

(Lower Ordovician, SW Sardinia, Italy), Revue de Micropaléontologie 51, 167–181.

Quesada C (1990a) Precambrian terranes in the Iberian Variscan Foldbelt. In: Strachan RA, Taylor GK (Eds), Avalonian and Cadomian geology of the North Atlantic. Blackie, New York, 109–133.

Quesada C (1990b) Precambrian successions in SW Iberia: their relationship to "Cadomian" orogenic events. In: D'Lemos RS, Strachan RA, Topley CG (eds), The Cadomian Orogeny. Geol Soc, London, Sp Publ 51: 353–362.

Quesada C (1991) Geological constraints on the Paleozoic tectonic evolution of tectonostratigraphic terranes in the Iberian Massif, Tectonophysics 185, 225–245.

Quesada C (1997) Evolución geodinámica de la Zona Ossa Morena durante el ciclo Cadomiense. In: Araújo AA, Pereira MF (eds.), Estudo sobre a geología da zona de Ossa Morena (Maciço Ibérico). Livro homenagem Prof. Francisco Gonçalves, University of Évora, 205–230.

Quesada C (2006) The Ossa-Morena zone of the Iberian Massif: a tectonostratigraphic approach to its evolution. Z Deuts Gesell Geowiss 157: 585–595.

Rábano I (1989) Trilobites del Ordovícico Medio del sector meridional de la Zona centroibérica española. Parte 1, Boletín Geológico y Minero 100, 307–338.

Rigby JK, Gutiérrez-Marco JC, Robardet M, Piçarra JM (1997) First articulated Silurian sponges from the Iberian Peninsula, Spain and Portugal, Journal of Paleontology 71, 554–563.

Robardet M (2002) Alternative approach to the Variscan Belt in southwestern Europe: Preorogenic palaeobiogeographical constraints, in Variscan-Appalachian dynamics: The building of the late Paleozoic basement (Martínez Catalán JR, Hatcher RD Jr, Arenas R, Díaz-Gacía F, eds), Geological Society of America Special Paper 364, 1–15, Boulder, Colorado.

Robardet M, Gutiérrez-Marco JC (1990) Sedimentary and faunal domains in the Iberian Peninsula during Lower Paleozoic times, in Pre-Mesozoic Geology of Iberia (Dallmeyer RD, Martínez García E, eds), Springer-Verlag, 383–395, Berlin-Heidelberg.

Robardet M, Gutiérrez-Marco JC (2002) Silurian, Chapter 5 in The Geology of Spain (Gibbons W, Moreno T, eds), The Geological Society, 51–66, London.

Robardet M, Gutiérrez-Marco JC (2004) The Ordovician, Silurian and Devonian sedimentary rocks of the Ossa Morena Zone (SW Iberian Peninsula, Spain), Journal of Iberian Geology 30, 73–92.

Robardet M, Weyant M, Laveine JP, Racheboeuf P (1986) Le Carbonifère inférieur du synclinal du Cerrón del Hornillo (Province de Séville, Espagne). Révue de Paléobiologie 5/1:71–90.

Robardet M, Weyant M, Brice D, Racheboeuf P (1988) Dévonien supérieur et Carbonifère inférieur dans le nord de la province de Séville (Espagne).Âge et importance de la première phase hercynienne dans la zone d'Ossa-Morena. CR Acad Sci Paris, Série II, 307:1091–1095.

Rodríguez S (ed) (1992) Análisis Paleontológico y Sedimentológico de la cuenca carbonífera de Los Santos de Maimona (Badajoz), Coloquios de Paleontología 44, 1–232.

Rodríguez S, Fernández-Martínez E, Cózar P, Valenzuela-Ríos JI, Pardo Alonso MV (2010) Stratigraphic succession, facies and depositional environment of Emsian reefal carbonates in the Ossa-Morena Zone (SW Spain), Neues Jahrbuch für Geologie und Paläontologie Abhandlungen 257, 69–83.

Rodríguez González R, Medina Varea P, González Lodeiro F, Martín Parra LM, Martínez Poyatos D, Matas J (2007) Microflora y conodontos del Mississippiense en la Fm Gévora (núcleo del Sinforme La Codosera-Puebla de Obando, SO de la Zona Centroibérica), Revista de la Sociedad Geológica de España 20, 71–88.

Rodríguez Pevida LS, Mira López M, Ortega Gironés E (1990) Mapa Geológico de España, 1:50.000: Hinojosa del Duque 833, 15–33, Instituto Geológico y Minero de España, 1-56, Madrid.

Rubio-Ordóñez A, Valverde-Vaquero P, Corretgé LG, Cuesta-Fernández A, Gallastegui G, Fernández-González M, Gerdes A (2012) An Early Ordovician tonalitic-granodioritic belt along the Schistose-Greywacke Domain of the Central Iberian Zone (Iberian Massif, Variscan Belt), Geological Magazine 149, 927–939.

Sá AA, Meireles CA, Coke C, Gutiérrez-Marco JC (2005) Unidades litoestratigráficas do Ordovícico da região de Trás-os-Montes (Zona Centro-Ibérica, Portugal), Comunicações Geológicas 92, 31–73.

Sá AA, Meireles CA, Gutiérrez-Marco JC, Coke C (2006) A sucessão de Ordovícico Superior de Trás-os-Montes (Zona Centro-Ibérica, Portugal) e sua correlação com Valongo e Buçaco, in Resumos alargados VII Congresso Nacional de Geologia (Mirão J, Balbino A, coords) 2, 621–624, Évora.

Sá AA, Gutiérrez-Marco JC, Piçarra, JM, García-Bellido DC, Vaz N, Aceñolaza GF (2011) Ordovician vs. "Cambrian" ichnofossils in the Armorican Quartzite of central Portugal, IGME, Cuadernos del Museo Geominero 14, 483–492.

Sá AA, Gutiérrez-Marco JC, Meireles CA, García-Bellido D, Rábano I (2014) A revised correlation of Lower Ordovician sedimentary rocks in the Central Iberian Zone (Portugal and Spain), in Strati 2013, at the cutting edge of Stratigraphy (Rocha RB, Pais J, Kulberg C, Finney S, eds), Springer Geology Series, 441–446, New York.

San José MA de (2006) The kernel of the Iberian block, Zeitschrift der Deutschen Gesellschaft für Geowissenschaften 157, 529–550.

Santos JA, Apalategui O, Carvajal A et al. (2003) Mapa Geológico de España, escala 1:50000, sheet no. 751: Villar del Rey. Instituto Geológico y Minero de España.

Sanz-López J, Blanco-Ferrera S (2012) Revisión estratigráfica del Misisipiense al Pensilvaniense más bajo de la zona Cantábrica y la posición de los límites entre los pisos, Geo-Temas 13, 90 (CD annex to Geotemas 13, 163–166).

Sanz-López J, Blanco-Ferrera S, Sánchez de Posada LC (2013) Conodont chronostratigraphic resolution and *Declinognathodus* evolution close to the Mid-Carboniferous Boundary in the Barcaliente Formation type section (NW Spain), Lethaia 46, 438–453.

Sanz-López J, Cózar P, Blanco-Ferrera S (2018) Discovery of a Mississippian–early Bashkirian carbonate platform coeval with condensed cephalopod limestone sedimentation in NW Spain, Geological Journal 53:2532–2557.

Sarmiento GN, Piçarra JM, Rebelo JA, Robardet M, Gutiérrez-Marco JC, Štorch P, Rábano I (1999) Le Silurien du synclinorium de Moncorvo (NE du Portugal): biostratigraphie et importance paléogéographique. Geobios 32:749–767.

Saupé F (1990) The geology of the Almadén mercury deposit. Econ Geol 85: 482–510.

Schemm-Gregory M, Piçarra J (2013) *Astraelenia saomamedensis* n. sp.—a new gigantic rhynchonellid species and its palaeobiogeographical implications for the Portalegre syncline (Central Portugal), Rivista Italiana di Paleontologia e Stratigrafia 119, 247–256.

Schermerhorn LJG, Kotsch S (1984) First occurrence of lawsonite in Portugal and tectonic implications. Comunicações do Instituto Geológico e Mineiro 70 (1):23–29.

Simancas JF, Martínez Poyatos DJ, Expósito I, Azor A, González Lodeiro F (2001) The structure of a major suture zone in the SW Iberian Massif: the Ossa Morena/Central Iberian contact. Tectonophysics 332:295–308.

Simancas JF, Carbonell R, González Lodeiro F, Pérez-Estaún A, Juhlin C, Ayarza P, Kashubin A, Azor A, Martínez Poyatos D, Almodóvar GR, Pascual E, Sáez R, Expósito I (2003) The crustal structure of the transpressionalVariscan Orogen of SW Iberia:

The IBERSEIS deep seismic reflection profile. Tectonics 22(6), 1062. https://doi.org/10.1029/2002tc001479.

Simancas JF, Tahiri A, Azor A, González Lodeiro F, Martínez Poyatos D, El Hadi H (2005) The tectonic frame of the Variscan-Alleghanian Orogen in Southern Europe and Northern Africa. Tectonophysics 398:181–198. https://doi.org/10.1016/j.tecto.2005.02.006.

Simancas JF, Carbonell R, González Lodeiro F, Pérez Estaún A, Juhlin C, Ayarza P, Kashubin A, Azor A, Martínez Poyatos D, Sáez R, Almodóvar GR, Pascual E, Flecha I, Martí D (2006) Transpressional collision tectonics and mantle plume dynamics: the Variscides of southwestern Iberia. In: Gee DG, Stephenson RA (eds), European Lithosphere Dynamics. Geological Society, London, Memoirs 32:345–354.

Soldevila Bartolí J (1992) La sucesión paleozoica en el sinforme de la Sierra de San Pedro (provincias de Cáceres y Badajoz, SO de España), Estudios Geológicos 48, 363–379.

Stampfli GM, von Raumer JF, Borel GD (2002) Paleozoic evolution of pre-Variscan terranes: from Gondwana to the Variscan collision, in Variscan-Appalachian dynamics: the building of the Late Paleozoic basement (Martínez Catalán JR, Hatcher RD, Arenas R, Díaz García F, eds), Geological Society of America Special Paper 364, 263–280.

Talavera C, Montero P, Martínez Poyatos D, Williams IS (2012) Ediacaran to Lower Ordovician age for rocks adscribed to the Schist-Graywacke Complex (Iberian Massif, Spain): Evidence from detrital zircon SHRIMP U-Pb geochronology, Gondwana Research 22, 928–942.

Talavera C, Montero P, Bea F, González Lodeiro F, Whitehouse M (2013) U-Pb Zircon geochronology of the Cambro-Ordovician metagranites and metavolcanic rocks of central and NW Iberia, International Journal of Earth Sciences 102, 1–23.

Teixeira RJS, Coke C, Gomes MEP, Corfu F, Dias R (2013) ID-TIMS U-Pb ages of Tremadocian-Floian ash fall tuff beds from Marão and Eucísia areas, Northern Portugal. In: William Smith Meeting 2013, London. Geological Society of London, pp 152–154.

Torsvik TH, Cocks LRM (2013) New global palaeogeographical reconstructions for the Early Palaeozoic and their generation, in Early Palaeozoic Biogeography and Palaeogeography (Harper DAT, Servais T, eds), Geological Society Memoirs 38, 5–24, London.

Torsvik TH, Cocks LRM (2017) Earth History and Palaeogeography, Cambridge University Press, 317 pp, Cambridge.

Toyos JM, Aramburu C (2014) El Ordovícico en el área de Los Barrios de Luna, Cordillera Cantábrica (NW de España), Trabajos de Geología 34, 61–96.

Vaz N (2010) Palinoestratigrafia da sequencia Ordovicico-Silúrica do Sinclinal Amêndoa-Mação, Ph.D. Thesis Universidade de trás-os--Montes e Alto Douro, Vila Real, 159 pp.

Videt B, Paris F, Rubino JL, Boumendjel K, Dabard MP, Loi A, Ghienne JF, Marante A, Gorini A (2010) Biostratigraphical calibration of third order Ordovician sequences on the northern Gondwana platform, Palaeogeography, Palaeoclimatology, Palaeoecology 296, 359–375.

Villaseca C, Merino Martínez E, Orejana D, Andersen T, Belousova E (2016) Zircon Hf signatures from granitic orthogneisses of the Spanish Central System: Significance and sources of the Cambro-Ordovician magmatism in the Iberian Variscan Belt. Gondwana Research 34, 60–83.

Wolf R (1980) The lower and upper boundary of the Ordovician System of some solected regions (Celtiberia, Eastern Sierra Morena) in Spain. Part I: The Lower Ordovician sequence of Celtiberia, Neues Jahrbuch für Geologie und Paläontologie Abhandlungen 160, 118–137.

Young TP (1989) Eustatically controlled ooidal ironstone deposition: facies relationships of the Ordovician open-shelf ironstones of Western Europe, in Phanerozoic Ironstones (Young TP, Taylor WEG, eds), Geological Society Special Publication 46, 51–63.

Young TP (1992) Ooidal ironstones from Ordovician Gondwana: a review, Palaeogeography, Palaeoclimatology, Palaeoecology 99, 321–347.

4 Variscan Suture Zone and Suspect Terranes in the NW Iberian Massif: Allochthonous Complexes of the Galicia-Trás os Montes Zone (NW Iberia)

J. R. Martínez Catalán, J. Gómez Barreiro, Í. Dias da Silva, M. Chichorro, A. López-Carmona, P. Castiñeiras, J. Abati, P. Andonaegui, J. Fernández-Suárez, P. González Cuadra, and J. M. Benítez-Pérez

Abstract

The NW Iberian Allochthon represents the suture of a peri-Gondwanan, Paleozoic ocean formed around the Cambro-Ordovician boundary but having registered renewed spreading during the Lower Devonian. The ocean separated a piece of continental crust detached from NW Gondwana from the northern and northwestern parts of present Africa. The separation was a consequence of slab roll-back of a wide, subducting oceanic lithosphere around 500 Ma. Early Variscan plate convergence closed the oceanic domain involving three subduction events between 400–365 Ma, and building an accretionary prism formed by the detached continental fragment, the new oceanic lithosphere and the external margin of Gondwana. The change of regime from subductive to collisional occurred at the Devonian-Carboniferous transition and was responsible for the emplacement of the Allochthon above the Central Iberian Autochthon.

4.1 Introduction

J. R. Martínez Catalán, J. Gómez Barreiro

The Allochthon of NW Iberia is the remnant of a huge nappe stack preserved as klippen in the core of late Variscan synforms and known as the **allochthonous complexes**. They consists of units mostly of peri-Gondwanan derivation, which receive local names, but can be correlated among the five existing allochthonous complexes, namely **Cabo Ortegal**, **Órdenes**, **Malpica-Tui**, **Bragança** and **Morais** (Figs. 4.1 and 4.2). The allochthonous units are classified in

Coordinator: J. R. Martínez Catalán.

J. R. Martínez Catalán (✉) · J. Gómez Barreiro · A.López-Carmona · J. M. Benítez-Pérez
Department of Geology, University of Salamanca, 37008 Salamanca, Spain
e-mail: jrmc@usal.es

J. Gómez Barreiro
e-mail: jugb@usal.es

A. López-Carmona
e-mail: alioli@usal.es

J. M. Benítez-Pérez
e-mail: jmbp@usal.es

Í. Dias da Silva
Faculty of Science, Instituto Dom Luiz, University of Lisbon, Campo Grande, Edifício C8, Piso 3, 1749-016 Lisbon, Portugal
e-mail: ipicaparopo@gmail.com

M. Chichorro
Department of Earth Sciences, Faculty of Science and Technology, New University of Lisbon, Campus de Caparica, Quinta da Torre, 2829-516 Caparica, Portugal
e-mail: ma.chichorro@fct.unl.pt

P. Castiñeiras · J. Abati · P. Andonaegui · J. Fernández-Suárez
Departamento de Petrología y Geoquímica, Instituto de Geociencias (UCM, CSIC), Universidad Complutense, 28040 Madrid, Spain
e-mail: castigar@ucm.es

J. Abati
e-mail: abati@geo.ucm.es

P. Andonaegui
e-mail: andonaeg@geo.ucm.es

J. Fernández-Suárez
e-mail: jfsuarez@geo.ucm.es

P. González Cuadra
Instituto Geológico y Minero de España, Ríos Rosas 23, 28003 Madrid, Spain
e-mail: pgc@usal.es

C. Quesada and J. T. Oliveira (eds.), *The Geology of Iberia: A Geodynamic Approach*, Regional Geology Reviews,
https://doi.org/10.1007/978-3-030-10519-8_4

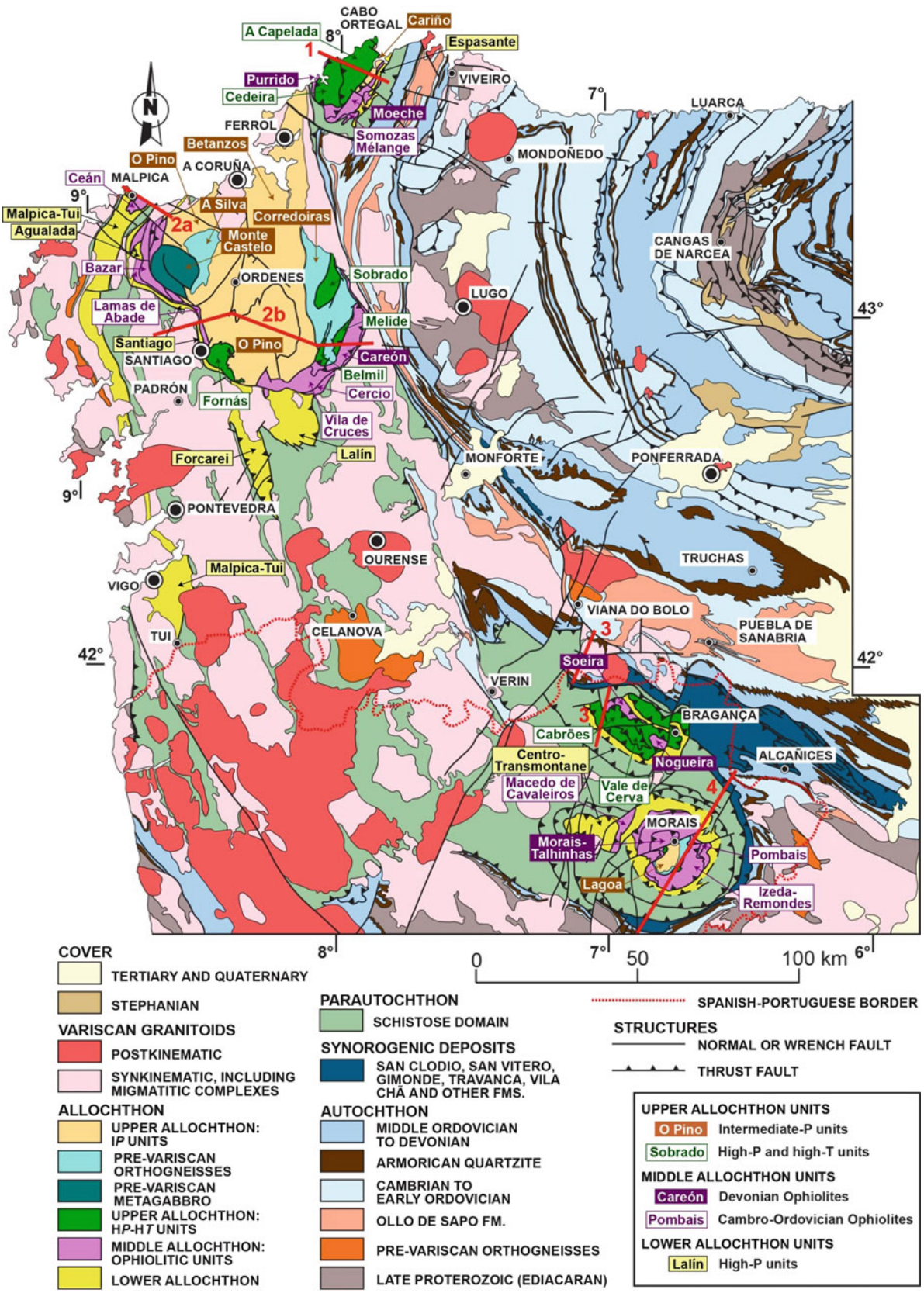

Fig. 4.1 Geological map of NW Iberia showing the allochthonous complexes and their units. The location of cross sections in Fig. 4.2 is indicated. Modified from Martínez Catalán et al. (2007)

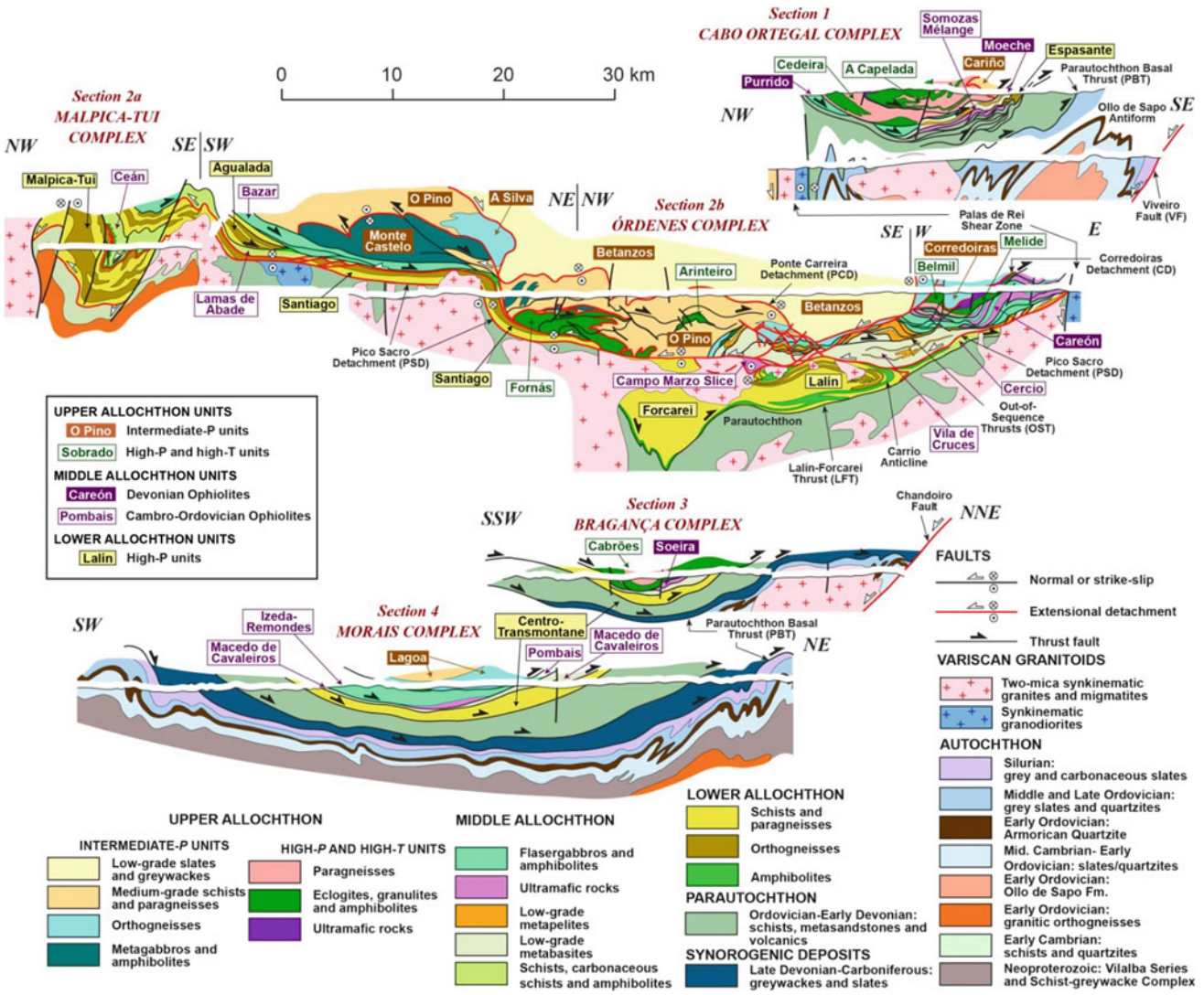

Fig. 4.2 Geological sections across central and eastern Galicia and northern Portugal showing the structure of the allochthonous complexes. The location of cross sections is indicated in Fig. 4.1. Modified from Martínez Catalán et al. (2007) and references therein

three groups based on their structural position in the nappe pile and their origin:

- The **Upper Allochthon** is a piece of the northern margin of Gondwana detached and drifted away during the Cambro-Ordovician opening of the Rheic oceanic realm.
- The **Middle Allochthon** is formed by lithospheric pieces of oceanic affinity or oceanic supracrustal sequences. They represent the suture of one of the oceans that formed part of the Rheic oceanic realm, and are often referred to as the ophiolitic units.
- The **Lower Allochthon** derives from distal parts of the Gondwanan continental margin.

In addition, an imbricate thrust sheet several kilometres thick separates the Allochthon from the Iberian Autochthon. It is known as the **Parautochthon** (Ribeiro et al. 1990a, b) or Schistose Domain in Galicia (NW Spain), and consists of Paleozoic metasedimentary and volcanic rocks. The Parautochthon has stratigraphic and igneous affinities with the Iberian autochthon of the Central Iberian Zone (Farias et al. 1987; Valverde-Vaquero et al. 2005; Dias da Silva et al. 2014), and no ophiolites occur within it or at its boundary with the Iberian autochthon. For these reasons, it is viewed as derived from a relatively distal part of the Gondwanan continental margin. The allochthonous complexes together with the Parautochthon form the **Galicia-Trás-os-Montes Zone** (GTMZ; Farias et al. 1987).

The nappe pile of the Allochthon is thought to have been generated in an early Variscan accretionary wedge, and its history is registered by the preserved tectonic fabrics, metamorphic associations and ages. Accretion took place

following a piggy back mode of thrust propagation, which implies that every new thrust fault carries the previously formed thrust sheets above. A higher position in the nappe stack means paleogeographically farther from the Autochthon, which was the later to be affected by thrusting. This propagation mode can be used to attempt approximate paleogeographic reconstructions. Accordingly, the Upper Allochthon is considered the more external and far-travelled of the terranes involved, while the Lower Allochthon would be the closer to Gondwana, and probably kept forming part of its northern margin.

During the Variscan collision, recumbent folding, renewed thrusting and extensional faulting affected the Allochthon and involved also the Parautochthon and Autochthon. As a result of faulting, the units of the three groups forming the Allochthon became thinned and dismembered, but in general, preserved the stacking order acquired at the accretionary wedge stage (Martínez Catalán et al. 1996, 1997; Gómez Barreiro et al. 2007).

In NW Iberia, several allochthonous units bear the imprint of closure of an oceanic realm. In some cases, it is the geochemical composition of igneous rocks, pointing to a supra-subduction zone setting. In others, it is the P-T conditions under which their oldest foliations developed. According to the latter, three subduction events have been recognized in relation with early Variscan convergence:

- The first affected some units of the Upper Allochthon, and probably reflect its accretion to a northern continental mass. It is dated at the Early-Middle Devonian transition (400–390 Ma).
- During the second, roughly coeval (ca. 395 Ma), an intraoceanic subduction zone created young Devonian oceanic lithosphere of the Middle Allochthon, and subsequently imbricated and accreted it during the following 10 Ma.
- The third subduction affected the old, Cambro-Ordovician ophiolitic units of the Middle Allochthon, its oceanic supracrustal units and the continental units of the Lower Allochthon. It is dated at 375–365 Ma and reflects oceanic closure and continental subduction.

Figure 4.3 shows the metamorphic evolution of representative units of the three allochthons. Units of the three groups, Upper, Middle and Lower Allochthon depict the subductive paths characterized by pressurization followed by nearly isothermal decompression (green, purple and yellow arrows respectively). Figure 4.4 tries to explain the different observations with a plate-tectonics model illustrating the Variscan Wilson cycle from opening to closure of the Rheic Ocean. It is probably an oversimplification of what really happened, but helps to understand the magmatic, metamorphic and structural history deduced from the different

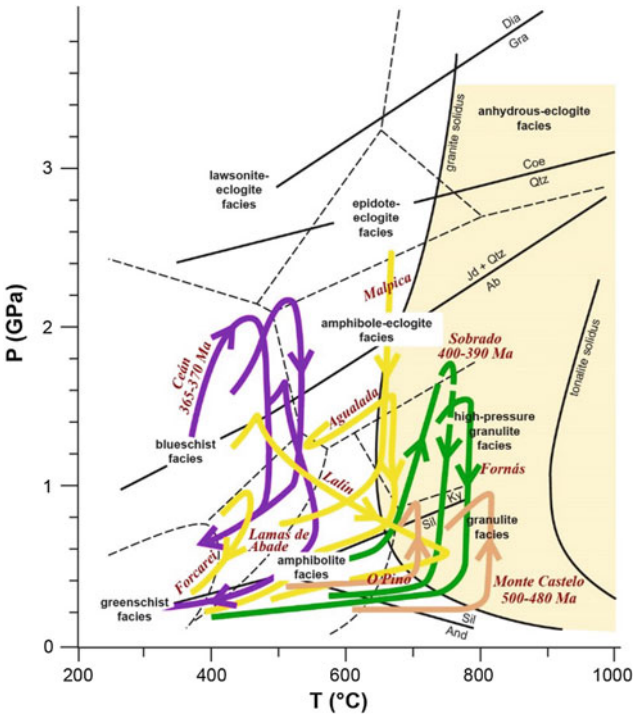

Fig. 4.3 Samples of P-T paths followed by the allochthonous units of Galicia. The Lower Allochthon (yellow arrows) generally records monocyclic P-T paths with pressurization followed by nearly isothermal decompression, but the Lalín Unit registered heating from an overlying hot source, probably the mantle wedge above the subduction zone. Some units of the Middle Allochthon (Ceán, Lamas de Abade, Vila de Cruces; purple arrows), recorded also high-P metamorphism. The Upper Allocthon recorded pressurization after strong heating in the intermediate-P units (Monte Castelo, O Pino; brown arrows), and strong pressurization along a subductive-type path, followed by nearly isothermal decompression, in the high-P and high-T units (Sobrado, Fornás; green arrows). After Ballèvre et al. (2014) and references therein

Allochthons and the Autochthon. Figures 4.1, 4.2, 4.3 and 4.4 will be referred to in the following sections, where the successive steps of the model of Fig. 4.4 will be explained.

4.2 The Lower Allochthon: The Stretched Continental Margin of Northern Gondwana

Í. Dias da Silva, M. Chichorro, J. Gómez Barreiro, A. López-Carmona

The Lower Allochthon (LA, Figs. 4.1 and 4.2, Table 4.1, Ballèvre et al. 2014) is exposed below the Middle and Upper Allochthons of the Galicia-Trás-os-Montes Zone (GTMZ) and tectonically overlies the lower grade domain known as Parautochthon or Schistose Domain (e.g. Ribeiro et al. 1990a, b; Farias et al. 1987). The LA records early Variscan

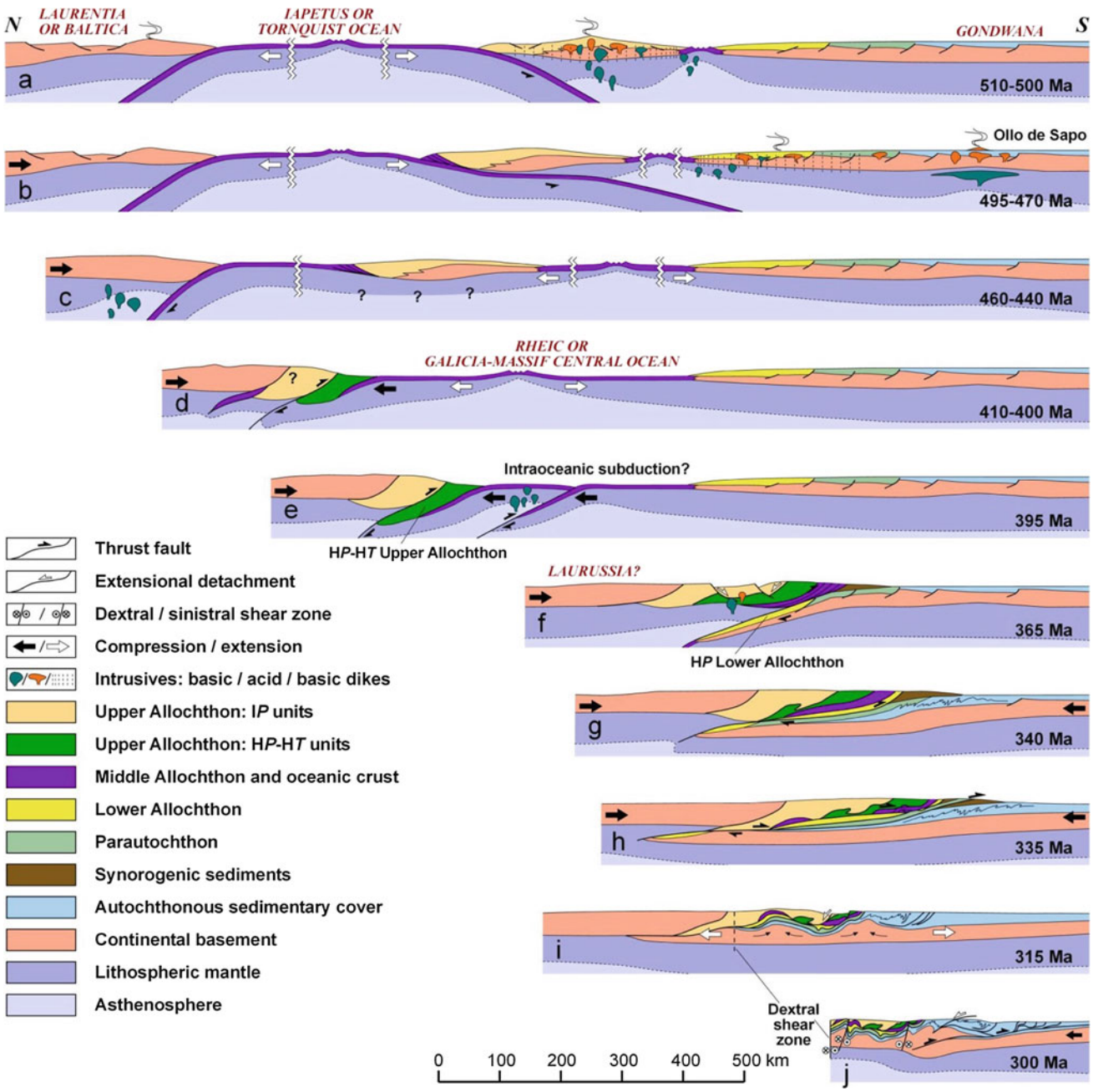

Fig. 4.4 Suggested stages in the tectonic evolution of NW Iberia, based on Martínez Catalán et al. (2009); **a** formation of a continental arc during the late Cambrian to Early Ordovician and its individualization of a peri-Gondwanan terrane by slab rollback; **b** possible flat subduction at the leading edge of the arc; **c** separation of the continental arc pulled by subduction to the N of old oceanic lithosphere and opening of an intervening ocean; **d** building of an accretionary prism by underthrusting and imbrication of the peri-Gondwanan terrane, whose trailing edge reached eclogite-facies conditions; **e** progressive closure of the ocean by intraoceanic subduction and formation of supra-subduction oceanic lithosphere; **f** subduction of outer edge of Gondwana; **g** locking of subduction due to buoyancy of continental crust and thrusting of Allochthon over the Parautochthon; **h** out-of-sequence thrusting of the Middle and Upper Allochthons over the Lower Allochthon, and thrusting the Parautochthon, with imbrication of the synorogenic deposits; **i** thrusting of more external parts of the belt, and collapse of the thickened crust, with formation of extensional detachments and gneiss domes; **j** late upright folding, strike-slip faulting, and thin-skinned tectonics in the foreland with underthrusting of its basement

high-pressure (HP) metamorphism, interpreted as the product of continental subduction at 370–365 Ma (Rodríguez et al. 2003; Abati et al. 2010; López-Carmona et al. 2014). It represents the outermost N-Gondwana continental margin, hyperextended during the opening of the Rheic Ocean and the drifting of the peri-gondwanan Upper Allochthon Cambro-Ordovician magmatic arc (e.g. Martínez Catalán et al. 2009).

Table 4.1 Lower Allochthon units of the NW Iberian Massif

		NW Iberian Massif			
Allochthonous complexes		Malpica-Tui	Órdenes	Cabo Ortegal	Bragança and Morais
Lower Allochthon	High-P units	Malpica-Tui	Agualada, Santiago, Lalín, Forcarei	Espasante	Lower Allochthonous Thrust Complex, Macedo de Cavaleiros Symplex[a]
	Temperature	High to middle-temperature			Low-temperature
	Ages	Neoproterozoic—Lower Ordovician			Ordovician-Devonian

[a]With transitional character, can be incorporated in the Middle Allochthon, as proposed in Sect. 4.3.1

The LA is currently exposed in all the allochthonous complexes of the GTMZ (Table 4.1) and, according to the metamorphic peak, can be grouped in high- to middle-temperature (HT-MT) units and low-temperature (LT) units. The HT-MT units are represented by the Malpica-Tui unit in the Malpica-Tui Complex, the Agualada, Santiago, Lalín and Forcarei units in the Órdenes Complex, and the Espasante unit, in the Cabo Ortegal Complex. The LT units surround the Morais and Bragança complexes in NE Portugal and are represented by the Centro-Transmontano Group (or Lower Allochthonous Thrust Complex), which includes the Macedo de Cavaleiros Formation (Pereira et al. 2006) and the Culminating Green-schists and Quartz-phyllites Formation (Ribeiro 1974; Ribeiro et al. 2013). Stratigraphic ages based on detrital zircon and igneous zircon geochronology in the HT units, point to a Neoproterozoic/Early Cambrian—Lower Ordovician age for both HT and LT groups (Díez Fernández et al. 2010). However, an Ordovician-Devonian age was proposed for the LT group without chronological constrains (Ribeiro et al. 2013).

4.2.1 The Lower Allochthon in Galicia

The Lower Allochthon can be separated in two tectonically juxtaposed sequences with different affinity, metamorphism and tectonostratigraphy "the lower sequence" and the "upper sequence" (Díez Fernández et al. 2010; López-Carmona et al. 2010). The upper HT-MT sequence (including the Ceán Unit; López-Carmona et al. 2010, 2013) is represented by a monotonous pile of glaucophane-chloritoid-bearing metapelites and mafic rocks with pseudomorphs after lawsonite with minor graphitic schists, metacherts, calc-silicate lenses, greywackes and quartzites (López-Carmona et al. 2013, 2014), and has been recently included in the Middle Allochthon as an "ocean-continent transitional domain" (Ballèvre et al. 2014).

The lower sequence occurs at the base of the nappe stack and comprises a thick metasedimentary sequence intruded by late Cambrian-Early Ordovician igneous rocks (e.g. Díez Fernández et al. 2010). The metasedimentary rocks include immature sandstones (greywackes) pelites, graphitic shales, impure carbonates, quartzites and sandstones, and in some instances, Bouma-type sequences can be recognized. This thick pile of sediments is unconformably overlaid by the Portela quartzites. The rocks of the lower sequence were transformed into paragneisses, schists, phyllites, carbonaceous schists, calc-silicate rocks, and meta-quartzites of the high-to mid-temperature group. One characteristic feature is the appearance of albite, oligoclase and garnet porphyroblasts.

The igneous rocks are (i) mafic dikes (alkali basalts; Marquínez García 1984; Rodríguez Aller 2005); (ii) a calc-alkaline suite formed by high-K granites, granodiorites and tonalites and (iii) an alkaline to peralkaline suite including metaluminous alkali-feldspar quartz-syenites and granites, peraluminous alkali-feldspar granites, and peralkaline granites (Rodríguez Aller 2005). During the Variscan Orogeny both magmatic series were metamorphosed into the eclogite facies conditions (Rodríguez Aller 2005; López-Carmona et al. 2014).

Knowing the west-directed component of subduction and the characteristics of each allochthonous unit of the GTMZ, everything suggests that the Middle Allochthon occupied an oceanward position compared to the Lower Allochthon before the Variscan collision (Martínez Catalán et al. 1996, 2009; Díez Fernández et al. 2012a, b). Thus, the Lower Allochthon is interpreted as a slice of a continental crust, whereas the Middle Allochthon is interpreted to represent a volcano-sedimentary sequence viewed as a more distal part of the same continental margin transitional to an oceanic domain (cf. Rodríguez et al. 2003; Díez Fernández et al. 2010; López-Carmona et al. 2010). The Lower Allochthon represents the outermost sections of the north Gondwana continental margin subducted beneath Laurussia during late Devonian (Martínez Catalán et al. 1996, 2009; Rodríguez et al. 2003; Abati et al. 2010; López-Carmona et al. 2014).

The youngest zircon age population for the greywackes of the lower sequence is 566 Ma, similar to the youngest population found in the Portela quartzites (557 Ma; Díez Fernández et al. 2010). The maximum depositional ages and the Precambrian zircon age spectra, especially the relative low proportion of Mesoproterozoic zircons in both assemblages, suggest proximity to the West African craton, with a

paleogeographic location estimated in the central part of the northern Gondwana margin (Díez Fernández et al. 2010). The turbiditic, then regressive character of the LA sequence, together with sedimentary geochemical data (Fuenlabrada et al. 2012), point to a geodynamic setting in a back-arc or retro-arc environment, close to the stretched continental margin and at some distance from a magmatic (Cadomian?) arc. The geochemistry also reflects the transition to a passive margin setting, reflecting the geodynamic changes in the N-Gondwana margin from back-arc to rifting/drifting during the late Ediacaran–middle Cambrian periods (Fuenlabrada et al. 2012). On the other hand, the maximum depositional ages of detrital zircons are quite similar to those observed in late Neoproterozoic and Early Cambrian sediments of Ossa Morena Zone (OMZ) and the zircon age spectra strongly supports the OMZ resemblance (Pereira et al. 2012). Therefore, the greywackes and the Portela quartzites may represent the transition from sin-orogenic Avalonian-Cadomian active margin sedimentation to the initial syn-rift sediments, apparently reflecting what is also observed in OMZ (Fuenlabrada et al. 2012; Díez Fernández et al. 2017).

The age of the metassediments is also constrained by the late Cambrian granitoids (~495 Ma) which intruded them, so that they must have been deposited between the late Ediacaran and the Furongian. The igneous intrusions include granitic orthogneisses and amphibolites which are highly flattened, folded and disposed parallel to the Variscan tectonic banding, thus marking the regional deformation associated to the HP-HT subductive event (Díez Fernández et al. 2011, 2012b).

The large variety of rift-related granitoids defined two compositional suites (Floor 1966, Rodríguez Aller 2005; Montero et al. 2009; Abati et al. 2010; Díez Fernández et al. 2012a): (i) an older and dominant calc-alkaline bimodal meta to peraluminous suite, represented by tonalites, granodiorites and granites (ca. 495–500 Ma), which includes the Agualada felsic gneisses (ca. 493 Ma), and (ii) a younger suite of alkaline and peralkaline granitoids (ca. 475–470 Ma for Malpica-Tui and ca. 482 Ma for the Galiñeiro peralkaline complex). A dike swarm of mafic rocks intruded mainly the calc-alkaline granitic series. Most of them are tholeiitic, but some are alkali basalts, probably related with the formation of the A-type granitoids with alkaline and peralkaline signatures (Montero et al. 2009 and references therein) and reflect mantle contribution to the LA magmatism possibly triggered by back-arc extension which ultimately led to the formation of the Rheic Ocean (Fig. 4.4, Díez Fernández et al. 2012a). Contrary to what is observed in the OMZ, only the late rift-related magmatism is noticed in the LA, being roughly coeval with the Cambro-Ordovician suite of CIZ and with the stage of the peralkaline magmatism observed in the NW of OMZ.

Summing up, the mainly metagreywacke and metapelite "lower sequence" (albite-bearing paragneisses and schists) of the LA represents an Ediacaran sedimentary pile in extension during the Cambrian-Ordovician transition while the Rheic oceanic lithosphere was being created. Considering the geochemical and tectonostratigraphic similarities between the LA in northwest Iberia and the southwestern OMZ (i.e. Évora Massif; Díez Fernández et al. 2017) it cannot be ruled out that they represent the same sedimentary basin and shared the same stratigraphic evolution in the outermost shelf of N-Gondwana. This margin was later dismembered due to Devonian subduction and exhumation, and to Carboniferous transcurrence during the Variscan orogeny. However, the dissimilar magmatic evolution and the age differences of magmatism suggest that they may represent different crustal portions positioned in slightly different paleogeographic contexts, as is also suggested by differences in εNd T_{DM} model ages (Fuenlabrada et al. 2012; Díez Fernández et al. 2017).

4.2.2 Lower Allochthon in NE Portugal

Recent investigations around the allochthonous complexes of NE Portugal have revealed that the magnitude of the originally proposed extension of the Lower Allochthon (LA; Lower Allochthonous Thrust Complex, according to Ribeiro et al. 1990a, b; Centro-Transmontano Group after Ribeiro et al. 2013) is much lower than expected, being most of it presently incorporated in the lower grade rocks of the Upper Parautochthon (Pereira et al. 2006; Rodrigues et al. 2013; Dias da Silva et al. 2014). In this way, we only will consider as part of the LA the units that are located between the Upper Parautochthon (structurally below) and the Middle Allochthon ophiolitic units (above) in Bragança and Morais complexes (Figs. 4.1 and 4.2; González-Clavijo et al. 2016).

The LA lithostratigraphic sequence in NE Portugal includes a mainly pelithic metasedimentary sequence showing an assorted suite of igneous rocks (sub-plutonic and volcanic; Ribeiro 1986, 1991; Ribeiro et al. 2013). According to Ribeiro et al. (2013 and references therein) the ages of the LA in Portugal could range from the Lower Ordovician to the Devonian (without further precision or chronological data), based in stratigraphic resemblances with sequences of other Variscan domains, such as in the OMZ (Ribeiro et al. 1990a, b). This age range does not make possible a direct correlation with the LA sequence of the Galician allochthonous complexes. However, the lack of age constraints of the LA in Portugal allows us to view it as representing a Neoproterozoic-Ordovician stratigraphic sequence, thus facilitating regional correlations along northwest Iberia and north-central Europe (e.g. Ballèvre et al. 2014).

The LA of NE Portugal shows relicts of blueschist facies metamorphism related to Variscan continental subduction, which were retrogressed into amphibolite (to the W of Morais) and greenschist (to the E) facies metamorphism during adiabatic exhumation associated to Variscan extensional detachments and out-of-sequence thrusts. Only one age of ~330 Ma was obtained for the HP-LT metamorphism in the LA of Morais (Gil Ibarguchi and Dallmeyer 1991), but it has been considered not reliable due to regional geological constrains (e.g. Navarro et al. 2003). Consequently, it is assumed a 375–365 Ma age for the HP metamorphism in the LA of NE-Portugal, as supported by isotopic dating in Galicia (Rodríguez et al. 2003; Abati et al. 2010).

As in Galicia, albite-oligoclase and garnet bearing schists are common in the LA as well as schists presenting glaucophane, crossite and/or lawsonite porphyroblasts (Schermerhorn and Kotsch 1984; Munhá et al. 1984; Ribeiro 1987, 1991).

Two LA laterally equivalent units are distinguished in NE Portugal:

- Surrounding the Morais and Bragança allochthonous complexes the **Culminating greenschist and quartz-phyllite Formation** (Ribeiro 1974; Ribeiro et al. 2013), also known as **Macedo de Cavaleiros Formation** in Pereira et al. (2006), is composed, from bottom-to-top, by dark-grey to dark-purple phyllites with black slates and siltite beds, greenish tuffs, felsic and mafic volcanic rocks, laminated phyllites and quartz-phyllites with immature quartzite lenses. This sequence is locally cut by felsic and metagabbro dykes. The mafic volcanic rocks show metamorphic albite-oligoclase, green amphibole (actinolite-tremolite), epidote, zoisite, clinozoisite and chlorite. Other minerals such as iron and titanium oxides, carbonates, titanite, muscovite, biotite, (hidro)grossular and apatite occur as accessory minerals (Ribeiro et al. 2013).
- To the W of the Morais Complex, the **Macedo de Cavaleiros Simplex** (Ribeiro 1974, 1986, 1991; Ribeiro et al. 1990a, b, 2013) comprehends two volcano-sedimentary sequences. The tectonically lower unit is the **Carrapatas Group**, which includes alkaline volcanics and peralkaline sub-volcanic rocks. It is overlaid by the more tholeiitic rocks of the **Macedo Group**.

The **Carrapatas Group**, is composed by four formations (Ribeiro 1987). At the base, the **Alto de Sequeira Formation** is formed by albite-bearing phyllites and quartz (+feldspathic) phyllites with minor volcanoclastic contribution. The stratigraphically overlaying **Facho Formation** includes massive peralkaline rhyolites at the base, gradually passing to banded rhyolites and basalt beds which occur sporadically at the top of this unit. Minor sedimentary contribution is associated to the felsic tuffs (i.e. banded rhyolites). The rhyolites of the Facho Formation present riebeckite, Mg-riebeckite and aegirine-augite, attesting their paralkaline character, also confirmed by their whole-rock geochemical signatures (Ribeiro 1987; Ribeiro et al. 2013). The local presence of crossite and garnet (andradite) are indicative of the HP event of Variscan metamorphism. This unit is overlain by the **Carrapatas Formation** which comprises mainly metabasaltic rocks (greenschists), with two metric-thick layers of peralkaline rhyolites at the base and top, scarce intermediate (andesitic) volcanics, purple chert and pelite beds. The uppermost unit of the Carrapatas Group is the **Alto de Casais Formation** being composed by felsic tuffs, with centimetric-thick pelitic layers towards the top and associated cherts. Geochemically, the rocks from the Carrapatas and the Facho formations match those from the Peso Formation of the Upper Parautochthon (Díez-Montes et al. 2015; Dias da Silva et al. 2016, 2017), pointing to the same geodynamic setting and possibly a Middle-Upper Ordovician age.

The **Macedo Group** presents at its base the **Madorra Formation** and the intrusive igneous rocks of the **Valbenfeito Complex**. The first is composed by greenish-grey to purple quartz and feldspar-rich phyllites. There are some beds of greenschists (basaltic rocks) and dark-purple cherts. Garnet porphyroblasts with andradite, grossular and almandine components have been described (Ribeiro 1987; Ribeiro et al. 2013). The **Valbenfeito Complex**, intrusive on the quartz-feldspathic rocks, is mainly composed by blastomylonitic gabbro dykes and thin and laterally discontinuous rhyolitic to andesitic dykes, where albite is the main component (Ribeiro 1987). These units are overlain by the **Macedo de Cavaleiros Formation** (*s.s.* after Ribeiro 1987 and Ribeiro et al. 2013), which is a monotonous unit, composed by amphibolites and greenschists (metabasalts and basaltic tuffs) with local intercalations of phyllites and quartz-feldspathic rocks like those of the Madorra Fm.

The lithostratigraphy of the Macedo de Cavaleiros Simplex shows a transitional character between the typical, mainly sedimentary LA sequence and the ophiolites of the Middle Allochthon (MA), as pointed by its geochemical patterns (Ribeiro 1987). The evolution from alkaline-transitional to tholeiitic can be viewed as the breakup of a highly stretched continental margin to form a true rift. In this way, the attribution to a specific unit (LA or MA) depends on the assumed criteria—hyperextended continental crust versus continental rift. Therefore, if a late Cambrian-Upper Ordovician age is assumed for the Macedo de Cavaleiros Simplex, it is correct to consider it as an equivalent to the "upper sequence" (or Ceán unit) in Malpica-Tui Complex (Díez Fernández et al. 2010; López-Carmona et al. 2014) and contemplate it as a Cambro-Ordovician ophiolitic unit of the MA, as proposed in Figs. 4.1 and 4.2).

4.3 Middle Allochthon: Paleozoic Ophiolites and Oceanic Terranes

J. Gómez Barreiro, J. R. Martínez Catalán

The ophiolitic units consist of dismembered slices of oceanic affinity that locally display high-pressure metamorphism. These include a diverse array of well-characterized oceanic complexes, with protolith ages clustering around the Cambro-Ordovician boundary and in the Lower Devonian. Some are true ophiolitic units, whereas others are interpreted as transitional to thinned continental crust. When Cambro-Ordovician and Devonian units occur together, the older occupy a lower structural position implying that they were located closer to the continental margin represented by the Autochthon (Martínez Catalán et al. 1996; Pin et al. 2006). The ophiolitic units receive local names, but can be correlated among the five existing allochthonous complexes of Cabo Ortegal, Órdenes, Malpica-Tui, Bragança and Morais (Table 4.2 and Figs. 4.1 and 4.2). They can be classified in two groups considering their relative structural position as Lower and Upper ophiolitic units (Arenas et al. 2007b; Arenas and Sánchez Martínez 2015). Here we favour a classification based on the protolith age, which results in a similar group of units but overcomes structural ambiguities when correlated to similar ophiolites abroad. Two groups of units are defined accordingly: Cambro-Ordovician and Early Devonian (Table 4.2).

4.3.1 Cambro-Ordovician Ophiolites

Among the Cambro-Ordovician units, three subgroups can be distinguished (Figs. 4.1 and 4.2):

- The Vila de Cruces and Bazar units, in the SE and W of the Órdenes Complex respectively, have a clear oceanic affinity. In northern Portugal, an equivalent of these units is probably represented by the Izeda-Remondes Unit of the Morais Complex.
- The Ceán, Cercio and Lamas de Abade units have been interpreted either as forming part of the Lower Allochthon (Díez Fernández et al. 2010; Gómez Barreiro et al. 2010a) or as oceanic units (Rodríguez Aller 2005). They are not ophiolitic in a strict sense, as they are essentially metasedimentary, but due to their transitional character and the observation that comparable units in the Armorican Massif are considered oceanic, they have been included in the Middle Allochthon (Ballèvre et al. 2014). The Portugal equivalents are the units of Macedo de Cavaleiros and Pombais, in the Morais Complex.
- The Somozas Mélange, which crops out to the E of the Cabo Ortegal Complex. Part of it has an ophiolitic character, but also includes a metasedimentary unit and blocks of amphibolites and orthogneisses of Cambro-Ordovician age (Arenas et al. 2009).

The **Vila de Cruces Unit** crops out to the SE of the Órdenes Complex, and consists of a tectonically repeated succession of metabasites and metapelitic phyllites and schists, with scarce and thin layers of granitic orthogneisses, serpentinites and metacherts. The dominant lithologies are greenschist-facies metabasites exhibiting intense deformation, though the occasional preservation of igneous textures suggests a metabasaltic origin with minor presence of coarse- to medium-grained gabbros. Metapelites dominate in the upper part, and greenschists in the middle and lower parts (Figs. 4.2 and 4.5). There are intercalations of tonalitic orthogneisses and metagabbros. The **Campo Marzo Slice**, formed by serpentinized ultramafic rocks, underlies the unit, and is viewed as a fragment of its original underlying mantle.

The main orthogneiss body of the Vila de Cruces Units has yielded a U-Pb age of 497 ± 4 Ma (Arenas et al. 2007a, b), a reference for the formation of the unit, although zircon ages around 1.2 Ga in metagabbros of the same unit point to inheritances. Most of the basic rocks plot in the fields of island-arc tholeiites, supra-subduction zone basalts, or destructive plate-margin basalts (Fig. 4.6). Abundances of the

Table 4.2 Middle Allochthon units of the NW Iberian Massif, including ophiolites and oceanic supracrustals

		NW Iberian Massif			
Allochthonous complexes		Cabo Ortegal	Órdenes	Malpica-Tui	Bragança and Morais
Middle Allochthon (Oceanic domain)	Devonian ophiolites	Purrido, MoechE	Careón		Morais-Talhinhas, Soeira-Nogueira
	Cambro-Ordovician ophiolites	Somozas Mélange	Villa de Cruces, Bazar		Izeda-Remondes
	Cambro-Ordovician oceanic supracrustals		Lamas de Abade, Cercio	Ceán	Macedo de Cavaleiros, Pombais

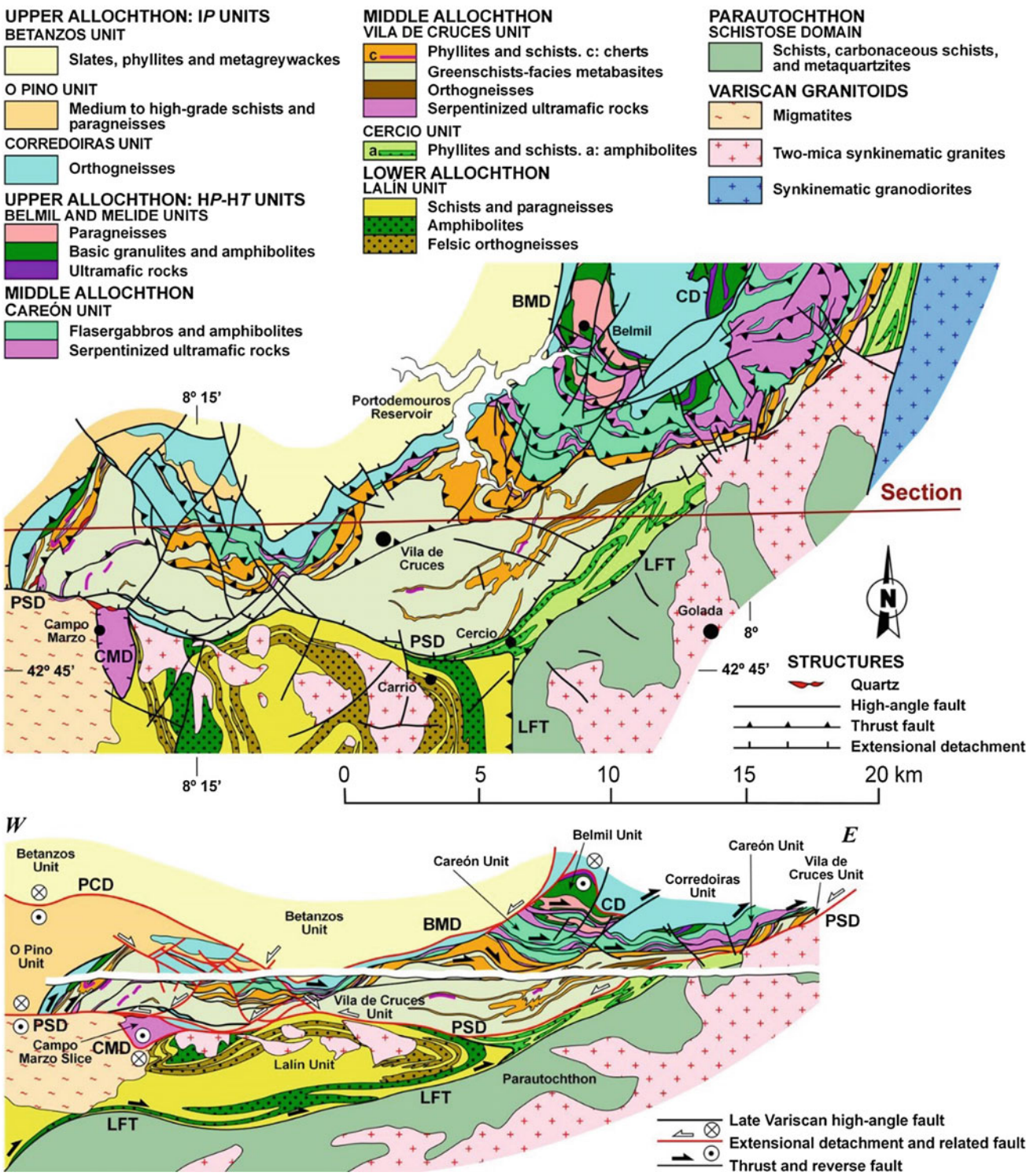

Fig. 4.5 Geological map and cross section of the Vila de Cruces and surrounding allochthonous units. LFT: Lalín-Forcarei thrust. Detachments: BMD: Boimorto; CD: Corredoiras; CMD: Campo Marzo; PCD: Ponte Carreira; PSD: Pico Sacro. After Arenas et al. (2007a)

most immobile trace elements in metagabbros mimic those of the greenschists, suggesting a similar tectonic setting (Arenas et al. 2007a). Both lithologies show a marked negative Nb anomaly, characteristic of magmas generated in a subduction zone (Pearce and Peate 1995; Pearce 1996). In the granitic orthogneisses, the immobile trace elements are typical of granitoids generated in volcanic arcs or supra-subduction zones (Pearce et al. 1984).

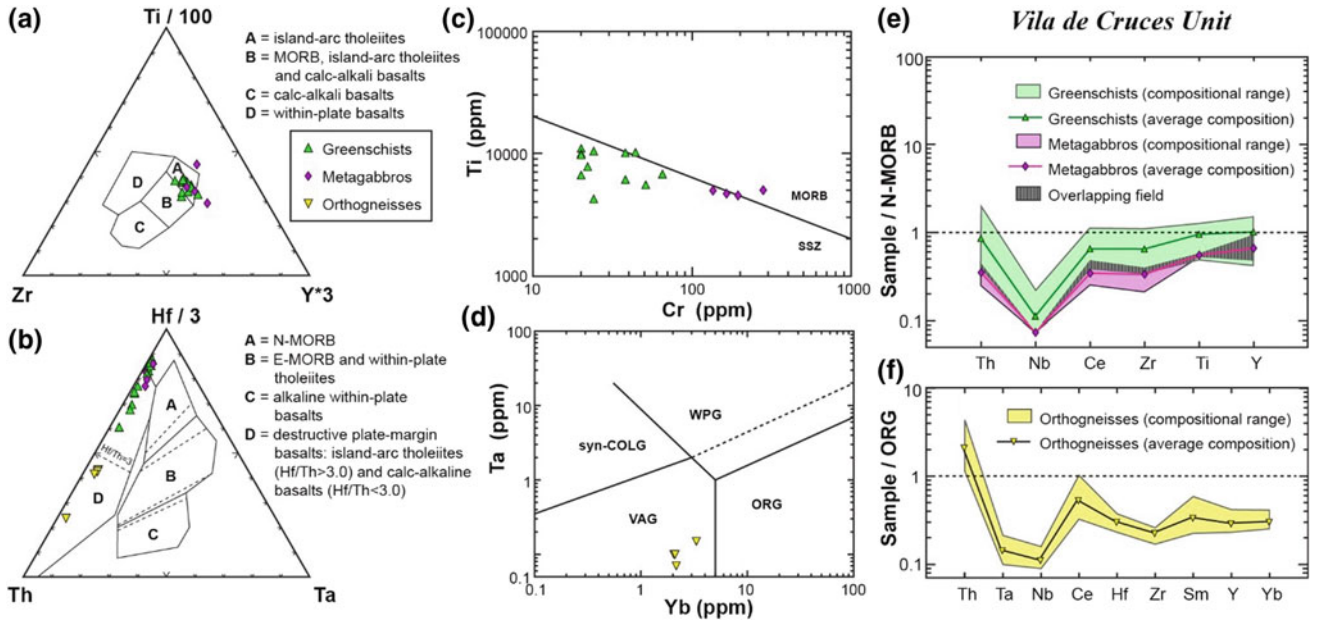

Fig. 4.6 Trace elements tectonic discrimination diagrams (**a**–**d**) and immobile trace element plots (**e**–**f**) for the Vila de Cruces Unit; **a** Ti-Zr-Y (Pearce and Cann 1973); **b** Th-Hf-Ta (Wood 1980); **c** Ti-Cr (Pearce 1975); **d** Ta-Yb (Pearce et al. 1984). **e** Greenschists and metagabbros. Normalizing values: N-MORB average composition (Pearce 1996); **f** Orthogneisses. Normalizing values: ORG average composition (Pearce et al. 1984). After Arenas et al. (2007a)

The **Bazar Unit** is located to the W of the Órdenes Complex (Figs. 4.1 and 4.2). Its thickness, up to 5000 m, and the presence of several thrust faults show that it is an imbricate (Gómez Barreiro and Martínez Catalán 2012). It is made up of monotonous metagabbroic amphibolite, and high-T amphibolites with a little deformed layer of gabbros, pegmatoid gabbros, pyroxenites, ultramafic rocks and minor tonalites and leucogabbros located close to the bottom (Díaz García 1990; Abati 2002). Relics of mafic granulites are preserved within the metagabbros, surrounded by high-T amphibolites (Arenas and Sánchez Martínez 2015). The geochemical features appear to be quite complex (Sánchez Martínez 2009). The common amphibolites and the metagabbros show compositions equivalent to island-arc tholeiites or N-MORB (Fig. 4.7) (Arenas and Sánchez Martínez 2015). However, the mafic granulites are transitional between mid-ocean ridge and within-plate basalts, with normalized trace element patterns similar to those of T-MORB generated in plume ridge interactions (Pearce 1996).

The unit was affected by an early high-T metamorphism that formed mafic granulites transitional between the low- and medium-P types. U-Pb zircon ages yielded two populations with mean values of 495 ± 2 Ma and 475 ± 2 Ma, interpreted as the ages of the gabbroic protolith and of the granulitic metamorphism respectively (Martínez et al. 2012). Hf isotope composition of these zircons points to juvenile mafic protolith without interaction with cortical sections (Martínez et al. 2012). The origin and meaning of the high-T metamorphic event are not clear. It is compatible with heating at the base of a magmatic arc, but can be interpreted also as related to subduction of a mid ocean ridge beneath (Arenas et al. 2007b; Sánchez Martínez 2009; Martínez et al. 2012; Arenas and Sánchez Martínez 2015). All in all, the lithological association, composition and temporal constraints suggest that the Bazar ophiolite could represent a section of a Cambro-Ordovician peri-Gondwanan ocean.

In northern Portugal, the Cambro-Ordovician ophiolites are represented by the **Izeda-Remondes Unit** of the Morais Complex (Figs. 4.1 and 4.2). This is essentially made of amphibolites, mylonitic amphibolites and greenschists, together with ultramafics cropping out at the base in the SE of the unit. The unit has been dated by Pin et al. (2006), who obtained a Sm–Nd correlation diagram that they interpreted as an isochron indicating an age of 447 ± 24 Ma.

The **Ceán**, **Cercio** and **Lamas de Abade** units share with the Vila de Cruces Unit part of the lithological association. They consist of a metapelitic sequence that intercalates mafic igneous rocks that in Ceán have N-MORB affinity (Rodríguez Aller 2005). The Ceán Unit has a middle Cambrian maximum depositional age (ca. 512 Ma), according to its youngest zircon age population, and has been interpreted to represent a distal paleoenvironment in a back-arc basin behind a Cambro-Ordovician volcanic arc (Díez Fernández et al. 2010, 2013). Vila de Cruces and Ceán underwent an early Variscan high-P metamorphic event (Arenas et al. 2007a), dated at

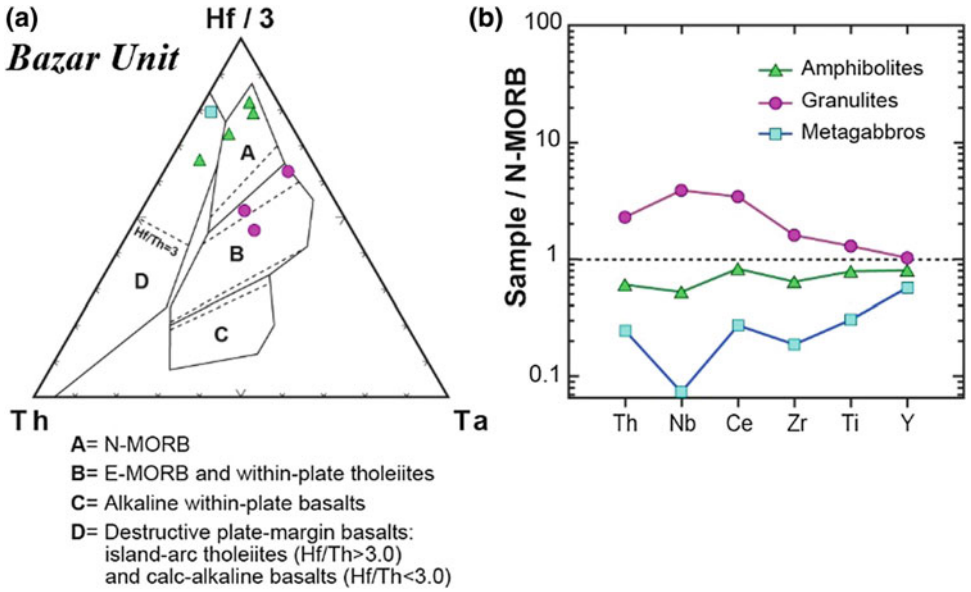

Fig. 4.7 Geochemical characteristics of the Bazar Unit; **a** Th-Hf-Ta diagram (Wood 1980) with projection of the metagabbroic amphibolites representing the most common lithology in the ophiolite, and the mafic granulites constituting rare minor bodies within the unit; **b** normal-mid-ocean-ridge basalts (N-MORB) normalized trace-element patterns (average composition); selected elements and normalized values after Pearce (1996). After Sánchez Martínez (2009) and Arenas and Sánchez Martínez (2015)

363 ± 2 Ma in the latter (López-Carmona et al. 2010, 2014). The units of **Macedo de Cavaleiros** and **Pombais** have a similar lithological association of phyllites, schists and basic metavolcanics, mostly in greenschist facies, although the latter includes alkaline metavolcanics (Pereira et al. 2003). All these units overlie tectonically the Lower Allochthon, which suggests that they were close or adjacent to each other. All of them represent a transition between the outermost attenuated continental margin and a more oceanic domain.

The **Somozas Mélange** crops out at the base of the Cabo Ortegal Complex (Figs. 4.1 and 4.2) as a tectonic mélange formed by three different rock subunits:

- An ophiolitic mélange consisting of igneous and sedimentary rocks mixed with serpentinites.
- A metasedimentary unit with phyllites and phyllonites, scarce conglomerates, marbles and quartzites.
- High-T metamorphic blocks consisting of several types of amphibolites and orthogneisses.

The ophiolitic part includes two different series of submarine metavolcanics, namely a group of basic to acid rocks of calc-alkaline affinity, and a group of metabasites with chemical compositions of island arc tholeiites (Fig. 4.8; Arenas et al. 2009).

In the Ti-Zr-Y diagram, the mélange samples plot in two separate groups. The first, including common volcanics, dikes and one gabbro sample, is located in or near the field of island-arc tholeiites. The second group, consisting of submarine metavolcanics and intermediate plutonic rocks, plots in the calc-alkaline basalts field (Fig. 4.8a). The Th Hf-Ta diagram allows the most accurate discrimination of subduction related rocks: all of the samples plot in the field of destructive plate margins due to their low Ta content (Fig. 4.8b). The classification in diagrams based on both mobile (silica and alkalis, Fig. 4.8c) and immobile (Ti, Zr, Nb and Y; Fig. 4.8d) elements supports the two different types of basic to intermediate metavolcanic rocks: the submarine metavolcanics can be classified as basaltic andesites whereas the common metavolcanic rocks are more similar to basalts. The projection in the MnO-TiO_2-P_2O_5 diagram strengthens the above interpretation for the origin for the mafic and intermediate samples, as they are located near the apex corresponding to supra-subduction zone rocks (Fig. 4.8e).

Two granitic rocks within the ophiolitic mélange were dated using U-Pb zircon geochronology at 527 ± 2 and 499 ± 1 Ma. In the metasedimentary unit, a conglomerate forms a large tectonic block included in serpentinites. The conglomerate yielded age populations of detrital zircons suggesting a provenance from the West African craton, with a large number of grains dated between ca. 630 and 464 Ma. These ages reflect the timing of a Pan-African event, but include the activity in the volcanic arc where the igneous lithologies of the mélange were generated. The maximum age of sedimentation for the conglomerate is estimated as latest Cambrian earliest Ordovician, and constraints the end of the magmatic activity in the volcanic-arc. Among the blocks of high-T rocks, an orthogneiss yielded a U-Pb

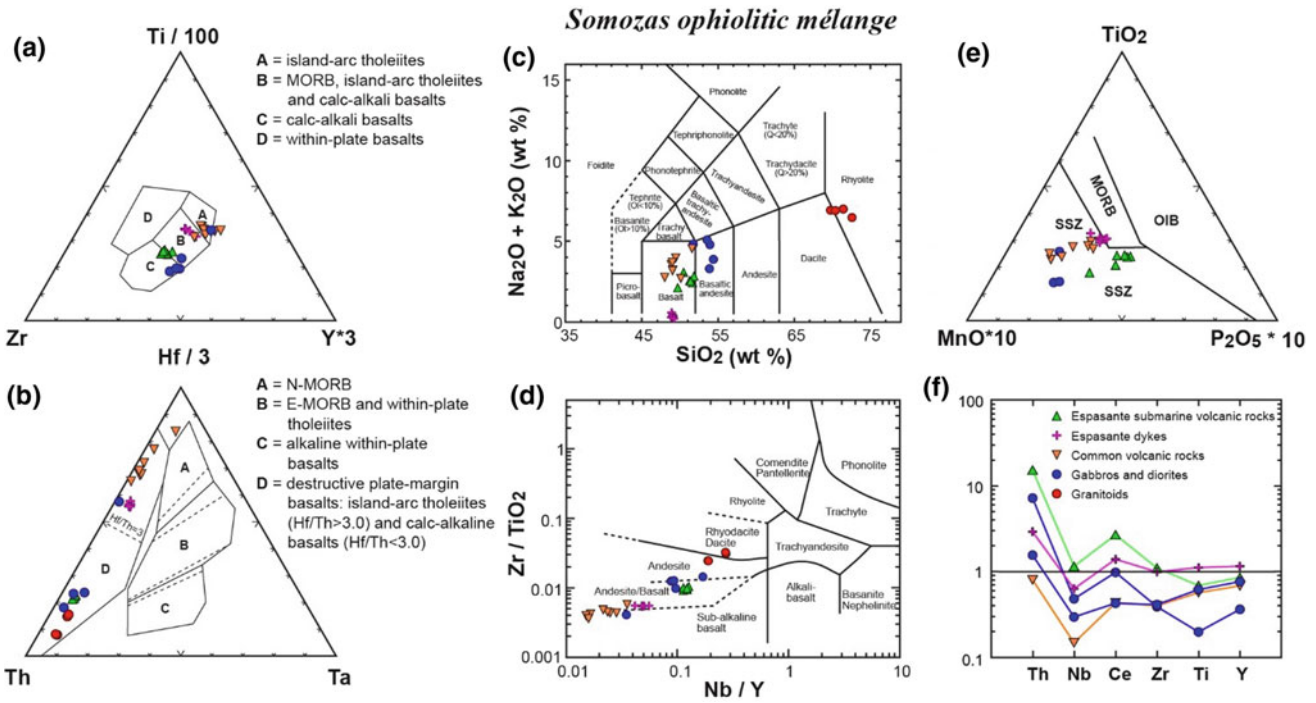

Fig. 4.8 Geochemical features of metaigneous low- to medium-T lithologies of the Somozas Mélange (tectonic blocks of high-T amphibolites and orthogneisses not included). **a** Ti-Zr-Y (Pearce and Cann 1973). **b** Th-Hf-Ta (Wood 1980). **c** Total alkalis versus silica (TAS) diagram (Le Maitre et al. 1989). **d** Zr/TiO_2-Nb/Y diagram (Winchester and Floyd 1977). **e** TiO_2-MnO-P_2O_5 diagram (Mullen 1983). After Arenas et al. (2009), except (**f**), after Arenas and Sánchez Martínez (2015)

protolith age of 485 ± 6 Ma, which is similar to other ages of igneous rocks in the Lower Allochthon of NW Iberia. All these data were provided by Arenas et al. (2009), according to whom, the protoliths of the mélange were generated in a mature volcanic arc located along the periphery of Gondwana between ca. 527 and 485 Ma. The mélange developed during the Late Devonian in a Variscan subduction zone beneath an ensemble of exhumed high-P units.

4.3.2 Early Devonian Ophiolites

Units of oceanic affinity dated between 405 and 395 Ma form part of the Middle Allochthon, occupying a structural position above the Cambro-Ordovician ophiolites. In Galicia, they are the Careón Unit, in the SE of the Órdenes Complex, and the Purrido and Moeche units, in the W and E of the Cabo Ortegal Complex respectively. In Trás-os-Montes, the group is represented by the Morais-Talhinhas Unit, in the N of the Morais Complex and probably also the Soeira-Nogueira Unit, in the Bragança Complex.

The **Careón Unit** is an incomplete but well exposed ophiolitic sequence occurring to the SE of the Órdenes Complex (Figs. 4.1, 4.2 and 4.5). It consists of three tectonic imbricates, the best preserved of which includes 600 m of metagabbros overlying 500 m of harzburgite (Díaz García et al. 1999b). The ultramafic rocks are highly serpentinized, but in the less retrograded rocks, a harzburgitic composition can be inferred. The transition between harzburgite and gabbro is abrupt and occurs along a surface without significant deformation and mostly parallel to the foliation of mafic and ultramafic rocks, that is considered the petrological paleo-Moho in the sense of Nicolas (1989). The gabbroic section is formed by a complex network of multiple intrusions of gabbro, wehrlite and wehrlite-gabbro transitional terms, and diabase to pegmatoid dikes.

The metabasites have compositions equivalent to tholeiitic basalts and plot mainly in the field of island arc tholeiites (Fig. 4.9a). According to the immobile trace elements, they show transitional characteristics between N-MORB and island-arc tholeiites (Fig. 4.9b; Sánchez Martínez et al. 2007a). Their immobile trace element patterns normalized to the average composition of N-MORB vary from flat and close to one to slightly fractionated or more depleted patterns. A negative Nb anomaly indicates an origin in a supra-subduction zone setting (Pearce 1996; Sánchez Martínez et al. 2007a).

A weakly deformed portion of a foliated plagioclase-rich gabbro was dated by U-Pb geochronology at 395 ± 2 Ma, considered the crystallisation age of the gabbro and evidence

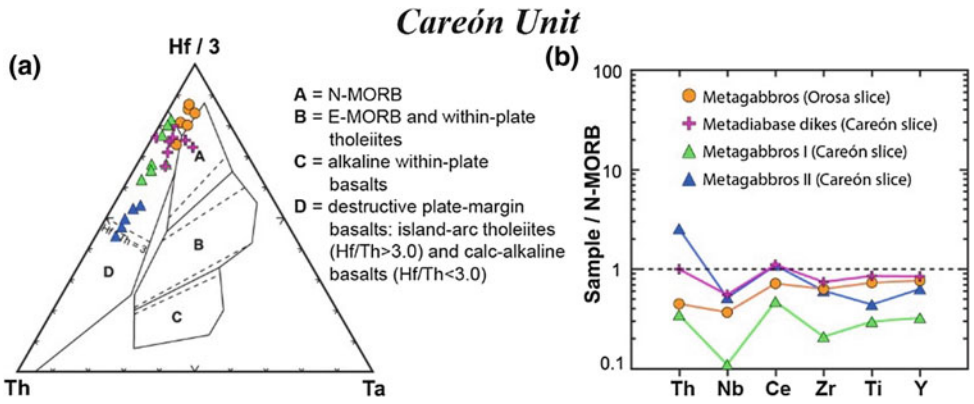

Fig. 4.9 **a** Th-Hf-Ta diagram (Wood 1980) for the most representative metabasites of the Careón ophiolite; **b** NMORB normalized trace element patterns of the average composition of each type of metabasite. Normalizing values are from Pearce (1996). After Sánchez Martínez et al. (2007a)

for oceanic crust generation by Early Devonian time (Díaz García et al. 1999b). A similar age of 395 ± 3 Ma was obtained in the Careón Unit by Pin et al. (2002), with εNd values for that age implying that these rocks were derived from a depleted mantle reservoir at the time of their formation, and are therefore juvenile. Initial εNd values ranging between +7.1 and +9.2 can be obtained for a crystallization age for Careón of 395 Ma from the Sm–Nd isotopic data of Pin et al. (2002). These values indicate that these rocks derived from a depleted mantle reservoir at the time of their formation, and are therefore juvenile.

Thermo-barometric estimations on garnet amphibolites located on top of the middle thrust sheet and interpreted as a metamorphic sole yielded 650 °C and 1.15 GPa, pointing to a subduction environment for ophiolite imbrication (Díaz García et al. 1999b). The amphibolite was dated at 376.8 ± 0.4 Ma (Dallmeyer et al. 1997), interpreted as a cooling age following the metamorphic thermal peak. This is slightly younger than the 390–380 Ma age reported for amphibolite facies metamorphism in ophiolitic units from Cabo Ortegal and the Portuguese complexes (Peucat et al. 1990; Dallmeyer et al. 1991).

Two different fabrics, an early high-T foliation and a subsequent lower-T foliation have been identified in two distinct crustal-scale shear zones of the middle ophiolitic thrust sheet. Combined quantitative texture analysis by electron backscattered diffraction and time-of-flight neutron diffraction carried out on the shear zones indicates that the regional lineation and shear zone kinematics (E-W, top-to-the E) represent fabrics developed essentially during intraoceanic subduction (Gómez Barreiro et al. 2010b).

The **Purrido Unit** is exposed in cliffs along the W of the Cabo Ortegal Complex (Figs. 4.1 and 4.2), where it consists of 300 m of homogeneous and well foliated massive amphibolites, locally bearing garnet (Vogel 1967). Geochemically, they classify as basalts in the Zr/Ti versus Nb/Y diagram (Fig. 4.10a) and as island-arc tholeiites in the Th-Hf-Ta diagram (Fig. 4.10b), which suggests generation in a supra-subduction zone setting (Sánchez Martínez 2009). The N-MORB normalized trace-element pattern is close to that of oceanic basalts, although somewhat depleted in Zr, Ti and Y, and exhibits the typical Nb anomaly of magmas generated in a subduction zone environment (Fig. 4.10c; Sánchez Martínez 2009; Sánchez Martínez et al. 2007b, 2011). Considering the homogeneous mafic character of the unit and its geochemical affinity, it can be derived from a gabbroic massif, perhaps part of the plutonic section of an arc-related ophiolite.

U-Pb zircon ages show a dominant Mesoproterozoic population with an age of 1155 ± 14 Ma and younger ages of 395 ± 3 Ma (Sánchez Martínez et al. 2006, 2011). Hf isotope data show that most Devonian zircons crystallized from a juvenile depleted mantle source, although some Devonian crystals show evidence of mixing with the Mesoproterozoic zircons. Whole rock Sm–Nd isotope data indicate also heterogeneity in composition, only compatible with the generation from two different sources. The Devonian mantle-derived magmatic source shows interaction with some Mesoproterozoic basement, either generated at a continent-ocean transition, or being the plutonic section of an arc-related ophiolite. Amphiboles of the prograde nematoblastic fabric were dated at 391 ± 6.6 Ma (Peucat et al. 1990; $^{40}Ar/^{39}Ar$ in a hornblende).

The **Moeche Unit** crops out in the E of the Cabo Ortegal Complex (Figs. 4.1 and 4.2). It shows the same dominant lithologies as the Vila de Cruces Unit, namely a sequence of greenschists with some alternations of phyllites and inclusions of metagabbros and serpentinites. However, U-Pb, LA-ICP-MS ages of zircons from a sample of mafic greenschist have yielded a maximum age of 400 ± 3 Ma (Arenas et al. 2014). The zircon ages suggest that the unit belongs to the group of Early Devonian ophiolites. The pervasively

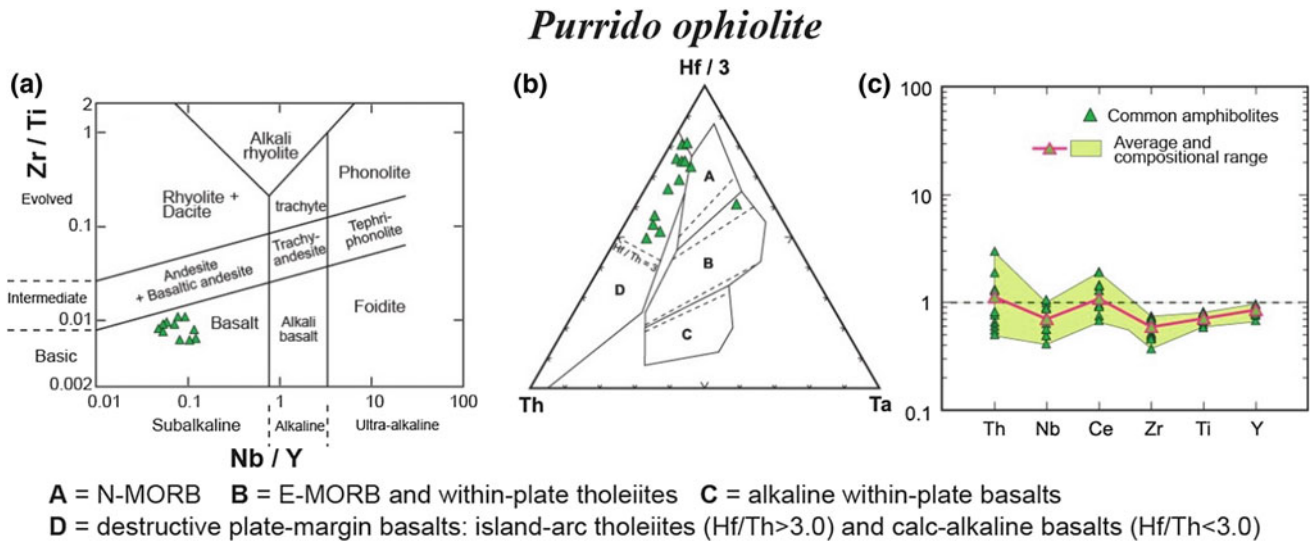

Fig. 4.10 Diagrams showing some relevant geochemical features of the Purrido amphibolites. **a** Zr/TiO_2-Nb/Y diagram (Winchester and Floyd 1977, modified by Pearce 1996); **b** Hf-Th-Ta diagram (Wood 1980); **c** N-MORB normalized trace element plot; normalizing values from Pearce (1996). After Sánchez Martínez (2009)

mylonitized character of Moeche and Vila de Cruces units masks their primary features, making them look similar to each other and suggesting a correlation that is not supported by age data. A 364 Ma $^{40}Ar/^{39}Ar$ age was obtained by Dallmeyer et al. (1997) for the mylonitic fabric of the Moeche Unit.

Analyses of the more representative metaigneous lithologies have been published by Sánchez Martínez et al. (2007b). The greenschists exhibit evidence of chemical variation, as is usual in sheared and metamorphosed metabasites, so that elements with the most immobile behaviour are most suitable for classification. The samples of the Moeche Unit plot in the Th-Hf-Ta diagram in a transitional position between island-arc tholeiites and N-MORB (Fig. 4.11a). The most immobile trace elements and with the highest discriminating power (Th, Nb, Ce, Zr, Ti and Y), normalized to an average tholeiitic N-MORB, depict quite flat spectra close to the average N-MORB concentrations, though slightly enriched (Fig. 4.11b). A small negative Nb anomaly points to a subduction zone component.

The **Morais-Talhinhas Unit** occurs in the northern half of the Morais Complex in Portugal. It consists largely of metaperidotites together with gabbroic rocks and minor felsic veins (Pin et al. 2006), whose U-Pb zircon ages range

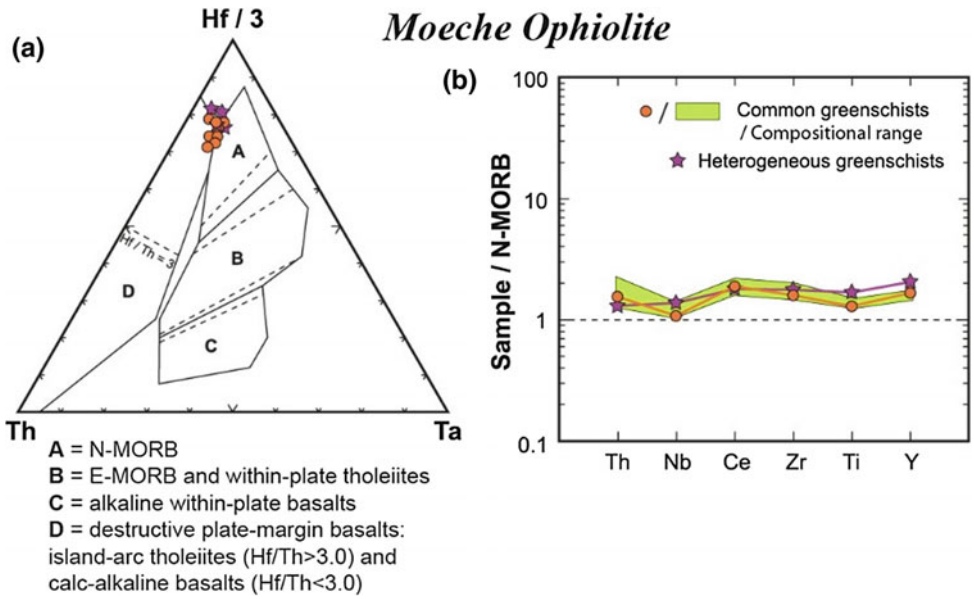

Fig. 4.11 Tectonic discrimination diagram and immobile trace element plots for the Moeche Unit; **a** Th-Hf-Ta diagram (Wood 1980); **b** N-MORB normalized trace element patterns of the most representative metabasites (Pearce 1996). After Sánchez Martínez et al. (2007b)

from 405 ± 1 to 396 ± 1 Ma (Pin et al. 2006). According to these authors, rocks from this unit have high Th/Nb ratios and elevated εNd values, reflecting generation above an intraoceanic subduction zone. The tectonometamorphic overprinting of the ophiolitic units, including imbrication with high- and medium-grade nappe units, was completed prior to ca. 385 Ma (Dallmeyer et al. 1991).

The **Soeira-Nogueira Unit** underlies the Upper Allochthon in the Bragança Complex (Ribeiro 1974; Marques et al. 1991–1992). It was described by the first author as consisting in basic, strongly foliated rocks, often showing metamorphic banding due to segregation of quartz-feldspathic bands. The texture is often mylonitic, and includes porphyroclasts of hornblende, plagioclase and epidote. No age data exist on this unit, but the previous description fits a similar facies rather common in the Careón Unit of the Órdenes Complex. Furthermore, the Soeira-Nogueira Unit overlies the greenschists that culminate the Lower Allochthon around the complexes of Morais and Bragança, and which probably are equivalents of the Vila de Cruces or the oceanic supracrustals of Galicia.

4.3.3 Geodynamic Implications of the Oceanic Terranes

Most of the Cambro-Ordovician ophiolites reflect in some way the opening of the Rheic Ocean, formed by pulling apart of the microcontinent Avalonia from the northern paleomargin of Gondwana. However, possibly none of these units in NW Iberia represent a true oceanic lithosphere, but rather the continent-ocean transition of an oceanic tract that may have not been the true, wide Rheic.

The continent-ocean transition is marked by the differences between the Lower Allochthon, which represents the attenuated continental crust of the outermost part of the margin, and the oceanic supracrustals of the Middle Allochthon. Metasandstones and Ordovician intrusive granitoids are abundant in the former while metapelites and basic volcanics form most of the latter (Díez Fernández et al. 2010). In turn, the Vila de Cruces and Izeda-Remondes units, where mafic rocks dominate and ultramafics occur, point to the transition toward a still more oceanic domain. Perhaps not fully oceanic indeed, as the presence of Mesoproterozoic zircons in metagabbros suggests inheritances from an old basement.

The whole picture reflects extension of the Gondwana margin, although the chemistry of the basic rocks of the Vila de Cruces Unit does not reflect a typical rift-related magmatism, but suggest a relationship with oceanic subduction. This is supported by the protoliths of the Somozas Mélange, generated in a volcanic arc in the periphery of Gondwana between the middle Cambrian and the lower most Ordovician (Arenas et al. 2009). To reconcile both observations, extension can be linked with opening of a back-arc basin behind a subduction zone. This is in agreement with the proposal of Winchester et al. (2002) that the closure of the Iapetus Ocean involved the development of two magmatic arcs, the Taconic arc in the Laurentian side and the Gander arc in the Gondwanan side. The Gander arc and associated subduction zones would have migrated toward Laurentia closing the Iapetus Ocean and simultaneously opening the Rheic Ocean behind. A similar process is illustrated in Fig. 4.4a–c, where the pulled-apart terrane that ultimately formed the Upper Allochthon would represent a lateral equivalent of Avalonia and the Gander arc.

The fitting of the Bazar Unit in that model has been debated. Following Martínez et al. (2012) and Arenas and Sánchez Martínez (2015), the unit would represent oceanic lithosphere derived from the Iapetus or Tornquist oceans instead of from the Rheic realm. But this would make an exception to the assumed regular stacking order of the allochthonous units, supposedly related to a piggy-back mode of thrust propagation and piling up. According to that mode, the lower is the position of one unit in the nappe pile, the closer was its paleogeographic position relative to the Autochthon. If so, a unit derived from the Iapetus or Tornquist oceans would occupy a position above the Upper Allochthon. Instead, the Bazar Unit forms part of the Middle Allochthon, as the rest of the units of oceanic affinity. The granulite-facies metamorphism might be related to subduction of a mid ocean ridge beneath, or due to heating at the base of a magmatic arc, according to Martínez et al. (2012). The latter interpretation is supported by two of the authors of that contribution for the intermediate-P units of the Upper Allochthon in the Órdenes Complex. This, together with the fact that the most abundant rocks of the unit may represent island-arc tholeiites, particularly the gabbro (which show a clear negative Nb anomaly; Fig. 4.7a), suggest that the Bazar Unit can be integrated in the model.

The Devonian ophiolites were generated during early Variscan plate convergence and closure of the Rheic Ocean, so that they cannot be related to the first part of a Wilson cycle. Their age, ca. 400 ± 5 Ma, is that of the high-P and high-T of the Upper Allochthon, suggesting that the associated extension should have been rather localized inside the Rheic realm. Geochemistry of the Morais Talhinhas and Careón units point to a supra-subduction zone setting (Pin et al. 2006; Sánchez Martínez et al. 2007a, b, 2011), and an intra-oceanic subduction has been proposed. This interpretation seems confirmed by the early high-T foliation developed in the Careón Unit, developed during intraoceanic subduction (Fig. 4.4e; Gómez Barreiro et al. 2010b).

4.4 Upper Allochthon: A Peri-Gondwanan Continental Terrane

J. R. Martínez Catalán, J. Gómez Barreiro, P. Castiñeiras, J. Abati, P. Andonaegui, J. Fernández-Suárez, P. González Cuadra, J. M. Benítez-Pérez

The Upper Allochthon occupies the core of all the Iberian allochthonous complexes except that of Malpica-Tui, where it has been completely eroded. It represents a continental piece separated from the northern margin of Gondwana during the late Cambrian, and registered volcanic-arc type magmatism at the Cambro-Ordovician transition. The ensemble comprises two groups of allochthonous units. The first group occupies the lower structural position, and its units display early Variscan metamorphism of high-P and high-T, granulite to eclogite facies. The units of the upper group underwent pre-Variscan metamorphism of intermediate-P type gradient, and include granulite, amphibolite, and greenschist facies. The age of the latter has been reported in NW Iberia as Cambro-Ordovician.

Both groups are considered parts of the same coherent terrane because no suture has been found between them, although a subtractive low-dipping detachment separates the intermediate-P from the underlying high-P and high-T units. In any case, the subdivision is meaningful for the interpretation of the respective histories of the two groups, which have a comparable lithological association but differ in their metamorphic evolution.

4.4.1 High-P and High-T Units

This group is well represented in Galicia (NW Spain), largely in the Cabo Ortegal Complex, and in four relatively small units in the Órdenes Complex (Figs. 4.1 and 4.2; Table 4.3). In Portugal, the group forms the core of the Bragança Complex and occurs in three small slices in the Morais Complex (Vale da Porca, Caminho Velho and Vinhas; Ribeiro 1974).

The **Cabo Ortegal Complex** offers the best occurrence of the high-P and high-T group of units, due to their extent and outcropping conditions. There, the group occurs in two large Variscan thrust sheets, the Cedeira Unit below, and A Capelada Unit above. Both show the same lithological association of basic granulites, amphibolites and felsic paragneisses, although A Capelada Unit includes also an ultramafic section and eclogite layers and lenses inside the paragneisses.

The **Cedeira Unit** consists of basic rocks (Candieira Fm.) below, and the paragneisses (Chimparra Gneisses) above (Figs. 4.12 and 4.13). The basic rocks of the **Candieira Fm.** occur in the granulite facies, but metagabbros with recognizable igneous textures are common as isolated bodies inside the paragneisses. The metagabbros occur also included as relicts in a heterogeneous ensemble of metabasic rocks where they alternate with high-T amphibolites and heterogeneously sheared retrogranulites (Azcárraga 2000). Garnet corona textures formed in the early stages of deformation, whereas a garnet-rich foliation developed during granulite-facies metamorphism. Subsequently, the rocks underwent significant retrogression during exhumation along shear zones developed under granulite and amphibolite facies conditions, and were strongly folded. Minor isoclinal folds, sheath folds, and superimposed folds were formed, and a major recumbent anticline hosts the Candieira Fm. at its core. The **Chimparra Gneisses** are derived from sedimentary protoliths, probably a monotonous greywacke succession, and underwent high-P granulite facies metamorphism followed by migmatization and mylonitization during exhumation.

A Capelada Unit contains the best exposure of the ultramafic lithospheric mantle, which crops out in the large overturned limb of the recumbent Uzal syncline (Figs. 4.12 and 4.13). The section contains a heterogeneous ensemble of ultramafic rocks with abundant pyroxenite layers alternating with spinel-bearing harzburgites and dunites. There are also abundant levels of garnet pyroxenites and chromite-rich layers, with high Pt-Pd concentrations toward the top of the

Table 4.3 Upper Allochthon units of the NW Iberian Massif

		NW Iberian Massif			
Allochthonous complexes		Cabo Ortegal	Órdenes	Bragança	Morais
Upper Allochthon	Low-grade units		Betanzos		
	Intermediate-P units	Cariño	O Pino, A Silva, Corredoiras, Monte Castelo		Lagoa
	High-P and high-T units	A Capelada, Cedeira	Sobrado, Melide, Belmil, Fornás, Arinteiro	Cabrões, Vale de Cervas	Vale da Porca, Caminho Velho, Vinhas

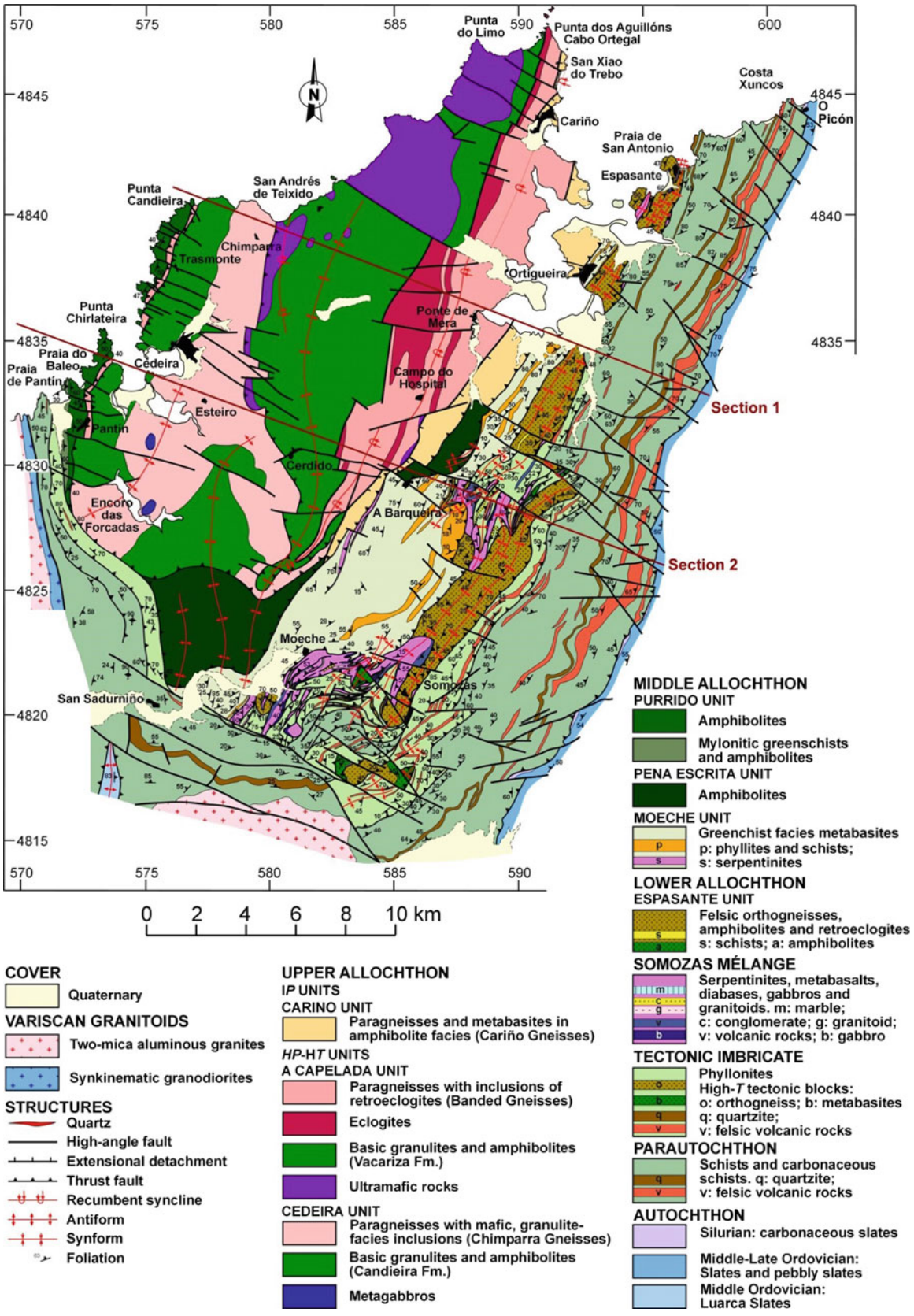

Fig. 4.12 Geological map of the Cabo Ortegal Complex based on Vogel (1967), Bastida et al. (1984) and Arenas et al. (2009)

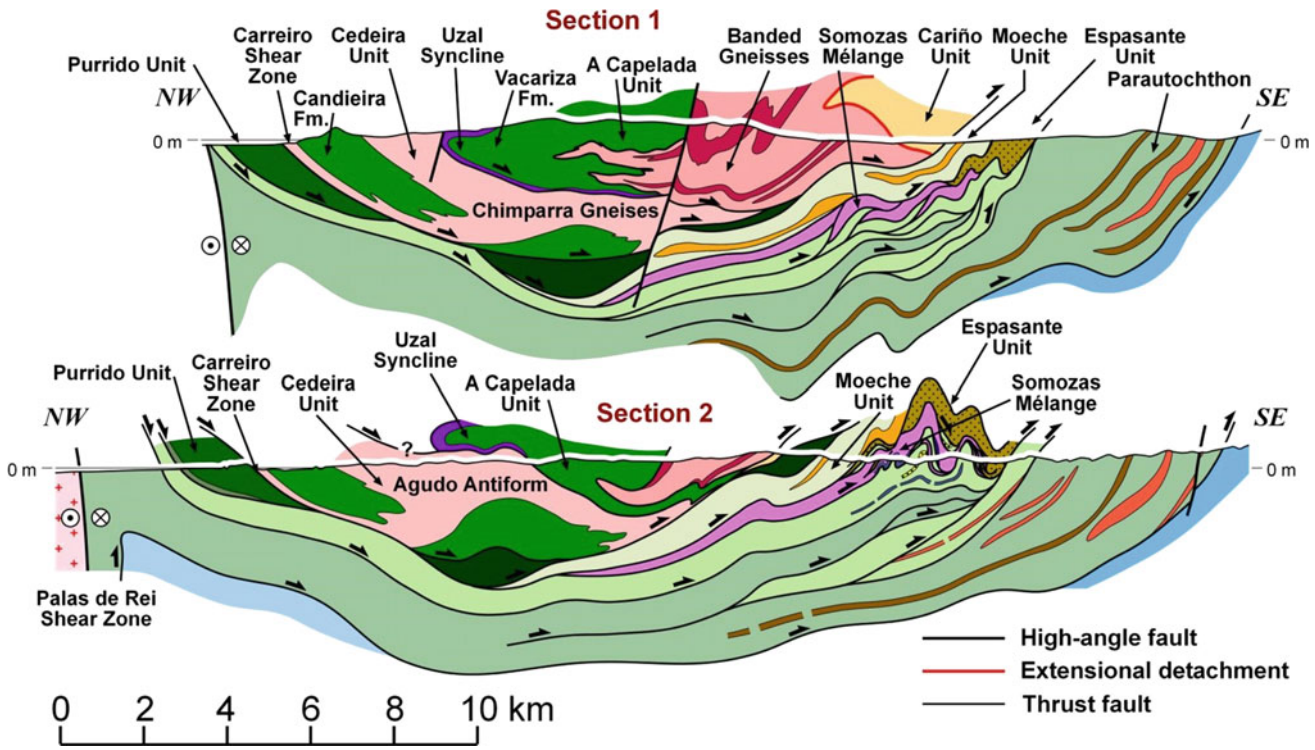

Fig. 4.13 Sections across of the Cabo Ortegal Complex. Their location is indicated in Fig. 4.12. Based on Marcos et al. (1984) and Arenas et al. (2009)

section (Girardeau et al. 1989; Moreno et al. 2001). The features of the ultramafic rocks point to an oceanic affinity (Girardeau and Gil Ibarguchi 1991). Sm–Nd isochron dating of the ultramafics yielded a protolith age of ca. 500 Ma, within the range of other magmatic protoliths in the unit, whereas the high-P and high-T metamorphism is 390 m.y. old, and responsible for the formation of garnet in pyroxenite layers (Santos et al. 2002). The ultramafic rocks are characteristic of a heterogeneous enriched upper mantle. Their nature and age suggest that they may represent the mantle root of a magmatic arc (Moreno et al. 2001; Santos et al. 2002), probably the wedge of lithospheric mantle above a subduction zone. Considering the harzburgitic nature of the dominant peridotites, it is possible that the initial subduction was intraoceanic. Pyroxenites are interpreted as partial melts of peridotite hydrated by upward fluxing of the descending oceanic slab.

The **Vacariza Fm.** occupies the intermediate section of A Capelada Unit. This is a heterogeneous ensemble of basic granulites, augen gneisses and some calc-silicate rocks (Vogel 1967; Puelles 2004). The most characteristic are the basic rocks with clinopyroxene and garnet (pyrigarnites) whose gabbroic protoliths have been dated at 490–520 Ma (Fernández-Suárez et al. 2007). These authors also report U-Pb ages on zircon representing a possible high-P and high-T metamorphic event ca. 404 ± 6 Ma old. Subsequently, the rocks underwent intense migmatization during their exhumation, dated between ca. 395 and 385 Ma (Fernández-Suárez et al. 2007), and which is coeval with a decompressive, often mylonitic, high-T fabric which obliterates the initial granulitic fabric.

The **Banded Gneisses**, occupy the core of the Uzal syncline (Fig. 4.13) and represent the uppermost formation of A Capelada Unit. Most of the formation consists of eclogite-facies paragneisses of pelitic-semipelitic composition, which registered peak metamorphic conditions of 750–800 °C and 2.0–2.3 GPa (Mendia Aranguren 2000). The formation includes a few thick layers and abundant inclusions of medium to coarse grained eclogites (Vogel 1967). The paragneisses underwent intense migmatization, followed by the development of a decompressive mylonitic foliation wrapping around the eclogite inclusions, which are often retrograded.

The Banded Gneisses are a polymetamorphic unit (Fernández-Suárez et al. 2002). They contain zircon, monazite, rutile and titanite that grew during two separate metamorphic events. The oldest event is latest Cambrian-Early Ordovician (500–480 Ma) and the younger took place in the Early-Middle Devonian (400–380 Ma). The first event is also identified in some units of the Órdenes Complex, where

it is recorded as an intermediate-P metamorphism linked to arc-related, voluminous Cambro-Ordovician magmatism combined with loading by crustal thickening (Abati et al. 1999, 2003, 2007).

The Devonian event can be correlated with the high-P and high-T event identified in the granulites of the Vacariza Fm. and other units of the Upper Allochthon. However, the Banded Gneisses and the eclogites have a tectonothermal evolution different from that of the pirygarnites of the Vacariza Fm., although eclogites and transitional types are found in the latter close to the contact with a band of eclogites at the bottom of the Banded Gneisses (Vogel 1967). This suggests that the contact is a major tectonic structure dating from early Variscan time, when subduction and accretion took place. Subsequently, the whole unit was progressively exhumed and affected by Variscan recumbent folding, thrusting, and late Variscan upright folding (Fig. 4.13).

In the **Órdenes Complex**, the high-P and high-T group is represented by the Sobrado, Melide, Belmil and Fornás units (Figs. 4.1, 4.2 and 4.14). The **Sobrado Unit** offers the most complete section. It occupies the core of a Variscan upright NE-SW antiformal stack formed by three horses (Fig. 4.14). The lower horse consists of highly serpentinized ultramafic rocks with some mafic inclusions and a 500 m thick layer of eclogites and related clinopyroxene-garnet rocks without primary plagioclase. The middle horse is a lens that contains up to 1000 m of migmatitic felsic gneisses (mainly paragneisses), with inclusions of high-P granulite-facies mafic rocks. U-Pb dating of zircons has yielded age populations typical of the West African craton, a maximum age of sedimentation around 510–490 Ma, and younger zircons and monazites clustering around 380 Ma.

Relicts of the igneous protoliths are neither preserved in the lower nor in the middle horses. Conversely, the upper horse includes migmatitic felsic gneisses and layers of mafic rocks derived from deformed and recrystallized gabbros that locally grade into undeformed varieties that preserve igneous textures (Pablo Maciá and Martínez Catalán 1984). The lower horse can be compared with the mafic and ultramafic parts of the Vacariza Fm. of A Capelada Unit in Cabo Ortegal, while the middle and upper horses correlate with the felsic and mafic parts of the Cedeira Unit (Chimparra Gneisses and Candieira Fm. respectively).

In the **Bragança Complex**, the units of this group are preserved in two adjacent late-Variscan synforms, where Marques et al. (1991–1992, 1996) identified three lithological types and two allochthonous units. The **Cabrões Unit** occupies the lower structural position, and consists of mafic granulites and paragneisses with eclogite boudins, similar to those of the A Capelada Unit in Cabo Ortegal. Also, some mafic and ultramafic intrusives occur, among which, the authors describe garnet-bearing and coronitic metagabbros. Above the Cabrões Unit, the **Vale de Cervas Unit** contains a similar association, but mafic and ultramafic intrusives are more abundant.

The gabbros of the high-P and high-T group are the most useful rock type for establishing the geotectonic setting of the units and their tectonometamorphic evolution. In the Cedeira Unit and the upper horse of the Sobrado Unit, they occur in several stages of transformation, from practically undeformed to coronitic metagabbros, high-P granulites and amphibolites (Arenas and Martínez Catalán 2002). In the less deformed gabbros, subophitic and diabase textures have been preserved, indicating an emplacement at relatively shallow crustal levels. Most of the gabbros are tholeiitic, and their geochemical signature has been compared to MORB (Gil Ibarguchi et al. 1990) and related to continental rifting (Galán and Marcos 1997). This contrasts with the geochemistry of the intrusives in the intermediate-P units of the overlying group and the ultramafic rocks at Cabo Ortegal, for which a generation in an arc setting has been suggested (Santos et al. 2002).

The metamorphic transformation of the gabbros started with formation of corona textures by reaction between all the ferromagnesian igneous phases and plagioclase. They have been studied in the Sobrado Unit, where three groups were established (subordinate phases in brackets): (I) amphibole + Opx; (II) (amphibole) + (Cpx) + Opx + Grt; (III) (amphibole) + Cpx + Opx + Grt (Arenas and Martínez Catalán 2002). The presence of high-P granoblastic granulites and the low Na-contents of clinopyroxene in the coronae indicate that the latter represent arrested stages during transformation to granulite. Different stages in the prograde metamorphic evolution are preserved in the three groups of coronae, which recorded P-T conditions increasing from group I to group III. The absence of textures related to subsequent cooling and/or decompression suggests that the coronae have not recorded any of these stages of the metamorphic evolution. Consequently, the prograde metamorphic evolution inferred from the coronae is compatible with a simple P-T path related with the burial of the unit. Figures 4.3 and 4.15 show the path established by thermobarometry applied to representative samples of types II and III coronae. The textures were generated during a drastic, nearly isothermal increase in pressure related with subduction. The highest P-T conditions reached 13–17 kbar and 660–770 °C.

Concerning the age of the basic igneous protholits, early Paleozoic ages (490–480 Ma) were obtained by Peucat et al. (1990; U-Pb on zircons) in the Cabo Ortegal Complex, and interpreted as dating the high-P and high-T metamorphism. More recent data have yielded 520–480 Ma in Cabo Ortegal and Órdenes, viewed as protolith ages (Ordóñez Casado et al. 2001), but that might in part reflect the imprint of a nearly contemporaneous metamorphic event (Fernández-Suárez et al. 2002, 2007). Similar ages, ranging 500–480 Ma have been obtained in the same rock-types in the Bragança Complex (Mateus et al. 2016).

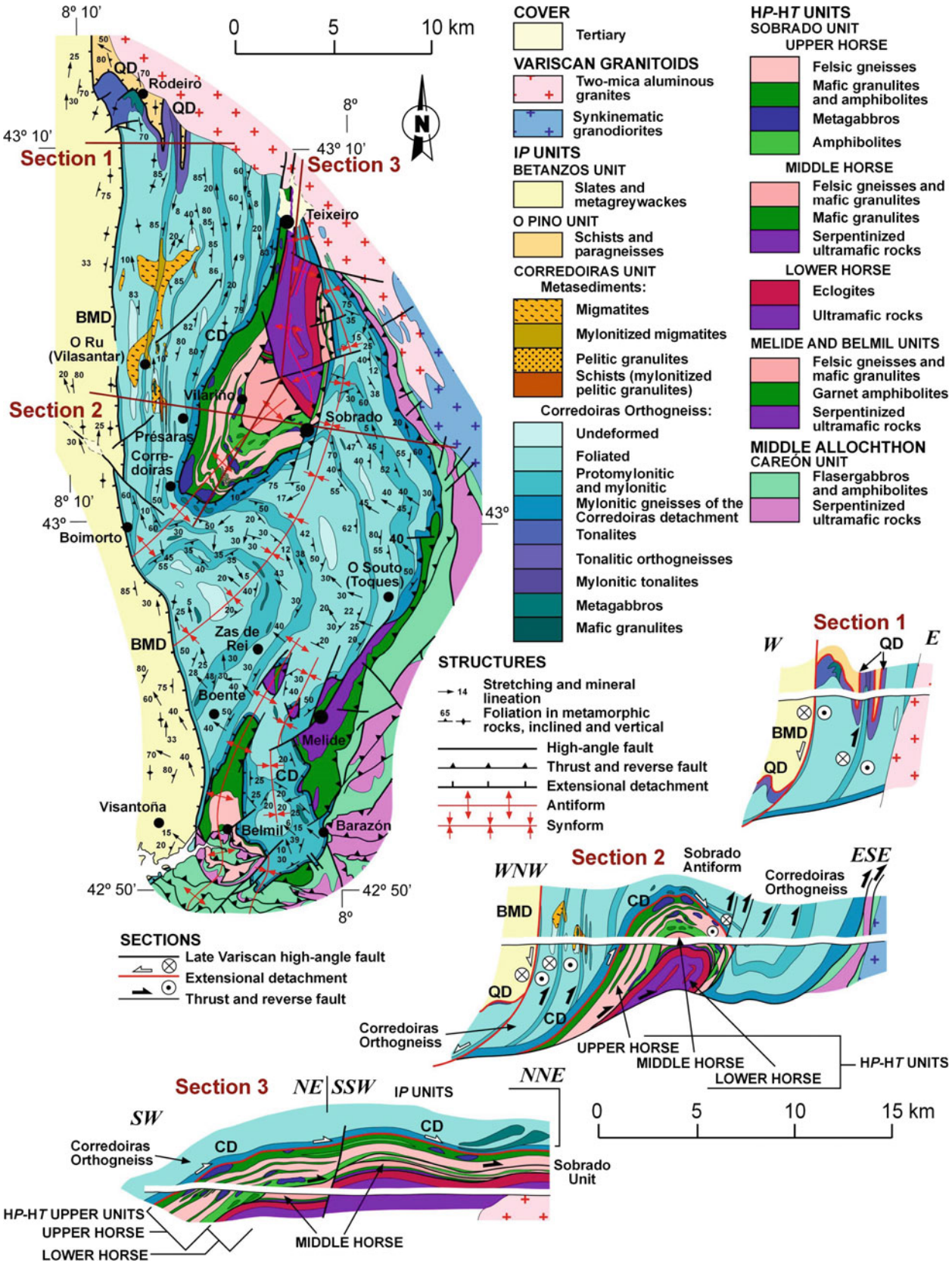

Fig. 4.14 Geological map and cross sections of the SE sector of the Órdenes Complex showing the relationships between the intermediate-P and the high-P and high-T units of the Upper Allochthon, represented by the Corredoiras Unit and the Sobrado, Melide and Belmil units respectively. After Arenas and Martínez Catalán (2002) and González Cuadra (2007). BMD, Boimorto detachment; CD, Corredoiras detachment; QD, Queimada detachment

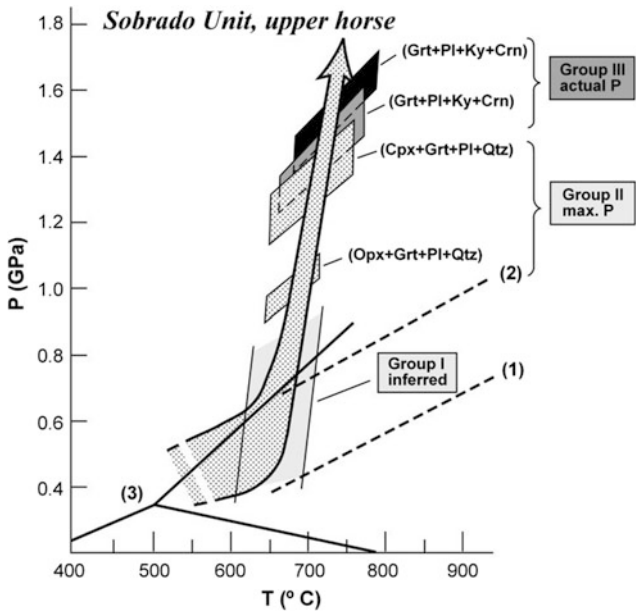

Fig. 4.15 P-T diagram showing thermobarometric data and interpreted P-T path for the mineral assemblages of coronae of the Sobrado Unit. (1) lower, and (2) upper conditions for the beginning of garnet stability in mafic granulites, after Ringwood and Green (1966) and Green and Ringwood (1967). (3) Al_2SiO_5 polymorphs stability after Holdaway (1971). After Arenas and Martínez Catalán (2002)

However, the main tectonothermal event in the Órdenes and Cabo Ortegal complexes, the high-P and high-T granulite and eclogite facies metamorphism that characterize the group occurred later, at 400–390 Ma (Schäfer et al. 1993; Santos Zalduegui et al. 1996; Ordóñez Casado et al. 2001; Fernández-Suárez et al. 2002, 2007). This Early-Middle Devonian metamorphic event, also identified in the Bragança Complex (Mateus et al. 2016), and which implied subduction, was followed by decompression and partial melting and then, successively, by a penetrative mylonitization in the amphibolite facies, recumbent folding, and finally thrusting under greenschist facies conditions (Vogel 1967; Marcos et al. 1984, 2002; Gil Ibarguchi et al. 1990; Arenas 1991; Girardeau and Gil Ibarguchi 1991; Mendia Aranguren 2000). The retrograde amphibolite-facies metamorphism has been dated at 390–380 Ma (Dallmeyer et al. 1991, 1997; Valverde Vaquero and Fernández 1996; Gómez Barreiro et al. 2006).

4.4.2 Intermediate-P Units

A thick sequence of terrigenous sediments intruded by Cambro-Ordovician gabbros and granitoids characterizes this group, whose units occupy the higher structural positions in the nappe pile. They reach the largest extension in the Órdenes Complex, but have been preserved also at the core of the Morais Complex and in the Cabo Ortegal Complex (Figs. 4.1 and 4.2).

In the **Órdenes Complex**, metamorphic grade ranges from the granulite facies in the lower units to the greenschist facies on top. Changes in metamorphic grade are abrupt and occur at both sides of extensional detachments (Díaz García 1990, 2000; Díaz García et al. 1999a; Abati 2002; González Cuadra 2007; Álvarez Valero et al. 2014). High-grade rocks occupying the lowermost position occur as massifs of metaigneous rocks: the Monte Castelo Unit (metagabbro) and the Corredoiras and A Silva units (orthogneisses). These are separated by subtractive detachments from the overlying O Pino Unit, which is essentially metasedimentary and mesozonal. A major low-dipping fault, the Ponte Carreira detachment (PCD), separates the schists and paragneisses of O Pino Unit from the uppermost, low-grade slates and greywackes of the Betanzos Unit (Fig. 4.2).

The **Monte Castelo Unit** is the largest of several gabbroic intrusions occurring in the Upper Allochthon (Figs. 4.16 and 4.17). It is formed by a massive two-pyroxene gabbro where three major compositional types have been distinguished: olivine gabbronorites, amphibole gabbronorites, and biotite gabbronorites. Textures vary from granular to intergranular and ophitic. The presence of olivine and the common ophitic textures point to a relatively shallow emplacement. Figure 4.18a shows the average contents of some elements of petrogenetic interest normalized to the composition of typical N-MORB (Andonaegui et al. 2002). The diagram shows patterns of weak enrichment in LIL elements and values close to one or slightly depleted in HFS and REE. The olivine gabbronorites exhibit an overall depletion in Zr, Ti and Y, characteristic of tholeiitic magmas generated in island arcs (Wilson 1989; Lapierre et al. 1992). In the Mn-Ti-P diagram (Mullen 1983), which is effective in discriminating between most basaltic types, the majority of samples plot in the island arc tholeiites field (Fig. 4.18b).

Granoblastic aluminous granulites occur in metapelitic enclaves up to 3 km long sparsely distributed in the gabbro (Figs. 4.16 and 4.17; Abati et al. 2003). Thermobarometric studies show an increase in pressure of 0.2–0.4 GPa at a nearly constant temperature of 800–825 °C during granulitization (Figs. 4.3, and 4.19, green path). Near its bottom, the gabbro is deformed by a prograde, granulite-facies shear zone which produced a complete recrystallization of the igneous components. These mafic granulites repeat the trend of isothermal pressurization of the metapelitic granulites. U-Pb analyses on zircons of the gabbro yielded a protolith age of 499 ± 2 Ma, whereas zircon rims in the shear zone yielded a concordia age of 482.6 ± 3.5 Ma reflecting granulite-facies metamorphism (Abati et al. 1999, 2007). Zircons and monazites in granulite-facies metapelites yielded ages of 505 ± 2 and 498 ± 2 Ma respectively, probably related to the intrusion, but rutiles in the same rocks gave ages of 380–390 Ma (Abati et al. 1999), about 100 Ma younger and indicating an early Variscan metamorphic imprint.

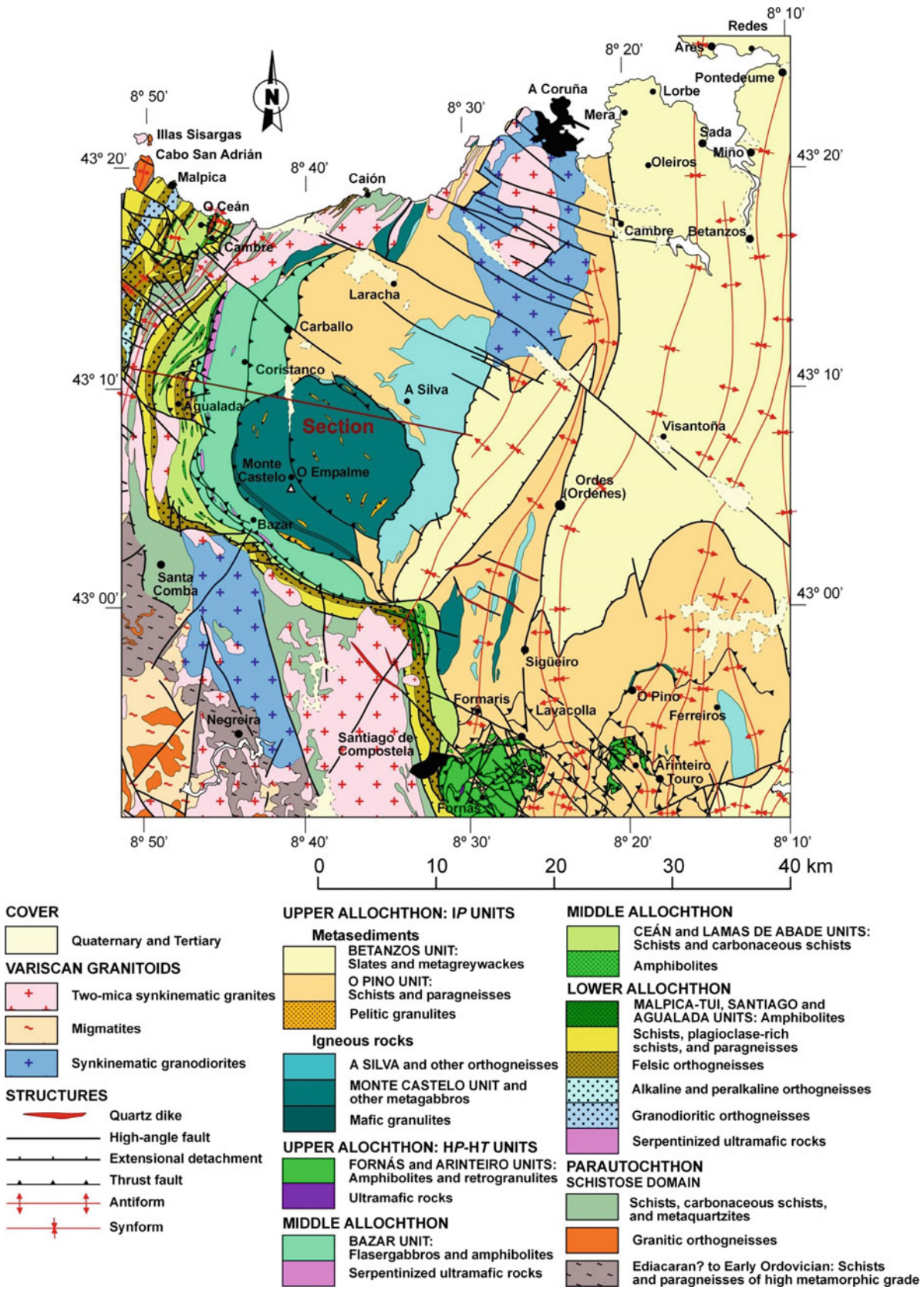

Fig. 4.16 Geological map of the NW and central sectors of the Órdenes Complex showing the relationships among the intermediate-P units of the Upper Allochthon, and with the Middle and Lower allochthons and the Parautochthon. A section across de Monte Castelo Unit is shown in Fig. 4.17

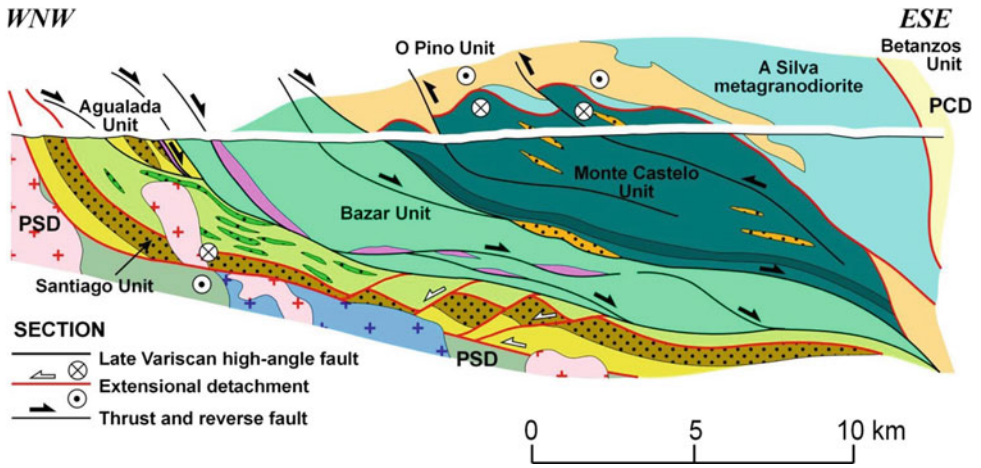

Fig. 4.17 Section across the western part of the Órdenes Complex. Modified after Abati et al. (2003). For location, see Fig. 4.16. PDS: Pico Sacro detachment; PCD: Ponte Carreira detachment

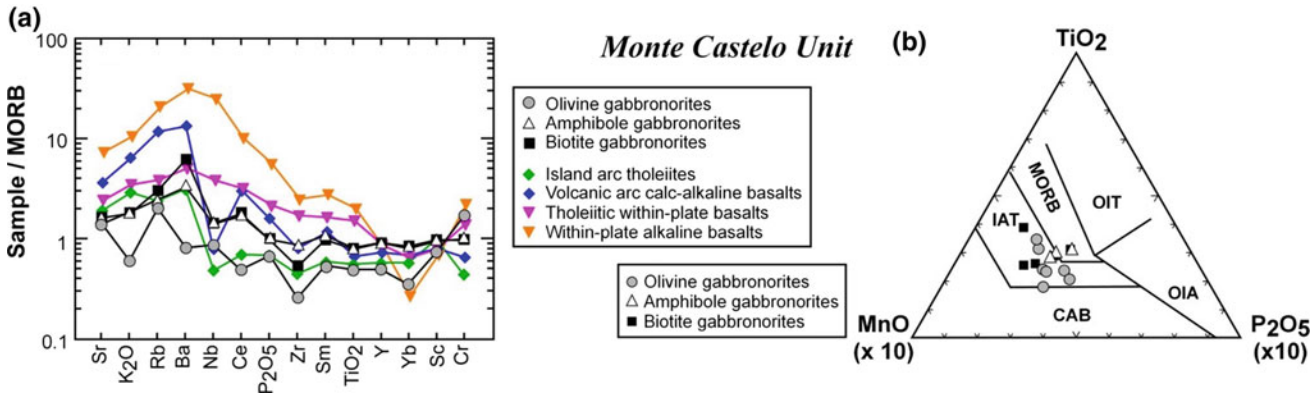

Fig. 4.18 **a** N-MORB normalized multi-element diagrams for the gabbroic rocks of the Monte Castelo Unit, compared with four basaltic types generated in different tectonic setting: island arc tholeiites, volcanic arc calc-alkaline basalts, tholeiitic within-plate basalts and within-plate alkaline basalts, from Pearce (1982); **b** TiO_2-MnO (×10)-P_2O_5 (×10) plot (Mullen 1983), for the same rocks. The diagram shows fields for ocean ridge basalts (MORB), ocean-island tholeiites (OIT), ocean-island alkali basalts (OIA), island-arc tholeiites (IAT) and calc-alkaline basalts (CAB). After Andonaegui et al. (2002)

The **Corredoiras Unit** is a coarse-grained orthogneiss of granodioritic to tonalitic composition that crops out in the E of the Órdenes Complex (Figs. 4.1, 4.2 and 4.14). Small bodies of gabbro occur close to the base of the unit, and diabase dikes occur sparsely distributed inside it. The orthogneiss was variably deformed during the Variscan Orogeny (Díaz García et al. 1999a; González Cuadra 2007), with at least two generations of ductile shear zones. The older of them produced mylonitic bands kinematically equivalent to thrust faults, with a dextral component of transcurrence. The younger shear zone is the Corredoiras detachment (CD), which placed the unit on top of the high-P and high-T units of Sobrado, Melide and Belmil (Fig. 4.14).

The chemical composition of the granitoid of this unit points to a generation above a subduction zone for tonalitic and gabbroic rocks, and to crustal influence in the case of granodiorites, all suggesting an ensialic island arc environment (Andonaegui et al. 2012). Most analyses of differently deformed orthogneisses in discrimination diagrams plot in the field of volcanic arc granites or show calc-alkaline affinity, although the metagabbros show tholeiitic affinity (Fig. 4.20a–d). The granodioritic and tonalitic orthogneisses show REE patterns typical of calc-alkaline rocks, with a characteristic Eu anomaly (Fig. 4.20e, f).

U-Pb dating on zircons yielded concordant ages of 500 ± 2 Ma (Abati et al. 1999) and 492 ± 3 Ma (Andonaegui et al. 2012), considered to represent the age of intrusion. Kilometer-scale xenoliths of hornfelses and migmatites occur inside the orthogneisses. The hornfelses reflect contact metamorphism, whereas migmatization is considered the product of regional metamorphism closely following the intrusion, because monazites included in biotite from the

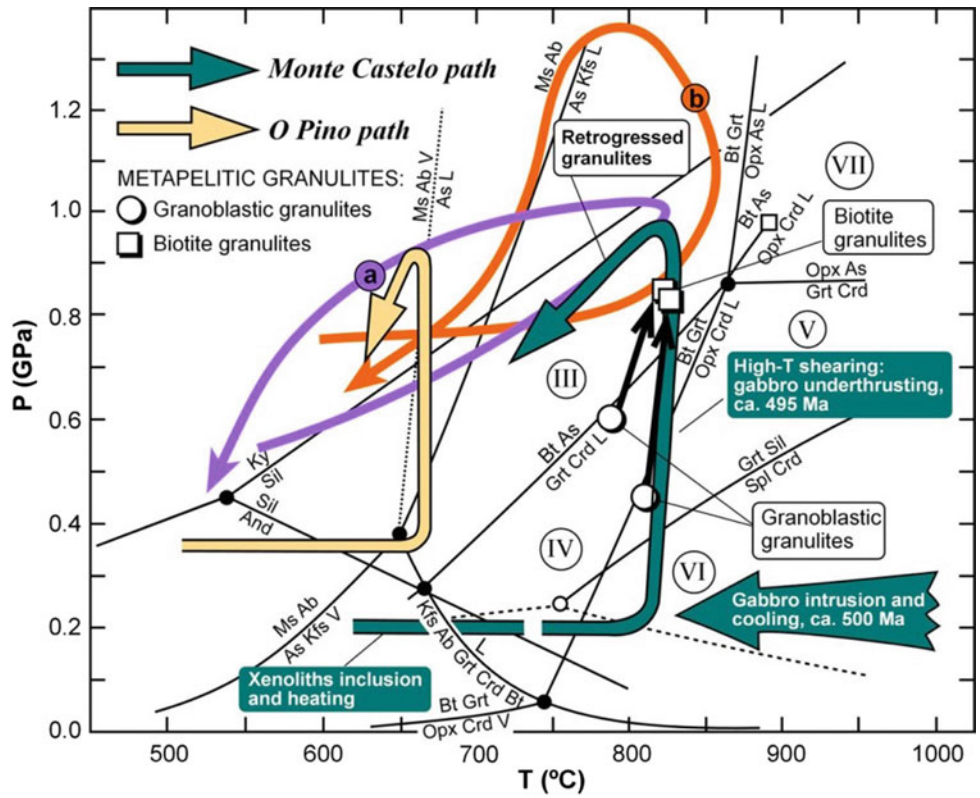

Fig. 4.19 Petrogenetic grid of Spear et al. (1999) showing the P-T path of aluminous granulite xenoliths in the Monte Castelo Unit, and the quantitative P-T estimations obtained with the TWQ method (circles and squares; Abati et al. 2003). The fragment of the path deduced by thermobarometry (black arrows) partially reproduces the path deduced using the petrogenetic grid. For comparison, two trajectories from granulites in terranes of intense magmatic injection are included (**a** Appel et al. 1998; **b** Baba 1998). Also shown is the P-T path obtained for the schists with Grt + St + Ky of the O Pino Unit by Castiñeiras (2005)

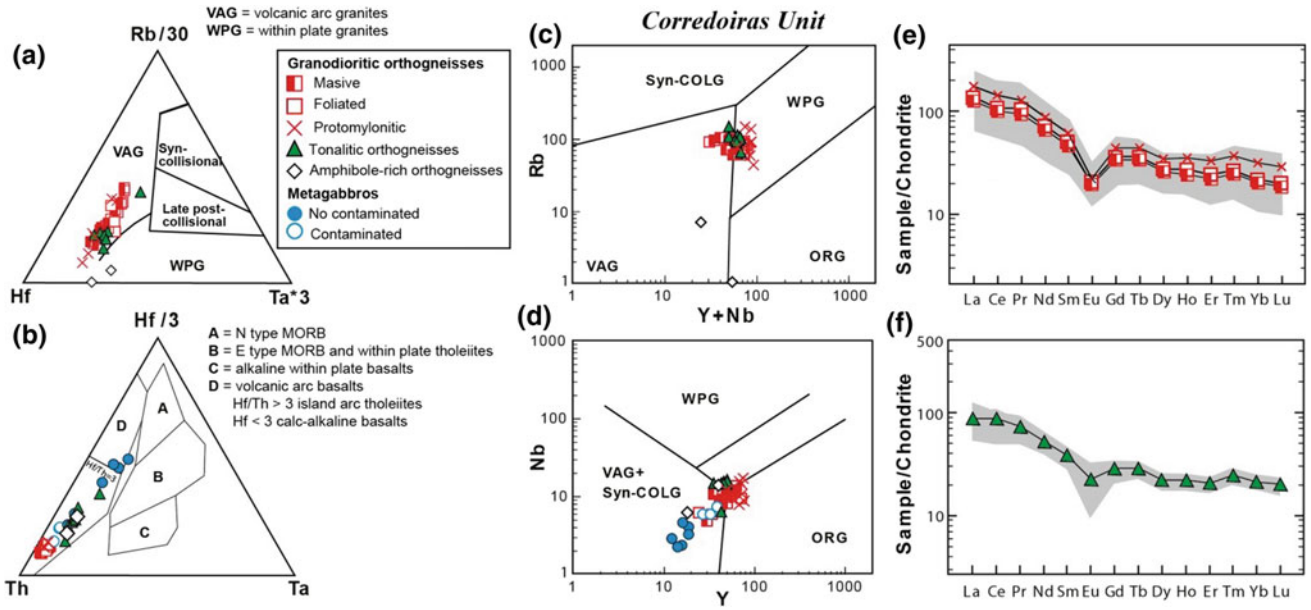

Fig. 4.20 Trace element discrimination diagrams for Corredoiras massif; **a** Rb-Hf-Ta diagram (Harris et al. 1986); **b** Hf-Th-Ta diagram (Wood 1980); **c** Rb-Y + Nb and **d** Nb-Y diagrams after Pearce et al. (1984); **e** Chondrite-normalized rare earth element plots for the granodioritic facies of the Corredoiras orthogneiss with different degrees of deformation: **f** Same for tonalitic facies. Normalizing values are from Nakamura (1974). Shading zone is the rank of total samples variation, and the individual lines correspond to the average of each type of rocks. After Andonaegui et al. (2012)

high-T association in migmatites yielded U-Pb ages of 493 ± 2 and 484 ± 2 Ma (Abati et al. 1999). Metapelites with a well preserved association of Grt + Opx + Bi is indicative of the intermediate-P granulite facies (González Cuadra 2007), and some gabbros show a Pl + Opx + Cpx paragenesis, also indicative of the granulite facies. This represents the same Cambro-Ordovician event identified in the Monte Castelo Unit.

Andonaegui et al. (2016) compared the geochemistry of the small gabbro intrusions at the base of the Corredoiras Unit with that of the Monte Castelo Unit, 45–55 km to the NW, using immobile element diagrams to determine the magmatic affinity of the mafic rocks. As both igneous assemblages are coeval, the authors consider them as formed in a single stage of development of a volcanic arc, but representing different parts of it. As geochemistry points out, the most primitive composition of Monte Castelo mafic body indicates a location within the volcanic arc closer to the trench, while the crustal affinity of Corredoiras igneous assemblage situates it closer to the mainland.

A Silva granodiorite is a metagranitoid that might represent the continuation of the Corredoiras Unit in the western limb of the large synform forming the Órdenes Complex, although cut and displaced by one or more extensional detachments (Díaz García et al. 1999a). It has yielded an imprecise age around 510 Ma (Castiñeiras et al. 2010), slightly older than that of the Corredoiras Unit. A comparable granodioritic massif occurs at the base of the **Lagoa Unit**, in the **Morais Complex**, and dated at 496 ± 3 Ma (Dallmeyer and Tucker 1993) and 484±10 Ma (Mateus et al. 2016).

O Pino Unit, in the Órdenes Complex, is a thick sequence of monotonous mesozonal schists and paragneisses intruded by relatively small bodies of gabbro and granitoids. It rests upon the high-grade metaigneous massifs of Monte Castelo and Corredoiras, from which it is separated by extensional detachments (Díaz García et al. 1999a; Abati 2002). It is also separated from the overlying low-grade Betanzos Unit by an extensional low-dipping fault, the Ponte Carreira detachment (PCD; Figs. 4.2, 4.16 and 4.17; Díaz García 2000).

The schists of the **Lagoa Unit**, in the center of the **Morais Complex**, and the **Cariño Unit**, occupying the core of the Uzal recumbent syncline in the **Cabo Ortegal Complex**, are the equivalent to the O Pino Unit (Figs. 4.2, 4.12 and 4.13). The Cariño Unit includes the San Xiao composite massif (gabbro, granodiorite and granite), whose geochemistry is calc-alkaline and characteristic of a volcanic arc setting (Castiñeiras et al. 2002; Castiñeiras 2005). U-Pb dating and Lu-Hf isotopic composition of zircons of the siliciclastic paragneisses, combined with Sm–Nd whole-rock analyses indicates a maximum depositional age of ca. 510 Ma and a probable derivation from a continental basement rather than a magmatic arc (Albert et al. 2015).

From the point of view of metamorphism, the Cariño and O Pino units represent a classical Barrovian pile, with metamorphic zones ranging from sillimanite below, to almandine above (Castiñeiras 2005). But kyanite is commonly found replacing andalusite pseudomorphs in O Pino Unit, indicating pressurization after heating, as in the Monte Castelo and Corredoiras units. Monazites from semipelitic paragneisses of the Barrovian sillimanite zone have yielded ages of 493 ± 1.3 and 496 ± 3 Ma (Abati et al. 1999), reflecting the Early Ordovician, regional metamorphic event. A P-T path for the O Pino Unit has been included in Figs. 4.3 and 4.19 for comparison.

The **Betanzos Unit** culminates the nappe stack in the Órdenes Complex, and consists of 2000–3000 m of metapelites and greywackes, with alternations of grey to black quartzites and a few conglomerates. Diabase dikes are common, and the metamorphic grade is always low. The facies and sedimentary structures indicate a turbiditic character (Matte and Capdevila 1978). The abundance of volcanic detrital components, when considered together with the chemistry of the Monte Castelo and Corredoiras units, suggest a volcanic arc environment, although the lack of volcanic rocks points to a dissected magmatic arc. The Betanzos Unit probably represents a forearc or back-arc basin fill. The metagreywackes have been investigated for detrital zircon ages, yielding three age populations of 2.5–2.4 Ga, 2.1–1.9 Ga and 610–480 Ma (Fernández-Suárez et al. 2003; Díaz García et al. 2010; Fuenlabrada et al. 2010), which establishes a maximum Cambro-Ordovician depositional age.

4.4.3 Geotectonic Meaning of the Upper Allochthon

The lithological association that characterizes the Upper Allochthon points to a thick and monotonous pelitic to greywacke succession of probable Cambrian age, intruded by a slightly younger, essentially bimodal Cambro-Ordovician plutonic suite. The geochemistry of the latter points to a volcanic-arc signature for the upper group of intermediate-P units, and to a tholeiitic affinity related to continental rifting for the lower group of high-P and high-T units. For the latter, however, the geochemistry of the ultramafic rocks in Cabo Ortegal is consistent with generation in the mantle wedge above a subduction zone.

Considering that the oceanic units of the Middle Allochthon underlie those of the Upper Allochthon and that no suture seems to separate the two groups established in the latter, we can interpret the Upper Allochthon as a peri-Gondwanan terrain pulled apart from the mainland around the Cambro-Ordovician boundary (Fig. 4.4a).

The coeval existence of a subduction zone suggests that the driving mechanism of terrane separation was slab roll-back of an old oceanic lithosphere, possibly that of the Iapetus or Tornquist oceans, that were undergoing closure at the time (e.g., Winchester et al. 2002). The latter is preferred because in reconstructions post-dating the late-Variscan dextral strike-slip motion between Laurussia and Gondwana, the European Variscides were partly situated to the S of Avalonia (in present-day coordinates). Removing the effects of dextral transcurrence, most of the Variscan Belt would be located to the S of Baltica, where the Tornquist suture is located (Martínez Catalán et al. 2007).

Terrane separation would have created a back arc (Fig. 4.4a–c), but the sedimentary succession closer to the mainland received essentially its detrital input from the continent, which is the case of the paragneisses of the Sobrado and Cariño units. Instead, the abundance of volcanic components in the uppermost Betanzos Unit, and the more juvenile isotopic signature (1 Ga vs. 1.7 Ga of the Cariño gneisses according to Nd depleted mantle model ages; Albert et al. 2015) suggest that this culminating unit of the NW Iberia nappe stack was facing the open ocean and subduction zone, while the Cariño and underlying units were closer to the opening back arc. This polarity also explains why the plutons of the upper group of units have arc affinities and those of the lower group suggest continental rifting.

The pre-Variscan metamorphic evolution of the intermediate-P units of the upper group—possibly also present in the lower group, but difficult to recognize due to Variscan overprint—is comparable to paths obtained in active plate margins (Appel et al. 1998; Baba 1998; Hiroi et al. 1998), characterized by pressurization in the sillimanite field, and a subsequent anticlockwise evolution (Figs. 4.3, and 4.19). The first part of the path is related to underplating by large plutons, resulting in an intense heating, whereas the subsequent burial implies severe crustal thickening.

The early Variscan high-P and high-T metamorphic event of the lower group is interpreted as the result of subduction under the upper group, which got rid of the high-P metamorphic imprint (Fig. 4.4d, e). The context was the creation of an accretionary wedge, which possibly developed at the southern margin of Laurussia (Martínez Catalán et al. 1997, 2007, 2009). The building of the wedge continued with the incorporation of the Middle and Lower allochthons during early Variscan convergence that resulted in closure of the intervening ocean. Underthrusting of these new units was coeval with the progressive exhumation of the Upper Allochthon, which continued during subsequent collision and emplacement above the NW Iberian Autochthon (Fig. 4.4e–h).

References

Abati J (2002). Petrología metamórfica y geocronología de la unidad culminante del Complejo de Órdenes en la región de Carballo (Galicia, NW del Macizo Ibérico). Laboratorio Xeolóxico de Laxe, Serie Nova Terra, 20, A Coruña, 269 pp.

Abati J, Dunning GR, Arenas R, Díaz García F, González Cuadra P, Martínez Catalán JR, Andonaegui P (1999). Early Ordovician orogenic event in Galicia (NW Spain): evidence from U-Pb ages in the uppermost unit of the Ordenes Complex. Earth and Planetary Science Letters, 165, 213–228.

Abati J, Arenas R, Martínez Catalán JR, Díaz García F (2003). Anticlockwise P-T path of granulites from the Monte Castelo Gabbro (Órdenes Complex, NW Spain). Journal of Petrology, 44, 305–327.

Abati J, Castiñeiras P, Arenas R, Fernández-Suárez J, Gómez Barreiro J, Wooden JL (2007). Using SHRIMP zircon dating to unravel tectonothermal events in arc environments. The early Paleozoic arc of NW Iberia revisited. Terra Nova, 19, 432–439.

Abati J, Gerdes A, Fernández-Suárez J, Arenas R, Whitehouse MJ, Díez Fernández R (2010). Magmatism and early-Variscan continental subduction in the northern Gondwana margin recorded in zircons from the basal units of Galicia, NW Spain. Geological Society of America Bulletin, 122 (1/2), 219–235.

Albert R, Arenas R, Gerdes A, Sánchez Martínez S, Fernández-Suárez J, Fuenlabrada JM (2015). Provenance of the Variscan Upper Allochthon (Cabo Ortegal Complex, NW Iberian Massif). Gondwana Research, 28, 1434–1448.

Álvarez Valero AM, Gómez Barreiro J, Alampi A, Castiñeiras P, Martínez Catalán JR (2014). Local isobaric heating above an extensional detachment in the middle crust of a Variscan allochthonous terrane (Órdenes complex, NW Spain). Lithosphere, 6, 409–418.

Andonaegui P, González del Tánago J, Arenas R, Abati J, Martínez Catalán JR, Peinado M, Díaz García F (2002). Tectonic setting of the Monte Castelo gabbro (Ordenes Complex, northwestern Iberian Massif): Evidence for an arc-related terrane in the hanging wall to the Variscan suture. In: Martínez Catalán, J.R., Hatcher, R.D., Arenas, R. and Díaz García, F. (Eds.), Variscan-Appalachian Dynamics: the Building of the Late Paleozoic Basement, Geological Society of America Special Paper, 364, 37–56.

Andonaegui P, Castiñeiras P, González Cuadra P, Arenas R, Sánchez Martínez S, Abati J, Díaz García F, Martínez Catalán JR (2012). The Corredoiras orthogneiss (NW Iberian Massif): Geochemistry and geochronology of the Paleozoic magmatic suite developed in a peri-Gondwanan arc. Lithos, 128–131, 84–99.

Andonaegui P, Sánchez-Martínez S, Castiñeiras P, Abati J, Arenas R (2016). Reconstructing subduction polarity through the geochemistry of mafic rocks in a Cambrian magmatic arc along the Gondwana margin (Órdenes Complex, NW Iberian Massif). International Journal of Earth Sciences, 105, 713–725.

Appel P, Möller A, Schenk V (1998). High pressure granulite facies metamorphism in the Pan-African belt of eastern Tanzania: P-T-t evidence against granulite formation by continent collision. Journal of Metamorphic Geology, 16, 491–509.

Arenas R (1991). Opposite P, T, t paths of Hercynian metamorphism between the upper units of the Cabo Ortegal Complex and their substratum (northwest of the Iberian Massif). Tectonophysics, 191, 347–364.

Arenas R, Martínez Catalán JR (2002). Prograde development of corona textures in metagabbros of the Sobrado window (Ordenes Complex, NW Iberian Massif). In: Martínez Catalán, J.R., Hatcher, R.D., Arenas, R. and Díaz García, F. (Eds.), Variscan-Appalachian

Dynamics: the Building of the Late Paleozoic Basement. Geological Society of America Special Paper, 364, 73–88.
Arenas R, Sánchez Martínez S (2015). Variscan ophiolites in NW Iberia: Tracking lost Paleozoic oceans and the assembly of Pangea. Episodes, 38, 315–333.
Arenas R, Martínez Catalán JR, Sánchez Martínez S, Fernández-Suárez J, Andonaegui P, Pearce JÁ, Corfu F (2007a). The Vila de Cruces Ophiolite: A remnant of the early Rheic Ocean in the Variscan suture of Galicia (NW Iberian Massif). Journal of Geology, 115, 129–148.
Arenas R, Martínez Catalán JR, Sánchez Martínez S, Díaz García F, Abati J, Fernández-Suárez J, Andonaegui P, Gómez Barreiro J. (2007b). Paleozoic ophiolites in the Variscan suture of Galicia (northwest Spain): distribution, characteristics and meaning. In: Hatcher, R.D., Jr., Carlson, M.P., McBride, J.H. and Martínez Catalán, J.R. (Eds.), 4-D framework of continental crust. Geological Society of America Memoir, 200, 425–444.
Arenas R, Sánchez Martínez S, Castiñeiras P, Jeffries TE, Díez Fernández R, Andonaegui P (2009). The basal tectonic mélange of the Cabo Ortegal Complex (NW Iberian Massif): a key unit in the suture of Pangea. Journal of Iberian Geology, 35, 85–125.
Arenas R, Sánchez Martínez S, Gerdes A, Albert R, Díez Fernández R, Andonaegui P (2014). Re-interpreting the Devonian ophiolites involved in the Variscan suture: U-Pb and Lu-Hf zircon data of the Moeche Ophiolite (Cabo Ortegal Complex, NW Iberia). International Journal of Earth Sciences, 103, 1385–1402.
Azcárraga J (2000). Evolución tectónica y metamórfica de los mantos inferiores de grado alto y alta presión del complejo de Cabo Ortegal. Laboratorio Xeolóxico de Laxe, Serie Nova Terra, A Coruña, 17, 346 pp.
Baba S (1998). Proterozoic anticlockwise P-T path of the Lewisian Complex of South Harris, Outer Hebrides, NW Scotland. Journal of Metamorphic Geology, 16, 819–841.
Ballèvre M, Martínez Catalán JR, López-Carmona A, Pitra P, Abati J, Díez Fernández R, Ducassou C, Arenas R, Bosse V, Castiñeiras P, Fernández-Suárez J, Gómez Barreiro J, Paquette JL, Peucat JJ, Poujol M, Ruffet G, Sánchez Martínez S (2014). Correlation of the nappe stack in the Ibero-Armorican arc across the Bay of Biscay: a joint French-Spanish project. In: Schulmann, K., Martínez Catalán, J. R., Lardeaux, J.M., Janousek, V. and Oggiano, G. (Eds.), The Variscan Orogeny: Extent, Timescale and the Formation of the European Crust. Geological Society Special Publication, 405, 77–113.
Bastida F, Marcos A, Marquínez J, Martínez Catalán JR, Pérez-Estaún A, Pulgar JA (1984). Mapa Geológico Nacional E. 1:200.000, 1, La Coruña. Instituto Geológico y Minero de España, Madrid.
Castiñeiras P (2005). Origen y evolución tectonotermal de las unidades de O Pino y Cariño (Complejos Alóctonos de Galicia). Laboratorio Xeolóxico de Laxe, Serie Nova Terra, 28, A Coruña, 279 pp.
Castiñeiras P, Andonaegui P, Arenas R, Martínez Catalán JR (2002). Descripción y resultados preliminares del plutón compuesto de San Xiao, Complejo de Cabo Ortegal (noroeste del Macizo Ibérico). Geogaceta, 32, 111–114.
Castiñeiras P, Díaz García F, Gómez Barreiro J (2010). REE-assisted U-Pb zircon age (SHRIMP) of an anatectic granodiorite: constraints on the evolution of the A Silva granodiorite, Iberian Allochthonous Complexes. Lithos, 116, 153–166.
Dallmeyer RD, Tucker RD (1993). U-Pb zircon age for the Lagoa augen gneiss, Morais Complex, Portugal: tectonic implications. Journal of the Geological Society, London, 150, 405–410.
Dallmeyer RD, Ribeiro A, Marques F (1991). Polyphase Variscan emplacement of exotic terranes (Morais and Bragança Massifs) onto Iberian successions: Evidence from $^{40}Ar/^{39}Ar$ mineral ages. Lithos, 27, 133–144.
Dallmeyer RD, Martínez Catalán JR, Arenas R, Gil Ibarguchi JI, Gutiérrez Alonso G, Farias P, Aller J, Bastida F (1997). Diachronous Variscan tectonothermal activity in the NW Iberian Massif: Evidence from $^{40}Ar/^{39}Ar$ dating of regional fabrics. Tectonophysics, 277, 307–337.
Dias da Silva I, Valverde-Vaquero P, González Clavijo E, Díez-Montes A, Martínez Catalán JR (2014). Structural and stratigraphical significance of U-Pb ages from the Mora and Saldanha volcanic complexes (NE Portugal, Iberian Variscides). In: Schulmann, K., Martínez Catalán, J.R., Lardeaux, J.M., Janousek, V. and Oggiano, G. (Eds.), The Variscan Orogeny: Extent, Timescale and the Formation of the European Crust. Geological Society, London, Special Publications, 405, 115–135.
Dias da Silva Í, Díez Fernández R, Díez-Montes A, González Clavijo E, Foster DA (2016) Magmatic evolution in the N-Gondwana margin related to the opening of the Rheic Ocean—evidence from the Upper Parautochthon of the Galicia-Trás-os-Montes Zone and from the Central Iberian Zone (NW Iberian Massif). International Journal of Earth Sciences 105 (4):1127–1151. https://doi.org/10.1007/s00531-015-1232-9.
Dias da Silva Í, González Clavijo E, Díez Montes A, Martínez Catalán JR, Gómez Barreiro J, Hoffmann M, Gärtner A (2017). Furongian-Late Ordovician volcanism in the Upper Parautochthon of the Galicia-Trás-os-Montes Zone (NE Portugal): Paleogeographic meaning and geodynamic setting. In: Ordovician Geodynamics: the Sardic Phase in the Pyrenees, Mouthoumet and Montagne Noire massifs. Álvaro, J.J., Casas, J.M. and Clausen, S. (Eds.), Géologie de la France 1 (4), 19–21.
Díaz García F (1990). La geología del sector occidental del Complejo de Órdenes (Cordillera Hercínica, NW de España). Laboratorio Xeolóxico de Laxe, Serie Nova Terra, 3, A Coruña, 230 pp.
Díaz García F (2000). Lithostratigraphy and structure of the A Coruña Unit. Uppermost units of the Variscan Belt, NW Spain. In: Variscan-Appalachian dynamics: the building of the Upper Paleozoic basement, Basement Tectonics 15, A Coruña, Spain, Program and Abstracts, 92–94.
Díaz García F, Martínez Catalán JR, Arenas R, González Cuadra P (1999a). Structural and kinematic analysis of the Corredoiras Detachment: evidence for early variscan orogenic extension in the Ordenes Complex, NW Spain. International Journal of Earth Sciences, 88, 337–351.
Díaz García F, Arenas R, Martínez Catalán JR, González del Tánago J, Dunning G (1999b). Tectonic evolution of the Careón ophiolite (Northwest Spain): a remnant of oceanic lithosphere in the Variscan belt. Journal of Geology, 107, 587–605.
Díaz García F, Sánchez Martínez S, Castiñeiras P, Fuenlabrada JM, Arenas R (2010). A peri-Gondwanan arc in NW Iberia. II: Assessment of the intra-arc tectonothermal evolution through U-Pb SHRIMP dating of mafic dykes. Gondwana Research, 17, 352–362.
Díez Fernández R, Martínez Catalán JR, Gerdes A, Abati J, Arenas R, Fernández-Suárez J (2010). U-Pb ages of detrital zircons from the Basal allochthonous units of NW Iberia: Provenance and paleoposition on the northern margin of Gondwana during the Neoproterozoic and Paleozoic. Gondwana Research, 18, 385–399.
Díez Fernández R, Martínez Catalán JR, Arenas R, Abati J (2011). Tectonic evolution of a continental subduction-exhumation channel: Variscan structure of the basal allochthonous units in NW Spain. Tectonics 30 (3):1–22. https://doi.org/10.1029/2010tc002850.
Díez Fernández R, Castiñeiras P, Gómez Barreiro J (2012a) Age constraints on Lower Paleozoic convection system: Magmatic events in the NW Iberian Gondwana margin. Gondwana Research 21 (4):1066–1079. https://doi.org/10.1016/j.gr.2011.07.028.
Díez Fernández R, Martínez Catalán JR, Arenas R, Abati J (2012b). The onset of the assembly of Pangaea in NW Iberia: Constraints on the kinematics of continental subduction. Gondwana Research 22 (1):20–25. https://doi.org/10.1016/j.gr.2011.08.004.

Díez Fernández R, Foster DA, Gómez Barreiro J, Alonso-García M (2013). Rheological control on the tectonic evolution of a continental suture zone: the Variscan example from NW Iberia (Spain). International Journal of Earth Sciences, 102, 1305–1319.

Díez Fernández R, Fuenlabrada JM, Chichorro M, Pereira MF, Sánchez-Martínez S, Silva JB, Arenas R (2017) Geochemistry and tectonostratigraphy of the basal allochthonous units of SW Iberia (Évora Massif, Portugal): Keys to the reconstruction of pre-Pangean paleogeography in southern Europe. Lithos 268–271 (Supplement C):285–301. https://doi.org/10.1016/j.lithos.2016.10.031.

Díez-Montes A, González-Clavijo E, Dias da Silva Í, Gómez Barreiro J, Martínez Catalán JR, Castiñeiras P (2015). Geochemical Evolution of Volcanism during the Upper Cambrian- Ordovician Extension of the North Gondwana Margin. In: X Congresso Ibérico de Geoquímica/XVIII Semana de Geoquímica, Alfragide, 2015. Laboratório Nacional de Geologia e Energia, pp 54–57.

Farias P, Gallastegui G, González-Lodeiro F, Marquínez J, Martín Parra LM, Martínez Catalán JR, Pablo Maciá JG, Rodríguez Fernández LR (1987). Aportaciones al conocimiento de la litoestratigrafía y estructura de Galicia Central. Memórias da Faculdade de Ciências, Universidade do Porto, 1, 411–431.

Fernández-Suárez J, Corfu F, Arenas R, Marcos A, Martínez Catalán JR, Díaz García F, Abati J, Fernández FJ (2002). U-Pb evidence for a polyorogenic evolution of the HP-HT units of the NW Iberian Massif. Contributions to Mineralogy and Petrology, 143, 236–253.

Fernández-Suárez J, Díaz García F, Jeffries TE, Arenas R, Abati, J (2003). Constraints on the provenance of the uppermost allochthonous terrane of the NW Iberian Massif: Inferences from detrital zircon U-Pb ages. Terra Nova, 15,138–144.

Fernández-Suárez J, Arenas R, Abati J, Martínez Catalán JR, Whitehouse MJ, Jeffries TE (2007). U-Pb chronometry of polymetamorphic high-pressure granulites: An example from the allochthonous terranes of the NW Iberian Variscan belt. In: Hatcher, R.D., Jr., Carlson, M.P., McBride, J.H. and Martínez Catalán, J.R. (Eds.), 4-D framework of continental crust. Geological Society of America Memoir, 200, 469–488.

Floor P (1966). Petrology of an aegirine-riebeckite gneiss-bearing part of the Hesperian Massif: the Galiñeiro and surrounding areas, Vigo, Spain. Leidse Geologische Mededelingen 36 (1):1–201.

Fuenlabrada JM, Arenas R, Sánchez Martínez S, Díaz García F, Castiñeiras P (2010). A peri-Gondwanan arc in NW Iberia. I: isotopic and geochemical constraints to the origin of the arc – A sedimentary approach. Gondwana Research, 17, 338–351.

Fuenlabrada JM, Arenas R, Díez Fernández R, Sánchez Martínez S, Abati J, López Carmona A (2012) Sm–Nd isotope geochemistry and tectonic setting of the metasedimentary rocks from the basal allochthonous units of NW Iberia (Variscan suture, Galicia). Lithos 148 (Supplement C):196–208. https://doi.org/10.1016/j.lithos.2012.06.002.

Galán G, Marcos A (1997). Geochemical evolution of high-pressure mafic granulites from the Bacariza formation (Cabo Ortegal complex, NW Spain): an example of a heterogeneous lower crust. Geologische Rundschau, 86, 355–539.

Gil Ibarguchi JI, Dallmeyer RD (1991) Hercynian blueschist metamorphism in North Portugal: tectonothermal implications. Journal of Metamorphic Geology 9 (5):539–549. https://doi.org/10.1111/j.1525-1314.1991.tb00547.x.

Gil Ibarguchi JI, Mendia M, Girardeau J, Peucat JJ (1990). Petrology of eclogites and clynopiroxene-garnet metabasites from the Cabo Ortegal Complex (northwestern Spain). Lithos, 25, 133–162.

Girardeau J, Gil Ibarguchi JI (1991). Pyroxenite-rich peridotites of the Cabo Ortegal Complex (Northwestern Spain): Evidence for large-scale upper-mantle heterogeneity. Journal of Petrology, 32 (Spec. Lherzolites Issue), 135–154.

Girardeau J, Gil Ibarguchi JI, Ben Jamaa N (1989). Evidence for heterogeneous upper mantle in the Cabo Ortegal Complex, Spain. Science, 245, 1231–1233.

Gómez Barreiro J, Martínez Catalán JR (2012). The Bazar shear zone (NW Spain): Microstructural and Time-of-Flight neutron diffraction analysis. In: Zucali, M., Spalla, M.I. and Gosso, G. (Eds.) Multiscale structures and tectonic trajectories in active margins, Journal of the Virtual Explorer, 41, (5), 1–24, https://doi.org/10.3809/jvirtex.2011.00296. Electronic Edition, ISSN 1441-8142.

Gómez Barreiro J, Wijbrans JR, Castiñeiras P, Martínez Catalán JR, Arenas R, Díaz García F, Abati J (2006). $^{40}Ar/^{39}Ar$ laserprobe dating of mylonitic fabrics in a polyorogenic terrane of NW Iberia. Journal of the Geological Society, London, 163, 61–73.

Gómez Barreiro J, Martínez Catalán JR, Arenas R, Castiñeiras P, Abati J, Díaz García F, Wijbrans JR (2007). Tectonic evolution of the upper allochthon of the Órdenes Complex (northwestern Iberian Massif): structural constraints to a polyorogenic peri-Gondwanan terrane. In: Linnemann, U., Nance, R.D., Kraft, P. and Zulauf, G. (Eds.).The evolution of the Rheic Ocean: From Avalonian-Cadomian active margin to Alleghenian-Variscan collision. Geologucal Society of America Special Paper, 423, 315–332.

Gómez Barreiro J, Martínez Catalán JR, Díez Fernández R, Arenas R, Díaz García F (2010a). Upper crust reworking during gravitational collapse: the Bembibre-Pico Sacro detachment system (NW Iberia). Journal of the Geological Society, London, 167, 769–784.

Gómez Barreiro J, Martínez Catalán JR, Prior D, Wenk HR, Vogel S, Díaz García F, Arenas R, Sánchez Martínez, S, Lonardelli I (2010b). Fabric development in a Middle Devonian Intraoceanic Subduction Regime: the Careón Ophiolite (Northwest Spain). Journal of Geology, 118, 163–186.

González-Clavijo E, Dias da Silva ÍF, Gutiérrez-Alonso G, Díez Montes A (2016). U/Pb age of a large dacitic block locked in an Early Carboniferous synorogenic mélange in the Parautochthon of NW Iberia: New insights on the structure/sedimentation Variscan interplay. Tectonophysics 681:159–169. https://doi.org/10.1016/j.tecto.2016.01.001.

González Cuadra P (2007). La Unidad de Corredoiras (Complejo de Órdenes, Galicia): Evolución estructural y metamórfica. Laboratorio Xeolóxico de Laxe, Serie Nova Terra, 33, A Coruña, 254 pp.

Green DH, Ringwood AE (1967). An experimental investigation of the gabbro-to-eclogite transformation and its petrological applications. Geochimica et Cosmochimica Acta, 31, 767–833.

Harris NBW, Pearce JA, Tindle AG (1986). Geochemical characteristics of collision-zone magmatism. In: Coward, M.P. and Ries, A. C. (Eds.), Collision Tectonics. Geological Society Special Publication, 19, 67–81.

Hiroi Y, Kishi S, Nohara T, Sato K, Goto J (1998). Cretaceous high-temperature rapid loading and unloading in the Abukuma metamorphic terrane, Japan. Journal of Metamorphic Geology, 16, 67–81.

Holdaway MJ (1971). Stability of andalusite and the aluminium silicate phase diagram. American Journal of Science, 271, 97–131.

Lapierre H, Ortiz LE, Abouchami W, Monod O, Coulon C, Zimmermann JL (1992). A crustal section in an intra-oceanic island arc: the Late Jurassic-Early Cretaceous Guanajuato magmatic sequence, central Mexico. Earth and Planetary Science Letters, 108, 61–77.

Le Maitre RW, Bateman P, Dudek A, Keller J, Lameyre Le Bas MJ, Sabine PA, Schmid R, Sorensen H, Streckeisen A, Wooley AR, Zanettin B (1989). A classification of igneous rocks and glossary of terms. Blackwell Scientific Publications, Oxford, 193 pp.

López-Carmona A, Abati J, Reche J (2010). Petrologic model of chloritoid-glaucophane schists from the NW Iberian Massif. Gondwana Research, 17, 377–391.

López-Carmona A, Pitra P, Abati J (2013): Blueschist-facies pelites from the Malpica-Tui Unit (NW Iberian Massif): phase equilibria

modeling and H_2O and Fe_2O_3 influence in high-pressure assemblages. Journal of Metamorphic Geology 31(3), 263–280. https://doi.org/10.1111/jmg.12018.

López-Carmona A, Abati J, Pitra P, Lee JKW (2014). Retrogressed lawsonite blueschists from the NW Iberian Massif: P-T-t constraints from thermodynamic modelling and $^{40}Ar/^{39}Ar$ geochronology. Contributions to Mineralogy and Petrology, 167, 1–20.

Marcos A, Marquínez J, Pérez-Estaún A, Pulgar JA, Bastida F (1984). Nuevas aportaciones al conocimiento de la evolución tectonometamórfica del Complejo de Cabo Ortegal (NW de España). Cuadernos do Laboratorio Xeolóxico de Laxe, 7, 125–137.

Marcos A, Farias P, Galán G, Fernández FJ, Llana-Fúnez S (2002). Tectonic framework of the Cabo Ortegal Complex: A slab of lower crust exhumed in the Variscan orogen (northwestern Iberian Peninsula). In: Martínez Catalán, J.R., Hatcher Jr., R.D., Arenas, R. and Díaz García, F. (Eds.), Variscan-Appalachian Dynamics: The Building of the Late Paleozoic Basement, Geological Society of America, Special Paper, 364, 125–142.

Marques FG, Ribeiro A, Pereira E (1991–1992). Tectonic evolution of the deep crust: Variscan reactivation by extension and thrusting of Precambrian basement in the Bragança and Morais massifs (Trás-os-Montes, NE Portugal). Geodinamica Acta, 5 (1–2), 135–151.

Marques FO, Ribeiro A, Munhá JM (1996). Geodynamic evolution of the Continental Allochthonous Terrane (CAT) of the Bragança Nappe Complex, NE Portugal. Tectonics, 15, 747–762.

Marquínez García JL (1984) La geología del área esquistosa de Galicia Central (Cordillera Herciniana, NW de España), vol 100. Memoria del Instituto Geológico y Minero de España. Instituto Geológico y Minero de España, Madrid.

Martínez Catalán JR, Arenas R, Díaz García F, Rubio Pascual FJ, Abati J, Marquínez J (1996). Variscan exhumation of a subducted Paleozoic continental margin: The basal units of the Ordenes Complex, Galicia, NW Spain. Tectonics, 15, 106–121.

Martínez Catalán JR, Arenas R, Díaz García F, Abati J (1997). Variscan acretionary complex of northwest Iberia: Terrane correlation and succession of tectonothermal events. Geology, 25, 1103–1106.

Martínez Catalán JR, Arenas R, Díaz García F, Gómez Barreiro J, González Cuadra P, Abati J, Castiñeiras P, Fernández-Suárez J, Sánchez Martínez S, Andonaegui P, Gónzalez Clavijo E, Díez Montes A, Rubio Pascual FJ and Valle Aguado, B. 2007. Space and time in the tectonic evolution of the northwestern Iberian Massif. Implications for the comprehension of the Variscan belt. In: Hatcher, R.D., Jr., Carlson, M.P., McBride, J.H. and Martínez Catalán, J.R. (Eds.), 4-D framework of continental crust. Geological Society of America Memoir, 200, 403–423.

Martínez Catalán JR, Arenas R, Abati J, Sánchez Martínez S, Díaz García F, Fernández-Suárez J, González Cuadra P, Castiñeiras P, Gómez Barreiro J, Díez Montes A, González Clavijo, E, Rubio Pascual FJ, Andonaegui P, Jeffries TE, Alcock JE, Díez Fernández R, López Carmona A (2009). A rootless suture and the loss of the roots of a mountain chain: the Variscan belt of NW Iberia. Comptes Rendus Geoscience, 341, 114–126.

Martínez SS, Gerdes A, Arenas R, Abati J (2012). The Bazar Ophiolite of NW Iberia: a relic of the Iapetus-Tornquist Ocean in the Variscan suture. Terra Nova, 24, 283–294.

Matte Ph, Capdevila R (1978). Tectonique en grands plis couchés et plissements superposés d'âge hercynien dans la série de Ordenes-Betanzos (Galice Occidentale). Cuadernos del Seminario de Estudios Cerámicos de Sargadelos, 27, 193–201.

Mateus A, Munhá J, Ribeiro A, Tassinari CCG, Sato K, Pereira E, Santos JF (2016). U-Pb SHRIMP zircon dating of high-grade rocks from the Upper Allochthonous Terrane of Bragança and Morais Massifs (NE Portugal); geodynamic consequences. Tectonophysics, 675, 23–49.

Mendia Aranguren MS (2000). Petrología de la Unidad Eclogítica del Complejo de Cabo Ortegal (NW de España). Laboratorio Xeolóxico de Laxe, Serie Nova Terra, 16, A Coruña, 424 pp.

Montero P, Bea F, Corretgé LG, Floor P, Whitehouse MJ (2009). U-Pb ion microprobe dating and Sr and Nd isotope geology of the Galiñeiro Igneous Complex: A model for the peraluminous/peralkaline duality of the Cambro-Ordovician magmatism of Iberia. Lithos 107 (3):227–238. https://doi.org/10.1016/j.lithos.2008.10.009.

Moreno T, Gibbons W., Prichard HM, Lunar R (2001). Platiniferous chromitites and the tectonic setting of ultramafic rocks in Cabo Ortegal (North West Spain). Journal of the Geological Society, London, 158, 601–614.

Mullen ED (1983). MnO/TiO2/P2O5: a minor element discriminant for basaltic rocks of oceanic environments and its implications for petrogenesis. Earth and Planetary Science Letters, 62, 53–62.

Munhá J, Ribeiro A, Ribeiro ML (1984) Blueschists in the Iberian Variscan Chain (Trás-os-Montes, NE Portugal). Comunicações dos Serviços Geológicos de Portugal 70 (1):31–5.

Nakamura N (1974). Determination of REE, Ba, Fe, Mg, Na, and K in carbonaceous and ordinary chondrites. Geochimica et Cosmochimica Acta, 38, 757–775.

Navarro NB, Maresch WV, Schertl H, Baumann A, Krebs M (2003) Petrology of the high-pressure "Basal Unit", Morais Complex, Northeast Portugal. Indian Journal of Geology 75 (1–4):9–37.

Nicolas A (1989). Structures of Ophiolites and Dynamics of Oceanic Lithosphere. Petrology and Structural Geology, 4. Kluwer, Dordrecht, 367 pp.

Ordóñez Casado B, Gebauer D, Schäfer HJ, Gil Ibarguchi JI, Peucat JJ (2001). A single Devonian subduction event for the HP/HT metamorphism of the Cabo Ortegal complex within the Iberian Massif. Tectonophysics, 332, 359–385.

Pablo Maciá JG, Martínez Catalán JR (1984). Estructura, petrología y evolución de la región de Sobrado de los Monjes (La Coruña). Cuadernos do Laboratorio Xeolóxico de Laxe, 7, 103–124.

Pearce JA (1975). Basalt geochemistry to investigate past tectonic environments on Cyprus. Tectonophysics, 25, 41–67.

Pearce JA (1982). Trace element characteristics of lavas from destructive plate boundaries. In: Thorpe RS (Ed.): Andesites, John Wiley & Sons, 525–548.

Pearce JA (1996). A users guide to basalt discrimination diagrams. In: Wyman DA (Ed.), Trace Element Geochemistry of Volcanic Rocks: Applications for Massive Sulphide Exploration. Short Course Notes. Geological Association of Canada, 12, 79–113.

Pearce JA, Cann JR (1973). Tectonic setting of basic volcanic rocks determined using trace element analyses. Earth and Planetary Science Letters, 19, 290–300.

Pearce JA, Peate DW (1995). Tectonic implications of composition of volcanic arc magmas. Annual Review of Earth Planetary Sciences, 23, 251–285.

Pearce JA, Harris NG, Tindle AG (1984). Trace element discrimination diagrams for the tectonic interpretation of granitic rocks. Journal of Petrology, 25, 956–983.

Pereira E, Ribeiro A, Oliveira DPS, Machado MJ, Moreira ME, Castro P (2003). Unidade de Pombais: - Ofiolito inferior do Maciço de Morais (NE de Trás-os-Montes Portugal). Ciências da Terra (UNL), Spec. Vol. V, CD.ROM B76-B80.

Pereira E, Pereira D, Rodrigues JF, Ribeiro A, Noronha F, Ferreira N, Sá CMd, Farinha Ramos J, Moreira A, Oliveira AF (2006). Notícia Explicativa da Folha 2 da Carta Geológica de Portugal à Escala 1:200.000. Instituto Nacional de Engenharia, Tecnologia e Inovação, Lisboa.

Pereira MF, Linnemann U, Hofmann M, Chichorro M, Solá AR, Medina J, Silva JB (2012) The provenance of Late Ediacaran and Early Ordovician siliciclastic rocks in the Southwest Central Iberian Zone: Constraints from detrital zircon data on northern Gondwana margin evolution during the late Neoproterozoic. Precambrian Research 192–195:166–189. https://doi.org/10.1016/j.precamres.2011.10.019.

Peucat JJ, Bernard-Griffiths J, Gil Ibarguchi JI, Dallmeyer RD, Menot RP, Cornichet J, Iglesias Ponce de León, M (1990). Geochemical and geochronological cross section of the deep Variscan crust: The Cabo Ortegal high-pressure nappe (northwestern Spain). Tectonophysics, 177, 263–292.

Pin C, Paquette JL, Santos Zalduegui JF, Gil Ibarguchi JI (2002). Early Devonian supra-subduction zone ophiolite related to incipient collisional processes in the Western Variscan Belt: The Sierra de Careón unit, Ordenes Complex, Galicia. In: Martínez Catalán, J.R., Hatcher, R.D., Arenas, R. and Díaz García, F. (Eds.), Variscan-Appalachian Dynamics: the Building of the Late Paleozoic Basement. Geological Society of America Special Paper, 364, 57–71.

Pin C, Paquette JL, Ábalos B, Santos FJ, Gil Ibarguchi JI (2006). Composite origin of an early Variscan transported suture: Ophiolitic units of the Morais Nappe Complex (north Portugal). Tectonics, 25, TC5001, 1–19.

Puelles P (2004). Deformación, metamorfismo y exhumación de las granulitas de alta presión de la Bacariza (Complejo de Cabo Ortegal, NO España). Laboratorio Xeolóxico de Laxe, Serie Nova Terra, 23, A Coruña, 411 pp.

Ribeiro A (1974). Contribution a l'étude tectonique de Trás-os-Montes Oriental. Memórias dos Serviços Geológicos de Portugal. Serviços Geológicos de Portugal, vol 24.

Ribeiro ML (1986). Geologia e petrologia da região a SW de Macedo de Cavaleiros. Tese de doutoramento, Universidade de Lisboa, Lisboa.

Ribeiro ML (1987) Petrogenesis of early paleozoic peralkaline rhyolites from the Macedo de Cavaleiros region (NE Portugal). Geologische Rundschau 76 (1):147–168. https://doi.org/10.1007/bf01820579.

Ribeiro ML (1991) Contribuição para o conhecimento estratigráfico e petrológico da região a SW de Macedo de Cavaleiros (Trás-os--Montes Oriental). Memórias dos Serviços Geológicos de Portugal, vol 30. Serviços Geológicos de Portugal, Lisboa.

Ribeiro A, Pereira E, Dias R, Gil Ibarguchi JI, Arenas R (1990a) Allochthonous Sequences. In: Dallmeyer RD, Garcia EM (eds) Pre-Mesozoic Geology of Iberia. Springer Berlin Heidelberg, Berlin, Heidelberg, 220–246. https://doi.org/10.1007/978-3-642-83980-1-15.

Ribeiro A, Quesada C, Dallmeyer RD (1990b). Geodynamic evolution of the Iberian Massif. In: Dallmeyer R.D. and Martínez García E. (Eds.), Pre-Mesozoic Geology of Iberia. Springer-Verlag, Berlín, 399–409.

Ribeiro A, Pereira E, Ribeiro ML, Castro P (2013). Unidades Alóctones da região de Morais (Trás-os-Montes oriental). In: Dias R, Araújo A, Terrinha P, Kullberg JC (eds) Geologia de Portugal, Vol. I - Geologia Pré-mesozoica de Portugal, 333–376.

Ringwood AE, Green DH (1966). An experimental investigation of the gabbro-eclogite transformation and some geophysical implications. Tectonophysics, 3, 383–427.

Rodrigues JF, Ribeiro A, Pereira E (2013) Complexo de Mantos Parautóctones do NE de Portugal:estructura interna e tectonoestratigrafia. In: Dias R, Araújo A, Terrinha P, Kullberg JC (eds) Geologia de Portugal, vol Vol. I - Geologia Pré-mesozoica de Portugal, 275–331.

Rodríguez Aller J (2005). Recristalización y deformación de litologías supracorticales sometidas a metamorfismo de alta presión (Complejo de Malpica-Tuy, NO del Macizo Ibérico). Laboratorio Xeolóxico de Laxe, Serie Nova Terra, 29, A Coruña, 572 pp.

Rodríguez J, Cosca MA, Gil Ibarguchi JI, Dallmeyer RD (2003). Strain partitioning and preservation of 40Ar/39Ar ages during Variscan exhumation of a subducted crust (Malpica–Tui complex, NW Spain). Lithos 70 (3–4):111–139. https://doi.org/10.1016/s0024-4937(03)00095-1.

Sánchez Martínez S (2009). Geoquímica y geocronología de las ofiolitas de Galicia. Laboratorio Xeolóxico de Laxe, Instituto Universitario de Xeoloxía, A Coruña, Spain, Serie Nova Terra, 37, 351 pp.

Sánchez Martínez S, Jeffries T, Arenas R, Fernández-Suárez J, García-Sánchez R (2006). A pre-Rodinian ophiolite involved in the Variscan suture of Galicia (Cabo Ortegal Complex, NW Spain). Journal of the Geological Society, London, 163, 737–740.

Sánchez Martínez S, Arenas R, Díaz García F, Martínez Catalán JR, Gómez Barreiro J, Pearce JA (2007a). Careón Ophiolite, NW Spain: Suprasubduction zone setting for the youngest Rheic Ocean floor. Geology, 35, 53–56.

Sánchez Martínez S, Arenas R, Andonaegui P, Martínez Catalán JR, Pearce JA (2007b). Geochemistry of two associated ophiolites from the Cabo Ortegal complex (Variscan belt of northwest Spain). In: Hatcher, R.D., Jr., Carlson, M.P., McBride, J.H. and Martínez Catalán, J.R. (Eds.), 4-D framework of continental crust. Geological Society of America Memoir, 200, 445–467.

Sánchez Martínez S, Arenas R, Gerdes A, Castiñeiras P, Potrel A, Fernández-Suárez J (2011). Isotope geochemistry and revised geochronology of the Purrido Ophiolite (Cabo Ortegal Complex, NW Iberian Massif): Devonian magmatism with mixed sources and involved Mesoproterozoic basement. Journal of the Geological Society, 168, 733–750.

Santos Zalduegui JF, Schärer U, Gil Ibarguchi JI, Girardeau J (1996). Origin and evolution of the Paleozoic Cabo Ortegal ultramafic-mafic complex (NW Spain): U-Pb, Rb-Sr and Pb-Pb isotope data. Chemical Geology, 129, 281–304.

Santos JF, Schärer U, Gil Ibarguchi JI, Girardeau J (2002). Genesis of pyroxenite-rich peritotite at Cabo Ortegal (NW Spain): geochemical and Pb-Sr-Nd isotope data. Journal of Petrology, 43, 17–43.

Schäfer HJ, Gebauer D, Gil Ibarguchi JI, Peucat JJ (1993). Ion-microprobe U-Pb zircon dating on the HP/HT Cabo Ortegal Complex (Galicia, NW Spain): preliminary results. Terra Abstracts, 5, 4, 22.

Schermerhorn LJG, Kotsch S (1984) First occurrence of lawsonite in Portugal and tectonic implications. Comunicações do Instituto Geológico e Mineiro 70 (1):23–29.

Spear FS, Kohn JM, Cheney JT (1999). P-T paths from anatectic pelites. Contributions to Mineralogy and Petrology, 134, 17–32.

Valverde-Vaquero P, Fernández FJ (1996). Edad de enfriamiento U/Pb en rutilos del Gneis de Chímparra (Cabo Ortegal, NO de España). Geogaceta, 20, 475–478.

Valverde-Vaquero P, Marcos A, Farias P, Gallastegui G, (2005). U-Pb dating of Ordovician felsic volcanism in the Schistose Domain of the Galicia-Trás-os-Montes Zone near Cabo Ortegal (NW Spain). Geológica Acta, 3, 27–37.

Vogel DE (1967). Petrology of an eclogite -and pyrigarnite- bearing polymetamorphic rock Complex at Cabo Ortegal, NW Spain. Leidse Geologische Mededelingen, 40, 121–213.

Wilson M (1989). Igneous Petrogenesis. London, Unwin Hyman, 466 pp.

Winchester JA, Floyd PA (1977). Geochemical discrimination of different magma series and their differentiation products using immobile elements. Chemical Geology, 20, 325–343.

Winchester JA, Pharaoh TC, Verniers J (2002). Palaeozoic amalgamation of Central Europe: an introduction and synthesis of new results

from recent geological and geophysical investigations. In: Winchester, J.A., Pharaoh, T.C. and Verniers, J. (Eds.), Palaeozoic Amalgamation of Central Europe. Geological Society Special Publication, 201, 1–18.

Wood DA (1980). The application of a Th-Hf-Ta diagram to problems of tectonomagmatic classification and to establishing the nature of crustal contamination of basaltic lavas of the British Tertiary Volcanic Province. Earth and Planetary Science Letters, 50, 11–30.

SW Iberia Variscan Suture Zone: Oceanic Affinity Units

5

C. Quesada, J. A. Braid, P. Fernandes, P. Ferreira, R. S. Jorge, J. X. Matos, J. B. Murphy, J. T. Oliveira, J. Pedro, and Z. Pereira

Abstract

The geology of SW Iberia records a sequence of geologic events from the Cambrian-Early Ordovician rifting and subsequent passive margin development along the southern flank of the Rheic Ocean, to onset of oblique (sinistral) subduction in the Devonian, followed by oblique terrane accretion, ocean closure/continental collision and orogenic collapse. As a result, SW Iberia contains the southernmost exposure of the Pangean suture in the European Variscides. This suture zone is characterized by a belt of dismembered oceanic-related rocks and HP metamorphic complexes which are tectonically juxtaposed with the Gondwanan passive margin to the north (OMZ) and with the exotic South Portuguese Terrane to the south, which is thought to be either a remnant of Avalonia or Meguma.

Coordinator: C. Quesada.

C. Quesada (✉)
Instituto Geológico y Minero de España, Ríos Rosas 23, 28003 Madrid, Spain
e-mail: quesada.cecilio@gmail.com

C. Quesada
Facultad de Ciencias Geológicas, Universidad Complutense, Madrid, Spain

J. A. Braid · J. B. Murphy
Department of Earth Sciences, Saint Francis Xavier University, Antigonish, NS B2G 2W5, Canada
e-mail: jbraid@stfx.ca

J. B. Murphy
e-mail: bmurphy@stfx.ca

P. Fernandes
CIMA - Centro de Investigação Marinha e Ambiental, Universidade do Algarve, Campus de Gambelas, 8005-139 Faro, Portugal
e-mail: pfernandes@ualg.pt

P. Ferreira · J. T. Oliveira
Laboratorio Nacional de Energia e Geologia (LNEG), Ap. 7586-Alfragide, 2611-901 Amadora, Portugal
e-mail: pedro.ferreira@lneg.pt

5.1 Introduction

C. Quesada, J. A. Braid, J. B. Murphy

It is generally agreed that the geology of SW Iberia records a sequence of geologic events from the Cambrian-Early Ordovician rifting and subsequent passive margin development along the southern flank of the Rheic Ocean, to onset of oblique (sinistral) subduction in the Devonian, followed by oblique terrane accretion, ocean closure/continental collision and orogenic collapse. As a result, SW Iberia contains the southernmost exposure of the Pangean suture in the European Variscides. This suture zone is characterized by a belt of dismembered oceanic-related rocks and HP metamorphic complexes (see Chap. 12 in this volume), which are tectonically juxtaposed with the Gondwanan passive margin to the north (OMZ) and with the exotic South Portuguese Terrane to the south, which is thought to be either a remnant

J. T. Oliveira
e-mail: josetomas.oliveira@gmail.com

R. S. Jorge
Faculdade de Ciências, IDL - Instituto Dom Luiz, Universidade de Lisboa, Campo Grande, Edifício C6, Piso 4, 1749-016 Lisbon, Portugal
e-mail: rjorge@fc.ul.pt

J. X. Matos
Laboratório Nacional de Energia e Geologia (LNEG), Centro de Estudos Geológicos e Mineiros do Alentejo, Bairro da Vale d'Oca, Ap. 14, 7600-020 Aljustrel, Portugal
e-mail: joao.matos@lneg.pt

J. Pedro
Instituto de Ciências da Terra, Departamento de Geociências da Universidade de Évora, 7000-671 Évora, Portugal
e-mail: jpedro@uevora.pt

Z. Pereira
Laboratório Nacional de Energia e Geologia (LNEG), Rua da Amieira, Ap. 1089, 4466-901 São Mamede de Infesta, Portugal
e-mail: zelia.pereira@lneg.pt

C. Quesada and J. T. Oliveira (eds.), *The Geology of Iberia: A Geodynamic Approach*, Regional Geology Reviews,
https://doi.org/10.1007/978-3-030-10519-8_5

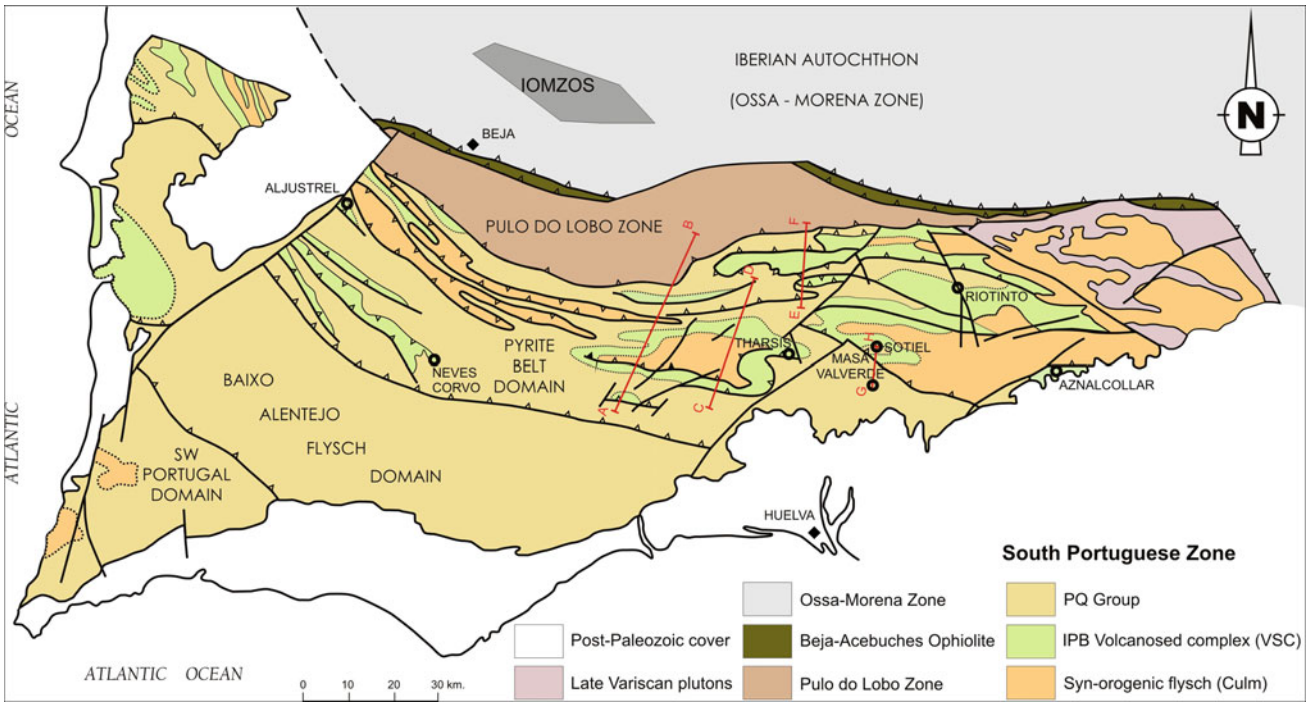

Fig. 5.1 Sketch geological map showing the location of the oceanic affinity units in SW Iberia. Due to structural complexity, only a polygonal outline of the main outcrops of the Internal Ossa Morena Zone Ophiolite Complexes (IOMZOS) is depicted (see Fig. 5.2 for more detail). Modified from Castroviejo et al. (2011)

of Avalonia (Martínez Catalán et al. 1997) or Meguma (Braid et al. 2011, 2012); see Chap. 6 in this volume for a detailed review and discussion.

Oceanic affinity sequences in the SW Iberia suture zone crop out in three different tectono-stratigraphic units, from south to north (Fig. 5.1):

(1) Pulo do Lobo Zone (PDL) of Quesada (1991) or Terrane (terminology used in this volume);
(2) Beja-Acebuches ophiolite belt (BAO; Munhá et al. 1986; Quesada et al. 1994);
(3) In an allochthonous nappe pile which overlies para-autochthonous OMZ sequences north of the main suture zone belt delineated by the other two units (so-called Internal Ossa Morena Zone Ophiolite Sequences-IOMZOS; Fonseca et al. 1999; Pedro 2004; Pedro et al. 2005, 2006, 2013).

With the exception of the Beja Acebuches Ophiolite, almost exclusively composed of E-to N-MORB metamafic and metaultrabasic rocks, metasediments occur associated to the ocean-floor affinity rocks in the other two units.

In structural terms, the PDL and BAO appear sandwiched (Fig. 5.1) with a south vergence between the OMZ (above and to the N) and the SPT (below and to the S). Noteworthy, apart from thrust components the deformation responsible for this structural arrangement includes an important sinistral component as is characteristic of the entire SW Iberia Variscan orogen (Ribeiro et al. 1990; Quesada 1991; and subsequent workers). In the case of the PDL and BAO oceanic exotic units this is envisaged as the result of their accretion to the upper plate during northward-directed (modern coordinates) sinistral subduction of the Rheic (?) Ocean (Ribeiro et al. 1990; Quesada 1991, 2006; Eden 1991; Quesada et al. 1994; Onézime et al. 2003). Recent finding of HP metamorphic relics in PDL rocks (Rubio Pascual et al. 2013) provides further support to the above interpretation. In turn, the IOMZOS appear disconnected from the main suture zone belt and occur imbricated within the so-called Cubito-Moura schist (also called Moura Phyllonitic Complex in Portugal), a tectonic mélange affected by HP located some tens of kilometers north of the southern boundary of the OMZ with the BAO. The Cubito-Moura schist outcrops for ca. 150 km but oceanic affinity rocks of the IOMZOS only occur in its western reaches in Portugal.

In the following sections we review and discuss the characteristics of the three units that contain oceanic affinity sequences, arranged according to the time of formation of their protoliths and the time of their accretion to the OMZ.

5.2 The Internal Ossa Morena Zone Ophiolitic Sequences

J. Pedro

5.2.1 Introduction

The Beja-Acebuches Ophiolite (Munhá et al. 1986) was the first reference to ophiolitic terranes in southwestern domains of OMZ, related with the closure of oceanic basins and continental collision during the Variscan Orogeny in Devonian and Carboniferous times (Matte 1991). According to this, the Beja-Acebuches Ophiolitic Complex (BAO) was interpreted as a thin amphibolite-serpentinite belt, metamorphosed and tectonically inverted, along the contact between the Ossa-Morena Zone and the South Portuguese Zone (Fig. 5.1), marking the SW-Iberia Variscan Suture and recording the closure of Rheic and related oceans through a subduction towards NNE (Fonseca and Ribeiro 1993; Quesada et al. 1994; Fonseca et al. 1999; Ribeiro et al. 2007, 2010). The geological data and tholeiitic to calk-alkaline geochemical features suggest that the BAO represents an ophiolite derived from a narrow and short-lived back-arc basin (Munhá et al. 1986; Quesada et al. 1994). Azor et al. (2008) obtained crystallization ages of ca. 332–340 Ma (SHRIMP U-Pb zircon) in BAO amphibolites and proposed a BAO generation from a narrow and very ephemeral oceanic-basin opened in Early Carboniferous times, after total consumption of the Rheic Ocean. Alternatively, Ribeiro et al. (2010) discussed the genesis of BAO and, based on Sm-Nd model ages, proposed a time-span of 400–370 Ma for the opening and closure of the Beja-Acebuches back-arc basin and an age of ca. 350 Ma for the ophiolitic complex emplacement onto the SW margin of OMZ, latter intruded by the Igneous Beja Gabroic Complex (ca. 350–340 Ma; Jesus et al. 2007). Regardless of the latter interpretation on the age and the BAO precursor basin, it is understandable that the BAO underlying the SW-Iberia Variscan Suture could not be correlated with the Rheic Ocean due to its derivation from a marginal oceanic basin.

In order to better understand the geodynamic meaning of the SW Iberia Variscan Suture, field work developed north of the BAO in inner domains of OMZ (Araújo et al. 1993) revealed the presence of klippes with sequences of ultramafic, mafic and meta-sedimentary rocks preserving the typical "oceanic lithosphere pseudostratigraphy", similar to those described for the classic ophiolites. These sequences—the Internal Ossa-Morena Zone Ophiolitic Sequences (IOMZOS)—are interpreted as an internal ophiolite representing remnants of the Rheic Ocean inside the OMZ (Fonseca et al. 1999; Pedro 2004; Pedro et al. 2005, 2006, 2013). They consists of metric to kilometric allochthonous and dismembered fragments of oceanic lithosphere, cropping out on top and/or imbricated inside the Moura Phyllonitic Complex (Fonseca et al. 1999; Pedro 2004; Araújo et al. 2005, 2013; Pedro et al. 2005, 2006, 2013; Ribeiro et al. 2010), that correspond to a basal tectonic mélange mainly formed by mica-schists and affected by high-P metamorphism during the Late Devonian (Araújo et al. 2005; Booth-Rea et al. 2006; Rosas et al. 2008; Rubio Pascual et al. 2013).

5.2.2 Geological Setting of the IOMZOS

The IOMZOS is formed by five ophiolitic fragments (i.e. Antas, Santana, Oriola, S. Lourenço and Vila Ruiva fragments; Fig. 5.2) defining a narrow and discontinuous WNW-ESE ophiolitic belt located 50–100 km to the north of the SW Iberia Variscan suture main belt. Shear zones and related structures preserved in the IOMZOS record micro-, meso- and macroscopic kinematic indicators which indicate transport and emplacement towards the north (present day coordinates) (Araújo et al. 2005, 2006, 2013; Ribeiro et al. 2010). Greenschist/amphibolite metamorphic recrystallisation and strong Variscan deformation overprinted these ophiolitic fragments and, in some cases, maked the sequences incomplete and difficult to recognize. However, detailed geological mapping supported by mineralogical and petrological/geochemical data (Pedro 2004) allowed the reconstruction of the different ophiolitic units, which are always separated by shear zones.

As a whole, the IOMZOS fragments preserve the typical "oceanic lithosphere pseudostratigraphy" matching those described for the classic ophiolites (Fig. 5.3). They include (from bottom to top): strongly serpentinised dunites and wehrlites, pyroxenite cumulates, metagabbros and flaser-gabbros, metagabbros intruded by metadoleritic dikes, metabasalts, and metacherts. The reconstruction of a complete oceanic lithosphere cross-section with a thin and discontinuous crustal structure, with sporadic stratiform pyroxenite cumulates as well as a section of serpentinised mantellic peridotite, that is often cut by pegmatoid metagabbro and metadolerite/metabasalt dikes, is the main geological evidence that the IOMZOS are remnants of the Rheic Ocean in SW Iberia.

5.2.3 Geochemistry and Petrogenesis

Pedro et al. (2010) presented detailed whole-rock geochemical data from IOMZOS metabasalts and metagabbros and discussed the geochemical fingerprints and petrogenesis of IOMZOS, in order to decipher their geotectonic settings.

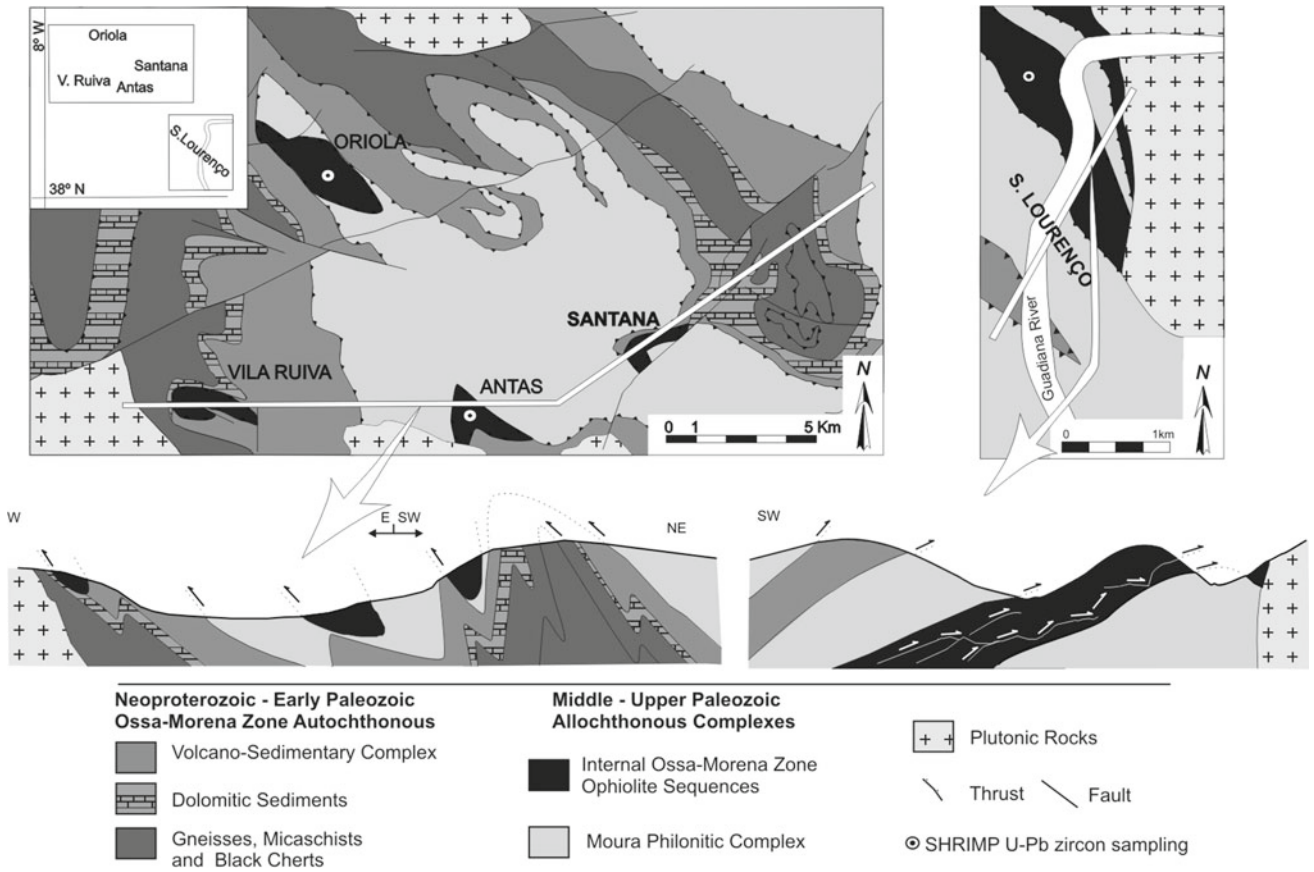

Fig. 5.2 Schematic geological map and interpretative cross-section of the Internal Ossa-Morena Zone Ophiolite Sequences, adapted after Pedro (2004)

Data from selected and representative metabasic rocks (Table 5.1) display SiO_2 (45.93–48.63 wt%) and alkali contents ($Na_2O + K_2O$ = 1.95 to 3.57 wt%) transitional between alkalic and sub-alkalic basalts (Middlemost 1975; Wilson 1989), while the Alkali Index (0.06–0.21) and Al_2O_3 contents (9.57–17.81 wt%) suggest tholeiitic affinities for the IOMZOS metabasic rocks (Middlemost 1975). Pedro et al. (2010) defined a general negative correlation between Fe_2O_3 tot and TiO_2 against mg# values, without a significant variation in SiO_2, which supports the tholeiitic affinities for the IOMZOS igneous protoliths, whereas the TiO_2 >0.7% sustain the assumption that the IOMZOS metabasic rocks are derived from MORB-type magmas with high Ti contents (Sun and Nesbitt 1978).

The IOMZOS metabasalts and metagabbros concentrations of Th (0.8 ± 0.7 ppm), Ta (0.7 ± 0.7 ppm), Zr (94.7 ± 32.4 ppm), Hf (2.3 ± 0.6 ppm), Ti (8423 ± 1931 ppm) and Y (23.7 ± 2.7 ppm) are comprised within the range of ocean-floor tholeiites (Pearce and Cann 1973; Wood 1980; Sun and McDonough 1989) in accordance with the above tholeiitic affinity suggested by the major elements. Variations in incompatible element ratios like Ti/Zr (93.1 ± 16.3) and Zr/Y (4.0 ± 1.4) and appropriate diagrammatic representation such as the Th-Hf-Ta discriminating diagram (after Wood 1980; Fig. 5.4) support the tholeiitic affinity of IOMZOS metabasic rocks. The data plotted in Fig. 5.4 show an affinity between the IOMZOS metabasic rocks and anorogenic oceanic basalts, ranging from N-MORB (less enriched) to Alkaline Within-Plate Basalts (more enriched) and do not suggest any orogenic geochemical signature for the IOMZOS metabasic rocks.

This anorogenic geochemical fingerprint of IOMZOS metabasic rocks is also well defined in the La/Nb and La/Th ratios. These pairs of elements (La/Nb = 1.05 ± 0.3; La/Th = 13.82 ± 4.8) show positive correlations between them, with coherent and progressive enrichment in LILE (Large Ion Lithophile Elements) and HFSE (High Field Strength Elements), without the typical LILE/HFSE decoupling observed in many orogenic basalts (Gill 1981; Pearce 1982, 1983; Wilson 1989; Miyashiro 1974; Juteau and Maury 1999). According to Pedro et al. (2010) the IOMZOS La/Nb and La/Th ratio variations define a geochemical transitional MORB (T-MORB) fingerprint for the IOMZOS metabasic rocks, with abundances and ratios between the reported

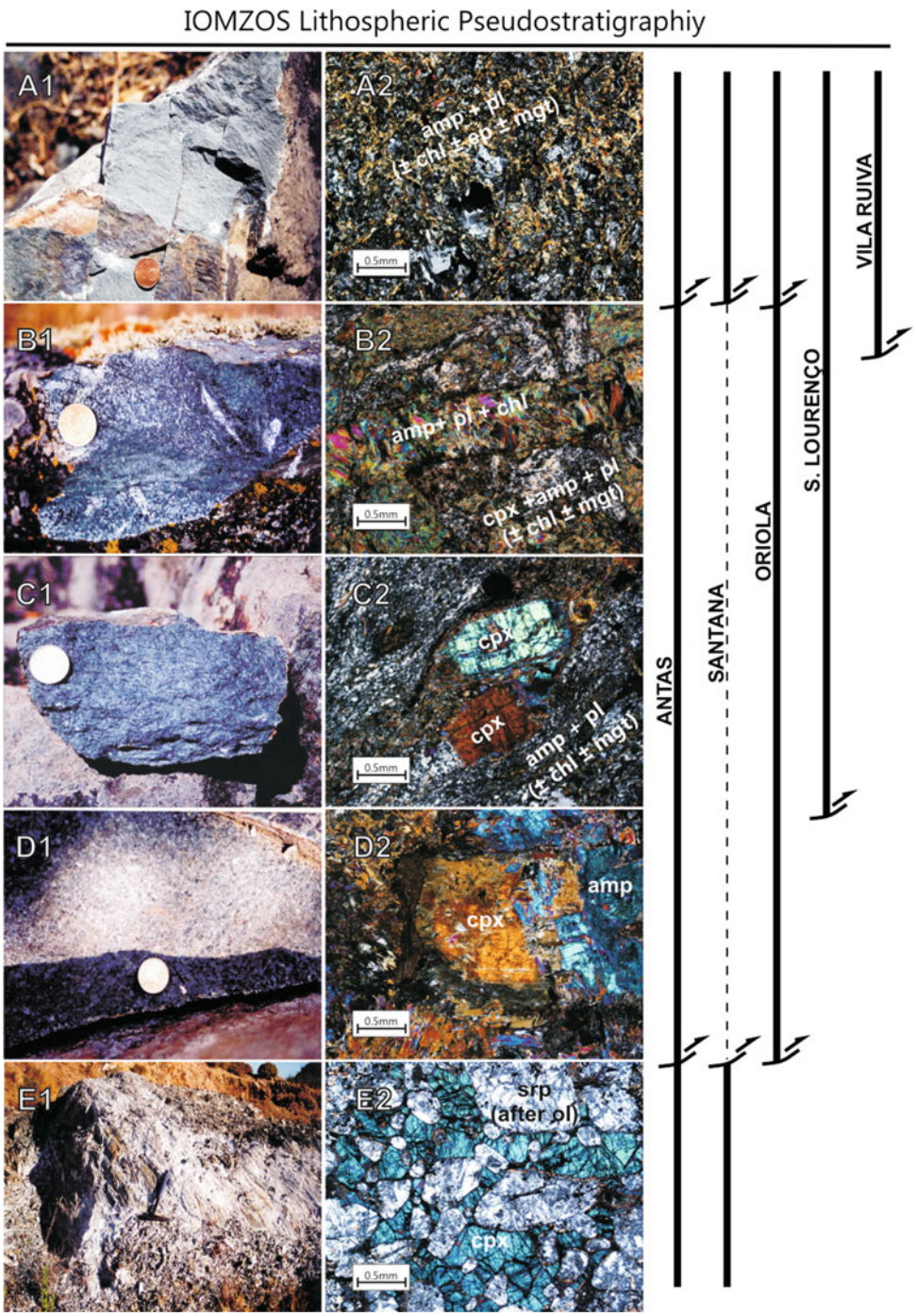

Fig. 5.3 Macro- (1) and microphotographs (2) of the reconstructed lithospheric sequence of the Internal Ossa-Morena Zone Ophiolite Sequences. **A** Metabasalts; **B** metagabbros intruded by metadolerite dikes; **C** metagabbros; **D** pyroxenite cumulates; and **E** strongly serpentinised peridotites (dunites). amp—amphibole; chl—chlorite; cpx—clinopyroxene; ep—epidote; mgt— magnetite; and srp—serpentine

values in the normal (N-MORB) and enriched (E-MORB) mid-oceanic ridge basalts (Sun et al. 1979; Sun 1980; Gill 1981; Wilson 1989; Flower 1991; Miyashiro 1974; Juteau and Maury 1999). Moreover, the observed low La/Nb (<2) and high La/Th (>10) ratios in the metabasic rocks of the IOMZOS are consistent with the reported values for the asthenospheric mantle (Sun and McDonough 1989; Green 1995; Pearce 2008), which provide an argument for derivation of the IOMZOS igneous protoliths from an asthenospheric mantle source.

The chondrite-normalised trace element and REE diagrams plotted on Fig. 5.5 show two main IOMZOS patterns, which are representative of the overall IOMZOS geochemistry (Pedro et al. 2010):

(i) Samples OR-4-2 and OR-4-3 with similar patterns to those commonly reported for N-MORB (Sun et al. 1979;

Table 5.1 Major and trace element composition of representative metabasalts and metagabbros from the Internal Ossa-Morena Zone Ophiolite Sequences (IOMZOS)

Outcran	ORIOLA		ANTAS	VILA RUIVA	ORIOLA	ANTAS	S. LOURENQC
	OR-4-2	OR-4-3	ANT-1-1	VR-1-1	OR-1-2	ANT-1-7	AF-3
Rock type wt%	B	B	B	B	GN	HG	HG
$Si0_2$	47.11	46.33	48.36	45.93	48.63	46.69	47.63
$Ti0_2$	0.94	1.22	1.99	1.98	1.63	1.41	1.35
AI_2O_3	15.61	16.77	14.65	16.59	9.57	16.20	17.81
$Fe_2O_3^{tot}$	10.27	10.19	10.38	9.95	12.09	8.77	8.49
MnO	0.18	0.21	0.17	0.17	0.22	0.15	0.17
MgO	7.71	7.22	7.08	7.91	10.35	7.96	6.71
CaO	13.94	13.89	13.01	9.09	13.72	10.81	11.37
Na_20	2.33	3.03	2.05	3.40	1.73	3.00	3.27
K_20	0.34	0.26	0.39	0.17	0.22	0.44	0.08
P_2O_s	0.07	0.11	0.30	0.32	0.14	0.21	0.20
LOI	1.33	0.67	1.28	3.84	0.97	1.99	2.06
mg #	49.61	48.16	47.21	51.04	52.89	54.34	50.89
A.I.	0.11	0.17	0.08	0.21	0.06	0.16	0.12
ppm							
Y	21.0	25.0	33.5	24.0	29.00	22.57	22.00
Zr	46	71	143	146	83.00	93.17	110.00
Nb	1.80	1.80	22.70	22.23	4.10	10.74	6.20
La	2.03	2.68	19.80	16.20	4.44	9.28	7.40
Ce	5.88	8.51	43.30	34.17	12.50	20.61	18.00
Pr	0.97	1.33	5.04	3.90	1.83	2.48	nd
Nd	5.95	8.65	23.00	18.15	10.80	11.90	12.00
Sm	2.19	3.06	5.62	4.47	3.61	3.22	3.10
Eu	0.84	1.21	1.93	1.51	1.22	1.19	1.14
Gd	2.93	3.92	5.97	4.54	5.20	3.56	nd
Tb	0.61	0.77	1.05	0.71	0.95	0.61	0.70
Dy	3.82	4.87	6.32	4.21	5.85	3.79	nd
Ho	0.81	1.03	1.25	0.84	1.24	0.83	nd
Er	2.48	3.02	3.59	2.46	3.74	2.32	nd
Tm	0.36	0.44	0.53	0.34	0.55	0.33	nd
Yb	2.30	2.69	3.25	2.06	3.46	2.04	2.06
Lu	0.34	0.40	0.48	0.29	0.52	0.30	0.33
Hf	1.40	2.00	3.60	3.30	2.40	2.18	2.30
Ta	0.10	0.08	1.42	1.72	0.24	0.87	0.50
Th	0.14	0.11	1.65	1.44	0.37	0.75	0.60
$(La/Sm)_{CN}$	0.60	0.57	2.27	2.34	0.79	1.86	1.54
$(La/Yb)_{CN}$	0.63	0.71	4.37	5.64	0.92	3.26	2.58
$(La/Th)_{CN}$	1.77	2.98	1.20	1.38	1.47	1.53	1.51
$(“m/Nb)_{CN}$	0.66	0.52	0.73	0.55	0.77	0.58	0.82

Rock type (Le Maitre et al. 1989): B-basalt, GN-gabbronorite, HG-hornblende gabbro
Data by ICP-MS at Activation Laboratories Lda–Canada
A.I. = $[(Na_2O + K_2O)/SiO_2 - 43) * 0.17]$ mg # = 100 * [MgO/(MgO + FeO)]

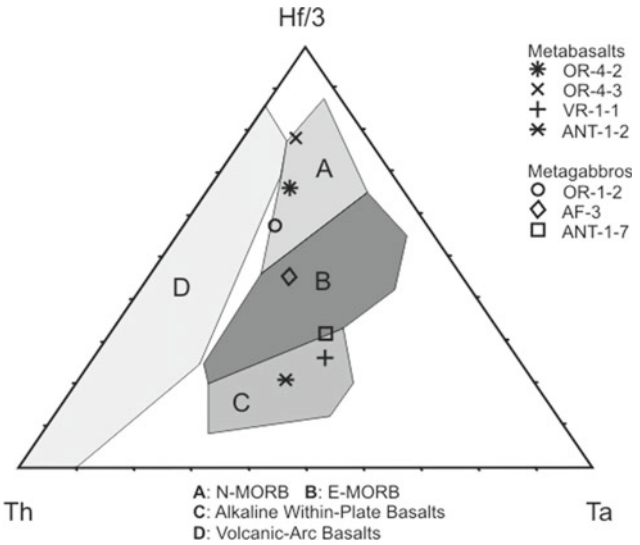

Fig. 5.4 Th-Hf-Ta ternary diagram (after Wood 1980) for the metabasic rocks of the Internal Ossa-Morena Zone Ophiolite Sequences

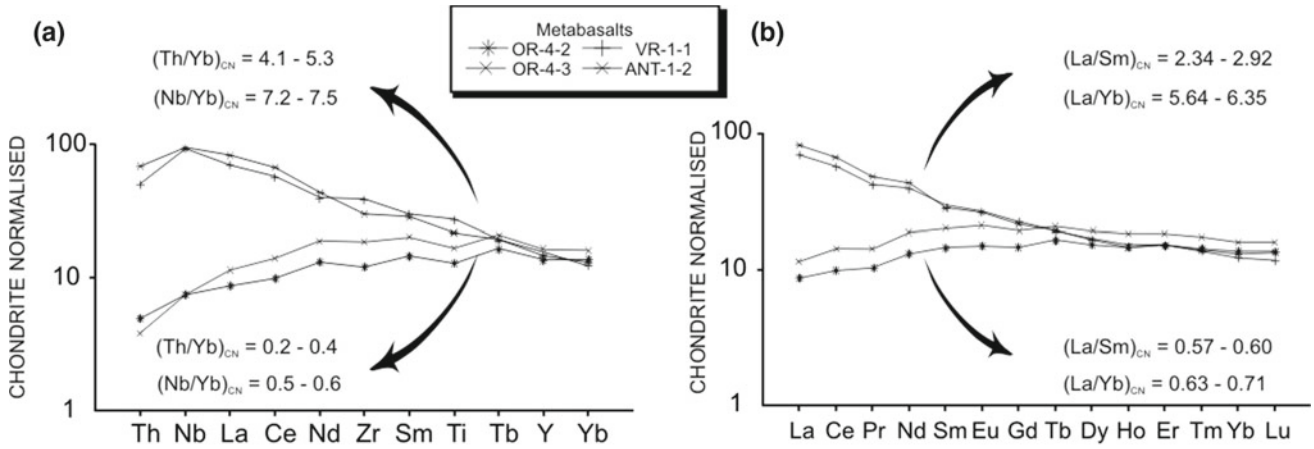

Fig. 5.5 Representative trace elements and REE chondrite-normalised diagrams for the Internal Ossa-Morena Zone Ophiolite Sequences. Normalising values after Sun et al. (1979), Sun and Nesbitt (1978) and Sun and McDonough (1989)

Sun 1980; Wilson 1989). They are slightly depleted in LREE with respect to MREE an HREE [$(La/Sm)_{CN}$ = 0.57–0.60, $(La/Yb)_{CN}$ = 0.63–0.71]. The LREE are somehow enriched relative to Nb and Th [$(La/Nb)_{CN}$ = 1.17–1.55 and $(La/Th)_{CN}$ = 1.77–2.98] while Th and Nb are depleted relative to Zr and Ti; and

(ii) Samples ANT-1-2 and VR-1-1 with patterns correlated with the E-MORB (Sun et al. 1979; Sun 1980; Wilson 1989). They are considerably enriched in the more incompatible elements (Th, Nb, La and Ce) relative to less incompatible elements (Zr, Ti, Y and Yb). The LREE are enriched relatively to MREE and HREE [$(La/Sm)_{CN}$ = 2.34–2.92, $(La/Yb)_{CN}$ = 5.64–6.35] and Nb is enriched with respect to Th and La [$(La/Nb)_{CN}$ = 0.76–0.88 and $(Th/Nb)_{CN}$ = 0.55–0.73].

According to Pedro et al. (2010) the overall IOMZOS samples have patterns between those two above mentioned patterns and are transitional between N-MORB and E-MORB, without any HFSE (Nb) negative anomaly. Therefore, the overall IOMZOS whole-rock geochemistry is consistent with a T-MORB geochemistry, ranging from N-MORB to E-MORB and supports the anorogenic tholeiitic geochemical fingerprint previously proposed for the igneous protoliths.

The use of incompatible elements ratios with a common denominator, like Th/Yb versus Nb/Yb and TiO_2/Nb versus Nb/Yb (Pearce 2008) is an useful methodology to highlight source features, melt effects and crustal contamination in oceanic metabasalts. On the Th/Yb versus Nb/Yb diagram (after Pearce 2008; Fig. 5.6a) the IOMZOS metabasic rocks

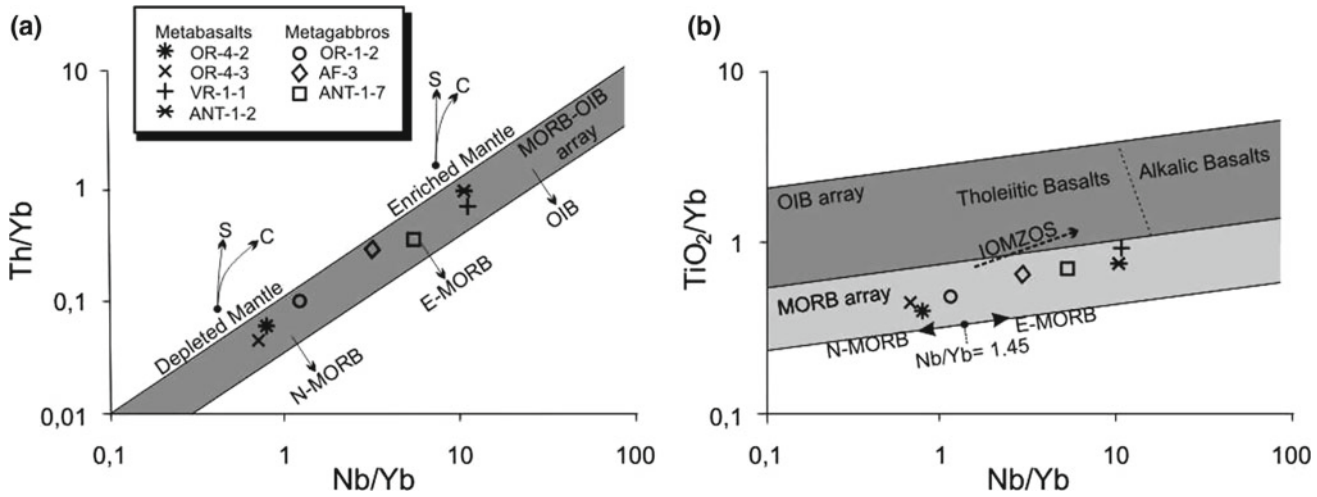

Fig. 5.6 **a** Th/Yb versus Nb/Yb and **b** TiO_2/Yb versus Nb/Yb diagrams (after Pearce 2008) for the Internal Ossa-Morena Zone Ophiolite Sequences. Arrows show the influence of subduction components (S) and crustal contamination (C)

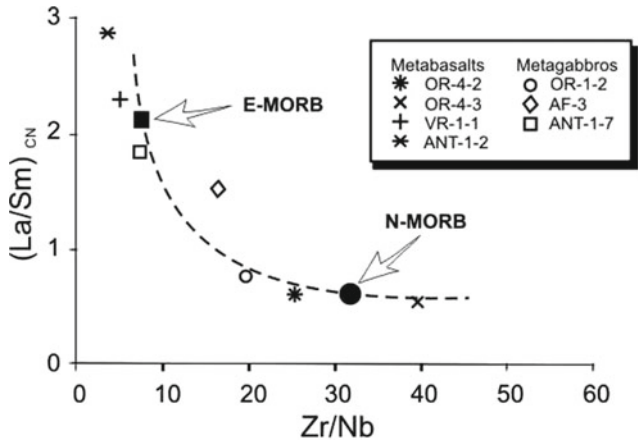

Fig. 5.7 $(La/Sm)_{CN}$ versus Zr/Nb diagram for the Internal Ossa-Morena Zone Ophiolite Sequences. The dashed line illustrates the expected compositional variation between E-MORB and N-MORB. MORB data from Sun et al. (1979); and Sun and McDonough (1989)

plot near the upper boundary of the MORB-OIB (Ocean Island Basalts) field. The ratios variation (Th/Yb = 0.34 ± 0.43; Nb/Yb = 4.53 ± 5.55) does not support any lithospheric contamination or subduction influence (high Th/Yb) but point to the IOMZOS mantle source(s) being heterogeneous and transitional between the N and E-MORB sources. In order to better constrain the IOMZOS mantle source in the TiO_2/Yb versus Nb/Yb variation diagram (after Pearce 2008; Fig. 5.6b) the IOMZOS metabasic rocks data scatter along the MORB array with a tenuous crosswise trend, from the MORB array to the tholeiitic OIB field. This fact together with the IOMZOS mantle source features, inferred from the Th/Yb and Nb/Yb variations, are coherent with a plume/proximal ridge interaction (Pearce 2008). In addition, the plume/ridge interaction is also supported by the $(La/Sm)_{CN}$ versus Zr/Nb variations (Fig. 5.7), corroborating the above mentioned IOMZOS geochemical features.

Pedro et al. (2010) proposed a heterogeneous mantle source with two-component mixing for IOMZOS petrogenesis: (i) an enriched component, similar to the E-MORB mantle source, with $(La/Sm)_{CN} > 2$ and Zr/Nb < 10; and (ii) a depleted component, similar to the N-MORB mantle source, with $(La/Sm)_{CN} < 1$ and Zr/Nb > 30. For both the data of Pedro et al. (2010) and the data of the present work, and despite the negligible effect of fractional crystallization and small variations in the degree of partial melting, the mantle source heterogeneity is interpreted as the foremost petrogenetic variable in IOMZOS petrogenesis. Indeed, the anorogenic tholeiitic geochemistry of the IOMZOS, transitional between N-MORB and E-MORB, indicates that the igneous protoliths of IOMZOS are genetically related with open ocean basins without orogenic influence and/or crustal contamination in their petrogenesis.

Several extensional magmatic events were often proposed for the OMZ Cambrian-Ordovician rifting evolution, invoking asthenospheric, lithospheric, and crustal magma sources (Sánchez-García et al. 2003, 2008, 2010; Chichorro et al. 2008; Linnemann et al. 2008). Nevertheless, these events are only representative of the initial rifting stages (primary budding stages), while the IOMZOS record an early/full divergent margin stage of the Rheic Ocean evolution, preserved in SW Iberia by obduction (Pedro et al. 2010; Ribeiro et al. 2010). This interpretation is supported by the following IOMZOS geological and whole-rock geochemical features: (1) presence of an oceanic lithosphere sequence; (2) considerable amounts of serpentinised peridotites (recording ocean-floor metamorphism; Pedro 2004); and (3) magma generation related to a plume-proximal ridge system (asthenospheric source).

5.2.4 SHRIMP U-Pb Zircon Dating

The still ongoing geodynamic interpretation of the IOMZOS requires U-Pb isotopic analyses (SHRIMP) to determine the protolith ages and to enlighten the genetic relation between IOMZOS and Rheic Ocean in SW-Iberia. Pedro et al. (2010) separated crystal zircons (6 crystals) from the coarse grained and less deformed metagabbroic rocks, in Antas, Oriola and S. Lourenço IOMZOS fragments (see Fig. 5.2 for sample location). The metagabbros (hornblende gabbros and gabbronorites) display the aforementioned N/E MORB geochemistry and are cogenetic with the overall IOMZOS magmatic suite. Zircon SHRIMP analyses yielded $^{206}Pb/^{238}U$–$^{207}Pb/^{235}U$ Concordia ages of 477 ± 8 Ma, 478 ± 7 Ma and 495 ± 9 Ma, respectively for Antas, Oriola and St. Lourenço IOMZOS fragments (Fig. 5.8a), with a weighted mean age of 482.5 ± 9.4 Ma (Pedro et al. 2010), suggesting that the IOMZOS could represent obducted diachronic (ca. 20 m.y.; Late Cambrian—Early Ordovician) Rheic's oceanic lithosphere. However, Pedro et al. (2010) discussed the achieved IOMZOS ages and proposed exclusion of the oldest age (497.5 ± 6.1 Ma; outlier spot) from the weighted mean average age in order to obtain a best fit 206Pb/238U weighted mean age of 479.6 ± 5.1 Ma with higher probability of concordance (Fig. 5.8b), and proposed the age of ca. 480 Ma as a reasonable estimate for the IOMZOS protolith age, due to the 482.5 ± 9.4 Ma (n = 6) and the 479.6 ± 5.1 Ma (n = 5) weighted mean average ages are statistically identical, indistinguishable within the analytical uncertainty and have the same geodynamic significance.

5.2.5 Discussion

The BAO (see below) and IOMZOS record obduction of oceanic lithosphere in SW Iberia during Devonian times, but only the IOMZOS may represent mature ophiolitic sequences originating from the Rheic Ocean (Pedro et al. 2005, 2006, 2010, 2013; Ribeiro et al. 2007, 2010), Several lines of evidence are in agreement with the geodynamic evolution model for the Rheic Ocean (Ribeiro et al. 2007, 2010) that allow correlation of the IOMZOS with the Rheic Ocean during the Early Ordovician: (i) the identification of a typical oceanic lithosphere sequence; (ii) the whole-rock geochemical data indicative of ocean-floor basalts geochemistry (plume-proximal ridge system) lacking any orogenic and/or crustal contamination signature; and (iii) the diachronic ages of 477 ± 8 to 495 ± 9 Ma that yield a weighted mean age of ca. 480 Ma.

We believe IOMZOS represent fragments of the Rheic Ocean floor, with typical oceanic lithosphere and passive margins that were not consumed by subduction during the Late Paleozoic and were emplaced onto SW Iberia by obduction. Therefore, two distinct passive margin magmatic events during the Early Paleozoic were recorded in OMZ, regarding distinct evolutionary stages of Rheic Ocean development:

(1) The OMZ Cambrian-Ordovician intracontinental rifting migration related with crustal contamination processes of the mantle sources, as recorded by shallow plutonic and volcanic rocks accompanied by coeval Early Paleozoic syn-rift sedimentary successions in the

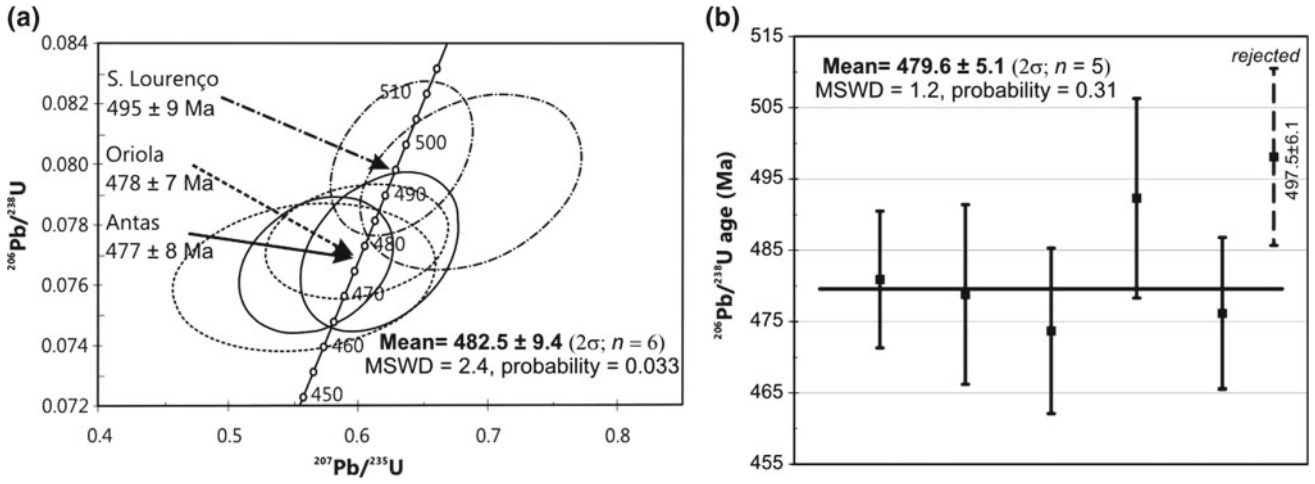

Fig. 5.8 **a** U-Pb concordia diagram of zircon SHRIMP data and weighted mean age (482.5 ± 9.4 Ma; n = 6) for the metagabbros of the Internal Ossa-Morena Zone Ophiolite Sequences (after Pedro et al. 2010); **b** Diagram of weighted mean average age of 479.6 ± 5.1 Ma (n = 5) for the metagabbros of the Internal Ossa-Morena Zone Ophiolite Sequences (after Pedro et al. 2010) with exclusion of the oldest age (497.5 ± 6.1 Ma, outlier spot)

autochthonous OMZ (Sánchez-García et al. 2003, 2008, 2010; Chichorro et al. 2008; Linnemann et al. 2008; see also Chap. 2 of this volume); and

(2) The IOMZOS, with an ocean lithospheric cross-section representing an early/full divergent margin stage, with tholeiitic ocean-ridge magmatism, preserved in the Middle—Upper Paleozoic OMZ allochthonous complexes tectonically superposed/imbricated with the Cubito-Moura schists. Only the IOMZOS should be viewed as remnants of the Rheic Ocean, and the protolith age of ca. 480 Ma should be regarded as a minimum age of Rheic Ocean opening in SW Iberia.

5.3 The Pulo do Lobo Terrane

5.3.1 The Mafic Rocks of the Pulo do Lobo Terrane

P. Ferreira, J. T. Oliveira

5.3.1.1 Geological Setting

The mafic rocks of the Pulo do Lobo Terrane occur associated to phyllites of the Pulo do Lobo Formation (PLF). In Portugal they are exposed along the NW-SE trending strip of Trindade-Alfarrobeira ca. 50 km in length (Fig. 5.9). Rock exposure is poor due to weathering and limited to road cuts or small stream valleys. In Spain they crop out in association with the Peramora Mélange which in turn is imbricated with phyllites ascribed to the Pulo do Lobo Formation (Eden 1991; Braid et al. 2011, 2012; Dahn et al. 2014) just at the core of the Los Ciries antiform (Fig. 5.9). In the present work emphasis is put on the study of the Alfarrobeira drill core in Portugal, ca. 50 m SE of Alfarrobeira farm. Samples of the Trindade-Alfarrobeira strip were previously studied by J. Munhá (in Quesada et al. 1994) although with imprecise localization. Geochemical and petrogenetic comparisons are made with the Peramora Mélange mafic rocks studied by Eden (1991) and Danh et al. (2014).

5.3.1.2 The Alfarrobeira ALF-2 Drill Core (PLA): Characterization, Sampling and Rock Petrography

The Alfarrobeira ALF-2 core was drilled by Sociedade Mineira Rio Artezia, Lda. in the PLF SE of Trindade village, Alentejo, Portugal (coordinates UTM: 29S 602080 E; 4190080 N). It crossed the initial 116 m in dark phyllites and thin-bedded siltstones and abundant contorted sweat-out quartz veinlets, all ascribed to the PLF (Fig. 5.10a). The remaining part of the drill core, which as a whole reach 450 m depth, is composed by light green to grayish metavolcanics and are intercalated with thin dark phyllite layers of the PLF (Fig. 5.10b). All the succession is affected by folding and a strong cleavage generally at 70–80° onto core axis, but lower inclinations are observed. The cleavage has a shear component, particularly visible in phyllites and thin-bedded siltstones (Fig. 5.10c) and is associated to the F2 regional tectonic episode.

The Alfarrobeira (PLA) mafic samples occur mainly as lava extensively affected by metamorphism, which has resulted in recrystallization of the primary igneous phases, and contain a typical mineral assemblage of greenschist metamorphic facies composed by amphibole (actinolite), plagioclase, chlorite, epidote, sphene, calcite and opaque minerals. These rocks display two types of textural varieties from strongly aphyric to microgranular (fine- to medium-grained). The well-developed cleavage (S2) is more clearly seen on the aphyric samples (Fig. 5.11a) and less well defined in the more granular rocks (Fig. 5.11b). These granular rocks are interpreted as rock ribbons bounded by S2 shear planes. Textural relics of primary igneous phases are

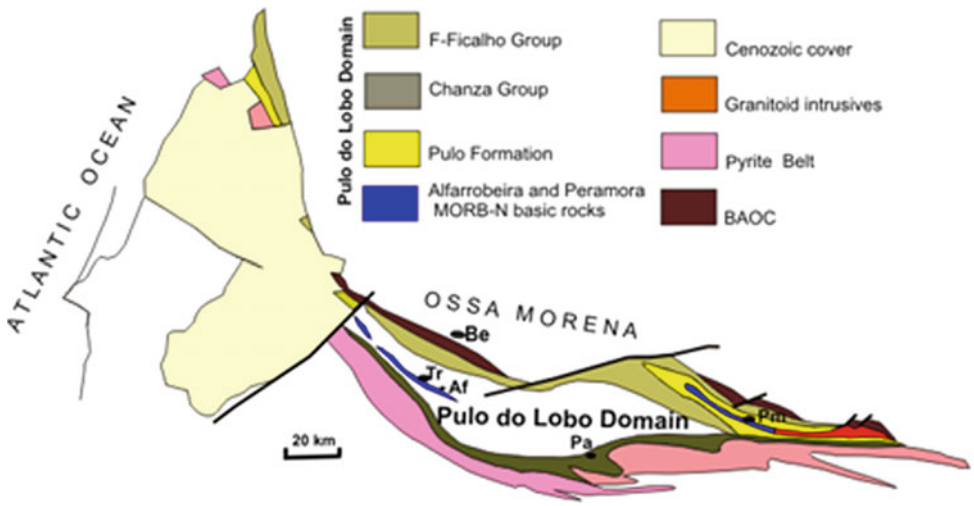

Fig. 5.9 Simplified geological map of the Pulo do Lobo Domain. Be-Beja; Tr-Trindade; Af-Alfarrobeira ALF-2 drill; Pa-Paymogo

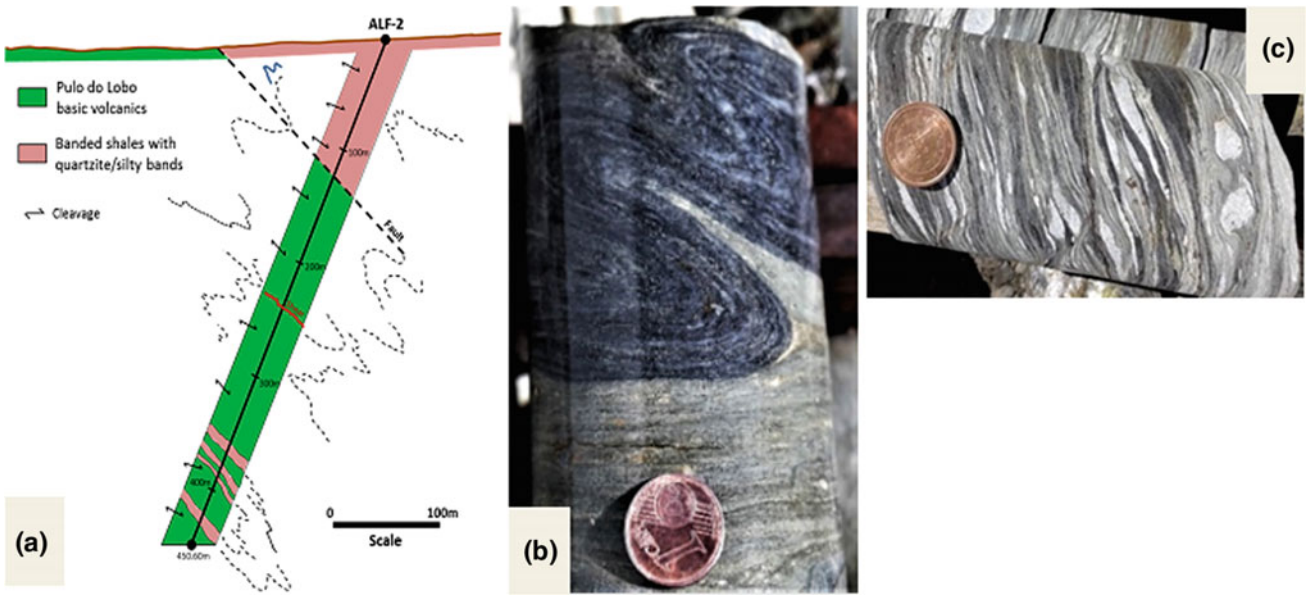

Fig. 5.10 **a** Schematic geological section of Alfarrobeira ALF-2 drill core (adapted from Sociedade Mineira Rio Artezia, Lda); **b** photograph of a core sample showing a F3 folded contact between the dark phyllites and the light green to grayish metavolcanics, both ascribed to the Pulo do Lobo Formation; **c** alternations of metavolcanic rocks and thin-bedded siltstones, phyllites and quartzites, affected by shearing cleavage with preserved quartzite ribbons

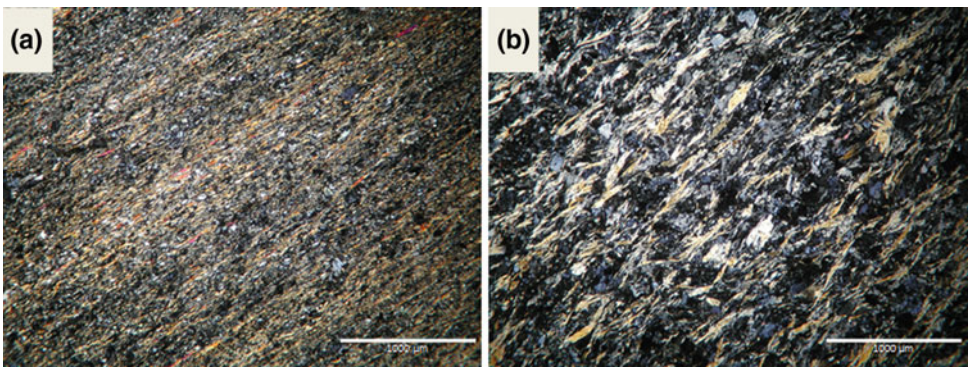

Fig. 5.11 Representative photomicrographs of Pulo do Lobo metavolcanics. **a** fine grained sample, rich in actinolite, with a well-developed cleavage **b** sample showing a coarser grain, richer in plagioclase and epidote, where two cleavages are observed

more easily recognized in the granular varieties and almost restricted to phenocrysts of plagioclase (up to 3–4 mm in size) totally transformed into albite + epidote. Subordinately, smaller and dispersed phenocrysts of clinopyroxene are completely transformed into actinolite. Variable amounts of amygdales and, more frequent, thin millimeter-scale veins, usually filled with calcite and epidote, are observed in many samples.

5.3.1.3 Analytical Methods and Data Quality Assessment

A group of 13 samples from the metavolcanic rocks crossed by Alfarrobeira ALF-2 drill core was selected for chemical characterization (Ferreira and Oliveira 2018), and their composition and sampling depths are presented in Table 5.2.

The whole rock major element concentrations of PLA were determined by X-Ray Fuorescence (XRF) at LNEG (S. Mamede de Infesta Campus, Porto, Portugal), whereas the trace element analyses (ICP-MS) were performed by Activation Laboratories Ltd. (Actlabs), Ancaster, Canada. Further analytical details and detection limits can be obtained from the authors. Analytical precision, assessed via analysis of a group of sample duplicates, was generally <2% for major elements and the reproducibility obtained for ICP-MS was globally better than 5%. The analytical control of accuracy was done by running Standard Reference Materials

Table 5.2 Volatile-free major and trace element bulk compositions from the metavolcanic rocks of Pulo do Lobo. All oxides in wt%; trace elements in ppm. LOI—Loss-on-ignition. All Fe as Fe_2O_3. Also shown the depths to which the different samples were collected along ALF-2 drill core

Safleff	ALF2-11	ALF2-15	ALF2-16	ALF2-17	ALF2-21	ALF2-24	ALF2-28	ALF2-30	ALF2-40	ALF2-41	ALF2-44	ALF2-47	ALF2-52
Deplh(m)	192.4	261.4	263.6	268.4	288.0	300.6	310.8	318.5	365.9	369.0	3B8.9	415.0	441.9
SiO_2	51.72	49.83	49.87	48.95	50.36	48.79	48.34	49.25	49.50	46.76	48.45	49.46	50.16
Al_2O_3	14.77	14.65	15.07	15.10	14.67	15.60	15.16	15.18	15.44	16.15	15.85	15.57	14.56
$Fe_2O_3^T$	10.02	10.81	10.87	11.18	10.67	10.60	9.99	10.62	10.88	10.27	10.72	11.20	10.55
MnO	0.16	0.18	0.17	0.18	0.17	0.16	0.16	0.17	0.16	0.16	0.17	0.16	0.18
CaO	10.56	12.53	12.06	12.43	11.44	12.79	14.82	1.49	11.15	16.49	12.50	9.65	11.05
MgO	7.57	7.75	7.66	8.27	8.11	8.37	7.96	8.40	8.69	7.66	8.53	8.89	8.16
Na_2O	3.42	2.51	2.55	2.21	2.84	2.16	2.01	2.18	2.52	0.99	2.09	3.07	3.41
K_2O	0.11	0.07	0.11	0,06	0.09	0.08	0.06	0.07	0.12	0.05	0.15	0.16	0.21
TiO_2	1.32	1.29	1.32	1.36	1.33	1,16	1.14	1.26	1.22	1.16	1.26	1.54	1.38
P_2O_5	0.10	0.10	0.11	0.11	0.11	0,09	0.09	0.10	0.09	0.10	0.10	0.12	0.12
LOI	2.53	2.01	1.82	2.42	1.92	2.58	2.78	2.01	2.71	2.58	2.57	2.51	3.02
Total	99.77	99.72	99.80	99.86	99.79	99.81	99.74	99.73	99.77	99.78	99.83	99.84	99.78
Cs	0.2	0.1	0.1	0.1	0.2	0.2	0.1	0.2	0.3	0.2	0.2	0.7	0.2
Rb	1	1	2	1	0.9	1	1	1	3	0.9	3	3	4
Ba	11	11	8	8	12	9	5	8	15	5	12	20	16
Sr	175	153	135	169	204	135	155	191	148	172	133	202	170
Y	28.0	27.6	29.3	29.4	28.8	24.4	24.7	26.8	25.5	26.6	26.6	30.9	29.0
Zr	74	72	73	76	75	63	64	70	66.5	63	70	89	78
Nb	2.4	1.9	2.0	2.2	2.6	1.6	1.4	1.8	1.6	1.5	1.9	3.2	2.0
Hf	2.1	2.0	2.0	2.1	2.0	1.6	1.8	2.0	1.9	1.6	2.0	2.2	2.1
Ta	0.19	0.16	0.19	0.20	0.18	0.14	0.16	0.20	0.14	0.11	0.15	0.26	0.16
Th	0.16	0,14	0.15	0.14	0.16	0.08	0.09	0.15	0.10	0.09	0.11	0.25	0.13
U	0.23	0.08	0.09	0.09	0.07	0.05	0.09	0.13	0.07	0.34	0.06	0.35	0.18
L_B	3.23	2.69	3.12	3.13	3.57	2.49	2.42	2.94	3.10	2.61	2.88	4.62	3.41
Ce	9.41	8.44	9.10	9.28	10.00	7.57	7.44	8.89	8.63	7.48	8.51	12.90	9.56

(continued)

Table 5.2 (continued)

Safleff	ALF2-11	ALF2-15	ALF2-16	ALF2-17	ALF2-21	ALF2-24	ALF2-28	ALF2-30	ALF2-40	ALF2-41	ALF2-44	ALF2-47	ALF2-52
Deplh(m)	192.4	261.4	263.6	268.4	288.0	300.6	310.8	318.5	365.9	369.0	3B8.9	415.0	441.9
Pr	1.55	1.44	1.49	1.50	1.55	1.23	1.22	1.50	1.36	1.27	1.39	1.97	1.53
Nd	8.44	7.48	8.21	8.17	8.39	6.99	6.73	7.93	7.22	7.10	7.55	10.40	8.46
Sm	3.05	2.95	3.05	3.28	3.04	2.65	2.50	2.72	2.64	2.68	2.79	3.42	2.99
Eu	1,17	1.08	1.16	1.10	1.23	0.99	0.92	1.05	1.07	1.07	1.11	1.34	1.07
Gd	4.22	4.18	4.33	4.39	4.14	3.48	3.56	3.91	3.69	3.74	335	4.61	4.10
Tb	1.77	0.77	0.76	0.81	0.80	0.65	0.66	0.73	0.70	0.71	0.72	0.85	0.75
Dy	4.94	4.88	5.27	5.06	5.06	4.19	4.46	4.83	4.63	4.55	4.73	5.42	4.95
Ho	1.55	1.03	1.09	1.11	1.09	0.89	0.92	0.99	0.92	0.96	0.98	1.12	1.04
Er	2.99	2.77	3.09	3.22	3.15	2.54	2.72	2.92	2.71	2.75	2.85	3.27	3.01
Tm	0.43	0.43	0.45	0.46	0.46	0.33	0.40	0.43	0.39	0.40	0.41	0.47	0.44
Yb	2.79	2.77	3.00	3.04	2.97	2.28	2.55	2.69	2.58	2.59	2.74	2.89	2.84
Lu	0.42	0.42	0.45	0.47	0.44	0.33	0.39	0.41	0.40	0.41	0.42	0.46	0.44
V	298	285	308	307	298	274	266	289	281	280	288	319	303
Cr	196	274	288	286	292	382	367	404	378	381	378	347	332
Co	41	45	47	45	41	48	49	48	47.5	46	49	40	41
Ni	56	52	52	59	59	66	72	66	66.5	65	71	66	65

(SRM's), and was commonly lower than 3% and 5% for major and trace elements, respectively. Detection limits vary from element to element, but for elements with low concentrations (apart Nb and Ta), such as REE, U, Th and Hf, limits typically fall within the range of 0.1–0.01 ppm.

5.3.1.4 Element Mobility, Geochemistry and Petrogenesis

The main characteristic of PLA geochemical data is the restricted variation in concentrations for most major oxides and trace elements whereas, for example, SiO_2 values range from 48.8 to 51.7% and Zr concentrations vary between 63 and 89 ppm (Table 5.2). This limited chemical variation can be observed in the bivariate diagrams of Fig. 5.12, where Zr is used as a differentiation index and plotted against various elements representing distinct geochemical groups.

When volcanic rock samples under study are geologically old, it is crucial to ensure that the original chemical compositions of the lavas were not modified by post-magmatic alteration processes, such as those associated to metamorphism, hydrothermal alteration and weathering. The evaluation of element mobility in the PLA samples can be assessed by the correlation obtained between major and trace elements with Zr, which is considered one of the least mobile elements (e.g. Floyd and Winchester 1978; Polat and Hofmann 2003). From the bivariate diagrams obtained (Fig. 5.12), it can be concluded:

(i) Almost all HFSE (Y, Nb, Ta, Hf, Th and Ti) show a strong correlation with Zr (Fig. 5.12d, f), with correlation coefficients (R^2) higher than 0.70, which is consistent with the relatively low mobility of these

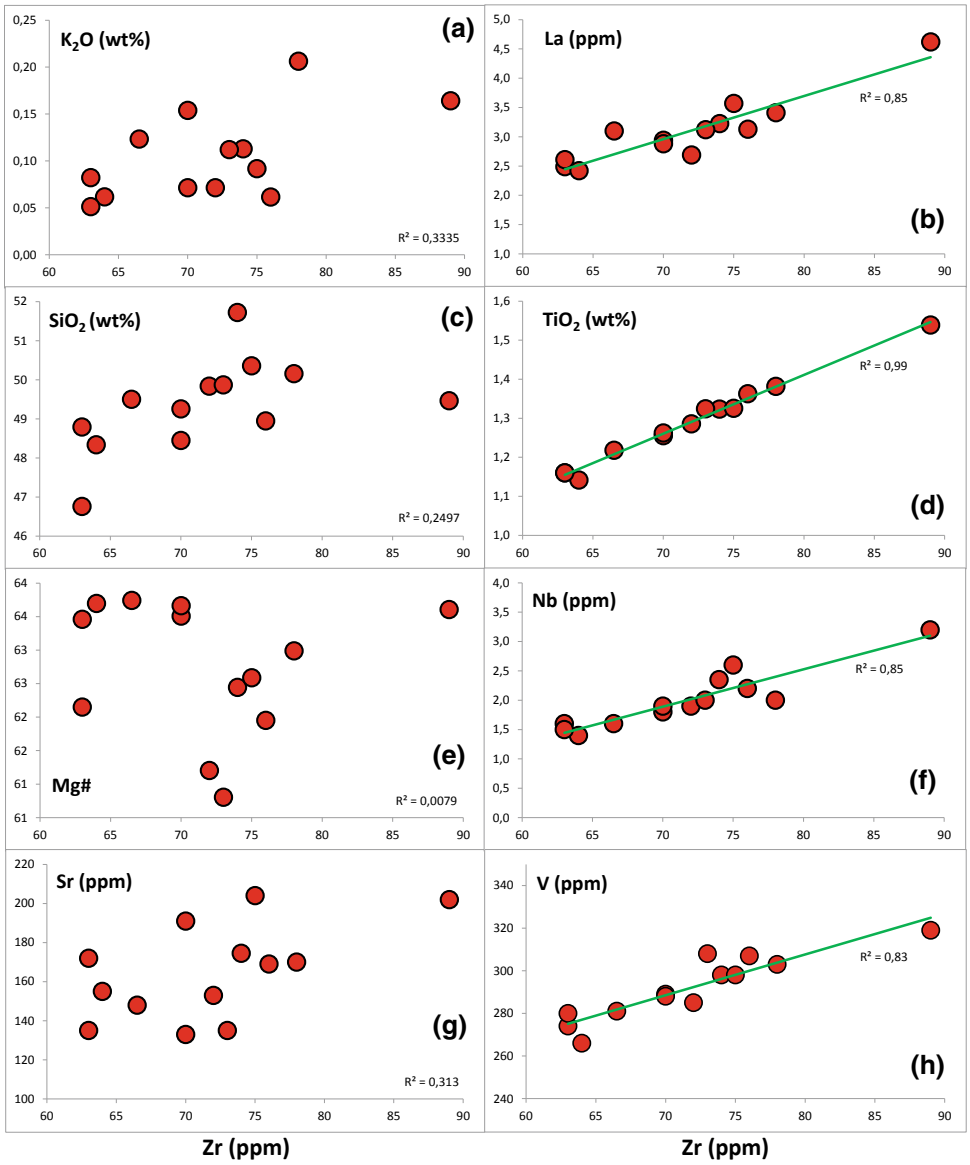

Fig. 5.12 Bivariate diagrams of selected elements (representing the distinct geochemical groups) plotted against Zr (considered the most immobile element) to highlight the effects of post-magmatic alteration in PLA samples

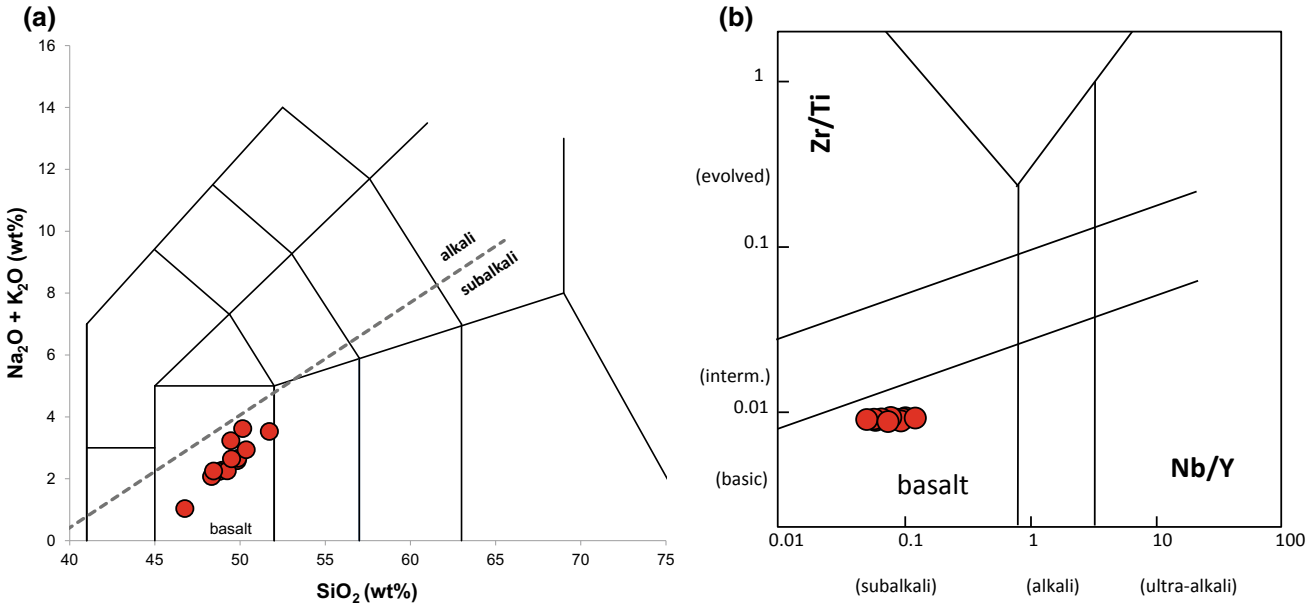

Fig. 5.13 Classification of Pulo do Lobo metavolcanic rocks using **a** the IUGS-recommended TAS diagram of Le Maitre (1989), with a dashed line (MacDonald and Katsura 1964) separating the alkali and subalkali fields; **b** an immobile element-based TAS proxy diagram from Pearce (1996), after Floyd and Winchester (1975). This second classification is more robust, but has lower discrimination degree. To be noted the coherence of the rock classification and subalkali character obtained on both diagrams, indicating that if silica and alkalis were mobile during alteration processes, these had a limited modification on the original overall magmatic concentrations

elements. Conversely, Sc and U do not establish any systematic trend with Zr;

(ii) All REE show strong correlation coefficient values with Zr, higher than 0.75 ($R^2 > 0.90$ for the LREE, including Ce, Pr and Nd), with exception of Yb, Lu and Eu (R^2 = 0.53, 0.60, 0.67, respectively) (Fig. 5.12b);

(iii) In respect to LILE (K, Rb, Sr, Cs, Ba), also highly incompatible elements in the magmatic systems, all are poorly correlated with Zr (K, Rb, Sr and Cs) with $R^2 < 0.38$, whereas Ba has $R^2 = 0.52$, supporting the hypothesis that none of these element concentrations represent their original magmatic contents (Fig. 5.12 a, g);

(iv) From the first transition metals, Cr, Co and Ni (which tend to be compatible in the magmas and, thus, decrease their abundance with differentiation), only Co presents a significant negative correlation with Zr ($R^2 = 0.60$); Cr and Ni concentrations also decrease as a function of Zr, but their correlation coefficients are not significant ($R^2 < 0.2$). Conversely, Vanadium is well, and positively, correlated against Zr ($R^2 = 0.83$; Fig. 5.12 h), pointing to the absence of Fe-Ti oxides (ilmenite or titano-magnetite) fractionation;

(v) Lastly, taking into account the major elements (Fig. 5.12c, e) it is worth to emphasize the absence of correlation when plotting Zr against SiO_2, MgO and Mg# (all frequently used as magma differentiation indexes in igneous petrology studies), meaning a possible mobility of Si, Fe and Mg during post-magmatic alteration processes. With the exception of P_2O_5, the rest of oxides are also poorly correlated against Zr.

Additionally, the range of loss-on-ignition values obtained for PLA (1.82–3.02 wt%) and the absence of any correlation with any major element or LILE concentrations, could mean that if these elements were mobile, their primary concentrations were only affected in a limited way.

Based on the arguments discussed above, it can be concluded that PLA samples have suffered the influence of post-magmatic alteration processes that have modified all LILE and most of the major element primary concentrations. Conversely, their HFSE (Zr, Y, Nb, Ta, Hf, Th, Ti), REE, Co and V contents are expected to represent magmatic concentrations and are the most reliable to established the geodynamic setting where the Pulo do Lobo magmas were generated.

Concerning the geochemical nomenclature used for volcanic rocks, all PLA metavolcanic samples are classified as basalts having a subalkaline affinity (Fig. 5.13a, b). This magmatic affinity is also supported by the low

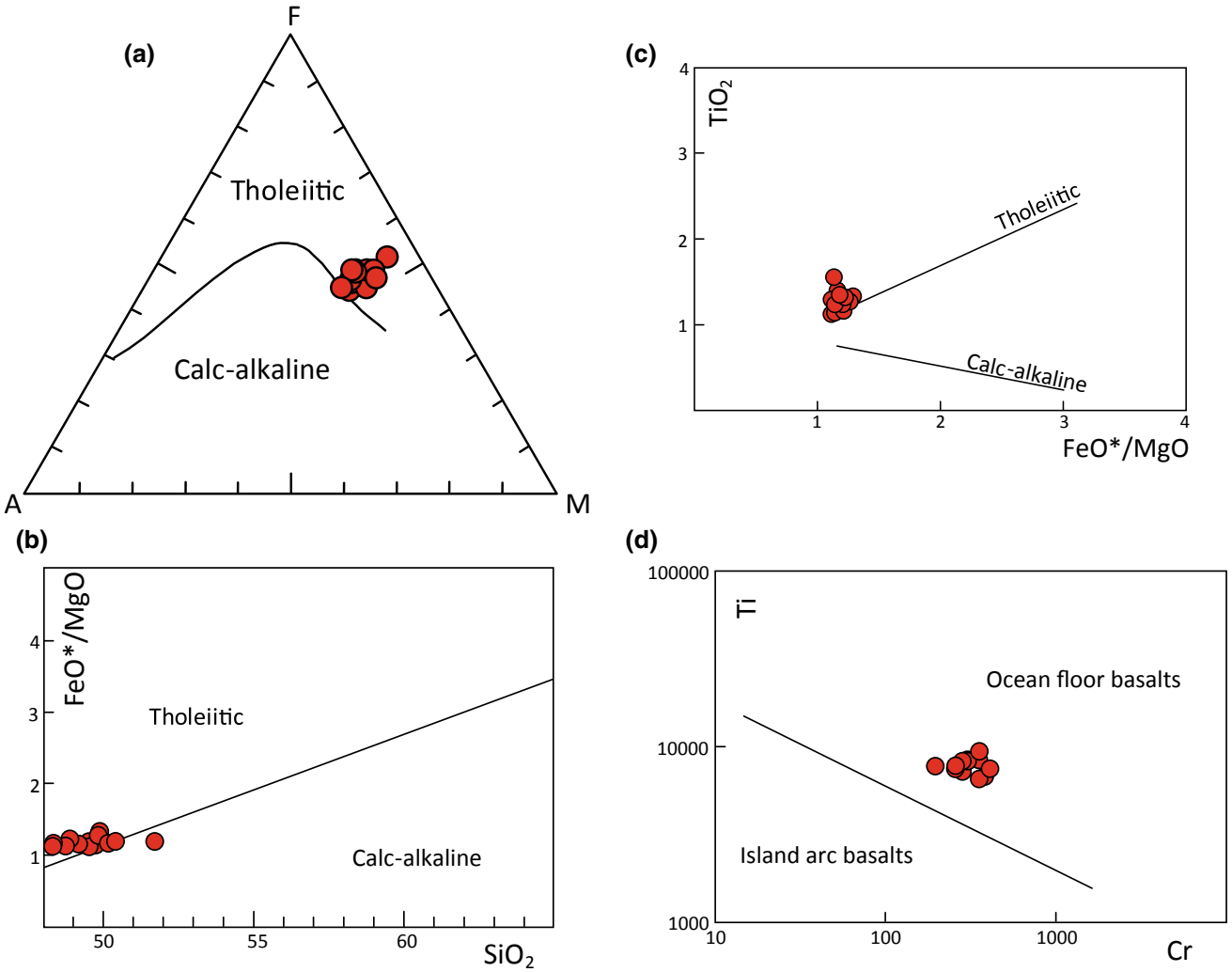

Fig. 5.14 Several discriminant diagrams for subalkaline magma series. **a** AFM diagram, where A = (Na_2O + K_2O), F = (FeO*) and M = (MgO). FeO* represents total iron expressed as FeO. The solid curved line divides tholeiitic and calc-alkaline fields of Irvine and Baragar (1971). **b** FeO*/MgO versus SiO_2 discrimination diagram with dividing line from Miyashiro (1974); all values in wt%. **c** FeO/MgO versus TiO_2 diagrams (Miyashiro 1974); all values in wt%. **d** Cr-Ti diagram for Pulo do Lobo metabasalts (after Pearce 1975); all values in ppm

concentrations of elements considered highly incompatible during melting of the mantle mineral assemblages, which include the LREE and the HFSE (e.g. Niu et al. 2011).

Volcanic rocks of the subalkaline magma series may be subdivided into a high alumina, or calc-alkaline series, and a low-K tholeiitic series. This discrimination can be achieved using the classical diagrams of Irvine and Baragar (1971) and Myashiro (1974), which show that all the PLA samples fall in the tholeiitic field (Fig. 5.14). These samples, plotted in the Pearce (1975) diagram, represent ocean floor basalts. All these discrimination diagrams have a more limited application when the chemical composition of the rocks have a restricted variation, such as observed in Pulo do Lobo metabasalts. However, in all diagrams the PLA are concordantly positioned in the tholeiitic fields.

Representative Masuda-Coryell plots of the REE data for the PLA metabasalts (Fig. 5.15) indicate that in all samples, with the exception of ALF2-47, the light-REE (LREE) are depleted with respect to the heavy-REE (HREE), compared to chondrites. The shape of these REE patterns is expressed in the chondrite-normalized $[La/Yb]_{cn}$ ratios <1 (sample ALF2-47 has a $[La/Yb]_{cn}$ = 1.15). All patterns are roughly sub-parallel, the ∑REE concentrations are low and their variation is limited (∑REE = 36.3–45.4 ppm). Sample ALF2-47 is the most differentiated metabasalt of all PLA samples, having the highest ∑REE value (53.3 ppm), and graphically is the only sample showing a normalized pattern separated, and above all the other sample patterns.

One of the most distinguished geochemical characteristics exhibited by PLA metabasalts is the smooth concave-down

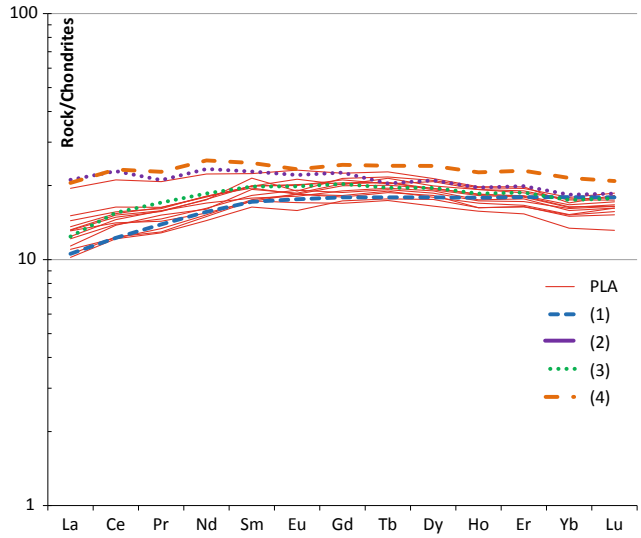

Fig. 5.15 Chondrite-normalized REE variations in Pulo do Lobo metabasalts. For comparison, typical patterns for several MORB averages are plotted: (1) N-MORB from Sun and McDonough (1989); (2) Global MORB and (3) N-MORB means from Arevalo and McDonough (2010); (4) N-MORB average from Gale et al. (2013). Normalizing chondrite values are from Sun and McDonough (1989)

chondrite-normalized REE patterns, reflecting the fact that they were derived from incompatible element-depleted mantle, an origin that is also attributed to the generation of N-MORB magmas (e.g. Langmuir et al. 1992; Workman and Hart 2005). In Fig. 5.15, the resemblance between all REE chondrite-normalized patterns of PLA samples and those representing N-MORB averages is clearly seen. For comparison we have used four average compositions for MORB: (1) N-MORB average chemical composition of Sun and McDonough (1989); (2) Global MORB average of Arevalo and McDonough (2010), which represents the global spectrum of MORB samples with a critically compiled collection of analyses from several high-quality, peer-reviewed data sets; (3) N-MORB average of Arevalo and McDonough (2010), which is a log-normal mean for the chemical abundances of (2), but only considered the MORBs with (La/Sm) < 1.00; 4) N-MORB mean of Gale et al. (2013), determined using a global data set compiled from previously published data, corresponding to the most likely basalt composition encountered along the oceanic ridges located >500 km from hot spots.

Other critical ratios are commonly used to express the degree of fractionation among REE, such as $[La/Sm]_{cn}$, for the LREE, and $[Tb/Yb]_{cn}$, for the HREE (Fig. 5.16). With the exception ALF2-47 (with $[La/Sm]_{cn}$ = 1.15 and $[Tb/Yb]_{cn}$ = 1,34), all PLA samples have $[La/Sm]_{cn}$ < 1 (0.70–0.86) and $[Tb/Yb]_{cn}$ between 1.15 and 1.26. A good correlation is observed in the covariation between $[La/Yb]_{cn}$ and $[La/Sm]_{cn}$ (Fig. 5.16a), but when plotting $[Tb/Yb]_{cn}$ as a function of $[La/Yb]_{cn}$ no correlation is obtained (Fig. 5.16b). Considering the Eu anomaly, expressed as Eu_{cn}/Eu^* (where Eu^* is $[Sm_{cn} \times Gd_{cn}]1/2$), the corresponding values vary between 0.89 and 1.06, meaning the existence of small negative and positive Eu anomalies, respectively.

Primordial Mantle normalized concentrations for PLA samples are shown in Fig. 5.17. The normalized patterns produced are roughly sub-parallel and a general depletion is apparent in the most incompatible elements comparatively to the least incompatible ones. As observed from the REE patterns, sample ALF2-47 produce a spidergram profile that is detached to higher normalized values from the rest of PLA samples, being more clearly seen in the most incompatible elements. In Fig. 5.17, primitive-mantle immobile trace elements for all PLA are plotted together with the several MORB means used in this study, for comparison. A first noticeable characteristic is the relatively flat patterns obtained for PLA in the least incompatible elements, from the middle region of the diagram to the right end, producing normalized element ratios closed to the unity; e.g.

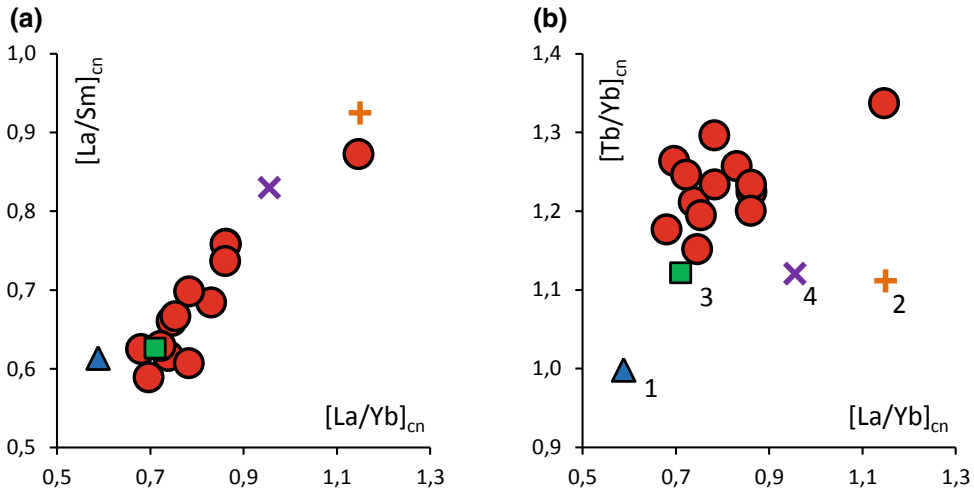

Fig. 5.16 Diagrams showing the correlation obtained between some key REE normalized ratios for Pulo do Lobo metabasalts: **a** $(La/Yb)_{cn}$ versus $(La/Sm)_{cn}$ and **b** $(La/Yb)_{cn}$ versus $(Tb/Yb)_{cn}$. Also projected some MORB averages (data source as in Fig. 5.15)

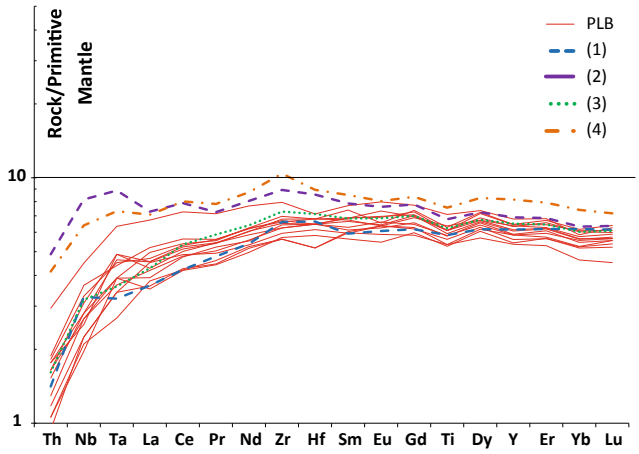

Fig. 5.17 Primitive mantle-normalized (Sun and McDonough 1989) trace element patterns for Pulo do Lobo metabasalts. Only the elements considered to be immobile were selected. Also shown for comparison the normalized patterns of four MORB averages (data source as in Fig. 5.15)

$(Hf/Yb)_{pmn}$ = 1.0–1.2; $(Nd/Y)_{pmn}$ = 0.9–1.1; $(Sm/Er)_{pmn}$ = 1.0–1.1, and indistinguishable from those presented by N-MORB mean compositions (Fig. 5.18). A second perceptible feature in Fig. 5.17 is the downward inclined normalized patterns produced in the left side of the diagram towards the most incompatible elements (from Zr to Th). This depletion is well expressed through more-to-less incompatible element ratios as, for example, $(Th/Zr)_{pmn}$ (0.19–0.37) and $(Nb/Hf)_{pmn}$ (0.34–0.63) that show values well below unity. These values are identical to those shown by the three N-MORB mean compositions considered (0.21–0.40, and 0.45–0.72, respectively for the two element ratios). Identical conclusion is taken when calculating the ratios among Nb, Zr and Y (Fig. 5.18).

The study of similarly incompatible element ratios in magmas allows to infer these ratios in their mantle sources, because the very low and similar mineral/liquid partition coefficients for these elements prevents their fractionation in the petrogenetic processes (e.g. Langmuir et al. 1992). The analysis of various PLA primitive mantle normalized ratios among the elements Th, Nb, Ta and La (such as, Th/Zr, Nb/Hf, Th/La, Th/Nb, Th/La, Nb/La, Ta/La and Nb/Ta) show a restricted variation for each element-pair (Fig. 5.18), supporting the origin of the PLA magmas from a relatively homogeneous mantle source. Additionally, there is clear evidence that these distinct element ratios are comparable to those presented by N-MORB averages, particularly to those established by Sun and McDonough (1989) and Arevalo and McDonough (2010).

Significant is the absence of any Nb-Ta anomaly in PLA, i.e. the relative depletion of Nb and Ta as compared to other highly incompatible elements. This anomaly is probably the most prominent geochemical feature of magmas produced in subduction zones (e.g. Pearce 1982). The absence of any Nb-Ta anomaly associated to the systematic location of PLA data points in the tholeiitic fields, defined in the several discrimination diagrams for the sub-alkali magmatic series (diagrams AFM, FeO/MgO vs. TiO_2, SiO_2 vs. FeO/MgO and Cr vs. Ti; Fig. 5.15), all support the hypothesis that PLA magmas were not associated to a tectonic setting under any influence of a subduction zone.

In conclusion, the shapes of chondrite normalized REE and primitive mantle normalized patterns as well as distinct element ratios, having either similar or distinct incompatibility degrees, shown by PLA basalts are indistinguishable from N-MORB. Globally, the chemical data obtained in this study for PLA show a strong depletion in the highly-incompatible elements, a characteristic that has been commonly explained to be a consequence of the progressive extraction of continental crust from the upper mantle, that must has begun billions of years ago, according to the radiogenic isotope ratio available data (e.g. Saunders et al. 1988; White 2015).

5.3.1.5 Tectono-Magmatic Trace Element Discrimination Diagrams

Trace element discrimination diagrams have been in use for some time as a means of fingerprinting the tectonic setting of eruption of basic volcanic rocks from the geological record (e.g. Pearce and Cann 1971, 1973). According to many authors (e.g. Wang and Glover 1992; Vermeesch 2006), the most common tectonic discrimination diagrams are not fully satisfactory, particularly if used in isolation, but when using a combination of two, three, or more diagrams, results are generally reasonable (Saccani 2015). In Fig. 5.19, PLA chemical data are plotted in several well-established and tested tectono-magmatic discriminant diagrams, suggesting a clear affinity with a Mid-Ocean Ridge environment.

Identical suggestion is gathered through the use of two diagrams (Fig. 5.20) frequently applied to discerning the tectonic setting of ophiolites and relating Nb, Th, Yb and Ti (Pearce 2008). In the first diagram (Fig. 5.20a), where Nb/Yb is plotted against Th/Yb, and which is particularly useful in highlighting crustal input and hence demonstrating an oceanic, non-subduction related setting, PLA metabasalts are positioned in the trend defined by all mid-ocean ridge and most ocean island basalts (MORB-OIB array). The two trends established in this diagram result from the decoupled behavior of Th and Nb during subduction processes: although both elements are highly incompatible and retain an almost constant ratio during mantle melting, Th is subduction-mobile but Nb is subduction-immobile during lithospheric plate dehydration. As a result, supra-subduction zone lavas and magmas that have assimilated continental crust (mostly derived by subduction) have high Th/Nb ratios. The absence of any trend of PLA samples extending from

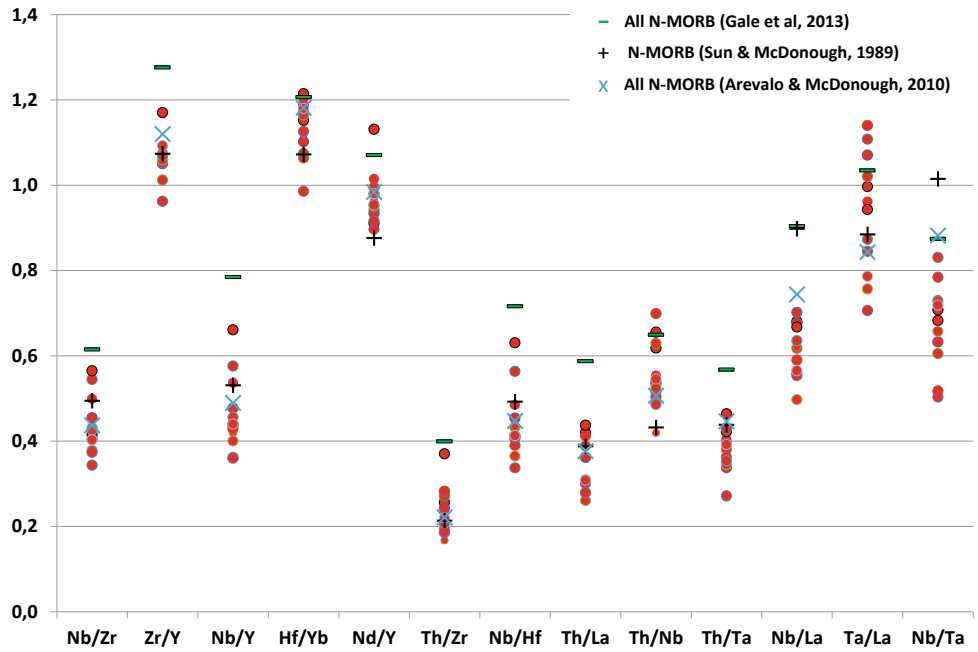

Fig. 5.18 Significant incompatible element ratios obtained in this study for Pulo do Lobo metabasalts. All values are normalized to Primitive Mantle (Sun and McDonough 1989). Ratios such as Nb/Zr, Zr/Y and Nb/Y have the most incompatible element in the numerator and represent an overall fractionation between the more and the less incompatible elements. Hf/Yb and Nd/Y ratios are a measure of the fractionation between the elements located in the middle region and those positioned on the right end of the spidergram shown in Fig. 5.17. Th/Zr and Nb/Hf ratios, both <1, express the depletion in the most incompatible elements (Th and Nb), located in the left side of the spidergram. The remaining ratios relate elements having similar incompatibility degree and, thus, are inferences of these element ratios in their mantle sources. This diagram emphasizes the limited variation in all these element ratios for PLA and their similarity between PLA and the N-MORB averages (data source as in Fig. 5.15)

the MORB-OIB array into the island arc field, which is frequently produced by samples from modern-day back-arc basins, is an important diagnostic feature to associate PLA to a mid-ocean ridge tectono-magmatic setting.

The second discriminant diagram (Fig. 5.20b), where Nb/Yb is plotted against TiO_2/Yb, is frequently used in association with the first diagram with the objective to subdivide the data points plotted along the MORB-OIB array. It is based on the decoupled behavior of Ti and Yb during deep mantle melting, where garnet is a stable mineral phase in the mantle peridotites (Yb is partitioned significantly into garnet producing primary melts with high Ti/Yb values). The distinction between the N-MORB and E-MORB types, characterized by having distinct degrees of enrichment in incompatible elements, is made through the Nb/Yb ratios, whereas Nb is more incompatible than Yb in the magmatic systems. It is evident from Fig. 5.20b that the Pulo do Lobo lavas plot as N-MORB.

In conclusion, and after using several well-established tectono-magmatic discriminant diagrams, build using various immobile elements, it can be concluded that Pulo do Lobo metabasalts are systematically plotted in compositional fields associated to ocean-floor basalts and are consistent with the inference that they could represent oceanic crust from an established spreading centre (N-MORB).

5.3.1.6 Other Published Geochemical Data from Pulo do Lobo Metavolcanics: Integration and Comparison with Data Obtained in This Work

Previous published geochemical data of metavolcanic rocks from the Pulo do Lobo Terrane are restricted to the PhD thesis of Eden (1991), its corresponding synthesis (Eden and Andrews 1990) and the papers by Quesada et al. (1994) and Dahn et al. (2014).

Eden (1991) presented 18 total rock analyses (obtained by XRF, with a limited range of analyzed trace elements) of which 6 were subsequently analyzed by Instrumental Neutron Activation (INAA) to quantify the REE and other important trace elements having low detection limits. These analyses were carried out in the exotic blocks that are preserved within a fine-grained mafic matrix of the Peramora Mélange, both structurally imbricated with sediments of the Pulo do Lobo Fm in Los Ciries antiform (Apalategui et al. 1983) These blocks have a mineral assemblage (actinolite, clinozoisite, chlorite, albite, quartz and opaque minerals) that

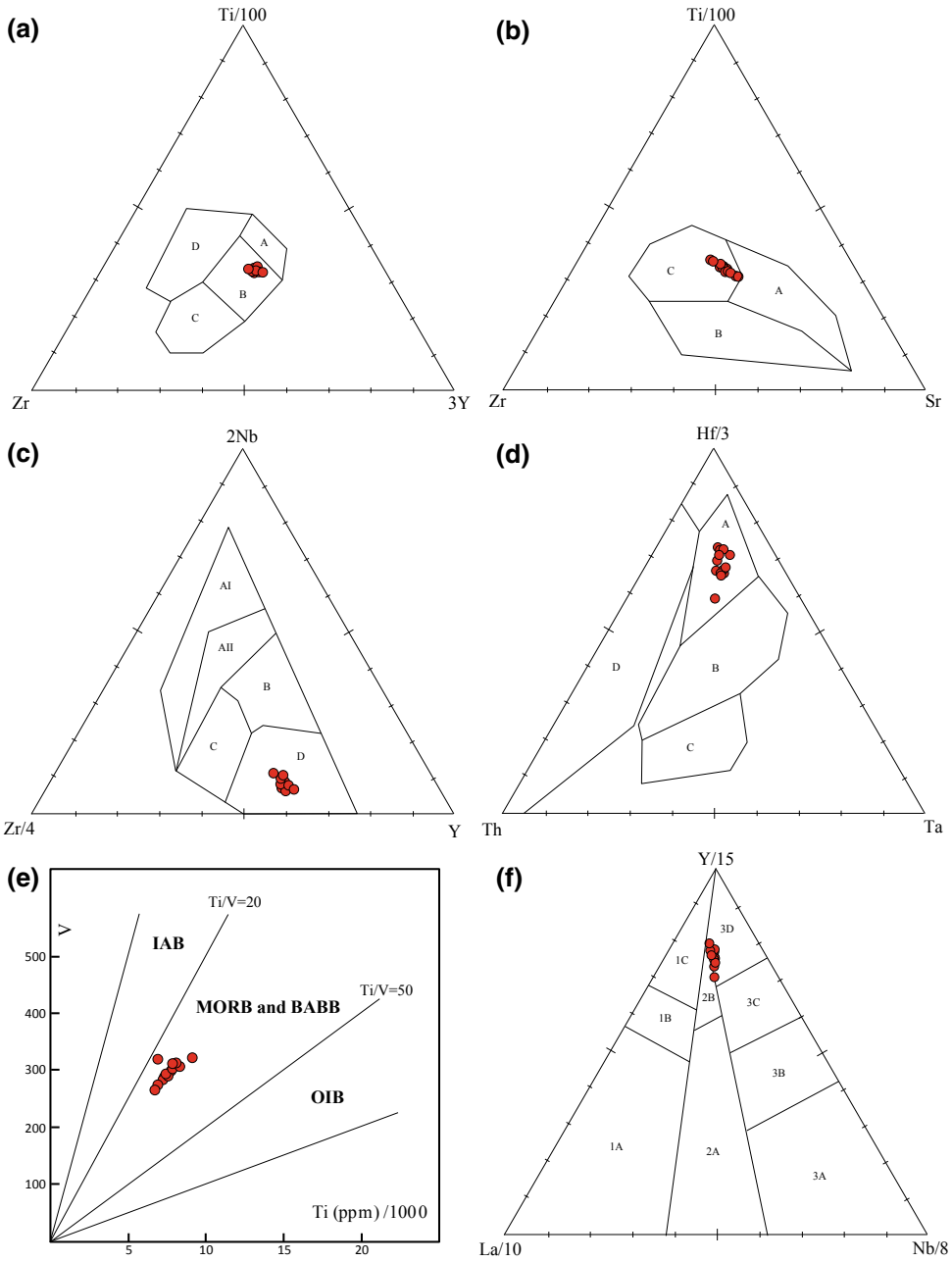

Fig. 5.19 Several tectonic setting discrimination diagrams used to assess the origin of Pulo do Lobo metabasalts. **a** Ti-Zr-Y diagram of Pearce and Cann (1973): A = island arc tholeiites; B = MORB, island arc tholeiites and calc-alkaline basalts; C = calc-alkaline basalts; D = within-plate basalts. **b** Ti-Zr-Sr diagram of Pearce and Cann (1973): A = island arc tholeiites; B = calc-alkaline basalts; C = MORB. **c** Zr-Nb-Y diagram of Meschede (1986): AI = within-plate basalts; AII = alkaline within-plate basalts and tholeiites; B = E-MORB; C = within-plate tholeiites and volcanic arc basalts; D = N-MORB and volcanic arc basalts. **d** Th-Hf-Ta diagram of Wood (1980): A = N-MORB; B = E-MORB and within-plate tholeiites; C = alkaline within-plate basalts; D = volcanic arc basalts. **e** Bivariate diagram correlating Ti and V (from Shervais 1982): IAB = island arc basalts; BABB = back-arc basin basalts; OIB = ocean-island basalts. **f** La-Y-Nb discriminant diagram of Cabanis and Lécolle (1989), where PLA samples are plotted in the 3D field (N-MORB), but in the border of field 2B (BABB)

is characteristic of greenschist facies metamorphism of a mafic protolith and according to Eden (1991) no internal foliation is visible. Taking into account the textural and mineralogical characteristics, associated to the field relationships and structural features, we relate these exotic blocks with the PLA metabasalts. All block samples from Eden (1991) are classified as subalkaline basalts having low Nb/Y (0.13–0.17) and Zr/Ti (=0.01–0.02) element ratios and low concentrations of elements considered highly incompatible during melting of the mantle mineral assemblages, which include the LREE and the HFSE. The tectonic discriminant diagrams using relatively immobile elements (Zr, Y, Nb, Ti, Cr) indicate that these metabasalts correspond generically to ocean floor basalts associated to Mid-Ocean Ridges.

The spidergrams produced from the Peramora samples (Eden 1991) were based on a limited number of elements (REE, Ta and Hf), and only the least differentiated samples (group i) are inside the range of patterns produced by PLA. Additionally, $(Ta/La)_{pmn}$ ratios obtained for Peramora samples range from 0.46 to 0.84 and are globally lower than the variation of PLA (0.71–1.07) and MORB averages previously considered (0.84–1.22). Thus, in comparison with the PLA samples, and considering the limited number of trace

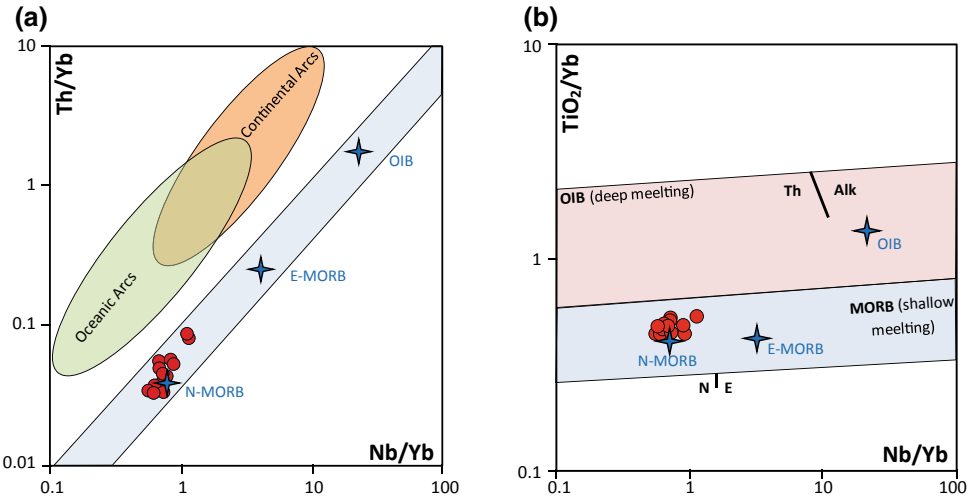

Fig. 5.20 Discriminant tectonic diagrams based on the relationships between Nb/Yb versus Th/Yb (**a**) and Nb/Yb versus TiO_2/Yb (**b**) (adapted from Pearce 2008). Diagram (**a**) is used in a first approach to distinguish magmas generated in a Mid-Ocean Ridge environment from those produced in a subduction zone setting. Pulo do Lobo metabasalts are positioned well within the MORB-OIB array (light-blue area) and located in the vicinity of N-MORB average composition (Sun and McDonough 1989). Diagram (**b**) is used to further detail the origin of basalts plotted in the MORB-OIB array, and PLA samples are positioned in the shallow melting field (light-blue area) and around N-MORB mean composition. Th = tholeiitic; Alk = alkaline; N = N-MORB; E = E-MORB

elements analyzed, it can be concluded that the Peramora metabasalts present a greater compositional variability in these elements (only the least LREE fractionated samples are indistinguishable from PLA), corresponding to distinct degrees of enrichment in incompatible elements, but which, in general, have geochemical affinities with MORB.

Dahn et al. (2014), presented major and trace element data as well as Nd isotopic ratios for three samples collected from the blocks belonging to the Peramora Mélange. The mineralogy of these blocks and their greenschist metamorphic facies are identical to those of the PLA samples. Geochemically they are classified as subalkaline basalts and when using various tectono-magmatic discriminant diagrams, based on relatively immobile elements, these metabasalts are consistently plotted in the fields corresponding to the ocean floor basalts with MORB affinity. The compositional variation of two block samples of Dahn et al. (2014) observed in the spidergrams and REE normalized patterns is similar to the range obtained for the PLA and the produced ratios between different incompatible elements (among REE and HFSE) are also identical to those observed for PLA. However a third Peramora sample is more enriched, having higher incompatible element concentrations, higher LREE/HREE fractionation and higher more-to-less incompatible element ratios (e.g. $(Th/La)_{pmn}$, $(Nb/La)_{pmn}$, $(Zr/Y)_{pmn}$, $(Ce/Hf)_{pmn}$), all typical of E-MORB. Additionally, Dahn et al. (2014) presented Nd isotopic ratios for Peramora blocks, obtaining a variation in $\varepsilon_{Nd(t\ =\ 360\ Ma)}$ between +6.4 and +8.5, which is also within the range presented by MORB (e.g. DePaolo 1981).

Quesada et al. (1994) presented the only geochemical study of the Trindade-Alfarrobeira metavolcanic basalts published so far. All studied samples (six in total) correspond to subalkaline basalts and are characterized by low incompatible element contents that are within the range of reported values for ocean floor tholeiites. Using distinct tectonic discriminant diagrams, all samples are positioned in the ocean floor/ MORB fields. Four samples display relatively flat REE patterns, but having LREE depletion relatively to MREE and HREE (giving $(La/Sm)_{CN}$ and $(La/Yb)_{CN}$ ratios <1). The other two samples are more REE fractionated and are LREE enriched comparatively to the other REE (producing $(La/Sm)_{CN}$ = 1.31–1.47 and $(La/Yb)_{CN}$ = 1.41–1.74). Distinct ratios among Zr, Y and Nb are also comparable to those commonly reported for MORB and identical to PLA samples. The patterns produced by the four most depleted samples, in the Primitive Mantle normalized spidergrams, are almost indistinguishable from those of PLA samples showing, however, slightly higher Th and Nb concentrations and normalized Th/Nb, Th/La and Nb/La ratios, comparatively to PLA.

In conclusion, all published chemical data for Pulo do Lobo Domain have MORB compositional affinity, but show distinct incompatible elements enrichment degrees. The majority of these samples globally have a geochemical composition similar to that presented by N-MORB.

However, a limited number of the metabasalts are more enriched and have chemical characteristics more similar to E-MORB.

5.3.1.7 Conclusions

The present detailed geochemical study is based on 13 samples of a drill core performed in the Trindade-Alfarrobeira strip of mafic rocks, Pulo do Lobo Terrane, Portugal. These rocks are interbedded in the Pulo do Lobo phyllites and both lithologies are affected by greenschist facies metamorphism and three episodes of tectonic deformation. Plotting the samples chemical analysis in classical discriminant diagrams shows that the mafic rocks are subalkaline basalts falling in the tholeiitic field and represent N-MORB type oceanic crust. The chondrite-normalized REE patterns, the trace element concentrations and their critical ratios together with the primordial mantle normalized patterns observed in PLA samples, all support this conclusion.

These results demonstrate that these rocks have clear geochemical affinity with the Peramora mafic rocks of the Los Ciries antiform, Spain (Eden 1991; Dahn et al. 2014). Furthermore, the Peramora basalts are imbedded in a mafic-shale matrix with oceanic-type composition, reinforcing so the oceanic character of these basalts (Dahn et al. 2014).

These mafic rocks have deserved distinct geodynamic interpretations, from true oceanic basalts (e.g. Quesada et al. 1994; Braid et al. 2010) to an intrusive basic vein system (e.g. Ribeiro et al. 2010; Pérez-Cáceres et al. 2015). As far as we are concerned, the vein interpretation is hard to reconcile with the structural and metamorphic history of the PLA rocks, common with the enveloping sediments, and the N-MORB geochemical signature. On the other hand, the latter do not discriminate between true large ocean or mature back-arc basin environments. A geodynamic interpretation depends on the regional geological context, a matter that will be discussed below in Sect. 5.5.

5.3.2 The Pulo do Lobo Terrane Stratigraphic Sequence

J. T. Oliveira, J. X. Matos, P. Fernandes, Z. Pereira, R. S. Jorge

5.3.2.1 Introduction

Geological mapping of the Pulo do Lobo Terrane shows that the Pulo do Lobo Formation occupies its central part (Fig. 5.21). North and South of this unit several clastic formations crop out, which are divided in Portugal into two lithostratigraphic groups: the Ferreira-Ficalho Group located to the North and the Chança Group situated to the South. The Ferreira-Ficalho Group is represented by three clastic Fms (Carvalho et al. 1976; Oliveira et al. 1986; Oliveira 1990), which in ascending stratigraphic order are: Ribeira de Limas, Santa Iria and Horta da Torre formations. The first two of these units were recognized and mapped in Spain (Apalategui et al. 1983, 1984). Later, the Ribeira de Limas and Santa Iria Fms were respectively correlated with La Giralda and Puerto Cañón formations (Eden 1991) or with the Flyschoid and Quartz-flyschoid units (Crespo-Blanc 1989), and the Horta da Torre Fm with the Ortoquartzites Fm (Crespo-Blanc 1989).The Chança Group, originally composed of three clastic units, i.e. Atalaia, Gafo and Represa formations (Pfefferkorn 1968; Cunha and Oliveira 1989; Oliveira 1990; Silva et al. 1990) is now revised excluding the Represa Fm, interpreted as part of the Iberian Pyrite Belt. The Atalaia Fm has not been identified in Spain so far. In spite of the strong tectonism that affects the entire succession, the composing lithostratigraphic units are easily recognized in the field. What follows is a synthesis of the present knowledge, following the nomenclature used in Portugal, which is far more referred to in the literature.

5.3.2.2 Pulo do Lobo Formation

The Pulo do Lobo Fm, also called Cumbres de Los Ciries Formation (Eden 1991) and Sierra de las Bañas Formation (Crespo-Blanc 1989), consists of highly sheared dark coloured schists, siltstones and quartzites and minor acidic intrusive veins. The schists, thin-bedded siltstones and fine-grained quartzite layers are predominant but the quartzite beds become progressively thicker at the upper part, both in the North and in the South of the unit exposure, reaching one meter in thickness and frequently presenting a phacoid geometry imposed by tectonic shearing (Fig. 5.22a). Abundant metamorphic exudation quartz veinlets are a typical feature of this Fm (Oliveira 1990). The unit thickness is unknown, probably of the order of several hundred meters. N-MORB mafic rocks occur intercalated in the metasedimentary succession, both in Portugal (Trindade-Alfarrobeira, described in above in Sect. 5.3.1) and Spain (Peramora Mélange in Los Ciries Antiform) (Munhá 1983; Apalategui et al. 1983; Eden 1991; Quesada et al. 1994; Crespo-Blanc and Orozco 1988, 1991; Dahn et al. 2014).

This unit is affected by three episodes of tectonic deformation with associated folding and related cleavages. The second episode is the most important, marked by NW-SE tight folding and strong associated SW-vergent cleavage frequently showing a shear component (Fig. 5.22b, c). The first episode is usually preserved as small scale intrafolial folds and related cleavage in microlithons of the second cleavage. The third episode is marked by vertical or SW

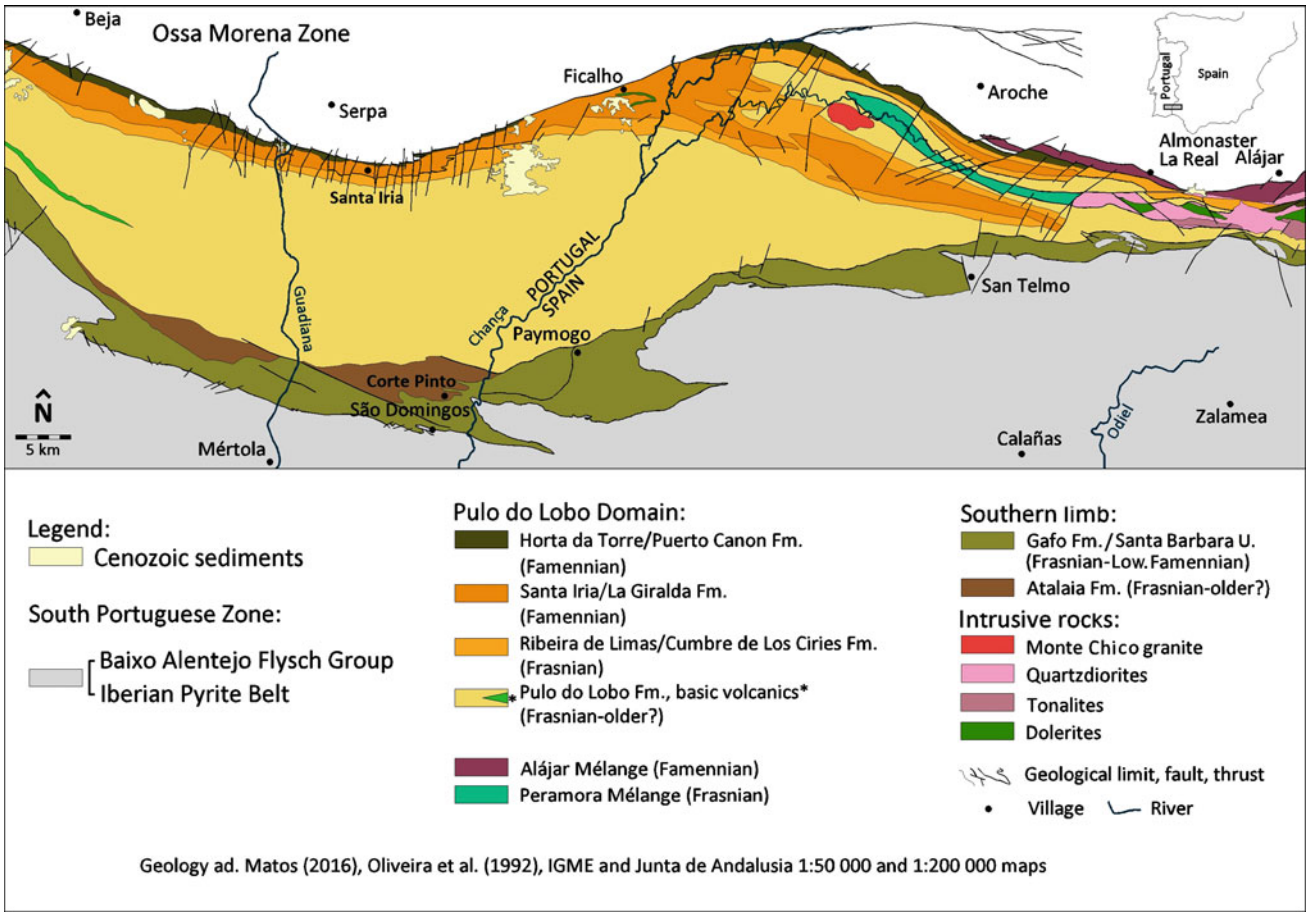

Fig. 5.21 Geological map of the Pulo do Lobo Domain (adapted from: Matos 2016; Oliveira 1992; Apalategui et al. 1983, 1984; Matas et al. 2010). Rectangles correspond to studied sectors shown in Fig. 5.23: **a** Serpa, **b** Peramora, **c** Almonaster, **d** Alájar

vergent folds without cleavage or restricted to the fold hinges (Silva et al. 1990; Eden 1991; Braid et al. 2010; Pérez-Cáceres et al. 2017).

Metamorphism is of upper greenschist-lower amphibolite facies (Munhá 1983; Eden 1991). More recently Rubio Pascual et al. (2013) found lawsonite pseudomorphs in the amphibolitic schists that enclose the mafic rocks of the Peramora Mélange which are linked to a first HP/LT episode of metamorphism (see Chap. 12 in this volume). This episode was later re-equilibrated by the regional greenschist facies metamorphism.

The Pulo do Lobo Fm was recently dated by palynomorphs in several locations both in Portugal and Spain (Pereira et al. 2018). In Portugal, south of Serpa region (Fig. 5.23) dark schists interbedded in the upper quartzites beds yielded a moderate to well preserved palynomorph assemblage assigned to the BM Biozone of mid Frasnian age. Characteristic spores of the assemblage are *Apiculiretusispora cf. brandtii, Aneurospora greggsii, Chelinospora concinna, Cristatisporites triangulatus, C. inusitatus, Cymbosporites magnificus, Emphanisporites rotatus, Geminospora lemurata, Grandispora cf. douglastownense, G. protea, Pustulatisporites rugulatus, Retusotriletes sp., Tholisporites densus, Tholisporites tenuis, Verruciretusispora dubia, V. loboziakii, Verruciretusispora sp., Verrucosisporites premnus and V. scurrus and the key species Verrucosisporites bulliferus*.

The same palynomorph biozone was also found in dark schists in Spain, south of Rosal de la Frontera and south of Aroche in the Los Ciries Antiform (Fig. 5.23), indicating contemporaneity of the upper levels of the Pulo do Lobo Fm in Portugal and Spain. All palynological productive samples contain common spore tetrads, scolecodonts, prasinophytes and rare acritarchs. Reworked Lower Devonian spores, e.g. the genera *Ambitisporites sp., Archaeozonotriletes sp., Camarozonotriletes sp. and Camarozonotriletes sextantii*, are also common.

In the Peramora Mélange at the core of Los Ciries Antiform (Fig. 5.23) dark schists in which the mafic metavolcanics and amphibolite schists are intercalated, near the bridge over the Peramora stream, also yielded a similar mid Frasnian spore assemblage. In apparent contradiction, the metasedimentary rocks of the Pulo do Lobo Fm in Los Ciries Antiform, and also the mafic matrix and the blocks of

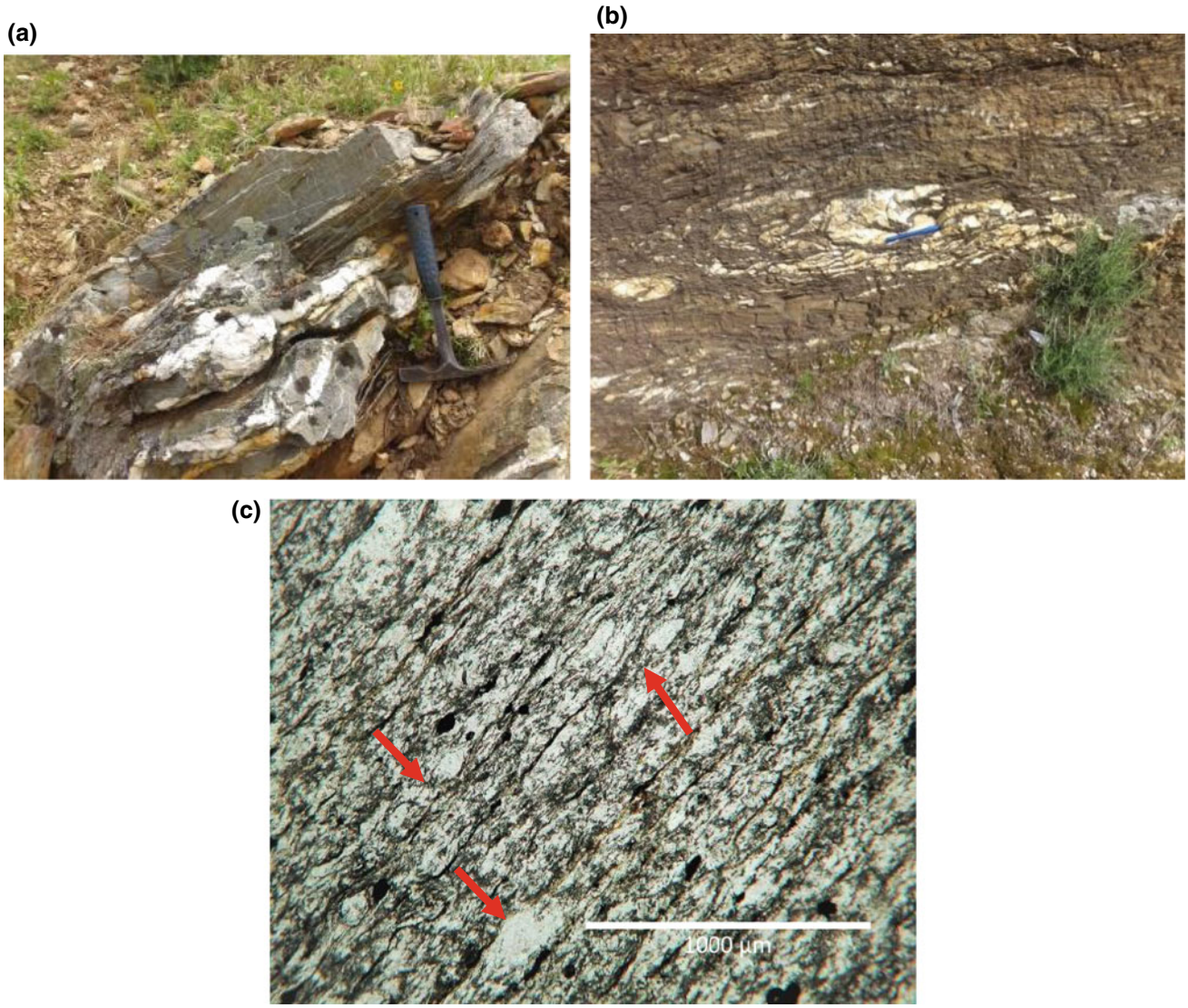

Fig. 5.22 **a** Quartzite beds with a phacoid geometry, Fonte Letreiro farm, near the Ribeira de Limas stream; **b** F3 quartz veinlet with the fold limbs affected by syn-F2 shearing, 100 m south of the Cobres river bridge, road Beja-Mértola; **c** thin-section, plain light, of a quartzite bed, Pulo do Lobo Formation, South sector, road cut 50 m south of Barranco dos Alcaides bridge, Corte de Pinto-Vila Nova de São Bento road; note the quartzite ribbons (red arrows) preserved between the planes of the shearing cleavage

the Peramora mélange provided some young detrital zircon grains dated (LA-ICPMS, U-Pb) at ca. 340–350 Ma (Tournaisian; youngest grain at 341.3 ± 7.5 Ma), which was primarily interpreted as the maximum depositional age of these Fms (Dahn et al. 2014). However, the own authors questioned the significance of these ages, since they are contradicted by post-deformation intrusion of the Monte Chico granite at ca. 345 Ma and gabbro at ca. 354 Ma (Gladney et al. 2014), and postulated that a process of Pb-loss may have taken place, probably connected to intrusion of the Gil-Márquez pluton to which the above mentioned granite and gabbro belong. Interestingly, those Lower Carboniferous ages were not found by Pereira et al. (2017) in the detrital zircon populations of two metagreywacke samples of the Pulo do Lobo Fm in Portugal, i.e. away from any thermal disturbance, and where the youngest detrital zircon grains, making only 1% of all grains, are ca. 531 Ma (Cambrian).

5.3.2.3 Ferreira—Ficalho Group

Ribeira de Limas Formation

This unit consists of dark schists intercalated with greywackes, quartzwackes and micaceous quartz-arenites, with ca. 100 m of structural thickness. Locally, minor fine-grained acidic volcanic rocks appear intercalated with the detrital rocks (Crespo-Blanc and Orozco 1988). The Ribeira de Limas Fm is found in stratigraphic continuity

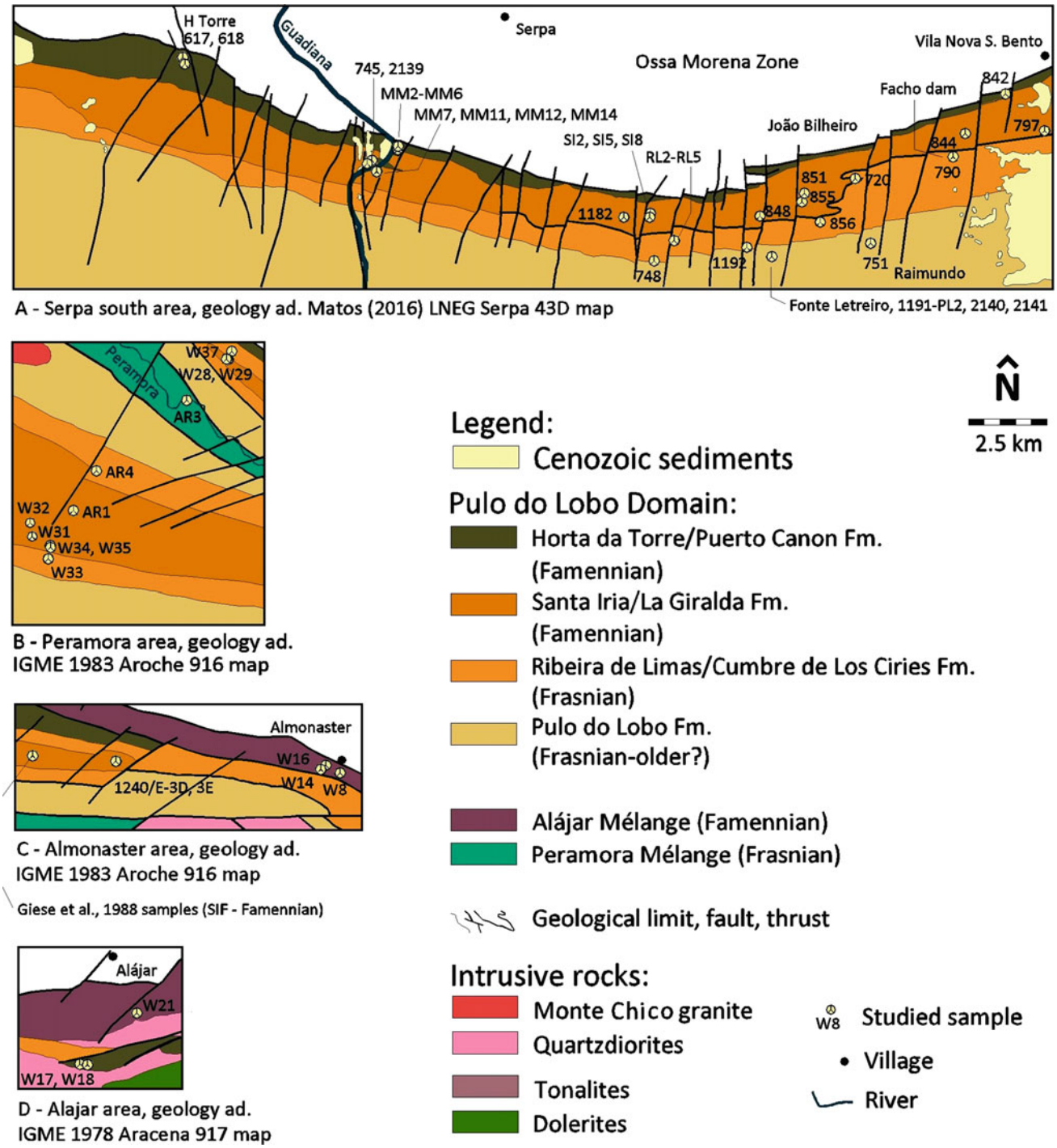

Fig. 5.23 Geological detail and sample location in the four areas studied. See location in Fig. 5.21 (adapted from Pereira et al. 2018)

with the Pulo do Lobo Fm, with which it shares the same three episodes of tectonic deformation, although it appears to be less metamorphosed (Pereira et al. 2006; Fig. 5.24a, b). The unit is affected by low-grade metamorphism with a quartz-muscovite-biotite paragenesis associated with the development of the penetrative tectonic cleavage of the second phase of deformation. Vitrinite reflection values obtained from dark schists is >3% Rr (Eden 1991) or range from ca. 4.0–4.4% Rr, indicating peak temperatures ca. 325–340 °C (Pereira et al. 2006). These temperatures are compatible with the metamorphic mineral paragenesis described above.

Dark schists sampled in several locations of the Ribeira de Limas Fm in Portugal (Fig. 5.23) yielded poor to

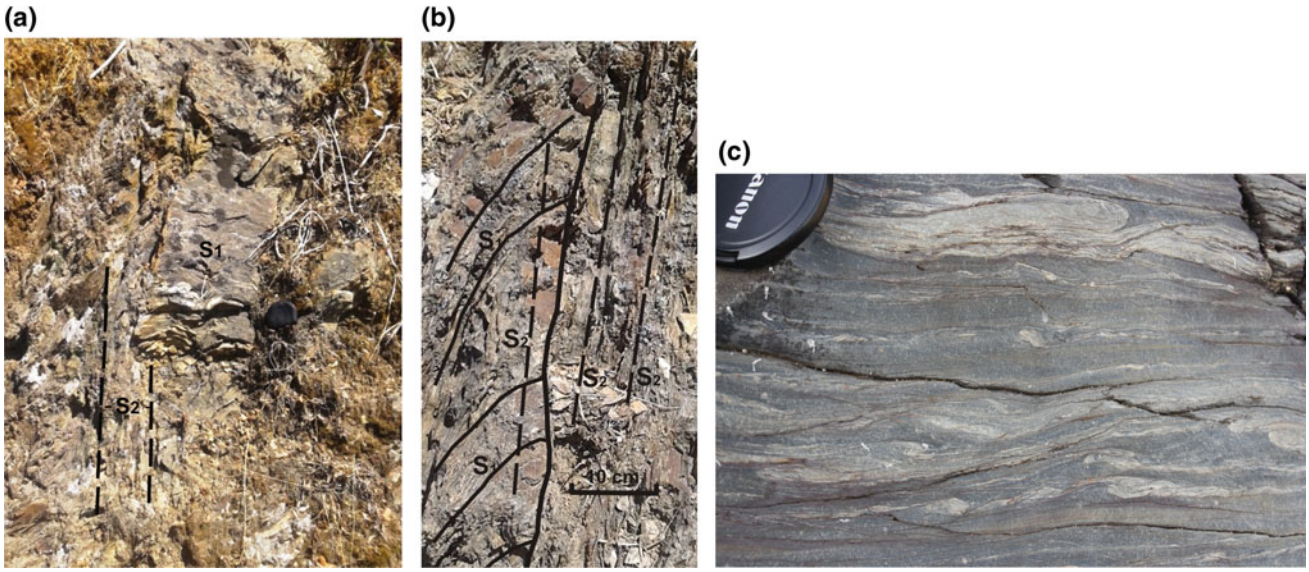

Fig. 5.24 **a** S1 cleavage of the F1 tectonic episode preserved in a quartzwacke bed and superimposed S2 cleavage of the F2 tectonic episode, Ribeira de Limas Fm, road-cut 100 m N of the Ribeira de Limas bridge, ca 8 Km SE of Serpa town; **b** F1 folds and associated cleavages, affected by S2 cleavage, Ribeira de Limas Fm, same local as A; **c** Close up of bedding of Santa Iria Formation with still preserved sedimentary features, slumps and linsen bedding, 750 m SW of the Misericórdia water mill, Guadiana River west bank

moderate preserved miospores assigned to the BM Biozone of mid Frasnian age (Pereira et al. 2006, 2018). This assemblage is similar to that recovered from the Pulo do Lobo Fm, including the reworked Lower Devonian miospores, prasinophytes and acritarchs. In terms of U-Pb zircon ages, a quartzwacke sample contains the youngest concordant zircon age of 947.6 ± 4.3 Ma (Braid et al. 2011). A much younger age of ca. 400 Ma (Emsian) was observed in another quartzwacke sample (Perez-Cáceres et al. 2017). U-Pb ages of detrital zircons were also studied by Pereira et al. (2017) who found the youngest age of 547.0 Ma (Ediacaran).

Santa Iria Formation

This Fm is composed of interbedded dark shales, siltstones, greywackes (Fig. 5.24c) and thin layers of tuffites (Crespo-Blanc 1989) that form a flysch type succession with a structural thickness in excess of 200 m. The unit unconformably overlies the Ribeira de Limas Fm (Carvalho et al. 1976; Oliveira 1990). The wackes contain clasts of sub-angular to sub-rounded quartz, plagioclase, detrital micas (biotite and muscovite) and fragments of acidic volcanic rock dispersed in a quartz-sericite matrix (Crespo-Blanc and Orozco 1988; Fig. 5.24d). This Fm is only affected by one episode of tectonic deformation represented by upright NW trending folds and associated spaced cleavage. The metamorphic paragenesis (biotite+muscovite+ chlorite+quartz) and organic maturation indicators (vitrinite reflectance) show that the metamorphism is of low greenschist grade (Pereira et al. 2006). Dark shales and siltstones, in Portuguese and Spanish outcrops of the Santa Iria Fm (Fig. 5.24) yielded well-preserved spore assemblages assigned to the VH Biozone of late Famennian age (Pereira et al. 2006, 2018). The assemblages include the key species *Grandispora echinata* together with *Ancyrospora* sp., *Apicfound uliretusispora verrucosa, Cristatisporites triangulatus, Cristicavatispora dispersa, Diducites* spp., *Emphanisporites annulatus, E. rotatus, Grandispora cornuta, Retusotriletes* spp., *Rugospora explicata, R. radiata, Teichertospora iberica* and *Vallatisporites hystricosus*. All samples contain also very rich assemblages of well-preserved prasinophytes and acritarchs.

U-Pb ages of detrital zircon from greywackes provided maximum depositional ages of 347.2 ± 5.5 Ma (Braid et al. 2011), ca. 345 Ma (Pérez-Cáceres et al. 2017) and ca. 370 Ma (Pereira et al. 2017). An important feature of this Fm is the presence of a Late Devonian—Early Carboniferous zircon population, making 32–40% of all detrital zircons, with peaks at ca. 347 Ma (Braid et al. 2011) and 375–365 Ma (Pérez-Cáceres et al. 2017). This conspicuous zircon population was not identified by Pereira et al. (2017), who reported a youngest Upper Devonian zircon population (380–370 Ma), forming only 5% of all detrital zircons.

The Santa Iria Fm is considered a syn-orogenic deposit and as such is also dealt with in Sect. 11.2.3, Chap. 11 of this volume.

Horta Da Torre Formation

This unit, firstly defined in Portugal (Oliveira et al. 1986), corresponds to the Orthoquartzite Fm in Spain (Crespo-Blanc 1989). It is exposed at the boundary with the OMZ for

more than 150 kms, of which ca 100 kms just in contact with the Beja-Acebuches Ophiolite Complex (Quesada et al. 1994). The lithological composition and thickness change in part due to the effect of the South Iberian Shear Zone (Crespo-Blanc and Orozco 1988, 1991) and the Ficalho-Valdedelarco Fault (Fig. 5.21). In the central region the dominant lithologies consist of dark shales, siliceous siltstones, greywackes and bioturbated micaceous sandstones (Oliveira et al. 1986). In Portugal, Santa Susana region (NW of the PLT, not represented in Fig. 5.21) and in Spain (sierras de Solana, Giralda, etc) sigmoidal shaped ortoquartzites are an important component, forming elongated hills parallel to the NW-striking dominant tectonic structure. The structural thickness changes from few tens to ca 700 m. The Horta da Torre Fm is affected by only one main tectonic episode with associated upright and NW trending folds and related cleavage. Late tectonic ductile-fragile shearing parallel to the South Iberian Shear Zone (Crespo-Blanc and Orozco 1988) is the main cause for the sigmoid geometry shown by the ortoquartzites according to Crespo-Blanc (1989). Metamorphism is of very low grade, similar to that of the Santa Iria Fm. Crespo-Blanc (1989) considered that the phacoid quartzites of the Alájar mélange (see below) belong to the Orthoquartzites Fm.

Black shales provided several productive samples with well-preserved assemblages of miospores assigned to the VH Biozone of late Famennian age. The assemblage contain *Grandispora echinata* together with *Ancyrospora sp., Apicfound uliretusispora verrucosa, Cristatisporites triangulatus, Cristicavatispora dispersa, Diducites spp., Emphanisporites annulatus, E. rotatus, Grandispora cornuta, Retusotriletes spp., Rugospora explicata, R. radiata, Teichertospora iberica and Vallatisporites hystricosus*. All samples are very rich in assemblages of well-preserved acritarchs and prasinophytes (Pereira et al. 2006, 2018). The assemblage is similar to that found in the Santa Iria Fm which is indicative that the unit may represent a shallower facies variation of the deep water Santa Iria Fm.

Alájar Mélange Formation

Following the definition by Eden (1991) this Fm is composed of a matrix of fine grained phyllites, enclosing variable sized and very pure massive orthoquartzites. Fine grained mylonites forming cm to m-thick zones occur and the ortoquartzites show sigmoidal geometry, the sigmoids reaching up to 30 m in length parallel to strike. These sigmoids correspond to disrupted original and continuous beds. This Fm also encloses local isolated and exotic blocks of serpentinised ultramafic rocks (dunites) altered to talc, which may reach some tens of meters in length, as well as blocks of marbles. According to Eden (1991) and Braid et al. (2010, 2011, 2012), this unit represents a true mélange, which Eden (1991) parallelizes with the Péramora mélange. As seen above, Crepo-Blanc (1989) includes this unit in her Orthoquartzite Fm whereas Pérez-Cáceres (2017) suggests that the serpentinised blocks and the marbles constitute true olistrostomes.

Dark phyllites that enclose the ortoquartzite sigmoids were sampled at three road-cuts (Almonaster la Real and Camino de Campofrio, Fig. 5.23). The samples provided a spore assemblage containing *Geminospora lemurata, Emphanisporites* sp., *Punctatisporites* sp., and *Retusotriletes* sp., and the late Famennian key species *Grandispora echinata*. All samples contain common to abundant well-preserved species of prasinophytes (*Cymatiosphaera* sp., *Leiosphaeridia* sp., *Maranhites* spp.), rare to common acritarch (*Crassiangulina* sp., *Veryhachium* sp., acritarch species A) and rare quitinozoan remains. This assemblage is quite similar to that recovered from the shales of the Horta da Torre Fm, both having the key species *Grandispora echinata* and as such they are assigned the same late Famennian age.

According to Braid et al. (2010, 2011, 2012), the Alájar mélange represents a syn-orogenic deposit, reason why it is also dealt with in Sect. 11.2.3, Chap. 11 of this volume.

5.3.2.4 Chança Group

Atalaia Formation

Thin-bedded schists and siltstones, quartwackes and quartzites are the main lithologies of this Fm (Pfefferkorn 1968; Carvalho et al. 1976; Oliveira 1982, 1990; Pereira et al. 2006). The quartzites consist of recrystallized quartz grains with, in lesser extent, biotite and muscovite (Fig. 5.25b). The quartzwackes have a few feldspars and a little more matrix. The unit has been mapped in the southern central area of the Pulo do Lobo Terrane, in Portugal, where it is preserved in two main outcrops with few tens of kms long sigmoidal geometry, probably bounded by thrust faults (Fig. 5.21). It has not been identified so far in Spain. The structural thickness changes from ca. 500 m to nil. The stratigraphic succession is affected by three episodes of tectonic deformation, similar in style to those observed in the underlying Pulo do Lobo Fm (Fig. 5.25a). Acidic and basic veins, few meters thick and few hundred meters long were intruded after the second episode of folding F2 but folded by the three tectonic episode F3 (Fig. 5.25c, d). As for the Pulo do Lobo Fm metamorphism is of the greenschist facies (Pereira et al. 2006).

The Atalaia Fm did not yield well preserved palynomorphs so far. A quartzite sample from the Atalaia Fm was studied by Pereira et al. (2017), who reported the youngest concordant zircons at age of 390.5 ± 4.7 Ma (Eifelian), which is interpreted as the maximum depositional age for this formation. The Atalaya Fm is considered

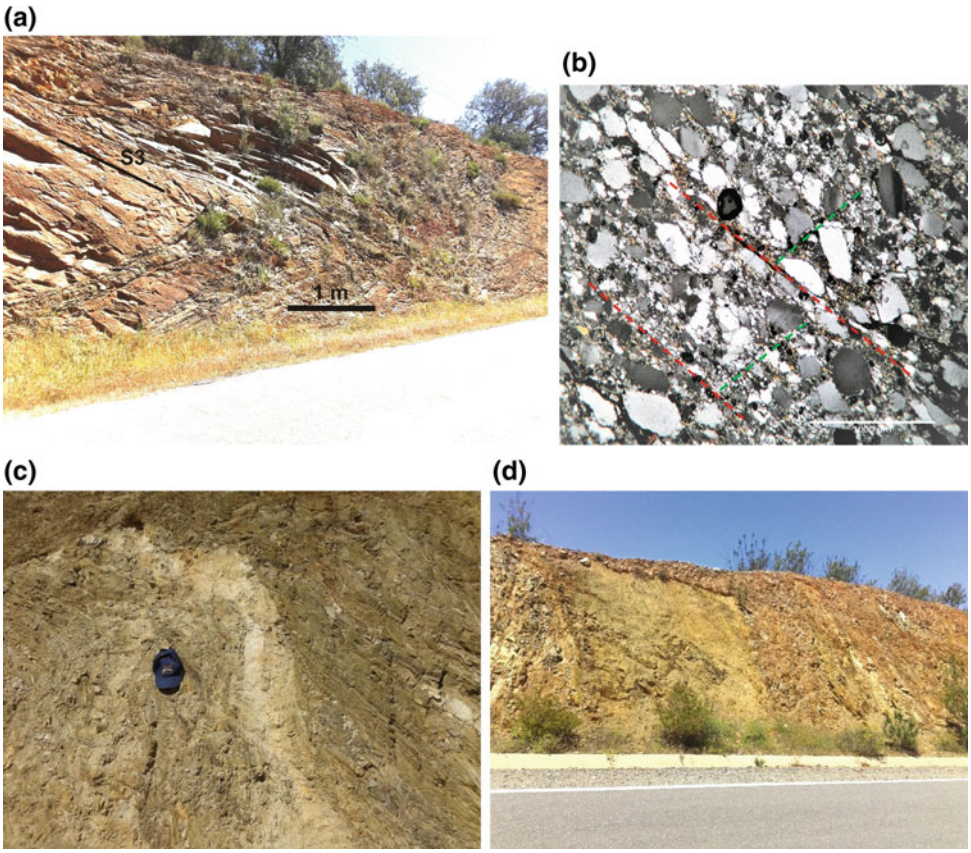

Fig. 5.25 **a** F3 NW vergent folds in the Atalaia Fm, km 49.7 road Mina de São Domingos-Serpa; **b** thin section view of a quartzite bed, cross-polarized light, Atalaia Formation, showing two cleavages:the strongest S2-red dashed lines; S1-green dashed lines, Giralda, road S. Domingos-Serpa, km 49.7; **c** post-F2 acidic vein folded by the F3 episode, road-cut 100 m south of Corte Pinto village; **d** post-F2 basic dyke, road cut 2 km north of Corte Pinto village

equivalent in the southern sector of the PLT to the Ribeira de Limas Fm in the northern sector.

Gafo Formation

The Gafo Fm is a succession of greywackes and interbedded slates, with minor intercalations of fine volcanoclastic sediments (tuffites), intruded by metric-thick felsic and mafic veins, several hundred meters long. The greywackes contain grains of acid and mafic volcanic rocks, quartz, feldspars and chert dispersed in a sericite + chlorite + quartz fine-grained matrix (Fig. 5.26c). Clasts of metamorphic rocks are less common and comprise fragments of schists and quartzites. In Portugal this unit is bounded to the South by the Represa Fm (not recognized in Spain) presently integrated in the Iberian Pyrite belt succession (see Chap. 6 in this volume). The Gafo Fm shows two NW trending main episodes of tectonic deformation (Fig. 5.26a) and associated cleavages and locally pre-cleavage first generation folds (Fig. 5.26b). The structural thickness may reach 500 m. Metamorphism is of low greenschist facies (Pereira et al. 2006).

In the recently published Geological Map of Spain, sheet Sevilla–Puebla de Guszmán, scale 1:200,000 (Matas et al. 2010), this unit is distinguished from the Santa Barbara Fm, and both are included in the Santa Barbara Group. Both units have very similar lithological characteristics and are separated by the Santa Barbara thrust fault.

In Portugal slates from the Gafo Fm provided poorly preserved miospores assigned to the upper part of the BM Biozone of mid Frasnian age (Pereira et al. 2006) but a recent revision points to the lowermost Famennian as indicated by the GF Biozone, which includes common *Grandispora famenensis* (the zonal specie), *Acinosporites* sp., *Aneurospora gregssii*, *Cristatisporites* sp., *Geminospora lemurata*, *Gradispora* sp., *Emphanisporites* sp., *Retusotriletes* spp, *Rugospora* sp., *Verrucosisporites premnus* and *V. scurrus*. All samples contain assemblages of acritarchs and prasinophytes.

The Gafo Fm exposed along the Chanza river yielded spore assemblages indicating a late Givetian to early Famennian age (Lake 1991). On the other hand, one sample taken from the Santa Barbara Fm gave a Tournaisian age (Rodríguez González in Matas et al. 2010).

A greywacke sample from the Gafo Fm yielded an U-Pb zircon age of 384 ± 6 Ma (Eifelian) for the youngest grain, which is assumed to represent the maximum depositional age for this Fm (Pereira et al. 2017) similar to that obtained

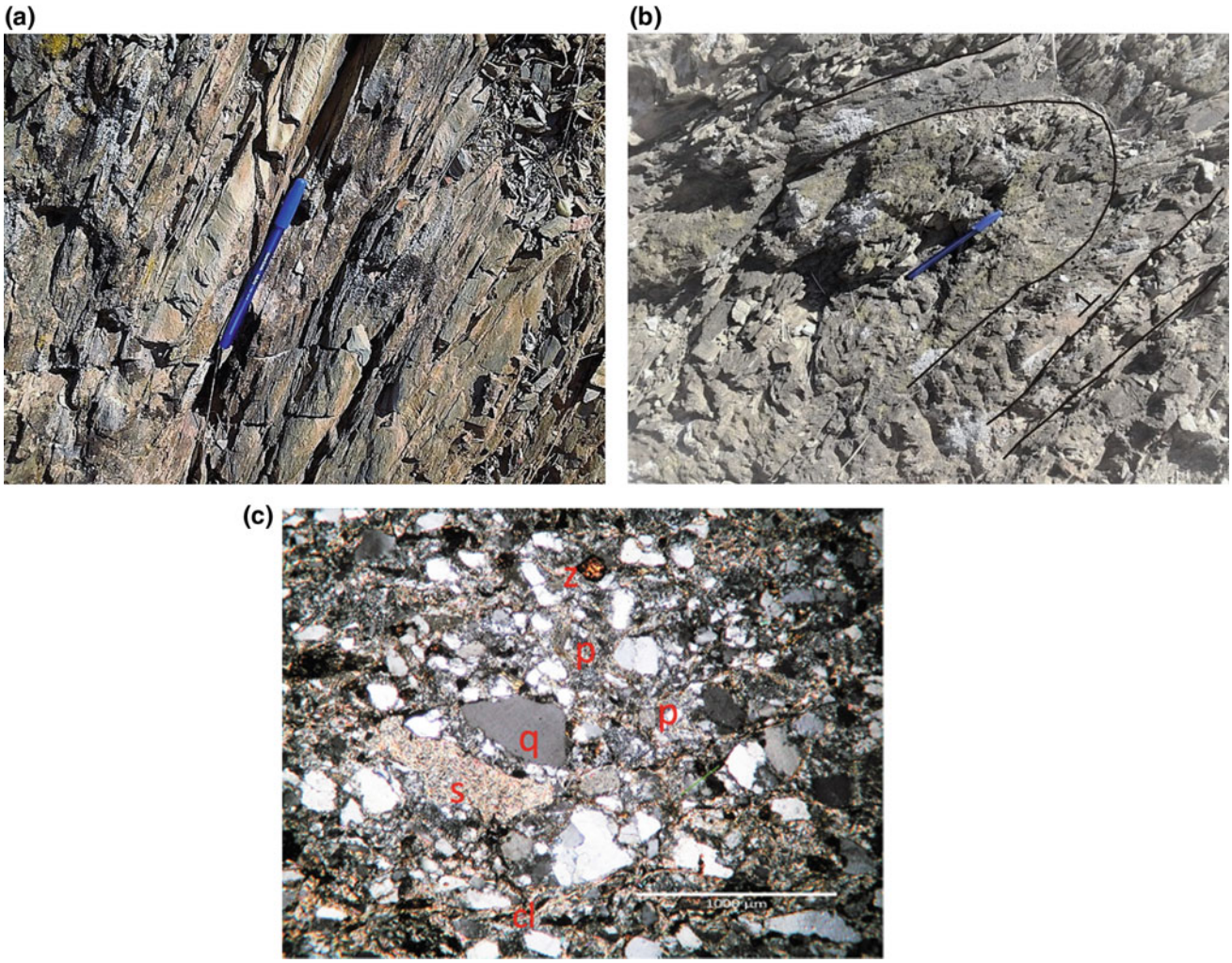

Fig. 5.26 **a** Gafo Fm siltstones and shales showing the L1 (S0^S1) lineation (top of the pen) folded by the S2 cleavage F1, road-cut Mina de São Domingos-Serpa, km 50.7; **b** fold in the Gafo Fm greywackes, S1 cleavage paralell to the pen, road-cut Mina de São Domingos-Serpa, km 51.2. The sedimentary polarity shows that this fold refolded a pre-F1 syn-sedimentary fold; **c** thin-section of a greywacke bed, cross-polarized light, Gafo Fm, Chança river, 300 m south of Volta Falsa old mine. Symbols: cl-chlorite; q-quartz; p-plagioclase; sh-shale clast; z-zircon

for the underlying Atalaia Fm. The age and geological interpretation of the Gafo and Santa Barbara Fms are still poorly understood and need further research.

5.3.2.5 Discussion on the Age and Sediment Provenance of the Pulo do Lobo Stratigraphic Units

Once palynostratigraphy and U-Pb absolute age in detrital zircon are the methodologies used to date the Pulo do Lobo Domain stratigraphic units and characterize sediment provenance, it seems appropriate to resume their basic principles.

Palynostratigraphy is an old branch of the earth sciences. Its techniques are well established, from the sample preparation to the definition of biozones and these are well constrained by other fossil groups, both macro and micro as, e.g. ammonoids and conodonts biostratigraphy (Streel 2009; Higgs et al. 2013). It deals with the study of a wide range of fossil microorganisms, of which miospores, prasinophytes and acritarchs, the biological groups that are treated in the present work. The structure of these microfossils proved to be resistant to metamorphism until the lower amphibolite facies and as such they can be used to date terrigenous sequences, including those affected by metamorphism. Palynostratigraphy is also an important tool in paleogeography and paleoclimatology reconstructions.

Detrital zircon investigation is a relatively recent branch of the earth sciences, with growing application in provenance studies and inference of maximum depositional age of sedimentary rocks based on U-Pb absolute age determinations. Zircon is known to resist to heat and corrosion and in general to the metamorphic and erosive process that occur in

the earth crust, retaining in its structure the geological events to which the crystal was subjected and whose age can be calculated using the U-Pb radiometry. However, under certain circumstances, particularly when the crystal is subjected to radiation (metamictization) or to the effect of metamorphic fluids, the crystal may modify its internal structure and Pb-loss by diffusion can occur with implications on age determinations (Gerdes and Zeh 2006, 2009).

As seen above the ages of the units that compose the Pulo do Lobo Domain show several discrepancies between the two methodologies, which are resumed in Table 5.3. For comparison the table also contains data from the South Portuguese Terrane.

Comparing the U-Pb detrital zircon ages and the palynological ages of the Pulo do Lobo Domain units, the results do not show a clear global tendency, i.e. there are units with palynological ages older than the U-Pb zircon ages, but in others the reverse may occur. Also for a given stratigraphic unit the U-Pb zircon ages are distinct, depending on the authors. In this case the results may possibly have been biased by sampling, number of grains studied (Anderson 2005) or even alteration of the zircon structure (Hay and Dempster 2009). Nonetheless, the results attained by both methodologies allow the following comments:

- The palynological ages obtained for the Horta da Torre, Ribeira de Limas and Gafo Formations are younger than the U-Pb maximum depositional ages and consequently may be considered stratigraphically valid and conforms the regional stratigraphic sequence.
- The Alájar Mélange has a mapping position very similar to that of the Horta da Torre Formation (according to Crespo-Blanc and Orozco 1988; Pérez-Cáceres et al. 2017, they are stratigraphically equivalent) and their shales yielded palynomorphs of the same age (late Famennian, Pereira et al. 2018). However, the quartzite phacoids and the associated schists yielded a U-Pb maximum depositional age of 440 My (Lower Silurian, Braid et al. 2011; Pérez-Cáceres et al. 2017), about ~80 Ma older than the palynological age. Since Silurian volcanism is not known in the South Portuguese Zone and in the Ossa Morena Zone (Gondwana margin), Laurentia, possibly the British Caledonides, was seen as the source of the Alájar quartzites (Braid et al. 2011). The marble and serpentine blocks that occur intercalated in this formation rise uncertainties. Assuming the late Famennian age of the unit, two possible hypotheses emerge for the origin of these blocks: (i) they are true syn-sedimentary olistoliths as suggested by Eden (1991) and Pérez-Cáceres et al. (2017); (ii) they were tectonically emplaced. Concerning the first hypothesis, the marble blocks can easily be interpreted as olistoliths derived from the Aracena Massif. The serpentinite blocks were seen as olistoliths coming from the Beja-Acebuches Ophiolite (Eden 1991; Pérez-Cáceres et al. 2015, 2017), implying that the blocks are older than the unit shaly matrix where they are intercalated, and consequently that the Beja-Acebuches Ophiolite (also known as Acebuches Amphibolites; Bard 1969; Bard and Moine 1979) is older than the late Famennian, hence in contradiction with the 340–332 Ma U-Pb zircon age determined by Azor et al (2008). The second hypothesis admits that the marble and the serpentine blocks may constitute slabs of respectively the Aracena Massif and of the Beja-Acebuches Ophiolite. The left lateral NW trending ductile-brittle shear zones that affect the unit, locally with a top to SW component (Crespo-Blanc 1989) and imbrication (Eden 1991) may have played an important role. Further research is needed concerning this hypothesis.
- For the Santa Iria Formation discrepancies occur between U-Pb absolute ages (345 Ma lower Visean, Pérez-Cáceres et al. 2017; 376 ± 4 Ma lower Famennian Pereira et al. 2017) and palynological age (late Famennian, Pereira et al. 2006, 2018). A late Famennian age is assumed to be the most probable age for this unit.

As seen above, the schists of the Pulo do Lobo Formation that frame the amphibolite schists and basic rocks of the Peramora Mélange, the lower unit of the Los Ciries Antiform, studied by Dahn et al. (2014) provided U-Pb maximum depositional age of 348.7 ± 3.8 My (upper Tournaisian) while schists recovered from the same local yielded a palynological mid Frasnian age, ca. 375 Ma (Pereira et al. 2018). Schists interbedded in the upper quartzites of the Pulo do Lobo Formation, in Serpa region, Portugal, indicate the same mid Frasnian age (Pereira et al. 2018). The U-Pb zircon maximum depositional age for the Pulo do Lobo Formation does not fit the stratigraphic sequence since it is younger than the palynological age of the stratigraphically overlying Ribeira de Limas Formation (mid Frasnian) and Santa Iria Formation (Late Famennian), the youngest regional unit, suggesting that a process of Pb-loss may have affected some zircon grains in the samples (Dahn et al. 2014). Putting all the things together the age of the Pulo do Lobo Fm. is mid Frasnian, although a slightly older age cannot be excluded.

- The presence of Lower Devonian taxa in the three units (Pulo do Lobo, Peramora Mélange and Ribeira de Limas formations) is here interpreted as a result of reworking from the same source. On the other hand, the Phyllite-Quartzite Group, the basal unit of the Iberian Pyrite Belt (see Chap. 6 of this volume) dated of

Table 5.3 Compilation of palynological and U-Pb detrital zircon ages in Pulo do Lobo Terrane units. *Sources* Oliveira et al. (1979), Oliveira et al. (1986), Giese et al. (1988), Pereira (1999), González et al. (2004), Pereira et al. (2006), (2008), (2012), (2017), Braid et al. (2011), Dahn et al. (2014), Pérez-Cáceres et al. (2015), (2017). Authors symbols: Oli-Oliveira et al.; Br-Braid et al.; ZP-Zélia Pereira et al.; PC-Perez-Cáceres et al.; Gie-Giese et al.; Dan-Danh et al.; FP-M Francisco Pereira et al.; GZ-González et al.

Domains	Stratigraphic. units	Authors	Nb samples	Total grains	U-Pb ages of detritic zircon populations (%)											Unit U-Pb age	Palynological age
					Visean	Tourn.	Up. Dev.	L-Mid Dev.	Silur.	Ordo.	Camb.	Neop.	Mesop.	Paleop.	Arch.		
P. do Lobo																	
	Santa Iria	Br, 2011	1	65	1 grain		32					30.0	12.0	21.0	5.0	347±5.5 (L. Visean)	
		PC, 2017	4	311	4.5		34.1		2.3		4.2	34.7	3.9	15.1	1.3	345.0 (L. Visean)	
		FP, 2017	1	78			5.0					65.0	4.0	26.0		376±4 (L. Famennian)	
		Z P, 2006															Up. Famen
		Gie, 1998															Up.Famen
	H. da Torre	PC, 2017	5	440					3.9		3.9	18.2	41.6	27.0	4.3	450.0 (Katian)	
		Oli, 1986															Up. Famen
	Alajar	Br, 2011	3	?					5.0				55-70	15-25	<10	438±4.38 (Aeronian)	
		PC, 2017														440.0 (Aeorian)	
		ZP, 2017															Up. Famen.
	Rib. Limas	Br, 2011	1	65									55.0	35.0	10	947.6±4 (Tonian)	
		PC, 2017	4	315				1.5			4.1	61.6	4.8	26.7	1.9	400.0 (Eifelian)	
		FP, 2017	1	80			5.0					62.0	5.0	23.0		547.0 (Ediacarian)	
		ZP, 2006															Mid Frasnian
	PM Mélange	Dan, 2014															
	Schist Pulo. Fm.		2	27					30.0			15.0	18.0		37.0	348.7±3.8 (Up.Tournai)	
	Amphib. Matrix		4	60	5.0				6.0				57.0		32.0	345.1±8.1 (L. Visean)	
	PM Mafic rocks		4	34	12.0					18.0			70.0			341.3±7.5 (Visean)	
	Imbricate schist		1	24				12					38.0		40.0	351.8±5.8 (Tournai)	
	Pulo do Lobo Fm.	FP, 2017									1.0	65.0	6.0	24.0	4.0	531.0 (L. Cambrian)	
		PC, 2015	2	17												333±/341±4 Up. Visean	
		Z P, 2017															Mid Frasnian
	Atalaia	FP, 2017	1	90				5.0			3.0	68.0	1.0	22.0	1.0	390±4.7 (L. Givetian)	
	Gafo	FP, 2017	1	81				5.0			2.0	68.0	1.0	22.0		390+-7.4	L. Famen
Pyrite Belt	Represa/ B.Homem	FP,2017	1	75			11.0			3.0	5.0	59.0	1 grain	16.0		372.6	Up. Famen
	PH. Quartzite	PC, 2017	2	126	7.9		24.6			1.6	3.2	46.8	1.6	11.0	3.2	Carbon ?	
		FP, 2012						1 grain	1.8	2.7	1.8	66.0	4.6	19.0	2.8	???	
		ZP,1999															Up. Famen
		ZP, 2008															Givetian
	Ronquilho	PC,2017	4					1.7	1.4		5.1	58.2	4.8	26.5		400-410	
Sw Portugal	Tercenas	FP, 2012	1				17.0		1 grain	1 grain	4.0	53.0	9.0	13.0	1 grain	367,2±6 (Famennian)	
		ZP, 1999															Up. Famen.

Givetian to late Famennian age based in palynomorphs, has the same type of reworked Lower Devonian spore signature (Pereira et al. 2008, 2009). It seems so that the source of the sediments and reworked palynomorphs of the Pulo do Lobo, Peramora, Ribeira de Limas and Atalaia (?) formations and the Phyllite-Quartzite Group was the same crustal block, which probably incorporated the South Portuguese Zone (see chap. 6 of this volume). It should be noted that Lower Devonian miospores are absent in the overlying and unconformable Horta da Torre, Santa Iria and Gafo Formations, suggesting that their sediments were derived from a distinct and unknown source.

- The floral and faunal associations of the South Portuguese Zone have clear affinities with those of the Avalonian Terrane (Loboziak and Streel 1981; Higgs et al. 2013; Oliveira et al. 1979; Korn 1997; Clayton et al. 2002) but a link with the Meguma terrane has also been suggested (Braid et al. 2012).
- It is worth noting that the youngest U-Pb zircon ages reported for the Peramora mafic rocks (both matrix and blocks; 341.3 ±7.5 Ma by Danh et al. 2014, 341 ± 3 Ma by Pérez-Cáceres et al. 2017) are younger than the embedding Pulo do Lobo Formation schists and all the overlying units, which led Pérez-Cáceres et al. (2017) to infer that the mafic rocks are intrusive in the stratigraphic succession. However, these rocks and the embedded Pulo do Lobo Formation schists appear to be affected by the same three tectonic episodes of folding and upper greenschist metamorphim prior to intrusion of the Gil Márquez pluton, whose older rocks are dated at ca. 354 Ma (Gladney et al. 2014). Accordingly, their N-MORB geochemical signature, the tectonic deformation and metamorphism and the age of the stitching Gil Márquez pluton seem to be incompatible with their possible intrusive character in the stratigraphic succession (for details, see Sect. 5.2). The amphibolite-in-shale matrix that encloses the mafic rocks has an oceanic crust signature (Eden 1991; Dahn et al. 2014), supporting the interpretation that the mafic rocks represent a true oceanic crust.

Comparing the U-Pb detrital zircon ages and the palynological ages of the Pulo do Lobo Domain units, the results do not show a clear global tendency, i.e. there are units with palynological ages older than the U-Pb zircon ages, but in others the reverse may occur. Also for a given stratigraphic unit the U-Pb zircon ages are distinct, depending on the authors. In this case the results may possibly have been biased by sampling, number of grains studied (Anderson 2005) or even alteration of the zircon structure (Hay and Dempster 2009). Nonetheless, the results attained by both methodologies allow the following comments:

The data summarized in Table 5.3 also shed some light on the sediments provenance of the Pulo do Lobo Domain units. The most impressive result is the high percentage of Neoproterozoic U-Pb zircon ages in all the units of the Pulo do Lobo Domain, except for the stratigraphically unconformable Horta da Torre (18%) and Santa Iria (∼30%, but 65% in FP) and the Pulo do Lobo schist (15%). The large percentage of Neoproterozoic ages conjugated with the small percentage of Mesoproterozoic ages (apart the contradictory ages obtained for the Ribeira de Limas Formation) suggest that the main source region of sediments of these units was the Cadomian Orogen of North Gondwana. The small percentage of Cambrian, Ordovician, Silurian ages is concentrated in the Horta da Torre, Alájar mélange and Santa Iria formations, which were laid down in a syn-collisional foreland basin. Assuming that this crustal block should have been docked to Laurussia during the late Silurian (Nance et al. 2012; Stampfli et al. 2002), the small percentage of U-Pb zircon Silurian age is surprising, owing to the voluminous volcanism that occurred in Laurussia at that time period (Stillman 1998).

All the units have small percentages of zircons of Lower-Mid Devonian ages (no data for the Horta da Torre and Alájar formations) suggesting that after docking to Laurussia units of this age were not deeply eroded during this time span. The Santa Iria Formation shows the highest percentage of Devonian age zircons (∼30%). This unit is the only one which has zircons of all the recorded ages, from the Archean to the Lower Carboniferous, reinforcing its interpretation as a syn-orogenic foreland basin flysch that probably received sediments from both the Gondwana and Laurussia margins (Braid et al. 2011).

Particular attention deserve the results obtained for the amphibolite matrix and mafic blocks of the Peramora Mélange. The respective 57% and 70% percentages of Neo and Mesoproterozoic U-Pb zircon ages are uncommon in rocks with N-MORB geochemical signature as these are. These results are highly suggestive of mantle contamination as is known in other oceanic domains (e.g. the SW Pacific; Buys et al. 2014). Also the similarities in percentages of U-Pb detrital zircon ages between the units of the Pulo do Lobo Terrane and those of the South Portuguese Terrane are quite impressive. The similarities are extensive to the Famennian palynological assemblages of the Horta da Torre, Santa Iria Formations and the Upper Devonian units of the South Portuguese Terrane (namely upper Phyllite-Quartzite Formation (Pereira et al. 2008, 2018), Represa/Barranco do Homem Formation (Pereira et al. 2008) in the Iberian Pyrite Belt, and Tercenas Formation (Pereira 1999;

Pereira et al. 2008) of SW Portugal. These assemblages together with the assemblages of the Ribeira de Limas and Gafo Formations show clear affinities with Avalonia (Clayton et al. 2002). Concluding, it seems plausible that the Pulo do Lobo and the South Portuguese terranes were in proximity at least since the mid-Frasnian.

5.3.2.6 Conclusions

Pereira et al (2006), based on lithological, palynological and low-grade metamorphic (vitrinite reflectance) data suggested stratigraphic equivalence between units of the northern and southern sector of the Pulo do Lobo Terrane, namely the Ribeira de Limas/Atalaia and the Santa Iria/Gafo formations. The actual palynological ages of these units (Pereira et al. 2018; this work), together with their tectonic history (Silva et al. 1990; Simancas 2004; Pérez-Cáceres et al. 2015) allow the division of the stratigraphic succession into two distinct groups of units. The lower, represented by the Pulo do Lobo and the overlying Ribeira de Limas/Atalaia formations share similar ages and the same three compressive tectonic episodes. The occurrence of N-MORB mafic rocks in the Pulo do Lobo Formation and the oceanic crust signature of the embedded schists (Eden 1991; Dahn et al. 2014) indicate that this group of units represents a true oceanic domain which was tectonically imbricated during two (and exclusive) post-mid Frasnian and pre-late Famennian compressive tectonic episodes, probably representing the accretionary prism related with the first collisional episodes of the Pulo do Lobo (Rheic?) Ocean closure.

The Horta da Torre/Santa Iria and Gafo formations form the upper group of units with Famennian palynological ages but quite different U-Pb detrital zircon ages. They represent syn-orogenic sequences unconformably superimposed on the first group of units. If they filled a single foreland basin covering the entire Pulo do Lobo Domain or distinct small basins located at its northern and southern sectors is still a matter of debate, needing further research (see Sect. 11.2.3, Chap. 11 of this volume for a discussion).

5.4 Beja-Acebuches Ophiolite

C. Quesada, J. A. Braid, J. B. Murphy

The first documented description of the Acebuches amphibolites was made by Bard (1969) in his excellent thesis. They occur along a narrow (less than 2 km wide on average) belt, tectonically sandwiched between the southernmost outcrops of the OMZ to the north (Évora-Aracena-Almadén de la Plata massifs) and to the Pulo do Lobo Terrane to the south (Fig. 5.1). Bard and Moine (1979) and Dupuy et al. (1979) published the first geochemical results on these rocks and demonstrated their tholeiitic MORB-like signature. These results attracted the interest of researchers working in both Portugal and Spain, as a result of which Munhá et al. (1986) were able to recognize that the Acebuches amphibolites share many characteristics with ophiolites and coined the term Beja-Acebuches Ophiolite (BAO) or Ophiolitic Complex. Subsequent studies (Fonseca and Ribeiro 1993; Quesada et al. 1994; Fonseca 1997) enabled recognizing a dismembered but rather complete pseudostratigraphy similar to other ophiolites and to modern oceanic lithosphere and indicated, for the first time, the existence of a Variscan suture in SW Iberia. This interpretation has been later on supported by finding of evidences of HP metamorphism in nearby units, which attest for subduction processes (see Chap. 12 of this volume and references therein).

The BAO is extremely dismembered along strike and displays an increasing metamorphic grade to the north. In the Spanish domain, the BAO is comprised primarily of amphibolite facies metabasalt and metagabbro (locally sheeted dikes also) whereas in Portugal ultramafic rocks, mylonitic gabbro, sheeted dike complexes and serpentinites are recognized (Quesada et al. 1994; Fonseca 1997). Although no location records an intact oceanic stratigraphy, all major components of a classic ophiolite sequence are found within the belt. This succession coupled with a MORB geochemical signature suggests these rocks are part of a relict oceanic crust and represent the local expression of a major Variscan suture (Munhá et al. 1986; Quesada et al. 1994). However, its formation and geodynamic history remain controversial (e.g. Munhá et al. 1986; Crespo-Blanc and Orozco 1988, 1991; Quesada 1991; Quesada et al. 1994; Castro et al. 1996a, b, 1999; Pin et al. 2008; Azor et al. 2008; Braid et al. 2012, 2018; Pérez Cáceres et al. 2015, 2017).

The geochemistry of the metabasic rocks in the ophiolite is normal to transitional MORB (Bard and Moine 1979, Quesada et al. 1994; Castro et al. 1996b) but with supra-subduction zone trace element characteristics, e.g. low Ti/Zr ratio, LILE and LREE enrichment, depletion in HFSE, profound decoupling between LILE and HFSE and some samples also showing a distinctive negative Nb anomaly; Quesada et al. 1994). Epsilon Neodymium data (t = 350 Ma) plot close to or above the depleted mantle curve at 7.9–9.2 (Castro et al. 1996b). Although geochemical data from the BAO are abundant, their interpretation is controversial. Bard (1977) proposed that the BAO represented either the very early stages in the development of a marginal volcanic arc or a ephemeral and narrow oceanic basin (intracontinental rifting). Quesada et al. (1994) interpreted the BAO to represent oceanic lithosphere formed within an intra-arc or back-arc marginal basin and Castro et al. (1996a, b) envisaged a mid-ocean ridge setting. However, recent SHRIMP U–Pb zircon age data for the BAO (ca. 332–340 Ma; Azor et al. 2008) indicate that its formation postdates many events recorded in the adjacent areas, among which the first

deformation phase and obduction of the IOMZOS (see above under Sect. 5.2) and HP rocks onto the OMZ, and accretion of the Pulo do Lobo units and intrusion of the Gil Márquez pluton into them (see above under Sect. 5.3) are most relevant.

The ages reported by Azor et al. (2008) were obtained from zircons showing the internal zoning (broadband oscillatory) and chemistry (high Th/U of 0.3–1.1) typical of magmatic zircons from mafic rocks, therefore their interpretation as dating the crystallization of the protolith seems plausible. If true, formation of the oceanic basin must have taken place very late in the history of the southern margin of OMZ (Gondwana), just before or even coeval with the onset of collision with the SPT, dated by the transformation of the latter into a foreland basin during the Late Visean, ca. 335 Ma (Oliveira 1990; Quesada 1991, 1998). These ages also fall within the age range interpreted by other authors to reflect penetrative deformation of the BAO and post-metamorphism cooling ages (Dallmeyer et al. 1993; Castro et al. 1999) following a major UHT-LP metamorphic event, accompanied by massive magmatic intrusion and extensional (transtensional) deformation that affected the southern units of the OMZ between ca. 350 Ma and 330 Ma (Pereira et al. 2016; see also Sect. Variscan Metamorphism in the Southwestern Ossa Morena Zone, Chap. 12 of this volume, and references therein).

Collectively, all the above data indicate that the BAO protolith basin was not an integral part of the main Rheic Ocean but, rather a marginal oceanic domain opened within the southern OMZ or, alternatively, at its margin with the already accreted Pulo do Lobo terrane units during a period of transient extensional (transtensional) deformation and HT-LP metamorphism. The suprasubduction signature of the BAO mafic rocks indicates that subduction beneath the OMZ margin was still active, i.e. collision with the SPT had not yet started. However, the data also prove that the BAO basin was extremely ephemeral, since their protolith crystallization ages (Azor et al. 2008) overlap within error with their post-metamorphic cooling ages (Dallmeyer et al. 1993; Castro et al. 1999), indicating that formation, deformation and metamorphism of the BAO rocks happened in a very short time period (anyhow unresolvable with the available radiometric ages). Recently, Murphy et al. (2015) and Braid et al. (2018) have proposed that the formation of the BAO occurred in a narrow and very ephemeral tract of oceanic-like crust, analogous to oceanic plates in the modern eastern Mediterranean sea. The narrowness of this domain is supported by the palynological (Pereira et al. 2006, see pevious section) and detrital zircon data (Braid et al. 2011; Dahn et al. 2014; Pérez-Cáceres et al. 2017; see also previous section), which show a sedimentary source from both Gondwana and Laurussia in the syn-orogenic overstep sequences demonstrating close proximity of the two continental plates at the time (see discussion in Sect. 5.3.2).

5.5 Discussion: Geodynamic Evolution of the Oceanic-Affinity Units in the SW Iberia Variscan Suture Zone

C. Quesada, J. A. Braid, J. B. Murphy

In the previous sections we have reviewed the three units which include oceanic affinity sequences (ophiolites sensu lato) along the SW Iberia Variscan suture zone. They represent distinct oceanic tracks with different ages and characteristics.

5.5.1 The Protoliths

The oldest unit concerning the age of its protoliths (ca. 480 Ma) corresponds to the Internal Ossa Morena Zone Ophiolitic Sequences (IOMZOS; see Sect. 5.2 above). The anorogenic tholeiitic geochemistry, transitional between N-MORB and E-MORB, indicates that the igneous protoliths of IOMZOS were genetically related with open ocean basins without orogenic influence and/or crustal contamination in their petrogenesis, and involved contribution of magmas derived from a depleted source (N-MORB) and an enriched source (E-MORB). A plume-ridge interaction environment within the Rheic Ocean is favored to account for all the geochemical characteristics.

The second unit corresponds to the Pulo do Lobo Terrane (Sect. 5.3). Ocean-floor mafic rocks represent only a small part of the currently exposed stratigraphic record of the PLT, which is largely dominated by sedimentary successions including pre-orogenic and syn-orogenic sequences. Precise dating of the protoliths of the mafic rocks in the PLT is not yet achieved but presence of inherited/xenocrystic zircon grains as young as Mississipian indicates that these rocks are younger than those of the IOMZOS (see discussion on the discrepancies between palynology based ages and detrital zircon ages in Sect. 5.3.2.5). In addition, the ages of the metasediments of the Pulo do Lobo Fm and the metasediments interleaved with the Peramora mélange are now soundly established by their palynological content as mid-Frasnian (Pereira et al. 2018), which given their intimate association to the mafic rocks suggests that the latter might not be much older. On the other hand, the N-MORB signature of the PLT mafic rocks, with absence of any suprasubduction zone characteristic indicate that their protoliths formed in a mature oceanic environment, probably belonging to the Rheic Ocean as suggested by their extremely depleted nature (Murphy et al. 2011). However, the minor presence of inherited/xenocrystic zircon grains (including Archean, Paleoproterozoic, Neoproterozoic and Paleozoic populations; Dahn et al. 2014) attests for some degree of contamination of the mantle magmas by

continental crust components, small enough though to enable changing the overall N-MORM composition. A scenario of extremely thin microcontinental plates within the Rheic Ocean, analogous to the current situation in the SW Pacific Ocean (Buys et al. 2014), could be applicable here.

Finally, the youngest oceanic unit in the SW Iberia suture zone corresponds to the Beja-Acebuches ophiolite (BAO), whose protoliths have been dated at ca. 340–332 Ma (Azor et al. 2008). Besides, the geochemical N- to T-MORB composition of the BAO rocks (Bard and Moine 1979; Quesada et al. 1994; Castro et al. 1996b) includes some supra-subduction zone trace element characteristics (Quesada et al. 1994; see above). These data indicate that the BAO protolith basin was not an integral part of the main Rheic Ocean but rather a marginal, back/intra-arc oceanic domain opened within the southern OMZ or, alternatively, at its margin with the already accreted Pulo do Lobo terrane.

5.5.2 The Accretion Processes

The three ophiolitic units not only differ on the nature and age of their protoliths but also on the nature and age of the processes that led to their respective accretion.

Association of the IOMZOS with typical Cambrian-Ordovician OMZ successions affected by HP metamorphism within the Cubito-Moura mélange unit (Rubio Pascua et al. 2013; Pérez-Cáceres et al. 2015; and references there in) links its accretion to a process of subduction of the leading edge of the OMZ beneath the IOMZOS protolith. The peak of HP metamorphism was dated at ca. 370 Ma ago and its post-collisional exhumation at ca. 360 Ma (Moita et al. 2005). These ages are identical within error to those of equivalent processes in NW Iberia, i.e. subduction of the Lower Allochthon of the Galicia Trás-os-Montes Zone (GTMZ) beneath the Middle Allochthon and subsequent exhumation onto the Parautochthon (see Chaps. 4, 10 and 12 in this volume, and references therein). Moreover, similar ca. 500–480 Ma old protoliths are known within the ophiolitic Middle Allochthon of the GTMZ (Martínez et al. 2012; see also Chap. 4 in this volume). The HP metamorphic event is interpreted as the result of westerly subduction of the leading edge of Gondwana beneath Laurussia and units previously accreted to it (i.e. the Upper Allochthon of the GTMZ), implying that Gondwana was in the lower plate during ocean closure and the subsequent collision (see Chaps. 4, 10 and 12 in this volume).

The WNW-ESE trending structural arrangement in SW Iberia lies almost at right angles to the presumed orientation of the Gondwanan margin in NW Iberia. However, if restoration of the late orogenic tightening of the Cantabrian arc (see Chap. 14 in this volume) is applied, the predominant sinistral transpressive deformation regime in SW Iberia during the entire Variscan orogeny (Brun and Burg 1982; Ribeiro et al. 1990; Quesada 1991, 2006, and subsequent workers) requires the existence of a corner effect between a promontory and a re-entrant in the Gondwanan margin that may have triggered escape of the Laurussian plate into the oceanic re-entrant once collision of the promontory started (Murphy et al. 2015, 2016; Braid et al. 2018). The present OMZ lied at the Gondwanan margin facing the re-entrant whereas its extension around the corner of the promontory was probably incorporated into the same subduction complex represented by the GTMZ Lower Allochthon and subsequentetly exhumed during the progression of collision. We firmly believe this was the way how the HP units in the Moura-Cubito mélange (probably representing an axhumed subduction channel) and the IOMZOS became exhumed onto parautochthonous OMZ. Therefore, accretion of the IOMZOS was related to processes taking place in frontal areas of the promontory, with Gondwana in the lower plate, and not with processes in the margin facing the adjacent re-entrant.

Once collision started, the OMZ was also forced to escape southeastwards, its displacement being accommodated by wrenching along the Badajoz-Córdoba shear zone and overriding of the oceanic part of the Gondwanan plate occupying the re-entrant (the future Pulo do Lobo "ophiolitic" unit (Quesada 1991, 2006). This overriding promoted a transformation of the pre-existing OMZ passive margin facing the re-entrant into an active one where discontinuous strongly oblique subduction is indicated by episodic arc growth on the southwestern OMZ since the mid-Devonian (Santos et al. 1987, 1990; Andrade et al. 1991), i.e. with Gondwana occupying the upper plate in this case (Fig. 5.27-1).

We envisage this scenario as the one responsible for the accretion of the Pulo do Lobo pro-orogenic units beneath the OMZ in an accretionary prism environment (Munhá et al. 1986; Quesada 1991, 2006; Quesada et al. 1994; Braid et al. 2010, 2011, 2012, 2018; Murphy et al. 2015). In this context, the Peramora mélange is interpreted as an ophiolitic mélange developed in a trench basin during accretion of an ocean floor basement sliver. Intrusion of arc-like gabbro and granitoids of the Gil Márquez pluton into already accreted and poly-deformed PLT units in the range 354–345 Ma (Gladney et al. 2014) attests for continuation of subduction until at least that time and provides a minimum age constraint to the accretion process (Fig. 5.27-3).

Finally, the much younger BAO protolith may have formed in a back/intra-arc setting right at the contact between the OMZ and already accreted PLT units (Fig. 5.27-4). Their protolith ages (ca. 340–332 Ma; Azor et al. 2008) fall within a period when the southwestern OMZ was undergoing an important extensional (transtensional)

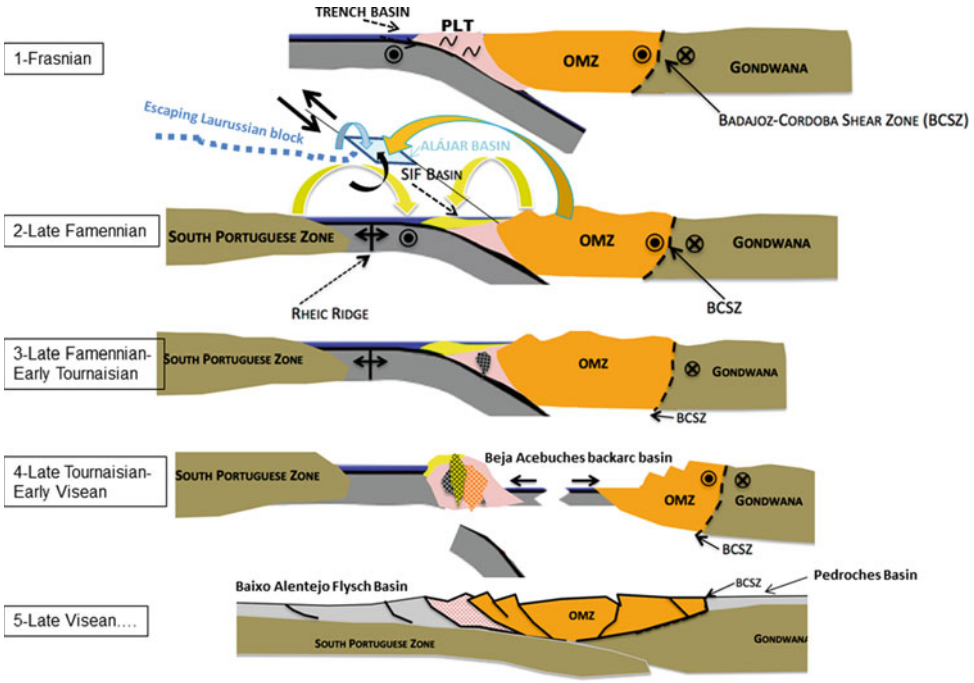

Fig. 5.27 Tectonic evolutionary cartoon showing the location of syn-orogenic basins in the future SW Iberia Variscan orogen since the onset of subduction beneath Gondwanan OMZ to final collision with the Laurussian SPT. 1, 2 and 3: Subduction stage: (1) formation of the Peramora mélange in the trench basin; (2) deposition of the Santa Iria flysch (SIF) in a forearc basin (sources indicated by yellow arrows) on top of already accreted PLT and, at some distance (out of the cross-section), arrival of an escaping Laurussian block (in whose shelf the Horta da Torre Fm was being deposited) to a pull-apart basin at a releasing bend; collapse of the basin margins gave rise to formation of the Alájar mélange; sources indicated by blue (exotic block), orange (OMZ) and black (oceanic lithosphere) buckled arrows; (3) arc growth on both OMZ and accreted PLT; (4) Rheic MOR collision with the trench, slab break-off and opening of the Beja-Acebuches backarc basin; (5) Collision stage: formation, migration and progressive inversion of the Baixo Alentejo foreland basin on the SPZ and the Pedroches foreland basin on the OMZ and CIZ

event accompanied by UHT-LP metamorphism and magmatic intrusion (Pereira et al. 2016; see also Sect. Variscan Metamorphism in the Southwestern Ossa Morena Zone, Chap. 12 of this volume, and references therein). The ages also overlap with those interpreted in connection to post-deformation/post-metamorphic cooling of the BAO rocks themselves and the adjacent OMZ units (Dallmeyer et al. 1993; Castro et al. 1999) and suggest that formation, deformation/accretion and exhumation all happened in a very short period of time. As for the formation of the BAO marginal basin we consider a mechanism of transtensional opening of a pull-apart oceanic domain at the margin between the OMZ and PLT during the afore-mentioned event of extensional (transtensional) deformation and UHT-LP metamorphism. Actually, the metamorphic regime within the BAO rocks was similar to the one recorded in OMZ rocks but with a ca. 200 °C smaller T peak (see Chap. 12 in this volume). This coincidence indicates that inversion of the BAO basin and accretion to the adjacent OMZ units took place under persistence of the HT-LP gradient.

All the overlapping ages discussed above also overlap with the age of the onset of collision in this SW margin of Iberia (the one facing the re-entrant), estimated at ca. 335 Ma ago on the basis of the transformation of the pre-existing passive margin of the South Portuguese Terrane (SPT) into a foredeep basin, which migrated southwards in front of a propagating south-vergent, thin-skin fold and thrust orogenic wedge over the SPT (Fig. 5.27-5; Oliveira 1990; Quesada 1991, 1998). Therefore, formation of the BAO immediately preceded the final closure of the Rheic Ocean relict in the re-entrant, which triggered inversion and accretion of the BAO during the initial collisional stages.

Detrital zircon data from the Alájar mélange published by Braid et al. (2011) further complicate the already complex scenario outlined in previous paragraphs. The data, mainly the presence of a ca. 440 Ma age population and absence of Neoproterozoic age populations characteristic of both the OMZ and the SPT, suggest that the Alájar Mélange and probably the Ribeira de Limas Fm contain blocks and sediments derived from crust that was excised from the Laurussian interior (see Fig. 5.27-2; probably the Southern

Uplands terrane of the British Caledonides; Braid et al. 2011). These hypotheses imply that the initial formation of the rocks incorporated in the suture zone and deformed during Variscan orogenesis was likely more complex than simple imbrication of primary Rheic oceanic lithosphere and ocean floor sedimentary rocks. During the final stages of Rheic ocean consumption, the remnants of this oceanic tract would not be the BAO, but instead the MORB-featured basalts included in the PLT.

The development of the SW Iberia suture zone and its relationship to other regions within the Variscan orogenic belt may be broadly analogous (Murphy et al. 2015) to the Mesozoic—Cenozoic development of the Mediterranean portion of the Alpine Iranian orogenic belt and the subduction of the Paleotethys and Neotethys oceans. This modern accretionary complex, developed nearly 100 My after initial collisional tectonics in the Alpine Chain commenced, may be analogous to the Pulo do Lobo accretionary prism.

Finally, it is worthwhile concluding that only two of the oceanic-affinity units present in SW Iberia (PLT mafic rocks and BAO) were linked to the evolution of the SW Iberia suture zone proper (i.e. the one facing the re-entrant), but only the PLT represents a primary vestige of the Rheic Ocean, accreted to the southern margin of the OMZ during a process of northerly subduction initiated in Mid-Devonian time. In turn, the BAO formed at a marginal back/intra-arc suprasubduction setting during the latest stages of Rheic Ocean closure, being soon inverted and imbricated with the adjacent OMZ units during initial collisional stages. Subsequent post-collisional evolution resulted in southward overriding, i.e. synthetic to the preexisting subduction zone, of the OMZ and accreted suture zone units onto the South Portuguese Terrane. On the other hand, we consider that the IOMZOS, which also likely represents a sliver of Rheic Ocean lithosphere, did not evolve within the SE Iberia suture zone as defined above. Instead, it may have evolved marginal to the westerly directed subduction zone that brought the leading edge of Gondwana to sink beneath Laurussia and units previously accreted to it, so beautifully documented in NW Iberia. Sensu stricto, the IOMZOS belonged to the Variscan suture zone complexes exposed in NW Iberia, which evolved with Gondwana occupying the lower plate. We explain the presence of this sliver of NW Iberia suture in the vicinity of the SW suture zone in connection to the progressive southeasterly escape of OMZ, which prevented its incorporation into the east propagating nappe pile that characterizes the NW Iberia Variscan orogen, being instead involved in the huge thick-skin sinistral duplex that characterizes the SW Iberia orogenic segment. This model provides an explanation to the contrasting vergence (N-NE in present coordinates) of the initial structures in the IOMZOS, Cubito-Moura mélange and southern OMZ autochthon (Quesada et al. 1994; Fonseca et al. 1999; Pedro 2004; Araújo et al. 2005, 2013; Pedro et al. 2005, 2006, 2013; Ribeiro et al. 2010) relative to the S-SW vergence of the structures formed in connection to the evolution of the SW Iberian orogen (Ribeiro et al. 1990; Quesada, 1991, 1998, 2006) so beautifully documented by the IBERSEIS seismic reflection profile (Simancas et al. 2003).

References

Anderson T (2005) Detrital zircons as traces of sedimentary provenance: limiting conditions from statistics and numerical simulations. Chem Geol 216, 249–270

Andrade AAS, Santos JF, Oliveira JT et al. (1991) Magmatismo orogénico na transversal de Odivelas-Santa Susana. XI Reun Geol Oeste Peninsular, Huelva, Excursion guide-book, 47–54

Apalategui O, Barranco E, Contreras Vázquez F, Roldán FJ (1983) Mapa Geológico de España. Sheet no. 916: Aroche. Instituto Geológico Minero España, Serv Pub Min Industria y Energia

Apalategui O, Barranco E, Delgado M, Roldan FJ (1984) Mapa Geológico de España. Sheet no. 917: Aracena. Instituto Geológico Minero España, Serv Pub Min Industria y Energia

Araújo A, Fonseca P, Munhá J (1993) Ossa - Morena Ophiolites. Terra Abstracts Supplement n. 6 (XII Reunião de Geologia do Oeste Peninsular), Terra Nova 5: 8

Araújo A, Fonseca P, Munhá J, Moita P, Pedro J, Ribeiro A (2005) The Moura Phyllonitic Complex: An Accretionary Complex related with obduction in the Southern Iberia Variscan Suture. Geodinamica Acta 18 (5): 375–388

Araújo A, Piçarra de Almeida J, Borrego J, Pedro J, Oliveira JT (2013) As Regiões Central e sul da Zona de Ossa Morena. In, Geologia de Portugal, Volume I, Geologia Pré-mesozóica de Portugal, Dias R, Araújo A, Terrinha P, Kullberg JC (Eds), Escolar Editora, 509–549

Arevalo R, McDonough WF (2010) Chemical variations and regional diversity observed in MORB. Chemical Geology, 271: 70–85

Azor A, Rubatto D, Simancas JF, González Lodeiro F et al. (2008) Rheic Ocean ophiolitic remnants in southern Iberia questioned by SHRIMP U-Pb zircon ages on the Beja-Acebuches amphibolites. Tectonics 27: TC5006. https://doi.org/10.1029/2008tc002306

Bard JP (1969) Le métamorphisme régional progressif des Sierras d'Aracena en Andalousie occidentale (Espagne). Sa place dans le segment sud-Ibérique. Thèse, Univ Montpellier, 1–398

Bard JP (1977) Signification tectonique des métatholéites d'affinité abyssale de la ceinture métamorphique de basse pression d'Aracena (Huelva, Espagne). Bull Soc Géol France (7) 19: 385–393

Bard JP, Moine B (1979) Acebuches amphibolites in the Aracena Hercynian metamorphic belt (southwest Spain): geochemical variations and basaltic affinities. Lithos, 12, 271–282

Booth-Rea G, Simancas JF, Azor A, Azañón JM, González-Lodeiro F, Fonseca P (2006) HP-LT Variscan metamorphism in the Cubito-Moura schists (Ossa-Morena Zone, southern Iberia). Comptes Rendus Geoscience 338: 1260–1267

Braid J, Murphy JB, Quesada C (2010) Structural analysis of an accretionary prism in a collisional setting, the late Paleozoic Pulo do Lobo Zone, South Iberia. Gondwana Research 17: 422–439

Braid JA, Murphy JB, Quesada C, Mortensen J (2011) Tectonic escape of a crustal fragment during the closure of the Rheic Ocean: U-Pb detrital zircon data from the Late Palaeozoic Pulo de Lobo and South Portuguese Zones, Southern Iberia. J Geol Soc Lond 168: 383–392

Braid JA, Murphy JB, Quesada C, Bickerton L, Mortensen JK (2012) Probing the composition of unexposed basement, South Portuguese

Zone, southern Iberia: implications for the connections between the Appalachian and Variscan orogens. Can J Earth Sci 49(4):591–613
Braid JA, Murphy JB, Quesada C, Gladney ER, Dupuis N (2018) Progressive magmatism and evolution of the Variscan suture in southern Iberia. Int J Earth Sci (Geol Runds) 107: 971–983
Brun JP, Burg JP (1982) Combined thrusting and wrenching in the Ibero-Armorican arc: a corner effect during continental collision. Earth and Planetary Science Letters 61:319–332
Buys J, Spandler C, Holm RJ, Richards SW (2014) Remnants of ancient Australia in Vanuatu: implications for crustal evolution in island arcs and tectonic development of the SW Pacific. Geology 42 (11):939–942
Cabanis B, Lécolle M (1989) Le diagramme La/10-Y/15-Nb/8: un outil pour la discrimination des séries volcaniques et la mise en évidence des processus de mélange et/ou de contamination crustale. Comptes Rendus de l'Académie des Sciences, 309: 2023–2029
Carvalho D, Correia M, Inverno C (1976) Contribuição para o conhecimento geológico do Grupo Ferreira-Ficalho. Suas relações com a Faixa Piritosa e o Grupo do Pulo do Lobo. Mem. Not. Mus. Lab. Min. Fac. Cienc. Coimbra 82: 145–169
Castro A, Fernández C, de la Rosa JD et al. (1996a) Triple-junction migration during Paleozoic plate convergence: the Aracena metamorphic belt, Hercynian massif, Spain. Geol Rundsch 85:180–185
Castro A, Fernández C, de la Rosa JD, Moreno-Ventas I, Rogers G (1996b) Significance of MORB-derived amphibolites from the Aracena metamorphic belt, Southwest Spain. J Petrol 37: 235–260
Castro A, Fernández C, El-Hmidi H et al. (1999) Age constraints to the relationships between magmatism, metamorphism and tectonism in the Aracena metamorphic belt, southern Spain. Int Jour Earth Sciences 88: 26–37
Castroviejo R, Quesada C, Soler M (2011) Post-depositional tectonic modification of VMS deposits in Iberia and its economic significance. Miner Depos 46:615–637
Chichorro M, Pereira MF, Díaz-Azpíroz M, Williams IS, Fernández C, Pin C, Silva JB (2008) Cambrian ensialic rift-related magmatism in the Ossa-Morena Zone (Évora - Aracena metamorphic belt, SW Iberian Massif) Sm-Nd isotopes and SHRIMP zircon U-Th-Pb geocronology. Tectonophysics 461: 91–113
Clayton G, Wicander R, Pereira Z (2002) Palynological evidence concerning the relative positions of Northern Gondwana and Southern Laurussia in latest Devonian and Mississippian times. In: Wyse Jackson, P. and Parkes, M.A. (eds), Studies in Palaeozoic palaeontology and biostratigraphy in honour of Charles Hepworth Holland. Special Papers in Palaeont 67: 45–56
Crespo-Blanc A (1989) Evolución geotectónica del contacto entre la Zona de Ossa-Morena y la Zona Surportuguesa en las sierras de Aracena y Aroche (Macizo Ibérico Meridional): un contacto mayor en la cadena hercínica europea. PhD thesis, Univ Sevilla
Crespo-Blanc A, Orozco M (1988) The Southern Iberian Shear Zone: a major boundary in the Hercynian folded belt. Tectonophysics 148: 221–227
Crespo-Blanc A, Orozco M (1991) The boundary between the Ossa-Morena and the South-portuguese Zones (southern Iberian Massif): a major suture in the European Hercynian chain. Geologische Rundschau 80: 691–702
Cunha T, Oliveira JT (1989) Upper Devonian Palynomorphs from the Represa and Phyllite-Quartzite Fm., Mina de Sao Domingos region, Southwest Portugal. Tectonostratigraphic implications. Bull Soc Belge Geol 98 (3/4): 295–309
Dahn DRL, Braid JA, Murphy JB, Quesada C, Dupuis N, McFarlane CRM (2014) Geochemistry of the Peramora Mélange and Pulo do Lobo schist: geochemical investigation and tectonic interpretation of mafic mélange in the Pangean suture zone, Southern Iberia. International Journal of Earth Sciences (Geol Rundsch) 103:1415–1431. https://doi.org/10.1007/s00531-014-1024-7
Dallmeyer RD, Fonseca PE, Quesada C, Ribeiro A (1993) 40Ar/39Ar mineral age constraints on the tectonothermal evolution of the Variscan Suture in SW Iberia. Tectonophysics 222: 177–194
DePaolo DJ (1981). Neodymium isotopes in the Colorado Front Range and crust–mantle evolution in the Proterozoic. Nature 291: 193–196
Dupuy C, Dostal J, Bard JP (1979) Trace element geochemistry of Paleozoic amphibolites from SW Spain. Tschermaks Min Petr Mitt 26:87–93
Eden CP (1991) Tectonostratigraphic analysis of the Northern Extent of the Oceanic Exotic Terrane, Northwestern Huelva Province, Spain. PhD thesis, Univ. Southampton, 281 p
Eden CP, Andrews JR (1990) Middle to Upper Devonian melanges in SW Spain and their relationship to the Meneage Formation in south Cornwall. Proceedings of the Ussher Society 7: 217–222
Ferreira PL, Oliveira JT (2018) Características geoquímicas dos metabasaltos do Pulo do Lobo provenientes da sondagem ALF-2, SE da aldeia da Trindade, Alentejo, Portugal. Geochemical characteristics of Pulo do Lobo metabasalts from ALF-2 drill core, SE of Trindade village, Alentejo, Portugal. XIV Congresso de Geoquímica dos Países de Língua Portuguesa. XIX Semana de Geoquímica. Abstract
Flower M (1991) Magmatic process in oceanic ridge and intraplate settings. In: PA Floyd (Ed), Oceanic Basalts. Blackie and Son, London, p. 116–147
Floyd PA, Winchester JA (1975) Magma Type and Tectonic Setting Discrimination Using Immobile Elements. Earth and Planetary Science Letters 27: 211–218
Floyd PA, Winchester JA (1978) Identification and discrimination of altered and metamorphosed volcanic rocks using immobile elements. Chemical Geology 21: 291–306
Fonseca P (1997) Dominios meridionais da Zona de Ossa-Morena e limites com a Zona Sul Portuguesa: metamorfismo de alta pressão relacionado com a sutura varisca ibérica. In: Aráujo AA, Pereira MF (eds), Grologia da Zona de Ossa-Morena (Maciço Ibérico), Livro homenagem Prof F Gonçalves. Univ Évora, 133–168
Fonseca P, Ribeiro A (1993) Tectonics of the Beja-Acebuches Ophiolite: a major suture in the Iberian Variscan Foldbelt. Geol Rundsch 82: 440–447
Fonseca P, Munhá J, Pedro J, Rosas F, Moita P, Araújo A, Leal N (1999) Variscan Ophiolites and High-Pressure Metamorphism in Southern Iberia. Ofioliti 24 (2): 259–268
Gale A, Dalton CA, Langmuir CH, Su Y, Schilling JG (2013) The mean composition of ocean ridge basalts. Geochemistry, Geophysics, Geosystems 14: 489–518
Gerdes A, Zeh A (2006) Combined U–Pb and Hf isotope LA-(MC-) ICP-MS analyses of detrital zircons: Comparison with SHRIMP and new constraints for the provenance and age of an Armorican metasedimentary Central Germany. Earth Plan Sci Letters 249: 47–61
Gerdes A, Zeh A (2009) Zircon formation versus zircon alteration. New insights from combined U-Pb and Lu-Hf in-situ LA-ICP-MS analyses, and consequences for the interpretation of Archean zircon from the Central Zone of the Limpopo Belt. Chem Geol 261: 230–243
Giese Y, Reitz E, Walter R (1988) Contributions to the stratigraphy of the Pulo do Lobo succession in Southwest Spain. Com Serv Geols Portugal 74: 79–84
Gill J (1981) Orogenic andesites and plate tectonics. Springer, Berlin, 390 p
Gladney ER, Braid JA, Murphy JB, Quesada C, McFarlane CRM (2014) U-Pb geochronology and petrology of the late Paleozoic Gil Márquez pluton: Magmatism in the Variscan suture zone, southern Iberia, during continental collision and the amalgamation of Pangea. Int J Earth Sci (Geol Runds) 103:1433–1451. https://doi.org/10.1007/s00531-014-1034-5

González F, Moreno C, López MJ, Dino R, Antonioli L (2004) Palinoestratigrafía del Grupo Pizarroso-Cuarcítico del sector oriental de la Faja Pirítica, SO de España. Rev Esp Micropaleontol 36: 2
Green TH (1995) Significance of Nb/Ta as an indicator of geochemical processes in the crust-mantle system. Chemical Geology 120: 347–359
Hay DC, Dempster DJ (2009) Zircon behavior during lower temperature metamorphism. J Petrol 50 (8): 1605
Higgs KH, Prestianni C, Streel M, Thorez J (2013) High resolution miospore stratigraphy of the Upper Famennian of eastern Belgium and correlation with the conodont zonation. Geol Belgica 16/1–2: 84–94
Irvine TN, Baragar WRA (1971) A guide to the chemical classification of the common volcanic rocks. Canadian Journal of Earth Sciences 8: 523–548
Jesus A, Munhá J, Mateus A, Tassinari C, Nutman A (2007) The Beja Layered Gabbroic Sequence (Ossa-Morena Zone, Southern Portugal): geochronology and geodynamic implications. Geodinamica Acta 20 (3): 139–157
Juteau T, Maury R (1999) The Oceanic Crust, from Accretion to mantle Recycling. Springer-Praxis, Berlin, 390 p
Korn D (1997) The Paleozoic ammonoids of the South Portuguese Zone. Mem Inst Geol Min Portugal 33: 1–131
Lake PA (1991) The Biostratigraphy and Structure of the Pulo do Lobo Domain within Huelva Province, Southwest Spain. PhD Thesis, Univ. of Southampton, 324 p
Langmuir CH, Klein EM, Plank T (1992) Petrological Systematics of Mid-ocean Ridge Basalts: Constraints on Melt Generation Beneath Ocean Ridges. In: Morgan JP, Blackman DK, Sinton JM (eds), Mantle flow and melt generation at mid-ocean ridges. American Geophysical Union Monograph Series 71: 183–280
Le Maitre RW (editor), Bateman P, Dudek A, Keller J. et al. (1989) A classification of Igneous rocks and Glossary of terms: Recommendations of the International Union of Geological Sciences, Subcommission of the Systematics of Igneous Rocks. Blackwell Scientific Publications, Oxford, 193 p
Linnemann U, Pereira MF, Jeffries T, Drost K, Gerdes A (2008) Cadomian Orogeny and the opening of the Rheic Ocean: New insights in the diachrony of geotectonic processes constrained by LA-ICP-MS U-Pb zircon dating (Ossa-Morena and Saxo-Thuringian Zones, Iberian and Bohemian Massifs), Tectonophysics 461: 21–43
Loboziak S, Streel M (1981) Miospores in Givetian to Lower Frasnian sediments dated by conodonts from the Boulonnais, France. Rev Palaeobot Palyno 29: 285–299
MacDonald GA, Katsura I (1964) Chemical Composition of Hawaiian Lavas. Journal of Petrology 5: 82–133
Martínez SS, Gerdes A, Arenas R, Abati J (2012) The Bazar Ophiolite of NW Iberia: a relic of the Iapetus-Tornquist Ocean in the Variscan suture. Terra Nova 24: 283–294
Martínez Catalán JR, Arenas R, Díaz García F, Abati J (1997) Variscan accretionary complex of northwest Iberia: terrane correlation and succession of tectonothermal events. Geology 25: 1103–1106
Matas J, Martín Parra LM, Rubio Pascual F et al. (2010) Mapa Geológico de España 1:200.000, sheet 75/74: Sevilla-Puebla de Guzmán. Instituto Geológico Minero España, Madrid
Matos JX (2016) Carta Geológica de Portugal 1/50 000: Sheet 43D Serpa, unpublished regional survey mapping. LNEG, Portugal
Matte P (1991) Accretionary history and crustal evolution of the Variscan Belt in western Europe. Tectonophysics 196: 309–339
Meschede M (1986) A method of discriminating between different types of mid-ocean ridge basalts and continental tholeiites with the Nb-Zr-Y diagram. Chemical Geology 56: 207–218
Middlemost EAK (1975) The basalt clan. Earth Sci Rev 11: 7–51
Miyashiro A (1974) Volcanic rock series in island arcs and active continental margins. American Journal of Science 274: 321–355
Moita P, Munhá J, Fonseca P, Pedro J, Tassinari C, Araújo A, Palacios T (2005) Phase equilibria and geochronology of Ossa Morena eclogites. Actas da XIV Semana de Geoquímica (VIII Congresso de Geoquímica dos Países de Língua Portuguesa) 2: 471–474
Munhá JM (1983) Low grade metamorphism in the Iberian Pyrite Belt Pyrite. Com Serv Geol Portugal 69: 3–35
Munhá J, Oliveira JT, Ribeiro A, Oliveira V, Quesada C, Kerrich R (1986) Beja-Acebuches Ophiolite: characterization and geodynamic significance. Maleo 2 (13): 31
Murphy JB, Cousens BL, Braid JA, Strachan RA, Dostal J, Keppie JD, Nance RD (2011) Highly depleted oceanic lithosphere in the Rheic Ocean: implications for Paleozoic plate reconstructions. Lithos 123 (1–4):165–175. https://doi.org/10.1016/j.lithos.2010.09.014
Murphy JB, Braid JA, Quesada C, Dahn D, Gladney E, Dupuis NE (2015) An eastern Mediterranean analogue for the Late Paleozoic evolution of the Pangean suture zone. In: Li ZX, Evans DAD, Murphy JB (eds), Supercontinent Cycles Through Earth History. Geol Soc London Spec Publ 424: 241–264. https://doi.org/10.1144/sp424.9
Murphy JB, Quesada C, Gutiérrez-Alonso G, Johnston, ST, Weil A (2016) Reconciling competing models for the tectono-stratigraphic zonation of the Variscan orogen in western Europe. Tectonophysics 681:209–219. https://doi.org/10.1016/j.tecto.2016.01.006
Nance RD, Gutiérrez-Alonso G, Keppie JD, Linnemann U, Murphy JB, Quesada C, Strachan RA, Woodcock NH (2012) A Brief History of the Rheic Ocean. Geosc Frontiers 3(2): 125–135
Oliveira JT (coordenador) (1992) Carta Geológica de Portugal 1/200 000, fl. 8. Noticia Explicativa. Serv Geol Portugal
Oliveira JT (1990) Stratigraphy and syn-sedimentary tectonism in the South Portuguese Zone.In: Dallmeyer RD, Martínez García E (eds), Pre-Mesozoic Geology of Iberia. Springer Verlag, 334–347
Oliveira JT, Horn M, Paproth E (1979) Preliminary note on the stratigraphy of the Baixo Alentejo Flysch Group, Carboniferous of Portugal and on the palaeogeographic development compared to corresponding units in Northwest Germany. Com Serv Geol Portugal 65: 151–68
Oliveira JT, Cunha TA, Streel M, Vanguestaine M (1986) Dating the Horta da Torre Fm., a new lithostratigraphic unit of the Ferreira-Ficalho Group, South Portuguese Zone: Geological consequences. Com Serv Geol Portugal 72 (1/2): 129–135
Onézime J, Charvet J, Faure M, Bourdier JC, Chavet A (2003) A new geodynamic interpretation for the South Portuguese Zone (SW Iberia) and the Iberian Pyrite Belt genesis. Tectonics 22 (4): 1–17
Pearce JA (1975) Basalt geochemistry used to investigate past tectonic environments on Cyprus. Tectonophysics 25: 41–67
Pearce JA (1982) Trace element characteristics of lavas from destructive plate boundaries. In: Thorpe RS (ed), Andesites: Orogenic Andesites and Related Rocks. John Wiley & Sons, 525–548
Pearce J (1983) Role of sub-continental lithosphere in magma genesis at active continental margins. In: Hawkesworth CJ, Nurry MJ (Eds), Continental Basalts and Mantle Xenoliths. Shiva Publishing, Nantwich, 230–249
Pearce JA (1996) A user's guide to basalt discrimination diagrams. Geological Association of Canada Special Publication 12: 79–113

Pearce JA (2008) Geochemical fingerprinting of oceanic basalts with applications to ophiolite classification and the search for Archean oceanic crust. Lithos 100: 14–48
Pearce JA, Cann JR (1971) Ophiolite origin investigated by discriminant analysis using Ti, Zr and Y. Earth and Planetary Science Letters 12: 339–349
Pearce JA, Cann JR (1973) Tectonic setting of basic volcanic rocks determined using trace element analyses. Earth and Planetary Science Letters 19: 290–300
Pedro J (2004) Estudo geológico e geoquímico das sequências Ofiolíticas Internas da Zona de Ossa-Morena (Portugal). PhD Thesis Évora Univ, 225 p
Pedro J, Araújo A, Fonseca P, Munhá J (2005) Internal Ossa-Morena Zone Ophiolitic Sequences: geodynamic implications for the evolution of the SW branch of the Iberian Variscan Chain. Cad. Lab. Xeol. de Laxe 30: 235–258
Pedro J, Araújo A, Fonseca P, Munhá J (2006) Ofiolitos e Metamorfismo de Alta Pressão. In: Dias R, Araújo A, Terrinha P, Kullberg JC (Eds), Geologia de Portugal no Contexto da Ibéria, Évora University, Évora (Portugal), 195–206
Pedro J, Araújo A, Fonseca P, Tassinari C, Ribeiro A (2010) Geochemistry and U-Pb zircon age of the internal Ossa-Morena zone ophiolite sequences: a remnant of Rheic ocean in SW Iberia. Ofioliti 35: 117–130
Pedro J, Araújo A, Fonseca P, Munhá J, Ribeiro A, Mateus A (2013) Cinturas Ofiolíticas e Metamorfismo de Alta Pressão no Bordo SW da Zona de Ossa Morena. In: Dias R, Araújo A, Terrinha P, Kullberg JC (Eds), Geologia Pré-mesozóica de Portugal v. 1, Escolar Editora, p 647–671
Pereira MF, Chichorro M, Johnston S, Gutiérrez-Alonso G, Silva JB, Linnemann U, Hofmann M, Drost K (2012) The missing Rheic Ocean magmatic arcs: provenance of synorogenic basins in SW Iberia. Gondwana Res 22: 882–891
Pereira MF, Castro A, Dias da Silva Í, Fernández C (2016) Granitic rocks of the European Variscan Belt: the case study of the Évora Massif (Alentejo, Portugal). 7 Congr Geol España, Geo-Guías 10: 89–107
Pereira MF, Gutiérrez-Alonso G, Murphy J B, Drost K, Gama C, Silva JB (2017) Birth and demise of the Rheic Ocean magmatic arc (s): Combined U-Pb and Hf isotope analyses in detrital zircon from SW Iberia siliciclastic strata. Lithos 278–281: 383–399
Pereira Z (1999) Palinoestratigrafia do Sector Sudoeste da Zona Sul Portuguesa. Com Serv Geol Portugal 86: 25–57
Pereira Z, Fernandes P, Oliveira JT (2006) Palinoestratigrafia do Domínio Pulo do Lobo, Zona Sul Portuguesa. Com Geol 93: 23–38
Pereira Z, Matos J, Fernandes P, Oliveira JT (2008) Palynostratigraphy and systematic palynology of the Devonian and Carboniferous successions of the South Portuguese Zone, Portugal. Mem Geol INETI 34, Lisboa, 181 p.
Pereira Z, Matos JX, Fernandes P, Jorge R, Oliveira JT (2009) New Lower Givetian age miospores of the Phyllite - Quartzite Group (São Francisco da Serra Anticline, Iberian Pyrite Belt - Portugal). CIMP Faro, UALG-LNEG, p. 75–78
Pereira Z, Fernandes P, Matos J, Oliveira JT, Jorge RS (2018) Stratigraphy of the Northern Pulo do Lobo Domain, SW Iberia Variscides: a palynological contribution. Geobios https://doi.org/10.1016/j.geobios.2018.04.001
Pérez-Cáceres I, Martínez Poyatos D, Simancas JF, Azor A (2015) The elusive nature of the Rheic Ocean suture in SW Iberia. Tectonics 34: 2429–2450
Pérez-Cáceres I, Martínez Poyatos DM, Simancas JF, Azor A (2017) Testing the Avalonian affinity of the South Portuguese Zone and the Neoproterozoic evolution of SW Iberia through detrital zircon populations. Gondwana Res 42: 177–192
Pfefferkorn HW (1968) Geologie des Gebietes zwichen Serpa und Mertola (Baixo Alentejo, Portugal. PhD thesis, Munster Forsch Geol Paläont 9: 2–143
Pin C, Fonseca PE, Paquette JL, Castro P, Matte Ph (2008) The ca. 350 Ma Beja Igneous Complex: A record of transcurrent slab break-off in the Southern Iberia Variscan Belt? Tectonophysics 461 (1–4): 356–377
Polat A, Hofmann AW (2003) Alteration and geochemical patterns in the 3.7–3.8 Ga Isua greenstone belt, West Greenland. Precambrian Research 126: 197–218
Quesada C (1991) Geological constraints on the Paleozoic tectonic evolution of tectonostratigraphic terranes in the Iberian Massif. Tectonophysics 185: 225–245
Quesada C (1998) A reappraisal of the structure of the Spanish segment of the Iberian Pyrite Belt. Mineralium Deposita 33: 31–44
Quesada C (2006) The Ossa-Morena Zone of the Iberian Massif: a tectonostratigraphic approach to its evolution. Z dt Ges Geowiss 157 (4): 585–595
Quesada C, Fonseca P, Munhá J, Oliveira JT, Ribeiro A (1994) The Beja - Acebuches Ophiolite (Southern Iberia Variscan fold belt): Geological characterization and geodynamic significance. Bol Geol Min 105: 3–49
Ribeiro A, Quesada C, Dallmeyer RD (1990) Geodynamic Evolution of the Iberian Massif. In: In: Dallmeyer RD, Martínez-García E (Eds), Pre-Mesozoic Geology of Iberia, Springer-Verlag, p. 398–409
Ribeiro A, Munhá J, Dias R, Mateus A, Pereira E, Ribeiro L, Fonseca P, Araújo A.,Oliveira JT, Romão J, Chaminé H, Coke C; Pedro JC (2007) Geodynamiv evolution of the Sw Europe Variscides. Tectonics 26, https://doi.org/10.1029/2006tc002058
Ribeiro A, Munhá J, Fonseca P E, Araujo A, Pedro JC, Mateus A, Tassinari C, Machado G, Jesus A (2010) Variscan ophiolite belts in the Ossa-Morena Zone (Southwest Iberia): Geological characterization and geodynamic significance. Gondwana Research 17 (2–3): 408–421
Rosas FM, Marques F, Ballèvre F, Tassinari C (2008) Geodynamic evolution of the SW Variscides: orogenic collapse shown by new tectonometamorphic and isotopic data from western Ossa-Morena Zone, SW Iberia. Tectonics 27: TC6008
Rubio Pascual, FJ, Matas J, Martín Parra LM (2013) High-pressure metamorphism in the Early Variscan subduction complex of the SW Iberian Massif. Tectonophysics 592: 187–199
Saccani E (2015) A new method of discriminating different types of post-Archean ophiolitic basalts and their tectonic significance using Th-Nb and Ce-Dy-Yb systematics. Geoscience Frontiers 6: 481–501
Sánchez-García T, Bellido F, Quesada C (2003) Geodynamic setting and geochemical signatures of Cambrian–Ordovician rift-related igneous rocks (Ossa-Morena Zone, SW Iberia). Tectonophysics 365: 233–255
Sánchez-García T, Quesada C, Bellido F, Dunning G, González de Tánago J (2008) Two-step magma flooding of the upper crust during rifting: The Early Paleozoic of the Ossa-Morena Zone (SW Iberia). Tectonophysics 461: 72–90
Sánchez-García T, Bellido F, Pereira MF, Chichorro M, Quesada C, Pin Ch, Silva JB. (2010) Rift-related volcanism predating the birth of the Rheic Ocean (Ossa-Morena zone, SW Iberia). Gondwana Research 17:392–407
Santos JF, Mata J, Gonçalves F, Munhá J (1987) Contribuição para o conhecimento geológico-petrológico da região de Santa Susana: O complexo vulcano-sedimentar da Toca da Moura. Comunicações Serviços Geológicos de Portugal 73: 29–48

Santos JF, Andrade AS, Munhá J (1990) Magmatismo Orogénico Varisco no limite meridional da Zona de Ossa-Morena. Comunicações Serviços Geológicos de Portugal 76: 91–124

Saunders AD, Norry MJ, Tarney J (1988) Origin of MORB and chemically-depleted mantle reservoirs: trace element constraints. Journal of Petrology 29: 415–445

Shervais JW (1982) Ti-V plots and the petrogenesis of modern and ophiolitic lavas. Earth Planetary Science Letters 59: 101–118

Silva JB, Oliveira JT, Ribeiro A (1990) South Portuguese Zone. Structural outline. In: Dallmeyer RD, Martínez García E (eds), Pre-Mesozoic Geology of Iberia. Springer Verlag, p. 348–362

Simancas JF (2004) Zona Sudportuguesa. In: Vera JA (ed), Geología de España, p. 199–201, SGE-IGME, Madrid, Spain.

Simancas JF, Carbonell R, González Lodeiro F, Pérez-Estaún A, Juhlin C, Ayarza P, Kashubin A, Azor A, Martínez Poyatos D, Almodóvar GR, Pascual E, Sáez R, Expósito I (2003) The crustal structure of the transpressionalVariscan Orogen of SW Iberia: The IBERSEIS deep seismic reflection profile. Tectonics 22 (6):1062. https://doi.org/10.1029/2002tc001479

Stampfli GM, von Raumer JF, Borel GD (2002) Paleozoic evolution of pre-Variscan terranes: from Gondwana to the Variscan collision. Geol Soc Am Spec Pap 364: 263–280

Stillman CJ (1998) Ordovician to Silurian volcanism in the Appalachian - Caledonian orogeny. Geological Society of London Special Publications London 38: 275–290

Streel M (2009) Upper Devonian miospore and conodont zone correlation in Western Europe. In: Königshof P (ed), Devonian Change: Case Studies in Palaeogeography and Palaeoecology. Geological Society London Special publications 314: 163–176

Sun S (1980) Lead isotopic study of young volcanic rocks from mid-ocean ridges, ocean islands and island arcs. Phil Trans R Soc A297: 409–445

Sun SS, McDonough WF (1989) Chemical and Isotopic Systematics of oceanic basalts: implications for Mantle Composition and Processes. In: Saunders AD, Norry MJ (Eds), Magmatism in the Ocean Basins. Geological Society, London, Special Publications 42: 313–345

Sun S, Nesbitt R (1978) Geochemical regularities and genetic significance of ophiolitic basalts. Geology 6: 689–693

Sun S, Nesbitt R, Sharaskin A (1979) Geochemical characteristics of mid-ocean ridge basalts. Earth Planet Sci Letters 44: 119–138

Vermeesch P (2006) Tectonic discrimination diagrams revisited. Geochemistry, Geophysics, Geosystems 7. https://doi.org/10.1029/2005gc001092

Wang P, Glover L (1992) A tectonics test of the most commonly used geochemical discriminant diagrams and patterns. Earth Science Reviews 33: 111–131

White WM (2015) Probing the Earth's Deep Interior Through Geochemistry. Journal Geochemical Perspectives 4: 95–251

Wilson M (1989) Igneous Petrogenesis: a Global Tectonic Approach. Chapman & Hall, London, 466 p

Wood DA (1980) The application of a Th-Hf-Ta diagram to problems of tectonomagmatic classification and to establishing the nature of crustal contamination of basaltic lavas of the British Tertiary volcanic province. Earth Planetary Science Letters 50: 11–30

Workman RK, Hart SR (2005) Major and trace element composition of the depleted MORB mantle (DMM). Earth Planetary Science Letters 231: 53–72

South Portuguese Terrane: A Continental Affinity Exotic Unit

6

J. T. Oliveira, C. Quesada, Z. Pereira, J. X. Matos, A. R. Solá, D. Rosa, L. Albardeiro, A. Díez-Montes, I. Morais, C. Inverno, C. Rosa, and J. Relvas

Abstract

The South Portuguese Terrane encompasses three major pre-orogenic mega-sequences: the Phyllite-Quartzite Group and the Tercenas Fm., the Volcanic-sedimentary Complex, and the Carrapateira Group, all three overlain by the syn-orogenic Baixo Alentejo Flysch Group, dealt with in Chap. 11. During the Mid-Late Devonian all the three mega-sequences belonged to an epicontinental sea. From the late Devonian to late Visean major changes took place: the region that became the IPB Domain was the locus of important lithospheric extension that led to the emplacement of important volumes of igneous rocks associated to a Volcanic-Sedimentary Complex, to which the VHMS ore deposits are associated; in Southwest Portugal the Tercenas Fm. shallow water sediments changed to a mixed-siliciclastic-carbonate shelf succession (Carrapateira Group); during the late Visean the extensional regime changed to crustal compression that caused the onset of huge deposits of flysch sediments (Baixo Alentejo Flysch Group) in successive depocenters migrating southward until the late Moscovian.

6.1 Introduction

J. T. Oliveira, C. Quesada

The South Portuguese Terrane (SPT) is part of the South Portuguese Zone, the southernmost division of the Iberian Massif initially proposed by Lotze (1945). The exposed

Coordinator: J. T. Oliveira.

J. T. Oliveira (✉) · A. R. Solá · C. Inverno
Laboratório Nacional de Energia e Geologia (LNEG), 2610-999 Amadora, Portugal
e-mail: josetomas.oliveira@gmail.com; tomas.oliveira@lneg.pt

A. R. Solá
e-mail: rita.sola@lneg.pt

C. Inverno
e-mail: carlos.inverno@lneg.pt

C. Quesada · A. Díez-Montes
Instituto Geologico y Minero de España, c/ Rios Rosas, 23, 28003 Madrid, Spain
e-mail: quesada.cecilio@gmail.com; quesada@ucm.es

A. Díez-Montes
e-mail: al.diez@igme.es

Z. Pereira
Laboratório Nacional de Energia e Geologia (LNEG), Ap. 1089. 4466- S., Mamede Infesta, Portugal
e-mail: zelia.pereira@lneg.pt

J. X. Matos · L. Albardeiro · I. Morais
Laboratório Nacional de Energia e Geologia (LNEG), Ap. 14, 7601-909 Aljustrel, Portugal
e-mail: joao.matos@lneg.pt

L. Albardeiro
e-mail: luis.albardeiro@lneg.pt

I. Morais
e-mail: igor.morais@lneg.pt

D. Rosa
Geological Survey of Denmark and Greenland, Oster Voldgade 10, Copenhagen, Denmark
e-mail: dro@geus.dk

C. Rosa
CRosa Geology Consulting, Qta Pedra Branca, Av. Casal Segulin, 1685-891 Famões, Portugal
e-mail: carlosiprosa@yahhoo.com

J. Relvas
Faculdade de Ciências, Universidade de Lisboa, Lisbon, Portugal
e-mail: jrelvas@fc.ul.pt

C. Quesada and J. T. Oliveira (eds.), *The Geology of Iberia: A Geodynamic Approach*, Regional Geology Reviews,
https://doi.org/10.1007/978-3-030-10519-8_6

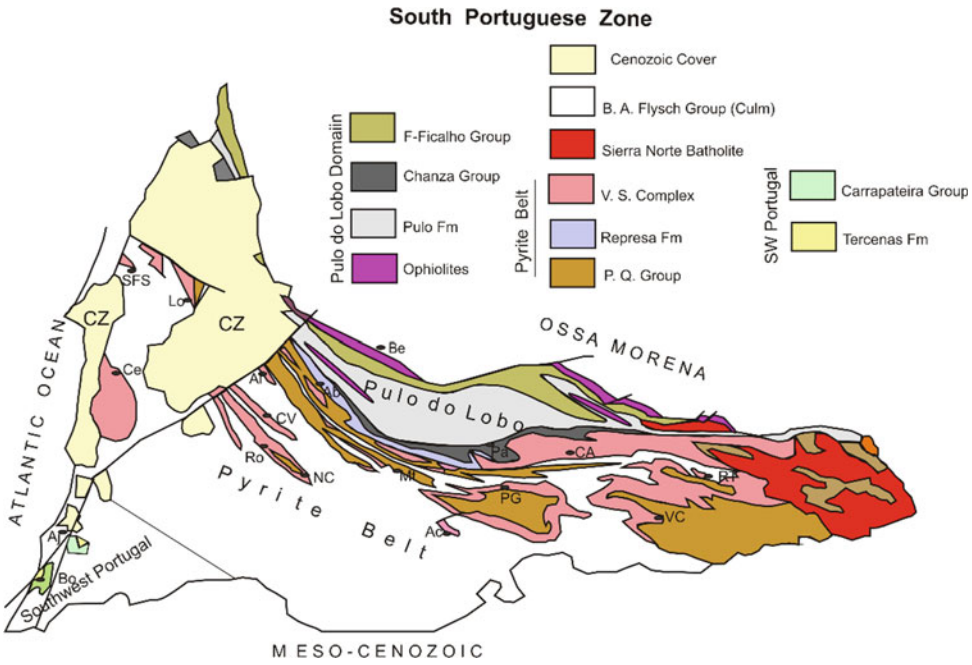

Fig. 6.1 Geological map of the South Portuguese Zone. Adapted from IGME/LNEG (2015). Symbols: Ab-Albernoa; Al-Aljustrel; Be-Beja; Bo-Bordeira; Ce-Cercal; CA-El Cerro de Andévalo; CV-Castro Verde; Lo-Lousal; Mt-Mértola; NC-Neves-Corvo; Pa-Paymogo; PG-Puebla de Guzmán; Ro-Rosário; RT-Rio Tinto; SFS-São Francisco da Serra; VC-Valverde del Camino; CZ-Cenozoic sedimentary

geological record in the South Portuguese Zone is restricted to Devonian and Carboniferous rocks, both metasedimentary and igneous, which has rendered rather difficult its correlation with other zones of the Iberian Massif or elsewhere. Despite this, it is a relatively well-known unit due to the fact that it hosts one of the largest volcanic-hosted massive sulphide (VHMS) metallogenic provinces in the world: the so-called Iberian Pyrite Belt (IPB), which has been attracting a mining interest for the last 5,000 years at least, especially during Roman Empire and since 19th century (Domergue 1983; Matos et al. 2008, 2011a). On the basis of significant stratigraphic, structural and metamorphic grade differences, four main domains have been proposed (Pfefferkorn 1968; Carvalho et al. 1971, 1976; Oliveira 1983, 1990), from north to south (Fig. 6.1): Pulo do Lobo, IPB, Baixo Alentejo Flysch Group and Southwest Portugal.

The wide application of geochemical studies and geodynamic models based on them made evident by the early nineteen eighties that the igneous rocks present in the Pulo do Lobo Domain had oceanic affinities (Bard and Moine 1979; Dupuy et al. 1979; Munhá et al. 1986). Besides, collaborative work undertaken at both sides of the Portugal-Spain border allowed recognition of an almost complete oceanic lithosphere stratigraphy within the so-called Acebuches amphibolite (Bard 1969), right at the contact with the Ossa-Morena Zone. This led Munhá et al. (1986, 1989) to interpret and rename it as Beja-Acebuches ophiolite, an interpretation that gained wide acceptance soon, mainly after publication of a thorough description by Quesada et al. (1994). The other divisions of the South Portuguese Zone referred to above share, at the base of the exposed stratigraphy, common mid-late Devonian shallow marine siliciclastic units (Phyllite-Quatzite Group—PQG; Schermerhorn 1971; Tercenas Formation—TF, Oliveira et al. 1985), indicating that they are underlain by continental crust. This is also supported by the compositions of the volcanic rocks in the IPB, which collectively derive from continental lithospheric sources (Munhá 1983a, b; Mitjavila et al. 1997; Díez-Montes and Bellido-Mulas 2008). As a whole, these continental divisions were incorporated in a single crustal block, the SPT (Ribeiro et al. 1990).

The nineteen eighties was also the time when, following developments in the North-American Cordillera (Coney et al. 1980), tectonostratigraphic terrane analysis was applied to many orogenic belts. This resulted in our case in the proposal of an "oceanic" Pulo do Lobo terrane, including the Beja-Acebuches ophiolite (Munhá et al. 1986, 1989), distinct to the SPT and the adjacent Ossa-Morena Zone, immediately north of it, both underlain by continental lithosphere. As a consequence, the Pulo do Lobo oceanic terrane was interpreted to delineate an oceanic suture between two continental blocks (Munhá et al. 1986, 1989; Ribeiro et al. 1990; Quesada 1991; Quesada et al. 1991, 1994).

Subsequent studies have provided evidence to ascribe the Pulo do Lobo oceanic terrane to the Paleozoic Rheic Ocean (Quesada 1996; Onézime et al. 2003; Braid 2011; Braid et al. 2010, 2011, 2012, 2018), whose closure was responsible for the collision between Gondwana and Laurussia that led to formation of the Variscan orogeny. In turn, the Ossa-Morena Zone as well as the northernmost zones within the Iberian Massif are being ascribed to Gondwana (Quesada 1991), whereas the "exotic" SPT, generally correlated with

Avalonia sensu lato (Quesada 1991; Quesada et al. 1994; Oliveira and Quesada 1998; Simancas et al. 2009; Pérez-Cáceres et al. 2017), has been recently ascribed to the Meguma terrane of the Appalachians, with which it shares similar provenance (detrital zircon) records (Braid 2011; Braid et al. 2011, 2012, 2018).

The major composing units of the SPT i.e. from north to south: IPB Baixo Alentejo Flysch and Southwest Portugal, exhibit contrasting stratigraphic records representing distinct paleogeographic domains in pre-orogenic times. During the mid-late Devonian all the domains belonged to an epicontinental sea. From the late Devonian to late Visean major changes took place: the region that became the IPB domain was the locus of important lithospheric extension that led to the emplacement of important volumes of igneous rocks associated to a Volcanic-Sedimentary Complex (VSC), to which the VHMS ore deposits are associated (Schermerhorn 1971; Barriga et al. 1997; Leistel et al. 1998a, b; Carvalho et al. 1999; Tornos 2006); the Southwest Portugal domain changed to a mixed-siliciclastic-carbonate shelf succession (Carrapateira Group; Oliveira 1983, 1990); during the late Visean the extensional regime in the IPB changed to crustal compression that caused the onset of the syn-orogenic Baixo Alentejo Flysch that accumulated huge deposits of flysch sediments in successive depocenters migrating southward until the late Moscovian (Oliveira 1983, 1990; Pereira 1997), in front of the propagating orogenic wedge after Variscan collision with the outer margin of Gondwana (Ribeiro et al. 1990; Quesada 1991, 1998). In order to put it in context with the other Variscan syn-orogenic basins in Iberia, this Baixo Alentejo Flysch basin is dealt with in Chap. 11 of this volume.

6.2 South Portuguese Terrane

J. T. Oliveira, C. Quesada, Z. Pereira, J. X. Matos

6.2.1 Pre-orogenic Mega-Sequences

6.2.1.1 Siliciclastic Open Platform (Epicontinental Sea)—Upper Devonian

The oldest mega-sequence is a siliciclastic open platform succession represented by the Phyllite-Quartzite Group (PQG) of the IPB Domain (Schermerhorn 1971) and the TF of SW Portugal Domain (Oliveira et al. 1985; Pereira 1997; Oliveira 1990). As a whole, it covered the entire depositional area of the SPT from the Givetian to the late Famennian, remaining until the Early Tournaisian in the Southwest Portugal domain (Oliveira et al. 2005, 2013; Pereira 1997; Pereira et al. 2008a, b).

The PQG occupies the core of the main complex antiformal structures that characterize the autochthonous/parautochthomous Southern Branch of the IPB, and is also a component of allochthonous sequences that overlie the IPB VSC and the Mértola Formation of the syn-orogenic Baixo Alentejo Flysch Group in the Intermediate and Northern branches of the IPB (Fig. 6.2).

Concerning the (para)autochthonous units, the PQG is divided in Portugal into the following composing units: the Phyllite-Quartzite Formation (PQF) (Schermerhorn 1971), which represents the most widespread unit (may assume local designations), the Barranco do Homem Formation and its equivalent Represa Formation (Oliveira 1990; Oliveira and Silva 1990) and the Nascedios and Forno da Cal

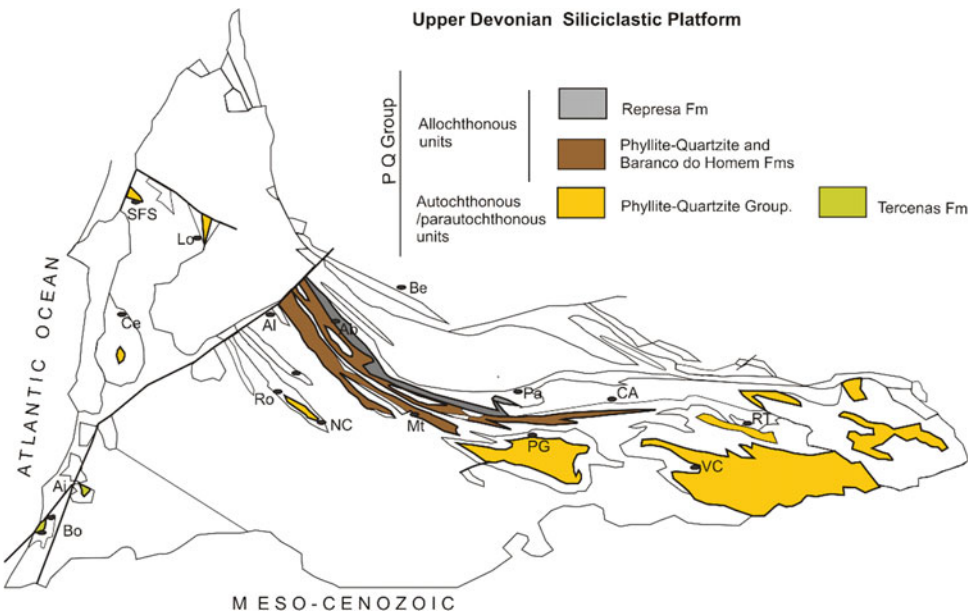

Fig. 6.2 The upper Devonian siliciclastic exposure in the SPT. Symbols as in Fig. 6.1

Limestones (Boogaard 1967; Boogaard and Schermerhorn 1981), representing deposition in distinct sedimentary environments. The largest PQG exposure occurs however in Spain, in the cores of the Puebla de Guzmán and Valverde Del Camino antiforms covering several thousands of Km but no formal composing units have been proposed (Fig. 6.1).

In general the autochthonous PQF is composed of a lower and middle part comprising mostly thin-bedded siltstones and fine-grained quartzite dispersed in dark shale, while there is a general tendency to build up metric to decametric thick packets of sandstones, mostly quartzite and quatzwacke beds whose thickness varies from 10 to 60 cm. The quartzites are dominant in the western outcropping area while the quartzwackes appear to be best represented in the east. Although the base of the lithologic succession is not known, the (structural) thickness of the exposed sequence is assumed to be of the order of 2,000 m. The thin-bedded lithofacies show frequently current ripples and meandering type trace fossils which suggest offshore deposition. The thicker beds exhibit several types of sedimentary structures (massive bedding, large scale planar and bimodal cross bedding, current and wave ripples, hummocky cross bedding (HCS), graded bedding, syn-sedimentary folds and sandstone balls) and occasional vertical and meandering burrows. In favourable situations, when the tectonic deformation is less strong, the thicker beds exhibit tabular and lenticular geometries with lengths that may reach few hectometers, probably representing coastal sand bars.

One of the best sections of the upper part of the succession is exposed in road cuts of the HV-5137 and HV-5131 roads, Berrocal region, Valverde Del Camino antiform. A detailed logging of this section recognized four lithofacies: dark shales, thin-bedded parallel laminated siltstones, single or amalgamated packets of tabular quartzites exhibiting HCS, and centimeter-thick graded beds of quartzwackes (Jorge et al. 2007a, b, c; Fig. 6.3a). The shales and thin-bedded lithofacies represent distal offshore sedimentation and the packets of quartzites and quartzwacke reflect frequent episodes of storm deposition above storm-wave base. The shales provided palynomorphs assigned to the VH (*A. verrucosa-V. hystricosus*) Miospore Biozone of late Famennian age (Jorge et al. 2007a, b, c).

In the extreme NW of the IPB, drill holes made at the core of the São Francisco da Serra anticline (Fig. 6.3b) and

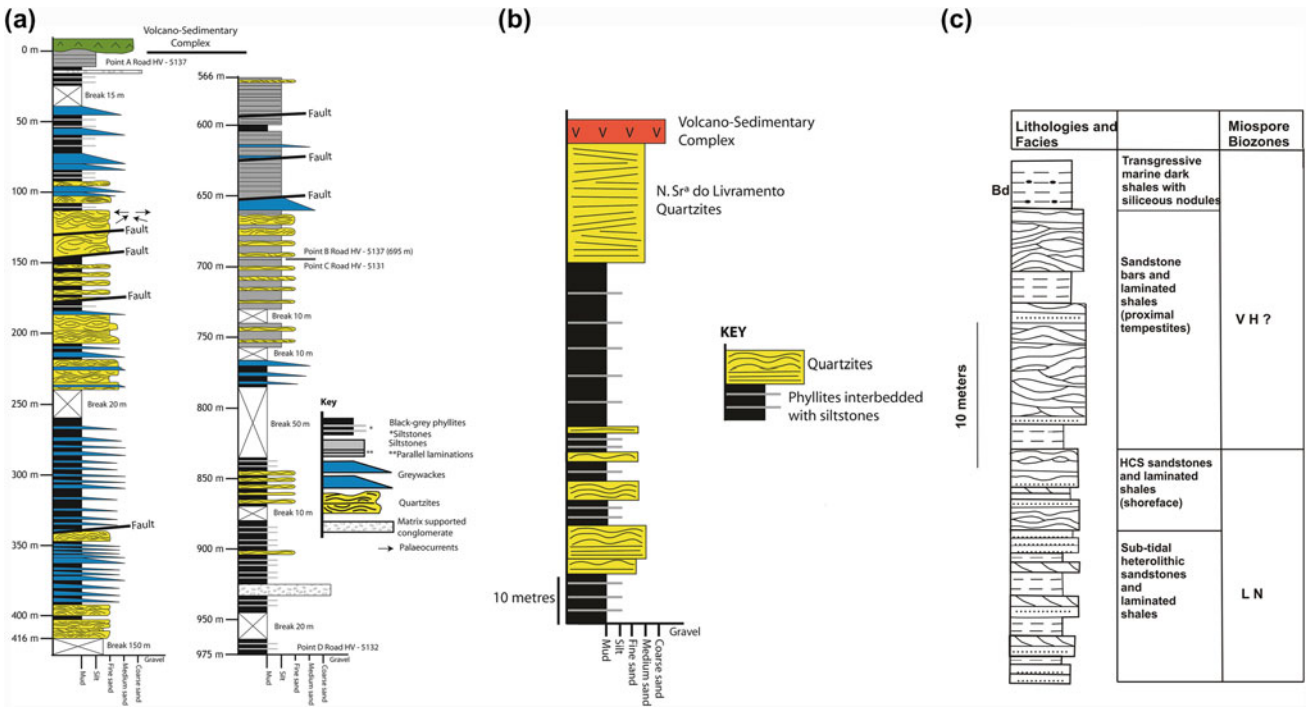

Fig. 6.3 **a** PQG environmental interpretation at Berrocal (Jorge et al. 2007a, b, c); **b** PQG facies interpretation based on drill core M1, São Francisco da Serra anticline (adapted from Pereira et al. 2010; Matos et al. 2014); **c** Pedra Ruiva facies interpretation, Tercenas Formation (modified from Moreno et al. 1996; Pereira 1997)

at the Lousal and Caveira old mines exhibit lithologic successions composed of alternations of packets of sandstones and thin-bedded heterolithic facies that are similar to those described at Berrocal. Shales recovered from these boreholes yielded miospores assigned to the upper part of AD Miospores Biozone, subzone Lem, of early Givetian age, based on the presence of *Geminospora lemurata*, the oldest age so far obtained for the PQG (Pereira et al. 2009, 2010; Matos et al. 2014).

Conglomerates may occasionally occur interbedded in the shallow water sandstone packets, the best studied being those exposed at Virgen de la Peña, Puebla de Guzmán antiform (Moreno and Saez 1990). These are clast-supported polymictic conglomerates containing sub-angular to rounded clasts of quartzite and other sandstones, 1–25 cm in diameter, and pebbles of Fe–Mn oxides, interpreted as channel-fill bodies associated to fan deltas. Subordinated mud-supported conglomerates composed of pebbles of quartzite dispersed in a shaly matrix are seen as flash flood episodes. Large scale gravity flows at the top of the PQG has also been described (Moreno et al. 1995, 1996). The flows are represented by matrix-supported conglomerates whose clasts have dimensions that range from few centimeters to several decimeters, and solely composed of angular shaped sandstone clasts dispersed in a shaly matrix (Fig. 6.4d). The clasts are lithologically similar to the PQG sandstones and show the same type of sedimentary features. These gravity flows are interpreted to have been derived from gravity sliding generated at the shoulders of uplifted PQG crustal blocks, which herald the onset of the extensional regime that prevailed during formation of the overlying VSC (Quesada 1998).

Angular and rounded clasts and boulders of siltstone, quartzite and quatzwacke occur dispersed in shales throughout the PQG but are more frequent in the allochthonous sheets (see below). Many clasts correspond to disrupted slabs of sandstone beds and fold hinges caused by tectonic shearing (Fig. 6.4a). That is, besides clasts associated to gravity flows, there are also clasts whose dispersion in shales is caused by strong shearing associated to the main regional cleavage.

The PQF shales yielded miospore ages range from the early Givetian, AD Biozone, subzone Lemurata (Pereira et al. 2010; Matos et al. 2014) through the late Givetian, TCo Biozone (Lake et al. 2000; González et al. 2004) to the mid late Famennian VCo (*D. versabilis-G. cornuta*) and VH (*A. verrucosa-V. hystricosus*) Miospore Biozones and Strunian LN (*V. nitidus*) Biozone (Oliveira et al. 2004; Pereira et al. 2008a, b, 2010, 2012; Matos et al. 2014).

Limestone lenses (mudstones and packstones) and nodules occur throughout at the top of the PQF, assuming in Portugal the designations of Nascedios (Pomarão anticline) and Forno da Cal (Rosario antiform) units. Their lengths rarely exceed one hundred meters and the thickness does not exceed ten meters. They have grey or brown colors when altered and frequently show crinoid articles. Rich conodont faunas provided early to middle Famennian ages (Boogaard 1963, 1967; Boogaard and Schermerhorn 1981). These limestones form mounds (bioherms) surrounded by black shales which together represent a few decameters-thick key horizon that marks a turning point in the basin infilling evolution from shallow energetic to more confined sedimentation. It is worth noting that this key horizon is overlain by the first manifestations of volcanism, i.e. the beginning of the extensional magmatic regime that led to the genesis of the VSC and related VHMS deposits.

The allochthonous PQG sedimentary packages in the IPB Northern branch are built up of shales, quartzites and quartzwackes which are structurally intercalated with VSC-type lithologies (siliceous shale, volcanogenic sediments, chert, Fe–Mn nodules and rare lenses and nodules of limestone) forming together sheet-like structures (Oliveira 1990; Oliveira and Silva 1990). These sheets structurally overlie hectometric thick sequences of the VSC, the Mértola and Freixial fms. and equivalent *Culm* turbidites in Spain (Fig. 6.2). The shales, siltstones, quartzites and quartzwackes display similar lithological compositions, sedimentary structures and ages as those of the (para)autochthonous PQF and as such they are considered stratigraphically equivalent to this unit. As it happens in the (para)autochthonous units, in appropriate tectonic conditions the packets of quartzite beds may form ridges, several hundred meters in length and few decameters-thick. Many of these ridges presently occupy the top of the hills. Disrupted quartzite beds (Fig. 6.4d) and shaly supported clasts and boulders of quartzite, quartzwacke and siltstone are common in almost all the sheet-like structures (Fig. 6.4c, e, f). The boulders may reach several meters in length and in many places they appear as tectonically disrupted folds.

The dispersion of clasts and boulders in several of these sheets may exhibit, in spite of shearing associated to the cleavage, crude coarsening (or fining) upward sedimentary arrangements which may reflect the inherited pre-orogenic sedimentary infilling. The Mata Filhos stream section (5 km NW Mértola) (Fig. 6.5a) is an example of a cross section showing alternations of tectonic origin of PQF sandstones and VSC volcanic rocks. Restoring the section by taking into account the normal stratigraphic order, i.e. VSC over the PQG, the fining upward sedimentary arrangement of the PQF lithologies and also the assumption that bigger PQF blocks at the base of the lithological sequence suggest gravity sliding close to a fault cliff, the result is the identification of four distinct structural blocks which are interpreted as being separated by gravitational faults generated in close relationship with successive extensional tectonic pulses (Fig. 6.5b). Subsequent tectonic inversion from extensional to compressive during the late Visean brought the stratigraphic pile to a

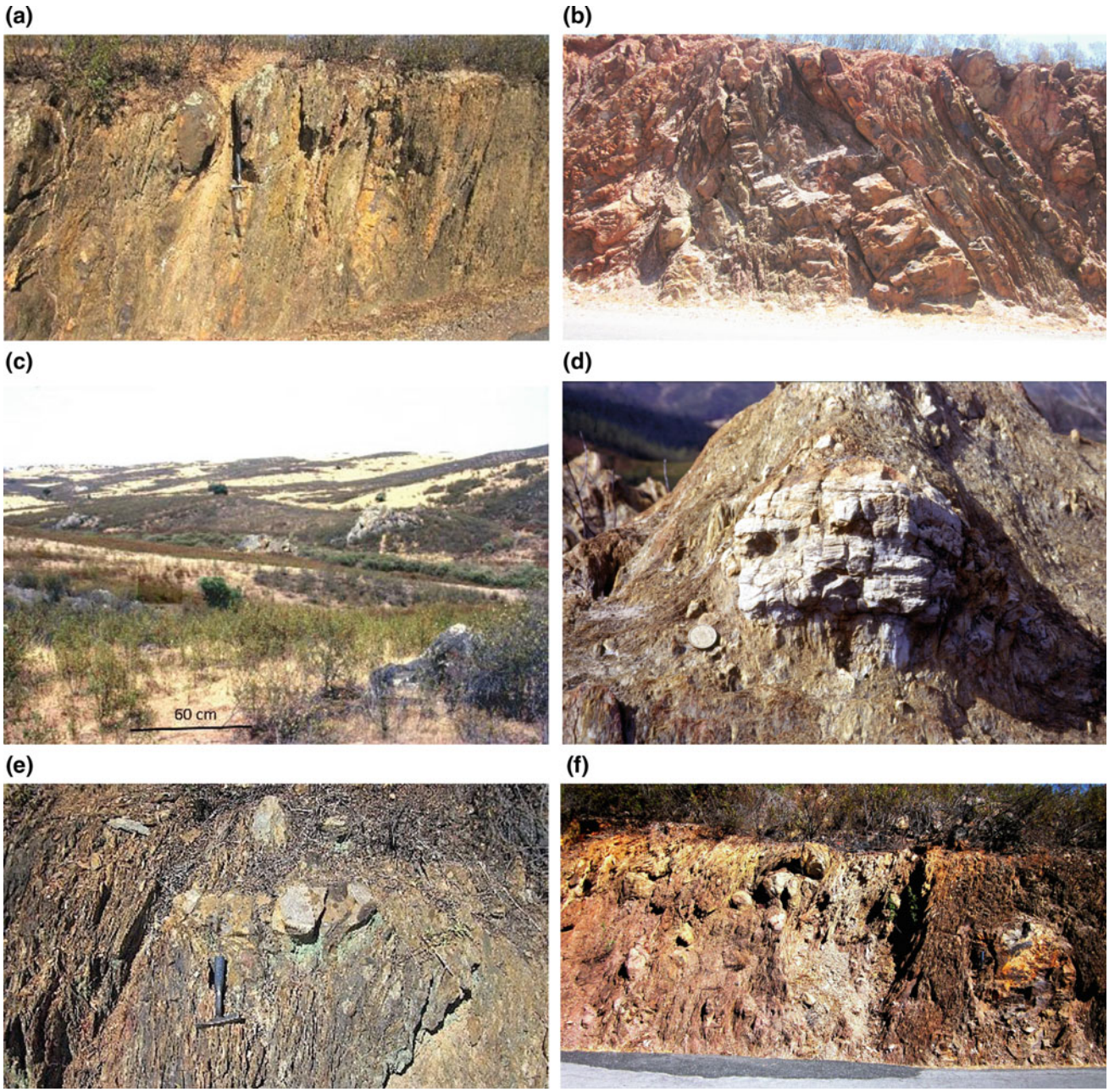

Fig. 6.4 Tectonically disrupted PQG beds: **a** round block of quartzite originated by shearing, left side, and a still preserved quartzite fold, right side, road Mertola-Corte Gafo, 4.8 km south of Corte Gafo village; **b** block of a quartzite bed preserved between undisrupted quartzite beds, road 2 km SW of Corvos village, Mértola nappe; **c** dispersed blocks of quartzite, Mata Filhos stream (see below); **d** gravity sliding of quartzites with cross bedding dispersed in shales, La Coronada, Sotiel, Valverde Antiform; **e** pre-cleavage rounded blocks of quartzite, forming true olistoliths, Galé-Cela nappe, road Mértola-Corte Gafo village, 4, 8 km south of this village; **f** olistrostomes composed of sandstone rounded blocks dispersed in shales, 1 km NW of Corvos village, road to Corte Sines, Mértola

vertical position and the reactivation of the gravitational faults as SW verging thrusts (Fig. 6.5c). Further compressive impulses led to the inversion of the stratigraphic sequence and brought the PQG to overly the CVS tectonic structure of the Northern Branch of the IPB may have resulted from a combination of syn-sedimentary olistrostomes and overthrust sheets (folded former thrusts). This is probably the case of the so-called Mértola and Galé-Cela nappes in Portugal (Silva et al. 1990; Oliveira and Silva 1990, 2007) and in all the Northern Branch of the Portuguese sector of the IPB (Oliveira coordenador 1982). In Spain they are part of the Duque unit (Santos Bonaño et al. 1982), here incorporated in the allochthonous redefined Northern Branch discussed ahead in the crustal extension mega-sequence.

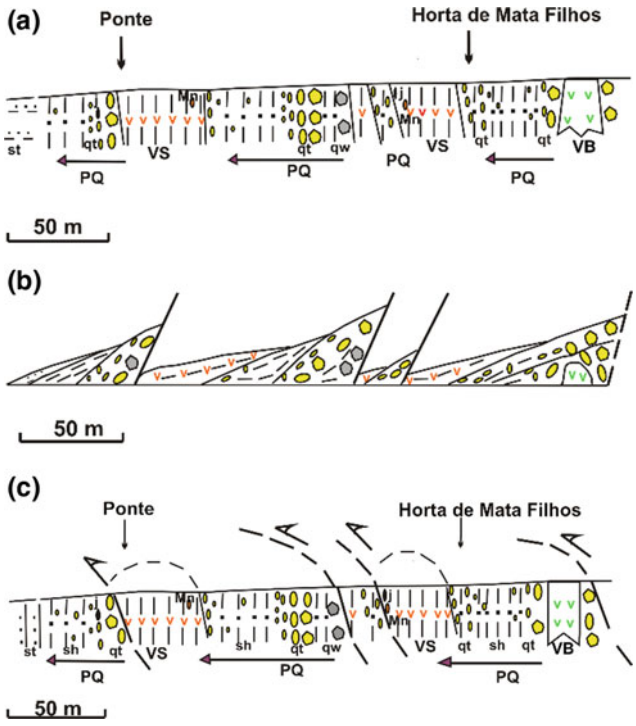

Fig. 6.5 **a** Cross section along the Mata Filhos stream, road Mértola-Beja, 5 km NW of Mértola. Symbols: St-shales and siltstones; VS-VSC shales and siliceous shales; VB-mafic volcanics; sh-shales; PQ-PQG shales with dispersed clasts and boulders of quartzites (qt) and quartzwackes (qw); Mn-manganese nodules and lenses; j-jaspers. **b** Restoring the Mata Filhos section based on the sedimentary polarity and the clasts dimensions and roundness. **c** Structural interpretation after the regional tectonic inversion

The shales that form the matrix of the olistrostomes provided only late Devonian palynomorph ages. However, as far as the basin(s) were widening during the early Carboniferous more gravity slides may have occurred. If this was the case the matrix supporting the clasts and boulders should have distinct Carboniferous ages, a situation never found until now. Clearly more detailed research is needed in order to clarify this important matter. Still referring to the Northern Branch, detailed mapping in the Mértola region, Portugal (Silva 1989; Oliveira and Silva 1990, 2007) allowed the identification of a hectometric thick succession composed of greywacke, quartzwacke, siltstone beds and shale to which the formal designation of Barranco do Homem Formation was given. The sandstone beds have thicknesses that range between 20 and 60 cm, are massive or show graded bedding. Ripple drift cross-lamination and bioturbation are common in the siltstones, particularly *Planolites* sp. and meandering burrows, of which rare *Nereites* sp. Further mapping recognized a large expression of this unit along the North Branch of the Portuguese part of the IPB (Oliveira coordenador 1982) always associated to the allochthonous sedimentary sheets.

Shales of the allochthonous PQG, including the Barranco do Homem Fm, yielded upper Famennian ages provided by miospore and acritarch assemblages, assigned to the VH (*A. verrucosa-V. hystricosus*) Miospore Biozone and Strunian palynomorph assemblages assigned to the LN (*V. nitidus*) Miospore Biozone (Cunha and Oliveira 1989; Matos et al. 2006; Pereira et al. 2007, 2008a, b; Faria et al. 2015) and rare ammonoids of *Clymenia* sp. (Oliveira 1990). Similar ages were also obtained from conodonts in the limestone lenses (Fantinet et al. 1976).

It should be noticed that thin-bedded silty/shale facies, reaching several hundred meters in thickness below VSC felsic volcanics are dominant in the unexposed PQG of the Rosario (Oliveira et al. 2013) and Cercal (Pereira et al. 2008a, b) antiforms, as shown by drill holes. In both cases the shales yielded palynomorphs assigned to the VH Miospore Biozone. The silty/shale facies may reflect the existence of deeper or confined areas in the siliciclastic platform in these areas.

Right at the boundary between the Pulo do Lobo Domain and the IPB Northern Branch the Represa Formation crops out. Previously considered to represent the upper unit of the Chança Group that forms the south limb of the Pulo do Lobo Domain (Oliveira 1990; Pereira et al. 2006), this interpretation is now being revised. The unit is bounded to the north by the Gafo Fm., a flyschoid unit dated as early Famennian (Pereira et al. 2008a, b) that has been integrated in the Pulo do Lobo Domain (Carvalho et al. 1976; Oliveira coordenador 1982; Pereira et al. 2006, 2008a, b, 2018). The boundary between the Represa and Gafo Fms is still poorly defined, needing more detailed mapping and research. The unit, first identified in the Mina de São Domingos region (Carvalho et al. 1976) was later recognized in the Guadiana river valley (Silva 1989) and further NW in Azinhalinho, SE of Albernoa village (Oliveira coordenador 1982). It is composed of decametric thick packets of quartzwacke beds showing Bouma's sedimentary structures intercalated in decametric thick successions containing siltstones, siliceous shales and occasional purple and green shales. Meandering type trace fossils can be observed at the bases of the siltstone beds. The unit is overlain by fine volcanogenic sediments in the Guadiana valley (Silva 1989) and by felsic volcanism, mostly composed of rhyolites and rhyodacites in the Azinhalinho region. These latter volcanics share the same geochemical signature and U/Pb zircon age to those of the IPB (Rosa et al. 2008). On the basis of its palynological content (see below) and its relationship with VSC lithologies, the Represa Fm. is now re-interpreted as a lateral equivalent of the Barranco do Homem Fm. and integrated in the PQG of the IPB. Samples recovered from shales in Mina de São Domingos and Azinhalinho regions yielded a diverse and well preserved assemblage of palynomorphs and acritarchs assigned to the VH (*A. verrucosa-V. hystricosus*) Miospore

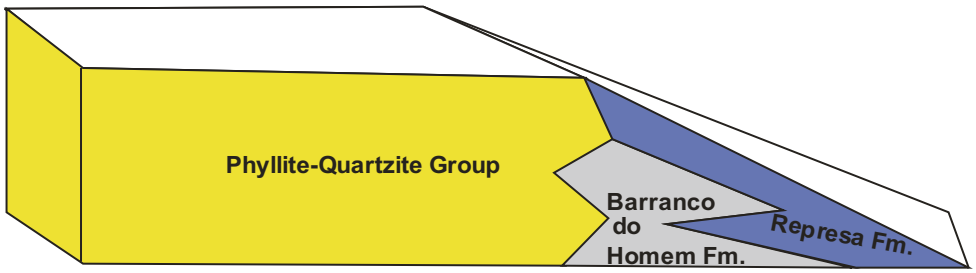

Fig. 6.6 Stratigraphic relationships between the PQG, the Barranco do Homem Fm. and the Represa Fm.

Biozone of late Famennian age (Cunha and Oliveira 1989; Matos et al. 2006; Pereira et al. 2006, 2008a, b). The palynological assemblage is composed of the same species as those identified in the upper part of the PQG succession and in the Barranco do Homem Fm. In the marine component of the Represa Fm. acritarchs and prasinophyte algae are dominant and abundant, suggesting a more distal depositional environment with respect to that of the PQG sensu stricto. Figure 6.6 shows an interpretative sketch of the units' relationship within the basin context.

Intrusive bodies of microdiorite and dolerite occur NE of the Azinhalinho and several small (hectometer to kilometer-size) intermediate to felsic plutons intrude the possible extension of the Represa Fm. in Spain (IGME 1:50.000 map, Paymogo; Gonzalo et al. 1978). However, the Represa Fm. has not been mapped as a distinct unit in Spain being integrated in the so-called Duque unit, which was interpreted as an allochthonous syn-sedimentary and tectonic mélange (Santos Bonaño et al. 1982). Besides the lithologies similar to those of the Represa Fm, the mélange incorporates also PQF-type quartzites, varied types of volcanic rocks, volcanogenic sediments, jaspers and purple shales. This rock assemblage is quite similar to that forming the above described sheet-like structures recognized in the Portuguese component of the Northern Branch.

The epicontinental sea facies are represented in the Southwest Portugal Domain by the TF which underlies the Carrapateira Group (CG) of Lower to Mid Carboniferous age. The TF crops out in the core of the Aljezur and Bordeira antiforms (Fig. 6.1) and the best exposures are found at the Atlantic coastal cliffs or inland in stream valleys. The unit is composed of two thickening and coarsening upward sedimentary sequences totaling ca. 100 m in thickness (base not exposed) (Oliveira et al. 1985). Each of these sequences is built up of heterolithic fine-grained sandstones and shales indicating a subtidal environment that grade upward to medium and coarse-grained graded sandstones, which were laid down in nearshore marine environments. The facies organization of the upper sequence is represented in Fig. 6.3c. The two sequences record two episodes of sea level change. The heterolithic facies of the lower sequence provided rare specimens of *Cymaclimenia* sp., which indicate a Famennian age, and poorly preserved pygidiums of trilobites and solitary corals which are usually linked to low energy environments (Oliveira et al. 1985). The upper sequence yielded miospores of the LN (*V. nitidus*) Biozone of late Famennian (Strunian) age and of the basal part of the VI (*C. cristifera*) Biozone in the upper tidal facies of Pedra Ruiva (Fig. 6.3c) indicating the base of the Tournaisian (Pereira et al. 1994; Pereira 1997, 1999). The breccia situated at the top of the Monte Novo section yielded a poorly preserved fauna of *Rugosochonetes* sp., *Syringotires* sp. and spiriferaces of early Carboniferous age (P. Racheboeuf in Oliveira et al. 1985). The age of the TF is therefore assigned to the late Famennian to early Tournaisian, based on palynomorphs and brachiopod faunas. That is, the Devonian/Carboniferous boundary in SW Iberia lies at the top of the heterolithic facies of the upper sequence (Pereira 1999; Pereira et al. 2007).

The sedimentary facies and ages yielded by miospore assemblages of the TF show close similarities with those of the PQG, although in SW Portugal the siliciclastic platform persisted until the early Tournaisian. This means that both depositional areas belonged to the same marine epicontinental sea. At this point it is worth noting that the miospore assemblages of the TF and the upper part of the PQG show close similarities with those recorded in the same stratigraphic interval in other areas of Western Europe, namely the British Isles, the Munster basin in Ireland, the Ardennes in Belgium and Rheinisches Schiefergebirge in Germany (Pereira et al. 1994). A comparison between SW Portugal and the Munster basin at the Devonian/Carboniferous boundary shows similar lithological successions and miospore assemblages (Pereira et al. 1994). All these areas are currently integrated in the Avalonian Terrane (Clayton et al. 2002).

6.2.1.2 Volcanic-Sedimentary Complex (Extensional Basins): Upper Devonian-Lower Carboniferous

The extensive and rather stable open siliciclastic platform where the PQG was deposited started to be subjected to active extensional processes during the Upper Devonian, leading to individualization of two basinal domains. To the south, the future Southwest Portugal domain (Fig. 6.1) remained as an open shelf where mixed

siliciclastic-carbonate successions were laid down until the Bashkirian CG. The northern part of the previous platform was intensely affected by lithosphere-through extension, as indicated by strong basin compartmentalization and massive bimodal volcanic activity (VSC) that characterize the IPB Domain (Fig. 6.1) of the SPT. Extensional deformation was already heralded during the late period of PQG deposition by the formation of the debris flows and olistrostomes outlined in the previous section, and was active until the late Visean, when the basin started to be inverted coeval to the onset of syn-orogenic flysch deposition (Baixo Alentejo Flysch Group). Both compressional inversion and flysch deposition progressively propagated southwards in front of an advancing orogenic wedge caused by the collision of the SPZ (s.l) with the outer margin of Gondwana (Ribeiro et al. 1990; Quesada 1991, 1998; Onézime 2001).

The boundary between the Southwest Portugal and the IPB domains is currently concealed beneath the syn-orogenic flysch units that make the Baixo Alentejo Flysch Domain (Fig. 6.1), rendering thus impossible to determine its characteristics and precise location.

The VSC Stratigraphic Sequence and Basin Development

Despite the strong structural complexity and penetrative internal deformation introduced by the collisional Variscan orogeny, it is possible to define IPB units with coherent VSC stratigraphic sequences. Those at larger scales, i.e. the Northern, Intermediate and Southern IPB branches (Figs. 6.7 and 6.8), may represent different lithospheric or crustal blocks whereas those at smaller scales most probably reflect deposition in sub-basins within those blocks, whose genesis is linked to the first stage of the regional tectonic extension. Volcanic eruption and sedimentation in the Northern and Southern IPB branches took place in submarine environments. However, recognition in Spain of very peculiar structural units in which felsic ignimbrites constitute the most part of the VSC volcanic record (El Almendro and Berrocal nappes; Quesada 1996, 1998) suggests that eruption in these units was largely subaerial or under an extremely thin water column (Routhier et al. 1980). One of these units, which is not exposed or at least not recognized so far in the Portuguese sector of the IPB, is structurally sandwiched in the Berrocal area between the Northern Branch nappes (above) and the parautochthonous Southern Branch units (below) occurring in the northern limb of the large Valverde del Camino antiform (Fig. 6.7). This geological situation led Quesada (1996, 1998) to interpret the existence of a syn-sedimentary relatively uplifted crustal block (Intermediate Domain in this author's terminology although the term Intermediate Branch is preferred herein for consistency) relative to both the Northern and Southern branches. This arrangement suggests an overall horst and graben structure during VSC times (Fig. 6.8). The syn-sedimentary horst and graben structure is also indicated at smaller scales by comparing the VSC thickness of various structural divisions within each of the Northern and Southern IPB branches (Quesada 1996, 1998). Note that the local variation of the volcanic units is common in submarine volcanic environments. The volcanic domes and cryptodomes can present a fast evolution in a short geological time, promoting significant lateral variation of facies. The evolution of these structures could be conditioned in the origin by structural distensive fault planes which facilitated the rise of lava flows. Due to the synthetic review character of this contribution the focus is placed on the general characteristics of the VSC in these three major divisions (Fig. 6.7), with exceptional incursions into more detailed scales only in those cases where the local characteristics are of a special significance (e.g. peculiar volcanic facies, paleontological or geochronological sites, sites with hydrothermal alteration and related stockwork and/or massive sulphide mineralization).

Common features of the VSC stratigraphy in the three IPB branches are: similar PQG sensu lato basement; alternation of volcanic and volcanoclastic rocks with sediments; submarine deposition and eruption in the Northern and Southern branches throughout the VSC versus subaerial to shallow marine environments in the Intermediate Branch; existence of a singular, radiolarian-bearing purple shale horizon near the top which marks the end of the extensional regime prevailing since late PQG times; lack of massive sulphide ore deposits in the upper VSC sequences with late Visean age. Palynological and geochronological data (e.g. Pereira et al. 2008a, b; Matos et al. 2011a, b; Oliveira et al. 2013; Sola et al. 2015; Albardeiro et al. 2017) shows a favourable correlation between the VHMS deposits and the lower VSC sequences present in the northern and southern IPB branches, with ages between Upper Famennian (Strunian) and early Tournaisian. Particular conditions in this geological period were favourable to an intense hydrothermal circulation and water/rock interaction, essential to the development of the massive sulphides and stockwork mineralizations >90 deposits.

VSC Stratigraphic Sequence of the Southern Branch

Despite the tectonic complexity, and apart the variability in space and time of the volcanic rocks that wedge out very rapidly, passing from hectometer thick accumulations to zero in only a few kilometers, the VSC stratigraphy share a general pattern in which the sedimentary and volcanogenic components are concerned. This is particularly evident for the Valverde and Puebla antiforms in Spain, and most of the

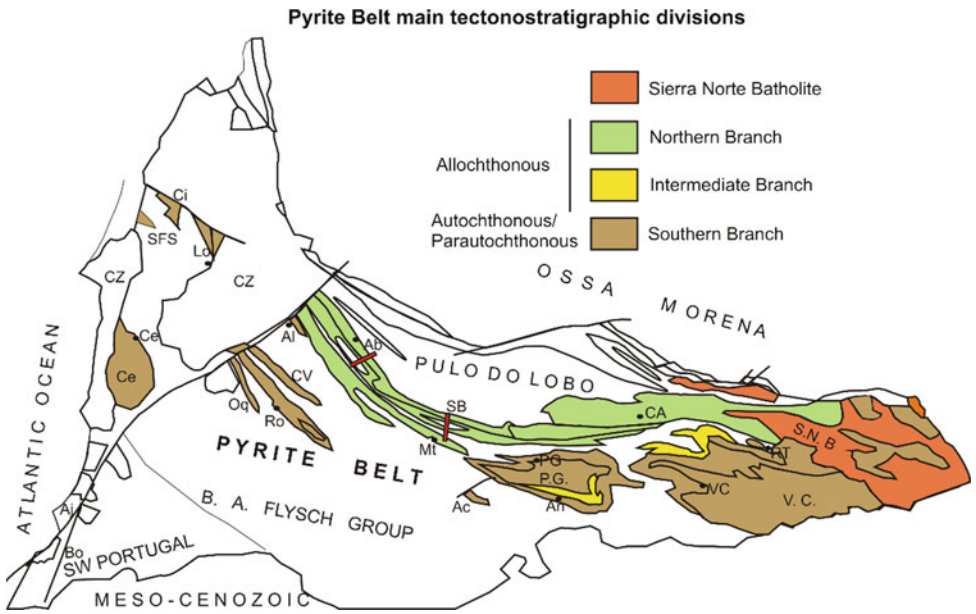

Fig. 6.7 Major tectono-stratigraphic divisions in the IPB

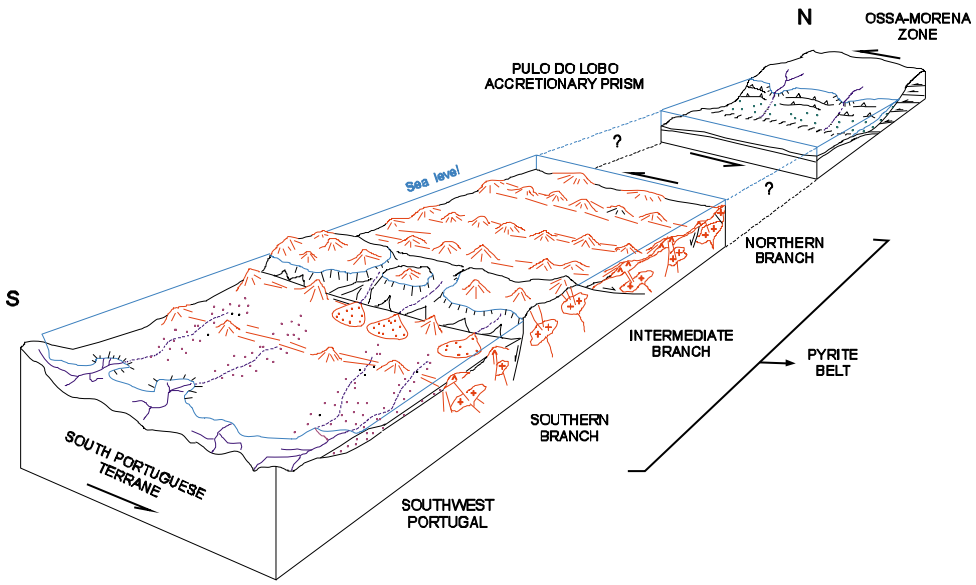

Fig. 6.8 Paleogeographic/paleotectonic sketch of the SPT showing the horst and graben structure inferred for the IPB in VSC times (adapted from Quesada 1996)

antiforms in Portugal. A singularity within this context is the Cercal antiform whose internal stratigraphy is somehow distinct (Pereira et al. 2008a, b). The VSC stratigraphic succession appears to be composed of three main tectono-stratigraphic sequences (TS1, TS2 and TS3; Fig. 6.9):

- TS0 in Fig. 6.9 corresponds to the upper part of the siliciclastic platform (PQG) that was subjected to intense tectonic extension.
- TS1, represented by the widespread bimodal volcanism that took place during the Upper Devonian-lower Carboniferous, which represent ca. 70% of all the volcanic

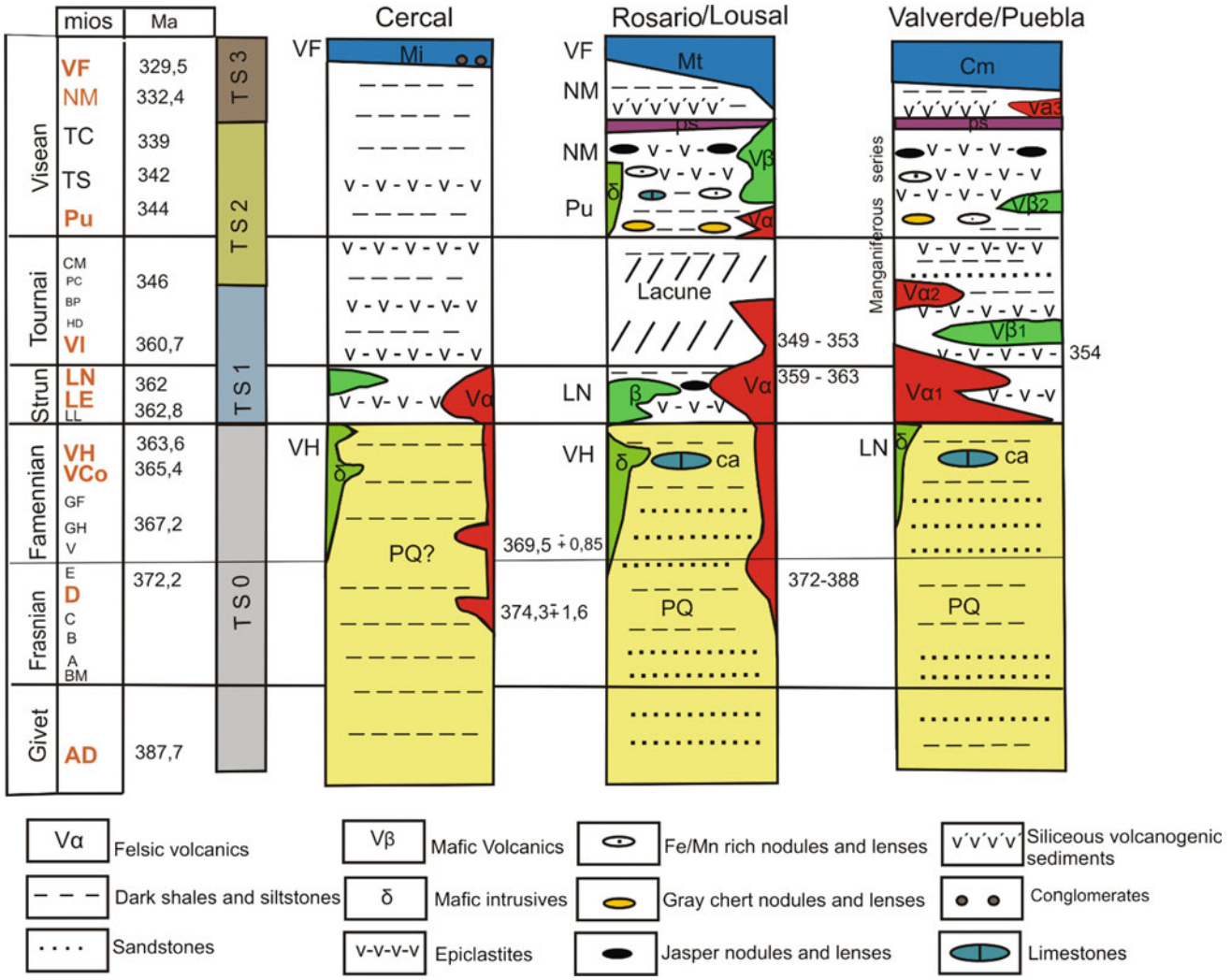

Fig. 6.9 Stratigraphic units in the IPB Southern Branch: PQ-Phyllite-Quartzite Group; ca-limestones; Vβ-mafic volcanic rocks; δ-mafic intrusives; Vα-felsic volcanic rocks; ps-purple shales; Cm-Culm flysch; Mt-Mértola Formation (∼Culm flysch in Spain); Mi-Mira Formation. Major tectono-stratigraphic sequences: T0, TS1, TS2 and TS3

activity in the entire IPB. Successive volcanic episodes are commonly bracketed by black shales.

- TS2, a succession composed of thin-bedded shales and siltstones in the western areas that change to shales and shallow water sandstones in the eastern areas, particularly in the northern limb of the Puebla and Valverde antiforms. Particular features of this sequence consist the occurrence of nodules rich in Fe/Mn oxides, jaspers and a basin scale marker bed the so called "pizarras moradas". In general terms, this sequence known in the literature as "*Série Manganesífera*".
- TS3, this megasequence is composed of volcanogenic sediments whose thickness changes from a few hundred to some tens of meters. The volcanogenic sediments which are usually associated to a late volcanic episode, grade upward and laterally to thin-bedded dark shales and greywackes that mark the beginning of the flysch sedimentation.

Owing to the extreme thickness and facies changes of the volcanic rocks it is not easy to describe a representative sections. Synthetic ideal columns, integrating data from

various sections across the antiforms are represented in Fig. 6.9. Details of each of these sequences are given below.

First Tectono-Stratigraphic Sequence (TS1)

In Spain the TS1 is well established and consists on:

- *Initial felsic volcanism (V1).* This is mainly rhyolitic/rhyodacitic in composition and is dominated by various types of tuffs and less abundant lavas. Thickness varies between ca. 200 m to zero. In places it rests directly on PQG rocks although in most localities it is preceded by a variably thick package of sediments (mainly black shales) and tuffites (first sedimentary sequence), which also exists laterally and on top of the volcanic rocks. The age of this volcanic event is mostly constrained by the Strunian palynomorphs present in the basal black shales and a single U–Pb zircon age of ca. 354 Ma from a tuff in the hanging wall of the Las Cruces ore deposit (Barrie et al. 2002). Significantly, the vast majority of VHMS ore deposits in this branch occur within this sequence associated to either volcanic rocks (Herrerías, Torerera deposits) or (most commonly) black shales (Tharsis, Sotiel-Migollas, Masa Valverde and Aznalcóllar deposits).
- *First mafic volcanism*. Although meter scale mafic sills occur throughout the VSC succession, decameter to hectometer thick piles of basaltic rocks postdate the first felsic volcanic event in the Southern Branch, i.e. the reverse order compared to the Northern and Intermediate branches (see below). These consist of vesicular, massive and locally pillowed lava flows and minor breccia and pyroclastic rocks, interbedded with dark gray shales. Intrusive dolerite sills are also present.
- *Second sedimentary sequence*. This is probably the most continuous and characteristic part of the VSC succession in the Southern Branch in Spain. It consists of predominant black and dark gray shales with abundant thin layers and nodules of iron and manganese, in which there are centimeter to decimeter (rarely meter) thick intercalations of (in order of abundance): fine-grained volcanic sediments, mature hummocky cross-bedded quartzites and quartzwackes, black to gray cherts and very rare crinoid-bearing carbonates. Thickness varies between 20 and 200 m. Conodonts found in the carbonates were attributed a early Visean age (Boogaard and Schermerhorn 1975).
- *Second felsic volcanism (V2).* This event is much more discontinuous than V1, with maximal representation in parts of the northern limbs of the Puebla de Guzmán and Valverde antiforms where it may reach up to 100 m in thickness, but commonly wedging out very rapidly. There it consists of various kinds of felsic volcanics, breccia, agglomerate and rare lava of rhyolite to dacite composition interbedded with shales and volcanic sediments. Pinkish colors are common.

In Portugal, the TS1 is best known in the antiforms hosting massive sulphide ores i.e. the Rosario, Lousal-Caveira and Aljustrel antiforms (Fig. 6.1). In Aljustrel the TS1 is incomplete since the boundary with the PQG shales and sandstones is not exposed and is not further commented.

The Rosario antiform, which hosts in its SE closure the Neves-Corvo mine, the most important IPB deposit considering mineralization volume and metal content (Barriga et al. 1997; Carvalho et al. 1999; Relvas et al. 2006a, b) is a complex tectonic structure deepening to SE, composed of several stacked thrust sheets intersected in several exploration drill holes and defined by seismic reflectors (Inverno et al. 2015; Carvalho et al. 2016). In spite of this complexity it is possible to recognize the stratigraphic succession due to the amount of data provided by dozens of drill holes and age determinations (palynology and geochronology). The TS1 is divided into two main sequences, separated by a stratigraphic lacune (Oliveira et al. 2004, 2013; Solá et al. 2015; Fig. 6.9):

- The lower VSC sequence overlies the PQF shales and quartzites and crinoidal limestones lenses at the upper part, which occupies the core of the antiform, followed upward by several episodes of felsic volcanic rocks (mostly rhyolites and less rhyodacites) which as a whole show variable thicknesses (500 m to zero). The felsic volcanic facies consist in two main types (Rosa et al. 2008, 2016): pumice rich facies, linked to submarine explosive volcanism, and coherent facies associated to domes and lava flows, also submarine. The felsic episodes are bracketed by black shales of the Neves Formation that yielded late Strunian (Upper Devonian) miospores of the LN and VH biozones (Pereira et al. 2008a, b). Mafic volcanic rocks, mostly spilites, microdiorites and dolerite sills also occur locally at the upper part of the PQG sequence. The limestone lenses provided conodonts of early Famennian age at Monte Forno da Cal (Boogaard and Schermerhorn 1981). U–Pb absolute ages in zircon of the felsic volcanic rocks show three magmatic episodes, respectively 372–388, 359–363 and 349–353 Ma, suggesting that the magmatic activity and the associated heat flow remained for at least 40 Ma (Oliveira et al. 2013; Solá et al. 2015; Albardeiro et al. 2017).

The Lousal-Caveira antiform (Fig. 6.1) is tectonically composed of several stacked thrust sheets which appear associated to two tectonically juxtaposed distinct crustal blocks. The western block incorporates the classical IPB

sequence here composed of PQF-type phyllites and quartzites, locally known as Corona Formation whose lower part yielded miospores of the AD Biozone of Givetian age, the oldest age so far obtained in the IPB (Pereira et al. 2010; Matos et al. 2014). The TS1 has many similarities with the succession described above for the Rosario antiform. The felsic volcanic rocks provided U–Pb ages of 361 Ma near the Caveira mine (Rosa et al. 2009).

The eastern block is composed of two tectonic sheets each one containing a sequence of PQF phyllites and quartzites overlain by mafic rocks, mostly basalts and dolerites (Azinheira de Barros geological map sheet, scale 1/50,000, LNEG, Oliveira et al. 2007). Each of these tectonic sheets has a thickness in excess of 500 m and the upper one is overlain by the late Visean turbidites of the Mértola Formation. This means that the VSC is solely represented by mafic rocks, the classical purple shales marker levels being absent.

Second Tectono-Stratigraphic Sequence (TS2)

In Spain the TS2 incorporates the *Third sedimentary sequence*, the so-called "*Pizarras vinosas*" which is overlain by the Radiolarian Purple Shale marker bed. The "*Pizarras vinosas*" sequence is another very characteristic unit in the Southern Branch of VSC. In terms of lithology it consists of a very monotonous alternation of shale and very fine-grained volcanic sediments with characteristic pinkish colors due to the presence of iron oxides. When fresh, the rocks are however dark gray to deep green. Thickness is very variable between 20 m and more than 80 m. Red to grey jaspers occur throughout but become thicker (locally up to 30 m in places) and more continuous right at the top of the succession. Jaspers contain high concentrations of manganese that have been mined out locally. Radiolarian fossils are frequently found in these shales. Joint surfaces commonly exhibit thin black seams of precipitated manganese minerals. In those places where the V2 volcanic rocks are not present, these "*pizarras vinosas*" rest directly over the second sedimentary sequence in an apparent transitional contact. In these cases, very common in the southern limbs of both the Puebla de Guzmán and Valverde antiforms, the two sedimentary sequences are mapped together under the informal name of "*manganesiferous series*" (Santos Bonaño and Contreras Vázquez 1983; Contreras and Santos 1982; Ramirez Copeiro del Villar and Navarro Vázquez 1982).

- *Second mafic volcanism*. This is only exposed in two relatively small areas: eastern closure of the Tharsis anticline and western closure of the Sotiel anticline, two second order structures of the major Puebla the Guzmán and Valverde anticlines, respectively. It consists of basaltic lava and pyroclastic rocks with a very peculiar green to purple color due to presence of abundant iron oxides, which locally reach nearly 100 m in thickness. Where present, this unit interfingers with the "*pizarras vinosas*" sequence.
- *Radiolarian purple shale*. As repeatedly said above, the radiolarian-bearing purple shale horizon forms the only continuous blanket that covered the entire IPB domain near the end of the VSC. In the Southern Branch it shows the same characteristics as those in the other branches, with thickness varying between a few meters up to 30 m. Manganese mineral seams along joints may derive from remobilization of the underlying "manganesiferous" formations.

In Portugal the TS2 coincides with the Upper VSC Sequence, defined in the Rosario Antiform. It is composed of thin-bedded dark shales and siltstones with phosphate nodules that laterally contain metric-thick volcanogenic sediments (Graça Formation). Upward, shales with nodules and metric lenses of gray cherts are overlain by shales with Fe/Mn nodules and decametric lenses of jasper, locally mined for Mn, which gradually change to pink siliceous shales (lithologically similar to the "*pizarras vinosas*" in Spain) forming the Grandaços Formation. The latter in turn is surmounted by purple and green shales, the so-called "Borra de Vinho" Formation equivalent to the Purple Shales unit in Spain. Within this upper sequence felsic volcanism is rare and mafic rocks are mostly represented by dolerite intrusions. The total thickness of the upper VSC is in excess of 300 m. Miospores of early late Visean (Pu Miospore Biozone) date the Graça Fm. and of late Visean (NM Miospore Biozone) the Grandaços Fm. (Oliveira et al. 2004, 2013, Pereira et al., 2008).

The TS2 sequence is also exposed, with minor lithological changes in the Lousal-Caveira, Grândola and São Francisco da Serra antiforms (Dias et al. 2016).

Third Tectono-Stratigraphic Sequence (TS3)

In Spain the TS3 corresponds to the *Third felsic volcanism (V3).* This is characterized as in most units of the other branches by an up to 60 m thick alternation of coarse to fine grained epiclastic layers and greenish shales. The epiclastic layers, of a predominant dacite composition, range between few mm and several decimeters in thickness and generally show fining upward grading; i.e. they were probably transported by turbidity currents but no obvious sequentiality appears to exist other than a progressive thinning and fining towards the top in the final meters.

In Portugal the TS3 volcanism maintain the same basic characteristics but the epiclastites appear to be more siliceous and lateral facies changes to more terrigenous sedimentation can be observed. It is known as the Aguia Fm. in

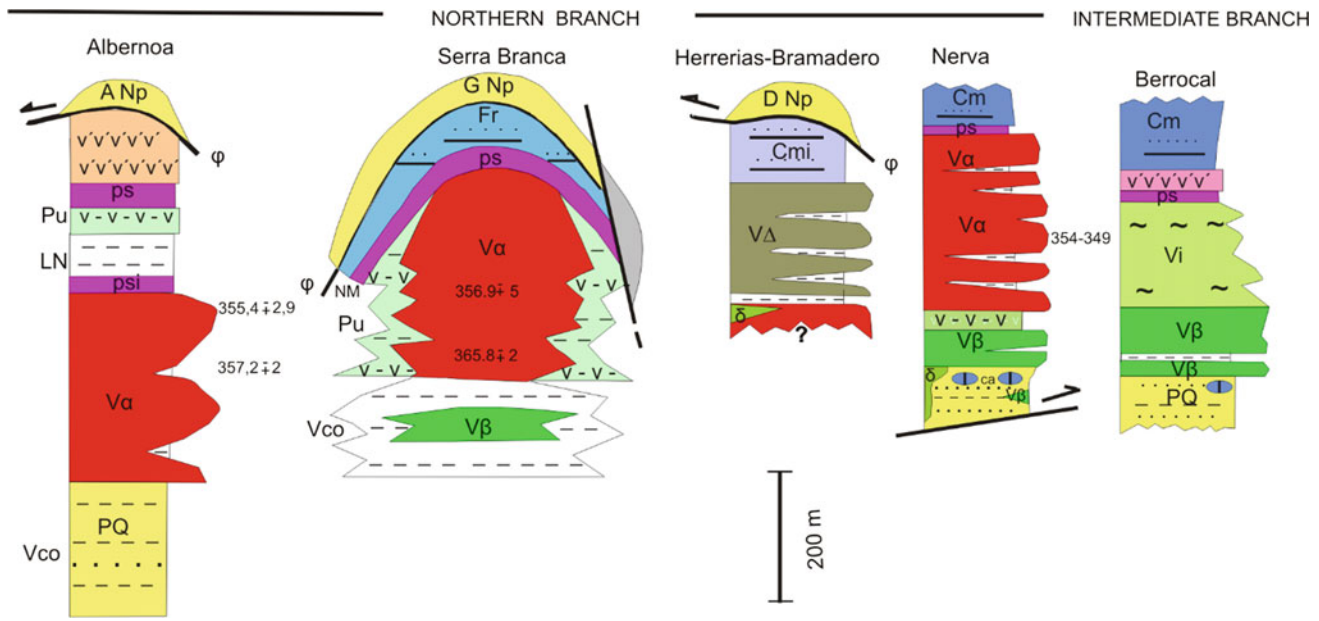

Fig. 6.10 Tectono-stratigraphic successions of selected nappes of the Northern Branch of the IPB. Symbols: Nappes: ANp-Albernoa nappe; GNp-Galé nappe; DNp-Duque nappe; Stratigraphic units: Cm-Culm flysch; Fr-Freixial Fm., turbidites; Cmi-Culm-type turbidites; ps-purple shales; Vα-felsic volcanic rocks; Vβ-mafic volcanics; δ-mafic intrusives; VΔ-intermediate volcanics; Vi-felsic ignimbrites; PQ-Phyllite-Quartzite Group; ca-limestones. Lithologies- as in Fig. 6.9

the Pomarão anticline and Godinho Formation defined in the Rosario antiform where it has provided miospores of late Visean age (Oliveira et al. 2013). This unit is conformably overlain by thin-bedded black shales and fine greywackes of late Visean age that mark the beginning of the Mértola Formation flysch sedimentation.

The Cercal antiform, the westernmost structure of the IPB is singular in several respects. The oldest outcropping rocks are rhyolites and rhyodacites, up to 200 m in thickness, dated at ca. 370 and 374 Ma, that occupy the core of the antiform (Rosa et al. 2009). Several boreholes drilled at the center of the antiform crossed a succession of thin bedded dark shales and siltstones with intercalations of mafic sills below the felsic rocks. The shales yielded miospores of late Famennian age, VH Biozone (Pereira et al. 2008a, b). This part of the succession is comparable with the TS1 of the other antiforms. The remaining part of the VSC is composed of a monotonous sequence of dark shales and minor volcanic sediments (São Luís Formation) followed by black shales with disseminated pyrite (Abertas Formation), with a total thickness of ca. 400 m that gradually passes to the turbidites of the Mira Formation (Carvalho 1976; Oliveira et al. 1986; Pereira et al. 2008a, b). The tradicional pink shales, purple shales and siliceous epiclastites marker levels are absent. The VF Biozone miospores (latest Visean) and the goniatites *Cravenoceras sp.* (early Serpukhovian) were found at the base of the Mira Formation turbidites (Oliveira et al. 1979; Pereira et al. 2008a, b).

VSC Stratigraphic Sequence of the Northern Branch

The largely allochthonous Northern branch of the IPB includes a series of refolded and thin (generally <2 km thick) rootless nappe-sheets overlying parautochthonous sequences incorporating mostly VSC lithologies. Together they extend in a roughly E-W to NW-SE direction for ca. 150 km and receive local names, from structural top to bottom: Galé-Cela and Mértola nappes in Portugal (Silva et al. 1990) Cerro de Andévalo, Paymogo and Herrerías-Bramadero nappes in the so-called Western Block in Spain, Rio Tinto nappe in the Spanish Central Block and Vicaría nappe in the Spanish Eastern Block (Quesada 1996, 1998). Unfortunately, the correlation between Portuguese and Spanish nappes is yet to be done. A comparison between tectono-stratigraphic successions of selected nappes (Fig. 6.10) is a first step towards their correlation.

Each of these regional scale structural units consists of one or several thrust sheets with contrasting internal stratigraphies, probably representing the inversion of smaller scale horst and graben divisions or sub-basins within this part of the IPB in VSC times. In the Spanish part of the IPB two rather different VSC successions are to be distinguished. The most widespread is exposed in the Cerro de Andévalo and Rio Tinto nappes (Quesada 1996, 1998), being most completely exposed within the so-called Nerva thrust sheet of the latter. The succession there, which is taken as representative of this type in the IPB Northern Branch, consists of (from bottom to top; Fig. 6.10):

(1) In apparent conformity with the underlying PQG rocks, the VSC succession starts with a deca- to hectometer thick package of mafic volcanic rocks, in which pillow lavas are seen locally. Several flows and/or sills are indicated by decimetric to metric-thick black shale interbeds whose contacts with the mafic volcanics are frequently peperitic, thus indicating eruption/intrusion into wet unconsolidated sediments (Boulter 1993a, b). Hyaloclastite breccias and rare pyroclastic tuffs occur in places.

(2) A meter to decameter package of dark colored shale with rare felsic epiclastic sandstone interbeds.

(3) Several hundred meters thick succession of felsic volcanic rocks, which makes most of the VSC stratigraphy in this unit. The most common lithologies are: flow-banded rhyolites/rhyodacites, rhyolite breccias and less abundant rhyolitic tuffs. Numerous decimeter to meter scale sedimentary and epiclastic interbeds separate individual flows and sills and, as within the mafic rocks, peperitic contacts are common (Boulter 1993a, b; Donaire et al. 1998). In general, volcanic lithologies largely outpace sedimentary rocks in all these units, although relative proportions vary from place to place. Locally, meter-thick basaltic sills intrude into the mostly felsic succession and, more rarely, some lava flows show evidence of mingling between mafic and felsic magmas, having there intermediate (dacite to andesite) overall compositions. These two features attest for coexistence and interaction of mafic and felsic magmas at this stage, both at the emplacement level (sills) and, deeper, in the underlying magma chambers (hybrid rocks). The sedimentary interbeds mostly consist of black to dark-grey shale in which centimeter to decimeter-thick graded layers of felsic epiclastic sandstones frequently occur. Grading and the lack of traction sedimentary structures in the epiclastites suggest prevalence of turbidite processes during their deposition in relatively deep (below storm wave base) or protected environments. Decimeter to meter thick red or black jasper horizons occur at various heights in the felsic pile, generally extending for some meters to some hectometers along strike. The most important jasper concentration occurs however right at the top of the succession, immediately below the overlying purple shale marker bed (see below) and frequently hosts Fe–Mn mineralizations, many of which have been historically mined. Scarce radiometric dating of various parts of this felsic sequence at several localities in Spain has provided ages ranging ca. 354–349 Ma (Barrie et al. 2002; Dunning et al. 2002) but much more geochronological work is still required.

(4) A meter to decameter thick package of radiolarian purple shale, the only VSC sedimentary unit that can be traced across the entire IPB.

(5) The top of the VSC succession (as in most of the IPB units) consists of an alternation of felsic to intermediate (dacitic and rarely andesitic) graded epiclastic sandstones and shales. The latter show purple colour near the base, suggesting a transition to the underlying purple shale, and progressively vary to greyish or greenish colors towards the top. This sequence is similar to the so-called Third Volcanism (V3) in the IPB Southern Branch (see above) and in the Rio Tinto nappe barely exceeds 25–30 m in thickness. Individual epiclastic sandstone layers vary between a few centimeters and several decimeters in thickness, whereas the intervening shales are generally thinner except towards the top where they progressively become thicker at the same time that the sandstones thin out, giving way to the basal, shale dominated sequence of the overlying *Culm* flysch. By far, the pre-purple shale horizon felsic volcanic succession and intervening sedimentary rocks referred to above host the largest concentration of VHMS ore deposits in the IPB, including the world-known Rio Tinto deposits with proven reserves in excess of 500 Mt, the largest found so far in the entire metallogenic province.

The only exception to the above representative succession is provided by VSC exposed within the so-called Herrerías-Bramadero nappe (Fig. 6.10), the structurally lowermost unit in the IPB Northern Branch in the Spanish Western Block (Quesada 1996, 1998). This is a unique unit in which a hectometer thick (up to ca. 250 m) package of mostly intermediate hybrid rocks occurs above the purple shale marker horizon. This volcanic package occupies the same stratigraphic position that the predominantly epiclastic V3 succession in the Southern and Intermediate branches but, besides being much thicker here, it is almost exclusively composed of hybrid lavas of predominant dacite and andesite compositions although some rhyolites and basalts also occur locally. As this unit mainly occurs in tectonic windows or a largely dismembered klippe in the hanging wall of the Herrerías mine, its base is unknown. The only rocks outcropping beneath the purple shale horizon correspond to rhyolites similar to those found at the same stratigraphic position in the remaining North Branch units, suggesting that probably the only significant difference resides in the massive post-purple shale volcanic event recorded in this unit exclusively. Owing to petrographic and geochemical similarities, Quesada (1997, unpublished IGME open-file report) interpreted this late massive volcanic succession as the

source of the V3 epiclastic successions so widely spread across the remaining of the IPB during the final stages of the VSC. Significantly, no ore deposits occur associated to this late volcanic event.

In Portugal, the Galé-Cela nappe is well exposed in the Guadiana valley, 6 kms north of Mértola. It comprises a parautochthonous VSC sequence and an allochthonous sheet-like package composed of sedimentary-dominated olistrostomes imbricated with VSC lithologies (Fig. 6.10). From bottom to top the parautochthonous sequence comprises (Oliveira et al. 2005; Rosa et al. 2006):

(a) Dark shales and interbedded mafic rocks, mostly basalts. The shales yielded miospores of late Famennian, VCo Biozone (Pereira et al. 2008a, b);
(b) A thick (400 m) pile of rhyodacitic lavas that show several interbedded episodes of rhyolitic pyroclasts with abundant fiamme. This volcanic sequence is disrupted by small cryptodomes of rhyolitic composition. Layers of volcanogenic sediments also occur between the lavas and the pyroclasts. U–Pb absolute ages in zircon recovered from the rhyolites gave 356.9 ± 5.0 and 365.8 ± 2.61 Ma (Rosa et al. 2009). This volcanic pile changes laterally to typical VSC dark shale and siliceous shale as shown by boreholes and detailed mapping. Miospores recovered from the dark shale indicate a early Visean age, Pu Miospore Biozone (Pereira et al. 2008a, b);
(c) Purple shale with variable thickness (5–20 m) resting directly on the volcanic pile. Detailed mapping indicates that to SW, in the absence of volcanic rocks, the purple shale overlies shales with interbedded Fe/Mn nodules, cherts and jaspers, pointing to stratigraphic equivalence to the Manganesiferorus Sequence of the South Branch;
(d) The Freixial Fm, ca. 150 m in thickness, which rests conformably on the purple shale. The unit consists of thin beds of greywacke, calcareous sandstone, volcanogenic sediments and shale. Miospores recovered from the shale yielded a late Visean age, NM biozone (Pereira et al. 2008a, b). The stratigraphic position of the Freixial Fm. is similar to that of the volcanogenic sediments that overly the purple shale marker bed in the Southern Branch (V3 in Spain). At a regional scale, the unit shows facies changes to thin-bedded shales, siltstones and greywackes.

Overlying this succession there is a structurally complex suite of lithologies, mostly composed of PQF-type quartzites, quartzwackes and shales which are imbricated with VSC shales, siliceous shales, tuffites, jaspers and scattered lenses of limestones. The latter yielded conodonts of late Tournaisian-early Visean age (W. Eder in Oliveira 1983; Boogaard 1963) The lithological imbrication has been interpreted as a tectonic nappe associated to a first fold and thrust episode with dominant tectonic transport to SW. This took place during the late Visean, underlining the change in tectonic regime from extensional to compressive (Silva et al. 1990; Oliveira and Silva 1990). As described above (see siliciclastic platform) the occurrence of olistrostomes intercalated in the lithological succession is indicative that gravity sliding may have played an important role. As far as we are concerned olistrostomes were probably triggered during the extensional regime and not after the first compressive tectonic episode as suggested by Silva et al. (2013).

The Albernoa nappe is less well understood owing to the less detailed mapping and poor rock exposure. The interpretation of the nappe succession is derived from the study of three boreholes (Oliveira et al. 2005; Pereira et al. 2008a, b; Rosa et al. 2006, 2009; Fig. 6.10). The stratigraphic sequence is composed, from bottom to top by: (1) PQF type quartzites and shales from which early Famennian miospores were recovered; (2) rhyodacites reaching 300 m in thickness, dated at 355.4 ± 2.69 Ma and 357.2 ± 2.60 Ma (Rosa et al. 2009), which are capped by (3) jasper lenses and purple shales; (4) dark shales and tuffites that yielded miospores of late Famennian age, VH Biozone; (5) shales and interbdded tuffites with miospores of early Visean age, Pu Biozone; (6) purple shales overlain by volcanogenic sediments with miospores of late Visean age, NM Biozone, which grade to (7) thin-bedded shales and siltstones (probably belonging to the base of the Méertola Fm.). The lithological sequence described above defines a NW trending antiform that is surrounded by imbricated PQF type shales and quartzites and isolated outcrops of dolerites, which as a whole are interpreted as an allochthonous nappe.

VSC Stratigraphic Sequence of the Intermediate Branch

As outlined above, the existence of an intermediate syn-sedimentary domain at VSC times was interpreted by Quesada (1996, 1998) to account for the predominance of ignimbrite volcanic rocks in certain areas of the IPB in Spain. Ignimbrites indicate eruption under (or close to) subaerial conditions, different to the entirely marine conditions prevailing in both the Northern and Southern IPB branches. Particularly, in the case of the Berrocal nappe located in this author's Central Block (Quesada 1996, 1998), its structural situation beneath the largely allochthonous Northern Branch nappes and above the parautochthonous Valverde nappe of the Southern Branch, suggests that the unit hosting the ignimbrites might have represented an uplifted block relative to both fringing units, and therefore, an overall horst and graben structure was interpreted to have existed during formation of the VSC (Fig. 6.8). Ignimbrites

also form the felsic part of the VSC in the El Almendro nappe occurring in the Spanish Western Block (Quesada 1996, 1998). The structural situation is however much more complex there, as this nappe occurs structurally interleaved between two Southern Branch nappes in the south and eastern parts of the large Puebla de Guzmán antiform (Fig. 6.7). The El Almendro nappe is internally imbricated (duplex structure), largely dismembered and wedges out laterally towards both east and west. Correlation of El Almendro and Berrocal nappes has been proposed by Quesada (1996, 1998), who interpreted the top thrust of the El Almendro nappe to be out-of-sequence but existence of another emerged horst within the Southern Branch cannot be ruled out.

Ignimbrites apparently are not exposed (or are extremely rare) on the Portuguese sector of the IPB. This can be related to either concealment beneath far-travelled out-of-sequence North Branch Variscan thrust sheets or relative floundering below sea level of the syn-sedimentary horst structure towards the west, preventing the formation of ignimbrites and making its identification much more difficult.

The VSC stratigraphic successions in this Intermediate Branch start by a variably thick package of mafic volcanic rocks. This is succeeded by a hectometer thick package of felsic ignimbrites, indicating eruption under subaerial conditions. The ignimbrite succession consists of many thinning and fining upward ash flow volcanics sequences, the basal parts of which are generally welded and locally show flow banding, rheomorphic folding and degassing vesicles. Presence of centimeter to decimeter size lithic clasts and fiamme at the basal part of some sequences suggests proximity to the eruption center. Individual ash flows range in thickness between few centimeters and several meters. Only the thicker flows include the welded basal part and despite the overall fining upward of the matrix, concentrations of large fiamme are frequently seen in apparently out-of-place position at intermediate heights of the welded part of some flows. Very commonly, a grain size jump is also detected at the boundary between the welded (gravel to coarse sand size in the matrix) and non-welded parts of the flows (medium sand to fine silt grain size). Compositions are predominantly rhyolitic but some dacitic ignimbrites also exist.

South of Berrocal village the ignimbrite sequence includes a several meters thick peculiar package of crystal-rich lithic tuffs with a characteristic purple color, which extends for several kilometers along strike. Several tuff events are indicated by superposed fining upward sequences, being the purple stain the peculiar common feature. The color is due to an abundance of iron oxides in the matrix of these rocks, interpreted as the result of percolation and precipitation through an overall unwelded succession of hydrothermal solutions similar to those giving rise to the abundant sulphide ore deposits in the other (submarine) IPB branches, here subjected to prevailing oxidizing conditions. Mafic sills intrude the ignimbrite succession at various places and locally develop thin contact metamorphic aureoles. The ignimbrites are overlain by the widespread radiolarian "purple shale" horizon, here only a few meters thick, whose presence attests for a return to overall submarine conditions. Finally, a few meters thick package of graded epiclastic sandstones, similar to those referred to above within the Northern Branch units and to the V3 in the Southern Branch units.

Only the felsic ignimbrite part of the VSC succession is preserved in El Almendro nappe (Quesada 1996, 1998). There, a complex duplex structure superposes three main thrust sheets, each of which consisting of a compositionally or texturally different ignimbrite sequence. The topmost thrust sheet exposes a very unique ignimbrite succession, made of several fully welded ash flows showing evidence of a hybrid nature. Both rhyolite and basaltic enclaves coexist in a vesicular amphibole-bearing matrix of dacite to andesite composition in which hybrid enclaves are also abundant. This rock suggests ongoing mingling between basaltic and rhyolitic melts in the underlying magma chamber at the time of eruption. However, the most striking characteristic of this upper ignimbrite sequence is the presence of very abundant, centimeter to decimeter long angular lithic clasts of quartz. The nature, shape and internal structure of these quartz clasts suggest derivation from hydrothermal quartz veins, which may have existed near the magma chamber walls before the eruption of these ignimbrites. The striking thing is their abundance rather than their presence, actually just another type of lithic fragment.

Characteristics and Petrogenesis of Volcanic and Plutonic Rocks in the IPB

A. R. Solá, D. Rosa, L. Albardeiro, A. Díez-Montes, I. Morais, C. Inverno, J. X. Matos, C. Rosa

Magmatism in the IPB (IPB) is represented by volcanic rocks of the Volcano-Sedimentary Complex (VSC) and by subvolcanic-plutonic rocks of the SNB that intruded the eastern IPB sequence (Fig. 6.1). The IPB volcanic rocks age range from Famennian to late Visean.

Physical Volcanology

Regional reconstructions of the volcanic and sedimentary facies architecture of the VSC of the IPB have defined that most felsic volcanic centres correspond to "lava–cryptodome–pumice cone volcanoes" (Rosa et al. 2010). The characteristics of the volcanic and sedimentary facies of the VSC indicate that the volcanoes have formed in submarine setting at variable water depth, the only exception being the

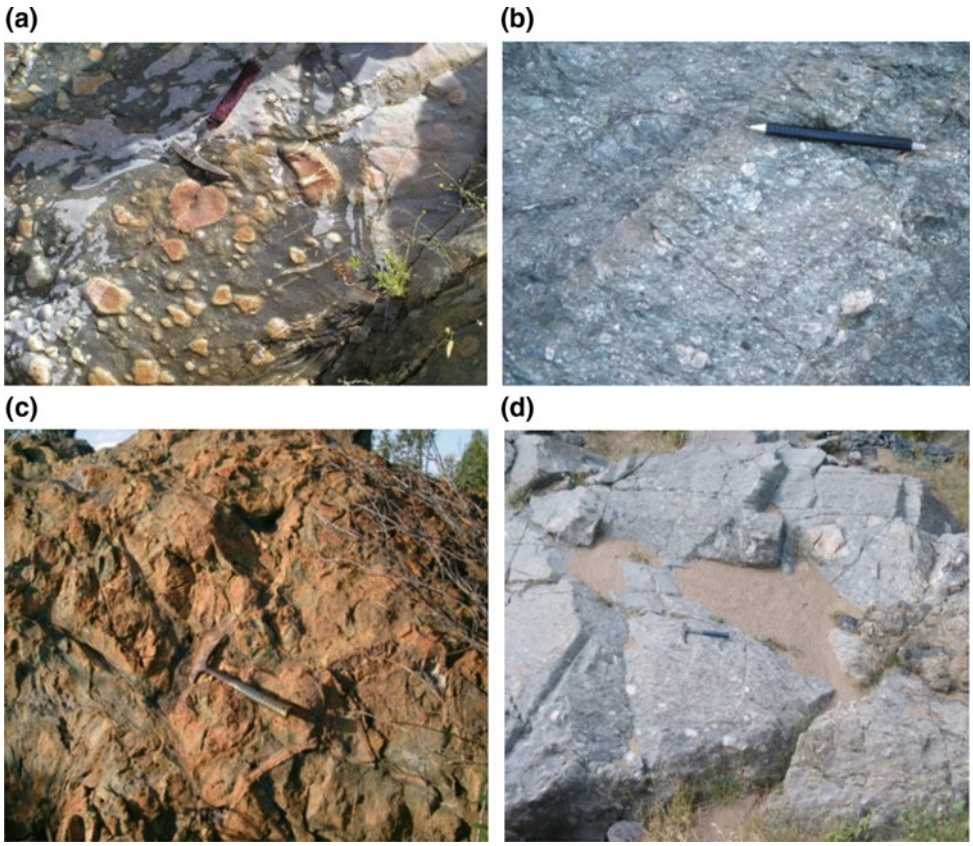

Fig. 6.11 IPB Volcanic Sedimentary Complex volcanic rocks: **a** monomictic rhyolitic breccia-in situ hyaloclastite (Terges creek, Albernoa); **b** Aljustrel mega crystals feldspar-quartz rhyolite unit (Água Industrial Dam, Aljustrel); **c** pillow lavas in basic volcanics (N-435 road, NW Rio Tinto); **d** pyroclastic unit with pumice (dark elongated elements) and dense volcanic clasts (white elements) (Guadiana River, Serra Branca). *Photo credits* C. Rosa (**a** and **d**); J. X. Matos (**b** and **c**)

volcanoes located in the Intermediate Branch. The volcanic centers are constructed by a variety of lithofacies that represent felsic lavas and domes, pyroclastic units, intrusions, and minor mafic lavas, locally showing pillows, and intrusions (Fig. 6.11; Rosa et al. 2010). The architecture of the felsic centers throughout the IPB comprises different combinations and proportions of these units (Rosa et al. 2010). The felsic lavas and domes can occur at several stratigraphic levels and are more voluminous than the pyroclastic units that were mostly sourced by them. The intrusions are minor and occur as shallow cryptodomes, partly extrusive cryptodomes and sills. The VSC also comprises well-defined beds of volcanogenic sandstones and breccias that overly or are interbedded in the volcanic centers, and extend laterally away from them. These units locally show graded bedding and load casts and may contain fossils. Their bedded nature indicate that they were deposited from water-supported gravity currents and compositionally are consistent as having been sourced from the clastic volcanic components of the lava, domes and pyroclastic units (Rosa et al. 2010).

Geochemical Composition

The volcanism within the VSC is mainly bimodal, with a predominance of felsic (dacitic to rhyolitic volcanics) over basic rocks (basalts and dolerites) at current exposure levels. Although subordinate on a regional scale, intermediate lavas (andesitic) also occur (Munhá 1983a, b; Mitjavila et al. 1997; Carvalho et al. 1999). However, it is important to mention that both chemical and mineralogical compositions in the IPB are strongly influenced by regional metamorphism and hydrothermal alteration (Munha and Kerrich 1980) as well as by secondary alteration stages related to massive sulphide mineralization, such as chloritization, sericitization and/or silicification (e.g. Neves-Corvo area, Relvas et al. 2006a, b). Rocks were subsequently regionally metamorphosed to the sub-greenschist facies. Thus, available geochemical data indicate significant redistribution of several major and trace elements during alteration processes, with implications for discussion of magmatic affinities and tectonic setting.

The bimodal nature of the IPB volcanism has been disputed by Carvalho et al. (1999) and Onézime et al. (2003), who considered that significant amounts of intermediate rock are present. This fact is significant for the geotectonic classification of the volcanism, once arc settings are typically dominated by intermediate rocks (andesites), whereas volcanism generated in extensional settings is generally bimodal. However, according to Rosa et al. (2004) the majority of intermediate compositions (andesites) are apparent, reflecting silica and alkali mobility along fracture networks and within the matrices of hyaloclastic breccias. This implies

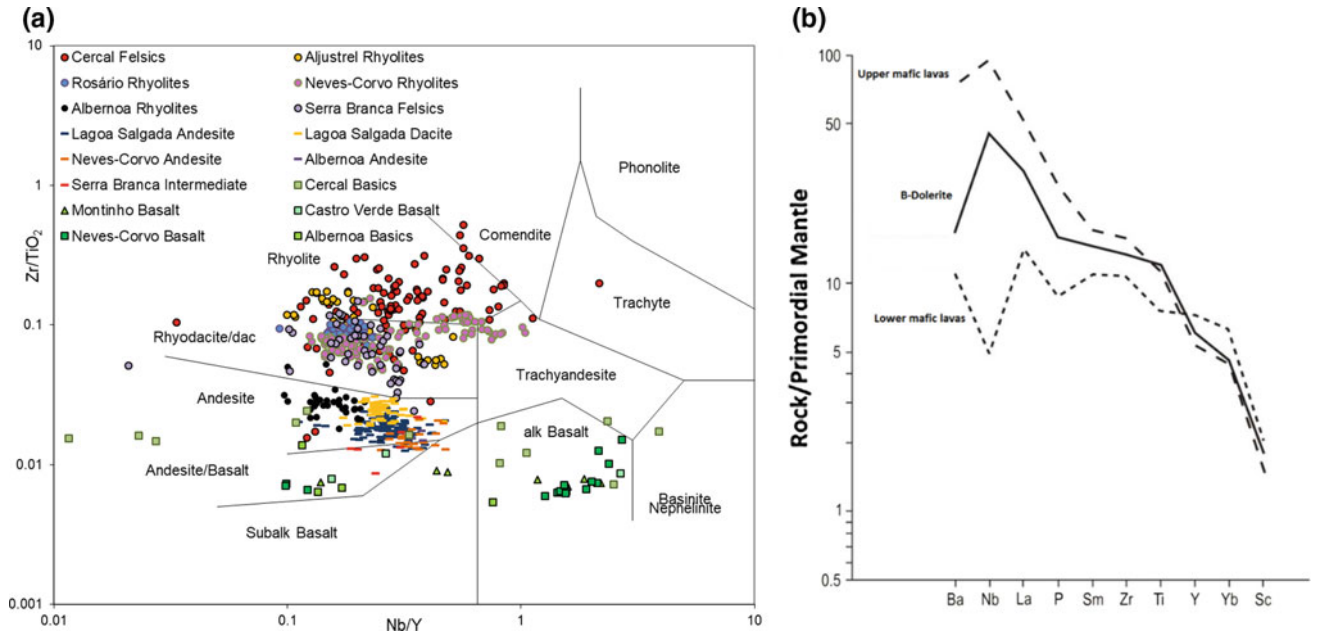

Fig. 6.12 **a** Zr/TiO_2 versus Nb/Y plot (Winchester and Floyd 1977) for the volcanic rocks from several sites along the Portuguese IPB including drill core and surface volcanic samples from the following areas: (i) Cercal area (Elf Aquitaine 1985); (ii) Lagoa Salgada (de Oliveira et al. 2011; Barrett 2013); (iii) Aljustrel (Barrett 2008); (iv) Montinho (Barrett 2010); (v) Rosário (Barrett nd); (vi) Neves-Corvo (Barrett 2008); (vii) Castro Verde (Barrett nd); (viii) Albernoa (Rosa et al. 2009); (ix) Serra Branca (Rosa et al. 2009; Albardeiro et al. 2018). **b** Trace elements abundances in IPB mafic rocks normalized to primordial mantle abundances (Sun and Nesbitt 1977; Wood et al. 1979) showing the compositional contrast between lower mafic lavas with tholeiitic affinities, and upper mafic lavas and intrusive equivalents (B-dolerites) with alkaline affinity (after Munhá 1983a, b)

dispersal of felsic or basic compositions when projected on the classification diagrams, thence a traditional bimodal nature of volcanism is favoured here. Consequently, the geochemistry results appear to confirm the petrographic classification. Reported problems regarding the application of geochemical and tectonic classification diagrams, interpreted as associated with anomalously low HFSE concentrations caused by low temperature crustal fusion, were also identified in some areas of the IPB (e.g., Albernoa and Serra Branca; Rosa et al. 2004, 2006).

A dataset compilation of available compositions of the VSC volcanic rocks is plotted in Fig. 6.12a (Albardeiro et al. 2018). The Zr/TiO_2 versus Nb/Y diagram indicates that most felsic rocks plot in the fields and along the boundary of the rhyolites and rhyodacites, with the exception of the Albernoa rhyolites (Fig. 6.12a) which fall in the andesite field, though Rosa et al. (2004) claimed as erroneous the classification as andesites due to anomalously high Ti and low Zr contents in these rocks, caused by low temperature crustal fusion. Apparently, with the exception of Aljustrel rhyolites, all sample sites are geochemically homogeneous. Highest Zr and Nb rich rocks (with lower TiO_2 and Y) are found in Cercal; intermediate values are found at Aljustrel, Rosário and Neves-Corvo rhyolites whereas lower ratios are found in the Serra Branca and Albernoa rhyolites and felsic rocks (Albardeiro et al. 2018).

Intermediate rocks fall almost exclusively within the andesite field. Some discrimination can be supported from Lagoa Salgada dacites to andesites, to Neves-Corvo andesite and to Serra Branca intermediate rocks. In the case of the intermediate rocks this trend is sustained by a decreasing Zr/TiO_2 ratio, due to either an increase in Ti content or an increase in Zr.

Regarding the basic rocks, a clear dispersion is observed. It appears though that an andesite to subalkali basalt group and an alkali basalt one can be identified. Within them, an increase in TiO_2/decrease in Zr seems to define a rough trend from Cercal to Montinho and to Neves-Corvo and, with less probability, to Albernoa basic rocks.

Based on geochemical characteristics of rocks and minerals, two main types of basic rocks are distinguished (Fig. 6.12b): (1) tholeiitic lavas (transitional to arc tholeiites), which crop out across the whole IPB, and (2) alkaline lavas and dolerites which are similar to recent within-plate basalts, more restricted to the western and southern regions of the IPB. According to Munhá (1983a, b) alkaline basalts are restricted to the upper part of the VSC volcanic sequence in the Portuguese sector. However, in the Spanish sector there is no evidence to justify the temporal evolution from tholeiitic to alkaline basalts (e.g. Mitjavila et al. 1997).

The tholeiitic lavas show a wide range of geochemical characteristics: those with medium La/Nb (1-2) and Y/Nb

(2-7) compositions are similar to recent continental tholeiites, whereas those with higher La/Nb (>2) and Y/Nb (>6) ratios have some affinities to arc-related basalts (Munhá 1983a, b; Thiéblemont et al. 1998). Alkaline affinity basalts show higher TiO_2 and P_2O_5, LREE and lower Y/Nb ratio (<1) (Fig. 6.12b).

The intermediate compositions (andesites) are spatially and temporally associated with tholeiitic basic lavas and fall into the field of normal calc-alkaline series (K_2O < 2.65 wt %; Munhá 1983a, b).

Overall felsic rocks range from dacite to high-Si rhyolites and belong to a calc-alkaline series. Rhyolites (and Sierra Norte Batholith leucogranites) show similar REE patterns displaying moderate LREE enrichment, with marked pronounced negative Eu anomalies, and relatively flat to slightly HREE enrichment (Munhá 1983a, b; Díez-Montes and Bellido-Mulas 2008). Dacites (and tonalites) are enriched in Al_2O_3, TiO_2, and P_2O_5 and display smaller negative Eu-anomalies relative to most rhyolites (e.g. Munhá 1983a, b).

The plutonic/subvolcanic (SNB) complex includes gabbro-diorite, quartzdiorite, tonalite, and granodiorite rocks (e.g. Schültz et al. 1987; de la Rosa 1992; Thiéblemont et al. 1998; Díez-Montes and Bellido-Mulas 2008). The geochemical similarities between the volcanic rocks of the VSC and the intermediate and felsic plutonic rocks of the SNB, together with the location and similar age, suggest that the VSC was approximately coeval and cogenetic with the plutonic rocks of the SNB (e.g. Schültz et al. 1987; Díez-Montes and Bellido-Mulas 2008). As a group, they define a low-Al TTG and high-HREE series (Arth et al. 1978), broadly equivalent to the FII dacite-rhyolite group of Lesher et al. (1986). The geochemical characteristics of felsic magmatism of SNB suggest that they were generated by fractionation partial melting of amphibolites at low pressures, involving plagioclase and pyroxene in the petrogenetic process without involvement of garnet, and with a significant contamination of crustal material (Díez-Montes and Bellido-Mulas 2008).

Petrogenesis

Although closely associated in space and time, the felsic and basic volcanic rocks had distinct sources and evolved independently; there is no evidence other than the sparse evidence for mixing and mingling described in previous sections that lithological transitions do occur; the volcanic centers are distinct, and the available geochemical and isotopic data refute any relationship by pure fractional crystallization between basalts, andesites and felsic rocks (e.g. Munhá 1983a, b; Mitjavila et al. 1997).

The basic rocks formed by partial melting of the asthenospheric mantle, whereas the felsic rocks derived from crustal anatexis during a major rifting event, possibly initiated by heat supplied by rising basic magmas (Munhá 1983a, b; Mitjavila et al. 1997; Thiéblemont et al. 1998; Carvalho et al. 1999) at low- to medium pressures and steep geothermal gradients. This makes the IPB different from other massive sulphide-bearing volcanic arc-related series and settings such as the Kuroko province (Leistel et al. 1998a, b).

Petrogenetic modeling of trace elements of the various basalts precludes an evolution solely by fractional crystallization and their diversity of compositions can be explained by a single mixing model between E- and N-MORB and assimilation of crustal material (Mitjavila et al. 1997). However, the mixing model between E- and N-MORB used to explain the origin of the most primitive basaltic rocks does not discriminate between the origin of both tholeiitic and alkaline affinities in the same magmatic context (Mitjavila et al. 1997). The existence of tholeiitic and alkaline affinities may be explained by different degrees of partial melting of a peridotitic mantle (Mitjavila et al. 1997), but according to Munhá (1983a, b) at least two different mantle sources are required to explain the compositional differences between the two major basaltic types.

Andesites were interpreted as due to contamination (mixing) between basaltic magmas and upper-crust material (Mitjavila et al. 1997), as supported by field and petrographic evidence.

Dacites and rhyolites exhibit enriched crustal signatures in their Nd and Sr isotopic systems, consistent with derivation from recycling of an older crust (Mitjavila et al. 1997) and the zircon inheritance provides direct evidence for older (Proterozoic to Ordovician) detrital components in their source rocks (Barrie et al. 2002; Rosa et al. 2001, 2009).

The diversity of chemical and Sr–Nd isotopic composition of dacites and rhyolites can mainly be explained either by differences in the composition of the source rocks or by different degrees of partial melting of upper-crust segments (e.g. Mitjavila et al. 1997). However, when plotted on the empirically derived tectonic discrimination diagrams of Pearce et al. (1984) most felsic rocks display volcanic arc signatures (VAG) instead of the extensional setting suggested by the geochemistry of mafic rocks and by the bimodal distribution of the volcanism. Since the HFSE used in these diagrams are immobile, this mismatch has been assigned to anomalously low HFSE contents, possibly caused by relatively low temperatures of crustal melting (Rosa et al. 2004, 2006). In addition, the speed of the partial melting process resulted in the production of felsic magmas that inherited the geochemical characteristics of their crustal protolith. This may explain the apparent contradiction between the calc-alkaline geochemical characteristics of the magmas and the inferred extensional (i.e. rift-related) tectonic setting.

Zircon Geochronology

Geochronology has proven the paleogeographic migration of volcanism (Barrie et al. 2002; Rosa et al. 2009). The age of

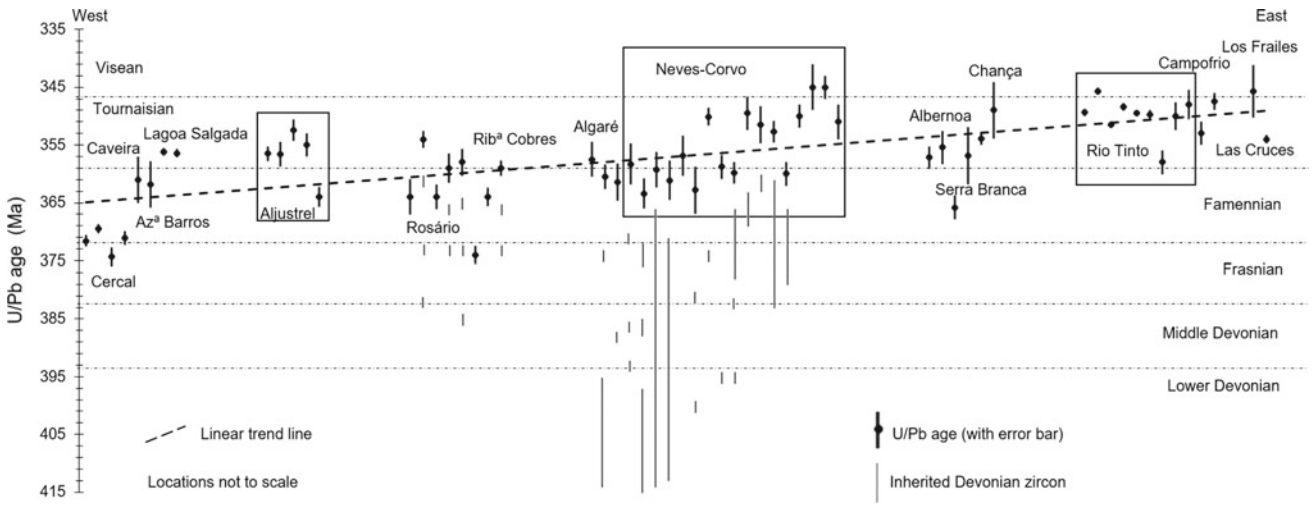

Fig. 6.13 Summary of zircon U–Pb magmatic and inherited ages of felsic volcanic rocks of IPB. Older (pre-Variscan) inherited ages are not represented. Based on: Nesbitt et al. (1999) (Los Frailes), Barrie et al. (2002) (Lagoa Salgada, Aljustrel, Campofrio, Las Cruces), Dunning et al. (2002) (Campofrio), Rosa et al. (2009) (Cercal, Caveira, Azinheira de Barros, Aljustrel, Albernoa, Serra Branca, Chança), Valenzuela et al. (2011) (Rio Tinto); Oliveira et al. (2013) (Rosário, Ribeira de Cobres); Solá et al. (2015) (Algaré, Neves-Corvo); Mello et al. (2017) (Rio Tinto)

the (felsic) volcanism has been reported as progressing from SW to NE (Rosa et al. 2009, Fig. 6.13). The oldest volcanism (ca. 371–374 Ma) is recorded at the Cercal antiform structure (western IPB region), while the Los Frailes felsic volcanic rocks, located in the eastern IPB region, have yielded an age of 345.7 ± 4.6 Ma, interpreted as representing the age of this VHMS deposit (Nesbitt et al. 1999). The compilation shown in Fig. 6.15 indicates duration of volcanism in the IPB for 24–35 Ma, and lasting for at least 14 Ma in a single location as documented in the Neves-Corvo VHMS deposit region (Solá et al. 2015; Albardeiro et al. 2017) and for at least 7 Ma at Aljustrel (Rosa et al. 2009). Zircon inheritance provides direct evidence for crustal derivation. The significant fraction of Devonian inherited zircon grains in Neves-Corvo and Rosário sectors provides direct evidence that the felsic volcanic rocks derived from the successive melting of pre-existing volcanic rocks and/or from juvenile immature sediments derived from them, probably included in PQF of Givetian to Strunian age (Pereira et al. 2008a, b; Matos et al. 2014) that lies immediately beneath the VSC. The link between the PQF. and related massive sulphide deposits have been suggested by Jorge et al. (2007a, b, c) based on Pb isotopic signatures, considering a leaching process of the siliciclastic basement by hydrothermal fluids. Moreover, the Hf protolith model ages of VSC and PQF are consistent with this hypothesis (Rosa et al. 2009). A compilation of geochronology and Hf isotope data of zircons from felsic volcanic rocks yields εHf values ranging between −14.4 and −0.2, and Hf protholith model ages ranging from 0.86 to 1.73 Ga (averaging 1.4 Ga) for source rocks involved in the genesis of felsic volcanics. This is compatible with a derivation from the melting of the PQF, which is immediately beneath the volcanic rocks and have the same distribution of inherited zircon U–Pb ages (Rosa et al. 2009).

Older, pre-Devonian zircon ages (Paleoproterozoic to Ordovician, not projected in Fig. 6.13) were also identified, reflecting a detrital component in the PQF. source rocks or an older basement beneath the PQF.

Relationship Between Volcanism and VHMS Genesis

The relationship between volcanism and VHMS genesis is still a matter of debate (Barriga et al. 1997; Carvalho et al. 1999). Geochemical and isotopic studies in local IPB sectors (e.g. Rosa et al. 2006, 2009; Valenzuela et al. 2011; Oliveira et al. 2013) give some insights into the nature of the felsic sources that host VHMS deposits, which could be tested as mineral exploration tools along the province.

Rosa et al. (2006) suggested that the existence of higher zircon and monazite saturation temperatures may be used as an exploration tool for VHMS deposits. This is because in this geological setting (attenuated continental lithosphere setting), hotter magmas tend to result from shallower melting and both factors favor the start and maintenance of convection cells that can generate VHMS deposits. For the Rosário–Neves-Corvo antiform (Oliveira et al. 2013) the magmatic heat flow should have been comparatively higher than in other sectors of the belt (e.g. Albernoa) where low temperatures of crustal fusion have been proposed as an explanation for unexpectedly low concentrations of high field strength elements in the felsic volcanic rocks (Rosa et al. 2004, 2006). The recycling of recently-formed igneous

rocks implies a sustained heat flow which is favourable for the development of giant VHMS deposits (>200 Mt of massive sulphides), such as those of Aljustrel and Neves-Corvo in Portugal or Rio Tinto, Tharsis, Aznalcóllar etc. in Spain. The occurrence of inherited Lower Devonian age zircons (~415 Ma) in felsic volcanic rocks in Neves-Corvo region, strongly suggests that at least locally, the magmatic activity was active for ~60 Ma (Fig. 6.13; Solá et al. 2015; Albardeiro et al. 2017). Such a long period of sustained heat flow would have promoted the long-lasting hydrothermal activity, favourable for the formation of giant VHMS deposits, formed by several ore lenses (7 in the case of Neves-Corvo and 6 in the case of Aljustrel). As mentioned by Rosa et al. (2009), the presence of recycled zircons in felsic volcanic rocks should therefore be considered a potential exploration criterion for VHMS deposits. Despite the temperature reached by the magmas (about 900 °C, calculated using the Ti-in-zircon thermometer, Codeço 2015) being high enough to dissolve all the available zircon (from the rock's zircon saturation temperature, 700–860 °C; Codeço 2015), the fact that the dissolution of zircon was incomplete can only be attributed to the kinetics of heat transfer to and from the magmas and would be possible only if melt production was rapid, from the beginning of melting (700 °C) to the thermal peak (900 °C). (e.g. Bea et al. 2007).

Isotopic and geochronological studies performed in the Rio Tinto-Nerva area by Valenzuela et al. (2011) show that younger, ~345 Ma felsic rocks, in the footwall of VHMS deposits exhibit lower εNd values relatively to the ~351 Ma hanging wall rocks (εNd variation from +0.3 to −2.68, respectively). The authors interpret that in the Rio Tinto-Nerva unit, crustal melting successively affected shallower, more evolved horizons in the crust and that low εNd values could be used as a proxy in mineral exploration studies.

It is also important to underline that the Neves-Corvo giant deposit is located within the alkaline "sub-province" (Thiéblemont et al. 1998), although whether this particular situation is responsible for the high potential of the deposit is not clear.

Tectonic Setting

Overall, the bimodal nature of the VSC, with continental tholeiites and the alkaline character of some lavas with only minor amounts of intermediate rocks points to a consensual extensional tectonic setting for the genesis of VSC (e.g. Munhá 1983a, b; Mitjavila et al. 1997; Thiéblemont et al. 1998; Rosa et al. 2004, 2006). Although basaltic alkaline magmas preserved their within-plate signature, the tholeiitic magmas display negative Nb anomalies that make them resemble VAB. However, these anomalies probably do not reflect a true subduction component, but rather result from assimilation of continental crust (Rosa et al. 2004). These basaltic magmas could have locally promoted crustal melting via underplating in the lower crust, yielding siliceous magmas. The fact that no arc related rocks were identified, with apparent arc signatures dismissed by the identification of crustal assimilation processes for the mafic rocks and low-temperature crustal melting for the felsic rocks, supports a model in which volcanism occurred in an attenuated continental lithosphere setting.

This is compatible with the model proposed by Silva et al. (1990) and Quesada (1991). In this model, the strike-slip tectonics within the continental crust of the South Portuguese Zone responsible for the opening of the sedimentary basin and associated volcanism was developed as a direct response to the oblique continental collision between the South Portuguese and the Ossa Morena zones. This transtensive tectonic regime would have favored the opening of pull-apart basins where bimodal volcanism, with the characteristics described above, would have occurred at a continental crust level due to localized extensional tectonics. Syn-volcanic tectonism caused increased geothermal gradients, and triggered the circulation and focused discharge of hydrothermal fluids which led to several syngenetic VHMS deposits. The IPB includes giant deposits such as Aljustrel and Neves-Corvo in Portugal and Rio Tinto and Tharsis in Spain (Fig. 6.1), which are related to long lasting focused submarine hydrothermal systems. These elevated rates of crustal melting could only have been caused by intrusion of mantle derived mafic magmas, most probably at the base of the crust. This scenario is consistent with a rifting regime in which crust and mantle were mechanically decoupled.

Geocronological data can also support the interpretation of the geotectonic evolution of the IPB. The compilation of magmatic zircon ages of felsic volcanic rocks associated with VHMS deposits (Rosa et al. 2009; Fig. 6.13) suggests that volcanism migrated within the basin perpendicularly to the suture, i.e. from southwest to the northeast (present day coordinates).

According to Rosa et al. (2009) this observation is not consistent with a model of central uplift and intense volcanic activity near what is now the Portuguese–Spanish border, with subsequent migration of the already formed volcanic edifices towards the basin margins, to the east and to the west, as suggested by Barrie et al. (2002). Instead, the inferred migration confirms the trend suggested by Carvalho (1976), based on the compilation of paleontological data obtained in the sediments enclosing the volcanic rocks. However, this trend should not be assigned as the result of northward-dipping subduction to the south of the IPB, as implied by Carvalho (1976), because of the widespread evidence linking the volcanism to extensional (i.e. rift-related) tectonic setting as described above.

The temporal evolution from tholeiitic to a more alkaline character of basaltic magmas (restricted to the upper part of

the VSC, Munhá 1983a, b) is the same as that of felsic volcanism at the Neves-Corvo region (Albardeiro et al. 2017 and references therein). The change to a more alkaline character of magmas towards the top of VSC sequence suggests that the distensive regime evolved to a more complex tectonic setting (transpressive regime; Silva et al. 1990). This also points to the possibility that towards the top of VSC (upper sequence) the rift had already ceased and was developing in a continental margin environment and consequently, with less favourable conditions for the VHMS formation (Albardeiro et al. 2017). This model could also explain the early Tournaisian age sedimentary hiatus recognized between the lower and upper sequences of the VSC in the Neves-Corvo region (Oliveira et al. 2004, 2013; Pereira et al. 2008a, b and references therein).

6.2.2 Outline Metallogeny of the IPB

J. Relvas, C. Quesada

6.2.2.1 Introduction

The IPB is one of the classical VHMS metallogenic provinces in the world, with more than eighty deposits, among which eight giant deposits, i.e. with resources in excess of 100 Mt, six world-class (30–100 Mt) and dozens of medium size and small deposits (Fig. 6.14). The Rio Tinto cluster alone originally hosted more than 500 Mt of massive sulphide and stockwork ores all together, whereas the seven orebodies already known in the Neves-Corvo camp (Neves, Corvo, Graça, Lombador, Zambujal, Monte Branco and Semblana orebodies) add more than 300 Mt of massive and stringer sulphides. The density and size of massive sulphide deposits in the IPB stand out among VHMS provinces worldwide (Large and Blundell 2000). More than 21 Mt of copper, 34 Mt of zinc, 12 Mt of lead and 0.8 Mt of gold are contained in about 2,500 Mt of massive and stringer sulphides distributed over 88 known deposits. These figures constitute the outstanding balance of 6–10 million years of highly productive ore-forming hydrothermal activity in this province, during the Upper Devonian-Lower Mississipian (Tornos 2006 and references therein). Notwithstanding, the exploration potential of the province is still very promising as indicated by the following facts: (i) many known deposits remain unexplored at depth; (ii) some were traditionally mined only for pyrite and their polymetallic content was commonly not recognized; and (iii) there is still potential for discovery through sophisticated structural analysis and exploration techniques of new blind deposits at depth, as suggested by discovery in the last 40 years of the blind Gavião, Lagoa Salgada, Neves-Corvo, Migollas, Los Frailes, Masa Valverde and Las Cruces deposits, and extensions to the old mines of Aguas Teñidas, Concepción, La Zarza and Tharsis.

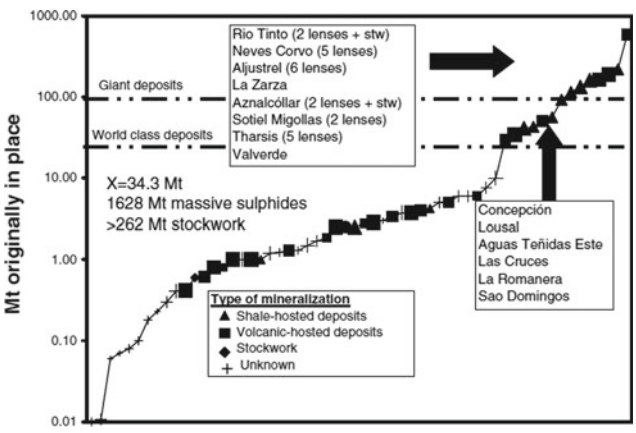

Fig. 6.14 Summary of size and characteristics of the most important deposits in the IPB (Adapted from Tornos et al. 2005)

6.2.2.2 VHMS Deposits in the IPB

Ore grades of the IPB deposits are generally between 0.4 and 1.85% Cu; 0.2–2.65% Pb; 0.5–3.9% Zn; 6.7–44.2 ppm Ag; 0.21–1.2 ppm Au (Leistel et al. 1998a and references therein). The average deposit in the IPB is strongly pyritic (30.1 Mt @ 0.85% Cu; 1.13% Zn; 0.53% Pb; 38.5 g/t Ag; 0.8 g/t Au; Tornos et al. 2000). Some deposits, however, possess moderate to high base metal contents (e.g. Neves-Corvo, Relvas et al. 2006a; Carvalho 2016; Las Cruces, Tornos et al. 2017). Sulphide mineralizations occur both in the volcanic-dominated Northern Branch (Aljustrel and São Domingos in Portugal; Rio Tinto, La Zarza, Aguas Teñidas, Concepción and Romanera in Spain) and the sediment-dominated Southern Branch (Lousal and Neves Corvo in Portugal; Tharsis, Sotiel-Migollas, Aznalcóllar-Los Frailes, Masa Valverde and Las Cruces in Spain), to mention only the giant and world-class deposits. This lithologic variation of the host sequences significantly constrained the styles of mineralization of the corresponding deposits (Tornos 2006). No sulphide deposits occur in the Intermediate Branch. Several deposits form an alignment in the Northern Branch and exhibit higher than average base metal and precious metal contents (Leistel et al. 1998a and references therein): Vuelta Falsa (1.27% Cu; 8.8% Zn; 20.7% Pb; 307 ppm Ag; 9.0 ppm Au), Nuestra Señora del Carmen (1.3% Cu; 10.3% Zn; 29.0% Pb; 153 ppm Ag; 1.0 ppm Au), Sierrecilla (1.5% Cu; 5.0% Zn; 12.60% Pb; 500 ppm Ag), San Telmo (1.2% Cu; 0.4% Zn; 12.60% Pb; 60 ppm Ag; 0.8 ppm Au), Lomero-Poyatos (0.5% Cu; 4.5% Zn; 7.5% Pb; 120 ppm Ag; 4.0 ppm Au). Special mention deserves the Neves-Corvo deposit, which is exceptionally rich in Cu and Sn. The extremely high Cu grades of its Cu and Cu–Sn ores place it among the richest copper deposits of the world. In addition, the Sn content and, specially, the Sn grade of the

Neves-Corvo tin ores are unique for a massive sulphide deposit compared with other stanniferous VHMS deposits such as the Geco, Kidd Creek and Lake Dufault deposits (£0.3% Sn, Superior Province, Canada), or the sediment-hosted Sullivan deposit (£2% Sn, British Columbia, Canada; Petersen 1986). No other IPB deposit contains such concentrations of tin, even though cassiterite and stannite are common accessory minerals in other deposits (Aye and Picot 1976).

Most IPB orebodies have lensoid morphology, but many of them were tectonically disrupted and/or stacked. The massive sulphide deposits are associated to variably large stockwork zones, both stringer type and disseminations. These, interpreted as feeder zones to the massive ores, were originally located at the footwall, but their original relationships and internal structures have been frequently modified due to the strong deformation during the Variscan orogeny (Tornos et al. 1998; Quesada 1998; Castroviejo et al. 2011). Also, the thickness of some stratiform massive sulphide deposits has been significantly altered due to tectonic stacking (Quesada 1998; Tornos et al. 1998; Castroviejo et al. 2011). Stratabound (e.g. Tharsis, Tornos et al. 1998; Neves-Corvo, Relvas et al. 2006a) to cone-shaped (e.g. Rio Tinto, García Palomero 1980; Aljustrel, Barriga and Fyfe 1988; Valverde, Toscano et al. 1993) ore-related hydrothermal alteration is classically zoned, with a chlorite (± pyrophillite ± donbasite) and/or quartz-rich core that is successively enveloped by sericite and paragonite-rich zones. The overall alteration/mineralization patterns in typical IPB deposits are characterized by low to moderate temperatures (70–270 °C), mildly acid conditions and low-sulphidation mineralogy (e.g., Relvas 1991; Barriga and Relvas 1993; Leistel et al. 1998a, b; Sánchez-España et al. 2000).

The overall ore mineralogy of both massive sulphides and stockwork ores is similar, consisting of dominant pyrite, sphalerite, galena and chalcopyrite, generally accompanied by accessory tetrahedrite-tennantite, cassiterite, pyrrhotite and numerous trace minerals including electrum (Strauss and Madel 1974; Aye and Picot 1976; Strauss et al. 1981; García Palomero 1980; Routhier et al. 1980; García de Miguel 1990; Marcoux et al. 1996; Gaspar 1991; Gaspar and Pinto 1991). In the Neves-Corvo deposit, cassiterite and other stanniferous minerals reach larger proportions in the Sn and Sn–Cu-rich ores (Pinto et al. 1994, 2013). In addition, Marcoux et al. (1996) found that the stockwork zone and the alteration zone at the base of some massive sulphides in the IPB contain bismuth and cobalt minerals not found in the overlying massive sulphides, being also enriched in gold. However, Marignac et al. (2003) interpreted that these might not be primary features but mainly due to remobilization during the Variscan deformation of the deposits.

VHMS deposits form in subaqueous environments by venting of hydrothermal fluids heated by magmatic activity, and commonly have stockwork/vein mineralization in their immediate footwall (Tornos et al. 2005 and references therein). This seafloor hydrothermal activity may give rise to sulphide mounds, stratiform exhalative and/or replacive bodies. In the IPB, a vast majority of the massive sulphides occur as stratiform bodies, thus largely representing exhalative types although the occurrence of replacive bodies (or parts of them) has been described as well (Tornos 2006; Relvas et al. 2006a). The frequent association of some IPB massive sulphides with fine-grained sediments (black shales) led Solomon and Quesada (2003) to consider them as brine-pool type; i.e. formed in anoxic bottom waters within bathymetric depressions (second order graben basins in our case). Besides physical isolation by flanking horsts, local anoxic conditions can also be self-induced by the exhalation and ponding of saline and reducing hydrothermal fluids (Sato 1972; Solomon et al. 2000; Tornos et al. 2005 and references therein). In the IPB, massive sulphide deposition occurred during the waning stages of felsic volcanic events within the variably thick VSC, characterized by a wide variety of felsic volcanic facies (see previous sections).

6.2.2.3 Fluids and Metals in the IPB Ore-Forming Systems

Most metals in typical IPB deposits are interpreted as being supplied by different extractions from similar crustal metal reservoirs. Lead isotope systematics of several IPB deposits show that, with the exception of Neves-Corvo, massive sulphides have an homogeneous lead isotopic composition ($^{206}Pb/^{204}Pb = 18.133 \pm 0.021$, $^{207}Pb/^{204}Pb = 15.622 \pm 0.015$, $^{208}Pb/^{204}Pb = 38.191 \pm 0.049$), which is similar to that of their felsic volcanic (VSC; Marcoux 1998; Relvas et al. 2001) and metasedimentary (PQG; Jorge et al. 2007a, b, c) host rocks. The fact that the deposits are isotopically homogeneous concerning the lead isotopes suggests that the hydrothermal fluids associated with transportation of lead to the surface must have equilibrated with the entire crustal segment involved before the deposition of the sulphides. Thus, the isotopic compositions of the deposits may represent the average composition of the South Portuguese crust during the latest Devonian-Mississipian period (Leistel et al. 1998a). Furthermore, the neodymium (Relvas et al. 2001), strontium (Tornos and Spiro 1999; Relvas et al. 2001; Tornos 2006) and osmium isotopes (Mathur et al. 1999; Munhá et al. 2005) indicate that the involvement of weakly radiogenic mantle sources was not relevant for the IPB metal budgets. Ore metals in these deposits are clearly of crustal derivation. The small thickness of the ore-hosting VSC (seldom exceeding 600 m; Relvas et al. 2006a; Tornos 2006) and the large predominance of sedimentary over

volcanic rocks in the overall footwall sequence, indicate that the most plausible source for the ore metals in the belt should have been the PQG metasediments and, eventually, their unknown basement. This conforms to the commonalities observed in metal ratios between these rocks and typical sulphide ores in the province (e.g., Tornos and Spiro 1999; Relvas et al. 2006a; Tornos 2006). Moreover, Jorge et al. (2007a, b, c) and Jorge (2010) have convincingly reported metal depletion accompanied by potassium metasomatism (and loss of CaO and Na_2O) in the PQG sediments.

Quartz fluid inclusions interpreted as being primary and representative of the IPB ore fluids are mostly aqueous and highly saline (3–12 eq. wt% NaCl; Almodóvar et al. 1998; Sánchez-España et al. 2003). Oxygen and hydrogen isotopic signatures of the IPB ore fluids are variably shifted relative to contemporary seawater values (e.g., Barriga and Kerrich 1984; Munhá et al. 1986; Sánchez-España et al. 2003; Relvas et al. 2006b). Notwithstanding, in most cases, data interpretations of these shifts point to isotope fractionation due to water-rock interaction, requiring no intervention of fluids other than deeply circulated seawater, connate waters equilibrated with the PQG siliciclastic sediments, low-grade dewatering fluids, or combinations among these (e.g., Munhá and Kerric 1981, 1986; Barriga and Fyfe 1998; Tornos and Spiro 1999; Relvas 2000; Tornos 2006; Relvas et al. 2006b). Some authors, like Sánchez-España et al. (2003) have proposed a major component of metals directly supplied by magmatic sources for the generality of the IPB deposits, based on the heavy oxygen isotope record and high salinities of many IPB ore fluids. However, the similar and regionally homogeneous radiogenic isotopic signatures and metal ratios showed by the ores and their footwall successions, combined with the shallow emplacement and, presumably, dry nature of the felsic magmatism that characterize the belt (Munhá 1983a, b; Mitjavila et al. 1997; Thiéblemont et al. 1998), suggest that magmatic metal contributions to the IPB ores should have been exceptional. Metal leaching of the footwall siliciclastic sequence was most likely the main mechanism of metal supply in typical IPB deposits.

The geotectonic setting of the IPB was a key factor in determining such highly prolific conditions for massive sulphide generation. Left-lateral strike-slip faulting induced by an oblique collision, created locally extensional conditions within a globally transpressive setting, allowing to the opening of an ensialic marine basin. Crustal thinning and magma underplating provided long-lasting high heat flow and high regional geothermal gradients (Silva et al. 1990; Quesada 1991, 1998; Quesada et al. 1991; Tornos et al. 2005). Tectonic extension favored the rise and shallow emplacement of super-heated, poorly fractionated, dominantly felsic magmas (Munhá 1983a, b; Mitjavila et al. 1997). High ambient heat promoted leaching reactions and, hence, the generation of metal-rich solutions in deep-seated hydrothermal aquifers. The felsic volcanism, the widespread emplacement of relatively shallow intrusive sills, and, especially, cooling of the hypabissal plutonic roots, energetically fed processes of compaction-induced dewatering from a thick, shale-dominated footwall succession, lateral migration and convection of hydrothermal fluids, metal-extraction reactions, fluid-rock geochemical and isotopic relative homogenization, and fault-controlled up flow and focused discharge of the resulting brines (Barriga 1990; Ribeiro et al. 1990; Marcoux 1998; Sáez et al. 1996, 1999; Relvas 2000; Tornos et al. 2002, 2005).

6.2.2.4 The Unique Geochemistry of the Neves Corvo Ores

The geochemistry of the Neves-Corvo ores contrasts with that of typical IPB deposits. The primary copper grades and the copper ratio of the Neves-Corvo ores (100 Cu/Cu + Zn = 50) significantly deviate from the IPB standards (15 < 100 Cu/Cu + Zn < 25). In addition, the total tin metal content (in excess of 0.3 Mt), the tin grades attained by the stringer and massive cassiterite ores (up to 60% SnO_2), coupled with the copper-tin metal association in the massive sulphide ores of Neves-Corvo are truly unique features among the IPB deposits known (Relvas et al. 2002). Nevertheless, the geochemical characteristics of the Neves Corvo footwall volcanic rocks (ranging from dacites to high-silica rhyolites) are similar to that of the remaining felsic volcanic centers of the IPB (Munhá et al. 1997; Rosa et al. 2008, 2010), and so it is the geochemical and lithological nature of the metasedimentary unit above which they lie (PQG; Jorge 2010).

Marcoux et al. (1996) documented accessory amounts of cassiterite in a number of IPB deposits, especially in the central and southernmost parts of the belt. In these deposits, cassiterite is practically devoid of HFSE, occurs as very small inclusions in sphalerite, their tin grades are very low (<300 ppm Sn; Leistel et al. 1994), and their tin metal contents is insignificant. Collectively, these features suggest a metal-leaching origin for the tin in these deposits. However, this is not the case in the Neves Corvo deposit. There, cassiterite is systematically rich in Fe, W, Ti and Sc, and has often high contents of Ta and Nb as well (Relvas 2000; Serranti et al. 2002; Huston et al. 2011), which mimics the trace element composition of granite-related cassiterite, and suggests a magmatic-affiliation for the Sn-bearing fluid in this deposit. In Neves Corvo, about two thirds of the tin occurs as relatively low grade (avg. 0.25% Sn) cassiterite dissemination associated with the high-temperature Cu-rich ores, indicating a genetic connection between tin and the Cu (±Au)-carrying ore fluids. Instead, the other third of the tin (*ca.* 100,000 tons of tin metal) occurs as an early generation of cassiterite precipitated as extremely high grade massive

cassiterite ores (± quartz ± pyrite) at or very near the seafloor, which was fed by independent tin stockworks related to syn-volcanic growth-faults (e.g. "tin corridor" of the Corvo orebody, Relvas et al. 2006a). The Neves Corvo massive and stringer cassiterite ores possess the highest tin grades ever reported in primary tin deposits on a worldwide basis. Blocks of massive cassiterite ore, weighting thousands of tons and averaging tin grades in excess of 25% Sn, were mined from the "tin corridor" of Corvo. Until 1997, more than 300,000 tons of massive and stringer cassiterite ores averaging 6, 72% Sn were exploited, mostly from that part of the deposit (Relvas et al. 2006a).

6.2.2.5 Tin Metallogenesis in Neves Corvo

The above conditions must have implied very special constraints imposed by the hydrothermal geochemistry of tin. The first constraint is that the uniquely high tin grades and the depositional characteristics of the massive cassiterite ores at Neves Corvo are inconsistent with a rock-buffered evolution for the tin-bearing fluid. As a matter of fact, it is widely acknowledged that greisenization is a very effective mechanism of tin extraction from a magmatic-hydrothermal tin-bearing fluid, but the maximum ore grade achieved by this process is relatively low because it is limited by the acid exchange capacity of the rock relative to the total acidity advected by the fluid (Heinrich 1990; Halter and William-Jones 1996). Heinrich (1990) calculated that, under rock-buffered chemical conditions, 99% of the initial Sn content of a fluid would precipitate at temperatures above 400 °C. He showed, however, that tin can easily be transported as stannous chloride complexes by a reduced and acidic magmatic-hydrothermal fluid to any low temperature depositional site, provided that fluid flow is rapid relative to the kinetics controlling chemical interaction with wall rocks (fluid-buffered transport), as it should happen in response to efficient fluid focusing mechanisms, like fault-related channelways. So, the fault-related depositional setting where massive and stringer cassiterite precipitated in the "tin corridor" of the Corvo orebody provided ideal conditions for extreme focusing of the fluid flow. Corroborating this, wall rock alteration related to the tin ore-forming episode is minimal and no cassiterite disseminations occur at depth (Relvas et al. 2006a).

Pb, Os and Nd isotopic signatures preserved in the stringer and massive cassiterite ores, imply external sources, which compare to those of granite-affiliated cassiterite (Relvas et al. 2001; Munhá et al. 2005; Jorge et al. 2007a, b, c). Distinct mixing arrays in the εNd (350 Ma) − Sm/Nd and $^{206}Pb/^{204}Pb$ – $^{207}Pb/^{204}Pb$ diagrams indicate that sulphide and tin ore deposition involved ore-forming solutions from different sources, which include significant incorporation of the typical VSC/PQG-derived hydrothermal components in the massive and stockwork sulphide ores, whereas highly radiogenic lead ($^{206}Pb/^{204}Pb$ = 18.50 to 35.03, $^{207}Pb/^{204}Pb$ = 15.65 to 16.78) and very low-εNd values (εNd (350 Ma) ≅ −9) preserved in tin ores require a predominant derivation from external sources, most probably magmatic (as metamorphic fluids are not suitable for tin metallogenesis; Lehmann 1991). Furthermore, pyrite separated from the Neves Corvo copper–tin ores have Re/Os ratios and osmium concentrations that are similar to those in pyrite from sulphide-rich stockwork ores, but their highly radiogenic initial $^{187}Os/^{188}O$ ratios (4.89–7.85) preclude derivation from the same sources as the remaining typical IPB sulphides.

As in Mt. Lyell (Markham 1968), Horne (Hannington et al. 1999a) and Kidd Creek (Hannington et al. 1999b), there is also a "bornite zone" at the Neves Corvo deposit (Pinto et al. 1994). In the bornite-rich ores, copper grade ascends to 39.6% Cu, auriferous mineralization occurs (together with Bi, As, Co, Cu, Sn, In, Hg, Te, Se and Sb), and the ore mineralogy locally warrants strong connection to high-sulphidation depositional conditions (bornite, tennantite, mawsonite, stannite, miharaite, carrolite, stromyerite, wittichinite) (Pinto et al. 1997, 2005). The bornite-rich ores expand the range of $^{206}Pb/^{204}Pb$ and $^{207}Pb/^{204}Pb$ values previously reported for the Neves Corvo ores, and Jorge et al. (2007a, b, c) have interpreted these data as reflecting extensive fluid mixing near the sites of ore deposition, the lead isotope compositions of the "bornite zone" being explained by the likely input of a magmatic fluid component.

In Neves Corvo, alteration mineralogy and geochemistry, coupled with oxygen and hydrogen isotopes clearly indicate that the Neves Corvo ore fluids were hotter and more acidic than typical IPB ore-forming fluids, but the overall low-sulphidation characteristics of the deposit are beyond debate. Unlike in typical porphyry-copper and epithermal systems, magmatic fluids associated to tin-rich granitic plutons are reduced and contain H_2S as the dominant vapor species. These circumstances imply that any magmatic fluid contribution to the Neves Corvo ore-forming system should not be expected to require assignment of its mineralogical record to predominant high-sulphidation characteristics.

A magmatic-hydrothermal model has been proposed for the genesis of this remarkable deposit (Relvas 2000; Relvas et al. 2001, 2006b; Huston et al. 2011; Carvalho 2016), but the formation of the Neves Corvo tin and copper mineralization still fuels a very interesting debate.

6.2.2.6 Other Types of Mineralization in the IPB

In addition to the sulphide deposits, more than 200 manganese deposits associated to jaspers occur in the IPB. They are widespread throughout the stratigraphy and generally very small. However, a large number of Mn deposits are hosted by the important jasper concentration at the top of the pre-purple shale marker horizon, including the Soloviejo deposit which is the largest known so far (Pinedo Vara 1963; Ramírez

Copeiro del Villar and Maroto 1995; Leistel et al. 1998b; Jorge et al. 2005). Manganese deposits are known in all three IPB branches and as the sulphides are thought to be exhalative (Leistel et al. 1998a). At the Aljustrel and Neves Corvo deposits, the jaspers were considered as pre-ore siliceous exhalites that acted as cap rocks, which would have prevented direct contact of the massive sulphides with unmodified seawater, therefore favoring sub-seafloor replacement mechanisms for sulphide deposition (Barriga and Fyfe 1988; Mirão et al. 1997). However, in other IPB massive sulphide deposits there are neither significant jasper caps, nor Mn deposits associated to the sulphide mineralization.

The IPB also hosts late-stage vein mineralizations of no economic significance in the PQG, in the VSC and even in the syn-orogenic *Culm* succession. Their mineralogy is clearly different from that of the syn-sedimentary massive sulphides and stockworks. There are veins comprising different mineral assemblages as follows (Sáez et al. 1987, 1988, 1989; Leistel et al. 1998a): quartz-galena-sphalerite (La Aurora), quartz-stibnite (La Esmeralda, Nerón), quartz-cassiterite-scheelite (Bajo Corumbel, La Palma del Condado), fluorite-galena-sphalerite-chalcopyrite (Los Angeles), and quartz-pyrite-chalcopyrite-grey copper (Lomochaparro, Valdeflores, Magalejo). The Pb isotopic composition of these mineralizations is more radiogenic than that of the massive sulphides, with $^{206}Pb/^{204}Pb > 18.27$ and $^{207}Pb/^{204}Pb < 15.613$ (Marcoux et al. 1992; Marcoux and Sáez 1994).

6.3 Carrapateira Group (Mixed Carbonate-Shale Platform)—Lower-Mid Carboniferous

Z. Pereira, J. T. Oliveira

The pre-orogenic stratigraphic sequence in the Southwest Portugal Domain comprises the TF at the base and the CG, the latter partially coeval to the VSC of the Pyrite Belt Domain. The TF., correlative to the PGG was already described above. The CG is well exposed in two small anticlines in the vicinity of Aljezur and Bordeira, of which the latter is best exposed in outcrops at the Atlantic coast (Fig. 6.15a). A comprehensive description of the stratigraphic sequence was presented in Oliveira et al. (1985), Ribeiro et al. (1987), Korn (1997), Pereira (1999), Pereira et al. (2007).

From base to top the CG stratigraphic sequence comprises the Bordalete, Murração and Quebradas Formations.

The Bordalete Fm. is best exposed at the Murração Beach (type section, Figs. 6.15 and 6.16). The unit is composed of a monotonous succession of dark grey to black shales, thin bedded siltstones and interbedded thin layers, lenses and nodules of calcisiltstones. At the upper levels, the black shales show pyritized burrows and the thin bedded siltstones and shales show large scale cross-stratification. Total thickness in the type section is ca. 200 m. The unit is dated of Tournaisian age, based on abundant fossil content

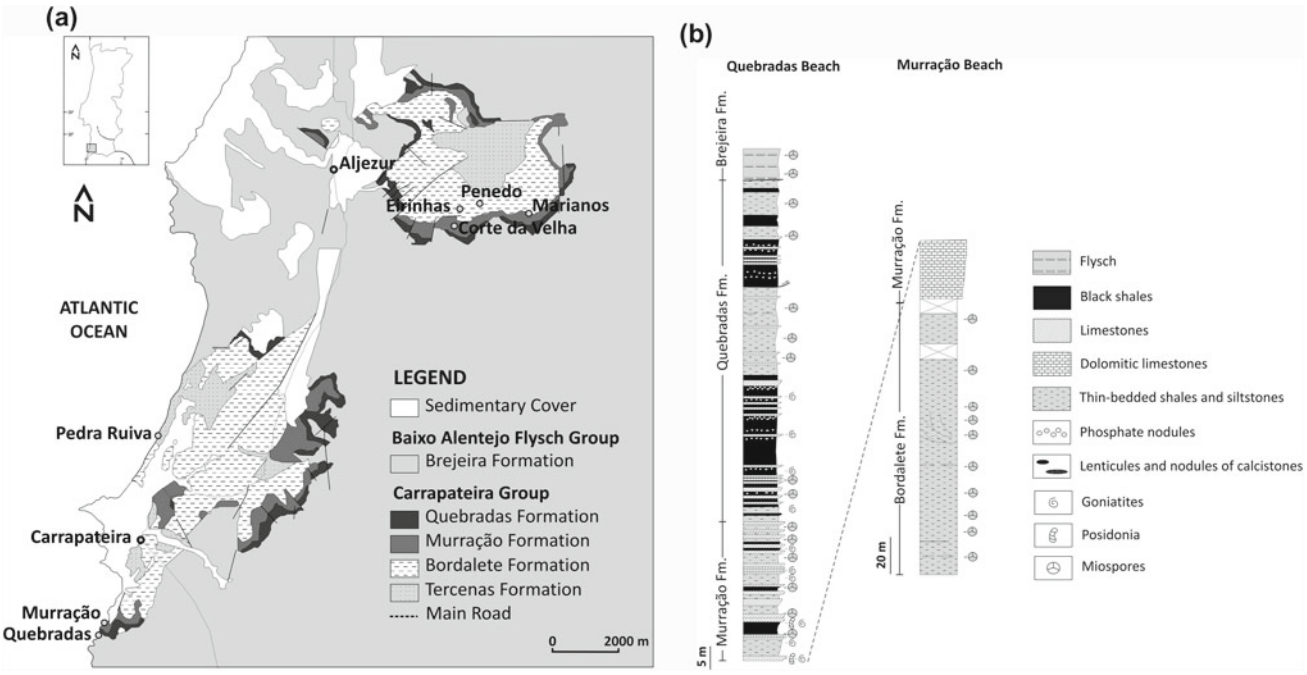

Fig. 6.15 **a** Geological map of Aljezur and Bordeira Antiforms (Adapted from Carta Geológica de Portugal, scale 1: 200,000, sheet 7); **b** stratigraphic log of the Carrapateira Group units

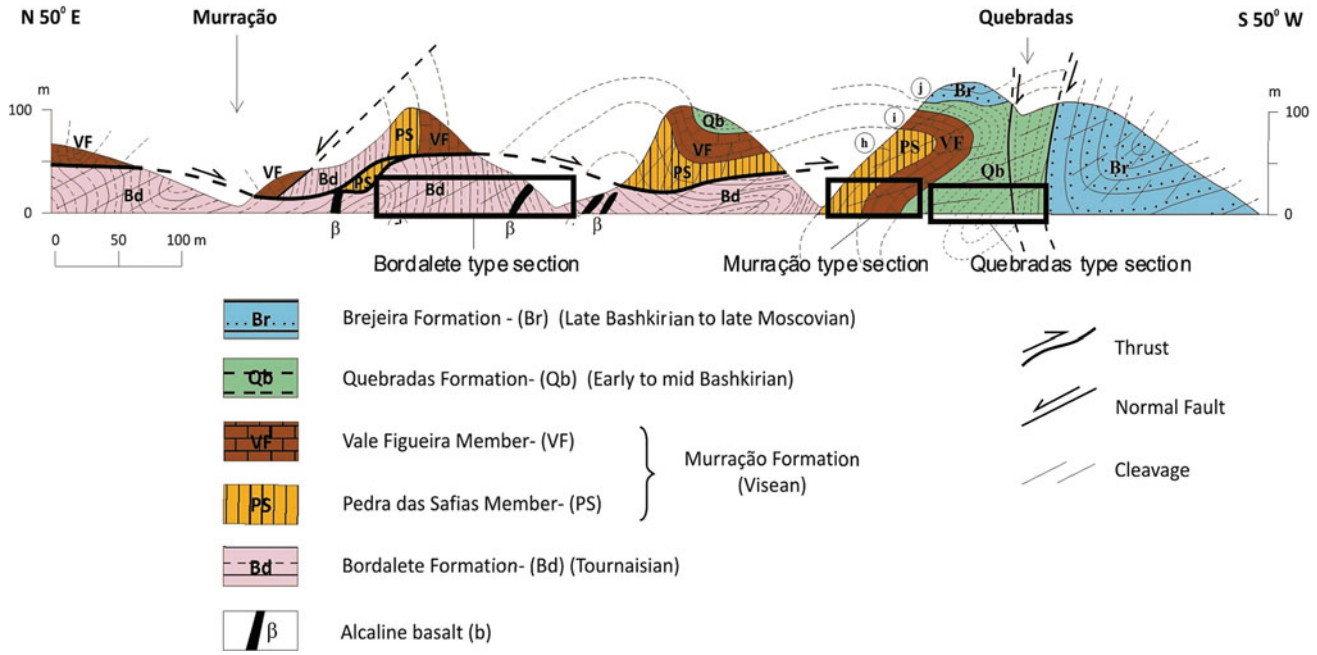

Fig. 6.16 Frontal part of the Carrapateira Trust along the coastal cliff of the Murração and Quebradas beaches (adapted from Ribeiro 1983). The type sections of the Bordalete, Murração end Quebradas Fms are outlined

composed of goniatites, trilobites and palynomorph assemblages, assigned to the VI (*C. cristifera*), HD (*U. distictus*) and PC (*S. claviger*) Miospore Biozones (Oliveira et al. 1985; Pereira 1999). At the top of this unit the CM Miospore Biozone of late Tournaisian age is missing, probably due to the presence of a hiatus. The lithological, sedimentological and fossil content of this formation suggests deposition in a quiet outer shelf marine environment following a generalized transgression during the Tournaisian.

The Murração Fm. has its type section located in the south cliff of the Murração beach and in the north cliff of the Quebradas beach (Figs. 6.15 and 6.16). From base to top, the first 30 m of the lithologic sequence comprise dark shales, bioclastic dolostones and marly limestones that correspond to the Pedra das Safias Member. The fossil content includes crinoids, corals, trilobites and rare goniatites (*Merocanites* sp.), indicating an early Visean age (Oliveira et al. 1985). The following 32 m that form the Vale Figueira Member are composed of dark-grey or black shales and nodular, sometimes dolomitic, limestones. The shales contain many specimens of *Posidonia becheri*. Goniatites are fairly frequent in some of the beds, allowing the identification of most of the goniatite zones of the late Visean (Oliveira et al. 1985; Korn 1997). The palynostratigraphic study of the Murração Fm. provided five miospore biozones of Visean age (Pereira 1999). The Pedra das Safias Member revealed strong dolomitization that erased the palynomorphs. Only in the Aljezur Antiform where the unit has a more shaly character, identification of the Pu (*L. pusilla*) Biozone and TS (*K. stephanephorus)* Biozone, of early Visean age, has been possible. The Vale Figueira Member allowed the identification of three miospore biozones assemblages, NM (*R. nigra*), SN (*S. nux*) and NC (*B. nitidus*) of late Visean age. Palynostratigraphic evidence indicates that the entire Visean may be represented in the Murração Fm., confirming the macrofauna age determinations (Pereira 1999; Pereira et al. 2007). The predominance of ammonoids and a scarce benthic community, with rare trilobites, brachiopods, echinoderms and rugose corals suggest that the Murração Fm. was laid down in an open and distal marine mixed carbonate/mud platform, deepening to the northeast as suggested by the unit more shaly character in the Aljezur Anticline. Herbig et al. (1999) recognized in SW Portugal the late Visean *Crenistia* event, which is well defined across the Avalonia Terrane.

The *Quebradas Formation* type section is exposed at the Quebradas Beach cliff (Figs. 6.11b and 6.12) where it forms the reverse limb of a frontal fold at the tip of the Carrapateira thrust (Fig. 6.12; Ribeiro 1983; Silva et al. 1990). The unit conformably overlies the Murração Fm. and is mainly composed of black shales with intercalations of carbonate layers and lenses, and conglomerate-like beds of phosphate nodules towards de upper part. The unit thickness is ca. 70 m. The unit is dated of Bashkirian as indicated by abundant ammonoid faunas representing the Biozones R1a to G1, (Oliveira et al. 1985; Korn 1997) and miospore assemblages ascribed to the early Bashkirian KV (*C. kosankei*) and FR (*R. reticulatus*) Miospore Biozones (Pereira 1997). In the type section

Serpukhovian faunal and floral assemblages were not identified suggesting a stratigraphic gap. However, in the Aljezur anticline the Serpukhovian is represented by the ammonoid *Eumorphoceras* sp.. The Quebradas Formation lithologies were laid down in a restricted marine environment of a mixed mud/carbonate platform, and the interbedded phosphatic nodules may well represent upwelling near its external border.

The first greywacke beds of the overlying Brejeira Formation (Baixo Alentejo Flysch Group, Fig. 6.16) in the Quebradas Section provided miospores assigned to the SL Miospore Biozone of mid Moscovian age. The absence of early Moscovian is due to a fault (Pereira 1999; Pereira et al. 2007).

References

Albardeiro L, Solá R, Salgueiro R, Morais I, Matos JX, Mendes M, Batista M J, Pereira Z, Inverno C, Oliveira D, Rosa D, Pacheco N (2017) Insights into timing of mineralization in the Neves-Corvo VMS deposit (IPB). Proceedings of the 14th SGA Biennial Meeting – Mineral Deposits to Discover, Québec City, Canada, 3, 989–992

Albardeiro L, Morais I, Solá R, Matos JX, Rosa D, Batista MJ, Pacheco N, Araujo V, Inverno C, Salgueiro R, Marques F, Mendes M, Pereira Z, Oliveira D (2018) Geochemical proxies as space and time indicators of the volcanism evolution in the Portuguese Iberian Pyrite Belt sector. XIV XIV Congresso de Geoquímica dos Países de Língua Portuguesa. XiX Semana de Geoquímica. Abstract Book, 19–22

Arth JG, Barker F, Peterman ZE, Friedman I (1978) Geochemistry of the Gabbro-Diorite-Tonalite-Trondhjemite Suite of southwest Finland and its Implications for the Origin of Tonalitic and Trondhjemitic Magmas. J Petrol, 19, 2, 289–316

Aye F, Picot P (1976) Sur les minéraux d'étain dans les amas sulfurés massifs: découverts récents, inventaire, gitologie. CR Acad Sci Paris 282, 1909–1912

Bard J P (1969) Le metamorphisme régional progressif des Sierras d'Aracena en Andalousie Occidentale (Espagne). Sa place dans le segment Sud-Ibérique. Thesis, Univ. Montpellier, 398

Bard J P, Moine B (1979) Acebuches amphibolites in the Aracena Hercynian metamorphic belt (southwest Spain): geochemical variations and basaltic affinities. Lithos 12, 271–282

Barrett T, no date. Lundin Mining/Somincor geochemical database. Unpub.

Barrett T (2008) Chemostratigraphy and petrography of volcanic rocks at the Neves-Corvo deposit, Portugal. Unpub. Rep, for Lundin Mining/Somincor

Barret TJ. Dawson GL, Maclean W (2008) Volcanic stratigraphy, alteration and sea floor setting of the Paleozoic Feitais massive sulfide deposit, Aljustrel, Portugal. Econ Geol 103, 215-239

Barrett T (2010) Lithogeochemestry and geological relations is selected regional drill holes and outcrops: Lundin Mining egional exploration program, Portugal. Unpub. Rep. for AGC and Somincor

Barrett T (2013) Chemostratigraphy petrography and alteration of the volcanic rocks at the Lagoa Salgada Deposit Portugal. Unpub. Explor Rep for Redcorp Ventures, Ltd.

Barrie CT, Amelin Y, Pascual E (2002) U-Pb geochronology of VMS mineralisation in the IPB. Mineral Deposita, 37, 684–703

Barriga FJAS (1990) Metallogenesis in the IPB. In: Dallmeyer RD and Martinez Garcia E (eds.) Pre-Mesozoic Geology of Iberia. Springer Verlag, 369–379

Barriga FJAS, Carvalho D (1997) Geology and VMS deposits of the IPB: guidebook series. Soc Econ Geol 27

Barriga FJAS, Fyfe WS (1988) Giant pyritic base-metal deposits: the example of Feitais, Aljustrel, Portugal. Chem Geol 69, 331–143

Barriga FJAS, Fyfe WS (1998) Multi-phase water-rhyolite interaction and ore fluid generation at Aljustrel, Portugal. Mineral Deposita 33, 188–207

Barriga FJAS, Kerrich R (1984) Extreme ^{18}O-enriched volcanics and ^{18}O-evolved marine water, Aljustrel, IPB: Transition from high to low Rayleigh number convective regimes. Geochem Cosmochem Acta 48, 1021–1031

Barriga FJAS, Relvas JMRS (1993) Hydrothermal Alteration as an Exploration Criterion in the IPB: Facts, Problems and Future. I Simpósio de Sulfuretos Polimetálicos da Faixa Piritosa Ibérica (Évora, Outubro 1993), APIMINERAL - Associação Portuguesa da Indústria Mineral

Bea F Montero P, González-Lodeiro F, Talavera C (2007) Zircon inheritance reveals exceptionally fast crustal magma generation processes in Central Iberia during the Cambro-Ordovician. J Petrol 48, 12, 2327–2339

Boogaard M (1963) Conodonts of Upper Devonian and Lower Carboniferous age from Southern Portugal. Geol Minjb 42, 8: 248–259

Boogaard M (1967) Geology of Pomarao region (Southern Portugal). Thesis. Graffisch Centrum Deltro. Rotterdam

Boogaard M, Schermerhorn LJG (1975) Conodont faunas from Portugal and southwestern Spain. Part 2.6 A Famennian conodont fauna at Cabezas del Pasto. Scripta Geol, 28, 1–36

Boogaard M, Schermerhorn LJG (1981) Conodont faunas from Portugal and Southwest Spain. A lower Famennian conodont fauna at Monte Forno da Cal (South Portugal). Scripta Geol 63, 1–16

Boulter C (1993a) Comparison of Rio Tinto, Spain, and Guaymas Basin, Gulf of California: An explanation of a supergiant massive sulfide deposit in an ancient sill-sediment complex. Geology 21, 801–804

Boulter C (1993b) High-level peperitic sills at Rio Tinto, Spain: Implications for stratigraphy and mineralization. Transactions of the Institution of Mining Metallurgy Section B, Applied Earth Science, 102, 30–38

Braid JA (2011) Dynamics of Allochthonous Terranes in the Pangean Suture Zone of Southern Iberia. Dalhousie University, PhD thesis

Braid JA, Murphy JB, Quesada C (2010) Structural analysis of an accretionary prism in a continental collisional setting, the Late Paleozoic Pulo do Lobo Zone, Southern Iberia. Gondwana Res17:422–439

Braid J A, Murphy B, Quesada C, Mortensen J K (2012) Probing the composition of the unexposed basement, South Portuguese Zone, Southern Iberia: implications for the connections between the Apalachian and the Variscan Orogens. Can J Earth Sci 49, 4, 591–613

Braid JA, Murphy JB, Quesada C, Mortensen J (2011) Tectonic scape of a crustal fragment during the closure of the Rheic Ocean: U-Pb detrital zircon data from the Late Palaeozoic Pulo do Lobo and South Portuguese Zones, Southern Iberia. J Geol Soc London 168, 383–392

Braid JA, Murphy JB, Quesada C, Gladney ER, Dupuis N (2018) Progressive magmatism and evolution of the Variscan suture in southern Iberia. Int J Earth Sci 107, 3, 971–983. https://doi.org/10.1007/s00531-017-1540-3

Carvalho D (1976) Considerações sobre o vulcanismo da região de Cercal-Odemira. Suas relações com a faixa piritosa. Com Serv Geol Portugal 60, 215–238

Carvalho JRS (2016) Zinc Metallogenesis, and Indium and Selenium Distribution at the Giant Neves Corvo Deposit, IPB Portugal. Unpublished PhD thesis, University of Lisbon, 550 pp

Carvalho D, Goinhas J, Oliveira V, Ribeiro A (1971) Observações sobre a geologia do Sul de Portugal e consequencias metalogenéticas. Estud Not Trav Serv Fomento Min 20:153-199

Carvalho, D., Correia, M., Inverno, C., 1976. Contribuição para o conhecimento geológico do Grupo Ferreira-Ficalho. Suas relações com a Faixa Piritosa e o Grupo do Pulo do Lobo. Memórias do Museu Laboratório Mineralógico Geológico da Faculdade de Ciências, Coimbra 82, 145–169.

Carvalho D, Barriga FJAS, Munhá J (1999) Bimodal siliciclastic systems: the case of the IPB. Rev Econ Geol, 8, 375–408

Carvalho J, Inverno C, Matos JX, Rosa C, Granado I, Branch T, Represas P, Carabaneanu L, Matias, L, Sousa, P (2016) Subsurface Mapping in the Iberian Pyrite Belt Using Seismic Reflection Profiling and Potential Field Data. Int J Earth Sci (Geol Rundsch). https://doi.org/10.1007/s00531-016-1340-1

Castroviejo R, Quesada C, Soler M (2011) Post-depositional tectonic modification of VMS deposits in Iberia and its economic significance. Miner Depos 46:615–637

Clayton G, Wicander R, Pereira Z (2002) Palynological evidence concerning the relative positions of Northern Gondwana and Southern Laurussia in latest Devonian and Mississippian times. In: Wyse Jackson P, Parkes MA (eds) Studies in Palaeozoic palaeontology and biostratigraphy in honour of Charles Hepworth Holland. Special Papers in Palaeontology 67, 45–56

Codeço M (2015) Estudo comparativo das sequências vulcânicas constituintes dos eixos Ervidel-Roxo e Figueirinha-Albernoa e respectiva relevância na prospecção de sulfuretos maciços polimetálicos. MSc. Thesis Fac Cien Univ Lisboa, 217 pp

Coney PJ, Jones DL, Monger JWH (1980) Cordilleran suspect terranes. Nature, 288, 329–333. https://doi.org/10.1038/288329a0

Contreras F, Santos A (1982) Mapa Geológco de España, E/1:50,000, Sheet 937: El Cerro de Andévalo. Instituto Geológico y Minero de España, 1–60

Cunha T, Oliveira JT (1989) Upper Devonian Palynomorphs from the Represa and Phyllite-Quartzite Fm Mina de Sao Domingos region Southwest Portugal, Tectonostratigraphic implications. Bull Soc Bel Geol 98, 3/4, 295–309

de Oliveira D et al. (2011) The Lagoa Salgada Orebody IPB Portugal. Econ Geol 106, 1111–1128

de la Rosa, J.D., 1992. Petrología de las rocas básicas y granitoides del batolito de la Sierra Norte de Sevilla, Zona Surportuguesa, Macizo Ibérico. Doctoral Thesis, Universidad de Sevilla, 312pp.

Dias R, Oliveira JT, Matos JX, Ressurreição R, Pereira Z, Machado S, Pais J, Manupella G (2016) Notícia Explicativa da Folha 42A Grândola. U Geologia, Hidrogeologia e Geologia Costeira, LNEG, 113p

Díez-Montes A, Bellido Mulas F (2008) Magmatismo TTGy Al-Ken la Zona Surportuguesa. Relaciones entre plutonismo y vulcanismo. VII Congreso Geológico de España. Las Palmas de Gran Canaria (España). Geo-Temas, 10, 1449–1452

Domergue C (1983) La mine antique d'Aljustrel (Portugal) et les tables de bronze de Vipasca. Conimbriga, XXII, 35

Donaire T, Toscano M, Pascual E (1998) Relaciones entre rocas volcánicas y plutónicas en el distrito minero de Riotinto, Faja Pirítica Ibérica, España. X Congreso Geológico de España Geo-Temas, 16, 1, 431–433

Dunning G, Diez Montes A, Matas J, Martin Parra L, Alamarza J, Donaire M (2002) Geocronologia U/Pb del volcanismo acido y granitoides dela Faja Piritica Iberica (Zona Surportuguesa). Geogaceta 32, 127–130

Dupuy C, Dostal J, Bard JP (1979) Trace elements geochemistry of Paleozoic amphibolites from SW Spain. Tschermarks Mineral Petrol Mitt, 26, 87–93

Eder W In: Oliveira JT (1983) The marine carboniferous of South Portugal: a stratigraphic and sedimentological approach. In: Lemos de Sousa MJ, Oliveira JT (eds) The Carboniferous of Portugal, Serv Geol Portugal 29: 3–38.

Elf Aquitaine 1985 Recherches pour metaux de premiere classe Baixo-Alentejo Portugal. Unpub Rep.

Fantinet D, Dreesen R, Dusar M, Termier G (1976) Faunes Famenniennes de certains horizons calcaires dans la formation quartzophylladique aux environs de Mertola (Portugal meridional). Com Ser Geol Portugal 60, 121–138

Faria R, Pereira Z, Matos JX, Rosa C, Caetano Alves MI, Oliveira JT (2015) Estudo palinostratigráfico do setor Malhadinha, região NE Alvares, concelho de Mértola, Faixa Piritosa Ibérica. Com Geol 102, 1, 5–11

García de Miguel JM (1990) Mineralogía paragénesis y sucesión de los sulfuros masivos de la Faja Pirítica en el suroeste de la Península Ibérica. Bol Geol Minero 101, 1, 73–105

García Palomero F (1980) Caracteres geológicos y relaciones morfológicas y genéticas delos yacimientos del anticlinal de Rio Tinto. Instituto Estudios Onubenses "Padre Marchena", Diputación Provincial Huelva, 1264 pp

Gaspar O (1991) Paragenesis of the Neves-Corvo volcanogenic massive sulphides. Com Serv Geol Portugal 77:27–52

Gaspar O, Pinto A (1991) Ore textures of Neves-Corvo volcanogenic massive sulphides and their implications for ore beneficiation. Min Mag 55, 417–422

González F, Moreno C, Lopez M J, Dino R, Antonioli L (2004) Palinoestratigrafia del Grupo Pizarroso-Quartzitico del sector oriental de la Faja Piritica SO de España. Rev Espan Micropal 36: 2.6

Gonzalo J, Locutura J, Sánchez A, Vázquez F (1978) Mapa Geológco de España, E/1:50,000, Sheet 936: Paymogo. Instituto Geológico y Minero de España, 1–29

Halter W, William-Jones AE (1996) The role of greisenization in cassiterite precipitation at the East Kemptville tin deposit Nova Scotia. Econ Geol 91:368–385

Hannington MD, Poulsen KH, Thompson JFH, Sillitoe RH (1999a) Volcanogenic gold and epithermal-style mineralization in the volcanic massive sulfides environment. In: Barrie CT, Hannington MD (eds) Volcanic-associated massive sulfide deposits: processes and examples in modern and ancient settings. Rev Econ Geol 8, 183–214

Hannington MD, Barrie CT, Bleeker W (1999b) The giant Kidd Creek volcanogenic massive sulfide deposit Western Abitibi Subprovince Canada: preface and introduction. Econ Geol Mon 10:1–30

Heinrich CA (1990) The chemistry of hydrothermal tin(-tungsten) ore deposition. Econ Geol 85:457–481

Herbig, H. G., Korn, D., Mestermann, 1999. Cresnitria Event and Asbian-Brigantian Transition in the South Portuguese Zone-Sea Level Control on a Hemipelagic Late Dinantian Platform. Facies, 41, pp. 183–196.

Huston, D.L., Relvas, J.M.R.S., Gemmell, J.B., Drieberg, S., 2011. The role of granites in volcanic-hosted massive sulphide ore-forming systems: An assessment of magmatic-hydrothermal contributions. Mineralium Deposita, 46, 5–6: 473–507.

IGME (1997) Estratigrafía de la parte Española de la Faja Pirítica Ibérica. Unpublished IGME open-file report, 89 pp

IGME/LNEG (2015) Roberto Rodriguez and Tomás Oliveira J (eds) Mapa Geológico de España y Portugal, scale 1: 1000.000. Madrid

Inverno C, Díez-Montes A, Rosa C, García-Crespo J, Matos J, García-Lobón JL, Carvalho J, Bellido F, Castello-Branco JM, Ayala C, Batista MJ, Rubio F, Granado I, Tornos F, Oliveira JT, Rey C, Araújo V, Sánchez-García T, Pereira Z, Represas P, Solá AR, Sousa P (2015) Introduction and Geological Setting of the IPB. In: P Weihed (ed) 3D, 4D and Predictive Modelling of Major Mineral Belts in Europe. Mineral Resource Reviews Springer. https://doi.org/10.1007/978-3-319-17428-0-9 191

Jorge RS (2010) Caracterização petrográfica, geoquímica e isotópica dos reservatórios metalíferos crustais, dos processos de extracção de metais e dos fluidos hidrotermais envolvidos em sistemas mineralizantes híbridos na Faixa Piritosa Ibérica. Unpublished PhD thesis Portugal Univ Lisbon, 324 pp

Jorge RS, Relvas JMRS, Barriga FJAS (2005) Silica Gel Microtextures in Siliceous Exhalites at the Soloviejo Manganese Deposit Spain. In: Mao J, Bierlein FP (eds) Mineral Deposit Research: Meeting the Global Challenge vol 1: Berlin, Germany. Springer-Verlag: 631–634

Jorge RS, Fernandes P, Pereira Z, Oliveira JT (2007a) A Late Fammenian age storm-dominated succession at Berrocal (IPB - Spain). In: Pereira Z, Oliveira JT, Wicander R (eds) CIMP Lisbon 07, Joint Meeting of Spores/Polen and Acritarch Subcomissions Abstracts. INETI, Lisbon

Jorge RS, Pinto AMM, Tassinari CCG, Relvas JMRS, Munhá J (2007b) VHMS metal sources in the IPB: new insights from Pb isotope data. In: Andrew et al (eds) Digging Deeper. Spec Pub Irish Ass Eco Geol: 097–1100

Jorge R, Pinto A, Tassinari C, Relvas J, Munhá J (2007c) VHMS metal sources in the IPB: new insights from Pb isotope data. Proc Ninth Biennial SGA Meeting Dublin, 097–1100

Korn, D., 1997. The Paleozoic ammoids of the South Portuguese Zone. Memorias do Instituto Geológico e Mineiro, Portugal 33, 131 p. Large, R., Blundell, D. (Eds.), 2000. Database on Global VMS districts.CODES-GEODE, 179 p.

Lake PA, Oswin WM, Marshall JEA (1998) A palynological approach to terrane analysis in South Portuguese Zone. Trabajos de Geologia Univ Oviedo 17: 125–131

Large RR, Blundell DL (2000) Database on Global VMS districts. Centre for Ore Deposit Research (CODES) Hobart Australia Univ Tasmania, 179 pp

Lehmann B (1991) Metallogeny of tin. In: Bhattacharji S, Friedman GM, Neugebauer HJ, Seilacher A (eds) Lecture Notes in Earth Science, Springer-Verlag, 211 pp

Leistel JM, Marcoux E, Thiéblemont D, Quesada C, Sánchez, A, Almodóvar GR, Pascual E, Sáez R (1998a) The volcanic-hosted massive sulphide deposits of the IPB. Miner Depos 33, 2–30

Leistel, JM, Marcoux E, Deschamps Y (1998b) Chert in the IPB. Miner Depos 33, 59–81

Leistel JM, Bonijoly D, Braux C, Freyssinet Ph, Kosakevitch A, Leca X, Lescuyer JL, Marcoux E, Milési JP, Piantone P, Sobol F, Tegyey M, Thiéblemont D, Viallefond L (1994) The massive sulphide deposits of the South Iberian Pyrite Province: Geological setting and exploration criteria. Bur Rech Géol Min 234, 236 pp

Lesher CM, Goodwin AM, Campbell IH, Gorton MP (1986) Trace-element geochemistry of ore-associated and barren felsic metavolcanic rocks in the Superior Province Canada. Can J Earth Sci 23, 222–237

Lotze F (1945) Zur Gliederung der Variszden der Iberich Meseta. Eotektobische Forschungen 6, 79–92

Marcoux E (1998) Lead isotope systematics of the giant massive sulphide deposits in the IPB. Miner Depos 33, 45–58

Marcoux E, Sáez R (1994) Geoquímica isotópica de plomo de las mineralizaciones hidrothermales tardihercínicas de la Faja Pirítica Ibérica. Bol Soc Esp Miner 17, 1, 202–203

Marcoux E, Leistel JM, Sobol F, Milési JP, Lescuyer JL, Leca X (1992) Signature isotopique du plomb des amas sulfurés de la province de Huelva Espagne: conséquences métallogéniques et géodynamiques. CR Acad Sci Paris 314 II, 1469–1476

Marcoux E, Moëlo Y, Leistel JM (1996) Bismuth and cobalt minerals: indicators of stringer zones to massive sulfide deposits IPB. Miner Depos 31, 1–26

Marignac C, Diagana B, Cathelineau M, Boiron MC, Banks D, Fourcade S, Vallance J (2003) Remobilisation of base metals and gold by Variscan metamorphic fluids in the south IPB: evidence from the Tharsis VMS deposit. Chem Geol 194, 143–165

Markham NL (1968) Some genetic aspects of the Mt Lyell mineralization. Miner Depos 3, 199–221

Mathur R, Ruiz J, Tornos F (1999) Age and sources of the ore at Tharsis and Río Tinto IPB from Re-Os isotopes. Miner Depos 34, 790–793

Matos J X, Pereira Z, Rosa C, Oliveira J T (2014) High resolution stratigraphy of the Phyllite-Quartzite Group in the northwest region of the IPB, Portugal. Com Geol vol 101, 489–493

Matos JX, Pereira Z, Oliveira V, Oliveira JT (2006) The geological setting of the Sao Domingos pyrite orebody, IPB. VII Congresso Nacional de Geologia, Estremoz, Univ Evora Portugal. Geologia de Portugal vol I, 13:5

Matos JX, Martins LP, Oliveira JT, Pereira Z, Batista MJ, Quental L (2008) Rota da pirite no sector português da Faixa Piritosa Iberica, desafios para um desenvolvimento sustentado do turismo geologico e mineiro. In: Paul Carrion (ed) Livro Rutas Minerales en Iberoamérica, Esc Sup Politecnica Guayaquil Equador, 136–155

Matos JX, Martins A, Rego M, Mateus A, Pinto A, Figueiras J, Silva E (2011a) Roman slag mine wastes distribution in the Portuguese sector of the Iberian Pyrite Belt. Actas V Cong. Int. Minería y Metalurgia Históricas SW Europeo, León, Libro Homenaje a Claude Domergue, Eds. J.M. Mata-Perelló, L.T. Iabat, M.N.F. Prieto, SEDPGYM Spain, 563–572 p. ISBN 978-99920-1-790-6

Matos JX, Pereira Z, Rosa CJP, Rosa DRN, Oliveira JT, Relvas JMRS (2011b) Late Strunian age: a key time frame for VMS deposit exploration in the Iberian Pyrite Belt. 11th Biennial SGA Meeting, Antofagasta, Chile, 790–792

Mirão JAP, Barriga FJAS, Noiva PC, Ferreira A (1997) Chemical sediments in the Neves-Corvo mine: the JC unit. Society of Economic Geologists, Neves-Corvo Field Conference, Lisbon, Portugal, Abstracts, 111

Mitjavila J, Martí J, Soriano C (1997) Magmatic evolution and tectonic setting of the IPB volcanism. J Petrol 38, 727–755

Moreno C, Saez R (1990) Sedimentacion marina somera en el devonico del anticlinorio de Puebla de Guzman, Faja Pirítica Iberica. Geogaceta, 8, 62–64

Moreno C, Sierra S, Saez R (1995) Mega-debris flows en el transito Devonico-Carbonico de la Faja Piritica. Geogaceta 17, 9–11

Moreno C, Pereira Z, Oliveira JT, Sierra S (1996) Sedimentacion litoral en el limite Devonico-Carbonico del Suroeste Portugues (Zona Sur Portuguesa). Geogaceta 20, 1:23–26

Munhá J (1983a) Hercynian magmatism in the IPB. In: Lemos de Sousa MJ, Oliveira JT (eds) The Carboniferous in Portugal. Mem Serv Geol Portugal 29, 39–81

Munhá J (1983b) Low grade metamorphism in the IPB Pyrite. Com Serv Geol Portugal 69, 3–35

Munha J, Kerrich R (1980) Sea water basalt interaction in spilites from the IPB. Contrib. Mineral. Petrol 73, 191–200

Munhá J, Kerric R (1981) Sea water-basalt interaction in spilites from the IPB. Contrib Miner Petrol 75, 15–19

Munhá J, Barriga FJAS, Kerrich R (1986) High ^{18}O ore-forming fluids in volcanic-hosted base metal massive sulfide deposits: geologic $^{18}O/^{16}O$ and D/H evidence from the IPB, Crandon, Wiscosin and Blue Hill, Maine. Econ Geol 81, 530–552

Munhá J, Oliveira JT, Ribeiro A, Quesada C, Fonseca P, Castro P (1989) Accreted terranes in southern Iberia: the Beja-Acebuches ophiolite and related oceanic sequences. 28th International Geological Congress, Washington, Abstr 2, 312–314

Munhá J, Pacheco N, Beliz A, Relvas JMRS, Hodder RW (1997) Physical and geochemical characterization of the Neves-Corvo felsic volcanism. Soc Econ Geol Neves-Corvo Field Conference, Lisbon, Portugal, May 11–14, 1997. Abstracts, 89

Munhá J, Relvas JMRS, Barriga FJAS, Conceição P, Jorge RCGS, Mathur R, Ruiz J, Tassinari CCG (2005) Os Isotopes Systematics in the IPB. In: Mao J, Bierlein FP (eds) Miner Depos Res, Meeting the Global Challenge vol 1, Berlin Germany. Springer-Verlag, pp 663–666

Nesbitt RW, Pascual, E, Fenning, CM, Toscano M, Sáez R, Almodóvar RG (1999) U-Pb dating of stockwork zircons from the eastern IPB. Jour Geol Soc London 156, 7–10

Oliveira J T (1983) The marine carboniferous of South Portugal: a stratigraphic and sedimentological Approach. In: Lemos Sousa MJ, Oliveira, JT (eds) The Carboniferous of Portugal. Ser Geol Port 29, 3–38

Oliveira JT (1990) Stratigraphy and syn-sedimentary tectonism in the South Portuguese Zone. In: Dallmeyer R D, Martinez Garcia E (eds) Pre-Mesozoic Geology of Iberia. Springer Verlag: 334–347

Oliveira J T, Horn M, Kullmann J, Paproth E (1985) Stratigraphy of the Upper Devonian and Carboniferous sediments of Southwest Portugal. CR X Inter Cong Strat Geo Carboniferous, Madrid 1, 1–17

Oliveira JT, Quesada C (1998) A comparison of stratigraphy and paleogeography of the South Portuguese Zone and South-West England European Variscides. Proc Ussher Soc (the Scottt Simpson invited lecture

Oliveira JT, Silva JB (1990) Carta Geologica de Portugal a escala 1:50000, Folha 46-D, Mertola. Serv Geol Portugal

Oliveira JT, Silva JB (2007) Noticia Explicativa da Folha 46-D-Mértola. Inst Nac Eng Geol, 46 pp

Oliveira JT, Horn M, Paproth E (1979) Preliminary note on the stratigraphy of the Baixo Alentejo Flysch Group Carboniferous of Portugal and on the palaeogeographic development compared to corresponding units in Northwest Germany. Com Serv Geol Portugal 65, 151–68

Oliveira JT coordenador (1982) Carta Geológica de Portugal 1/200 000 fl. 8. Not Expl. Serv Geol Portugal

Oliveira JT, Cunha TA, Streel M, Vanguestaine M (1986) Dating the Horta da Torre Fm a new lithostratigraphic unit of the Ferreira-Ficalho Group South Portuguese Zone geological consequences. Com Serv Geol Portugal 72, 1/2, 129–135

Oliveira JT, Pereira Z, Rosa C, Rosa D, Matos J (2005) Recent advances in the study of the stratigraphy and the magmatism of the IPB Portugal. In: Carosi R, Dias R, Iacopini D, Rosenbaum G (eds) The southern Variscan belt. Journal of the Virtual Explorer Edition 19, 9, 1441–8142

Oliveira JT, Pereira Z, Carvalho P, Pacheco N, Korn, D (2004) Stratigraphy of the tectonically imbricated lithological succession of the Neves Corvo mine area, IPB, Portugal. Miner Depos 39, 4, 422–436

Oliveira JT, Fernandes P, Dias RP, Pais J (2007) Notícia explicativa da folha 42-B, Azinheira de Barros. LNEG

Oliveira JT, Rosa C J P, Pereira Z, Rosa D R N, Matos J X, Inverno C MC, Andersen T (2013) Geology of the Rosário-Neves Corvo antiform IPB Portugal: New insights from physical volcanology palynostratigraphy and isotope geochronology studies. Miner Depos 48, 6, 749–766

Onézime J, Chavet J, Faure M, Bourdier JC, Chavet A (2003) A new geodynamin interpretation for the South Portuguese Zone (SW Iberia) and the IPB genesis. Tectonics 22, 4, 1–17

Pearce JA, Harris NBW, Tindle AG (1984) Trace element discrimination diagrams for the tectonic interpretation of granitic rocks. J Petrol 25, 956–983

Pereira Z (1997) Palinologia e petrologia orgânica do sector SW da Zona Sul Portuguesa. Tese de Doutoramento. Fac Cien Univ Porto, 260 pp

Pereira Z (1999) Palinoestratigrafia do Sector Sudoeste da Zona Sul Portuguesa. Com Serv Geol Portugal 86: 25–57

Pereira Z, Clayton G, Oliveira JT (1994) Palynostratigraphy of the Devonian-Carboniferous Boundary in Southwest Portugal. Ann Soc Geol Belgique 117, 1, 189–199

Pereira Z, Fernandes P, Oliveira JT (2006) Palinoestratigrafia do Domínio Pulo do Lobo, Zona Sul Portuguesa. Com Geol Inst Nac Eng Tec Inov Lisboa 93, 23–38

Pereira Z, Matos JX, Fernandes P, Oliveira JT (2007) Devonian and Carboniferous palynostratigraphy of the South Portuguese Zone Portugal: An overview. Com Geol Inst Nac Eng Tec Inov Lisboa, 94: 53–79

Pereira Z, Matos JX, Fernandes P, Oliveira JT (2008a) Palynostratigraphy and systematic palynology of the Devonian and Carboniferous successions of the South Portuguese Zone, Portugal. Mem Geol Inst Nac Eng Tec Inov Lisboa, 34, 181 pp

Pereira Z, Matos, JX, Fernandes P, Oliveira JT (2008b). New data on the late Famennian miospore assemblage of the Cercal Anticline (westernmost IPB area), Portugal. AbstractVolume12th International Palynological Congress (IPC-XII 2008) 8th International Organisation of Palaeobotany Conference (IOPC-VIII 2008) Joint Congress Bonn 2008: 219–220

Pereira Z, Matos, JX, Fernandes, P, Jorge R, Oliveira JT (2009) New Lower Givetian age miospores of the Phyllite - Quartzite Group (São Francisco da Serra Anticline IPB Portugal). CIMP Faro UALG-LNEG, p 75–78

Pereira Z, Matos JX, Fernandes P, Oliveira JT (2010) Qual a idade mais antiga da Faixa Piritosa? Nova idade Givetiano inferior para o Grupo Filito-Quartzítico (Anticlinal de S. Francisco da Serra, Faixa Piritosa). Revista Electrónica de Ciencias da Terra, Geosciences On-line Journal ISSN 1645-0388, 17, 13, 1–4

Pereira Z, Matos J, Rosa C, Oliveira JT (2012) Palynostratigraphic importance of the Strunian in the IPB. Joint Meeting of the 45th Annual Meeting of American Association Stratigraphic Palynology (AASP) - The Palynological Society and Meeting of Internacional Commission of Paleozoic Microflora (Cimp), Lexington, KY, USA, Abstract Book, 42–43

Pereira Z, Fernandes P, Matos JX, Oliveira JT, Jorge RS (2018) Stratigraphy of the Northern Pulo do Lobo Domain, SW Iberia Variscides: a palynological contribution. Geobios. https://doi.org/10.1016/j.geobios.2018.04.001

Pérez-Cáceres, I., Poyatos,D. M., Simancas, J. F., Azor A., 2017. Testing the Avalonian affinity of the South Portuguese Zone and the Neoproterozoic evolution of SWIberia through detrital zircon populations. Gondwana Research 42, 177–192.

Petersen EU (1986) Tin in volcanogenic massive sulfide deposits: an example from the Geco mine Manitouwadge district Ontario Canada. Econ Geol 81, 323–342

Pfefferkorn H W (1968) Geologie des Gebietes zwichen Serpa und Mertola (Baixo Alentejo Portugal. (PhD thesis) Munster Forsch Geol Palaont 9, 2–143

Pinedo Vara I (1963) Piritas de Huelva (su historia minería y aprovechamiento) Summa (ed) Madrid, 1003 pp

Pinto A, Bowles JFW, Gaspar OC (1994) The mineral chemistry and textures of wittichenite miharaite carrolite mawsonite and In-Bi-Hg tennantite from Neves-Corvo Portugal. Procof XVI Gen Meet IMA Pisa Italy, p 329

Pinto A, Ferreira A, Bowles JFW, Gaspar OC (1997) Mineralogical and textural characterization of the Neves-Corvo ores: metallogenetic implications. Neves Corvo Field Conference Abstracts Soc Econ Geol Lisbon, pp 90

Pinto A, Relvas JMRS, Barriga FJAS, Munhá J, Pacheco N, Scott SD (2005) Gold mineralization in recent and ancient volcanic-hosted massive sulphides: the PACMANUS field and the Neves-Corvo deposit. In: Mao J, Bierlein FP (eds) Miner Depos Res: Meeting Global Challenge vol 1 Berlin, Germany. Springer-Verlag, pp 683–686

Pinto A, Relvas JMRS, Carvalho JRS, Pacheco N, Liu Y (2013) Mineralogy and distribution of indium and selenium metals within zinc-rich ore types of the Neves Corvo deposit Portugal. Goldschmidt Conference, Aug 25–30, 2013. Florence, Italy

Quesada C (1991) Geological constraints on the Paleozoic tectonic evolution of tectonostratigraphic terranes in the Iberian Massif. Tectonophysics 185, 225–245

Quesada C (1996) Estructura del sector español de la Faja Piritica: implications para la exploración de yacimientos. Bol Geol Min vol 107–3, 4: 265–268

Quesada C (1998) A reappraisal of the structure of the Spanish segment of the IPB. Miner Depos 33, 31–44

Quesada C, Bellido F, Dallmeyer RD, Gil Ibarguchi JI, Oliveira JT, Pérez Estaún A, Ribeiro A, Robardet M, Silva JB (1991) Terranes within the Iberian Massif: correlations with West African sequences. In: Dallmeyer RD, Lecorché JP (eds) The West African Orogens and Circum-Atlantic correlations. Berlin Heidelberg New York Springer-Verlag, pp 267–293

Quesada C, Fonseca P, Munha J, Oliveira JT, Ribeiro A (1994) The Beja-Acebuches Ophiolite: geological caracterization and geodynamic significance. Bol Geol Min España 105, 3–49

Ramírez Copeiro del Villar J, Maroto Aranda S (1995) Metodología de investigación aplicada a los yacimientos de manganeso en Huelva. Bol Geol Min 106, 2, 125–135

Ramirez Copeiro del Villar J, Navarro Vázquez (1982) Mapa Geológco de España, E/1:50,000, Sheet 960: Valverde del Camino. Instituto Geológico y Minero de España, 1–77

Relvas JMRS (1991) Estudo Geológico e Metalogenético da Área de Gavião Baixo Alentejo. Unpublished MSc thesis Portugal Univ Lisbon, 248 pp

Relvas JMRS (2000) Geology and metallogenesis at the Neves-Corvo deposit Portugal. Unpublished PhD thesis Portugal Univ Lisbon, 319 pp

Relvas JMRS, Tassinari CCG, Munhá J, Barriga FJAS (2001) Multiple sources for ore-forming fluids in the Neves-Corvo VHMS deposit of the IPB (Portugal): strontium neodymium and lead isotope evidence. Miner Depos 36, 416–427

Relvas JMRS, Barriga FJAS, Pinto A, Ferreira A, Pacheco N, Noiva P, Barriga G, Baptista R, Carvalho D, Oliveira V, Munhá J, Hutchinson RW (2002) The Neves-Corvo deposit, IPB Portugal: impacts and future 25 years after the discovery. Soc Econ Geol, Special Publication 9, 155–176

Relvas JMRS, Barriga FJAS, Ferreira A, Noiva PC, Pacheco N, Barriga G (2006) Hydrothermal alteration and mineralization in the Neves-Corvo volcanic-hosted massive sulfide deposit Portugal. I Geology, Mineralogy, Geochemistry. Economic Geology, 101, 4, 753–790

Relvas JMRS, Barriga FJAS, Longstaffe F (2006b) Hydrothermal alteration and mineralization in the Neves-Corvo volcanic-hosted massive sulfide deposit Portugal. II: Oxygen, Hydrogen and Carbon isotopes. Econ Geol 101, 791–804

Ribeiro A (1983) Structure of the Carrapateira Nappe in the Bordeira área, Sw Portugal. In: ML Sousa and J T Oliveira (eds) The Carboniferous of Portugal. Mem. 29, Serv. Geol. Portugal

Ribeiro A, Oliveira JT, Ramalho M, Ribeiro Ml, Silva (1987) Notícia Explicativa da Folha 48-D, Bordeira. Serv. Geol. Portugal, Lisboa

Ribeiro A, Quesada C, Dallmeyer RD (1990) Geodynamic evolution of the Iberian Massif. In: Dallmeyer RD, Martínez García E (edts) Pre-Mesozoic Geology of Iberia. Berlin-Heidelberg-New York Springer-Verlag: 399–409

Rosa C, Oliveira, V, Matos J, Martins L, Oliveira J (2001). Mapa metalogenético do Sul de Portugal, esc. 1/500000. IGM.

Rosa D, Finch A, Andersen T, Inverno C (2009) U–Pb geochronology and Hf isotope ratios of magmatic zircons from the Iberian PyriteBelt. Mineral Petrol 95, 47–69

Rosa C, McPhie J, Relvas JMRS, Pereira Z, Oliveira T, Pacheco N (2008) Facies analysis and volcanic setting of the giant Neves Corvo massive sulfide deposit IPB Portugal. Miner Depos 43, 449–466

Rosa C, McPhie J, Relvas J M R S (2010) Type of volcanoes hosting the massive sulfide deposits of the IPB. J Volcanol Geotherm Res 194, 4, 107–126

Rosa D, Inverno C, Oliveira V, and Rosa C, (2004) Geochemistry of volcanic rocks Albernoa area IPB Portugal. Inter Geol Rev, 46, 366–383

Rosa D, Inverno C, Oliveira V, Rosa C (2006) Geochemistry and geothermometry of volcanic rocks from Serra Branca IPB Portugal. Gondwana Res 10, 328–339

Rosa C, Mcphie J, Relvas JMRS (2016) Distinguishing peperite from other sediment-matrix igneous breccias: lessons from the IPB. J Volcanol Geotherm Res 315, 28–39

Routhier P, Aye F, Boyer C, Lécolle M, Molière P, Picot P, Roger G (1980) La ceinture sud-ibérique à amas sulfurés dans sa partie espagnole médiane, Tableau géologique et métallogénique, Synthèse sur le type amas sulfurés volcano-sédimentaires. 26th Int. Geol. Congr. Paris. Mém BRGM 94, 265 pp

Sáez R, Pascual E, Almodóvar GR, Rodríguez-Gordillo J (1987) Mineralizaciones de Sn-W en La Palma del Condado (Huelva): nota previa. Mem Mus Labor Miner Geol Fac Cien Porto 1:249–273

Sáez R, Almodóvar GR, Pascual E (1988) Mineralizaciones estratoligadas de scheelita en la Faja Pirítica del Suroeste Ibérico. Bol Soc Españ Miner 11, 1, 135–141

Sáez R, Requena A, Fernández-Caliani JC, Almodóvar GR (1989) Control estructural de las mineralizaciones de Sn-W-As del bajo Corumbel La Palma del Condado Huelva. Stvdia Geologica Salmanticensia 4, 189–203

Sáez R, Almodóvar GR, Pascual E (1996) Geological constraints on massive sulfide genesis in the IPB. Ore Geol Rev 11:429–451

Sáez R, Pascual F, Toscano M, Almodóvar GR (1999) The Iberian type of volcano-sedimentary massive sulfide deposits. Miner Depos 34, 549–570

Sánchez-España J, Velasco F, Yusta I (2000) Hydrothermal alteration of felsic volcanic rocks associated with massive sulphide deposition in the northern IPB (SW Spain). Appl Geochem 15, 1265–1290

Sánchez-España J, Velasco F, Boyce AJ, Fallick AE (2003) Source and evolution of ore-forming fluids in northern IPB massive sulphide deposits (SW Spain): evidence from fluid inclusions and stable isotopes. Miner Depos 38:519–537

Santos Bonaño A, Contreras Vázquez F (1983) Mapa Geológco de España, E/1:50,000, Sheet 959: Calañas. Instituto Geológico y Minero de España, 1–87

Santos Bonaño A, Feanández Alonso A, Quesada C (1982) Mapa Geológco de España, E/1:50,000, Sheet 958: Puebla de Guzmán. Instituto Geológico y Minero de España, 1–57

Sato T (1972) Behaviours of ore forming solutions in seawater. Min Geol 22, 31–42

Schermerhorn L (1971) An outline stratigraphy of the IPB. Bol Geol Min España, 82/ 3–4, 239–268

Schütz, W., Ebneth, J., Meyer, K.D., 1987. Trondhjemites, tonalites and diorites in the South Portuguese Zone and their relations to the vulcanites and mineral deposits of the Iberian Pyrite Belt. Geologische Rundschau, 76(1), 201–212.

Serranti S, Ferrini V, Masi U, Cabri LJ (2002) Trace-element distribution in cassiterite and sulfides from rubané and massive ores of the Corvo deposit Portugal. Canad Mineral 40, 815–835

Silva JB (1989) Estrutura de uma geotransversal da Faixa Piritosa Vale do Guadiana, Estudo de tectónica pelicular em regime de deformação não coaxial. Tese Doutoramento Fac Cienc Univ Lisboa

Silva JB, Oliveira JT, Ribeiro A (1990) Structural outline of the South Portuguese Zone. In: Dallmeyer RD, Martínez García (eds) Pre-Mesozoic geology of Iberia. Berlin Springer-Verlag: 348–362.6

Silva, J.B., Pereira, F., Chichorro, M., 2013. Estrutura das áreas internas da Zona Sul Portuguesa, no contexto do Orógeno Varisco. In: Dias, R., Araujo, A., Terrinha, P., Kullberg, J.C. (Eds.), Geologia de Portugal, Chapter II.2.8. Escolar Editora, Lisboa, pp. 767–786.

Simancas JF, Tahiri A, Azor A, González Lodeiro F, Martínez Poyatos D, El Hadi H (2009) The tectonic frame of the Variscan-Alleghanian orogen in southern Europe and northern Africa. Tectonophysics 398, 181–198

Solá AR, Salgueiro R, Pereira Z, Matos JX, Rosa C, Araújo V, Neto R, Lains JA (2015) Time span of the volcanic setting of the Neves-Corvo VMS deposit. Abs X Cong Iber Geochim 122–125

Solomon M, Quesada C (2003) Zn-Pb-Cu massive sulfide deposits: Brine-pool types occur in collisional orogens, black smoker types occur in back arc and/or arc basins. Geology 31, 12, 1029–1032

Solomon M, Tornos F, Gaspar OC, Inverno C (2000) Construction of the massive pyritic ore deposits of the IPB: an explanation involving brine pools sulfur deficient ore fluids and tin granites. In: Gemmell J B, Pongratz J (eds) Volcanic environments and massive sulfide deposits Program and Abstracts. CODES Hobart, 201–202

Strauss GK, Madel J (1974) Geology of massive sulfide deposits in the Spanish-Portuguese Pyrite Belt. Geol Rundsch 63, 191–211

Strauss GK, Roger G, Lécolle M, Lopera E (1981) Geochemical and geologic study of the volcano-sedimentary sulfide orebody of La Zarza Huelva Province Spain. Econ Geol 76, 1975–2000

Sun S, Nesbitt R (1977) Chemical heterogeneity of the Archaean mantle composition of the earth and mantle evolution. Earth Planet Sci Lett 35, 429–448

Thiéblemont D, Pascual E, Stein G (1998) Magmatism in the IPB: petrological constraints on a metallogenic model. Miner Depos 33, 98–110

Tornos F (2006) Environment of formation and styles of volcanogenic massive sulfides: the IPB. Ore Geol Rev 28, 259–307

Tornos F, Spiro B (1999) The genesis of shale-hosted massive sulfides in the IPB. In: Stanley et al (eds) Mineral Deposits: Processes to Processing, Rotterdam Balkema: 605–608

Tornos F, González Clavijo E, Spiro BF (1998) The Filon Norte orebody (Tharsis IPB): a proximal low-temperature shale-hosted massive sulphide in a thin-skinned tectonic belt. Miner Depos 33, 150–169

Tornos F, Barriga FJAS, Marcoux E, Pascual E, Pons JM, Relvas, JMRS, Velasco F (2000) The IPB. In: Large R, Blundell D (eds) GEODE database on global VMS districts. Centre for Ore Deposit Research (CODES) Hobart Australia, Univ Tasmania, 19–52

Tornos F, Casquet C, Relvas JMRS, Barriga FJAS, Sáez R (2002) The relationship between ore deposits and oblique tectonics: the SW Iberian Variscan belt. In: Blundell DJ, Neubauer F, von Quadt A (eds) The timing and location of major ore deposits in an evolving orogeny. Geol Soc London Spec Pub 204, 179–198

Tornos F, Casquet C, Relvas JMRS (2005) Transpressional tectonics lower crust decoupling and intrusion of deep mafic sills: a model for the unusual metallogenesis of SW Iberia. Ore Geol Rev 27, 133–163

Tornos F, Velasco F, Slack JF, Gómez C (2017) The high-grade Las Cruces copper deposit Spain: a product of secondary enrichment in an evolving basin. Miner Depos 52, 1–34

Almodóvar GR, Sáez R, Pons J, Maestre A, Toscano, M, Pascual, E (1998) Geology and genesis of the Aznalcóllar massive sulphide deposits, IPB, Spain. Mineral Deposita 33, 111–136

Toscano M, Almodóvar R, Sáez R (1993) Hydrothermal alteration related to the "Masa Valverde" massive sulphide deposit IPB Spain. In: Fenoll Hach-Ali P, Torres-Ruiz J, Gervilla F (eds) Current Research in Geology applied to Ore Deposits Granada, 389–392

Valenzuela A, Donaire T, Pin Ch, Toscano M, Hamilton MA, Pascual E (2011) Geochemistry and U–Pb dating of felsic volcanic rocks in the Riotinto–Nerva unit, IPB, Spain: crustal thinning, progressive crustal melting and massive sulphide genesis. J Geol Soc, London, 168, 717–731

Wood DA, Tarney J, Varet J, Saunders AD, Bougault H, Joron JL, Trenil M, Cann, JR (1979) Geochemistry of basalts drilled in the North Atlantic by IPOD Leg 49: implications for mantle heterogeneity. Earth Planet Sci Lett 42, 77–97

The Finisterra-Léon-Mid German Cristalline Rise Domain; Proposal of a New Terrane in the Variscan Chain

7

N. Moreira, J. Romão, R. Dias, A. Ribeiro, and J. Pedro

Abstract

This chapter characterizes the Finisterra Terrane, enhancing its differences from the neighbouring Iberian Terrane. The contact between these terranes is the Porto-Tomar-Ferreira do Alentejo Shear Zone, a major lithospheric structure whose complex Variscan evolution remains debatable. The lithostratigraphic, tectono-metamorphic and magmatic features observed in the Finisterra Terrane show that it was an independent terrane during the Devonian. This situation changed during the Mississippian, when the main features of the Finisterra and the Iberian Terranes became similar, which indicates that both terranes evolved together since the Carboniferous times. The similarities of the Finisterra Terrane with the Central European Variscan domains, namely the Léon Block and the Mid-German Crystalline Rise, enable us to propose a new tectono-stratigraphic terrane (Finisterra-León-MGCR Terrane), which defines an arcuate pattern compatible with the Ibero-Armorican Arc.

Coordinator: N. Moreira.

N. Moreira (✉) · R. Dias · J. Pedro
Earth Sciences Institute (ICT), Pole of the Évora University and Departamento de Geociências ECTUE, Rua Romão Ramalho, nº 59, 7000-671 Évora, Portugal
e-mail: nmoreira@estremoz.cienciaviva.pt

R. Dias
e-mail: rdias@uevora.pt

J. Pedro
e-mail: jpedro@uevora.pt

N. Moreira · R. Dias
Laboratório de Investigação de Rochas Industriais e Ornamentais da Escola de Ciências e Tecnologia, Universidade de Évora (LIRIO-ECTUE), Convento das Maltezas, 7100-513 Estremoz, Portugal

J. Romão
Laboratório Nacional de Energia e Geologia, UGCG, Estrada da Portela, Apartado 7586—Zambujal, 2720 Alfragide, Portugal
e-mail: manuel.romao@lneg.pt

A. Ribeiro
Museu Nacional de História Natural e da Ciência, Departamento de Geologia, Faculdade de Ciências, Instituto Dom Luiz (IDL), Edifício C6, Piso 4, Campo Grande, 1749-016 Lisbon, Portugal
e-mail: aribeiro@fc.ul.pt

7.1 Introduction

The Iberian Massif presents a well-developed arcuate pattern, in close relationship with the genesis of the Ibero-Armorican Arc (Fig. 7.1a; Dias et al. 2016). Its internal domains, with a WNW-ESE to NW-SE general trend (e.g. Dias et al. 2013; Moreira et al. 2014), are westerly interrupted by one of the most important Iberian Variscan structures, the Porto-Tomar-Ferreira do Alentejo shear zone (Fig. 7.1b; PTFSZ). The geodynamic interpretation of this shear zone, with polyphase tectonic deformation, is controversial. Indeed, it has been interpreted as an active lithospheric-scale shear zone since the early Devonian (Dias and Ribeiro 1993), possibly reactivating an older structure (Cadomian?) (Ribeiro et al. 2007, 2013). However, an alternative interpretation suggests that the PTFSZ has been active only during the Mississippian as a dextral transcurrent shear zone (Pereira et al. 2010; Martínez Catalán 2011; Gutiérrez-Alonso et al. 2015).

Whatever the meaning of the PTFSZ, it is clear that PTFSZ marks a major boundary between a western crustal block—Finisterra Block—and the adjacent Central Iberian (CIZ) and Ossa-Morena (OMZ) Zones, both from Iberian Terrane (Fig. 7.1b; Ribeiro et al. 2007), each one with distinct geological features and geodynamical evolution, at least, during the Palaeozoic. This work presents a geological overview of the western block of PTFSZ, which has been used as the base to discuss and propose the Finisterra Block as a new terrane in the Iberian Variscides. The geological affinities between this block, the Léon Block and Mid German Crystalline Rise seems to indicate an independent terrane within the Variscan Chain.

C. Quesada and J. T. Oliveira (eds.), *The Geology of Iberia: A Geodynamic Approach*, Regional Geology Reviews,
https://doi.org/10.1007/978-3-030-10519-8_7

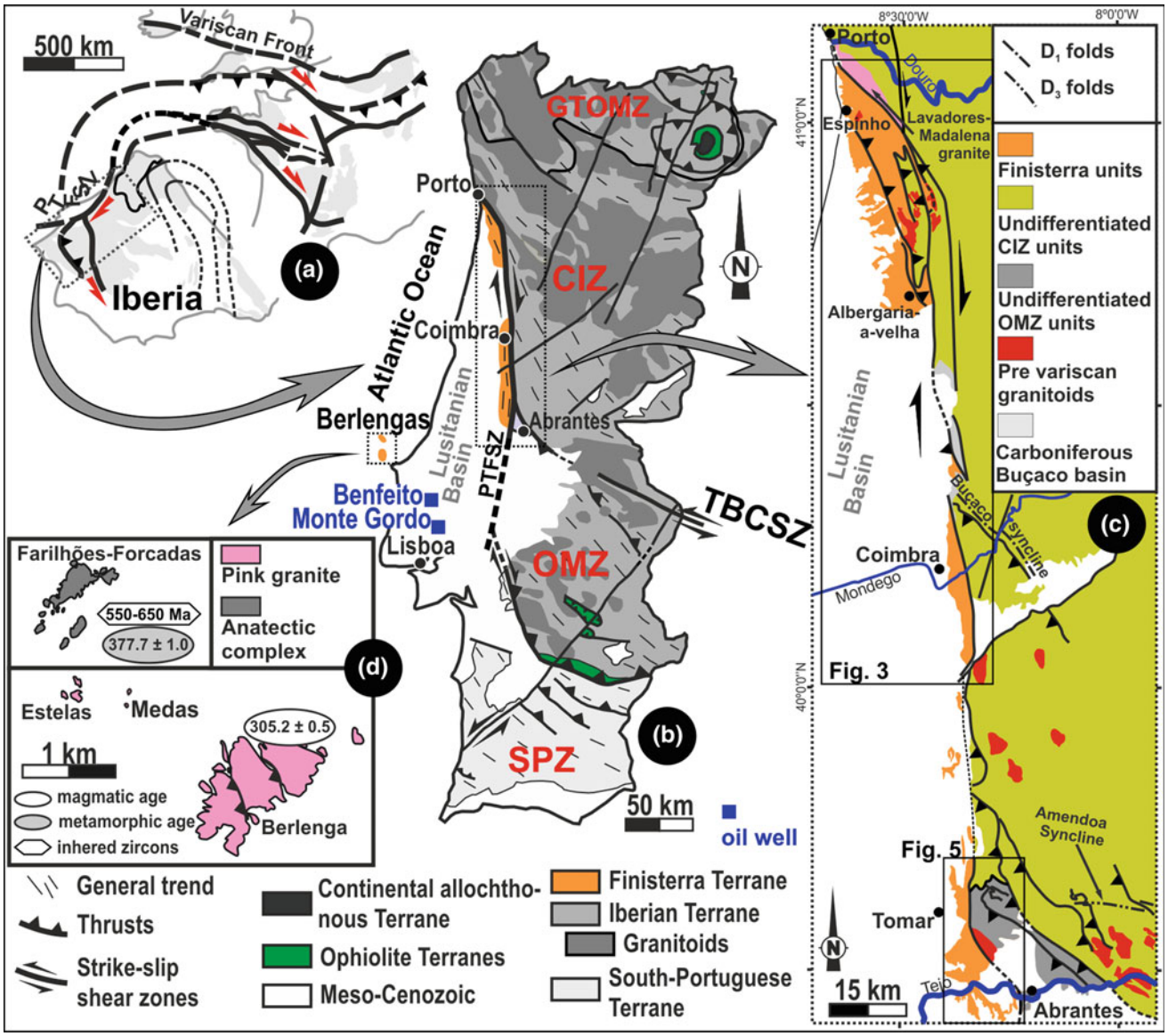

Fig. 7.1 The Finisterra block in the context of the Iberian Variscides: **a** The Ibero-Armorican arc (adapted from Dias et al. 2016); **b** General overview of Finisterra block (adapted from Ribeiro et al. 2013); **c** The Finisterra outcrops in the vicinity of PTFSZ (adapted from Chaminé et al. 2003a; Romão et al. 2014, 2016; Moreira 2017); **d** The Berlengas archipelago geological features (adapted from Bento dos Santos et al. this volume)

7.2 Tectonostratigraphy of the Finisterra Bock

West of the PTFSZ, low and high-grade tectonostratigraphic units are defined in four sectors (Porto-Espinho-Albergaria-a-Velha, Coimbra, Abrantes-Tomar and Berlengas Archipelago; Fig. 7.1c, d; Chaminé et al. 2003a, b; Ferreira Soares et al. 2007; Ribeiro et al. 2013; Romão et al. 2013, 2016; Moreira et al. 2016a, b; Bento dos Santos et al. this volume). The continuity between these sectors is not observable due to the overlying Meso-Cenozoic sedimentary cover (Fig. 7.1b). An overview of the tectonostratigraphic succession of these sectors is shown in Fig. 7.2.

7.2.1 The Porto-Espinho-Albergaria-a-Velha and Coimbra Sectors

Four pre-Mesozoic tectonostratigraphic units were defined between Porto, Albergaria-a-Velha and Coimbra (Figs. 7.2 and 7.3; Chaminé 2000; Chaminé et al. 2003a, b; Pereira

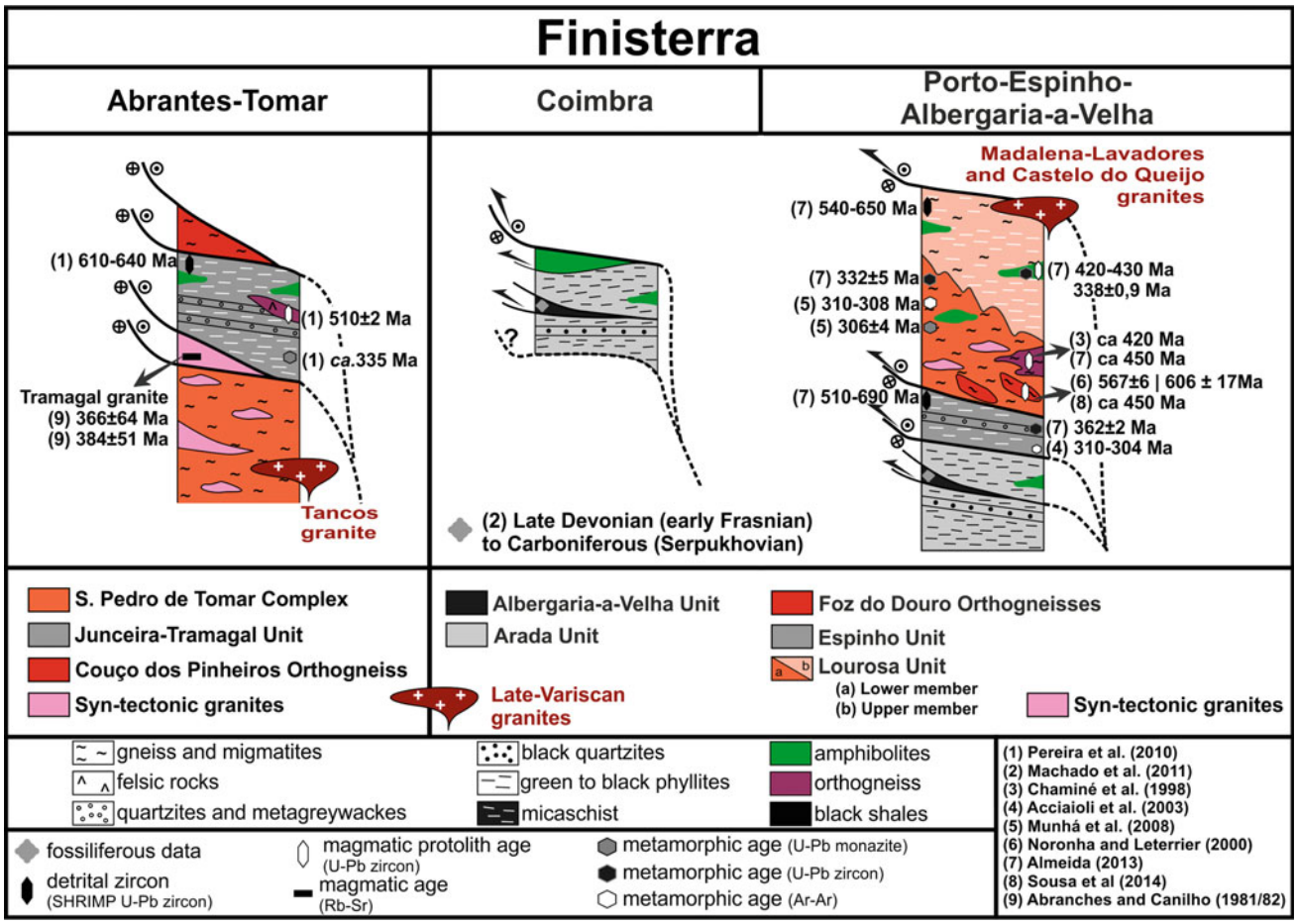

Fig. 7.2 Simplified tectonostratigraphic successions of Finisterra sectors (see references in the text)

et al. 2007; Machado et al. 2008, 2011; Ribeiro et al. 2013). The boundaries between these units are always Variscan shear zones.

7.2.1.1 Lourosa Unit

Two members were individualized in the Lourosa Unit (Fig. 7.2): the lower member mostly composed of migmatites, ortho- and paragneisses and the upper member dominated by (garnet-)biotite-micaschists (Chaminé 2000; Chaminé et al. 2003a). This high-grade unit is considered of Neoproterozoic in age (Chaminé 2000), but this age appears to be doubtful according to more recent data. Indeed, detrital zircon population obtained in a granite and a paragneiss from this unit provided a Lower Cambrian to Ediacarian para-derived protolith age (540–650 Ma; U–Pb in zircon, LA–ICP–MS), however some Upper Cambrian-Ordovician to Devonian zircons were also recognized (Fig. 7.4a; Almeida 2013; Almeida et al. 2014). The younger ages may result from analytical problems, U–Pb re-equilibrium during high temperature (HT) metamorphism or, alternatively, may indicate Palaeozoic ages of some of the para-derived lithotypes. Furthermore, the granite and paragneiss inhered zircon populations are distinct (Almeida 2013): while the paragneiss contains Mesoproterozoic populations, in the granite such ages are absent (Fig. 7.4a). This difference has paleogeographic importance and will be discussed.

Both members have (olivine-)amphibolites and amphibolic schists with geochemical signature similar to within-plate to MORB basalts (Montenegro de Andrade 1977; Silva 2007; Aires and Noronha 2010) and some orthogneisses. Lower Devonian protolith ages were obtained for mafic amphibolite (392 ± 2 Ma; U–Pb, LA–ICP–MS in zircons; Almeida et al. 2014), although older concordant ages were also obtained in these ortho-derived rocks (ca. 420–430 Ma; Almeida 2013). Therefore, Silurian-Devonian ages could be ascribed to these amphibolites or at least part of them. Concerning the orthogneisses, several ages were obtained for their protolith: Ordovician (459 ± 7 Ma; U–Pb, LA–ICP–MS in zircon; Almeida 2013), Silurian (420 ± 4 Ma in Lourosela and 419 ± 4 Ma in Souto Redondo; U–Pb, TIMS in zircon; Chaminé et al. 1998) and Upper Devonian-Mississippian (353 ± 10 Ma; U–Pb, LA–

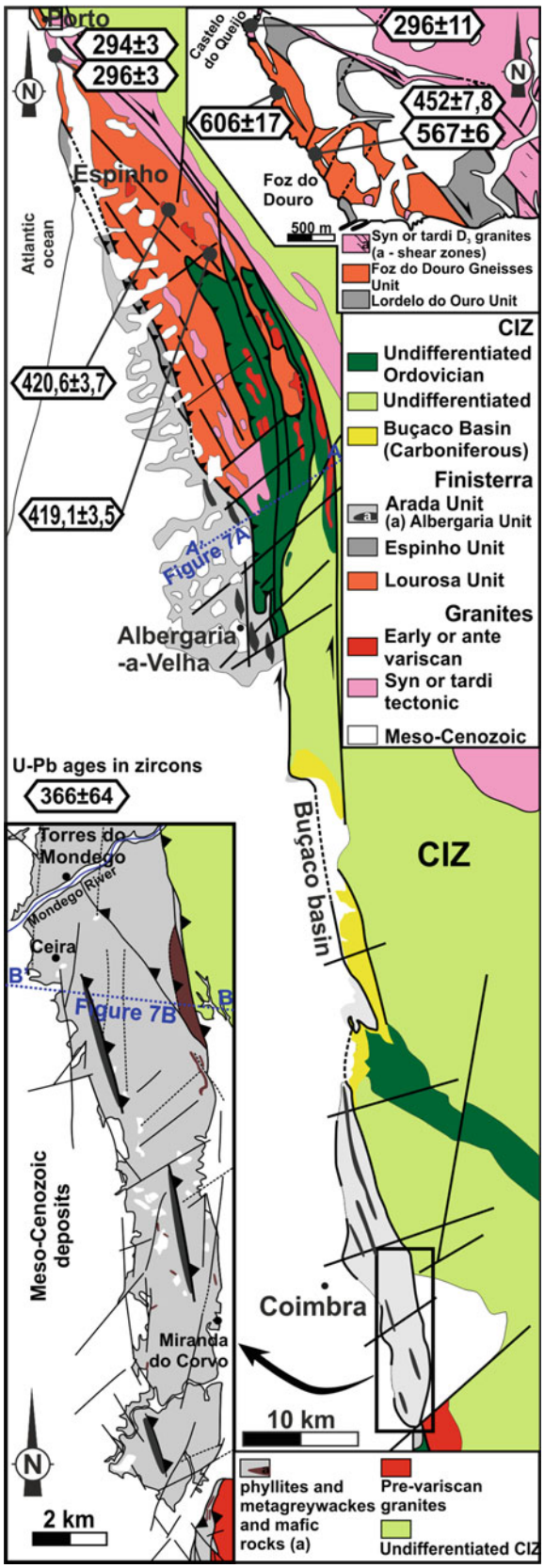

Fig. 7.3 Simplified geological map and geochronological data for the Porto-Espinho-Albergaria-a-Velha and Coimbra sectors (blue lines correspond to the cross sections of Figs. 7A, 7B; adapted from Chaminé et al. 2003a; Ferreira Soares et al. 2005; Pereira et al. 2007; LNEG 2010; Machado et al. 2011; Dinis et al. 2012)

ICP–MS in zircons; Almeida 2013). Mississippian metamorphic ages were obtained in a gneiss and an amphibolite (332 ± 5 Ma and 339 ± 1 Ma; U–Pb in zircons—SHRIMP and LA–ICP–MS respectively; Almeida 2013).

7.2.1.2 Foz Do Douro Gneissic Unit

The Foz do Douro Gneissic Unit comprises tonalitic and granitic ortogneisses with intercalations of mylonites, paragneisses, micaschists and amphibolites. The amphibolites have tholeiitic MORB geochemical affinity (Noronha and Leterrier 1995, 2000) and their Sm–Nd isotopic fingerprint suggest a Mesoproterozoic model age (TDM; ca. 1050 Ma; Noronha and Leterrier 2000). This unit is considered a geological equivalent of the Lourosa Unit described above, based on its lithological, geochemical and structural features (Chaminé et al. 2003a).

The oldest record of magmatism in the Finisterra Block has been reported in the orthogneisses of this unit (Fig. 7.2), namely an Ediacarian age for its protoliths (567 ± 6 Ma in biotitic orthogneiss and 606 ± 17 Ma in augen felsic gneisses; U–Pb, isotopic dilution in zircons; Noronha and Leterrier 2000). However, more recently, the protolith of the biotitic orthogneiss was re-evaluate, yielding an Upper Ordovician age (452 ± 8 Ma; U–Pb, SHRIMP in zircons; Sousa et al. 2014), leaving room to protolith age uncertainties.

The eastern boundary of Foz do Douro Gneissic Unit is underlined by a contact with a narrow band of micaschists and quartz-tectonites (locally named Lordelo do Ouro Unit; Fig. 7.3), which is affected by a pervasive dextral shearing, being considered as the local expression of the PTFSZ (Ribeiro et al. 2009). The strong similarities between the Lordelo do Ouro Unit and the micaschists interlayered in the Foz do Douro Gneisses Unit indicate that both units are part of the Finisterra Block.

NW-SE trending late-tectonic Variscan granites (Castelo do Queijo and Lavadores-Madalena) intrude the northernmost boundary of the Lourosa Unit and the Foz do Douro Gneissic Unit (Fig. 7.3; Chaminé et al. 2003a; LNEG 2010). This magmatism is Late Carboniferous—Permian in age: 296 ± 11 Ma for the Castelo do Queijo granite (U–Pb, LA–ICP–MS in zircons; Martins et al. 2014) and 296 ± 3 Ma (U–Pb, LA–ICP–MS in zircons), 294 ± 3 Ma (U–Pb, SHRIMP in zircons) and 298 ± 11 Ma (U–Pb, isotopic dilution in zircons) for the Lavadores-Madalena granite (Martins et al. 2011, 2014).

7.2.1.3 Espinho Unit

The Espinho Unit outcrops to the West of the Lourosa Unit (Fig. 7.3) and it is composed of a narrow band of staurolite-garnet-biotite micaschists, locally with intercalations of (mylonitic garnet-)quartzites (Fig. 7.2; Chaminé 2000; Chaminé et al. 2003a). Two HT metamorphic events

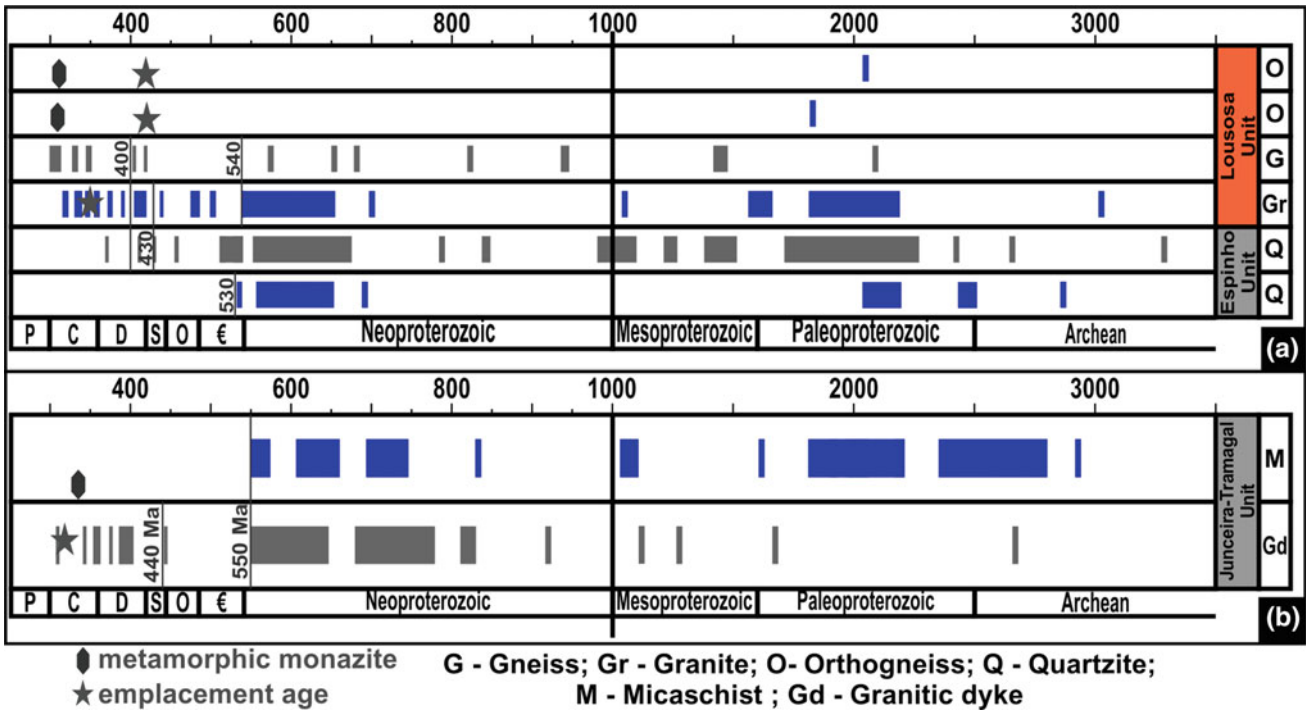

Fig. 7.4 Simplified pattern of the zircon populations of Finisterra sectors (the grey colours outline the samples with Mesoproterozoic populations): **a** Lourosa and Espinho Units (geochronological data from Chaminé et al. 1998; Almeida 2013; Almeida et al. 2014); **b** Junceira-Tramagal Unit ($^{207}Pb/^{206}Pb$ ages obtained by Pereira et al. 2010)

are recorded in the paragenesis of garnet quartzites: the first reaches the sillimanite zone while in the second one the staurolite zone was attained (Fernández et al. 2003).

Geochronological data recovered from the quartzites (U–Pb, LA–ICP–MS in zircons; Almeida 2013; Almeida et al. 2014) indicate a Lower Cambrian protolith age (510–690 Ma is the youngest population of inhered zircons). However, as in the Lourosa Unit, Ordovician and Silurian-Devonian ages were also obtained in zircons displaying detrital morphologies (Fig. 7.4a; Almeida 2013; Almeida et al. 2014). These data may be biased by the same reasons as those described for the Lourosa Unit. Some quartzites do not present Mesoproterozoic zircon populations, while in others such populations are representative (Fig. 7.4a), as it was also emphasized in Lourosa Unit.

An Upper Devonian metamorphic event (362 ± 2 Ma; U–Pb LA–ICP–MS in zircon) is recorded in the mentioned quartzite layers (Almeida 2013; Almeida et al. 2014).

7.2.1.4 Arada Unit

This unit (Fig. 7.3) is composed of black to green phyllites, metagreywackes, black quartzites and mafic rocks with a tholeiitic geochemical fingerprint (Silva 2007), which are affected by chlorite-biotite zone metamorphism (Ferreira Soares et al. 2007). The lithological resemblances of this unit with the Ediacarian "Série Negra" of the OMZ have been proposed by some authors (Beetsma 1995; Chaminé 2000; Chaminé et al. 2003a; Ferreira Soares et al. 2007; Pereira et al. 2007). However, the absence of the black chert (flint) horizons, typical of the "Série Negra", is assumed to represent a distinct feature of the Arada Unit. The age of this lithological succession is open to debate, although it is considered as Neoproterozoic (Beetsma 1995; Chaminé 2000; Ferreira Soares et al. 2007).

7.2.1.5 Albergaria Unit

The Albergaria Unit crops out as narrow bands within the Arada unit (Figs. 7.2 and 7.3; Chaminé et al. 2003b). It is composed of very low-grade (low anchizone; Chaminé et al. 2003b) black shales and siltstones, which yielded Laurussia-akin acritarch assemblages of Frasnian-Serpukhovian age (Chaminé et al. 2003b; Machado et al. 2008, 2011). This unit is tectonically deformed by a single deformation episode while the older Arada Unit is deformed by two episodes. This fact combined with the distinct metamorphism shown by these units indicates the existence of an unconformity between them. Both units were tectonically imbricated during Pennsylvanian.

7.2.2 The Abrantes-Tomar Sector

In the Abrantes-Tomar sector, a N-S to NNW-SSE elongate high-grade tectonostratigraphic succession was recently defined (Fig. 7.5; Romão et al. 2013, 2016; Moreira et al. 2016a, b; Moreira 2017). The contact between the tectonostratigraphic units is always underlined by Variscan shear zones.

7.2.2.1 Pedro de Tomar Complex

The S. Pedro de Tomar Complex represents the basal unit of the Abrantes-Tomar sector. To the East, this complex contacts with the Junceira-Tramagal Unit, while to the West it is covered by the Meso-Cenozoic formations (Fig. 7.5). This complex is characterized by medium to fine-grained strongly deformed para- and ortho-gneisses, interlayered with micaschists, mylonites and migmatites. The most representative lithotypes are paragneisses with sillimanite zone metamorphism (Fig. 7.6a). The orthogneisses are generally less deformed and clearly related to the anatexis and melting of para-derived rocks. The feldspars present undulose extinction and dynamic recrystallization which, coupled with the presence of sillimanite, suggests minimum temperatures around 500–600 °C (Passchier and Trouw 2005; Bucher and Grapes 2011). Some gneisses result from migmatitic processes superimposed by a strong high-strain dextral shearing, giving rise to the gneissic foliation.

The protolith and metamorphic ages of these gneisses and migmatites are uncertain, being considered respectively of Neoproterozoic and Mississippian in age when compared with the overlying Tramagal-Junceira Unit (see below).

The high-grade tectonostratigraphic units are intruded by the syn-tectonic N-S elongated Tramagal and Casal Pinheiro granites (Romão et al. 2013, 2016; Moreira 2017). These are two mica granites with tourmaline and sillimanite, which indicates their peraluminous character and anatetic nature (e.g. Clarke 1981; Pesquera et al. 2012). A Mississippian emplacement age is assumed to these granites, because they are controlled by the second deformation episode, showing hot-plastic dextral shearing coeval of their crystallization (Fig. 7.6c). The field data are in accordance with inaccurate geochronological data of Tramagal granite (366 ± 64 Ma and 384 ± 51 Ma; Rb/Sr method, respectively in whole rock and in biotite; Abranches and Canilho 1981/82).

A post-tectonic porphyritic two-mica granite, not affected by ductile deformation, intrudes the S. Pedro de Tomar Complex (Fig. 7.5; Tancos Granite). Geochronological data shows an Early Permian age to its cooling based on K–Ar (294 ± 5 Ma, biotite and 290 ± 2 Ma, muscovite; Neves et al. 2007) and Rb–Sr (312–293 Ma, biotite; Mendes 1967/68) methods.

7.2.2.2 Junceira-Tramagal Unit

The Junceira-Tramagal Unit crops out in a narrow N-S to NNW-SSE 40 km long band from Ferreira do Zêzere to Tramagal (Fig. 7.5). This unit is composed of garnet and staurolite-garnet micaschists, subordinate metagreywackes, metaquartzwackes and black schists. Early HT (Variscan?) migmatization occurs near the Tramagal Granite and this migmatization could derive from the palingenesis of older deformed (Cadomian?) migmatites, also displayed in the Neoproterozoic units of the OMZ East of Abrantes (Henriques et al. 2015). The micaschists paragenesis is dominated by biotite + muscovite + quartz + plagioclase + opaque minerals ± K-feldspar. Millimetric to centimetric garnet and staurolite porphyroblasts were generated during the metamorphic peak conditions, being ascribed to the amphibolite facies (staurolite zone; Fig. 7.6b).

Geochronological data (U–Pb, LA–ICP–MS in zircons; Pereira et al. 2010) indicate an Ediacarian protolith age for the para-derived lithotypes of the Junceira-Tramagal Unit (550–660 Ma is the most recent population of inhered zircons) and a Mississippian metamorphic episode (ca. 335–330 Ma). Neoproterozoic (700–750 and ca. 830 Ma) Mesoproterozoic (1050–1150 Ma), Paleoproterozoic (ca. 1650 and 1880–2200 Ma) and Paleoproterozoic-Archean (2350–2900 Ma) inhered zircon populations were also found (Fig. 7.4b).

Ortho-derived lithotypes are also found in this unit, namely:

- Amphibolite dykes with green amphibole + plagioclase + opaque minerals ± quartz, typical of the amphibolite facies, and with unknown age;
- Quartz-feldspatic orthogneisses, sometimes with mylonitic textures, interpreted as the result of the tectono-metamorphism affecting felsic-rich rocks (pegmatitic dykes?), present Lower Cambrian protolith ages (510.3 ± 2.0 Ma; U–Pb, LA–ICP–MS in zircons; Fig. 7.5; Pereira et al. 2010);
- (Micro-)granitic dykes, less deformed than the quartz-feldspatic orthogneisses and cutting the gneissic foliation, with Pennsylvanian age (318.7 ± 1.2 Ma; U–Pb, LA–ICP–MS in zircons; Pereira et al. 2010). Several zircon populations were found in this granite dyke (Fig. 7.4a), with emphasis on the Silurian-Carboniferous (ca. 350–420 Ma) and the Mesoproterozoic (ca. 1100, 1270 Ma) ages.

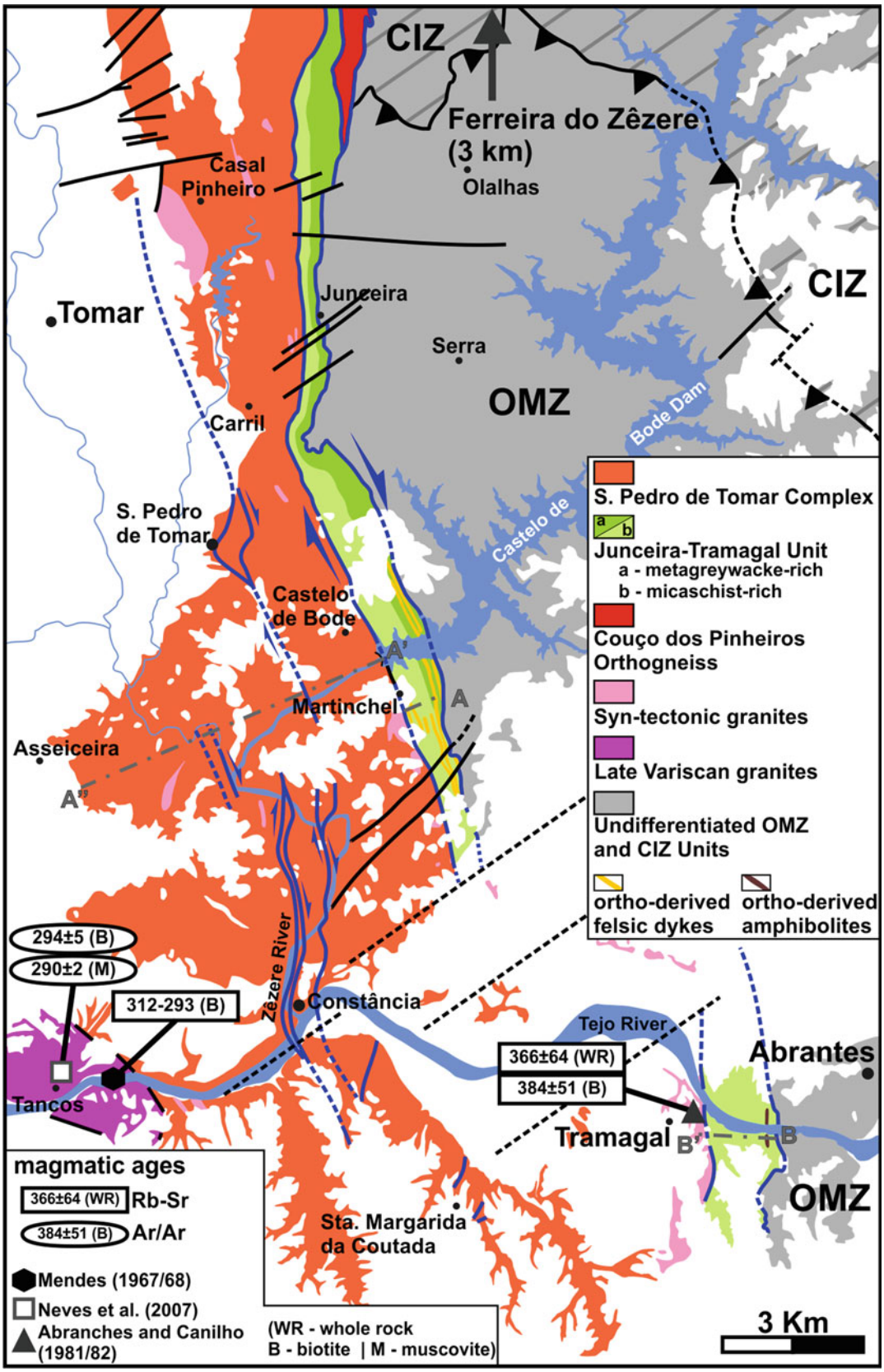

Fig. 7.5 Simplified geological map of the Abrantes-Tomar sector and published geochronological ages (grey lines show the location of the Fig. 7.7c cross sections)

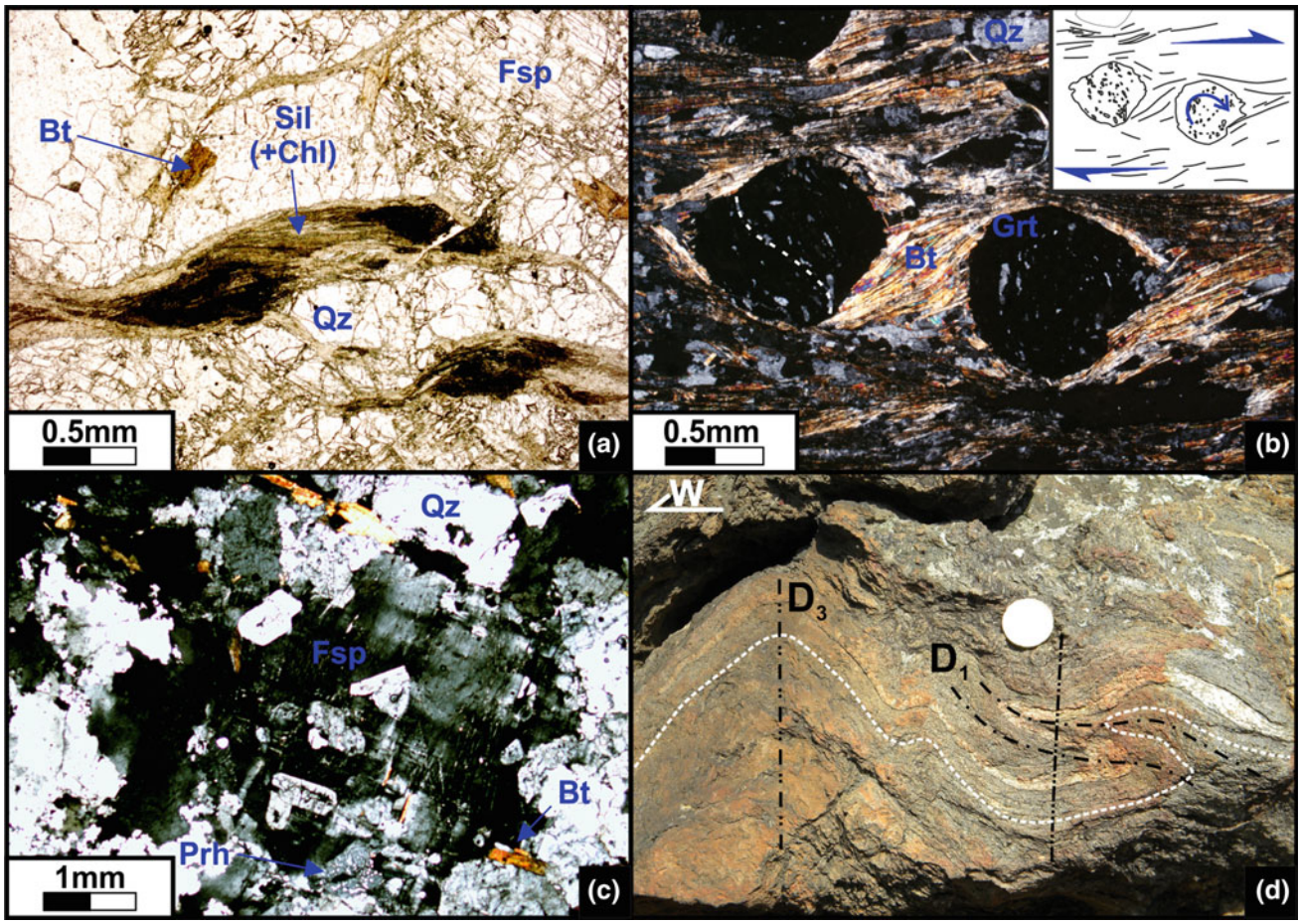

Fig. 7.6 Petrographic and structural representative features of the Abrantes-Tomar sector (Bt—biotite; Sil—sillimanite; Chl—chlorite; Fsp—feldspar; Qz—quartz; Grt—garnet; Prh—perthite): **a** Sillimanite partially retrograded to chlorite in gneisses of the S. Pedro de Tomar Complex (parallel nicols); **b** Syn-tectonic poikilitic garnets in micaschists of the Junceira-Tramagal Unit, showing dextral synthetic spinning (crossed nicols); **c** Deformed plagioclase crystal of the Tramagal Granite (crossed nicols); **d** Refolded D_1 recumbent fold in micaschists of the Junceira-Tramagal Unit

7.2.2.3 Couço Dos Pinheiros Orthogneiss

The Couço dos Pinheiros Orthogneiss is a strongly stretched N-S body (Fig. 7.5), whose gneissic texture is composed of millimetric-thick felsic-rich layers (quartz and feldspars *s.l.*) and iron-magnesium rich silicates. The presence of sigma shaped K-feldspar porphyroblasts and strongly stretched quartz ribbons indicate an intense ductile dextral deformation. The gneiss is intruded by less deformed felsic coarse-grained dykes, possibly with similar ages to those described in the micro-granitic dykes cutting the Junceira-Tramagal Unit.

The origin and age of the Couço dos Pinheiros Orthogneiss is unknown. The petrographic and structural similarities with the S. Pedro de Tomar Complex suggest a pre-orogenic origin for this orthogneiss and a Neoproterozoic-Lower Cambrian age could be considered. However, an Ordovician to Devonian age should not be excluded, because similar ages were obtained in the pre-orogenic magmatism of northern Finisterra sectors previously described.

7.2.3 The Berlengas Archipelago Sector

The Berlengas Archipelago is composed of granites, gneisses and micaschists. It was considered a "suspect" terrane due its position W of the Lusitanian Basin (Fig. 7.1b; Ribeiro et al. 1991). The similarities with the lithotypes of Abrantes-Tomar sector led us to consider this archipelago as part of the Finisterra Block. In the Farilhões and Forcadas islands outcrops an anatectic complex with gneisses, migmatites and micaschists, while in the Berlengas, Estelas and

Medas islands a pink granite is the most representative lithotype (Fig. 7.1d; Valverde Vaquero et al. 2010a, b; Bento dos Santos et al. this volume).

The Farilhões metatexites highlight a HT metamorphism (sillimanite zone) with Upper Devonian age (377 ± 1 Ma; U–Pb, TIMS in monazites; Valverde Vaquero et al. 2010a, b; Bento dos Santos et al. this volume). Some relics in these metatexites show previous prograde metamorphism reaching granulite facies (P = 8.6 ± 1 kbar; T = 915 ± 50 °C; Bento dos Santos et al. 2010; this volume). Inhered zircon populations indicate a Neoproterozoic para-derived protolith (Bento dos Santos et al. this volume).

The Berlengas granite (Fig. 7.1d) was initially considered of Permian age (280 ± 15 Ma; $^{87}Rb/^{86}Sr$ in whole rock; Priem et al. 1965), but recent geochronological data indicates a Pennsylvanian age (307.4 ± 0.8 Ma; U–Pb, ID–TIMS in monazite and zircon; Valverde Vaquero et al. 2010a, b), being only affected by Tardi-Variscan deformation (Fig. 7.1d; Ribeiro et al. 1991; Dias et al. 2017a).

7.3 Structure and Metamorphism

The sectors described above share a common structural framework characterized by a predominant N-S Variscan trend parallel to the PTFSZ, with NNW-SSE deflections in the vicinity of Porto and Abrantes (Fig. 7.1c). The Abrantes inflection, between Martinchel and Tramagal (Fig. 7.5), is related to a deca-kilometric-scale sheath fold that resulted from the interaction between the Tomar-Badajoz-Cordoba Shear Zone (TBCSZ) and the PTFSZ (Ribeiro et al. 2009; Moreira et al. 2011, 2013). The Porto inflection is ascribed to the strike irregularities of the PTFSZ, which generated a restraining band (Ribeiro et al. 2013). Both inflections are compatible with an early activity of the PTFSZ, at least since the beginning of the Variscan Orogeny (Dias and Ribeiro 1993).

Two ductile Variscan deformation episodes (D_1 and D_2) are interpreted as a progressive tectonic process (Ribeiro et al. 1995; Chaminé 2000; Ribeiro et al. 2013) that affects all sectors and units, with the exception of the younger Albergaria Unit, which does not show the D_1 episode (Ribeiro et al. 2013). Frequently, the D_1 and D_2 ductile structures are overprinted by a brittle to brittle-ductile deformation event (D_3).

The D_1 episode consists of recumbent West quadrant facing folds, with low dipping hinges and a pervasive S_1 foliation, being expressed in all the Finisterra sectors (Figs. 7.6d and 7.7; Pereira et al. 1980, 2007; Ribeiro et al. 1980, 1995, 2013; Chaminé 2000; Ferreira Soares et al. 2007; Moreira et al. 2016a; Moreira 2017). Several features are considered coeval with the D_1 tectonic episode:

- The extremely flattened garnets in the Espinho Unit developed in the HT sillimanite zone (P = 4–5 kbar; T = 700 ± 50 °C; Fernández et al. 2003);
- The early metamorphic ages in the same unit (ca. 360 Ma; Almeida et al. 2014);
- The early HT migmatites in the Abrantes-Tomar sector (Moreira 2017);
- The sillimanite zone metamorphism of the Farilhões migmatites (ca. 380 Ma; Bento dos Santos et al. this volume);
- The Upper Silurian-Devonian magmatism of Lourosa Unit (ca. 420 Ma; Chaminé et al. 1998);
- The Late Silurian-Devonian metamorphic overgrowths in inherited zircon (Fig. 7.4; Pereira et al. 2010; Almeida et al. 2014).

This event took place before the deposition of the Frasnian-Serpukhovian black shales of the Albergaria Unit where D_1 structures are absent (Ribeiro et al. 2013). However, a previous Cadomian episode cannot be excluded (Ferreira Soares et al. 2007; Ribeiro et al. 2013).

The D_2 episode is marked by folds with an associated East dipping pervasive S_2 cleavage (sometimes mylonitic), subparallel to the PTFSZ (Fig. 7.7). The presence of a sub-horizontal to low plunging X_2 stretching mineral lineation highlights the dominant dextral transcurrent component (Ribeiro et al. 1980, 2013; Chaminé 2000; Moreira et al. 2016a). The intensity of the D_2 deformation increases eastward towards the PTFSZ where the D_1 structures are often transposed (Chaminé 2000; Moreira et al. 2016a). The Finisterra Block units are always bounded by D_2 shear zones.

The D_2 episode generated a staurolite zone HT metamorphic paragenesis in the Espinho Unit (with garnet overgrowth and staurolite porphyroblasts—P = 3–6 kbar; T = 600 ± 30 °C; Fernández et al. 2003), in the Lourosa Unit migmatites (garnet + sillimanite + K-feldspar + biotite ± muscovite + melt assemblage—P = 8 ± 0.7 kbar; T = 730 ± 25 °C, Acciaioli et al. 2003; Munhá et al. 2008) and in the micaschists of the Junceira-Tramagal Unit (syn-kinematic growth of garnet, with poikilitic structures, and staurolite Fig. 7.6b; Moreira 2017). The D_2 metamorphic event partially resets the previous D_1 HT metamorphic event (Fernández et al. 2003; Moreira et al. 2016a; Moreira 2017). The D_2 tectono-metamorphic event is considered Mississippian in age (ca. 340–315; Pereira et al. 2010; Almeida et al. 2014). The syn-tectonic Carboniferous Tramagal granite (Abranches and Canilho 1981/82) is coeval with the D_2 event (Fig. 7.6c; Romão et al. 2013, 2016; Moreira et al. 2016a). However, this deformation episode do not affect the granitic dykes (318.7 ± 1.2 Ma; Pereira et al. 2010) that are intrusive in the Junceira-Tramagal Unit.

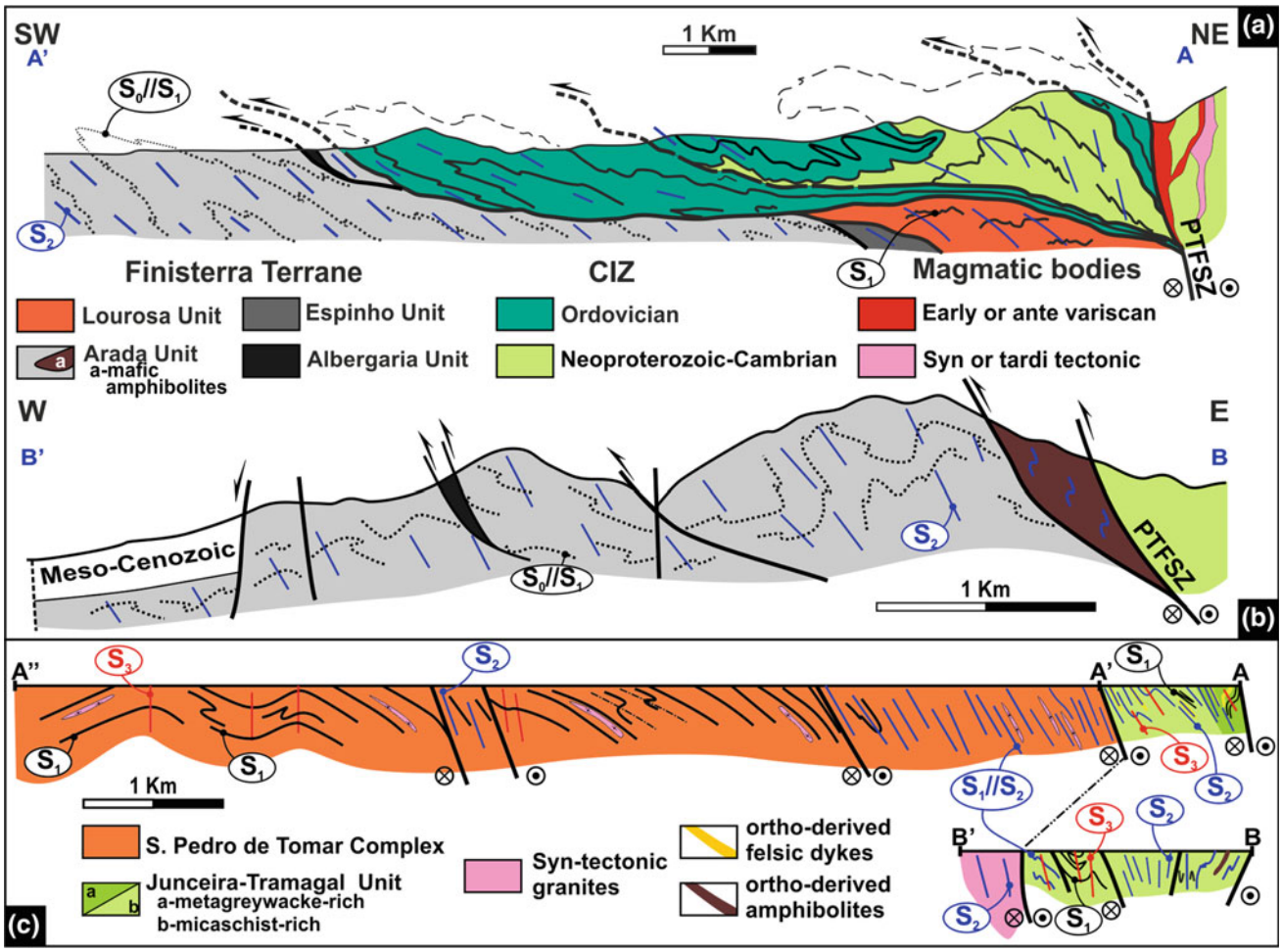

Fig. 7.7 Simplified cross-sections in the Finisterra block: **a** Main structural features of Porto-Espinho-Albergaria sector (see location in Fig. 7.3; adapted from Pereira et al. 2007); **b** Main structural features of Coimbra sector (see location in Fig. 7.3; adapted from Ferreira Soares et al. 2005; Machado et al. 2011); **c** Main structural features of Abrantes-Tomar sector (see location in Fig. 7.5)

The last Variscan deformation episode (D_3) is characterized by the development of folds subparallel to the PTFSZ and faults, generated in brittle-ductile to brittle conditions, frequently associated with the reactivation of D_2 N-S shear zones or the top-to-SW thrusts generated during D_1/D_2 (Ribeiro et al. 2013; Moreira 2017). In the Abrantes-Tomar sector (Moreira 2017) the intensity of the D_3 folds increases towards the PTFSZ, where the open D_3 folds become tight slightly W vergence and with a weak low-grade axial planar cleavage (Fig. 7.7c).

The D_3 deformation event is constrained by the 310–305 Ma Ar–Ar ages obtained in micas of the para-derived rocks of the Espinho and Lourosa Units (Acciaioli et al. 2003; Munhá et al. 2008; Gutiérrez-Alonso et al. 2015) and the 295 Ma of the late-tectonic Tancos, Castelo do Queijo and Madalena-Lavadores granites (Neves et al. 2007; Martins et al. 2011, 2014). However, the Madalena-Lavadores granite is affected by brittle N-S dextral faults (Ribeiro et al. 2015) that result from Late Variscan and/or Meso-Cenozoic tectonic deformations.

7.4 Distinctive Features of Finisterra Block

The individualization of a lithospheric terrane must be supported by stratigraphic, tectonic, metamorphic and magmatic data, emphasizing a distinct geodynamical evolution (Coney et al. 1980). In the author's opinion the Finisterra Block fulfil these conditions because (Fig. 7.8):

(i) It has its own tectonostratigraphic succession composed of:
- Neoproterozoic-Lower Cambrian high-grade assemblage with a basal gneissic-migmatite

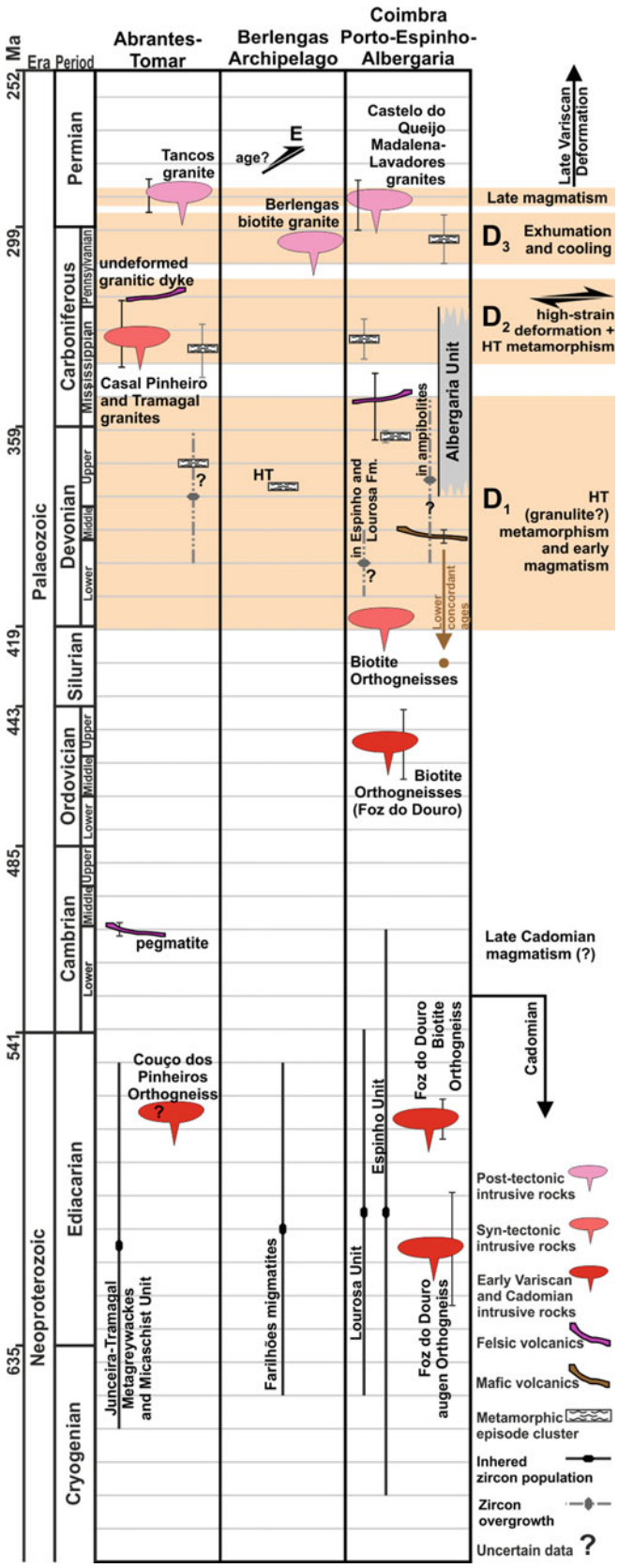

Fig. 7.8 Geological and geochronological synthesis of Finisterra block (see text for references)

complex (Foz do Douro Gneiss, Farilhões, S. Pedro de Tomar and Lourosa Units) and an upper staurolite-garnet-micaschists succession (Espinho and Junceira-Tramagal Units);
  - A low-grade assemblage, where the Lower Devonian-Carboniferous Albergaria Unit is discordant over the more deformed and metamorphosed Neoproterozoic Arada Unit.

(ii) The high-grade assemblage shows predominance of Archean, Paleoproterozoic and Neoproterozoic detrital zircon populations. Some lithotypes show the lack of Mesoproterozoic ages (Fig. 7.4), which is a distinctive feature of the North Gondwana margin (Fernández-Suárez et al. 2002; Linnemann et al. 2008; Pereira et al. 2008, 2011, 2012a, b; Talavera et al. 2012; Orejana et al. 2015). However, the presence of Mesoproterozoic zircons in some of the samples (Fig. 7.4; Pereira et al. 2010; Almeida 2013; Almeida et al. 2014) indicates a more complex evolution of these units, with different sources for the clastic sediments of the Finisterra Block. Moreover, the presence of rare (and dubious?; Pereira et al. 2010) Ordovician and Silurian detrital zircons (Pereira et al. 2010; Almeida et al. 2014) could indicate that part of these units are Palaeozoic.

(iii) The Lower Cambrian carbonate sedimentation typical of the OMZ (e.g. Oliveira et al. 1991) and the Ordovician siliciclastic sedimentation recognized in the CIZ (e.g. Dias et al. 2013) are not recognized in any of the Finisterra tectonostratigraphic units.

(iv) The mafic and ultramafic Silurian/Devonian magmatism with intra-plate to MORB geochemistry interlayered in high-grade and Arada Units (Fig. 7.8; e.g. Noronha and Leterrier 2000; Silva 2007; Almeida et al. 2014) is not observed in the Iberian Terrane (e.g. Mata and Munhá 1990; Sánchez-García et al. 2008; Pedro et al. 2010).

(v) The low anchizone marine black shales and siltstones of the Albergaria Unit with Laurussia-type acritarch assemblages of Frasnian-Serpukhovian age (Chaminé et al. 2003b; Machado et al. 2008, 2011) are not recognized, neither in the Iberian Terrane nor in the South Portuguese Terrane. Indeed:
  - the lack of marine sedimentation during Frasnian is one of the distinctive features of Iberian Terrane (e.g. Oliveira et al. 1991; Dias et al. 2013; Moreira and Machado this volume), although continental successions with similar ages are found in the lower parauthochton of Galiza-Trás-os-Montes Zone (GTOMZ; Martínez-Catalán et al. 2008).
  - in Pulo do Lobo Domain of the South Portuguese Terrane, the marine sedimentation with Frasnian acritarch assemblages have Avalonia affinities (Oliveira et al. 2013; Pereira et al. 2018).

(vi) An Eo-Variscan HT metamorphic event (Fig. 7.8) is recognized in the high-grade tectonostratigraphic units of the Finisterra Block (ca. 420–350 Ma). This event could explain the pre-Carboniferous HT paragenesis observed in Espinho Unit (Fernández et al. 2003), with stretched garnets representative of extremely HT metamorphism (Ji and Martignole 1994), the Silurian-Devonian zircon overgrowths observed in these high-grade units (Pereira et al. 2010; Almeida 2013; Almeida et al. 2014), the metamorphic ages obtained in Farilhões metatexites (ca. 380 Ma; Valverde Vaquero et al. 2010a, b; Bento dos Santos et al. this volume) and in Espinho Unit (ca. 360 Ma; Almeida 2013; Almeida et al. 2014). This HT metamorphic event is not recognized in the Iberian Variscides, where similar ages are only found in the high pressure (HP) metamorphism in the OMZ (Moita et al. 2005) and the HP-granulitic metamorphism of the GTOMZ (e.g. Gómez Barreiro et al. 2007; Mateus et al. 2016; Puelles et al. 2017).

(vii) The Eo-Variscan Silurian magmatism recognized in the Lourosa Unit (ca. 420 Ma; Chaminé et al. 1998) is absent in the Iberian Terrane.

(viii) There is also a strong structural contrast between the Finisterra block and the Iberian Terrane. The oldest D_1 deformation of the Finisterra Block, although highly disturbed by the Carboniferous tectono-metamorphic events, shows N-S oriented recumbent folds with top-to-W transport and rooted in the PTFSZ (Fig. 7.7). Such geometry has no equivalent in the Iberian Terrane, where a NW-SE general trend prevails during early episodes of deformation (Fig. 7.1b; Dias et al. 2013, 2016; Moreira et al. 2014). This early deformation episode is considered contemporaneous of the Silurian-Devonian Finisterra metamorphic event.

Since the Carboniferous, the Finisterra Block and Iberian Terranes share a common geodynamical evolution:

- The Mississippian D_2 HT metamorphic event of Finisterra is synchronous of the HT event described in the Iberian Terrane (Bea et al. 2006; Castiñeiras et al. 2008; Pereira et al. 2012c), where a dextral shearing related to the D_2 evolution of PTFSZ is also observed (Ribeiro et al. 2014; Dias et al. 2017b; Moreira and Dias 2018);
- In the Pennsylvanian, the Finisterra and Iberian Terranes were both pervasively deformed by regional D_3 shear zones (Gutiérrez-Alonso et al. 2015);
- The Late Pennsylvanian sediments of the Buçaco Basin, located in the western border of CIZ near the Finisterra Block (Fig. 7.3), show some Silurian-Devonian and Mesoproterozoic inhered zircon populations (Dinis et al. 2012). The absence of such zircons ages in the CIZ, led to

propose a long source for such populations (Dinis et al. 2012). An alternative proposal is to consider that these sediments were fed by both Finisterra and Iberian Terranes;

- The Upper Pennsylvanian-Permian granitic magmatism is represented in the Finisterra Block (e.g. the Tancos, Castelo do Queijo and Madalena-Lavadores; Figs. 7.2, 7.3 and 7.5; Neves et al. 2007; Martins et al. 2011, 2014) and in the Iberian Terrane (e.g. Pinto and Andrade 1987; Sant'Ovaia et al. 2013).

7.5 The Finisterra Block in the Context of the European Variscides

The geodynamics of the Finisterra Block cannot be dissociated from the evolution of the European Variscides. However, the continuity of the narrow Finisterra Block is not obvious because its boundary with the Iberian Terrane is marked by a lithospheric shear zone (the PTFSZ) and is separated from the Central European Variscides by the Ibero-Armorican Arc (Dias et al. 2016), which was disrupted during the opening of the Atlantic Ocean. In spite of these difficulties, the main geological features of the Finisterra Block support correlations with the Léon Domain and the Mid-German Crystalline Rise (MGCR), in a similar way to what has already been proposed (Mateus et al. 2016).

7.5.1 The Léon Domain

The Léon Domain (also called Léon-Normanian Domain; Ballèvre et al. 2009) is the northernmost domain of the Armorican Massif (Fig. 7.9a; Ballèvre et al. 2009; Faure et al. 2010), whose "exotic" nature was emphasized long ago (Balé and Brun 1986; Le Corre et al. 1989). The boundary between the Léon and the Armorican domains (Fig. 7.9b) is considered either in the Elorn fault (Ballèvre et al. 2009) or in the Le Conquet-Penzé Shear Zone (Faure et al. 2010). The highly deformed Precambrian and Palaeozoic rocks are structured in a complex stack of nappes as follows (Fig. 7.9c, d; Faure et al. 2005, 2010; Schulz et al. 2007; Ballèvre et al. 2009):

- A parautochthonous unit of paragneisses intruded by the Lower-Middle Devonian Plounevez-Lochrist and

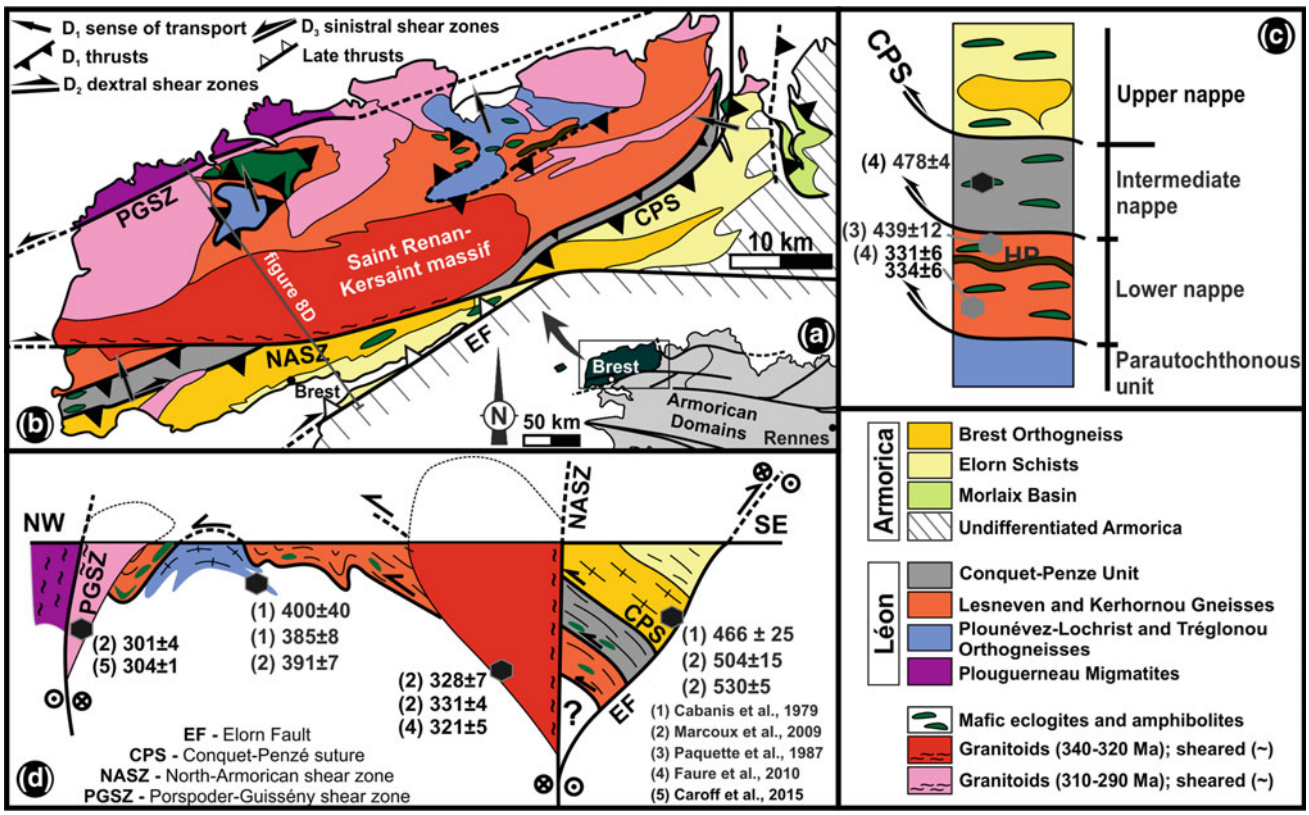

Fig. 7.9 The Léon Domain geological setting: **a** The Léon block and its geological relationship with the Armorican Domain (adapted from Ballèvre et al. 2009); **b** Simplified geological map (adapted from Faure et al. 2010; Schulz 2013); **c** Simplified tectonostratigraphic nappe stack organization (see text for geochronological references); **d** Simplified cross-section (see text for geochronological references; adapted from Ballèvre et al. 2009; Faure et al. 2010; Schulz 2013)

Tréglonou Augen orthogneisses (ca. 400–380 Ma; Fig. 7.9d; Cabanis et al. 1979; Marcoux et al. 2009), affected by intense migmatization during the late Carboniferous (ca. 320–310 Ma; Schulz 2013).

- A lower nappe consisting of garnet-sillimanite gneisses and micaschists (Lesneven and Kerhornou gneisses) with a Proterozoic para-derived protolith (Schulz et al. 2007; Schulz 2013), as well as mafic tholeiites (amphibolites, pyroxenites, serpentinites and eclogites; Balé and Brun 1986; Faure et al. 2010). Eclogite metamorphism of Silurian age (439 ± 12 Ma; Fig. 7.9c; Paquette et al. 1987), Upper Mississippian HT migmatization (ca. 335–330 Ma; Faure et al. 2010) and/or Pennsylvanian (ca. 310–300 Ma; Schulz et al. 2007) ages have been described.
- An intermediate nappe, where biotite-garnet-staurolite micaschists (Conquet-Penzé Micaschists) with a Neoproterozoic protolith and Carboniferous metamorphism (ca. 340–305 Ma; Schulz et al. 2007; Faure et al. 2010; Schulz 2013) predominates. Metacherts, quartzites, conglomeratic lenses and Ordovician amphibolites and Early Ordovician meta-gabbros (Fig. 7.9c; Faure et al. 2010) are also present.
- An upper nappe represented by the Late Proterozoic Elorn Schists (greenschists facies; Ballèvre et al. 2009; Faure et al. 2010), which were intruded by the Cambrian-Early Ordovician Brest orthogneiss with granodiorite composition (Fig. 7.9c, d; Deutsch and Chauris 1965; Cabanis et al. 1979; Marcoux et al. 2009). The Elorn Schists are ascribed to the Armorican Massif basement (Faure et al. 2010).

Two magmatic events took place during the Carboniferous:

- The oldest (340–320 Ma; Cabanis et al. 1979; Faure et al. 2010; Marcoux et al. 2009; Le Gall et al. 2014) composed of calc-alkaline granites and granodiorites (Balé and Brun 1986);
- The youngest (310–290 Ma; Cabanis et al. 1979; Marcoux et al. 2009; Caroff et al. 2015), located in the northern sectors, consisting of sub-alkaline granitoids (Balé and Brun 1986).

Three main tectono-metamorphic events affect the Léon Domain, generating an ENE-WSW to NE-SW global trend (Fig. 7.9b). The early event (D_1) is linked to the emplacement to NNW of nappes (Fig. 7.9b, d; Faure et al. 2010; Balé and Brun 1986). The HP metamorphism registered in the lower nappe is considered previous to the D_1 episode (Bradshaw et al. 1967; Faure et al. 2010), so constraining the timing of this episode to Late Silurian (?)-Devonian.

The HT D_2 episode, which deeply reworks the D_1 fabrics (Balé and Brun 1986; Le Corre et al. 1989; Faure et al. 2005; 2010), is associated to the E-W dextral North-Armorican shear zone (NASZ; Fig. 7.9b; Balé and Brun 1986; Schulz et al. 2007; Faure et al. 2010) and reactivate the Elorn Fault (Faure et al. 2005). This episode is coeval of the Mississippian HT metamorphic event (Schulz et al. 2007; Faure et al. 2010, Schulz 2013) and the first plutonic suite (ca. 340–320 Ma). In the lower nappe, where the D_2 is weaker, the D_2 migmatization and melting postdates the eclogite metamorphism (Faure et al. 2010).

The D_3 episode is restricted to the northern sectors (Fig. 7.9b; Le Corre et al. 1989; Marcoux et al. 2009; Caroff et al. 2016). It is closely linked to the NE-SW Porspoder-Guissény sinistral shear zone (Fig. 7.9b, d; Le Corre et al. 1989), which controls the second episode of magmatism and the Plouguerneau migmatites (Fig. 7.9; Ballèvre et al. 2009; Caroff et al. 2015). The metamorphic ages obtained in the migmatites (ca. 330 Ma—U–Pb in monazites, Marcoux et al. 2009; 311 ± 14 Ma; Schulz 2013) and in the mylonites of the Porspoder-Guissény shear zone (293 ± 3 Ma—Ar/Ar in muscovites, Marcoux et al. 2009) constrain this deformation episode between 330 and 290 Ma, which seems to indicate that the migmatization was initiated during D_2 episode.

7.5.1.1 The Mid-German Crystalline Rise

The Mid-German Cristaline Rise (MGCR; Fig. 7.10a; sometimes also called Mid-German Cristaline High) forms the northern sector of the Saxo-Thuringian Domain. It is mostly composed of medium- to high-grade gneisses, migmatites and plutonic rocks, exposed in small basement outcrops with general NE-SW trend (Ruhla—Fig. 7.10b, Kyffhäuser—Fig. 7.10c, Spessart or Odenwald Crystalline Complexes—Fig. 7.10d; Zeh and Will 2010).

The metamorphism reaches HT conditions (amphibolite-granulite facies) during the Mississippian (340–320 Ma; Nasir et al. 1991; Todt et al. 1995; Will and Schmädicke 2003; Zeh et al. 2003, 2005). This event is coeval with the emplacement of several plutonic bodies (Reischmann and Anthes 1996; Anthes and Reischmann 2001; Zeh et al. 2005). Older ages were obtained in the Odenwald Crystalline Complex (349 ± 14 and 430 ± 43 Ma; Will et al. 2017), suggesting, at least, one early HT episode associated to magmatism. This complex also contains retrograde eclogites derived from within-plate to MOR basalts (Scherer et al. 2002, Will and Schmädicke 2001, 2003) with a Silurian/Lower Devonian protolith age (Fig. 7.10; 410–400 Ma; Zeh and Will 2010). The HP metamorphism of these eclogites is dated of Upper Devonian (357 ± 6 Ma; Scherer et al. 2002), although some resetting could have occurred during the Mississippian retrograde metamorphism (Scherer et al. 2002). Similar metamorphic ages were obtained, not only in the Odenwald Complex

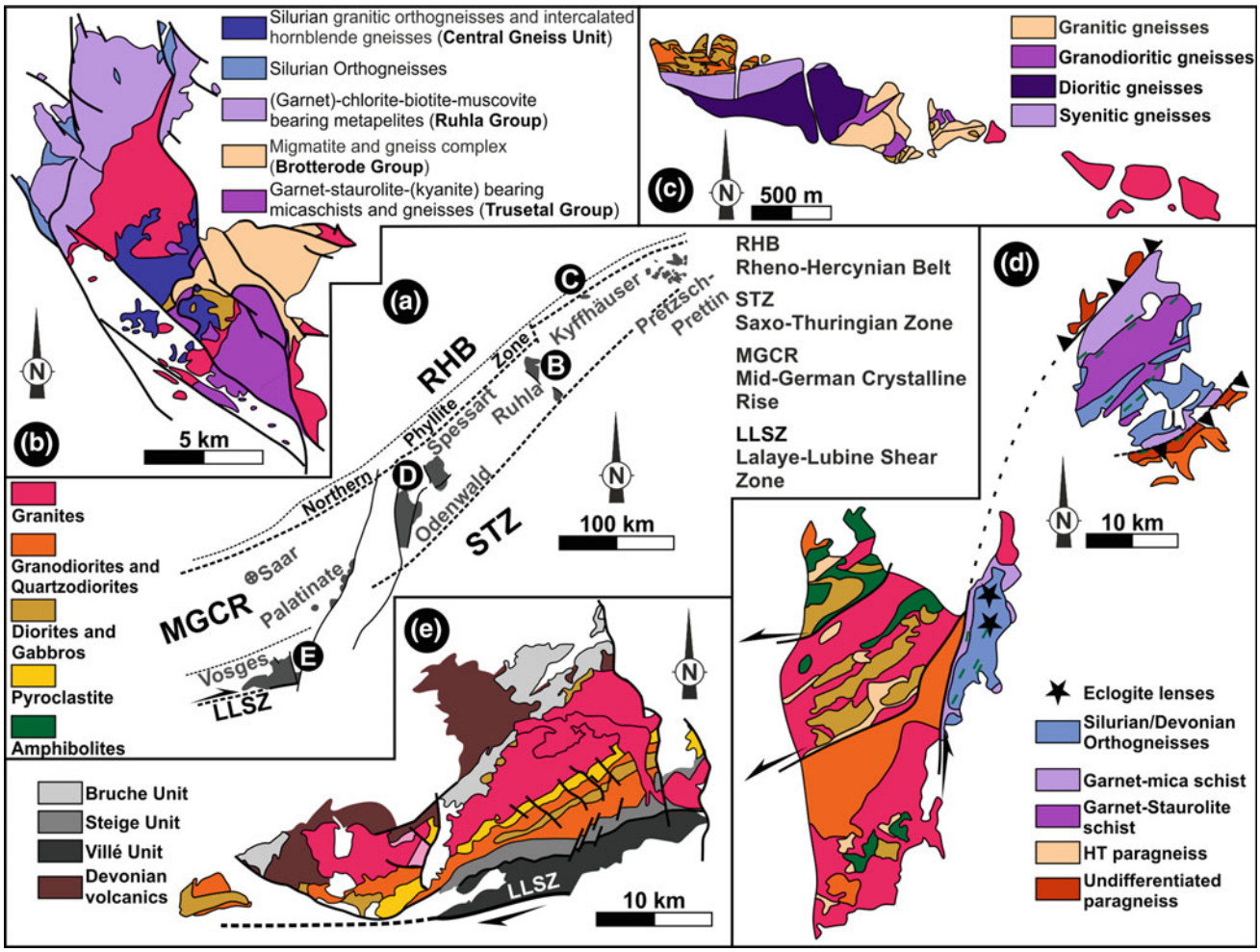

Fig. 7.10 Simplified geological maps of the MGCR (adapted from Zeh and Will 2010): **a** General relation between the crystalline complexes; **b** The Ruhla Complex; **c** The Kyffhäuser Complex; **d** The Spessart and Odenwald Complexes; **e** The Vosges Complex

(375 ± 5 Ma; Todt et al. 1995), but also in the Ruhla one (357 ± 5 and 352 ± 8 Ma; Zeh et al. 2003), but in these cases the association with the HP metamorphic event is not identified (Zeh and Will 2010). The Upper Devonian metamorphism is coeval with the felsic and mafic-intermediate plutonism (Kirsch et al. 1988; Reischmann and Anthes 1996; Zeh et al. 2005).

The MGCR plutonism is not restricted to the above mentioned events, having a wider temporal range: Late Cambrian-Early Ordovician (Anthes and Reischmann 2001), Silurian-Devonian (ca. 420–410 Ma; Dombrowski et al. 1995; Zeh et al. 2003) and Pennsylvanian-Early Permian (310–290 Ma; Anthes and Reischmann 2001). The geological meaning of this plutonism is not treated in the present work.

Detrital zircon populations in the para-derived gneisses and migmatites (Zeh et al. 2001, 2003, 2005; Gerdes and Zeh 2006; Zeh and Gerdes 2010) and some ortho-derived gneisses (Anthes and Reischmann 2001) show two distinct patterns in the Ruhla Crystalline Complex (Fig. 7.10b): samples where Mesoproterozoic populations are absent (Brotterode Group) and samples where the Mesoproterozoic populations are significant (Ruhla Group).

The Vosges complex has a distinct geological history because low-grade metamorphic units are dominant, namely (Fig. 7.10e; Franke 2000; Zeh and Will 2010):

- The Villé Unit, composed of late Cambrian to early Ordovician metapelitic to meta-psammitic schists and quartzites;
- The Steige Unit, a monotonous Ordovician to Silurian shallow marine metapelitic succession, which thrust the Villé Unit;
- The Bruche Unit, a sedimentary and tectonic mélange comprising Frasnian black shales and Fammenian to early Carboniferous shelf and slope sediments, grey-wackes and conglomerates, as well as calc-alkaline volcanic rocks.

The Bruche Unit is only affected by a Carboniferous tectono-metamorphic event, while the Steige and Villé Units

have a previous deformation episode (Skrzypek et al. 2014). All these sequences were intruded by diorites and granites during the Carboniferous times.

7.6 The Finisterra-Léon-MGCR Terrane; a Proposal

This proposal is based on the stratigraphic, metamorphic, magmatic and structural comparison between the Finisterra, Léon and MGCR blocks which share remarkable affinities. They are resumed below:

(i) An Eo-variscan plutonic event (ca. 420–360 Ma), represented by Devonian granites, is described in the three domains (Cabanis et al. 1979; Chaminé et al. 1998; Dombrowski et al. 1995; Marcoux et al. 2009). In the MGCR and Finisterra blocks this magmatism is partially coeval with HT amphibolite-granulite metamorphism (ca. 390–360 Ma; Zeh and Will 2010; Bento dos Santos et al. this volume). Late Silurian-Devonian felsic magmatism and metamorphism are rare in European Variscides, a period generally associated with eclogite and granulite facies conditions (Moita et al. 2005; Gómez Barreiro et al. 2007; Ballèvre et al. 2009; Schulz 2013; Mateus et al. 2016; Puelles et al. 2017).

(ii) These early magmatic and HT metamorphic processes were contemporaneous of a complex structural deformation. The older deformation is characterized by N-facing folds and thrusts in the MGCR and Léon domains (Faure et al. 2010; Zeh and Will 2010) and W-facing in the Finisterra Block (Fig. 7.11), a kinematics compatible with the arcuate structure of Ibero-Armorican Arc (Fig. 7.11; Dias et al. 2016).

(iii) A Silurian-Devonian HP metamorphism with eclogites was also described in the Léon and MGCR domains. These eclogites, which were retrograded during the Carboniferous HT events, are older in the Léon Domain (Silurian; Paquette et al. 1987) than in the MGCR (Upper Devonian; Scherer et al. 2002). Although the age of the MGCR HP rocks are

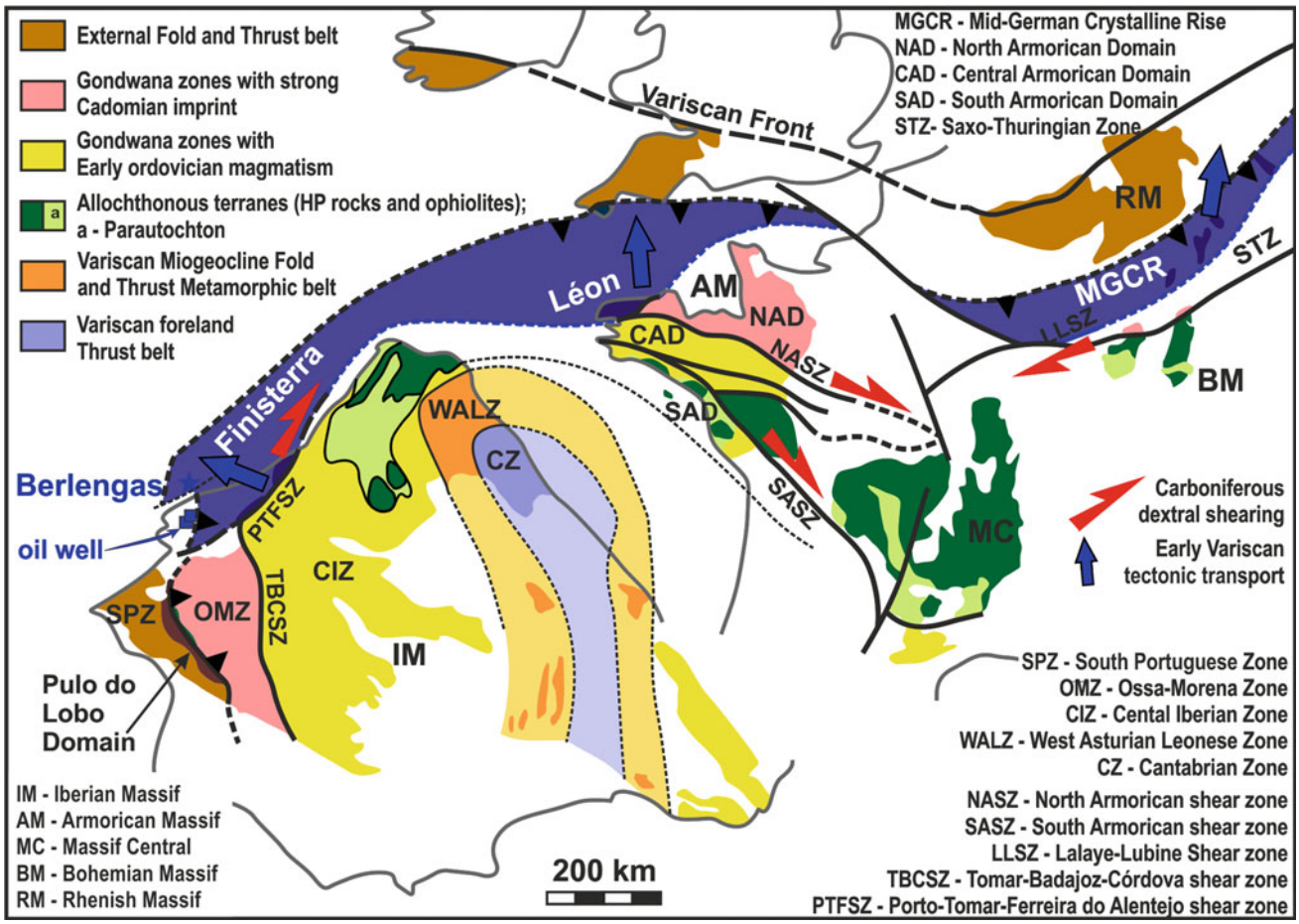

Fig. 7.11 The Finisterra-Leon-MGCR Terrane in the context of the European Variscides (adapted from Ribeiro et al. 2007; Dias et al. 2016; Franke and Dulce 2017)

debatable, this suggests a diachronic Variscan subduction during Upper Silurian-Devonian, which may have controlled the early tectono-metamorphic stages of the Finisterra-Léon-MGCR Terrane (Rheic or Rheno-Hercynian Ocean subduction?). Nevertheless, the presence of distinct subductions of two different oceans (e.g. Franke and Dulce 2017) could not be excluded. Eclogites have not been described in the Finisterra Block, probably due to the scarcity of detailed metamorphic studies and/or to the Meso-Cenozoic sedimentary cover of the Lusitanian Basin, which hide a great part of the Finisterra Block (Fig. 7.1b).

(iv) Mafic and ultramafic magmatism, contained in the HT metamorphic units, occurs in all domains, although without well age constrain. The within-plate to MORB geochemistry signature of this magmatism may be the expression of extensional processes during Cambrian-Ordovician, or even Silurian, related with Variscan Ocean(s) opening;

(v) A similar diversity of lithotypes and the ages of the magmatic and metamorphic events can be found in the Continental Allochthonous Terrane of NW Iberia (Fig. 7.1b; Gómez Barreiro et al. 2007; Mateus et al. 2016). This suggests that this terrane could have been rooted in the Finisterra-Léon-MGCR Terrane and not in Armorica as usually considered (e.g. Ballèvre et al. 2009). This possibility is compatible with the spatial position of Finisterra-Léon-MGCR Terrane in the Ibero-Armorican Arc (Fig. 7.11) and with the SSE nappe transport of the Continental Allochthonous Terrane (Ribeiro et al. 2007).

(vi) Regarding the inhered zircon distribution in the Finisterra, Léon and MGCR Domains, although having in mind the scarcity of studies in León Domain, a common behaviour of the Mesoproterozoic ages is found in all the domains (Gerdes and Zeh 2006; Marcoux et al. 2009; Pereira et al. 2010; Zeh and Gerdes 2010; Almeida et al. 2014), which consist in the existence of samples with and without abundant Mesoproterozoic zircon populations. As the Mesoproterozoic gap is one of the most distinctive feature of Gondwana-derived metasediments (Zeh and Gerdes 2010; Pereira 2014), this seems to indicate distinct sources during the siliciclastic sedimentation, i.e. from Gondwana and Laurussia-Baltica(?) where Mesoproterozoic ages are common (Murphy et al. 2004; Pollock et al. 2007; Kuznetsov et al. 2014; Petersson et al. 2015).

(vii) On the other hand, the Late Devonian-Lower Carboniferous marine acritarch found in the Albergaria Unit of the Finisterra Block show close affinities to that of the Rhenish Massif usually associated to Laurussia (Fig.2.7.11; Machado et al. 2008). This association is reinforced by the Caledonian Laurrusia source of the Devonian clastic sedimentation of the Rhenish realm (Franke 2000).

Putting all things together it seems plausible that the Finisterra, Léon and MGCR blocks were attached together to Gondwana until the Neoproterozoic-Lower Cambrian and were close to Laurussia during the Late Devonian-Lower Carboniferous time. This implies the migration of the Finisterra-Léon-MGCR towards Laurussia as an independent peri-Gondwana Terrane, separated from Gondwana by an ocean realm as indicated by the Silurian-Lower Devonian mafic rocks with MORB signature recognised in the Léon and MGCR (and Finisterra?) Domains.

Therefore, the boundaries of these blocks deserve also a close look:

(i) As seen above, the eastern boundary of the Finisterra Block is marked by the PTFSZ (Fig. 7.11; Ribeiro et al. 2007), interpreted as a transform fault with polyphasic deformation at least since the early Variscan Cycle (Ribeiro et al. 2007). Available geophysical data (Silva et al. 2000) suggest that its western boundary is hidden below the Meso-Cenozoic sedimentary cover of the Lusitanian Basin, while its SE continuation is established using the presence of South Portuguese Zone lithotypes found in oil well cores (Benfeito and Monte Gordo; Figs. 7.1b and 7.11; Ribeiro et al. 2013);

(ii) The southern boundary of the Léon Domain is considered the Le Conquet-Penzé Shear Zone whose interpretation is debated, either representing an oceanic suture or the closure of a basin with thinned continental crust (Fig. 7.9b; Faure et al. 2010). Its northern boundary is assumed to represent the Rheic suture zone (Faure et al. 2010).

(iii) The MGCR boundaries are almost totally covered by Permian to Quaternary sediments (Zeh and Will 2010). The contact with the southern Moldanubian Zone corresponds to the Lalaye-Lubine dextral shear zone (LLSZ), superimposed on a previous deformation (Fig. 7.10; Skrzypek et al. 2014). The geodynamical interpretation of this major shear zone is not consensual, seen either as a suture, or as an early Variscan detachment reactivated during Carboniferous (Skrzypek et al. 2014). The northern boundary is not exposed but is indirectly assumed to be placed south of the Northern Phyllite Zone correlated with the Pulo do Lobo Domain of the South Portuguese Zone (Fig. 7.10; Franke and Dulce 2017).

Thus, the northernmost boundary of the Finisterra-León-MGCR Terrane should represent a Variscan Oceanic suture (Fig. 7.11; Rheic and/or Rheno-Hercynian Oceanic Suture?; Franke 2000; Faure et al. 2010; Franke and Dulce 2017). However, its southernmost boundary with Gondwana derived Terranes (Armorica and Iberia) is debatable and two distinct interpretations coexist:

- An active transform margin expressed by the PTFSZ, which connects the SW Iberian suture with the northern European suture(s), mainly the Le Conquet-Penzé Suture (and/or Paleotethys suture);
- A suture zone of a minor Palaeozoic Ocean (or a stretched continental crust basin) opened during Palaeozoic times, as it was proposed for León Block (Faure et al. 2010).

The first hypothesis could explain the absence of HP rocks in the Finisterra Block and its appearance in León Block and MGCR. In turn, the second one could explain the abundant Ordovician to Silurian mafic and ultramafic rocks with geochemistry similar to MORB to within-plate basalt in all domains (Faure et al. 2010; Zeh and Will 2010; Almeida et al. 2014), as well as the Upper Silurian to Devonian HP metamorphic event in León Block and MGCR (Paquette et al. 1987; Scherer et al. 2002).

Since Mississippian, the Finisterra-León-MGCR Terrane and the other peri-Gondwana terranes show similar metamorphic and magmatic events, suggesting a common evolution. This is compatible with the beginning of the collision between Gondwana and Laurentia (Ribeiro et al. 2007; Moreira et al. 2014; Dias et al. 2016). In Mississippian times, all these terranes were affected by major dextral shear zones (e.g. PTFSZ, NASZ and LLSZ). The pervasive HT metamorphism, with melting generation related to the collisional process, are superimposed on previous events and almost obliterates the early Variscan events in the Finisterra-Léon-MGCR Terrane.

The Neoproterozoic magmatism and metamorphism of Finisterra and Léon Domains (ascribable to the Cadomian event) and the presence of Late Cambrian-Early Ordovician magmatism, also seems to indicate the Northern Gondwana affinities for this composite Terrane. Assuming a possible Cadomian suture in the Espinho Unit, the PTFSZ could be interpreted as a Variscan transform fault reactivating an earlier Cadomian structure, connecting two segments of a Cadomian suture in the TBCSZ and in the northern sector of Finisterra.

Thus, the Finisterra-Léon-MGCR Terrane only has a distinct evolution of Northern peri-Gondwana realm during Early Palaeozoic times (Ordovician to Upper Devonian).

Acknowledgements The authors recognize the excellent work of Tomás Oliveira as editor, which greatly help to improve this paper. They also acknowledge the funding provided to the ICT and to IDL, under contract with FCT (the Portuguese Science and Technology Foundation; respectively UID/GEO/04683/2013 and UID/GEO/50019/2013). Noel Moreira acknowledges Fundação Gulbenkian for the financial support through the "Programa de Estímulo à Investigação 2011" and Fundação para a Ciência e a Tecnologia, through the PhD grant (SFRH/BD/80580/2011).

References

Abranches MCB, Canilho MH (1981/82) Determinação de idade pelo método Rb–Sr de granitos portugueses. Mem Acad Cienc Lisboa 24:17–31.

Acciaioli MH, Santos JF, Munhá JM, Cordani GG, Couto A, Sousa P (2003) Idades Ar–Ar em micas de metapelitos da zona de Espinho: Datação do Metamorfismo relacionado com a F3 Varisca. IV Congresso Ibérico de Geoquímica (Coimbra) abstract book, 161–163.

Aires S, Noronha F (2010) O anfibolito olivínico do Engenho Novo (Norte de Portugal) revisitado. X Congresso de Geoquímica dos Países de Língua Portuguesa and XVI Semana de Geoquímica abstract book, 69–77.

Almeida N (2013) Novos dados geocronológicos do Terreno Finisterra no Sector entre Espinho e Albergaria-a-Velha, Portugal. MSc Thesis (unpublished), University of São Paulo, 98 p.

Almeida N, Egydio Silva M, Fonseca PE, Bezerra MH, Basei M, Chaminé HI, Tassinari C (2014) Novos dados geocronológicos do Finisterra. Comunicações Geológicas 101(I):31–34.

Anthes G, Reischmann T (2001) Timing of granitoid magmatism in the eastern Mid-German Crystalline Rise. J Geodyn 31:119–143. https://doi.org/10.1016/s0264-3707(00)00024-7.

Balé P, Brun JP (1986) Les complexes métamorphiques du Léon (NW Bretagne): un segment du domaine éo-hercynien sud armoricain translaté au Dévonien. Bull Soc Geol Fr 2:471–477.

Ballèvre M, Bosse V, Ducassou D, Pitra P (2009) Palaeozoic history of the Armorican Massif: models for the tectonic evolution of the suture zones. C R Geosci 341:174–201. https://doi.org/10.1016/j.crte.2008.11.009.

Bea F, Montero PG, Gonzalez-Lodeiro F, Talavera C, Molina JF, Scarrow JH, Whitehouse MJ, Zinger T (2006) Zircon thermometry and U–Pb ion-microprobe dating of the gabbros and associated migmatites of the Variscan Toledo Anatectic Complex, Central Iberia. J Geol Soc 163:847–855. https://doi.org/10.1144/0016-76492005-143.

Beetsma JJ (1995) The late Proterozoic/Paleozoic and Hercynian crustal evolution of the Iberian Massif, N Portugal, as traced by geochemistry and Sr-Nd-Pb isotope systematics of pre-Hercynian terrigenous sediments and Hercynian granitoids. PhD Thesis (unpublished), Vrije Universiteit, Amsterdam.

Bento dos Santos T, Ribeiro ML, González Clavijo E, Díez Montes A, Solá AR (2010) Geothermobarometric estimates and P-T paths for migmatites from Farilhões Islands, Berlengas Archipelago, W Portugal. VIII Congresso Nacional de Geologia, Braga. E-Terra 16 (11). Available online: http://e-terra.geopor.pt.

Bento dos Santos T, Valverde Vaquero P, Ribeiro ML, Solá AR, Clavijo EG, Díez Montes A, Dias da Silva I (this volume) The Farilhões Anatectic Complex (Berlengas Archipelago). In Quesada C, Oliveira JT (Ed) The Geology of Iberia: a geodynamic approach. Springer (Berlin), Regional Geology Review series.

Bradshaw JD, Renouf JT, Taylor RT (1967) The development of Brioverian structures and Brioverian|Palaeozoic relationships in west Finistere (France). Geologische Rundschau 56:567–96. https://doi.org/10.1007/bf01848744.

Bucher K, Grapes M (2011) Petrogenesis of Metamorphic Rocks. Springer-Verlag, 8th Ed, 428 p.

Cabanis B, Peucat J, Michot J, Deutsch S (1979) Remise en cause de l'existence d'un socle orthogneissique antécambrien dans le pays de Léon (domaine Nord-armoricain); étude géochronologique par les méthodes Rb/Sr et U/Pb des orthogneiss de Tréglonou et de Plouvenez-Lochrist. Bull BRGM 4:357–364.

Caroff M, Labry C, Le Gall B, Authemayou C, Bussin Grosjean D, Guillong M (2015) Petrogenesis of late-Variscan high-K alkali-calcic granitoids and calc-alkalic lamprophyres: the Aber-Ildut/North-Ouessant complex, Armorican massif, France. Lithos 238:140–155. https://doi.org/10.1016/j.lithos.2015.09.025.

Caroff M, Le Gall B, Authemayou C, Grosjean DB, Labry C, Guillong M (2016) Relations between basalts and adakitic/ felsic intrusive bodies in a soft substrate environment: The South Ouessant Visean basin in the Variscan belt, Armorican Massif, France. Can J Earth Sci 53(4):441–456. https://doi.org/10.1139/cjes-2015-0230.

Castiñeiras P, Villaseca C, Barbero L, Martín Romera C (2008) SHRIMP U–Pb zircon dating of anatexis in high-grade migmatite complexes of Central Spain: implications in the Hercynian evolution of Central Iberia. Int J Earth Sci 97:35–50. https://doi.org/10.1007/s00531-006-0167-6.

Chaminé HI (2000) Estratigrafia e estrutura da Faixa Metamórfica de Espinho—Albergaria-a-Velha (Zona de Ossa Morena: Implicações geodinâmicas). PhD Thesis (unpublished), University of Porto, Portugal, 497 p.

Chaminé HI, Leterrier J, Fonseca PE, Ribeiro A, Lemos de Sousa MJ (1998) Geocronologia U/Pb em zircoes e monazites de rochas ortoderivadas do sector Espinho—Albergaria-a-Velha (Zona de Ossa Morena, NW de Portugal). In: Azeredo, A. (Ed). Abstracts of V Congresso Nacional de Geologia. Comun Inst Geol Min 84 (1):B115–B118.

Chaminé HI, Gama Pereira LC, Fonseca PE, Noronha F, Lemos de Sousa MJ (2003a) Tectonoestratigrafia da faixa de cisalhamento de Porto-Albergaria-a-Velha-Coimbra-Tomar, entre as Zonas Centro-Ibérica e de Ossa-Morena (Maciço Ibérico, W de Portugal). Cad Lab Xeol Laxe 28:37–78.

Chaminé HI, Pereira G, Fonseca P, Pinto de Jesus A, Rocha F, Moco L, Fernandes J, Flores D, Gomes C, Araújo A, Soares de Andrade A (2003b) Tectonostratigraphy of middle and upper Palaeozoic black-shales from the Porto-Tomar-Ferreira do Alentejo shear zone (W Portugal): new perspectives on the Iberian Massif. Geobios 36:649–663. https://doi.org/10.1016/j.geobios.2003.03.002.

Clarke DB (1981) The mineralogy of peraluminous granites; a review. The Canadian Mineralogist 19(1): 3–17.

Coney P, Jones DL, Monger JWH (1980) Cordilleran suspect terranes. Nature 288:329–333. https://doi.org/10.1038/288329a0.

Deutsch S, Chauris L (1965) Age de quelques formations cristallophylliennes et granitiques du Pays de Léon (Finistère). C R Acad Sci Paris 260:615–617.

Dias C, Martins HCB, Almeida A, Sant'Ovaia H, Ribeiro MA (2017b) Características da Faixa Metamórfica Porto-Viseu e a sua relação com a Zona de Cisalhamento Porto-Tomar. VII Congresso Jovens Investigadores em Geociências, LEG 2017 Abstract book, Estremoz, 191–195.

Dias R, Ribeiro A (1993) Porto-Tomar shear zone, a major structure since the beginning of the Variscan orogeny. Comun Inst Geo. Mineiro 79: 29–38.

Dias R, Ribeiro A, Coke C, Pereira E, Rodrigues J, Castro P, Moreira N, Rebelo J (2013) Evolução estrutural dos sectores setentrionais do autóctone da Zona Centro-Ibérica. In Dias R, Araújo A, Terrinha P, Kullberg JC (Ed) Geologia de Portugal (vol 1), Escolar Editora 73–147.

Dias R, Ribeiro A, Romão J, Coke C, Moreira N (2016) A review of the arcuate structures in the Iberian Variscides; constraints and genetical models. Tectonophysics 681:170–194. https://doi.org/10.1016/j.tecto.2016.04.011.

Dias R, Moreira N, Ribeiro A, Basile C (2017a) Late Variscan Deformation in the Iberian Peninsula; A late feature in the Laurasia-Gondwana Dextral Collision. Int J Earth Sci 106(2):549–567. https://doi.org/10.1007/s00531-016-1409-x.

Dinis P, Andersen T, Machado G, Guimarães F (2012) Detrital zircon U–Pb ages of a late-Variscan Carboniferous succession associated with the Porto-Tomar shear zone (West Portugal): Provenance implications. Sediment Geol 273–274:19–29. https://doi.org/10.1016/j.sedgeo.2012.06.007.

Dombrowski A, Henjes-Kunst F, Höhndorf A, Kröner A, Okrusch M, Richter P (1995) Orthogneisses in the Spessart Crystalline Complex, Northwest Bavaria: witnesses of Silurian granitoid magmatism at an active continental margin. Geol Rundsch 84:399–411. https://doi.org/10.1007/bf00260449.

Faure M, Bé Mézème E, Duguet M, Cartier C, Talbot J (2005) Paleozoic tectonic evolution of Medio-europa from the example of the French Massif Central and Massif Armoricain. In Carosi R, Dias R, Iacopini D, Rosenbaum G (Ed) The southern Variscan belt. J Virt Explor 19:5. https://doi.org/10.3809/jvirtex.2005.00120.

Faure M, Sommers C, Melleton J, Cocherie A, Lautout O (2010) The Léon domain (French Massif armoricain): a westward extension of the Mid-German Crystalline Rise? Structural and geochronological insights. Int J Earth Sci 99:65–81. https://doi.org/10.1007/s00531-008-0360-x.

Fernández FJ, Chaminé HI, Fonseca P E, Munhá JM, Ribeiro A, Aller J, Fuertes-Fuentes M, Borges FS (2003) HT-fabrics in a garnet-bearing quartzite from Western Portugal: geodynamic implications for the Iberian Variscan Belt. Terra Nova 15(2):96–103. https://doi.org/10.1046/j.1365-3121.2003.00472.x.

Fernández-Suárez J, Gutierrez-Alonso G, Jeffries TE (2002) The importance of along-margin terrane transport in northern Gondwana: Insights from detrital zircon parentage in Neoproterozoic rocks from Iberia and Brittany. Earth Planet Sci Lett 204:75–88. https://doi.org/10.1016/s0012-821x(02)00963-9.

Ferreira Soares AF, Marques J, Rocha R, Cunha PP, Duarte LV, Sequeira A, Sousa MB, Pereira E, Gama Pereira LC, Gomes E, Santos JR (2005) Carta Geológica de Portugal à escala 1:50.000, Folha 19-D Coimbra-Lousã. LNEG.

Ferreira Soares AF, Marques J, Sequeira A (2007) Notícia Explicativa da Carta Geológica de Portugal à escala 1:50.000, Folha 19-D Coimbra-Lousã. LNEG, 71p.

Franke W (2000) The Mid-European segment of the Variscides: tectonostratigraphic units, terrane boundaries and plate tectonic evolution. In Franke W, Haak V, Oncken O, Tanner D (Ed) Quantification and modelling in the Variscan Belt, Geol Soc London Spec Publ 179:35–61. https://doi.org/10.1144/gsl.sp.2000.179.01.05.

Franke W, Dulce JC (2017) Back to sender: tectonic accretion and recycling of Baltica-derived Devonian clastic sediments in the Rheno-Hercynian Variscides. Int J Earth Sci 106(1):377–386 https://doi.org/10.1007/s00531-016-1408-y.

Gerdes A, Zeh A (2006) Combined U–Pb and Hf isotope LA-(MC)-ICP-MS analyses of detrital zircons: comparison with SHRIMP and new constraints for the provenance and age of an Armorican metasediment in Central Germany. Earth Planet Sci Lett 249:47–61. https://doi.org/10.1016/j.epsl.2006.06.039.

Gómez Barreiro J, Martínez Catalán JR, Arenas R, Castiñeiras P, Abati J, Díaz García F, Wijbrans, JR (2007) Tectonic evolution of the upper allochthon of the Órdenes Complex (northwestern Iberian Massif): Structural constraints to a polyorogenic peri-Gondwanan terrane. Geological Society of America Special Paper 423:315–332.

Gutiérrez-Alonso G, Collins AS, Fernández-Suárez J, Pastor-Galán D, González-Clavijo E, Jourdan F, Weil AB, Johnston ST (2015) Dating of lithospheric buckling: $^{40}Ar/^{39}Ar$ ages of syn-orocline

strike–slip shear zones in northwestern Iberia. Tectonophysics 643:44–54. https://doi.org/10.1016/j.tecto.2014.12.009.

Henriques SBA, Neiva AMR, Ribeiro ML, Dunning GR, Tajčmanová L (2015) Evolution of a Neoproterozoic suture in the Iberian Massif, Central Portugal: new U–Pb ages of igneous and metamorphic events at the contact between the Ossa Morena Zone and Central Iberian Zone. Lithos 220–223:43–59. https://doi.org/10.1016/j.lithos.2015.02.001.

Ji S, Martignole J (1994) Ductility of garnet as an indicator of extremely high temperature deformation. J Struct Geol 16(7) 985–996. https://doi.org/10.1016/0191-8141(94)90080-9.

Kirsch H, Kober B, Lippolt HJ (1988) Age of intrusion and rapid cooling of the Frankenstein gabbro (Odenwald, SW Germany) evidenced by $^{40}Ar/^{39}Ar$ and single zircon $^{207}Pb/^{206}Pb$ measurements. Geol Rundsch 77:693–711. https://doi.org/10.1007/bf01830178.

Kuznetsov NB, Meert JG, Romanyukc TV (2014) Ages of detrital zircons (U/Pb, LA–ICP–MS) from the Latest Neoproterozoic–Middle Cambrian(?) Asha Group and Early Devonian Takaty Formation, the Southwestern Urals: A test of an Australia-Baltica connection within Rodinia. Precambrian Research 244:288–305. https://doi.org/10.1016/j.precamres.2013.09.011.

Le Corre C, Balé P, Geoget Y (1989) Le Léon: un domaine exotique au Nord-Ouest de la chaîne varisque armoricaine. Geodin Acta 3:57–71. https://doi.org/10.1080/09853111.1990.11105200.

Le Gall B, Authemayou C, Ehrhold A, Paquette J-L, Bussien D, Chazot G, Aouizerat A, Pastol Y (2014) LiDAR offshore structural mapping and U/Pb zircon/monazite dating of Variscan strain in the Léon metamorphic domain, NW Brittany. Tectonophysics 630:236–250. https://doi.org/10.1016/j.tecto.2014.05.026.

Linnemann U, Pereira MF, Jeffries T, Drost K, Gerdes A (2008) Cadomian Orogeny and the opening of the Rheic Ocean: new insights in the diacrony of geotectonic processes constrained by LA–ICP–MS U–Pb zircon dating (Ossa-Morena and Saxo-Thuringian Zones, Iberian and Bohemian Massifs). Tectonophysics 461:21–43. https://doi.org/10.1016/j.tecto.2008.05.002.

LNEG (2010) Geological map of Portugal at 1:1.000.000, 3rd Ed, Laboratório Nacional de Energia e Geologia, Lisboa.

Machado G, Vavrdová M, Fonseca PE, Chaminé H, Rocha F (2008) Overview of the Stratigraphy and initial quantittive Biogeographical results from the Devoniano of the Albergaria-a-Velha Unit (Ossa-Morena zone, W Portugal). Acta Musei Nationalis Pragae 64 (2–4):109–113.

Machado G, Francu E, Vavrdová M, Flores D, Fonseca PE, Rocha F, Gama Pereira LC, Gomes A, Fonseca M, Chaminé, HI (2011) Stratigraphy, palynology and organic geochemistry of the Devonian-Mississippian metasedimentary Albergaria-a-Velha Unit (Porto-Tomar Shear Zone, W Portugal). Geological Quarterly 55 (2):139–164.

Marcoux E, Cocherie A, Ruffet G, Darboux JR, Guerrot C (2009) Géochronologie revisitée du dôme du Léon (Massif armoricain, France). Géologie de la France 2009 (1):19–40.

Mateus A, Munhá J, Ribeiro A, Tassinari CCG, Sato K, Pereira E, Santos JF (2016) U–Pb SHRIMP zircon dating of high-grade rocks from the Upper Allochthonous Terrane of Bragança and Morais Massifs (NE Portugal); geodynamic consequences. Tectonophysics 675:23–49. https://doi.org/10.1016/j.tecto.2016.02.048.

Martínez Catalán J (2011) Are the oroclines of the Variscan belt related to late Variscan strike-slip tectonics? Terra Nova 23:241–247. https://doi.org/10.1111/j.1365-3121.2011.01005.x.

Martínez Catalán J, Fernández-Suárez J, Meireles C, González-Clavijo E, Belousova E, Saeed A (2008) U–Pb detrital zircon ages in synorogenic deposits of the NW Iberian Massif: interplay of syntectonic sedimentation and thrust tectonics. J Geol Soc Lond 165:687–698. https://doi.org/10.1144/0016-76492007-066.

Martins HCB, Sant'Ovaia H, Abreu J, Oliveira M, Noronha F (2011) Emplacement of the Lavadores granite (NW Portugal): U/Pb and AMS results. C R Geosci 343(6):387–396. https://doi.org/10.1016/j.crte.2011.05.002.

Martins HCB, Ribeiro MA, Sant'Ovaia H, Abreu J, Garcia de Madinabeitia S (2014) SHRIMP and LA-ICPMS U–Pb zircon geochronology of post-tectonic granitoid intrusions in NW of Central Iberian Zone. Comunicações Geológicas 101 (I):147–150.

Mata J, Munhá J (1990) Magmatogénese de metavulcanitos câmbricos do nordeste alentejano: os estádios iniciais de "rifting" continental. Com Serv Geol Portugal 76:61–89.

Mendes F (1967/1968) Contribution à l'étude géochronologique, par la méthode au strontium, des formations cristallines du Portugal. Bol Mus Labor miner Geol Fac Ciênc 11(1):3–155.

Moita P, Munhá J, Fonseca PE, Pedro J, Tassinari C, Araújo A, Palacios T (2005) Phase equilibria and geochronology of Ossa Morena eclogites. XIV Semana de Geoquimica/VIII Congresso de geoquimica dos Paises de Lingua Portuguesa (abstract book) 2:471–474.

Montenegro de Andrade M (1977) O Anfibolito olivínico do Engenho Novo (Vila da Feira). Com Serv Geol Portugal 61:43–61.

Moreira N (2017) Evolução Geodinâmica dos sectores setentrionais da Zona de Ossa-Morena no contexto do Varisco Ibérico. PhD thesis (unpublished), University of Évora, 433p.

Moreira N, Dias R (2018) Domino structures as a local accommodation process in shear zones. J Struct Geol 110:187–201. https://doi.org/10.1016/j.jsg.2018.01.010.

Moreira N, Machado G (this volume) Devonian sedimentation in Western Ossa-Morena Zone and its geodynamic significance. In Quesada C, Oliveira JT (Ed), The Geology of Iberia: a geodynamic approach. Springer (Berlin), Regional Geology Review series.

Moreira N, Pedro J, Dias R, Ribeiro A, Romão J (2011) Tomar-Badajoz-Córdoba shear zone in Abrantes sector; the presence of a kilometric sheath fold?. Deformation mechanisms, Rheology and Tectonics abstract book, Oviedo, Spain, 90.

Moreira N, Dias R, Romão J, Pedro JC, Ribeiro A (2013) Influência da Zona de Cisalhamento Porto-Tomar-Ferreira do Alentejo na região de Abrantes; uma estrutura de primeira ordem à escala do Orógeno Varisco na Ibéria. In Moreira N, Pereira I, Couto F, Silva H (Ed), III CJIG, LEG 2013 and 6th PGUE abstract book, Estremoz, Portugal 161–165.

Moreira N, Araújo A, Pedro JC, Dias R (2014) Geodynamic evolution of Ossa-Morena Zone in SW Iberian context during the Variscan Cycle. Comunicações Geológicas 101 (I):275–278.

Moreira N, Romão J, Pedro J, Dias R, Ribeiro A (2016a) The Porto-Tomar-Ferreira do Alentejo Shear Zone tectonostratigraphy in Tomar-Abrantes sector (Portugal). In IX Congreso Geológico de España special volume. Geo-Temas 16(1):85–88.

Moreira N, Romão J, Dias R, Pedro JC, Ribeiro A (2016b) Tectonostratigraphy proposal for western block of Porto-Tomar Shear zone; the Finisterra Terrane. Abstract book of Workshop on Earth Sciences 2016, Évora (Portugal).

Munhá J, Mendes MH, Santos JF, Tassinari C, Cordani U, Nutman AP (2008) Timing and duration of migmatization recorded in Ovar-Espinho metamorphic belt (northern sector of Ossa-Morena Zone, Porto-Tomar Shear Zone). XI Congresso de Geoquímica dos PLP abstract book, 111.

Murphy JB, Fernández-Suárez J, Keppie JD, Jeffries TE (2004) Contiguous rather than discrete Paleozoic histories for the Avalon and Meguma terranes based on detrital zircon data. Geology 32:585–588. https://doi.org/10.1130/g20351.1.

Nasir S, Okrusch M, Kreuzer H, Lenz H, Höhndorf A (1991) Geochronology of the Spessart crystalline complex, Mid-German Crystalline Rise. Mineral Petrol 44:39–55. https://doi.org/10.1007/bf01167099.

Neves L, Pereira A, Macedo C (2007) Alguns dados geoquímicos e geocronológicos (K-Ar) sobre o plutonito granítico de Tancos (Portugal Central). XV Semana—VI Congresso Ibérico de Geoquímica abstract book, 137–140.

Noronha F, Leterrier J (1995) Complexo metamórfico da Foz do Douro. Geoquímica e geocronologia. Resultados preliminares. Abstract book of IV Congresso Nacional de Geologia. Mem Mus Lab Min Geol Fac Ciênc Univ Porto, 4:769–774.

Noronha F, Leterrier J (2000) Complexo Metamórfico da Foz do Douro (Porto). Geoquímica e Geocronologia. Revista Real Academia Galega de Ciências XIV:21–42.

Oliveira JT, Oliveira V, Piçarra J (1991) Traços gerais da evolução tectono-estratigráfica da Zona de Ossa Morena, em Portugal: síntese crítica do estado actual dos conhecimentos. Comun Serv Geol Port 77:3–26.

Oliveira JT, Relvas J, Pereira Z, Matos J, Rosa C, Rosa D, Munhá J, Fernandes P, Jorge R, Pinto A (2013) Geologia Sul portuguesa, com ênfase na estratigrafia, vulcanologia física, geoquímica e mineralizações da faixa piritosa. In Dias R, Araújo A, Terrinha P, Kullberg JC (Ed) Geologia de Portugal (vol 1), Escolar Editora 673–767.

Orejana D, Martínez EM, Villaseca C, Andersen T (2015) Ediacaran–Cambrian paleogeography and geodynamic setting of the Central Iberian Zone: Constraints from coupled U–Pb–Hf isotopes of detrital zircons. Precambrian Research 261:234–251. https://doi.org/10.1016/j.precamres.2015.02.009.

Paquette JL, Balé P, Ballèvre M, Georget Y (1987) Géochronologie et géochimie des éclogites du Léon: nouvelles contraintes sur l'évolution géodynamique du Nord-Ouest du Massif armoricain. Bulletin de Minéralogie 110:683–696.

Passchier CW, Trouw RAJ (2005) Microtectonics. 2nd Ed, Springer, 382p.

Pedro JC, Araújo A, Tassinari C, Fonseca PE, Ribeiro A (2010) Geochemistry and U–Pb zircon age of the Internal Ossa-Morena Zone Ophiolite Sequences: a remnant of Rheic Ocean in SW Iberia. Ofioliti 35 (2):117–130. https://doi.org/10.4454/ofioliti.v35i2.390.

Pereira E, Gonçalves LS, Moreira A (1980) Carta Geológica de Portugal à Escala de 1:50.000—Folha 13-D Oliveira de Azemeis and Explanatory Note. Serviços Geológicos de Portugal. Lisboa.

Pereira E, Rodrigues JF, Gonçalves S, Moreira A, Silva A (2007) Carta Geológica de Portugal à escala 1:50.000, Folha 13-D Oliveira de Azemeis. LNEG.

Pereira MF (2014) Potential sources of Ediacaran strata of Iberia: a review. Geodinamica Acta 1(1):1–14. https://doi.org/10.1080/09853111.2014.957505.

Pereira MF, Chichorro M, Williams IS, Silva JB (2008) Zircon U–Pb geochronology of paragneisses and biotite granites from the SW Iberian Massif (Portugal): Evidence for a paleogeographic link between the Ossa-Morena Ediacaran basins and the West African craton. In Liégeois JP, Nasser E (Ed) The boundaries of the West African Craton. Geol Soc London Spec Publ 297:385–408. https://doi.org/10.1144/sp297.18.

Pereira MF, Silva JB, Drost K, Chichorro M, Apraiz A (2010) Relative timing of the transcurrent displacements in northern Gondwana: U–Pb laser ablation ICP-MS zircon and monazite geochronology of gneisses and sheared granites from the western Iberian Massif (Portugal). Gondwana Res 17(2–3):461–481. https://doi.org/10.1016/j.gr.2009.08.006.

Pereira MF, Chichorro M, Sola AR, Silva JB, Sanchez-Garcia T, Bellido F (2011) Tracing the Cadomian magmatism with detrital/inherited zircon ages by in-situ U–Pb SHRIMP geochronology (Ossa-Morena Zone, SW Iberian Massif). Lithos 123(1–4):204–217. https://doi.org/10.1016/j.lithos.2010.11.008.

Pereira MF, Solá AR, Chichorro M, Lopes L, Gerdes A, Silva JB (2012a) North-Gondwana assembly, break up and paleogeography: U–Pb isotope evidence from detrital and igneous zircons of Ediacaran and Cambrian rocks of SW Iberia. Gondwana Res 22 (3–4):866–881. https://doi.org/10.1016/j.gr.2012.02.010.

Pereira MF, Linnemann U, Hofmann M, Chichorro M, Solá AR, Medina J, Silva JB (2012b) The provenance of Late Ediacaran and Early Ordovician siliciclastic rocks in the Southwest Central Iberian Zone: Constraints from detrital zircon data on northern Gondwana margin evolution during the late Neoproterozoic. Precambrian Research 192–195:166–189. https://doi.org/10.1016/j.precamres.2011.10.019.

Pereira MF, Silva JB, Chichorro M, Ordóñez-Casado B, Lee JKW, Williams IS (2012c) Early Carboniferous wrenching, exhumation of high-grade metamorphic rocks and basin instability in SW Iberia: constraints derived from structural geology and U–Pb and ^{40}Ar-^{39}Ar geochronology. Tectonophysics 558–559:28–44. https://doi.org/10.1016/j.tecto.2012.06.020.

Pereira Z, Fernandes P, Matos JX, Jorge RCGS, Oliveira JT (2018) Stratigraphy of the Northern Pulo do Lobo Domain, SW Iberia Variscides: A palynological contribution. Geobios. https://doi.org/10.1016/j.geobios.2018.04.001.

Pesquera A, Torres-Ruiz J, García-Casco A, Gil-Crespo PP (2012) Evaluating the Controls on Tourmaline Formation in Granitic Systems: a Case Study on Peraluminous Granites from the Central Iberian Zone (CIZ), Western Spain. Journal of Petrology 54(3):609–634. https://doi.org/10.1093/petrology/egs080.

Petersson A, Scherstén A, Andersson J, Möller C (2015) Zircon U–Pb and Hf - isotopes from the eastern part of the Sveconorwegian Orogen, SW Sweden: implications for the growth of Fennoscandia. Geol Soc London Spec Publ 289:281–303. https://doi.org/10.1144/sp389.2.

Pinto MCS, Andrade, AAS (1987) Geocronologia dos granitóides da Zona de Ossa-Morena no contexto do Arco Ibero-Armoricano. Geociências 2(1/2):95–103.

Pollock JC, Wilton DHC, van Staal CR, Morrissey KD (2007) U–Pb detrital zircon geochronological constraints on the Early Silurian collision of Ganderia and Laurentia along the Dog Bay Line: The terminal Iapetan suture in the Newfoundland Appalachians. American Journal of Science 307(2):399–433. https://doi.org/10.2475/02.2007.04.

Priem HNA, Boelrijk NAIM, Verschure RH, Hebeda EH (1965) Isotopic ages of two granites on the Iberian continental margin: The Traba Granite (Spain) and the Berlenga Granite (Portugal). Geologie en Mijnbow 44e:353–354.

Puelles P, Beranoaguirre A, Ábalos B, Gil Ibarguchi JI, García de Madinabeitia S, Rodríguez J, Fernández-Armas S (2017) Eclogite inclusions from subducted metaigneous continentalcrust (Malpica-Tui Allochthonous Complex, NW Spain): Petrofabric, geochronology, and calculated seismic properties. Tectonics 36:1376–1406. https://doi.org/10.1130/b30226.1.

Reischmann T, Anthes G (1996) Geochronology of the Mid-German Crystalline Rise west of the River Rhine. Geol Rundsch 85:761–774. https://doi.org/10.1007/bf02440109.

Ribeiro A, Pereira E, Severo L (1980) Análise da deformação da zona de cisalhamento Porto-Tomar na transversal de Oliveira de Azemeis. Comum Serv Geol Portugal 66:3–9.

Ribeiro A, Silva JB, Dias R, Romão J (1991) The Berlenga Suspect Terrane and the spatial and temporal end of the Variscan Orogene. Abstract book of III Congresso Nacional de Geologia, Coimbra, 70.

Ribeiro A, Pereira E, Chaminé HI, Rodrigues J (1995) Tectónica do megadomínio de cisalhamento entre a Zona de Ossa-Morena e a Zona Centro-Ibérica na região de Porto-Lousã. In Sodré Borges F, Marques M (coord) IV Congresso Nacional de Geologia, Porto. Men Mus Labor Miner Geol 299–303.

Ribeiro A, Munhá J, Dias R, Mateus A, Pereira E, Ribeiro L, Fonseca PE, Araújo A, Oliveira JT, Romão J, Chaminé HI, Coke C, Pedro JC (2007) Geodynamic evolution of the SW Europe

Variscides. Tectonics 26 (6):TC6009. https://doi.org/10.1029/2006tc002058.

Ribeiro A, Pereira E, Fonseca PE, Mateus A, Araújo A, Munhá J, Romão J, Rodrigues JF (2009) Mechanics of thick-skinned Variscan overprinting of Cadomian basement (Iberian Variscides). CR Geosciences 341 (2–3):127–139. https://doi.org/10.1016/j.crte.2008.12.003.

Ribeiro A, Romão J, Munhá J, Rodrigues J, Pereira E, Mateus A, Araújo A (2013) Relações tectonostratigráficas e fronteiras entre a Zona Centro-Ibérica e a Zona Ossa-Morena do Terreno Ibérico e do Terreno Finisterra. In Dias R, Araújo A, Terrinha P, Kullberg JC (Ed) Geologia de Portugal (vol 1), Escolar Editora 439–481.

Ribeiro MA, Martins HCB, Sant'Ovaia H, Dória A, Ferreira J, Areias M (2014) Evolução tectono-metamórfica, migmatização e magmatismo sin-tectónico na região do Porto (NW Portugal). Comunicações Geológicas 101 (I):297–300.

Ribeiro MA, Areias M, Ferreira J, Martins H, Sant'Ovaia H (2015) Geological and petrological constraints on the variscan evolution of the NW area of Port-Viseu Belt. The Variscan belt: correlations and plate dynamics. Géologie de la France (Variscan 2015 special issue, Rennes) 2015(1):119–120.

Romão J, Moreira N, Pedro JC, Mateus A, Dias R, Ribeiro A (2013) Contribuição para o conhecimento das unidades tectono-estratigráficas do Terreno Finisterra na região de Tomar. In Moreira N, Dias R, Araújo A (Ed) Geodinâmica e Tectónica Global; a Importância da cartografia geológica, 9ª Conferência Anual do GGET-SGP Abstract book, Estremoz, 87–91.

Romão J, Moreira N, Dias R, Pedro J, Mateus A, Ribeiro A (2014) Tectonoestratigrafia do Terreno Ibérico no sector Tomar-Sardoal-Ferreira do Zêzere e relações com o Terreno Finisterra. Comunicações Geológicas 101 (I):559–562.

Romão J, Manupella G, Barbosa B, Pereira E, (2016). Carta Geológica de Portugal, na escala de 1:50 000. Folha 27-B (Tomar). Laboratório Nacional de Energia e Geologia, Lisboa.

Sánchez-García T, Quesada C, Bellido F, Dunning GR, González de Tánago J (2008) Two-step magma flooding of the upper crust during rifting: the Early Palaeozoic of the Ossa Morena Zone (SW Iberia). Tectonophysics 461:72–90. https://doi.org/10.1016/j.tecto.2008.03.006.

Sant'Ovaia H, Martins H, Noronha F (2013) Oxidized and reduced Portuguese Variscan granites associated with W and Sn hydrothermal lode deposits: magnetic susceptibility results. Comunicações Geológicas 100(1):33–39.

Scherer EE, Mezger K, Münker C (2002) Lu–Hf ages of high pressure metamorphism in the Variscan fold belt of southern Germany. Goldschmidt Conference Abstract, Geochim Cosmochim Acta Suppl 66:A677.

Schulz B (2013) Monazite EMP–Th–U–Pb age pattern in Variscan metamorphic units in the Armorican Massif (Brittany, France). German Journal of Geosciences 164:313–335. https://doi.org/10.1127/1860-1804/2013/0008.

Schulz B, Krenn E, Finger F, Brätz H, Klemd R (2007) Cadomian and Variscan metamorphic events in the Léon Domain (Armorican massif, France): P-T data and EMP monazite dating. In The evolution of the Rheic ocean from Avalonian-Cadomian active margin to Alleghenian-Variscan collision. Geol Soc London Spec Publ 423:267–285. https://doi.org/10.1130/2007.2423(12).

Silva S (2007) Estudo geoquímico de metabasitos da ZOM e da ZCI aflorantes na região Centro-Norte de Portugal. MsC Thesis (unpublished), University of Aveiro, 180 p.

Silva EA, Miranda JM, Luis JF A. Galdeano A (2000) Correlation between the Palaeozoic structures from West Iberian and Grand Banks margins using inversion of magnetic anomalies. Tectonophysics 321:57–71. https://doi.org/10.1016/s0040-1951(00)00080-9.

Skrzypek E, Schulmann K, Tabaud AS, Edel JB (2014) Palaeozoic evolution of the Variscan Vosges Mountains. In Schulmann K, Martínez Catalán JR, Lardeaux JM, Janousek V, Oggiano G (Ed) The Variscan Orogeny: Extent, Timescale and the Formation of the European Crust. Geol Soc London Spec Publ 405:45–75. https://doi.org/10.1144/sp405.8.

Sousa M, Sant'Ovaia H, Tassinari C, Noronha F (2014) Geocronologia U–Pb (SHRIMP) e Sm-Nd do ortognaisse biotítico do Complexo Metamórfico da Foz do Douro (NW de Portugal). Comunicações Geológicas 101(I):225–228.

Talavera C, Montero P, Martínez Poyatos D, Williams IS (2012) Ediacaran to Lower Ordovician age for rocks ascribed to the Schist–Graywacke Complex (Iberian Massif, Spain): Evidence from detrital zircon SHRIMP U–Pb geochronology. Gondwana Res 22:928–942. https://doi.org/10.1016/j.gr.2012.03.008.

Todt WA, Altenberger U, von Raumer JF (1995) U–Pb data on zircons for the thermal peak of metamorphism in the Variscan Odenwald, Germany. Geol Rundsch 84:466–472. https://doi.org/10.1007/bf00284514.

Valverde Vaquero P, Bento dos Santos T, González Clavijo E, Díez Montes A, Ribeiro ML, Solá R (2010a) Geochronology and P-T-t paths of the Berlengas Archipelago rocks, W Portugal. 2010 Goldschmidt Conference, Knoxville (E.U.A.), Geochim Cosmochim Acta, 74, 12, 1, A1070.

Valverde Vaquero P, Ribeiro ML, González Clavijo E, Díez Montes A, Bento Dos Santos T (2010b) Idades preliminares U–Pb (ID–TIMS) das Ilhas Berlengas (Portugal). VIII Congresso Nacional de Geologia, Braga. E-Terra 13(8). Available online: http://e-terra.geopor.pt.

Will TM, Schmädicke E (2001) A first report of retrogressed eclogites in the Odenwald Crystalline Complex: evidence for high-pressure metamorphism in the Mid-German Crystalline Rise, Germany. Lithos 59:109–125. https://doi.org/10.1016/s0024-4937(01)00059-7.

Will TM, Schmädicke E (2003) Isobaric cooling and anti-clockwise P–T paths in the Variscan Odenwald Crystalline Complex. J Metamorph Geol 21:469–480. https://doi.org/10.1046/j.1525-1314.2003.00453.x.

Will TM, Schulz B, Schmädicke E (2017) The timing of metamorphism in the Odenwald–Spessart basement, Mid-German Crystalline Zone. Int J Earth Sci 106(5):1631–1649. https://doi.org/10.1007/s00531-016-1375-3.

Zeh A, Gerdes A (2010) Baltica- and Gondwana-derived sediments in the Mid-German Crystalline Rise (Central Europe): implications for the closure of the Rheic ocean. Gondwana Res 17:254–263. https://doi.org/10.1016/j.gr.2009.08.004.

Zeh A, Will TM (2010) The Mid-German Crystalline Rise. In: Linnemann U, Romer RL (Ed) Pre-Mesozoic geology of Saxo-Thuringia–From the Cadomian active margin to the Variscan orogen. Schweizerbart, Stuttgart, 195–220.

Zeh A, Brätz H, Millar IL, Williams IS (2001) A combined zircon SHRIMP and Sm-Nd isotope study on high-grade paragneisses from the Mid-German Crystalline Rise: Evidence for northern Gondwanan and Grenvillian provenance. J Geol Soc 158:983–994. https://doi.org/10.1144/0016-764900-186.

Zeh A, Williams IS, Brätz H, Millar IL (2003) Different age response of zircon and monazite during the tectonometamorphic evolution of a high grade paragneiss from the Ruhla Crystalline Complex, Central Germany. Contrib. Mineral. Petrol. 145:691–706. https://doi.org/10.1007/s00410-003-0462-1.

Zeh A, Gerdes A, Will TM, Millar IL (2005) Provenance and Magmatic-Metamorphic Evolution of a Variscan Island-arc Complex: Constraints from U–Pb dating, Petrology, and Geospeedometry of the Kyffhäuser Crystalline Complex, Central Germany. Journal of Petrology 46:1393–1420. https://doi.org/10.1093/petrology/egi020.

Palaeozoic Basement of the Pyrenees

8

J. M. Casas, J. J. Álvaro, S. Clausen, M. Padel, C. Puddu, J. Sanz-López, T. Sánchez-García, M. Navidad, P. Castiñeiras, and M. Liesa

Abstract

In the Pyrenees, the Cambrian-Lower Ordovician strata represent a quiescent time span with no remarkable tectonic activity, followed by a late Early-Mid Ordovician episode of uplift and erosion that led to the formation of the Sardic unconformity. Silurian sedimentation was widespread and transgressive followed by a Devonian succession characterized by a complex mosaic of sedimentary facies. Carboniferous pre-Variscan sediments (Tournaisian-Viséan cherts and limestones) precede the arrival of the synorogenic siliciclastic supplies of the Culm flysch at the Late Serpukhovian. All this succession was subsequently affected by the Serpukhovian-Bashkirian (Variscan) collision, as a result of which, the Palaeozoic rocks were incorporated into the northeastern branch of the Ibero-Armorican Arc.

8.1 Introduction

J. M. Casas, J. J. Álvaro

In the Pyrenees, the aftermath of the late Ediacaran-early Terreneuvian magmatism, related to the Cadomian subduction, records the transition to passive-margin conditions. Cambrian-Lower Ordovician strata represent a quiescent time span with no remarkable tectonic activity, followed by a late Early-Mid Ordovician episode of uplift and erosion that led to the formation of the Sardic unconformity. Uplift was accompanied by magmatic activity that pursuit until the Late Ordovician, the latter coinciding with an extensional pulse that developed normal faults and controlled the record of post-Sardic sediments infilling palaeorelief depressions (the significance of this magmatism and tectonic activity is still

Coordinators: J. M. Casas, J. J. Álvaro.

J. M. Casas (✉)
Departamento de Dinàmica de la Terra i de l'Oceà-Institut de Recerca Geomodels, Universitat de Barcelona, Martí Franquès s/n, 08028 Barcelona, Spain
e-mail: casas@ub.edu

J. J. Álvaro
Instituto de Geociencias (CSIC-UCM), Dr. Severo Ochoa 7, 28040 Madrid, Spain
e-mail: jj.alvaro@csic.es

S. Clausen
UMR 8198 EEP CNRS, Université de Lille 1, Bâtiment SN5, Avenue Paul Langevin, 59655 Villeneuve d'Ascq Cedex, France
e-mail: sebastien.clausen@univ-lille1.fr

M. Padel
BRGM, 3 Avenue Claude Guillemin, 45100 Orléans, France
e-mail: m.padel@brgm.fr

C. Puddu
Departamento de Ciencias de la Tierra, Universidad de Zaragoza, Pedro Cerbuna 12, 50009 Zaragoza, Spain
e-mail: claudiapuddugeo@gmail.com

J. Sanz-López
Dpto. de Geologia, Universidad de Oviedo, Jesus Arias de Velasco s/n, 33005 Oviedo, Spain
e-mail: jasanz@geol.uniovi.es

T. Sánchez-García
Departamento Investigación Recursos Geológicos, Área Recursos Minerales y Geoquímica, Instituto Geológico y Minero de España, Ríos Rosas 23, 28003 Madrid, Spain
e-mail: t.sanchez@igme.es

M. Navidad · P. Castiñeiras
Departamento de Petrología y Geoquímica, Universidad Complutense de Madrid, Novais 12, 28040 Madrid, Spain
e-mail: navidad@geo.ucm.es

P. Castiñeiras
e-mail: castigar@ucm.es

M. Liesa
Departament de Mineralogia, Petrologia i Geologia aplicada, Universitat de Barcelona, Martí Franquès s/n, 08028 Barcelona, Spain
e-mail: mliesa@ub.edu

C. Quesada and J. T. Oliveira (eds.), *The Geology of Iberia: A Geodynamic Approach*, Regional Geology Reviews,
https://doi.org/10.1007/978-3-030-10519-8_8

under debate; see Sect. 8.3). Silurian sedimentation was widespread and transgressive, sealing the Sardic uplift palaeorelief and Late Ordovician rifting pulsation, followed by a Devonian succession characterized by a complex mosaic of sedimentary facies. Tournaisian-Viséan cherts and limestones represent the Carboniferous pre-Variscan sediments, preceding the arrival of the synorogenic siliciclastic supplies of the Culm flysch at the Late Serpukhovian. All this succession was subsequently affected by the Serpukhovian-Bashkirian (Variscan) collision, as a result of which, the Palaeozoic rocks were incorporated into the northeastern branch of the Ibero-Armorican Arc. In this chapter, we update data and interpretations from these Palaeozoic rocks of the Pyrenees, with a new proposal for the lower Cambrian-Ordovician stratigraphy and an update of the Upper Ordovician, Silurian, Devonian and pre-Variscan Carboniferous stratigraphy. Exposed data emphasize the affinity of the Pyrenean basement rocks with that of the neighbouring Sardinia, Mouthoumet and Montagne Noire-French Central Massif domains, as well as its differences with the Palaeozoic evolution of the Iberian Massif.

In the Pyrenees, the pre-Variscan Palaeozoic rocks constitute a 3–4 km-thick succession that crops out in the backbone of the cordillera (Fig. 8.1). These rocks form an elongated strip unconformably overlain by Mesozoic and Cenozoic rocks, which lie geographically disconnected from neighbouring outcrops of the Catalan Coastal Range to the south, the Mouthoumet and Montagne Noire (southern French Central) massifs to the north, and Sardinia to the east. Palaeozoic rocks are involved in three main Alpine thrust sheets, the so-called Lower Structural Units (Muñoz 1992) named Nogueres, Orri and Rialp thrust sheets. These units form an antiformal stack with their basal thrusts north-dipping or subvertical in the northern side of the chain, subhorizontal in the central part, and south-dipping in the southern contact with the Mesozoic-Cenozoic cover. In the description that follows, we will focus on the Palaeozoic rocks of the Nogueres and Orri units, which constitute a complete pre-Variscan succession, ranging in age from Cambrian to Carboniferous. Exposures of the Rialp unit only occur in a small tectonic window of the central Pyrenees.

Transverse (N-S-trending) displacement related to the Alpine deformation is about 150–160 km (Muñoz 1992), so the original Palaeozoic basin should be located northward from present-day arrangement. Moreover, the Alpine deformation gave rise to important horizontal axes rotation related to antiformal stack development. In contrast, Alpine metamorphism is absent and internal deformation is moderated. As a result, the original characteristics of the Palaeozoic rocks may be confidently reconstructed in the Pyrenees. As discussed below, other pre-Alpine movements may be also envisaged in order to obtain a reliable original Early Palaeozoic palaeoposition of the Pyrenenan domain and to establish its geodynamic relationship with the neighbouring Variscan Sardinia, Mouthoumet and Montagne Noire-French Central Massif domains.

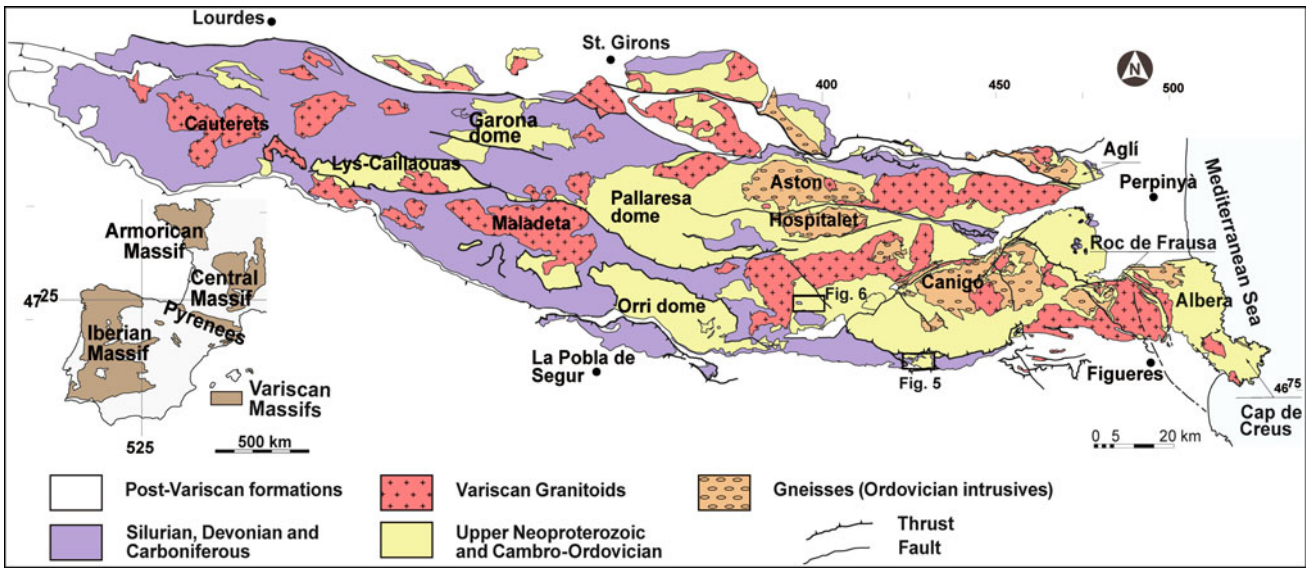

Fig. 8.1 Simplified geological map of the Pyrenees with the location of the massifs mentioned in the text

8.2 Cambro-Ordovician (pre-Sardic) Stratigraphy: Jujols Group

J. J. Álvaro, J. M. Casas, S. Clausen, M. Padel

The Jujols Group (Fig. 8.2) was firstly described by Cavet (1957) as the Jujols Schists, comprising a monotonous succession of alternating shale and sandstone overlying the Canaveilles Series in the northern Canigó massif. Cavet (1957) attributed an Ordovician age to the Jujols Schists, which then included what is now considered as Upper Ordovician conglomerates and volcanic deposits. These are underlain by a significant erosive unconformity and angular discordance representative of the Sardic Phase, and therefore excluded from the Jujols Group (Laumonier 1988). According to Cavet (1957), the base of the Jujols Schists was characterized by the presence of grey shales with carbonate nodules and quartzite interbeds. As reported in Chap. 2, the Jujols Group overlies the Cadomian volcanic activity reported in the Canaveilles Group.

In this contribution, we follow Padel (2016) and Padel et al. (2018) updating revision of the Jujols Group in the Eastern Pyrenees based on new stratigraphic data and geometric relationships (Fig. 8.2). These authors propose a subdivision of the Jujols Group into the Err, Valcebollère and Serdinya formations. The base of the Jujols Group coincides with the base of the Err Formation (Fig. 8.2), which onlaps an inherited palaeorelief formed by the Pic de la Clape Formation to the south of the Canigó massif (see Chap. 2). Where the Pic de la Clape volcanosedimentary complexes are absent, the Err Formation conformably overlies the Olette Formation. The top of the Jujols Group is highlighted by the Middle-Upper (*pars*) Ordovician hiatus associated with the Sardic Phase. The thickness of the group can be estimated at about 3–4 km.

The Err Formation (Fig. 8.2) is a relatively monotonous shale-dominated unit, up to about 2000 m thick. It consists of grey, brownish and greenish shales and centimetre-to-decimetre thick, fine-grained sandstones locally punctuated by gravelly sandstones. The latter never exceed 10 m in thickness and can be observed in the Puigmal area, near the summit of the Puigmal d'Err and at the Pic de la Clapa, where they overlie the Puig Sec Member. These sandstones are also well developed in the Aspres and Conflent areas.

The Valcebollère Formation (Fig. 8.3) consists of a lower massive-to-bedded limestone-to-marble package (up to 300 m thick), overlain and passing westward to a 15–200 m thick, shale/carbonate alternation that changes upsection into green shales bearing carbonate nodules. The thickness of the formation and its carbonate content diminish northward disappearing to the north of the Canigó massif. Despite the absence of archaeocyaths, several outcrops exhibit typical plano-convex exposures and microbial framebuilding textures (e.g., Gorges de la Fou in the Vallespir-Roc de Frausa area, and isolated bioherms close to Valcebollère village; Fig. 8.3 a–d) characteristic of reefal complexes. In the Aspres area, the Courbis Limestone of the Valcebollère Formation has yielded the acritarch *Archaeodiscina* cf. *umbonulata* Volkova, 1968. *A. umbonulata* is a cosmopolitan species ranging approximately from Cambrian Age 3 to early Cambrian Age 4 (Laumonier et al. 2015; T. Palacios, pers.com. 2016). Associated with the Courbis Limestone, some centimetric layers of grainy phosphorites have been identified, for the first time, marking the topmost part of the Valcebollère Formation.

The Serdinya Formation consists of a roughly 1500 m thick rhythmic alternation of shale and sandstone beds. Layers are 1 mm to several cm thick, change in colour from grey to characteristic light green or light brown grey to greenish, and exhibit sedimentary structures representative of tidal-to-storm influence (Fig. 8.4a). Sandstones up to 1 m thick occur at the top of the formation, exhibiting graded bedding, load casts and cross bedding (Fontfrède Member) (Fig. 8.4b). The Serdinya Formation conformably overlies the Valcebollère Formation (in some areas sealing hydrothermally induced karstic features, such as in the Roques Blanques section along the road N260; Fig. 8.3e–g) and is topped by the Sardic unconformity (Fig. 8.4c). Acritarchs recovered from the uppermost part of the Serdinya Formation in the southern Canigó massif has yielded a broad Furongian-Early Ordovician microphytoplancton assemblage (Casas and Palacios 2012). Ichnoassemblages recorded in the La Molina area, although not chronostratigraphically diagnostic, show a low-to-moderate ichnodiversity (Gámez et al. 2012). A maximum depositional age of ca. 475 Ma can be proposed for the quartzites of the Fonfrède Member in the La Rabassa dome, on the basis on the youngest detrital zircon population (Margalef et al. 2016).

Considering a Cambrian Fortunian age for the base of the Err Fomation, and a Furongian-Early Ordovician age for the top of the Serdinya Formation (Fig. 8.2), a broad Cambrian-earliest Ordovician age can be envisaged for the entire Jujols Group. As discussed below, it should be noted that Middle Ordovician sedimentary rocks have not yet been described in the Pyrenees.

8.3 Upper Ordovician Succession

J. J. Álvaro, J. M. Casas, C. Puddu

The Upper Ordovician succession of the Central and Eastern Pyrenees, well known after the works of Cavet (1957) and Hartevelt (1970), constitutes a broad fining-upward megasequence bearing a key limestone-marlstone interbed

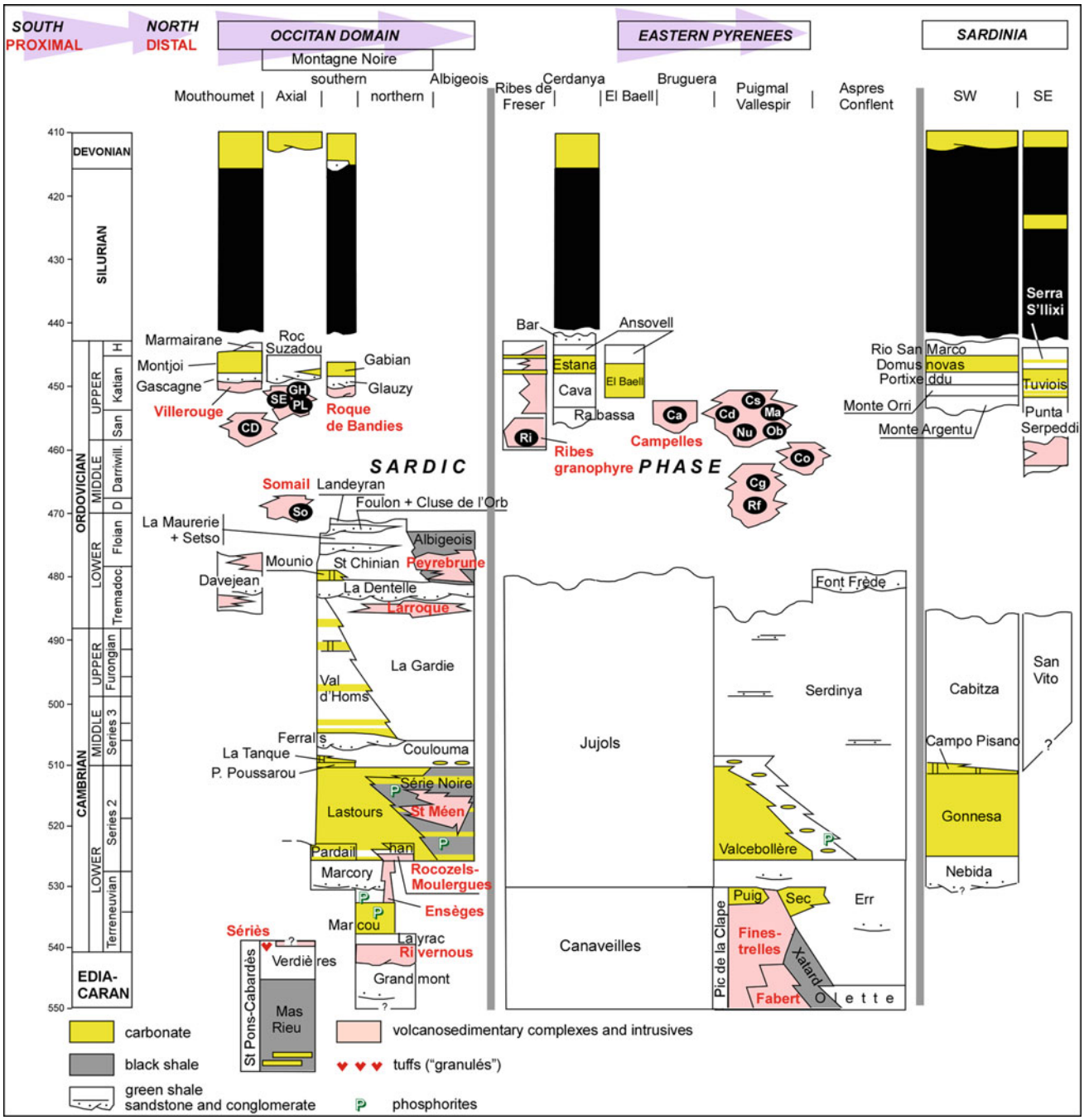

Fig. 8.2 Stratigraphic comparison of the Cambro-Ordovician successions from the Occitan Domain (Montagne Noire and Mouthoumet), Eastern Pyrenees and Sardinia. So: Somail orthogneiss (471 ± 4 Ma, Cocherie et al. 2005); SE: Saint Eutrope gneiss (455 ± 2 Ma, Pitra et al. 2012); GH: Gorges d'Heric orthogneiss (450 ± 6 Ma, Roger et al. 2004); Pl: Pont de Larn orthogneiss (456 ± 3 Ma, Roger et al. 2004); Ri: Ribes granophyre (458 ± 3 Ma, Martínez et al. 2011); Ca: Campelles ignimbrites (ca. 455 Ma, Martí et al. 2014); Cs: Casemí gneiss (446 ± 5, 452 ± 5 Ma, Casas et al. 2010); Cd: Cadí gneiss (456 ± 5 Ma, Casas et al. 2010); Ma: Marialles microdiorite (453 ± 4 Ma, Casas et al. 2010); Nu: Núria gneiss (457 ± 4 Ma, Martínez et al. 2011); Qb: Queralbs gneiss (457 ± 5 Ma, Martínez et al. 2011); Co: Cortalets metabasite (460 ± 3 Ma, Navidad et al. submitted); Cg: Canigó gneiss (472–462 Ma, Cocherie et al. 2005, Navidad et al. 2018); Rf: Roc de Frausa gneiss (477 ± 4, 476 ± 5 Ma, Cocherie et al. 2005; Castiñeiras et al. 2008)

and marked thickness variations, ranging between 100 and 1000 m. Hartevelt (1970) defined five formations, which can be recognized with some lithologic variations all across most part of the cordillera (Fig. 8.2). Furthermore, various volcanic and volcanosedimentary complexes crop out in different areas (Robert and Thiébaut 1976), although

Fig. 8.3 **a** Field aspect of a hectometre-size, microbial bioherm of the Valcebollère Formation cropping out in the vicinity of the homonymous village; *co*: core, *f*: flank. **b** Detail of boxed area in **a** showing the intertonguing contact (arrowed) of the core (white) and flank (grey). **c** Detail of boxed area in **a** illustrating the distant core/flank contact. **d** Biohermal flank composed of elongated marble clasts embedded in a silty (brownish) matrix; scale = 4 cm. **e** Contact (arrowed) of massive marbles (Valcebollère Fm) and bedded sandy shales (Serdinya Fm) marked by ferrigenous crusts. **f** Photomicrograph of the contact marked in **e** showing a fissure network of hydrothermal veins infilled with hematite, goethite and ankerite sealed (top) by a clean sparry mosaic of calcite (marble); scale = 2 mm. **g** Valcebollère/Serdinya transition characterized by the presence of unselected marble nodules "floating" in a shaly matrix (facies named "schistes troués" in France and "facies rizada" in Spain)


(a)
(b)
(c)
(d)
(e)
(f)
(g)
(h)
(i)

◀ **Fig. 8.4** **a** Convoluted alternations of centimetre-thick sandstones and shales showing amalgamation of migrating bars and storm-induced processes; Serdinya Formation at La Molina. **b** Burrowing surfaces of soft-bodied metazoan suspensivores marking low-sedimentation events; Font Frède Member at Camporells. **c** Angular discordance separating the Serdinya Formation (left) and the Rabassa conglomerates (right) at Talltendre. **d** Alluvial-to-fluvial trough cross-stratified conglomerates and sandstones of the Rabassa Formation at Talltendre. **e**, **f** Hydrothermal dykes infilled with quartz marking the outlines of the half-grabens infilled with the Rabassa conglomerates at La Molina. **g** Field aspect of the Rabassa conglomerate rich in subangular hydrothermal quartz clasts; La Molina. **h** Top of the Katian El Baell Formation at its stratotype unconformably overlain by the Hirnantian Ansovell Formation. **i** Detail of the El Baell limestones showing echinoderm-rich packstones with scattered, partially articulated columns

radiometric ages are necessary to distinguish between Sardic-related and post-Sardic (Upper Ordovician) volcanogenic events.

Unconformably overlying the Sardic-related palaeotopography, the Rabassa Conglomerate Formation is made up of reddish-purple, unfossiliferous conglomerates with sharp lateral thickness variations, from zero to 200 m. Conglomerates are composed of subrounded to well-rounded clasts rich in slates, quartzites and vein quartz, up to 50 cm in diameter, embedded in a green-purple granule-sized matrix (Fig. 8.4d). Their massive-to-channelized sets are interpreted as alluvial-to-fluvial deposits (Hartevelt 1970). Due to its stratigraphic position, this author attributed the Rabassa conglomerates to the Sandbian-Early Katian (former Caradoc).

The overlying Cava Formation, 100–800 m thick, which either cover the Sardic unconformity or the Rabassa Conglomerate Formation, is made up of feldspathic conglomerates and sandstones in the lower part, grading upwards into variegated shales and fine-grained sandstones, with strongly burrowed quartzites in the uppermost part (Belaustegui et al. 2016). A contemporaneous volcanic influence is distinct in the southwestern part of the Canigó massif, where ash levels, andesites and metavolcanic rocks are embedded (e.g., in Ribes de Freser; Muñoz 1985). Brachiopods, bryozoans and echinoderms are locally abundant, concentrated in fine-grained sandstones of the middle part of the formation, based on which, Gil-Peña et al. (2004) attributed a Katian (former late Caradoc-early Asghill) age to this formation.

The Estana Formation, which lies above the Cava Formation, consists of limestones and marly limestones, up to 10 m thick. The unit constitutes a good stratigraphic marker bed, the so-called "schistes troués", "Grauwacke à *Orthis*" and "Caradoc limestones" of French and Dutch geologists. Conodonts, brachiopods, bryozoans and echinoderms are abundant, yielding a Katian (former mid Ashgill; Gil-Peña et al. 2004) age for the development of echinoderm-bryozoan meadows on shelly, offshore-dominated substrates.

The "Ansovell" Formation (Ansobell sensu Hartevelt 1970) unconformably overlies the Estana limestone and consists of blackish shales with common slumping and convoluted layers close to the base and minor quartzite interlayers in the uppermost part. Where the Estana Formation tapers off, the Ansovell shales directly overlie the Cava sandstones. Finally, the Bar Quartzite Formation marks the top of the Upper Ordovician as a quartzitic layer, 5–10 m thick. An Hirnantian age (former late Ashgill) was proposed for the Ansovell and Bar formations by Hartevelt (1970), and confirmed by Roqué et al. (2017). Westward, in the Orri, Pallaresa and Garona domes, Gil-Peña et al. (2000, 2004) reported a calcareous conglomerate, up to 8 m thick, directly capping the erosive unconformity that marks the Estana/Ansovell contact, and attributed it to a Hirnantian glacial event.

Thickness of the Upper Ordovician succession diminishes northward, across the Massana anticline and the Aston and Ospitalet domes. In these areas, the Rabassa conglomerates are absent, whereas the Estana limestone attains its maximum thickness, about 70 m (Margalef 2015).

In the Ribes de Freser area (south of the Canigó massif, Eastern Pyrenees), an Upper Ordovician succession, different from the above-mentioned one, is located. There, several Alpine structural units form an antiformal stack bounded to the north by the out-of-sequence Ribes-Camprodon thrust. In this antiformal stack, three Alpine units (named Ribes de Freser, El Baell and Bruguera) exhibit a characteristic Upper Ordovician succession (Fig. 8.5). Restoration of the Alpine deformation allows us to situate the Bruguera unit in a pre-Alpine northernmost position, the El Baell unit in an intermediate setting, and the Ribes de Freser unit would lie originally in a southernmost one.

The Ribes de Freser unit is predominantly made up of volcanic and volcanosedimentary rocks (Fig. 8.5) (Robert and Thiébaut 1976; Ayora 1980; Robert 1980; Muñoz 1985; Martí et al. 1986), with a variable thickness ranging from 600 to 1200 m. Its lower part consists of dioritic bodies and volcanosedimentary rocks, whereas rhyolitic lava flows and ignimbrites predominate in the central part, and ash levels, ignimbrites and volcaniclastic rocks form its upper part. A granophyric body, dated as 458 ± 3 Ma (Martínez et al. 2011), intruded into the lower part of the succession. The volcanic activity was mainly explosive and had a calc-alkaline affinity reflecting crustal melting (Martí et al. 1986).

The El Baell unit, in turn, comprises a 300 m-thick succession entirely composed of limestones, marly limestones ("schistes troués") and shales (Robert 1980; Muñoz 1985). Three limestone-dominated thickening-upward sequences, up to 30 m thick, can be distinguished. Conodonts and crinoids allowed Robert (1980) to attribute an early Katian (former Caradoc) age to the beds forming this unit (Fig. 8.4h, i).

The Bruguera unit lies on the top of the El Baell unit and is composed of a 200 m-thick undated slate-dominated

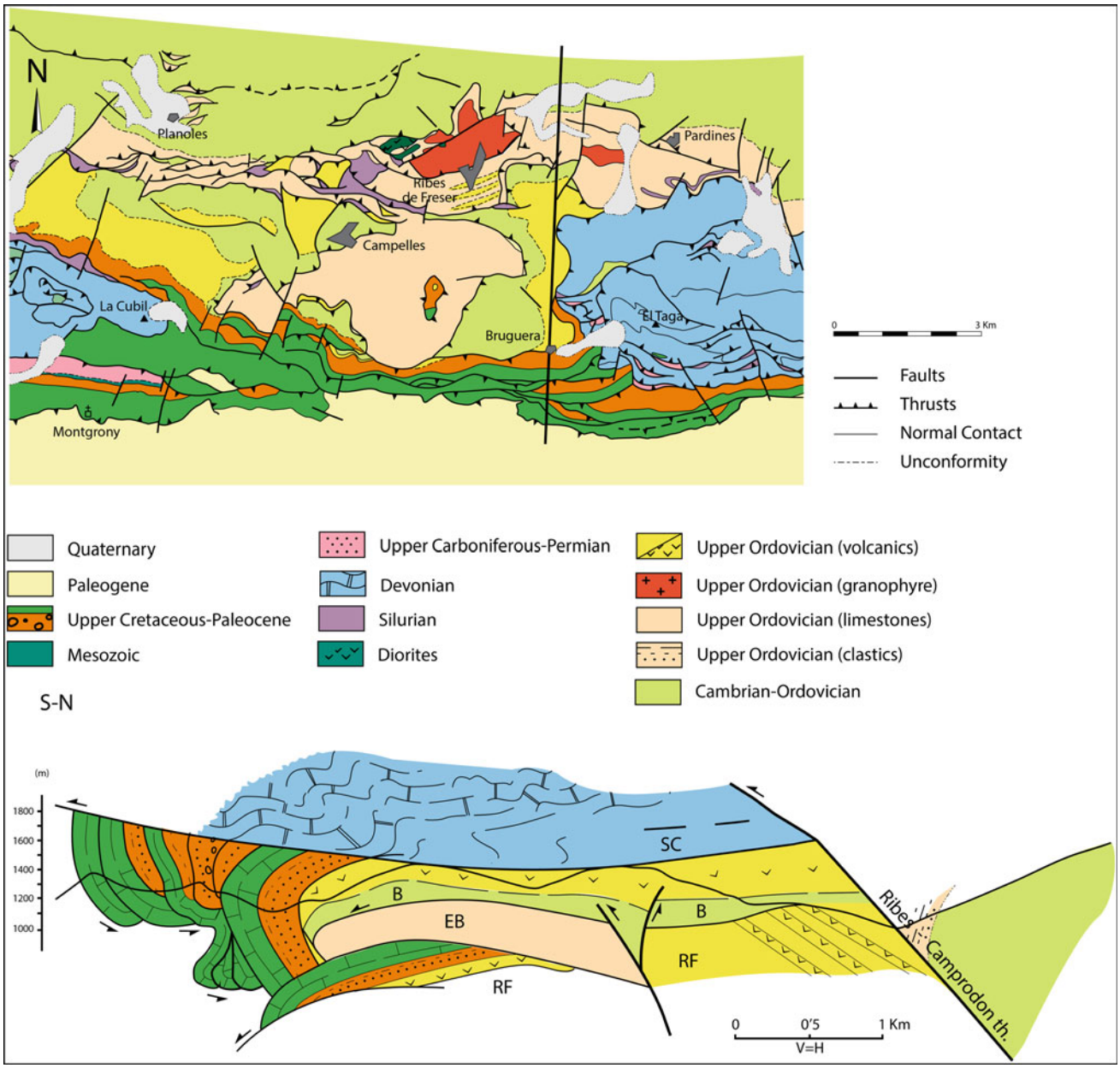

Fig. 8.5 Cross-section of the Freser river antiformal stack with the Ribes de Freser (RF), El Baell (EB) and Bruguera (B) units. After Muñoz (1985) modified. See location on Fig. 8.1

succession, pre-Variscan (Cambrian-Ordovician?) in age, overlain by a volcanic complex (Muñoz 1985). The latter consists of rhyolitic ignimbrites and andesitic lava flows, recently dated at ca. 455 Ma (Martí et al. 2014), an age similar to that of the Ribes granophyre cropping out in the Ribes de Freser unit.

After Santanach's (1972a) work, it is widely accepted that the Upper Ordovician succession lies unconformably over either the Jujols or Canaveilles groups (García-Sansegundo and Alonso 1989; Den Brok 1989; Kriegsman et al. 1989; Poblet 1991; Muñoz and Casas 1996; García-Sansegundo et al. 2004; Casas and Fernández 2007). However, the origin of this unconformity has been object of several interpretations. Santanach (1972a) in the Canigó massif and García-Sansegundo et al. (2004) in the Garona dome attributed the Sardic unconformity to basement tilting, related to of a Late Ordovician faulting episode and subsequent erosion. In the Lys-Caillaouas massif, Den Brok (1989) and Kriegsman et al. (1989) proposed the existence of a pre-Variscan deformation event. A pre-Upper Ordovician folding episode has been also suggested as related to the unconformity on the southern Canigó massif (Casas 2010; Casas et al. 2012).

However, the meaning of this deformation episode is unclear: it is related neither to metamorphism nor cleavage development, although it seems related to uplift, widespread emersion and considerable erosion before the onset of Upper Ordovician deposition. As a result, the Upper Ordovician rocks directly onlap different formations of the pre-Sardic succession, ranging from the upper Neoproterozoic to the Lower Ordovician in the Central and Eastern Pyrenees (Santanach 1972a; Laumonier and Guitard 1986; Cirés et al. 1994).

Based on the above-reported maximum depositional age of the Jujols Group (ca. 475 Ma) and the ca. 455 Ma U–Pb age for the Upper Ordovician volcanic rocks directly overlying the Sardic unconformity in the Bruguera unit (Martí et al. 2014), a time gap of about 20 m.y. can be estimated for the Sardic Phase. Similar gaps are found in SW Sardinia (ca. 18 m.y.), the type area where the original unconformity was described, where the discontinuity is constrained by well-dated Upper Ordovician metasediments overlying upper Tremadoc-lower Floian(?) strata (Barca et al. 1987; Pillola et al. 2008).

The Sardic uplift (whatever its origin) was necessarily followed by a succession of Late Ordovician extensional pulsations, which preceded and were contemporaneous with the opening of grabens and half-grabens infilled with the alluvial-to-fluvial Rabassa Conglomerate Formation. At outcrop scale, a synsedimentary hydrothermal activity is associated with the onset of decametre-sized normal faults lined with quartz veins and dykes, which subsequently feed the Rabassa conglomerates as vein quartz pebbles (Fig. 8.4 e–g). At cartographic scale, a detailed geological map of the La Cerdanya area reveals a set of normal faults sharply affecting the thickness of the Rabassa and Cava formations (Fig. 8.6) (Casas and Fernández 2007; Casas 2010; Puddu and Casas 2011). The faults are steep and currently exhibit broad N-S to NNE-SSW trending. In most cases, their hangingwall is the eastern block despite the presence of some antithetic faults; maximum throws of about 0.2–0.9 km can be recognized. Displacement progressively diminishes upward and fades out in the Cava rocks (Fig. 8.6). Based on these orientations, an E-W extension (in present day coordinates) can be proposed. The original orientation of the faults cannot be pinpointed owing to subsequent deformation events, although an original N-S orientation can be proposed. This orientation probably prevented the faults from being inverted during subsequent Variscan and Alpine deformation events, although the faults probably suffered rotations on horizontal E-W axes during these deformation episodes. On the other hand, sharp variations in the thickness of the Upper Ordovician succession have been reported by several authors (Llopis Lladó 1965; Hartevelt 1970; Speksnijder 1986). Hartevelt (1970) documented variations from 200 to more than 850 m in the thickness of the Cava Formation: e.g., eastward from La Seu d'Urgell, the thickness of the Rabassa and Cava formations attain more than 800 m before sharply diminishing to some tens of metres within a few kilometres (Casas and Fernández 2007). There, the maximum observed thickness occurs associated with the maximum grain size of the conglomerates (pebbles exceeding 50 cm in diameter are common). Variations in thickness and grain size can be attributed to palaeorelief formation controlled by fault activity and subsequent erosion of uplifted palaeotopographies, with subsequent infill controlled by alluvial fan and fluvial deposition.

A set of roughly E-W oriented normal faults originally limited the Ribes de Freser, El Baell and Bruguera units, nucleated the contemporaneous active volcanism reported in the Ribes de Freser and Bruguera units, and the high patterns

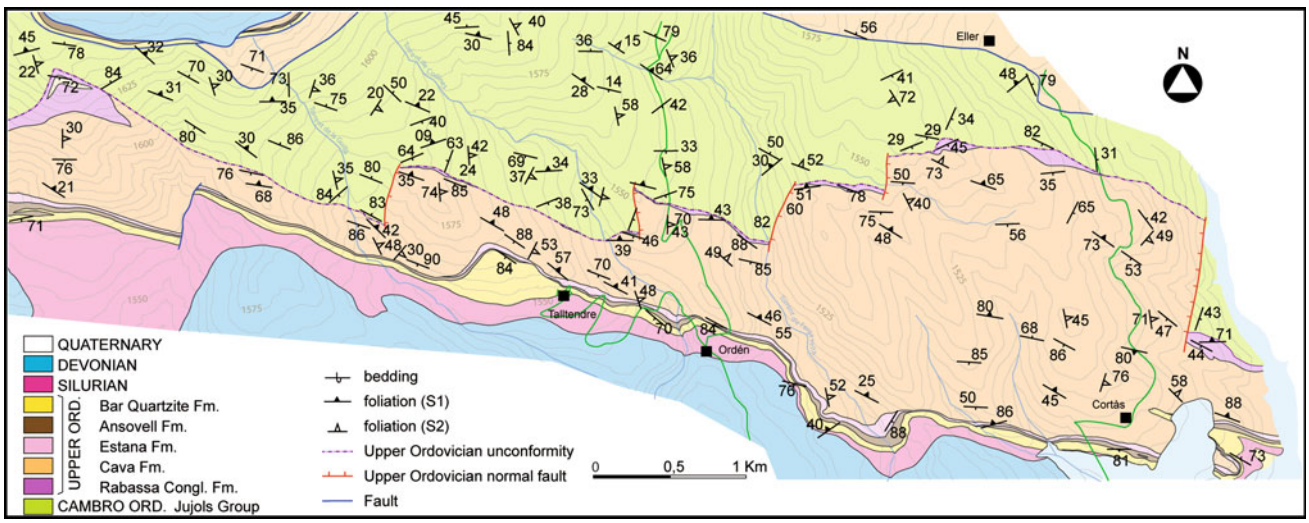

Fig. 8.6 Geological map of the Talltendre area, north of Bellver de Cerdanya; modified from Puddu and Casas (2011). See location on Fig. 8.1

of Katian carbonate productivity on an unstable epeiric platform, now preserved in the El Baell unit. These E-W oriented faults seemingly coexisted with the aforementioned N-S normal faults. The former faults were probably inverted during subsequent Variscan and Alpine tectonics, whereas the latter ones, because of their unfavourable orientation, are preserved and currently recognizable.

8.4 Ordovician Magmatism

J. J. Álvaro, J. M. Casas, C. Puddu, T. Sánchez-García, M. Navidad, P. Castiñeiras, M. Liesa

Successive Ordovician magmatic pulsations are well documented in the pre-Variscan basement of the Pyrenees (Fig. 8.1). According to radiometric data, magmatism lasted about 30 m.y., from ca. 477 to 446 Ma. Although the magmatic activity seems to be continuous, two peaks can be distinguished at 473–472 Ma and 457 Ma (Fig. 8.7). Based on geochronological and geochemical data, two different magmatic complexes can be distinguished: latest Early-Mid Ordovician and Late Ordovician in age.

(i) *Latest Early and Mid Ordovician magmatism*

During Early to Mid Ordovician times, the magmatic activity gave rise to the intrusion of voluminous aluminous granites, about 500–3000 m in size and emplaced into the Canaveilles and Jujols strata. They constitute the protoliths of the large laccolithe-shaped, orthogneissic bodies that crop out at the core of the domal massifs that punctuate the backbone of the Pyrenees. These are, from west to east, the Aston (470 ± 6 Ma, Denèle et al. 2009; 467 ±2 Ma, Mezger and Gerdes 2016), Hospitalet (472 ± 2 Ma, Denèle et al. 2009), Canigó (472 ± 6 to 467 ± 7 Ma, Cocherie et al. 2005), Roc de Frausa (477 ± 4 Ma, Cocherie et al. 2005; 476 ± 5 Ma, Castiñeiras et al. 2008) and Albera (470 ± 3 Ma, Liesa et al. 2011) massifs (Fig. 8.8), which exhibit a dominant Floian-Dapingian age. It should be noted that only a minor representation of basic coeval magmatic rocks are exposed (e.g., Cortalet metabasite). The acidic volcanic equivalents have been reported in the Albera massif, where subvolcanic rhyolitic porphyroid rocks yielded similar ages than those of the main gneissic bodies: 465 ± 4, 472 ± 3, 473 ± 2 and 474 ± 3 Ma (Liesa et al. 2011; Liesa unpubl.). Other acidic products are represented by the rhyolitic sills of Pierrefite (Calvet et al. 1988) (Fig. 8.8). Granites are medium to coarse grained and exhibit porphyritic textures with rapakiwi K-feldspars.

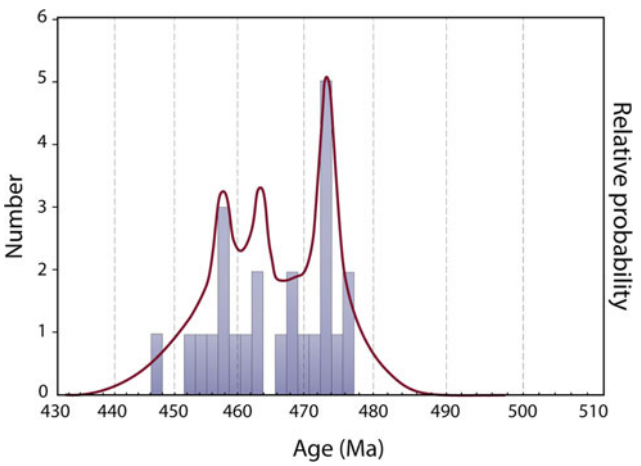

Fig. 8.7 Relative probability plot of the geochronological ages of the Ordovician magmatism of the Pyrenees. Data after Deloule et al. (2002); Cocherie et al. (2005); Castiñeiras et al. (2008); Denèle et al. (2009); Casas et al. (2010); Liesa et al. (2011); Martínez et al. (2011); Mezger and Gerdes (2016); Navidad et al. (2018) and Liesa et al. (unpublsh.). n = 25

The rocks selected for geochemical analysis have suffered from variable degrees of metamorphism and hydrothermalism, so only the most inmobiles elements have been taken into account. We have differentiated three geochemical assemblages: the Cortalets metabasite, the Volcanic Assemblage A and the Gneissic Assemblage A. Some of the differentiated assemblages are based on very few samples and further sampling could modify the geochemical signature documented below.

The Cortalets metabasite (Metabas A in Fig. 8.9) shows low silica content (43.22%) and high FeO_t (10.05), MgO (9.43%) and CaO (12.16%) values. It is metaluminous (A/CNK = 0.64) and subalkaline in the Pearce's diagram (1996) (Fig. 8.9a). REE patterns present slightly more fractionated values for LREE (La_n/Sm_n = 1.54) than HREE (Gd_n/Yb_n = 1.19), without Eu anomalies and an almost flat arrangement for HREE (Fig. 8.10a). This suggests the lack of plagioclase fractionation and garnet in the melt. Nb, Sr and Ti positive anomalies are distinct in the spider-diagram of Palme and O'Neil (2004) (Fig. 8.10b) reflecting the possible influence of mantle-derived magmas lacking plagioclase and magnetite in the melt. The metabasite exhibits average values of La/Nb, (average = 0.54), Th/Nb (0.06), Th/La (0.12), Nb/Y (0.60), Zr/Nb (5.89) and Nb/Yb (5.81) close to the Lower Continental Crust parameters of Rudnick and Gao (2004), and Th/Yb (average = 0.37) values close to the Ocean Island Basalt of Sun and McDonough (1989) (Fig. 8.11a). In the Wood's (1980) tectonic discrimination diagram, the analysis plots in the arc-basalt domain (Fig. 8.12a), while the Pearce's (2008) diagram informs about crustal contamination (Fig. 8.12b). The TiO_2/Yb versus Nb/Yb diagram (Fig. 8.12c) shows E-MORB character. All geochemical characteres may reflect primitive mantle-derived melts with crustal contamination at their origin. Further samples are necessary to confirm this interpretation.

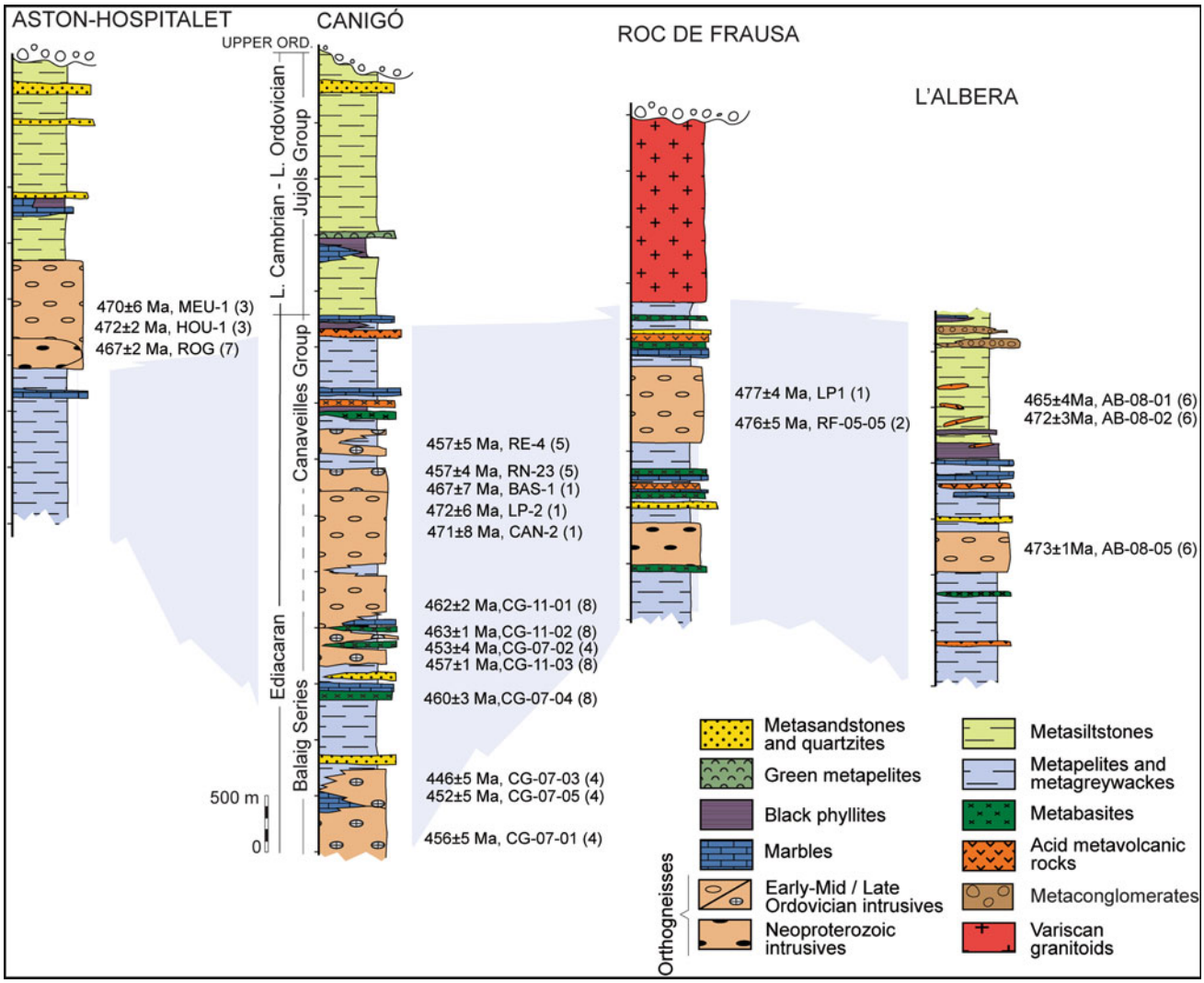

Fig. 8.8 Synthetic stratigraphic logs of the pre-Upper Ordovician rocks from the Aston-Hospitalet, Canigó, Roc de Frausa and Albera massifs with the location of the geochronological data of the protoliths of the Ordovician gneisses: (1) Cocherie et al. (2005); (2) Castiñeiras et al. (2008); (3) Denèle et al. (2009); (4) Casas et al. (2010); (5) Martínez et al. (2011); (6) Liesa et al. (2011); (7) Mezger and Gerdes (2016) and (8) Navidad et al. (2018). Stratigraphic data from Guitard (1970), Santanach (1972b), Ayora and Casas (1986), Liesa and Carreras (1989) and Liesa et al. (2011)

The Volcanic Assemblage A includes 6 samples from the Albera (Liesa et al. 2011) and Pierrefite (Calvet et al. 1988) massifs. They show a narrow range of SiO_2 content ($70.09 < SiO_2 < 74.87$) and peraluminous (A/CNK = 2.03 − 1.12) and subalkaline features, with an average content of Nb/Y = 0.32 (Fig. 8.9a). REE patterns present more fractionated values for LREE ($La_n/Sm_n = 2.63$) than HREE ($Gd_n/Yb_n = 1.32$) being $(La/Yb)_n = 5.88$. The average Eu anomalies show moderate negative values (0.68) reflecting plagioclase crystallization (Fig. 8.10c). It should be noted that this assemblage presents two subsets, one with a distinct enrichment in HREE and a flat slope, and another with a moderate slope in HREE. This suggests different magmatic sources for both subsets. In the spider-diagram of Palme and O'Neil (2004), they show negative anomalies of Nb, Sr and Ti (Fig. 8.10d). The overall chondrite-normalized pattern is close to the values of the Upper Continental Crust of Rudnick and Gao (2004), and display slight enrichments in Th/Nb (average = 1.13) and Th/La (average = 0.56), and depletion in La/Nb (average = 2.43), Th/Yb (average = 3.50) and Nb/Yb (average = 3.06) ratios close to EMORB values (3.5 values of Sun and McDonough 1989) (Fig. 8.11b). In the tectonic diagram of Pearce et al. (1984), the samples plot in the volcanic arc-I type field (Fig. 8.13a). In the Zr versus TiO_2 diagram of Syme (1998), they plot in the arc association (Fig. 8.13b). No εNd values are yet available for this

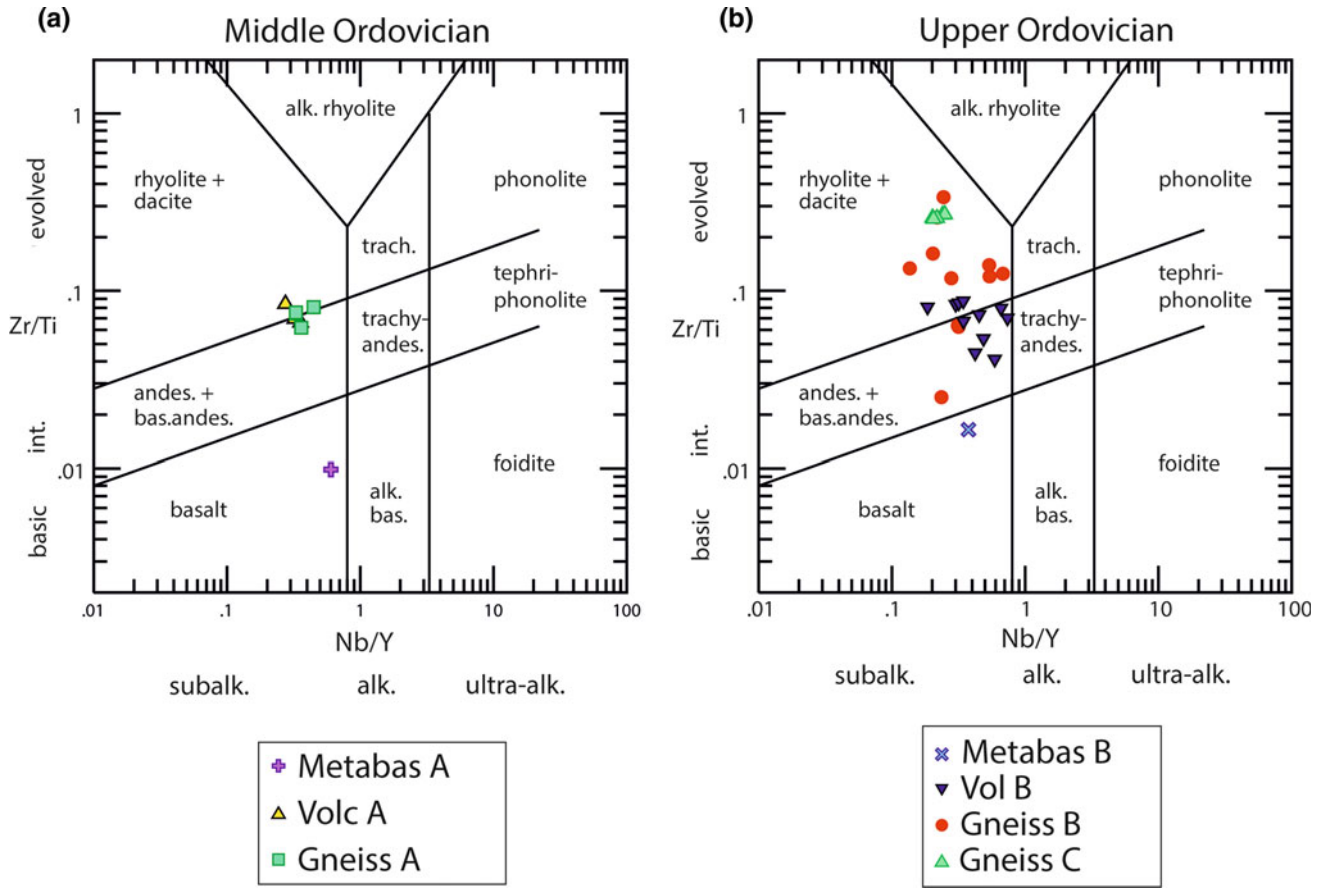

Fig. 8.9 Zr/Ti versus Nb/Y diagram (Pearce 1996). **a** Uppermost Lower-Middle Ordovician rocks; **b** Upper Ordovician rocks (data after Robert and Thiébaut 1976; Calvet et al. 1988; Castiñeiras et al. 2008; Navidad et al. 2010; Liesa et al. 2011; Navidad et al. 2018)

assemblage. All these geochemical data suggest a calc-alkaline magmatic source from active margin environments related to the first stages of extension, as pointed out by Calvet et al. (1988).

The Gneissic Assemblage A includes 4 samples of the Roc de Frausa (Castiñeiras et al. 2008), Albera (Liesa et al. 2011) and Canigó (Navidad et al. 2018) massifs. They show SiO_2 contents ranging between 67.17 and 73.62%. They are peraluminous (A/CNK = 1.20 − 1.10) and subalkaline, with an average content of Nb/Y = 0.37 (Fig. 8.9a). REE patterns present more fractionated values for LREE (La_n/Sm_n = 3.13) than for HREE (Gd_n/Yb_n = 1.43) being $(La/Yb)_n$ = 6.52. The average Eu anomalies show moderate negative values (0.39) reflecting plagioclase crystallization (Fig. 8.10c). In the spider-diagram of Palme and O'Neil (2004), they show negative anomalies of Nb reflecting crustal magmas, Sr and Ti (Fig. 8.10d) suggesting fractionation of plagioclase and Fe–Ti oxides, respectively. The overall chondrite-normalized pattern is close to the values of the Upper Continental Crust of Rudnick and Gao (2004), with slight enrichment in the Th/Nb (average = 1.13) and Th/La (average = 0.56) ratios, and depletion in the La/Nb (average = 2.43), Th/Yb (average = 3.50) and Nb/Yb (average = 3.06) ratios close to EMORB values (3.5 values of Sun and McDonough 1989) (Fig. 8.11b). In the tectonic diagram of Pearce et al. (1984), the samples plot in the volcanic arc-I type field (Fig. 8.13a), whereas in the Zr versus TiO_2 diagram of Syme (1998) they plot in the arc association (Fig. 8.13b). No εNd values are available for this assemblage. All the geochemical characters outlined above indicate that they are similar to the above-reported volcanic assemblage, so these rocks were mainly derived from a continental crustal source. Navidad et al. (2010) suggested that crustal recycling would account for the volcanic arc signature of these samples. This signature was probably inherited by melting of a pre-existing Neoproterozoic-Lower Palaeozoic calc-alkaline crust.

(ii) *Late Ordovician magmatism*

A Late Ordovician magmatic pulse yielded a varied suite of magmatic rocks. Small granitic bodies are emplaced in the Canaveilles and Jujols strata of the Canigó massif and constitute the protoliths of the Cadí, Casemí and Núria

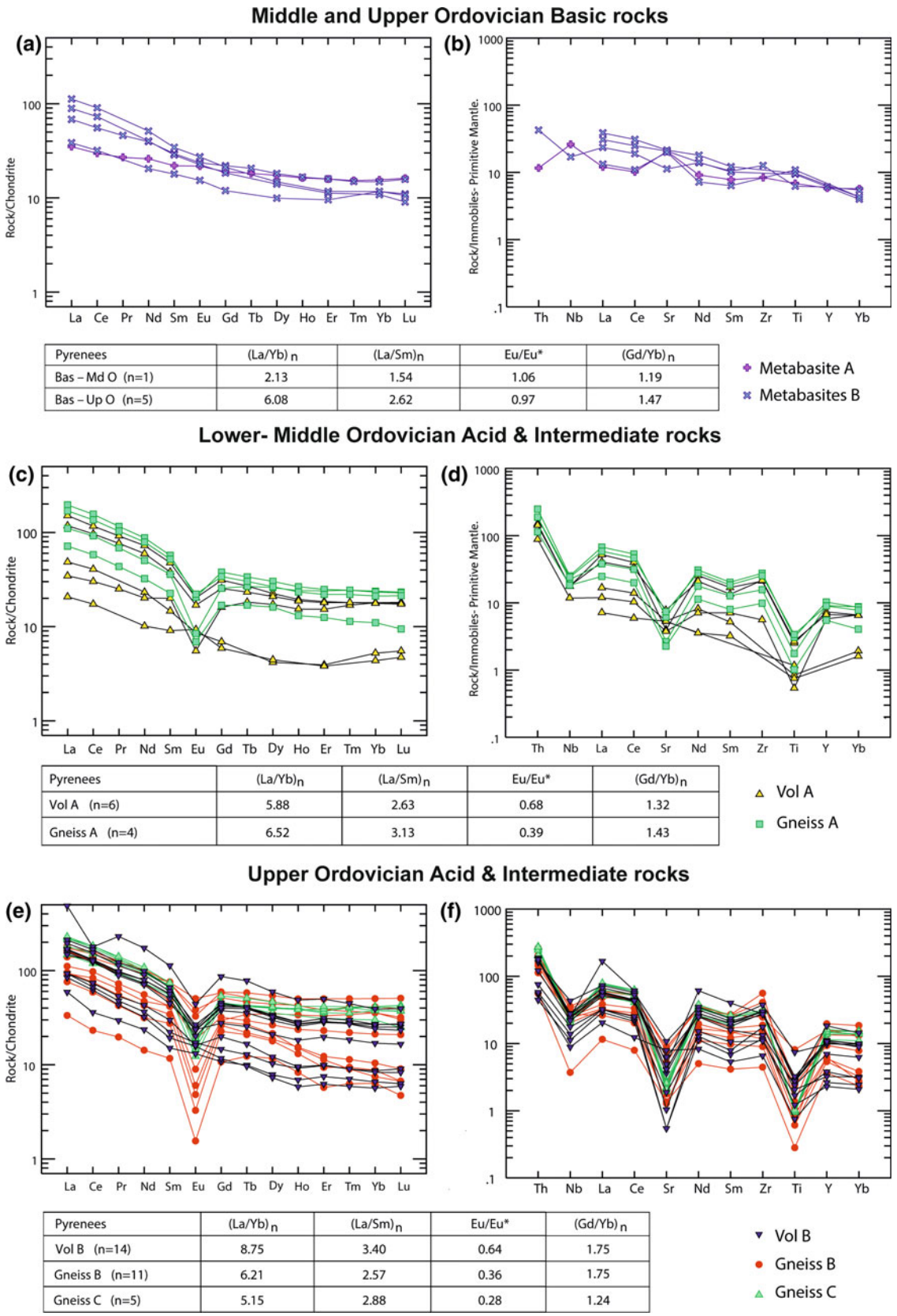

Pyrenees	$(La/Yb)_n$	$(La/Sm)_n$	Eu/Eu*	$(Gd/Yb)_n$
Bas – Md O (n=1)	2.13	1.54	1.06	1.19
Bas – Up O (n=5)	6.08	2.62	0.97	1.47

Pyrenees	$(La/Yb)_n$	$(La/Sm)_n$	Eu/Eu*	$(Gd/Yb)_n$
Vol A (n=6)	5.88	2.63	0.68	1.32
Gneiss A (n=4)	6.52	3.13	0.39	1.43

Pyrenees	$(La/Yb)_n$	$(La/Sm)_n$	Eu/Eu*	$(Gd/Yb)_n$
Vol B (n=14)	8.75	3.40	0.64	1.75
Gneiss B (n=11)	6.21	2.57	0.36	1.75
Gneiss C (n=5)	5.15	2.88	0.28	1.24

Fig. 8.10 Geochemical features; **a** chondrite-normalized REE patterns for basic Middle and Upper Ordovician rocks; **b** spider-diagram for basic Middle and Upper Ordovician rocks; **c** chondrite-normalized REE patterns for acid and intermediate Middle Ordovician rocks; **d** spider-diagram for acid and intermediate Middle Ordovician rocks **e** chondrite-normalized REE patterns for acid and intermediate Upper Ordovician rocks; **f** spider-diagram for acid and intermediate Upper Ordovician rocks. (Chondrite normalizing values of Sun and McDonough 1989 and Primitive Mantle normalizing values of Palme and O'Neil 2004)

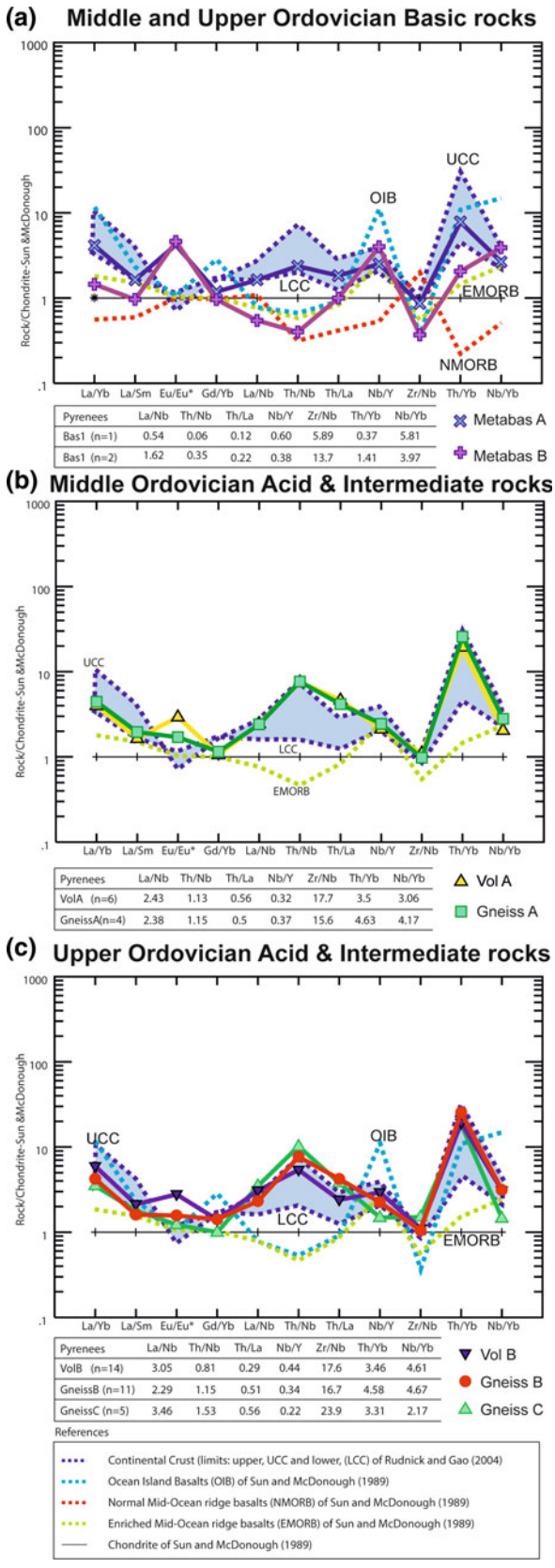

Fig. 8.11 Chondrite-normalized isotope ratios patterns (Sun and McDonough 1989). **a** mafic Middle and Upper Ordovician rocks; **b** acid and intermediate Middle Ordovician rocks; **c** acid and intermediate Upper Ordovician rocks. Blue area: Continental crust values of Rudnick and Gao (2004)

gneisses. The Cadí gneiss (Guitard 1970), dated at 456 ± 5 Ma by Casas et al. (2010), is an aluminous metagranite body with petrographic characteristics similar to those of the Canigó gneiss; it represents the lowest structural unit recognized in the Canigó massif (Fig. 8.8). The Casemí gneiss (Guitard 1970) is a tabular body up to 1000 m thick mainly made up of fine-grained biotitic and amphibolic granitic gneisses. Geochronological data indicate a Late Ordovician age for the protolith of this orthogneiss (446 ± 5 and 452 ± 5 Ma Ma, SHRIMP U–Pb in zircon, Casas et al. 2010). In the southern Canigó massif, the protoliths of the Núria granitic gneiss and the homonymous augen gneiss (Santanach 1972b) also yield Late Ordovician ages (457 ± 4 and 457 ± 5 Ma, respectively, Martínez et al. 2011). Moreover, metre-scale thick bodies of metadiorite are interlayered in the micaschists of the Balaig series, which has also yielded a Late Ordovician age for the formation of its protolith (453 ± 4 Ma, SHRIMP U–Pb in zircon, Casas et al. 2010) (Fig. 8.8).

Coeval calc-alkaline volcanic rocks (ignimbrites, andesites and volcaniclastic rocks) are interbedded in the Upper Ordovician of the Ribes de Freser and Bruguera units. The lower part of the Ribes de Freser unit is made up of dioritic bodies and volcaniclastic rocks, whereas rhyolitic lava flows and ignimbrites predominate in the central part, and ash levels, ignimbrites and volcaniclastic rocks constitute its upper part. The Ribes granophyric body, dated at 458 ± 3 Ma by Martínez et al. (2011), crops out at the base of the Upper Ordovician. On the other hand, the rhyolitic ignimbrites and andesitic lavas of the Bruguera unit have been recently dated at ca. 455 Ma by Martí et al. (2014). This volcanism was mainly explosive and displays a calc-alkaline affinity (Martí et al. 1986). Based on their geochemical data, we have differentiated four Upper-Ordovician magmatic assemblages: the metabasites B, the Volcanic Assemblage B and the Gneissic Assemblages B and C.

The metabasites B include 5 samples of the Marialles diorite (Navidad et al. 2010) and the alkali-pillow basalts of the Pierrefite massif (Calvet et al. 1988). They are undersaturated with SiO_2, whose content ranges from 47.3 to 52.4 wt%. Most of them are metaluminous (average A/CNK ratio = 0.98), although a sample (25-1) from the Pierrefite massif presents a value of 1.47. In the Pearce's diagram (1996), the assemblage plots in the subalkaline field (Fig. 8.9b), whereas the Pierrefite samples are alkaline in the Shervais (1982) diagram with Ti/V values = 100 to 50. The REE patterns present more fractionated values for LREE (La_n/Sm_n = 2.62) than HREE (Gd_n/Yb_n = 1.47), without Eu anomalies and higher slopes that the Cortalets metabasites (Fig. 8.10e) suggesting little plagioclase fractionation. Most of them show Nb, Sr and Ti negative anomalies in the spider diagram of Palme and O'Neil (2004) (Fig. 8.10b). This

assemblage displays a different behaviour in the La/Nb, Th/Nb, Th/La, Zr/Nb (depleted) and Nb/Y (enriched) ratios that the Cortalet metabasite. The Th/La, Zr/Nb and Th/Yb values are close to the Ocean Island basalts of Sun and McDonough (1989), while the Nb/Y value is close to the Upper Continental Crust of Rudnick and Gao (2004), and the Th/Nb ratio is close to the NMORB values of Sun and McDonough (1989) (Fig. 8.11a). In the tectonic discrimination diagram of Wood (1980), this assemblage plots in the Ocean Island Basalts domain (Fig. 8.12a), in the Pearce's (2008) diagram in the MORB array (Fig. 8.12b), and in the TiO_2/Yb versus Nb/Yb diagram (Fig. 8.12c) the dataset shows a distinct E-MORB character. The Sm–Nd isotopic data obtained from the Marialles sample are given in Table 8.1 and plotted in Fig. 8.14. The reference age considered for the emplacement of the Marialles diorite is 453 Ma (Navidad et al. 2010). The analysed sample shows a $^{147}Sm/^{144}Nd$ ratio of 0.1474, slightly negative εNd values (−0.8) and a TDM age of 1.18 Ga. This value could indicate that their protoliths were derived from mantle melts with heterogeneous crustal contamination (Navidad et al. 2010). In summary, the geochemical data discussed above could reflect a more primitive origin mantle-derived but with crustal contamination at their origin.

The Volcanic Assemblage B includes 14 samples from the Els Metges volcanic tuffs, Les Gavarres epiclastic ash (Navidad et al. 2010) and the Ribes de Freser rhyolitic lavas (Robert and Thiébaut 1976). Although no geochemical data are available, we suggest including in this assemblage the Bruguera volcanic rocks due to their similar field characteristics. This assemblage shows a SiO_2 content ranging between 86.06 and 62.98%. They are peraluminous (A/CNK = 3.63 − 1.04) and subalkaline, with an average content of Nb/Y = 0.44 (Fig. 8.9b). REE patterns present more fractionated values for LREE (La_n/Sm_n = 3.40) than HREE (Gd_n/Yb_n = 1.75) being $(La/Yb)_n$ = 8.75. The average Eu anomalies show negative values (0.64) reflecting plagioclase crystallization (Fig. 8.10e). In the spider-diagram of Palme and O'Neil (2004), they show negative anomalies of Nb, Sr and Ti (Fig. 8.10f). Overall chondrite-normalized pattern are close to the values of the Upper Continental Crust of Rudnick and Gao (2004), with slight enrichment in the La/Nb (average = 3.05) and Zr/Nb (average = 17.6) ratios, and depletion in the Th/Nb (average = 0.81), Th/La (average = 0.29), Nb/Y (average = 0.44), Th/Yb (average = 3.46) and Nb/Yb (average = 4.61) ratios (Fig. 8.11c). In the tectonic diagram of Pearce et al. (1984), most of samples plot in the volcanic arc-I type field and the anomalous rift field (Fig. 8.13c). In the Zr versus TiO_2 diagram of Syme (1998), most of samples plot in the arc association (Fig. 8.13d). The volcanic tuffs of Les Gavarres show an $^{147}Sm/^{144}Nd$ isotope ratio ranging between 0.1410 and 0.1372 and εNd between −5.1 and −4.8, indicating a crustal origin (Navidad et al. 2010). Similar isotopic values have been obtained by Martínez et al. (2011) for the Ribes granophyre (εNd −2.6) indicating also a crustal origin.

The Gneissic Assemblage B includes 11 samples from the Canigó and Cadí gneisses, (Canigó massif, Navidad et al. 2010; Navidad et al. 2018). Although no geochemical data are available, we suggest including here the Núria gneisses. The assemblage shows a SiO_2 content between 76.42 and 56.47%. The samples are peraluminous (A/CNK = 1.24 − 0.64) and subalkaline, with an average content of Nb/Y = 0.34 (Fig. 8.9b). REE patterns present more fractionated values for LREE (La_n/Sm_n = 3.13) than HREE (Gd_n/Yb_n = 1.43) being $(La/Yb)_n$ = 6.38. The average Eu anomalies show moderate negative values (0.36) reflecting plagioclase crystallization (Fig. 8.10e). In this assemblage, two subsets can be distinguished, one with flat slope and another with negative slope. This could indicate two different magmatic sources. In the spider-diagram of Palme and O'Neil (2004), they show negative anomalies of Nb, Sr and Ti (Fig. 8.10f). The overall chondrite-normalized pattern is close to the values of the Upper Continental Crust of Rudnick and Gao (2004), with a slight enrichment in the Th/Nb (average = 1.15), Th/La (average = 0.51) and Zr/Nb (average = 16.7) ratios and depletion in the La/Nb (average = 2.29) and Th/Yb (average = 4.58) values. The Nb/Y (average = 0.34) value is close to the Lower Continental Crust of Rudnick and Gao (2004) (Fig. 8.11c). In the tectonic diagram of Pearce et al. (1984), the samples plot in the volcanic arc-I type field and the anomalous rift field (Fig. 8.13c). In the Zr versus TiO_2 diagram of Syme (1998), the samples plot both in the arc association (Fig. 8.13d) and the extensional field. The Cadí orthogneisses show a Nd isotope ratio (0.5118) similar to the most differentiated assemblage (Casemí, Gneissic Assemblage C; see below) and a higher negative isotopic signature with εNd negative values (−4.2 to −5.2) (Fig. 8.14) than these gneisses (Gneissic Assemblage C) suggesting a crustal origin (Navidad et al. 2010). Similar isotopic values have been obtained by Martínez et al. (2011) for the Núria gneisses (εNd between −3.0 and −4.7). All the geochemical characters outlined above indicate that this assemblage was mainly derived from different magmas of continental crustal source.

The Gneissic Assemblage C includes 5 samples from the Casemí and Canigó gneisses (Canigó massif, Navidad et al. 2010). They present more silica and alkalis and less Al, Fe and Mg than the Gnesissic Assemblage B. They show a narrow range of composition (73.62% < SiO_2 < 75.02%) and are peraluminous (A/CNK = 1.24 − 0.64) and subalkaline, with an average content of Nb/Y = 0.22 (Fig. 8.9b). The REE pattern is similar to the subset with flat slope of HREE in the Gneissic Assemblage B, with more fractionated

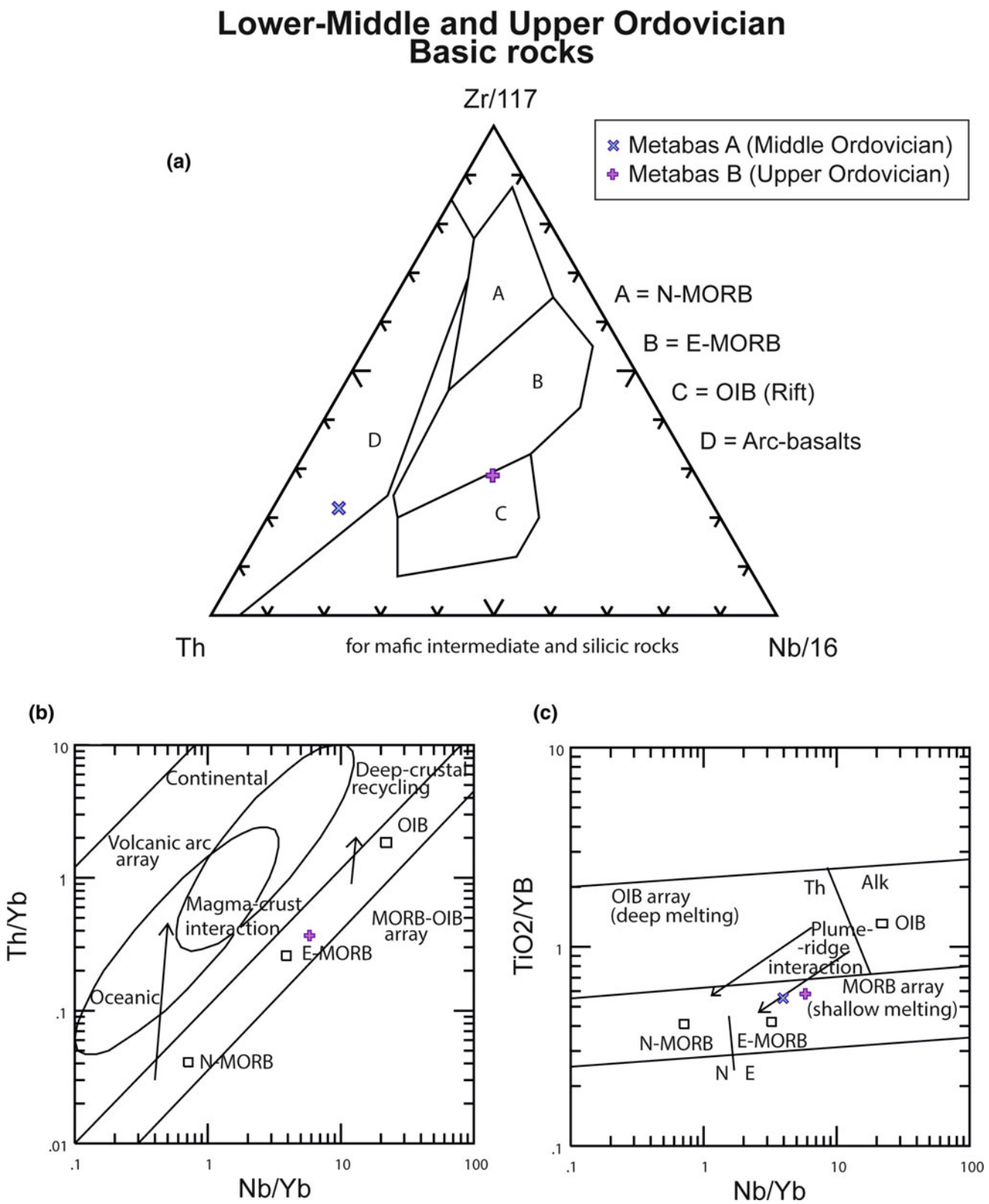

Fig. 8.12 Tectonic discriminating diagram of basic rocks. **a** Wood (1980); **b** Th/Yb versus Nb/Yb of Pearce (2008); **c** TiO_2/ Yb versus Nb/Yb of Pearce (2008)

Table 8.1 Sr–Nd isotopic data of the Upper Ordovician magmatic rocks of the Pyrenees (data after Navidad et al. 2010 and Martínez et al. 2011). (Bas B: Metabasites B; Gneiss B: Gneisssic Assemblage B; Gneiss C: Gneisssic Assemblage C; Vol B: Volcanic assemblage B)

Sample	Unit rock	Litology	Sm	Nd	$^{147}Sm/^{144}Nd$	$^{143}Nd/^{144}Nd$	$^{143}Nd/^{144}Nd_{age}$	eNd_0	eNd_{age}	Age (Ma)	Tdm (Ga)	$(^{87}Sr/^{86}Sr)_0$	$(^{87}Sr/^{86}Sr)_{age}$	Author
CG-07-02a	Marialles (Bas B)	Diorite	4.51	18	0.1508	0.51246	0.512014	−3.5	−0.6	453	1.18	0.736385	0.731345	2
C96767aQ2	Canigó (Gneiss B)	Bt orthogneiss	10.45	47	0.1338	0.5123	0.511909	−6.6	−3	445.9	1.41	0.770513	0.660161	2
CG-07-01a	Cadí (Gneiss B)	Orthogneiss	7.3	34	0.1292	0.51223	0.511841	−8	−4.2	456.1	1.47	0.736385	0.708542	2
100768	Canigó (Gneiss B)	Amph. orthogneiss	11.3	48	0.1417	0.51236	0.511941	−5.5	−2.3	445.9	1.45	0.720992	0.707661	2
100786	Canigó (Gneiss B)	Bt orthogneiss	6.41	22	0.1754	0.51239	0.511878	−4.8	−3.5	445.9	2.63	0.817270	0.690857	2
C-96940F	Canigó (Gneiss B)	Amph. orthogneiss	11.57	47	0.1482	0.51238	0.51195	−5	−2.2	445.9	1.53	0.720939	0.708524	2
C-770288	Canigó (Gneiss B)	Amph. orthogneiss	11.46	43	0.1604	0.51233	0.51186	−6	−4	445.9	2.04	0.718292	0.709528	2
RE-2	Núria (Gneiss B)	Augen gneiss	7.07	35.1	0.1217	0.51226	0.511901	−7.4	−3	450	1.47	–	–	1
RE-10	Núria (Gneiss B)	Augen gneiss	2.4	9.9	0.1468	0.51231	0.51188	−6.3	−3.5	450	1.9	–	–	1
RN-16	Núria (Gneiss B)	Two-mica gneiss	2.74	10.14	0.1634	0.51234	0.511855	−5.9	−4	450	2.45	–	–	1
RN-26	Núria (Gneiss B)	Two-mica gneiss	6.18	27.13	0.1377	0.51227	0.511865	−7.2	−3.8	450	1.76	–	–	1
RN-27	Núria (Gneiss B)	Two-mica gneiss	0.86	1.88	0.2765	0.51264	0.511825	0	−4.7	450	–	–	–	1
GRF-05-1A	Ribes (Gneiss B)	Granophyre	8.51	37.09	0.1381	0.51233	0.511927	−5.9	−2.6	450	1.66	–	–	1
CG-07-05a	Casemí (Gneiss C)	Bt orthogneiss	11.29	50	0.1359	0.51239	0.511991	−4.8	−1.2	451.6	1.27	0.745438	0.696910	2
CG-07-03a	Casemí (Gneiss C)	Bt orthogneiss	8.36	34	0.148	0.5124	0.511969	−4.6	−1.7	445.9	1.48	0.742716	0.702258	2
100766	Canigó (Gneiss C)	Bt orthogneiss	10.3	44	0.1409	0.51241	0.511998	−4.5	−1.4	445.9	1.32	0.754248	0.706702	2
NF-29a	Les Gavarres (Vol B)	Volcanic tuff	8.67	37	0.141	0.51223	0.511806	−8	−4.8	455.2	1.71	0.733067	0.703181	2
NF-32	Les Gavarres (Vol B)	Volcanic tuff	7.75	34	0.1372	0.51221	0.511802	−8.3	−4.9	455.2	1.65	0.726113	0.707025	2
NF-63	Les Gavarres (Vol B)	Volcanic tuff	8.57	37	0.1394	0.51221	0.511789	−8.4	−5.1	455.2	1.71	0.729263	0.705315	2

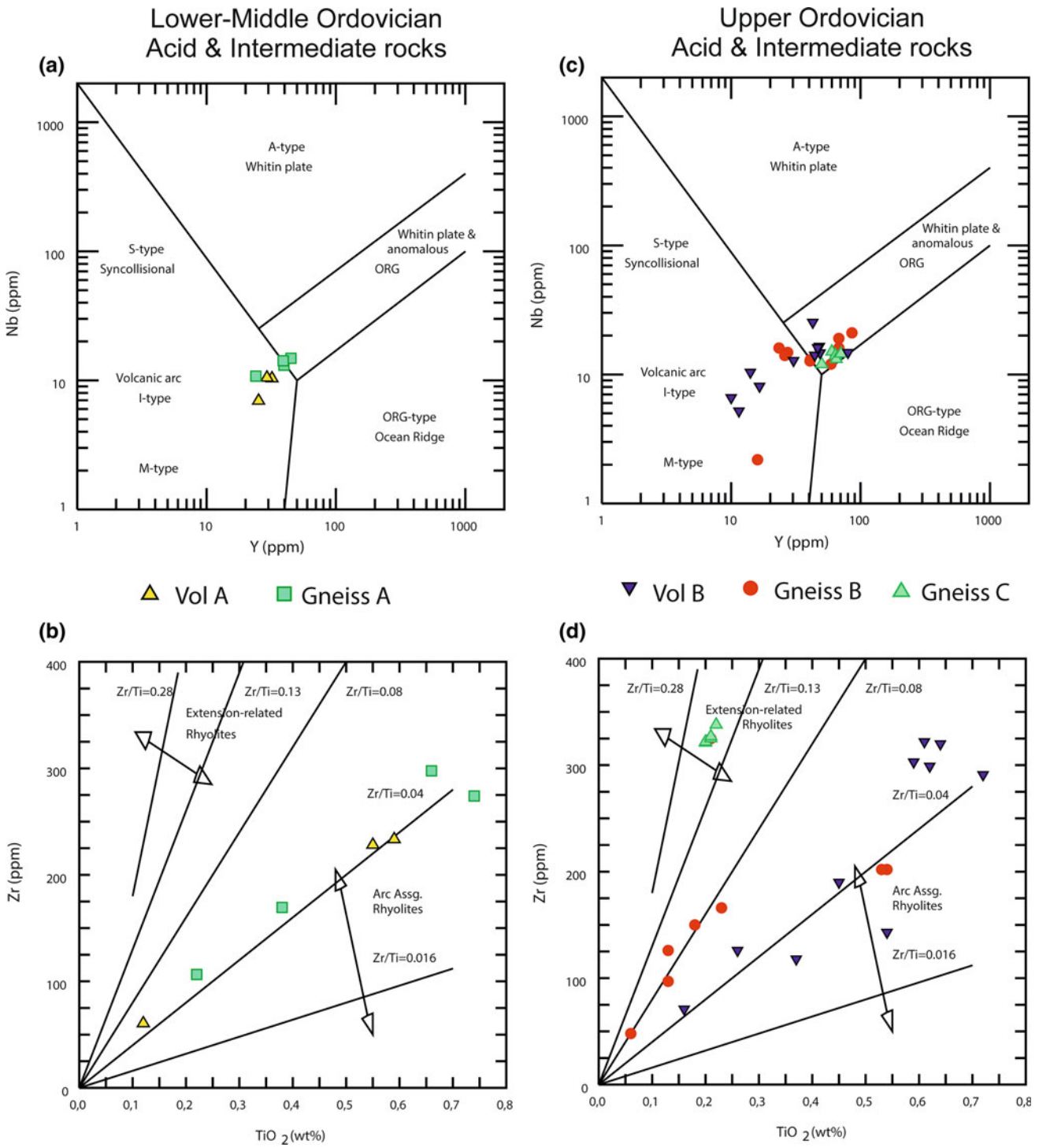

Fig. 8.13 Tectonic discriminating diagram of acid and intermediate rocks. **a** and **c** Y versus Nb diagram (Pearce et al. 1984); **b** and **d** Zr versus TiO_2 diagram (Syme 1998)

values for LREE (La_n/Sm_n = 3.13) than HREE (Gd_n/Yb_n = 1.43), being $(La/Yb)_n$ = 6.38. The average Eu anomalies show moderate negative values (0.36) reflecting plagioclase crystallization (Fig. 8.10e). In the spider-diagram of Palme and O'Neil (2004), they show negative anomalies of Nb, Sr and Ti (Fig. 8.10f). Overall chondrite-normalized pattern close to the values of the Upper Continental Crust of Rudnick and Gao (2004) values with slight enrichment in the Th/Nb (average = 1.15), Th/La (average = 0.51) and Zr/Nb (average = 16.7) and depletion in the

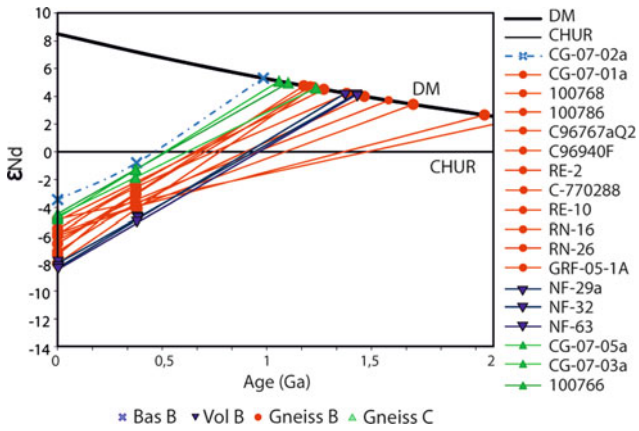

Fig. 8.14 εNd versus age diagram (DePaolo and Wasserburg 1976; DePaolo 1981) for the Upper Ordovician magmatic rocks of the Pyrenees (data after Navidad et al. 2010; Martínez et al. 2011). Depleted mantle evolution calculated according to DePaolo (1981)

La/Nb (average = 2.29) and Th/Yb (average = 4.58) ratios. The Nb/Y (average = 0.34) value is close to the Lower Continental Crust of Rudnick and Gao (2004) (Fig. 8.11c). This suggests a certain degree of crustal contamination and recycling of materials. In the tectonic diagram of Pearce et al. (1984), the samples plot in the volcanic arc-I type field and the anomalous rift (Fig. 8.13c). In the Zr versus TiO_2 diagram of Syme (1998), the data plot in the extensional field (Fig. 8.13d). The initial Nd isotope ratio of the Casemí gneiss ($^{147}Sm/^{144}Nd$ between 0.1480 and 0.1359 and εNd between −1.9 and −1.3) indicates that their protoliths were derived from mantle melts with heterogeneous crustal contamination (Navidad et al. 2010). Castiñeiras et al. (2011) reached similar conclusions on the basis of zircon composition. Despite their different age, the zircons from the Cadí orthogneiss and the Albera gneiss exhibit similar characteristics. The zircon composition suggests that this mineral grew in a melt formed by anatexis of continental crust. In contrast, zircons from the Casemí gneiss and the metadiorite point out that the mantle was involved in the origin of these rocks. Extrapolations of εNd data back to the depleted mantle curve yield TDM values varying between 1.3 and 1.5 Ga (Navidad et al. 2010; Martínez et al. 2011; Fig. 8.14, Table 8.1). The absence of inherited zircons from these ages led the authors to interpret these values as the result of the melting of a Neoproterozoic source mixed with Palaeoproterozoic components.

All geochemical characteristics broadly suggest crustal sources in their parental magmas. According to Navidad et al. (2010), the whole-rock geochemistry shows that the Upper Ordovician orthogneiss of the Canigó massif are compositionally uniform. As fractionation processes cannot be recognized, crustal contamination of mantle melts is the most probable process accounting for the formation of the various geochemical datasets (Casemí biotite and amphibole orthogneisses, and metadiorite).

It should be noted that the latest Early-Mid Ordovician magmatism is coincident with the pre-Late Ordovician episode of uplift and erosion that led to the formation of the Sardic unconformity. Uplift was followed by an extensional pulse that developed normal faults, directly affecting the onset of the basal unconformity and controlling deposition of the (post-Sardic) Upper Ordovician strata and coeval Late Ordovician magmatic activity.

Early and Late Ordovician ages have also been obtained in magmatic bodies from the French Massif Central, such as in the Axial Zone of the Montagne Noire (Somail orthogneiss: 471 ± 4 Ma, Cocherie et al. 2005; Pont de Larn and Gorges d'Heric orthogneisses: 456 ± 3 Ma and 450 ± 6 Ma, Roger et al. 2004; Saint Eutrope gneiss: 455 ± 2 Ma, Pitra et al. 2012). As in the Pyrenees, the emplacement of Late Ordovician felsic granitic bodies is coeval in the Montagne Noire with a tholeiitic volcanic activity originated by melting of mantle and crustal lithosphere and infilling of rifting branches preserved on the southern Montagne Noire (Álvaro et al. 2016). These authors also describe a similar Late Ordovician volcanism in the Mouthoumet massif and relate it to the end of the Sardic Phase and the opening of rift branches linked to those developed on the southern Montagne Noire.

8.5 Correlation with Surrounding Areas and Other Northern Gondwanan Domains

J. J. Álvaro, J. M. Casas, S. Clausen, M. Padel, C. Puddu

To the west of the Canigó massif, the Jujols Group extends as far as the Noguera Pallaresa and Ribagorçana rivers, where the Serdinya Formation may be correlated with the Seo Formation defined by Hartevelt (1970) in the Orri Dome. In the La Pallaresa dome, the La Massana antiform and the western slopes of the Aston and Hospitalet domes, a siliciclastic-dominated succession, more than 4000 m thick, was subdivided into three formations by Laumonier et al. (1996), from bottom to top: the Alós d'Isil, Lleret-Bayau and Alins formations. The Alós d'Isil and Alins formations are dominated by shales, locally alternating with thin- to medium-grained sandstones, and are separated by the metasandstones and marbles of the Lleret-Bayau Formation. Despite the lack of any geochronologic or biostratigraphic control, we suggest that the Pallaressa succession should be correlated with the Jujols Group, being the Alós d'Isil, Lleret-Bayau and Alins triad equivalent to the Err, Valcebollère and Serdinya formations, respectively (Fig. 8.9). In the same way, the Jujols Group may be correlated with

the pre-Sardic rocks of the Garona Dome, which have been subdivided into three terms by García-Sansegundo and Alonso (1989), from bottom to top: the Urets beds, the Bantaillou limestone and the Orlà beds. Again, these terms may be equivalent to the Err, Valcebollère and Serdinya formations, respectively.

In contrast, the Jujols Group cannot be easily recognized in the easternmost Cap de Creus, where some geochronological ages of Cadomian magmatic rocks constrain the depositional ages of the pre-Sardic succession from ca. 570 to 542 Ma. In the Albera massif, alternating layers of metapelites and metapsamites form the uppermost part of a metasedimentary succession that is crosscut by a network of acidic subvolcanic porphyritic dykes, which constrain its minimum depositional age to 465–472 Ma (Liesa et al. 2011). This uppermost part can be tentatively correlated with the Jujols Group, although coarse-grained terms (sandstone and conglomerate) are locally abundant in the Albera massif.

The only Cambrian shelly fossils reported until present in the Pyrenees occur in an Alpine thrust sheet of the Terrades area. Abad (1988) described the presence of archaeocyathan patch reefs, alternating with green to brownish shales in an up to 50 m thick succession, and assigned the sponges to the Cambrian Age 3. A complete taxonomic study by Perejón et al. (1994) confirmed a late Cambrian Age 3. The detailed preservation of pristine microfacies and microbial textures in these limestone strata, contrasting with the traditional marble aspect of any carbonate bed of Cambrian age, is in accordance with the allochthonous provenance of this Alpine thrust slice: the Cambrian limestones of the Salut slice thrust Eocene strata and are, in turn, unconformably overlain by Eocene strata (Pujadas et al. 1989). Biogeographic affinities of the archaeocyaths point to strong similarities with similar assemblages from SW Sardinia (Matoppa Formation of the Nebida Group) (Perejón et al. 1994). A pre-Alpine northward setting, in a lateral prolongation of the archaeocyath-bearing carbonates cropping now in SW Sardinia and southern Montagne Noire, may be envisaged.

Since the pioneer work of Cavet (1957), the Ediacaran-Lower Ordovician succession of the Pyrenees has been traditionally compared to fossiliferous successions from the neighbouring southern Montagne Noire. These lithostratigraphic correlations between both Variscan massifs have remained, up to recently, the main way to interpolate the age of the Canaveilles and Jujols groups (Cavet 1957; Laumonier et al. 1996, 2004). The stratigraphic framework of the Montagne Noire has recently been updated (Álvaro et al. 1998, 2014) and better constrained based on recent chronostratigraphic (Devaere et al. 2013, 2014) and geochronologic studies (Roger et al. 2004; Pitra et al. 2012; Padel et al. 2017). As a result, the Valcebollère Formation and, as suggested above, the Lleret Bayau Formation and the Bentaillou limestone from the Central Pyrenees, can be confidently considered as representative of the characteristic Cambrian Age 3–4 episode of subtropical carbonate production highlighted by the Pardailhan and Lastours formations in the Montagne Noire (Álvaro et al. 2010; Devaere et al. 2014) (Fig. 8.2). The upper part of the Valcebollère Formation (limestone/shale alternations and monotonous shales bearing carbonate centimetre-thick nodules) is lithologically equivalent to the La Tanque-Coulouma transition. A distinct lithological difference between the Eastern Pyrenees and the Montagne Noire is marked by the absence, in the former, of the Guzhangian (regional Languedocian) regression represented by the onset of the Ferrals Formation (Álvaro et al. 2007). This sandstone-dominated formation, representative of prograding shoal complexes, is absent in the Eastern Pyrenees (Fig. 8.2). The regression recorded by the input of sandstones marking the uppermost part of the Serdinya Formation (Font Frède Member) may represent the onset of the early Tremadocian regression marked, in the Montagne Noire, by the La Dentelle Formation.

In SW Sardinia, the 1500–3000 m thick Cambrian-Lower Ordovician succession is subdivided into the Nebida, Gonnesa and Iglesias groups (Pillola 1990). The lower siliciclastic deposits of the Sa Tuvara Member (Matoppa Formation, Nebida Group) should represent a lateral equivalent of the Err (Eastern Pyrenees) and Marcory (Montagne Noire) formations (Fig. 8.2). The upper carbonate and siltstone alternations of the Matoppa Formation have yielded a Cambrian Age 3–4 fauna (Pillola 1990) which was correlated with the Pardailhan Formation of Montagne Noire (Álvaro et al. 2010). The Matoppa Formation is conformably overlain by the Punta Manna Formation, the uppermost heterolithic unit of the Nebida Group. The following Gonnesa Group, mainly composed of massive archaeocyathan-bearing carbonates, is correlatable with the Pardailhan and Lastours formations (Álvaro et al. 2010). The upper part of the Matoppa Formation, the Punta Manna Formation and the Gonnesa Group were deposited during the Cambrian Epoch 2 and are interpreted as lateral equivalents of the Valcebollère Formation and the La Salut thrust slice (Fig. 8.2). The carbonate sequence of the Gonnesa Group is overlain by the Iglesias Group, which begins with the carbonate-shale alternations and/or nodular limestones of the Campo Pisano Formation that can be considered as a lateral equivalent of the Coulouma Formation (Álvaro et al. 2010) and the upper part of the Valcebollère Formation. The Campo Pisano Formation (Cambrian Series 2–3 transition; Pillola 1990) is conformably overlain by the terrigenous rocks of the Cambrian Series 3-Lower Ordovician Cabitza Formation, correlated herein with the Serdinya Formation.

In SW Sardinia, according to Loi et al. (1995), a regressive trend culminating with local coarse-grained sandstones, is recognized in the middle member of the Cabitza Formation (sensu Gandin and Pillola 1985; Pillola

1989), biostratigraphically represented by the so-called CAB-4 fossil assemblage, correlatable with the late Languedocian. This sandy-dominant level might represent the Ferrals regression, but somewhat delayed in time. The Acerocare Regressive Event is proposed close to the Cambrian-Ordovician boundary, which lies at the so-called Cabitza "tubi" part and is directly overlain by the first occurrence of Tremadocian graptolites (CAB-6; Loi et al. 1995). Therefore, the lack of the Guzhangian Ferrals Formation regression in the Eastern Pyrennes, present in the Iberian Peninsula, the Montagne Noire and somewhat diachronous in SW Sardinia, might be related to peneplanation of source areas, unable to yield coarse-grained sediments.

The Sardic unconformity recognized in Sardinia and the Pyrenees could be considered as a correlation element for both areas. Such as the Sardic unconformity, the Upper Ordovician successions that follow this unconformity are broadly comparable. In Sardinia, two post-Sardic sequences have been recognized, reported at the SW and SE of the island. The SW Sardinian sequence starts with a conglomerate-to-sandstone, fining-upward package, followed by a sandy-siltstone succession characterized by two late Katian key-levels: the fossiliferous Portixeddu Formation and the carbonate-dominated Domusnovas Formation. The SE Sardinian sequence starts with conglomeratic deposits and volcanic products of Mid Ordovician age, topped by a terrigenous and volcanoclastic complex characterized by a fossiliferous lower Katian level (Punta Serpeddì Formation), and an upper-Katian key carbonate level, the Tuviois Formation (Fig. 8.2). Based on their lithology, fossil record and age, the SW Sardinian sequence is comparable to the Hartevelt's (1970) sequence of the Eastern Pyrenees, where the Rabassa Conglomerate Formation is the corresponding of the Monte Argentu Formation (Sandbian), the Cava Formation (Katian) represents the Monte Orri (Early Katian) and Portixeddu formations (Late Katian), while the Estana Formation (Late Katian) is the lateral equivalent of the Domusnovas Formation (Late Katian). The Ansovell and Bar formations broadly represent the Rio San Marco counterpart (Hirnantian).

The SE Sardinian sequence could be comparable to that cropping out in the Ribes de Freser area. In the Bruguera unit, the Upper Ordovician volcanites that overlie the Sardic unconformity are similar to the volcanic products that overlie the Sardic unconformity in the SE Sardinian sequence. The basal tuffs of the Ribes de Freser unit may correspond to the volcanites of SE Sardinia that overlie the Sardic unconformity, while the Katian sediments that cover the former tuffs represent the Punta Serpeddì Formation (lower Katian) followed by limestones comparable to the Tuviois Formation. The thickness, facies and fossil record of the limestones in the El Baell unit are different from the two above-reported Sardinian sequences. These limestones could be comparable only in age with the Estana Formation (Eastern Pyrenees), the Domusnovas Formation (SW Sardinia) or the Tuviois Formation (SE Sardinia) (Fig. 8.2).

The south-north, proximal-distal palaeogeographic trend recorded in the Lower Palaeozoic of the eastern Pyrenees is repeated across the Mouthoumet and Axial Zone-southern-northern (proximal-to-distal) Montagne Noire transect. Moreover, the biogeographic affinity displayed by the archaeocyaths of the Alpine Salut thrust sheet, and the comparative analysis of zircon provenance (Padel 2016) point to closer palaeogeographic affinities between the Pyrenees and Sardinia than between the Pyrenees and the Montagne Noire. As a result, in addition to the estimated 150–160 km accumulated in a south-north Alpine displacement of the Pyrenean thrust sheets, other pre-Alpine movements may be envisaged to solve the present-day relationship between the Pyrenees and the Occitan Domain (sensu Álvaro et al. 2016). Dextral shearing along the southern branch of the South Armorican Shear Zone, between 315 and 305 Ma (Martínez Catalán 2012 and references therein), may account for an original westernmost position of the Montagne Noire and the French Central Massif in pre-Variscan, Early Palaeozoic times.

The inner peri-Gondwanan massifs that form the eastern branch of the Variscan Ibero-Armorican Arc (Southern Armorican, Pyrenean and Occitan Domains and lateral prolongation into Corsica and Sardinia) offer a common geodynamic framework during Early Palaeozoic times. They differ from the Iberian Massif (western branch of the same arc) by the absence of Cadomian deformation, the record of Cadomian felsic-dominated volcanic activity crossing the Ediacaran-Cambrian boundary interval, a significant episode of carbonate productivity capping the top of palaeohorsts and volcanosedimentary edifices during Terreneuvian times, the lack of the Toledanian phase (marking the rift/drift transition in parts of the Iberian Peninsula) and the common record of the Sardic phase. The latter is characterized by intrusion of granites in the Pyrenees and the Axial Zone of the Montagne Noire, contemporaneously with the opening of Katian rifting branches and the record of a basaltic-dominated, tholeiitic magmatism in the Mouthoumet and Cabrières klippes (southern Montagne Noire). The palaeorelief generated as a result of the Sardic uplift was succeeded by extensional pulses, tilting, discontinuous erosion of the pre-Sardic basement, and infill of the new palaeorelief with alluvial-to-fluvial deposits, volcanosedimentary complexes and final sealing of the whole palaeotopography during Silurian to Early Devonian times.

The interpretation of the Sardic phase as (i) the onset of a Mid Ordovician arc that developed in North Gondwana as a consequence of subduction of oceanic crust under continental crust (Andean-type convergence; see Di Pisa et al. 1992; Carmignani et al. 2001; Stampfli et al. 2002; Buzzi et al. 2007;

Funedda and Oggiano 2009), (ii) a change from symmetric to asymmetric opening conditions of the Rheic Ocean leading to local crustal fusion, or (iii) the onset of a rift/drift unconformity similar to the Toledanian one recorded in the Iberian massif, is still open to future discussion.

8.6 Silurian, Devonian and pre-Variscan Carboniferous

J. Sanz-López

The Pyrenean successions show a great spatial variation on the distribution of sedimentary facies, particularly during the Devonian, where a plethora of local lithostratigraphic units have been differentiated (Fig. 8.15). Consequently, detailed description and reference to the original studies are here avoided, since it overpasses the subject of this synthesis. It may be found in extended and recent publications (Dégardin 1988; Sanz-López 1995, 2002a, b, 2004; Dégardin et al. 1996; Delvolvé et al. 1996; García-López et al. 1996; Majesté-Menjoulas et al. 1996; García-Alcalde et al. 2002). Sanz-López (2002a, 2004) described several sedimentary domains modifying the previous Devonian facies-area defined in the Pyrenean Axial zone (Mirouse 1966; Mey 1967, 1968; Boersma 1973; Zwart 1979) and the Basque massifs (Heddebaut 1975) (Fig. 8.16). The western margin of the preserved basin is characterized by the occurrence of a sedimentary hiatus between the Ordovician and Upper Devonian rocks (Basque Cinco Villas domain, CVd; Fig. 8.15). The southern margin is interpreted since shallow-water carbonate platforms are located in a southern belt (Fig. 8.16), and siliciclastic systems were fed from the current south (the Cantabro-Ebroan massif after Mey 1967; Llopis Lladó et al. 1968; Requadt 1974; Carls 1988). An intra-Devonian, or Devonian-late Tournaisian hiatus, is usually recognized in the southernmost successions (Mirouse 1966). Subsidence rates were decreasing and, in parallel, deep-water conditions were increasing along the marginal southern belt from west to east; from the southern Alduides-Mendibeltza to the Sallent, Baliera, Sierra Negra and el Comte domains (AMd, Sd, Bd, SNd and ECd; Fig. 8.16). The norhern belt represents a deep-water epicontinental basin where a condensed carbonate sedimentation prevailed (Northern and Eastern domains, Nd and Ed), although shallow-water facies with sedimentary hiatus also occur in the westernmost part (Ferrières domain, Fd). Among the southern and northern belts, an asymmetric central trough (Central domain, Cd) differentiated from the Eifelian to the Tournaisian (Fig. 8.15). The highest subsidence was located at the southern margin probably in relation to fault activity, mainly in the early Frasnian, when the occurrence of extensional listric faults bounding some blocks was interpreted (Majesté-Menjoulas et al. 1991). The siliciclastic supplies filling this trough came from the west highly subsiding area (AMd). Siliciclastic input piled up in the southern part of the trough and disappeared toward the east and the north.

The Silurian sedimentation was onlapping and transgressive, covering the Late Ordovician rifting basins throughout the Pyrenees. Deposition of black carbonaceous shales (Lower Graptolitic Shales after Schmidt 1931 in Fig. 8.15; 70–180 m thick) on a poorly oxygenated bottom sea characterized the Pyrenees as other Variscan areas of southern Europe and northern Africa (García-López et al. 1996). Late Rhuddanian to Aeronian (Llandovery) graptolites are traditionally the lowermost described in black shales of many Pyrenean sections (Dégardin 1988). Late Hirnantian (latest Ordovician) and basal Llandovery graptolites are known in a single locality (Roqué Bernal et al. 2017). The early Llandovery may be recorded by sandy shales without graptolites or by shallow-water deltaic sandstones of the Bar Formation in the southern part of the Central and Eastern Pyrenees. The drowning of this sandy platform seems to have been diachronous, because Aeronian-Telychian graptolites and Llandovery conodonts were described from the transition interval (Llopis Lladó 1969; Sanz-López and Sarmiento 1995). Furthermore, black shales are usually a common detachment horizon.

Condensed carbonate and/or reworking beds with mainly mollusks recorded occasional oxygenation events in the deep basin (Orthoceras Limestone after Dalloni 1913). It may constitute a composite horizon, 5–15 m thick, with Gorstian-Lutfordian (Ludlow) conodonts, although upper Wenlock to lower Prídolí beds are also known (García-López et al. 1996; Sanz-López et al. 2002c). Locally, condensed crinoidal limestones with corals were interpreted as an early Wenlock sedimentary high in the central Pyrenees (Marxant Limestone after Sanz-López and Palau 2000). In the southern, central Pyrenees, ochre condensed and bioturbated carbonates of type Ockerkalk replaced to the Orthoceras Limestone between the early Ludlow and the latest Prídoli (Llessui Formation and Toloriu Limestone; see Sanz-López et al. 2002c). This Ockerkalk facies was deposited on swells or ridges areas and could be in the subsurface of the Ebro basin, because it crops out in the Catalan Coastal Range and is known in the External Nappe zone of Sardinia.

The carbonate deposition and oxygenation of the sea-bottom in the Axial zone coincided with the arrival of distal siliciclastic deposits from the Ludlow in the higher subsiding Basque AMd (Arnéguy Formation; Requadt 1974). There, a shoaling interval is recognized trough Prídolí and early Lockhovian shallow-water faunas (Heddebaut 1975; Requadt 1974). At this time, it corresponds with the east extension of the distal siliciclastic sedimentation

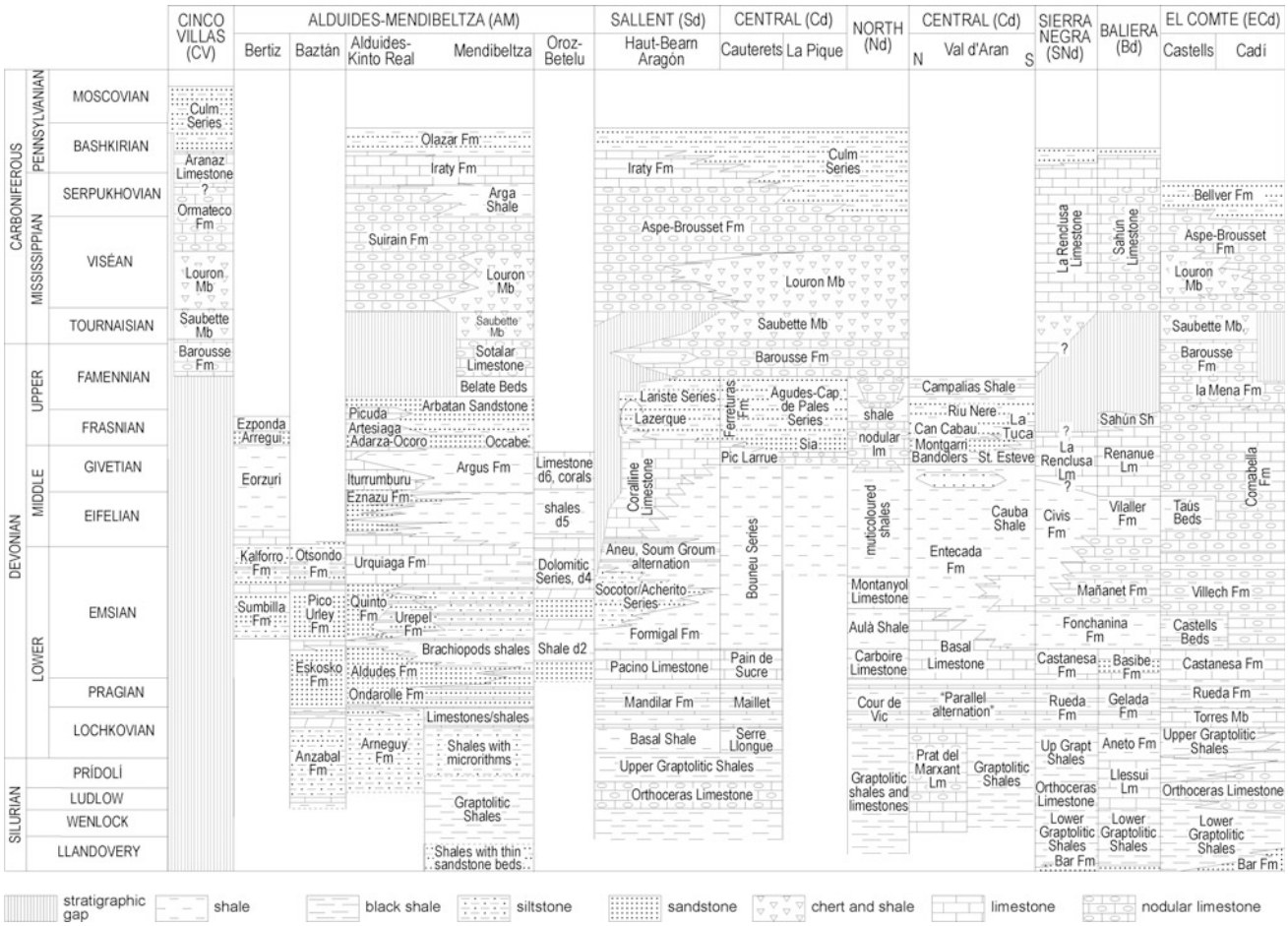

Fig. 8.15 Correlation chart among the Silurian to Middle Pennsylvanian lithostratigraphic units described in the different sedimentary domains. Explanation of units is in the text

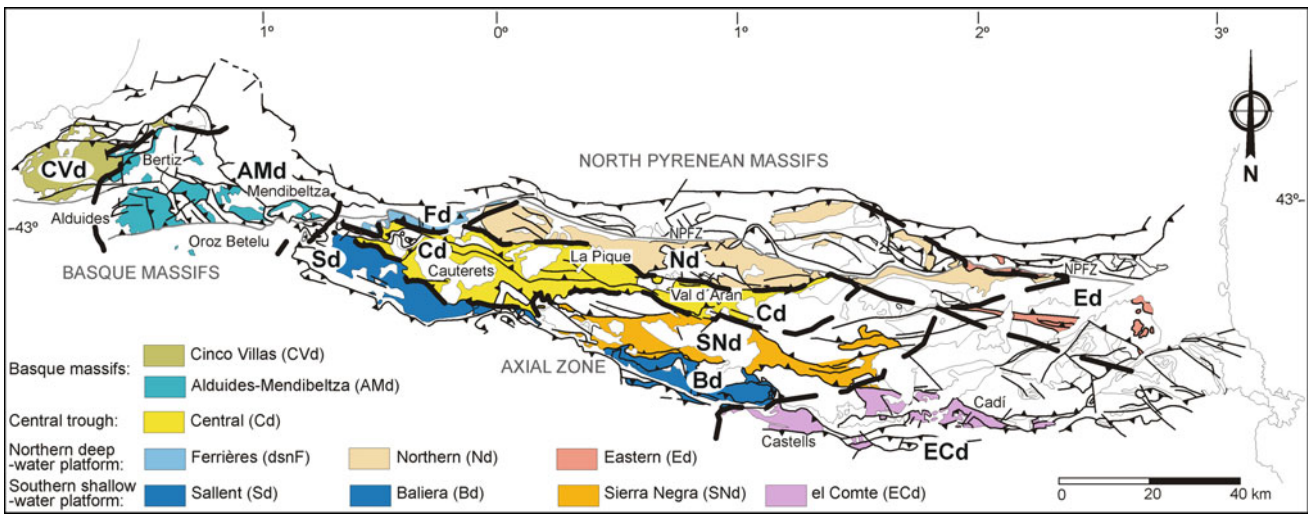

Fig. 8.16 Geological sketch of the Paleozoic rocks in the Pyrenees (Basque massifs, Axial zone and North Pyrenean massifs-north of the North Pyrenean Fault zone, NPFZ) showing the sedimentary domains differentiated for the Silurian to Middle Pennsylvanian rocks

eastward in the Axial zone (Serre Llongue Shale in the Sd, Aneto Formation in the Bd; 40–80 m thick), although black shale and limestone (Upper Graptolitic Shales; 20–40 m) were restricted to the oxygen depleted basin (Sd, SNd and ECd) and condensed crinoidal limestone deposited on sedimentary highs (ECd). Prídolí to early Lochkovian conodonts, graptolites, chitinozoans and a varied of invertebrate fauna are known (Dégardin 1988; Sanz-López et al. 1999).

A highstand sea-level interval ended the prevalent stratified water and black shale deposition in the Pyrenean Basin. It is recorded in the Torres Member of the ECd (Rueda Formation; 10–20 m thick) or the equivalent units locally described in the Bd, Nd and Ed. It consists of condensed carbonate hemipelagic sedimentation with bioturbated sea-bottom and occasional hardground development. A high resolution conodont zonation spans the mid to late Lochkovian (Valenzuela-Ríos et al. 2015). In the western part of the basin (AMd), shallow water sedimentation corresponds to crinoidal limestones and shales with brachiopods (200 m thick; Klarr 1974).

Siliciclastic input and high subsidence occurred in the AMd during the Pragian (200–700 m of sandstones, shales and quartzites of the Ondarelle and Aldudes formations) in coincidence with a change from extremely hot Lochkovian to hot and humid Pragian climate conditions according to Slavík et al. (2016), and a worldwide sea level lowering (Johnson et al. 1985). A well-oxygenated basin recorded the development of a vast extended Pragian ramp with a distal siliciclastic component (limestones and shales of the Mandilar, Gelada and Rueda formations, 50–120 m thick).

The Aldudes siliciclastic system was retrograding during the late Pragian-early Emsian in the western AMd, and was replaced by 100–200 m of "Brachiopod Shale" (Klarr 1974). In most parts of the Pyrenees, a carbonate ramp with moderate subsidence was onset (Basibé, Castanesa and Pacino formations; 30–60 m thick). In the Central Pyrenees, a late Pragian siliciclastic wedge prograded northward (San Silvestre Member of the Basibé Formation in the Bd). The carbonate platform shows early Emsian local coralline growth developed on sedimentary highs (ECd; Sanz-López 1995).

An important deepening of the sedimentation occurred during the early Emsian, but it was subdivided into several pulses (from the Middle *P. excavatus* to the Upper *P. nothorperbonus* conodont Zones; Sanz-López 2002a, b; Martínez-Pérez and Valenzuela-Ríos 2014). Shallow-water mixed siliciclastic-carbonate sedimentation was located in the AMd (Quinto and Urepel formations, 500–600 m thick), while shaly input extended in the Central Pyrenees (Formigal Formation in the Sd, Fonchanina Formation in the Bd and SNd, Aulà Shales in the Nd; Fig. 8.15). Shale sedimentation was replaced by condensed limestone with dacrioconarids in the ECd (less than 30 m thick of the Castells Beds). In the late Emsian, a prevailing carbonate sedimentation with reefal development occurred in the AMd (Urquiaga Formation; 500 m). The reduction of mud supply into the southern Pyrenees is related to hemipelagic carbonate sedimentation with deep-water dacrioconarids, ostracods and ammonoids in the Bd and SNd (Mañanet Formation; 280 m thick; García-López et al. 1990). More condensed and carbonate deposition is recorded by the Villech Formation in the distal Eastern Pyrenees (ECd; 35–70 m thick). Local changes among successions were related to the location in the basin and slopes of sedimentary highs where limestone with coral biostromes may occur (Dalloni 1930; Cavet 1957). A drowning event was recognized at the top of the Villech Fomation (upper Emsian) and followed by the progradation of resedimented carbonate of the Comabella Formation in the ECd (Sanz-López 1995; Montesinos and Sanz López 1999). Late Emsian to basal Eifelian distal siliciclastic wedges arrived to the Western Pyrenees (Socotor and Acherito Beds in the Sd and Fd) and limestone beds yielded brachiopods from the Emsian-Eifelian interval (Requadt 1974; Juch and Schafer 1974; García-Alcalde et al. 2002). Distal siliciclastic deposits were sedimented in the deepest and subsiding areas of the Central Pyrenees (Vilaller Formation in the Bd and SNd; Boneu and Entecada formations in the Cd).

The early Eifelian corresponds to a new episode of siliciclastic progradation characterized by sandstones rich in iron oxides in the southern part of AMd (Eznazu Formation, about 200 m in thickness). Thick successions of shales extended along the Central Pyrenees (Vilaller, Boneu and Entecada formations) as a wedge of condensed shales and marls with abundant dacriconarids in the deep-water nodular limestones of the Comabella Formation deposited in the Ed and the ECd (Taús Beds in Montesinos and Sanz López 1999).

High subsidence and growth of shallow-water reefal limestone is recorded during the latest Eifelian to early Givetian in the Sd and Fd, the Coral Limestone (150–500 m thick; Mirouse 1966; Joseph and Tsien 1975; Joseph et al. 1980, 1984). It seems to be equivalent to the Iturrumburu Limestone in the southernmost part of the AMd (Chesterikoff 1964; Wirth 1967). The prograding of outer carbonate platform above shales is also recorded from the latest Eifelian in the Bd (Renanué Formation in the central Pyrenees). Slope-apron carbonate bodies were prograding above hemipelagic carbonates derived from reefal biostromes in the ECd.

The mid-Givetian to early Frasnian interval corresponds to the decreasing in the distal siliciclastic sources and highstand sea level. Reefal growth extended to the southern margin of the Cd (Sant Esteve Limestone) and deep-water carbonate sedimentation (dacrioconarid limestone) occurred in the central trough, the Northern and Eastern Pyrenees

(Bandolers, Gabiedou and Pic de Larrue limestones; Perret et al. 1972; Bodin 1988; Palau and Sanz 1989; García-López et al. 1991). The shale sedimentation was confined to the western highly subsiding margin of the basin in the AMd (Argus Shale, 800–1000 m thick).

Differential subsidence increased probably in relation with extensional tectonics and an early Frasnian compartmented palaeogeography has been suggested (Raymond 1987; Sanz-López 1995). The proximal siliciclastic deep sea-fan deposits occurred in the southern margin of the high subsiding trough in the Cd (Les Bordes Sandstone; Kleinsmiede 1960). The input should be located at the west, concretely in the AMd, where early Frasnian 800–1500 m of shallow-water sandstones and shales deposited as deltaic systems (Irurita Group; de Boer et al. 1974). The trough is not recognizable eastwards, in the Tor–Casamanya syncline, where Givetian to Frasnian nodular limestones and shales were recently described (Clariana 2015). The siliciclastic supplies decreased in the middle Frasnian, but high subsidence continued as shale deposition in the AMd (500 m thick of the Artesiaga Shale). In this line, the Givetian coralline reefal development in the southern belt was retrograding southwards from the Middle-Middle *M. asymmetricus* conodont zones (Sd, Bd and southern ECd), may be in relation to the tilting of the southern basin margin. Siliciclastic facies and carbonates resedimented beds deposited in the outer platform (Lazerque and Lariste series, Ferreturas Formation, Sahún Shale) and arrived to the southern part of the Cd (La Tuca Shale and limestone), whereas distal deep sea fans deposits filled the central and northern parts of the central trough (Riu Nere Sandstone and shale, Tourmalet unit). Condensed and deep-water hemipelagic limestone deposited laterally in the epicontinental basin of the Nd, Ed and ECd. Frasnian intraformational breccias, slope deposits and local reefal growth suggest the occurrence of swollen areas probably bounded by faults in the ECd (Sanz-López 1995, 2002b). Shallow-water sandstones and bioclastic limestones with brachiopods and corals (Arbartán and Picuda formations; 60–120 m thick) suggest a late Frasnian shoaling in the AMd.

The uppermost Frasnian deepening pulse is characterized by poorly oxygenated shale sedimentation, which included tempestite limestone beds in the lower Famennian of the AMd (Belate Beds, 30 m thick). It is not differentiated in the outer platform deposits of the Sd and in the distal siliciclastic turbidites of the Cd. A deepening horizon corresponding to shales with carbonate nodules and ammonoids was described in the hemipelagic north and east carbonate sedimentation, and deep-water nodular limestone buried coralline limestone in successions of the Comabella Formation (ECd; Sanz-López 2002b).

The Frasnian/Famennian boundary was correlated with a condensed shale horizon in the Comabella Formation, where a sharp change in the conodont and ostracod faunas occurred in relation to the global Kellwasser Event (Sánchez de Posada et al. 2008). In the Cadí nappe, the Frasnian/Famennian boundary is located at the base of the La Mena Formation, red limestone with brachiopod shoals and derived tempestistes deposited on sedimentary highs (Sanz-López 2002b). The succession shows a lower–middle Famennian deepening sequence, where cephalopod "Griotte" limestone deposited on the slope and basin. The La Mena Formation is a condensed, reddish, nodular limestone with cephalopods (12–30 m thick) deposited in the basinal area of the ECd, Ed and part of the Nd (Bouquet and Stoppel 1975; Cygan 1979). At time, anoxic deep-water black shale sedimentation with resedimented limestone beds deposited in the central trough (Campalias Shale) and in the AMd (Belate Beds), whereas siliciclastic beds of the Ferreturas Formation seems to be the lateral equivalent in the southern Pyrenean belt.

The Barousse Formation consists of nodular cephalopod-bearing limestones (25–70 m thick) deposited during the mid Famennian to the early Tournaisian. It formed a deep-water, starved, carbonate ramp extending along mostly of the Pyrenees, including the CVd (where it is above Ordovician rocks). This formation marks the beginning of the onlap on the Cantabro-Ebroian block and predated its burial in the upper Tournaisian. The Barousse Formation lacks or is locally preserved, as bioclastic or crinoidal limestone, in the southern part of the Sd. The upper part of the Barousse Formation includes ash and cherts beds in the Sd and AMd (Soques Chert after Perret 1993). At the top, the Boyer et al. (1974)'s horizon B is a continuous shale less than 1 m in thickness (2 m in the deep basin of the Cd) and equivalent to the Rhenish Hangenberg Shale. It is associated with the latest Famennian, global, cooling event and the life extinction crisis (Walliser 1996). The base of the Boyer et al. (1974)'s limestone C of the Barousse Formation (about 2 m thick) corresponds to a worldwide eustatic rise post-glacial horizon close to the lower boundary of the Carboniferous according to conodont faunas (Boyer et al. 1974; Sanz-López 1995, 2002c; Kaiser et al. 2008). The top of this limestone provided mid Tournaisian conodonts (*Siphonodella cooperi* or *S. crenulata* zones).

Above, the Saubette Chert consists of black radiolarian cherts and shales with horizons of phosphatic nodules (Perret 1993). A mid to late Tournaisian age is derived from radiolarians, crustaceans and ammonoids in coincidence with the conodonts obtained in the limestone above and below the chert unit (Delépine 1935; Goumerlon 1987). These poorly oxygenated sediments extended throughout the Pyrenees in coincidence with the worldwide Lower Alum Shale event or Mid-Tournaisian event described by Walliser (1996). It lacks on the southern marginal area and on the sedimentary highs in relation to the tilting of the southern Devonian platform and to extensional tectonics in the Sd and Fd. These areas

were drowned by condensed sandy transgressive bioclastic limestones (lowest part of the Aspe-Brousset Formation) with late Tournaisian and reworked Devonian conodonts (Perret 1993; Perret and Weyant 1994). Consequently, the onlap of the marginal area was contemporaneous with the deposition of the upper part of the Saubette Chert in the basin. Tournaisian cherts or limestones are directly overlying different Cambrian to Upper Devonian rocks in the adjacent Palaeozoic outcrops of the current western Mediterranean Sea (Aiguafreda Formation of the Catalonian Coastal Range, cherts and siliceous shales in the Minorque Island and the lower member of the Falcoña Formation in the Betic Chains) indicating a subdivided basin maybe in relation to extensional faults (Raymond and Lethiers 1990). An intra-Tournaisian hiatus and erosion has also been recognized in the Cantabrian zone (Sanz-López and Blanco-Ferrera 2012). The mid–late Tournaisian starved basins recorded episodic high planktonic productivity and poorly oxygenated bottom-sea, far of siliciclastic supplies and locally related to submarine volcanism. In the southern Catalonian Coastal Range, lava flows derived from alkali basalts solidified in shallow-waters marine setting in an intraplate extensional context (Melgarejo and Martí 1989; Melgarejo 1992).

Complete deep-water sedimentation above sedimentary highs had a maximum flooding event at the late Tournaisian (*Scaliognathus anchoralis* Conodont Zone). Sedimentation of condensed, nodular to massive, cephalopod limestones (Aspe-Brousset Formation; 25–30 m thick) recorded an increase in the oxygen content of the sea-bottom respect to the mid Tournaisian (Perret 1976; Sanz-López 2002b). A similar episode is known in the Cabrières klippes (Montagne Noire), the Valls unit (Catalonian Coastal Range) and the Cantabrian Mountains, and corresponds to the Avins Event in the Dinant Basin (Poty 2007). Sedimentation of cherts and siliceous shales with inter-bedded graded tuff layers (Louron Member) deposited above the Saubette Chert in the deep part of the Pyrenean basin, including the CVd, eastern AMd, Cd and locally the Nd and ECd (Krylatov 1963; Crilat 1983; Sanz-López 1995). The lower-middle Viséan cherts are replaced by condensed cephalopod limestone on the swollen areas in a similar line to the described in the Cantabrian Mountains and the Montagne Noire (cherts of the Lavandera Member in the Alba Formation; Colonnes Formation, respectively). The basinal, starved, Tournaisian to lower Viséan chert sedimentation in known in other adjacent Palaeozoic outcrops of the current western Mediterranean Sea—region (Catalonian Coastal Range, Minorque Island, Betic Chains and the Palentine nappes of the Cantabrian Mountains). In all these areas, centimetre-thick fine-grained tuffaceous clayey horizons occurred and suggest volcanism in relation with a faulted, subdivided basin.

Condensed nodular carbonate sedimentation of the Aspe-Brousset Formation extended in the Pyrenees and the western Mediterranean area from the mid to late Viséan (*G. praebilineatus* to *G. bilineatus* conodont zones). A deeper sedimentation corresponds to the limestone and siliceous shales (Larbont facies of Clin 1959) in the northeastern part of the Pyrenees (ECd, Cd and Nd). There, the top of the Aspe-Brousset Formation provided conodonts and ammonoid considered late Viséan or early Serpukhovian. This limestone-shale sedimentation was described in the Catalonian Coastal Range (el Papiol Formation; 10–12 m thick) and in Minorque (Bourrouilh 1983; Martínez Chacón et al. 2003). Rich endemic trilobite, brachiopods and coral faunas adapted to quiet water conditions in soft, muddy sea bottom muddy bottoms are known (Martínez Chacón et al. 2003; Plusquellec et al. 2007; Gandl et al. 2015). Shallow-water carbonate shelves grew up north of the Pyrenees during the Viséan and the Serpukhovian. It is preserved in the Mouthoumet massif ("Calcaires à algues et foraminifers" Formation in Bessière and Schulze 1984) and as deposits derived as calciturbidites and debris flows in the Montagne Noire (Colonnes Formation and Puech Capel Formation in Korn and Feist 2007). The arrival of synorogenic siliciclastic supplies of the Culm flysch ended the carbonate sedimentation. It occurred in the late Serpukhovian drowning episode recorded at the top of the Aspe-Brousset Formation in the southern central and western Pyrenees (Sd, Bd and AMd). Late Viséan to late Serpukhovian clasts and olistoliths from shallow-water carbonate platforms were reworked in the synorogenic flysch deposits of the Montagne Noire and Pyrenees (Delvolvé et al. 1996; Vachard et al. 2016).

References

Abad A (1988) El Cámbrico inferior de Terrades (Gerona). Estratigrafía, facies y paleontología. Batallería 2:47–56.

Álvaro JJ, Courjault-Radé P, Chauvel JJ, Dabard MP, Debrenne F, Feist R, Pillola GL, Vennin E, Vizcaïno D (1998) Nouveau découpage stratigraphique des séries cambriennes des nappes de Pardailhan et du Minervois (versant sud de la Montagne Noire, France). Géol Fr 1998 (2):3–12.

Álvaro JJ, Ferretti F, González-Gómez C, Serpagli E, Tortello MF, Vecoli, M, Vizcaïno D (2007) A review of the Late Cambrian (Furongian) palaeogeography in the western Mediterranean region, NW Gondwana. Earth-Sci Rev 85:47–81.

Álvaro JJ, Monceret E, Monceret S, Verraes G, Vizcaïno D (2010) Stratigraphic record and palaeogeographic context of the Cambrian Epoch 2 subtropical carbonate platforms and their basinal counterparts in SW Europe, West Gondwana. Bull Geosci 85:573–584.

Álvaro JJ, Bauluz B, Clausen S, Devaere L, Imaz AG, Monceret E, Vizcaïno D (2014) Stratigraphy of the Cambrian–Lower Ordovician volcanosedimentary complexes, northern Montagne Noire, France. Stratigraphy 11:83–96.

Álvaro JJ, Colmenar J, Monceret E, Pouclet A, Vizcaïno D (2016) Late Ordovician (post-Sardic) rifting branches in the North Gondwanan Montagne Noire and Mouthoumet massifs of southern France. Tectonophysics 681:111–123.

Ayora C (1980) Les concentrationes metàl·liques de la Vall de Ribes. PhD, Univ. Barcelona.

Ayora C, Casas JM (1986) Strabound As-Au mineralization in pre-Caradocian rocks from the Vall de Ribes, Eastern Pyrenees, Spain. Mineralium Deposita 21:278–287.

Barca S, Carmignani L, Cocozza T, Franceschelli M, Ghezzo C, Memmi I, Minzoni N, Pertusati PC, Ricci CA (1987) The Caledonian events in Sardinia. In The Caledonian Orogen-Scandinavian and related areas. In: Gee DG, Sturt BA (eds) John Wiley ans Sons Ltd, p 1195–1199.

Belaustegui Z, Puddu C, Casas JM (2016) New ichnological data from the lower Paleozoic pf the Central Pyrenees: presence of *Artrophycus brogniartii* (Harlam, 1832) in the Upper Ordovician Cava Formation. Geo-Temas 16:271–274.

Bessière G, Schulze H (1984) Le Massif de Mouthoumet (Aude, France): nouvelle définition des unités structurales et essai d'une reconstruction paléogéographique. Bull Soc géol Fr 26:885–894.

Bodin J (1988) Le Dévonien inférieur et moyen des Pyrénées ariégeoises et centrales. Biostratigraphie, séries hétéropiques et mise en évidence de nappes hercyniennes précoces. Doc BRGM 153:1–255.

Boer HU de, Krausse MF, Mohr K, Pilger A, Requadt H (1974) La région de magnésite d'Eugui dans les Pyrénées Occidentales espagnoles: Une explication de la carte géologique. Pirineos 111:21–39.

Boersma KT (1973) Devonian and Lower Carboniferous biostratigraphy, Spanish Central Pyrénées. Leidse Geol Meded 49:303–377.

Bouquet C, Stoppel D (1975) Contribution à l'étude du Paléozoïque des Pyrénées centrales (Hautes vallées de la Garonne et d'Aure). Bull BRGM (sec 1) 1:7–61.

Bourrouilh R (1983) Estratigrafía, sedimentología y tectónica de la isla de Menorca y del noreste de Mallorca (Baleares). La terminación nororiental de las Cordilleras béticas en el Mediterráneo occidental. Mem IGME 99, Madrid.

Boyer F, Krylatov S, Stoppel D (1974) Sur le problème de l'existence d'une lacune sous les lydiennes à nodules phosphatés du Dinantien des Pyrénées et de la Montagne Noire (France, Espagne). Geol J (B) 9:1–60.

Buzzi L, Funedda A, Gaggero L, Oggiano G (2007) Sr-Nd isotope, trace and REE element geochemistry of the Ordovician volcanism in the southern realms of the Variscan belt. EGU General Assembly 2007, Wien, 15–20 April 2007, Abstract.

Calvet Ph, Lapierre E, Charvet J (1988) Diversité du volcanisme ordovicien dans la région de Pierrefitte (Hautes Pyrénées): rhyolites calco-alcalines et basalts alcalins. C R Acad Sci Paris 3078: 805–812.

Carls P (1988) The Devonian of Celtiberia (Spain) and Devonian paleogeography of SW Europe. Can Soc Petrol Geol Mem 14: 421–464.

Carmignani L, Oggiano G, Barca S, Conti P, Salvadori I, Eltrudis A, Funedda A, Pasci S (2001) Geologia della Sardegna. Note illustrative della Carta Geologica della Sardegna a scala 1:200.000. Memorie Descrittive della Carta Geologica d'Italia, Servizio Geologico 60:1–283. Instituto Poligrafico e Zecca dello Stato, Roma.

Casas JM (2010) Ordovician deformations in the Pyrenees: new insights into the significance of pre-Variscan ('sardic') tectonics. Geol Mag 147: 674–689.

Casas JM, Fernández O (2007) On the Upper Ordovician unconformity in the Pyrenees: New evidence from the La Cerdanya area. Geol Acta 5:193–198.

Casas JM, Palacios T (2012) First biostratigraphical constraints on the pre-Upper Ordovician sequences of the Pyrenees based on organic-walled microfossils. C R Géosci 344:50–56.

Casas JM, Castiñeiras P, Navidad M, Liesa M, Carreras J (2010) New insights into the Late Ordovician magmatism in the Eastern Pyrenees: U-Pb SHRIMP zircon data from the Canigó massif. Gondwana Res 17:317–324.

Casas JM, Queralt P, Mencos J, Gratacós O (2012) Distribution of linear mesostructures in oblique folded surfaces: Unravelling superposed Ordovician and Variscan folds in the Pyrenees. J Struct Geol 44:141–150.

Castiñeiras P, Navidad M, Liesa M, Carreras J, Casas JM (2008) U-Pb zircon ages (SHRIMP) for Cadomian and Lower Ordovician magmatism in the Eastern Pyrenees: new insights in the pre-Variscan evolution of the northern Gondwana margin. Tectonophysics 46:228–239.

Castiñeiras P, Navidad M, Casas JM, Liesa M, Carreras J (2011) Petrogenesis of Ordovician magmatism in the Pyrenees (Albera and Canigó Massifs) determined on the basis of zircon minor and trace element composition). J Geol 119:521–534.

Cavet P (1957) Le Paléozoïque de la zone axiale des Pyrénées orientales françaises entre le Roussillon et l'Andorre. Bull Serv Carte géol Fr 55:303–518.

Chesterikoff A 1964 Note sur l'existence d'un palédôme dans la région de Burguete-Arive-Arrieta (Pyrénées basques espagnoles) et ses relations métallogéniques avec les mineralizations périphériques. Bull Soc géol Fr (6) 8:225–232.

Cirés J, Casas JM, Muñoz JA, Fleta J, Barbera M (1994) Memoria explicativa del mapa geológico de España a escala 1:50.000, hoja de Molló (n°218). ITGE, Madrid.

Clariana P (2015) Estratigrafía, estructura y su relación con el metamorfismo de la Zona Axial pirenaica en la transversal del Noroeste de Andorra y comarcas del Pallars Sobirá y el Alt Urgell (Lleida). Dissertation, University of Oviedo.

Clin M (1959) Etude géologique de la haute chaine des Pyrénées Centrales entre le cirque de Troumouse et le cirque du Lys. Dissertation, University of Nancy.

Cocherie A, Baudin Th, Autran A, Guerrot C, Fanning C.M, Laumonier B (2005) U-Pb zircon (ID-TIMS and SHRIMP) evidence for the early Ordovician intrusion of metagranites in the late Proterozoic Canaveilles Group of the Pyrenees and the Montagne Noire (France). Bull Soc géol Fr 176:269–282.

Crilat S (1983) Le Devonien supérieur et le Carbonifère inférieur des Pyrénées et de la Montagne Noire (Frasnien, Famennien, Tournaisien). Newsl IGCP 5:231–254.

Cygan C (1979) Etude de conodontes dévoniens des Pyrénées et du massif de Mouthoumet. Dissertation, University of Toulouse.

Dalloni M (1913) Stratigraphie et tectonique de la région des Nogueras (Pyrénées centrales). Bull Soc géol Fr (sér 4) 1:243–263.

Dalloni M (1930) Etude géologique des Pyrénées Catalanes. An Fac Sci Marseille 26, 3:1–373.

Dégardin JM (1988) Le Silurien des Pyrénées. Biostratigraphie. Paléogéographie. Bull Soc géol Nord 15:1–355.

Dégardin JM (coord) et al (1996) Ordovicien supérieur-Silurien. In: Barnolas A, Chiron JC, Guérangué B (eds) Synthèse géologique et géophysique des Pyrénées vol 1. Editons BRGM-ITGE, Orléans, Madrid, pp 211–233.

Delépine G (1935) Contribution a l'étude de la faune du Dinantien des Pyrénées Deuxième partie: la faune de Mondette. Bull Soc géol Fr (sér 5) 5:171–189.

Deloule E, Alexandrov P, Cheilletz A, Laumonier B, Barbey P (2002) In-situ U-Pb zircon ages for Early Ordovician magmatism in the eastern Pyrenees, France: the Canigou orthogneisses. Int J Earth Sci 91:398–405.

Delvolvé JJ et al (1996) Carbonifère à faciès Culm In Barnolas A, Chiron JC (eds) Synthèse géologique et géophysique des Pyrénées vol 1. Editions BRGM-ITGE, Orléans, Madrid, pp 303–338.

Den Brok SWJ (1989) Evidence for pre-Variscan deformation in the Lys Caillaouas area, Central Pyrenees, France. Geol Mijnbouw 68:377–380.

Denèle Y, Barbey P, Deloule E, Pelleter E, Olivier Ph, Gleizes G (2009) Middle Ordovician U-Pb age of the Aston and Hospitalet orthogneissic laccoliths: their role in the Variscan evolution of the Pyrenees. Bull Soc géol Fr 180:209–221.

DePaolo DJ (1981) Neodymiun isotopes in the Colorado Front range and crust-mantle evolution in the Proterozoic. Nature 291:193–196.

DePaolo DJ, Wasserburg GJ (1976) Nd isotopic variations and petrogenetic models. Geophys Res Lett 3 (5):249–252.

Devaere L, Clausen S, Steiner M, Álvaro JJ, Vachard D (2013) Chronostratigraphic and palaeogeographic significance of an early Cambrian microfauna from the Heraultia Limestone, northern Montagne Noire, France. Palaeonto Electr 16(2), 17A:1–91.

Devaere L, Clausen S, Monceret E, Vizcaïno D, Vachard D, Genge MC (2014) The tommotiid *Kelanella* and associated fauna from the early Cambrian of southern Montagne Noire (France): implications for Camenellan phylogeny. Palaeontology 57:979–1002.

Di Pisa A, Gattiglio M, Oggiano G (1992) Pre–Hercynian magmatic activity in the nappe zone (internal and external) of Sardinia: evidence of two within plate basaltic cycles. In Carmingnani L, Sassi F P (eds) Contributions to the Geology of Italy with Special Regard to the Paleozoic Basements. Newsletter IGCP no. 276:107–116.

Funedda A, Oggiano G (2009) Outline of the Variscan basement of Sardinia. In: Corradini C, Ferretti A, Štorch P (eds) The Silurian of Sardinia. Volume in Honour of Enrico Serpagli. Rendicontti della Società Paleontologica Italiana 3:23–35.

Gámez Vintaned JA, de Gibert JM, Casas JM (2012) First ichnological data from the pre-Upper Ordovician rocks of the Pyrenees. Geo-Temas 13.

Gandin A, Pillola GL (1985) Biostratigrafia e sedimentologia della Formazione di Cabitza nell'Iglesiente. In: Gruppi di lavoro del CNR: "Paleozoico" e "Evoluzione magmatica e matemorfica della costra fanerozoica". Riunione Scientifica Siena, 13–14 Decembre 1985, 30–31.

Gandl J, Ferrer E, Magrans J, Sanz-López J (2015) Trilobiten aus dem Unter-Karbon des Katalonischen Küstengebirges (NE-Spanien). Abh Senckenberg Ges Naturforsch 571, Schweizerbart and Borntraeger Science Publishers, Stuttgart.

García-Alcalde JL, Carls P, Pardo-Alonso MV, Sanz-López J, Soto FM, Truyols-Massoni M, Valenzuela-Ríos JI (2002) Devonian. In: Gibbons W, Moreno MT (eds) The Geology of Spain. Geol Soc London, pp 67–91.

García-López S, García-Sansegundo J, Arbizu M (1990) Datos estratigráficos y paleontológicos de la sucesión devónica del área del río Baliera (Zona Axial, Pirineos centrales españoles). Geogaceta 7:33–35.

García-López S, García-Sansegundo J, Arbizu M (1991) Devonian of the Aran Valley Synclinorium, Central Pyrenees, Spain: Stratigraphical and Paleontological data. Acta Geol Hisp 26 (1):55–66.

García-López, S, Rodríguez-Cañero R, Sanz-López J, Sarmiento GN, Valenzuela-Ríos JI (1996) Conodontos y episodios carbonatados en el Silúrico de la Cadena hercínica meridional y el Dominio Sahariano. Rev Esp Paleontol, num extr: 33–57.

García-Sansegundo J, Alonso JL (1989) Stratigraphy and structure of the southeastern Garona Dome. Geodin Acta 3:127–134.

García-Sansegundo J, Gavaldà J, Alonso JL (2004) Preuves de la discordance de l'Ordovicien supérieur dans la zone axiale des Pyrénées: exemple de dôme de la Garonne (Espagne, France). C R Géosci 336:1035–1040.

Gil-Peña I, Sanz-López J, Barnolas A, Clariana P (2000) Secuencia sedimentaria del Ordovícico superior en el margen occidental del domo del Orri (Pirineos Centrales). Geotemas 1:187–190.

Gil-Peña I, Barnolas A, Villas E, Sanz-López J (2004) El Ordovícico Superior de la Zona Axial. In Vera JA (ed) Geología de España. SGE-IGME, Madrid, p 247–249.

Goumerlon F (1987) Les radiolaires tournaisiens des nodules phosphatés de la Montagne Noire et des Pyrénées Centrales. Systematique-Biostratigraphie-Paleobiogeographie. Biostratigraphie du Paléozoïque 6:1–172.

Guitard G (1970) Le métamorphisme hercynien mésozonal et les gneiss œillés du massif du Canigou (Pyrénées orientales). Mém BRGM 63:1–353.

Hartevelt JJA (1970) Geology of the upper Segre and Valira valleys, central Pyrenees, Andorra/Spain. Leid Geol Meded 45:167–236.

Heddebaut C (1975) Etudes géologiques dans les Massifs paléozoïques basques (résumé de thèse). Bull BRGM 4 (2):5–30.

Johnson JG, Klapper G, Sandberg CA (1985) Devonian eustatic fluctuations in Euramerica. Geol Soc Am Bull 96:567–587.

Joseph, J, Brice D, Mouravieff N (1980) Données paléontologiques nouvelles sur le Frasnien des Pyrénées centrales et occidentales: implications paléogéographiques. Bull Soc Hist Nat Toulouse 116:16–41.

Joseph J, Mirouse R, Perret MF (1984) Calcaires dévoniens et carbonifères du Monte Tobazo (Pyrénées aragonaises, Huesca, Espagne). Acta Geol Hisp 19:149–166.

Joseph J, Tsien HH (1975) Calcaires mésodévoniens et leurs faunes de tétracoralliaires en haute vallée d'Ossau (Pyrénées Atlantiques). Bull Soc Hist Nat Toulouse 111:179–202.

Juch D, Schafer D (1974) L'Hercynien de Maya et de la vallée d'Arizakum dans la partie orientale du massif de Cinco-Villas (Pyrénées Occidentales de Espagne). Pirineos 111:41–58.

Kaiser S I, Steuber T, Becker RT (2008) Environmental change during the Late Famennian and Early Tournaisian (Late Devonian–Early Carboniferous) implications from stable isotopes and conodont biofacies in southern Europe. In: Aretz M, Herbig H-G, Somerville ID (eds) Carboniferous Platforms and Basins. Geol J 43:241–260.

Klarr K (1974) La structure géologique de la partie sud-est du Massif des Aldudes-Quinto Real (Pyrénées Occidentales). Pirineos 111:59–67.

Kleinsmiede WJF (1960) Geology of the valle d'Aran (Central Pyrenees). Leidse Geol Meded 25:129–245.

Korn D, Feist R (2007) Early Carboniferous ammonoid faunas and stratigraphy of the Montagne Noire (France). Fossil Record 10:99–124.

Kriegsman LM, Aerden DGAM, Bakker RJ, den Brok SWJ, Schutjens PMTM (1989) Variscan tectonometamorphic evolution of the eastern Lys-Caillaouas massif, Central Pyrenees-evidence for late orogenic extension prior to peak metamorphism. Geol Mijnbouw 68:323–333.

Krylatov S (1963) Note préliminaire sur les jaspes dinantiens des Pyrénées et leur cortège). Bull Soc géol Fr (sér 7) 5:393–400.

Laumonier B (1988) Les groupes de Canaveilles et de Jujols (''Paléozoïque inférieur'') des Pyrénées orientales – arguments en faveur de l'âge essentiellement Cambrien de ces séries. Hercynica 4:25–38.

Laumonier B, Guitard G (1986) Le Paléozoïque inférieur de la moitié orientale de la Zone Axiale des Pyrénées. Essai de synthèse. C R Acad Sci Paris 302:473–478.

Laumonier B, Abad A, Alonso JL, Baudelot S, Bessière G, Besson M, Bouquet C, Bourrouilh R, Brula P, Carreras J, Centène A, Courjault-Radé R, Courtessole R, Fauconnier D, García-Sansegundo J, Guitard G, Moreno-Eiris E, Perejón A, Vizcaïno D (1996) In: Barnolas A, Chiron JC (eds) Synthèse géologique et géophysique des Pyrénées. Tome 1: Cycle hercynien. Cambro-Ordovicien. BRGM-ITGE, Orléans-Madrid. p 157–209.

Laumonier B, Autran A, Barbey P, Cheilletz A, Baudin T, Cocherie A, Guerrot C (2004) Conséquences de l'absence de socle cadomien sur l'âge et la signification des séries pré-varisques (anté-Ordovicien supérieur) du sud de la France (Pyrénées, Montagne Noire). Bull Soc géol Fr 175:105–117.

Laumonier B, Calvet M, Wiazemsky M, Barbey P, Marignac C, Lambert J, Lenoble JL (2015) Notice explicative de la Carte géologique de la France (1/50.000), feuille Céret (1096). BRGM, Orléans.

Liesa M, Carreras J (1989) On the structure and metamorphism of the Roc de Frausa Massif (Eastern Pyrenees). Geodin Acta 3:149–161.

Liesa M, Carreras J, Castiñeiras P, Casas JM, Navidad M, Vilà M (2011) U-Pb zircon age of Ordovician magmatism in the Albera Massif (Eastern Pyrenees). Geol Acta 9:1–9.

Loi A, Pillola GL, Leone F (1995) The Cambrian and Early Ordovician of south-western Sardinia. In: 6th Paleobenthos International Symposium, October, 25–31 1995. Rendiconti del Seminario della Facoltà di Scienze dell'Università di Cagliari (suppl. vol. 65): 63–81.

Llopis Lladó N (1965) Sur le Paléozoïque inférieur de l'Andorre. Bull Soc géol Fr 7:652–659.

Llopis Lladó N (1969) Estratigrafía del Devónico de los valles de Andorra. Mem R Acad Cien Art Barcelona 39:219–290.

Llopis Lladó N, de Villalta JF, Cabanas R, Pelaez Pruneda JR, Vilas L (1968) Le Dévonien de l'Espagne. Int Symp Devonian System, Calgary (1967) 1, pp 171–187.

Majesté-Menjoulas C, Debat C, Mercier A (1991) Les massifs anciens des Pyrénées. Sci Geol Bull 44:337–369.

Majesté-Menjoulas C, Ríos LM (coord) et al (1996) Dévonien-Carbonifère inférieur. In: Barnolas A, Chiron JC, Guérangué B (eds) Synthèse géologique et géophysique des Pyrénées vol 1. Editons BRGM-ITGE, Orléans, Madrid, pp 235–301.

Margalef A (2015) Estudi estructural i estratigràfic del sud d'Andorra. PhD, Univ. Barcelona.

Margalef A, Castiñeiras P, Casas JM, Navidad M, Liesa M, Linnemann U, Hofmann M, Gärtner A (2016) Detrital zircons from the Ordovician rocks of the Pyrenees: Geochronological constraints and provenance. Tectonophysics 681:124–134.

Martí J, Muñoz JA, Vaquer R (1986) Les roches volcaniques de l'Ordovicien supérieur de la région de Ribes de Freser-Rocabruna (Pyrénées catalanes): caractères et signification. C R Acad Sci Paris 302:1237–1242.

Martí J, Casas JM, Guillén N, Muñoz JA, Aguirre G (2014) Structural and geodynamic constraints of Upper Ordovician volcanism of the Catalan Pyrenees. Gondwana 15 Abstracts book, 104.

Martínez F, Iriondo A, Dietsch C, Aleinikoff JN, Peucat JJ, Cirès J, Reche J, Capdevila R (2011) U-Pb SHRIMP-RG zircon ages and Nd signature of lower Paleozoic rifting-related magmatism in the Variscan basement of the Eastern Pyrenees. Lithos 127:10–23.

Martínez Catalán JR (2012) The Central Iberian arc, an orocline centered in the Iberian Massif and some implications for the Variscan belt. Int J Earth Sci 101:1299–1314.

Martínez Chacón ML, Winkler Prins CF, Sanz-López J, Ferrer E, Magrans J (2003) Braquiópodos misisípicos de los alrededores de Barcelona (Cadenas Costeras Catalanas, NE España). Rev Esp Paleontol 18:189–204.

Martínez-Pérez C, Valenzuela-Ríos JI (2014) New Lower Devonian polygnathids (Conodonta) from the Spanish Central Pyrenees, with comments on the early radiation of the group. J Iber Geol 40:141–155.

Melgarejo JC (1992) Estudio geológico y metalogenético del Paleozoico del sur de las Cordilleras Costeras Catalanas. Mem ITGE 103.

Melgarejo JC, Martí J (1989) El vulcanisme bàsic del Carbonífer inferior de la serra de Miramar. Acta Geol Hisp 24:131–138.

Mey PHW (1967) The Geology of the upper Ribagorzana and Baliera valleys, Central Pyrenees, Spain. Leidse Geol Meded 41:153–220.

Mey PHW (1968) Evolution of the Pyrenean Basins during the Late Paleozoic. Internat Symp Devonian System, Calgary (1967) 1, pp 1157–1166.

Mezger J, Gerdes A (2016) Early Variscan (Visean) granites in the core of central Pyrenean gneiss domes: implications from laser ablation U-Pb and Th-Pb studies. Gondwana Res 29:181–198.

Mirouse R (1966) Recherches géologiques dans la partie occidentale de la zone primaire axiale des Pyrénées. Mém Carte géol Fr, Paris.

Montesinos JR, Sanz López J (1999) Ammonoideos del Devónico Inferior y Medio en el Pirineo Oriental y Central. Antecedentes históricos y nuevos hallazgos. Rev Esp Paleontol, num extr: 97–108.

Muñoz JA (1985) Estructura alpina i herciniana a la vora sud de la zona axial del Pirineu oriental. PhD, Univ. Barcelona.

Muñoz JA (1992) Evolution of a continental colision belt: ECORS-Pyrenees crustal balanced cross-section. In: Mc Clay KR (ed) Thrust Tectonics, Chapman & Hall, London, p 235–246.

Muñoz JA, Casas JM (1996) Tectonique préhercynienne. In: Barnolas A, Chiron JC (eds) Synthèse géologique et géophysique des Pyrénées, BRGM-ITGE, Orléans-Madrid, p 587–1589.

Navidad M, Castiñeiras P, Casas JM, Liesa M, Fernández-Suárez J, Barnolas A, Carreras J, Gil-Peña I (2010) Geochemical characterization and isotopic ages of Caradocian magmatism in the northeastern Iberia: insights into the Late Ordovician evolution of the northern Gondwana margin. Gondwana Res 17:325–337.

Navidad M, Casas J M, Castiñeiras P, Liesa M, Belousova E, Proenza J, Aiglsperger Th (2018) Ordovician magmatism in northern Gondwana: Evolution based on new U-Pb geochronology, whole-rock geochemistry, and Nd isotopes in orthogneisses and metabasic rocks from the Eastern Pyrenees. Lithos 314–315, 479–496.

Padel M (2016) Influence cadomienne dans les séries pré-sardes des Pyrénées Orientales: approche géochimique, stratigraphique et géochronologique. PhD Thesis. University of Lille I.

Padel M, Álvaro JJ, Clausen S, Guillot F, Poujol M, Chichorro M, Monceret E, Pereira MF, Vizcaïno D (2017) U-Pb laser ablation ICP-MS zircon dating across the Ediacaran-Cambrian transition of the Montagne Noire, southern France. Comptes Rendus Geoscience 349:380–390.

Padel M, Clausen S, Álvaro JJ, Casas JM (2018) Review of the Ediacaran-Lower Ordovician (pre-Sardic) stratigraphic framework of the Eastern Pyrenees, southwestern Europe. Geol Acta 16, 339–355.

Palau J, Sanz J (1989) The Devonian units of the Marimanya Massif and their relationship with the Pyrenean Devonian facies areas. Geodin Acta 3:171–182.

Palme H, O'Neill HSC (2004) Cosmochemical estimates of mantle composition. In: RW Carlson (ed) The mantle and core. Treatise on Geochemistry. HD Holland, HD, Turekian KK (eds), Elsevier-Pergamon, Oxford, 2:1–38.

Pearce JA (1996) Sources and setting of granitic rocks. Episodes 19 (4):120–125.

Pearce JA (2008) Geochemical fingerprinting of oceanic basalts with applications to ophiolite classification and the search for Archean oceanic crust. Lithos 100:14–48.

Pearce JA, Harris NBW, Tindle AG (1984) Trace element discrimination diagrams for the tectonic interpretation of granitic rocks. J Petrol 25:956–983.

Perejón A, Moreno Eiris E, Abad A (1994) Montículos de arqueociatos y calcimicrobios del Cámbrico Inferior de Terraldes, Gerona (Pirineo Oriental, España). Bol R Soc Esp Hist Nat (Sec Geol) 89:55–95.

Perret MF (1976) Une transgression dinantienne dans les Pyrénées occidentales: datation micropaléontologique et analogies. C R somm Soc géol Fr 6:257–259.

Perret MF (1993) Recherches micropaléontologiques et biostratigraphiques (Conodontes – Foraminifères) dans le Carbonifère pyrénéen. Strata 21, Toulouse.

Perret MF, Weyant M (1994) Les biozones à conodontes du Carbonifère des Pyrénées. Comparaisons avec d'autres régions du globe. Geobios 27:689–715.

Perret MF, Joseph J, Mirouse R, Mouravieff A (1972) Un précieux jalon chronostratigraphique dans le Paléozoïque pyrénéen: la datation des "Calcaires rubanés" du Pic Larrue (Hautes Pyrénées). C R Acad Sci Paris D 274:2439–2442.

Pillola GL (1989) Données lithologiques et stratigraphiques sur le Cambrien et le Trémadoc de l'Iglesiente (SE de la Sardaigne). In : Sassi FP, Bourrouilh R (eds) IGCP Project no. 5, Correlation of Prevariscan and Variscan events of the Alpine-Mediterranean Mountain Belt. Newsletter 7, 228–239.

Pillola GL (1990) Lithologie et Trilobites du Cambrien inférieur du SW de la Sardaigne (Italie): implications paléobiogéographiques. C R Acad Sci Paris 310:321–328.

Pillola GL, Piras S, Serpagli E (2008) Upper Tremadoc-Lower Arenig? Anisograptid-Dichograptid fauna from the Cabitza Formation (Lower Ordovician, SW Sardinia, Italy). Rev Micropal 51:167–181.

Pitra P, Poujol M, Den Driessche JV, Poilvet JC, Paquette JL (2012) Early Permian extensional shearing of an Ordovician granite: The Saint-Eutrope "C/S-like" orthogneiss (Montagne Noire, French Massif Central). C R Géosci 344:377–384.

Plusquellec Y, Fernández-Martínez E, Sanz-López J, Soto F, Magrans J, Ferrer E (2007) Tabulate corals and stratigraphy of Lower Devonian and Mississippian rocks near Barcelona (Catalonian Coastal Ranges, Northeast Spain). Rev Esp Paleontol 22:175–192.

Poblet J (1991) Estructura herciniana i alpina del versant sud de la zona axial del Pirineu central. PhD thesis, Univ. Barcelona.

Poty E (2007) The Avins event: a remarkable worldwide spread of corals at the end of the Tournaisian (Lower Carboniferous). In Hubmann B, Piller WE (eds) Fossil corals and sponges. Graz 2003. Schriften erdwiss Komm (Oesterreichische Akad Wiss) 17, Wien, pp 231–250.

Puddu C, Casas JM (2011) New insights into the stratigraphy and structure of the Upper Ordovician rocks of the la Cerdanya area (Pyrenees). In: Gutiérrez-Marco JC, Rábano I, García-Bellido D (eds) Ordovician of the World. Cuad. Museo Geomin 14:441–445.

Pujadas J, Casas JM, Muñoz JA, Sàbat F (1989) Thrust tectonics and Paleogene syntectonic sedimentation in the Empordà area (southeastern Pyrenees). Geodin Acta 3:195–206.

Raymond D (1987) Le Dévonien et le Carbonifère inférieur du sud-ouest de la France (Pyrénées, Massif de Mouthoumet, Montagne Noire): sédimentation dans un bassin flexural en bordure sud de la Chaîne de collision varisque. Geol Rundsch 76:795–803.

Raymond D, Lethiers F (1990) Signification géodynamique de l'événement radiolaritique dinantien dans les zones externes sud-varisques (Sud de la France et Nord de l'Espagne). C R Acad Sci Paris 310:1263–1269.

Requadt H (1974) Aperçu sur la stratigraphie et le facies du Devonien inferieur et le moyen dans les Pyrénées Occidentales d'Espagne. Pirineos 111:109–127.

Robert JF (1980) Etude géologique et métallogénique du Val de Ribas sur le versant espagnol des Pyrénées Catalanes. PhD, Univ. Besançon.

Robert JF, Thiébaut J (1976) Découverte d'un volcanisme acide dans le Caradoc de la région de Ribes de Freser (Prov. de Gérone). C R Acad Sci, Paris 282:2050–2079.

Roger F, Respaut JP, Brunel M, Matte Ph, Paquette JL (2004) Première datation U-Pb des orthogneiss œillés de la zone axiale de la Montagne Noire (Sud du Massif central): nouveaux témoins du magmatisme ordovicien dans la chaîne varisque. C R Géosci 336:19–28.

Roqué Bernal J, Štorch P, Gutiérrez-Marco JC (2017) Bioestratigrafía (graptolitos) del límite Ordovícico-Silúrico en los Pirineos orientales (curso alto del río Segre, Lleida). Geogaceta 61:27–30.

Rudnick RL, Gao S (2004) Composition of the Continental Crust. In: Rudnick, RL (ed) The Crust. Treatise on Geochemistry. Holland HD, Turekian KK (eds), Elsevier-Pergamon, Oxford, 3:1–64.

Sánchez de Posada LC, Sanz-López J, Gozalo R (2008) Ostracod and conodont faunal changes across the Frasnian-Famennian boundary at Els Castells, Spanish central Pyrenees. Rev Micropal 51: 205–219.

Santanach PF (1972a) Sobre una discordancia en el Paleozoico inferior de los Pirineos orientales. Acta Geol Hisp 7:129–132.

Santanach PF (1972b) Estudio tectónico del Paleozoico inferior del Pirineo entre la Cerdaña y el río Ter. Acta Geol Hisp 7:44–49.

Sanz-López J (1995) Estratigrafía y bioestratigrafía (Conodontos) del Silúrico superior–Carbonífero inferior del Pirineo Oriental y Central. Dissertation, University of Barcelona.

Sanz-López J (2002a) Devonian and Carboniferous pre-Stephanian rocks from the Pyrenees. In: García-López S, Bastida F (eds) Palaeozoic conodonts from northern Spain. Eight International Conodont Symposium held in Europe. Publ IGME, Cuad Mus Geomine 1, Madrid, pp 367–389.

Sanz-López J (2002b) Devonian and Lower Carboniferous rocks from the Cadí nappe (eastern Pyrenees). In: García-López S, Bastida F (eds) Palaeozoic conodonts from northern Spain. Eight International Conodont Symposium held in Europe. Publ IGME, Cuad Mus Geomin, Madrid 1:419–438.

Sanz-López, J, Gil-Peña I, Rodríguez-Cañero R (2002c) Conodont content and stratigraphy of the Llessui Formation from the south central Pyrenees. In: García-López S, Bastida F (eds) Palaeozoic conodonts from northern Spain. Eight International Conodont Symposium held in Europe. Publ IGME, Cuad Mus Geomin 1, Madrid, pp 391–401.

Sanz-López J (2004) Silúrico, Devónico y Carbonífero pre- y sin-varisco en Geología de los Pirineos. In: Vera JA (ed.) Geología de España. SGE-IGME, Madrid, pp 250–254.

Sanz-López J, Blanco-Ferrera S (2012) Revisión estratigráfica del Misisipiense al Pensilvaniense más bajo de la zona Cantábrica y la posición de los límites entre los pisos. Geo-Temas 13:90 (annexed CD: 163–166).

Sanz-López J, Palau J (2000) Conodontos del Wenlock del macizo del Marimanya, Pirineo central. 1st Congr Iber Paleontol, 16th J Soc Esp Paleontol, Évora, pp 278–279.

Sanz-López J, Sarmiento GN (1995) Asociaciones de conodontos del Ashgill y del Llandovery en horizontes carbonatados del valle del Freser (Girona). 11th J Paleontol, Tremp, pp 157–160.

Sanz-López J, Valenzuela-Ríos JI, García-López S, Gil Peña I, Robador A (1999) Nota preliminar sobre la estratigrafía y el contenido en conodontos del Prídolí-Lochkoviense inferior en la unidad de els Castells (Pirineo central). Temas Geol-Min ITGE 26 (2), pp 638–642.

Schmidt H (1931) Das Paläozoikum der spanischen Pyrenäen. Abh Ges Wiss K 3 5, Göttingen.

Shervais J (1982) Ti-V plots and the petrogenesis of modern and ophiolitic lavas. Earth and Planetary Sci Letters 59:101–118.

Slavík L, Valenzuela-Ríos JI, Hladil J, Chadimová L, Liao J-C, Hušková A, Calvo H, Hrstka T (2016) Warming or cooling in the Pragian? Sedimentary record and petrophysical logs across the Lochkovian-Pragian boundary in the Spanish central Pyrenees: Palaeogeogr Palaeoclim Palaeocol 449, 300–320.

Speksnijder A (1986) Geological analysis of Paleozoic large-scale faulting in the south-central Pyrenees. Geol Ultraiectina 43.

Stampfli GM, von Raumer JF, Borel GD (2002) Paleozoic evolution of pre–Variscan terranes: from Gondwana to the Variscan collision. In: Martínez Catalán JR, Hatcher RD, Arenas R, Díaz García F

(eds) Variscan–Appalachian Dynamics: the Building of the Late Paleozoic Basement. Geol Soc Am, Spec Pap 364:263–280. Boulder, Colorado.

Sun SS, McDonough WF (1989) Chemical and isotopic systematics of oceanic basalts; implications for mantle composition and processes. In: Saunders AD, Norry MJ (eds) Magmatism in the Ocean Basins. Geol Soc London, Spec Vol 42: 429–448.

Syme EC (1998) Ore-associated and barren rhyolites in the central Flin Flon Belt: Case study of the Flin Flon mine sequence. Manitoba Energy and Mines, Open File Rep OF98-9:1–32.

Vachard D, Cózar P, Aretz M, Izart A (2016) Late Viséan–Serpukhovian foraminifers in the Montagne Noire (France): Biostratigraphic revision and correlation with the Russian substages. Geobios 49:469–498.

Valenzuela-Ríos JI, Slavík L, Liao J-C, Calvo H, Hušková A, Chadimová L (2015) The middle and upper Lochkovian (Lower Devonian) conodont successions in key peri-Gondwana localities (Spanish Central Pyrenees and Prague Synform) and their relevance for global correlations. Terra Nova 27:409–415.

Walliser OH (1996) Global events in the Devonian and Carboniferous, In: Walliser OH (ed) Global events and event stratigraphy in the Phanerozoic. Springer-Verlag, Berlin, pp 225–250.

Wirth M (1967) Zur Gliederung des höheren Paläozoikums (Givet-Namur) im Gebiet des Quinto Real (West pyrenäen) mit Hilfe von Conodonten). N J Geol Palaeont Abh 127:179–244.

Wood D (1980) The application of a Th-Hf-Ta diagram to problems of tectonomagmatic classification and to establishing the nature of crustal contamination of basaltic lavas of the British Tertiary volcanic province. Earth Planet Sci Lett 50:11–30.

Zwart HJ (1979) The Geology of the Central Pyrenees. Leidse Geol Meded 50:1–74.

Paleozoic Basement and Pre-Alpine History of the Betic Cordillera

9

A. Martín-Algarra, A. García-Casco, M. T. Gómez-Pugnaire, A. Jabaloy-Sánchez, C. Laborda-López, V. López Sánchez-Vizcaíno, S. Mazzoli, P. Navas-Parejo, V. Perrone, R. Rodríguez-Cañero, and A. Sánchez-Navas

Abstract

Palaeozoic rocks in the Betic Cordillera are widespread in the Maláguide, Alpujárride and Nevado-Filábride complexes of its Internal Domain. The Malaguide stratigraphic successions record a deepening trend during the post-rift evolution of a divergent continental margin that was paleogeographically related to the Northern Paleotethys from the latest Ordovician to the Early Carboniferous. Since the Serpukhovian it evolved to a convergent margin with Culm-like synorogenic sedimentation. Also probably at that time most of the Nevado-Filábride and Alpujárride rocks were affected by a Variscan tectonometamorphic evolution that was followed by latest Variscan local granite emplacement at ca. 300–280 Ma.

9.1 Introduction: State of the Art and Main Controversies

A. Martín-Algarra

In the Betic Cordillera Cadomian basement rocks and Cambrian-Ordovician successions have not been recognized, and very limited evidence of Precambrian marine sediments has been found only in the Nevado-Filábride Complex.

Coordinator: Agustín Martín-Algarra.

A. Martín-Algarra (✉) · P. Navas-Parejo · R. Rodríguez-Cañero
Departamento de Estratigrafía y Paleontología, Facultad de Ciencias, Universidad de Granada, 18071 Granada, Spain
e-mail: agustin@ugr.es

P. Navas-Parejo
e-mail: pilarnpg@geologia.unam.mx

R. Rodríguez-Cañero
e-mail: charorc@ugr.es

A. Martín-Algarra · A. García-Casco · M. T. Gómez-Pugnaire · C. Laborda-López · V. López Sánchez-Vizcaíno · A. Sánchez-Navas
Departamento de Mineralogía y Petrología, Instituto Andaluz de Ciencias de la Tierra (IACT), Universidad de Granada (UGR)-Consejo Superior de Investigaciones Científicas (CSIC), Avenida de las Palmeras 4, 18100 Armilla, Granada, Spain
e-mail: agcasco@ugr.es

M. T. Gómez-Pugnaire
e-mail: teresa@ugr.es

C. Laborda-López
e-mail: claborda@ujaen.es

V. López Sánchez-Vizcaíno
e-mail: vlopez@ujaen.es

A. Sánchez-Navas
e-mail: asnavas@ugr.es

A. García-Casco · M. T. Gómez-Pugnaire · A. Sánchez-Navas
Departamento de Mineralogía y Petrología, Universidad de Granada, 18071 Granada, Spain

A. Jabaloy-Sánchez
Departamento de Geodinámica, Universidad de Granada, 18071 Granada, Spain
e-mail: jabaloy@ugr.es

V. López Sánchez-Vizcaíno
Departamento de Geología, Escuela Politécnica Superior, Universidad de Jaén, Alfonso X el Sabio 28, 23700 Linares, Spain

S. Mazzoli
Dipartimento di Scienze della Terra, dell'Ambiente e delle Risorse (DiSTAR), Università di Napoli Federico II, Complesso di Monte S. Angelo, Via Cinthia 21, 80126 Naples, Italy
e-mail: stefano.mazzoli@unina.it

Present Address:
P. Navas-Parejo
Estación Regional del Noroeste, Instituto de Geología, UNAM, 83240 Hermosillo, Mexico

V. Perrone
Dipto di Scienze Geologiche e Tecnologie Chimiche e Ambientali, Università di Urbino, Località Crocicchia, 61029 Urbino, Italy
e-mail: vincenzo.perrone@uniurb.it

C. Quesada and J. T. Oliveira (eds.), *The Geology of Iberia: A Geodynamic Approach*, Regional Geology Reviews,
https://doi.org/10.1007/978-3-030-10519-8_9

Nonetheless, geochronological data from detrital and magmatic zircon reworked in younger sedimentary, metamorphic and magmatic rocks from different complexes reveal that the Betic Paleozoic successions were originally related to crustal segments that were previously involved in the Cadomian subduction and followed by Cambrian-Ordovician magmatic events, as observed in many other North-Gondwanic regions. Solid although yet limited biostratigraphic data from the Maláguide Complex reveals, however, a well-developed marine basin since, at least, the latest Ordovician. The Silurian-Devonian Maláguide sediments are widespread, relatively diversified and systematically pelagic, although clasts of Devonian to Carboniferous shallow-water carbonates are also present in uppermost Devonian and Carboniferous deep-water clastics. The Maláguide successions record a deepening trend during the post-rift evolution of a divergent continental margin that was paleogeographically related to Paleotethyan margins preserved in other Alpine regions. After some limited basin unstability during the Frasnian-Famennian, the margin reached its mature post-drif stage, dominated by thermal subsidence, in Early Carboniferous time, with deposition of Tournaisian radiolarian cherts and Visean conodont limestones. Since then, an important tectonic event marked the onset of the synorogenic (Late) Variscan evolution in the Maláguide Complex. It was followed by deposition of thick clastic wedges, showing the classical Culm facies, which started to be deposited since the Serpukhovian or, more probably, after the beginning of the Bashkirian. Also probably during that time most of the Nevado-Filábride and Alpujárride rocks were affected by an intense Variscan tectonometamorphic evolution, which was followed by latest Variscan local granite emplacement at ca. 300–280 Ma. However, many aspects of the Betic pre-Mesozoic evolution remain controversial.

The Paleozoic successions and pre-Alpine geological history of the Betic Cordillera (Fig. 9.1) are poorly known. Paleozoic rocks are rarely present in the ***External Zones*** and the ***Campo de Gibraltar Flysch Complex*** and mostly as reworked sedimentary components in younger successions. On the contrary, they are widely present in the ***Internal Zones***, below Mesozoic successions (frequently metamorphosed) of many Alpine thrust nappes. The lithological monotony, scarcity of fossils, intensity and style of deformation, and metamorphism make difficult to recognize the original features of the different successions and, consequently, unravelling their Paleozoic history. Notwithstanding controversial aspects, recent studies make increasingly evident that (i) the intense Alpine evolution that overprints the Paleozoic features of Betic successions has not completely erased them, and that (ii) their pre-Alpine history can be reconstructed, at least partially.

Paleozoic rocks in the ***External Zones*** practically do not exist in outcrop. Only a few, decametre to hectometre sized fragments of putative Paleozoic rocks have been documented within the Antequera Subbetic Chaotic Complex, isolated within mélange-type rocks dominated by brecciated Triassic gypsum (Peyre 1974). In spite of lacking outcrops, a general consensus exists about the nature of the Paleozoic basement rocks below the *Prebetic* and *Subbetic* cover thrust sheets of the External Zones: seismic and some deep well data certainly show that they constitute the south-eastern prolongation of the Variscan Iberian Massif. This basement was thinned during the opening of the Mesozoic ***Southern Iberian Paleomargin***, which was the paleogeographic realm where the terrains of the External Zones were originally deposited (Vera 2004).

The Betic (and Rifian) Internal Zones constitute, at least in wide parts (see below), the outcropping crustal segment of the same lithosphere than that of the Alboran sea and, together with the basement of the Alboran Sea, they are included, since Andrieux et al. (1971), in the same tectonostratigraphic terrane, named ***Alboran Block*** or ***Domain*** (Balanyà and García-Dueñas 1987; Guerrera et al. 1993; Gómez-Pugnaire et al. 2012; Behr and Platt 2012; Augier et al. 2013). The Betic Internal Zones are subdivided in four Alpine thrusts sheet complexes named, from the deepest to the highest, ***Nevado-Filábride***, ***Alpujárride*** and ***Maláguide***, in addition to a group of ***Frontal Units*** located along the boundary between the Internal and External Zones (Vera 2004). The Nevado-Filábride, Alpujárride and Maláguide complexes constitute the main body of the Internal Zones forming an antiformal nappe stack of pre-Mesozoic and Meso-Cenozoic rocks, whereas the Frontal Units are exclusively made of post-Paleozoic cover rocks. The lithosphere of the Alboran Sea is made of a strongly thinned continental crust constituted by Alpujárride- and Maláguide-like terrains. In addition, the upper units of the Alpujárride Complex include the largest outcropping bodies in the World of subcontinental mantle rocks, the Ronda peridotites. The characterization and interpretation of the *pre-Alpine* processes that affected the Paleozoic successions associated with the peridotites play a crucial role for understanding of the *Alpine* geodynamic evolution of these mantle slices.

The pre-Mesozoic lithologic successions of the Betic Internal Zones are strongly deformed and affected by metamorphism of different grade (Vera 2004). Those of the Maláguide Complex yet preserve many original sedimentary features and fossils that allow accurate stratigraphic dating and environmental interpretation. Those of the Nevado-Filábride and Alpujárride complexes, however, are fully constituted by metamorphic rocks, mainly pelito-psammitic metasediments, with subordinate metaconglomerates, marbles and, occassionally, volcanic, subvolcanic and plutonic rocks, either acid and intermediate or mafic and ultramafic. The latter were transformed by the metamorphism to gneisses and amphibolites (or eclogites) and serpentinites,

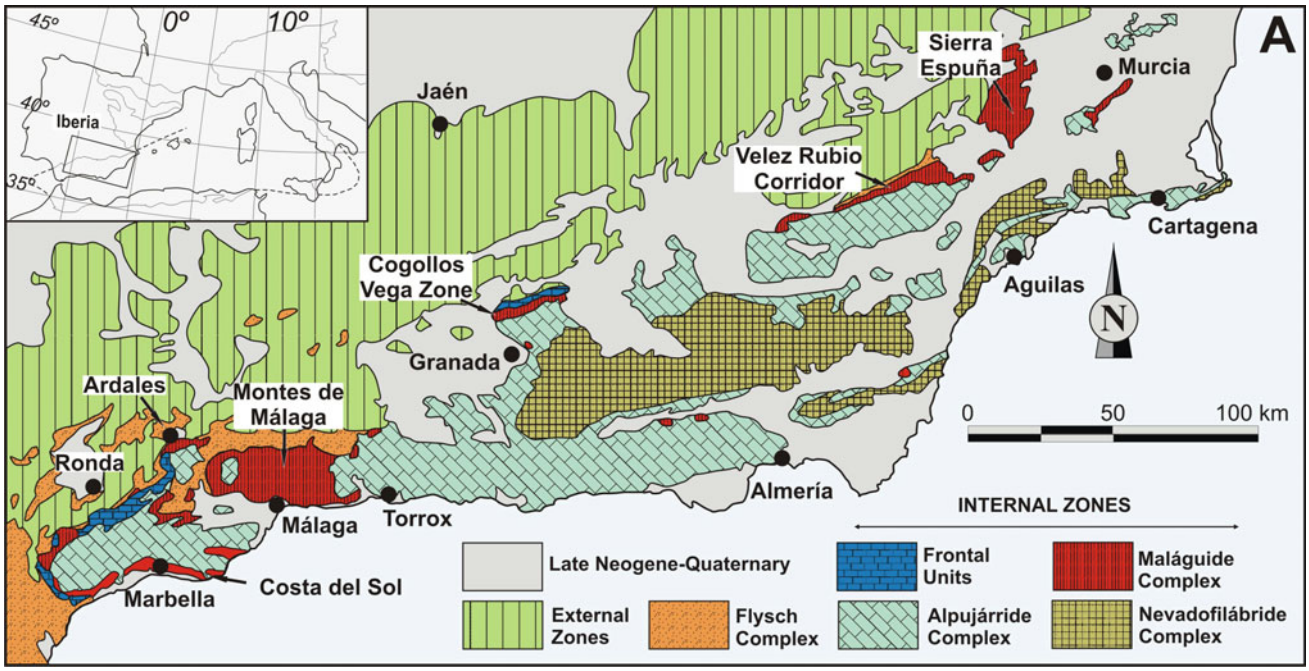

Fig. 9.1 Main divisions of the Internal Zones of the Betic Cordillera

respectively. These successions lack fossils, except in some localized outcrops. The combined stratigraphic-petrologic-structural analysis of the oldest metasedimentary successions of the three complexes and geochronologic dating from gneisses of diverse units, in particular by U-Pb zircon dating, make increasingly evident that they were affected by pre-Alpine (Variscan and maybe older) tectonic, metamorphic and magmatic events.

The main controversies on the Betic pre-Mesozoic successions deal with: (1) the stratigraphic interpretation and correlation of rock successions; (2) the distinction among petrographic and deformational features related to pre-Alpine and to Alpine events; (3) the significance of geochronological ages obtained from different rock types and by different methods; (4) the integration of available data in crustal/lithosphere scale geodynamic models compatible with the pre-Alpine and Alpine plate tectonic evolution.

It is yet unclear if the stratigraphy and paleogeographic evolution of the Betic Paleozoic terrains must be related to continental paleomargins and basins associated with the plate tectonic evolution of the Rheic Ocean, like those of the Iberian Massif, or to margins and basins associated with the evolution of the Prototethys and Paleotethys Oceans, as it is accepted for most Paleozoic terrains of the Alpine belt (Stampfli and Borel 2004; Stampfli et al. 2013 and references therein). Actually, most–but not all–Internal Betic Paleozoic successions show much stronger geological affinities with coeval succession of other Alpine areas (Alps, Maghrebides, Apennines, Carpathians…) than with those of the Variscan Iberian or Nord-African Paleozoic Massifs of the foreland of the Alpine-Mediterranean belts (Martín-Algarra et al. 2000, 2004; Rodríguez-Cañero et al. 2010; Navas-Parejo 2012; Rodríguez-Cañero and Martín-Algarra 2014).

It is also unclear the timing and mode of exhumation of the Alpujárride subcontinental mantle rocks. The tectonic emplacement of the Ronda peridotites accounted in the frame of a subduction-related Alpine metamorphism of early Miocene age that also involved Mesozoic covers of the Alpujárride Complex and of some Frontal Units of the Internal Zones (Nieves Unit in particular: Mazzoli and Martín-Algarra 2011; Mazzoli et al. 2013). But this emplacement involved *extremely thinned* pre-Mesozoic Alpujárride crustal successions, in which recent geochronological data are demonstrating the existence of pre-Alpine HP and HT metamorphic and anatectic events (Sánchez-Navas et al. 2017 and references therein). Consequently, some authors interpret that the important thinning that affects the Alboran Domain crust could be at least partially *inherited* since (late) Paleozoic time and that it would not be *exclusively* related to Alpine extensional collapse of a previously thickened lithosphere as interpreted by most authors (e.g., Précigout et al. 2013; Gueydan et al. 2015; Frasca et al. 2017; Williams and Platt 2017, and references therein). The Paleozoic tectonometamorphic signatures of the Betic Paleozoic successions must have conditioned the Alpine evolution at crustal and lithospheric scales. The real problem arises from incomplete understanding of the role played by each orogeny in the configuration of the Internal Betic realms.

9.1.1 Controversies Related to the Stratigraphy and Structure of the Nevado-Filábride Complex

The Nevado-Filábride Complex is usually divided into two main groups of units that are grouped in the ***Veleta*** and ***Mulhacén*** tectonic ensembles (Puga et al. 1974, 2002). There is no agreement, however, neither on the cartographic distribution of these units nor on their lithological succession and stratigraphy, and even some authors reject this twofold subdivision and interpret the whole complex as a single tectonic unit (González-Casado et al. 1995; García-Dueñas et al. 1998a, b; Sanz de Galdeano and López-Garrido 2016a; Sanz de Galdeano et al. 2016; Santamaría-López and Sans de Galdeano 2018). The occurrence of Variscan magmatic rocks in the graphite bearing lower successions of the Mulhacén (Sierra Nevada), and in equivalent units of eastern areas, is well constrained, and the Paleozoic age of the host metasediments unanimously accepted. Moreover, some Veleta-type graphite-rich low-grade metapelites and black marble horizons have provided Paleozoic and older fossils (see below). Nevertheless, the interpretation of most upper Mulhacén successions, which are lithologically very heterogeneous, is controversial (see Sect. 2.1).

Different types of micaschists quartzites, calcschits and marbles constitute the predominant lithotypes in the Mulhacén successions (Puga 1977, 1990; Estévez and Pérez-Lorente 1974; Díaz de Federico et al. 1979; Gómez-Pugnaire 1981; Puga et al. 2002, 2011; Gómez-Pugnaire et al. 2012). The schists sometimes are dark-coloured, graphite bearing and/or biotite-rich, but also light-coloured, muscovite-rich and/or chlorite-rich. The marbles are locally massive, quite pure and several hundred of metres thick, but they are also, and mostly, impure and alternate with different types of metapelites, calcschists and amphibolites. Typically, these successions also include former magmatic rocks bodies, both felsic and mafic, with ultramafic lenses, all now systematically metamorphosed under high-P conditions. The felsic rocks are massive and layered orthogneisses, the latter frequently very rich in tourmaline (Nieto 1996; Nieto et al. 2000; Martínez-Martínez et al. 2010; Gómez-Pugnaire et al. 2012, and references therein). The felsic rocks have provided late Paleozoic magmatic U-Pb zircon ages (see Sect. 9.4). The massive orthogneisses are associated with graphite-rich metapelites unanimously interpreted as Paleozoic metasediments. Nevertheless, the layered gneissic lithotypes appear in the uppermost part of the Nevado-Filábride succession. They are commonly intercalated within light-coloured metasediments, including marble horizons in its upper part, which underlie a thick metasedimentary, mainly carbonatic succession, whose age is considered as, essentially, Permian although some authors have interpreted these layered lithotypes as Permian-Triassic vulcanoclastic rocks (Andriessen et al. 1991; Nieto 1996; Nieto et al. 2000). The mafic rocks are mainly amphibolites or amphibolitized eclogites with locally well preserved magmatic features evidencing that their protoliths were gabbros or basalts, sometimes pillowed (Morten and Puga 1984; Morten et al. 1987; Bodinier et al. 1987; Puga 1990; Gómez-Pugnaire and Muñoz 1991; Puga et al. 1989a, b, 1995, 1997, 1999, 2005, 2011, 2017). The ultramafic rocks are serpentinites and harzburgite metaperidotites (Burgos et al. 1980; Jabaloy-Sánchez et al. 2015 and references therein). The age of the mafic and ultramafic rocks and, especially, that of the upper Mulhacén metasedimentary successions is controversial. According to stratigraphic correlations with the Triassic Alpujárride succession, most authors interpret that the age of the metasediments (mainly marbles, sometimes bearing gypsum) above the layered gneisses and associated rocks reached the Permian-Triassic (Gómez-Pugnaire and Cámara 1990; De Jong and Bakker 1991; Gómez-Pugnaire et al. 1994). Other authors interpret part of the impure marbles and calcschists as Jurassic-Cretaceous metasediments originally deposited in deep marine environments deposited within an oceanic branch of the Western Tethys (Tendero et al. 1993; Puga et al. 2017), but others consider the same metasediments as part of the Paleozoic succession (Gómez-Pugnaire et al. 2012). Nevertheless, very recent studies on detrital zircon data on both sides of the Gibraltar Arc, coeval to the writing of this chapter, tend to accept the post-Paleozoic age (Triassic and younger) of at least part of the upper Mulhacén successions (Jabaloy-Sánchez et al. 2018; see also Azdimousa et al. 2019).

The geological meaning of the mafic and ultramafic Nevado-Filábride rocks is also another important unsolved topic because there is not agreement about the geodynamic and paleogeographic meaning of the original magmatism: for some authors it was only related to a continental rifting, for others the rifting progressed to seafloor spreading related to the Mesozoic opening of the Tethys and would be responsible for producing an ophiolitic succession (Puga et al. 2017, Lozano-Rodríguez 2018, and references therein). The upper Mulhacén mafic and ultramafic rocks and related metasediments would then constitute ophiolitic relics of a thinned *Mesozoic* lithosphere now tectonically sandwiched between continental crust successions belonging to opposite continental margins and Mesozoic plates, and transformed in a subduction-related tectonometamorphic mélange. In any case, there is increasing evidence supporting that most of the Nevado-Filábride Complex must be excluded from the Alboran Domain lithosphere, and that its lower part must be interpreted as a crustal section of the Iberian lithosphere now outcropping in a tectonic window in the very core of the Betic orogen.

9.1.2 Controversies Related to the Other Complexes of the Betic Internal Zones

One of the main controversies involving structurally higher Betic internal complexes deals with the distinction of pre-Alpine tectonometamorphic signatures in Alpujárride rocks that were strongly affected by Alpine metamorphism. Actually, different and sometimes contradictory PTt paths have been proposed for the metamorphic evolution of Alpujárride rocks. According to recent petrological research and geochronological dating, a polymetamorphic and polyorogenic Alpine and pre-Alpine history, Variscan in particular, is becoming increasingly evident in the Alpujárride Paleozoic rocks (Zeck and Whitehouse 1999, 2002; Zeck and Williams 2001; Sánchez-Navas et al. 2012, 2014, 2016, 2017; Acosta-Vigil et al. 2014; Barich et al. 2014; Ruiz-Cruz and Sanz de Galdeano 2014a, b). Moreover, the importance of the Variscan Orogeny in the Maláguide Complex, the highest one in the Alpine tectonic stack, is clearly highlighted by the local preservation of pre-Alpine thrust sheets involving stratigraphically different Paleozoic successions (Martín-Algarra et al. 2009a, b), but this is usually ignored or underestimated (e.g. Williams and Platt 2017).

Another controversy deals with correlation of the Paleozoic (and post-Paleozoic) Internal Betic successions with other Iberian and Alpine terrains in North Africa, Apennines and Alps. If a Jurassic-Cretaceous ocean opened within the Nevado-Filábride Complex to the SE of Iberia before the onset of the proper Alpine Orogeny, the Paleozoic and younger terrains of the (true) Alboran Domain tectonic units would be originally located far towards the east, then in areas closer to the Alps and to the Apennines than to Iberia, and this putative ocean would have its continuation towards the Alps (compare Gómez-Pugnaire et al. 2000, 2004, 2012, with Puga et al. 2002, 2011, 2017). Consequently, the pre-Alpine (Variscan and older) evolution of these terrains (including upper Nevado-Filábride units and the whole Alpujárride and Maláguide complexes) should be different from that of the Iberian Variscan terranes and related units of the Nevado-Filábride Complex.

The paleogeography, geodynamics and tectonometamorphic evolution of the Alboran Domain is controversial during the Meso-Cenozoic (cf. Vol. 3, Ch. 7) but these aspects are practically unknown in pre-Mesozoic time, indeed. Actually, the proper existence of the Betic Palaeozoic terrains is neglected in widely difussed models devoted to the Palaeozoic evolution of the Alpine and Variscan regions in Southern Europe and North Africa, or misunderstood with that of other Iberian Variscan terranes (e.g. Von Raumer et al. 2002, 2003; Stampfli and Borel 2004; Sampfli and Hochard 2009; Stampfli et al. 2002, 2011, 2013; Torsvik and Cocks 2013). Only a few recent papers deal with this problem and they are mainly focused on the paleogeography of Maláguide sedimentary successions, whose stratigraphy and the understanding of their palaeogeographic and geodynamic evolution in relation to other Alpine Paleozoic terranes are rapidly improving (Rodríguez-Cañero et al. 2010, 2013; Navas-Parejo 2012; Navas-Parejo et al. 2008, 2009a, b, 2011, 2012a, b, 2015a, b; Somma et al. 2013; Rodríguez-Cañero and Martín-Algarra 2014).

In relation to the pre-Alpine tectonometamorphic evolution, recent studies are demonstrating that the effects of the pre-Alpine metamorphism and magmatism were very intense in the Alpujárride pre-Mesozoic successions. In addition, a probable pre-Alpine rise of the Ronda-Beni Bousera peridotites, and their emplacement in the shallow lithosphere in relation to a very important late Variscan crustal thinning, is becoming increasingly evident since some seminal papers (Reuber et al. 1982; Michard et al. 1997; see Sánchez-Navas et al. 2017 and references therein). In a different way, some authors have proposed that the Ronda peridotites were exhumed at surface in early Mesozoic time (Sanz de Galdeano and Ruiz-Cruz 2016; Sanz de Galdeano and López--Garrido 2016b) and that the Alpujárride continental crust rocks lying above them were previously affected by UHP metamorphism responsible for diamond and coesite within garnets (Ruiz-Cruz 2011b; Ruiz-Cruz and Sanz de Galdeano 2012b, 2013, 2014a, b). Accordingly, the Alpujárride pre-Alpine tectonometamorphic evolution and crustal thinning should be deeply re-evaluated. Moreover, the signatures related to the pre-Alpine emplacement of the peridotites at the base of the Alpujárride crustal succesions must be clearly distinguished from those related to the well documented Alpine thrust emplacement of the ultramafic slices within the upper Alpujárride crustal segment.

9.2 Pre-Mesozoic Successions of the Nevado-Filábride Complex

A. Martín-Algarra, M. T. Gómez-Pugnaire,
A. Jabaloy-Sánchez, R. Rodríguez-Cañero,
V. López Sánchez-Vizcaíno, P. Navas-Parejo,
C. Laborda-López

The Nevado-Filábride Complex is mainly exposed in the core of three main E–W trending antiforms and in separate outcrops toward the East (Fig. 9.1). Several tectonic subdivisions with diferent local names have been proposed. The most commonly used nomenclature distinguishes two tectonic ensembles (Puga and Díaz de Federico 1976; Puga et al. 1974, 2002): Veleta (footwall) and Mulhacén (hangingwall), which are subdivided in smaller tectonic units by other authors (Nijhuis 1964; Voet 1967; Bicker 1966; Egeler and Simon

1969; Puga et al. 1974, 2002; Kampschuur 1975; Vissers 1981; Bakker et al. 1989; De Jong and Bakker 1991; Martínez-Martínez et al. 2002; Gómez-Pugnaire et al. 2012, etc.). Both include thick and monotonous successions of graphite-bearing dark schists (locally including other subordinate rock types) of undisputable Paleozoic and older age. The dark schists of both the "*Veleta Succession*" and the "*Lower Mulhacén Succession*" are unanimously interpreted as pre-Alpine basements affected by Variscan metamorphism and overprinted by Alpine metamorphism. The "*Upper Mulhacén Successions*" are lithologically much more varied, structurally very complex and of controversial age and origin: they are dominated by light-coloured schists and marbles, and by magmatic rocks, both acid and mafic, also including some small ultramafic tectonic lenses. They have been classically interpreted as part of a Permo-Triassic and perhaps younger Alpine sedimentary cover (Egeler and Simon 1969; Puga et al. 2002), but other authors interpret that they are of exclusively Paleozoic age (Gómez-Pugnaire et al. 2000, 2004, 2012).

9.2.1 Veleta Succession

A. Jabaloy-Sánchez, A. Martín-Algarra, R. Rodríguez-Cañero, P. Navas-Parejo, C. Laborda-López

The Veleta Succession is several kilometres thick, partly due to tectonic causes, and characterized by monotonous graphite-rich fine-grained black schists and phyllites, with increasingly abundant quartzites towards the top of the succession (Jabaloy-Sánchez 1993; Martínez-Martínez 1986; Puga et al. 2002, 2004). Ocasionally, the schists intercalate laterally discontinuous graphite-rich black marbles (Puga 1971; Puga and Díaz de Federico 1976; Díaz de Federico et al. 1979; Vissers 1981; Martínez-Martínez 1986; Álvarez-Lobato and Aldaya 1985), decimetres to a few metres thick bands of rhyolitic orthogneisses (Nieto et al. 2000) and sparse amphibolite lenses that, according to their compositional and isotopic features, correspond to former basaltic magmas generated in intracontinental mantle settings (Puga et al. 2002).

The black schists of the Veleta Succession in Sierra de Baza provided probable Neoproterozoic acritarchs (*Gloecapsomorpha* sp. and *Trematospahaeridium* sp.: Gómez-Pugnaire et al. 1982). The graphite–rich marbles are rare in the Veleta Succession of Sierra Nevada but in Sierra de Baza and in the Águilas-Cartagena region they are frequent and have provided pre-Mesozoic fossils. In the latter sector, the carbonate levels are locally thick (from 0.5 to 5 m). They concentrate in the middle part of the graphite-rich schists and have provided Devonian (Emsian-Eifelian) macrofossils: chaetetids (Lafuste and Pavillon 1976), crinoids and unclassifiable remnants of rugose corals, cephalopods, gastropods, brachiopods, trilobites and other fossils (Laborda-López et al. 2015a, b). In the Sierra the Baza, a low-grade metamorphic succession formed by fine-grained black schists very rich in graphite, including thin-bedded dark marbles and thick quartzites towards the top, underlies typical Veleta schists. The marbles have recently provided the first conodonts of the Nevado-Filábride Complex, of early Bashkirian age (*Declinognathodus inaequalis* Zone: Rodríguez-Cañero et al. 2018) and the quartzites contain well-preserved sedimentary structures (graded laminae, current ripples, parallel and cross bedding: Jabaloy-Sánchez 1993). These new data allow interpreting the Veleta Succession in the Aguilas-Cartagena area as deposited in marine (mainly terrigenous, subordinately carbonatic) shallow platform environments above storm base during the Devonian (Laborda-López et al. 2015b). In the Sierra de Baza the Late Carboniferous sedimentation accounted in deeper environments under calm and poorly oxygenated to anoxic bottom water conditions, although the seabottom was occassionally affected by slow bottom currents (Rodríguez-Cañero et al. 2018).

9.2.2 Lower Mulhacén Succession

A. Martín-Algarra, M. T. Gómez-Pugnaire, A. Jabaloy-Sánchez

The Lower Mulhacén Succession is made, predominantly, of dark coloured graphite-rich schists with subordinate quartzites, quite similar to those of the Veleta Succession but without amphibolite lenses. The most significant difference is the local presence, in the Mulhacén black schists, of very large (cm-to dm-sized) and sometimes very well preserved pre-Alpine minerals (for details see Sect. 9.3.2) generated under static metamorphic conditions (Díaz de Federico and Puga 1976; Gómez-Pugnaire and Sassi 1983; Díaz de Federico et al. 1990). These porphyroblasts (Fig. 9.2) preserve microstructures defining two pre-Alpine phases of blastesis/deformation (Estévez and Pérez-Lorente 1974). Nonetheless, in most outcrops (in particular in the Sierra de Filabres) the porphyroblasts are strongly deformed, flattened, stretched and pseudomorphosed by micaceous lenses forming large white spots along rock surfaces defining the Alpine foliation (Puga et al. 1975; Díaz de Federico and Puga 1976; Puga et al. 2002, 2004). Hectometre sized ortogneissic (metagranite) bodies also appear locally included within these black schists (Nijhuis 1964; Bicker 1966). In the largest known (kilometre-sized) body, which is found in the eastern Sierra de Filabres (*Lubrín-Bedar Gneiss*), the original plutonic and pegmatoid magmatic structures are locally well preserved in spite of the intense Alpine deformation (see Sect. 9.4).

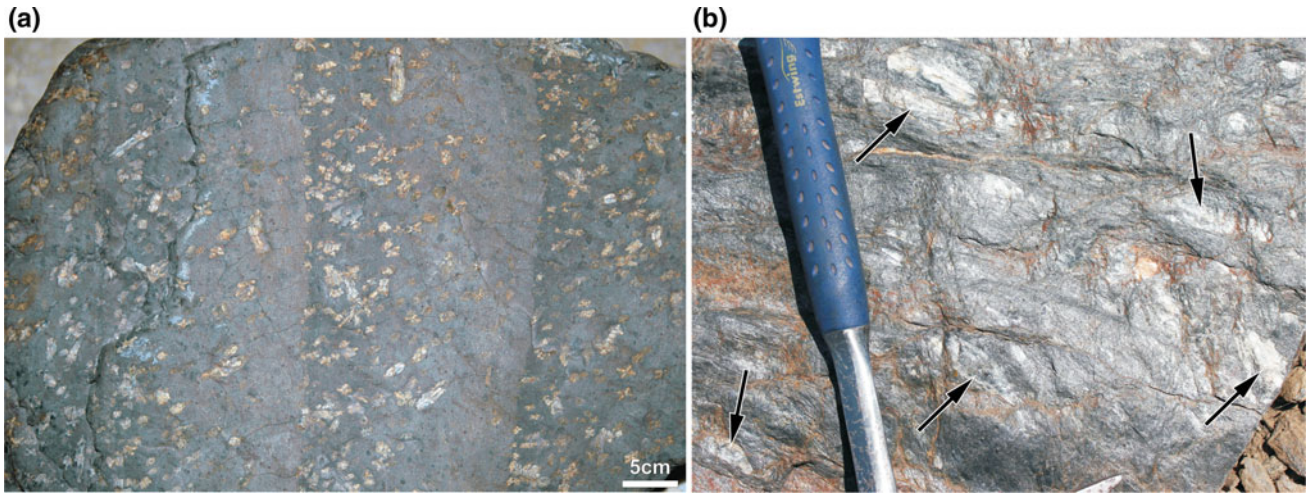

Fig. 9.2 Field views of pre-Alpine minerals of the Mulhacén Paleozoic succession: **a** grahite-rich schist with palm-like disoriented andalusite chiastolites (now fully transformed to Alpine kyanite), garnet, staurolite and chloritoid (smaller spots within the black matrix). **b** Alpine foliation surface showing white spots (arrows) corresponding to flattened and strongly sheared pre-Alpine andalusite crystals now transformed to fine-grained aggregates of Alpine muscovite and kyanite

9.2.3 Upper Mulhacén Succession

A. Martín-Algarra, M. T. Gómez-Pugnaire,
A. Jabaloy-Sánchez, V. López Sánchez-Vizcaíno

Above the black schists of the Lower Mulhacén Succession, a thick succession of light-coloured micaschists and quartzites constitutes the ***Tahal Schists*** (Nijhuis 1964; Kampschuur 1975; De Jong and Bakker 1991). Near to its base, this succession locally bears laterally discontinuous and *strongly deformed metaconglomerate lenses* (Fig. 9.3a), which probably constitute the base of a continental, probably alluvial succession unconformably deposited on their substratum of black schists (Gómez-Pugnaire et al. 2000). The widest outcrops of the proper Tahal Schists appear in the central part of the Sierra de Filabres (Vissers 1981). They constitute a thick (800–1000 m) monotonous sequence of silvery-gray muscovite schists with intercalated blue gray and white thick-to thin-layered quartzites, which are more abundant in the lower part of the succession. The quartzites frequently preserve cross lamination, cross bedding (Fig. 9.3b), ripples and bioturbation (De Jong and Bakker 1991; Gómez-Pugnaire et al. 2000). Silvery light gray metapelites with rare intercalations or marbles (>1 m thick) and calc-schists become predominant towards the top, although quartzites are always present. Some gneissic bodies with associated tourmaline-and garnet-skarns boudins and layers of garnet-tourmaline micaschists also appears in the upper part, as well as dikes of metabasites (Gómez-Pugnaire et al. 2012).

The Tahal Schists change upwards to a laterally discontinuous and usually *strongly brecciated calcite-dolomite marble succession, locally bearing gypsum and scapolite* (Gómez-Pugnaire et al. 1994; Puga et al. 1996), as well as metabasite lenses and dikes intruding different types of fine-grained schists and calc-schists. This complex lithologic ensemble has received many different local names (Nijhuis 1964; Voet 1967; Vissers 1981; De Jong and Bakker 1991; Puga et al. 1996; Martínez-Martínez et al. 2002; Puga et al. 2004 and references therein). This succession was deposited in evaporitic, probably coastal environments. The tectonic versus sedimentary origin of this succession and its age are controversial: (i) tectonic brecciation of evaporite-bearing Permian-Triassic rocks (Leine 1968; Vissers 1981); (ii) brecciation resulting from partial dissolution of rocks with high content of soluble salts (Duplaix and Fallot 1960; Jabaloy-Sánchez 1993; Gómez-Pugnaire et al. 1994); (iii) hybrid origins (Leine 1968; Bourgois 1979; Orozco et al. 1999); or (iv) deposition of an intra-orogenic volcano-sedimentary andesitic succession of Paleogene age that was subsequently tectonically brecciated (Puga et al. 1996). The presence of high-pressure minerals (kyanite-talc-phengite pseudomorphs) formed during the first high-pressure alpine metamorphic event in the very fine-grained metapelites does not fit well with the latter interpretation, however.

The uppermost part of the Upper Mulhacén succession is dominated by massive and pure calcitic and dolomitic marbles that overlie a heterogeneous succession of calcschists alternating with impure marbles, garnet micaschists (sometimes rich in graphite), chloritic and amphibolic micaschists, layered tourmaline-rich gneisses, metabasites and, occassionally, serpentinites. These lithologies show rapid lateral and vertical changes due to both stratigraphic and tectonic causes, the later resulting from intense syn- to postmetamorphic folding. Massive and pure calcitic and/or dolomitic marbles with white and/or banded white-gray colours are predominant in the uppermost part of the succession (***Macael Marbles***). Thinly to

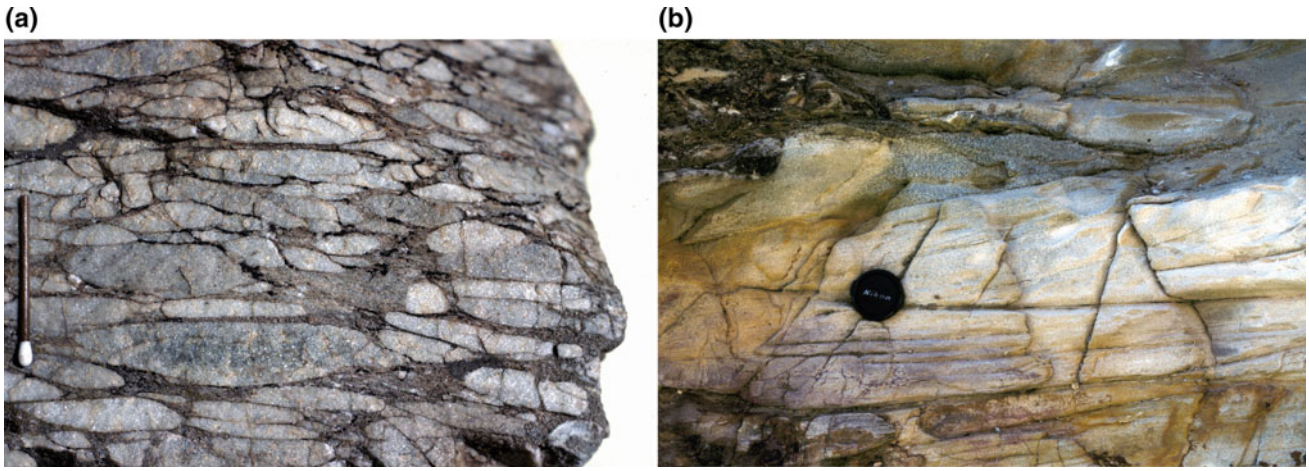

Fig. 9.3 Field views of the Tahal succession: **a** Stretched metaconglomerate of the lower part of the Tahal Schists succession (Sierra de Filabres). **b** Quartzites showing well preserved cross bedding (outcrop near Lubrin)

medium layered impure marbles lacking evaporites and rich in rounded detrital quartz grains, are essentially calcitic, usually dark coloured (grayish, brownish). They appear closely related to metabasites and serpentinites, and are associated with different types of yellowish-greenish calc-schists and micaschists with some quartzite horizons. They also, locally include a few meters thick bands of garnet-bearing, graphite-rich slightly calcareous dark schists. In the Cóbdar area the brown marbles include very thin layers with epidote, phengite, chlorite, amphibole, garnet, titanite and rutile, and some of them have unusually high Cr contents (López Sanchez-Vizcaíno et al. 1995) probably derived from detrital grains. In the same area, the impure marbles and calcschists intercalate a few metres thick bands of micaschists rich in graphite, and contain quartz nodules and bands (Fig. 9.4). These rocks bear rounded fine sand-sized detrital quartz grains and have provided ankeritic objects evoking marine pelagic microfossil remnants (Tendero et al. 1993): their size and shape in thin sections suggest mid-Cretaceous planktonic foraminifera, among them some fitting with *Helvetoglobotruncana helvetica* BOLLI, of Turonian age (Fig. 9.5). Nonetheless, this attribution is controversial, as Gómez-Pugnaire et al. (2000) interpret these remnants as benthic foraminifers of a wide geological time span.

9.3 Pre-Alpine Metamorphism in the Nevado-Filábride Complex

M. T. Gómez-Pugnaire, A. Martín-Algarra, A. Jabaloy-Sánchez, V. López Sánchez-Vizcaíno

There is a general consensus about the existence of a pre-Alpine (Variscan) tectonometamorphic evolution in the Nevado-Filábride Complex. Nevertheless, some authors interpret that the Veleta Succession was exclusively affected by pre-Alpine metamorphism (Gómez-Pugnaire and Franz 1988) whereas others consider that the pre-Alpine event was also overprinted by Alpine metamorphic events (Puga et al. 2002) or interpret the whole evolution of the Veleta successions as related to, exclusively, an Alpine polyphasic evolution (Augier et al. 2005a; Behr and Platt 2012). The dark micaschists and quartzites of the Lower Mulhacén Succession show clear evidence of polyorogenic metamorphism that is unanimously accepted: these rocks underwent Variscan LP/IT metamorphism, which was overprinted by HP Alpine metamorphism (Puga and Díaz de Federico 1976; Gómez-Pugnaire and Sassi 1983; Puga et al. 2002; Martínez-Martínez et al. 2002).

9.3.1 Veleta Succession

M. T. Gómez-Pugnaire, V. López Sánchez-Vizcaíno

The Veleta rocks are dark, fine-grained micachists and quartzites, with garnet, chloritoid, plagioclase, white mica, green and brown-red chlorite, quartz, graphite, ilmenite, zircon, tourmaline and apatite; small amounts of biotite and stilpnomelane intergrowths are also locally present (Nijhuis 1964; Vissers 1981; Martínez-Martínez 1986). Phase relationships of the main minerals are sketched in Fig. 9.6. These rocks are affected by four deformational events. Dominant fabrics are related to D_2 and produced isoclinal folds and a penetrative schistosity (S_2) subparallel to the axial planes of folds and to lithological contacts (Fig. 9.6c). This S_2 is poorly preserved but it is locally visible mainly within porphyroblasts (Puga and Díaz de Federico 1976; Vissers 1981). The D_3 deformational episode produces asymmetrical folds and, locally, a less penetrative

Fig. 9.4 Marbles of the Upper Mulhacén successions at Cóbdar

crenulation foliation S_3 (Fig. 9.6d). The D_4 event generated open folds with an associated crenulation cleavage S_4.

Large and small chloritoid crystals are rich in inclusions of graphite and ilmenite defining the folded S_1. Undeformed (Fig. 9.6f), sigmoidal (Fig. 9.6e) or folded graphite and quartz inclusion (S_1, Fig. 9.6b) appear within plagioclase porphyroblasts. Garnet porphyroblasts show undeformed, folded or sigmoidal helicitic inclusion patterns of graphite and quartz (Fig. 9.6a), and, sometimes, inclusion-free rims. Some garnet including S_1 and apparently rotated, with deformational pressure shadows and flattening of the main schistosity, were interpreted as syn-S_2 to post-S_2 (Gómez--Pugnaire and Franz 1988).

Figures 9.7 and 9.8 show variations in chemical composition of garnet and chloritoid respectively. For comparison, they also include data of the same minerals, both pre-Alpine and Alpine, from Mulhacén rocks (Gómez-Pugnaire and Sassi 1983; Puga et al. 2002). Peak temperatures were crudely estimated around 400–450 °C for the main assemblage, without significant changes in the evolution of the metamorphic grade (Gómez-Pugnaire and Franz 1988). However, the oligoclase rim of the albite cores and the inclusion-free garnet rims would indicate a T-increase after recrystallization (Eeckhout and Konert 1983; Vissers 1981). It is noteworthy that similar chemical compositions are found in the inclusion-free garnet rims and in garnets recrystallized during Alpine metamorphism (see discussion below on controversies).

Low P conditions are generally accepted for the pre-Alpine metamorphism that affected the Veleta Succession (Puga and Díaz de Federico 1976; Gómez-Pugnaire and Sassi 1983; Gómez-Pugnaire and Franz 1988). Puga et al. (2002) estimated $P \approx 3$ kb from the low-Si phengite in white micas found in pressure shadows of porphyroblasts. This agrees with chemical composition of the mineral assemblage and allows distinguishing this metamorphism from the HP Alpine metamorphism found in the Mulhacén rocks. Actually, systematic high-Fe contents in some minerals such as chloritoid and garnet are chemically incompatible with the high-Mg content found in the same minerals when formed in relation to the Alpine metamorphism (Figs. 9.7a, b and 9.8).

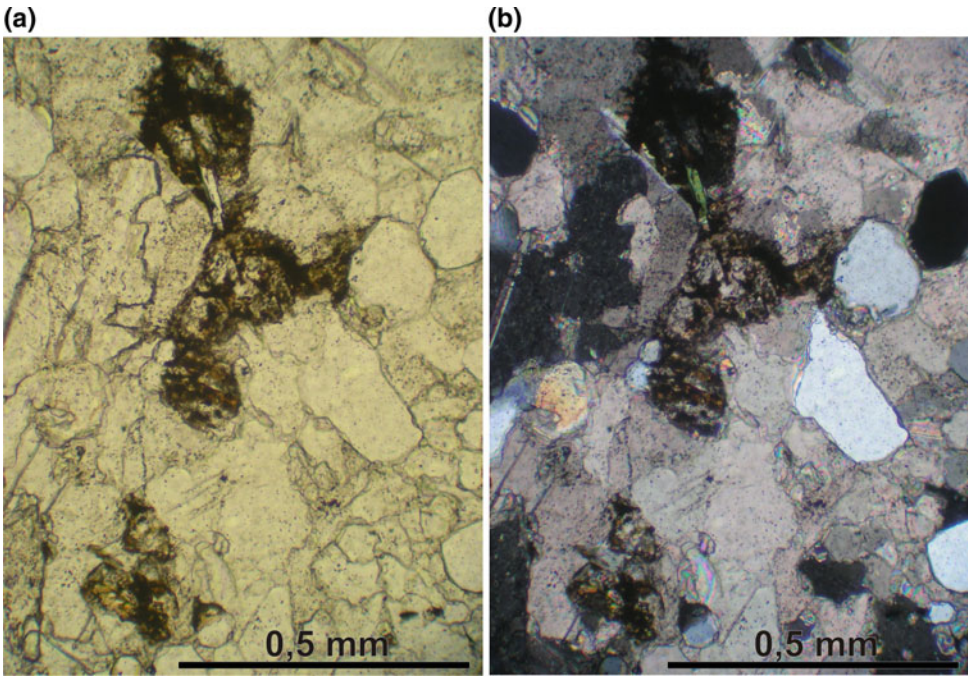

Fig. 9.5 Thin section of impure marbles near Cóbdar, with subrounded detrital quartz grains and one ankeritic object whose size and shape fits exactly with the axial section of the planktonic foraminifer *Helvetoglobotruncana helvetica* BOLLI, of Turonian age (Tendero et al. 1993)

Recent estimates using Raman spectrometry in carbonaceous materials of the Veleta Succession and local equilibria of chlorite-phengite pairs (Vidal and Parra 2000) yield P–T conditions of 450–530 °C at 12–14 kbar followed by heating and decompression reaching a maximum temperature of 530 °C at 8–10 kbar (Augier et al. 2005b). Behr and Platt (2012) also used Raman spectrometry in Sierra Alhamilla to quantify the temperature peak at the top of the Veleta succession, obtaining an average T = 493 °C. These authors attributed this metamorphic event in the Veleta rocks to the Alpine cycle. In addition, isopleth thermobarometry and pseudosections obtained from compositional zoning of garnet from Veleta schists (Aerden et al. 2013) indicate prograde metamorphic paths from ca. 5 kb/500 °C to 10 kb/550 °C, with P peak between 7 and 12 kbar. The pressure peak was calculated from garnet inclusion-free overgrowths that are interpreted to be Alpine. This would probably explain the overlap of some Veleta garnets in the field of the Alpine garnet of the Mulhacén rocks (Fig. 9.7b; full dots).

9.3.2 Lower Mulhacén Succession

M. T. Gómez-Pugnaire, A. Jabaloy-Sánchez, A. Martín-Algarra

The graphite-bearing micaschists of the lowest part of the Lower Mulhacén Succession include LP/IT mineral parageneses consisting of andalusite, chloritoid, staurolite, garnet, biotite, white micas, chlorite, quartz, magnetite and rutile. This assemblage, unanimously interpreted as Variscan, was overprinted by the HP/LT Alpine metamorphism (Puga and Díaz de Federico 1976; Gómez-Pugnaire and Sassi 1983; Martínez-Martínez 1986). The most striking feature of the Variscan mineral assemblage is the large size and the euhedral habit of porphyroblasts such as chloritoid, staurolite and andalusite (up to several cm long) and the very fine-grained matrix in the less overprinted samples (Fig. 9.9).

In the alpine overprint kyanite replaces andalusite; pre-Alpine sericite is found in rim and cracks of large porphyroblasts of andalusite and staurolite, and is replaced by Mg-chloritoid + garnet; garnet crystallized after biotite, and a pyrope-rich corona occurs overgrowing almandine-rich euhedral core of porphyroblastic garnets. The chemical composition of pre-Alpine garnet and choritoid is very similar to that described in the Veleta Succession. Both assemblages are typically rich in FeO compared with the Mg-rich Alpine minerals (Figs. 9.8a, b and 9.9). Peak pressures and temperatures recorded by phase relationships and the conventional geobarometric method are in the range of 2–4 kb and 500–600 °C (Puga and Díaz de Federico 1976; Gómez-Pugnaire and Sassi 1983).

9.3.3 Variscan Pre-Magmatic UHP Metamorphism in the Nevado-Filábride Complex?

M. T. Gómez-Pugnaire

Ruiz-Cruz et al. (2015, 2016) and Ruiz-Cruz and Sanz de Galdeano (2017) have reported diamond inclusions in

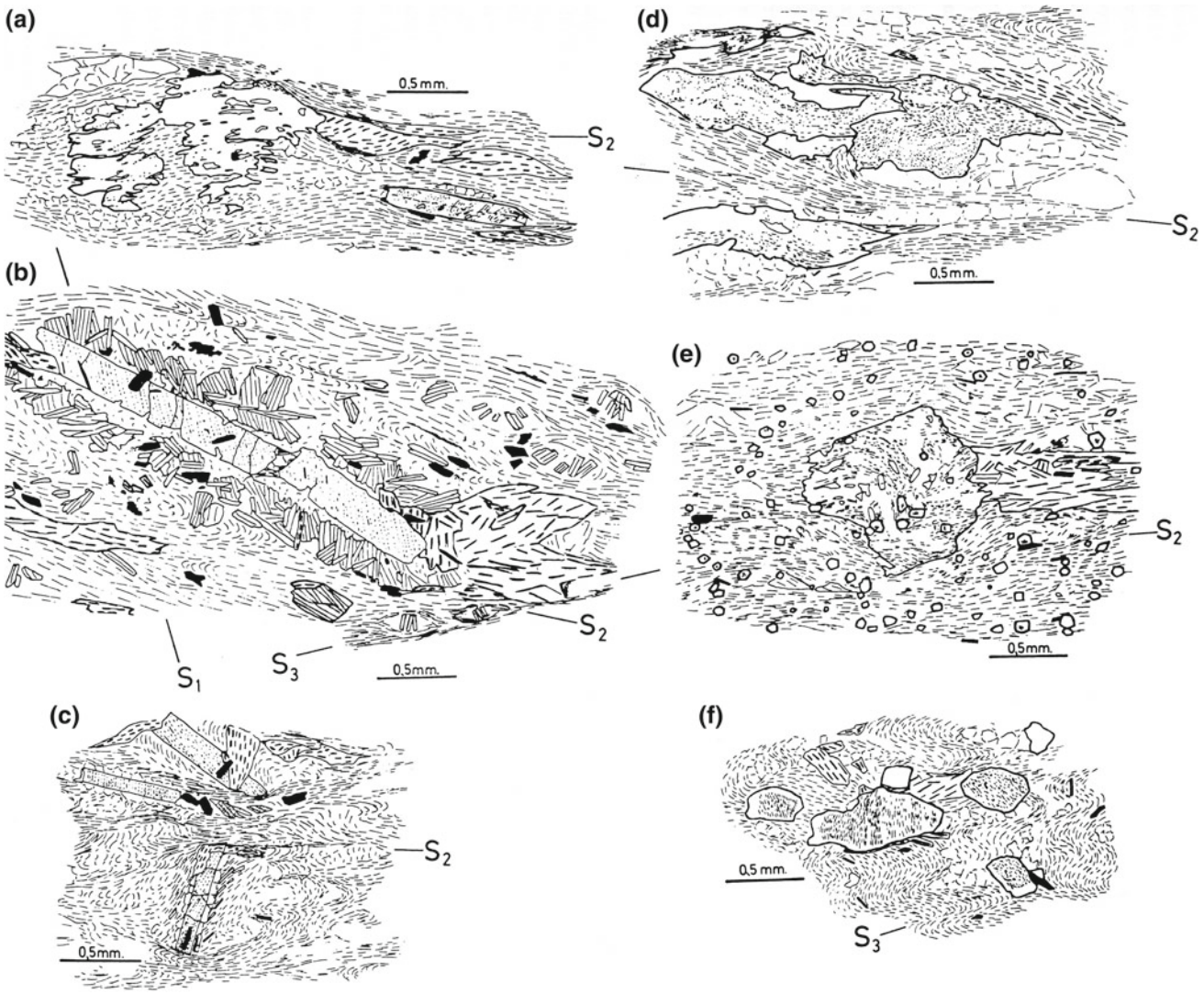

Fig. 9.6 Drawings illustrating phase relationships of porphyroblasts in the Veleta Succession. **a** Garnet (left) with S-inclusion pattern, chlorite (thick dashed) and chloritoid (slightly folded and irregular inclusion pattern), quartz and white mica. **b** Cracked chloritoid with undeformed inclusion pattern defining S_1, surrounded by small chloritoid crystals (thin dashed) and partly replaced by oxychlorite (thick dashed). **c** Irregular distribution of chloritoid porphyroblasts with partly continuous, partly discontinuous internal inclusion pattern. **d** Albite blast with irregular shape growing parallel to S_2 and a mostly continuous inclusion pattern of an early crenulation. **e** S-shaped inclusion pattern in albite with small garnets and chlorite to the right of the blast. **f** Albite blasts in a mica rich matrix, affected by S_3 crenulation, and with a narrow inclusion-free rim (from: Gómez-Pugnaire and Franz 1988)

apatite from different Nevado-Filábride rocks in Sierra Nevada, which they interpret as related to a pre-Alpine UHP metamorphism in the Nevado-Filábride Complex. The studied apatite comes from biotitic gneisses dated by $^{238}U/^{206}Pb$ in zircon as 285 ± 3 Ma. Based on petrographic and SEM analyses, and on geochemical data from biotite gneisses, these authors distinguished several generations of minerals that they attributed respectively to pre-magmatic, magmatic (Hercynian) and metamorphic (Alpine) events. Apatite concentrated in biotite-rich layers is closely associated with poorly preserved garnet interpreted as pre-magmatic on the base of garnet zoning pattern and isopleth thermobarometry. The coexistence of garnet and apatite suggests their common pre-magmatic origin, and the presence of diamond inclusions in apatite would indicate that UHP metamorphism might have affected source rocks before melting and latter gneissic recrystallization. The interpretations by Ruiz-Cruz and co-workers have important objections that are discussed by the authors themselves. One is related to distinguishing true diamond inclusions from artifacts produced by contamination during sample preparation, although the authors ruled out this possibility. The second objection relates to the easy metamorphic recrystallization of apatite below 500 °C, and to the possible dissolution of

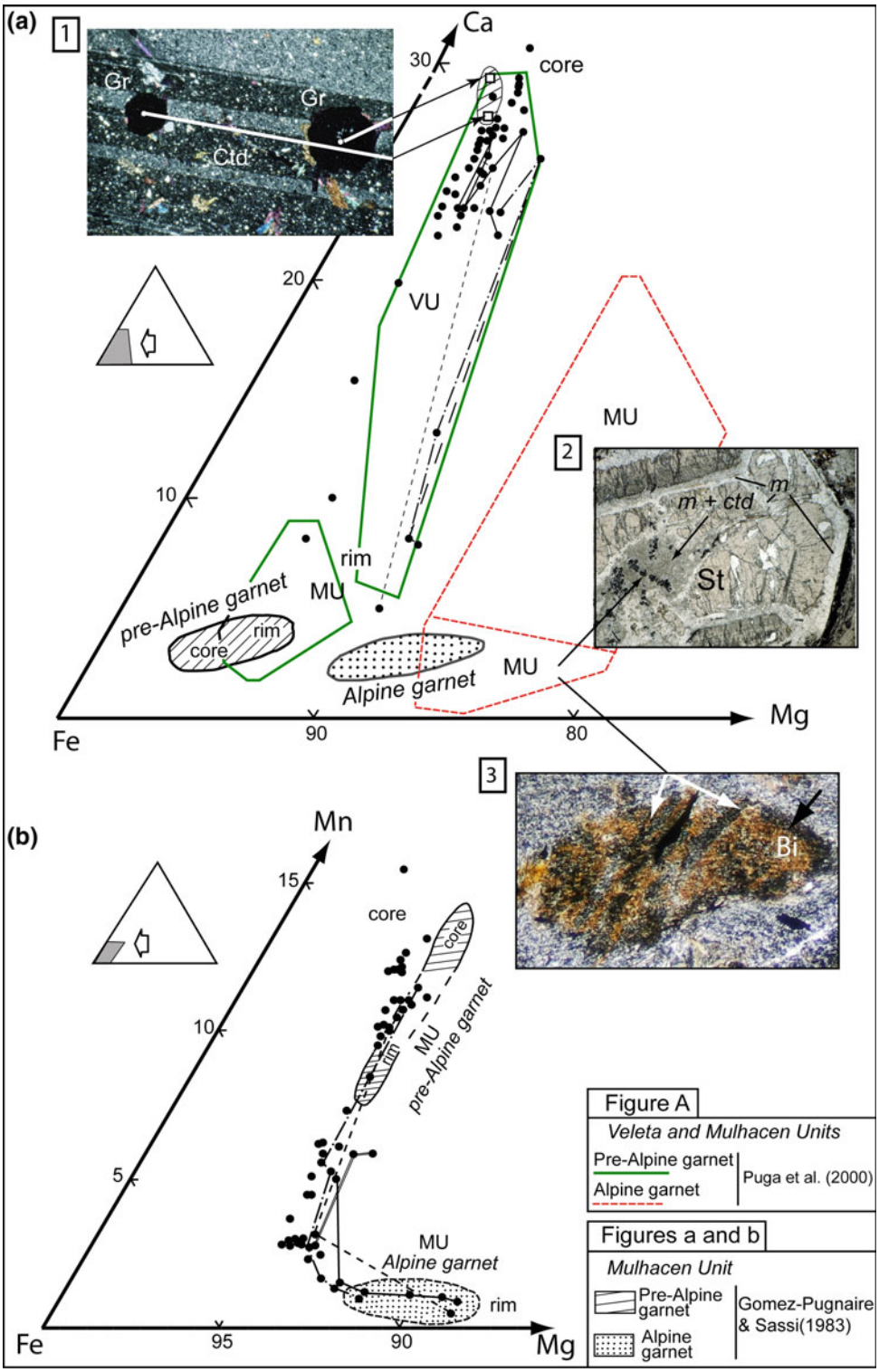

Fig. 9.7 Chemical composition of garnets: **a** Ca–Fe–Mg; **b** Mn–Fe–Mg of the Veleta and Mulhacén schists (VS and full dots, and MS, respectively). Lines connect point analyses along compositional profiles. Empty squares represent chemical compositions of euhedral garnet (cores) included within large pre-Alpine chloritoid poikiloblasts (insert picture 1). Mineral abbreviations according to Whitney and Evans (2010). Modified from Gómez-Pugnaire and Franz (1988), with analyses of the Mulhacén Alpine and Pre-Alpine garnets from other studies (insert in the lower right corner). See text for details

apatite during partial melting (Hammerli et al. 2014; Bea and Montero 1999). Nonetheless, Ruiz-Cruz et al. (2016) report several occurrences of apatite that persisted melting in eclogites and under crustal anatexis conditions (e.g. Puchelt and Emmermann 1976; Bingi et al. 1996). To avoid possible misinterpretations, geochemical data of well-characterized apatite domains must be used to testify the preservation or re-equilibration of the pre-magmatic apatite during anatexis. In any case, the existence of UHP conditions in the Nevado-Filábride Complex, if confirmed, would have very

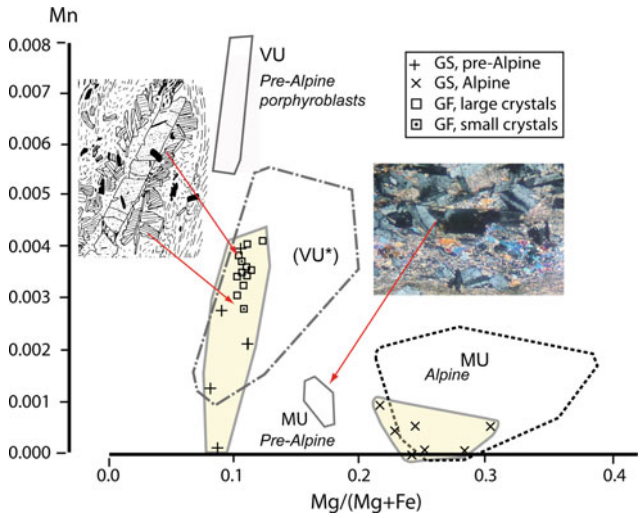

Fig. 9.8 Chemical composition of chloritoid (modified from Gómez-Pugnaire and Franz 1988; yellow shaded areas; GF) compared with data from Gómez-Pugnaire and Sassi (1983; GS) and Puga et al. (2002). VU: Veleta; MU; Mulhacén; VU*: interpreted as Alpine garnet by Puga et al. (2002)

important consequences not only for understanding the geological evolution of the Nevado-Filábride Complex but also for that of the Betic Cordillera as a whole, and must be carefully checked in future research.

9.3.4 Controversial Aspects on the Metamorphism Affecting the Veleta Successions

M. T. Gómez-Pugnaire, V. López Sánchez-Vizcaíno

There is a general agreement on the polymetamorphic character of the Lower Mulhacén Succession: the main low-pressure assemblage has been overprinted by other metamorphic parageneses chemically similar to those related to the Alpine metamorphism. In the Veleta Succession, however, most if not all the metamorphism is considered to be of Alpine age by some authors, despite of the metamorphic regime is similar to that of pre-Alpine metamorphism in the Lower Mulhacén Succession (Gómez-Pugnaire and Franz 1988). Nevertheless, the lower metamorphic degree, the lack of index minerals and strong retrogression do not allow reaching conclusive estimates for the P-T conditions that affected the Veleta Succession. For this reason, the consistence of some data addressed to identify HP Alpine metamorphic conditions in the Veleta Succession, as proposed by some recent studies, is discussed below.

Puga and Díaz de Federico (1976) and Vissers (1981) proposed a polymetamorphic history of the Veleta Succession from folded inclusion patterns found in large chloritoid porphyroblasts. They attributed an Alpine age to the main deformational event (D_2) and assumed a pre-Alpine age for the porphyroblasts. Since folded inclusions are similar in chloritoids of the matrix, they can also be interpreted as resulting from porphyroblasts growth while pre-Alpine S_1 was developing. Alpine HP conditions in the Veleta schists have been calculated on the base of the Si content (a.p.f.u) in phengite (Puga et al. 2002; Augier et al 2005b). Phengite component of muscovite is a function not only of pressure but also of the composition and this barometer can only be used in metapelites of specific compositional systems: KMASH (phengite + quartz + K-feldspar + biotite + H_2O) and KFASH (phengite + almandine + kyanite + quartz + H_2O; Massonne and Szpurka 1997). Assemblages containing feldspar, biotite and kyanite do not coexist with phengite in the Veleta schists, however. Additionally, the pyrophyllite substitution in muscovite should be considered because this substitution can be so large that geobarometry solely based on Si content can result in pressure overestimation (Essene 1989; Agard et al. 2011). By applying the chlorite-phengite multiequilibria thermobarometric method recent studies have concluded that the low-grade Veleta micaschists were affected by HP Alpine metamorphism (Augier et al. 2005b; Booth-Rea et al. 2005). Nevertheless, this method requires ascertaining whether adjacent mineral phases are in chemical equilibrium, which is extremely difficult to prove, in practice, in low-grade rocks, especially when they are strongly retrogressed like the Veleta schists. Recent attempts to reproduce these results from Veleta rocks of Sierra Alhamilla have actually failed (Behr and Platt 2012).

Scattered K/Ar and $^{40}Ar/^{39}Ar$ ages obtained from the Veleta Succession, ranging from the Early Jurassic to the Early Miocene, have been interpreted as related to Alpine metamorphic events (De Jong 1991, 1993a, b, 2003; Puga et al. 2004; Behr and Platt 2012). These ages are difficult to reconcile with much more robust results recently obtained from multiple geochronometers that constrain the peak of metamorphism in the Nevado-Filábride Complex to the early-middle Miocene (15.0 ± 0.6 Ma: López Sanchez-Vizcaíno et al. 2001; 18.2 ± 0.8 Ma and 16.8 ± 0.3 Ma: Platt et al. 2006; 17.3 ± 0.4 Ma: Gómez-Pugnaire et al. 2012; 20.1 ± 1.1 Ma: Kirchner et al. 2016).

RAMAN thermometry on carbonaceous material in the graphite schists shows that the shear zone at the Veleta-Mulhacén contact superposes the higher-T Lower Mulhacén Succession onto lower-T Veleta Succession (Augier et al. 2005b; Platt et al. 2006; Behr and Platt 2012; Booth-Rea et al. 2015). The inverted metamorphic gradient was classically interpreted as a result of a late-stage thermal overprint before Alpine nappe emplacement (De Roever and Nijhuis 1964; Vissers 1981; Bakker et al. 1989) and, recently, as formed during subduction of the cold Nevado-Filábride Complex beneath the hot thin Alboran

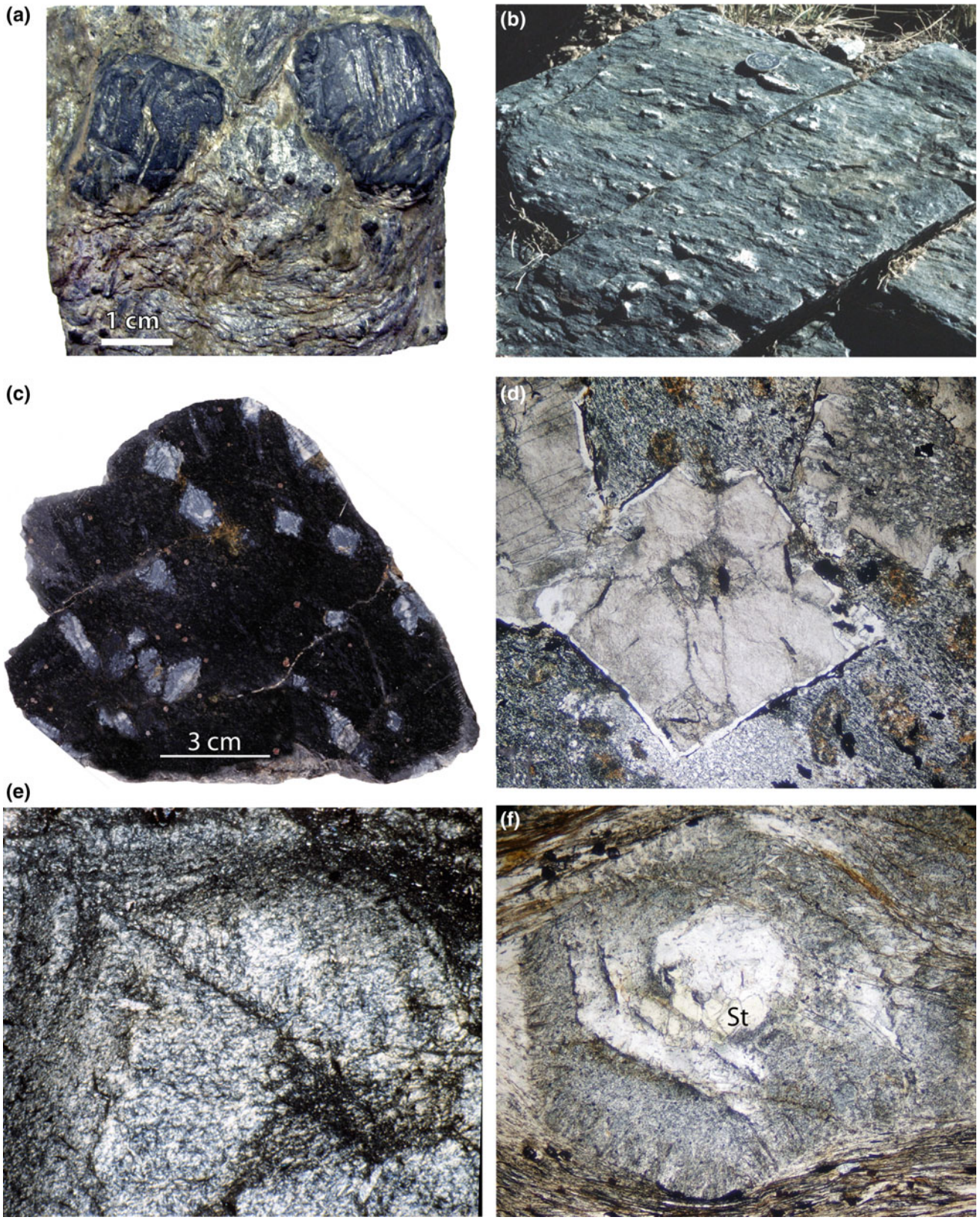

Fig. 9.9 Pre-Alpine minerals of the pre-Mesozoic Mulhacén dark schists. **a** Large chloritoid porphyroblasts with garnet inclusions. **b** Field view of elongated staurolite crystals. **c** Pseudomorphs of euhedral andalusite crystals in fine-grained schists with euhedral garnet. **d** Microphotography of the same sample as C showing euhedral chiastolite pseudomorphs and biotite flakes (plane-polarized light). **e** Cross-polarized photography of chiastolitic andalusite fully replaced by tiny Alpine kyanite crystals. **f** Petrographical image of a large staurolite crystal almost completely replaced by Alpine chloritoid and muscovite (plane-polarized light). Mineral abbreviations after Whitney and Evans (2010)

lithosphere (Behr and Platt 2012). In any case, the upper part of the Veleta Succession must have been affected, at least locally, by the metamorphic evolution related to the latest Alpine deformational events responsible for the ductile shear zone that separates it from the overlying Lower Mulhacén Succession: thin oligoclase rims of plagioclase and overgrowths of garnet could be the metamorphic products of this process. The temperature calculated from the rocks involved in the shear zone ranges between 493 and 510ºC (Augier et al. 2005b; Behr and Platt 2012), which is in the same range of the temperature calculated for the main event of the regional metamorphism of the Veleta Succession.

In summary, inaccuracies associated with the methods used lead to conclude that, for the moment, the estimated P-T conditions and age (pre-Alpine vs. Alpine) for the metamorphism underwent by the Veleta rocks should be taken with caution. This brings into question the widespread attribution of the Veleta metamorphism to the sole Alpine orogeny. If the main metamorphic processes would be related mainly to the Variscan Orogeny, the interpretation of the Veleta successions as a pre-Alpine basement involved in the Alpine orogeny only at a relatively late stage (Gómez-Pugnaire and Franz 1988) would be reinforced. Consequently, the rocks of the Veleta Succession might correspond to the prograde lower temperature segment of the pre-Alpine PT path while those of the Lower Mulhacén Succession would represent the peak PT conditions of the Variscan metamorphism.

9.4 Paleozoic Magmatism of the Nevado-Filábride Complex

M. T Gómez-Pugnaire, A. Jabaloy-Sánchez, V. López Sánchez-Vizcaíno

In addition to the above-mentioned metasediments, the Mulhacén Successions include different types of magmatic rocks strongly affected by the Alpine metamorphism (orthogneisses, metabasites and serpentinites). This section deals with acidic orthogneisses, whose latest Paleozoic magmatic age is demonstrated by geochronological data. Metamorphosed acidic igneous rock bodies of variable dimensions are commonly found throughout the Nevado-Filábride successions (Nijhuis 1964; Puga et al. 2002; Nieto 1996; Gómez-Pugnaire et al. 2012; Martínez-Martínez et al. 2010). In the Veleta Succession, Puga et al. (2002) mention the local presence of dm-to m-thick lenses of undated rhyolitic orthogneisses. In the Lower and Upper Mulhacén Successions, Gómez Pugnaire et al. (2012) and Ruiz-Cruz et al. (2016) distinguished gneisses with two different compositions: (1) peraluminous leucocratic gneisses, with textures that ranged from metagranites (Fig. 9.10a), augen gneisses and even-grained gneisses depending of the different degree of deformation and metamorphism, which affected the granites, and (2) strongly peraluminous biotite-rich gneisses. The largest outcrop of the type 1 gneisses is exposed in the Sierra de los Filabres near to El Chive and Bédar (Fig. 9.10), where evidences of contact metamorphism and metasomatism in the country metasediments are common.

Nieto et al. (2000) and Puga et al. (2002) distinguished among syncollisional and postcollisional peraluminous leucocratic gneisses. The latter type consists of tourmaline-rich layered gneisses made of alternating centimeter-to metre-thick leucocratic layers, with Na- and K-feldspar, and quartz, and melanocratic lithotypes with phengite, green biotite, epidote and tourmaline (Díaz de Federico et al. 1990; Nieto 1996; Nieto et al. 2000; Torres-Ruiz et al. 2003; Gómez-Pugnaire et al. 2012). They were interpreted as metarhyolites and meta-volcanoclastic rocks (Nieto et al. 2000; Puga et al. 2002), and have been dated by K/Ar as Triassic in age (Andriessen et al. 1991; Nieto 1996; Nieto et al. 2000). The same rocks, however, have provided Paleozoic zircon ages (Martínez-Martínez et al. 2010; Gómez-Pugnaire et al. 2012) and the alternation of dark and light layers can be also explained by segregation during deformation by ductile shear zones. Most compositional data of the gneisses protoliths plot in the *anatectic* (syn- and post-orogenic) granitoid field in the R1–R2 multicationic diagram of Batchelor and Bowden (1985), whereas some of the biotite gneiss samples and one leucocratic gneiss display very high R1 and plot in the compositional field of the Nevado-Filábride metapelites (Gómez-Pugnaire et al. 2012; Ruiz-Cruz et al. 2016). All geochemical data suggest a derivation of gneisses by melting of a crustal parent. Additionally, the presence of detrital zircon cores with different zoning patterns in all dated gneisses (Gómez-Pugnaire et al. 2012) indicates metasedimentary rather than igneous sources. The high A/CNK ratio, high SiO_2, low CaO, high LILE, and REE patterns, are comparable to other peraluminous, post-collisional granitic bodies in the European Variscan orogen. The sequence can be interpreted within the context of the late Variscan extension that generates magmatic activity between 295 and 240 Ma (Gómez-Pugnaire et al. 2012; Ruiz-Cruz et al. 2016).

The age of the igneous rocks indicates the minimum age of the host rocks if relationships between them prove to be original. Rb/Sr whole rock dating and U-Pb SHRIMP dating of magmatic zircons from gneisses from the Upper Mulhacén Successions near the marbles yield and age of 247 ± 11 and 301 ± 7 Ma respectively (Table 9.1: Gómez-Pugnaire et al. 2000, 2004). Martínez-Martínez et al. (2010) reported U-Pb LA-ICPMS ages of 314 ± 7 Ma and 304 ± 23 Ma in gneisses from one outcrop studied by Gómez-Pugnaire et al. (2004) in Sierra Nevada, but disagree with the interpretation of field relationships between the gneisses and the country

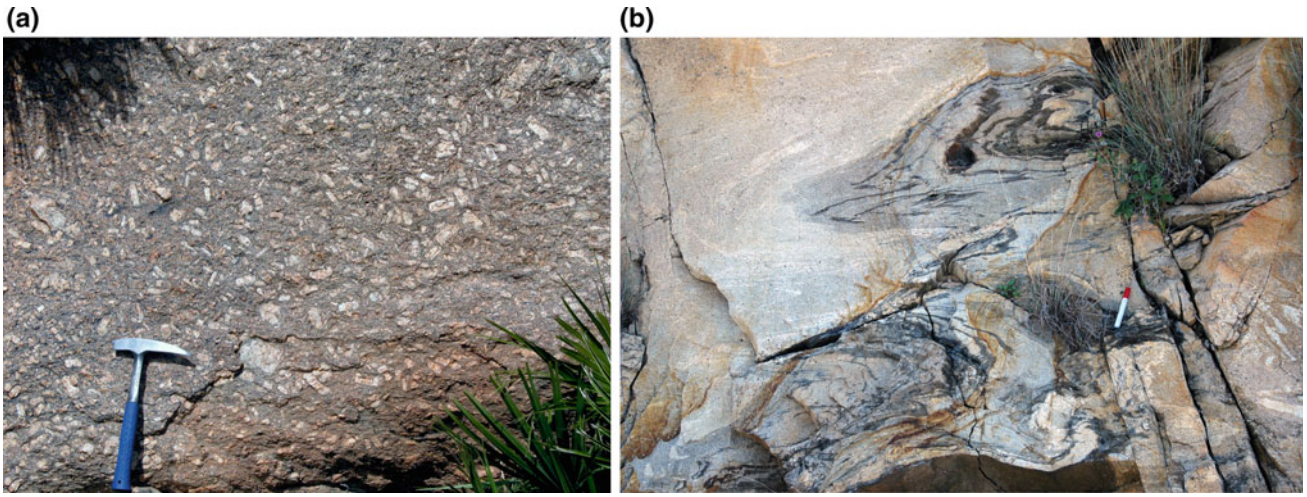

Fig. 9.10 **a** Undeformed metagranite from the Monda outcrop. **b** Strongly deformed gneiss from the Bédar outcrop

rocks (upper marbles) made by the previous authors. The intense thinning of the Upper Mulhacén Successions makes difficult assessing the relationships of this gneiss body and marbles in this locality. Nevertheless, thick marble layers from the Sierra de los Filabres underlie, with obvious stratigraphic relationships, a tourmaline gneiss complex yielding and age of 291 ± 3 Ma to Gómez-Pugnaire et al. (2012, their Fig. 9.3). The same authors also reported U-Pb SHRIMP dating of zircons from metagranites and gneisses intruded in the Lower Mulhacén Succession and associated with metasediments of the Upper Mulhacén Successions (Fig. 9.11) up to the base of the marbles that characterize their highest part (Table 9.1). Ruiz-Cruz and Sanz de Galdeano et al. (2017) have reported slightly younger ages (286 ± 3 Ma) in equivalent rocks in Sierra Nevada.

9.5 Pre-Mesozoic Successions and Pre-Alpine Evolution of the Alpujárride Complex

A. Sánchez-Navas, A. Martín-Algarra, A. García-Casco, S. Mazzoli

The stratigraphic successions of the Alpujárride Complex (Fig. 9.11) yet preserve abundant Triassic fossils, in spite of having been affected by Alpine metamorphism (cf. Vol. 3, Ch. 7), but they have not provided any pre-Mesozoic fossil. So, the Paleozoic and/or older stratigraphic age of many Alpujárride rocks is primarily based on lithostratigraphic correlation. The mineral paragenesis and metamorphic conditions of the Alpujárride rocks change depending on their stratigraphy (pre-Mesozoic vs. Mesozoic), lithology (pelitic-psammitic *vs.* carbonate), tectonic position within the Alpujárride nappe stack (lower, intermediate, upper), or regional location (eastern, central, western). In general, the metamorphic grade in the Lower Alpujárrides is lower than in the Intermediate and Upper Alpujárrides, and it is the highest in the western sectors where the Upper Alpujárride pre-Mesozoic rocks directly overlie the Ronda ultramafic massifs. The main lithological and petrological features of the pre-Mesozoic Alpujárride successions are quite constant, with only minor changes from the Lower to the Upper Alpujárrides, although they are much better developped and thicker in the latter. Actually, the Upper Alpujárrides are dominantly made of pre-Mesozoic rocks (Fig. 9.12) because Triassic and eventually younger rocks above them are exclusively present close to the Internal-External Zone boundary, along a narrow and strongly imbricated belt below the Maláguide Complex (Didon et al. 1973; Martín-Algarra et al. 1995; Sanz de Galdeano et al. 1995a, b, 2001).

The pre-Mesozoic Alpujárride successions are predominantly made of dark brown and gray metapelites and metapsammites, usually rich in graphite (Gr; mineral abbreviations after Whitney and Evans 2010) but not as much as in their Nevado-Filábride counterparts. The metapelites are fine-grained schists in the upper part, and become progressively coarser-grained downwards. In their middle and lower part, the schists include mm to occasionally cm-sized porfiroblasts, especially of garnet (Grt), chloritoid (Cld), plagioclase (Pl) and andalusite (And), which mainly concentrate in discrete, pelitic horizons and in quartz (Qz)-rich veins (Fig. 9.12e, f). Deeper levels also contain staurolite (St), kyanite (Ky), fibrolite (Fi) and, occasionally, prismatic sillimanite (Sil). In some Intermediate and especially Upper Alpujárride units, the coarsest-grained schists gradually change downwards to gneisses and migmatites (Fig. 9.12a–d), with local evidence of partial melting. Consequently, the pre-Mesozoic Alpujárride rocks were affected by a metamorphism of gradually increasing grade

Table 9.1 Field occurrence, petrography and age of some gneiss samples (modified from Gómez-Pugnaire et al. 2012)

Area	Locality	Sample	Country rocks	Field occurrence	Magmatic ages (U-Pb) zircon
Eastern Sierra de Filabres	*El Chive*	**CHIVE-2**	**Bottom of gneiss**: light schists, marbles, metabasites, metaevaporites and serpentinites **Top of gneiss**: dark- and light-coloured schists, serpentinites and marbles. Skarn with eclogitic assemblages in the border	*Chive:* porphyritic gneiss with feldspar megacrystals *Bédar:* tectonite	291 ± 3 Ma
	Bédar	**BED-3**			283 ± 4 Ma
Western Sierra de Filabres	*El Pocico*	**PC-3**	Uppermost light schists and marbles. Small dikes of metabasites	Stretching lineation and parallel folds	283 ± 4 Ma
		PC-4	Light micaschists		
	Charches	CHA-1[(1)]	Replacement tourmalinites, dark and light micaschists and marbles	Small and strongly sheared even-grained layers and lenses augen textured, abundant tourmaline nodules	247 ± 11 Ma[(1)] (Rb/Sr whole rock)
Central Sierra de Filabres	*Líjar River*	**LR-3**	Marble layers (1 m thick) and dark and light micaschists. Skarn boudins (~40 cm thick)	Small banded body, 4–5 m thick	295 ± 3 Ma
Eastern Sierra Nevada	*Cerro Blanco*	**CB-4**	Uppermost marbles and metaserpentinites. Skarn rocks in the contact	75 m thick body. Banded structure. Well-developed mylonitic foliation	279 ± 5 Ma
Western Sierra Nevada	*Sierra Nevada road*	SAB-00[(2)]	Host tourmalinites, dark, light micaschists and marble. Skarn like rocks in the original intrusive contacts	Augen and even-grained layers	301 ± 7 Ma[(2)]
	Prado del Cebollar	**CEB-3**	Graphite-bearing schists. Dismembered skarns transformed to eclogites	Lens (10 × 40 m) of alternating leucocratic and melanocratic layers. Augen texture and even-grained layers, parallel to the foliation	285 ± 3 Ma

downwards, with highest-grade conditions locally associated with anatexis in the deepest structural levels.

The Alpujárride pre-Mesozoic rocks show a polymetamorphic and polyorogenic pre-Alpine and Alpine evolution (Sánchez-Navas et al. 2017 and references therein). In the Upper Alpujárrides of the central sector (Fig. 9.1) the lowest known pre-Mesozoic rocks make part of the *Torrox Gneissic Complex* (TGC: Fig. 9.12). The TGC is made of several types of gneissic rocks bearing muscovite (Ms) biotite (Bt), K-feldspar (Kfs), Grt, Al-silicates (Als) and, subordinately, cordierite (Crd). The ortho- or paraderivated origin of the TGC, the Alpine or pre-Alpine age of the high-T metamorphism that affect it, and the precise metamorphic conditions reached during both evolutions are controversial (Cuevas et al. 1989; García-Casco 1993; García-Casco et al. 1993; Zeck and Williams 2001; Zeck and Whitehouse 2002). Traditionally considered of fully Alpine metamorphic age, recent detailed petrologic and geochronologic studies show, however, that the TGC evolved from pre-Mesozoic granitic rocks (Fig. 9.12a, b) that were affected by a pre-Alpine high T metamorphism responsible for migmatization and for intrusion of granitic pegmatite dikes bearing And at 283 ± 16 Ma, according to SHRIMP zircon dating (Sánchez-Navas et al. 2014; Fig. 9.12c).

The TGC and its schistose envelope were strongly deformed and metamorphosed during the Alpine Orogeny under medium- to high-grade metamorphic conditions at around 20–22 Ma (Zeck et al. 1989; García-Casco et al. 1993; García-Casco and Torres-Roldán 1996, 1999; Sánchez-Navas 1999). Ruiz-Cruz and Sanz de Galdeano (2012b, 2013, 2014a, b) affirm that the Torrox gneisses and other Grt-bearing high-grade gneisses in Ceuta and immediately above the Ronda peridotites would have been affected by ultrahigh P metamorphism producing coesite and microdiamond, although this has been considered doubtfull in the Ronda area by Massonne (2014).

At outcrop scale, the main tectonic fabric of the Alpujárride pre-Mesozoic schists above the TGC, and of equivalent rocks in other Alpujárride units, is a metamorphic foliation, which is generally sub-parallel to the lithologic contacts. This foliation includes one older foliation and is strongly folded and partially or totally transposed by at least one (probably two) new foliation(s). These foliations are usually named S_1 (oldest), S_2 (main) and S_3 (youngest) and

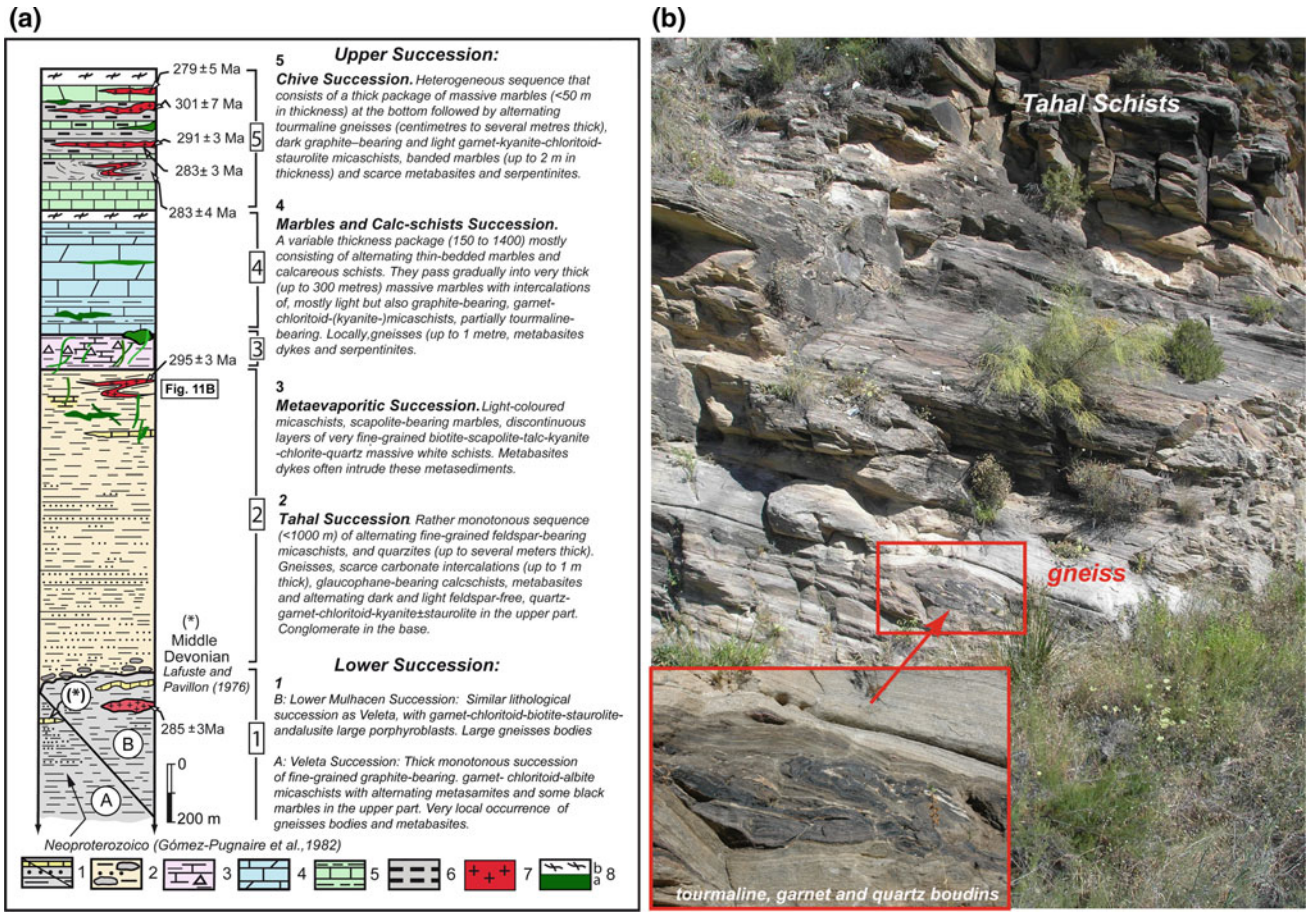

Fig. 9.11 **a** Lihological successions of the Nevado-Filábride Complex and location of the dated gneisses bodies. **b** A gneiss body embedded in the marbles and schists of the Upper Mulhacen Successions (see location in Fig. 9.11a)

were formed during prograde evolutions from low- to medium- to high-grade metamorphic stages during a polycyclic, polyphasic and plurifacial tectonometamorphic evolution, ending with retrograde evolutions. The S_1 and S_2 foliations and the associated minerals (see below) are also found in pelitic enclaves included within the most evidently granitic lithotypes of the TGC, dated as Early Permian (Sánchez-Navas et al. 2017). Consequently, these foliations must be related to a prograde pre-Alpine tectonometamorphic cycle that culminated with crustal anatexis and granite emplacement in latest Variscan (Hercynian) time. The S_3 foliation crosscuts all gneissic lithotypes of the TGC including, in particular, the latest Variscan pegmatite dikes and their discordant intrusive contacts with the enclosing rocks (Sánchez-Navas et al. 2014). Consequently, this S_3 foliation is usually considered as Alpine. Hereafter, these pre-Alpine (S_1, S_2) and Alpine (S_3) foliations will be named S_{1V} S_{2V} and S_A, respectively.

The oldest pre-Alpine foliation of the pre-Mesozoic schists (S_{1V}) is rarely visible at outcrop scale but it is commonly found under the microscope, delineated by Gr, opaque minerals and fine-grained micas, in lensoid domains bounded by later foliations, or as oriented inclusions within relict minerals that grew synkinematically and/or postkinematically with respect to S_{1V}: Grt, Ky, St, and (only in the upper levels of the succession) Cld (Fig. 9.13a–d). These relict minerals usually appear strongly dissolved and deformed by the later foliations (Sánchez-Navas et al. 2012, 2014, 2016, 2017).

The S_{2V} was associated with the synkinematic blastesis of the largest Bt and Ms crystals visible within these rocks. It was clearly overprinted by static blastesis of the largest minerals visible at the naked eye (mm to cm sized), And in particular (Figs. 9.12f, 9.13d-e-f). It is also statically overprinted by disoriented Ms and, especially, by red Bt crystals, Pl and, in the deepest parts of the succession affected by the highest metamorphic grade, by Cdr (Fig. 9.13b), which is intimately associated with And and usually appears, under the microscope, strongly pinnitized (Sánchez-Navas et al. 2012, 2014).

In most outcrops where the pre-Mesozoic Alpujárride schists are coarse-grained the And quite evidently grew

Fig. 9.12 Field views of Upper Alpujárride pre-Mesozoic rocks from the Torrox Gneissic Complex (**a**–**d**) and surrounding high-grade metapelites (**f**), and of the Benamocarra Unit (**e**): **a** Porphyritic orthogneiss yet preserving the magmatic texture of the granite protolith, which is intruded by a pegmatite dike, the whole affected by intense folding. **b** Well preserved granite texture, with large undeformed porphyroblasts of Kfs. **c** Late Variscan granitic dike dated by zircon SHRIMP at 283 ± 16 Ma, intruding intensely deformed gneisses in the outer part of the TGC; SHRIMP data of this dike, which is affected by a later sillimanite-bearing foliation, also record an Alpine event at ca 22 Ma. **d** Intensely folded leucocratic and melanocratic bands of the TGC close to the contact with surrounding metapelites. **e** Disoriented pre-Alpine Ky crystals partially transformed to pre-Alpine pink And cristals within a small Qz seggregation in dark schists of the Benamocarra Unit). **f** Close-up of dark (graphite-rich) pelitic bands lying directly on the gneisses shown in (**d**), full of large Variscan pink And crystals that are strongly deformed along the Alpine foliation, and partially transformed to a whitish aggregate of Alpine Ky and Ms

statically on the best visible foliation planes S_{2V}, forming palm-like aggregates and, in the coarsest-grained lithotypes, also forming chiastolites up to several cm long and, sometimes, nearly 1 cm thick (Figs. 9.12f and 9.13f). Nevertheless, a careful examination of the outcrops and thin sections reveal that the post-S_{2V} And as well as all the other above mentioned minerals in relation to the S_{1V} and S_{2V} foliations, are systematically deformed and sheared along the Alpine foliation S_A (Fig. 9.12f), which is frequently the most evident at outcrop scale, although it can be locally difficult to distinguish it from the S_{2V}.

A typical feature of the pre-Mesozoic schists, especially in the Upper Alpujárride units, is the presence of Qz plus albite (Ab)-rich veins. These are discordant with respect to a previous foliation (probably S_{2V}) but are usually strongly deformed and parallelized to the most evident foliation at oucrop scale (S_A). Along most of the succession-but not in its highest and finest-grained levels-these veins frequently contain pink And, sometimes forming well-preserved rosettes of disoriented crystals. In some veins, but much less frequently, there also appear large blue Ky crystals (Fig. 9.12e) that are replaced by pink And, which evidently postdate the Ky (Fig. 9.13d), during a prograde Variscan metamorphic evolution (Sánchez-Navas et al. 2016). The formation of blue Ky and its partial or total replacement by pink And within the veins has been tentatively correlated with the prograde evolution (Fig. 9.14) that affects their schistose matrix and that was responsible for the pre-Alpine syn- to postkinematic blastesis (with respect to S_{1V}) of variscan Ky (Ky_V), followed by S_{2V}-related deformation and, finally, by the post-S_{2V} blastesis of And, which replaced partially or totally the syn- to post-S_{1V} previous Ky (Ky_V). The same reaction has been found in pelitic enclaves included within ortogneisses of the TGC, which evidence a pre-Alpine evolution that produced a high-T metamorphism of pre-Permian metasediments (Sánchez-Navas et al. 2017). In the deepest parts of the Upper Alpujárride successions this tectonometamorphic evolution was followed by anatexis under moderate to high P, followed by decompression and granite emplacement at the end of the Variscan Orogeny (near to the Carboniferous-Permian boundary) whereas lower P and T are recorded in the upper structural levels represented by the Benamocarra Unit and the Maláguide Paleozoic successions (Fig. 9.14). In any case, these veins, and the pink And within them, as well as the And within both the schistose matrix and the enclaves included in the TGC orthogneisses, have been also strongly affected by the S_A-related deformation: the And within these rocks appears stretched, sheared and crushed to form granular aggregates of small sized cataclastic And and fine-grained Ms, and partially transformed to fine-grained Alpine Ky (Sánchez-Navas et al. 2012, 2017).

The development of S_A is associated with a generalised grain size reduction that affects most previous minerals, especially micas, and that produces Alpine Ky (Ky_A) plus Grt, and Fi in deeper structural levels. This foliation is mainly defined by fine-grained phengitic Ms and Bt plus strongly stretched Qz bands that are locally associated with neoformed Als from larger minerals (Ky and/or Fi, which forms, in particular, from the post-S_{2V} And crystals and from the pelitic matrix), and by retrograde chlorite Chl (Sánchez-Navas et al. 2012, 2014, 2016). The Ky_A is of much lesser size than the pre-Alpine Ky_V and, together with Fi, it clearly postdates the post-S_{2V} pre-Alpine And. In the Upper Alpujárrides of the central sector (Torrox area) the S_A foliation is associated with dominantly top-to-the-W shear zones, and records an evolution from kyanite-grade ductile shear zones, to Chl-bearing low-grade S-C mylonites, to brittle duplexes produced by west-directed imbrication (Sánchez-Navas et al. 2017).

At present, it is unclear if staurolite also formed synkinematically with kyanite and garnet in relation to the S_A-related Alpine tectonometamorphic event, or not (see, however, Williams and Platt 2017). It is also yet unclear if Alpine Ky and Fi formed coevaly and in relation to the *same* foliation, or not. Actually, Fi formation from And could also develop during the latest stages of a *prograde* pre-Alpine evolution at low P, as a consequence of the development of and extensional foliation under high-T conditions in relation to the widespread and well-documented latest Variscan extensional collapse, which accounted, essentially and everywhere, during the early Permian. This hypothesis does not fit, however, with higher P mineral asssemblages predating pre-Alpine And in the enclaves within the TGC nor in the surrounding schists (Sánchez-Navas et al. 2017, and Fig. 9.14). In the pre-Mesozoic Alpujárride schists, St usually appears strongly corroded and associated with the previous Ky (syn-S_{1V} to post S_{1V} above-mentioned), being both included, together with Grt and with Cld (when present), within post-S_{2V} And. In relation to Grt, the picture is also complicated: the compositional mapping of zoned Grt from pre-Mesozoic schists belonging to Upper Alpujárride units (García-Casco 1993; see also Ruiz-Cruz 2011a, b and Sánchez-Navas et al. 2012) and also to Intermediate Alpujárride units (Manjón-Cabeza et al. 2014) show complex compositional patterns, including relatively sharp boundary zones between cores and overgrowths, and chemical reversals at the boundaries, which clearly record two superimposed metamorphic events: pre-Alpine (cores) and Alpine (rims). On the contrary, garnets from Permo-Triassic schists overlying the pre-Mesozoic black schists in Intermediate Alpujárride units are unzoned and they only record, obviously, Alpine events (Manjón-Cabeza et al. 2014). The blastesis of the pre-Alpine Grt cores accounted under high-gradient

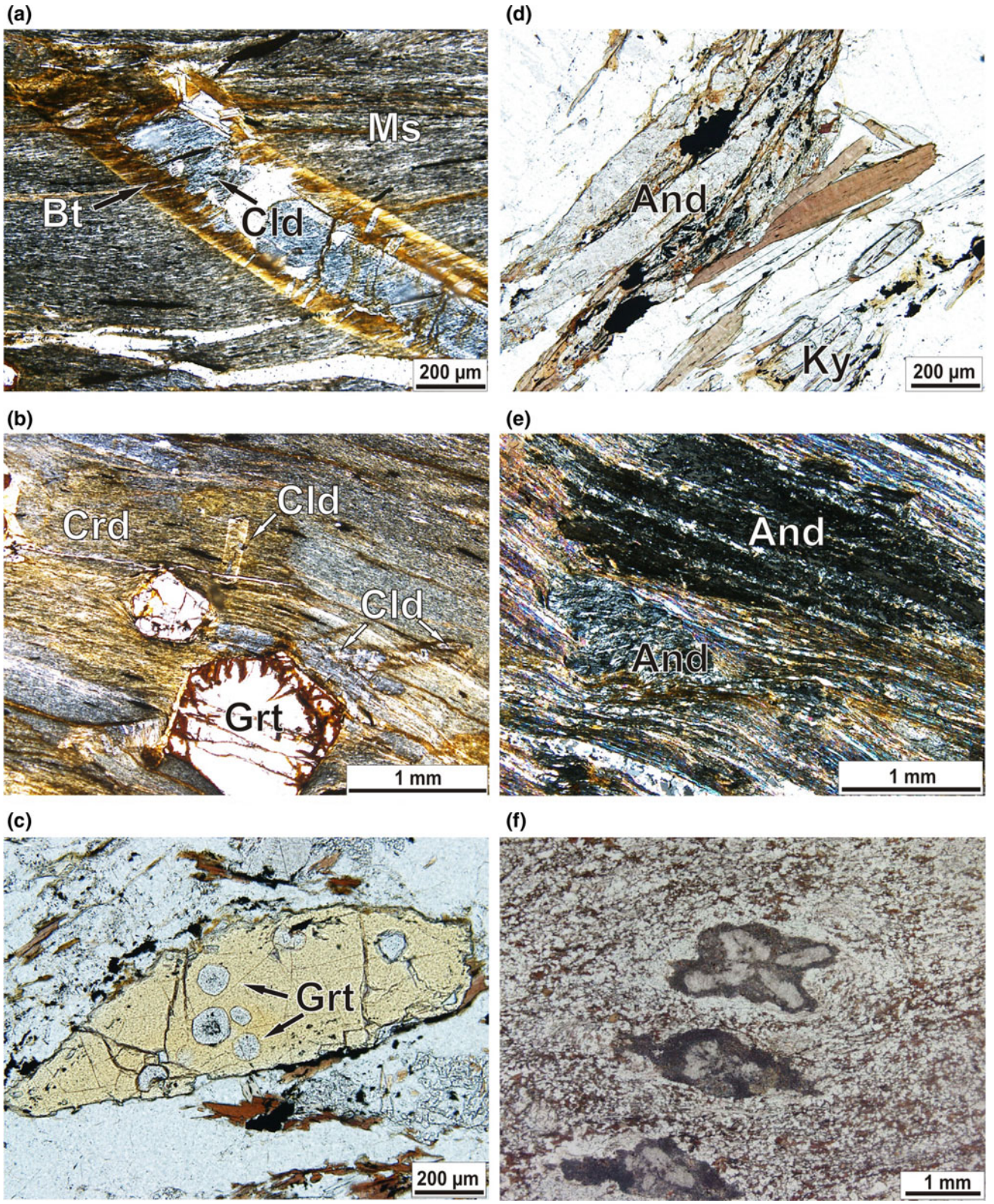

Fig. 9.13 Optical image with parallel nicols (**a**–**d** and **f**) and with crossed nicols (**e**) of black Gr-rich Upper Alpujárride metapelites (**a**-**b**-**e**: Benamocarra Unit, upper part of the succession; (**c**-**d**-**f**): Torrox Unit, lower part of the succession, immediately above the TGC). **a** Slightly deformed pre-Alpine Cld prism, partially transformed to Alpine Bt, Ms and opaque phases, within a foliated fine-grained matrix (S_{1V} foliation). **b** Pre-Alpine Cld and Grt porphyroblasts enclosed by altered pre-Alpine Crd. **c** Pre-Alpine St porphyroblast including small rounded Grt. **d** Pre-Alpine And pseudomorphs after Ky and relict Ky (lower part of the image). **e** Gr-rich domain corresponding to sheared And ghost, with a pre-Alpine chiastolite remnant on the left, wrapped by syn-S_A Qz, Bt and Ms. **f** Post S_{2V} pre-Alpine And chiastolites transformed to Alpine Ky at their rims, affected by the S_A foliation and surrounded by a mantle composed by Alpine Ms (lighter regions)

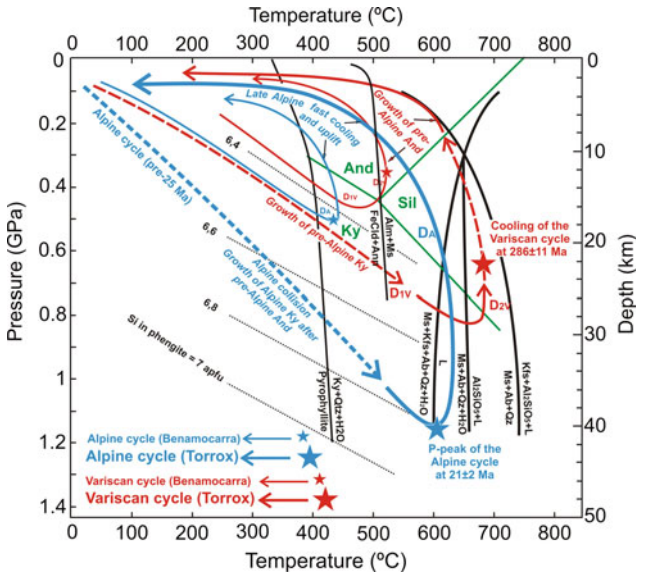

Fig. 9.14 Tentative pressure-temperature-time (P-T-t) Variscan (red) and Alpine (blue) paths of the lowest and upper parts of the pre-Mesozoic successions in the central Upper Alpujárrides, corresponding, respectively, to the Torrox and Benamocarra units (Sánchez-Navas et al. 2016, 2017), based on relevant reactions for partial melting and granitic melt crystallization in the symplified NKASH system (White et al. 2001), Si isopleths in muscovite-phengite solid solution in the KMASH system (Massonne and Schreyer 1987) and the phase diagram for Al_2SiO_5 polymorphs (Holdaway 1971). The garnet-in reaction is defined by the Fe end-member reaction: Fe-Cld + Ann = Alm + Ms (Spear and Cheney 1989). Dashed lines correspond to poorly defined parts of the P-T-t paths. The main pre-Alpine (D_{1V}, D_{2V}) and Alpine (D_A) deformation phases and growth episodes of kyanite (Ky) and andalusite (And) are also indicated

conditions, sometimes producing layeritic growth. After a sharp stop in its growth, the rims made of Alpine Grt formed, starting with sharp Ca-enrichments related to a marked P-increase, followed by a gradual P-decrease associated with a T-increase that reached maximum values during the final growth of the rims, probably during the Early Miocene.

The uppermost, finest-grained part of the pre-Mesozoic Alpujárride schists does not contain visible minerals at the naked eye or these minerals are strongly retromorphosed: they are represented by Gr-rich black spots in which the original mineralogy can be recognized with great difficulty and only occasionally under the microscope. These rocks, either when spotted or finest-grained, are indistinguishable from those that constitute the lowest part of the Maláguide Paleozoic succession. Consequently, in wide areas of the Montes de Malaga (especially in their eastern part: Fig. 9.1) and of the Costa del Sol, delineating the contact among typical Upper Alpujárride schists in lower tectonic position (*Benamocarra Unit:* Sánchez-Navas et al. 2016) and typical Maláguide Paleozoic rocks (*Piar Group*, see below) becomes an extremely difficult or simply impossible task. Actually, in these areas, the pre-Mesozoic Alpujárride schists seem to change, gradually upwards, to the lowest siliciclastic formations of the Maláguide Paleozoic, which are only slightly affected by metamorphism (*Morales Formation*). Nonetheless, a detailed study of the Benamocarra schists allows recognizing an equivalent evolution to that to the deepest part of the Upper Alpujárride succession represented by the TGC, but at low-P/medium-T metamorphic conditions (Fig. 9.14) that Sánchez-Navas et al. (2016) interpreted in relation to a late Variscan instead of a late Alpine extensional collapse as it is usually accepted for Alpujárride pre-Mesozoic rocks in most studies.

In the western Upper Alpujárrides and in their Sebtide counterparts the downwards-increasing metamorphic grade of the pre-Mesozoic crustal successions is evidently related to the emplacement of the Ronda and Beni Bousera ultramafic bodies. The crustal succession is detached from the underlying peridotites and related mafic rocks by an extensional ductile shear zone (Balanyà and García-Dueñas 1987; Balanyà et al. 1993, 1997; Argles et al. 1999). It is totally equivalent to the Alpujárride pre-Mesozoic successions above discussed. Actually, it constitutes a quite complete but extremely thinned crustal section (ca. 6 km at present), with transitional boundaries among successive lithotypes that are, from top to bottom, the same as those present in eastern areas. Nonetheless, in addition to the low-to medium-to high-grade metapelites and quartzites, a thick belt of pelitic migmatitic gneisses and Grt-bearing granulitic gneisses, associated with leucocratic magmatic differentiates, surrounds the contact of the crustal succession with the peridotites (Loomis 1972, 1975; Torres-Roldán 1981). The Grt-bearing rocks close to the peridotites are coarse-grained and banded, show granoblastic and blastomilonitic textures, and are made of Qz-Fds-Bt-rich bands bearing Kfs, Ky, Grt and Plg, with late prismatic Sil, Crd and hercinite replacing Grt. The Grt in these rocks shows the same zoning observed in Grt from the equivalent rocks previously mentioned. Monazite dating of the Grt cores demonstrates that the high-grade rocks attached to the peridotites are also polymetamorphic, and that they record a late Variscan high T event; in addition, Grt rims record a sharp Alpine P-increase followed by T-rise reaching its peak during the Miocene (Massonne 2014; see Montel et al. 2001 for equivalent rocks in the Moroccan Sebtides).

The Grt-bearing rocks at the hangingwall of the peridotites gradually evolve upwards to pelitic migmatitic gneisses by decreasing Fd and increasing Bt, by disappearing Sil, which is replaced by Fi, and by appearing Ms and St, the latter always wrapped around by a foliation (probaly

S_{2V}) and frequently replaced by And. The associated migmatite layers are stromatic and fluidal metatexites (Barich et al. 2014). The same rocks are found in the pelites located at the footwall of the peridotites (Blanca-type units). They show medium-to coarse-grained leucosomes forming cm- to dm-thick layers that are usually parallelized to the most evident foliation or that are slightly discordant to it. The melanosomes are medium- to fine-grained, and richer in Bt, Pl and Sil, with Grt mostly replaced by Crd (Torres-Roldán 1983; Acosta-Vigil et al. 2014, 2016; Bartoli et al. 2016). They evolve gradually outwards of the contact with the peridotites to the same schistose succession above discussed.

Both the Upper Alpujárride crustal succession and, especially, the peridotites located in its footwall, constitute the hangingwall of the Intermediate Alpujárrides (*Blanca-type units*) and of the Frontal *Nieves Unit* (Martín-Algarra 1987; Mazzoli and Martín-Algarra 2011). As a consequence of this lithosphere scale hot thrust, the Triassic to Lower Miocene locally fossiliferous successions below the peridotites were transformed to high-grade marbles and calc-schists, and their associated pelitic intervals, especially those of pre-Mesozoic age, were partially melted under high-grade conditions (Mazzoli and Martín-Algarra 2011, 2014; Mazzoli et al. 2013). Consequently, the presence of migmatitic gneisses with leucocratic differentiates is quite common not only in the crustal succession above the peridotites but also in rocks belonging to the tectonic units at the footwall of the Ronda peridotites, both pre-Mesozoic and Meso-Cenozoic. This high-T metamorphism and the related peridotite emplacement and deformation within the Alpujárride Complex and also in the Sebtides are evidently Alpine (Bouybaouène et al. 1998; Michard et al. 2006; Afiri et al. 2011; Ruiz-Cruz and Sanz de Galdeano 2012a). Moreover, stratigraphic data demonstrate that the age of this Alpine event is latest Aquitanian-early Burdigalian (Martín-Algarra and Estévez 1984) then at about 22–18 Ma, and this is confirmed by different radiometric dating methods applied to different Alpujárride-Sebtide rocks either above or below the peridotites (Priem et al. 1979; Zeck et al. 1989, 1992; Monié et al. 1991, 1994; Morillon et al. 1996; Sosson et al. 1998; Sánchez-Rodríguez and Gebauer 2000; Platt and Whitehouse 1999; Whitehouse and Platt 2003; Platt et al. 2003, 2005, 2006, 2013; Esteban et al. 2004, 2011a, b, 2013; Janots et al. 2006; Negro et al. 2006; Rossetti et al. 2010; Azdimousa et al. 2014; Sánchez-Navas et al. 2014; Gueydan et al. 2015) and also to the mafic layers within the peridotites themselves (Zindler et al. 1983; pyroxenite layers in Beni Bousera provide slighghtly older ages: Blichert-Toft et al. 1999). Nevertheless, zircon and monazite dating and detailed petrological and isotopic studies in both the peridotites (e.g. Pearson and Nowell 2004; González-Jiménez et al. 2017) and in the crustal rocks related to them reveal a much more complex picture, and provide increasingly stronger support for an early emplacement of the Ronda-Beni Bousera ultramafic slices at shallow lithospheric levels since, at least, latest Variscan time (Michard et al. 1997; Montel et al. 2001; Massonne 2014; Acosta-Vigil et al. 2014, 2016).

In the Guadaiza and Albornoque tectonic windows the migmatitic gneisses below the peridotites include abundant lithoclasts and enclaves coming from diverse Alpujárride lithologies, including also marbles (Lundeen 1978; Torres-Roldán 1983; Martín-Algarra 1987; Esteban et al. 2011a, b). The SHRIMP dating of zircon from these rocks indicates partial melting events at ca. 20–22 Ma (Esteban et al. 2011a). Downwards from the peridotites these rocks grade to dark (pre-Mesozoic) schists with abundant And that include, in their geometrically lowest part, gneissic bodies similar to the Torrox Gneissic Complex above mentioned (e.g., the *Istan gneiss*). Compositionally, these rocks are strongly deformed granites or granodiorites bearing Crd, Sil and And, and have provided magmatic pre-Alpine zircon ages (ca. 290–280 Ma: Acosta-Vigil et al. 2014).

In the highest tectonic units of the Intermediate Alpujárrides of the western (Blanca-type) and central sectors (Tejeda Unit), the dark schists unanimously considered of pre-Mesozoic stratigraphic age support a thick lithologic ensemble of much controversial age. It is made of light-coloured, gray to greenish schists and quartzites very rich in Chl and epidote and locally bearing Grt, blue amphibole, Cld and Als, which gradually changes upwards to a thick carbonate succession rich in tremolite and phlogopite and locally bearing also scapolite (Torres-Roldán 1974, 1978). The light-coloured schists and quartzites are classically interpreted as Permian to earliest Triassic probably vulcanosedimentary continental to coastal metasediments, and the overlying marbles as marine Triassic deposits (Blumenthal 1927; Torres-Roldán 1974; Delgado et al. 1981; Vera 2004). They are sometimes thicker than 500 m and include, in its lower part, leucocratic differentiates and, upwards, metabasite bodies that are also present within the lower part of the overlying carbonate succession, and that are usually interpreted in relation to the Triassic rifting. Nevertheless, these rocks have also been considered to be of pre-Mesozoic age, Cambrian, or pre-Cambrian, by some authors (Blumenthal 1949; Boulin 1970) although they have provided, up to now, only Alpine geochronological ages (Monié et al. 1991, 1994; Platt and Whitehouse 1999; Platt et al. 2003; Esteban et al. 2011a).

9.6 Pre-Mesozoic Successions of the Maláguide Complex

A. Martín-Algarra, R. Rodríguez-Cañero, P. Navas-Parejo, A. Jabaloy-Sánchez, S. Mazzoli, V. Perrone

9.6.1 General Features of the Maláguide Complex

A. Martín-Algarra, A. Jabaloy-Sánchez

The Maláguide Complex (Blumenthal 1927; Fallot 1948; Durand-Delga 1968; Vera 2004) includes the highest tectonic units of the Alpine thrust stack formed by the Betic Internal Zones (Fig. 9.1). It is made, essentially, of Ordovician (and older?) to Carboniferous deep marine turbiditic terrigenous clastics, with subordinate horizons of conglomerates, pelagic carbonates (sometimes conodont-bearing) and radiolarian cherts (Fig. 9.15). Shallow marine Paleozoic rocks are only represented by clasts of Frasnian to Bashkirian limestones included in uppermost Devonian and Upper Carboniferous conglomerates (Herbig 1984; Rodríguez-Cañero and Martín-Algarra 2014). Above them, an angular unconformity below Triassic continental red beds testifies for tectonic events related to the Variscan Orogeny (Foucault and Paquet 1971; Cuevas et al. 2001; Martín-Algarra et al 2009b). However, this was neglected in the Vélez Rubio area due to the intensity of the Alpine deformation that affects the Maláguide successions (Roep 1974).

The main outcrops of the Maláguide Complex locate in the Malaga area and in the Costa del Sol but also forming a narrow belt from W to E (Fig. 9.1) along the Internal-External Zone boundary (IEZB) in the Serranía de Ronda (Blumenthal 1927, 1930, 1949), in the Cogollos Vega Zone (Blumenthal 1928; Blumenthal and Fallot 1935), in the Velez Rubio Corridor and in Sierra Espuña (Fallot 1948). Small, scattered Maláguide outcrops S of the Sierras Nevada and Filabres and around the Sierras Cabrera and Alhamilla (Bodenhausen et al. 1967; Durand-Delga 1968), testify for its presence onto the thrust stack in the eastern Internal Zones before recent erosion (Fig. 9.1).

The Maláguide Complex thrusts over the Alpujárride Complex, although the original tectonic contact between them has been strongly modified by extensional tectonics in most sites, and now usually corresponds to an extensional detachment (Aldaya et al. 1991; Lonergan and Platt 1995; Fernández-Fernández et al. 2007). The top of the Maláguide Complex is an unconformity below Burdigalian deep clastic deposits (Viñuela Group: Martín-Algarra 1987) that predate back-thrusting of the Campo de Gibraltar Flysch Complex during the mid-Miocene Internal-External continental collision.

The structure of the Maláguide Complex is not fully understood in most sites. Several Alpine thrust slices are certainly present in several areas, but the main Maláguide outcrops of the Montes de Malaga and Costa del Sol (Fig. 9.1) seems to constitute, essentially, a single Alpine unit, with only some Alpine thrusts of limited lateral continuity and overstep. On the contrary, in the Maláguide outcrops close to the IEZB several Alpine thrusts bound at least three independent Alpine tectonic units (Roep and Mac Gillavry 1962; Geel 1973; Martín-Algarra 1987; Martín-Algarra et al. 2009b). Nevertheless, the exact number, continuity and extent, detailed stratigraphic features, correlation and kinematics of these tectonic units are not completely solved. The lowest one was slightly touched by the Alpine metamorphism and bears transitional stratigraphic and tectonometamorphic signatures towards the underlying Alpujárride terrains (Sanz de Galdeano et al. 1995a, b, 1999). The Alpine metamorphism is absent, or of very low-grade, in the overlying Maláguide units (Ruiz-Cruz 1997; Ruiz-Cruz and Nieto 2002; Ruiz-Cruz and Rodríguez-Jiménez 2002).

Stratigraphic and structural criteria clearly demonstrate the existence of pre-Alpine deformation of the Maláguide Paleozoic successions: an unconformity below continental redbeds (Saladilla Formation: Roep 1972) and above much more intensely deformed Paleozoic deep marine sediments is locally well preserved (Fig. 9.16a) in spite of later intense Alpine deformation and thrusting (Fig. 9.16b). Moreover, remnants of Variscan thrust slices (Fig. 9.17) are yet locally preserved *within* some Maláguide Alpine thrust masses in the Ardales area (Martín-Algarra et al. 2009a, b). These Alpine and Variscan thrust slices along the IEZB show slightly different Palaeozoic stratigraphy and facies, making evident that Maláguide successions come from diverse palaeogeographic realms. Studies on the Maláguide Paleozoic succession confirm that most horizons of fossiliferous Ordovician (Hirnantian) to Devonian (Famennian) limestones come from outcrops located in the outermost Maláguide outcrops and in the highest tectonic units (both Alpine and pre-Alpine) located along the IEZB and in the northern and western sectors of the largest Maláguide outcrops of the Montes de Málaga and the Costa del Sol (Herbig 1983, 1984, 1985; Rodríguez-Cañero et al. 2010; Navas-Parejo 2012). According to lithofacies criteria these outcrops represent the proximal (shallower) sectors of the Paleozoic basin. On the contrary, the distal (deep) area of the basin corresponds to the classical Maláguide stratigraphy, dominated by turbidites (Fig. 9.15). The later stratigraphy is also found in the structurally lowest Maláguide Alpine (and pre-Alpine) units outcropping along the IEZB and in the southern and eastern outcrops of this complex in the Montes de Malaga and the Costa del Sol.

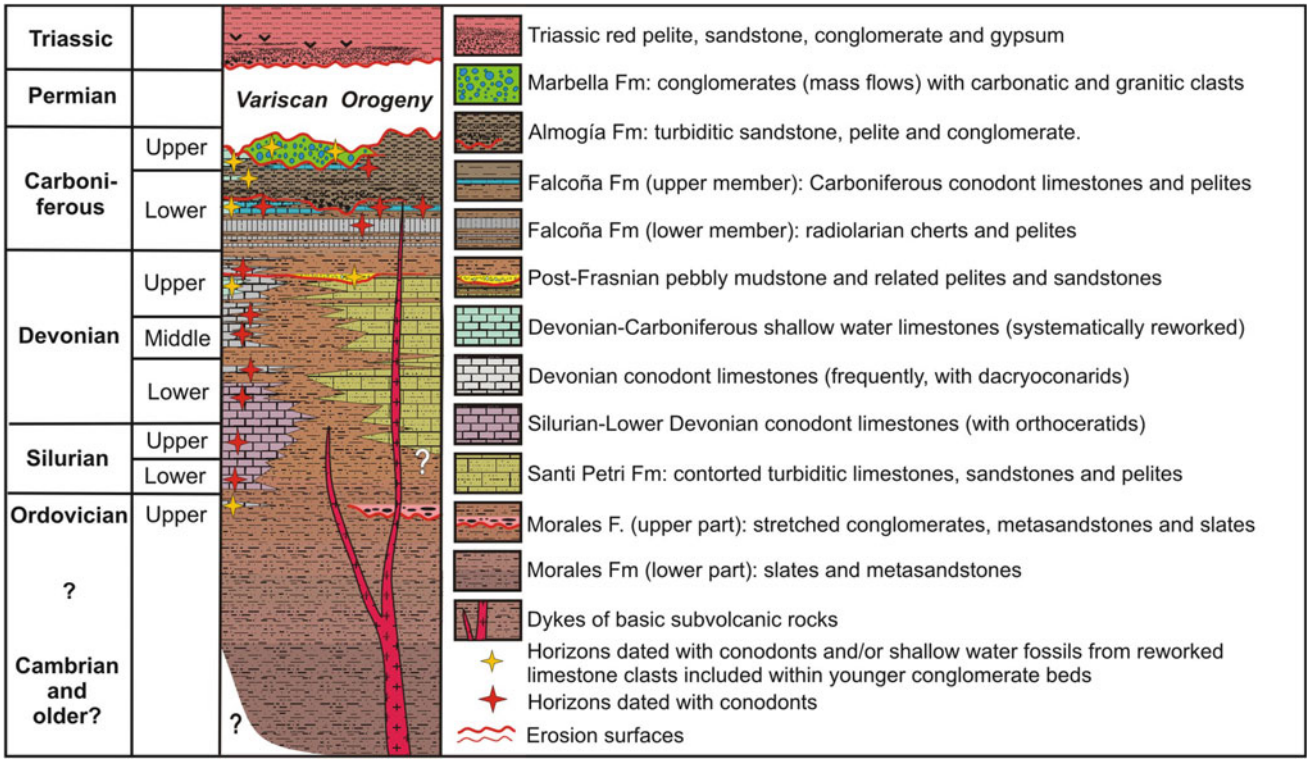

Fig. 9.15 Synthetic stratigraphy of the Maláguide Complex

9.6.2 Paleozoic (Piar Group)

A. Martín-Algarra, R. Rodríguez-Cañero, P. Navas-Parejo, V. Perrone

The Maláguide Paleozoic rocks are included in the Piar Group (Martín-Algarra 1987), previously considered as a formation (Soediono 1971; Geel 1973). This includes several thick Ordovician (and older?) to Carboniferous formations constituted by deep marine pelites and distal turbiditic litharenitic sandstones (Fig. 9.15). Subordinate fine- and coarse-grained conglomerate horizons essentially correspond to feeder channels of the turbidite systems. In addition to these predominant deep-sea terrigenous-clastics there also appear other much thinner formations made of pelagic carbonates, with different facies depending on their age, and of radiolarian cherts. The carbonates provide autochthonous fossils, mainly conodonts, from the Upper Ordovician (Hirnantian: Rodríguez-Cañero et al. 2010) up to the Upper Carboniferous (Bashkirian: Navas-Parejo et al. 2012b). They have provided also other biostratigraphically useful macro and microfossils: orthoceratid cephalopods (Silurian-lowermost Devonian: Blumenthal 1930), tintinnids (Silurian: Hermes 1966) and dacryoconarids (Devonian: Blumenthal 1930; Geel 1973; Herbig 1985; Navas-Parejo 2012). Radiolarian cherts have provided Lower Carboniferous radiolarians (O'Dogherty et al. 2000). Devonian-Carboniferous corals and other shallow marine fossils have been also found but exclusively within carbonate clasts from younger Paleozoic conglomerates (Blumenthal 1949; Boulin and Lys 1968; Geel 1973; Buchroithner et al. 1980; Herbig 1983, 1984, 1986, 1992; Herbig and Mamet 1985; Mamet and Herbig 1990; Rodríguez-Cañero and Martín-Algarra 2014).

The classical lithostratigraphy of the Piar Group was defined in the Montes de Malaga (Mon 1971; Herbig 1983, 1984) with five pre-Devonian to Upper Carboniferous formations named, from bottom to top: *Morales, Santi Petri, Falcoña, Almogía and Marbella formations* (Fig. 9.15). The Morales and Santi Petri Fms lack fossils but the latter underlies the well-dated beds of the Falcoña Fm: Tournaisian radiolarian cherts and Visean conodont limestones (Rodríguez-Cañero and Guerra-Merchán 1996; O'Dogherty et al. 2000). The Almogía and Marbella Fms contain Paleozoic fossils, but reworked, as they have been found within carbonate clasts in Carboniferous conglomerates.

The existence of fossiliferous Ordovician, Silurian and Devonian rocks in addition to Carboniferous formations is only demonstrated from thin horizons of condensed conodont-bearing limestones with diverse pelagic facies that are occasionally found associated with pelites and fine-grained sandstones (Kockel 1959; Kockel and Stoppel 1962; Rodríguez-Cañero 1993a). The lithostratigraphic correlation of these limestones with the classical Maláguide

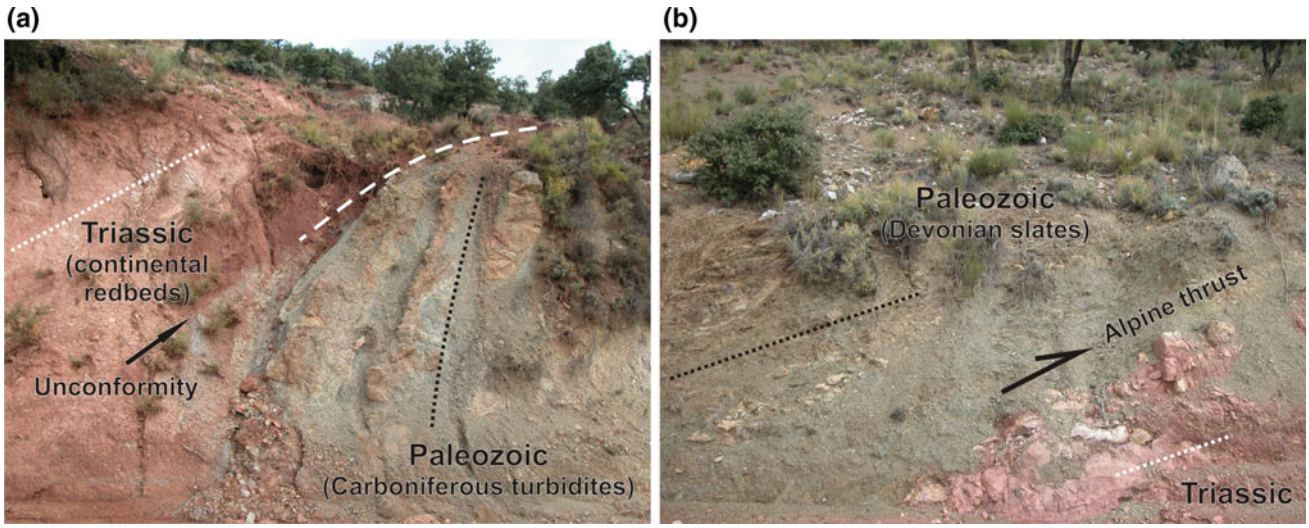

Fig. 9.16 **a** Unconformity below Triassic continental redbeds (Saladilla Fm) and steeply dipping Carboniferous turbiditic conglomerates and sandstones alternating with pelites (Almogía Fm). **b** Alpine thrust of Devonian deep-marine pelites onto Triassic continental redbeds. Both images come from La Solana outcrop in the Cogollos Vega Zone (see Fig. 9.1 and, for details, Fig. 9.2b in Navas Parejo et al. 2015)

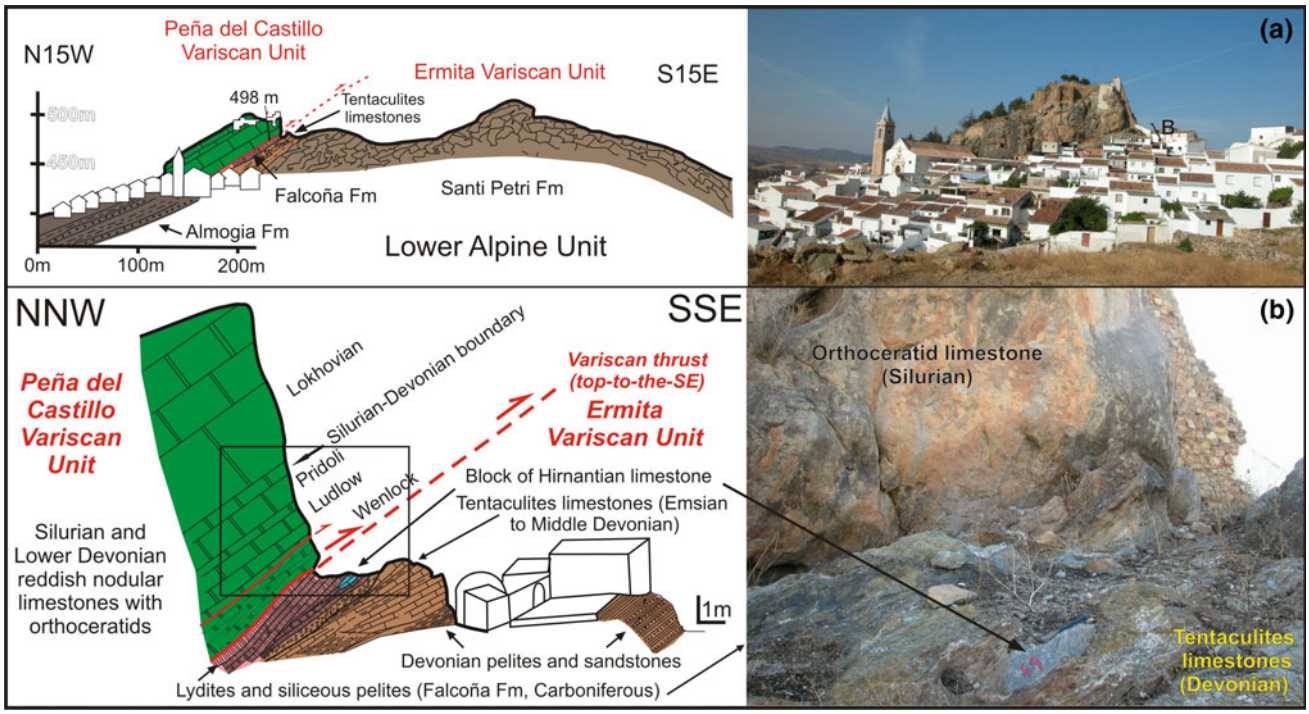

Fig. 9.17 **a** Geological section through the Ardales Castle Rock, showing two Variscan thrust units within the lower Maláguide Alpine Unit in the area. **b** Close-up of the thrust contact between the lower (Peña del Castillo) and upper (Ermita) Variscan units. This Variscan thrust emplaces Silurian limestones (dated by conodonts) onto bedded cherts correlated to the Carboniferous Falcoña Fm. The cherts stratigraphically underlie Visean conodont limestones (not present in this section but dated in a site located a few hundred of metres to the West: Navas-Parejo et al. 2012a). The Falcoña Fm cherts stratigraphically overlie a brecciated and laterally discontinuous lens of Tentaculites limestone, dated by conodonts as Emsian to Middle Devonian, which overlies foliated pelites and sandstones from the uppermost beds of the Santi Petri Fm. At that site, the beds just below the cherts, which are brecciated and rich in Fe-crusts, include one block of limestone that has provided the youngest Ordovician (Hirnantian) conodont association in Iberia (labelled with the red number 69, longest arrow, see text for details) Modified from Martín-Algarra et al. (2009a, b), and from Rodríguez-Cañero et al. (2010)

lithostratigraphy below the well-dated Falcoña Formation is far to be completely solved. Actually, these pre-Carboniferous limestones should be included in independent formations, which remain yet formally undefined. In addition, these pre-Carboniferous conodont-bearing limestones only appear in the highest tectonic units of the Maláguide Complex outcropping along the IEZB, in the outermost Maláguide outcrops in the Montes de Malaga (Almogía area) and in the western Costa del Sol (Marbella).

The stratigraphy of the Piar Group reveals two main evolutionary stages. The first stage comprises pre-Hirnantian to upper Visean-lower Serpukhovian) pre-orogenic sediments (with respect to the Variscan Orogeny). Their mainly deep marine facies, dominated by siliciclastic and calciclastic turbidites (Morales and Santi Petri Fms) relates most Maláguide outcrops to distal areas of a continental margin during its post-rift and syn-drift evolution. The sedimentation in the proximal areas of this margin was dominated by fine-grained clastics including the above-mentioned conodont-bearing condensed limestones. The basin became deepest, tectonically stable and morphologically homogeneous during the deposition of the Tournaisian-Visean cherts and conodont limestones (Falcoña Fm). The siliciclastic turbidites and conglomerates (Culm facies: Almogía and Marbella Fms) were deposited during the second stage, in relation to the Variscan synorogenic evolution of a convergent margin before its final orogenic deformation in Late Carboniferous time.

Dykes of mafic subvolcanic rocks (dolerites) that are usually interpreted to be arc tholeites of Tertiary age (Torres-Roldán et al. 1986; Turner et al. 1999; Esteban et al. 2013) crosscut the Benamocarra Unit and the lowest Maláguide formations (Morales to Falcoña), either in the southern and eastern Maláguide outcrops in the province of Malaga (Fig. 9.15) or in the lowest Maláguide units along the IEZB in the Velez Rubio Corridor (Fernández-Fernández et al. 2007). Nevertheless, the dikes have never been found along the IEZB in the provinces of Malaga and Granada nor in the upper Maláguide units of the Velez Rubio Corridor, in the western Maláguide outcrops of the Costa del Sol or in the northwestern areas of the Montes de Malaga (Almogía area). The dikes never crosscut the Almogía and Marbella Fms, or conodont-bearing limestones older than those of Visean age of the Falcoña Fm in the central Montes de Malaga. Mafic volcanics and dikes of subvolcanic rocks (but different to those above-mentioned) are locally found within Triassic continental red beds, however.

9.6.3 Pre-Orogenic Evolution

A. Martín-Algarra, R. Rodríguez-Cañero, P. Navas-Parejo

The ***Morales Formation*** (Mon 1971) includes the lowest deposits of the Piar Group. It is usually considered pre-Devonian and, maybe, pre-Silurian in age and constitutes a thick (>1 km in the eastern Montes de Malaga) monotonous pelitic-psammitic succession (Fig. 9.18a). It shows intense deformation and low-grade metamorphic overprint, both pre-Alpine and Alpine, which certainly increase downwards from anchimetamorphic to low-grade to medium-grade metamorphic rocks (Ruiz-Cruz 1997; Ruiz-Cruz and Nieto 2002).

In addition to the dikes of basic subvolcanics mentioned above, the pelites of the lower part of the Morales Fm typically include mm- to cm-sized graphite-rich black spots with increasing size downwards, that correspond to sericiticed andalusite, chloritoid and garnet (Orozco and Gálvez 1979; Gálvez and Orozco 1980). These Alpujárride-like spotted schists are identical to those included in the Benamocarra Unit that outcrops below the Maláguide Complex in the eastern Montes de Malaga (Sánchez-Navas et al. 2016). This suggests gradual lithological transition from Paleozoic Alpujárride (Benamocarra) to Maláguide rocks in this region where, actually, it is practically impossible to precisely locate in the field a tectonic contact between typical Maláguide and Alpujárride rocks.

In spite of widespread pre-Alpine foliations (see below), the psammites of the Morales Formation locally preserve sedimentary structures (scours marks, cross lamination, graded beds) and locally intercalate decimetre to metre-thick beds of black turbiditic limestones (Fig. 9.18c) made of crinoid bioclasts, testifying for the marine origin of this formation. The stratigraphic upper part of the succession includes metre- to decametre thick horizons of *stretched conglomerates* (Fig. 9.18b) constituted mainly by clasts of quartzites, but pelites, sandstones, black cherts, recrystallized limestones, schists and gneisses are also present.

The ***Santi Petri Formation*** (Mon 1971) lies above the Morales Fm in rapid but gradual lithological transition. It is up to several hundred of metres thick but it laterally changes notably due to tectonic causes. Its most typical lithofacies is known as ***calizas alabeadas***, that is, warped/contorted limestones (Fig. 9.18d, e). These are intensely folded, finely terrigenous turbiditic limestones that vertically and laterally change to calcareous greywackes and pelites showing very similar features to those of the upper part of the Morales Fm. Typically, these rocks are black or dark-grey coloured when fresh, brown-greenish when weathered, thin to medium-bedded (Fig. 9.18f) and crosscut by numerous white veins filled with calcite and/or quartz. They contain frequent incomplete Bouma sequences, rippled surfaces (Fig. 9.18g) and sole marks (Fig. 9.18h, i) that evidence their distal turbiditic origin. They have not provided yet any fossil and remain undated, but are usually considered to be of late Devonian age, as they are always located stratigraphically below the Falcoña Fm, of well-dated Carboniferous age (Tournaisian-Visean).

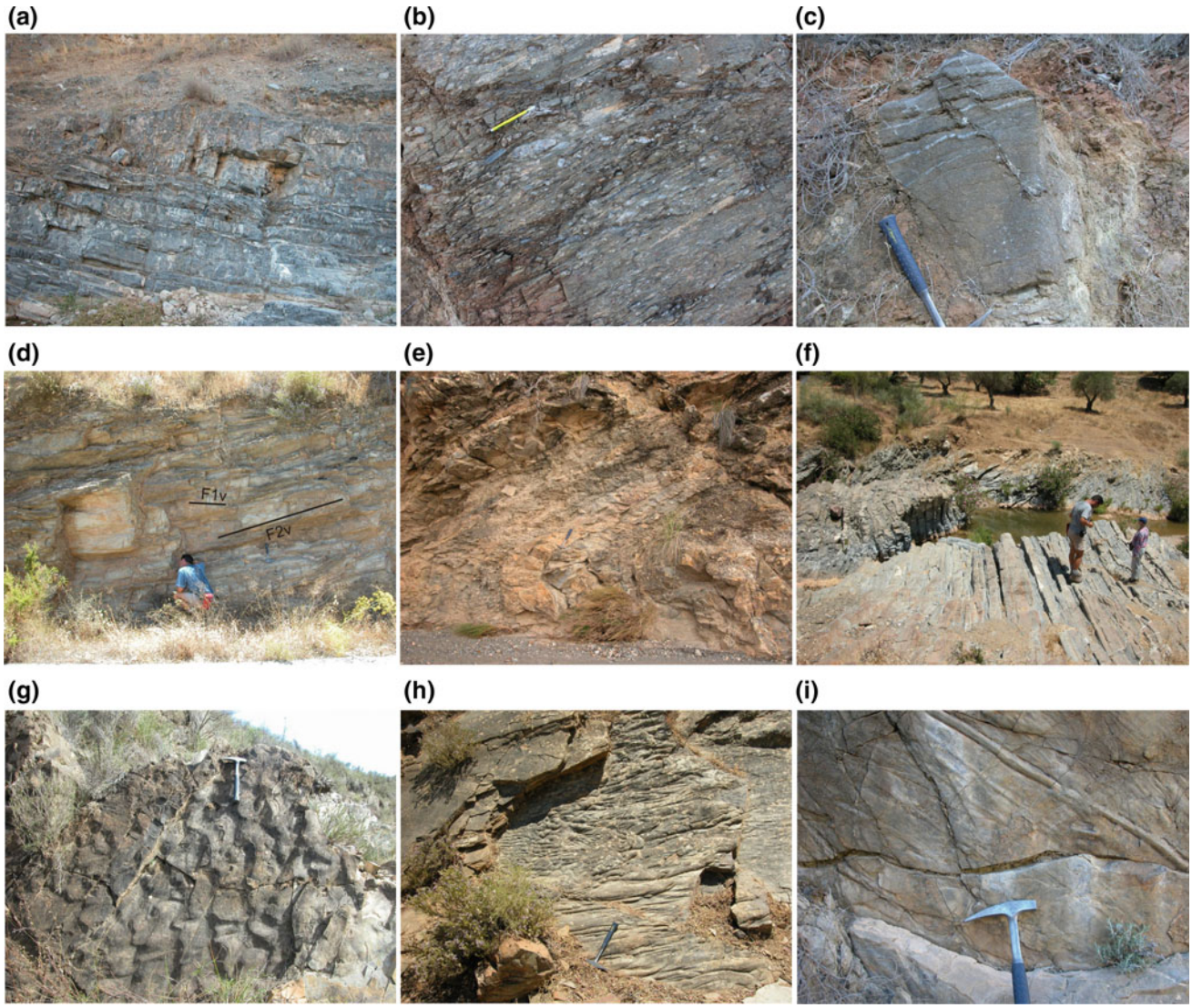

Fig. 9.18 Field views of the Morales (**a**–**c**) and Santi Petri (**d**–**i**) Formations. (**a**–**d**) and (**f**) come from the Montes de Málaga; (**e**, **g**–**i**) from the Vélez Rubio Corridor. **a** Well-bedded sandstones. **b** Stretched conglomerate. **c** Turbiditic limestone rich in crinoid debris. **d** Typical aspect of the "calizas alabeadas" (contorted limestones) facies, which is, mainly, a result of superimposed folding of variscan age (F1v, older, and F2v, younger). **e** Recumbent fold with well-developed axial plane foliation in alternating pelites and limestones. **f** Moderately folded distal turbiditic succession of alternating limestones, sandstones and pelites. **g** Rippled bed surface atop of a turbidite bed. **h** Sole marks, mainly flute and bounce casts. **i** Grooved sole of a turbidite bed

The Falcoña Fm has been also well characterized in all the outermost Maláguide outcrops in the western Montes de Malaga (Almogía area: Kockel 1959, Kockel and Stoppel 1962; Rodríguez-Cañero 1993a, b, 1995), the westernmost Costa del Sol (Marbella area, Arroyo de la Cruz: Herbig 1985) and, especially, in those mainly belonging to the highest Alpine Maláguide units outcropping along the IEZB, from west to east: Algatocín and Ardales-Chorro areas (Kockel 1959, 1964; Kockel and Stoppel 1962; Rodríguez-Cañero et al. 1997; Martín-Algarra et al 2009a; Cogollos Vega Zone Navas-Parejo et al. 2011, 2015a, b; Velez Rubio Corridor (Navas-Parejo 2012). In the higher Alpine Maláguide units of the latter areas, the Morales and Santi Petri Fms do not exist stratigraphically below the Falcoña Fm: they are replaced by a succession dominated by pelites, with subordinate thin- to medium-bedded sandstones that occasionally include laterally discontinuous ***conodont-bearing limestone lenses*** of Silurian and Devonian age. The original stratigraphic thickness of these conodont-bearing limestones has been strongly reduced by intense tectonic stretching in most sites but, locally (e.g. the Ardales Castle Rock: Fig. 9.17), they are up to several tens of metres thick. Their existence demonstrates that the Maláguide palaeogeography changed laterally from deeper, basinal

siliciclastic or mixed siliciclastic/carbonatic turbiditic environments (represented by the Morales Fm and, especially, by the Santi Petri Fm) to less deep successions including condensed pelagic limestones and alternating platy limestones and pelites. Regional outcrop distribution suggests that deepest successions were located towards the SE (in present-day coordinates) and that they evolved to less deep areas towards the NW within the same continental margin.

Ordovician conodonts have been only found at Ardales (Rodríguez-Cañero et al. 2010; Sarmiento et al. 2011), in *one* sample coming from a boulder of recrystallized bioclastic limestone (Fig. 9.17b), firstly observed and differentiated, but not dated, by Blumenthal (1930). It is included within siliceous–ferruginous–calcareous claystones associated with a laterally discontinuous calcareous breccia horizon lying below well bedded cherts that correlate to the Falcoña Fm and that lie onto a decametre-sized Devonian (Emsian) *Tentaculites* limestone lens (Rodríguez-Cañero 1993a), which probably resulted from submarine sliding and resedimentation (Martín-Algarra et al. 2009a). The original stratigraphic location within the Maláguide succession of the Ordovician beds from which this block was eroded is unknown. Interestingly, the block contains a rich Hirnantian conodont fauna showing remarkable differences with coeval Iberian conodont associations, but strong palaeobiogeographic affinities with Austroalpine-South-Alpine coeval faunas found in the Uggwa and Wolayer Fms (Rodríguez-Cañero et al. 2010; see also Sarmiento et al. 2011, Schönlaub 1988). This Hirnantian fauna indicates deposition (of the limestone bed where the block come from) in cold-water marine environments at high latitudes like coeval deposits in the Alps, but not in glaciomarine settings like those present in the Variscan areas of the Iberian massif at that time (Rodríguez-Cañero et al. 2010; Sarmiento et al. 2011).

Silurian and lowermost Devonian conodonts have been found in red, brown and grey nodular limestones (Fig. 9.19a) bearing orthoceratids and scyphocrinites, with biomicritic microfacies including bioclasts of trilobites, cephalopods, crinoids, ostracods and tintinnids (Hermes 1966). The thickest outcrop is that of the Ardales Castle Rock (Fig. 9.17a) where Rodríguez-Cañero (1993a; see also García-López et al. 1996; Martín-Algarra et al. 2009a; Rodríguez-Cañero et al. 1997, 2010) identified diverse conodont biozones, from the Llandovery to the Pragian. Equivalent facies and faunas have been found also in the Serranía de Ronda, the Montes de Málaga (Kockel 1959, 1964; Kockel and Stoppel 1962) and the Vélez Rubio Corridor (Van den Boogaard 1965). These Silurian to Lower Devonian beds were deposited in distal ramp to pelagic high bottom environments, with condensed sedimentation of moderate depth, at middle latitudes, within a divergent continental margin related to the Paleotethys opening (Herbig 1992).

Lower and Middle Devonian conodont bearing limestones also contain, commonly, abundant dacryoconarids (*Tentaculites* limestone facies). These facies are frequently formed by platy limestones interlayered with pelites (Fig. 9.19b), sometimes reddish-pinkish or varicoloured although they locally constitute a few metres thick calcareous horizons of alternating thin to medium-bedded grey limestones and grey to pinkish nodular limestones (Fig. 9.19c) including thin pelitic partings and platy limestones sometimes crowded with dacryoconarids. Geel (1973) differentiated the reddish shales as a "variegated phyllite member" within her Piar Formation that she frequently found in relation to her *Tentaculites* limestone member, but similar pelites also appear associated with conodont-bearing Carboniferous limestones belonging to the Falcoña Fm (Navas-Parejo et al. 2015b).

The Upper Devonian beds show equivalent features, but they are much poorer in dacryoconarids during the Frasnian. A stratigraphic gap (Fig. 9.19d) is systematically detected at the base of Famennian beds (Fig. 9.19f), usually the richest conodont-bearing horizons within the Maláguide Complex (Rodríguez-Cañero 1993b, 1995). This gap records the Frasnian-Famennian crisis (Kellwasser event) in the Maláguide Complex (Rodríguez-Cañero 1993b) and is associated with Fe-rich crusts and nodules (Fig. 9.19d) and with redeposited horizons (pebbly mudstones and coarse-grained carbonate turbidites). The latter provide abundant carbonate clasts with shallow marine to pelagic microfacies (including oolites, corals, stromatoporoids, ostracods, algae, crinoids, etc.), and with Frasnian conodont biofacies indicating shallow marine to moderately deep to very deep depositional settings (Fig. 9.20). These clasts were eroded from late Devonian carbonate platforms formed under warm subtropical climate, and from laterally related and deeper pelagic beds, during a period of tectonic instability of the Maláguide basin, as it is also frequently observed worldwide during the Frasnian-Famennian crisis (Rodríguez-Cañero and Martín-Algarra 2014, and references therein). The Devonian shallow carbonate platform was, however, totally dismantled.

In the northwestern Montes de Malaga, a few metres thick -sometimes reddish or pinkish, sometimes dark-coloured- pelitic interval above the Santi Petri Fm includes some horizons of calcareous greywackes ("*serie Rana*" of Kockel and Stoppel 1962). This interval gradually changes upwards to the ***Falcoña Formation*** (Herbig 1983), which includes a thin (usually a few metres, up to 20 m at most) but conspicuous Lower Carboniferous chert-limestone interval. The cherts are much more commonly found than the related limestones, and are well bedded in thin to very thin beds (Fig. 9.19f). Although their original color was black or dark gray, occassionally reddish, and yet preserve abundant but usually flattened and recrystallised radiolarians

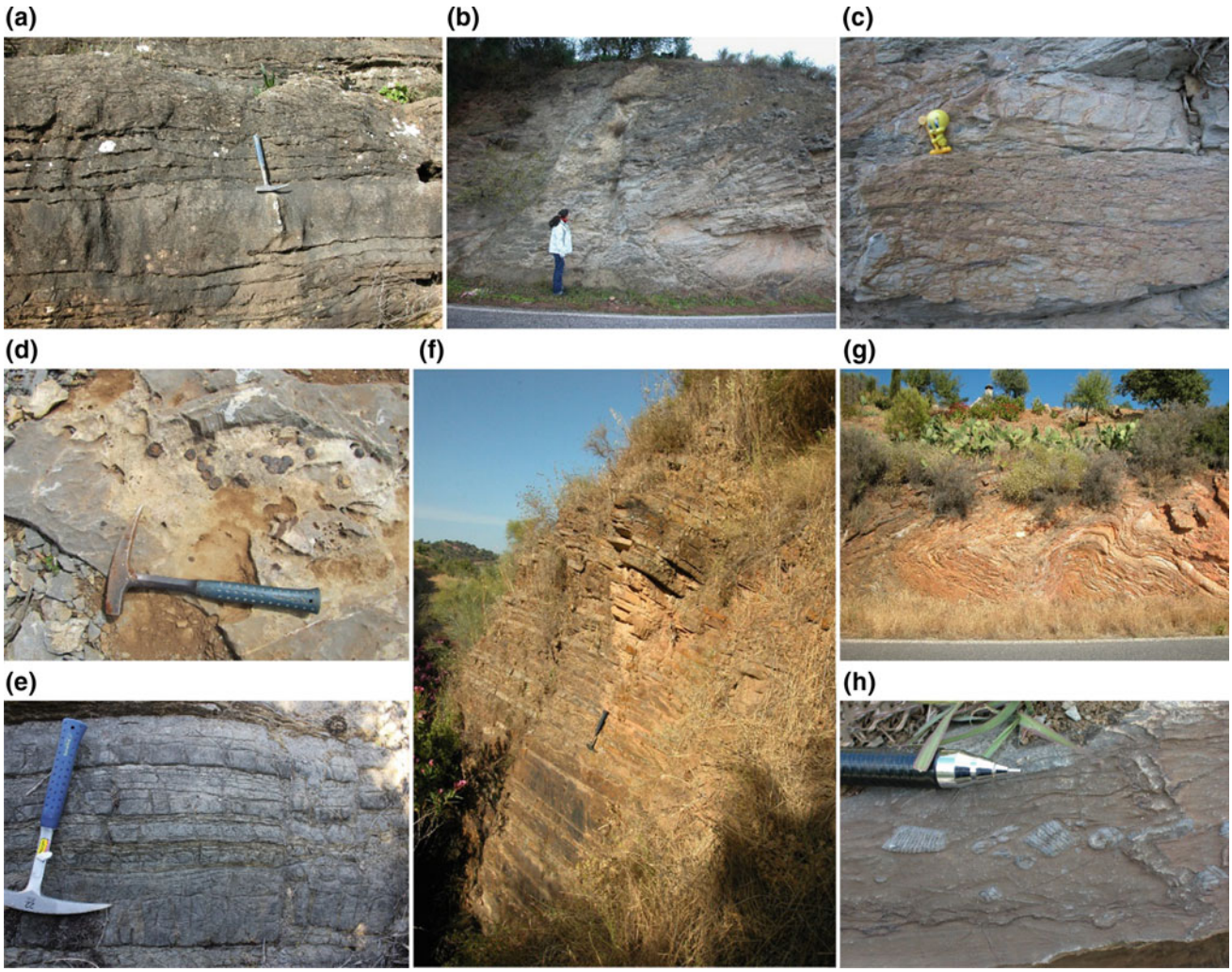

Fig. 9.19 Silurian-Devonian conodont limestones and related facies (**a**–**e**) and Falcoña Formation (**f**–**h**). **a** Silurian nodular limestones (Arroyo de las Viñas section, Ardales). **b** Lower Devonian platy and nodular limestones alternating with thin shale partings (Almogía). **c** Close-up of a nodular limestone of the same outcrop as B (Tweety for scale is 4 cm high). **d** Fe-rich discontinuity surface onto uppermost Frasnian beds encrusted by Fe-rich nodules and patinas covered by Famennian limestones, which delineates the Kellwasser event at Almogía. **e** Alternating calcarenitic and micritic slightly nodular Famennian beds (Arroyo de la Cruz, Marbella). **f** Gradual very well bedded transition from uppermost Devonian pelites to Tournaisian dark radiolarian cherts (lydites) of the lower member of of the Falcoña Fm in its type area (Cortijo de la Falcoña, Montes de Málaga). **g** Strongly folded lydites of the lower member of the Falcoña Fm (Montes de Málaga, old road Málaga-Casabermeja). **h** Crinoid stems in Visean limestones of the upper member of the Falcoña Fm (Montes de Málaga)

(O'Dogherty et al. 2000), the radiolarian cherts (lydites) are commonly transformed to fine-grained reddish-orangish quartzites, usually intensely folded (Fig. 9.19g). The lydites constitute the lower member of the Falcoña Formation and are commonly found in all areas, in spite of being laterally discontinuous due to intense folding, shearing and boudinage (Orozco and Gálvez 1979; Gálvez and Orozco 1979, 1980). Above the cherts, the upper member of the Falcoña Fm. is made of micritic limestones sometimes including dark grey chert (and quartz) nodules and stretched crinoid stems (Fig. 9.19h). Thinly bedded limestones interlayered with calcareous slates gradually change upwards to pelites overlying the Falcoña Fm. In the type section, the cherts provided Tournaisian radiolarians and the limestones Visean conodonts (Rodríguez-Cañero 1993a; Rodríguez-Cañero and Guerra-Merchán 1996; O'Dogherty et al. 2000). Consequently, this formation is well dated as Lower Carboniferous. This is confirmed in many other sites (Navas-Parejo et al. 2008, 2012a, 2015a, b).

The Falcoña Fm is present in all Maláguide outcrops and tectonic units. Actually, it is a key horizon for stratigraphic correlation among Maláguide Paleozoic successions bearing the Morales and Santi Petri Fms and those without them but bearing Ordovician-Silurian-Devonian limestones with

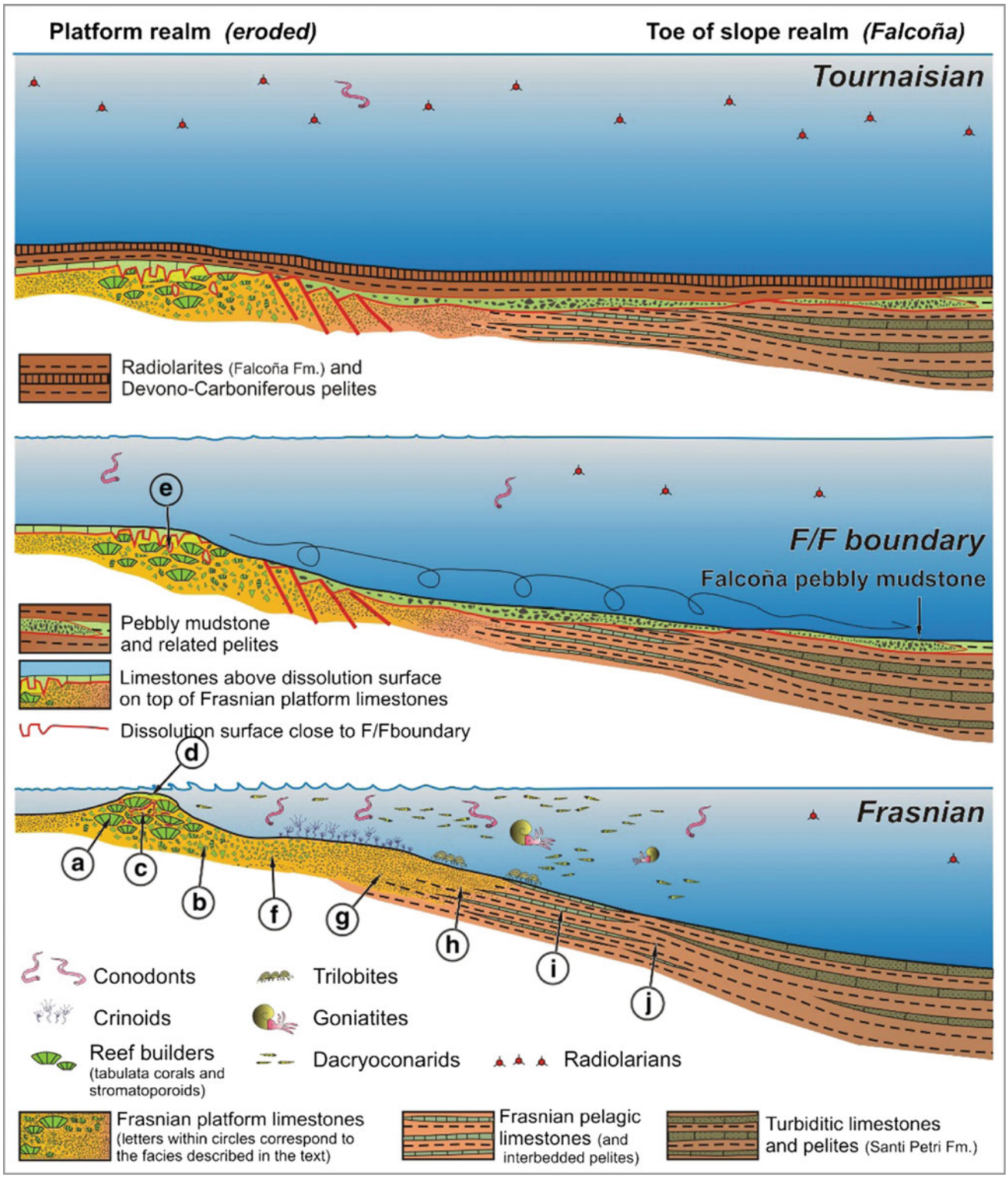

Fig. 9.20 Model on the sedimentary evolution of the Maláguide basin in the frame of a Paleotethyan margin during the Late Devonian and Early Carboniferous, with a shallow marine proximal area distally connected with a turbiditic deep basin where the Santi Petri Fm and related facies were being deposited. The shallow water area collapsed during a tectonic event related to the Frasnian/Famennian crisis, and was dismantled to produce the pebbly mudstone horizon at the base of the Falcoña Fm. During the successive Tournaisian deepening the bottom irregularities attenuated and a widespread deposition of radiolarites accounted everywhere in the Maláguide basin (modified from Rodríguez-Cañero and Martín-Algarra 2014)

conodonts (Fig. 9.15). In the central-eastern Montes de Malaga, in the Costa del Sol and in the tectonically lower Maláguide units along the IEZB the Falcoña Fm is well dated but the stratigraphic age of the underlying Santi Petri and Morales Fms is controversial or at least uncertain. Most field data point to a late Devonian age for the Santi Petri Fm and probably also for the upper part of the Morales Formation (Rodríguez-Cañero and Martín-Algarra 2014). Nevertheless, intense tectonic folding does not preclude other possibilities. Actually, the existence of reverse limbs affecting the contact between the Santi Petri and Falcoña Fms can be locally demonstrated and, in many areas, the lithological similarities among the Almogía (see below) and the Morales Fms make difficult to distinguish among them if the Falcoña Fm is absent and the Santi Petri Fm stratigraphically reversed.

After the tectonic disturbances recorded by the Kellwasser event, the deposition of the Falcoña Fm represents a period of tectonic quiescence dominated by thermal subsidence in the Maláguide basin (Fig. 9.20). The previously formed marine bottom irregularities were levelled and a marked deepening of the whole basin led to radiolarian-rich sedimentation below the CCD and to deposition of the siliceous member (lydites) of the Falcoña Fm during the Tournaisian (O'Dogherty et al. 2000). After siliceous sedimentation a lowering CCD was responsible for deposition of pelagic limestones sometimes including chert nodules and isolated crinoid stems with Visean conodonts and deep (*Gnathodus*) biofacies (Rodríguez-Cañero and Guerra-Merchán 1996). A similar vertical facies evolution is commonly observed in many other European Variscan regions.

When the successions are more complete and tectonically less disturbed, the upper member of the Falcoña Fm changes, rapidly but gradually, to a pelitic succession with identic features to those of the finer-grained facies of the Almogía Fm. In addition, a carbonate horizon intercalated between pelites similar to those of the Almogía Fm has recently provided the youngest conodont association found in the Maláguide Complex, of early Bashkirian age (Navas-Parejo et al. 2012b). Then, the Maláguide sedimentation shows deep-water basinal facies from the Tournaisian up to the earliest Bashkirian. In addition, the existence of Visean to Early Bashkirian shallow marine carbonate platform environments in the Maláguide realm (now dismantled) or close to it is also revealed by carbonate clasts with shallow marine facies and fossils found, ocassionally, in the conglomerates of the overlying Almogía Fm and, especially and systematically, in those of the Marbella Fm (Buchroithner et al. 1980; Herbig 1984, 1986; Herbig and Mamet 1985; Mamet and Herbig 1990).

9.6.4 Syn-orogenic Evolution

A. Martín-Algarra, R. Rodríguez-Cañero, P Navas-Parejo, S. Mazzoli, V. Perrone

The Variscan evolution in the Maláguide Complex started with deposition of the *Almogía Fm* and culminated after deposition of the *Marbella Fm*, which are usually attributed to the synorogenic Culm facies. Their deposition evidence the progressive erosional dismantling of *previously deformed* Paleozoic and/or older successions, as well as that of Devonian-Carboniferous carbonate platforms probably formed on them and/or on laterally related successions now outcropping in the Rif (Chalouan 1986; Chalouan and Michard 1990, 2004). These sediments were redeposited within turbiditic synorogenic basins from the latest Early Carboniferous to the Late Carboniferous. After that, the main (late) Variscan deformation accounted in the Maláguide Complex, as revealed by a marked unconformity below the Triassic beds of the Saladilla Fm.

The starting deposition of the Almogía Fm was associated with the post-Visean onset of the (frequently coarse-grained) siliciclastic sedimentation everywhere within the Maláguide basin (Figs. 9.15 and 9.21a–e). Moreover, although stratigraphic and tectonic relationships between the Falcoña and Almogía Fms are frequently masked by poor outcrop exposures or by faulting, a marked contrast in the tectonic style and/or in the intensity of tectonic deformation can be observed between them: the Falcoña Fm beds are usually much more intensely folded than, and are laterally discontinuous below, the Almogía Fm. This suggests that an unconformity exists between them and that the Maláguide basin was probably affected by important tectonic events since the Serpukhovian or, more probably after the early Bashkirian, although this is not precisely dated. Actually, the Almogía Fm only provides redeposited Devonian and Early Carboniferous conodont faunas that have been extracted from carbonate clasts included in the conglomerate horizons that frequently (but not always) characterize its stratigraphic lowest part. Recent zircon dating indicates predominant Cambro-Ordovician and older magmatic ages for most clasts of crystalline rocks within these conglomerates although a few zircon grains with Permian ages have also been obtained (Esteban et al. 2017), but these younger ages need to be confirmed and/or re-evaluated.

The ***Almogía Fm*** is a several hundred of metres thick succession of siliciclastic turbidites dominated by fine-grained pelites and greywackes with undeterminable plant remains and Bouma sequences, which commonly include also subordinate conglomeratic horizons (Blumenthal 1930, 1949; Soediono 1971; Mon 1971; Geel 1973; Herbig

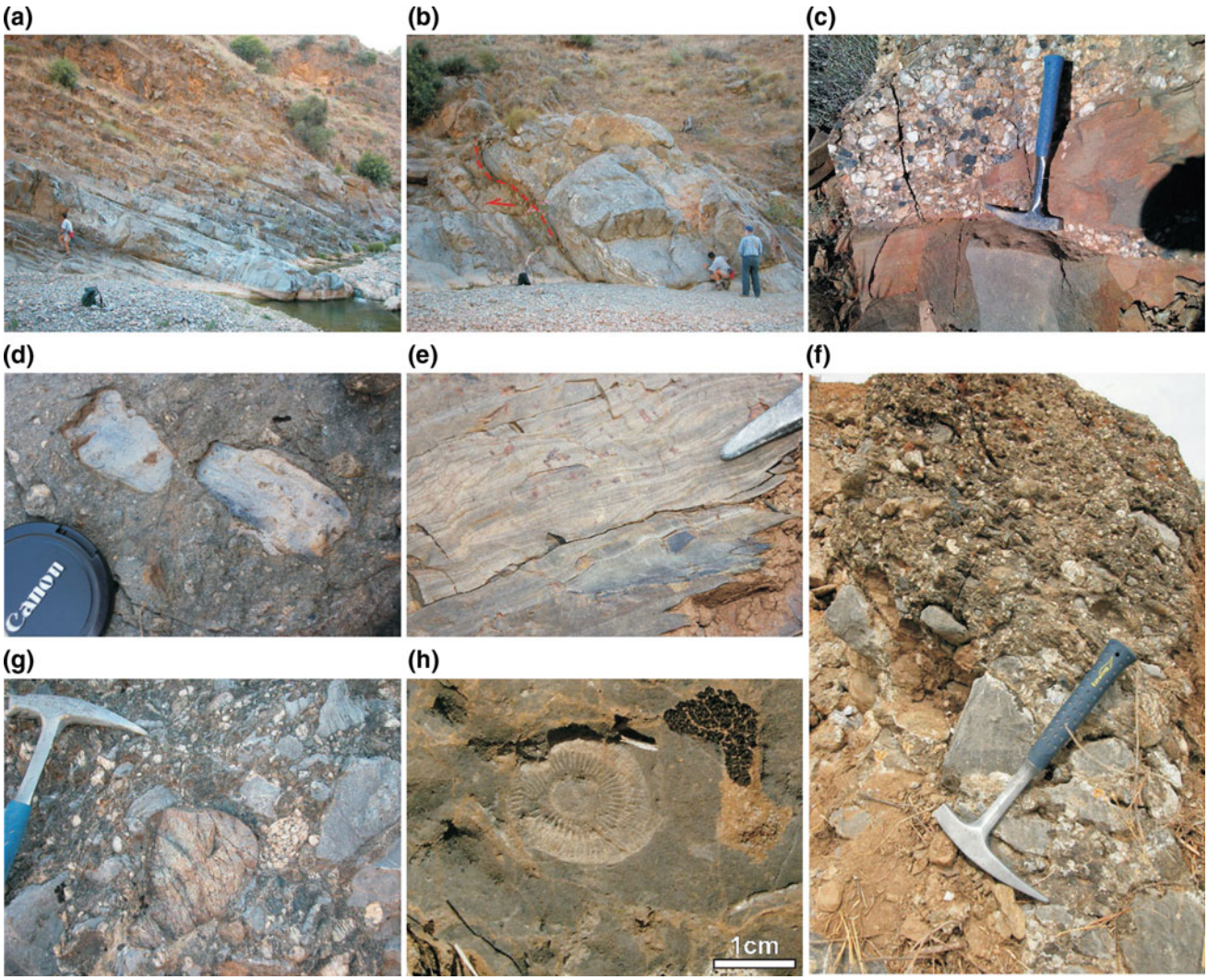

Fig. 9.21 Field views of the Almogía Formation, mostly Retamares member (**a**–**d**), in the Montes de Malaga (**a**, **b**, **e**), Costa del Sol (**d**) and Vélez Rubio Corridor (**c**), and of the Marbella Formation in the Montes de Málaga (**f**, **g**), and Vélez Rubio (**h**). **a** Thinning and fining-upwards turbiditic succession (mainly greywackes with subordinate conglomerates. **b** Channeled conglomerate bed that buries a synsedimentary normal fault. **c** Channeled conglomerate beds including black clasts of lydite eroded from the Falcoña Fm) and white clasts of quatzites and of granites. **d** Clasts of Tentaculites limestone included in a microconglomeratic matrix. **e** Fine-grained rippled sandstone in a stratigraphically reversed turbidite bed. **f** Typical outcrop of coarse-grained and normally graded Marbella Fm conglomerates including clasts of Visean to lowermost Bashkirian shallow marine limestones. **g** Close-up of a Marbella Fm conglomerate, where rounded clasts of granites and angular clasts of limestones are clearly visible. **h** Detail of a coral included in a limestone clast

1983, 1984; Martín-Algarra 1987; Herbig and Statteger 1989; Mayoral et al. 2018). The succession is organized as a thinning- and fining-upwards turbiditic megasequence, whose lower part is dominated by greywackes sometimes forming normally graded beds up to several metres thick stacked in metre to decametre thick thinning and fining upwards sequences (Fig. 9.21a) with commonly channeled bases (Fig. 9.21b) filled with coarse- to very coarse-grained conglomerates (Fig. 9.21c) and/or finer conglomeratic to coarse-grained amalgamated sanstone beds with commonly scoured bases. Its upper part is dominated by fine-grained olive-green pelites with subordinate interlayered thin greywacke beds. Laterally discontinuous coarser-grained conglomeratic beds (from granule up to cobble, rarely boulder size) with clasts usually subrounded to well rounded, are also frequently present in the greywackes of the lower part of the formation, which is known as Retamares Member (Kockel and Stoppel 1962). The later beds can be up to several metres thick and include clasts eroded from the underlying succession, among them clasts of pelagic limestones with Devonian and Carboniferous conodonts (Fig. 9.21d) and, especially, of black chert (Fig. 9.21d) and of greywackes eroded from the

Falcoña Fm and from older formations. In addition, clasts of crystalline rocks, mostly granitoids and gneisses of unknown provenance are frequently present. The conglomerate and thickest sandstone beds, with erosional (channeled and scoured) bases and that are normally graded, indicate deposition in channelled areas of a deep clastic system, whereas the finer-grained and thinner bedded greywackes and the related pelites indicate outermost areas of deep sea fans and/or basin plain environments. Heavy mineral spectra and clastic provenance analysis indicate a tectonically active source that was in very rapic tectonic rise, certainly forming a nascent orogenic belt related to the development of a rapidly evolving convergent margin (Herbig and Statteger 1989). Nevertheless, basin unstability atenuated gradually with time as indicated by the thinning and fining upwards megasequential evolution. Recent palaeoichnological data from the eastern Montes de Málaga indicate that the sequence became shallower upwards (Mayoral et al. 2018).

The ***Marbella Fm*** is dominated by coarse to very coarse-grained olistostromic conglomerates that systematically include granitic, gneissic and especially carbonatic clasts of cobble to boulder size, frequently with reverse grading although normal grading is also present (Fig. 9.21f). Finer grained facies are constituted by silicliclastic turbidites mixed with some carbonate components. The Marbella Fm conglomerates shows deep erosional bases on the Almogía Fm, whose upper part is systematically much finer-grained, and were certainly deposited by debris flows (Herbig 1984; Martín-Algarra 1987). The carbonate clasts are commonly abundant and sometimes huge (Fig. 9.21f, g), and contain shallow marine fossils like corals (Fig. 9.21h), bivalves, benthic foraminifera, algae etc., that allow precise biostratigraphic dating and reconstructing diverse Visean to Early Bashkirian shallow marine environments that are now totally dismantled (Boulin and Lys 1968; Boulin 1970; Geel 1973; Buchroithner et al. 1980; Herbig 1984, 1986; Herbig and Mamet 1985; Mamet and Herbig 1990). The common presence -and locally abundance- of clasts of gneisses, granites (Fig. 9.21g), quartzites and metapelites in the Marbella Fm is particularly remarkable, as well as that subordinate of rare metabasites and mafic plutonic rocks that are also occasionally present. This reveals a deep and renewed erosion of a pre-Variscan (Early Paleozoic and/or older) crystalline basement that was being affected by rapid tectonic rise and orogenic deformation after a period of tectonic quiescence during sedimentation of the upper part of the Almogía Fm. Again, this is a typical feature of synorogenic deposits, as also revealed by the spectrum of heavy mineral data that, as in the case of the Almogía Fm, show contrasting clastic provenance signatures with respect to those of the underlying preorogenic deposits (Herbig and Statteger 1989; Henningsen and Herbig 1990).

9.6.5 Variscan Tectonics and Metamorphism in the Maláguide Complex

A. Martín-Algarra, S. Mazzoli, V. Perrone

The importance and intensity of the Variscan versus Alpine tectonics in the Maláguide Complex have been debated (Foucault and Paquet 1971; Roep 1974; Orozco and Gálvez 1979; Gálvez and Orozco 1979, 1980; Cuevas et al. 2001). Nonetheless, in spite of the intense Alpine deformation affecting basement and cover together, the Maláguide Paleozoic shows strong tectonic deformation and mild metamorphic recrystallization that are absent in the cover. The marked depositional contrasts between deep marine Paleozoic successions and overlying Triassic continental red beds also indicates that the Maláguide Paleozoic was affected by intense Variscan deformations, whose kinematics, timing and relationships with the tectonometamorphic evolution at deeper structural levels (Alpujárride Complex) are still poorly understood.

In relation to the Variscan tectonometamorphic evolution, the composition of chlorite in the rocks on both sides of the unconformity reveals an abrupt increase in the temperature of the metamorphism in the rocks successions belonging to the Paleozoic Piar Group with respect to the Triassic Saladilla Formation (Ruiz-Cruz 1997). In addition, the Alpine metamorphic overprint is demonstrated by the gradual evolution of the crystalchemical parametres of other mineral phases in both successions, in particular by the IC index and by the evolution of the kaolinite polymorphs (Ruiz-Cruz 1997). Concerning the Variscan tectonometamorphic evolution, IC values = 0.32–0.25 corresponding to the deep anchizone characterize the Morales Fm, whose lowest beds, bearing vermiculite, biotite, paragonite or chloritoid, are of of evident metamorphic origin. In areas close to Malaga, in rocks bearing ghosts of andalusite and garnet at the very base of typical Maláguide successions the IC values <0.25 clearly indicate epizonal metamorphism (Ruiz-Cruz and Rodríguez-Jiménez 2002). Mineral associations in the same rocks indicate $T \approx 500$ ºC and $P \approx 5$ kbar for the pre-Alpine metamorphism (Ruiz Cruz and Nieto 2002), compatible with those deduced for the underlying Benamocarra rocks (Sánchez-Navas et al. 2016).

The Variscan tectonics in the Maláguide Complex is evidenced by major scale structures (folds, thrusts and faults) that are not yet well featured neither cartographically nor regionally, and by several generations of meso- and microstructures like isoclinal and crenulation folds and other associated ductile deformation structures (axial plane foliations, stretching and crenulation lineations) and by fragile structures that are absent in the Saladilla Formation (Martín-Algarra et al. 2009b). In addition, as stated above, the

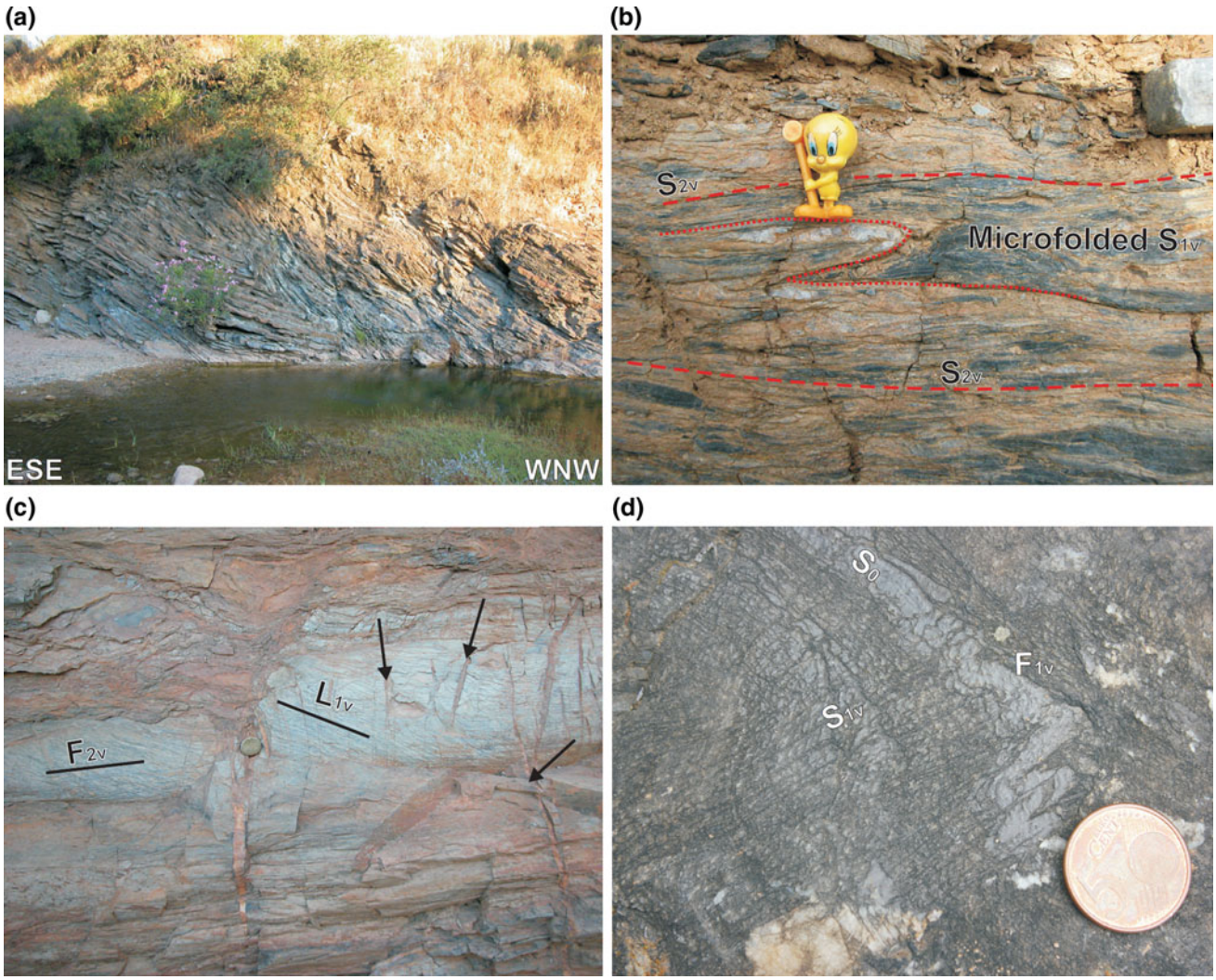

Fig. 9.22 Variscan structures of the Maláguide Complex. **a** Markedly assymmetric (E-vergent) fold by heterogeneous simple shear oblique to S_0 (top-to-the-SE reverse motion) affecting thin-bedded mixed carbonatic siliciclastic turbidites of the Santi Petri Fm. **b** Two variscan foliations within the Morales Fm metapelites: the slaty cleavage S_{2v} is roughly axial planar with respect to hosting folds of the S_{1v}. **c** Lineation (L_{1v}) affected by the second phase of folding F_{2v}; the arrows point to extensional quatz-filled joints related to F_{2v} folds. **d** Microfolds (F_{1v}) folding the bedding (S_0) and related foliation (S_{1v}) in Visean limestones dated with conodonts at that site (Falcoña Fm)

Maláguide Paleozoic succession shows two parts with different style and intensity in deformation between Visean and older pelagites and turbidites and post-Visean clastics. Pre-Culm deposits (pre-Almogía Fm) form deep marine successions deposited in proximal to distal areas of a divergent Paleotethyan margin that were affected by the first important Variscan deformation. The synorogenic siliciclastic sediments with Culm facies (Almogía and Marbella Fms) record marked synsedimentary instability that affected the Maláguide margin since mid-Carboniferous time, and were affected by the main latest Variscan (Hercynian) deformation.

In the Morales Fm and in the Santi Petri Fm at least two Variscan foliations are present. The Variscan deformation is characterized by a markedly asymmetric, E-vergent folding (Fig. 9.22a) related to heterogeneous simple shear oblique to S_0, with top-to-the-SE reverse motion (Martín-Algarra et al. 2009b). A slaty cleavage develops in the pelitic beds, which is roughly axial planar with respect to hosting F_{1V} folds, as well as a lineation (L_{1V}). These structures (Fig. 9.22a, b) are affected by a second phase of folding (F_{2V}), which refolded previous (F_{1V}, S_{1V}, L_{1V}) structures (Fig. 9.22c) and produced a new cleavage (S_{2V}), which locally becomes the main foliation, and a mostly W plunging lineation (L_{2V}). This occurred within the framework of the same progressive deformation, as suggested by a general coaxiality of fold structures. The same type of folds, also E-verging, are well documented in the Lower Carboniferous radiolarites (Falcoña Fm) and in the related Visean limestones (Fig. 9.22d). Nevertheless, the style and intensity of the deformation

affecting the Culm-like deposits is quite different from what it is usually observed in the pre-Culm sediments. These deposits are usually much less deformed than the pre-Culm deposits and their more pelitic lithotypes document only one clear foliation, corresponding to the S_{2V} of the underlying beds. In addition, they are affected by numerous faults that document a roughly E-W extension (Fig. 9.21b).

Finally, two stratigraphically different types of pre-Carboniferous successions have been recently recognized in the Maláguide Complex, mainly in the outcrops along the IEZB (Martín-Algarra et al. 2009a; Navas-Parejo 2012; Rodríguez-Cañero and Martín-Algarra 2014; Navas-Parejo et al. 2015b), and they usually make part of independent Alpine tectonic units that overprint a previous Variscan thrust nappe structure. In the Ardales area, the pre-Alpine structure has been demonstrated by cartographic, stratigraphic and structural criteria as formed by two Variscan thrust units (Fig. 9.17), where the proximal facies constitute the hanging wall unit and the distal facies the footwall units (Martín-Algarra et al. 2009a). Structural analysis indicates that the contact between these Variscan units is an E-directed thrust and that the internal structure of the lower Variscan unit is consistent with bulk noncoaxial strain dominated by top-to-the-E shearing (Martín-Algarra et al. 2009b).

Additional evidence on the Variscan evolution of the Maláguide Complex and neighbour areas is indirectly obtained from granitic and gneissic clasts that are commonly present in much younger deposits, in particular in those of late Oligocene to Aquitanian age included in the Ciudad Granada Group. These clasts are identical to several types of late Variscan granites and related moderately alpinised metamorphic lithotypes that are commonly present within the Calabria-Peloritani pre-Mesozoic basements and that are currently dated as latest Carboniferous to earliest Permian (Martín-Algarra et al. 2000, and references therein).

References

Acosta Vigil A, Barich A, Bartoli O, Garrido CJ, Cesare C, Remusat L, Poli S, Raepsaet C (2016) The composition of nanogranitoids in migmatites overlying the Ronda peridotites (Betic Cordillera, S Spain): the anatectic history of a polymetamorphic basement. Contributions to Mineralogy and Petrology 171:24. https://doi.org/10.1007/s00410-016-1230-3.

Acosta-Vigil A, Rubatto D, Bartoli O, Cesare B, Meli S, Pedrera A, Azor A, Tajčmanová L (2014) Age of anatexis in the crustal footwall of the Ronda peridotites, S Spain. Lithos 210–211:147-167. https://doi.org/10.1016/j.lithos.2014.08.018

Aerden DGAM, Bell TH, Puga E, Sayab M, Lozano JA, Díaz de Federico A (2013) Multi-stage mountain building vs. relative plate motions in the Betic Cordillera deduced from integrated microstructural and petrological analysis of porphyroblast inclusion trails. Tectonophysics 587:188–206. https://doi.org/10.1016/j.tecto.2012.11.025

Afiri A, Gueydan F, Pitra P, Essaifi A, Précigout J (2011) Oligo-Miocene exhumation of the Beni-Bousera peridotite through a lithosphere-scale extensional shear-zone, Geodinamica Acta 24:49–60. https://doi.org/10.3166/ga.24.49-60

Agard P, Augier R, Monie P (2011) Shear band formation and strain localization on a regional scale: evidence from anisotropic rocks below a major detachment (Betic Cordilleras, Spain). Journal of Structural Geology 33:114–131. https://doi.org/10.1016/j.jsg.2010.11.011

Aldaya F, Alvarez F, Galindo-Zaldívar J, González-Lodeiro F, Jabaloy A, Navarro-Vilá F (1991) The Maláguide-Alpujárride contact (Betic Cordilleras, Spain): A brittle extensional detachment. Comptes Rendus de l'Académie des Sciences Paris II 313:1447–1453.

Álvarez-Lobato F, Aldaya F (1985) Las unidades de la Zona Bética en la región de Águilas-Mazarrón (Prov. de Murcia). Estudios Geológicos 41:139–146. http://estudiosgeol.revistas.csic.es/index.php/estudiosgeol/article/view/698/726

Andriessen PAM, Hebeda EH, Simon OJ, Verschure RH (1991) Tourmaline K-Ar ages compared to other radiometric dating systems in Alpine anatectic leucosomes and metamorphic rocks (Cyclades and southern Spain). Chemical Geology 91:33–48. https://doi.org/10.1016/0009-2541(91)90014-I

Andrieux J, Fontboté J, Mattauer M (1971) Sur un modèle explicatif de l'Arc de Gibraltar. Earth and Planetary Science Letters 12:191–198. https://doi.org/10.1016/0012-821X(71)90077-X

Argles TW, Platt JP, Water DJ (1999) Attenuation and excision of a crustal section during extensional exhumation: the Carratraca Massif, Betic Cordillera, Southern Spain. Journal of the Geological Society London, 156:149–162. http://dx.doi.org/10.1144/gsjgs.156.1.0149

Augier R, Agard P, Monié P, Jolivet L, Robin C, Booth-Rea G. (2005a) Exhumation, doming and slab retreat in the Betic Cordillera (SE Spain): in situ 40Ar/39Ar ages and P-T-d-t paths for the Nevado-Filábride complex. Journal of Metamorphic Geology 23:357–81. https://doi.org/10.1111/j.1525-1314.2005.00581.x

Augier R, Booth-Rea G, Agard P, Monié P, Martínez-Martínez JM, Jolivet L, Azañón JM (2005b) Exhumation constraints for the lower Nevado-Filabride Complex (Betic Cordillera, SE Spain): a Raman thermometry and Tweequ multiequilibrium thermobarometry approach. Bulletin de la Société Géologique de France 76:403–416. https://doi.org/10.2113/176.5.403

Augier R, Jolivet L, Do Couto D, Negro F (2013) From ductile to brittle, late- to post-orogenic evolution of the Betic Cordillera: Structural insights from the northeastern Internal zones. Bulletin de la Société Géologique de France 184:405–425. https://doi.org/10.2113/gssgfbull.184.4-5.405

Azdimousa A, Bourgois J, Poupeau,G, Vázquez M, Asebriy L, Labrin E (2014) Fission track thermochronology of the Beni Bousera peridotite massif (Internal Rif, Morocco) and the exhumation of ultramafic rocks in the Gibraltar Arc. Arabian Journal of Geosciences 7:1993–2005. https://doi.org/10.1007/s12517-013-0924-3

Azdimousa A, Jabaloy-Sánchez A, Talavera C, Asebriy, González-Lodeiro F, Evans NJ (2019) Detrital zircin U-Pb ages in the Rif Belt (Northern Morocco): Paleogeographic implicatons. Gondwana Research 70:133–150. https://doi.org/10.1016/j.gr.2018.12.008

Balanyà JC, García-Dueñas V (1987) Les directions structurales dans le Domaine d'Alborán de part et d'autre du Détroit de Gibraltar. Comptes Rendus de l'Académie des Sciences Paris 304:929–932.

Balanyà JC, Azañón JM, Sánchez-Gómez M, García-Dueñas V (1993) Pervasive ductile extension, isothermal decompression and thinning of the Jubrique unit in the Paleogene (Alpujárride Complex, western

Betics, Spain). Comptes Rendus de l'Académie des Sciences Paris 316:1595–1601.
Balanyà JC, García-Dueñas V, Azañón JM, Sánchez-Gómez M (1997) Alternating contractional and extensional events in the Alpujarride nappes of the Alboran Domain (Betics, Gibraltar Arc). Tectonics 16:226–238. https://doi.org/10.1029/96TC03871
Bakker HE, De Jong K, Helmers H, Biermann C (1989) The geodynamic evolution of the Internal Zone of the Betic Cordillera (South-east Spain); a model based on structural analysis and geothermobarometry. Journal of Metamorphic Geology 7:359–381. https://doi.org/10.1111/j.1525-1314.1989.tb00603.x
Barich A, Acosta-Vigil A, Garrido CJ, Cesare B, Tajčmanová L, Bartoli O (2014) Microstructures and petrology of melt inclusions in the anatectic sequence of Jubrique (Betic Cordillera, S Spain): implications for crustal anatexis. Lithos 206–207:303–320. https://doi.org/10.1016/j.lithos.2014.08.003
Bartoli O, Acosta-Vigil A, Tajčmanová L, Cesare B, Bodnar RJ (2016) Using nanogranitoids and phase equilibria modeling to unravel anatexis in the crustal footwall of the Ronda peridotites (Betic Cordillera, S Spain). Lithos 256–257:282–299. https://doi.org/10.1016/j.lithos.2016.03.016
Batchelor RA, Bowden P (1985) Petrogenetic interpretation of granitoids series using multicationic parameters. Chemical Geology 48:43–55. https://doi.org/10.1016/0009-2541(85)90034-8
Bea F, Montero P (1999) Behavior of accessory phases and redistribution of Zr, REE, Y, Th, and U during metamorphism and partial melting of metapelites in the lower crust, an example from the Kinzigite Formation of Ivrea–Verbano, NW Italy. Geochimica Cosmochimica Acta 63:1133–1153. https://doi.org/10.1016/S0016-7037(98)00292-0
Behr WM, Platt JP (2012) Kinematic and thermal evolution during two-stage exhumation of a Mediterranean subduction complex. Tectonics 31:TC4025. https://doi.org/10.1029/2012TC003121
Bicker RE (1966) Geological investigations in the region west of Antas and Cuevas del Almanzora, south-eastern Spain. PhD Thesis University of Amsterdam 124 p.
Bingen B, Demaiffe D, Hertogen J (1996) Redistribution of rare earth elements, thorium, and uranium over accessory minerals in the course of amphibolite to granulite facies metamorphism: the role of apatite and monazite in the orthogneisses from southwestern Norway. Geochimica Cosmochimica Acta 60:1341–1354. https://doi.org/10.1016/0016-7037(96)00006-3
Blichert-Toft J, Albarède F, Kornprobst J (1999) Lu-Hf isotope systematics of garnet pyroxenites from Beni Bousera, Morocco: implications for basalt origin. Science 283:1303–1306. https://doi.org/10.1126/science.283.5406.1303
Blumenthal M (1927) Versuch einer tektonischen Gliederung der betischen Cordillera von Central-und Südwest (Andalusien). Eclogae Geologicae Helvetiae 20:487–532.
Blumenthal M (1928) L'éxistence du Bétique de Malaga dans la région de Grenade. Comptes Rendus de l'Académie des Sciences Paris 187:1059–1062.
Blumenthal M (1930) Beiträge zur Geologie der betischen Cordillere beiderseits des Rio Guadalhorce (Prov. Malaga). Eclogae Geologicae Helvetiae 23:41–289.
Blumenthal M (1949) Estudio geológico de las cadenas costeras al oeste de Málaga entre el río Guadalhorce y el río Verde. Boletín del Instituto Geológico y Minero de España 52:11–203.
Blumenthal M, Fallot P (1935) Observations géologiques sur la Sierra Arana entre Grenade et Guadix. Memorias de la Real Sociedad Española de Historia Natural 17:5–74.
Bodenhausen JWA, Fontboté JM, Simon OJ (1967) Sur la présence d'éléments du Bétique de Malaga au Sud de la Sierra Nevada (près de Cherín, Espagne meridionale). Geologie en Mijnbouw 44:251–253.
Bodinier JL, Morten L, Puga E, Díaz de Federico A (1987) Geochemistry of metabasites from the Nevado-Filabride Complex, Betic Cordilleras, Spain: relicts of a dismembered ophiolitic sequence. Lithos 20:235–245. https://doi.org/10.1016/0024-4937(87)90011-9
Booth-Rea G, Azañón JM, Martínez-Martínez JM, Vidal O, García--Dueñas V (2005) Contrasting structural and P-T evolutions of tectonic units in the southeastern Betics: key for understanding the exhumation of the Alboran Domain HP/LT crustal rocks (Western Mediterranean). Tectonics 21. http://dx.doi.org/10.1029/2004TC001640.
Booth-Rea G, Martínez-Martínez, JM Giaconia F (2015) Continental subduction, intracrustal shortening, and coeval upper-crustal extension: PT evolution of subducted south Iberian paleomargin metapelites (Betics, SE Spain). Tectonophysics 663:122–139. https://doi.org/10.1016/j.tecto.2015.08.036
Boulin J (1970) Les Zones Internes des Cordillères Bétiques de Málaga à Motril (Espagne méridionale). PhD Thesis Université de Paris, Annales Hébert et Haug Travaux de Géologie de la Faculté des Sciences de Paris 10:1–237.
Boulin J, Lys M (1968) Nouveaux repères paléontologiques dans le Carbonifère des Monts de Málaga (Espagne méridionale). Comptes Rendus de l'Académie des Sciences Paris (D) 266:1561–1563.
Bourgois J (1979) Origine sédimentaire des "polymict rauhwackes": formation post-triasique impliquée dans les nappes internes bétiques (Espagne méridionale). Comptes Rendus sommaires de la Societé géologique de France 1:26–29. https://pubs.geoscienceworld.org/sgf/bsgf/article-abstract/169/2/153/88084
Bouybaouène ML, Goffé B, Michard A (1998). High-pressure granulites on top of the Beni Bousera peridotites, Rif belt, Morocco: A record of an ancient thickened crust in the Alboran domain. Bulletin de la Societé Géologique de France 169:153–162. https://pubs.geoscienceworld.org/sgf/bsgf/article-abstract/169/2/153/88084
Buchroithner MF, Flügel E, Flügel HW, Stattegger K (1980) Mikrofazies, Fossilien und Herkunft der Kalk-Gerölle im Karbon-"Flysch" der Betischen Kordilleren, Spanien. Facies 2:1–54. https://link.springer.com/article/10.1007/BF02536462
Burgos J, Díaz de Federico A, Morten L, Puga E (1980) The ultramafic rocks from the Cerro del Almirez, Sierra Nevada Complex, Betic Cordilleras, Spain: preliminary report. Cuadernos de Geología Universidad de Granada 11:157–165.
Chalouan A (1986) Les nappes Ghomarides (Rif septentrional, Maroc): un terrain varisque dans la chaîne alpine. PhD Thesis Université Louis Pasteur, Strasbourg 317 p.
Chalouan A, Michard A (1990) The Ghomaride nappes, Rif Coastal Chain, Morocco: a Variscan chip in the Alpine Belt. Tectonics 9:1565–1583. https://doi.org/10.1029/TC009i006p01565
Chalouan A, Michard A (2004) The Alpine Rif Belt (Morocco): A Case of Mountain Building in a Subduction-Subduction-Transform Fault Triple Junction. Pure and Applied Geophysics 161:489–519. https://link.springer.com/article/10.1007/s00024-003-2460-7
Cuevas J, Navarro-Vilá F, Tubía JM (1989) Interprétation des cisaillements ductiles vers le NE dans le gneiss de Torrox (Complexe Alpujarride, Cordillères Bétiques). Geodinamica Acta 3:107–116. https://doi.org/10.1080/09853111.1989.11105178
Cuevas J, Navarro-Vilá F, Tubía JM (2001) Evolución estructural poliorogénica del complejo Maláguide (Cordilleras Béticas). Boletín Geológico y Minero, 112:47–57. http://www.igme.es/boletin/2001/112_3-2001/4-ARTICULO EVOLUCION.pdf
De Jong K (1991) Tectono-metamorphic studies and radiometric dating on the Betic Cordilleras (SE Spain). PhD Thesis University of Amsterdam 204 p.
De Jong K (1993a) Tectono-metamorphic and chronologic development of the Betic Zone (SE Spain) with implications for the geodynamic evolution of the western Mediterranean area.

Proceedings of the Koninklijke Nederlandse Akademie van Wetenschappen B 96:295–333.
De Jong K (1993b) The tectono-metamorphic evolution of the Veleta Complex and the development of the contact with the Mulhacen Complex (Betic Zone, SE Spain). Geologie en Mijnbouw 71:227–237.
De Jong K (2003) Very fast exhumation of high-pressure metamorphic rocks with excess ^{40}Ar and inherited ^{87}Sr, Betic Cordilleras, southern Spain. Lithos 70:91–110. https://doi.org/10.1016/S0024-4937(03)00094-X
De Jong K, Bakker HE (1991) The Mulhacen and Alpujarride Complex in the eastern Sierra de los Filabres, SE Spain: Lithostratigraphy. Geologie en Mijnbouw 70:93–103.
De Roever WP, Nijhuis HJ (1964) Plurifacial alpine metamorphism in the eastern Betic Cordilleras (SE Spain) with special reference to the genesis of glaucophane. Geologische Rundschau 53:324–336. https://link.springer.com/article/10.1007/BF02040754
Delgado F, Estévez A, Martín JM, Martín-Algarra A (1981) Observaciones sobre la estratigrafía de la formación carbonatada de los mantos alpujárrides (Cordilleras Béticas). Estudios Geológicos 37:45–57.
Díaz de Federico A, Gómez-Pugnaire MT, Puga E, Sassi FP (1979) New problems in the Sierra Nevada Complex (Betic Cordilleras, Spain). Neues Jahrbuch für Geologie und Paläontologie Monatshefte 10:577–585.
Díaz de Federico A, Puga E (1976): Estudio geológico del Complejo de Sierra Nevada, entre los meridianos de Lanjarón y Pitres. Tecniterrae 9:1–10.
Díaz de Federico A, Torres-Roldán R, Puga E (1990) The rock series of the Betic substratum. Documents et Travaux IGAL 12–13:19-29.
Didon J, Durand-Delga M, Kornprobst J (1973) Homologies géologiques entre les deux rives du détroit de Gibraltar. Bulletin de la Societé Géologique de France (7) 15/2:77–105. https://doi.org/10.2113/gssgfbull.S7-XV.2.77
Duplaix S, Fallot P (1960) Les "konglomeratische Mergel" des Cordillères Bétiques. Bulletin de la Societé Géologique de France 7(II):308–317. https://doi.org/10.2113/gssgfbull.S7-II.3.308
Durand-Delga M (1968) Coup d'oeil sur les unités malaguides des Cordillères Bétiques. Comptes Rendus de l'Académie des Sciences Paris 266:190–193.
Eeckhout BvD, Konert G (1983) Plagioclase porphyroblast growth and its relation to the Alhamilla unit (Sierra Alhamilla, Betic Cordilleras, SE Spain). Journal of Metamorphic Geology 1:227–249. https://doi.org/10.1111/j.1525-1314.1983.tb00273.x
Egeler CG, Simon OJ, (1969) Sur la tectonique de la zone bétique (Cordillères Bétiques, Espagne). Etude basée sur la recherche dans le secteur compris entre Almería et Vélez Rubio. Verhandelingen der Koninklijke Nederlandse Akademie van Wetenschappen Afh Natuurkunde 25–3:1–90.
Essene EJ (1989) The current status of thermobarometry in metamorphic rocks. In: Daly JS, Cliff RA, Yardley BWD (eds) Evolution of Metamorphic Belts, Geological Society London Special Publication 43:1–44. https://doi.org/10.1144/GSL.SP.1989.043.01.02
Esteban JJ, Cuevas J, Tubía JM, Gutiérrez-Alonso, Larionov A, Sergeev S, Hofmann M (2017) U–Pb detrital zircon ages from the Paleozoic Marbella Conglomerate of the Malaguide Complex (Betic Cordilleras, Spain). Implications on Paleotethyan evolution. Lithos 290–291:34-47. https://doi.org/10.1016/j.lithos.2017.07.022
Esteban JJ, Cuevas J, Tubía JM, Sergeev S, Larionov A (2011a) A revised Aquitanian age for the emplacement of the Ronda peridotites (Betic Cordilleras, southern Spain). Geological Magazine 48:183–187. https://doi.org/10.1017/S0016756810000737
Esteban JJ, Sánchez-Rodríguez L, Seward D, Cuevas J, Tubía JM (2004) The late thermal history of the Ronda area, southern Spain. Tectonophysics 398:81–92. https://doi.org/10.1016/j.tecto.2004.07.050
Esteban JJ, Tubía JM, Cuevas J, Vegas N, Sergeev S, Larionov A (2011b) Peri-Gondwanan provenance of pre-Triassic metamorphic sequences in the western Alpujarride nappes (Betic Cordillera, southern Spain). Gondwana Research 20:443–449. https://doi.org/10.1016/j.gr.2010.11.006
Esteban JJ, Tubía JM, Cuevas J, Seward D, Larionov A Sergeev S, Navarro-Vilá F (2013) Insights into extensional events in the Betic Cordilleras, southern Spain: New fission-track and U–Pb SHRIMP analyses. Tectonophysics 603:179–188. https://doi.org/10.1016/j.tecto.2013.05.027
Estévez A, Pérez-Lorente F (1974) Estudio geológico del sector de Cáñar-Soportújar, vertiente meridional de Sierra Nevada. Estudios Geológicos 30:515–541.
Fallot P (1948) Les Cordillères Bétiques. Estudios Geológicos 8:83–172.
Fernández-Fernández EM, Jabaloy-Sánchez A, Nieto F, González-Lodeiro F (2007) The structure of the Maláguide Complex near Vélez Rubio (Eastern Betic Cordillera, SE Spain). Tectonics 26:TC4008. https://doi.org/10.1029/2006tc002019.
Foucault A, Paquet J (1971). Sur l'importance d'une tectogénèse hercynienne dans la région centrales des Cordilléres bétiques (S de la sierra Arana, prov. de Grenade, Espagne). Comptes Rendus de l'Académie des Sciences Paris 272:2756–2758.
Frasca G, Gueydan F, Poujol M, Brun JP, Parat F, Monié P, Pichat A, Mazier S (2017) Fast switch from extensional exhumation to thrusting of the Ronda Peridotites (South Spain). Terra Nova 29:117–126. https://doi.org/10.1111/ter.12255
Gálvez R, Orozco M (1979) Strain determinations using deformed Radiolaria; Malaguide Complex, southern Spain. Acta Geologica Hispanica, 14:129–134. https://core.ac.uk/download/pdf/39071354.pdf
Gálvez R, Orozco M (1980) Estructuras de superposición complejas en la Cordillera Bética (Región de los Montes de Málaga). Boletin Geológico y Minero, 91:697–704.
García-Casco A (1993) Evolución metamórfica del Complejo Gneísico de Torrox y series adyacentes (Alpujárrides centrales). PhD Thesis Universidad de Granada 456 p. http://hdl.handle.net/10481/28865.
García-Casco A, Sanchez-Navas A, Torres-Roldán RL (1993) Disequilibrium decomposition and breakdown of muscovite in high PT gneisses, Betic alpine belt (southern Spain). American Mineralogist 78:158–177. http://www.minsocam.org/ammin/AM78/AM78_158.pdf
García-Casco A, Torres-Roldán RL (1996) Disequilibrium Induced by Fast Decompression in St-Bt-Grt-Ky-Sil-And Metapelites from the Betic Belt (southern Spain). Journal of Petrology 37:1207–1240. https://doi.org/10.1093/petrology/37.5.1207
García-Casco A, Torres-Roldán RL (1999) Natural metastable reactions involving garnet, staurolite and cordierite: Implications for petrogenetic grids and the extensional collapse of the Betic-Rif Belt. Contributions to Mineralogy and Petrology 136:131–153. https://link.springer.com/article/10.1007/s004100050528
García-Dueñas V, Martínez-Martínez JM, Orozco M, Soto JI (1988a) Plis-nappes, cisaillements syn- à postmétamorphiques et cisaillements ductiles-fragiles en distension dans les Nevado-Filabres (Cordillères Bétiques, Espagne). Comptes Rendus de l'Académie des Sciences Paris 307:1389–1395.
García-Dueñas V, Martínez-Martínez JM, Soto JI (1988b) Los Nevado-Filábrides, una pila de pliegue-mantos separados por zonas de cizalla. II Congreso Geológico de España Simposios Granada 17–26.
García-López S, Rodríguez-Cañero R, Sanz-López J, Sarmiento G, Valenzuela-Ríos JI (1996) Conodontos y episodios carbonatados en el Silúrico de la Cadena Hercinica meridional y del Dominio Sahariano. Revista Española de Paleontología N° Extraordinario:33–57. https://eprints.ucm.es/29918/1/03. Garci-a-Lo-pez et al.pdf

Geel T (1973) The geology of the Betic of Málaga, the Subbetic and the zone between these two units in the Vélez Rubio area (southern Spain). GUA Papers of Geology Series 1 5:1–181.

Gómez-Pugnaire MT (1981) Evolución del metamorfismo alpino en el Complejo Nevado-Filábride de la Sierra de Baza (Cordilleras Béticas, España). Tecniterrae 41:1–130.

Gómez-Pugnaire MT, Braga JC, Martín JM, Sassi FP, del Moro A (2000) Regional implications of a Palaeozoic age for the Nevado-Filabride cover of the Betic Cordillera, Spain. Schweizerische Mineralogische und Petrographische Mitteilungen 80:45–52. http://doi.org/10.5169/seals-60949

Gómez-Pugnaire MT, Cámara F (1990) La asociación de alta presión distena + talco + fengita coexistente con escapolita en metapelitas de origen evaporítico (Complejo Nevado-Filábride, Cordilleras Béticas). Revista de la Sociedad Geológica de España 3:373–384. http://www.sociedadgeologica.es/archivos/REV/3(3-4)/Art11.pdf

Gómez-Pugnaire MT, Chacón J, Mitrofanov F, Timofeev V (1982) First report on pre-Cambrian rocks in the graphite-bearing series of the Nevado-Filábride Complex (Betic Cordilleras, Spain). Neues Jahrbuch für Geologie und Palaeontologie Monatshefte 3:176–180.

Gómez Pugnaire MT, Franz G (1988) Metamorphic evolution of the Palaeozoic series of the Betic Cordilleras (Nevado-Filábride complex SE Spain) and its relationship with the Alpine orogeny. Geologische Rundschau 77:619–640. https://link.springer.com/article/10.1007/BF01830174

Gómez-Pugnaire MT, Franz G, López Sánchez-Vizcaíno V (1994) Retrograde formation of NaCl-scapolite in high pressure metaevaporites from the Cordilleras Béticas (Spain). Contributions to Mineralogy and Petrology 116:448–461. https://link.springer.com/article/10.1007/BF00310911

Gómez-Pugnaire MT, Galindo-Zaldívar J, Rubatto D, González-Lodeiro F, López Sánchez-Vizcaíno V, Jabaloy A (2004) A reinterpretation of the Nevado-Filábride and Alpujárride Complex (Betic Cordillera): field, petrography and U-Pb ages from orthogneisses western Sierra Nevada, S Spain. Schweizerische Mineralogische und Petrographische Mitteilungen 84:303–322. https://hdl.handle.net/1885/35845

Gómez-Pugnaire M, Muñoz M (1991) Al-rich xenoliths in the Nevado-Filabride metabasites; evidence for a continental setting of this basic magmatism in the Betic Cordilleras (SE Spain). European Journal of Mineralogy 3:193–198. https://doi.org/10.1127/ejm/3/1/0193

Gómez-Pugnaire MT, Rubatto D, Fernández-Soler JM, Jabaloy A, López Sánchez- Vizcaíno V, González-Lodeiro F, Galindo-Zaldívar J, Padrón-Navarta JA (2012) U–Pb geochronology of Nevado–Filábride gneisses: evidence for the Variscan nature of the deepest Betic complex (SE Spain). Lithos 146–147:93-111. https://doi.org/10.1016/j.lithos.2012.03.027

Gómez-Pugnaire MT, Sassi FP (1983) Pre-Alpine metamorphic features and alpine overprints in some parts of the Nevado-Filabride basement (Betic Cordilleras, Spain). Memorie di Scienze Geologiche 36:49–72.

González-Casado JM, Casquet C, Martínez-Martínez JM, García-Dueñas V (1995) Retrogade evolution of quartz segregations from the Dos Picos shear zone in the Nevado-Filabride Complex (Betic chains, Spain); evidence from fluid inclusions and quartz c-axis fabrics. Geologische Rundschau 84:175–186. https://link.springer.com/article/10.1007/BF00192249

González-Jiménez JM, Marchesi C, Griffin WL, Gervilla F, Belousova EA, Garrido CJ, Romero R, Talavera C, Leisen M, O'Reilly SY, Barra F, Martin L (2017) Zircon recycling and crystallization during formation of chromite- and Ni-arsenide ores in the subcontinental lithospheric mantle (Serranía de Ronda, Spain). Ore Geology Reviews 90:193–209. https://doi.org/10.1016/j.oregeorev.2017.02.012

Guerrera F, Martín-Algarra A, Perrone V (1993) Late Oligocene-Miocene syn- late-orogenic successions in Western and Central Mediterranean Chains from the Betic Cordillera to the Southern Apennines. Terra Nova 5:525–544. https://doi.org/10.1111/j.1365-3121.1993.tb00302.x

Gueydan F, Pitra P, Afiri A, Poujol M, Essaifi A, Paquette JL (2015) Oligo- Miocene thinning of the Beni Bousera peridotites and their Variscan crustal host rocks, Internal Rif, Morocco. Tectonics 34:1244–1268. https://doi.org/10.1002/2014TC003769

Hammerli J, Kemp AIS, Spandler C (2014) Neodymium isotope equilibration during crustalmetamorphism revealed by in situ microanalysis of REE-rich accessory minerals. Earth and Planetary Science Letters 392:133–142. https://doi.org/10.1016/j.epsl.2014.02.018

Henningsen D, Herbig HG (1990) Die karbonischen Grauwacken der Malagiden und Menorcas im Vergleich (Betische Kordillere und Balearen, Spanien). Zeitschrift der Deutschen Geologischen Gesellschaft 141:13–29. https://www.schweizerbart.de/papers/zdgg_alt/detail/141/54507

Hermes J (1966) Tintinnids from the Silurian of the Betic Cordilleras, Spain. Revue de Micropaléontologie 8:211–214.

Herbig HG (1983) El Carbonífero de las Cordilleras Béticas. In: Díaz M (ed) Carbonífero y Pérmico de España X Congreso Internacional de Estratigrafía y Geología del Carbonífero Madrid 343–356.

Herbig HG (1984) Rekonstruktion eines nicht mehr existenten Sedimentations-Raums: die Kalk-Gerölle im Karbon Flysch der Malagiden (Betische Kordillere, Südspanien). Facies 11:1–108. https://link.springer.com/article/10.1007/BF02536907

Herbig HG (1985) An Upper Devonian limestone slide block near Marbella (Betic Cordillera, Southern Spain) and the palaeogeographic relations between Malaguides and Menorca. Acta Geologica Hispanica 20:155–178. http://revistes.ub.edu/index.php/ActaGeologica/article/view/4397/5484

Herbig HG (1986) Rugosa und Heterocorallia aus Obervise Geröllen der Marbella Formation (Betische Kordillere, Suedspanien). Palaeontogische Zeitschrift 60:189–225. https://link.springer.com/article/10.1007/BF02985668

Herbig HG (1992) Carboniferous paleogeography of the West-Mediterranean Paleotethys. Comptes Rendus Onzième Congrès International de Stratigraphie et de Géologie du Carbonifère, Bejing 1987, 4 (1989), 186–196; Nanjing.

Herbig HG, Mamet B. (1985) Stratigraphy of limestone boulder, Marbella Formation (Betic Cordillera, southern Spain). Comptes Rendus Dixième Congrès International de Stratigraphie et de Géologie du Carbonifère Madrid 1983 1:199–212.

Herbig HG, Statteger K (1989) Late Palaeozoic heavy mineral and clast modes from the Betic Cordillera (southern Spain): transition from a passive to an active continental margin. Sedimentary Geology 63:93–108. https://doi.org/10.1016/0037-0738(89)90073-0

Holdaway MJ (1971) Stability of andalusite and the alumino-silicate phase diagram. American Journal of Science 271:97–131. http://www.ajsonline.org/content/271/2/97.full.pdf

Jabaloy-Sánchez A (1993) La estructura de la región occidental de la Sierra de los Filabres (Cordilleras Béticas). PhD Thesis Universidad de Granada. Monografica Tierras del Sur 9:1–200. https://doi.org/10.1016/j.lithos.2005.06.008

Jabaloy-Sánchez A, Gómez-Pugnaire MT, Padrón-Navarta JA, López Sánchez-Vizcaíno V, Garrido CJ (2015) Subduction- and exhumation-related structures preserved in metaserpentinites and associated metasediments from the Nevado–Filábride Complex (Betic Cordillera, SE Spain). Tectonophysics 644–645:40–57. https://doi.org/10.1016/j.tecto.2014.12.022

Jabaloy-Sánchez A, Talavera C, Gómez-Pugnaire MT, López Sánchez-Vizcaíno V, Vázquez-Vílchez M, Rodríguez-Peces MJ, Evans NJ (2018) U-Pb ages of detrital zircons from the Internal

Betics: a key to deciphering paleogeographic provenance and tectono-stratigraphic evolution. Lithos 318–319:244–266. https://doi.org/10.1016/j.lithos.2018.07.026

Janots E, Negro F, Brunet F, Goffè B, Engi M, Bouybaouene ML (2006) Evolution of the REE mineralogy in HP-LT metapelites of the Sebtides complex, Rif, Morocco: Monazite stability and geochronology, Lithos 87:214–234. https://doi.org/10.1016/j.lithos.2005.06.008

Kampschuur W (1975) Data on thrusting and metamorphism in the eastern Sierra de los Filabres: Higher Nevado-Filabride unitsand the glaucophanictoc greenschists facies. Tectonophysics 27:51–81. https://doi.org/10.1016/0040-1951(75)90048-7

Kirchner KL, Behr WM, Loewy S, Stockli DF (2016) Early Miocene subduction in the western Mediterranean: Constraints from Rb-Sr multimineral isochron geochronology. Geochemistry Geophysics Geosystems 17:1842–1860. https://doi.org/10.1002/2015gc006208.

Kockel F (1959) Conodontos del Paleozoico de Málaga. Notas y Comunicaciones del Instituto Geológico y Minero de España 53:149–164.

Kockel F (1964) Die Geologie des Gebietes zwischen dem Río Guadalhorce und dem Plateau von Ronda (Südspanien). Geologisches Jahrbuch 81:413–480.

Kockel F, Stoppel D (1962) Nuevos hallazgos de conodontos y algunos cortes en el Palaeozoico de Málaga (Sur de España). Notas y Comunicaciones del Instituto Geológico y Minero de España 68:133–170.

Laborda-López C, Aguirre J, Donovan SK (2015a) Surviving metamorphism: taphonomy of fossil assemblages in marble and calc-silicate schist. Palaios 30:668–679. http://dx.doi.org/10.2110/palo.2015.013

Laborda-López C, Aguirre J, Donovan SK, Navas-Parejo P, Rodríguez S (2015b) Fossil assemblages and biochronology of metamorphic carbonates of the Nevado-Filábride Complex from the Águilas tectonic arc (SE Spain). Spanish Journal of Palaeontology 30:275–292. https://core.ac.uk/download/pdf/33108856.pdf

Lafuste MLJ, Pavillon MJ (1976) Mise en évidence d'Eifélien daté au sein des terrains métamorphiques des zones internes des Cordillères bétiques. Intérêt de ce nouveau repère stratigraphique. Comptes Rendus de l'Académie des Sciences Paris II 283:1015–1018.

Leine L (1968) Rauhwackes in the Betic Cordilleras, Spain: Nomenclature, description and genesis of weathered carbonate breccias of tectonics origin. PhD Thesis University of Amsterdam 112 p.

Lonergan L, Platt JP (1995) The Malaguide-Alpujarride boundary: a major extensional contact in the Internal Zone of the eastern Betic Cordillera, SE Spain. Journal of Structural Geology 17:1655–1671. https://doi.org/10.1016/0191-8141(95)00070-T

Loomis TP (1972) Diapiric emplacement of the Ronda high-temperature ultramafic intrusion, Southern Spain. Geological Society of America Bulletin 83:2475–2496. https://doi.org/10.1130/0016-7606(1972)83[2475:DEOTRH]2.0.CO;2

Loomis TP (1975) Tertiary mantle diapirism, orogeny and plate tectonic east of Strait of Gibraltar. American Journal of Science 275:1–30. https://doi.org/10.2475/ajs.275.1.1

López Sánchez-Vizcaíno V, Rubatto D, Gómez-Pugnaire MT, Trommsdorff V, Müntener O (2001) Middle Miocene high-pressure metamorphism and fast exhumation of the Nevado–Filábride Complex, SE Spain. Terra Nova 13:327–332. https://doi.org/10.1046/j.1365-3121.2001.00354.x

López Sánchez-Vizcaíno V, Franz G, Gómez-Pugnaire MT, (1995) The behaviour of Cr during metamorphism of carbonate rocks from the Nevado-Filabride Complex, Betic Cordilleras, Spain. Canadian Mineralogist 33:85–104. https://doi.org/10.1046/j.1365-3121.2001.00354.x

Lozano-Rodríguez JA (2018) Estudio petrológico, geoquímico y geocronológico comparado de las ofiolitas de la Sierra de baza con otras ofiolitas béticas. PhD Thesis University of Granada. http://digibug.ugr.es/handle/10481/54877

Lundeen M (1978) Emplacement of the Ronda Peridotite, Sierra Bermeja, Spain. Geological Society of America Bulletin 89:172–180. https://doi.org/10.1130/0016-7606(1978)89<172:EOTRPS>2.0.CO;2

Mamet BL, Herbig HG (1990) The algae *Pseudodonezella* n. gen. and *Eovelebitella occitanica* Vachard, 1974 from Southern Spain (Carboniferous, Betic Cordillera). Revista Española de Micropaleontología 22:199–211.

Manjón-Cabeza Córdoba A, García-Casco A, Sánchez- Navas A, Martín-Algarra A (2014) Evidencias de metamorfismo policíclico (pre-Alpino y Alpino) en granates de metapelitas de la Unidad de Tejeda (Alpujárride Intermedio, Cordillera Bética). Revista de la Sociedad Geológica de España 27:327–336. http://www.sociedadgeologica.es/archivos/REV/27(1)/art21_327-336%20RSGE27_1.pdf

Martín-Algarra A (1987) Evolución Geológica Alpina del Contacto Entre las Zonas Internas y la Zonas Externas de la Cordillera Bética. PhD Thesis Universidad de Granada 1171 p.

Martín-Algarra A, Estévez A (1984) La Brèche de la Nava; dépôt continental synchrone de la structuration pendant le Miocène inférieur des zones internes de l'ouest des Cordillères Bétiques. Comptes Rendus de l'Académie des Sciences Paris, 299:463–466.

Martín-Algarra A, Rodríguez-Cañero R, O'Dogherty L, Sánchez-Navas A, Ruiz-Cruz MD (2004) Complejo Maláguide. Estratigrafía. Paleozoico ¿y más antiguo? (Grupo Piar). In: Vera JA (ed) Geología de España SGE-IGME Madrid 401–404.

Martín-Algarra A, Mazzoli S, Perrone V, Rodríguez-Cañero R, Navas-Parejo P (2009a) Variscan tectonics in the Malaguide Complex (Betic Cordillera, Southern Spain): stratigraphic and structural Alpine versus Pre-Alpine constraints from the Ardales Area (Province of Málaga). I. Stratigraphy. Journal of Geology 117:241–262. https://doi.org/10.1086/597364

Martín-Algarra A, Mazzoli S, Perrone V, Rodríguez-Cañero R (2009b) Variscan tectonics in the Malaguide Complex (Betic Cordillera, Southern Spain): stratigraphic and structural Alpine versus Pre-Alpine constraints from the Ardales Area (Province of Málaga). II. Structure. Journal of Geology 117:263–284. https://doi.org/10.1086/597365

Martín-Algarra, A. Messina A, Perrone V, Russo S, Maate A, Martín-Martín M (2000) A lost realm in the internal domains of the Betic-Rif orogen (Spain and Morocco). Evidence from conglomerates and consequences for alpine geodinamic evolution. Journal of Geology 108:447–467. https://doi.org/10.1086/314410

Martín-Algarra A, Solé de Porta N, Maate A (1995) El Triásico del Maláguide-Gomáride (Formación Saladilla, Cordillera Bética Occidental y Rif Septentrional). Nuevos datos sobre su edad y significado paleogeográfico. Cuadernos de Geología Ibérica 19:249–278. http://revistas.ucm.es/index.php/CGIB/article/view/CGIB9595110249A/2563

Martínez-Martínez JM (1986) Evolución tectono-metamórfica del Complejo Nevado-Filábride en el sector entre Sierra Nevada y Sierra de los Filabres (Cordilleras Béticas). Cuadernos de Geología Universidad de Granada 13:1–194.

Martínez-Martínez JM, Soto JI, Balanyá JC (2002) Orthogonal folding of extensional detachments: structure and origin of the Sierra Nevada elongated dome (Betics, SE Spain). Tectonics 21. https://doi.org/10.1029/2001tc001283.

Martínez-Martínez JM, Torres-Ruiz J, Pesquera A, Gil-Crespo PP (2010) Geological relationships and U-Pb zircon and 40 Ar/39Ar tourmaline geochronology of gneisses and tourmalinites from the Nevado–Filabride complex (western Sierra Nevada, Spain): tectonic implications. Lithos 119:238–250. https://doi.org/10.1016/j.lithos.2010.07.002

Massonne HJ (2014) Wealth of P-T-t information in medium-high grade metapelites: Example from the Jubrique Unit of the Betic Cordillera, S Spain. Lithos 208–209:137-157. https://doi.org/10.1016/j.lithos.2014.08.027

Massonne HJ, Schreyer W (1987) Phengite geobarometry based on limiting assemblage with K-feldspar, phlogopite and quartz. Contributions to Mineralogy and Petrology 96:212–224. https://link.springer.com/article/10.1007/BF00375235

Massonne HJ, Szpurka Z (1997) Thermodynamic properties of white micas on the basis of high-pressure experiments in the systems K_2O-MgO-Al_2O_3-SiO_2-H_2O and K_2O-FeO-Al_2O_3-SiO_2-H_2O. Lithos 41:229–250. https://doi.org/10.1016/S0024-4937(97)82014-2

Mayoral EJ, Gámez Vintaned JA, Diez, JB, Liñán E (2018) Carboniferous trace fossils from Vélez-Málaga (Maláguide Complex, Betic Cordillera, SE Spain). Spanish Journal of Palaeontology 33:89–104. www.sepaleontologia.es/revista/anteriores/SJP (2018) vol. 33/vol. 1/5 Mayoral et al (web).pdf

Mazzoli S, Martín-Algarra A (2011) Deformation partitioning during transpressional emplacement of a "mantle extrusion wedge": the Ronda peridotites, western Betic Cordillera, Spain. Journal of the Geological Society London 168:373–382. https://doi.org/10.1144/0016-76492010-126

Mazzoli S, Martín-Algarra A, Reddy SM, López Sánchez-Vizcaíno V, Fedele L, Noviello A (2013) The evolution of the footwall to the Ronda subcontinental mantle peridotites: insights from the Nieves Unit (western Betic Cordillera). Journal of the Geological Society (London) 170:385–402. https://doi.org/10.1144/jgs2012-105

Michard A, Goffé B, Bouybaouenne ML, Saddiqi O (1997) Late Hercynian–Mesozoic thinning in the Alboran domain; metamorphic data from the northern Rif, Morocco. Terra Nova 9:171–174. https://doi.org/10.1046/j.1365-3121.1997.d01-24.x

Michard A, Negro F, Saddiqi O, Bouybaouene ML, Chalouan A, Montigny R, Goffé B (2006) Pressure–temperature–time constraints on the Maghrebide mountain building: evidence from the Rif–Betic transect (Morocco, Spain), Algerian correlations, and geodynamic implications. Comptes Rendus de l'Académie des Sciences Paris II 338:92–114. https://doi.org/10.1016/j.crte.2005.11.011

Mon R (1971) Estudio geológico del extremo occidental de los Montes de Málaga y de la sierra de Cártama (prov. de Málaga). Boletín Geológico y Minero 82:132–146.

Monié P, Galindo-Zaldívar J, González-Lodeiro F, Goffé B, Jabaloy A (1991) $^{40}Ar/^{39}Ar$ geochronology of Alpine tectonism in the Betic Cordilleras (southern Spain). Journal of the Geological Society London 148:288–297. https://jgs.lyellcollection.org/content/jgs/148/2/289.full.pdf

Monié P, Torres Roldan RL, García Casco A (1994) Cooling and exhumation of the Western Betic Cordilleras, $^{40}Ar/^{39}Ar$ thermochronological constraints on a collapsed terrane. Tectonophysics 238:353–379. https://doi.org/10.1016/0040-1951(94)90064-7

Montel JM, Kornprobst J, Vielzeuf D (2001) Preservation of old U–Th–Pb ages in shielded monazite; example from the Beni Bousera Hercynian kinzigites (Morocco). Journal of Metamorphic Geology 18:335–342. https://doi.org/10.1046/j.1525-1314.2000.00261.x

Morten L, Bargossi GM, Martínez-Martínez JM, Puga E, Díaz de Federico A (1987) Metagabbro and associated eclogites in the Lubrin area, Sierra Nevada Complex, Spain. Journal of Metamorphic Geology 5:155–174. https://doi.org/10.1111/j.1525-1314.1987.tb00377.x

Morten L, Puga E (1984) Blades of olivines and orthopyroxenes in ultramafic rocks from the Cerro del Almirez, Sierra Nevada Complex, Spain: relics of quench-textured harzburgites. Neues Jahrbuch für Mineralogie Monatshefte 5:211–218.

Morillon AC, Bourgois J, Poupeau G, Sosson M (1996) Exhumation au Miocène inférieur des unités Alpujarrides de Los Reales et d'Ojen (Cordillères bétiques, Espagne) à partir de l'étude des traces de fission sur apatites. Comptes Rendus de l'Académie des Sciences Paris 322:885–891.

Navas-Parejo P (2012) Paleozoic stratigraphy and palaeogeography of the Malaguide Complex (Betic Cordillera) and other Western Mediterranean related domains (Calabria-Peloritani Terrane). PhD Thesis Universidad de Granada 235 p. http://digibug.ugr.es/bitstream/handle/10481/23780/21454292.pdf

Navas-Parejo P, Rodríguez-Cañero R, Martín-Algarra A (2008) Conodontos del Carbonífero maláguide en Vélez Rubio (Cordillera Bética, SE Spain). Geo-Temas 10:1273–1276.

Navas-Parejo P, Rodríguez-Cañero R, Somma R, Martín-Algarra A, Perrone V (2009a) The Frasnian Upper Kellwasser event and a lower Famennian stratigraphic gap in Calabria (southern Italy). Palaeobiodiversity and Palaeoenvironments 89:111–118. https://link.springer.com/article/10.1007/s12549-009-0006-4

Navas-Parejo P, Somma R, Martín-Algarra A, Perrone V, Rodríguez--Cañero R (2009b) First record of Devonian Orthoceratid-bearing limestones in Southern Calabria (Italy). Comptes Rendus Palevol 8:365–373. https://doi.org/10.1016/j.crpv.2009.01.001

Navas-Parejo P, Martín-Algarra A, Martínez-Pérez C (2011) Primeros datos sobre la presencia de conodontos del Emsiense (Devónico Inferior) en el Complejo Maláguide de la provincia de Granada. Paleontologia i Evolució Memòria especial 5:425–429.

Navas-Parejo P, Martín-Algarra A, Rodríguez-Cañero R (2012a) Conodontos del Carbonífero en el Complejo Maláguide de la región de Ardales (Cordillera Bética occidental). In: Martínez-Pérez C, Furió M, Santos-Cubedo A, Poza B. (eds) Paleodiversity and Paleoecology of Iberian Ecosystems, Sot de Chera (Valencia), X EJIP (Encuentro de Jóvenes Investigadores en Paleontología), Book of Abstracts/Libro de Resúmenes 52–54.

Navas-Parejo P, Rodríguez-Cañero R, Martín-Algarra A (2012b) Primer registro de un horizonte estratigráfico hemipelágico con conodontos del Carbonífero Superior en el Complejo Maláguide (Cordillera Bética oriental). Geogaceta 52:81–84. http://www.sociedadgeologica.es/archivos/geogacetas/geo52/art20.pdf

Navas-Parejo P, Somma R, Martín-Algarra A, Rodríguez-Cañero R, Perrone V (2015a) Conodont-based stratigraphy in the Devonian of the SerreMassif (southern Italy). Stratigraphy 12:1–21. http://www.micropress.org/microaccess/stratigraphy/issue-316/article-1925

Navas-Parejo, P, Rodríguez-Cañero R, Martín-Algarra A (2015b) New conodont data from a Devonian-Carboniferous succession in the central sector of the Betic Cordillera (SE Spain). Spanish Journal of Palaeontology 30:133–145. https://www.sepaleontologia.es/revista/anteriores/REP%20%282015%29%20vol.%2030/11%20Navas-Parejo%20et%20al%20color%20web-.pdf

Negro F, Beyssac O, Goffé B, Saddiqi O, Bouybaouène ML (2006) Thermal structure of the Alboran Domain in the Rif (northern Morocco) and the Western Betics (southern Spain). Constraints from Raman spectroscopy of carbonaceous material. Journal of Metamorphic Geology 24:309–327. https://doi.org/10.1111/j.1525-1314.2006.00639.x

Nieto JM (1996) Petrología y geoquímica de los ortogneises del Complejo del Mulhacén, Cordilleras Béticas. PhD Thesis Universidad de Granada 211 p.

Nieto JM, Puga E, Díaz de Federico A (2000) Late Variscan pyroclastic rocks from the Mulhacén Complex (Betic Cordillera, Spain). In: Leyrit H, Montenat Ch (eds) Volcaniclastic Rocks, from magmas to sediments. Gordon and Breach Science Publishers Amsterdam 217–234.

Nijhuis HJ (1964) Plurifacial Alpine Metamorphisn in the Southeastern Sierra de los Filabres South of Lubrín, SE Spain. PhD Thesis University of Amsterdam 151 p.

O'Dogherty L, Rodríguez-Cañero R, Gursky HJ, Martín-Algarra A, Caridroit M (2000) New data on Lower Carboniferous stratigraphy and palaeogeography of the Malaguide Complex (Betic Cordillera,

southern Spain). Comptes Rendus de l'Académie des Sciences Paris IIa 331:1–9. https://doi.org/10.1016/S1251-8050(00)01455-5

Orozco M, Gálvez R (1979) The development of folds in bedded chert and related rocks in the Malaguide Complex, southern Spain. Tectonophysics 56:277–295. https://doi.org/10.1016/0040-1951(79)90086-6

Orozco M, Molina JM, Crespo-Blanc A, Alonso-Chaves FM (1999) Palaeokarst and rauhwacke development, mountain uplift and subaerial sliding of tectonic sheets (northern Sierra de los Filabres, Betic Cordilleras, Spain). Geologie en Mijnbouw 78:103–117. https://link.springer.com/article/10.1023/A:1003610431688

Pearson DG, Nowell GM (2004) Re-Os and Lu-Hf Isotope Constraints on the Origin and Age of Pyroxenites from the Beni Bousera Peridotite Massif: Implications for Mixed Peridotite-Pyroxenite Mantle Sources. Journal of Petrology 45:439–455. https://doi.org/10.1093/petrology/egg102

Peyre Y (1974) Géologie d'Antequera et de sa région (Cordillères Bétiques, Espagne). PhD Thesis Université de Paris 528 p.

Platt JP, Argles TW, Carter A, Kelley SP, Whitehouse MJ, Lonergan L (2003) Exhumation of the Ronda peridotite and its crustal envelope: constraints from thermal modelling of a P–T–time array. Journal of the Geological Society London 160:655–676. https://doi.org/10.1144/0016-764902-108

Platt JP, Behr WM, Johanesen K, Williams JR (2013) The Betic-Rif arc and its Orogenic Hinterland: A review. Annual Review of Earth and Planetary Science 41:313–357. https://doi.org/10.1146/annurev-earth-050212-123951

Platt JP, Kelley SP, Carter A, Orozco M (2005) Timing of tectonic events in the Alpujárride Complex, Betic Cordillera, southern Spain. Journal of the Geological Society (London) 162, 451–462. https://doi.org/10.1144/0016-764903-039

Platt JP, Anczkiewicz R, Soto JI, Kelley SP, Thirlwall M (2006) Early Miocene continental subduction and rapid exhumation in the western Mediterranean. Geology 34:981–984. https://doi.org/10.1130/G22801A.1

Platt JP, Whitehouse MJ (1999) Early Miocene high-temperature metamorphism and rapid exhumation in the Betic Cordillera (Spain): evidence from U-Pb zircon ages. Earth and Planetary Science Letters 171:591–605. https://doi.org/10.1016/S0012-821X(99)00176-4

Précigout J, Gueydan F, Garrido CJ, Cogné N, Booth-Rea G (2013) Deformation and exhumation of the Ronda peridotite (Spain). Tectonics 32:1011–1025. https://doi.org/10.1002/tect.20062

Priem HNA, Boelrijk NAIM, Hebeda EH, Oen IS, Verdurmen EAT, Verschure RH (1979) Isotopic dating of the emplacement of the ultramafic masses in the Serrania de Ronda. Contributions to Mineralogy and Petrology 70:103–109. https://link.springer.com/article/10.1007/BF00371876

Puchelt H, Emmermann R (1976) Bearing of rare earth patterns of apatites from igneous and metamorphic rocks. Earth and Planetary Science Letters 31:279–286. https://doi.org/10.1016/0012-821X(76)90220-X

Puga E (1971) Investigaciones petrológicas en Sierra Nevada Occidental. PhD Thesis Universidad de Granada 269 p.

Puga E (1977) Sur l'existence dans le complexe de la Sierra Nevada (Cordillère Bétique, Espagne du sud) d'éclogites et sur leur origine probable à partir d'une croûte océanique mésozoique. Comptes Rendus de l'Académie des Sciences Paris 285:379–1382.

Puga E (1990) The Betic Ophiolitic Association (Southeastern Spain). Ofioliti 15:97–117.

Puga E, Díaz de Federico A (1976) Metamorfismo polifásico y deformaciones alpinas en el Complejo de Sierra Nevada (Cordilleras Béticas). Implicaciones geodinámicas. In: Reunión sobre la Geodinámica de la Cordillera Bética y del Mar de Alborán, Secretariado de Publicaciones Universidad de Granada 79–114.

Puga E, Díaz de Federico A, Fontbote, JM (1974) Sobre la individualización y sistematización de las unidades profundas de la Zona Bética. Estudios Geológicos 30:543–548.

Puga E, Fontboté JM, Martín-Vivaldi JL (1975) Kyanite pseudomorphs after andalusite in polymetamorphic rocks of Sierra Nevada (Betic Cordillera, Southern Spain). Schweizerische Mineralogische und Petrographische Mitteilungen 55:227–241.

Puga E, Díaz de Federico A, Bargossi GM, Morten L (1989a) The Nevado–Filabride metaophiolitic association in the Cóbdar region (Betic Cordillera, SE Spain): preservation of pillow structures and development of coronitic eclogites. Geodinamica Acta 3:17–36. https://doi.org/10.1080/09853111.1989.11105172

Puga E, Díaz de Federico A, Fediukova E, Bondi M, Morten L (1989b) Petrology, geochemistry and metamorphic evolution of the ophiolitic eclogites and related rocks from the Sierra Nevada (Betic Cordilleras, Southeastern Spain), Schweizerische Mineralogische und Petrographische Mitteilungen 69:435–455.

Puga E, Díaz de Federico A, Demant A (1995) The eclogitized pillows of the Betic Ophiolitic Association: relics of the Tethys ocean floor incorporated to the Alpine Chain after subduction. Terra Nova 7:32–43. https://doi.org/10.1111/j.1365-3121.1995.tb00665.x

Puga E, Nieto JM, Diaz de Federico A, Portugal E, Reyes E (1996) The intra-orogenic Soportujar Formation of the Mulhacén Complex; evidence for the polyciclic character of the Alpine orogeny in the Betic Cordilleras. Eclogae Geologicae Helvetiae 89:129–162.

Puga E, Bodinier JL, Díaz de Federico A, Morten L, Nieto JM (1997) Pseudo-spinifex meta-ultramafic rocks containing eclogitized rodingite dykes in the Betic Ophiolitic Association (SE Spain): evidence of Alpine subduction following an ocean-floor metasomatic process. Quaderni di Geodinamica Alpina e Quaternaria 4, 98–99.

Puga E, Nieto JM, Díaz de Federico A, Bodinier JL, Morten L (1999) Petrology and metamorphic evolution of ultramafic rocks and dolerite dykes of the Betic Ophiolitic Association (Mulhacén Complex, SE Spain): evidence of Eo-Alpine subduction following an ocean-floor metasomatic process. Lithos 49:107–140. https://doi.org/10.1016/S0024-4937(99)00035-3

Puga, E., Díaz de Federico, A. y Nieto, J.M. (2002): Tectonostratigraphic subdivision and petrological characterization of the deepest complexes of the Betic one: a review. Geodinamica Acta 15:23–43. https://doi.org/10.1080/09853111.2002.10510737

Puga E, Díaz de Federico A, Martín-Algarra A, González-Lodeiro F, Estévez A, Jabaloy A (2004). Complejo Nevado-Filábride. Sucesiones litológicas y petrología. In: Vera JA (ed) Geología de España SGE-IGME Madrid 424–427.

Puga E, Fanning CM, Nieto JM, Díaz de Federico A (2005) New recrystallisation textures in zircons generated by ocean-floor and eclogite facies metamorphism: a cathodoluminescence and U–Pb SHRIMP study with constraints from REE elements. Canadian Mineralogist 43:183–202. https://doi.org/10.2113/gscanmin.43.1.183

Puga E, Fanning CM, Díaz de Federico A, Nieto JM, Beccaluva L, Bianchini G, Diaz-Puga MA (2011) Petrology, geochemistry and U-Pb geochronology of the Betic Ophiolites: inferences for Pangea break-up and birth of the Westernmost Tethys Ocean. Lithos: 124:255–272. https://doi.org/10.1016/j.lithos.2011.01.002

Puga E, Díaz de Federico A, Fanning CM, Nieto JM, Rodríguez Martínez-Conde JA, Díaz-Puga MA, Lozano JA, Bianchini G, Natali C, Beccaluva L. (2017) The Betic Ophiolites and the Mesozoic Evolution of the Western Tethys. Geosciences 2017 7:31. https://doi.org/10.3390/geosciences7020031.

Reuber I, Michard A, Chalouan A, Juteau T, Jermoumi B (1982) Structure and emplacement of the Alpine-type peridotites from Beni Bousera, Rif, Morocco: A polyphase tectonic interpretation, Tectonophysics 82:231–251. https://doi.org/10.1016/0040-1951(82)90047-6

Rodríguez-Cañero R (1993a) Contribución al Estudio de los Conodontos del Paleozoico del Complejo Maláguide (Cordillera Bética). Unpublished PhD Thesis, Universidad de Málaga 474 p.

Rodríguez-Cañero R (1993b) Presencia del evento de extinción Frasniense en el Complejo Maláguide (Cordillera Bética), detectado mediante fauna de conodontos. In: Gonzalez Donoso J.M. (ed): Comunicaciones de las IX Jornadas Paleontológicas Sociedad Española de Paleontología Málaga Spain 13–17.

Rodríguez-Cañero R (1995) El género Palmatolepis Ulrich y Bassler (Conodonta) y su aplicación para el reconocimiento de biozonas y biofacies en el Devónico superior del Complejo Maláguide (Cordillera Bética, España). Revista Española de Paleontología 10:3–23. http://www.sepaleontologia.es/revista/anteriores/REP%20Homenaje%20G.%20Colom%20%281995%29/00.%20Rodri%C2%81guez%20Cannero.pdf

Rodríguez-Cañero R, García-López S, Sarmiento GN (1997) Conodontos siluro-devónicos de la Peña de Ardales (Complejo Maláguide, Cordillera Bética). In: Grandal d'Anglade A, Gutiérrez Marco JC, Santos Hidalgo A (eds) Comunicaciones de las XIII Jornadas Paleontológicas Sociedad Española de Paleontología A Coruña Spain 92–94.

Rodríguez-Cañero R, Guerra-Merchán A (1996) Nuevos datos sobre la fauna de conodontos y la edad de la Formación Falcoña (Complejo Maláguide, Cordillera Bética). Revista de la Sociedad Española de Paleontología 11:235–246. http://www.sepaleontologia.es/revista/anteriores/REP%20%281996%29%20vol.%2011/2/10.%20Rodriguez-Canero%20&%20Guerra-Merchan.pdf

Rodríguez-Cañero R, Jabaloy-Sánchez A, Navas-Parejo P, Martín-Algarra A (2018) Linking Palaeozoic palaeogeography of the Betic Cordillera to the Variscan Iberian Massif: new insight through the first conodonts of the Nevado-Filábride Complex. International Journal of Earth Sciences 107:1791–1806. https://link.springer.com/article/10.1007/s00531-017-1572-8

Rodríguez-Cañero R, Martín-Algarra A (2014) Frasnian/Famennian crisis in the Malaguide Complex (Betic Cordillera, Spain). Terra Nova 26:38–54. https://doi.org/10.1111/ter.12068

Rodríguez-Cañero R, Martín-Algarra A, Sarmiento GN, Navas-Parejo P (2010) First Late Ordovician conodont fauna in the Betic Cordillera (South Spain): a palaeobiogeographical contribution. Terra Nova 22:330–340. https://doi.org/10.1111/j.1365-3121.2010.00954.x

Rodríguez-Cañero R, Navas-Parejo P, Somma R, Martín-Algarra A, Perrone V (2013) First finding of upper Silurian and Lower Devonian conodonts from the Peloritani Mts (Sicily, southern Italy). Bollettino della Società Paleontologica Italiana, 52:113–121. http://paleoitalia.org/media/u/archives/05_Rodriguez_Canero_et_al_2013_BSPI_522.pdf

Roep TB (1972) Stratigraphy of the "Permo-Triassic" Saladilla formation and its tectonic setting in the Betic of Malaga (Vélez Rubio region, SE Spain). Proceedings of the Koninklijke Nederlandse Akademie van Wetenschappen 75:223–247.

Roep TB (1974) The Hercynian diastrophism in the Betic of Malaga, SE Spain: a discussion. Geologie en Mijnbow 53:245–247.

Roep TB, MacGillavry HJ (1962) Preliminary note on the presence of distinct tectonic units in the Betic of Malaga of the Vélez Rubio region (SE Spain). Geologie en Mijnbouw 41:423–429.

Rossetti F, Theye T, Lucci F, Bouybaouene ML, Dini A, Gerdes A, Phillips D, Cozzupoli D (2010) Timing and modes of granite magmatism in the core of the Alboran Domain, Rif chain, northern Morocco: implications for the Alpine evolution of the western Mediterranean. Tectonics 29(2):TC2017. https://doi.org/10.1029/2009tc002487.

Ruiz-Cruz MD (1997) Very low-grade chlorite with anomalous chemistry and optical properties from the Malaguide Complex (Betic Cordilleras, Spain). Canadian Mineralogist 35:923–935. https://pubs.geoscienceworld.org/canmin/article-standard/35/4/923/12909

Ruiz-Cruz MD (2011a) NH_4-bearing micas in poly-metamorphic Alpujárride micaschists and gneisses from the central zone of the Betic Cordillera (Spain): tectono-metamorphic and crystal-chemical constraints. Mineralogy and Petrology 101:225–244. https://doi.org/10.1007/s00710-011-0146-x

Ruiz-Cruz MD (2011b) Origin of atoll garnet in schists from the Alpujárride Complex (Central zone of the Betic Cordillera, Spain): Implications on the PT evolution. Mineralogy and Petrology 101:245–261. https://link.springer.com/article/10.1007/s00710-011-0147-9

Ruiz-Cruz MD, Nieto F (2002) Condiciones P-T de estabilidad de las fases vermiculíticas en metaclastitas de la zona de Málaga (Cordillera Bética). Boletín de la Sociedad Española de Mineralogía 25:95–96.

Ruiz-Cruz MD, Rodríguez-Jiménez P (2002) Correlation between crystallochemical parameters of phyllosilicates and mineral facies in very low-grade metasediments of the Betic Cordilleras, Spain: a synthesis. Clay Minerals 37:169–185. https://doi.org/10.1180/0009855023710026

Ruiz-Cruz MD, Sanz de Galdeano C (2012a) Amphibole-derived evidence of medium P/T metamorphic ratio in Alpujárride and Federico "HP" units (Western Betic-Northern Rif, Spain and Morocco): Possible interpretations. International Journal of Earth Sciences 101:221–238. https://link.springer.com/content/pdf/10.1007%2Fs00531-011-0672-0.pdf

Ruiz-Cruz MD, Sanz de Galdeano C (2012b) Diamond and coesite in ultrahigh-pressure–ultrahigh-temperature granulites from Ceuta, Northern Rif, northwest Africa. Mineralogical Magazine 76:683–70. https://doi.org/10.1180/minmag.2012.076.3.17

Ruiz-Cruz MD, Sanz de Galdeano, (2013) Coesite and diamond inclusions, exsolution microstructures and chemical patterns in ultrahigh pressure garnets from Ceuta (Northern Rif, Spain). Lithos 177:184–206. https://doi.org/10.1016/j.lithos.2013.06.004

Ruiz-Cruz MD, Sanz de Galdeano C (2014a) Garnet variety and zircon ages in UHP meta-sedimentary rocks from the Jubrique zone (Alpujárride Complex, Betic Cordillera, Spain): evidence for a pre-Alpine emplacement of the Ronda peridotite. International Geology Review, 56:845–868. https://doi.org/10.1080/00206814.2014.904759

Ruiz-Cruz MD, Sanz de Galdeano C (2014b) Petrology of microdiamond-bearing schists from the Torrox unit, Betic Cordillera, Spain. European Journal of Mineralogy 25:919–933. https://dx.doi.org/10.1127/0935-1221/2013/0025-2337

Ruiz-Cruz MD, Sanz de Galdeano C (2017) Genetic significance of zircon in orthogneisses from Sierra Nevada (Betic Cordillera, Spain). Mineralogical Magazine 81:77–101. https://doi.org/10.1180/minmag.2016.080.072

Ruiz-Cruz MD, Sanz de Galdeano C, Santamaría A. (2015) Petrology and Thermobarometric Estimates For Metasediments, Orthogneisses, and Eclogites From the Nevado-Filábride Complex In the Western Sierra Nevada (Betic Cordillera, Spain). Canadian Mineralogist 53:1083–1107. https://doi.org/10.3749/canmin.1500037

Ruiz-Cruz MD, Sanz de Galdeano C, Santamaría A. (2016) Geochemical Signatures and Inclusions in Apatite as Markers of a Hidden Ultrahigh-Pressure Event (Betic Cordillera, Spain). Journal of Geology 124:277–292. https://doi.org/10.1086/685508

Sánchez-Navas A (1999) Sequential kinetics of a muscovite-out reaction: a natural example. American Mineralogist 84:1270–1286. https://doi.org/10.2138/am-1999-0905

Sánchez-Navas A, Oliveira-Barbosa RdC, García-Casco A, Martín-Algarra A (2012). Transformation of andalusite to kyanite in the Alpujarride Complex (Betic Cordillera, S Spain): Geologic implications. Journal of Geology 120:557–574. https://www.jstor.org/stable/10.1086/666944

Sánchez-Navas A, García Casco A, Martín-Algarra A (2014) Pre-alpine discordant granitic dikes in the metamorphic core of the Betic Cordillera. Tectonic implications. Terra Nova 26:477–486. https://doi.org/10.1111/ter.12123

Sánchez-Navas A, García Casco A, Mazzoli S, Martín-Algarra A (2017) Polymetamorphism in the Alpujarride Complex, Betic Cordillera, south Spain Journal of Geology 125:637–657. https://doi.org/10.1086/693862

Sánchez-Navas A, Macaione E, Oliveira-Barbosa RdC, Messina A, Martín-Algarra A (2016) Transformation of kyanite to andalusite in the Benamocarra Unit (Betic Cordillera, Spain). Kinetics and petrological significance. European Journal of Mineralogy 28:337–353. https://www.schweizerbart.de/papers/ejm/detail/28/85988/

Sánchez-Rodríguez L, Gebauer D (2000) Mesozoic formation of pyroxenites and gabbros in the Ronda area (southern Spain), followed by Early Miocene subduction metamorphism and emplacement into the middle crust: U-Pb sensitive high-resolution ion microprobe dating of zircon. Tectonophysics 316:19–44. https://doi.org/10.1016/S0040-1951(99)00256-5.

Santamaría-López A, Sanz de Galdeano C (2018) SHRIMP U–Pb detrital zircon dating to check subdivisions in metamorphic complexes: a case of study in the Nevado–Filábride complex (Betic Cordillera, Spain). International Journal of Earth Sciences, 107:2539–2552. https://doi.org/10.1007/s00531-018-1613-y

Sanz de Galdeano C, Andreo B, García-Tortosa FJ, López-Garrido AC (2001) The Triassic palaeogeographic transition between Alpujarride and Malaguide Complexes, Betic-Rif Internal Zones (S Spain, N Morocco). Palaeogeography Palaeoclimatology Palaeoecology 167:157–173. https://doi.org/10.1016/S0031-0182(00)00236-4

Sanz de Galdeano C, Delgado F, López-Garrido AC (1995a) Estructura del Alpujárride y del Maláguide al NW de Sierra Nevada (Cordillera Bética). Revista de la Sociedad Geológica de España 8:239–250. http://www.sociedadgeologica.es/archivos/REV/8(3)/Art09.pdf

Sanz de Galdeano C, Delgado F, López-Garrido AC (1995b) Unidades Alpujárrides y Maláguides al NE de Granada (Cordillera Bética). Geogaceta 18:27–29. http://www.sociedadgeologica.es/archivos/geogacetas/Geo18/Art07.pdf

Sanz de Galdeano C, López Garrido AC (2016a) The Nevado-Filábride Complex in the western part of Sierra de los Filabres (Betic Internal Zone): structure and lithologic succession. Boletín Geológico y Minero 127:823–836. http://www.igme.es/boletin/2016/127_4/BGM_127-4_Art-5.pdf

Sanz de Galdeano C, López-Garrido AC (2016b) Geometry of the contact of the peridotites of Sierra Alpujata with the Sierra Blanca succession (Alpujarride Complex, Betic Internal Zone). Geogaceta 60:7–10. http://www.sociedadgeologica.es/archivos/geogacetas/geo60/geo60_02p7_10.pdf

Sanz de Galdeano C, López Garrido AC, Santamaría-López A (2016) Major scale structure of the marbles situated between Cóbdar and Macael (Nevado-Filábride Complex, Betic Cordillera, Almeria province Spain), and general stratigraphic arrangement. Revista de la Sociedad Geológica de España 29:107–116. http://www.sociedadgeologica.es/archivos/REV/29(2)/RSGE_29(2)_art7.pdf

Sanz de Galdeano C, López-Garrido AC, Andreo B (1999) The stratigraphic and tectonic relationships of the Alpujarride and Malaguide complexes in the western Betic Cordillera (Casares, prov. of Malaga, South Spain). Comptes Rendus de l'Académie des Science Paris 328:113–119. https://doi.org/10.1016/S1251-8050(99)80006-8

Sanz de Galdeano C, Ruiz-Cruz MD (2016) Late Palaeozoic to Triassic formations unconformably deposited over the Ronda peridotites (Betic Cordilleras): Evidence for their Variscan time of crustal emplacement. Estudios Geológicos 72(1). http://dx.doi.org/10.3989/egeol.42046.368.

Sarmiento GN, Gutiérrez-Marco JC, Rodríguez-Cañero R, Martín-Algarra A, Navas-Parejo P (2011): A brief summary of Ordovician conodont faunas from the Iberian Peninsula. In: Gutiérrez-Marco JC, Rábano I, García-Bellido D (eds.), Ordovician of the World. Cuadernos del Museo Geominero 14:505–514. Instituto Geológico y Minero de España Madrid. http://digital.csic.es/bitstream/10261/61081/1/ORDOVICIAN OF THE WORLD_505_514.pdf

Schönlaub HP (1988) The Ordovician-Silurian boundary in the Carnic Alps of Austria. In: Cocks LRM, Rickards RB (eds.) A Global Analysis of the Ordovician-Silurian Boundary. Bulletin of the British Museum (Natural History) Geology 43:95–100.

Soediono H (1971) Geological investigations in the Chirivel area, province of Almería - southeastern Spain. PhD Thesis University of Amsterdam 144 p.

Somma R, Navas-Parejo P, Martín-Algarra A, Rodríguez-Cañero R, Perrone V, Martínez-Pérez C (2013) Paleozoic stratigraphy of the Longi-Taormina Unit (Peloritanian Mountains, southern Italy). Stratigraphy 10:127–152. http://www.micropress.org/microaccess/stratigraphy/issue-299/article-1824

Sosson M, Morillon AC, Bourgois J, Féraud G, Poupeau G, Saint-Marc P (1998) Late exhumation stages of the Alpujarride Complex (western Betic Cordilleras, Spain): new thermo-chronological and structural data on Los Reales and Ojen nappes. Tectonophysics 285:253–273. https://doi.org/10.1016/S0040-1951(97)00274-6

Spear FS, Cheney JT (1989) A petrogenetic grid for pelitic schists in the system SiO_2–Al_2O_3–FeO–MgO–K_2O–H_2O. Contributions to Mineralogy and Petrology 101:149–164. https://link.springer.com/article/10.1007/BF00375302

Stampfli GM, Borel GD (2004) The TRANSMED Transects in Space and Time: Constraints on the Paleotectonic Evolution of the Mediterranean Domain. In: Cavazza W, Roure F, Spakman W, Stampfli GM, Ziegler P (eds) The TRANSMED Atlas: the Mediterranean Region from Crust to Mantle. Springer Verlag 53–80 (and CD ROM). https://link.springer.com/chapter/10.1007/978-3-642-18919-7_3

Stampfli GM, Hochard C (2009) Plate tectonics of the Alpine realm. In: Murphy JB, Hynes AJ, Keppie JD (eds) Ancient orogens and modern analogues. Geological Society, London, Special Publications 327:89–111. https://doi.org/10.1144/SP327.6

Stampfli GM, Hochard C, Vérard C, Wilhem C, von Raumer J (2013) The formation of Pangea. Tectonophysics 593:1–19. https://doi.org/10.1016/j.tecto.2013.02.037

Stampfli GM, von Raumer J, Borel G (2002) Paleozoic evolution of pre-Variscan terranes: from Gondwana to the Variscan collision. In: Martinez Catalan JR, Hatcher Jr RD, Arenas R, Díaz García F (eds) Variscan-Appalachian Dynamics: the Building of the Late Paleozoic Basement. Geological Society of America Special Paper 364:263–280. https://doi.org/10.1130/0-8137-2364-7.263

Stampfli GM, von Raumer J, Wilhem C (2011) The distribution of Gondwana derived terranes in the early Paleozoic. In: Gutiérrez--Marco JC, Rábano I, García-Bellido D (eds) The Ordovician of the World. Cuadernos del Museo Geominero 14:567–574. Instituto Geológico y Minero de España Madrid.

Tendero JA, Martín-Algarra A, Puga E, Díaz de Federico A (1993) Lithostratigraphie des métasédiments de l'association ophiolitique Nevado-Filabride (SE Espagne) et mise en evidence d'objets ankéritiques évoquant des foraminiféres planctoniques du Crétacé: conséquences paléogéographiques. Comptes Rendus de l'Académie des Sciences Paris 316:1115–1122.

Torsvik TH, Cocks LRM (2013) Gondwana from top to base in space and time. Gondwana Research 24:999–1030. https://doi.org/10.1016/j.gr.2013.06.012

Torres-Roldán RL (1974) El metamorfismo progresivo y la evolución de la serie de facies en las metapelitas alpujárrides al SE de Sierra

Almijara (sector central, Cordilleras Béticas, España). Cuadernos de Geología Universidad de Granada 5:21–77.

Torres-Roldán RL (1978): Scapolite-bearing and related rocks calc-silicate layers from the Alpujarride series (Betic Cordilleras of southern Spain). Geologische Rundschau 67:342–355. https://doi.org/10.1007/BF01803272

Torres-Roldán RL (1981) Plurifacial metamorphic evolution of the Sierra Bermeja peridotite aureole (Southern Spain). Estudios Geológicos 37:115–133.

Torres-Roldán RL (1983) Fractionated melting of metapelite and further crystal melt equilibria. The example of the Blanca unit migmatite complex, north of Estepona (southern Spain). Tectonophysics 96:95–123. https://doi.org/10.1016/0040-1951(83)90246-9

Torres-Roldán RL Polli, G, Peccerillo A (1986) An Early Miocene arc tholeitic magmatic dike event from the Alboran Sea. Evidence for precollisional subduction and back-arc crustal extension in the westernmost Mediterranean. Geologische Rundschau 75:219–234. https://doi.org/10.1007/BF01770190

Torres-Ruiz J, Pesquera A, Gil-Crespo PP, Velilla N (2003) Origin and petrogenetic implications of tourmaline-rich rocks in the Sierra Nevada (Betic Cordillera, southern Spain). Chemical Geology 197:55–86. https://doi.org/10.1016/S0009-2541(02)00357-1

Turner SP, Platt JP, George RMM, Kelley SP, Pearson DG, Nowell GM (1999) Magmatism associated with orogenic collapse of the Betic-Alboran domain, SE Spain. Journal of Petrology 40:1011–1036. https://doi.org/10.1093/petroj/40.6.1011

Van den Boogaard M (1965) Two conodont faunas from the Paleozoic of the Betic of Malaga near Velez Rubio. Proceedings of the Koninklijke Nederlandse Akademie van Wetenschappen Amsterdam B 68–1:33-37.

Vera JA (ed) (2004) Geología de España. SGE-IGME, Madrid.

Vidal O, Parra T (2000) Exhumation paths of high-pressure metapelites obtained from local equilibria for chlorite-phengite assemblages. Geological Journal 35:139–161. https://doi.org/10.1002/gj.856

Vissers RLM (1981) A structural study of the Central Sierra de los Filabres (Betic Zone, SE Spain), with emphasis on deformational processes and their relation to the Alpine Metamorphism. GUA Papers of Geology, 15:1–154.

Voet HW (1967) Geological investigations in the northern Sierra de Filabres around Macael and Cóbdar, south-eastern Spain. PhD Thesis University of Amsterdam, 122 p.

Von Raumer J, Stampfli GM, Borel GD, Bussy F (2002) The organisation of pre-Variscan basement areas at the north-Gondwanan margin. International Journal of Earth Sciences 91:35–52. https://doi.org/10.1007/s005310100

Von Raumer JF, Stampfli GM, Bussy F (2003). Gondwana-derived microcontinents- the constituents of the Variscan and Alpine collisional orogens. Tectono physics 365:7–22. https://doi.org/10.1016/S0040-1951(03)00015-5

White RW, Powell R, Holland TJB (2001) Calculation of partial melting equilibria in the system Na_2O–CaO–K_2O–FeO–MgO–Al_2O_3–SiO_2–H_2O (NCKFMASH). Journal of Metamorphic Geology 19:139–153. https://doi.org/10.1046/j.0263-4929.2000.00303.x

Whitehouse MJ, Platt JP (2003) Dating high-grade metamorphism-constraints from rare-earth elements in zircon and garnet. Contributions to Mineralogy and Petrology 145:61–74. https://link.springer.com/content/pdf/10.1007%2Fs00410-002-0432-z.pdf

Whitney DL, Evans BW (2010) Abbreviations for names of rock-forming minerals. American Mineralogists 95:185–187. http://minsoc.ru/FilesBase/Whitney_p185_10.pdf

Williams JR, Platt JP (2017) Superposed and refolded metamorphic isograds and superposed directions of shear during late orogenic extension in the Alborán Domain, southern Spain. Tectonics 36:756–786. https://doi.org/10.1002/2016TC004358

Zeck HP, Albat F, Hansen BT, Torres-Roldán RL, García-Casco A, Martín-Algarra A (1989) A 21 ± 2 Ma age for the termination of the ductile alpine deformation in the internal zone of the Betic cordilleras, South Spain. Tectonophysics 169:215–220. https://doi.org/10.1016/0040-1951(89)90196-0

Zeck HP, Monié P, Villa IM, Hansen BT (1992) Very high rates of cooling and uplift in the Alpine belt of the Betic Cordilleras, southern Spain. Geology 20:79–82. https://doi.org/10.1130/0091-7613(1992)020<0079:VHROCA>2.3.CO;2

Zeck HP Whitehouse MJ (1999) Hercynian, Pan-African, Proterozoic and Archean ion-microprobe zircon ages for a Betic-Rif core complex, Alpine belt, W Mediterranean: consequences for its P-T-t path. Contributios to Mineralogy and Petrology 134:134–149. https://doi.org/10.1007/s004100050474

Zeck HP Whitehouse MJ (2002) Repeated age resetting in zircons from Hercynian-Alpine polymetamorphic schists Betic-Rif tectonic belt, S. Spain/ a U-Th-Pb ion microprobe study. Chemical Geology 182:275–292. https://doi.org/10.1016/S0009-2541(01)00296-0

Zeck HP, Williams IS (2001) Hercynian Metamorphism in Nappe Core Complexes of the Alpine Betic–Rif Belt, Western Mediterranean—a SHRIMP Zircon Study. Journal of Petrology 42:1373–1385. https://doi.org/10.1093/petrology/42.7.1373

Zindler A, Staudigel H, Hart, SR, Endres R, Goldstein S (1983) Nd and Sr isotopic study of a mafic layer from Ronda ultramafic complex. Nature 304:226–230. Ihttps://www.nature.com/articles/304226a0.pdf

Deformation and Structure

10

A. Azor, Í. Dias da Silva, J. Gómez Barreiro, E. González-Clavijo, J. R. Martínez Catalán, J. F. Simancas, D. Martínez Poyatos, I. Pérez-Cáceres, F. González Lodeiro, I. Expósito, J. M. Casas, P. Clariana, J. García-Sansegundo, and A. Margalef

Abstract

The Variscan deformation in the Iberian Massif is related to the large-scale plate tectonic scenario that drove to the destruction of the Rheic and other intervening oceans, to finally form the Pangea Supercontinent. The Northern Iberian Massif structure consists in an East-vergent orogenic wedge developed at the footwall of a rootless oceanic suture. The collisional architecture of this wedge has been strongly modified by extensional tectonics in the hinterland and orocline formation affecting the whole domain. The Southwestern Iberian Massif transect contains two orogenic sutures cropping out at both boundaries of the OMZ and shows a general transpressive character of the whole collisional evolution, as well as an Early Carboniferous transtensional/extensional stage that gave way to flysch sedimentation, voluminous bimodal magmatism and oblique left-lateral extensional shearing.

10.1 Introduction

A. Azor, Í. Dias da Silva

This section is devoted to the main Variscan structures of the Iberian Massif. The structures described here were associated with the large-scale plate tectonic scenario that drove to

Coordinators: A. Azor and Í. Dias da Silva.

A. Azor (✉) · J. F. Simancas · D. Martínez Poyatos · I. Pérez-Cáceres · F. González Lodeiro
Departamento de Geodinámica, Facultad de Ciencias, Universidad de Granada, Campus de Fuentenueva s/n, 18071 Granada, Spain
e-mail: azor@ugr.es

J. F. Simancas
e-mail: simancas@ugr.es

D. Martínez Poyatos
e-mail: djmp@ugr.es

I. Pérez-Cáceres
e-mail: perezcaceres@ugr.es

F. González Lodeiro
e-mail: lodeiro@ugr.es

Í. Dias da Silva
Faculty of Science, Department of Geology, Instituto Dom Luiz, University of Lisbon, Campo Grande, Edifício C1, Piso 1, 1749-016 Lisbon, Portugal
e-mail: ipicaparopo@gmail.com

J. Gomez Barreiro · J. R. Martínez Catalán
Departamento de Geodinámica, Facultad de Ciencias, University of Salamanca, Plaza de la Merced, s/n, 37008 Salamanca, Spain
e-mail: jugb@usal.es

J. R. Martínez Catalán
e-mail: jrmc@usal.es

E. González-Clavijo
Unidad de Salamanca, Instituto Geológico y Minero de España, Plaza de la Constitución, 1, Planta 3ª, 37001 Salamanca, Spain
e-mail: e.clavijo@igme.es

I. Expósito
Departamento de Ciencias Ambientales, Universidad Pablo de Olavide, Seville, Spain
e-mail: iexpram@upo.es

J. M. Casas
Departamento de Dinàmica de la Terra i de l'Oceà, Institut de Recerca Geomodels, Universitat de Barcelona, Martí Franquès s/n, 08028 Barcelona, Spain
e-mail: casas@ub.edu

P. Clariana
Instituto Geológico y Minero de España, Unidad de Zaragoza, Manuel Lasala, 44, 9ºB, 50006 Zaragoza, Spain
e-mail: p.clariana@igme.es

J. García-Sansegundo
Departamento de Geología, Universidad de Oviedo, Jesús Arias de Velasco, s/n, 33208 Oviedo, Spain
e-mail: jgsansegundo@uniovi.es

A. Margalef
Centre d'Estudis de la Neu i de la Muntanya d'Andorra, Institut d'Estudis Andorrans, Av. Rocafort 21-23, 3ª planta, 600 Sant Julià de Lòria, Andorra
e-mail: amargalef.cenma@iea.ad

C. Quesada and J. T. Oliveira (eds.), *The Geology of Iberia: A Geodynamic Approach*, Regional Geology Reviews,
https://doi.org/10.1007/978-3-030-10519-8_10

the destruction of the Rheic and other intervening oceans, to finally form the Pangea Supercontinent. The number and nature of the terranes involved in this complex collisional evolution in Iberia can be discussed on the basis of their tectono-metamorphic aspects since each one preserves singular features, though keeping in mind that they were deformed during the same orogenic cycle. However, Variscan-related deformation was highly diachronic in Iberia, with deformation starting in Early-Middle Devonian time in the supposedly inner orogenic domains—such as the Ossa-Morena Zone and the Galicia-Trás-os-Montes Zone—and, much later, during the Early Pennsylvanian in most of the external domains represented today by the South Portuguese and Cantabrian zones.

Due to the complexity and variety of the Variscan structures, we will describe separately the Northern and Southwestern sectors of the Iberian Massif, each one comprising some of the classic tectono-stratigraphic zones defined in earlier works. The Northern Iberia transect includes the Galicia-Trás-os-Montes Zone (GTMZ), the northern Central Iberian Zone (CIZ), the West-Asturian Leonese Zone (WALZ) and the Cantabrian Zone (CZ), while the Southwestern Iberia transect comprehends the southern CIZ, the Ossa-Morena Zone (OMZ) and the South Portuguese Zone (SPZ).

These two transects have a number of structural particularities that justify their separate treatment. Thus, Northern Iberia attests an orogenic wedge with a general east vergence, where the collisional architecture has been strongly modified by extensional tectonics in the hinterland and orocline formation affecting the whole domain. As for Southwestern Iberia, two orogenic sutures have been featured at both boundaries of the OMZ, with a general transpressive character of the whole collisional evolution and an Early Carboniferous transtensional/extensional stage that gave way to flysch sedimentation, voluminous bimodal magmatism and oblique left-lateral extensional shearing. The boundary between the two transects is a Late Variscan extensional shear zone that separates two segments of the CIZ with contrasting structural style: to the north, the deformation was complex with compressional and extensional events; to the south the deformation of the CIZ was relatively simple, the only penetrative structures being km-scale upright folds formed during Middle Carboniferous compression.

10.2 Northern Iberia

Í. Dias da Silva, J. Gómez Barreiro, E. González-Clavijo, J. R. Martínez Catalán

It is widely accepted that the Variscan orogeny was the result of the collision of Laurussia and Gondwana during the Late Paleozoic. In Northern Iberia, a complete section of the belt exposes not only the Variscan collisional structures, but also relics of the previous continental convergence, which attest the accretion of arc-related units and the consumption of the Rheic Ocean and related basins (Gómez Barreiro et al. 2007; Martínez Catalán et al. 2009; Ballèvre et al. 2014; Martínez Catalán et al. 2014). Pre-collisional evidences are somewhat fragmentary and limited to the allochthonous units of the Galicia-Trás-os-Montes Zone (GTMZ), being designated here as early-Variscan. Strictly speaking, collision started after the ocean between the approaching continents was consumed. First evidences of ocean consumption appear at ca. 405–376 Ma in some ophiolites of the Middle Allochthon, with supra-subduction zone imprint and ductile fabrics developed in a subduction environment (Dallmeyer et al. 1997; Díez García et al. 1999; Sánchez Martínez et al. 2007; Gómez Barreiro et al. 2010a). The subduction of the outermost margin of Gondwana eventually marks the final closure of the Rheic Ocean occurred at 375–365 Ma. This stage was coeval to the high-P metamorphism in the Lower Allochthon (Van Calsteren et al. 1979; Santos Zalduegui et al. 1995; Rodríguez et al. 2003; Abati et al. 2010; López-Carmona et al. 2014).

Deformation during the collisional stage is considered Variscan and includes crustal thickening and thinning with several generations of structures that can be grouped as contractional (C_1, C_2 and C_3) and extensional (E_1 and E_2; Martínez Catalán et al. 2014). These structures were defined in the Autochthon, but also affected the Allochthon, which was emplaced during C_2. The deformation of the Allochthon previous to its emplacement is quite unique for each group of units, reflecting pre- and Early-Variscan events. Once the continental subduction of Gondwana locked, deformation transferred to the autochthon. The first structures were east-verging overturned and recumbent folds, followed by thrusts and synorogenic extensional detachments. The age of each deformation phase is progressively younger towards the foreland, thus indicating a diachronic trend across the orogen (Dallmeyer et al. 1997).

10.2.1 Early-Variscan Deformation

J. Gómez Barreiro, J. R. Martínez Catalán, Í. Dias da Silva

An early Variscan history of convergence and accretion is preserved in the different units of the Allochthon as metamorphic assemblages and deformation fabrics. The progressive accretion of terranes was a continuous tectonothermal process progressing from NW to SE (in present-day coordinates), which is reflected in the progressively younger ages of metamorphism and deformation from the Upper to the Lower Allochthon (Martínez Catalán et al. 2009; Ballèvre et al. (2014).

In the Upper Allochthon, the main, high-P and high-T metamorphism is characterized by high-P granulite and eclogite facies dated at 400–390 Ma (Schäfer et al. 1993; Santos Zalduegui et al. 1996; Ordóñez Casado et al. 2001; Fernández-Suárez et al. 2007). This event implied Early-Middle Devonian subduction (Gil Ibarguchi et al. 1990, 1999; Mendia Aranguren 2000), and eventually accretion to a large continental mass (Laurussia?) or another terrane (Martínez Catalán et al. 2009; Ballèvre et al. 2014). The age of the high-P and high-T event and its geodynamic meaning has been a subject of debate (Gómez Barreiro et al. 2006), and a limited number of exhumative fabrics show Late Silurian-Early Devonian ages, which may suggest an older (pre-Variscan) age for the high-P and high-T metamorphism (Gómez Barreiro et al. 2006; Arenas et al. 2013). Whether or not the pre-Variscan record is restricted to some units, the age for high-P and high-T metamorphism in the Upper Allochthon is connected to early Variscan convergence, i.e. it is previous to the Variscan collision.

Major thrusts and extensional detachments produced decompression and partial melting subsequent to the high-P and high-T event in the Upper Allochthon, giving way to a penetrative deformation occurred under amphibolite facies conditions. This deformation produced exhumation and the tectonic attenuation of the original pile (Martínez Catalán et al. 2002; Gómez Barreiro et al. 2007; Álvarez-Valero et al. 2014). The retrograde amphibolite-facies metamorphism has been dated at 390–380 Ma (Dallmeyer et al. 1991, 1997; Gómez Barreiro et al. 2006). Subsequently, the Upper Allochthon underwent mylonitization under lower amphibolite facies conditions, followed by recumbent folding and thrusting under greenschist facies conditions (Vogel 1967; Marcos et al. 1984; Gil Ibarguchi et al. 1990; Girardeau and Gil Ibarguchi 1991; Mendia Aranguren 2000).

In the underlying Middle Allochthon (oceanic domain), three different groups of units can be distinguished (Ballèvre et al. 2014). Among them, the Cambro-Ordovician ophiolite of Bazar was affected by early low- to medium-P granulites facies metamorphism dated at around 475 ± 2 Ma (Sánchez Martínez et al. 2012). The origin and meaning of this metamorphic event are not clear, having been interpreted as related to subduction of a very young oceanic lithosphere, with an eventual consumption of a mid-ocean ridge (Arenas et al. 2007b; Sánchez Martínez 2009; Sánchez Martínez et al. 2012). However, the main deformation fabric (amphibolite facies) seems to be kinematically related to the Variscan emplacement (Gómez Barreiro and Martínez Catalán 2012).

In the Devonian Ophiolites, a prograde amphibolite facies metamorphism occurred at 395–380 Ma. P-T conditions in mylonites reached 625–680 °C and 1.1–1.2 GPa, pointing to imbrication in a subduction setting (Díaz García et al. 1999). This metamorphism reflects the understacking of oceanic lithosphere related to the closure of the intervening ocean. Thrust imbrication occurred at ca. 380 Ma (Peucat et al. 1990; Dallmeyer et al. 1991, 1997), when the 395 Ma old oceanic lithosphere was still hot, producing metamorphic soles (Díaz García et al. 1999). Fabric analysis by neutron diffraction and EBSD in thrust-related shear zones showed plastic deformation of hornblende and plagioclase (>600 °C), an observation coherent with an intraoceanic subduction scenario (Gómez Barreiro et al. 2010a). A consistent E-W oriented lineation and top-to-the-E shearing were found in the mylonites, tentatively reflecting a convergence vector in present-day coordinates. Overall, an accretionary prism was being built at a plate boundary where convergence concentrated.

The Cambro-Ordovician ophiolites that witnessed back-arc spreading at the Gondwana margin were the next to be incorporated to the accretionary wedge. A relatively early high-P metamorphism has been identified in some of them, such as the Vila de Cruces and Ceán Units (Arenas et al. 2007a). This metamorphism has been dated at 370–360 Ma (López-Carmona et al. 2010, 2014). The stacking of the Middle and Lower Allochthon is spatially and temporally related, resulting in exhumation between 365–350 Ma. Meanwhile the Somozas Mélange was developed in the Variscan subduction zone, probably about Late Devonian. Some evidences suggest the shear zone where the tectonic mélange was originated remained active as a major tectonic boundary until the imbrication with the Parautochthon (Arenas et al. 2009; Arenas and Sánchez Martínez 2015).

The subduction of the Gondwana outermost edge, represented by the Lower Allochthon, occurred at about 380–370 Ma (Van Calsteren et al. 1979; Santos Zalduegui et al. 1995; Rodríguez et al. 2003; Abati et al. 2010; López-Carmona et al. 2014). This Late Devonian event developed eclogites and blueschists, with peak pressures between 1.5–2.2 GPa (Munhá et al. 1984; Arenas et al. 1995, 1997; Gil Ibarguchi 1995; Rubio Pascual et al. 2002; Rodríguez et al. 2003; López-Carmona et al. 2010, 2014), and marks the last stage of subduction-related Eo-Variscan convergence. Early exhumative fabrics are constrained at ca. 370–360 Ma (Rodríguez et al. 2003; López-Carmona et al. 2014), and show a consistent top-to-the-E shearing, with the development of major ductile thrusts and recumbent folds (Díez Fernández et al. 2011).

10.2.2 Variscan Deformation

Í. Dias da Silva, J. Gómez Barreiro, E. González-Clavijo, J. R. Martínez Catalán

The Laurussia-Gondwana convergence after the closure of the oceanic realm took place in a collisional regime that can be considered as the **Variscan Orogeny** in a strict sense.

Recumbent and overturned folds and large thrust sheets thickened the continental crust, which subsequently underwent orogenic collapse and a Late-Variscan episode of upright folding. The Variscan stages C_1, C_2 and E_1 (Martínez Catalán et al. 2014) are all highly diachronic, with ages getting younger from the allochthonous units towards the Autochthon, and from the CIZ towards the CZ, thus revealing an eastward progression of the orogenic front (Fig. 10.1; Dallmeyer et al. 1997). The last Variscan contractional episode (C_3) has been recently associated with orocline development (Martínez Catalán 2011a; Shaw et al. 2012; Weil et al. 2013; Gutiérrez-Alonso et al. 2015).

The Variscan deformation started after the development of the greenschist facies foliation in the Middle Allochthon (e.g. Moeche and Vila de Cruces units; 363–367 Ma; Dallmeyer et al. 1997) and the continental subduction of the Lower Allochthon (365 Ma; Rodríguez et al. 2003). Large scale thrusts, recumbent folds and detachment faults (Gómez Barreiro et al. 2007, 2010b; Díez Fernández and Martínez Catalán 2012) allowed a top-to-the-E exhumation of the Allochthon onto the not subducted outer Gondwana shelf, represented by the **Upper Parautochthon** (Martínez Catalán et al. 1997; Díez Fernández et al. 2012a; Rodrigues et al. 2013; Dias da Silva et al. 2014). Continuous deformation led to the development of a thrust system that overprinted the older system related to the formation of the accretionary wedge where the Allochthon was originally stacked (Martínez Catalán et al. 2002). So, the Variscan thrust system was out-of-sequence, and responsible for the thinning of the orogenic wedge, as well as the unrooting and final emplacement of the Upper and Middle allochthons onto the Lower Allochthon. This event was immediately followed by low-angle detachments that brought the whole Allochthon further inland onto the Upper Parautochthon (Martínez Catalán et al. 1997; Gómez Barreiro et al. 2007, 2010b; Díez Fernández et al. 2012a).

The arrival of the Variscan tectonic front to the autochthonous domains is marked by the *first contractional Variscan stage* (C_1). The S_1 axial planar foliation in the CIZ near the allochthonous complexes yielded a ^{40}Ar–^{39}Ar age

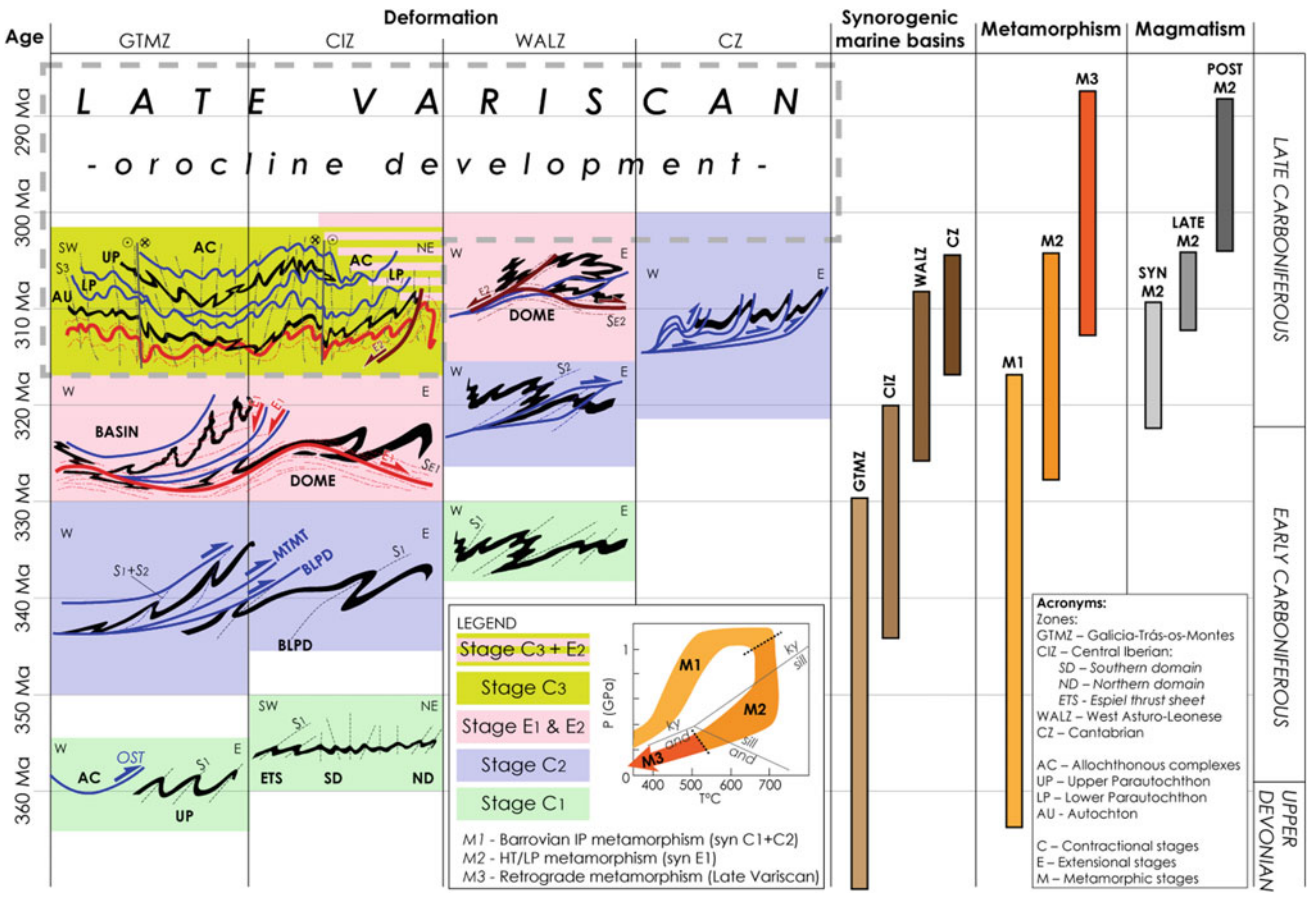

Fig. 10.1 Summary of Variscan deformation, magmatism, synorogenic marine sedimentation and metamorphism in Northern Iberia. Deformational ages and metamorphism are younger towards external orogenic zones, from the GTMZ to the CZ. The migration of synorogenic marine basins developed in the foreland follows the arrival of the tectonic front into more external domains. Based in Dallmeyer et al. (1997), Martínez Catalán et al. (2014, 2016a, b)

of 359 Ma (Dallmeyer et al. 1997). The major C_1 structures are recumbent, overturned and upright folds developed under low-grade, medium-P conditions. C_1 folds in the Upper Parautochthon are often very tight and recumbent, with low-dipping long limbs and vertical or overturned short limbs, indicating north-east to south-east vergence (Rodrigues et al. 2013; Dias da Silva 2014). In the structurally underlying Autochthon (CIZ), C_1 folds are similar yet less abundant and show centrifuge vergence with respect to the allochthonous complexes of Bragança and Morais (Aerden 2004; Dias da Silva 2014; Martínez Catalán et al. 2014), evidencing a close relation to the piggy-back emplacement of the GTMZ onto the CIZ (Fig. 10.2).

Far from the allochthonous complexes, C_1 folds are heterogeneously distributed and may be sub-parallel to late-Variscan C_3 folds. The geometry and attitude of C_1 folds in the CIZ allowed the individualization of two domains (Fig. 10.2; Díez Balda et al. 1990; Martínez Catalán et al. 2004b; Dias et al. 2013):

- **The northern domain** corresponds to the Domain of Recumbent Folds of Díez Balda et al. (1990), being characterized by NE- and E-vergent recumbent and overturned folds.
- **The southwestern domain** is equivalent to the Domain of Vertical Folds of Díez Balda et al. (1990), being characterized by upright and SW- to NE-vergent folds.

In the northern domain, recumbent C_1 folds are refolded by nearly homoaxial but steep C_3 structures, which makes easy to distinguish them from each other. In the southern domain, however, many of the folds presumed to be C_1 are actually C_3 structures (Aerden 2004; Martínez Catalán 2011a, b). In fact, this domain includes large areas with very low C_1 strain (spaced, very low-grade, even missing S_1 cleavage, large wavelength/low amplitude upright C_1 folds). This contrasts with the regularly spaced C_3 folds common in the southern domain, generally showing a well-developed axial planar, slaty or crenulation cleavage, and which are fully comparable to C_3 folds of the northern domain.

These facts do not invalidate the established subdivision in two domains, as the southern one is clearly characterized by upright folds, and although many of them are C_3, the extant C_1 folds are upright too, apart from the southernmost domain of the CIZ, where a couple of large recumbent folds exists (Espiel thrust sheet, Fig. 10.2; Azor et al. 1994a, b; Martínez Poyatos 1997).

The main criterion to identify a fold as C_1 is the evidence that it is oblique to and/or folded by a later fold. The attitude of C_3 folds in the northern and southern domains delineates the Ibero-Armorican Orocline (IAO). But in several places of the southern domain, the previous folds are clearly oblique, and their folded axial surfaces delineate another arc, the Central Iberian Orocline (CIO) with a curvature opposite to that of the IAO, and which is also delineated by magnetic anomalies (Fig. 10.2; Ardizone et al. 1989; Aerden 2004; Martínez Catalán 2011a, b).

In the northern domain, overturned and recumbent C_1 folds, the largest of which is the Mondoñedo nappe, developed facing the foreland, represented by the CZ (Martínez Catalán et al. 2003) (Fig. 10.2). Ductile deformation started in the CIZ at the Devonian-Carboniferous boundary (ca. 359 Ma) and migrated inland reaching the eastern limit of the WALZ at about 336 Ma (Dallmeyer et al. 1997). Crustal thickening was followed by erosion and sedimentation, which occurred yet in the innermost orogenic areas (Figs. 10.1 and 10.4a–c). Shallow marine foreland basins were established over an erosional surface that exposed the previous C_1 folds (Martínez Catalán et al. 2016a, b). Sedimentary provenance studies indicate contribution from the northern Gondwana terranes imbricated in the Allochthon, and from autochthonous sequences eroded in the peripheral bulge (Martínez Catalán et al. 2004a, 2008; Dias da Silva et al. 2015b; González-Clavijo et al. 2016). With the migration of the basin depocenter towards the foreland, the oldest Upper Devonian-early Carboniferous synorogenic deposits were rapidly incorporated at the base of the allochthonous complexes of Bragança and Morais immediately after their sedimentation (Martínez Catalán et al. 2016a, b), thus defining the Lower Parautochthon (Figs. 10.1 and 10.2; Rodrigues et al. 2013; Dias da Silva et al. 2015b). The youngest synorogenic marine units are Late Carboniferous and were placed unconformably on top of the CZ pre-Variscan stratigraphic sequences (Pérez-Estaún et al. 1988; Pastor-Galán et al. 2013).

The continued thrusting of the allochthonous pile onto the Autochthon promoted the south-eastward thin-skinned, piggy-back emplacement of the Upper Parautochton over the foreland basins and the autochthon, using the Main Trás-os-Montes-Thrust as the first order thrust of the *second contractional Variscan stage* (C_2; Figs. 10.1, 10.2, 10.3 and 10.4; Ribeiro et al. 1990). Subsequently, these basins were detached towards the CIZ, sliding on the Silurian strata generating the Basal Lower Parautochthon Detachment (Dias da Silva 2014; Dias da Silva et al. 2015b; González Clavijo et al. 2016). This allowed the tectonic elimination of parts of the stratigraphic sequence of all the involved units and produced the current wedge-like, open-to-the-east shape of the Lower Parautochthon below the Upper Parautochthon in the Morais and Bragança complexes (Fig. 10.2; Dias da Silva et al. 2014).

The C_2 event across northern Iberia was active during 350–330 Ma in the GTMZ and its boundary with the CIZ (Fig. 10.1). It produced the duplication of the pre-Variscan

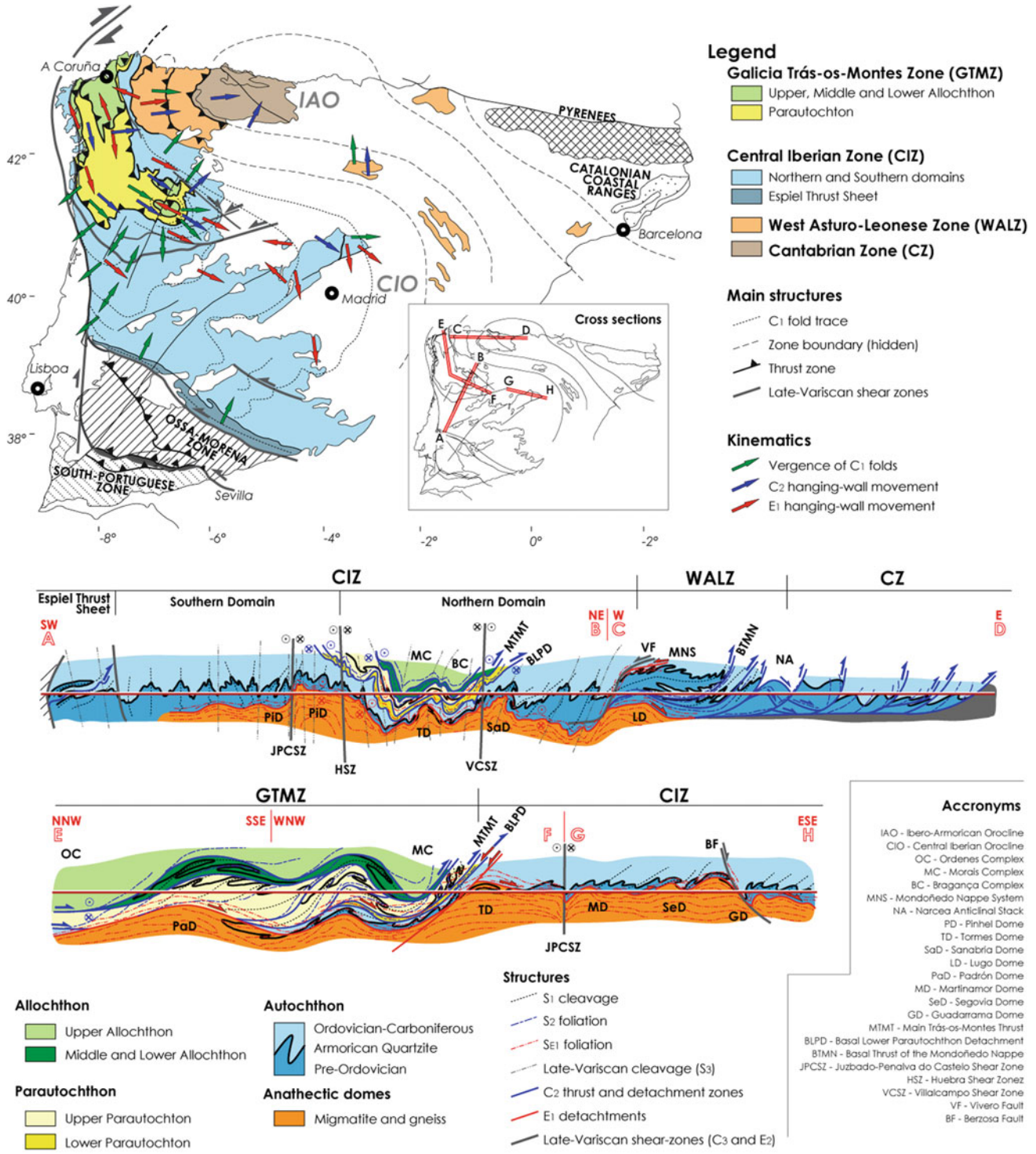

Fig. 10.2 Map of Iberia and simplified cross-sections with the main Variscan structures (modified from Ribeiro 1986; Pereira 1989; Díez Balda et al. 1990; González-Clavijo et al. 1993; Escuder Viruete et al. 1994; Martínez Catalán et al. 2004c; Martínez Poyatos et al. 2004a, b; Díez-Montes 2007; González-Clavijo and Diez Montes 2008; Moreira et al. 2010; Dias et al. 2013; Rodrigues et al. 2013a, b; Rubio Pascual et al. 2013a, b; Dias da Silva 2014; Martínez Catalán et al. 2014; Díez Fernández and Pereira 2016, and references there in). Granitic bodies have been omitted for a better view of the structures in map and sections

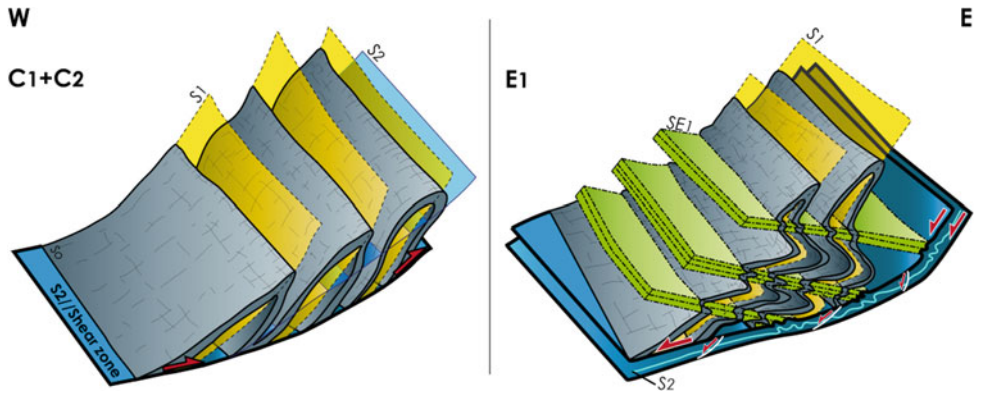

Fig. 10.3 Deformation sketches for the Upper Parautochthon (GTMZ), showing the initial compressional stages (C_1 and C_2) and related fabrics (S_1 and S_2) that produced tight ESE verging folds latter cut across by C_2 thrusts that increased the original flattening. The right-hand sketch depicts the effect of the E_1 stage in the Upper Parautochthon, where a sub-vertical pure-shear component produced a flat-lying pervasive crenulation cleavage (S_{E1}), axial planar to E_1 folds that wriggled the steeper C_1 folds. Along C_2 thrusts, E_1 deformation produced simple shear with top-to-the-WNW hanging-wall movement, opposite to the emplacement kinematics during C_2, evidencing the backward movement of the allochthonous complexes and the formation of tectonic depressions where they are currently preserved (adapted from Dias da Silva 2014)

stratigraphic record of northern Gondwana by means of the Main Trás-os-Montes-Thrust. This event was recorded in the GTMZ by the appearance of lawsonite in the uppermost structural levels of the Upper Parautochthon (Schermerhorn and Kotsch 1984), and by the blastesis of crossite and barroisite in the Lower Allochthon of Morais at ca. 330 Ma (Gil Ibarguchi and Dallmeyer 1991). This late-Visean age reveals that the upper allochthonous units were still being moved under very cold conditions, adding local extra-pressure to the underlying units (Fig. 10.4b). At the same time, the pressure peak of Barrovian-type metamorphism was attained beneath the allochthonous pile in the CIZ, roughly defining the maximum reach of the exotic terranes onto the northern Iberian autochthon (Escuder Viruete et al. 1994; Díez-Montes 2007; Martínez Catalán et al. 2014; Rubio Pascual et al. 2016).

The orogen-parallel emplacement of the allochthonous terranes along C_2 shear zones (Fig. 10.4b) was estimated at ≈200 km (Alcock et al. 2015). The derived thin-skinned dragging of the wedge was responsible for the nucleation of the Central Iberian Orocline (CIO; Martínez Catalán et al. 2014). The axial zone of this mega structure is currently defined by the sub-horizontal dragging and vertical axis rotations that produced the centrifuge vergence of C_1 folds (Figs. 10.2 and 10.4b) around the Morais and Bragança allochthonous complexes (Dias da Silva 2014), as well as the N-S striking, east-vergent C_1 folds in the Sierra de Guadarrama (Macaya et al. 1991; Rubio Pascual et al. 2013a, b).

The overburden created during the initial contractional stages triggered the synorogenic extensional collapse known as the *first extensional Variscan stage* (E_1; Martínez Catalán et al. 2014; Alcock et al. 2015), due to thermal relaxation, isostatic rebound and exhumation of the middle crust (Figs. 10.1 and 10.4c). Anathectic domes were formed, and oval-shaped structural basins developed interspersed among them, forming an egg carton structural pattern where the allochthonous complexes were preserved in the more depressed basins (Gómez Barreiro et al. 2007; Martínez Catalán et al. 2007, 2014). A wide variety of crust-derived melts were formed and gradually emplaced in the upper structural levels from E_1 to Late-Variscan times (e.g. Martínez 1974; López-Moro et al. 2012).

The anathectic domes are bounded on top by low-dipping extensional detachments, C_2 shear zones of subtractive character with different hanging wall kinematics (Fig. 10.3; Martínez Catalán et al. 2003). The E_1 structures allowed the thinning of the Variscan crust and M_1 metamorphic zones, being concomitant with the development and telescoping of M_2 isograds (Escuder Viruete 1993; Díez Balda et al. 1995; Martínez Catalán et al. 2003; Díez-Montes 2007; Gómez Barreiro et al. 2010b; Díez Fernández et al. 2012b; Díez Fernández and Pereira 2016; Dias da Silva 2014). The M_2 zonation is represented by three metamorphic units in the hanging-wall of the anathectic domes. These are based on the appearance of aluminium-silicate porphyroblasts grown coeval with the S_{E1} foliation and characterize a Buchan-type metamorphic evolution (Escuder Viruete 1993; Díez Balda et al. 1995; Arenas and Martínez Catalán 2003; Dias da Silva 2014). From bottom to top, these units are:

- **Lower Gneiss Unit**: Composed by gneissic rocks with sillimanite + k-feldspar (high amphibolite facies metamorphism).
- **Intermadiate Schist Unit**: Formed by sillimanite and andalusite + staurolite bearing schists.

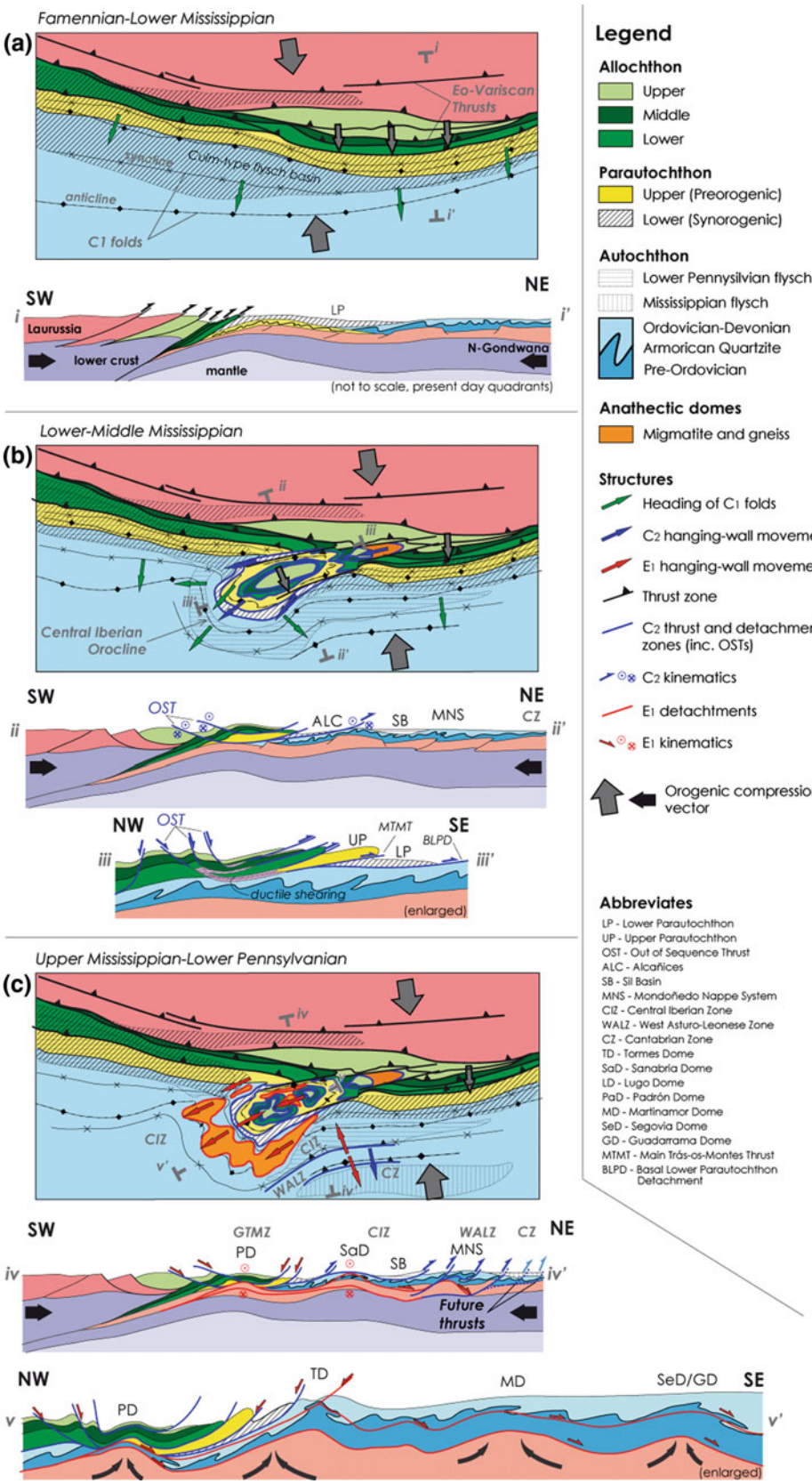
Famennian-Lower Mississippian
(a)
Eo-Variscan Thrusts
Culm-type flysch basin
synclines
anticline
C1 folds
SW
NE
Laurussia
lower crust
mantle
LP
N-Gondwana
(not to scale, present day quadrants)
Lower-Middle Mississippian
(b)
Central Iberian Orocline
OST
ALC
SB
MNS
CZ
NW
SE
UP
LP
MTMT
BLPD
ductile shearing
(enlarged)
Upper Mississippian-Lower Pennsylvanian
(c)
CIZ
WALZ
CZ
GTMZ
PD
SaD
SB
MNS
Future thrusts
TD
MD
SeD/GD
(enlarged)
Legend
Allochthon
Upper
Middle
Lower
Parautochthon
Upper (Preorogenic)
Lower (Synorogenic)
Autochthon
Lower Pennysilvian flysch
Mississippian flysch
Ordovician-Devonian Armorican Quartzite
Pre-Ordovician
Anathectic domes
Migmatite and gneiss
Structures
Heading of C1 folds
C2 hanging-wall movement
E1 hanging-wall movement
Thrust zone
C2 thrust and detachment zones (inc. OSTs)
C2 kinematics
E1 detachments
E1 kinematics
Orogenic compressional vector
Abbreviates
LP - Lower Parautochthon
UP - Upper Parautochthon
OST - Out of Sequence Thrust
ALC - Alcañices
SB - Sil Basin
MNS - Mondoñedo Nappe System
CIZ - Central Iberian Zone
WALZ - West Asturo-Leonese Zone
CZ - Cantabrian Zone
TD - Tormes Dome
SaD - Sanabria Dome
LD - Lugo Dome
PaD - Padrón Dome
MD - Martinamor Dome
SeD - Segovia Dome
GD - Guadarrama Dome
MTMT - Main Trás-os-Montes Thrust
BLPD - Basal Lower Parautochthon Detachment

◀ **Fig. 10.4** Evolutionary sketch for the Variscan deformations in Northern Iberia, modified from Dias da Silva (2014) and Dias da Silva et al. (2015a). **a** Initial thrusting in the hinterland with flysch sedimentation in both back-arc and foreland basins. The main transport direction (grey arrows) is perpendicular to the orogenic trend. C_1 is more intense near the axial zones of the orogenic wedge and weaker in the external zones represented today by the Iberian Autochthon (CIZ, WALZ and CZ); **b** The gravitational instability in the more active zones led to the formation of out-of-sequence thrusts (OSTs) that unrooted the Upper, Middle and Lower Allochthon onto the Upper Parautochthon sub-parallel to the structural grain. These movements were the consequence of a thin-skinned emplacement of a laterally extruded wedge from the hinterland towards the Iberian Autochthon, dragging the foreland basins in its footwall. C_1 folds in the Upper Parautochthon and in the autochthon were dragged and rotated due to the emplacement of the GTMZ wedge, thus wrapping them around the main C_2 thrusts and detachment faults and nucleating the Central Iberian Orocline (CIO). In the outer rim of this orocline, synorogenic flysch sedimentation occurred in basins covering partially eroded C_1 folds (e.g. Sil Basin); **c** The overburden of the Allochthon in N-Iberia induced synorogenic collapse with the formation of anatectic core complexes (domes) that allowed the exhumation of deep-settled rocks and the consequent backward movement of the allochthonous pile. Hanging wall kinematics was parallel to the orogenic trend and C_2 shear zones, evidencing an extension-dominated regime in N-Iberia during these stages. New C_2 thrusts, with kinematics matching the main orogenic transport direction (grey arrows) were formed in the more external domains (e.g. Mondoñedo Nappe System), showing the arrival of the Variscan tectonic front there. This led to the detachment of the previous synorogenic basins and the migration of the foreland basin towards the CZ. At the end of C_2 stage in the WALZ, E_1 structures collapsed the $C_1 + C_2$ systems, forming dome structures and propagating C_2 front into new regions (the CZ), previously to the development of the Ibero-Armorican Orocline (not represented)

- **Upper Slate Unit**: Composed at the base by chiastolite-bearing schists, in the middle by biotite-rich schists and by chloritic slates at the transition to areas outside the influence of E_1 (absence of S_{E1} flat-lying crenulation cleavage).

The formation of the metamorphic domes in the Autochthon of NW Iberia at 330–320 Ma caused dragging and parallelization of C_1 folds and S_1 cleavage to the extensional detachments in the hanging-wall units of the migmatitic cores, where E_1 fabrics obliterated almost completely the previous structures (Escuder Viruete et al. 1994, 1999; Díez Balda et al. 1995; Valle Aguado et al. 2005; Bea et al. 2009; Pesquera et al. 2009; Rubio Pascual et al. 2013a, b). Furthermore, E_1 doming folded the C_2 thrusts, and the extensional detachments continued the thinning of the Allochthon, that started during the early Variscan building of the accretionary wedge (Figs. 10.2 and 10.4c). The kinematics of E_1 detachments is variable and includes top-to-the-N and NW motions in several parts of the GTMZ, producing backward movements of the allochthonous thrust stack (Dias da Silva 2014). Some of these detachments reactivated previous C_2 shear zones. There, simple shear deformation mechanisms dominated, in contrast with the sub-vertical pure-shear regime component present between the detachments, where flat-lying crenulation cleavage and related sub-horizontal axial-plane folds developed, as for instance, in the Upper and Lower Parautochthon of NE Portugal (Fig. 10.3; Dias da Silva 2014).

Synchronously with the E_1 movements in the CIZ and GTMZ, a C_2 thrust system evolved inland leading to the unrooting of C_1 recumbent folds such as the Mondoñedo nappe (Martínez Catalán et al. 2003) at ca. 336–321 Ma (Dallmeyer et al. 1997). During C_2 (Figs. 10.2 and 10.4c), thick- to thin-skinned tectonics with eastward kinematics favoured the exhumation of deep settled rocks and the duplication of the Variscan basement in the WALZ (Gutiérrez-Alonso 1996; Martínez Catalán et al. 2003).

After the important E_1 extensional collapse and crustal equilibration, a *third contractional Variscan stage* produced a new generation of folds (C_3) that affected the whole Iberian Massif, and in particular the GTMZ and CIZ. Folds are well developed where a previous horizontal layering existed, and an associated crenulation cleavage (S3) formed where the previous regional foliation (S_1, S_2 or S_{E1}) was subhorizontal. C_3 folds reached a size similar to that of many C_1 folds, and some of the largest folds were nucleated on previous E_1 domes. They are commonly vertical or steeply inclined, and only occasionally overturned. A nearly horizontal stretching lineation developed often parallel to C_3 fold axes. These folds occur frequently in close relation with ductile, strike-slip shear zones, either dextral or sinistral (Iglesias Ponce de León and Choukroune 1980) but can also be seen far from them. In central and NW Iberia, the folds commonly show an axial planar attitude in relation to the Central Iberian Orocline and are considered coeval and genetically linked to tightening of this arc (Martínez Catalán 2011a, b).

Later on, a *second extensional Variscan stage* (E_2) produced detachment structures that assisted the exposition of high-grade rocks in the upper crust, leading to partial melting and formation of new domes (Arenas and Martínez Catalán 2003; Martínez Catalán et al. 2003). The $E_1 + E_2$ gravitational collapse in the WALZ forced the progression of the C_2 front into the CZ at about 312–300 Ma, producing a thin-skinned piggy-back imbricated sequence typical of externally orogenic regions (Pérez-Estaún et al. 1988; Pastor-Galán et al. 2013, 2014).

10.2.3 Remarks on the Formation of the Central Iberian Orocline

Í. Dias da Silva, J. Gómez Barreiro, E. González-Clavijo

Post-E_1 deformations (i.e. younger than 318 Ma, C_3 and E_2; Martínez Catalán et al. 2014) can be considered coeval with orocline development in Iberia (Pastor-Galán et al. 2018). However, if the Ibero-Armorican Orocline (Dias and Ribeiro 1995; Weil et al. 2001) is restored to a pre-bucking stage, C_2 and E_1 structures in the GTMZ and CIZ show an obliquity of almost 90° with respect to their equivalents in the WALZ (Fig. 10.4c). It is also noticeable that the structures that nucleated the CIO in the CIZ must be previous to the Upper Pennsylvanian-early Permian wrapping around the CZ (Pastor-Galán et al. 2011).

The restored position reveals the N-Iberian transect as a lineal orogen (Weil et al. 2010; Pastor-Galán et al. 2011; Shaw et al. 2012; Pastor-Galán et al. 2015), exposing the remarkable similarity of the eastward kinematics along the basal C_2 thrusts in the GTMZ and the E_1 flat-lying shear-zones, both running sub-parallel to the orogenic trend and C_1 fold axes in the CIZ (Dias da Silva 2014; Rubio Pascual et al. 2016). This means that the post-C_1 Variscan deformation in this region was dominated by the regional orogenic extensional vector (Fig. 10.4a). These parallel-to-the-orogen movements forced the wrapping of C_1 folds around C_2 and E_1 structures to nucleate the CIO (Fig. 10.4b, c; Pastor Galán et al. 2018; Dias da Silva et al. 2018). Therefore, the arcuate aspect of C_1 fold trends in the CIZ must be considered as a primary trait in relation to the buckling of the Ibero-Armorican Orocline, with bending produced due to thin-skinned tectonics. Opposingly, C_2 and E_2 shear-zones in the WALZ and C_2 structures in the CZ are perpendicular to the C_1 folds (Martínez Catalán et al. 2003, 2014) and are clearly related with the main orogenic contractional vector that also produced the C_1 folds (Fig. 10.4a). So, they did not promote changes in the original trend of C_1 axes (Fig. 10.4b, c).

These macroscale structural aspects are in agreement with the parallel display of the Namurian magnetic declination data in the northern, core and southern sectors of the CIO, including the WALZ and CZ (Pastor-Galán et al. 2016), and argue against the idea of a large scale secondary buckling, nucleated around the Morais Complex, formed coevally with the IAO (Martínez Catalán 2011a; Shaw et al. 2012; Weil et al. 2013).

The different geometrical relationships between deformation stages in GTMZ-CIZ and in WALZ-CZ, can be explained by lateral progradation of a thin-skinned tectonic wedge bearing the allochthonous complexes previously piled in the Eo-Variscan accretion prism (Fig. 10.4a; Dias da Silva et al. 2018). The unrooting of this tectonic pile was possibly due to a corner effect in the orogenic front (Martínez-Catalán 1990; Dias da Silva 2014). It promoted the parallel-to-the-orogen extrusion of the Upper, Middle and Lower allochthons over the Parautochthon and CIZ by the means of out-of-sequence thrusts and detachments from the late Devonian until early-late Carboniferous time (Fig. 10.4b; Dias da Silva et al. 2015a). The continuous contractional regime allowed the formation of a new set of C_2 thrusts in the WALZ and CZ during the late-Carboniferous, which are synchronous with the E_1 detachments in the CIZ and consequently unrelated to those responsible by the emplacement of the GTMZ extrusion wedge over the CIZ (Fig. 10.4c). They are a direct response to the increasing proximity of the more orogenically active zones in N-Iberia during the latest stages of the Variscan continental collision and, therefore, they are parallel and intrinsically associated with the orogenic-scale compressional vector.

10.3 Southwestern Iberia

A. Azor, J. F. Simancas, D. Martínez Poyatos, I. Pérez-Cáceres, F. González Lodeiro, I. Expósito

This part of the Variscan Massif comprises the Central Iberian Zone (CIZ) south of the Toledo extensional shear zone, the Ossa-Morena Zone (OMZ) and the South Portuguese Zone (SPZ) (Fig. 10.2). The structural evolution of this region attests a number of particular features regarding the timing, kinematics and number of tectonic episodes. Thus, unlike the CIZ north of Toledo (Northern Iberia, this chapter), the southern CIZ exhibits relatively simple Carboniferous upright folding and low metamorphic grade, with the exception of a narrow band located just north of the boundary with the OMZ. More importantly, from the Pedroches Carboniferous Basin to the south, distinguishing structural characteristics of Southwestern Iberia with respect to Northern Iberia refer to the presence of an intracollisional Early Carboniferous transtensional stage that gave way to widespread basin development and magmatism, and the transpressive character of the whole collisional Variscan evolution, with left-lateral movements being probably dominant over orthogonal ones. These two particular features are probably related to the large-scale plate tectonic scenario that controlled the Variscan evolution of Southwestern Iberia (see below).

10.3.1 Variscan Structure of the Southern Central Iberian Zone

The region described in this section (Fig. 10.5a) mostly coincides with the Lusitanian-Alcudian Zone originally defined by Lotze (1945). The southern Central Iberian Zone (CIZ) is characterized by large outcrops of the pre-Ordovician Schist-Greywacke Complex (locally called 'Alcudian'), unconformably overlaid by an Ordovician-Devonian passive-margin succession. The most outstanding Variscan structures are NW-SE trending upright folds that depict the cartographic pattern (Fig. 10.5).

Pre-Variscan deformations have also been described and related to either Cadomian (Late Ediacaran) or Toledanic (Middle-Late Cambrian) tectonic events that gave way to regional unconformities. In the Schist-Greywacke Complex, the Cadomian deformation produced folds in the Lower Alcudian succession, without associated foliation and metamorphism; the Upper Alcudian succession unconformably covers the lower succession giving way to the so-called intra-Alcudian unconformity (Ortega and González Lodeiro 1986; Palero 1993). Talavera et al. (2015) have tentatively dated the Cadomian event in this region by using detrital zircon population ages, which show a time gap of ~20 Ma (575–555 Ma) between the maximum depositional ages of the two Alcudian successions. In the southernmost CIZ, the Cadomian unconformity has been recognized in the core of the Peraleda Anticline (Fig. 10.5; Llopis et al. 1970; Capdevila et al. 1971), where the Ediacaran rocks show a low- to medium-grade foliation dated at 560–540 Ma (Blatrix and Burg 1981; Dallmeyer and Quesada 1992; Henriques et al. 2015). To conclude, the Cadomian tectonothermal imprint seems to be present in the southernmost CIZ, while to the north only the intra-Alcudian unconformity has been found, lacking any evidence of Cadomian penetrative deformation and metamorphism. This contrast is accompanied by a different Ediacaran stratigraphy, with the Serie Negra in the southernmost CIZ and the Schist-Greywacke Complex to the north. In this respect, Pérez-Cáceres et al. (2017) have argued in favor of a hidden Cadomian suture beneath the Pedroches basin.

Another unconformity (Toledanian) is usually observed as a low-angle obliquity between pre-Ordovician and lowermost Ordovician rocks (Fig. 10.5). This unconformity is

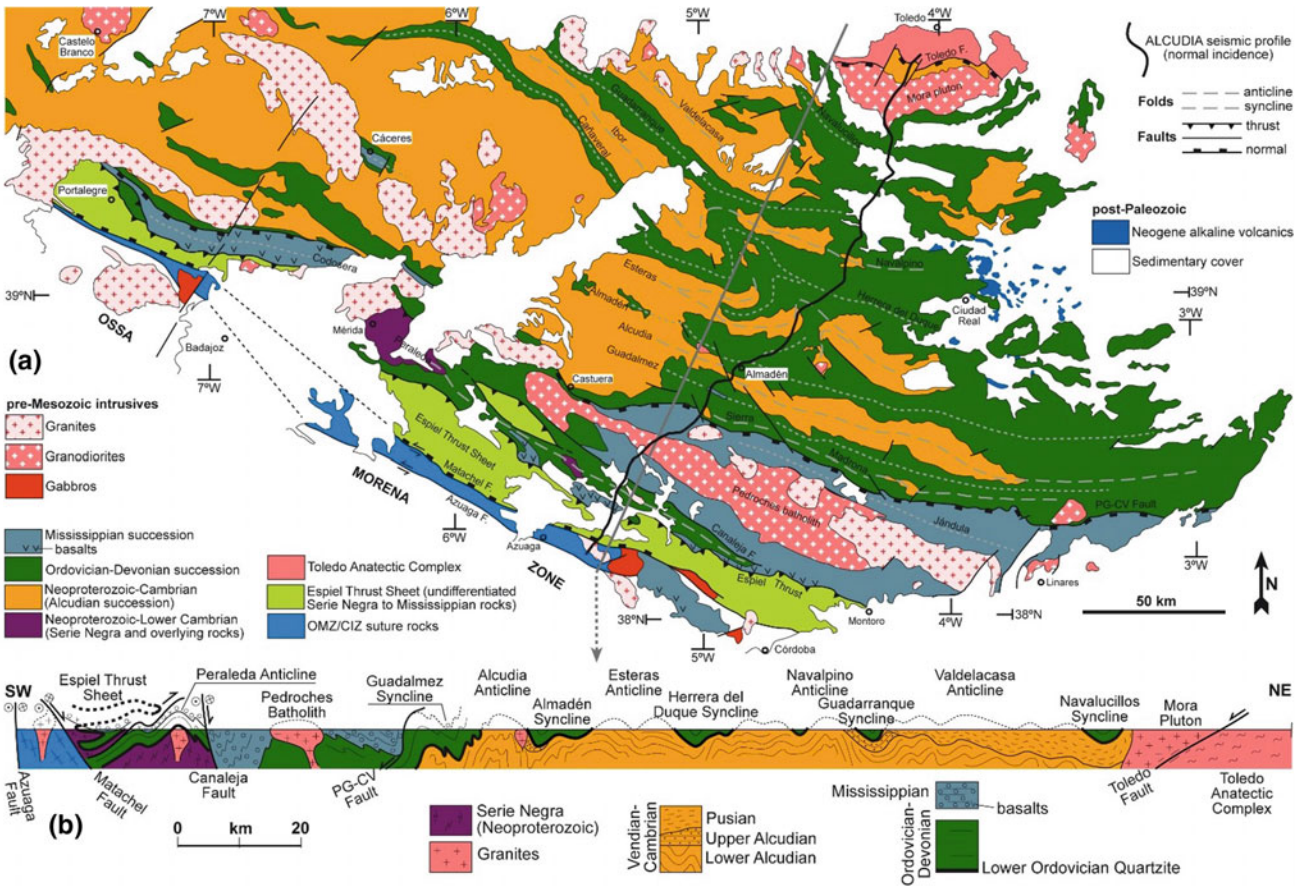

Fig. 10.5 **a** Geological map of the study area, showing the Espiel Thrust Sheet (Fig. 10.6) and the ALCUDIA seismic profile (Fig. 10.7). **b** Geological cross-section (modified from Martínez Poyatos et al. 2012)

probably due to fault-related tilting and/or gentle folding occurred at Middle/Late Cambrian time. Furthermore, sudden changes in thickness of the lowermost Ordovician formation point to the existence of a paleorelief at that time (McDougall et al. 1987).

The first Variscan deformation is pre-Visean (probably Late Devonian) in age, having only affected the Espiel Thrust Sheet, an allochthonous unit located at the southernmost CIZ next to the boundary with the OMZ (Fig. 10.5). Here, the Ediacaran to Lower/Middle Devonian succession was deformed by syn-metamorphic recumbent folds and related ductile shearing (Azor et al. 1994a; Martínez Poyatos 1997; Martínez Poyatos et al. 1995a, b and 1998a). The recumbent folds strike NW-SE and display NE vergence, with overturned limbs that can exceed 15 km (Fig. 10.6). The rocks show a penetrative planar-linear fabric parallel to the axial planes of the folds. The stretching lineation is parallel to the fold axes, while asymmetrical structures reveal top-to-the-SE kinematics. The metamorphic conditions range from the chlorite zone in the NW to the sillimanite zone in the SE, with a low- to intermediate-pressure gradient (Martínez Poyatos et al. 2001). These eo-Variscan structures are interpreted as formed during the transpressional OMZ/CIZ collision, being the NE-vergent folds of the southernmost CIZ retro-vergent structures with respect to the coeval SW-vergent folds in the OMZ (e.g., Simancas et al. 2001). The recumbent folds of the CIZ were unconformably covered by Lower Carboniferous sediments (Fig. 10.6).

A transtensional scenario characterized SW Iberia in the Early Carboniferous (e.g. Simancas et al. 2003). In the southern CIZ, subsidence led to the accumulation of a thick flysch succession (the Culm-facies Pedroches Basin; Gabaldón et al. 1985) that widely crops out along a NW-SE trending band located to the North of the OMZ/CIZ boundary (Fig. 10.5). The visible thickness of this basin exceeds 6000 m. Basaltic volcanism accompanied the beginning of the sedimentation mostly in the SW part of the basin, attesting significant lithospheric thinning (Armendáriz et al. 2008). Additional evidence of transtensional crustal thinning is given by the left-lateral to normal, high- to low-temperature, ductile- to brittle shearing recorded at the OMZ/CIZ boundary (Azor et al. 1994b).

In the Espiel Thrust Sheet, the Culm-facies sedimentation ceased at Late Visean time, being replaced by shallowing-upward sequences at Namurian (paralic facies) and Westphalian (limnic facies) time, with erosional episodes in-between (Fig. 10.6f). These changes in sedimentation have been related to the progressive uplift of the Espiel Thrust Sheet during its NE displacement (Martínez Poyatos et al. 1998b; Fig. 10.6c). The cartographic overlap of the Espiel Thrust Sheet onto its relative para-autochthon does not exceed 12 km, but the total displacement might have been greater since the thrust superposed highly deformed and metamorphosed rocks onto a still undeformed succession.

All of the previous structures were deformed by the km-scale NW-SE trending upright folds that dominate the cartographic pattern in the whole southern CIZ (Fig. 10.5). To the NW, the synclines are narrow, while the corresponding anticlines are large and dome-shaped. To the SE, the appearance of domes and basins and hook-shaped fold interferences (Martínez Rius 1983; Vergés 1983; Fig. 10.5a) have been interpreted as fold rotation due to later NW-SE oriented sinistral shearing (Aller et al. 1986; Ortega 1986), or superimposed NE-SW oriented folding (Aerden 2004; Martínez Catalán 2011a, b). The strain related to this folding episode was weak, with development of an axial-plane slaty cleavage in the metapelitic rocks and occasional rough partition in the quartzites. The occurrence of foliation transecting some of the folds suggests that folding was accompanied by some transcurrent simple shear component (Aller et al. 1986; Dias and Ribeiro 1991). The associated regional metamorphism was of very low- to low-grade, with a low- to intermediate-pressure gradient (López Munguira et al. 1991; Martínez Poyatos et al. 2001).

The late Variscan deformation in the CIZ is characterized by transcurrent ductile-brittle shear zones and low-angle extensional shear zones. The most important of these shear zones are located in the northern and central CIZ (Juzbado-Penalva left-lateral shear zone, Tormes, Salamanca and Berzosa detachments; Fig. 10.2). In the southern CIZ, two important extensional shear zones have been reported, namely the Toledo and Puente Génave/Castelo de Vide (PG-CV) shear zones (Fig. 10.5). The Toledo shear zone (Hernández Enrile 1991; Barbero 1995) separates very low-grade metasediments and granites (the Mora pluton) in the hanging wall from the Toledo Anatectic Complex in the footwall. The shear zone is made up of 350 m of mylonites with superposed cataclasites, breccias and a sharp fault surface atop. The activity of the Toledo shear zone is late- to post-Variscan ($\geq$280 Ma) according to apatite fission-track data (Barbero et al. 2005). The footwall (Toledo Anatectic Complex; Barbero et al. 1995) is composed of granulite facies migmatitic pelites, orthogneisses and diverse granitoids, emplaced before and during the metamorphic climax (800 $\pm$ 50 °C, 4–6 Kbar). Ion-microprobe U–Pb on zircon data have revealed that melting processes occurred at $\approx$340 Ma, while mafic bodies intruded at 307 Ma (Bea et al. 2006). The PG-CV shear zone (Martín Parra et al. 2006) bounds to the North the main Mississippian outcrops in the Pedroches Basin (Fig. 10.5). The shear zone dips to the South and at surface coincides with Silurian black shales, which appear transformed to phyllonites. In the eastern part, the PG-CV shear zone is characterized by ductile deformation affecting the pre- to syn-kinematic Santa Elena pluton ($\sim$320 Ma; U/Pb zircon unpublished data), where S-C

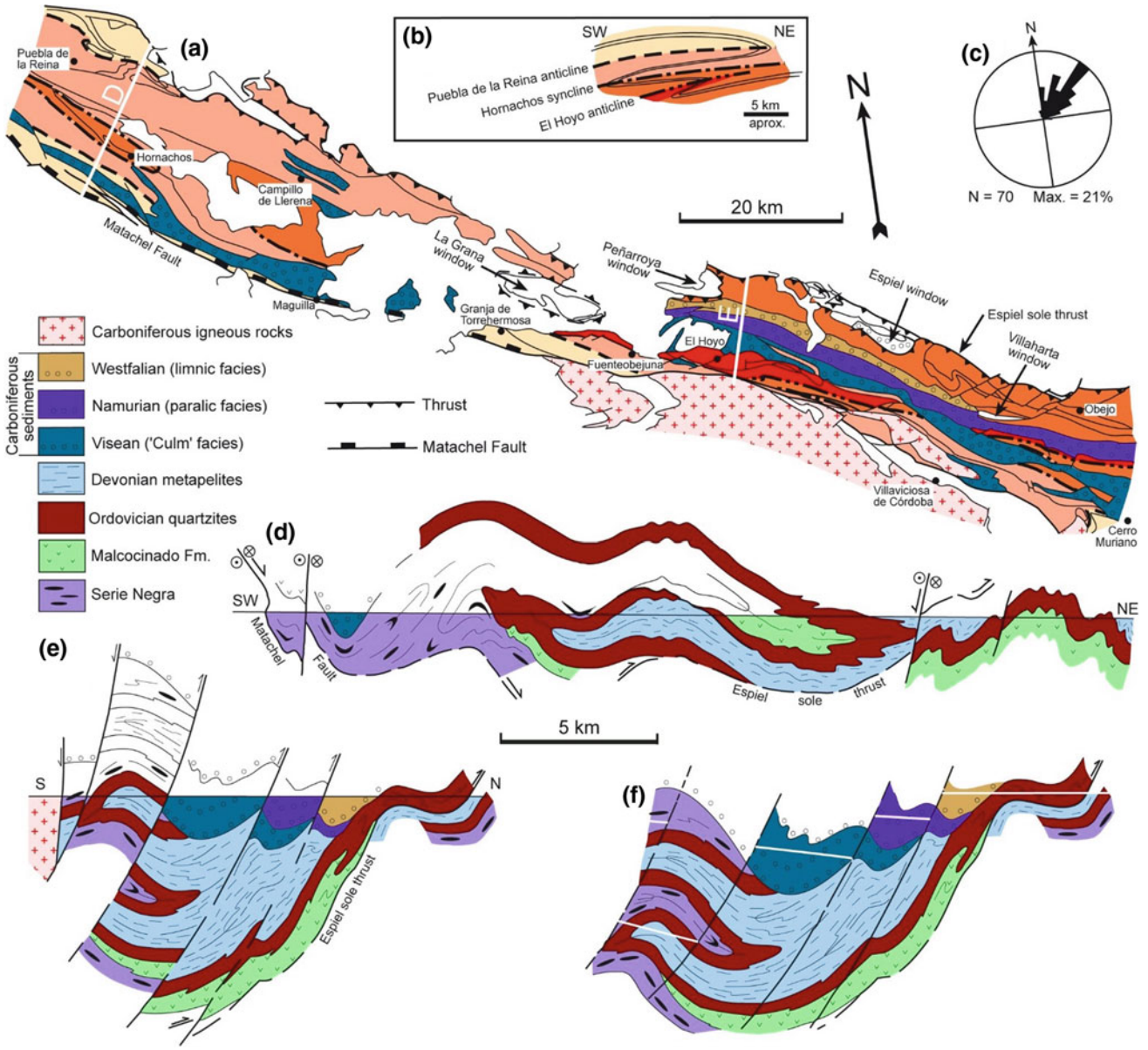

Fig. 10.6 Structure of the central and eastern sectors of the allochthonous Espiel Thrust Sheet (for location, see Fig. 10.5). **a** Map showing the recumbent folds, the overlying Carboniferous sequences, and the underlying tectonic windows of the para-authochthonous. **b** Sketch section of the recumbent folds (same colors of the fold-limbs and axial traces as in the map). **c** Rose diagram of striations of the Espiel sole thrust. **d** and **e** Geological cross-sections (located on **a**). **f** Cross-section **e** with restored late faults, showing the interpreted original disposition of the Carboniferous sequences

structures indicate top-to-the-South kinematics. The shear zone also generated two km-scale drag folds (Fig. 10.5).

The knowledge of the crustal structure of the southern CIZ has been improved by recent geophysical investigations. The ALCUDIA deep seismic reflection profile (Martínez Poyatos et al. 2012) has provided with a high-resolution 2D crustal section from the OMZ/CIZ boundary to the Toledo Anatectic Complex (Fig. 10.7). The Moho discontinuity is subhorizontal and located at 10 s (~30 km). The reflectivity of the upper crust is not very intense, probably due to the dominant monotonous lithologies (Schist-Greywacke Complex and granite intrusions), though the variably dipping reflectors correlate well with surface geology. By contrast, intense reflectivity in the middle-lower crust is depicted by numerous high-amplitude and laterally coherent events, suggesting a fine banded/laminated/sheared fabric. This

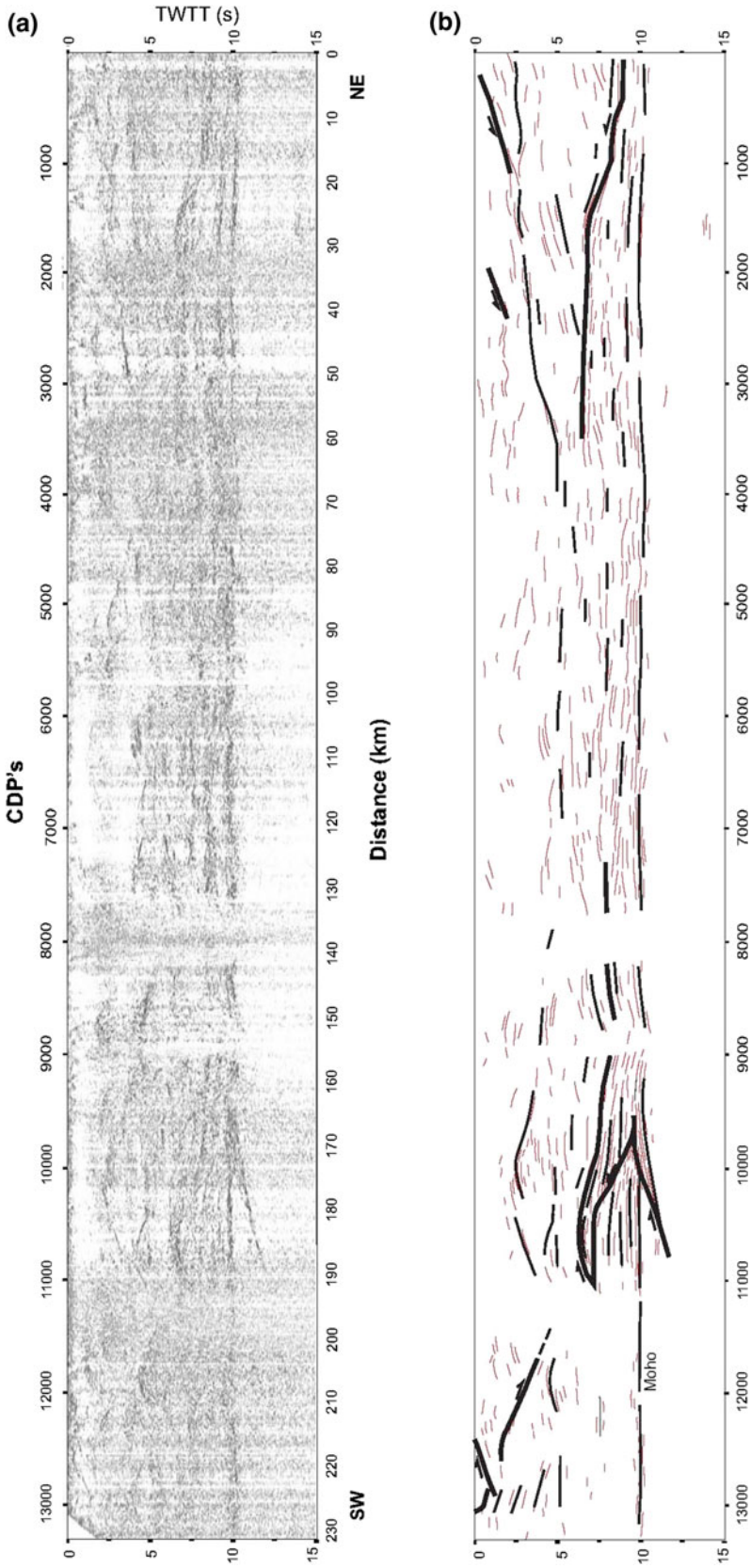

Fig. 10.7 **a** Coherency filtered stacked image of the ALCUDIA deep seismic reflection profile (see Fig. 10.5a for location; modified from Martínez Poyatos et al. 2012). **b** Line drawing of the most conspicuous reflectivity (in light red) and large-scale tectonic interpretation

pervasive seismic fabric is subhorizontal in the central part of the section, while it reveals two large-scale contractional structures at both ends of the seismic profile. Thus, the northern end lower crust depicts a South-directed flat-ramp-flat thrust geometry located below the Toledo shear zone, while the lower crust below the Pedroches basin shows a conspicuous tectonic wedge that involves the Moho and the upper mantle. The interpretation of these two specific lower crustal structures accounts for 65 km of shortening. Interestingly, a similar value of shortening is homogeneously distributed in the upper crust through the relatively simple train of Carboniferous km-scale upright folds (Fig. 10.5b). Therefore, the ALCUDIA seismic image shows that, in an intracontinental orogenic crust, the upper and lower crust may react differently to shortening in different sectors, which is taken as evidence of decoupling. The detachment would coincide with the reflectivity contrast located at 4–5 s, which would likely separate an upper crust made up of metasediments and granite intrusions from a laminated crystalline basement. Moreover, the lower-crustal thrust in the northern end of the profile produced thickening, which, in turn, gave way to upper crustal extension (the Toledo and Mora normal faults) above the thrust (Fig. 10.7b). Differently, the thickening produced by the lower crustal tectonic wedge in the southern part of the profile resulted only in antiformal doming above the wedge (Fig. 10.7b) without upper crustal extension, probably because the thickening here took place on a previously attenuated crust (the Early Carboniferous transtensional event that formed the Pedroches Basin).

A wide-angle reflection profile coincident with the ALCUDIA one (Ehsan et al. 2015) has allowed to obtain a high-resolution P-wave seismic velocity model of the CIZ crust from the OMZ/CIZ boundary to the southern border of the Spanish Central System. The model shows the detailed position of the Moho as a sharp P-wave velocity contrast from 7.2 to 8.0 km/s, which gradually deepens from 31 km in the southern end of the profile to 36 km in its northern end. The boundary between the upper and mid-lower crust is characterized by a P-wave velocity contrast from 6.2 to 6.6 km/s in the south (at ~13 km depth) and 6.4 to 6.6 km/s to the north (at ~20 km depth), which is interpreted as a decoupling zone that represents lithological/rheological variations.

10.3.2 Variscan Structure of the Ossa-Morena Zone

The Ossa-Morena Zone (OMZ) stands out in the Iberian Massif mostly drawing on stratigraphic, magmatic, and structural grounds. From a stratigraphic point of view, both Ediacaran and Lower Paleozoic Sequences in the OMZ are quite distinctive with respect to other Variscan Zones in the Iberian Massif. Regarding magmatism, the OMZ is distinguished by the relative abundance of late Ediacaran and Middle Cambrian to Ordovician volcanic and plutonic rocks.

On a large scale, the Variscan structure of the OMZ must be viewed as a continental piece deformed in-between two suture contacts, namely the contact with the CIZ (Burg et al. 1981; Azor et al. 1994b; Simancas et al. 2001) and the contact with the SPZ (Bard 1977; Crespo-Blanc and Orozco 1988; Fonseca and Ribeiro 1993; Quesada et al. 1994; Castro et al. 1996; Azor et al. 2008; Pérez-Cáceres et al. 2015). These two contacts are interpreted as suture zones that allowed subduction to balance the shortening accumulated in upper crustal structures (e.g., Simancas et al. 2013). Subduction at the OMZ/CIZ boundary seems to have accommodated most of the shortening in the OMZ interior, while the OMZ/SPZ boundary must account for the shortening measured in the SPZ.

The crustal structure of the OMZ is very well constrained from seismic surveys (Simancas et al. 2003; Palomeras et al. 2009), which have clarified two main facts: (1) the shortening estimated from the observed structures in the field and the upper crustal seismic section must be compensated at a mid-crustal detachment, without entering the lower crust; (2) the flat Moho at ≈10 s is obviously younger than the Variscan orogeny, which implies that the two putative subduction slabs at both boundaries of the OMZ have not been imaged, their polarity being therefore inferred from the vergence of the Variscan structures and the location of oceanic-like crustal remnants and high-pressure metamorphic belts.

The description of the Variscan structures in the OMZ is presented below in three subsections dealing with the two suture boundaries and the interior of the zone. The subsection devoted to the description of the OMZ/SPZ boundary will only deal with the emplacement of the Beja-Acebuches amphibolites; the Carboniferous collisional evolution will be addressed together with the SPZ (see Sect. 10.3.3) since it started at the boundary with the OMZ and propagated to the SW, thus affecting the whole SPZ.

10.3.2.1 The Boundary Between the Ossa-Morena and Central Iberian Zones

The OMZ/CIZ contact (Fig. 10.8) has been considered a suture of the Variscan orogen according to its metamorphic and tectonic evolution (Burg et al. 1981; Matte 1986; Azor et al. 1994b; Simancas et al. 2001, 2002; Pereira et al. 2010a, b, 2012). This is further supported by the change of the structural vergence through the OMZ/CIZ boundary, with NE-vergent recumbent folds and thrusts in the southernmost CIZ (see Sect. 10.3.1) and SW-vergent recumbent folds and thrusts in the OMZ (Martínez Poyatos 1997; Simancas et al.

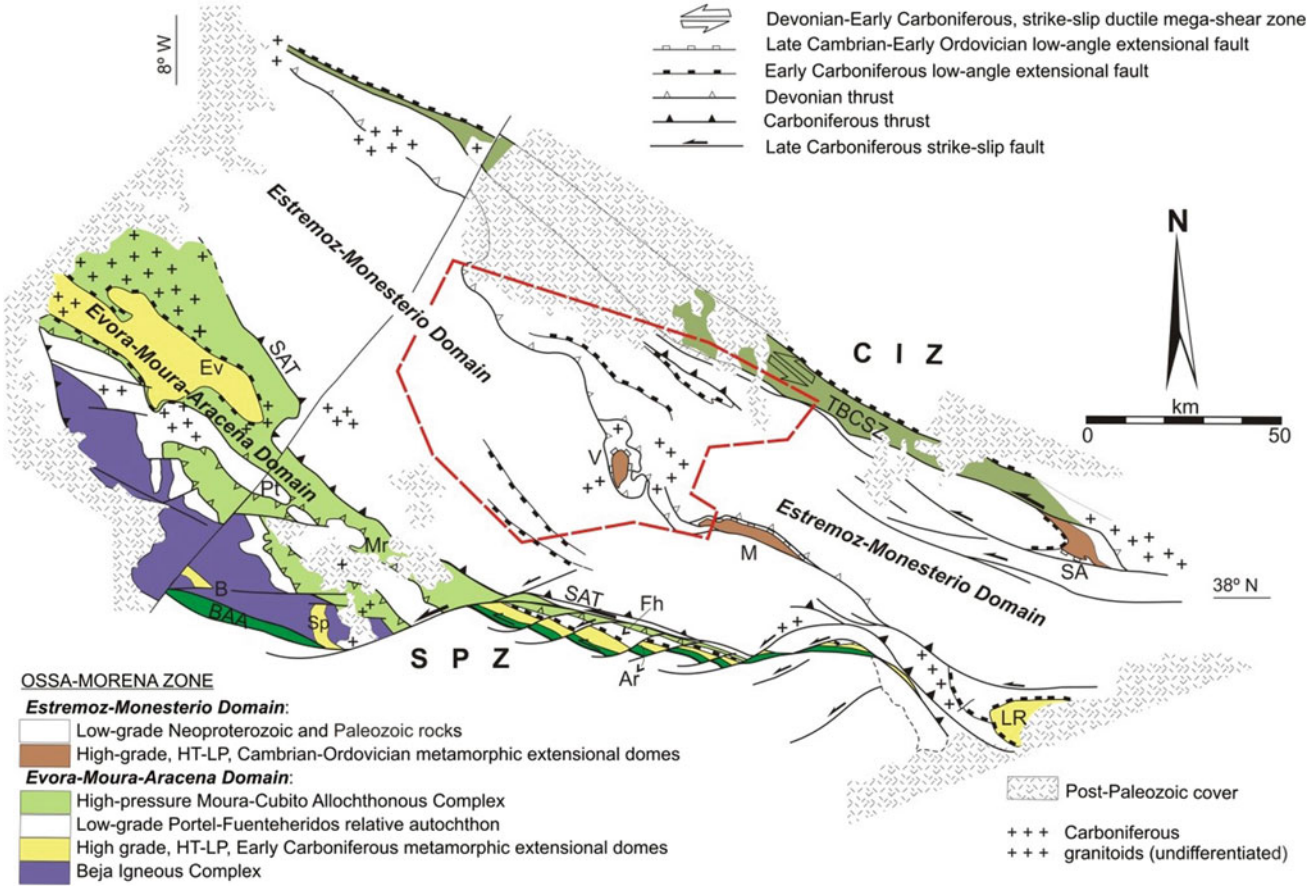

Fig. 10.8 Domains of the Ossa-Morena Zone. The inset at the central part of the Estremoz-Monesterio Domain locates the geological map shown in Fig. 10.10. Abbreviations: Ar, Aracena; B, Beja; BAA, Beja-Acebuches Amphibolites; CIZ, Central Iberian Zone; Ev, Evora; Fh, Fuenteheridos; LR, Lora del Río; M, Monesterio; Mr, Moura; Pt, Portel; SA, Sierra Albarrana; SAT, Santo Aleixo Thrust; Sp, Serpa; SPZ, South Portuguese Zone; TBCSZ, Tomar-Badajoz-Córdoba Shear Zone; V, Valuengo

2001; Expósito et al. 2002), as well as by the IBERSEIS and ALCUDIA seismic profiles that have imaged a NE-dipping slab down to the middle crust (Simancas et al. 2003; Martínez Poyatos et al. 2012). All these data emphasize the importance of this tectonic boundary and, together with the available geochemical and geochronological data, point to the possible existence of some sort of narrow oceanic realm between the OMZ and CIZ in Lower Palaeozoic times. Actually, the geochemical and geochronological data of sheet-shaped strongly deformed bodies of basic rocks included in this contact showed the existence of two groups corresponding to (i) dikes intruded into a continental basement during the late Precambrian Cadomian orogeny, and (ii) fragments (currently tectonic lenses) of an Early Paleozoic oceanic-like crust (Ordóñez Casado 1998; Gómez-Pugnaire et al. 2003).

The boundary between the OMZ and the CIZ was first set up as a major left-lateral and subvertical ductile shear zone, namely the Tomar-Badajoz-Córdoba Shear Zone (TBCSZ; Burg et al. 1981; Matte 1986), running for 300 km in SW Iberia with a NW-SE orientation (Fig. 10.8). According to some authors, the TBCSZ would represent a polyorogenic terrane that underwent a high-pressure, high-temperature Late Precambrian (Cadomian) metamorphism, followed by a low-grade Late Palaeozoic one (Variscan) (Quesada 1990; Abalos et al. 1991, 2002; Eguiluz et al. 2000; Ribeiro et al. 2007). Nevertheless, a good number of geochronological and structural data indicate that the metamorphic evolution of the TBCSZ is entirely Variscan in age (Azor et al. 1993, 1994b; Ordóñez Casado 1998; Pereira et al. 2010a, 2012). This narrow band of highly sheared and distinctively metamorphosed rocks is made up of rocks that are neither represented in the CIZ to the NE nor in the OMZ to the SW.

The TBCSZ consists in metasediments, orthogneisses, amphibolites and minor serpentinites organized in a sequence in which the structural top is located to the NE. The lower part of the sequence is dominated by orthogneisses and amphibolites with minor metasediment intercalations (mainly migmatites). The amphibolites appear intercalated with the different orthogneissic and migmatitic

lithologies, showing hectometre- to kilometre-scale along-strike lengths (López Sánchez-Vizcaíno et al. 2003). By contrast, the upper part is dominated by metasedimentary rocks (garnet-bearing micaschists with minor quartzite intercalations) and only a few orthogneissic bodies. The geochronological ages available for the orthogneisses range from Middle Cambrian to Middle Ordovician (see Simancas et al. 2004, for a review). Orthogneisses of similar ages and geochemical signatures are also found in the interior of the OMZ, the entire CIZ and the allochthonous complexes of the Galicia-Tras-Os-Montes Zone, having been generally attributed to the rifting episode that marks the onset of the Variscan cycle (e.g. Expósito et al. 2003; Sánchez García et al. 2003; Simancas et al. 2004; Díez Fernández et al. 2015).

The metamorphic evolution of the lower part of the TBCSZ is characterized by an initial high-pressure/intermediate-temperature event (Abalos et al. 1991) with peak-pressure conditions of ≈19 kbar and 550 °C, followed by a high-pressure/high-temperature one with peak temperatures of ≈725 °C (López Sánchez-Vizcaíno et al. 2003). Subsequently, these rocks were retrogressed to intermediate pressures, but maintaining the high-temperature conditions (amphibolite- and migmatite-facies assemblages). Finally, retrogression reached greenschist-facies conditions and the rocks were exhumed to the upper crust. The upper part of the TBCSZ recorded only intermediate-pressure/intermediate-temperature conditions (the micaschists contain garnet and rare kyanite; Abalos 1990; Azor 1994; Azor et al. 1997) with peak pressures of ≈10 kbar and temperatures of ≈500 °C. The high-pressure metamorphism recorded in the TBCSZ can be related to Variscan underthrusting beneath the southern border of the CIZ in an early compressional stage whose structural record became completely obliterated by the later shearing that penetrates the whole subducted unit (see below). This shearing produced the retrogression of the high-pressure assemblages first to amphibolite- and then to greenschist-facies assemblages while the rocks were being exhumed to upper-crustal levels (Azor et al. 1994b; Simancas et al. 2001).

The available geochronological data on the metamorphic evolution of the TBCSZ mostly constrain the temperature-peak conditions (≈340 Ma) and the subsequent retrogression to amphibolite (≈335 Ma) and greenschist (≈330 Ma) facies conditions (Blatrix and Burg 1981; Quesada and Dallmeyer 1994; Ordóñez Casado 1998; Pereira et al. 2010a, b). Peak pressure (eclogite facies) would have taken place probably some million years before (Late Devonian?) peak temperature.

The structure of the TBCSZ as observed in the field basically consists in a NW-SE oriented km-scale cartographic band of strongly sheared rocks, which are affected by minor later folds and cut across by later NW-SE striking brittle faults (Figs. 10.8 and 10.9). Thus, ductile shearing

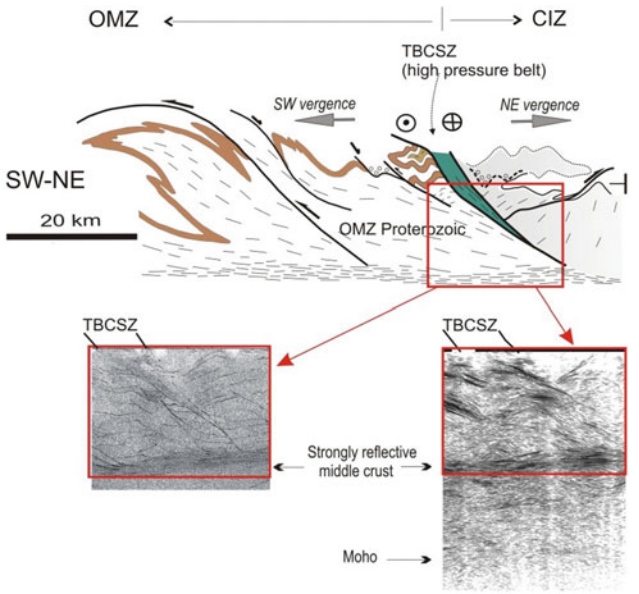

Fig. 10.9 Geological cross-section and seismic windows of the Tomar-Badajoz-Córdoba Shear Zone. The windows correspond to two different processings of the IBERSEIS deep seismic reflection profile (Simancas et al. 2003). CIZ, Central Iberian Zone; OMZ, Ossa-Morena Zone; TBCSZ, Tomar-Badajoz-Córdoba Shear Zone

penetrated the whole unit, giving way to an intense planar-linear fabric. The mylonitic foliation strikes on average NW-SE with dominant steep dips to the NE, in accordance with NE-dipping seismic reflectors (Fig. 10.9; Simancas et al. 2003, 2016). The stretching lineation is subhorizontal, or gently plunging either to the NW or to the SE. Shear criteria indicate a left-lateral sense of movement when the foliation is steeply dipping and top-to-the-NW when the foliation dips moderately to the NE. The total ductile left-lateral displacement along the TBCSZ has been estimated at ≈150 km by applying different simple shear models (Pérez-Cáceres et al. 2016).

Two later fold generations have been recognized in the TBCSZ, both of them with axes parallel to the stretching lineation, i.e. NW-SE. The first folds show SW-dipping axial surfaces, being responsible for the observed dip changes of the main foliation at different transects; the second folds are upright and have only been observed locally. The final cartographic pattern of the TBCSZ is due to an episode of brittle faulting, which constrains the observed thickness to be between 5 and 15 km (Figs. 10.8 and 10.9). To the SW, the gneissic and migmatitic lithologies appear cut by a prominent subvertical left-lateral fault, namely the Azuaga Fault (Azor 1994). To the NE, the micaschists of the upper part of the TBCSZ are cut by the Matachel Fault, which dips to the NE and has a normal component, i.e. it downthrows the southernmost CIZ rocks (Azor et al. 1994b).

To understand the tectonic meaning of the shearing affecting the whole TBCSZ rocks, we need to consider its

metamorphic evolution, with higher temperature and pressure conditions recorded in the lower part, keeping also in mind that these rocks are geometrically below lower grade rocks of the southernmost CIZ. These considerations led Azor et al. (1994b) to claim that the left-lateral shearing affecting the whole TBCSZ rocks must have, in addition to the obvious and dominant left-lateral movement, a normal (extensional/transtensional) component that contributed to the final exhumation of the rocks now exposed. Therefore, this shearing can be framed in the Early Carboniferous transtensional intraorogenic episode that affected the whole SW Iberian Massif.

The seismic expression of the TBCSZ rocks is quite prominent and mostly consists in a wedge of northeast dipping reflectivity that strongly contrasts and cuts across the seismic fabric at both sides (Fig. 10.9). The reflectivity of the TBCSZ rocks shows a lower part characterized by high-amplitude energy, which probably corresponds to orthogneisses and amphibolites, while the less reflective upper part with wavy reflections corresponds to the micaschists. Truncation of reflections along the northern border of the TBCSZ defines the Matachel fault (Fig. 10.9).

10.3.2.2 The Interior of the Ossa-Morena Zone

To better describe the structure of the OMZ interior we will divide it into two domains, namely the Estremoz-Monesterio domain to the north and the Evora-Moura-Aracena domain to the south, separated by the Santo Aleixo thrust (Fig. 10.8). Both domains share NW-SE structural grain and SW-vergent folds and thrusts (e.g., Vauchez 1975; Expósito 2000; Simancas et al. 2001; Expósito et al. 2002). However, the rocks of the Estremoz-Monesterio domain exhibit only very low or low-grade Variscan metamorphism, while in the Evora-Moura-Aracena domain low-pressure/high-temperature metamorphic rocks crop out in the core of transtensional Carboniferous dome-shaped sectors.

The Estremoz-Monesterio Domain

The general structure of this domain is well observed at its central sector (Figs. 10.8 and 10.10), where the cartographic information is quite good and the geometry of the different structures very well known (Expósito 2000; Expósito et al. 2002). The Variscan deformation consists in two compressional stages separated by a transtensional one that occurred at Early Carboniferous time. Moreover, at two localized areas, structural and metamorphic features attributed to a rift-related Cambrian-Ordovician event have been detected (Fig. 10.8).

Cambrian-Ordovician Extensional Domes

The Late Cambrian—Early Ordovician time-span in the OMZ corresponds to a rifting stage that presumably preceded and/or was coeval to the initial development of the Rheic Ocean (e.g., Sánchez García et al. 2003; Simancas et al. 2004; Etxebarria et al. 2006; Díez Fernández et al. 2015). This tectonic interpretation is mainly based on the stratigraphic and magmatic record, but two dome-shaped sectors, namely Valuengo-Monesterio and Sierra Albarrana (Fig. 10.8), have preserved tectonic fabrics and low-pressure/high-temperature metamorphic assemblages of Cambrian-Ordovician age, which are ascribable to this pre-Variscan rifting episode (Expósito et al. 2003; Azor et al. 2012).

The Valuengo-Monesterio metamorphic outcrops form a discontinuous and narrow NW-SE oriented alignment (Fig. 10.8) of low-pressure/high-temperature (mostly migmatitic) rocks previously attributed to Cadomian (Eguiluz 1987) or Variscan (Apraiz 1998) orogenic events. From a tectonic point of view, the low-pressure/high-temperature assemblages are associated with a mylonitic fabric, which, in turn, has been interpreted as due to an extensional ductile shearing with top-to-the-north (present-day coordinates) sense of movement (Expósito et al. 2003). The mylonitic fabric and the telescoped metamorphic isograds appear folded by the recumbent folds of the first Variscan deformation (see below), while the age of syn-extensional igneous bodies is Cambrian–Early Ordovician (ca. 530–500 Ma; Expósito et al. 2003). On a broad scale, this tectonothermal event can be viewed as related to crustal and lithospheric extension occurred in the OMZ during the pre-orogenic rifting stage.

The Sierra Albarrana area also features a low-pressure/high-temperature metamorphic zonation with a central migmatitic zone, which has been attributed to the Cadomian (Garrote 1976) or the Variscan orogeny (González del Tánago and Arenas 1991; Azor and Ballèvre 1997). The migmatites have yielded late Cambrian—early Ordovician ages (≈497–481 Ma; Azor et al. 2012) that can be interpreted in the same way as in the Valuengo-Monesterio area (Fig. 10.8). However, an intense Variscan tectonothermal imprint (Dallmeyer and Quesada 1992; Azor et al. 2012) has also been recognized, thus hindering the structural characterization of the Early Paleozoic rift-related event.

Variscan Structures

The first Variscan structures are recumbent km-scale NE-SE oriented SW-vergent folds, whose axial traces show rather complex map patterns due to the interference with later upright folds (Fig. 10.10). The main recumbent fold in the OMZ is the Olivenza anticline, which shows in its core the

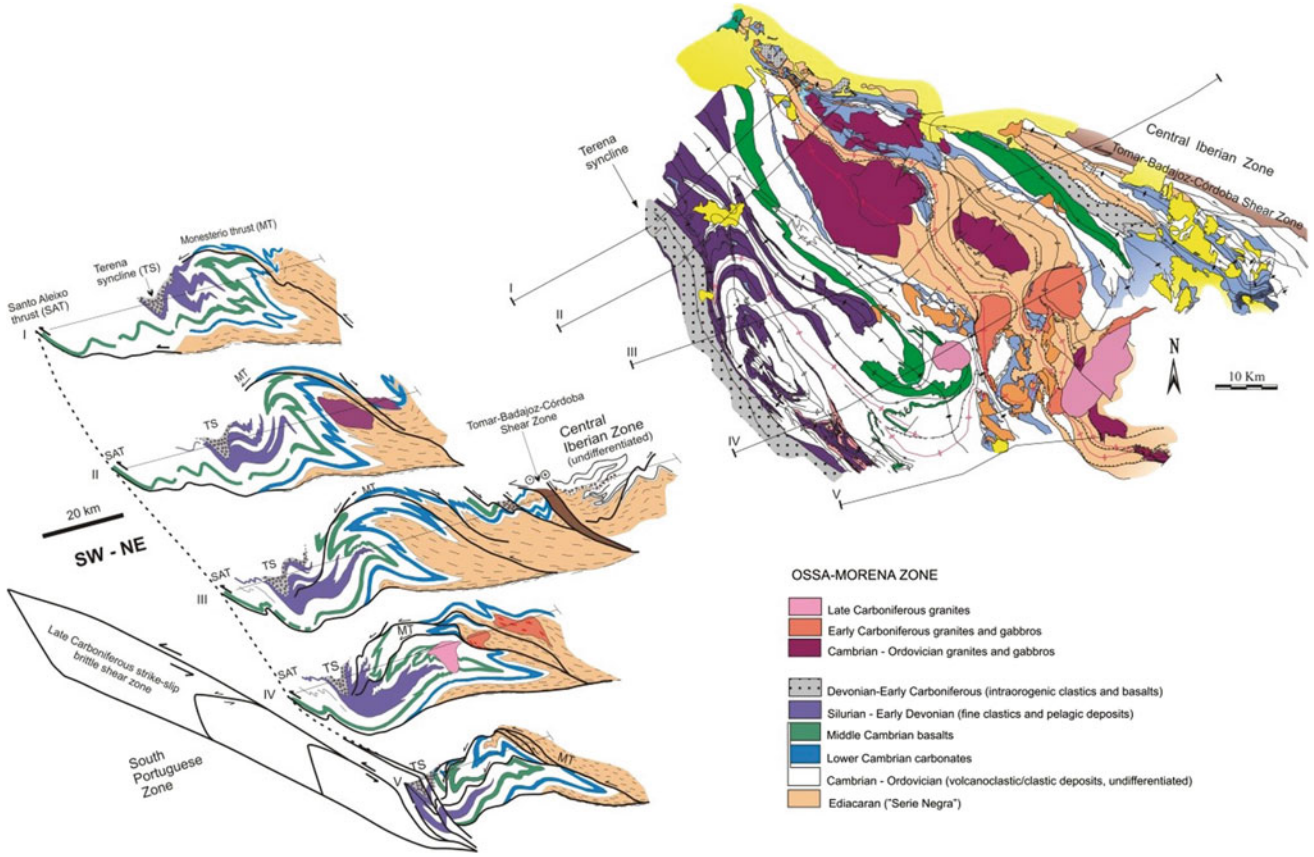

Fig. 10.10 Geological map and cross-sections of the central part of the Estremoz-Monesterio Domain (modified from Expósito 2000)

uppermost Ediacaran Serie Negra rocks. The younger rocks affected by this folding episode are the Lower Devonian ones that crop out in the core of the synclines. The fabric associated to this folding is dominantly planar (slaty cleavage), though at times a faint mineral or stretching lineation can also be observed. The slaty cleavage depicts the axial plane of the recumbent folds, while the mineral/stretching lineation usually forms a high angle with the fold axes (Expósito et al. 2002). This folding episode probably started at Early Devonian time according to the age of the older syn-orogenic sediments in the Terena basin (Piçarra 1998; Pereira et al. 1999; Rocha et al. 2010). The time gap between these early syn-orogenic sediments and the underlying deformed rocks is minimal, but the existence of an unconformity in-between has been demonstrated through detailed structural mapping (Fig. 10.10; Expósito 2000; Expósito et al. 2002; Azor et al. 2004).

The recumbent folds are cross-cut by SW-directed thrusts (Fig. 10.10) generated as a continuation of the same shortening episode. The most important of these structures is the Olivenza-Monesterio thrust (Eguiluz 1987; Expósito 2000; Expósito et al. 2002), which shows a ductile-brittle fault zone with a prominent planar-linear fabric. The kinematic indicators associated with this fabric indicate top-to-the-SSW displacement, which has been estimated in ≈20 km according to cartographic criteria (Expósito 2000). The IBERSEIS deep seismic reflection profile imaged the Olivenza-Monesterio thrust as a highly to moderately dipping structure rooted in the middle crust (Simancas et al. 2003).

The Early Carboniferous transtensional intrarorogenic episode already described in the southernmost CIZ and the TBCSZ also affected the OMZ interior, giving way in the Estremoz-Monesterio domain to low- to high-angle normal faults and several sedimentary basins (Expósito 2000; Expósito et al. 2002; Simancas et al. 2003). Among these basins, the Santos de Maimona (Giese et al. 1994), Toca da Moura and Cabrela basins (Oliveira et al. 2006) are entirely related to the Early Carboniferous intraorogenic extension, while the Terena basin (currently a tight synform extending along most of the OMZ) is a complex sedimentary trough. Thus, the Terena outcrop exhibits two unconformities: the older one is at the base of the syn-orogenic flysch-type sediments of Early Devonian age, which are nearly coeval with the pre-orogenic Early Devonian to Silurian deformed rocks (Piçarra 1998; Pereira et al. 1999; Expósito 2000;

Expósito et al. 2002); the second unconformity is at the base of Early Carboniferous deposits that may overlie either the former flysch or pre-orogenic Lower Paleozoic deformed rocks (Giese et al. 1994; Boogaard and Vázquez 1981; Expósito 2000; Expósito et al. 2002; Azor et al. 2004).

The Variscan collision was resumed after the transtensional stage, giving way to large-scale, open to tight, NW-SE oriented folds (Figs. 10.8 and 10.10), and high-angle reverse faults. These folds are generally upright and have an associated axial plane foliation consisting in a slaty cleavage in the Mississippian metapelitic rocks and a variably developed crenulation cleavage in the already deformed pre-Carboniferous lithologies. The axes of these second generation folds form a small angle with the axes of the Devonian recumbent folds, while the axial planes of the first and second generation folds should have made a high angle in origin. This fact, together with the lack of cylindrism of the structures, gave way to complex interference fold patterns (Expósito 2000, Expósito et al. 2002; Fig. 10.10). Finally, strike-slip left-lateral faults developed mostly at both boundaries of the OMZ.

The Evora-Moura-Aracena Domain

This domain constitutes the southernmost part of the OMZ (Fig. 10.8). Three different units have been differentiated drawing on the Variscan contrasting tectonometamorphic evolution and the structural position, namely the low-grade para-autochthonous Portel-Fuenteheridos unit, the high-grade/low-pressure Evora-Aracena unit, and the high-pressure Moura-Cubito unit (Fig. 10.8). Moreover, the so-called Beja Igneous Complex constitutes a voluminous outcrop of Early Carboniferous plutonic rocks at the southern border of the OMZ (Jesus et al. 2007; Pin et al. 2008).

Portel-Fuenteheridos Unit

This unit features the classical stratigraphy of the OMZ, with the Ediacaran Serie Negra, the latemost Ediacaran Malcocinado formation and the Cambrian succession. The structure of this unit is similar to the one observed in the Estremoz-Monesterio domain, with two generations of superposed folds, i.e. first generation recumbent folds affected by upright second generation ones. The Portel-Fuenteheridos unit constitutes the para-autochthon of the overlying allochthonous high-pressure Moura-Cubito Moura unit, while an Early Carboniferous low-angle normal fault system separates the Portel-Fuenteheridos unit from the underlying high-grade/low-pressure Evora-Aracena unit (Figs. 10.8 and 10.11).

Evora-Aracena Unit

This unit crops out as NW-SW elongated structural domes in the Evora, Aracena and Lora del Río sectors, being characterized by high-temperature/low-pressure (amphibolite to granulite facies) metamorphism occurred at 345–335 Ma (Bard 1977; Crespo-Blanc 1989; Apraiz and Eguiluz 2002; Díaz Azpiroz et al. 2004; Pereira et al. 2009a, b). Despite the dominant high-grade rocks and the intense deformation, some of the original lithologies are still recognizable and correspond to the classical Ediacaran to Cambrian succession of the OMZ. The dominant structure is a widespread NW-SE oriented moderate to steeply-dipping mylonitic foliation with a gently-plunging stretching lineation, generally coaxial with the later fold axes. Reliable shear criteria have not been described yet due to poor exposure and overprinting by subsequent deformation. However, normal to left-lateral movements seem to dominate, which have been interpreted as compatible with an oblique extensional scenario (Pereira et al. 2009a, b).

Moura-Cubito Unit

The Moura-Cubito unit tectonically overlies the Portel-Fuenteheridos para-autochthon (Fig. 10.11). This unit is mainly constituted by micaschists, though at some places includes tectonic intercalations of different rock-types such as MORB metabasites, eclogitic metabasites, marbles, gneisses and black schists. All of these rock types, except the MORB-type metabasites, can be correlated with less deformed and metamorphosed lithologies of the Ediacaran and Early Paleozoic formations of the autochthonous OMZ. Thus, this unit was considered as an allochthonous complex constituted by the scraped off-cover of the OMZ continental margin, with some small fragments of oceanic crust (Fonseca et al. 1999; Araújo et al. 2005; Ribeiro et al. 2010). Regarding the MORB-featured metabasites, the only available protolith age is Ordovician (ca. 480 Ma; Pedro et al. 2010), thus being compatible with a Rheic Ocean attribution.

The metamorphic evolution of the Moura-Cubito unit has been established drawing on the eclogite and blueschist facies assemblages preserved in metabasites, as well as from PT calculations performed on the metapelitic assemblages. Thus, the eclogitic assemblages led Fonseca et al. (1999) to propose peak conditions of ≈16 kbar and 650 °C. The blueschist assemblages have yielded P between 11 and 12 kbar and T between 300 and 450 °C (Fonseca et al. 1999; Rubio Pascual et al. 2013a). In the metapelites, chlorite—white K-mica—quartz ± chloritoid multi-equilibrium calculations yielded peak pressure conditions in the range 9–12 kbar at temperatures of 300–400 °C (Booth-Rea et al. 2006; Ponce et al. 2012). All of these data show a high-pressure/intermediate- to low-temperature metamorphic event in the Cubito-Moura unit, which attests an early collisional stage (see below) tentatively attributed to the Late Devonian (371 ± 17 Ma; Moita et al. 2005).

In the Moura-Cubito unit, the first deformational event recognized in metapelites is represented by a fabric

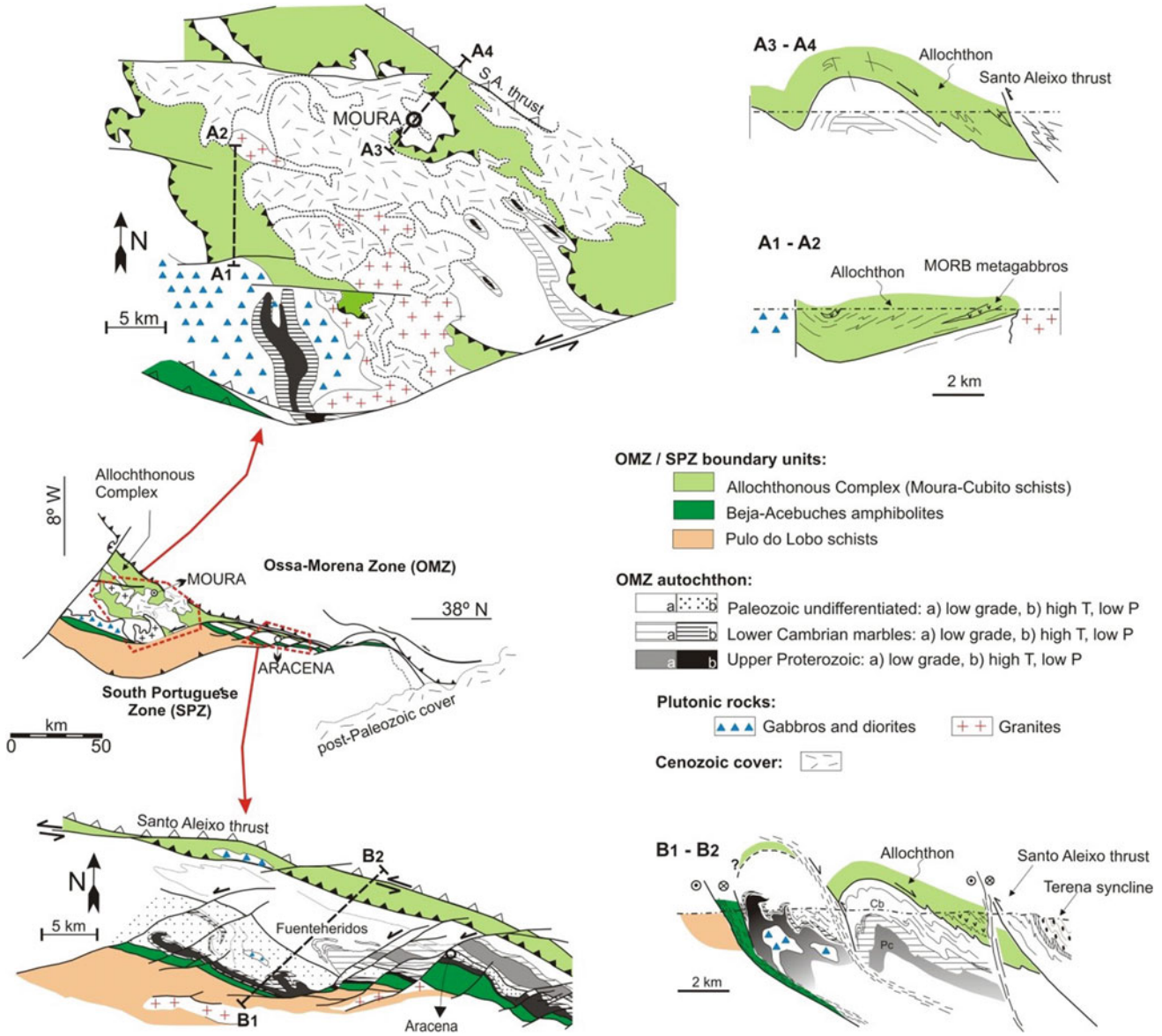

Fig. 10.11 Simplified geological maps of two sectors of the Evora-Moura-Aracena Domain, illustrating the structural relationships between the high-pressure Moura-Cubito unit and the Portel-Fuenteheridos relative autochthon. Note also the high-temperature/low-pressure metamorphic belt that is the structurally lower part of the autochthon

characterized by stretching/mineral lineation (L_1) and foliation (S_1), which would have been formed during the early exhumation of the HP-LT rocks. L_1 is well preserved only in early metamorphic quartz veins, while S_1 is a relict microstructure in the metapelites (Booth-Rea et al. 2006; Ponce et al. 2012). The present-day trend of L_1 concentrates between N90 °E and N110 °E. However, L_1 is affected by tight second phase folds, resulting in an ≈N70 °E original orientation after unfolding (Ponce et al. 2012). Quartz microfabric points to top-to-the-east movement (Fig. 10.12), thus attesting an oblique left-lateral collisional scenario in SW Iberia since the very beginning of the Variscan orogeny. A kinematically different mylonitic fabric observed in some metabasites of the Moura-Cubito unit (Araújo et al. 2005) has been interpreted as representing an Early Carboniferous extensional event (Rosas et al. 2008). A second deformational event produced a very penetrative crenulation cleavage (S_2), which transposes the previous S_1 without associated stretching or mineral lineation. Mesoscopic folds of this second deformation trend around N135 °E. Later penetrative deformation gave way to upright folds, sometimes with an axial-plane crenulation foliation (S_3).

To conclude, the Moura-Cubito is considered at present to contain the only remains of Rheic Ocean

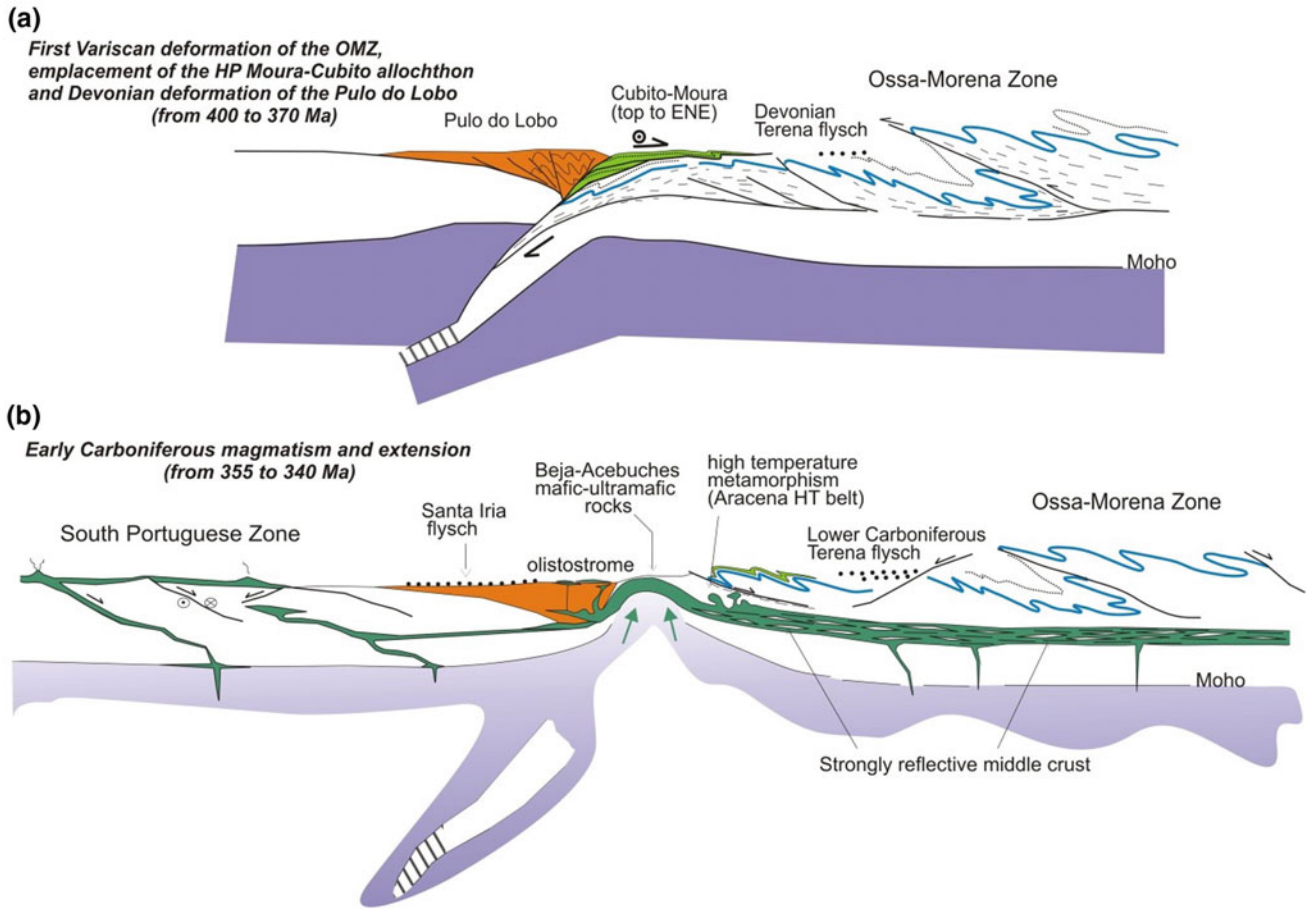

Fig. 10.12 Geological sketch illustrating the Devonian evolution of the Ossa-Morena Zone and its boundary with the South Portuguese Zone (A), and the extensional and magmatic episode of Early Carboniferous age

subduction/obduction and early collision in SW Iberia. The envisaged tectonic scenario is one with subduction of the OMZ continental margin below the SPZ just following the disappearance of the Rheic oceanic realm in Devonian time (Fig. 10.12). On a larger scale, this subduction is the consequence of the collision between Avalonia (represented by the SPZ; Simancas et al. 2005; Pérez-Cáceres et al. 2017) and Gondwana or Armorica (represented by the OMZ), after the closing of the intervening Rheic Ocean.

The Boundary Between the Ossa-Morena and South Portuguese Zones

The boundary between the OMZ and the SPZ (Fig. 10.8) has been traditionally interpreted as the main Variscan suture, i.e. a remnant of the closure of the Rheic Ocean and the subsequent collision of the Avalonian border of Laurussia with the complex border of Gondwana (e.g., Crespo-Blanc and Orozco 1988; Fonseca and Ribeiro 1993; Fonseca et al. 1999; Simancas et al. 2003; Araújo et al. 2005; Pérez-Cáceres et al. 2015). This interpretation has been sustained by the presence of three units with oceanic and/or high-pressure rocks, namely the Moura-Cubito unit (see above), the Beja-Acebuches (BA) unit, and the Pulo do Lobo unit. Nevertheless, recent geochronological and structural data have questioned the ophiolitic interpretation of the BA and the accretionary prism interpretation of the Pulo do Lobo units as related to the closure and subduction of the Rheic Ocean in pre-Carboniferous times (Azor et al. 2008, 2009; Pérez-Cáceres et al. 2015). Instead, both units contain Carboniferous protoliths and show a Carboniferous deformation that propagated from the OMZ/SPZ southwards into the SPZ. Accordingly and for clarity of the exposition, the deformation of these two units will be presented in connection with the evolution of the South Portuguese Zone (see Sect. 10.3.3—Variscan structure of the South Portuguese Zone). Therefore, this subsection will only summarize the geochronology, origin (igneous emplacement) and tectonic significance of the BA unit.

The BA unit crops out as a 0.5–2 km-wide strip (Fig. 10.8) of metamafic rocks (from greenschists to metagabbros, locally ultramafic rocks), continuous along the OMZ/SPZ boundary (Bard 1977; Fonseca and Ribeiro 1993;

Quesada et al. 1994; Castro et al. 1996). SHRIMP U–Pb zircon ages from MORB-featured rocks of this unit range from 332 to 340 Ma, having been interpreted as corresponding to the crystallization of the mafic protoliths (Azor et al. 2008, 2009). A first and direct implication of these Early Carboniferous ages is that the BA unit can no longer be viewed as an ophiolite belonging to the Rheic Ocean suture, since this oceanic domain was presumably closed in Devonian times. Accordingly, our preferred interpretation for the BA unit is that it represents a narrow and very ephemeral realm of oceanic-like crust that opened in Early Carboniferous times, after total consumption of the Rheic Ocean (Fig. 10.12). On the contrary, Murphy et al. (2016) have suggested that the Ocean Rheic lithosphere might have survived until Early Carboniferous times in SW Iberia due to the existence of an oceanic re-entrant along the Gondwana margin. It must be stressed however that the presence of collisional structures of Devonian age in the Cubito-Moura unit can be argued to undermine this hypothesis. Furthermore, the palynological content of Upper Devonian and Lower Carboniferous sediments at both sides of the BA unit is similar (Pereira et al. 2006a, b), thus suggesting that the OMZ and SPZ were already welded in Late Devonian time.

The ages reported for the BA metamafic protoliths (340–332 Ma) are slightly younger or virtually coincident with other published ages of mafic, intermediate and felsic rocks outcropping close to the OMZ/SPZ boundary and in the interior of the OMZ (354–335 Ma for the Gil Marquez pluton; Gladney et al. 2014; 355–345 Ma for the Beja Gabbros; Pin et al. 2008; Jesus et al. 2007; 335–320 Ma for the Cuba-Alvito gabbro-diorites; Jesus et al. 2007; 344–335 Ma for the Evora Massif granitoids; Pereira et al. 2015; 352–338 Ma for the Santa Olalla del Cala plutonic complex; Romeo et al. 2006; Ordóñez Casado et al. 2008; 338–335 Ma for the Burguillos del Cerro plutonic complex; Cambeses 2015), thus highlighting the importance of this Early Carboniferous magmatic event.

Despite the reassessment of the significance of the BA unit and the Pulo do Lobo unit, the OMZ/SPZ boundary might still represent a cryptic Rheic suture (Pérez-Cáceres et al. 2015). On this view, the high-pressure metamorphic event recorded in the Cubito-Moura unit, together with the small and dispersed fragments of MORB-featured mafic rocks (480 Ma, Pedro et al. 2010) included in this unit, remain as the only putative Rheic-related suture rocks.

10.3.3 Variscan Structure of the South Portuguese Zone

The South Portuguese Zone (SPZ) constitutes the southernmost part of the Iberian Massif (Fig. 10.2), being characterized by its restricted stratigraphic range from the Givetian to the Pennsylvanian (Schermerhorn 1971; Oliveira 1990; González et al. 2004; Pereira et al. 2008). It can be divided into three main belts, namely (from north to south) the Pulo do Lobo Belt, the Iberian Pyrite Belt and the Flysch Belt, each one featuring distinctive stratigraphy and deformation (Fig. 10.13). The older rocks (Givetian-Frasnian metasediments) crop out at the Pulo do Lobo Belt (Pulo do Lobo and Ribeira de Limas formations; Pereira et al. 2008) and the eastern Iberian Pyrite Belt (Ronquillo formation; Simancas 1983; González et al. 2004; Pérez-Cáceres et al. 2017). These siliciclastic rocks have undergone a complex polyphase deformation and low-grade metamorphism, being unconformably overlain by upper Famenian-lower Carboniferous metasediments and volcanic rocks only affected by Carboniferous deformations. The Iberian Pyrite Belt attests the most complete (Givetian to Serpukhovian) and lithologically varied stratigraphy, while the Flysch Belt is a thick clastic sequence of Mississippian to Pennsylvanian age (Fig. 10.13).

The first deformation event recognized in the oldest rocks of the SPZ took place at Late Devonian time, affecting only the Givetian-Frasnian schists of the Pulo do Lobo Belt and the Ronquillo formation of the Iberian Pyrite Belt (Figs. 10.12 and 10.13). This event was separated from the Carboniferous deformations by a transtensional magmatic event that gave way to the Tournaisian-early Visean Volcanosedimentary Complex with associated giant sulphide deposits. The orogenic shortening was resumed at late Visean time, migrating from the northern border of the SPZ to the south and being heralded by flysch deposits that are progressively younger southwards (Oliveira 1990).

10.3.3.1 Devonian Deformation

The geometric and kinematic features of the Late Devonian deformation in the SPZ remain obscure, since only a relic foliation (S1) inside microlithons of the main foliation (S2) has been recognized. S1 is usually seen at high angle with the S2 planes, thus suggesting a high angle between the axial planes of their respective folds. Accordingly and because the second folds have northward vergence (see below), the first Devonian deformation in the SPZ might have originated southward vergence folds. A major structure that could be coeval with the poorly visible Devonian deformation of the SPZ is the allochthonous complex (Cubito-Moura unit) tectonically emplaced onto the southern OMZ, just north of the Pulo do Lobo belt (Figs. 10.11 and 10.12).

The classic tectonic context given to the Devonian deformation around the SPZ/OMZ boundary has been a northward directed subduction (SPZ underneath OMZ), with the Pulo do Lobo metasediments and the associated metabasalts representing an accretionary prism (Silva et al. 1990; Eden 1991; Braid et al. 2010a, b). However, the Pulo do

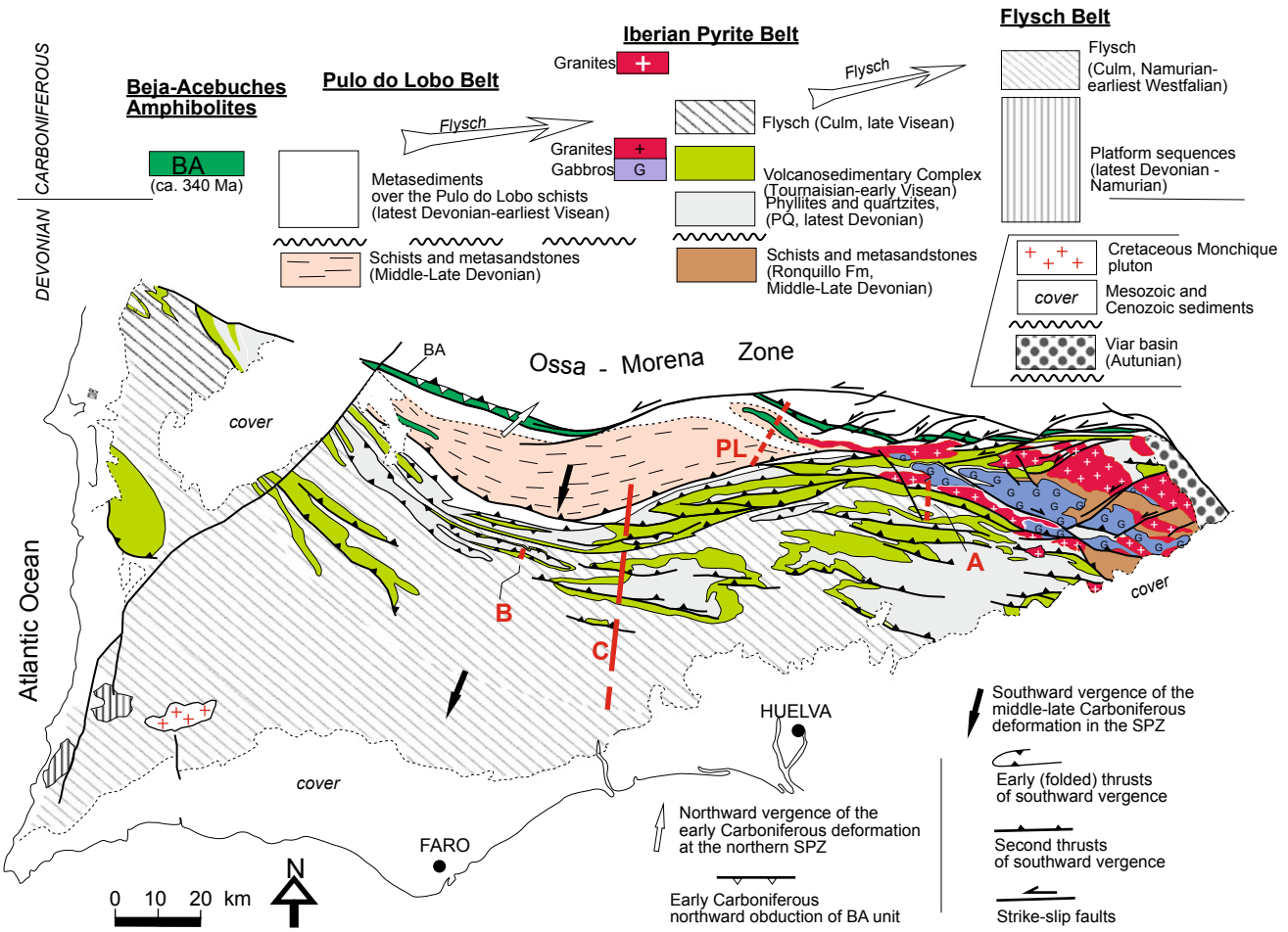

Fig. 10.13 General structural map of the South Portuguese Zone with the three belts distinguished on stratigraphic and tectonic grounds. Cross-section PL is shown in Fig. 10.15, while cross-sections A, B and C are shown in Fig. 10.16

Lobo Devonian sediments are not pelagic, they did not undergo high-pressure metamorphism (only lawsonite pseudomorphs have been locally reported by Rubio Pascual et al. 2013a) and their embedded metabasalts, previously interpreted as slivers of the Rheic Ocean floor, seem to be indeed early Carboniferous intrusions (Dahn et al. 2014; Murphy et al. 2015; Pérez-Cáceres et al. 2015). Thus, an alternative tectonic scenario for the Devonian deformation recorded at the SPZ/OMZ boundary may be one with southward subduction of the OMZ continental margin, giving way to synthetic northward exhumation of high-pressure rocks onto the OMZ margin (Cubito-Moura unit) and antithetic southward development of a sedimentary prism represented by the Givetian-Frasnian rocks of the Pulo do Lobo and Ronquillo formations (Fig. 10.12; Pérez-Cáceres et al. 2015).

10.3.3.2 Early Carboniferous Transtensional and Magmatic Stage

In the SPZ, this transtensional magmatic event is represented by the Tournaisian-early Visean volcanosedimentary complex that hosts huge sulphide deposits, which are interpreted by most authors as the consequence of a pervasive rifting event (e.g. Schermerhorn 1971; Munhá et al. 1983; Oliveira 1990; Barrie et al. 2002; Thiéblemont et al. 1998; Valenzuela et al. 2011). Moreover, at the eastern SPZ there are remarkable volumes of gabbros, diorites and granitic rocks coeval with the volcanics of the volcanosedimentary complex (Simancas 1983; Barrie et al. 2002; Dunning et al. 2002; de la Rosa and Castro 2004). Plausibly, the Early Carboniferous rifting event would have created a fracture network that influenced the subsequent transpressional

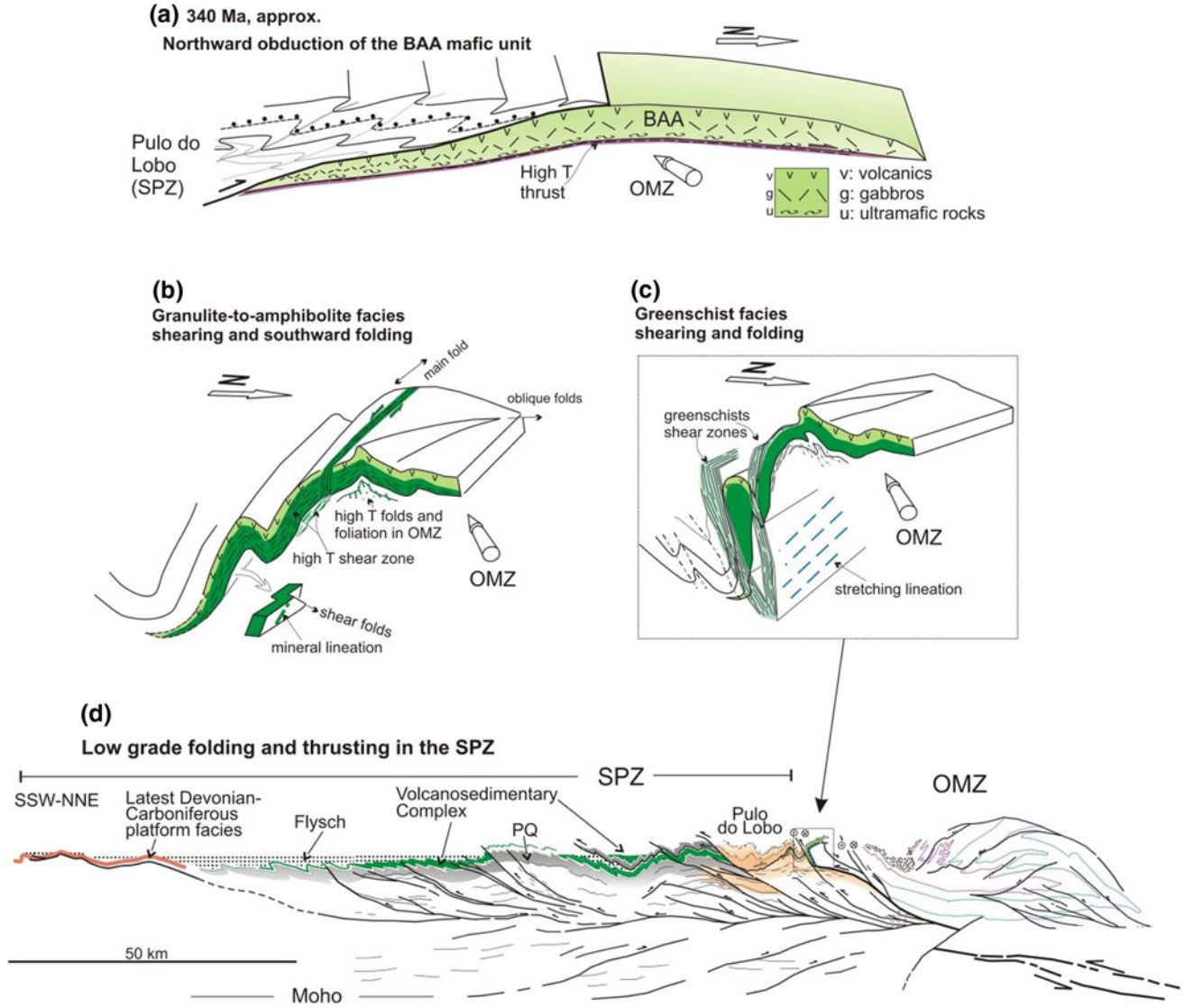

Fig. 10.14 Geological sketches illustrating the Carboniferous evolution of the Ossa-Morena/South Portuguese boundary and the deformation inside the South Portuguese Zone

structures. In this regard, seismic imaging of the SPZ shows high-amplitude reflection patterns similar to the ones characterizing the volcanosedimentary complex, but subparallel to some of the thrust structures. Such reflections were interpreted as subvolcanic bodies intruded along preexisting extensional faults and joints (Schmelzbach et al. 2008). More recently, many specific thrust structures at outcrop have been interpreted as reactivated normal faults (Martín-Izard et al. 2016).

10.3.3.3 Carboniferous Tectonic Inversion

The transpressional tectonic inversion that followed the transtensional early Carboniferous stage gave way to the structures that typify the deformation of the SPZ. Two main deformational events of opposite regional vergence can be distinguished: (i) the first one is characterized by a set of northward-directed structures affecting only the northern part of the SPZ and the southern border of the OMZ; (ii) the second event originated south-vergent structures that affected the entire SPZ (Fig. 10.14).

10.3.3.4 North-Vergent Structures at the SPZ/OMZ Boundary

At the southern border of the OMZ, this event gave way to the northward tectonic emplacement (obduction) of the Beja-Acebuches Amphibolitic unit onto the Evora-Aracena high-temperature/low-pressure metamorphic belt (Fig. 10.14a) (Fonseca and Ribeiro 1993; Pérez-Cáceres et al. 2015). The obduction would have taken place at granulite-facies

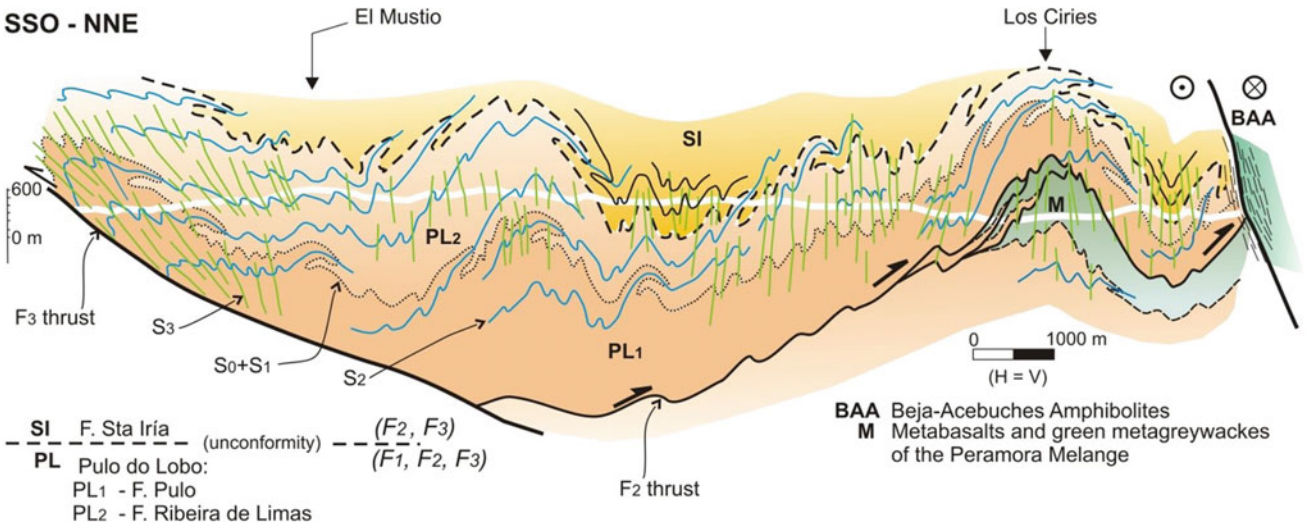

Fig. 10.15 Geological cross-section of the central part of the Pulo do lobo Belt (located as PL in Fig. 10.13)

conditions, according to relic fabrics preserved at the base of the obducted rocks (Figueiras et al. 2002). To the south, the Pulo do Lobo Belt of the SPZ exhibits north-vergent folds ascribable to this event; these folds constitute the second penetrative deformation in the Givetian-Frasnian rocks (S_2 foliation; Fonseca 2005; Martínez Poza et al. 2012; Pérez-Cáceres et al. 2015) and the first one in the overlying uppermost Devonian-lower Carboniferous formations (Fig. 10.15). This event might also have produced the so-called Peramora mélange (Eden 1991), which Pérez-Cáceres et al. (2015) have reinterpreted as a tectonic imbrication of Devonian Pulo do Lobo phyllites and a mafic-derived olistostromic unit (Fig. 10.15).

10.3.3.5 South-Vergent Late Visean to Moscovian Deformation in the SPZ

The BA unit that marks the SPZ/OMZ boundary generally dips to the north. Thus, this early Carboniferous (Azor et al. 2008) mafic unit has been usually viewed as a geometrically simple (though intensely sheared) lens of oceanic-like crust thrust onto the SPZ (Crespo-Blanc and Orozco 1988; Díaz Azpiroz and Fernández 2005; Díaz Azpiroz et al. 2006). However, the ophiolitic pseudostratigraphy of the BA unit suggests tectonic inversion (Quesada et al. 1994; Simancas et al. 2003), while structural mapping in the Guadiana section has demonstrated that it forms a south-vergent overturned fold, namely the Quintos fold (Fig. 10.14b, c; Pérez-Cáceres et al. 2015). The inception of this major fold marks the beginning of the southward-directed left-lateral transpressional deformational wave that dominated the Carboniferous collision in the SPZ (Fig. 10.14d; Pérez-Cáceres et al. 2015, 2016).

The evolution of the Quintos fold started at high-temperature amphibolite facies conditions. $^{40}Ar/^{39}Ar$ dating of amphiboles from the BA unit has yielded metamorphic ages between 328 and 346 Ma (Dallmeyer et al. 1993; Castro et al. 1999), not different within error from the U–Pb protholith ages of 332–340 Ma (Azor et al. 2008). This probably means that the crystallization of these mafic rocks at Visean time was immediately followed by the tectonic inversion that gave way first to their northward obduction and then to the Quintos fold. As the southern limb of the fold rotated and increased dip, oblique left-lateral shearing concentrated on it, thus developing a shear zone that evolved from amphibolite- to greenschist-facies conditions (Crespo and Orozco 1988; Quesada et al. 1994; Díaz Azpiroz and Fernández 2005; Pérez-Cáceres et al. 2015) (Fig. 10.14b, c).

South of the Beja-Acebuches Amphibolites, the Givetian-Frasnian rocks of the Pulo do Lobo Belt exhibit a third penetrative deformation (the second one in the overlying uppermost Devonian-lower Carboniferous sedimentary rocks), consisting in upright to south-vergent folds and thrusts that can be correlated with the south-vergent deformation at the SPZ/OMZ boundary (Pérez-Cáceres et al. 2015; Fig. 10.15). U–Pb dating of different facies of the Gil Márquez pluton in the Pulo do Lobo Belt apparently constrain the age of this deformation between 345 Ma (deformed facies) and 335 Ma (undeformed facies) (Gladney et al. 2014); furthermore, U–Pb dating of metavolcanic rocks at the northern Pulo do lobo Belt affected by low-temperature ductile shearing has yielded ages of 337–345 Ma (Pérez-Cáceres et al. 2015). Accordingly, the deformational wave would have attained the Pulo do Lobo Belt at 335–337 Ma, then migrating southwards.

South of the Pulo do Lobo Belt, the Carboniferous deformation that characterizes the whole SPZ (Oliveira et al. 1992;

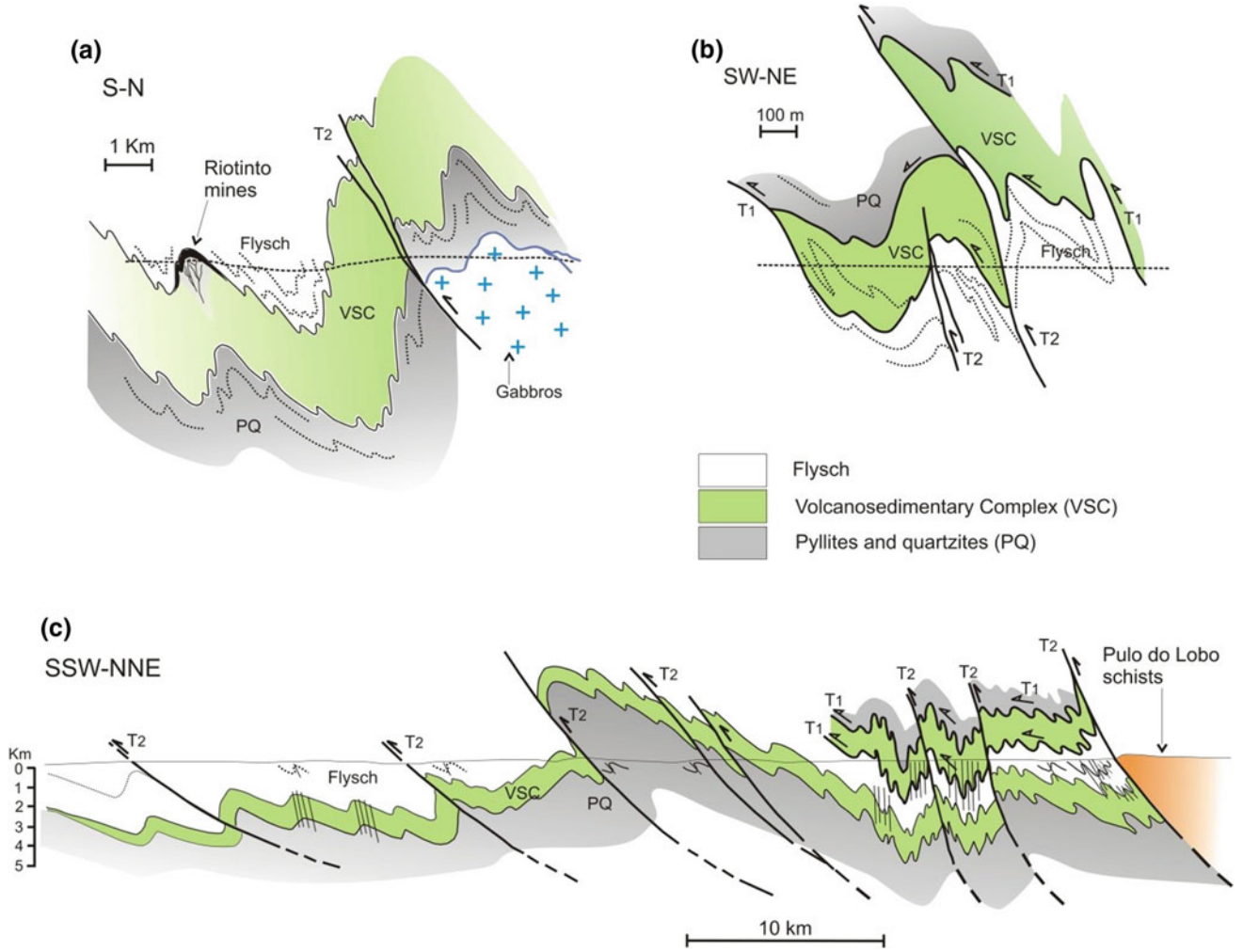

Fig. 10.16 Three geological cross-sections illustrating the structure of the South Portuguese Zone. See location in Fig. 10.13. Cross-section B, around the Mértola area, is based on mapping by Silva et al. (1990), while cross-section C is modified from Soriano and Casas (2002)

Matas et al. 2010) constitutes a south-vergent fold-and-thrust belt detached at a mid-crustal level, as imaged in the IBERSEIS deep seismic experiment (Fig. 10.14d; Simancas et al. 2003). This deformation was preceded by the deposition of flysch-type syn-orogenic deposits with progressively younger ages southwards, thus showing the migration of the deformation (Oliveira 1990): deformation started at late Visean time in the northern Iberian Pyrite Belt and reached the southwest corner of the SPZ at Moscovian time. Deformation is particularly complex at the northern border of the SPZ, where folds and thrusts of a first generation are deformed by a second generation of coaxial tight folds (S2 foliation) and thrusts (Fig. 10.16b, c; Schermerhörn and Stanton 1969; Ribeiro and Silva 1983; Silva et al. 1990; Soriano and Casas 2002). To the south, the structure tends to be simpler with a prevailing single generation of overturned tight folds and thrusts and a second generation of dominantly coaxial upright folds (Fig. 10.16), though detailed studies reveal that the set of thrusts may be locally complex (e.g., Oliveira et al. 2004; Mantero et al. 2011). Accordingly, two penetrative superposed cleavages are frequently found at the northern SPZ, while to the south a single slaty cleavage is sometimes accompanied by poorly penetrative crenulations or disjunctive cleavages. Fold axes show variable plunge even at local scale, and a faint high-pitch stretching lineation is usually visible in pyroclastic rocks (Simancas 1986).

A brittle strike-slip fault system stands out on the geological map of the OMZ/SPZ boundary, penetrating the easternmost SPZ (Fig. 10.13; Simancas 1983; Quesada 1991; Crespo-Blanc 1992; Pérez-Cáceres et al. 2015). The age of these faults is late Pennsylvanian, since they affect Pennsylvanian granitoids but are covered by the Autunian sediments of the El Viar basin (Fig. 10.13; Sierra and Moreno 2004). E-W to NE-SW trending left-lateral faults largely dominate, the summed slip having been estimated at ≈80 km. The development of this brittle strike-slip shear

zone around the SPZ/OMZ boundary might have been coeval with the latest deformation at the southwesternmost SPZ (Carrapateira thrust; Silva et al. 1990).

The deformation in the SPZ displays a number of features supporting a global transpressional tectonic scenario (Pérez-Cáceres et al. 2016): (i) the left-lateral dominant component of the Visean ductile shearing at the SPZ/OMZ boundary; (ii) the left-lateral oblique kinematics of some thrusts in the SPZ interior; (iii) the oblique trend of fold axial traces with respect to the trend of the SPZ/OMZ boundary (Fig. 10.13); and (iv) the Late Pennsylvanian, left-lateral strike-slip brittle shearing around the SPZ/OMZ boundary.

10.4 Discussion

The structure of Southwestern Iberia was intensely debated in the 90 s regarding the age of the main deformation and metamorphic events in the southernmost CIZ, the CIZ/OMZ boundary, and the OMZ interior. As previously stated, an increasing number of geochronological and structural data favor that both the main structures and the associated metamorphism are Variscan in age (e.g., Azor et al. 1993; Ordóñez Casado 1998; Pereira et al. 2010a, b, 2012), while the Cadomian orogeny is mainly witnessed by the presence of subduction-related Ediacaran plutonic and volcanic rocks (e.g., Bandrés et al. 2002; Henriques et al. 2015). A tectonometamorphic Cadomian imprint has only been demonstrated at a very few localities (Blatrix and Burg 1981; Dallmeyer and Quesada 1992).

A new discussion regarding the structure of the OMZ comes from a recent proposition that considers it as a Variscan mega-nappe spreading from the Allochthonous Complexes of NW Iberia (Díez Fernández and Arenas 2015, 2016; Arenas et al. 2016a; Díez Fernández et al. 2016) and also covering the Central System and most of the southern Central Iberian Zone. These authors claim that the same pile of allochthonous units recognized in NW Iberia (e.g. Martínez Catalán et al. 2009; Arenas et al. 2016b) also exists in the OMZ, thus proposing a huge nappe emplaced eastward at Early Carboniferous time (Díez Fernández and Arenas 2016; Díez Fernández et al. 2016) onto the Gondwana margin. This hypothesis is exclusively based on the correlation of high-pressure metamorphic "belts" and MORB-type metabasites from NW to SW Iberia, which would be part of a single and huge high-pressure and ophiolitic allochthonous complex, i.e. they would attest a single suture, instead of two as considered by other authors (e.g. Matte 1991; Simancas et al. 2002). This proposal has a number of structural and kinematic inconsistencies that were already stated by Simancas et al. (2016). Basically, the two main flaws come from the fact that both field and seismic data clearly show that the large-scale structure of the OMZ is not an open synform and from the absence of Variscan structures (folds, thrusts or shear zones) congruent with the needed kinematics of emplacement. Moreover, Early Carboniferous time is a transtensional stage in the whole SW Iberian Massif with widespread basin formation, magmatism (see below) and top-to-the-NW shearing in the TBCSZ.

Apart from the above topics, there are two striking features in SW Iberia as compared with northern Iberia and the Variscan Massifs in Europe, namely the Early Carboniferous transtensional stage that interrupted the collisional evolution, and the left-lateral component that accompanied the whole tectonic evolution. Regarding the Early Carboniferous evolution, a good deal of stratigraphical, tectonometamorphic and magmatic data reported in the above subsections point to a general transtensional or extensional scenario after the Devonian collisional structures (NE-vergent recumbent folds in the southernmost CIZ and SW-vergent folds and thrust in the OMZ interior). From north to south, we have described the following coeval features: thick sedimentation and basaltic volcanism in the southernmost CIZ (Pedroches basin), left-lateral and extensional shearing at the TBCSZ that drove the exhumation of previously subducted rocks (eclogites), basin development with accompanying mafic volcanism and normal faulting in the OMZ interior (Santos de Maimona, Terena and Toca da Moura basins), formation of low-pressure/high-temperature extensional domes in the southern OMZ (Évora, Aracena and Lora del Rio metamorphic outcrops), ephemeral oceanic-crust generation (BA unit), mafic to acid magmatism in the OMZ (e.g., Burguillos del Cerro pluton) and at the OMZ/SPZ boundary (Beja Igneous Complex), and abundant bimodal volcanism and plutonism in the SPZ interior (Volcanosedimentary Complex and gabroic-granitic plutons of the easternmost SPZ). The plausible tectonic scenario is one where transtension/extension would have given way to a variably thinned continental lithosphere (e.g., Simancas et al. 2001, 2003; Pereira et al. 2012; Pérez-Cáceres et al. 2015; Cambeses 2015). A plume-type mantle upwelling interfering with the collisional process (Simancas et al. 2003, 2006) or a slab break-off (Pin et al. 2008) have been two tentative geodynamic hypotheses proposed to account for the intraorogenic transtensional/extensional and magmatic event in SW Iberia. Similar events of late Devonian-early Carboniferous age have also been described in other areas of the Variscan orogen (Franke 2006, 2014; Simancas et al. 2009; Franke et al. 2011), pointing towards a large-scale geodynamic explanation. In this respect, Franke (2014) has suggested a mantle anomaly related to the propagation of the Paleotethys Ocean south of the main outcrops of the Variscan belt.

The Variscan evolution of SW Iberia is also characterized by a left-lateral component of deformation that contrasts with the dextral component recognized in most of the regions of the Orogen (e.g., Shelley and Bossière 2000).

This left-lateral component in SW Iberia suggests oblique convergence of its three continental terranes (CIZ, OMZ and SPZ). Thus, deformation was partitioned into thin bands dominated by strike-slip kinematics, namely the northern and southern boundaries of the OMZ, and broader regions combining frontal shortening and left-lateral displacements, namely the OMZ and the SPZ interiors (e.g., Pérez-Cáceres et al. 2016 and references therein). This evolution has been classically related to the formation and tightening of the Ibero-Armorican Arc (Matte and Ribeiro 1975; Brun and Burg 1982), though the reassessment of this orocline as an essentially early Permian structure (Weil et al. 2000) has questioned this interpretation. An alternative explanation for the left-lateral movements in SW Iberia was provided by considering a Paleogeographic Avalonian promontory that collided with the northern Gondwana margin (Simancas et al. 2005). An approximate assessment of the left-lateral transpressional deformation in SW Iberia has been performed by Pérez-Cáceres et al. (2016), obtaining a total collisional convergence that surpasses 1000 km, most of them corresponding to left-lateral displacements parallel to terrane boundaries.

10.5 The Pyrenees

J. M. Casas, P. Clariana, J. García-Sansegundo, A. Margalef

The pre-Variscan Palaeozoic and Ediacarian basement rocks of the Pyrenees record a polyphase deformation essentially related to the main period of Variscan crustal thickening and a low pressure-high temperature metamorphism. In these rocks evidence of Eo-Variscan deformation or high pressure metamorphism related to subduction during the early Variscan convergence is lacking and most palaeogeographic reconstructions suggest that the Variscan domains of the Pyrenees may be equivalent to the northern branch of the Ibero-Armorican Arc (Julivert and Martinez 1983; Matte 1986; Martínez Catalán 2011a, b; García-Sansegundo et al. 2011; Aguilar 2013 and references therein). Deformational structures formed during this event differ significantly all along the Pyrenees, and as a consequence a comprehensive scheme integrating all the available data is lacking. In this contribution we briefly present the main characteristics of the Variscan deformation in the medium to high-grade metamorphic areas, in the low-grade infra-Silurian rocks and in the non-metamorphic or low-grade Silurian, Devonian and Carboniferous successions.

The pre-Variscan Palaeozoic rocks of the Pyrenees form an elongated strip unconformably overlain by Mesozoic and Cenozoic rocks, geographically disconnected from neighbouring outcrops of the Catalan Coastal Range to the south, the Mouthoumet and Montagne Noire (southern French Central massifs) to the north, Sardinia to the east and Iberian Massif to the west. Palaeozoic rocks are involved in three main Alpine thrust sheets, the so-called Lower Structural Units (Muñoz 1992) that provoked important N-S displacements, so the original position of the Palaeozoic rocks should be located northward from present-day arrangement. Moreover, the Alpine deformation gave rise to important rotation related to antiformal stack development. In contrast, Alpine metamorphism is absent and internal deformation is moderated. As a result, the original characteristics of the Variscan deformation may be confidently reconstructed in the Pyrenees. Other pre-Alpine movements may be also envisaged in order to obtain a reliable original Early Palaeozoic palaeoposition of the Pyrenenan domain and to establish its affinities with the neighbouring Variscan Sardinia, Mouthoumet and Montagne Noire-French Central Massif domains.

A pervasive foliation is the main deformational structure in the medium- to high-grade metasediments and the gneissic bodies derived from Ordovician and Cadomian granitoids. This foliation ($S_{1\text{-}2}$) is a composite fabric developed prior to coeval with the Variscan regional metamorphism, being associated with an E-W to NE-SW oriented stretching lineation. $S_{1\text{-}2}$ is folded by later E–W to NW–SE upright folds, and as a result is the mesostructure that depicts the Aston-Hospitalet, Canigó, Roc de Frausa and Albera gneissic domes all along backbone of the chain. According to Clariana and García-Sansegundo (2009) and García-Sansegundo et al. (2011), in the Garona dome and the Pallaresa massif S_1 is a slaty cleavage only developed in the Cambro-Ordovician succession and not related to folds, i.e. it is pre-Variscan and probably related to extensional tectonics; in these rocks, S_2 is associated with N-verging recumbent folds (Fig. 10.17) formed at Carboniferous time according to the available geochronological ages for the regional metamorphism (ca. 320–315 Ma in the Roc de Frausa massif; Aguilar et al. 2014) and granitoids (ca. 339–336 Ma in the Garona dome and Aston Massif (Mezger and Gerdes 2016).

In the low-grade pre-Silurian rocks, a pervasive crenulation cleavage (S_3) is also the main Variscan deformational structure. The relationship between this cleavage and $S_{1\text{-}2}$ is uncertain. However, in the easterm part of Pallaresa massif in the central Pyrenees, south of Aston massif and north of the Tor-Casamanya syncline, Clariana et al. (2009) and Clariana and García-Sansegundo (2009) described a subvertical S_3 crenulation cleavage deforming $S_{1\text{-}2}$ (Fig. 10.17). In this area, S_3 is the axial plane of E-W trending upright folds and becomes the main cleavage in the Pallaresa massif, the Tor-Casamanya and Llavorsí synclines and the Rabassa and Orri domes (Speksnijder 1986; Poblet 1991; Clariana and García-Sansegundo 2009; Margalef and Casas 2016) (Fig. 10.17). S_3 exhibits a fan-like attitude near to the

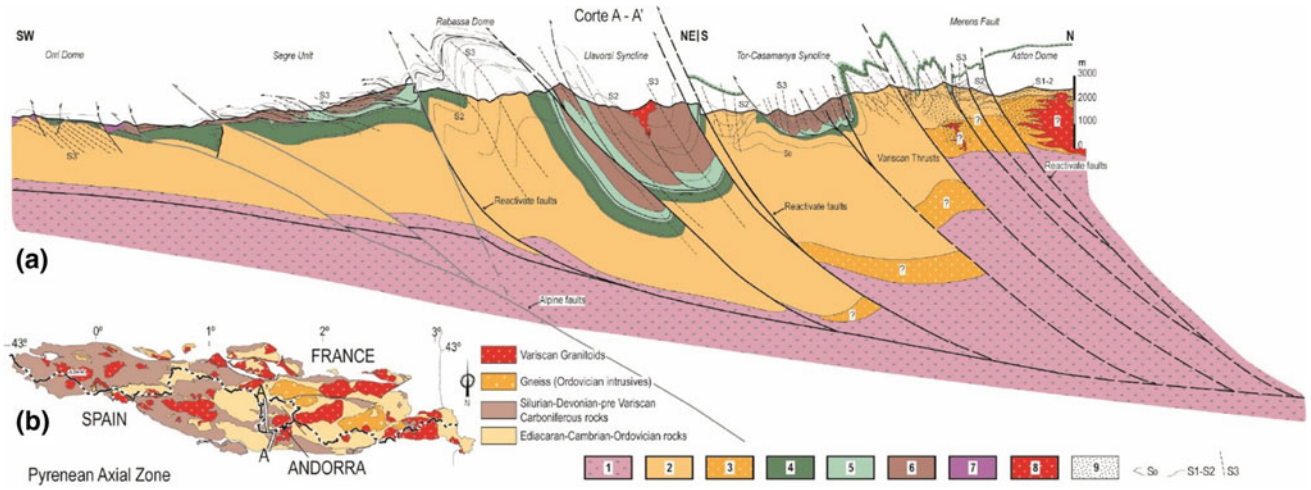

Fig. 10.17 **a** Geological cross-section across the central Pyrenees showing the main Variscan and Alpine structures. 1. Undifferentiated Neoproterozic-Paleozoic rocks; 2. Paleozoic Pre-Upper Ordovician metasediments; 3. Aston orthogneiss (Ordovician intrusives); 4. Upper Ordovician rocks; 5. Silurian rocks; 6. Devonian rocks; 7. Late-Variscan Andesites (Carboniferous-Permian); 8 Synorogenic and Late-Variscan granitoids; 9. Amphibolite facies Variscan metamorphism. Alpine faults according to Muñoz (1992) **b** Simplified geological map of the Neoproterozoic-Paleozoic rocks of the Pyrenees. A-A′ geological cross-section in (**a**)

southern contact with the post-Variscan rocks due to the Alpine rotations linked to thrust sheet stacking (Fig. 10.17; Muñoz 1992). In the Eastern Pyrenees, the relationship between $S_{1\text{-}2}$ and S_3 in the low and medium to high-grade rocks is not so clear, mainly due that both mesostructures are intensely folded and, as a consequence, S_3 does not exhibit a regular attitude as in the Central Pyrenees. Moreover, some folds previous to this cleavage have been described (Laumonier and Guitard 1978; Cirés et al. 1990; Poblet 1991; Capellà and Bou 1997). Their age is not well constrained, some of them may be related to pre-Variscan (Ordovician?) deformations (Den Brok 1989; Casas 2010), and others may represent the expression in the low-grade metamorphic rocks of the D_2 deformation in the medium or high-grade rocks.

South directed thrusts are well developed in the Silurian, Devonian and Carboniferous successions (Fig. 10.17; Hartevelt 1970; Casas et al. 1989, among others). Some of the thrusts sharply diminish displacement and die out in the Carboniferous rocks, thus confirming their syn-orogenic character. The basal detachment is located at the base of the Silurian black shales. Although most of thrusts are south-directed, some north-directed ones can be recognized too. In the southern limb of the D_3 megastructures, as the Rabassa dome (Fig. 10.17), thrusts and the lower detachment dip to the south. In turn, thrusts cut fold-related cleavage. Thus, in the post-Silurian rocks thrust development must have been broadly coeval with D_3 folds in the low-grade pre-Silurian rocks. Thrusts and folds gave rise to a shortening of about 60%, whereas the shortening related to the same deformational events in the pre-Silurian rocks does not exceed 50%, thus highlighting a vertical strain partitioning (Margalef and Casas 2016). This shortening difference between the pre- and post-Silurian rocks should be resolved with a deepening detachment level northwards of the Axial Zone. Moreover, part of this shortening difference may be accommodated by a Variscan reactivation of some of the pre-Variscan, Ordovician, normal faults (Casas 2010).

In the eastern and central Pyrenees, D_3 deformational episode occurred at 330–319 Ma, according to the age of syn-orogenic Carboniferous Culm deposits (latest Visean to Serpukhovian: Sanz-López et al. 2006; Namurian: Delvolvé 1981, Delvolvé and Perret 1989, Delvolvé et al. 1993, Trias et al. 2014). A westward migration of the age of the deformation may be proposed on the basis of the age of the Culm deposits in the westernmost Cinco Villas massif (Middle Westphalian, Moscovian, Delvolvé and Perret 1989, Delvolvé et al. 1993) (Fig. 10.6). Moreover, a maximum depositional ages of 336 ± 2 Ma and 356 ± 9 Ma have been obtained from U–Pb on detrital zircons in Carboniferous rocks (Martínez et al. 2015), and a minimum age, in turn, is provided by the age of the crosscutting granites (Andorra-Mont Lluís granodiorite, dated as 305 ± 3 Ma by Romer and Soler 1995, 305 ± 5 Ma by Maurel et al. 2004 and 301.5 ± 1.9 Ma by Pereira et al. 2014; Maladeta and Lys-Caillaouas plutons, dated as 301.7 ± 7.3 Ma and 300 ± 2 Ma by Martínez et al. 2015 and Esteban et al. 2015 respectively). The presence of undeformed granitoid cobbles in Culm conglomerates confirms a pre-latest Visean igneous activity in the Pyrenees (Soulcem and Bosost granites, ca. 339–336 Ma according to Mezger and Gerdes 2016), significantly different from the much younger late

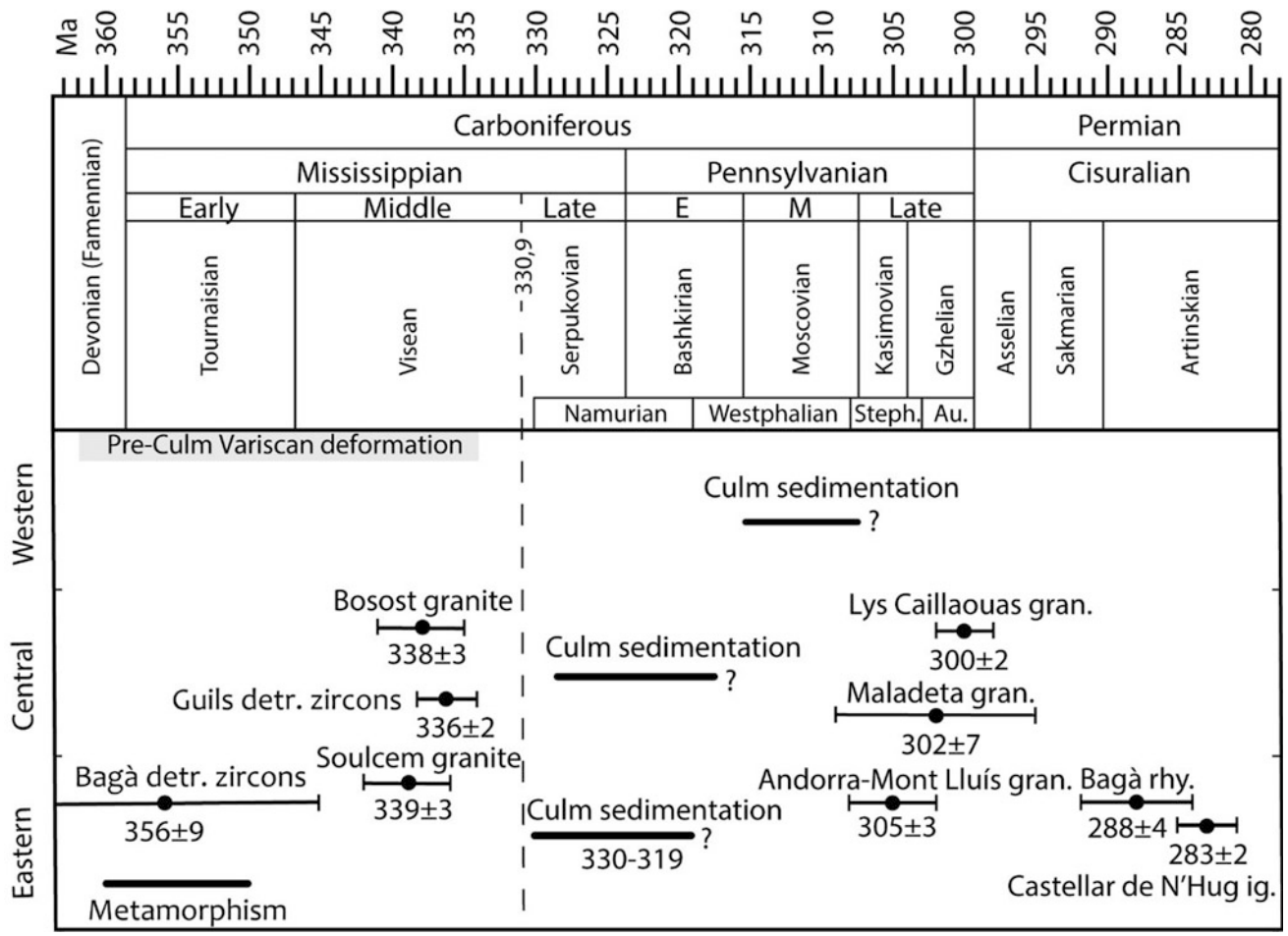

Fig. 10.18 The date of the Variscan deformation in the Pyrenees based on the ages of the Culm sedimentation (biostratigraphic data of the eastern Pyrenees: Trias et al. 2014; central Pyrenees: Delvolvé 1981; Delvolvé and Perret 1989; Delvolvé et al. 1993 and western Pyrenees: Delvolvé and Perret 1989), the crosscutting Andorra-Mont Lluís granodiorite (Romer and Soler 1995), Maladeta granodiorite (Martínez et al. 2015) and Lys-Caillaouas granite (Esteban et al. 2015), the unconformable Bagà rhyolite (Martínez et al. 2015) and Castellar de N'Hug ignimbrite (Pereira et al. 2014), the youngest detrital zircon population from Guils and Bagà (Martínez et al. 2015), the Bossost and Soulcem granites that may provide the undeformed cobbles of igneous rocks (Mezger and Gerdes 2016), and the Mississippian Variscan metamorphism (Martínez et al. 2015)

Carboniferous magmatism (ca. 312–305 Ma). In contrast, the presence of strongly foliated schist and gneiss cobbles (Martínez et al. 2015) suggests the existence of pre-Culm Variscan ductile deformation. This pre-Culm deformation may be related to $S_{1\text{-}2}$ formation in the medium- to high-grade metamorphic rocks, as confirmed by the ca. 360–350 Ma metamorphic ages obtained by Martínez et al. (2015) (Fig. 10.18).

From the stated above, two consequences arise. In one hand, extends the time available for Variscan deformational phases in the metamorphic areas of the Pyrenees to the Tournaisian-Visean. On the other hand, highlights the importance of the correlation between the structures developed in $D_{1\text{-}2}$ and D_3 events. Although this correlation is hampered by the different expression of each of these events in the low-grade and medium- to high-grade metamorphic rocks, recent studies on zones where $D_{1\text{-}2}$ and D_3 structures and their relationships are recognized may provide an important progress in this matter.

References

Abalos B (1990) Cinemática y mecanismos de la deformación en régimen de transpresión. Evolución estructural y metamórfica de la Zona de Cizalla Dúctil de Badajoz-Córdoba. PhD Thesis, University of the Vasque Country

Abalos B, Gil Ibarguchi JI, Eguiluz L (1991) Cadomian subduction/collision and Variscan transpression in the Badajoz-Córdoba shear belt, southwest Spain. Tectonophysics 199: 51–72

Abalos B, Carreras J, Druguet E, Escuder Viruete J, Gómez Pugnaire MT, Lorenzo Álvarez S, Quesada C, Rodríguez-Fernández LR, Gil Ibarguchi JI (2002) Variscan Tectonics. In: Gibbons W, Moreno T (eds.) The Geology of Spain, Geological Society of

London, 155–183.Aerden DGAM (2004) Correlating deformation in Variscan NW-Ibéria using porphyroblasts; implications for the Ibero Armorican Arc. Journal of Structural Geology 26 (1):177–196. https://doi.org/10.1016/s0191-8141(03)00070-1

Abati J, Gerdes A, Fernández Suárez J, Arenas R, Whitehouse MJ, Díez Fernández R (2010) Magmatism and early-Variscan continental subduction in the northern Gondwana margin recorded in zircons from the basal units of Galicia, NW Spain. Geological Society of America Bulletin 122 (1–2):219–235. https://doi.org/10.1130/b26572.1

Aerden DGAM (2004) Correlating deformation in Variscan NW-Ibéria using porphyroblasts; implications for the Ibero Armorican Arc. Journal of Structural Geology 26 (1):177–196. https://doi.org/10.1016/S0191-8141(03)00070-1

Aguilar C (2013) P–T–t–d constrains on the Late Variscan evolution of the Eastern Pyrenees. Ph.D. thesis. Universitat de Barcelona

Aguilar C, Liesa M, Castiñeiras P, Navidad M (2014) Late Variscan metamorphic and magmatic evolution in the eastern Pyrenees revealed by U–Pb age zircon dating. Journal of the Geological Society London 171 (2): 181–192

Alcock JE, Martínez Catalán JR, Rubio Pascual FJ, Díez Montes A, Díez Fernández R, Gómez Barreiro J, Arenas R, Dias da Silva Í, González-Clavijo E (2015) 2-D thermal modeling of HT-LP metamorphism in NW and Central Iberia: Implications for Variscan magmatism, rheology of the lithosphere and orogenic evolution. Tectonophysics 657:21–37. https://doi.org/10.1016/j.tecto.2015.05.022

Aller J, Bastida F, Ortega E, Pérez-Estaún A (1986) Aportación al conocimiento estructural del Sinclinal de Almadén. Boletín Geológico y Minero 97: 608–621

Álvarez-Valero AM, Barreiro JG, Alampi A, Castiñeiras P, Martínez Catalán JR (2014) Local isobaric heating above an extensional detachment in the middle crust of a Variscan allochthonous terrane (Órdenes complex, NW Spain). Lithosphere 6 (6):409–418. https://doi.org/10.1130/l369.1

Apraiz A (1998) Geología de los macizos de Lora del Rio y Valuengo (Zona de Ossa-Morena). Evolución tectonometamórfica y significado geodinámico. PhD Thesis, University of the Vasque Country

Apraiz A, Eguiluz L (2002) Hercynian tectono-thermal evolution associated with crustal extension and exhumation of the Lora del Río metamorphic core complex (Ossa-Morena zone, Iberian Massif, SW Spain). Interational Journal of Earth Sciences 91: 76–92. https://doi.org/10.1007/s005310100206

Araújo A, Fonseca P, Munhá J, Moita P, Pedro J, Ribeiro A (2005) The Moura Phyllonitic Complex: An accretionary complex related with obduction in the southern Iberia Variscan suture. Geodinamica Acta 18(5): 375–388

Arenas R, Martínez Catalán JR (2003) Low-P metamorphism following a Barrovian-type evolution. Complex tectonic controls for a common transition, as deduced in the Mondoñedo thrust sheet (NW Iberian Massif). Tectonophysics 365:143–164. https://doi.org/10.1016/s0040-1951(03)00020-9

Arenas R, Sánchez Martínez S (2015) Variscan ophiolites in NW Iberia: Tracking lost Paleozoic oceans and the assembly of Pangea. Episodes 38, 315–333

Arenas R, Rubio Pascual FJ, Díaz García F, Martínez Catalán JR (1995) High pressure micro-inclusions and development of an inverted metamorphic gradient in the Santiago Schists (Ordenes Complex, NW Iberian Massif, Spain): evidence of subduction and syn-collisional decompression. Journal of Metamorphic Geology, 13, 141–164

Arenas R, Abati J, Catalán JRM, García FD, Pascual FJR (1997) P-T evolution of eclogites from the Agualada Unit (Ordenes Complex, northwest Iberian Massif, Spain): Implications for crustal subduction. Lithos 40 (2):221–242. https://doi.org/10.1016/S0024-4937(97)00029-7

Arenas R, Martínez Catalán JR, Sánchez Martínez S, Fernández-Suárez J, Andonaegui P, Pearce JA, Corfú F (2007a) The Vila de Cruces ophiolite: A remnant of the early Rheic Ocean in the Variscan suture of Galicia (northwest Iberian Massif). The Journal of Geology 115:129–148

Arenas R, Martínez Catalán JR, Sánchez Martínez S, Díaz García F, Abati J, Fernández Suárez J, Andonaegui P, Gómez-Barreiro J (2007b) Paleozoic ophiolites in the Variscan suture of Galicia (northwest Spain): distribution, characteristics and meaning. In: Hatcher, R.D., JR., Carlson, M.P., McBride, J.H., Martínez Catalán, J.R. (Eds.), 4-D framework of continental crust. Geological Society of America Memoir, 200, 425–444

Arenas R, Sánchez Martínez S, Castiñeiras P, Jeffries TE, Díez Fernández R, Andonaegui P (2009) The basal tectonic mélange of the Cabo Ortegal Complex (NW Iberian Massif): a key unit in the suture of Pangea. Journal of Iberian Geology, 35, 85–125

Arenas R, Sánchez Martínez S, Gerdes A, Albert R, Díez Fernández R, Andonaegui P (2013) Re-interpreting the Devonian ophiolites involved in the Variscan suture: U–Pb and Lu–Hf zircon data of the Moeche Ophiolite (Cabo Ortegal Complex, NW Iberia). International Journal of Earth Sciences:1–18. https://doi.org/10.1007/s00531-013-0880-x

Arenas R, Díez Fernández R, Rubio Pascual FJ, Sánchez Martínez S, Martín Parra LM, Matas J, González del Tánago J, Jiménez-Díaz A, Fuenlabrada JM, Andonaegui P, Garcia-Casco A (2016a) The Galicia–Ossa-Morena Zone: Proposal for a new zone of the Iberian Massif. Variscan implications. Tectonophysics 681: 135–143. https://doi.org/10.1016/j.tecto.2016.02.030

Arenas R, Sánchez Martínez S, Díez Fernández R, Gerdes A, Abati J, Fernández-Suárez J, Andonaegui P, González Cuadra P, López Carmona A, Albert R, Fuenlabrada JM, Rubio Pascual FJ (2016b) Allochthonous terranes involved in the Variscan suture of NW Iberia: A review of their origin and tectonothermal evolution. Earth-Science Reviews 161: 140–178. https://doi.org/10.1016/j.earscirev.2016.08.010

Armendáriz M, López-Guijarro R, Quesada C, Pin C, Bellido F (2008) Genesis and evolution of a syn-orogenic basin in transpression: Insights from petrography, geochemistry and Sm–Nd systematics in the Variscan Pedroches basin (Mississippian, SW Iberia). Tectonophysics 461 (1):395–413. https://doi.org/10.1016/j.tecto.2008.02.007

Azor A (1994) Evolución tectonometamórfica del límite entre las zonas Centroibérica y de Ossa-Morena (Cordillera Varisca, SO de España). PhD Thesis, University of Granada

Azor A, Ballèvre M (1997) Low-Pressure Metamorphism in the Sierra Albarrana Area (Variscan Belt, Iberian Massif). Journal of Petrology 38: 35–64

Azor A, González Lodeiro F, Simancas JF (1993) Cadomian subduction/collision and Variscan transpression in the Badajoz Córdoba Shear belt (SW Spain): a discussion on the age of the main tectonometamorphic events. Tectonophysics 217: 343–346

Azor A, González Lodeiro F, Martínez Poyatos D, Simancas JF (1994a) Regional significance of kilometric-scale NE-vergent recumbent folds associated with E- to SE-directed shear on the southern border of the Central Iberian Zone (Hornachos-Oliva region, Variscan belt, Iberian Peninsula). Geologische Rundschau 83: 377–387

Azor A, González Lodeiro F, Simancas JF (1994b) Tectonic evolution of the boundary between the Central Iberian and Ossa-Morena zones (Variscan belt, southwest Spain). Tectonics 13: 45–61

Azor A, Simancas JF, Expósito I, Gonzalez Lodeiro F, Martínez Poyatos D (1997) Deformation of garnets in a low-grade shear zone. Journal of Structural Geology 19: 1137–1148

Azor A, Expósito I, Gonzalez Lodeiro F, Simancas JF, Martínez Poyatos D (2004) Zona de Ossa-Morena. Estructura y metamorfismo. In: Vera JA (ed) Geología de España, SGE-IGME, Madrid, 173–189

Azor A, Rubatto D, Simancas JF, González Lodeiro F, Martínez Poyatos D, Martín Parra LM, Matas J (2008) Rheic Ocean ophiolitic remnants in Southern Iberia questioned by SHRIMP U-Pb zircon ages on the Beja-Acebuches amphibolites. Tectonics 27: TC5014. https://doi.org/10.1029/2009tc002527

Azor A, Rubatto D, Marchesi C, Simancas JF, González Lodeiro F, Martínez Poyatos D, Martín Parra LM, Matas J (2009) Reply to comment by C. Pin and J. Rodriguez on "Rheic Ocean ophiolitic remnants in southern Iberia questioned by SHRIMP U-Pb zircon ages on the Beja-Acebuches amphibolites". Tectonics 28: TC5014: https://doi.org/10.1029/2009tc002527

Azor A, Simancas JF, Martínez Poyatos DJ, Montero P, Bea F, Gonzalez Lodeiro F, Gabites J (2012) Nuevos datos geocronológicos sobre la evolución tectonometamórfica de la Unidad de Sierra Albarrana (Zona de Ossa-Morena, SO de Iberia). VIII Congreso Geológico de España, Geo-Temas 13

Ballèvre M, Martínez Catalán JR, López Carmona A, Pitra P, Abati J, Díez Fernández R, Ducassou C, Arenas R, Bosse V, Castiñeiras P, Fernández-Suárez J, Gómez Barreiro J, Paquette JL, Peucat JJ, Poujol M, Ruffet G, Sánchez Martínez S (2014) Correlation of the nappe stack in the Ibero-Armorican arc across the Bay of Biscay: a joint French-Spanish project. Geological Society, London, Special Publications:77–113. https://doi.org/10.1144/sp405.13

Bandrés A, Eguíluz L, Gil Ibarguchi JI, Palacios T (2002) Geodynamic evolution of a Cadomian arc region: the northern Ossa-Morena zone, Iberian massif. Tectonophysics 352: 105–120. https://doi.org/10.1016/s0040-1951(02)00191-9

Barbero L (1995) Granulite-facies metamorphism in the Anatectic Complex of Toledo, Spain: Late hercynian tectonic evolution by crustal extension. Journal of the Geological Society 152(2): 365–382. https://doi.org/10.1144/gsjgs.152.2.00365

Barbero C, Villaseca C, Rogers G, Brown PE (1995) Geochemical and isotopic disequilibrium in crustal melting: An insight from the anatectic granitoids from Toledo, Spain. Journal of Geophysical Research 100(B8): 15745–15765. https://doi.org/10.1029/95jb00036

Barbero C, Glasmacher UA, Villaseca C, López García JA, Martín Romera C (2005) Long-term thermo-tectonic evolution of the Montes de Toledo area (Central Hercynian Belt, Spain): constraints from apatite fission track analysis. International Journal of Earth Sciences 94: 193–203. https://doi.org/10.1007/s00531-004-0455-y

Bard JP (1977) Signification tectonique des me´tatholeites d'affinite´ abyssale de la ceinture de basse pression d'Aracena (Huelva, Espagne), Bulletin de la Société Géologique de France 19: 385–393

Barrie CT, Amelin Y, Pascual E (2002) U-Pb Geochronology of VMS mineralization in the Iberian Pyrite Belt. Mineralium Deposita 37: 684–703. https://doi.org/10.1007/s00126-002-0302-7

Bea F, Montero P, Talavera C, Zinger A (2006) A revised Ordovician age for the Miranda do Douro orthogneiss, Portugal. Zircon U–Pb ion-microprobe and LA-ICPMS dating. Geologica Acta 4 (3):395–401. https://doi.org/10.1344/105.000000353

Bea F, Pesquera A, Montero P, Torres-Ruiz J, Gil-Crespo PP (2009) Tourmaline 40Ar/39Ar chronology of tourmaline-rich rocks from Central Iberia dates the main Variscan deformation phases. Geologica Acta 7 (4):399–412. https://doi.org/10.1344/105.000001446

Blatrix P, Burg JP (1981) $^{40}Ar/^{39}Ar$ dates from the Sierra Morena (Southern Spain): Variscan metamorphism and Cadomian orogeny. Neues Jahrb Mineral Monatsh 10: 470–478

Boogaard M, Vázquez F (1981) Conodont faunas from Portugal and Southwester Spain. Part 5. Lower Carboniferous conodonts at Santa Olalla de Cala (Spain). Scripta Geologica 61: 1–8

Booth-Rea G, Simancas JF, Azor A, Azañón JM, Gonzalez Lodeiro F, Fonseca P (2006). HP-LT Variscan metamorphism in the Cubito-Moura schists (Ossa-Morena Zone, southern Iberia). Comptes Rendus Geosciences 338(16): 1260–1267. https://doi.org/10.1016/j.crte.2006.08.001

Braid JA, Murphy JB, Quesada C (2010a) Structural analysis of an accretionary prism in a continental collisional setting, the Late Paleozoic Pulo do Lobo Zone, Southern Iberia. Gondwana Research 17: 422–439. https://doi.org/10.1016/j.gr.2009.09.003

Braid JA, Murphy JB, Quesada C (2010b) Structural analysis of an accretionary prism in a continental collisional setting, the Late Paleozoic Pulo do Lobo Zone, Southern Iberia. Gondwana Research17 (2–3), 422–439. https://doi.org/10.1016/j.gr.2009.09.003

Brun JP, Burg JP (1982) Combined thrusting and wrenching in the Ibero-Armorican arc: a corner effect during continental collision. Earth and Planetary Sciences Letters 61: 319–332

Burg JP, Iglesias M, Laurent P, Matte P, Ribeiro A (1981) Variscan intracontinental deformation: The Coimbra-Córdoba Shear zone (SW Iberian Peninsula). Tectonophysics 78: 161–177

Cambeses A (2015) Ossa-Morena Zone Variscan 'calc-alkaline' hybrid rocks: interaction of mantle- and crustal-derived magmas as a result of intra-orogenic extension-related intraplating. PhD Thesis, University of Granada

Capdevila R, Matte P, Paredes J (1971) La nature du Précambrien et ses relations avec le Paleozoïque dans la Sierra Morena centrale (Sud de l'Espagne). Comptes Rendus Académie des Sciences de Paris 273: 1359–1362

Capellà I, Bou O (1997) La estructura del domo de la Rabassa y del sector oriental del sinclinal de Llavorsi (Pirineo central). Estudios Geológicos 53: 121–133

Casas JM (2010) Ordovician deformations in the Pyrenees: new insights into the significance of pre-Variscan ('sardic') tectonics. Geological Magazine 147: 674–689

Casas JM, Domingo F, Poblet J, Soler A (1989) On the role of the Hercynian and Alpine thrusts in the Upper Paleozoic rocks of the Central and Eastern Pyrenees. Geodinamica Acta 3: 135–147

Castro A, Fernández C, de la Rosa J, Moreno-Ventas I, Rogers G (1996) Significance of MORB-derived amphibolites from the Aracena Metamorphic belt, Southwest Spain. Journal of Petrology 37/2: 235–260. https://doi.org/10.1093/petrology/37.2.235

Castro A, Fernández C, El-Hmidi H, El-Biad M, Díaz M, de la Rosa JD, Stuard F (1999) Age constraints to the relationships between magmatism, metamorphism and tectonism in the Aracena metamorphic belt, southern Spain. International Journal of Earth Sciences 88: 26–37. https://doi.org/10.1007/s005310050243

Cirés J, Alías G, Poblet J, Casas JM (1990) La estructura del anticlinal de La Masana (Hercínico del Pirineo central). Geogaceta 8: 42–44

Clariana P, García-Sansegundo J (2009) Variscan structure in the eastern part of the Pallaresa massif, Axial Zone of the Pyrenees (NW Andorra). Tectonic implications. Bulletin Societé géolgique France 180 (6): 501–511

Clariana P, García-Sansegundo J, Gavaldà J (2009) The structure in the Bagneres de Luchon and Andorra cross sections (Axial Zone of the central Pyrenees). Trabajos de Geología, Universidad de Oviedo 29: 175–181

Crespo-Blanc A (1989) Evolución geotectónica del contacto entre la Zona de Ossa-Morena y la Zona Surportuguesa en las sierras de Aracena y Aroche (Macizo Ibérico meridional): un contacto mayor en la Cadena Hercínica europea. PhD Thesis, University of Sevilla

Crespo-Blanc A (1992) Structure and kinematics of a sinistraltranspressive suture between the Ossa-Morena and the South Portuguese Zones, South Iberian Massif. Journal of the Geological Society, London, 149:401–411

Crespo-Blanc A, Orozco M (1988) The Southern Iberian Shear Zone: a major boundary in the Hercynian folded belt. Tectonophysics 148: 221–227

Dahn DRL, Braid JA, Murphy JB, Quesada C, Dupuis N, McFarlane CRM (2014) Geochemistry of the Peramora Mélange and Pulo do Lobo schist: geochemical investigation and tectonic interpretation of mafic mélange in the Pangean suture zone, Southern Iberia. International Journal of Earth Sciences 103(5): 1415–1431. https://doi.org/10.1007/s00531-014-1024-7

Dallmeyer RD, Quesada C (1992) Cadomian vs. Variscan evolution of the Ossa-Morena Zone (SW Iberia): filed and $^{40}Ar/^{39}Ar$ mineral age constrains. Tectonophysics 216: 339–364

Dallmeyer RD, Ribeiro A, Marques F (1991) Polyphase Variscan emplacement of exotic terranes (Morais and Bragança Massifs) onto Iberian successions: Evidence from 40Ar/39Ar mineral ages. Lithos 27 (2):133–144. https://doi.org/10.1016/0024-4937(91)90025-g

Dallmeyer RD, Fonseca P, Quesada C, Ribeiro A (1993) 40Ar/39Ar mineral age constraints for the tectonothermal evolution of a Variscan suture in southwest Iberia. Tectonophysics 222: 177–194

Dallmeyer RD, Martínez Catalán JR, Arenas R, Gil Ibarguchi JI, Gutiérrez-Alonso G, Farias P, Bastida F, Aller J (1997) Diachronous Variscan tectonothermal activity in th NW Iberia Massif: Evidence from 40Ar/39Ar dating of regional fabrics. Tectonophysics 277 (4):307–337. https://doi.org/10.1016/s0040-1951(97)00035

de la Rosa JD, Castro A (2004) Magmatismo de la Zona Sudportuguesa. In: Vera JA (ed) Geología de España. SGE-IGME, Madrid, 215–222

Delvolvé JJ (1981) Arguments en faveur de l'âge namurien du Culm des Pyrénées Centrales françaises. C.R. Acad. Sc.Paris, 293: 219–222

Delvolvé JJ, Perret MF (1989) Variations de l'âge des sédiments calcaires et "Culm" carbonifère dans la chaîne varisque du Sud de la France: migration de l'orogenèse varisque. Geodinamica Acta (Paris) 3: 117–126

Delvolvé JJ, Souquet P, Vachard D, Perret MF, Aguirre P (1993) Caractérisation d'un bassin d'avant-pays dans le Carbonifère des Pyrénées: faciès, chronologie de la tectonique synsédimentaire. C.R. Acad. Sci. Paris, t. 316, Série II: 959–966

Den Brok SWJ (1989) Evidence for pre-Variscan deformation in the Lys Caillaouas area, Central Pyrenees, France. Geologie en Mijnbouw 68: 377–380

Dias da Silva Í (2014) Geología de las Zonas Centro Ibérica y Galicia—Trás-os-Montes en la parte oriental del Complejo de Morais, Portugal/España, vol 45. Serie Nova Terra, vol 45. Instituto Universitario de Geología "Isidro Parga Pondal"—Área de Xeoloxía e Minería do Seminario de Estudos Galegos, Coruña

Dias da Silva Í, Valverde-Vaquero P, González-Clavijo E, Díez-Montes A, Martínez Catalán JR (2014) Structural and stratigraphical significance of U–Pb ages from the Mora and Saldanha volcanic complexes (NE Portugal, Iberian Variscides). Geological Society, London, Special Publications 405:115–135. https://doi.org/10.1144/sp405.3

Dias da Silva Í, González-Clavijo E, Díez-Montes A Lateral escape tectonics in the Variscan Orogen: A new approach for the emplacement of the Allochthonous terranes and for the birth of the Central Iberian Orocline. In: Pitra P, Ballèvre M, Martínez Catalán JR (eds) Variscan 15 - The Variscan belt: Correlations and plate dynamics, Rennes, 2015a. BRGM/SGF, pp 48–49

Dias da Silva Í, Linnemann U, Hofmann M, González-Clavijo E, Díez-Montes A, Martínez Catalán JR (2015b) Detrital zircon and tectonostratigraphy of the Parautochthon under the Morais Complex (NE Portugal): implications for the Variscan accretionary history of the Iberian Massif. Journal of the Geological Society 172 (1):45–61. https://doi.org/10.1144/jgs2014-005

Dias da Silva Í, González-Clavijo E, Díez Montes A, Gómez Barreiro J The NW Iberia Allochthonous domain envisaged as a Variscan lateral extrusion fan-like structure: local and orogenic-scale implications. In: EGU General Assembly 2018, Vienna, 2018. Geophysical Research Abstracts, pp EGU2018-2738

Días R, Ribeiro A (1991) Finite strain analysis in a transpressive regime (Variscan autochthon, northeast Portugal). Tectonophysics 191: 389–397

Dias R, Ribeiro A (1995) The Ibero-Armorican Arc: A collision effect against an irregular continent? Tectonophysics 246 (1–3):113–128. doi:https://doi.org/10.1016/0040-1951(94)00253-6

Dias R, Ribeiro A, Coke C, Pereira E, Rodrigues JF, Castro P, Moreira N, Rebelo JA (2013) Evolução estructural dos sectores setentrionais do Autóctone da Zona Centro-Ibérica. In: Dias R, Araújo A, Terrinha P, Kullberg JC (eds) Geologia de Portugal, vol Vol. I—Geologia Pré-mesozoica de Portugal. pp 73–147

Díaz Azpiroz M, Fernández C (2005) Kinematic analysis of the southern Iberian shear zone and tectonic evolution of the Acebuches metabasites (SW Variscan Iberian Massif). Tectonics 24(3): TC3010. https://doi.org/10.1029/2004tc001682

Díaz Azpiroz M, Castro A, Fernández C, López S, Fernández Caliani JC, Moreno-Ventas I (2004) The contact between the Ossa-Morena and the South Portuguese zones. Characteristics and significance of the Aracena metamorphic belt, in its central sector between Aroche and Aracena (Huelva). Journal of Iberian Geology 30: 23–51

Díaz Azpiroz M, Fernández C, Castro A, El-Biad M (2006) Tectonometamorphic evolution of the Aracena metamorphic belt (SW Spain) resulting from ridge-trench interaction during Variscan plate convergence. Tectonics 25: TC1001. https://doi.org/10.1029/2004tc001742

Díaz García F, Martínez Catalán JR, Arenas R, González Cuadra P (1999) Early Ordovician orogenic event in Galicia (NW Spain): evidence from U–Pb ages in the uppermost unit of the Ordenes Complex. International Journal of Earth Sciences 88:337–351. https://doi.org/10.1007/s005310050269

Díez Balda MA, Vegas R, González Lodeiro F (1990) Structure. In: Dallmeyer RD, Martínez García E (eds) Pre-Mesozoic Geology of Iberia. Springer-Verlag, Germany, pp 172–188

Díez Balda MA, Martínez Catalán JR, Ayarza Arribas P (1995) Syn collisional extensional collapse parallel to orogenic trend in a domain of steep tectonics: The Salamanca Detachment Zone (Central Iberian Zone, Spain). Journal of Structural Geology 17 (2):163–182. https://doi.org/10.1016/0191-8141(94)e0042-w

Díez Fernández R, Arenas R (2015) The Late Devonian Variscan suture of the Iberian Massif: A correlation of high-pressure belts in NW and SW Iberia. Tectonophysics 654: 96–100. https://doi.org/10.1016/j.tecto.2015.05.001

Díez Fernández R, Arenas R (2016) Reply to Comment on "The Late Devonian Variscan suture of the Iberian Massif: A correlation of high-pressure belts in NW and SW Iberia". Tectonophysics 670: 155–160. https://doi.org/10.1016/j.tecto.2015.11.033

Díez Fernández R, Martínez Catalán JR (2012) Stretching lineations in high-pressure belts: the fingerprint of subduction and subsequent events (Malpica–Tui complex, NW Iberia). Journal of the Geological Society 169 (5):531–543. https://doi.org/10.1144/0016-76492011-101

Díez Fernández R, Pereira MF (in press) Extensional orogenic collapse captured by strike-slip tectonics: Constraints from structural geology and UPb geochronology of the Pinhel shear zone (Variscan orogen, Iberian Massif). Tectonophysics. https://doi.org/10.1016/j.tecto.2016.10.023

Díez Fernández R, Martínez Catalán JR, Arenas R, Abati J (2011) Tectonic evolution of a continental subduction-exhumation channel: Variscan structure of the basal allochthonous units in NW Spain. Tectonics, 30, TC3009, 1–2

Díez Fernández R, Martínez Catalán JR, Arenas R, Abati J (2012a) The onset of the assembly of Pangaea in NW Iberia: Constraints on the kinematics of continental subduction. Gondwana Research 22 (1):20–25. https://doi.org/10.1016/j.gr.2011.08.004

Díez Fernández R, Martínez Catalán JR, Gómez Barreiro J, Arenas R (2012b) Extensional flow during gravitational collapse: A tool for setting plate convergence (Padrón migmatitic dome, Variscan belt, NW Iberia). The Journal of Geology, 120, 83–103

Díez Fernández R, Pereira MF (2016) Extensional orogenic collapse captured by strike-slip tectonics: Constraints from structural geology and UPb geochronology of the Pinhel shear zone (Variscan orogen, Iberian Massif). Tectonophysics 691:290-310. https://doi.org/10.1016/j.tecto.2016.10.023

Díez Fernández R, Pereira MF, Foster DA (2015) Peralkaline and alkaline magmatism of the Ossa-Morena zone (SW Iberia): Age, source, and implications for the Paleozoic evolution of Gondwanan lithosphere. Lithosphere 7: 73–90. https://doi.org/10.1130/l379.1

Díez Fernández R, Arenas R, Pereira MF, Sánchez-Martínez S, Albert R, Martín Parra LM, Rubio Pascual FJ, Matas J (2016) Tectonic evolution of Variscan Iberia: Gondwana–Laurussia collision revisited. Earth-Science Reviews 162: 269–292. https://doi.org/10.1016/j.earscirev.2016.08.002

Díez García F, Arenas R, Martínez Catalán JR, González del Tánago J, Dunning GR (1999) Tectonic Evolution of the Careón Ophiolite (Northwest Spain): A Remnant of Oceanic Lithosphere in the Variscan Belt. The Journal of Geology 107 (5):587–605. https://doi.org/10.1086/314368

Díez-Montes A (2007) *La geología del Dominio "Ollo de Sapo" en las comarcas de Sanabria y Terra do Bolo*, vol 34. Nova Terra, 2007 edn. Instituto Universitario de Geología "Isidro Parga Pondal" - Área de Xeoloxía e Minería do Seminario de Estudos Galegos, La Coruña

Dunning GR, Díez-Montes A, Matas J, Martín Parra LM, Almarza J, Donaire M (2002) Geocronología U/Pb del volcanismo ácido y granitoides de la Faja Pirítica Ibérica (Zona Surportuguesa). Geogaceta 32: 127–130

Eden CP (1991) Tectonostratigraphic analysis of the northern extent of the oceanic exotic terrane, Northwestern Huelva Province, Spain. PhD thesis, University of Southampton, England, 293 p

Eguiluz L (1987) Petrogénesis de rocas ígneas y metamórficas en el antiforme de Burguillos Monesterio. Macizo Ibérico. PhD Thesis, University of Granada

Eguiluz L, Gil Ibarguchi JI, Ábalos B, Apraiz A (2000) Superposed Hercynian and Cadomian orogenic cycles in the Ossa-Morena Zone and related areas of the Iberian Massif. Geological Society of America Bulletin 112: 1398–1413

Ehsan SA, Carbonell R, Ayarza P, Martí D, Martínez Poyatos D, Simancas, JF, A A, Ayala C, Torné M, Pérez-Estaún A (2015) Lithospheric velocity model across the Southern Central Iberian Zone (Variscan Iberian Massif): The ALCUDIA wide-angle seismic reflection transect. Tectonics 34: 535–554. https://doi.org/10.1002/2014tc003661

Escuder Viruete J (1993) Mylonitic fabric development and tectonothermal model associated with variscan crustaextension, Northwest Salamanca, Spain (Iberian Hercinian Belt). BRGM France (219):66

Escuder Viruete J (1999) Hornblende-bearing leucosome development during syn-orogenic crustal extension in the Tormes Gneiss Dome, NW Iberian Massif, Spain. Lithos 46 (4):751–772. https://doi.org/10.1016/s0024-4937(99)00002-x

Escuder Viruete J, Arenas R, Martínez Catalán JR (1994) Tectonothermal evolution associated with Variscan crustal extension, in the Tormes Gneiss dome (NW Salamanca, Iberian Massif, Spain). Tectonophysics 238:1–22

Esteban JJ, Aranguren A, Cuevas J, Hilario A, Tubía JM, Larionov A, Sergeev S (2015) Is there a time lag between the metamorphism and emplacement of plutons in the Axial Zone of the Pyrenees? Geological Magazine 152: 935–941.https://doi.org/10.1017/s001675681500014x

Etxebarria M, Chalot-Prat F, Apraiz A, Eguíluz L (2006) Birth of a volcanic passive margin in Cambrian time: Rift paleogeography of the Ossa-Morena Zone, SW Spain. Precambrian Research 147: 366–386. https://doi.org/10.1016/j.precamres.2006.01.022

Expósito I (2000) Evolución Estructural de la mitad septentrional de la Zona de Ossa-Morena, y su relación con el límite Zona de Ossa-Morena/ Zona Centroibérica. PhD Thesis, University of Granada

Expósito I, Simancas JF, González Lodeiro F, Azor A, Martínez Poyatos DJ (2002) La estructura de la mitad septentrional de la Zona de Ossa-Morena: deformación en el bloque inferior de un cabalgamiento cortical de evolución compleja. Revista de la Sociedad Geológica de España 15(1–2): 3–14

Expósito I, Simancas JF, González Lodeiro F, Bea F, Montero P, Salman K (2003) Metamorphic and deformational imprint of Cambrian-Lower Ordovician rifting in the Ossa-Morena Zone (Iberian Massif, Spain). Journal of Structural Geology 25: 2077–2087

Fernández-Suárez J, Arenas R, Abati J, Martínez Catalán JR, Whitehouse MJ, Jeffries TE (2007) U-Pb chronometry of polymetamorphic high-pressure granulites: An example from the authochtonous terranes of the NW Iberian Variscan belt. In: Hatcher Jr. RD, Carlson MP, McBride JH, Martínez Catalán JR (eds) 4D Framework of Continental Crust, vol 200. Geological Society of America, pp 469–488. https://doi.org/10.1130/2007.1200(24)

Figueiras J, Mateus A, Gonçalves MA, Waerenborgh J, Fonseca P (2002) Geodynamic evolution of the South Variscan Iberian Suture as recorded by mineral transformations. Geodinamica Acta 15:45–61

Fonseca P (2005) O terreno acrecionário do Pulo do Lobo: implicaçoes geodinâmicas da sutura com a Zona de Ossa-Morena (SW da Cadeia Varisca Ibérica). Cadernos do Laboratorio Xeolóxico de Laxe 30:213–222

Fonseca P, Ribeiro A (1993) Tectonics of the Beja-Acebuches Ophiolite: a major suture in the Iberian Variscan Foldbelt. Geologische Rundschau 82: 440–447

Fonseca P, Munhá J, Pedro J, Rosas F, Moita P, Aráujo A, Leal N (1999) Variscan Ophiolites and High-Pressure Metamorphism in Southern Iberia. Ofioliti 24: 259–268

Franke W (2006) The Variscan orogen in Central Europe: construction and collapse. In: Gee DG, Stephenson RA (eds) European Lithosphere Dynamics, Geological Society, London, Memoirs, 32: 333–343

Franke W (2014) Topography of the Variscan orogen in Europe: failed–not collapsed. International Journal of Earth Sciences 103:1471–1499. https://doi.org/10.1007/s00531-014-1014-9

Franke W, Doublier MP, Klama K, Potel S, Wemmer K (2011) Hot metamorphic core complex in a cold foreland. International Journal of Earth Sciences 100(4): 753–758. https://doi.org/10.1007/s00531-010-0512-7

Gabaldón V, Garrote A, Quesada C (1985) Geología del Carbonífero Inferior del Norte de la Zona de Ossa-Morena. Introducción a la excursión. Temas Geológico-Mineros, IGME, 101–137

García-Sansegundo J, Poblet, J, Alonso JL, Clariana P (2011). Hinterland – foreland zonation of the Variscan orogen in the Central Pyrenees: comparison with the northern part of the Iberian

Variscan Massif. *Geological Society of London*, Special Publications, 349, pp. 169–184

Garrote A (1976) Asociaciones minerales del núcleo metamórfico de Sierra Albarrana (Prov. de Córdoba). Sierra Morena Central. Memórias e Noticias Publ Mus Lab Mineral Geol Univ Coimbra 82: 17–39

Giese U, Walter R, Von Winterfled C (1994) Geology of the southwestern Iberian Meseta II: the Aracena Metamorphic belt between Almonaster la Real and Valdelarco, Huelva province (SW Spain). Neues Jahrbuch für Geologie und Paläontologie, Abhandlung, 192/3: 333–360

Gil Ibarguchi JI (1995) Petrology of jadeite-metagranite and associated orthogneiss from the Malpica-Tuy allochthon (Northwest Spain). European Journal of Mineralogy, 7, 403–415

Gil Ibarguchi JI, Dallmeyer RD (1991) Hercynian blueschist metamorphism in North Portugal: tectonothermal implications. Journal of Metamorphic Geology 9 (5):539–549. https://doi.org/10.1111/j.1525-1314.1991.tb00547.x

Gil Ibarguchi JI, Mendia M, Girardeau J, Peucat JJ (1990) Petrology of eclogites and clinopyroxene-garnet metabasites from the Cabo Ortegal Complex (northwestern Spain). Lithos 25 (1):133–162. https://doi.org/10.1016/0024-4937(90)90011-o

Gil Ibarguchi JI, Abalos B, Azcárraga J, Puelles P (1999) Deformation, high-pressure metamorphism and exhumation of ultramafic rocks in a deep subduction/collision setting (Cabo Ortegal, NW Spain). Journal of Metamorphic Geology, 17, 747–764

Girardeau J, Gil Ibarguchi JI (1991) Pyroxenite-rich peridotites of the Cabo Ortegal Complex (Northwestern Spain): Evidence for large-scale upper-mantle heterogeneity. Journal of Petrology, 32 (Spec. Lherzolites Issue), 135–154

Gladney ER, Braid JA, Murphy JB, Quesada C, McFarlane CRM (2014) U–Pb geochronology and petrology of the late Paleozoic Gil Marquez pluton: magmatism in the Variscan suture zone, southern Iberia, during continental collision and the amalgamation of Pangea. International Journal of Earth Sciences 103: 1433–1451. https://doi.org/10.1007/s00531-014-1034-5

Gómez Barreiro J, Martínez Catalán JR (2012) The Bazar shear zone (NW Spain): Microstructural and Time-of-Flight neutron diffraction analysis. Journal of the VIrtual Explorer, 41, paper 5

Gómez Barreiro J, Wijbrans JR, Castiñeiras P, Martínez Catalán JR, Arenas R, Díaz García F, Abati J (2006) 40Ar/39Ar laserprobe dating of mylonitic fabrics in a polyorogenic terrane of NW Iberia. Journal of the Geological Society 163 (1):61–73. https://doi.org/10.1144/0016-764905-012

Gómez Barreiro J, Martínez Catalán JR, Arenas R, Castiñeiras P, Abati J, Díaz García F, Wijbrans JR (2007) Tectonic evolution of the upper allochtonon of the Órdenes complex (Northwestern Iberian Massif): Structural constraints to a poligenic peri-Gondwanan terrane. Geologic Society of America—Special paper 423:315–332. https://doi.org/10.1130/2007.2423(15)

Gómez Barreiro J, Martínez Catalán JR, Prior D, Wenk H, Vogel S, Díez García F, Arenas R, Sánchez Martínez S, Lonardelli I (2010a) Fabric Development in a Middle Devonian Intraoceanic Subduction Regime: The Careón Ophiolite (Northwest Spain). The Journal of Geology 118 (2):163–186. https://doi.org/10.1086/649816

Gómez Barreiro J, Martínez Catalán JR, Díez Fernández, R., Arenas, R., Díaz García, F. (2010b) Upper crust reworking during gravitational collapse: the Bembibre-Pico Sacro detachment system (NW Iberia). Journal of the Geological Society, London, 167, 769–784

Gómez-Pugnaire MT, Azor A, Fernández-Soler JM, López Sánchez--Vizcaíno V (2003) The amphibolites from the Ossa-Morena/Central Iberian Variscan suture (southwestern Iberian Massif): geochemistry and tectonic interpretation. Lithos, 68: 23–42. https://doi.org/10.1016/s0024-4937(03)00018-5

González-Clavijo E, Díez Balda MA, Álvarez F (1993) Structural study of a semiductile strike-slip system in the Central Iberian Zone (Variscan Fold Belt, Spain): Structural controls on gold deposits. Geologische Rundschau 82 (3):448–460. https://doi.org/10.1007/bf00212409

González-Clavijo E, Díez Montes A (2008) Procesos tardi-variscos en la Zona Centro Ibérica. Las bandas de cizalla subverticales del Domo de Tormes. Geo-Temas 10:445-448

González-Clavijo E, Dias da Silva Í, Gutiérrez-Alonso G, Díez Montes A (2016) U/Pb age of a large dacitic block locked in an early carboniferous synorogenic mélange in the parautochthon of NW Iberia: New insights on the structure/sedimentation variscan interplay. Tectonophysics first online (TECTO-126895):11. https://doi.org/10.1016/j.tecto.2016.01.001

González del Tánago J, Arenas R (1991) Anfibolitas granatíferas de Sierra Albarrana Córdoba). Termobarometría e implicaciones para el desarrollo del metamorfismo regional. Revista Sociedad Geológica de España 4: 251–269

González F, Moreno C, López MJ, Dino R, Antonioli L (2004) Palinoestratigrafía del Grupo Pizarroso-Cuarcítico del sector más oriental de la Faja Pirítica Ibérica, SO de España. Revista Española de Micropaleontología 36:279–304

Gutiérrez-Alonso G (1996) Strain partitioning in the footwall of the Somiedo Nappe: structural evolution of the Narcea Tectonic Window, NW Spain. Journal of Structural Geology 18 (10):1217–1229. https://doi.org/10.1016/s0191-8141(96)00034-x

Gutiérrez-Alonso G, Collins AS, Fernández-Suárez J, Pastor-Galán D, González-Clavijo E, Jourdan F, Weil AB, Johnston ST (2015) Dating of lithospheric buckling: 40Ar/39Ar ages of syn-orocline strike–slip shear zones in northwestern Iberia. Tectonophysics 643:44–54. https://doi.org/10.1016/j.tecto.2014.12.009

Hartevelt JJA (1970) Geology of the upper Segre and Valira valleys, central Pyrenees, Andorra/Spain. Leidse Geologische Mededelingen 45: 167–236

Henriques SBA, Neiva AMR, Ribeiro ML, Dunning GR, Tajčmanová L (2015) Evolution of a Neoproterozoic suture in the Iberian Massif, Central Portugal: New U-Pb ages of igneous and metamorphic events at the contact between the Ossa Morena Zone and Central Iberian Zone. Lithos 220–223: 43–59. https://doi.org/10.1016/j.lithos.2015.02.10001

Hernández Enrile JL (1991) Extensional tectonics of the Toledo ductile-brittle shear zone, central Iberian Massif. Tectonophysics 191: 311–324

Jesus AP, Munhá J, Mateus A, Tassinari C, Nutman, AP (2007) The Beja Layered Gabbroic Sequence (Ossa-Morena Zone, Southern Portugal): geochronology and geodynamic implications. Geodinamica Acta 20: 139–157. https://doi.org/10.3166/ga.20.139-157

Julivert M, Martínez FJ (1983). Estructura de conjunto y visión global de la Cordillera Herciniana. En Comba JA (ed.) Libro Jubilar JM Ríos. Geología de España, Tomo I. Instituto Geológico y Minero de España, Madrid: 612—631

Laumonier B, Guitard G (1978) Contribution à l'étude des tectoniques superposes hercyniennes dans les Pyrénées orientales: le problème des plissements précoces dans le synclinal de Villefranche. Revue géographie physique et géologie dynamique 20: 177–212

Llopis N, San José MA, Herranz P (1970) Notas sobre una discordancia posiblemente precámbrica al SE de la provincia de Badajoz y sobre la edad de las series paleozoicas circundantes. Boletín Geológico y Minero 81: 586–592

López-Carmona A, Abati J, Reche J (2010) Petrologic model of chloritoid-glaucophane schists from the NW Iberian Massif. Gondwana Research, 17, 377–391

López-Carmona A, Abati J, Pitra P, Lee JW (2014) Retrogressed lawsonite blueschists from the NW Iberian Massif: P–T–t constraints from thermodynamic modelling and 40Ar/39Ar

geochronology. Contributions to Mineralogy and Petrology 167 (3):1–20. https://doi.org/10.1007/s00410-014-0987-5

López Munguira A, Nieto F, Sebastián Pardo E, Velilla N (1991) The composition of phyllosilicates in Precambrian low-grade metamorphic, clastic rocks from the Southern Herperian Massif (Spain) used as an indicator to metamorphic conditions. Precambrian Research 53: 267–279

López-Moro FJ, López-Plaza M, Romer RL (2012) Generation and emplacement of shear-related highly mobile crustal melts: the synkinematic leucogranites from the Variscan Tormes Dome, Western Spain. International Journal of Earth Sciences 101:1273–1298. https://doi.org/10.1007/s00531-011-0728-1

López Sánchez-Vizcaíno V, Gómez-Pugnaire MT, Azor A, Fernández-Soler JM (2003) Phase diagram sections applied to amphibolites: a case study from the Ossa-Morena/Central Iberian Variscan suture (Southwestern Iberian Massif). Lithos 68: 1–21. https://doi.org/10.1016/s0024-4937(03)00017-3

Lotze F (1945) Zur Gliederung der Varisziden der Iberischen Meseta. Geotekt Forsch 6: 78–92

Macaya J, González-Lodeiro F, Martínez-Catalán JR, Alvarez F (1991) Continuous deformation, ductile thrusting and backfolding of cover and basement in the Sierra de Guadarrama, Hercynian orogen of central Spain. Tectonophysics 191 (3):291–309. https://doi.org/10.1016/0040-1951(91)90063-x

Mantero EM, Alonso-Chaves FM, García-Navarro E, Azor A (2011) Tectonic style and structural analysis of the Puebla de Guzmán Antiform (Iberian Pyrite Belt, South Portuguese Zone, SW Spain). In: Poblet J, Lisle RJ (eds) Kinematic Evolution and Structural Styles of Fold-and-Thrust Belts. Geological Society, London, Special Publications, 349, 203–222. https://doi.org/10.1144/sp349.11

Marcos A, Marquínez J, Pérez-Estaún, A, Pulgar JA, Bastida F (1984) Nuevas aportaciones al conocimiento de la evolución tectonometamórfica del Complejo de Cabo Ortegal (NW de España). Cuadernos do Laboratorio Xeolóxico de Laxe, 7, 125–137

Margalef A, Casas JM (2016) Corte geológico compensado del sur de Andorra: aportaciones a la estructura varisca del Pirineo central. Geo-Temas 16 (1): 61–63

Martín Parra LM, González Lodeiro F, Martínez Poyatos D, Matas J (2006) The Puente Génave-Castelo de Vide shear zone (southern Central Iberian Zone, Iberian Massif): geometry, kinematics and regional implications. Bulletin de la Société Géologique de France 177(4): 191–202. https://doi.org/10.2113/gssgfbull.177.4.191

Martínez JF (1974) Petrografía, estructura y geoquímica de los diferentes tipos de granitoides del NW de Salamanca (Cordillera Herciniana, España). Trabajos de Geología 7:61–141

Martínez FJ, Dietsch C, Aleinikoff J, Cirés J, Arboleya ML, Reche J, Gómez-Gras D (2015) Provenance, age, and tectonic evolution of Variscan flysch, southeastern France and northeastern Spain, based on zircon geochronology. Geological Society America Bulletin 128 (5–6): 842–859

Martínez Catalán JR (2011a) Are the oroclines of the Variscan belt related to late Variscan strike-slip tectonics? Terra Nova 23 (4):241–247. https://doi.org/10.1111/j.1365-3121.2011.01005.x

Martínez Catalán JR (2011b) The Central Iberian arc, an orocline centered in the Iberian Massif and some implications for the Variscan belt. International Journal of Earth Sciences 101 (5):1299–1314. https://doi.org/10.1007/s00531-011-0715-6

Martínez Catalán JR, Arenas R, Díaz García F, Abati J (1997) Variscan accretionary complex of northwest Iberia: Terrane correlation and succession of tectonothermal events. Geology 25 (12):1103–1106. https://doi.org/10.1130/0091-7613(1997)025%3c1103:vaconi%3e2.3.co;2

Martínez Catalán JR, Díaz García F, Arenas R, Abati J, Castiñeiras P, González Cuadra P, Gómez Barreiro J, Rubio Pascual F (2002) Thrust and detachment systems in the Ordenes Complex (northwest Spain): Implications for the Variscan-Appalachian geodinamics. In: Martínez Catalán JR, Hatcher Jr. RD, Arenas R, Díaz García F (eds) Variscan-Appalachian dynamics: The building of the late Palaeozoic basement. Geological Society of America, Boulder, pp 163–182

Martínez Catalán JR, Arenas R, Díez Balda MA (2003) Large extensional structures developed during the emplacement of a crystalline thrust sheet: the Mondoñedo nappe (NW Spain). Journal of Structural Geology 25 (11):1815–1839. https://doi.org/10.1016/s0191-8141(03)00038-5

Martínez Catalán JR, Fernández-Suárez J, Jenner GA, Belousova E, Díez Montes A (2004a) Provenance constraints from detrital zircon U-Pb ages in the NW Iberian Massif: implication for Palaeozoic plate configuration and Variscan evolution. Journal of the Geological Society 161 (3):463–476. https://doi.org/10.1144/0016-764903-054

Martínez Catalán JR, González Lodeiro F, González-Clavijo E, Fernández Rodríguez C, Díez Montes A (2004b) Estructura. In: Vera JA (ed) Geología de España. SGE-IGME, Madrid, pp 75–78

Martínez Catalán JR, Martínez Poyatos D, Bea F (2004c) Zona Centro Ibérica. In: Vera JA (ed) Geología de España. SGE-IGME, Madrid, pp 69–72

Martínez Catalán JR, Arenas R, Díaz García F, González Cuadra P, Gómez Barreiro J, Abati J, Castiñeiras P, Fernández-Suárez J, Sánchez Martínez S, Andonaegui P, González-Clavijo E, Díez Montes A, Rubio Pascual F, Valle Aguado B (2007) Space and time in the tectonic evolution of the northwestern Iberian Massif: Implications for the Variscan belt. In: Hatcher Jr. RD, Carlson MP, McBride JH, Martínez Catalán JR (eds) 4-D Framework of Continental Crust. Geologic Society of America, Boulder, pp 403–423

Martínez Catalán JR, Fernández-Suárez J, Meireles C, González-Clavijo E, Belousova E, Saeed A (2008) U-Pb detrital zircon ages in sinorogenic deposits of the NW Iberian Massif (Variscan belt): Interplay of Devonian-Carboniferous sedimentation and thrust tectonics. Journal of the Geological Society 165 (3):687–698. https://doi.org/10.1144/0016-76492007-066

Martínez Catalán JR, Arenas R, Abati J, Sánchez Martínez S, Díaz García F, Fernández-Suárez J, González Cuadra P, Castiñeiras P, Gómez Barreiro J, Díez Montes A, González-Clavijo E, Rubio Pascual F, Andonaegui P, Jeffries TE, Alcock JE, Díez Fernández R, López Carmona A (2009) A rootless suture and the loss of the roots of a mountain chain: The Variscan Belt of NW Iberia. CR Geoscience 341 (2–3):114-126. https://doi.org/10.1016/j.crte.2008.11.004

Martínez Catalán JR, Rubio Pascual FJ, Montes AD, Fernández RD, Barreiro JG, Dias Da Silva Í, Clavijo EG, Ayarza P, Alcock JE (2014) The late Variscan HT/LP metamorphic event in NW and Central Iberia: relationships to crustal thickening, extension, orocline development and crustal evolution. Geological Society, London, Special Publications 405 (1):225–247. https://doi.org/10.1144/sp405.1

Martínez Catalán JR, Gómez Barreiro J, López-Carmona A, Castiñeiras P, Díez Fernández R, Andonaegui P, Fernández-Suárez J, Abati J, González Cuadra P, Rubio Pascual FJ, Díez-Montes A and González Clavijo E (2016a). Variscan 2015 - The Variscan belt: correlations and plate dynamics. Field Guide - NW Iberian Massif (Galicia): The nappe stack from the Autochthon to the Upper Allochthon. Special meeting of the French & Spanish Geological Societies. Third field trip: A Coruña, 12–18 June 2016. 142 pp. ISBN-13 978-84-608-8840-6

Martínez Catalán JR, González-Clavijo E, Meireles C, Díez Fernández R, Bevis J (2016b) Relationships between syn-orogenic sedimentation and nappe emplacement in the hinterland of the Variscan belt in NW Iberia deduced from detrital zircons. Geological Magazine 153 (1):38–60. https://doi.org/10.1017/s001675681500028x

Martín-Izard A, Arias D, Arias M, Gumiel P, Sanderson DJ, Castañon C, Sánchez J (2016) Ore deposit types and tectonic evolution of the Iberian Pyrite Belt: From transtensional basins and magmatism to transpressional and inversion tectonics. Ore Geology Reviews 79:254–267. https://doi.org/10.1016/j.oregeorev.2016.05.011

Martínez Poyatos D, Azor A, González Lodeiro F, Simancas JF (1995a) Timing of the Variscan structures on both sides of the Ossa Morena/Central Iberian contact (south-west Iberian Massif). Comptes Rendus de l'Académie des Sciences de Paris 321(II): 609–615

Martínez Poyatos D, Simancas JF, Azor A, González Lodeiro F (1995b) La estructura del borde meridional de la Zona Centroibérica en sector suroriental de la provincia de Badajoz. Revista de la Sociedad Geológica de España 8: 41–50

Martínez Poyatos D (1997) Estructura del Borde Meridional de la Zona Centroibérica y su relación con el contacto entre las Zonas Centroibérica y de Ossa-Morena. PhD Thesis, University of Granada.

Martínez Poyatos D, Simancas J, Azor A, Lodeiro FG (1998a) La estructura del borde meridional de la Zona Centroibérica (Macizo Ibérico) en el Norte de la Provincia de Córdoba. Revista de la Sociedad Geológica de España 11:87–94

Martínez Poyatos D, Simancas JF, Azor A, González Lodeiro F (1998b) Evolution of a Carboniferous piggyback basin in the southern Central Iberian Zone (Variscan Belt, SE Spain). Bulletin de la Société Géologique de France 169: 573–578

Martínez Poyatos D, Nieto F, Azor A, Simancas JF (2001) Relationships between very low-grade metamorphism and tectonic deformation: examples from the southern Central Iberian Zone (Iberian Massif, Variscan Belt). Journal of the Geological Society 158: 953–968. https://doi.org/10.1144/0016-764900-206

Martínez Poyatos D, Díez Balda MA, Macaya J, González Lodeiro F, Martínez Catalán JR, Vegas R (2004a) El acortamiento varisco inicial. In: Vera JA (ed) Geología de España. SGE-IGME, Madrid, pp 84–87

Martínez Poyatos D, Gutiérrez Marco JC, Prado Alonzo MV, Rábano I, Sarmiento GN (2004b) La Secuencia Paleozoica postcámbrica. In: Vera JA (ed) Geología de España. SGE-IGME, Madrid, pp 81–83

Martínez Poyatos D, Carbonell R, Palomeras I, Simancas JF, Ayarza P, Martí D, Azor A, Jabaloy A, González Cuadra P, Tejero R, Martín Parra LM, Matas J, González Lodeiro F, Pérez-Estaún A, García Lobón JL, Mansilla L (2012) Imaging the crustal structure of the Central Iberian Zone (Variscan Belt): The ALCUDIA deep seismic reflection transect. Tectonics 31 (3):n/a-n/a. https://doi.org/10.1029/2011tc002995martínez

Martínez Poza I, Martínez Poyatos D, Simancas JF, Azor A (2012) La estructura varisca de la Unidad del Pulo o Lobo (SO del Macizo Ibérico) en las transversales de Aroche y Rosal de la Frontera (Huelva). Geogaceta 52:21–24

Martínez Rius A (1983) Estudio geométrico de pliegues cónicos y su aplicación a la terminación occidental del sinclinal de Guadalmez. In: Geología de España, Libro Jubilar JM Ríos, IGME, Madrid, 3: 177–192

Matas J, Martín Parra, LM, Rubio Pascual FJ, Roldán FJ, Martín Serrano A (2010) Mapa Geológico de España escala 1:200 000, Sevilla-Puebla de Guzmán. IGME, Madrid

Matte P (1986) Tectonics and Plate Tectonics Model for the Variscan Belt of Europe. Tectonophysics 126: 329–374

Matte P (1991) Accretionary history and crustal evolution of the Variscan belt in Western Europe. Tectonophysics 196: 309–337

Matte P, Ribeiro A (1975) Forme et orientation de l'ellipsoïde de déformation dans la virgation hercynienne de Galice. Relations avec le plissement et hypothèses sur la genèse de l'arc ibéro-armoricain. Comptes Rendus de l'Académie des Sciences de Paris 280: 2825–2828

Maurel O, Respaut J-P, Monié P, Arnaud N, Brunel M (2004) U–Pb emplacement and 40Ar/39Ar cooling ages of the eastern Mont-Louis granite massif (Eastern Pyrenees, France). Compte Rendu Geoscience 336: 1091–1098

McDougall N, Brenchley PJ, Rebelo JA, Romano M (2009) Fans and fan deltas—precursors to the Armorican Quartzite (Ordovician) in western Iberia. Geological Magazine 124 (4):347–359. https://doi.org/10.1017/S0016756800016678

Mendia Aranguren M (2000) Petrología de la unidad eclogítica del Complejo de Cabo Ortegal (NW de España), vol 16. Serie Nova Terra, vol 16. Instituto Universitario de Geología "Isidro Parga Pondal" - Área de Xeoloxía e Minería do Seminario de Estudos Galegos, Coruña

Mezger J, Gerdes A (2016) Early Variscan (Visean) granites in the core of central Pyrenean gneiss domes: implications from laser ablation U-Pb and Th-Pb studies. Gondwana Research Gondwana Research 29:181–198

Moita P, Munhá J, Fonseca P, Pedro J, Tassinari C, Araújo A, Palacios T (2005) Phase equilibria and geochronology of Ossa-Morena eclogites. Actas do XIV Semana de Gequímica / VIII Congresso de geoquímica dos Países de Língua Portuguesa 2: 471–474

Moreira N, Búrcio M, Dias R, Coke C (2010) Partição da deformação Varisca nos sectores de Peso da Régua e Vila Nova de Foz Côa (Autóctone da Zona Centro Ibérica). Comunicações Geológicas:147–162

Munhá J (1983) Hercynian magmatism in the Iberian Pyrite Belt. In: Sousa MJL, Oliveira JT (eds), The Carbonferous of Portugal. Memórias dos Serviços Geológicos de Portugal 29:39–81

Munhá J, Ribeiro A, Ribeiro ML (1984) Blueschists in the Iberian Variscan Chain (Trás-os-Montes: NE Portugal). Comunicaçoes dos Serviços Geológicos de Portugal, 70, 31–53

Muñoz JA (1992) Evolution of a continental colision belt: ECORS-Pyrenees crustal balanced cross-section. In: K. R. Mc Clay (Ed.), Thrust Trectonics, London: Chapman & Hall. 235–246

Murphy JB, Braid JA, Quesada C, Dahn D, Gladney E, Dupuis NE (2015) An eastern Mediterranean analogue for the Late Paleozoic evolution of the Pangean suture zone. In: Li, Z.X., Evans, D.A.D., Murphy, J.B. (ed), Supercontinent Cycles Through Earth History. Geological Society of London Special Publication 424. https://doi.org/10.1144/sp424.9

Murphy JB, Quesada C, Gutiérrez-Alonso G, Johnston SJ, Weil A (2016) Reconciling competing models for the tectono-stratigraphic zonation of the Variscan orogen in Western Europe. Tectonophysics 681: 209–219

Oliveira JT (1990) The South Portuguese Zone. Stratigraphy and Synsedimentary Tectonism. In: Dallmeyer RD, Martínez García E (eds), Pre-Mesozoic Geology of Iberia. Springer, Berlin, 334–347

Oliveira JT, Ramalho M, Antunes MT, Monteiro JH (1992) 5ª ediçao da Carta Geológica de Portugal à escala 1:500 000. Serviços Geológicos de Portugal

Oliveira JT, Pereira Z, Carvalho P, Pacheco N, Korn D (2004) Stratigraphy of the tectonically imbricated lithological succession of the Neves Corvo mine area, Iberian Pyrite Belt, Portugal. Mineralium Deposita 39:422–436. https://doi.org/10.1007/s00126-004-04152-2

Oliveira JT, Relvas JMRS, Pereira Z, Munhá J, Matos JX, Barriga FJAS, Rosa CJ (2006) O Complexo Vulcano-Sedimentar de Toca da Moura-Cabrela (Zona de Ossa-Morena); Evoluçao tectono-estratigráfica e mineralizaçoes associadas. In: Días R, Araújo A, Terrinha P, Kullberg JC (eds) Geologia de Portugal no contexto da Iberia, Univ. Évora, Évora, 181–193

Ordóñez Casado B (1998) Geochronological studies of the Pre-Mesozoic basement of the Iberian Massif: the Ossa Morena

zone and the Allochthonous Complexes within the Central Iberian zone. PhD Thesis, ETH Zurich

Ordóñez Casado B, Gebauer D, Schäfer HJ, Ibarguchi JIG, Peucat JJ (2001) A single Devonian subduction event for the HP/HT metamorphism of the Cabo Ortegal complex within the Iberian Massif. Tectonophysics 332 (3):359–385. https://doi.org/10.1016/s0040-1951(00)00210-9

Ordóñez Casado B, Martin-Izard A, García-Nieto J (2008) SHRIMP-zircon U–Pb dating of the Ni–Cu–PGE mineralized Aguablanca gabbro and Santa Olalla granodiorite: Confirmation of an Early Carboniferous metallogenic epoch in the Variscan Massif of the Iberian Peninsula. Ore Geology Reviews 34: 343–353. https://doi.org/10.1016/j.oregeorev.2008.03.002

Ortega E (1986) Geology and metallogeny of the Almadén area, Centro. Iberian Zone, Spain. En: Van Wambeke (Ed.): Remote sensing in mineral exploration. Report Eur 11317: 147–173

Ortega E, González Lodeiro F (1986) La discordancia intra-Alcudiense en el dominio meridional de la Zona Centroibérica. Breviora Geológica Astúrica 27: 27–32

Palero FJ (1993) Tectónica pre-hercínica de las series infraordovícicas del anticlinal de Alcudia y la discordancia intraprecámbrica en su pate oriental (sector meridional de la Zona Centroibérica). Boletín Geológico y Minero 104: 227–242

Palomeras I, Carbonell R, Flecha I, Simancas JF, Ayarza P, Matas J, Martínez Poyatos D, Azor, A, González Lodeiro F, Pérez-Estaún A (2009) Nature of the lithosphere across the Variscan orogen of SW Iberia: Dense wide-angle seismic reflection data. Journal of Geophysical Research 114: B02302. https://doi.org/10.1029/2007jb005050

Pastor-Galán D, Gutiérrez-Alonso G, Weil AB (2011) Orocline timing through joint analysis: Insights from the Ibero-Armorican Arc. Tectonophysics 507 (1–4):31–46. https://doi.org/10.1016/j.tecto.2011.05.005

Pastor-Galán D, Gutiérrez-Alonso G, Fernández-Suárez J, Murphy JB, Nieto F (2013) Tectonic evolution of NW Iberia during the Paleozoic inferred from the geochemical record of detrital rocks in the Cantabrian Zone. Lithos 182–183:211–228. https://doi.org/10.1016/j.lithos.2013.09.007

Pastor-Galán D, Martín-Merino G, Corrochano D (2014) Timing and structural evolution in the limb of an orocline: The Pisuerga–Carrión Unit (southern limb of the Cantabrian Orocline, NW Spain). Tectonophysics 622:110–121. https://doi.org/10.1016/j.tecto.2014.03.004

Pastor-Galán D, Groenewegen T, Brouwer D, Krijgsman W, Dekkers MJ (2015) One or two oroclines in the Variscan orogen of Iberia? Implications for Pangea amalgamation. Geology 43 (6):527–530. https://doi.org/10.1130/g36701.1

Pastor-Galán D, Dekkers MJ, Gutiérrez-Alonso G, Brouwer D, Groenewegen T, Krijgsman W, Fernández-Lozano J, Yenes M, Álvarez-Lobato F (2016) Paleomagnetism of the Central Iberian curve's putative hinge: Too many oroclines in the Iberian Variscides. Gondwana Research 39:96–113. https://doi.org/10.1016/j.gr.2016.06.016

Pastor-Galán D, Dias da Silva ÍF, Groenewegen T, Krijgsman W (2018) Tangled up in folds: tectonic significance of superimposed folding at the core of the Central Iberian curve (West Iberia). International Geology Review Published online: 8 Jan 2018:1–16. https://doi.org/10.1080/00206814.2017.1422443

Pedro J, Araújo A, Fonseca P, Tassinari C, Ribeiro A (2010) Geochemistry and U-Pb zircon age of the internal Ossa-Morena ophiolite sequences: a remnant of Rheic Ocean in SW Iberia. Ofioliti 35 (2): 117–130. https://doi.org/10.4454/ofioliti.v35i2.390

Pereira E (1989) Carta Geológica de Portugal à escala 1:50.000, Folha 10-A (Celorico de Basto). Serviços Geológicos de Portugal

Pereira Z, Piçarra JM, Oliveira JT (1999) Lower Devonian Palynomorphs from the Barrancos region, Ossa-Morena Zone, Portugal. Bolletino della Società Paleontologica Italiana 38(2–3): 239–245

Pereira MF, Silva JB, Chichorro M (2006a) Maciço de Évora. In: Días R, Araújo A, Terrinha P, Kullberg JC (eds) Geologia de Portugal no contexto da Iberia, Univ. Évora, Évora, 173–180

Pereira Z, Oliveira V, Oliveira JT (2006b) Palynostratigraphy of the Toca da Moura and Cabrela Complexes, Ossa Morena Zone, Portugal. Geodynamic implications. Review of Palaeobotany and Palynology 139(1–4): 227–240. https://doi.org/10.1016/j.revpalbo.2005.07.008

Pereira Z, Matos J, Fernandez P, Oliveira JT (2008) Palynostratigraphy and systematic palynology of the Devonian and Carboniferous successions of the South Portuguese Zone, PORTUGAL. Memórias Geológicas do Instituto Nacional de Engenharia, Tecnologia e Innovaçao 34

Pereira MF, Chichorro M, Williams IS, Silva JB, Fernández C, Díaz-Azpiroz M, Apraiz A, Castro A (2009a) Variscan intra-orogenic extensional tectonics in the Ossa-Morena Zone (Évora–Aracena–Lora del Río metamorphic belt, SW Iberian Massif): SHRIMP zircon U–Th–Pb geochronology. In: Murphy JB, Keppie JD, Hynes AJ (eds) Ancient Orogens and Modern Analogues. Geological Society, London, Special Publications 327: 215–237. https://doi.org/10.1144/sp327.11

Pereira MF, Chichorro M, Williams IS, Silva JB, Fernández C, Díaz-Azpiroz M, Aparaiz A, Castro C (2009b) Variscan intra-orogenic extensional tectonics in the Ossa-Morena Zone (Évora-Aracena-Lora del Río metamorphic belt, SW Iberian Massif): SHRIMP zircon U–Th–Pb geochronology. In: Murphy JB, Keppie JD, Hynes AJ (eds), Ancient Orogens and Modern Analogues. Geological Society, London, Special Publications 327:215–237. https://doi.org/10.1144/sp327.11

Pereira MF, Apraiz A, Chichorro M, Silva JB, Armstrong RA (2010a) Exhumation of high-pressure rocks in northern Gondwana during the Early Carboniferous (Coimbra–Cordoba shear zone, SW Iberian Massif): Tectonothermal analysis and U–Th–Pb SHRIMP in-situ zircon geochronology. Gondwana Research 17(2–3): 440–460. https://doi.org/10.1016/j.gr.2009.10.001

Pereira MF, Silva JB, Drost K, Chichorro M, Apraiz A (2010b) Relative timing of transcurrent displacements in northern Gondwana: U–Pb laser ablation ICP-MS zircon and monazite geochronology of gneisses and sheared granites from the western Iberian Massif. Gondwana Research 17(2–3: 461–481. https://doi.org/10.1016/j.gr.2009.08.006

Pereira MF, Chichorro M, Silva JB, Ordóñez-Casado B, Lee, JKW, Williams IS (2012) Early carboniferous wrenching, exhumation of high-grade metamorphic rocks and basin instability in SW Iberia: Constraints derived from structural geology and U–Pb and ^{40}Ar–^{39}Ar geochronology. Tectonophysics 558–559: 28–44. https://doi.org/10.1016/j.tecto.2012.06.020

Pereira MF, Castro A, Chichorro M, Fernández C, Díaz-Alvarado J, Martí J, Rodríguez C (2014) Chronological link between deep-seated processes in magma chambers and eruptions: Permo-Carboniferous magmatism in the core of Pangaea (Southern Pyrenees). Gondwana Research 25: 290–308

Pereira MF, Chichorro M, Moita P, Santos JF, Solá AMR, Williams IS, Silva JB, Armstrong RA (2015) The multistage crystallization of zircon in calc-alkaline granitoids: U–Pb age constraints on the timing of Variscan tectonic activity in SW Iberia. International Journal of Earth Sciences 104: 1167–1183. https://doi.org/10.1007/s00531-015-1149-3

Pérez-Cáceres I, Martínez Poyatos D, Simancas JF, Azor A (2015) The elusive nature of the Rheic Ocean suture in SW Iberia. Tectonics 34: 2429–2450. doi:https://doi.org/10.1002/2015tc003947

Pérez-Cáceres I, Martínez Poyatos D, Simancas JF, Azor A, González Lodeiro F (2016) Oblique collision and deformation partitioning in the SW Iberian Variscides. Solid Earth 7: 857–872. https://doi.org/10.5194/se-7-857-2016

Pérez-Cáceres I, Martínez Poyatos D, Simancas JF, Azor A (2017) Testing the Avalonian affinity of the South Portuguese Zone and the Neoproterozoic evolution of SW Iberia through detrital zircon populations. Gondwana Research 42: 177–192. https://doi.org/10.1016/j.gr.2016.10.010

Pérez-Estaún A, Bastida F, Alonso JL, Marquínez J, Aller J, Alvarez-Marrón J, Marcos A, Pulgar JA (1988) A thin-skinned tectonics model for an arcuate fold and thrust belt: The Cantabrian Zone (Variscan Ibero-Armorican Arc). Tectonics 7 (3):517–537. https://doi.org/10.1029/tc007i003p00517

Pesquera A, Torres-Ruiz J, Gil-Crespo PP, Roda-Robles E (2009) Multistage boron metasomatism in the Alamo Complex (Central Iberian Zone, Spain): Evidence from field relations, petrography, and 40Ar/39Ar tourmaline dating. American Mineralogist 94 (10):1468–1478. https://doi.org/10.2138/am.2009.3100

Peucat JJ, Bernard-Griffiths J, Ibarguchi JIG, Dallmeyer RD, Menot RP, Cornichet J, De Leon MIP (1990) Geochemical and geochronological cross section of the deep Variscan crust: The Cabo Ortegal high-pressure nappe (northwestern Spain). Tectonophysics 177 (1–3):263–292. https://doi.org/10.1016/0040-1951(90)90285-g

Piçarra JM (1998) First Devonian graptolites from Portrugal. In: Gutiérrez-Marco JC, Rábano I (eds) Proceedings 6th International Graptolite Conference (GWG-IPA) & 1998 Field Meeting, IUGS Subcomission on Silurian Stratigraphy. Temas Geológico-Mineros ITGE, 23: 242–243

Pin C, Fonseca PE, Paquette JL, Castro P, Matte P (2008) The ca. 350 Ma Beja Igneous Complex: A record of transcurrent slab break-off in the Southern Iberia Variscan Belt? Tectonophysics 461 (1–4): 356–377. https://doi.org/10.1016/j.tecto.2008.06.001

Poblet J (1991) Estructura herciniana i alpina del vessant sud de la zona axial del Pirineu central. Ph.D. thesis, Universitat de Barcelona

Ponce C, Simancas JF, Azor A, Martínez Poyatos DJ, Booth-Rea G, Expósito I (2012) Metamorphism and kinematics of the early deformation in the Variscan suture of SW Iberia. Journal of Metamorphic Geology 30(7): 625–638. https://doi.org/10.1111/j.1525-1312.10.2012.1000988.x

Quesada C (1990) Precambrian successions in SW Iberia: their relationship to Cadomian orogenic events. In: D'Lemos RS, Strachan RA, Topley CG (eds) The Cadomian Orogeny, Special Publication of the Geological Society of London 51: 353–362

Quesada C (1991) Geological constraints on the Paleozoic tectonic evolution of tectonostratigraphic terranes in the Iberian Massif. Tectonophysics 185:225–245

Quesada C, Dallmeyer RD (1994) Tectonothermal evolution of the Badajoz-Córdoba shear zone (SW Iberia): characteristics and 40Ar/39Ar mineral age constrains. Tectonophysics 231: 195–213

Quesada C, Fonseca PE, Munhá J, Oliveira JT, Ribeiro A (1994) The Beja-Acebuches Ophiolite (Southern Iberia Variscan Fol. Belt): Geological characterization and geodynamic significance. Boletín Geológico y Minero 105: 3–49

Ribeiro ML (1986) Geologia e petrologia da região a SW de Macedo de Cavaleiros. Universidade de Lisboa, Lisboa

Ribeiro A, Silva JB (1983) Structure of the South Portuguese Zone. In: Sousa MJL, Oliveira JT (eds), The Carbonferous of Portugal. Memórias dos Serviços Geológicos de Portugal 29:83–89

Ribeiro A, Pereira E, Dias R (1990) Allochtonous sequences—Structure in the Northwest of the Iberian Peninsula. In: Dallmeyer RD, Martínez García E (eds) Pre-Mesozoic Geology of Iberia. Springer-Verlag, Germany, pp 222–236

Ribeiro A, Munhá J, Dias R, Mateus A, Pereira E, Ribeiro L, Fonseca P, Araújo A, Oliveira JT, Romão J, Chaminé H, Coke C, Pedro J (2007) Geodynamic evolution of the SW Europe Variscides. Tectonics 26: TC6009. https://doi.org/10.1029/2006tc002058

Ribeiro A, Munhá J, Fonseca PE, Araújo A, Pedro JC, Mateus A, Tassinari C, Machado G, Jesus A (2010) Variscan ophiolite belts in the Ossa-Morena Zone (Southwest Iberia): Geological characterization and geodynamic significance. Gondwana Research 17: 408–421. https://doi.org/10.1016/j.gr.2009.09.005

Rocha R, Pereira Z, Araújo A (2010) Novos dados bioestratigráficos (miosporos) na Formação de Terena—Implicações para a interpretação estrutural (Rio Ardila, Barrancos). VIII Congresso Nacional de Geologia de Portugal, Revista Electrónica de Ciências da Terra 17

Rodríguez J, Cosca MA, Gil Ibarguchi JI, Dallmeyer RD (2003) Strain partitioning and preservation of 40Ar/39Ar ages during Variscan exhumation of a subducted crust (Malpica–Tui complex, NW Spain). Lithos 70 (3–4):111–139. https://doi.org/10.1016/s0024-4937(03)00095-1

Rodrigues JF, Ribeiro A, Pereira E (2013) Complexo de Mantos Parautóctones do NE de Portugal: estructura interna e tectonoestratigrafia. In: Dias R, Araújo A, Terrinha P, Kullberg JC (eds) Geologia de Portugal, Vol. I—Geologia Pré-mesozoica de Portugal, pp 275–331

Romeo I, Capote R, Tejero R, Lunar R, Quesada C (2006) Magma emplacement in transpression: The Santa Olalla Igneous Complex (Ossa-Morena Zone, SW Iberia). Journal of Structural Geology 28: 1821–1832.10. https://doi.org/10.1016/j.jsg.2006.06.007

Romer RL, Soler A (1995) U-Pb age and lead isotopic characterization of Au-bearing skarn related to the Andorra granite. Mineralium Deposita 30: 374–383

Rosas FM, Marques FO, Ballèvre M, Tassinari C (2008) Geodynamic evolution of the SW Variscides: orogenic collapse shown by new tectonometamorphic and isotopic data from western Ossa-Morena Zone, SW Iberia. Tectonics 27: TC6008. https://doi.org/10.1029/2008tc002333

Rubio Pascual FJ, Arenas R, Díaz García F, Martínez Catalán JR, Abati J (2002) Eclogites and eclogite-amphibolites from the Santiago Unit (Ordenes Complex, NW Iberian Massif, Spain): a case study of contrasting high-pressure metabasites in a context of crustal subduction. In: Martínez Catalán, J.R., Hatcher, R.D., Arenas, R., Díaz García, F. (Eds.), Variscan-Appalachian Dynamics: the Building of the Late Paleozoic Basement, Geological Society of America, Special Paper, 364, 105–122.10

Rubio Pascual FJ, Matas J, Martín Parra LM (2013a) High-pressure metamorphism in the Early Variscan subduction complex of the SW Iberian Massif. Tectonophysics 592: 187–199. https://doi.org/10.1016/j.tecto.2013.02.022

Rubio Pascual FJ, Arenas R, Martínez Catalán JR, Rodríguez Fernández LR, Wijbrans JR (2013b) Thickening and exhumation of the Variscan roots in the Iberian Central System: Tectonothermal processes and 40Ar/39Ar ages. Tectonophysics 587:207–221. https://doi.org/10.1016/j.tecto.2012.1010.005

Rubio Pascual FJ, López-Carmona A, Arenas R (2016) Thickening vs. extension in the Variscan belt: P–T modelling in the Central Iberian autochthon. Tectonophysics 681:144–158. https://doi.org/10.1016/j.tecto.2016.02.10033

Sánchez García MT, Bellido F, Quesada C (2003) Geodynamic setting and geochemical signatures of Cambrian-Ordovician rift-related igneous rocks (Ossa-Morena Zone, SW Iberia). Tectonophysics 365: 233–255

Sánchez Martínez, S (2009) Geoquímica y geocronología de las ofiolitas de Galicia. Laboratorio Xeolóxico de Laxe, Instituto

Universitario de Xeoloxía, A Coruña, Spain, Serie Nova Terra, 37, 351 pp
Sánchez Martínez S, Arenas R, Díaz García F, Martínez Catalán JR, Gómez-Barreiro J, Pearce JA (2007) Careón ophiolite, NW Spain: Suprasubduction zone setting for the youngest Rheic Ocean floor. Geology 35 (1):53–56. https://doi.org/10.1130/g23024a.1
Sánchez Martínez S, Gerdes A, Arenas R, Abati J (2012) The Bazar Ophiolite of NW Iberia: a relic of the Iapetus-Tornquist Ocean in the Variscan suture. Terra Nova, 24, 283–292.10
Santos Zalduegui JF, Schärer U, Gil Ibarguchi JI (1995) Isotope constraints on the age and origin of magmatism and metamorphism in the Malpica-Tuy allochthon, Galicia, NW Spain. Chemical Geology 121 (1):91–103. https://doi.org/10.1016/0009-2541(94)00123-p
Santos Zalduegui JF, Schärer U, Gil Ibarguchi JI, Girardeau J (1996) Origin and evolution of the Paleozoic Cabo Ortegal ultramafic-mafic complex (NW Spain): U–Pb, Rb–Sr and Pb–Pb isotope data. Chemical Geology 129 (3):281–302.10. https://doi.org/10.1016/0009-2541(95)00144-1
Sanz-López J, Perret MF, Vachard D (2006) Silurian to Mississipian series of the eastern Catalan Pyrenees (Spain), updated by conodonts, foraminifers and algae. Geobios 39: 709–725
Schäfer, H.J., Gebauer, D., Gil Ibarguchi, J.I., Peucat, J.J. 1993. Ion-microprobe U-Pb zircon dating on the HP/HT Cabo Ortegal Complex (Galicia, NW Spain): preliminary results. Terra Abstracts, 5, 4, 22.10
Schermerhorn LJG (1971) An outline stratigraphy of the Iberian Pyrite Belt. Boletín Geológico y Minero 82:239–268
Schermerhörn LJG, Stanton WI (1969) Folded overthrust at Aljustrel (South Portugal). Geological Magazine 106:130–141
Schermerhorn LJG, Kotsch S (1984) First occurrence of lawsonite in Portugal and tectonic implications. Comunicações do Instituto Geológico e Mineiro 70 (1):23–29
Schmelzbach C, Simancas JF, Juhlin C, Carbonell R (2008) Seismic reflection imaging over the South Portuguese Zone fold-and-thrust belt, SW Iberia. Journal of Geophysical Research 113, B08301. https://doi.org/10.1029/2007jb00534
Shaw J, Johnston ST, Gutiérrez-Alonso G, Weil AB (2012) Oroclines of the Variscan orogen of Iberia: Paleocurrent analysis and paleogeographic implications. Earth and Planetary Science Letters 329–330:60–70. https://doi.org/10.1016/j.epsl.2012.02.014
Shelley D, Bossière G (2000) A new model for the Hercynian Orogen of Gondwanan France and Iberia. Journal of Structural Geology 22: 757–776. https://doi.org/10.1016/s0191-8141(00)00007-9
Sierra S, Moreno C (2004) Cuenca Pérmica del Viar. In: Vera JA (ed), Geología de España. SGE-IGME, Madrid, 214–215
Silva JB, Oliveira JT, Ribeiro A (1990) The South Portuguese Zone. Structural Outline. In: Dallmeyer RD, Martínez E (eds), Pre-Mesozoic Geology of Iberia. Springer, Berlin, 334–362
Simancas JF (1983) Geología de la extremidad oriental de la Zona Sudportuguesa. PhD Thesis University of Granada, Spain
Simancas JF (1986) La deformación en el sector oriental de la Zona Sudportuguesa. Boletín Geológico y Minero 97:148–159
Simancas JF, Martínez Poyatos D, Expósito I, Azor A, González Lodeiro F (2001) The structure of a major suture zone in the SW Iberian Massif: the Ossa-Morena/Central Iberian contact. Tectonophysics 332: 295–308
Simancas JF, González Lodeiro F, Expósito I, Azor A, Martínez Poyatos D (2002) Oppsoite subduction polarities connected by transform faults in the Iberian Massif and western European Variscides. In: Martínez Catalán JR, Hatcher RD, Arenas R, Díaz García F (eds) Variscan-Appalachian dynamics: The building of the late Paleozoic basement. Geological Society America, Special Paper 364: 253–262
Simancas JF, Carbonell R, González Lodeiro F, Pérez-Estaún A, Juhlin C, Ayarza P, Kashubin A, Azor A, Martínez Poyatos D, Almodóvar GR, Pascual E, Sáez R, Expósito I (2003) The crustal structure of the transpresional Variscan Orogen of the SW Iberia: The IBERSEIS Deep Seismic Reflection Profile. Tectonics 22(6): 1062. https://doi.org/10.1029/2002tc001479
Simancas F, Expósito I, Azor A, Martínez Poyatos D, González Lodeiro F (2004) From the Cadomian orogenesis to the Early Paleozoic Variscan rifting in Southwest Iberia. Journal of Iberian Geology 30: 53–71
Simancas JF, Tahiri A, Azor A, González Lodeiro F, Martínez Poyatos D, El Hadi H (2005) The tectonic frame of the Variscan–Alleghanian orogen in Southern Europe and Northern Africa. Tectonophysics 398: 181–198. https://doi.org/10.1016/j.tecto.2005.02.006
Simancas JF, Carbonell R, González Loderio F, Pérez Estaún A, Juhin C, Ayarza P, Kashubien A, Azor A, Martínez Poyatos D, Sáez R, Almodóvar GR, Pascual E, Flecha I, Martí D (2006). Transpressional collision tectonics and mantle plume dynamics: the Variscides of southwestern Iberia. In: Gee DG, Stephenson RA (eds) European Lithosphere Dynamics, Geological Society, London, Memoirs, 32: 345–354
Simancas JF, Azor A, Martínez-Poyatos D, Tahiri A, El Hadi H, González-Lodeiro F, Pérez-Estaún A, Carbonell R (2009) Tectonic relationships of Southwest Iberia with the allochthons of Northwest Iberia and the Moroccan Variscides. Comptes Rendus Geoscience 341: 103–113. https://doi.org/10.1016/j.crte.2008.11.003
Simancas JF, Ayarza P, Azor A, Carbonell R, Martínez Poyatos D, Pérez-Estaún A, González Lodeiro F (2013) A seismic geotraverse across the Iberian Variscides: Orogenic shortening, collisional magmatism, and orocline development. Tectonics 32: 417–432. https://doi.org/10.1002/tect.20035
Simancas JF, Azor A, Martínez Poyatos DJ, Expósito I, Pérez-Cáceres I, González Lodeiro F (2016) Comment on "The Late Devonian Variscan suture of the Iberian Massif: A correlation of high-pressure belts in NW and SW Iberia. Tectonophysics 654, 96–100" by R. Fernández and R. Arenas. Tectonophysics 666: 281–284. https://doi.org/10.1016/j.tecto.2015.07.040
Soriano C, Casas JM (2002) Variscan tectonics in the Iberian Pyrite Belt, South Portuguese Zone. International Journal of Earth Sciences.91:882–896. https://doi.org/10.1007/s00531-001-0253-8
Speksnijder A (1986) Geological analysis of Paleozoic large-scale faulting in the south-central Pyrenees. Geologica Ultraiectina: 43
Talavera C, Martínez Poyatos D, González Lodeiro F (2015) SHRIMP U–Pb geochronological constraints on the timing of the intra-Alcudian (Cadomian) angular unconformity in the Central Iberian Zone (Iberian Massif, Spain). International Journal of Earth Sciences 104:1739–1757. https://doi.org/10.1007/s00531-015-1171-5
Thiéblemont D, Pascual E, Stein G (1998) Magmatism in the Iberian Pyrite Belt: petrological constraints on a metallogenic model. Mineralium Deposita 33:98–110
Trias S, Martín-Closas C, Casas JM (2014) New palaeobotanical data in the Lower Carboniferous of the Eastern Pyrenees: Implication for the aging of the Variscan deformation. Résumés de la 24e Réunion des Sciences de la Terre: 187–188
Valenzuela A, Donaire, T, Pin C, Toscano M, Hamilton MA, Pascual E (2011) Geochemistry and U-Pb dating of felsic volcanic rocks in the Riotinto-Nerva unit, Iberian Pyrite Belt, Spain: crustal thinning, progressive melting and massive sulphide genesis. Journal of the Geological Society, London, 168:717–731. https://doi.org/10.1144/0016-76492010-081
Valle Aguado B, Azevedo MR, Schaltegger U, Martínez Catalán JR, Nolan J (2005) U-Pb zircon and monazite geochronology of Variscan magmatism related to syn-convergence extension in Central Northern Portugal. Lithos 82 (1–2):169–184. https://doi.org/10.1016/j.lithos.2004.12.012

Van Calsteren PWC, Boelrijk NAIM, Hebeda EH, Priem HNA, Den Tex E, Verdurmen EAT, Verschure RH (1979) Isotopic dating of older elements (including the Cabo Ortegal mafic-ultramafic complex) in the Hercynian orogen of NW Spain: Manifestations of a presumed Early Paleozoic mantle-plume. Chemical Geology 24 (1):35–56. https://doi.org/10.1016/0009-2541(79)90011-1

Vauchez A (1975) Tectoniques tangeantielles superposées dans la segment hercynien Sud-bérique: Les nappes et plis couchés de la region d'Alconchel-Fregenal de la Sierra (Badajoz). Boletín Geológico y Minero 86: 573–580

Vergés J (1983) Estudio del complejo vulcano-sedimentario del Devónico y de la estructura de la terminación oriental del sinclinal de Almadén (Ciudad Real). In: Geología de España, Libro Jubilar JM Ríos, IGME, Madrid, 3: 215–229

Vogel, DE (1967) Petrology of an eclogite -and pyrigarnite- bearing polymetamorphic rock Complex at Cabo Ortegal, NW Spain. Leidse Geologische Mededelingen, 40, 121–213

Weil AB, van der Voo R, van der Pluijm BA, Parés JM (2000) The formation of an orocline by multiphase deformation: a paleomagnetic investigation of the Cantabria–Asturias Arc (northern Spain). Journal of Structural Geology 22: 735–756. https://doi.org/10.1016/s0191-8141(99)00188-1

Weil AB, Van der Voo R, Van der Plujim BA (2001) Oroclinal bending and evidence against the Pangea megashear: The Cantabria-Asturias arc (northern Spain). Geology 29 (11):991–994. doi: https://doi.org/10.1130/0091-7613(2001)029<0991:obaeat>2.0.co;2

Weil AB, Gutiérrez-Alonso G, Conan J (2010) New time constraints on lithospheric-scale oroclinal bending of the Ibero-Armorican Arc: a palaeomagnetic study of earliest Permian rocks from Iberia. Journal of the Geological Society 167:127–145. https://doi.org/10.1144/0016-76492009-002

Weil AB, Gutiérrez-Alonso G, Johnston ST, Pastor-Galán D (2013) Kinematic constraints on buckling a lithospheric-scale orocline along the northern margin of Gondwana: A geologic synthesis. Tectonophysics 582:25–49. https://doi.org/10.1016/j.tecto.2012.10.006

Synorogenic Basins

11

J. T. Oliveira, E. González-Clavijo, J. Alonso, M. Armendáriz, J. R. Bahamonde, J. A. Braid, J. R. Colmenero, Í. Dias da Silva, P. Fernandes, L. P. Fernández, V. Gabaldón, R. S. Jorge, Gil Machado, A. Marcos, Óscar Merino-Tomé, N. Moreira, J. Brendan Murphy, A. Pinto de Jesus, C. Quesada, B. Rodrigues, I. Rosales, J. Sanz-López, A. Suárez, E. Villa, J. M. Piçarra, and Z. Pereira

Abstract

Synorogenic basins formed in all lithospheric units involved in the Variscan orogeny, i.e. the Gondwanan and Laurussian continental margins and also in the oceanic realm. However, examples of the latter are only preserved in SW Iberia. On the other hand, synorogenic deposits of the Gondwanan foreland are only preserved in NW Iberia, whereas remains of both continental margins exist in SW Iberia. Record of Variscan synorogenic basins also exists in basement exposures within the

Coordinators: J. T. Oliveira and E. González-Clavijo.

J. T. Oliveira (✉) · J. M. Piçarra · Z. Pereira
Laboratório Nacional de Energia e Geologia (LNEG), 2610-999 Amadora, Portugal
e-mail: joetomas.oliveira@gmail.com; tomas.oliveira@lneg.pt

J. M. Piçarra
e-mail: jose.picarra@lneg.pt

Z. Pereira
LNEG. Laboratório Nacional de Energia e Geologia, Ap. 1089.4466-S., Mamede Infesta, Portugal
e-mail: zelia.pereira@lneg.pt

E. González-Clavijo
Instituto Geológico y Minero de España-Unidad de Salamanca, Azafranal 48, 1º A., 37001 Salamanca, Spain
e-mail: e.clavijo@igme.es

J. L. Alonso · J. R. Bahamonde · L. P. Fernández · A. Marcos · Ó. Merino-Tomé · J. Sanz-López · E. Villa
Departamento de Geología, Universidad de Oviedo, C/Arias de Velasco s/n, 33005 Oviedo, Spain
e-mail: jlalonso@geol.uniovi.es

J. R. Bahamonde
e-mail: jrbaham@geol.uniovi.es

L. P. Fernández
e-mail: lpedro@geol.uniovi.es

A. Marcos
e-mail: marcos@geol.uniovi.es

Ó. Merino-Tomé
e-mail: omerino@geol.uniovi.es

J. Sanz-López
e-mail: sanzjavier@uniovi.es

E. Villa
e-mail: evilla@geol.uniovi.es

M. Armendáriz · V. Gabaldón · C. Quesada · I. Rosales
Instituto Geológico y Minero de España, Ríos Rosas 23, 28003 Madrid, Spain
e-mail: maiderad@gmail.com

V. Gabaldón
e-mail: vicente.gabaldon@gmail.com

C. Quesada
e-mail: quesada.cecilio@gmail.com

I. Rosales
e-mail: i.rosales@igme.es

J. A. Braid · J. Brendan Murphy
Department of Earth Sciences, Saint Francis Xavier University, B2G 2W5 Antigonish, NS, Canada
e-mail: jbraid@stfx.ca

J. Brendan Murphy
e-mail: bmurphy@stfx.ca

J. R. Colmenero
Departamento de Geología, Universidad de Salamanca, Plaza/La Merced s/n, 37008 Salamanca, Spain
e-mail: colme@usal.es

Í. D. da Silva · R. S. Jorge
Faculdade de Ciências, Instituto Dom Luiz, Universidade de Lisboa, Campo Grande, Ed. C8, 1749-016 Lisbon, Portugal
e-mail: ipicaparopo@gmail.com

R. S. Jorge
e-mail: rjorge@fc.ul.pt

C. Quesada and J. T. Oliveira (eds.), *The Geology of Iberia: A Geodynamic Approach*, Regional Geology Reviews,
https://doi.org/10.1007/978-3-030-10519-8_11

Alpine realm that occupies the eastern half of the Iberian Peninsula and the Balearic Islands. These, which are less known and in some cases of uncertain affinities, are described in a separate section.

11.1 Introduction

J. T. Oliveira, E. González-Clavijo

The onset and subsequent evolution of the Variscan orogeny gave rise to the formation of synorogenic basins that recorded the response of the involved lithospheric units to the new conditions. As repeatedly stated in previous sections, the Variscan orogeny was the result of the closure of the Rheic Ocean during the late Palaeozoic, which led to the collision of the continents Laurussia and Gondwana that culminated the amalgamation of the supercontinent Pangea. In Iberia, evidence of the oceanic suture zone is exposed in both the NW and SW segments of the Variscan orogen, with highly contrasting characteristics: far-travelled nappe pile in the NW versus strongly transpressive in the SW Iberian Massif. In response to such contrast in tectonic regimes, the conditions under which synorogenic basins developed vary significantly from one orogenic segment to the other, thence the convenience to deal with them separately.

Synorogenic basins formed in all lithospheric units involved, i.e. the Gondwanan and Laurussian continental margins and also in the oceanic realm. However, examples of the latter are only preserved in SW Iberia. On the other hand, synorogenic deposits are only preserved in the Gondwanan foreland in NW Iberia, whereas they are preserved on both continental margins in SW Iberia.

Record of Variscan synorogenic basins also exist in basement exposures within the Alpine realm which that occupies the eastern half of the Iberian Peninsula and the Balearic Islands. These, which were probably located far away from the hinterland of the Variscan orogen sensu stricto, i.e. the continent-continent collision of the two continental margins facing the Rheic Ocean, are thought to pertain to the area of influence of the Paleotethys margin of Gondwana and are described in a separate section. However, our current knowledge of the Carboniferous synorogenic strata of the Pyrenees shows that the of the synorogenic successions are closely linked with those of the foreland basin developed during the Variscan orogeny above the continental margin of Gondwana and facing the growing Variscan orogen. As J. Sanz indicates in chap. 11.4 (and previous contributions of this author and others), there are striking similarities in the stratigraphy of those successions and the synorogenic strata of the Cantabrian Zone in NW Spain.

P. Fernandes · B. Rodrigues
CIMA - Centro de Investigação Marinha e Ambiental, Universidade do Algarve, 8005-139 Faro, Portugal
e-mail: pfernandes@ualg.pt

B. Rodrigues
e-mail: bmrodrigues@sapo.pt

G. Machado
Galp Exploração e Produção, R. Tomás da Fonseca, Torre A, 10º Piso, 1600-209 Lisbon, Portugal
e-mail: machadogil@gmail.com

N. Moreira
Laboratório de Investigação de Rochas Industriais e Ornamentais (LIRIO), University of Évora, Estremoz Pole, Convento das Maltezas, 7100-513 Estremoz, Portugal
e-mail: geo.noel.87@gmail.com

N. Moreira
Earth Sciences Institute (ICT), Pole of the University of Évora, Rua Romão Ramalho, nº 59, 7000-671 Évora, Portugal

A. Pinto de Jesus
Departamento de Geociências, Ambiente e Ordenamento do Território, University of Porto, Rua Campo Alegre 687, 4169-007 Porto, Portugal
e-mail: arypintojesus@gmail.com

A. Súarez
Instituto Geológico y Minero de España-Unidad de León, Avda. La Real, 24006 León, Spain
e-mail: a.suarez@igme.es

11.2 Synorogenic Basins in the NW Iberia Variscan Orogen

11.2.1 Foreland Basin at the Galicia Trás-os-Montes—Central Iberian Zones Limit: Culm-Type and Flyschoid Sequences Enclosing Olistostromes

E. González-Clavijo, Í. Dias da Silva

At the NW Central Iberian Zone (CIZ) around the allochthonous Galicia-Trás-os-Montes Zone (GTMZ), some Variscan synorogenic units crop out preserved in different structural positions, which contribute to preserve this type of sediments in this deeply eroded part of the orogenic belt (Martínez Catalán et al. 2008). The structures holding these sedimentary deposits are of two types: (i) the core of late Variscan synclines (C3), as in the Sil Synform (Fig. 11.1A) and the Valongo area (Fig. 11.1B); and (ii) in an intervening structural unit between the allochthonous GTMZ and the autochthonous CIZ known as the Parautochthon (PA), which is a set of imbricated horses stacked during the earlier Variscan events, as it is observed around the Bragança and Morais allochthonous complexes (Fig. 11.1C).

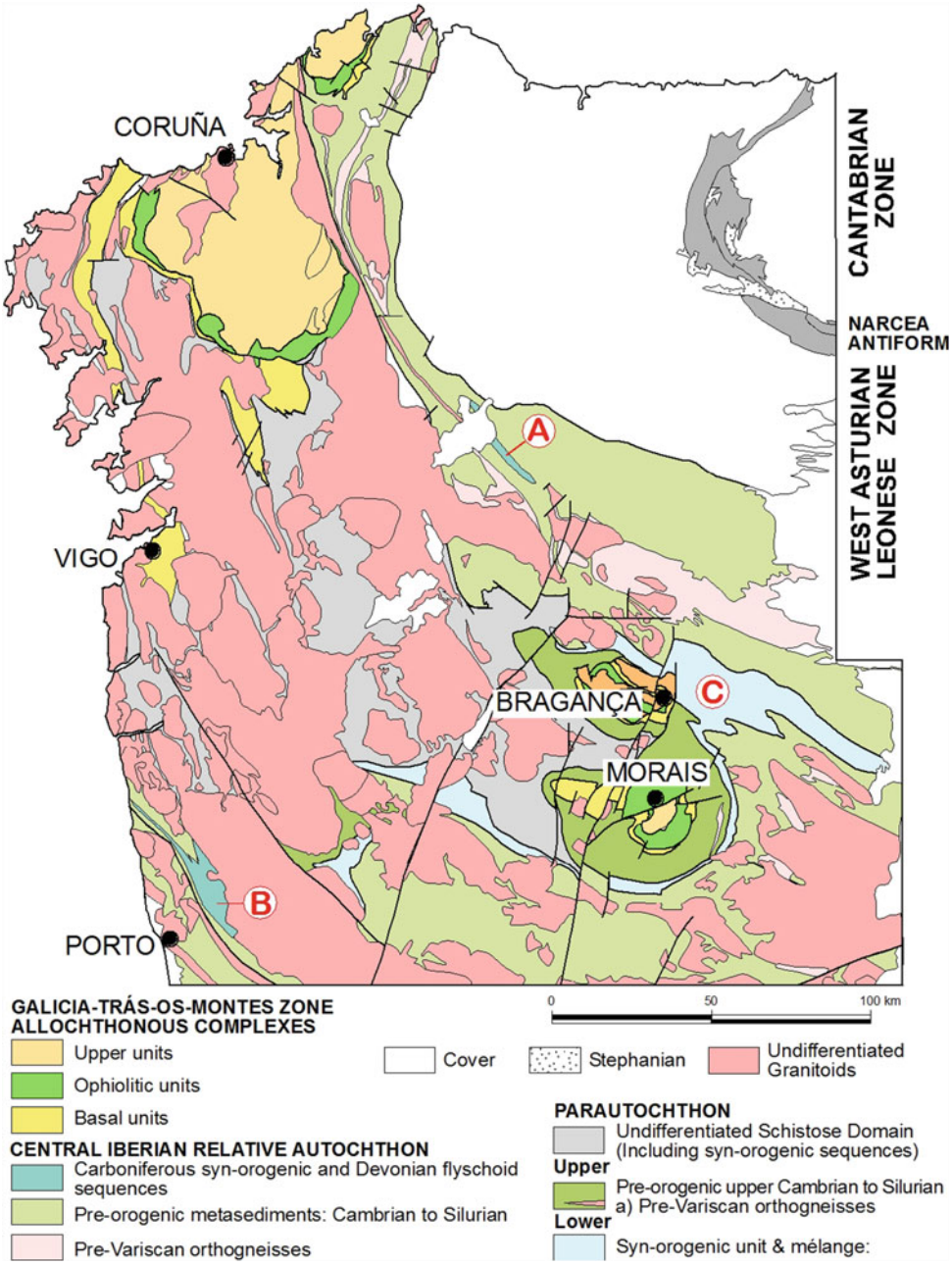

Fig. 11.1 Simplified map of NW Iberia enclosing the Central Iberian and Galicia Tras-os-Montes Variscan zones boundary and the stratigraphic sequences considered synorogenic in the region. **A** and **B** Late Variscan synclines on CIZ; **C** lower Parautochthon tectonic slice

These lithostratigraphic units were traditionally considered of Silurian–Devonian age on base of fossil findings (Martínez García 1972; Teixeira and Pais 1973; Aldaya et al. 1976; Moro Benito 1980; Quiroga 1980; Truyols-Massoni and Quiroga 1981; Sarmiento et al. 1997; González Clavijo et al. 1997; Piçarra et al. 2006) and palynomorphs (Pereira et al. 1999a, 2000; Pereira 2006; Pereira and Oliveira, 2003a). The stratigraphic sequence preserved in the Sil synform (San Clodio Fm) was, however, considered of turbiditic nature and Carboniferous age since Riemer (1963, 1966) works. New studies on detrital zircon ages of the synorogenic sequences have constrained the ages as Carboniferous (Martínez Catalán et al. 2016, and references therein). Consequently, the flora and fauna findings must be interpreted as inherited from the source area.

11.2.1.1 Synorogenic Sequence Characteristics

These synorogenic metasediments, both authenticated and postulated, are known under diverse lithostratigraphic names. A synthetic relation is shown on Table 11.1, displaying the main sedimentary characteristics and the referenced age. All the sequences considered display sedimentary characteristics resembling the European Culm facies.

1. In the synorogenic parautochthon (PA) (Fig. 11.1C) variable size blocks (up to several hundred meters long) entering the basin from the directly overridden nappe have been described around the Bragança and Morais Allochthonous Complexes (Martínez García 1972; Aldaya et al. 1973, 1976; Ribeiro and Ribeiro 1974; Dias da Silva et al. 2014; González Clavijo et al. 2016).

Table 11.1 Lithostratigraphic units bearing synorogenic sedimentary characteristics in the NW Iberia. Number code indicates the age determination method. Data from: Da Silva Domingo (2004); Dias da Silva et al. (2015a); LNEG (2010); Meireles (2013); Martínez Catalán et al. (2004); Martínez Catalán et al. (2008); Martínez Catalán et al. (2016); Pereira (2006); Piçarra and Rebelo (1997); Pereira et al. (1999a); Ribeiro and Ribeiro (1974); Romariz (1969)

Autochthon (CIZ)		Lower Parautochthon (GTMZ)				
San Clodio	Telheiras Sobrado	Mouquim Canadelo	Santos Curros	Casal do Rato	Meirinhos	Vila Chã
Turbiditic pelites and graywackes, minor lidites at the base and thin coal seams	Flyschoid phyllites and metagraywackes	Phyllites, metasiltites and metagraywackes, upper levels of tuffites	Turbiditic phyllites and metagraywackes	Turbiditic phyllites, siltites and metagraywackes	Layered and black schists, quartzwackes; olistoliths and slumps	phyllites and metagraywackes with lidites and quartzites
Pennsylvanian[1]	Middle-Upper Devonian[2]	Lower Devonian[4]	Lower Devonian[4]	Lower Devonian[4]	Llandovery-Wenlock[2]	Carboniferous[1]
Chronostratigraphy determination by: 1. Detrital zircon 2. Fossils 3. Palynomorphs 4. Stratigraphic position		Travanca	Gimonde	Rabano	San Vitero	Almendra
		Flyschoid phyllites and metagraywackes olistoliths	Flyschoid phyllites and metagraywackes, wild-flysch	Turbiditic phyllites and metagraywackes, olistoliths	Turbiditic phyllites and graywackes, conglomerates, slumps	Turbiditic phyllites and calcarenites, conglomerates
		Middle Devonian or younger[1]	Upper Devonian Carboniferous[1–3]	Visean or younger[1]	Tournaisian or younger[1]	Visean or younger[1]

Accordingly, a major division of facies can be envisaged: (i) a bedded flyschoid sequence witnessing for continent-continent foredeep turbiditic succession deposited in a low-slope environment (González Clavijo 2006); and (ii) block-in-matrix discontinuous bodies (olistostromes in Fig. 11.2) placed in diverse locations and representing varied scenarios. Some are precursory olistostromes (Festa et al. 2016) emplaced by cohesive debris-flows and/or block avalanches in migrating foredeep basins (Fig. 11.2), which recorded depositional deactivation and formed before the advance of the thrust-related deformation following incorporation of the synorogenic sequence to the collisional belt.

Another type corresponds to olistostromal carpets (Pini et al. 2004), which consists of coalescing aprons formed by debris flows and avalanches in front of an advancing nappe, subsequently overridden by the allochthonous units during the orogenic progression (Fig. 11.2).

11.2.1.2 Sedimentation and Thrust Tectonics Interplay

The second compressive event (C2) of the general Variscan orogenic frame in NW Iberia is related to formation of thrust structures (González Clavijo and Martínez Catalán 2002). C2 deformation and related thermal events are diachronic, being older in the GTMZ and progressively younger to the

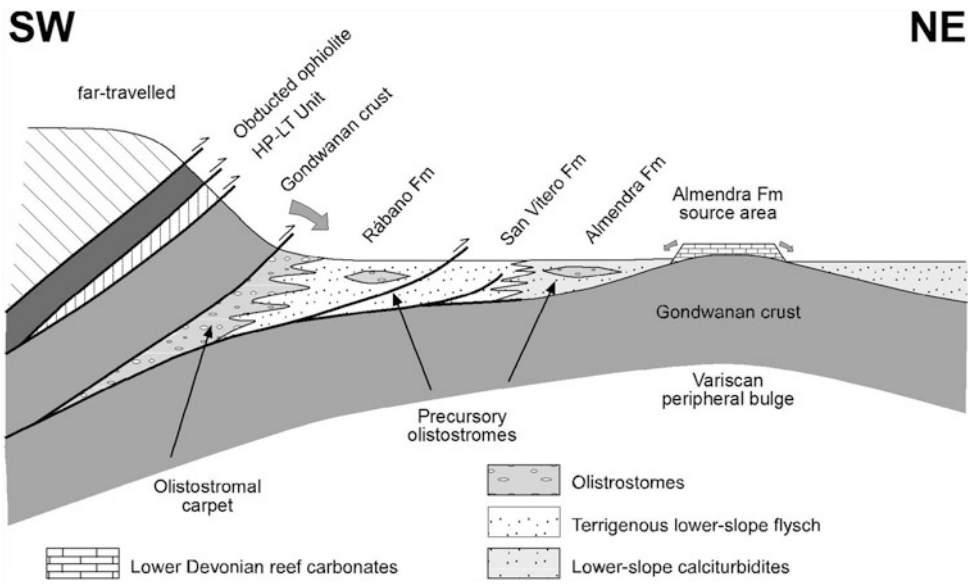

Fig. 11.2 Sketch of the Variscan foredeep basin and thrusting evolution during Tournaisian–Visean times. The erosion of the forebulge reef carbonates and the formation of calciturbidites inside the basin (Almendra Fm.) are shown

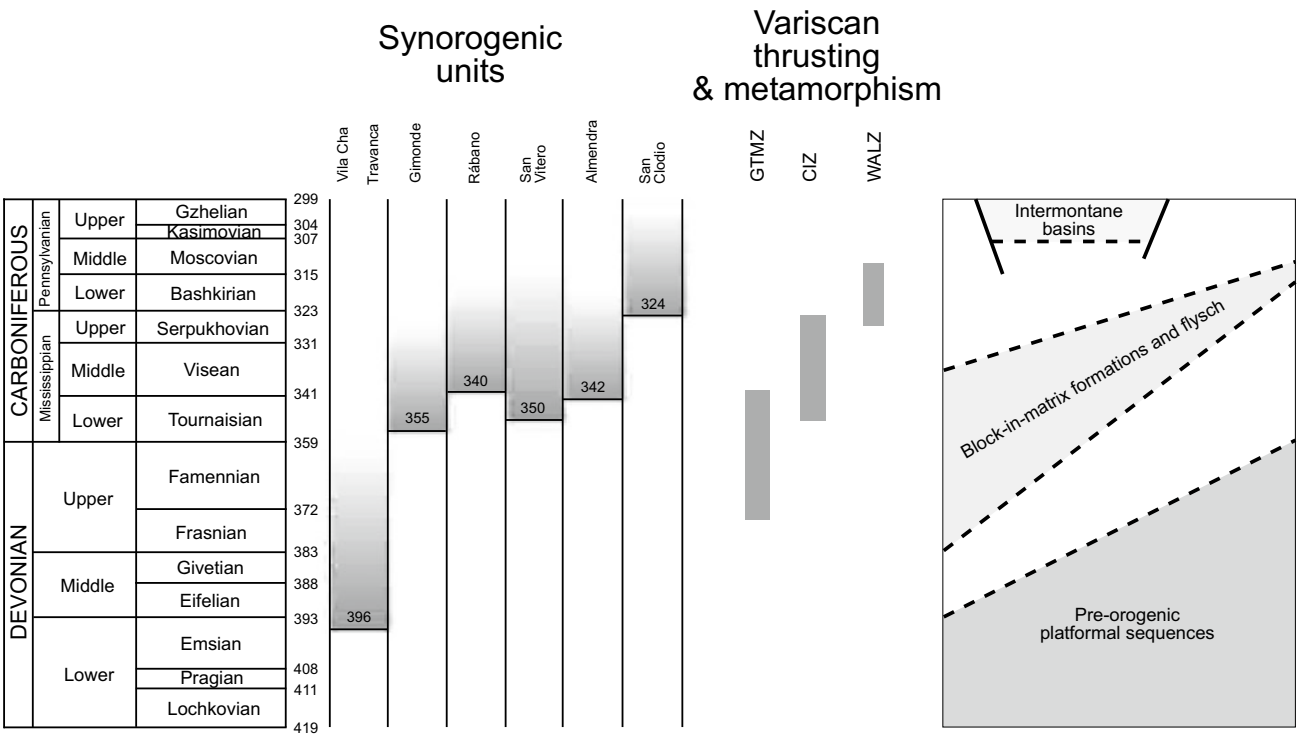

Fig. 11.3 Chronographic correlation of the NW Iberia Variscan synorogenic units and the early Variscan thrusting. Ages from Dias da Silva et al. (2015a), Martínez Catalán et al. (2016) and Dallmeyer et al. (1997)

CIZ and West Asturian-Leonese Zone (WALZ) (Dallmeyer et al. 1997); producing radiometric ages which are almost coeval to sedimentation of the flyschoid sequences ages (Fig. 11.3). This synchronicity upholds the genetic relationship between advance of the Variscan deformation front and the flyschoid sedimentation in the foredeep trough. The underlying structural units yield progressively younger ages thus supporting the migration of the synorogenic basin depocentre towards the foreland mirroring the orogenic-front advance. Consecutive synorogenic wedges were incorporated to the Variscan belt by thrusting between them, and incorporated onto the pre-orogenic passive margin sequences by a basal detachment (Fig. 11.2).

The detached lowermost structural unit displays special characteristics as its stratigraphic sequence is made of calciturbidites (Almendra Fm) of Visean or younger age according to its detrital zircon record (Martínez Catalán et al. 2008), but containing Lower Devonian fossils and coral fragments in the limestones (Sarmiento et al. 1997; González Clavijo 2006). The source area for this unit remains unknown, since Devonian carbonates do not crop out in the northern CIZ. The most likely explanation is to postulate a reefal limestone platform on top of the peripheral bulge (Fig. 11.2), subsequently eroded and redeposited in the basin during the orogenic progression and displacement of the bulge towards the foreland. Similar erosive processes of the forebulge have been considered to explain the erosion of the pre-orogenic CIZ sequence in the Sil synform area, where the synorogenic San Clodio Fm. lies on top of the reverse limb of a major early Variscan (C1) recumbent fold developed in the pre-orogenic unit (Martínez Catalán et al. 2016).

The youngest zircon ages support that thrusting and related sedimentation occurred during the Mississippian, with a maximum in the Tournaisian–Visean (355–350 Ma) at the internal imbricates and a minimum at Serpukhovian time (323 Ma) in the most external areas (Sil synform; Martínez Catalán et al. 2016).

11.2.1.3 Detrital Zircon Studies and Provenance Areas

Detrital zircon population studies on some of the Variscan synorogenic sequences allow unravelling the source areas for these low-grade meta-sediments. Zircon populations in the synorogenic sequences have been compared to the gathered on the superimposed allochthons (GTMZ) and the underlying autochthon (CIZ) by Martínez Catalán et al. (2016) and Dias da Silva et al. (2015a). The comparison shows that the allochthons (active orogenic margin) were the dominant source of detritus, on basis of: (i) the scarcity of Mesoproterozoic and Tonian zircons; (ii) the relative

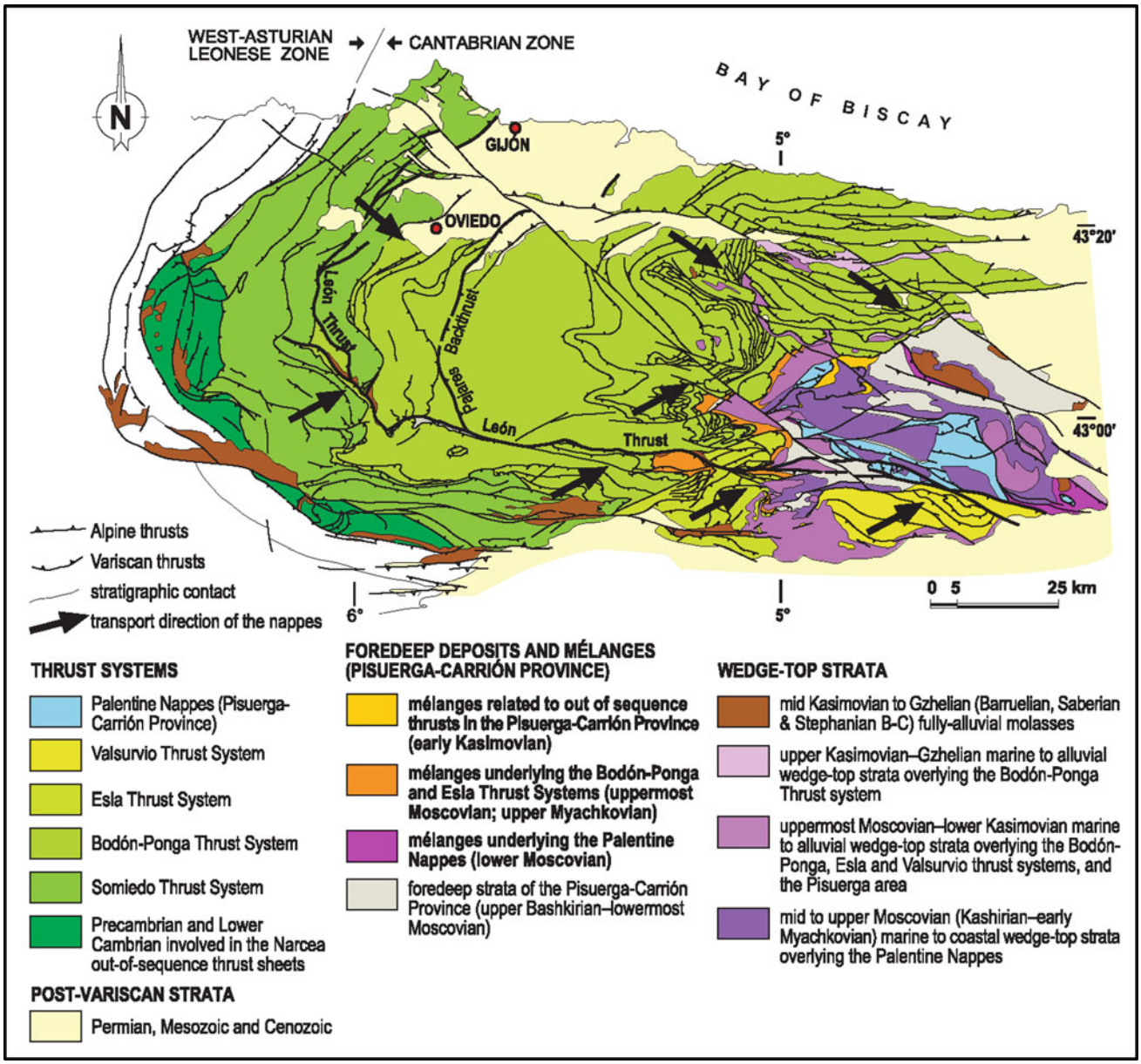

Fig. 11.4 Structural sketch and division of the Cantabrian Zone into geological domains (Alonso et al. 2009), showing location of the mélanges (Alonso et al. 2015). Arrows indicate the transport direction of the thrusts after Arboleya (1981), Bastida et al. (1984), Alonso (1987a), Alonso et al. (1989), Alvarez Marrón (1989), Heredia (1991), Bulnes and Marcos (1994) and own data. Mélanges underlying the Palentine nappes, Esla and Bodón-Ponga thrust systems and wedge-top successions are indicated

abundance of Paleozoic pre-Variscan populations, which points to sedimentary provenance from nearby, poorly recycled areas; and (iii) the existence of early-Variscan and Variscan zircons. However, the above proposed erosion and incorporation of sediments from the Variscan peripheral bulge to the trough flysch-type deposits backs some additional input from the uplifted passive margin (CIZ).

Provenance indicated by zircon populations suggests source from, with contributions from the West Africa craton, the Saharan metacraton (or Hoggar megasuture), the Trans-Saharan fold belt, and probably the Arabian-Nubian shield (Gómez Barreiro et al. 2007; Bea et al. 2010; Díez Fernández et al. 2010; Drost et al. 2011; Fernández-Suárez et al. 2014). Far-travelled clastic sediments from terranes exposed to the south of the Arabian craton and Arabian-Nubian shield, like the East Africa orogen, are included by Shaw et al. (2014) and Dias da Silva et al. (2015b) following Meinhold et al. (2011) and

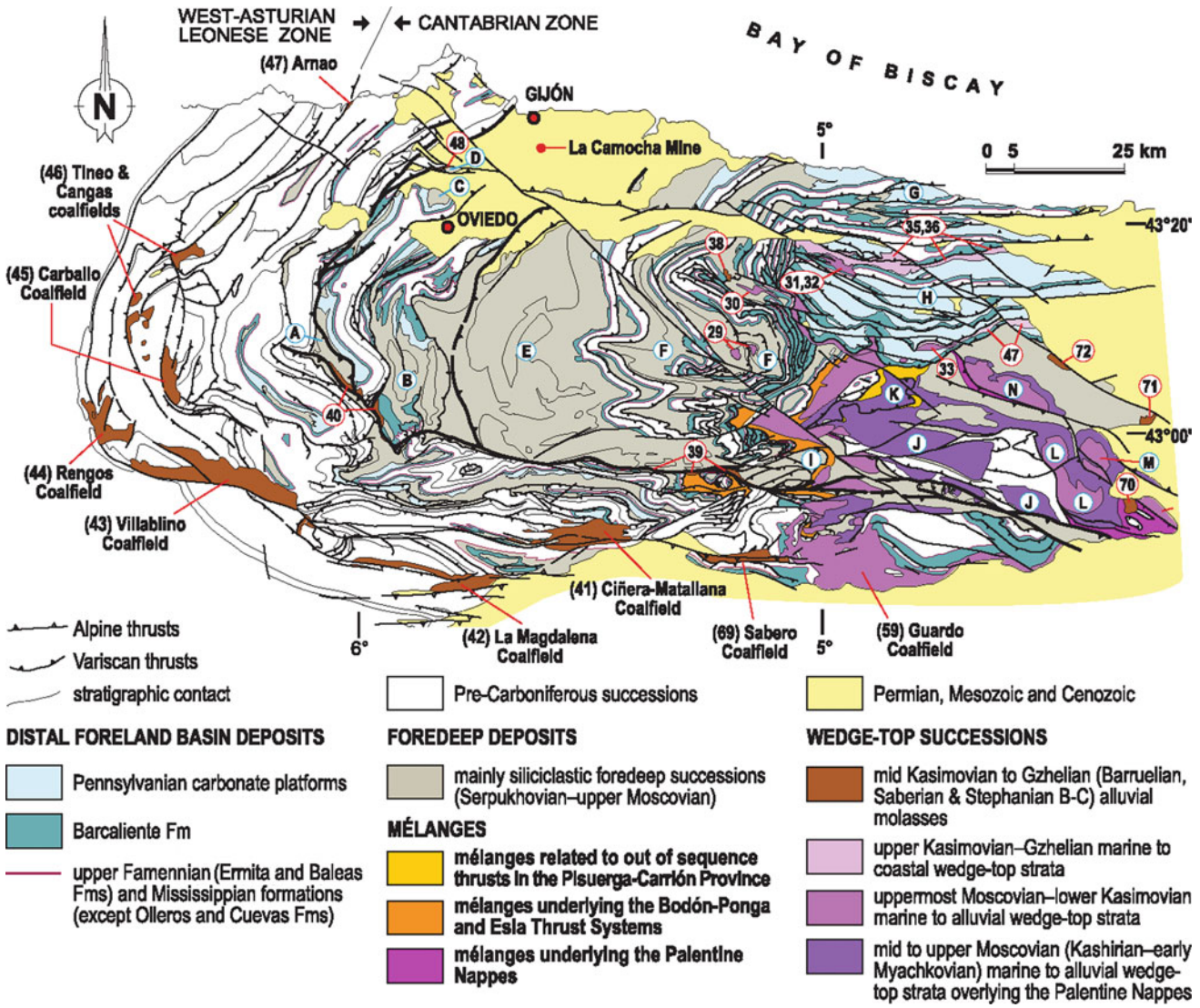

Fig. 11.5 Schematic geological map of the CZ showing the distribution of Carboniferous successions (modified from Alonso et al. 2015). The location of the main coalfields and stratigraphic successions mentioned in the text and in Fig. 11.5 are indicated. A. Teverga; B. Quirós; C. Naranco syncline; D. Santo Firme; E. Central Asturian coalfield; F. Ponga nappe; G. Cuera area; H. Picos de Europa area; I. Lois-Ciguera area; J. Lechada syncline; K. Coriscao syncline; L. Casavegas-Castillería syncline; M. Redondo syncline; N. Central Liébana-Viorna syncline; 29. San Juan de Beleño and Tiaordos peak; 30. Sebarga; 31. Gamonedo Fm.; 32. Demúes Fm.; 33. Las Llacerias Fm.; 34. Áliva Fm. and equivalents; 35. Puentellés Fm.; 36. Cavandi Fm.; 37. Lebeña Fm.; 38. Fontecha succession; 39. Canseco-Rucayo succession; 40. Puerto Ventana succession; 41. Ciñera-Matallana coalfield succession; 42. La Magdalena coalfield succession; 43. Villablino coalfield succession; 44. Rengos coalfield succession; 45. Carballo coalfield succession; 46. Tineo and Cangas coalfield succession; 47. Arnao coalfield succession; 48. Ferroñes; 59. Guardo coalfield succession; 69. Sabero coalfield succession; 70. Peña Cildá succession; 71. Pico Cordel succession; 72. Puente Pumar succession

Meinhold et al. (2013) on a superfan proposal, which allows a detrital provenance from very remote zones of Gondwana.

The synorogenic deposits at the GTMZ-CIZ edge create an intervening structural unit under the Morais and Bragança complexes, later folded by the late Variscan deformation events. This structural unit (PA) is the lowest and youngest imbricate of the stack of nappes that constitutes the allochthonous GTMZ (Ries and Shackleton 1971; Ribeiro 1974; Schermerhorn and Kotsch 1984), and it mimics, inside itself, the general piggy-back structure, incorporating the more external and younger synorogenic sequences into the lower slices. On this basis we consider that they record the early Variscan thrust progression onto the Gondwana (lower plate) passive margin leading to the closure of a foredeep basin in a continent-continent collision.

11.2.2 Foreland Basin at the Cantabrian Zone: Evolution from the Distal Foreland Basin Successions to Wedge-Top Deposition and the Tightening of the Ibero-Armorican Arc

O. Merino-Tomé, J. L. Alonso, J. R. Bahamonde, L. P. Fernández, A. Marcos, J. R. Colmenero, E. Villa, A. Suárez

The Cantabrian Zone (CZ) is the external domain of the Variscan Orogen in the NW Iberian Peninsula (Lotze 1945) and it is characterized by thin-skinned tectonics (De Sitter 1962; Julivert 1971; Pérez-Estaún et al. 1988; Alonso et al. 2009, 2015). It is constituted by several major thrust systems (Somiedo, Bodón-Ponga and Esla thrust systems) that were emplaced after the Palentine nappes of the Pisuerga-Carrión province (Alonso et al. 2009) (Fig. 11.4). These thrust systems comprise both pre-orogenic Cambrian to Upper Devonian strata and synorogenic upper Famennian (uppermost Devonian) to Upper Pennsylvanian successions. The latter accumulated in the distalmost part of a very broad marine foreland basin developed on the Gondwana lithosphere during the Variscan Orogeny (Julivert 1978; Marcos and Pulgar 1982; Águeda et al. 1991; Bahamonde et al. 2015).

11.2.2.1 Synorogenic Successions of the CZ

The stratigraphy of the upper Famennian-Carboniferous synorogenic successions is synthesized in Colmenero et al. (2002), Sánchez de Posada et al. (2002) and Fernández et al. (2004). In the Somiedo, Bondón-Ponga, Esla and Valsurvio units these successions rest above a low-angle unconformity of latest Devonian age, which has been interpreted as the result of erosion of the migrating peripheral bulge of the basin by Keller et al. (2007). Nevertheless, this unconformity has not being recognized in the Palentine nappes of the Pisuerga-Carrión unit. The synorogenic successions fit the classical flysch-to-molasse evolution described in foreland basins and their strata can be classified into five main groups according to their location within the foreland basin system following the terminology used by DeCelles and Giles (1996) (see Fig. 11.5): (a) distal (foreland margin) strata; (b) foredeep infill, comprising from deep-water turbiditic successions to shallow-water–alluvial deposits; (c) mélanges, which appear as carpets beneath or ahead of submarine thrust systems; (d) unconformable successions accumulated on top of advancing thrust nappes and representing wedge-top successions, including the youngest fully alluvial successions. The first two groups are best represented in the Somiedo, Bodón-Ponga, Esla and Valsurvio units. Mélanges occur exclusively in the Pisuerga-Carrión unit. Marine to coastal wedge-top successions characterize the frontal part of the Bodón-Ponga and Esla thrust systems and the Palentine nappes of the Pisuerga-Carrión province. Finally, Stephanian (Kasimovian and Gzhelian) alluvial molasses occur on the Pisuerga-Carrión, Esla, Somiedo and Bondón-Ponga units of the CZ as well as in the adjacent WALZ.

11.2.2.2 Distal (Foreland Margin) Strata of the Somiedo, Bodón-Ponga, Esla and Valsurvio Units

The synorogenic successions commence with uppermost Famennian and Mississippian marine sediments with a very broad distribution that accumulated in the distal areas of the basin (Sánz-López et al. 2007). From base to top, this succession comprises conglomerates and sandstones (Ermita Fm), crinoidal grainstones embracing the Devonian-Carboniferous boundary (Baleas Fm), black shales (Vegamián Fm), red nodular limestones, radiolarites and black laminated calci-mudstones, red shales and marlstones (Alba Fm) (Comte 1959; Van Adrichem Boogaert 1967; Wagner et al. 1971; Kullmann et al. 1977; Reüther 1977; Wendt and Aigner 1985; Sanz-López 2004; Sanz-López and Blanco-Ferrera 2012a) (Fig. 11.6). Overlying the Alba Fm., the Barcaliente Fm. (Wagner et al. 1971) consists of black laminated calci-mudstones reaching some 150–350 m in thickness (Figs. 11.6 and 11.7) embracing the Mississipian–Pennsylvanian boundary (Sánz-López and Blanco-Ferrera 2013).

At the top of the Barcaliente Fm., the Valdeteja and Picos de Europa Fms represent microbial carbonate platforms developed locally in the basin that were progressively buried by terrigenous sediments sourced from the hinterland (corresponding to the foredeep infill successions). The age of these carbonate platforms range from the early-late Bashkirian, in the areas located closer to the orogen, to the early Kasimovian in the Picos the Europa area, which represents the distalmost preserved areas of the basin (Fig. 11.6). They have been studied and described in detail in the southern branch of the CZ (Eichmüller 1985; Chesnel et al. 2016a, b), in the Sierra del Cuera and Picos de Europa (Bahamonde et al. 1997a, b, 2000, 2004, 2007, 2008; Della Porta et al. 2002a, b, 2003, 2004; Kenter et al. 2003; Van der Kooij et al. 2007) and in the Sierra del Sueve (Bahamonde et al. 2014). Synchronously with the development of these carbonate platforms, in the surrounding basinal settings, pelagic limestone strata and condensed red shales, including locally manganese nodules, accumulated in the surrounding basinal settings during Bashkirian times. These pelagic limestones have been assigned either to the Barcaliente Fm. (Señares Mb; Sánz-López and Blanco-Ferrera 2012b) or to the Ricacabiello Fm., the latter also comprises the overlying condensed red shales (Sjerp 1967; Eichmüller 1985) (Fig. 11.6).

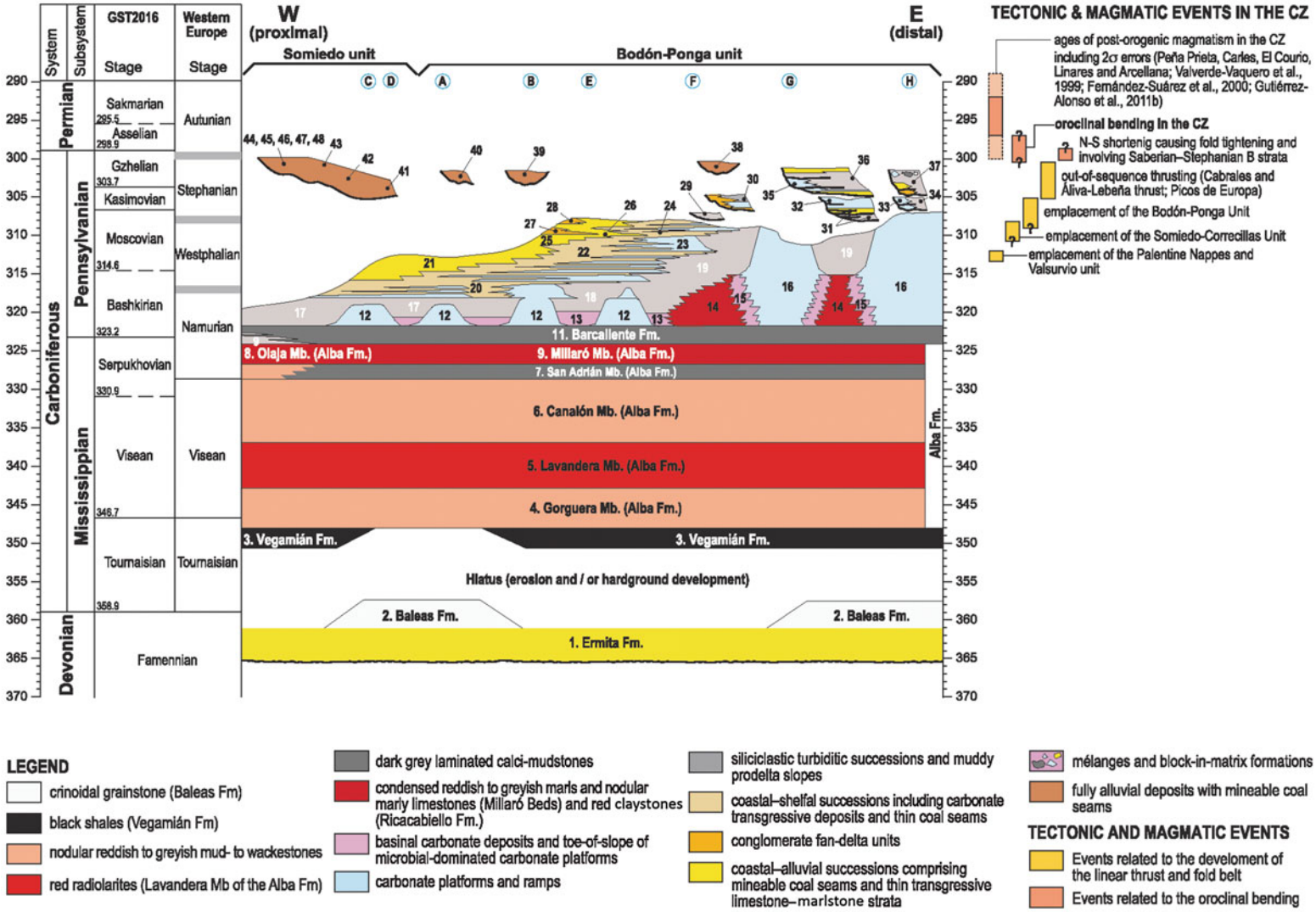
System
Subsystem
GST2016
Stage
Western Europe
Stage
Permian
Sakmarian
Asselian
Autunian
Carboniferous
Pennsylvanian
Gzhelian
Kasimovian
Moscovian
Bashkirian
Stephanian
Westphalian
Namurian
Mississippian
Serpukhovian
Visean
Tournaisian
Visean
Tournaisian
Devonian
Famennian
295.5
298.9
303.7
314.6
323.2
330.9
346.7
358.9
W
(proximal)
E
(distal)
Somiedo unit
Bodón-Ponga unit
C
D
A
B
E
F
G
H
11. Barcaliente Fm.
8. Olaja Mb. (Alba Fm.)
9. Millaró Mb. (Alba Fm.)
7. San Adrián Mb. (Alba Fm.)
6. Canalón Mb. (Alba Fm.)
5. Lavandera Mb. (Alba Fm.)
4. Gorguera Mb. (Alba Fm.)
Alba Fm.
3. Vegamián Fm.
3. Vegamián Fm.
Hiatus (erosion and / or hardground development)
2. Baleas Fm.
2. Baleas Fm.
1. Ermita Fm.
TECTONIC & MAGMATIC EVENTS IN THE CZ
ages of post-orogenic magmatism in the CZ including 2σ errors (Peña Prieta, Carles, El Courio, Linares and Arcellana; Valverde-Vaquero et al., 1999; Fernández-Suárez et al., 2000; Gutiérrez-Alonso et al., 2011b)
oroclinal bending in the CZ
N-S shortenig causing fold tightening and involving Saberian–Stephanian B strata
out-of-sequence thrusting (Cabrales and Áliva-Lebeña thrust; Picos de Europa)
emplacement of the Bodón-Ponga Unit
emplacement of the Somiedo-Correcillas Unit
emplacement of the Palentine Nappes and Valsurvio unit
LEGEND
crinoidal grainstone (Baleas Fm)
black shales (Vegamián Fm)
nodular reddish to greyish mud- to wackestones
red radiolarites (Lavandera Mb of the Alba Fm)
dark grey laminated calci-mudstones
condensed reddish to greyish marls and nodular marly limestones (Millaró Beds) and red claystones (Ricacabiello Fm.)
basinal carbonate deposits and toe-of-slope of microbial-dominated carbonate platforms
carbonate platforms and ramps
siliciclastic turbiditic successions and muddy prodelta slopes
coastal–shelfal successions including carbonate transgressive deposits and thin coal seams
conglomerate fan-delta units
coastal–alluvial successions comprising mineable coal seams and thin transgressive limestone–marlstone strata
mélanges and block-in-matrix formations
fully alluvial deposits with mineable coal seams
TECTONIC AND MAGMATIC EVENTS
Events related to the develoment of the linear thrust and fold belt
Events related to the oroclinal bending

Fig. 11.6 Synthetic chronostratigraphic diagram showing the stratigraphy of Carboniferous successions in the Somiedo and Bodón-Ponga units of the CZ defined by Alonso et al. (2009) with indication of the main tectonic events recorded both in the internal and external areas of the Variscan orogen (Modified from Merino-Tomé et al. 2007). A. Teverga; B. Quirós; C. Naranco syncline; D. Santo Firme; E. Central Asturian coalfield; F. Ponga nappe; G. Cuera area; H. Picos de Europa area (see Fig. 11.5 for location). **Distal foreland basin successions**: 1. Ermita Fm.; 2. Baleas Fm.; 3. Vegamián Fm.; 4. Gorguera Mb; 5. Lavandera Mb; 6. Canalón Mb; 7. San Adrián Mb; 8. Olaja Mb; 9. Millaró Beds; 11. Barcaliente Fm.; 12. Valdeteja Fm.; 13. Señares Mb; 14. Ricacabiello Fm.; 15. Valdeteja and Picos de Europa Fms. (toe-of-slope and basinal deposits); 16. Valdeteja Fm. and Picos de Europa Fms. **Foredeep infill successions**: 10. Olleros Fm.; 17. Pinos Mb and Villanueva beds; 18. Fresnedo Fm.; 19. Beleño Fm.; 20. La Majúa Mb; 21. Candemuela Mb; 22. Lena Group (Central Asturian Coalfield); 23. Escalada Fm. (I); 24. Fito Fm. and Escalada Fm. (II); 25. Canales Fm.; 26. Sama Group (Central Asturian Coalfield); 27. Mieres Conglomerate Fm.; 28. Olloniego Conglomerate Fm. **Marine to coastal wedge-top successions** (see Fig. 11.5 for location): 29. San Juan de Beleño and Tiatordos peak; 30. Sebarga; 31. Gamonedo Fm.; 32. Demúes Fm.; 33. Las Llacerias Fm.; 34. Áliva Fm. and equivalents; 35. Puentellés Fm.; 36. Cavandi Fm.; 37. Lebeña Fm. **Wedge-top alluvial successions** (see Fig. 11.5 for location): 38. Fontecha succession; 39. Canseco-Rucayo succession; 40. Puerto Ventana succession; 41. Sabero and Ciñera-Matallana coalfield succession; 42. La Magdalena coalfield succession; 43. Villablino coalfield succession; 44. Rengos coalfield succession; 45. Carballo coalfield succession; 46. Tineo and Cangas coalfield succession; 47. Arnao coalfield succession; 48. Ferroñes succession. Ages of systems, stage and substage boundaries according to GST2016 (Ogg et al. 2016). Correlation of Westphalian and Stephanian stages and substages of Western European regional scale after Wagner and Álvarez-Vázquez (1991, 2010), Wagner et al. (2002), Knight and Wagner (2014)

11.2.2.3 Foredeep Infill

The foredeep successions were sourced mainly from the erosion of the growing Variscan chain (Águeda et al., 1991; Colmenero and Prado 1993; Colmenero et al. 2002; Pastor-Galán et al. 2013a, b) and overlie the strata accumulated in the distal margin of the foreland basin. They have a diachronous age, which reflects the foreland-ward migration of the mountain front and the basin depocentre (Julivert 1978; Marcos and Pulgar 1982; Barba and Colmenero 1994). The base of these strata range in age from the early Serphukovian in the Alba syncline to the latest Bashkirian-early Moscovian in the Ponga nappe and they can reach up to 6,000 m in thickness in the Central Asturian Coalfield belonging to the Bodón-Ponga unit. Their stratigraphy and sedimentology has been described in a number of publications (García Loygorri et al. 1971; Bowman 1985; Horvath 1985; Fernández et al. 1988; Águeda et al. 1991; Salvador 1993; Bahamonde and Colmenero 1993; Fernández 1993; Barba and Colmenero 1994; Wagner and Álvarez-Vázquez 1995; Corrochano et al. 2012a, b; Bahamonde et al. 2015).

In general terms, this infill displays a shallowing and coarsening upward trend from: (a) deep-water turbiditic deposits and 500–1,000 m-thick clay-dominated slope and prodeltaic wedges (e.g. Olleros and Cuevas Fms; Cervera Fm., Potes and Prioro Groups, Pinos Mb of the San Emiliano Fm. including the Villanueva beds, the Fresnedo and Beleño Fms); (b) siliciclastic shallow-water to alluvial strata, generally arranged in tens to hundreds meter-thick cyclothems, containing deltaic and alluvial coals and commonly marine limestones deposited during marine transgressions (La Majúa and Candemuela Mbs of the San Emiliano Fm; Levinco to Oscura packages of the Central Asturian coalfield and Fito Fm); to (c) thick fan-delta successions (Mieres and Olloniego Fms). A particular feature of the foreland basin of the CZ is the development of thick carbonate platforms in the distal sectors of the delta-built marine shelf (e.g. Escalada and Bachende Fms; Corrochano et al. 2012a; Bahamonde et al. 2015).

11.2.2.4 Mélanges

The mélanges of the CZ occur as up to km-thick carpets resting on foredeep or wedge-top marine successions. They underlie the Bodón-Ponga, Esla and Palentine thrust systems and also some out-of-sequence thrusts in the Pisuerga-Carrión province. They have been interpreted as originated by sliding and slumping of submarine steep slopes at the orogenic front (Alonso et al. 2006, 2015). These mélanges are mostly composed of broken formations (boudinaged sequences) of Late Carboniferous age and scattered 'exotic' blocks derived from older Paleozoic formations, sourced from the front of advancing nappes, and intercalated subordinate chaotic block-in-matrix deposits (olistostromes in the sense of Pini 1999).

The mélange underlying the Bodón-Ponga thrust system occurs ahead of the trace of the sole thrust in the Riaño-Maraña area and in the Porma valley (Alonso et al. 2006; see details therein; Figs. 11.4 and 11.5). The mélange underlying the Esla thrust system is exposed in the headwaters of the Cea valley ahead of this thrust system (Figs. 11.4 and 11.5). It comprises olistostromes with blocks of Devonian (Alonso 1987a) and late Mississippian (Arboleya 1978) limestones derived from the Esla nappe, and of disrupted successions displaying hydroplastic extension fractures (Alonso et al. 2015).

The Perapertú Fm. (Wagner and Wagner-Gentis 1963) represents the mélange carpet associated with the Palentine thrust system (Alonso et al. 2015). It is at least one km thick and contains blocks of variable size and age, including Devonian blocks derived from the Palentine nappes and blocks of Carboniferous sandstones and limestones (up to early Moscovian in age) (Wagner and Wagner-Gentis 1963; Ginkel 1965; Frets 1965; Wagner 1971b; Kullman 1960). The mélange also includes fragments of the lower Pennsylvanian Brezo limestones, which occur in the Valsurvio thrust system and in the southern border of the Palentine nappes. The San Julian and Revilla 'klippes' (Wagner 1955, 1971a), which are up to several kilometers in size, may be

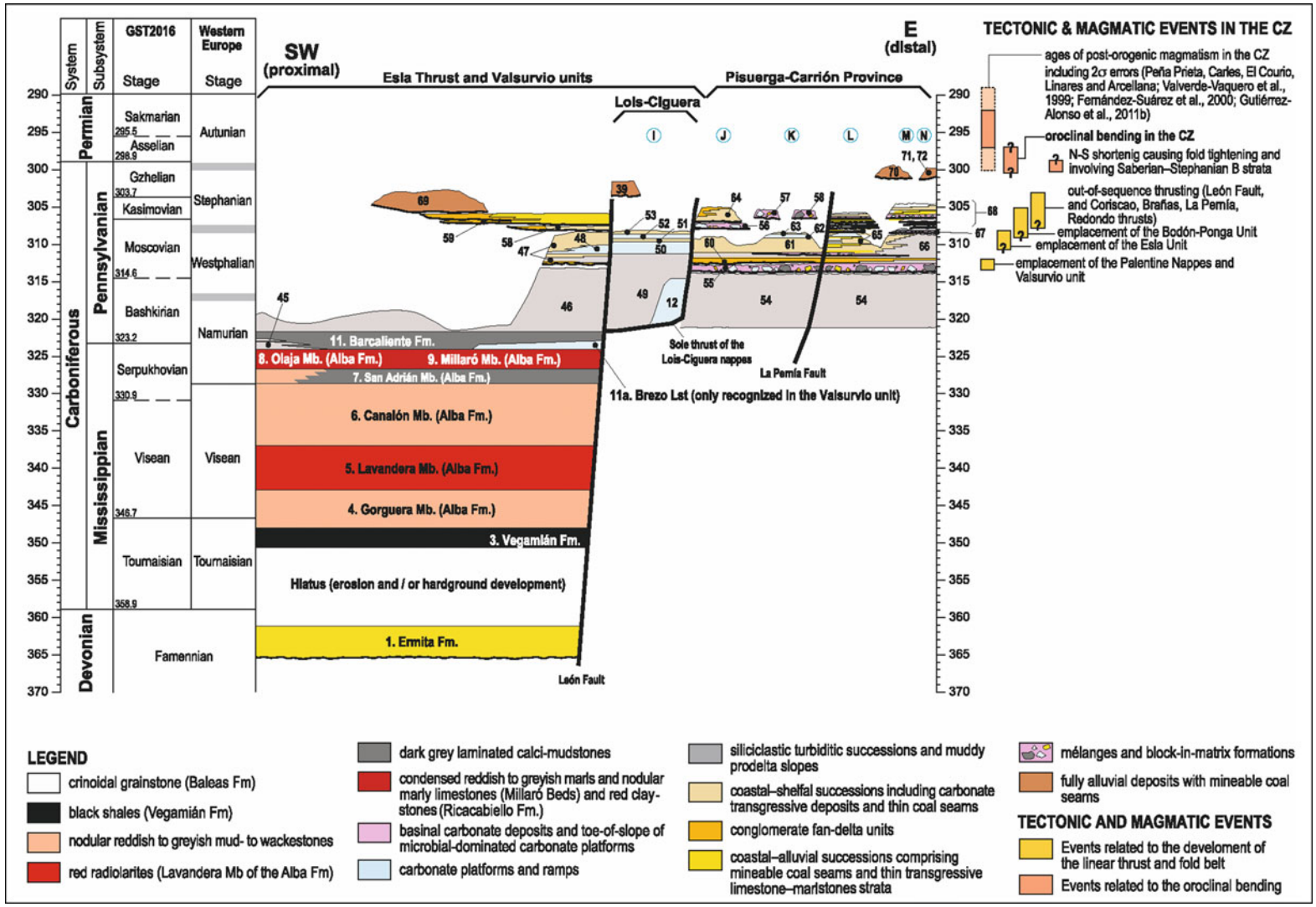
System
Subsystem
GST2016
Stage
Western Europe
Stage
Permian
Carboniferous
Pennsylvanian
Mississippian
Devonian
Sakmarian
Asselian
Gzhelian
Kasimovian
Moscovian
Bashkirian
Serpukhovian
Visean
Tournaisian
Famennian
Autunian
Stephanian
Westphalian
Namurian
Visean
Tournaisian
295.5
298.9
303.7
314.6
323.2
330.9
346.7
358.9
SW
(proximal)
E
(distal)
Esla Thrust and Valsurvio units
Pisuerga-Carrión Province
Lois-Ciguera
I
J
K
L
M
N
11. Barcaliente Fm.
8. Olaja Mb. (Alba Fm.)
9. Millaró Mb. (Alba Fm.)
7. San Adrián Mb. (Alba Fm.)
6. Canalón Mb. (Alba Fm.)
5. Lavandera Mb. (Alba Fm.)
4. Gorguera Mb. (Alba Fm.)
3. Vegamián Fm.
Hiatus (erosion and / or hardground development)
1. Ermita Fm.
Soie thrust of the Lois-Ciguera nappes
La Pernía Fault
11a. Brezo Lst (only recognized in the Valsurvio unit)
León Fault
TECTONIC & MAGMATIC EVENTS IN THE CZ
ages of post-orogenic magmatism in the CZ including 2σ errors (Peña Prieta, Carles, El Courio, Linares and Arcellana; Valverde-Vaquero et al., 1999; Fernández-Suárez et al., 2000; Gutiérrez-Alonso et al., 2011b)
oroclinal bending in the CZ
N-S shortenig causing fold tightening and involving Saberian–Stephanian B strata
out-of-sequence thrusting (León Fault, and Coriscao, Brañas, La Pernía, Redondo thrusts)
emplacement of the Bodón-Ponga Unit
emplacement of the Esla Unit
emplacement of the Palentine Nappes and Valsurvio unit
LEGEND
crinoidal grainstone (Baleas Fm)
black shales (Vegamián Fm)
nodular reddish to greyish mud- to wackestones
red radiolarites (Lavandera Mb of the Alba Fm)
dark grey laminated calci-mudstones
condensed reddish to greyish marls and nodular marly limestones (Millaró Beds) and red clay-stones (Ricacabiello Fm.)
basinal carbonate deposits and toe-of-slope of microbial-dominated carbonate platforms
carbonate platforms and ramps
siliciclastic turbiditic successions and muddy prodelta slopes
coastal–shelfal successions including carbonate transgressive deposits and thin coal seams
conglomerate fan-delta units
coastal–alluvial successions comprising mineable coal seams and thin transgressive limestone–marlstones strata
mélanges and block-in-matrix formations
fully alluvial deposits with mineable coal seams
TECTONIC AND MAGMATIC EVENTS
Events related to the develoment of the linear thrust and fold belt
Events related to the oroclinal bending

Fig. 11.7 Synthetic chronostratigraphic diagram showing the stratigraphy of Carboniferous successions in the Esla unit and the Pisuega-Carrión province with indication of the main tectonic events recorded both in the internal and external areas of the Variscan orogen. I. Lois-Ciguera area; J. Lechada syncline; K. Coriscao syncline; L. Casavegas-Castillería syncline; M. Redondo syncline; N. Central Liébana-Virona syncline (see Fig. 11.5 for location). **Distal foreland basin successions**: 1. Ermita Fm.; 3. Vegamián Fm.; 4. Gorguera Mb; 5. Lavandera Mb; 6. Canalón Mb; 7. San Adrián Mb; 8. Olaja Mb; 9. MIllaró Beds; 11. Barcaliente Fm.; 12. Yordas Lmst Fm. **Foredeep infill successions**: 45. Cuevas Fm.; 46. Prioro Group and Cervera Fm.; 47. Pando Group; 48. Pando Lmst Fm.; 49. Lois shales Fm.; 50. Bachende Fm.; 51. Dueñas Fm.; 52. Ciguera Lmst Fm.; 53. Ciguera Sh Fm.; 54. Cervera Fm. = Potes and Prioro Gr. **Mélanges** (see Fig. 11.5 for location): 55. Carmen-Perapertú Fm. (mélange underlying the Palentine nappes); 56. Maraña Fm. (mélange underlying the Esla and Bodón-Ponga thrust systems); 57. Remoña and Brañas olistostromes; 58. Coriscao olistostrome. **Marine to coastal wedge-top successions** (see Fig. 11.5 for location): 58, Conjas-mental Gr; 59. Cea Gr (Guardo Coalfield succession); 60. Curavacas Fm.; 61. Lechada-Vegacerneja Fms., Ferreras Fm. and Ves Lmst; 62. Panda Limestone; 63. Pandetrave Fm.; 64. Pontón and Valdeón Grs; 65. Vañes Fm., Vergaño Fm., Coterraso, Camasobres and Peña Maldrigo Lmts; 66. Mogrovejo Gr = Lechada Fm.; 67. Covarres Fm.; 68. Ojosa, Rozo, Verdeña, San Salvador, Brañosera and Barruelo Fms., Sierra Corisa, Agujas and Peña del Abismo Lmts. **Wedge-top alluvial successions** (see Fig. 11.5 for location): 39, Canseco-Rucayo coalfield successions; 69. Sabero coalfield succession; 70. Peña Cildá succession; 71. Pico Cordel succession; 72. Puente Pumar succession. Ages of systems, stage and substage boundaries according to GST2016 (Ogg et al. 2016). Correlation of Westphalian and Stephanian stages and substages of Western European regional scale after Wagner and Álvarez-Vázquez (1991, 2010), Wagner et al. (2002), Knight and Wagner (2014)

interpreted either as a remnant of a previously continuous thrust sheet, or as megablocks slipped down into the basin (Alonso et al. 2015).

The so-called Brañas-Remoña and Coriscao olistostromes (Savage 1961; Maas 1974), described in detail by Maas and van Ginkel (1983), have been interpreted as block-in-matrix formations (BIMF) related to out-of-sequence thrusts involving the wedge-top basin of the Palentine nappes (Alonso et al. 2015) (Figs. 11.4 and 11.5). They contain Devonian and Mississippian limestone blocks sourced from the Palentine nappes as well as limestone blocks of Bashkirian to earliest Kasimovian age (Maas and van Ginkel 1983), yielding thus a minimum earliest Kasimovian age for these mélanges (middle Cantabrian stage; Maas and van Ginkel 1983).

11.2.2.5 Wedge-Top Successions

Unconformable strata ranging from deep-water turbiditic deposits and block-in-matrix formations to deltaic and fan-deltaic successions and small carbonate ramps occur on the frontal sector of the Bodón-Ponga thrust system (e.g. Sebarga and Sobrefoz in the Ponga nappe, and the Gamonedo-Cabrales, Covadonga, Áliva, Lebeña and Ándara areas of the Picos de Europa mountains; Merino Tomé et al. 2006, 2007, 2009a, b; Alonso et al. 2015), as well as on the Esla thrust system (Helmig 1965; Alonso 1987a), and on the Palentine nappes of the Pisuerga-Carrión province (Van Veen 1965; Rodríguez Fernández 1994; Martín-Merino et al. 2014) (Figs. 11.5, 11.6 and 11.7). In the Pisuerga area, these successions range in age from the early Moscovian (Kashirian) to Kasimovian (=Duckmantian to Barruelian) (Van veen 1965; Martín Merino et al. 2014) and overlie the so-called Palentine unconformity. They show near the base the remarkable and laterally continuous conglomerate beds of the Curavacas Fm., which represents a large fan-delta system (Colmenero et al. 1988). In the case of the Esla and Bodón-Ponga thrust systems, the age of these successions ranges from the latest Moscovian (late Myachkovian) to the Gzhelian (=late Asturian to Stephanian B).

These strata represent the remnants of piggy-back basins developed on the frontal thrust nappes of the advancing orogen. During the latest Moscovian (late Myachkovian), Kasimovian and Gzhelian, the main depocenters of the basins consisted of growth synclines in front of thrust-related anticlines, which eventually served as the nucleation areas for narrow carbonate-ramp systems. The sedimentary successions are commonly arranged in unconformity-bounded sequences (see references cited above).

Very thick (up to several thousand m in thickness) alluvial molasses with local marine incursions, which on the basis of floral remains have been assigned to the Cantabrian, Barruelian, Saberian and Stephanian B stages (Kasimovian to Gzhelian), unconformably overlie the thrust systems of the CZ and the WALZ (Corrales 1971; Wagner 1971a; Heward 1978; Knight 1983; Wagner and Winkler Prins 1985a; Colmenero et al. 2002; Fernández et al. 2004; Wagner and Álvarez-Vázquez 2010; Wagner and Castro 2011) (Figs. 11.4 and 11.5). They contain numerous mineable coal seams that were exploited in many coalfields (see Figs. 11.4 and 11.5), which represent the remnants of broader sedimentary basins. In fact, stratigraphic and paleontological studies carried out in the Sabero, Ciñera-Matallana and La Magdalena coalfields show that these currently isolated outcrops might correspond to the sedimentary infill of a single and larger sedimentary basin (Wagner and Castro 2011). The thick sedimentary pile preserved records very high subsidence rates affecting broad areas of the orogenic wedge. These strata postdate the emplacement of the major tectonic units in the CZ. Nevertheless, it is worth mentioning that they were coetaneous with ongoing deformation and sedimentation on the Picos de Europa area, which lasted until Gzhelian times.

11.2.2.6 The Variscan Deformation in the CZ

The CZ records a complex structural evolution that culminated with the lithospheric-scale orocline bending giving rise to the Ibero-Armorican Arc. This evolution has been described in two main steps: (a) the development of an initial linear thrust and fold belt and (b) a late oroclinal bending related to N-S shortening (Ries and Shackleton 1971; Alonso 1987a; Stewart 1995; Van der Voo et al. 1997; Weil et al. 2000, 2013a, b; Kollmeier et al. 2000; Gutiérrez Alonso et al. 2004; Weil 2006).

11.2.2.6.1 Thrust Nappe Emplacement (Early Moscovian to Early Gzhelian)

Thrust-nappe emplacement in the CZ took place mostly in submarine conditions (Alonso et al. 2006, 2015) and the upper thrust-belt surface was close to sea level over extensive areas of the orogenic wedge (at least until mid-Kasimovian times) allowing for the development of the marine wedge-top basins that are preserved in the Bodón-Ponga, Esla thrust systems (Alonso 1987a; Merino-Tomé et al. 2009a) and in the Pisuerga-Carrión province (Martín Merino et al. 2014). The age of the thrust-system development can be accurately constrained on the basis of the age of the mélanges and of the wedge-top successions associated to the frontal area of each thrust system.

The earliest record of tectonic deformation in the CZ corresponds to the emplacement of the Palentine nappes (van Veen 1965) and the Valsurvio unit during the early Moscovian (Alonso et al. 2015). A minimum age of latest Vereian or even early Kashirian can be estimated for this tectonic event considering the presence in the associated mélange of the Perapertú Fm. of limestone blocks containing fusulinids of the *Profusulinella* B zone of late Vereian–early Kashirian age (Ginkel 1965). According to Martín-Merino et al. (2014), unconformable wedge-top basins covered the Palentine nappes showing good examples of related out-of-sequence thrust-propagation growth folds in a submarine environment, particularly during the latest Moscovian (late Myachkovian) and early Kasimovian.

The Esla and Somiedo and Bodón-Ponga thrust systems emplaced during the late Moscovian, that is, later than the emplacement of the Palentine nappes but in part synchronously with ongoing deformation and thrusting in the Pisuerga area. The Esla thrust system was emplaced on a shallow-marine basin during the late Moscovian and after its emplacement it was immediately covered by a fan-delta succession of early Stephanian (latest Moscovian-early Kasimovian) age (Alonso 1987a). According to the inferred age of the related mélange deposits and the age of the frontal wedge-top successions, the Bodón-Ponga unit was emplaced during the late Moscovian (Myachkovian) and early Kasimovian (Krevyakinian-Khamovnikian) (Alonso et al. 2006, 2015; Merino-Tomé et al. 2007, 2009a, b). The emplacement of the Somiedo thrust system preceeded that of the Bodón-Ponga but, according to the character of the youngest foredeep successions exposed in the underlying Bodón nappe, it could have not started earlier than the early Kashirian. The development of the large fan deltas of the Mieres and Olloniego conglomerate Fms during the latest Podolian and early-mid Myachkovian in the Central Asturian Coalfield (Bodón-Ponga unit) is probably related with the subaerial emplacement of the more advanced nappes of the Somiedo thrust system (Fernández et al. 1988).

During Kasimovian to early Gzhelian times, in a late stage of the development of the linear fold and thrust belt, some outstanding out-of-sequence thrusting breached the nappe pile increasing tectonic shortening and thickening of the orogenic wedge (Alonso et al. 2009). The main examples are the León thrust fault and the related Pajares backthrust (Alonso et al. 2009), but other out-of-sequence thrusts developed in the frontal area of the Bodón-Ponga thrust system in the Picos de Europa area (Merino-Tomé et al. 2009a), and ahead of them, in the Pisuerga Carrión (Maas and Van Ginkel 1983; Alonso et al. 2015). At this time, marine sedimentation continued on the frontal areas of the orogenic wedge (e.g. marine synorogenic successions of the Picos de Europa area and Pisuerga-Carrión province).

11.2.2.6.2 The Formation of the Ibero-Armorican Arc (Gzhelian to Early Permian)

The oroclinal bending of a primarily linear thrust and fold belt, which represents the last episode of Variscan deformation in the CZ, started around the early Gzhelian and ended during the earliest Permian. The age of this process is deduced considering the age of the main thrust systems, including the out-of-sequence León thrust (Alonso et al. 2009), of the linear fault-and-thrust belt, the paleomagnetic data (Hirt et al. 1992; Parés et al. 1994; Stewart 1995; van der Voo et al. 1997; Weil et al. 2000, 2001; Weil 2006, among others) and the joint analyses by Pastor-Galán et al. (2011, 2014). Analogue modeling (Pastor-Galán et al. 2012) and the available geological data allow inferring that the Ibero-Armorican Arc formation was a fast thick-skinned lithospheric-scale process (Gutiérrez-Alonso et al. 2004, 2011a, 2011b; Pastor-Galán et al. 2013b; Johnston et al. 2013). This process caused the tightening and reorientation of previous thrust-related folds (Alonso 1989; Stewart 1995; Weil 2006), the overturning of thrusts in the southern part of the CZ (Alonso et al. 1991) and the fold tightening that involved the Saberian to Stephanian B molasses (latest Kasimovian and Gzhelian). According to Gutiérrez-Alonso et al. (2004) and Pastor-Galán et al. (2012), the onset of lithospheric-scale shortening in the core of the arc might have produced a thickened mantle lithospheric root and lower-crust duplication that could have induced subsidence over broad areas of the CZ allowing the formation of the Saberian to Stephanian B basins (e.g. El Bierzo, Tormaleo, Villablino, Tineo, Rengos, Cangas del Narcea, Carballo, Peña Cildá and Pico Cordel).

11.3 Synorogenic Basins in the Southern Iberian Massif

J. T. Oliveira, C. Quesada

The Variscan orogen in the southern half of the Iberian Massif is characterized by sinistral transpressional processes throughout its evolution. The area affected by this left-lateral regime of convergence includes the southern part of the Central Iberian Zone (CIZ), the Ossa Morena Zone (OMZ) and the South Portuguese Zone (SPZ) (see Fig. 11.8). The most salient element in this part of the Variscan orogen is

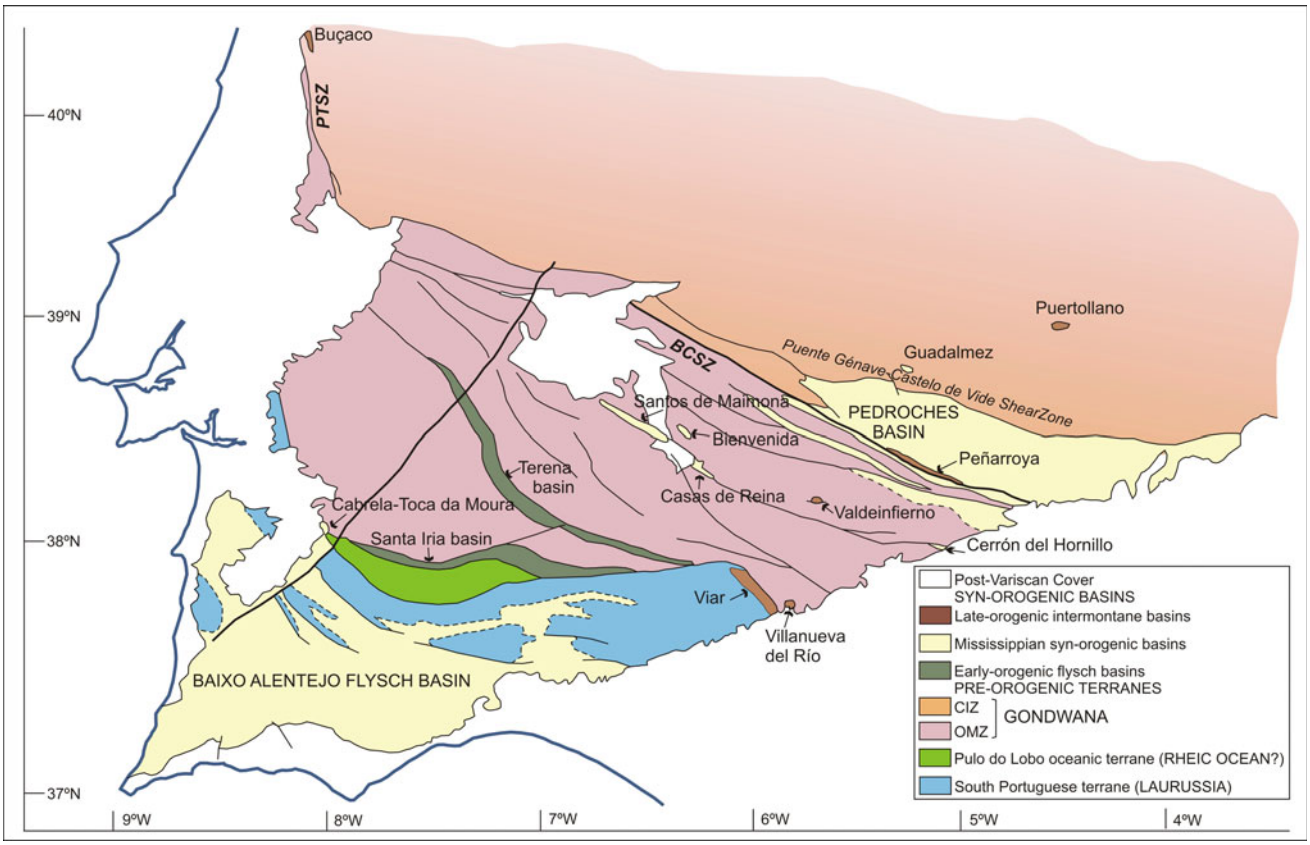

Fig. 11.8 Map location of the main outcrops of Variscan synorogenic basins in SW Iberia (PTSZ: Porto-Tomar shear zone; BCSZ: Badajoz-Córdoba shear zone)

the presence of a suture zone, materialized by the oceanic affinity Pulo do Lobo terrane (PLT) that separates the Laurussian affinity South Portuguese terrane (SPT) from the other zones belonging to the margin of Gondwana. At odds with the northern Iberian Massif, where collisional deformation started in late Early to Middle Devonian times (Arenas et al. 2016 and references therein), collision between the South Portuguese terrane and the outer margin of Gondwana in the southern Iberian Variscan orogen probably started in the Late Devonian (pre-Famennian), sequentially migrated laterally along the Gondwanan margin while still in presence of relic oceanic lithosphere, and was finally completed by the late Visean (Ribeiro et al. 1990; Quesada 1991, Quesada and Dallmeyer 1994; Pereira et al. 2006; Braid et al. 2018).

The sinistral transpressional regime that governed the tectonic evolution of the southern Iberian Massif has been interpreted in connection with the existence of a reentrant in the Gondwanan continental margin, which favoured tectonic escape of marginal continental units (Quesada 1991, 2006; Murphy et al. 2015). Specially, the OMZ, which occupied the thinned outermost continental margin of Gondwana and whose northern boundary (Badajoz-Córdoba shear zone) formed by sinistral Variscan reactivation of a previous suture zone, may have been forced to escape from the zones already undergoing collision since the very onset of this process, as represented by the northern Iberian Variscan orogen (i.e. in late Early Devonian times). Tectonic escape would have been accommodated by sinistral displacement along the Badajoz-Córdoba shear zone and correlatives in the northern part and by overriding onto the oceanic lithosphere of the adjacent reentrant located to the south (Quesada 1991, 2006). This interpretation is given support by the transformation of the previous southern passive margin into an active one, as indicated by punctuated emplacement of volumetrically minor but significant subduction-related igneous rocks on the southern OMZ in the Middle Devonian-early Visean timespan (Santos et al. 1987, 1990). This fact implies a northerly polarity of subduction with Ossa Morena as upper plate at this time, opposite to the overall situation in the northern Iberian orogen where the Gondwanan plate was always the lower one. In its escaping journey, the OMZ would have started to be deformed and to develop its prominent sinistral strike-slip duplex structure (Fig. 11.8) as well as the first synorogenic basins, despite the fact that collision had not yet commenced at its southern margin. However, the most important synorogenic basins formed in late Visean times when collision with the SPZ finally reached this area, giving rise to two opposite-verging peripheral foreland basins: the S-propagating Baixo Alentejo Flysch Group basin onto the SPT (Oliveira 1990) and

the N-propagating Pedroches basin (Gabaldón et al. 2004, Armendáriz 2008) to the north of the OMZ and extending into the Central Iberian Zone (Fig. 11.8).

Synorogenic basins also formed within the suture zone proper, i.e. the Pulo do Lobo terrane (Santa Iria Flysch basin), interpreted as an extremely imbricated accretionary prism (Quesada 1991; Quesada and Dallmeyer 1994; Braid et al. 2010). According to the regional geodynamic environment, the following synorogenic basins are to be recognized in the southern Iberian Massif (Figs. 11.8 and 11.9):

1. Southwestern OMZ intra-arc basin (Devonian-Early Mississippian) and successor Mississippian flysch basins (Toca da Moura and Cabrela);
2. Retro-arc Terena Flysch basin (Early Devonian-early Visean) in the south-central OMZ;
3. Fore-arc/trench basins in the PLT suture zone (Frasnian-Famennian)
4. Valdeinfierno intermontane basin (late Tournaisian) in northern OMZ;
5. Pedroches basin (late Tournaisian-Serpukhovian) in the northernmost OMZ and the southern CIZ), and Central OMZ basin (including the outcrops at Los Santos de Maimona, Bienvenida, Casas de Reina and Cerrón del Hornillo);
6. Baixo Alentejo Flysch Group basin (late Visean-Moscovian) in the SPT;
7. Late-orogenic intermontane basins: Peñarroya-Belmez-Espiel, Villanueva del Río y Minas and Santa Susana (Westphalian) in the OMZ; Puertollano (Stephanian) in the CIZ; Viar and related outcrops (late Stephanian-early Permian) in the SPZ and southeastern OMZ.

All the above basins were reviewed in contributions by Lemos de Sousa and Wagner (1983), Quesada (1983), Quesada and Garrote (1983), Gabaldón et al. (1985a, b),

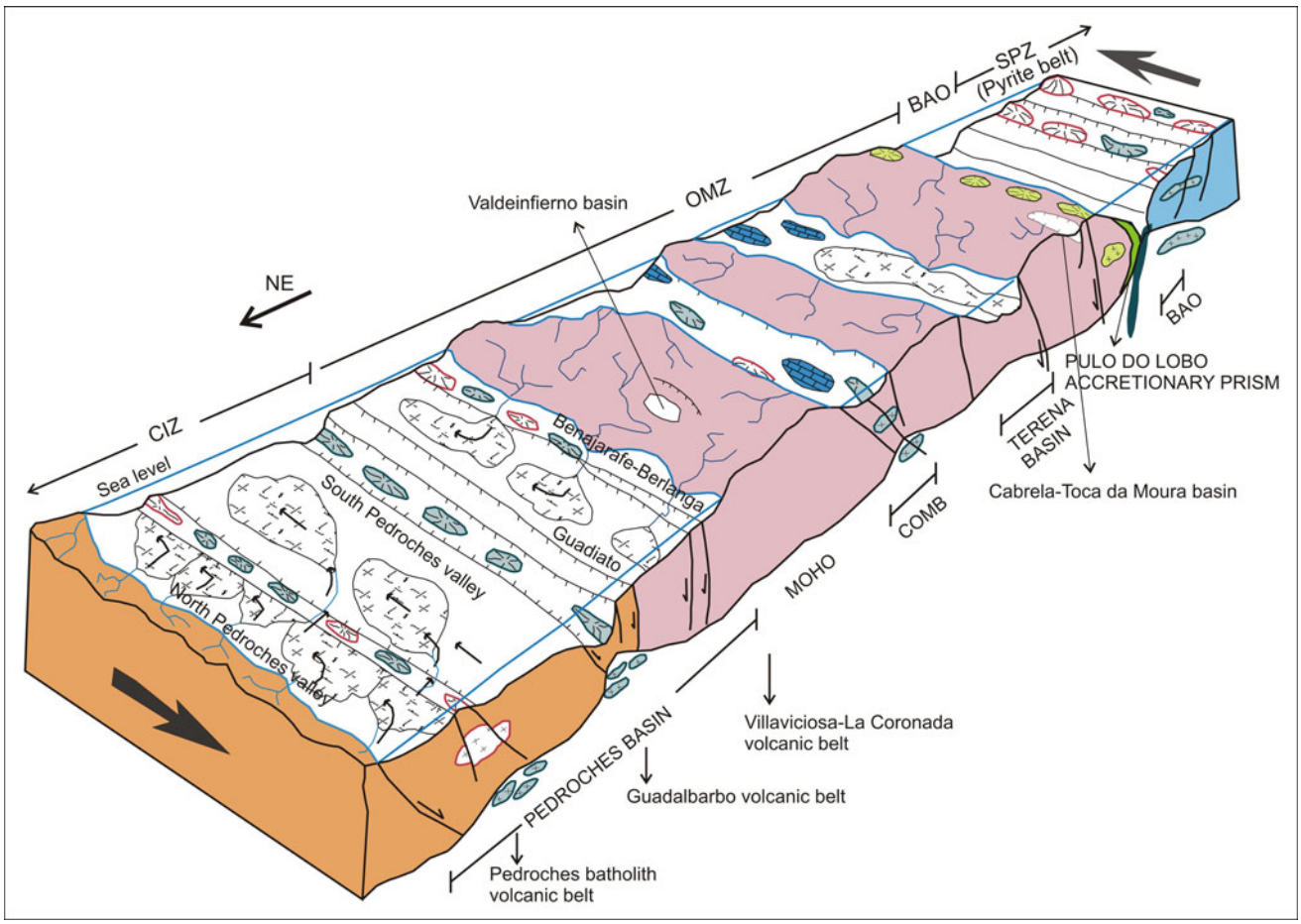

Fig. 11.9 Idealized block diagram showing the main synorogenic basins existing in SW Iberia immediately prior to the onset of collision (i.e. ca. 335 Ma ago). Names in the Pedroches basin correspond to the main structural units described in the text. Legend: barbed ovoids represent volcanic buildups (red: felsic; blueish grey: mafic; green: intermediate arc-related); bricked ovoids: carbonate platforms; cross-bearing ovoids: plutons (same colour code as the volcanics); cross-hatched envelopes: tempestitic/turbiditic sand lobes. Singular acronyms: BAO: Beja-Acebuches oceanic basin; COMB: Central Ossa-Morena basin

Oliveira (1983, 1990) and Quesada et al. (1990), among others, and an update of their main characteristics and evolution is briefly outlined below.

11.3.1 Devonian Intra-arc Basin in the Southwestern Ossa Morena Zone and Its Geodynamic Significance

N. Moreira, G. Machado

Devonian carbonate sediments are poorly developed in the OMZ. In the south-west branch of this zone, several Devonian limestone occurrences are known and its description, regional framework and significance are the subject of this subsection.

11.3.1.1 Regional Overview of Devonian Sedimentary Rocks in the OMZ and Neighboring Regions

From the Ordovician to the Early Devonian the sedimentation in the OMZ took place in general in a passive margin setting (Quesada et al. 1990; Robardet and Gutiérrez-Marco 1990, 2004). This is recorded in metasedimentary rocks cropping out in areas from Portalegre to Córdoba and more to the south in the Barrancos-Estremoz area (Robardet and Gutiérrez-Marco 1990, 2004; Oliveira et al. 1991; Piçarra 2000), Terena syncline (Piçarra 2000) and Valle, Venta de Ciervo and Cerrón del Hornillo synclines in Spain (Robardet and Gutiérrez-Marco 1990, 2004). Most of the Paleozoic rocks are siliciclastic, varying from proximal inner-shelf deposits to deep fan turbidites (Oliveira et al. 1991; Piçarra 2000; Borrego et al. 2005). Lower Devonian reefal and other carbonate sedimentation in the OMZ is rare, but reported by May (1999) and Rodríguez et al. (2007) in Spain and Piçarra (2000) and Piçarra and Sarmiento (2006) in Portugal. Middle Devonian metasedimentary rocks are very rare in the OMZ. This has been explained by a generalized uplift of this area during the Middle Devonian, creating a regional scale hiatus, as a consequence of the first pulses of the Variscan orogeny (Robardet and Gutiérrez-Marco 1990; 2004; Oliveira et al. 1991). In southwestern OMZ, several scattered occurrences of reefal and peri-reefal carbonates were described near Cabrela (Boogaard 1972, 1983; Ribeiro 1983; Pereira and Oliveira 2003a; Pereira et al. 2006), and within the Beja Igneous Complex around the Odivelas water reservoir (Conde and Andrade 1974; Machado et al. 2009, 2010; Fig. 11.10). Other rare occurrences of limestones in the same domain are reported near the contact area with the South Portuguese Zone (SPZ) around the Caeirinha mine and Pena (Pereira et al. 2006; Oliveira et al. 2013), shown to be Middle Devonian in age (Machado and Hladil 2010).

Together with the reefal and peri-reefal sediments, these occurrences frequently have interbedded or spatially related black cherts (with radiolarite lenses), tuffites and marly limestones.

During the Late Devonian and Carboniferous, the sedimentation is controlled by the pulses and geometry of the oblique convergence occurring between the SPZ and the OMZ in a synorogenic phase (Quesada et al. 1990).

11.3.1.2 Magmatism in Southwestern Ossa Morena Zone

In the southwesternmost domains of the OMZ, a suite of magmatic rocks is present, generally included in the so-called Beja Igneous Complex (e.g. Andrade 1983; Oliveira et al. 1991; Jesus et al. 2007, 2016). This igneous complex includes: plutonic (e.g. Beja Layered Gabbroic Sequence) and volcanic rocks (e.g. Toca da Moura and Cabrela VS complexes) related with different stages of a convergent process between OMZ and the South Portuguese Zone (e.g. Jesus et al. 2007; Ribeiro et al. 2010; Fig. 11.10). This suite presents a Devonian-Carboniferous range of ages, distinct magmatic natures and consequently distinctive geodynamic significances.

The description of the magmatism is not the objective of this section, thus only two distinct volcanic units will be briefly described because they present key features of the western OMZ carbonate sedimentation general framework:

- Rebolado basalts (Peroguarda Unit; e.g. Andrade et al. 1976; Santos et al. 1990);
- Toca da Moura and Cabrela VS complexes (e.g. Pereira et al. 2006; Oliveira et al. 2013).

Andrade et al. (1976) divided the magmatic rocks in the Odivelas-Alvito cross section in three distinct complexes: Odivelas, Peroguarda and Faro-Alvito. The Odivelas and Faro-Alvito complexes are mainly composed by plutonic rocks, with gabbro-diorite or granitic composition and a Carboniferous age (Andrade et al. 1976; Pin et al. 2008; Jesus et al. 2007, 2016). In turn, the Peroguarda complex is mainly composed by mafic to intermediate volcanic rocks. This complex is subdivided in three units, among which the Rebolado basalts (OD-6 in Santos et al. 1990 nomenclature). This unit is spatial and stratigraphically associated with the (Lower-) Middle Devonian limestones in Covas Ruivas and Cortes locations (Conde and Andrade 1974; Andrade et al. 1976; Machado et al. 2009, 2010; Moreira et al. 2010; Figs. 11.10 and 11.11), presenting a mafic to intermediate nature with abundant effusive lithotypes and tephra rocks (Santos et al. 1990; Silva et al. 2011). These basalts exhibit low grade hydrothermal metamorphism (Andrade et al.

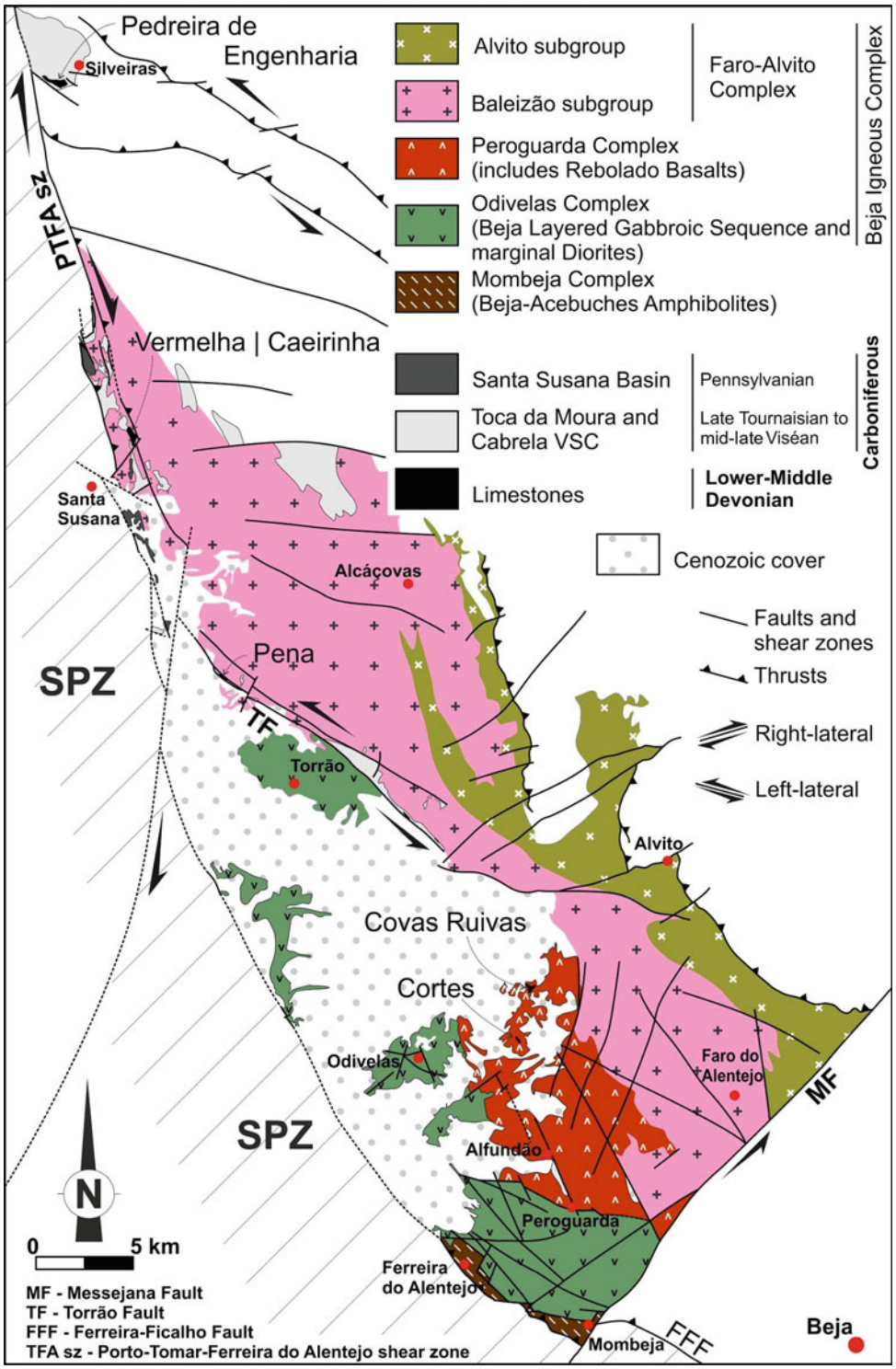

Fig. 11.10 Simplified geological sketch map of western OMZ emphasizing magmatic and Late Paleozoic sedimentary rocks (adapted from Geological Map of Portugal at 1:500.000 scale (1992); Andrade et al. 1976; Santos et al. 1990; Oliveira et al. 2013; Machado et al. 2012; Jesus et al. 2016)

1976; Santos et al. 1990; Silva et al. 2011), which does not obliterate the original volcanic textures.

Santos et al. (1990) refers a spatial association between the Peroguarda and Odivelas complexes, showing plutonic facies in the SW border (Odivelas complex) which laterally pass to the volcanic ones in the NE branch (Peroguarda complex). Recent studies (Jesus et al. 2016) also show a NW-SE to WNW-ESE magmatic layering in the Odivelas complex (designated as Layered Gabbroic Sequence by the authors), which is congruent with Santos et al. (1990) data. However, the Odivelas complex is Carboniferous in age (Jesus et al. 2007, 2016; Pin et al. 2008). Geochemical data suggests that the mafic-intermediate sub-alkaline volcanic rocks contained in the Rebolado Basalts unit present significant similarities with the typical orogenic volcanic arc magmatism, exhibiting a low-K tholeiitic to calc-alkaline signature (Santos et al. 1990; Silva et al. 2011). However, Santos et al. (1990) remark a slight difference between two sectors: the Odivelas-Penique, in the north, where the calc-alkaline signature is more pronounced, while the Alfundão-Peroguarda sector presents a predominant tholeiitic nature. Recently, Santos et al. (2013) supported this distinction based on isotopic data (Sm–Nd and Rb–Sr isotope pairs). The data provide evidence of common (or very similar) mantle sources for the mafic magmas in both sectors, although the Odivelas-Penique group shows some evidences of crustal assimilation.

The Toca da Moura and Cabrela VS complexes are located adjacent to the southwestern border of the OMZ (Fig. 11.10). These complexes are composed of a sequence of slightly deformed pelites, siltstones and greywackes, interbedded with felsic, intermediate and basic volcanic rocks, although felsic volcanics are predominant in the Cabrela Basin (e.g. Pereira et al. 2006; Oliveira et al. 2013). At the base of the sequence, conglomeratic levels are identified (Ribeiro 1983; Oliveira et al. 1991). In both complexes, Devonian limestones (Boogaard 1983; Machado and Hladil 2010) are also present. However, its geometric and stratigraphic relation with the siliciclastic sedimentation is poorly constrained (Oliveira et al. 1991, 2013). Pereira and Oliveira (2003a) suggest these limestones are, at least in part, olistoliths. The Toca da Moura and Cabrela complexes are coeval, providing miospore associations which indicate a late Tournaisian to middle-late Visean age (Pereira and Oliveira 2003b; Pereira et al. 2006; Oliveira et al. 2013; Lopes et al. 2014). These complexes were deposited over a well-structured Silurian (?) basement defining an angular unconformity (Pereira and Oliveira 2003a; Pereira et al. 2006).

In the Toca da Moura complex, Santos et al. (1987) characterized basalt, dolerite, andesite and rhyodacite rocks. All these rocks present a low grade metamorphism related to late Variscan deformation episodes. The same authors established the orogenic calc-alkaline geochemical signature of these volcanic series, explaining the diversity of lithotypes in connection with fractional crystallization processes. The Cabrela felsic volcanics (rhyodacites; Chichorro 2006) present geochemical similarities with the previously described Toca da Moura volcanics and some felsic and intermediate dykes intruded in the Évora Massif (Chichorro 2006), also showing a calc-alkaline signature. According to Chichorro (2006), this volcanism may represent the effusive member of the widespread plutonism in the Évora Massif.

11.3.1.3 Lower-Middle Devonian Rocks in the Southwestern OMZ Intra-arc Basin

Despite the relevance of the initial paleontological work carried out by Boogaard (1972, 1983) and Conde and Andrade (1974), who studied the limestone occurrences in western OMZ, there is still a big gap on the knowledge of these units, notably on the range of the sedimentation ages,

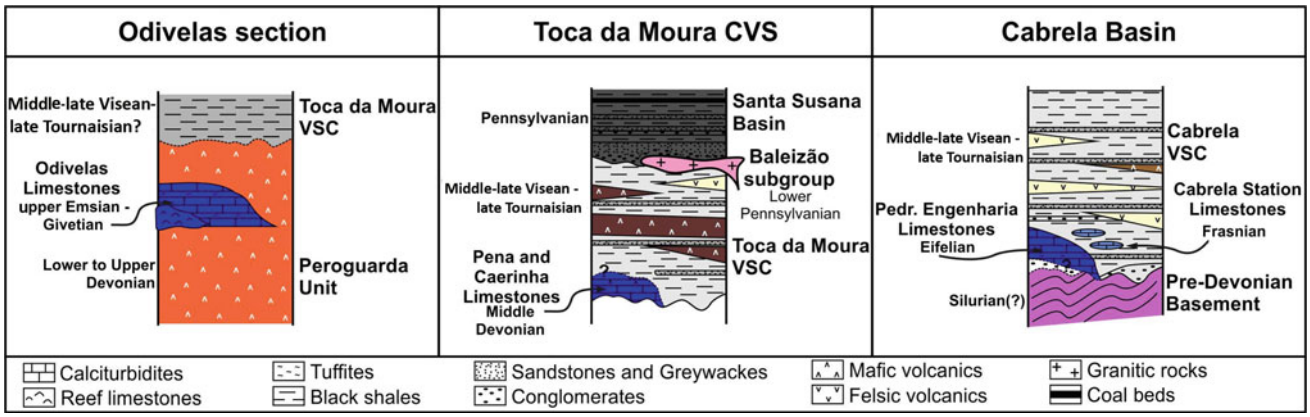

Fig. 11.11 Schematic stratigraphic sections at the Odivelas, Toca da Moura and Cabrela areas (based on data from Carvalhosa 1977; Ribeiro 1983; Oliveira et al. 1991, 2013; Chichorro 2006; Pereira et al. 2006; Machado et al. 2009, 2010; Machado and Hladil 2010; Moreira et al. 2010)

integration with other occurrences in neighboring regions and especially their geodynamic significance.

The Odivelas Limestone and correlatable units are presently found scattered in from the Odivelas reservoir area (Ferreira do Alentejo) in the South to the Cabrela village in the North (Vendas Novas and Montemor-o-Novo). Most of the known occurrences are aligned NNW-SSE close to the OMZ-SPZ boundary (Fig. 11.10). Other, spatially restricted occurrences of carbonate rocks, cherts, tuffites and marls are known further to the east (Vidigueira area), but these may represent older Cambrian (?) rocks.

Each of the occurrences is composed by loose boulders, small quarries and natural outcrops scattered in areas usually less than 1 km 2. They are found interbedded or spatially associated with the Rebolado basalts (see below) or Toca da Moura and Cabrela complexes rocks which are volumetrically much more important (Fig. 11.11).

The vast majority of the known limestone occurrences are composed by crinoidal wackestones (up to 90% crinoidal fragments) with subordinate proportions of other bioclasts such as forams, tantaculitids, ostracods, bryozoans, corals and stromatoporoids (Figs. 11.11, 11.12b, g, i). Associated with this lithofacies fine-grained calcimudstones with abundant peloids (up to 75%) occur. These have occasional mixing of coarser grains such as crinoidal fragments, tentaculites and radiolarians. These two lithofacies are interbedded (dm to m-thick beds) and generally interpreted as calciturbidites, in more distal (calcimudstones) or more proximal (wackestones) settings. While this is clear in continuous outcrops such as Covas Ruivas (Machado et al. 2010) the interpretation is only tentative in localities with small discontinuous outcrops, as Pena and Caeirinha. The origin of the carbonate material is most likely a reef system updip. This is corroborated by the highly diversified reef fauna found in the few, very coarse carbonate breccias. The only locality with bioherm/biostromal facies (Figs. 11.11 and 11.12h) is Cortes, where very coarse grained packstone-grainstones (locally rudstones and boundstones) with abundant crinoids, rugose and tabulate corals, brachiopods and stromatoporoids occur in the central part of the outcrop area. The fossil association is indicative of latest Eifelian to earliest Givetian ages (Machado et al. 2009). Unpublished conodont work by the authors confirms the age determination. This central area is surrounded by calciturbidite facies (Machado et al. 2009). Cortes and Covas Ruivas occurrences constitute the Odivelas Limestone s.s.

In some of the localities (Pena, Caerinha, Cabrela) these lithofacies are overprinted by intense dolomitization and/or silicification (Machado and Hladil 2010; Moreira et al. 2016). Nevertheless, crinoid columnal sections and remnants of the original facies are partially preserved and allow petrographic and biostratigraphical work to be conducted (Fig. 11.12i).

Other notable lithofacies present are tuffites interbedded with the calciturbidites. These form cm-thick beds, frequently cherty or with millimetric carbonate lenses, which in some levels have radiolarians, tentaculites and ostracod shells (Figs. 11.11 and 11.12b–e). These are always volumetrically less relevant than the carbonates and are interpreted as hemipelagic sediments. They also occur in the volcaniclastic sequences of the Rebolado basalts, that under and overlay the limestones (Fig. 11.11 and 11.12c). The tuffites have been described in detail in the Odivelas reservoir area (Machado et al. 2010). In the Cabrela area, both calciturbidite and (possible) tuffites seem macroscopically identical, but have not been studied petrographically (Figs. 11.11 and 11.12j).

As briefly described above, nearly all the known occurrences of the Odivelas Limestone and correlatable units are Middle Devonian in age. A notable exception is the very base of the sequence in Covas Ruivas which includes the youngest Emsian (Early Devonian) conodont biozone (*patulus*) and ranges to the *australis* biozone. The presence of crinoid ossicles of *Gasterocoma* sp. and *Cupressocrinities* sp. (and dominance over other crinoids) is quite distinctive of many of these localities (except in Covas Ruivas), indicating a late Eifelian to early Givetian age. The presence of large limestone boulders, Frasnian in age (Boogaard 1983), within the Mississippian Toca da Moura and Cabrela complexes and often spatially associated with Middle Devonian limestone outcrops (Eifelian; Boogaard 1972) is puzzling. Frasnian carbonate rocks are not known in the area, thus the source area of the boulders (likely olistoliths) is currently unknown. Possibly the carbonate sedimentation continued in some areas from the Early–Middle Devonian into the Frasnian. A reanalysis of the limestone boulders in the basal conglomerates and other scattered limestone occurrences in the Cabrela area is underway and will shed light on this subject.

Recent work performed by Moreira et al. (2016) also shows clear similarities between the $^{87}Sr/^{86}Sr$ ratio signature presented in Pena, Cortes and Covas Ruivas limestones (ratio value lower than 0,70800) with the global values defined for Early-Middle Devonian times (Veizer et al. 1999; McArthur et al. 2012). However, the Pedreira da Engenharia dolomitized limestones, with similar age and genesis, present higher $^{87}Sr/^{86}Sr$ values (0,70972), which, according to Moreira et al. (2016), could be the result of secondary dolomitization processes.

Thus the sedimentation of the Odivelas limestone and correlatable units occurred in an interval between the latest Emsian to the early Givetian, possibly extending into the Frasnian.

The current distribution of Devonian limestones reflects their original disposition, but also post deposition processes, tectonic and possibly sedimentary. Their current small areal extent is likely a consequence of their original limited extent,

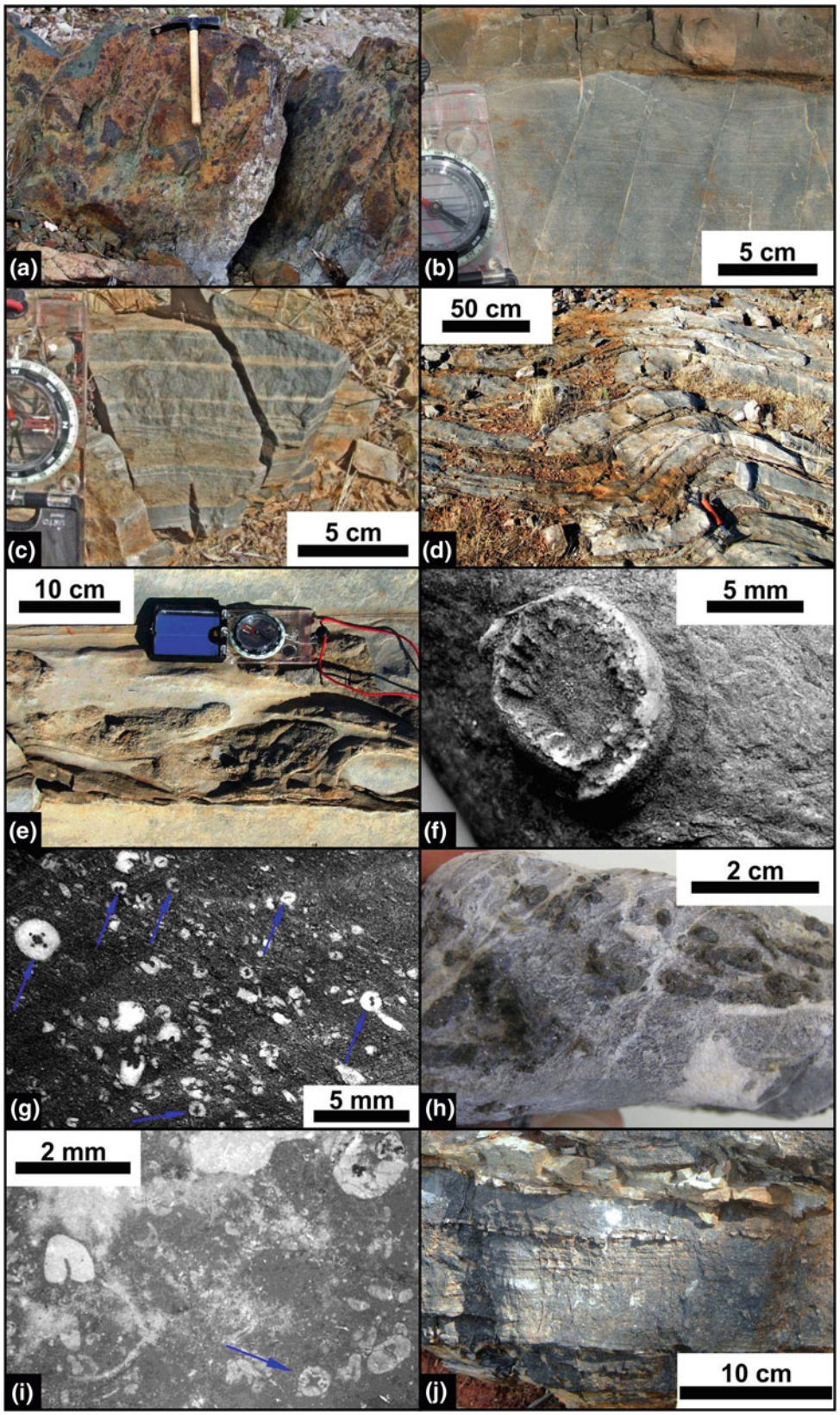
(a)
(b)
5 cm
(c)
5 cm
50 cm
(d)
10 cm
(e)
5 mm
(f)
(g)
5 mm
2 cm
(h)
2 mm
(i)
(j)
10 cm

Fig. 11.12 Outcrop and polished slabs photographs of the Odivelas limestone and correlatable units; **a–e** Covas Ruivas locality: **a** Pyroclastic rocks below the first calciturbidite beds; **b** detail of calciturbidite bed (note fining upward character and cross bedding on top) and sharp contact with the tuffite bed above (adapted from Machado et al. 2010); **c** thinly bedded tuffite near the base of the calciturbidite sequence (adapted from Machado et al. 2010); **d** alternation of calciturbidites (thicker lighter beds) and tuffites (thinner darker beds) gently folded; **e** convolute bedding showing a mix of tuffite material (darker) in a calciturbidite bed as evidence of slope syn-sedimentary deformation; **f–h** Cortes locality: **f** *Pseudamplexus* sp. coral weathered out in loose limestone boulder (adapted from Machado et al. 2009); **g** Crinoidal limestone with small cupressocrinitid and gasterocomids columnals (arrows), polished slab (adapted from Machado et al. 2009); **h** packstone with amphiporids (high relief) and crinoidal, brachiopod and ostracod fragments; **i** Caeirinha locality. Crinoidal limestone with small cupressocrinitid columnals (arrow), thin section (adapted from Machado and Hladil 2010); **j** Cabrela locality. Pedreira de Engenharia Fm. Calciturbidite bed with fining upward trend and sharp contact with the (?) hemipelagic sediment above. Note similarity with B

but also the result of erosional processes of Devonian rocks (along with older and younger Paleozoic rocks) in the Alentejo peneplain.

While in Odivelas area the limestone rocks are clearly in situ (stratigraphically bounded by Rebolado volcanics; Figs. 11.11 and 11.12a), the other occurrences along the western border of the OMZ may be tectonically displaced, as in the Cabrela and Toca da Moura complexes. The limestones interpreted as olistoliths in these complexes (which are at least partially Frasnian in age) and the limestone boulders in the basal conglomerate of the Toca da Moura complex show that during the Mississippian the Odivelas limestone was being eroded.

Although the Devonian limestone outcrops are few and small, in Covas Ruivas two distinct episodes of folding can be discriminated (Moreira et al. 2010), which seem to represent the most recent (Carboniferous?) deformation events. However, the post-depositional tectonics in western OMZ is clearly dominated by brittle to brittle-ductile structures. Three main families can be highlighted: (1) N-S to NNW-SSE right-lateral faults, which also mark the limit between the OMZ and SPZ near Cabrela and in the late-orogenic Santa Susana Carboniferous basin; (2) WNW-ESE to W-E faults, including the Torrão and Ferreira-Ficalho faults, and (3) NE-SW sinistral faults, genetically associated to the large Messejana fault (Fig. 11.10). These faults were active during the Variscan cycle (e.g. Moreira et al. 2010, 2014; Machado et al. 2012), and possibly some of them could control the Carboniferous sedimentation. However, some of these families have Meso-Cenozoic reactivation (e.g. Pimentel and Azevedo 1994; Cabral 2012), which further complicates the structural pattern and partially obliterates its kinematic record during the post-Devonian evolution of southwestern OMZ.

11.3.1.4 Global Events and Intercontinental Correlation

The Basal Choteč Event (BCE) is a global event which corresponds to a transgressive pulse just above the Emsian-Eifelian boundary. In carbonate slope conditions this is materialized by suboxic organic-rich sediments and lower carbonate sedimentation rates. These sediments are frequently overlain by coarse bioclastic calciturbidites or debris-flow carbonate breccias (e.g. Berkyová et al. 2008; Chlupáč and Kukal 1986). This sequence of lithologies is precisely what is observed in the Covas Ruivas section from upper *partitus* to *costatus* conodont biozones, consistent with the BCE ages of other localities around the world. The magnetic susceptibility record is also consistent and correlatable with other sections such as Lone Mountain, Nevada USA; Issemour, Morocco; Red Quarry, Barrandian Czech Republic and Khoda-Kurgan Gorge, Uzbekistan (see Machado et al. 2010 and references therein for details).

The end-Eifelian Kačák-otomari Event is another anoxic event which is potentially recorded in a small (2 m thick) calciturbidite section in the Cortes locality. The organic-rich limestones with chert nodules, low magnetic susceptibility magnitudes and pattern, correlatable with other sections in the Czech Republic (Hladil et al. 2006) are tentative, but not definitive indications of the record of this event (see Machado et al. 2009 for details).

Overall, the age, local palaeogeographical setting associated with volcanic buildings, the reef fauna and even the timing and nature of the magmatism are strikingly similar to other areas in Variscan Europe, notably the Rhenish area (Braun et al. 1994; Königshof et al. 2010) in Germany, Horní Benešov in Moravia (Hladil et al. 1994; Galle et al. 1995) and neighboring regions (Krebs 1974). These occurrences are part of the peri-Laurussian realm of the inner side of the Variscan tectonic facies belt. In both Cortes (late Eifelian-early Givetian) and Covas Ruivas (early Eifelian) the reef fauna is particularly diversified, containing elements which that are typical of the Rhenish area, but also Peri-Gondwana elements (Machado et al. 2009, 2010).

11.3.1.5 Geodynamic Evolution: Implications to SW Iberia Variscides

Local and Regional Paleogeography

Considering the known lithofacies, both carbonate and volcaniclastic, the fossil content and their stratigraphic and spatial relationships, the local paleogeography can be modelled with significant detail. Reef systems developed around the top of volcanic edifices (Fig. 11.13) where their top would be close enough to the sea surface to allow colonization and development of reef building taxa. These were

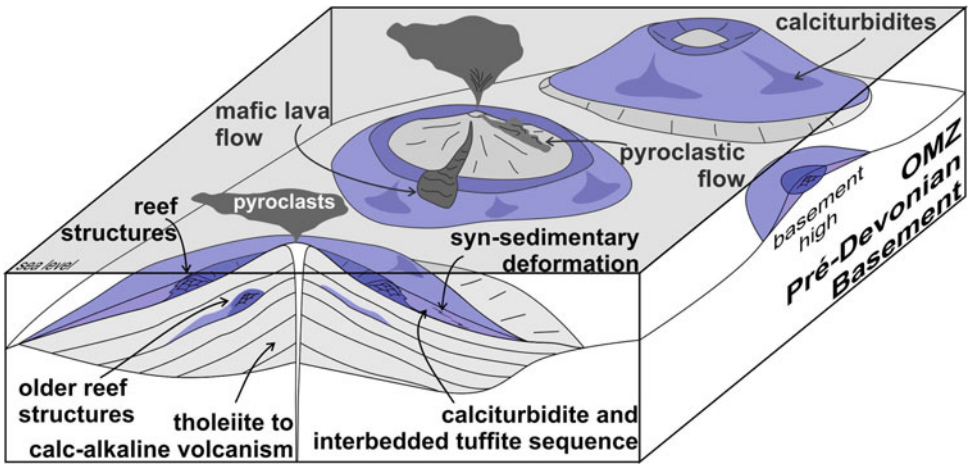

Fig. 11.13 Latest Early Devonian to Middle Devonian schematic model of the local/regional paleogeography of the Odivelas-Cabrela area in southwestern OMZ

probably isolated reefs, not larger than a few km across, possibly forming atolls and perhaps small detached carbonate platforms where the seabed morphology allowed it. On the flanks of the volcanic edifices, coeval peri-reefal sedimentation occurred, essentially as calciturbidites, extending at least to the base of slope. Overall, the basin can be interpreted as intra-arc.

Volcanic and volcaniclastic rocks pre-date and post-date carbonate sedimentation and constitute the majority of the rocks filling the accommodation space in the basin, succeeded by younger rocks (Cabrela and Toca da Moura complexes?). In the Cabrela area, the absence of direct evidence for coeval volcanic rocks suggests these reefs and consequent peri-reefal sedimentation could also develop in basement highs (Fig. 11.13).

According to Andresen et al. (2003), the formation of calciturbidites is influenced by several factors, among which sea level fluctuations and local slope and seafloor topography stand out, although some calciturbidite sequences are directly related to tectonic activity. In southwestern OMZ, the tectonic environment and the seafloor topography seem to be coupled during the Devonian. The subduction process, which probably began during the Early Devonian (see below) generated a volcanic arc and seafloor elevations (basement highs) (Fig. 11.14a). Over these volcanic and tectonic reliefs, under the previous mentioned favorable environmental conditions, reef systems could develop that would be eroded/dismantled along their edges, generating deposition of calciturbidite sequences on the slopes (Fig. 11.13), including occasional debris-flow breccias and syn-sedimentary deformation (Fig. 11.12e).

11.3.1.6 Subduction Timing: A Proposal to the Devonian Evolution of SW Iberia

The beginning of oblique subduction process of the Rheic Ocean under the OMZ margin is poorly constrained. Although it is considered that the process began during the Devonian (e.g. Ribeiro 1983; Quesada 1990, 1991; Oliveira et al. 1991; Moreira et al. 2014), some authors consider that it may even started at the time of the Silurian-Devonian boundary (e.g. Ribeiro et al. 2010). Stratigraphic (e.g. Oliveira et al. 1991; Machado et al. 2010; Araújo et al. 2013),

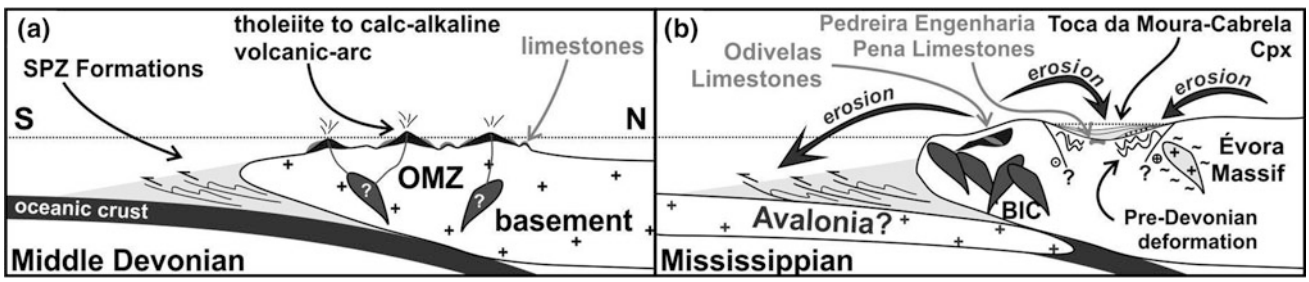

Fig. 11.14 Schematic model of Devonian-Mississippian evolution of the OMZ southwest branch. N and S are current coordinates: **a** development of proximal volcanic arc with growth of reef structures, related to subduction during the Middle Devonian; **b** beginning of continental collision process, with emplacement of large plutonic bodies (BIC). The Devonian volcanic arc and limestones are partially eroded, feeding the OMZ and SPZ synorogenic Mississippian basins

magmatic (e.g. Costa et al. 1990; Santos et al. 1990; Moita et al. 2005a; Silva et al. 2011), metamorphic (e.g. Quesada and Dallmeyer 1994; Moita et al. 2005b; Pedro et al. 2013) and structural (e.g. Ribeiro 1983; Araújo et al. 2005, 2013) data clearly show the presence of tectono-metamorphic events during Devonian times.

The sedimentary and biostratigraphic data described above are consistent with crustal uplift of the OMZ during Early Devonian (at least during the Emsian; circa 400 Ma) times, possibly related to the beginning of the subduction process (Moreira et al. 2014). Indeed, the characteristic euxinic marine sedimentation of the Silurian times (Black Shale Series; e.g. Piçarra 2000; Araújo et al. 2013) is replaced by shallow carbonate sedimentation in central OMZ (Ferrarias and Barrancos) although here the age is poorly constrained (Late Silurian to Devonian), because the sedimentary record is fragmentary (e.g. Piçarra 2000; Piçarra and Sarmiento 2006; Araújo et al. 2013). This trend is possibly present in the Odivelas sector, but the sedimentary record is incomplete. The carbonate sedimentation in the SW branch of the OMZ seems to persist until the Frasnian, although only some remobilized limestones were found in the Cabrela VS Complex (Boogaard 1983; Pereira and Oliveira 2003a, b; Pereira et al. 2006).

The Devonian magmatism, poorly represented in the OMZ, can be observed in the Peroguarda Unit. Although there are no geochronological data which supports its Devonian age, the presence of Lower-Middle Devonian limestones interbedded with the Rebolado Basalts (Oliveira et al. 1991; Moreira et al. 2010) constrains its age. The orogenic low-K tholeiitic to calc-alkaline geochemical signature of the Rebolado Basalts (e.g. Santos et al. 1990, 2013; Silva et al. 2011) seems to indicate that proximal volcanic arc magmatism is represented by this unit. With (Late) Devonian age and far from the subduction zone, a calc-alkaline to shoshonitic magmatism is developed in Veiros-Vale Maceira (Central OMZ; Costa et al. 1990; Moita et al. 2005a). The geochemical and spatial arrangement of Devonian magmatism suggests that subduction related magmatic activity migrated to the north, assigning a north polarity to the Rheic subduction under the OMZ, extending up to 365 Ma—Famennian (e.g. Moita et al. 2005a; Araújo et al. 2013).

Recent geochronological studies Braid et al. (2011; Pereira et al. 2012a; Rodrigues et al. 2015; Pérez-Cáceres et al. 2016, 2017), based on detrital zircons content in OMZ and SPZ Carboniferous synorogenic sedimentary sequences, show large populations of Devonian inherited zircons, which may represent an indirect evidence of subduction-related magmatism during this period. The Mississippian Cabrela Basin siliciclastics provide two Devonian inherited zircon clusters, with Eifelian-Givetian and Famennian ages, respectively (Pereira et al. 2012a). Similar clusters are also obtained in the SPZ Mississippian turbidites of Mértola and Mira Formations (Pereira et al. 2012a; Rodrigues et al. 2015), although in Mira Formation, only the latter cluster (Famennian) is present. These SPZ units possibly have a source area in southwestern OMZ (Jorge et al. 2013). In turn, in the Pulo do Lobo terrane the flyschoid Santa Iria Formation presents a Late Devonian cluster of inherited zircons (Braid et al. 2011; Pérez-Cáceres et al. 2016, 2017), while the Ribeira de Limas and Ronquillo Formations yielded Early Devonian (Emsian) inherited zircons that represent the youngest Devonian population in these units (Pérez-Cáceres et al. 2016, 2017).

The previous mentioned data are in agreement with ages attributed to Peroguarda Unit volcanism, which seems to represent a preserved section of volcanic arc magmatism in the SW branch of the OMZ, related with subduction processes and supporting the existence of a magmatic arc during Devonian times. This was partly eroded during the Mississippian, intruded by younger plutonic rocks composing the Beja Igneous Complex and finally eroded by recent peneplanation.

Also the metamorphic ages obtained from high pressure-low-temperature (HP-LT) metamorphic rocks, in the SW border of the OMZ, are in agreement with a Devonian subduction process. Geochronological data indicate a Famennian age to the baric peak of this HP-LT metamorphism (371 ± 17 Ma; Sm/Nd isochronous whole rock-garnet; Moita et al. 2005b; Pedro et al. 2013), materializing the active subduction processes.

After the genesis and development of volcanic arc magmatism and the related carbonate sedimentation, the collision process between SPZ and the OMZ began during the Mississippian (probably during the Tournaisian; e.g. Jesus et al. 2007, 2016; Ribeiro et al. 2010; Moreira et al. 2014; Fig. 11.14b). During this period, the magmatic activity became intense in the Beja Igneous Complex (Pin et al. 2008; Jesus et al. 2007, 2016), and also in the Évora Massif (Chichorro 2006; Pereira et al. 2015).

During the Mississippian (Fig. 11.14b) accommodation space in the southwestern OMZ basin was enhanced in response to ongoing collision, the infill being dominated by turbidite sedimentation and volcaniclastics (Toca da Moura and Cabrela VS complexes; e.g. Ribeiro 1983; Pereira et al. 2006). The previously deformed OMZ substrate and arc sequences were eroded, feeding these basins as indicated by the lenses of Frasnian limestones found in the western border of the Cabrela basin (Cabrela Station limestones), which some authors interpret as olistholiths within Mississippian turbidites (Pereira and Oliveira 2003a; Pereira et al. 2006; Oliveira et al. 2013). In the Cabrela VS complex, fragments of granites and slates are described in the basal conglomerate (Ribeiro 1983; Oliveira et al. 1991; Pereira et al. 2006), emphasizing the unconformity between the Cabrela VS Complex and the previous deformed sequence, consequently dating the first deformation episode as earlier than Late Devonian.

In turn, the Toca da Moura and Cabrela complexes calc-alkaline Carboniferous volcanism may not represent the

real volcanic arc magmatism, but the remains of the processes after the subduction stop, i.e. during the collision, as mentioned by Santos et al. (1987). This magmatism could be related with the Beja Igneous Complex emplacement or the Évora Massif activity (Fig. 11.14b) as proposed by Chichorro (2006).

Acknowledgements

Noel Moreira acknowledges Fundação Calouste Gulbenkian for financial support, the FCT (Portuguese Science and Technology Foundation) PhD grant (SFRH/BD/80580/2011) and the funding provided by the Institute of Earth Sciences (ICT), under contract with FCT (UID/GEO/04683/2013).

11.3.2 Terena Flysch Basin (Late Early Devonian-Early Visean)

J. T. Oliveira, C. Quesada, J. M. Piçarra, Z. Pereira

The Terena flysch represents the oldest synorogenic deposits known in the Gondwanan units of the Iberian Massif, providing evidence for the onset of deformation related to the Variscan orogeny. Its main exposure lies along the core of a long (ca. 150 km) and narrow sigmoidal shape syncline that extends from west of Estremoz in Portugal to southwest of Santa Olalla del Cala in Spain (Terena syncline; Fig. 11.15). Other exposures are located towards the eastern extremity of the syncline, both north and south of it (Fig. 11.15). Most of the contacts of the synorogenic succession are currently faulted, rendering the recognition of the original relationships with the surrounding units a very difficult task. With a local single exception that will be described below, structural complexity also prevents recognition of any of the basin margins, whose original location and geometry are completely unknown. At present all the outcrops of the Terena flysch only occur within the southern units of the Ossa Morena Zone.

The basin is mostly filled by a flysch succession dominated by greywackes and shales with turbidite characteristics. Locally, conglomerates (generally matrix-supported) and chaotic olistostromes also occur as well as minor volcanic rocks mainly towards the east. Pre-orogenic successions occur in contact with the Terena flysch encompassing the Cambrian, Ordovician, Silurian and Lower Devonian. This pre-orogenic succession is affected by low-grade metamorphism not exceeding the chlorite zone. The basin deserved attention due to the excellent content of Silurian graptolite faunas in olistoliths interbedded with the turbidites (Delgado 1908, Piçarra 2000) and Lower Devonian macrofaunas of crinoids, corals, bryozoans, bivalves (Perdigão et al. 1982, Le Menn et al. 2002) and plant remains (Teixeira 1951).

The interpretation of the Terena flysch within the context of the Variscides has been the aim of some controversy, particularly in what the age and structure is concerned. Firstly considered of Lower Devonian age by Teixeira (1951) based on plant remains, this interpretation was criticized by Schermerhorn (1971) who assumed that the plant remains are poorly preserved and do not allow a good classification. This author admit an Upper Devonian to Lower Carboniferous age for the unit and suggests that it is a lateral equivalent of the Santa Iria Formation in the north limb of the Pulo do Lobo Anticline and of the Culm flysch in the South Portuguese Zone, both of which he considered of Lower Carboniferous age.

More recent data provided by palynomorphs and graptolites (Pereira et al. 1999a, b) indicate a Lower Devonian age for most of the flysch succession outcropping along the Terena syncline at least in Portugal. However, Upper Devonian to Lower Carboniferous conodonts, echinoderms and brachiopods found in the easternmost exposures where carbonates are more abundant, prove that deposition of the Terena flysch may have lasted until at least late Tournaisian-early Visean times (Boogaard and Vázquez 1981; Weyant et al. 1988; Giese et al. 1994). On the basis of this age difference Giese et al. (1994) and Expósito (2000) proposed a division of the Terena Flysch into a lower succession of lower Devonian age (Terena Formation proper as defined in Portugal), and an upper succession, more varied lithologically (*Upper Terena* member in Spain; Matas et al. 2010). Whether there was a progressive migration of depocenters towards the southeast or we deal with two distinct successions separated by a variably wide time gap will be discussed below.

The Terena flysch basin was also interpreted as a through filled with sandy turbidites that rest unconformably on a previously structured substrate (Ribeiro et al. 1979; Perdigão et al. 1982; Oliveira et al. 1991) an interpretation that will also be discussed below.

11.3.2.1 Stratigraphy

As outlined above, the largest outcrop of the Terena flysch forms the core of the Terena syncline, a very asymmetric second phase structure with subvertical to moderately N-verging axial plane cleavage. This structure appears to be the only affecting the flysch succession. Although the contacts with the adjacent pre-orogenic successions are frequently faulted, primary relationships are locally exposed mainly along the southern limb. There, basal flysch strata paraconformably overly an incomplete Silurian succession belonging to the so-called Xistos com Nódulos Formation (Fig. 11.16). On the northern synclinal limb, a higher part of the flysch succession is faulted against a complexly refolded succession including Silurian ("Xistos com Nódulos" Formation in Portugal, "Pizarras negras y liditas" in Spain) and Lower Devonian rocks (Xistos Raiados and Russianas

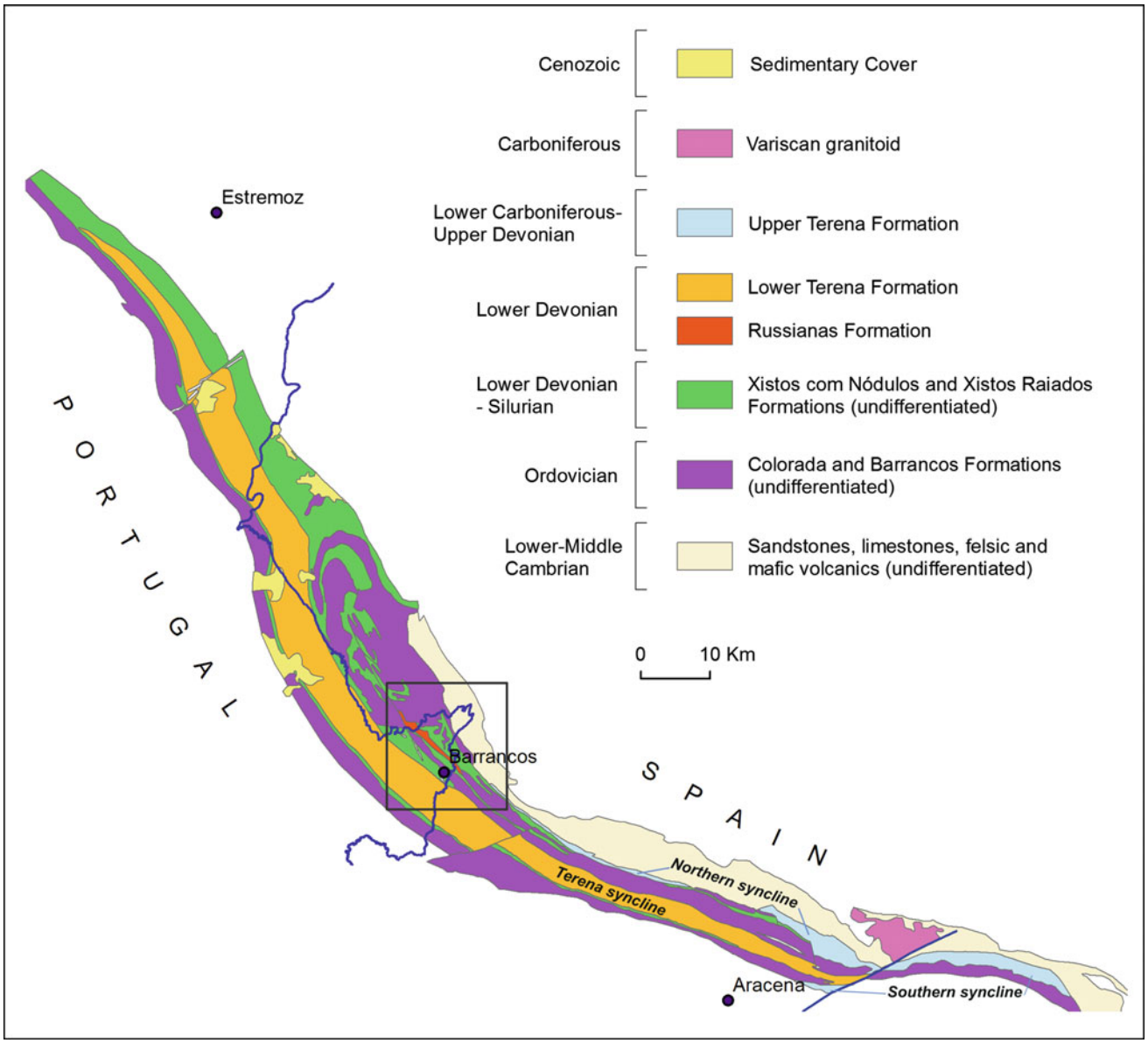

Fig. 11.15 Schematic map showing the distribution of Terena flysch outcrops in south central OMZ

Formations). Only rocks of the Lower Devonian *Lower Terena* succession (Terena Formation sensu stricto) have been recognized so far within the Terena syncline. The lack of palynological studies on the Spanish part of the syncline leaves open the possibility that younger turbidites belonging to the *Upper Terena* succession may also exist there.

The Terena syncline has an abrupt end towards the east, where it is cut by the Zufre fault, a regionally important late-stage NE-SW trending sinistral fault. This fault also forms the eastern termination of the flysch outcrop located north of the Terena syncline (Fig. 11.15). There, only the *Upper Terena* succession is thought to occur (Matas et al. 2010) but, again, the lack of systematic paleontogical studies casts some doubts on this statement. The same is applicable to the southernmost belt where the flysch crops out (Fig. 11.15). Both flysch exposures have yielded Late Devonian and Early Carboniferous fossils, which have led most authors to include them in the *Upper Terena* succession.

11.3.2.1.3 Lower Terena Succession (Terena Formation Sensu Stricto)

This unit occupies the core of the Terena syncline and consists of a flysch succession dominated by alternations of greywackes and shales, and limited intercalations of conglomerates. The sand/shale ratio varies across the basin. In the southwest flank the greywackes are thick-bedded, frequently amalgamated, show typical Bouma sequences, and the sand/shale ratio is >1. Fining and coarsening upward cycles

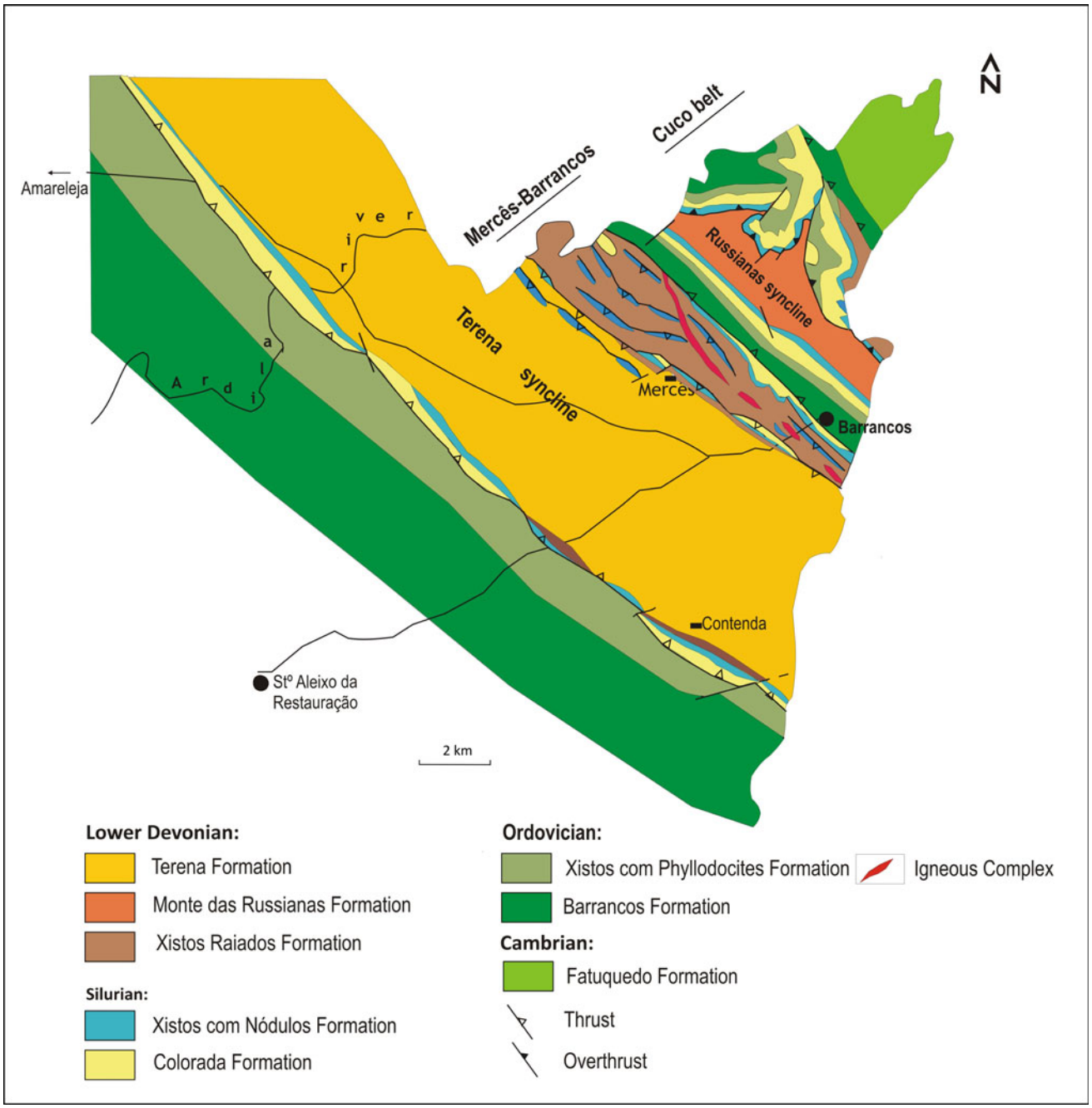

Fig. 11.16 Geological map of Barrancos region

are common and may attain 50 m in thickness. The lithological sequence becomes progressively more thinner-bedded towards the center of the syncline. Polygenic conglomerates occur some tens to one hundred meters above the southwestern base of the sequence, usually in lenticular rock bodies 150–200 m long and maximum 20 m in thickness, forming a strip of at least 20 km in length. They show up to 5 cm size clasts and pebbles of quartz, quartzite, lydite, shale, and in places (S of the Granja village) broken remnants of crinoids, bryozoans and corals, all dispersed in a greywacke matrix. Some clasts show evidence of pre-depositional deformation fabrics. Polygenic conglomerates also crop out in the center of the syncline, although with much less dimensions. They are of pebbly-mudstone type with clasts of quartz, lydite, quartzite, greywacke, slate with two cleavages, deformed and cleaved limestone and felsic volcanic rocks, all supported by a shaly matrix. The limestone clasts provided poorly preserved *Tentaculites* sp (Perdigão et al. 1982).

In the northeast flank of the syncline the flysch sequence shows a sand/shale ratio <1, the greywacke beds are centimeter-thick and the intervals with shales in the sedimentary package are thicker than in the west flank, frequently above 20 m. No conglomerates are known. Still in this flank, lenticular outcrops containing quartzite, lydite and black shale, few meters wide and reaching up to 100 m in length are intercalated in the flysch sequence. These rocks, usually imbricated with the flysch are interpreted as olistoliths. Towards the east, centimeter-to-decimeter thick limestone lenses locally occur interbedded with the siliciclastic turbidites but they have not yielded any identifiable fossil remains so far. Available paleocurrent data indicate a predominance of ESE and WSW directions (Apalategui et al. 1990), i.e. roughly parallel to the orientation of the Terena syncline.

The northern boundary of the Terena syncline is locally characterized by a fault-bounded belt in which a set of meter-to-decameter thick igneous dikes (both felsic and mafic) intrude into a complex tectonically imbricated rock association. This includes, the Silurian Xistos com Nódulos Fm., the Lower Devonian Xistos Raiados Fm., limestones that provided near Barrancos poorly preserved crinoid fragments and enigmatic breccia of unknown age incorporating clasts of limestone, slate, mafic and acidic volcanic rocks. This NNW-ESE belt is known in Portugal by the name of *Igneous complex* and can be followed as a rosary of outcrops for ca. 60 km (from near the east termination of the Estremoz antiform to few kilometers southwest of Encinasola in Spain).

The Terena Fm. yielded graptolites (*Monograptus hercynicus*; Fig. 11.17b) and miospores of Lochkovian age at its base, and of Praguian, Praguian-Emsian transition and Emsian ages in several places in the central area of the syncline (Pereira et al. 1999b). Lower Devonian plant remains (*Psylophita*, according to Teixeira 1951) can also be found in the greywacke beds as well as meandering ichnofossils such as *Helminthopsis, Gyrochorte, Protopaleodictyon*. Collectively, these paleontological findings allow establishing a Lower Devonian age (Lochkovian to Emsiam) for the Terena Fm. This is a very interesting point, since this spread of ages largely overlaps the ages of the pre-orogenic Xistos Raiados and Russianas formations outcropping immediately to the north of the Terena syncline. A possible interpretation of this apparent contradiction will be discussed below.

11.3.2.1.4 Upper Terena Succession

As already outlined, this rock succession is only exposed with certainty at the cores of two second Variscan phase synclines located few kilometers north and south of the Terena syncline in easterly parts of the Ossa Morena Zone in Spain (Fig. 11.15). This succession has not been distinguished so far within the latter syncline. Siliciclastic turbidites, compositionally similar to those in the Terena Fm., form the most common lithology by far, thence its attribution to the Terena flysch succession. The southern contacts of this *Upper Terena* succession in both synclines are generally faulted but on the contrary the northern contacts locally preserve original unconformable relationships over previously deformed pre-orogenic successions. The northern syncline (Fig. 11.15) is particularly interesting in this respect, as it shows discontinuous exposure for ca. 50 km (from near

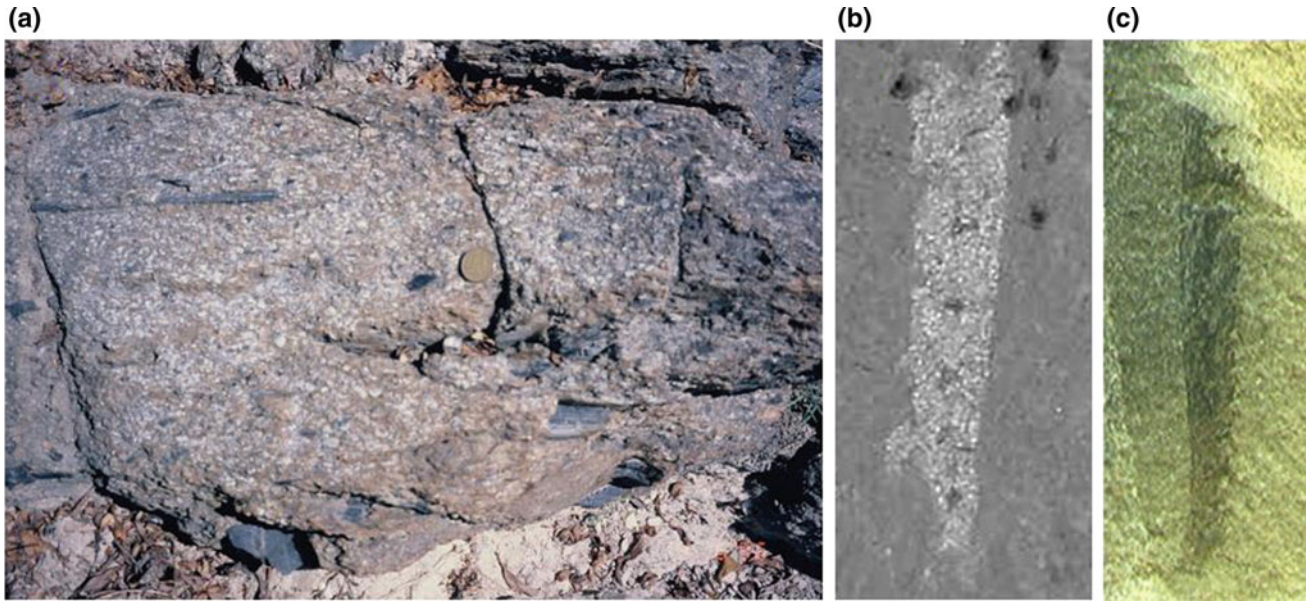

Fig. 11.17 **a** Close up of the conglomerates interbedded in the flysch showing dark shales and lydites of the Xistos com Nódulos Fm. dispersed in a conglomerate rich in well-rounded clasts and grains of quartz; **b** *Monograptus hercynicus* sp, Terena Fm. flysch, Mercês farm; **c** *Monograptus uniformis* sp, Xistos Raiados Fm., Mercês farm

Cumbres de San Bartolomé in the west up to immediately southwest of Santa Olalla del Cala where the Zufre fault marks the eastern end of the exposure) of the basal unconformable contact of the flysch succession over various Cambrian formations recumbently folded previously. When exposed, the basal unconformity is overlain by discontinuous lenses of polymict conglomerates succeeded upwards by classical Bouma sequence turbidites, in which other meter-thick conglomerate layers occur interbedded locally. Many clasts and cobbles carry pre-depositional tectonic fabrics. Locally, crinoid-bearing detrital limestones appear above the basal conglomerates (Apalategui et al. 1979). The most striking feature of this *Upper* Terena succession is exposed along the ridge and slopes of Sierra del Álamo (ca. 5 km south of Cumbres de San Bartolomé) where an impressive breccia unit occurs interbedded with the turbidites (Álamo breccia; Bard 1965). The breccia extends with a WNW-ESE orientation for ca. 5 km and reaches a maximum thickness of ca. 700 m. Most of the breccia has a massive chaotic structure but towards both top and bottom it forms tabular bodies (decimeter to decameter in thickness) separated by turbidite packages. The matrix has greywacke nature and wraps around the (mostly) angular clasts. These vary between centimeters to decameters in size and mainly include all the lithologies present in the underlying Cambrian succession that generally show pre-depositional deformation structures such as cleavages and folds (Apalategui et al. 1990; Giese et al. 1994). Other clasts include greywacke, slates, Silurian black cherts and crenulated phyllites resembling those of the Ordovician Barrancos Fm. Rare but significant crinoid-bearing limestone clasts also occur, in which Giese et al. (1994) reported presence of Upper Devonian corals and probably derive from the above mentioned carbonates overlying the basal conglomerate. Presence of this thick chaotic breccia suggests proximity to a basin margin at this stage or to an intrabasinal active fault scarp.

The southern syncline (Fig. 11.15) shows a similar succession but with some differences, among which more abundant and thicker carbonate horizons. This is the only belt of Terena flysch that does not disappear when cut by the Zufre fault, being displaced 8–10 km in a sinistral sense and extending for some further 20 km eastwards. The basal unconformable contact of the succession rests in this case over deformed slates and mafic metavolcanic rocks of the Ordovician Barrancos Fm. and Ribera de Huelva volcanics, respectively. The first strata over the unconformity correspond to arkosic sandstones and conglomerates, being succeeded by several decameter thick packages of crinoid-bearing carbonates interbedded with green shales and marls. Towards the top, the carbonates show a transition to diluted turbidites which give way to a classical Bouma sequence turbidite succession (several hundred meters thick) with interbedded matrix-supported conglomerates. Noticeably, only Ordovician, Silurian and possibly Devonian lithologies are represented in the clasts, with a remarkable absence of the Cambrian rocks so abundant in the Álamo breccia, which suggests different sources for the two marginal synclines. Concerning the age of this *Upper Terena* succession, the carbonates yielded conodont faunas of late Tournaisian-early Visean age in the outcrops located west of the Zufre fault (Boogaard and Vázquez 1981) and of Famennian age in those located east of the fault (Weyant et al. 1988). Besides, Giese et al. (1994) reported bryozoans, echinoderms, gastropods and plant remains of early Carboniferous age, therefore suggesting an overall Late Devonian-early Carboniferous age (Matas et al. 2010).

11.3.2.2 Basin Formation and Tectono-Stratigraphic Development

Confirmation of the Lower Devonian age of the Terena Fm., including rocks as old as Lochkovian (ca. 415 Ma), provides evidence for initiation of the Variscan orogeny some tens of million years earlier than previously recognized in the Gondwanan side of the orogen. However, the geodynamic scenario at this stage remains a matter of speculation as: (i) typical basin margin facies are nor preserved anywhere along the Terena syncline, thus preventing recognition of the size, orientation and geometry of the basin at this early stage; (ii), the flysch basin developed coeval to persistence of passive margin platform sedimentation throughout the Gondwanan margin in the Iberian Massif, including the Ossa Morena Zone northeast of the Terena basin as discussed below; and (iii) from the very base, conglomerates in the Terena Fm. include traceable clasts carrying pre-depositional deformation fabrics despite the fact that no clear angular unconformity is discernible when the original contact is exposed. By Upper Devonian time, the *Upper Terena* succession exposed in the two marginal synclines clearly rests unconformable onto previously deformed pre-orogenic sequences. Since the two flysch successions never occur in contact and the paleontological evidence is very meagre in Spain, it is so far impossible to decipher the stratigraphic relationship between the *Lower* and *Upper Terena* successions.

In order to frame the Terena Basin tectono-stratigraphic development it seems appropriate to take into account the sedimentary and tectonic situation existing in the Ossa Morena Zone immediately before, and during the formation and evolution of the Terena basin. During the Silurian the sedimentation was platformal, fine-grained, euxinic and full of life everywhere. Graptolites were the dominant faunas and the assemblages recovered in Barrancos area, as well as in the Valle and Cerrón del Hornillo synclines located to the NE, cover all the Silurian graptolite biozones. Bivalves, trilobites, crinoids, ostracods, cephalopods, conodonts and solitary corals can be also found across the sedimentary sequence (Jaeger and Robardet 1979; Robardet and Gutiérrez Marco

2002, 2004; Loydell et al. 2015; see also Chap. 3-Passive margins, this volume). The marine and euxinic platform that predominated during the Silurian deepened locally at the location of the present southern Ossa Morena Zone during the Lower Devonian generating a trough where the flysch sedimentation was accumulated (Terena Fm). All along the northeastern regions of this trough, euxinic graptolite sedimentation continued during the Early Devonian (Lochkovian) which gave way during the Praguian and the Emsian to thin-bedded shale and siltstone sedimentation (Xistos Raiados Fm.), locally with detritic limestone intercalations (Russianas Fm.), rich in benthic faunas of trilobites, ostracods, bivalves, corals and abundant brachiopods (Perdigão et al. 1982; Le Menn et al. 2002; Robardet and Gutiérrez-Marco 2004). After a Mid Devonian gap, sedimentation went on in this northeastern areas as shown by deposition of, still platformal, shales, calcareous sandstones and limestones, preserved in the core of the Valle syncline, and which provided rich faunas of brachiopods, bivalves and conodonts of Famennian age (Robardet and Gutiérrez-Marco 2004). By the Late Devonian, deposition of the *Upper Terena* succession proceeded over an already deformed substrate. At this stage the basin may have likely been smaller in size, having a margin at the location of the regionally important Juromenha-Hinojales fault, which may have shed the locally derived Cambrian clasts of the Álamo breccia. Perhaps, the Mid Devonian gap referred to above might be the expression in the foreland of the propagation of the first Variscan deformation phase, which may have reached the Terena basin and its adjacent passive margin at that time.

The existence of fossil remains of crinoids, bryozoans and corals in the polygenic conglomerates interbedded in the Terena Fm. close to its southwestern base, suggests provenance from nearby (?) Lower Devonian sediments removed by erosion. The more proximal flysch accumulation in the western flank of the Terena syncline, together with the occurrence of lenticular polygenic conglomerates, interpreted as channel lobes, suggest sedimentary provenance from an uplifted block in the western areas, probably in connection with the N-trending first Variscan shortening episode discussed below. Furthermore, a litho-geochemical study of the Terena greywackes suggests presence of arc volcanics in the source (Borrego et al. 2005; Borrego 2009). This could only be situated in the western regions of the Terena trough since marine platformal sedimentation persisted in the eastern regions during the Devonian, as seen above. In fact, relics of Lower Devonian magmatic arc rocks exist at the southwesternmost tip of the Ossa Morena Zone.

Perdigão et al. (1982) recognized the existence of two episodes of folding and associated cleavages in the Barrancos region. The first episode is underlined by N-S trending, W vergent, recumbent folds, in which the incipient cleavage is restricted to the hinges, being the overturned limbs frequently laminated by thrusting. The same authors also postulated that the expression of the tectonic deformation depends on the structural level: in the upper structural level, cleavage is absent; in the lower structural level the cleavage is restricted to the fold hinges. In turn the second deformation event developed in deeper structural levels, trended NW-SE and developed steeply dipping, slightly asymmetric folds and a very penetrative axial plane cleavage. The clasts of slates with two cleavages, folded and cleaved limestones and felsic volcanics that compose the conglomerates interbedded in the flysch from the very base indicate erosion from a pre-Terena tectonically deformed substrate. Following the same authors, the Terena Fm. is only affected by the second episode of tectonic deformation, and this led them to assume that this unit rests unconformably on the underlying units. Consequently they concluded that the first episode of tectonic deformation is post- Russianas Fm. and pre-Terena flysch deposition, that is, of Mid Devonian age, while the second episode with associated strong cleavage postdates Terena flysch deposition. This interpretation can be no longer sustained on the basis of the following data: (1) when exposed along the southwestern limb of the Terena syncline, the basal contact of the Terena Fm. appears paraconformable over Silurian strata, if there is a sedimentary gap it is not related to any penetrative deformation of the substrate in the flysch depositional area; (2) according to the available paleontological evidence at least a part of the Terena Fm. is coeval to the platformal Xistos Raiados/Russianas formations, therefore juxtaposition of two originally separated paleogeographic domains is indicated rather than stratigraphic superposition as interpreted by Perdigão et al. (1982). Figure 11.18 is the authors' visualization of the Terena basin in Barrancos region during the late Lower Devonian, i.e. at the time when the Terena Fm. was being deposited, which may be applied to the rest of the basin. It is based on the following: (a) basin asymmetry is indicated by continuous sedimentation in the eastern areas and erosion in the western areas, in this case related with uplifting; (b) this uplifting may have been caused by propagation of eastward facing thrust faulting during the first Variscan deformation phase; (c) in response to thrust loading a crustal depression was generated and filled with the Terena flysch sourced in the frontal area of the thrust faulted block, with the sedimentation keeping pace with the faults activity; (d) in the eastern (passive) margin of this depression limited crustal instability affected the Xistos Raiados, Russianas and Terena Fms depositional areas triggering westward gravity sliding, presently preserved as olistoliths; (e) thrusting finally reached the Terena basin giving way to the first E-W compressional tectonic episode which generated folds and weak cleavage. However this episode is only expressed by open folds in the Terena Fm. (upper structural level).

The aforementioned basin asymmetry mimics that of many foreland basins developed in front and as a consequence of a

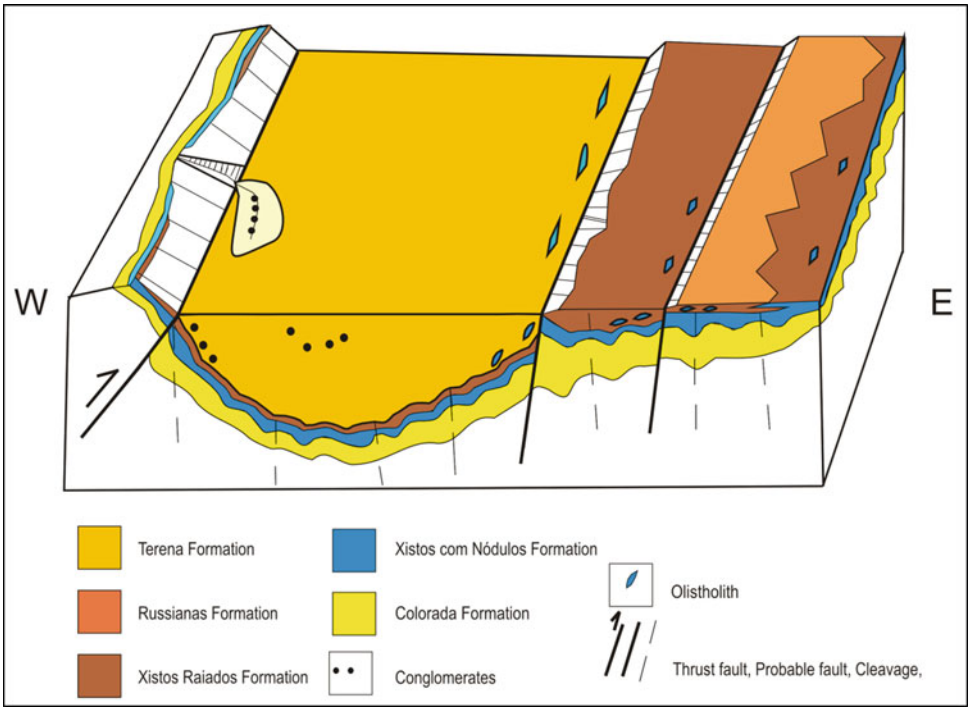

Fig. 11.18 Sketch block-diagram showing the structural control of the basin where the Terena flysch was deposited

propagating thrust wedge. In our case, the active margin is clearly located to the west of the trough whereas to the east, the basin floor probably ramped gently towards the platformal areas not yet reached by the load imposed by the orogenic wedge. Eventual elastic rupture on the passive margin may have triggered forebulge uplift and the instability responsible for the gravitational collapse emplacement of olistoliths within the flysch basin. Propagation of the deformation wave would have progressed ideally from west to east, which is supported by the facies asymmetry in this direction (more proximal in the west and more distal in the east) and the increasing proportion of carbonate interbeds in the Terena Fm. towards the east (presumed passive margin). Presence of previously deformed clasts in conglomerates, traceable to the underlying pre-orogenic rocks, can be easily explained by progressive involvement in the orogenic wedge of those formations and eventually even older parts of the basin fill. Exposure at the surface of those deformed rocks would have allowed their erosion and subsequent transport into the flysch basin, itself not yet reached by the deformation wave.

We do not know for sure whether such easterly propagation progressed continuously from the Terena Fm. into the *Upper Terena* succession. The fact that the latter was deposited clearly after the platformal areas located to the NE of the Terena syncline were affected by the first deformation event, suggests that most likely there was a break in between the two, probably encompassing the Mid Devonian, during which the first Variscan event would have deformed the entire southern Ossa Morena, including the *Lower Terena* basin. Deposition of the *Upper Terena* succession, only preserved in eastern areas, probably took place in a smaller successor basin and lasted at least for the Famennian-early Visean timespan. At this stage the flysch basin was clearly controlled by NW-SE faults such as the Juromenha-Hinojales fault, which neatly defines a basin margin at least during deposition of the Álamo breccia. Probably the faults bounding the so-called *Igneous complex* that mark the northern boundary of the Terena syncline were also active then. However, the predominant turbidite facies are very similar to those in the Terena Fm. and their provenance, away from local supply near the northeastern margin, appears to have remained the same. Finally, the whole region was affected by the second and more penetrative Variscan deformation event, responsible for the pervasive deformation of both flysch successions, starting in post-Early Visean time.

In conclusion, it is suggested that the Terena Flysch trough originated as the distal expression of an ongoing subduction related episode that occurred between the Ossa Morena Zone (Gondwana) and the Pulo do Lobo Oceanic Domain during the Lower Devonian. This tectonic process propagated from west to east and developed an orogenic wedge growing in the same direction. The load imposed on the previous passive margin by the propagating wedge would have caused subsidence and nucleation of a foredeep where turbidites and associated sediments would have been

shed from the propagating active margin (Terena basin). Towards the east, flysch would onlap onto pre-existing platform successions. The deformation wave reached the entire area by the Mid Devonian and caused a first structuration of the Terena Fm., mild though (no cleavage) due to its upper crustal, near surface location. No evidence exists within the Terena basin present exposures for the period comprised between the first deformation and the onset of deposition of the *Upper Terena* succession in Late Devonian (Famennian) times. Whatever the case, flysch deposition resumed with similar characteristics by that time, although presence of interbedded relatively thick carbonate platform successions probably suggests less deep environments at this stage. Finally, the second Variscan deformation event took place in the late Mississippian-Pensylvanian interval. This event in interpreted as a result of the final closure of the Pulo do Lobo oceanic domain, which brought the South Portuguese terrane (Laurussia) to collide with the Ossa Morena Zone (Gondwana), causing the present-day NW-SE structures that characterize the SW Iberia Variscan orogen.

11.3.3 Trench/Fore-arc Basins in the PLT Suture Zone (Frasnian-Famennian)

J. Braid, J. B. Murphy, C. Quesada

Synorogenic deposits are also preserved within the Pulo do Lobo terrane, which materializes the Variscan suture zone in SW Iberia. However, their characterization is generally extremely difficult owing to the pervasive polyphase deformation and mutual imbrication that affect the oldest exposed sequences. The only exception being the Santa Iria flysch (late Famennian) that unconformably covers the other, previously imbricated and polyphase deformed units (Carvalho et al. 1976; Oliveira 1990; Braid et al. 2010, 2011).

Within the presently exposed PLT successions several units exhibit some features diagnostic of a synorogenic character. From older to younger, these are: the Peramora mélange (middle Frasnian), the Alájar mélange (late Famennian) and the Santa Flysch (also late Famennian).

11.3.3.1 Peramora Mélange

Exposure of this unit is currently limited to the core of Los Ciries antiform (south of Aroche) where it is repeatedly imbricated with Pulo do Lobo Fm. schists, forming a complex duplex structure (Braid et al. 2010; Dahn et al. 2014). First defined by Eden (1991), the Peramora mélange is a chaotic deposit consisting of centimeter-to-meter size blocks embedded in a greenish matrix of mafic composition. Microgabbro, basalt and greywacke are the clast-forming lithologies, which apparently do not carry any preexistent internal tectonic fabric. At odds, the matrix is extremely polydeformed and retrograded to a greenschist facies paragenesis (Eden and Andrews 1990; Eden 1991, Braid et al. 2010; Dahn et al. 2014). The fact that the rocks in the clasts do not show any internal tectonic fabric supports the interpretation of this mélange as a primarily sedimentary one; although with enhanced fragmentation during subsequent imbrication with the Pulo do Lobo Fm. schists.

The composition of the matrix exhibits the characteristics of typical N-MORBs and is identical to that of the mafic clasts (Eden 1991; Braid et al. 2010; Dahn et al. 2014), suggesting that both clasts and matrix probably derive from a common oceanic basaltic protolith. The composition of the mafic blocks and matrix of the Peramora mélange mimics that of the more massive metabasalts occurring along the Alfarrobeira-Trindade belt in the Portuguese western reaches of the PLT, also associated with Pulo do Lobo Fm. schists and which could be a similar protolith to that existing at the source of the mélange, which is to be considered of an ophiolitic type. Sm–Nd data reported by Dahn et al. (2014) show highly positive values (+7.9 to +9.1), which suggest an ultradepleted nature. The extremely depleted signature of these basaltic rocks is claimed to be a characteristic of the MORBs associated to the Rheic Ocean (Murphy et al. 2011, 2014).

The schists (Pulo do Lobo Fm.) imbricated with the Peramora mélange yielded a mid Frasnian age palynomorphs association and the same age is assigned to the mélange (Pereira et al. 2018). This is in apparent contradiction with the youngest detrital zircon grains (ca. 348 Ma-late Tournaisian) found in the matrix and Pulo do Lobo schists by Dahn et al. (2014), which are younger than the unconformably overlying Santa Iria flysch (late Famennian) and an intrusive gabbro (ca. 354 Ma-early Tournaisian) of the Gil Márquez pluton (Gladney et al. 2014; Braid et al. 2018), therefore, impossible! The latter authors interpret these younger ages as due to partial rejuvenation via Pb-loss of those zircon grains, probably in connection with post-deposition fluid-assisted shearing, while Dahn et al. (2014) proposed Pb-loss induced by heating associated to emplacement of the Gil Márquez pluton. In addition to these younger zircon grains, a distinctive feature of both the Peramora mélange and Pulo do Lobo Fm. schist is the presence of a significant population of Mesoproterozoic grains (Dahn et al. 2014), also found in other lithostratigraphic units of the PLT (e.g. Ribeira de Limas Fm. and Alájar mélange; Braid et al. 2011; Pérez-Cáceres et al. 2016, 2017). This age population is extremely rare or absent in the two bounding terranes (i.e. the Gondwanan-affinity OMZ to the north of the PLT and the Laurussian-affinity SPT to the south of it). With different relative proportions, all units contain Neoproterozoic, Paleoproterozoic and minor Archean zircon populations (Braid 2011; Braid et al. 2011, 2012; Dahn et al. 2014; Pérez–Cáceres et al. 2017). Presence of zircon, even in small amounts, in primitive N-MORB basalts, specially showing such a spread of ages is rare, suggests a xenocrystic nature of the grains and requires assimilation of continental crustal-derived rocks or

sediments by the basaltic liquid. Similar cases have been described in the recent SW Pacific Ocean by Buys et al. (2014). In our case, owing to the similar detrital zircon age distribution, we favor a process of assimilation of the Pulo do Lobo schist protolith by the magma during its emplacement, which we interpret to represent abyssal sediments laid down directly over the oceanic crust. Assimilation must have been very minor, though, to allow preservation of the highly-depleted geochemical characteristics of the basalts.

The sparse occurrence of the Peramora mélange prevents any attempt to characterize the basin in which it was deposited. Following Quesada et al. (1994) we favor a trench-type basin (Stage 1 in Fig. 11.19) as a likely option on the basis of the following facts: (i) recent finding of HP-metamorphic relics in samples of the Peramora mélange (Rubio Pascual et al. 2013), indicating subduction of this sequence to a certain depth, and (ii) its pervasive polyphase deformation and retrogression to lower pressure, greenschist facies conditions, which may have happened during both the subduction stage and its exhumation and accretion to the upper (Gondwana) plate. These facts provide support to the interpretation by Quesada et al. (1994) and Braid et al. (2010), among others, of the PLT as an accretionary prism, but one with a predominant sinistral strike-slip strain component (Stage 1 in Fig. 11.19).

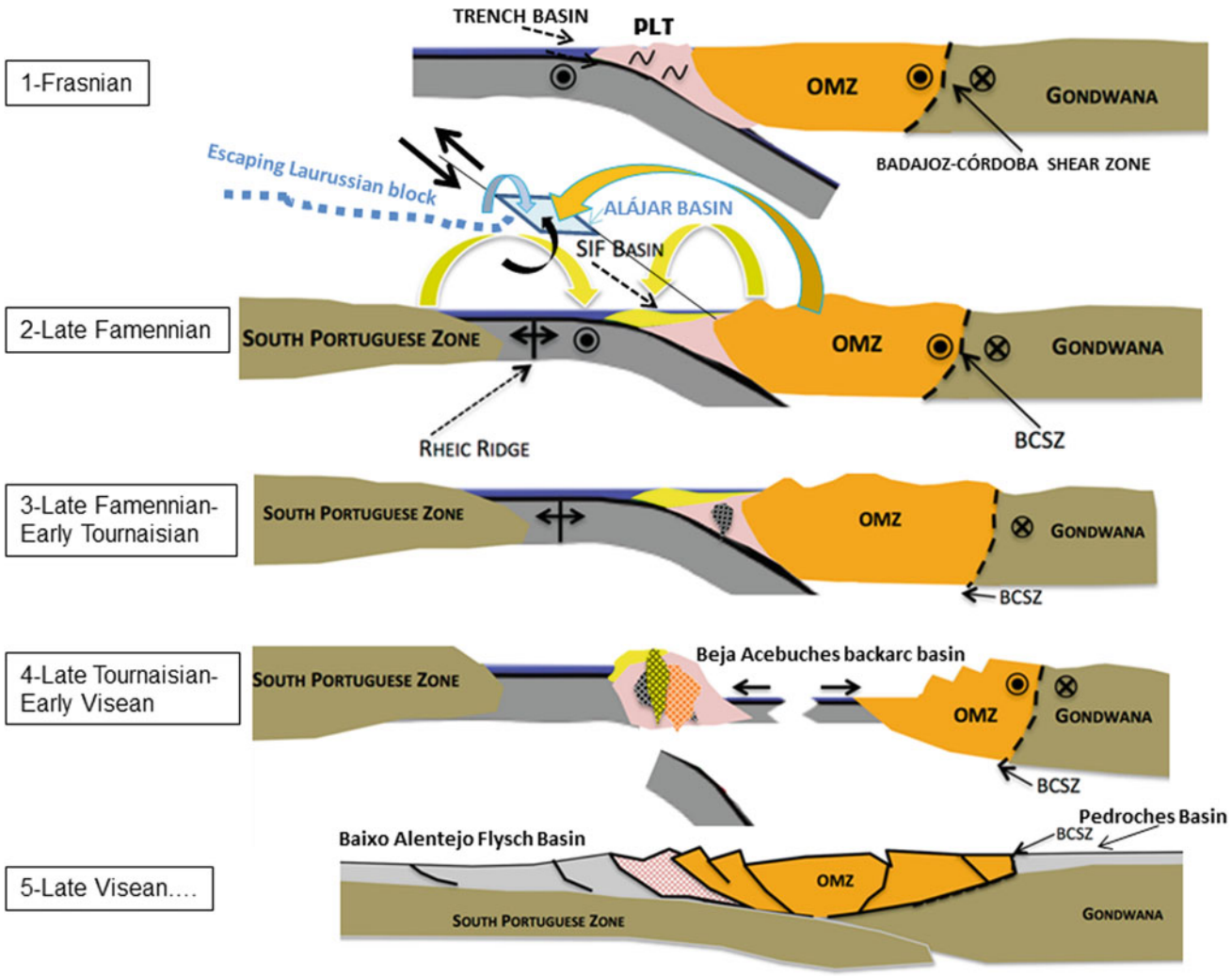

Fig. 11.19 Tectonic evolutionary cartoon showing the location of synorogenic basins in the future SW Iberia Variscan orogen since the onset of subduction beneath Gondwanan OMZ to final collision with the Laurussian SPT. 1, 2 and 3: Subduction stage: (1) formation of the Peramora mélange in the trench basin; (2) deposition of the Santa Iria flysch (SIF) in a forearc basin (sources indicated by yellow arrows) on top of already accreted PLT and, at some distance (out of the cross-section), arrival of an escaping Laurussian block (in whose shelf the Horta da Torre Fm. was being deposited) to a pull-apart basin at a releasing bend; collapse of the basin margins gave rise to formation of the Alájar mélange; sources indicated by blue (exotic block), orange (OMZ) and black (oceanic lithosphere) buckled arrows; (3) arc growth on both OMZ and accreted PLT; (4) Rheic MOR collision with the trench, slab break-off and opening of the Beja-Acebuches backarc basin (5) Collision stage: formation, migration and progressive inversion of the Baixo Alentejo Flysch foreland basin on the SPZ and the Pedroches foreland basin on the OMZ and CIZ

11.3.3.2 Alájar Mélange

Also defined by Eden (1991), this unit is being the subject of intense debate. The Alájar mélange is only recognized in Spain, as the northernmost structural unit in the eastern half of the PLT exposure. To the west and always in a northernmost position within the PLT, the coherent Horta da Torre Fm. (Oliveira et al. 1986) crops out, showing similar lithological characteristics. Both the Horta da Torre Fm. and Alájar mélange occupy the footwall of the so-called South Iberian shear zone (Crespo-Blanc and Orozco 1988, 1991), a predominantly sinistral fault zone but with a thrust component of displacement, through which the Beja-Acebuches ophiolite and Ossa Morena Zone overthrust the PLT. The contact zone between the two is obscured by late displacements along the Ficalho fault.

Eden (1991) and Braid et al. (2010) described the Alájar mélange as composed of a matrix of fine-grained phyllites wrapping around ortoquartzite blocks of variable sizes (from millimeters to some tens of decametres, more rarely hectometers). Fine-grained mylonites form millimetric-to-metric-thick shear zones anastomosing around the quartzite bodies that show sigmoidal geometries, the sigmoids reaching up to hectometres in length parallel to strike. Importantly, however, the Alájar mélange also locally contains meter-thick matrix supported cobble-size conglomerates (debris flows) and isolated exotic blocks (from few centimetres up to some tens of meters in length) of serpentinised ultramafic rocks, gabbro and marbles, the latter resembling the Cambrian marbles of the Aracena massif cropping out in the hanging wall of the South Iberian shear zone. Lithological similarity of the main protoliths of the Alájar mélange, mainly the quartzites, to those of the coherent Horta da Torre Fm. together with the fact that they occupy the same structural position led some authors to interpret them as the same lithostratigraphic unit, the mélange being formed by tectonic disruption of the preexistent coherent succession (Crespo-Blanc and Orozco 1988, 1991; Crespo-Blanc 1989; Pérez–Cáceres et al. 2017). Tectonic shearing and disruption are undebatable but, alone, they cannot explain the presence of either the debris flows or the exotic (marble, serpentinite and gabbro) blocks. Following Eden (1991) we suggest that the Alájar mélange had a sedimentary origin, probably sourced in the lithologically similar Horta da Torre Fm., being subsequently deformed and further disrupted within the area affected by the South Iberian shear zone.

Dark-color phyllite samples from the matrix of the Alájar mélange have yielded a late Famennian spore assemblage rather similar to that found in the Horta da Torre Fm. (Pereira et al. 2018) supporting the existence of a link between the two. These and other recently obtained palynological results from various lithostratigraphic units in the PLT prove that the Alájar mélange is much younger than the Peramora mélange (mid Frasnian) and invalidate the interpretation by Eden (1991) who considered both mélanges as originated in similar conditions but involving different sources. Again, as in the case of the Peramora mélange and other formations within the PLT, this soundly established palynological age frame is in apparent contradiction with existence of some younger detrital zircon grains in them (Braid et al. 2011, 2012; Dahn et al. 2014; Pérez–Cáceres et al. 2016, 2017). Partial Pb-loss during deformation is also to be interpreted in all these cases.

The most intriguing finding in the detrital zircon record obtained from the Alájar mélange (both matrix and quartzite clasts) and also from the Ribeira de Limas Fm. of the PLT is however its outstanding difference with respect to those published from both sides of the PLT, i.e. the OMZ to the north and the SPT to the south (Braid 2011; Braid et al. 2011, 2012; Pérez-Cáceres et al. 2017). The most important zircon population in the mélange samples is Mesoproterozoic in age (55–70% of the analized grains), which is extremely rare or absent in the record of both OMZ and SPT. In addition, a minor (<5%) though significant population of early Silurian age (ca. 440 ma) is fully unknown in the bounding zones (OMZ and SPT), whereas the most abundant (Neoproterozoic) population in the two latter zones is absent or minor in the Alájar mélange, (Braid 2011; Braid et al. 2011; Pérez-Cáceres et al. 2017). The closest match of this detrital zircon record is found with the Southern Uplands unit of the British Caledonides, posing an unexpected question about their possible mutual link. This is interpreted by Braid et al. 2011, 2012 in connection with a process of tectonic escape along a transform zone of a Laurussian block into an oceanic reentrant that existed south of the Iberian margin of Gondwana. Eventually, the transform may have reached the outer margin of the OMZ (Gondwana), juxtaposing the two continental masses. Further detrital zircon studies on the Alájar mélange and on other PLT units, the Horta da Torre Fm. in particular, are required to confirm this finding and substantiate the correlation indicated by the palynomorphs record.

At present all the boundaries of the Alájar mélange exposure are faulted, preventing characterization of the type of basin in which it was deposited. A possibility, suggested here under the perspective of sinistral escape along a transform margin, is a pull-apart type basin developed at a releasing bend (Stage 2—out of section—in Fig. 11.19). In this context, the presently exposed Alájar mélange may have had a main source in the Laurussian (Southern Uplands correlative) block carrying the Horta da Torre Fm., exposed or near surface. Collapse of the latter at the basin margin may have triggered large landslides giving rise to formation of the mélange, whereas collapse of the other basin margins, OMZ or eventually oceanic lithosphere, would have delivered olistoliths (marbles, and gabbro and serpentinite, respectively) that may have episodically reached the part of the basin represented by the presently exposed Alájar mélange.

11.3.3.3 Santa Iria Flysch Basin

The Santa Iria flysch Fm. was defined by Carvalho et al. (1976) as the upper unit of the Ferreira-Ficalho Group. At odds with the remaining lithostratigraphic units exposed in the PLT that are polyphase deformed, the Santa Iria flysch is only affected by a single-phase NW trending upright folding and associated axial-plane pressure-solution cleavage, thence its interpretation as a late, unconformable unit, despite the fact that almost all contacts with the other units are presently faulted or unexposed at least in Spain. In Portugal, Carvalho et al. (1976) and Oliveira (1990) described unconformable superposition over the Ribeira de Limas Fm.

The Santa Iria Fm. is composed of alternating dark shales, siltstones, greywackes and (minor) thin layers of tuffites (Crespo Blanc 1989), showing turbiditic characteristics and reaching at least 200 m of preserved structural thickness. Dark shales and siltstones in Portuguese and Spanish outcrops of the Santa Iria Fm. yielded well-preserved palynomorph assemblages assigned to the VH Miospore Biozone of late Famennian age (Pereira et al. 2006, 2018).

The detrital zircon record in the Santa Iria flysch displays the widest age range recorded in the PLT, including a variety of Proterozoic populations (ca. 30% Neoproterozoic, ca. 12% Mesoproterozoic and ca. 21% Paleoproterozoic) with only a minor (<5%) Archean population (Braid et al. 2011; Pereira et al. 2017; Pérez-Cáceres et al. 2017). However, the most abundant zircon population, making 32–40% of the analyzed grains, is of Late Devonian-early Carboniferous age, with a strong peak at ca. 347 Ma in Braid's sample and a 375–365 Ma broader peak in Pérez Cáceres's samples. The latter authors interpret this late Devonian-early Carboniferous population as derived from a cryptic magmatic arc (Pereira et al. 2012a), whose volcanic part is now eroded in the PLT but whose plutonic root is exposed in parts of the Sierra Norte batholith (e.g. oldest phases in the Gil Márquez pluton; Gladney et al. 2014; Braid et al. 2018). Alternatively, the referred zircons may have derived from the modest arc (both plutonic and volcanic parts) exposed in the southwestern OMZ. Again, some detrital zircon grains show younger ages than the late Famennian age assigned to the Santa Iria flysch on the basis of its palynological content. In this particular case, and although partial rejuvenation of the zircon ages is also likely, Pérez-Cáceres et al. (2017) interpret that palynomorph reworking is more plausible and suggest a somewhat younger (Tournaisian) age for the flysch.

Concerning the type of basin, a forearc turbidite basin is here suggested following Braid et al. (2018) (Stage 2 in Fig. 11.19). According to all the above referred authors a mixture of sources (SPZ, PLT, exotic Laurussian block and OMZ, plus the possible Devono-Carboniferous arc) appears to have supplied detritus to the basin, suggesting proximity of all the players at that time.

11.3.4 Valdeinfierno Intermontane Basin (Late Tournaisian)

V. Gabaldón, C. Quesada

First described by Mallada (1898–1927) and Carbonell (1917) this small basin ($\sim$20 km^2 of outcrop area) is located within the so-called Sierra Albarrana domain of the northern Ossa Morena Zone (Chacón et al. 1974; Delgado Quesada et al. 1977). Despite its small size, it has however very important paleogeographic and paleotectonic significance. Concerning paleogeography, its entire fill corresponds to various types of terrestrial deposits, among which cobble to block size breccia form the most common lithology (Gabaldón et al. 1983, 1985a, b; Broutin et al. 1983b; Quesada and Garrote 1983). Since the pioneer work by Jongmans (1949) and Jongmans and Meléndez (1950) a Mississippian age is assigned to the basin fill, later on refined as late Tournaisian by Wagner (1978) and Garrote and Broutin (1979) on the basis of its paleoflora and palynomorphs. Elsewhere in SW Iberia rocks of this age correspond to marine successions (see under the previous and the next subsections), this fact providing the only direct evidence for an uplift event that affected at least the northern part of the OMZ. Such uplift is also indirectly indicated in the southern Central Iberian Zone and the central and northern parts of the OMZ by the important erosional and angular unconformity that makes the base of the various Lower Carboniferous basins dealt with herein. In contrast, the southern OMZ was not affected apparently by this uplift event, mainly at the location of the Terena Flysch basin, where marine conditions persisted until at least early Visean time (Boogaard and Vázquez 1981). Uplift and denudation is interpreted in connection with the transpressional deformation produced during the southeasterly escape of the OMZ (Dallmeyer and Quesada 1992; Quesada and Dallmeyer 1994).

The stratigraphic record preserved in the Valdeinfierno basin consists of five superposed sequences (Fig. 11.20), adding to 1,200 m in thickness, whose characteristics and sedimentological interpretation are as follows (Gabaldón et al. 1983, 1985a, b; Gabaldón and Quesada 1986):

- *Sequence I.* A basal regolith developed over polydeformed, greenschist grade metapelites and metasandstones of the Azuaga Fm. (Delgado Quesada 1971; Ediacaran-early Cambrian?) gives way to a 10–20 m thick succession made of matrix-supported breccia (debris flows) gradually passing upwards to channelized clast-supported conglomerates. The breccias are interpreted as gravitationally-driven deposits forming an apron at the foot of a syn-sedimentary fault scarp. In turn, the overlying conglomerates probably represent proximal alluvial fan deposits.

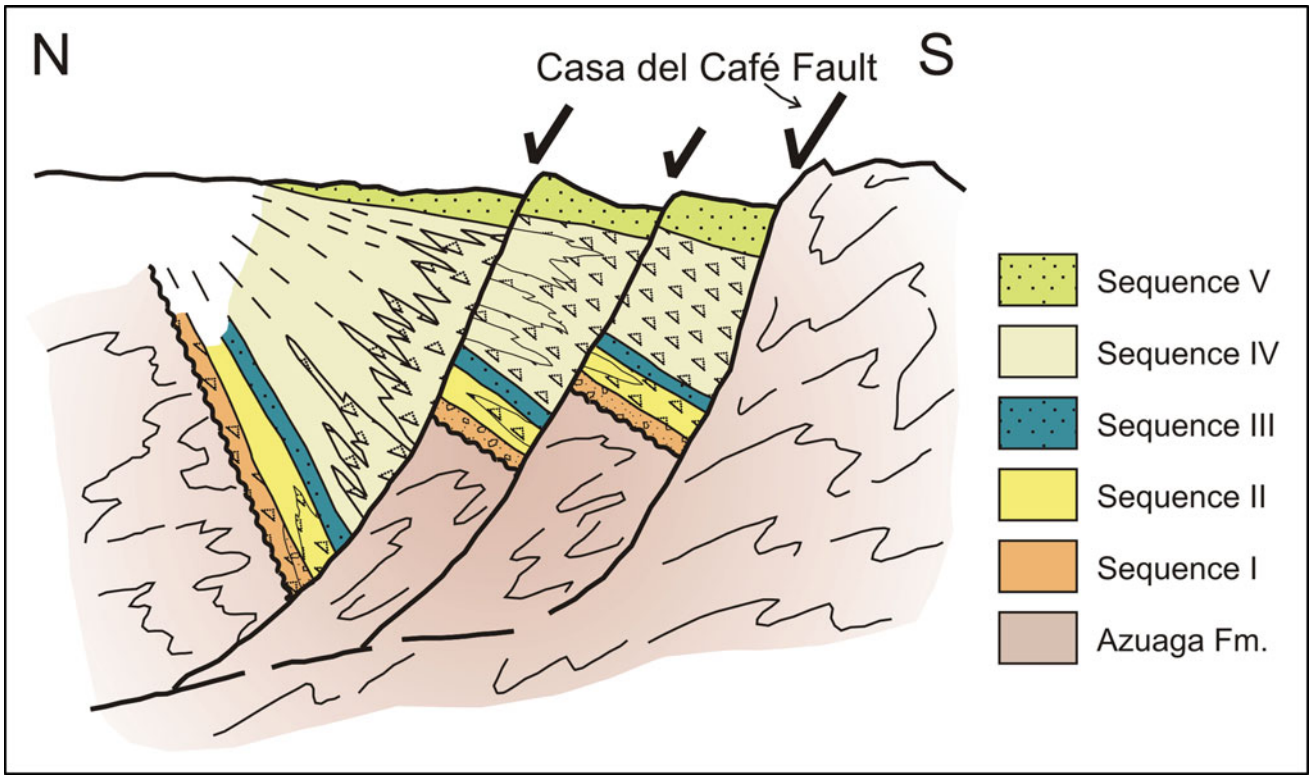

Fig. 11.20 Sketch evolutionary model of the Valdeinfierno basin fill (Symbols: Saw-tooth line: basal unconformity; triangles: breccia deposits; dots: fluviatile deposits; blank: lacustrine and marsh deposits; hatch lines: bedding attitude)

- *Sequence II*. Ca. 50 m thick succession of laminated mudstones (varves) alternating with either isolated strata or meter-scale thickening and coarsening upwards turbidite sequences. Frequent intercalations of decimeter-thick breccia layers and slumped beds also occur as well as several coal beds, the most important of which were mined out up to the nineteen sixties. This sequence is considered the result of autochthonous mud settling in a lake, frequently interrupted by arrival of turbidity currents and debris flows sourced in the active basin marginal faults. The latter eventually filled some parts of the lake, leading to development of marsh areas where the coals formed.
- *Sequence III*. Channel-fill sandstone bodies interfingering with massive mudstones in which numerous rootlet beds generally occur beneath mm- to cm-thick coal seams. The total thickness of this alluvial plain sequence ranges from 30–50 m.
- *Sequence IV*. This makes the thickest part of the basin fill (ca. 800 m) and consists of meter-thick tabular breccia layers and (frequently slumped) turbidites interbedded with fine-grained siltstone and mudstone alternations that have yielded numerous remains of the fresh water crustacean *Euestheria striata* (Wagner 1978). This sequence is interpreted as a return to renewed lacustrine conditions linked to tectonic reactivation. This would have caused floundering of the basin floor and formation of one or several intrabasinal fault scarps where the turbidites and slumps incorporating parts of the previous basin fill would have had their sources.
- *Sequence V*. Another fluviatile deposit with similar characteristics as *Sequence III*.

At odds with other Mississippian basins in the area (see below) that are penetratively deformed, no cleavage or folding other than syn-sedimentary slump folds affects the synorogenic succession at Valdeinfierno. It is however faulted and tilted in the hanging wall of a curvilinear normal fault (Casa del Café fault; Azor 1994), which appears to have played a major role in the nucleation and subsequent evolution of this hemigraben or asymmetric graben basin as suggested by a progressive upwards dip decrease of the tilted succession (progressive unconformity, see Fig. 11.20). Other authors (Roldán García 1983; Roldán García and Rodríguez Fernández 1986–1987) interpret a mechanism of pull-apart in the origin of this basin, something very likely in the context of transpression that dominated the Variscan orogeny in this part of Iberia.

11.3.5 Pedroches Basin and Correlatives (Mississippian)

M. Armendáriz, C. Quesada, V. Gabaldón, I. Rosales

Every isolated exposure of Carboniferous rocks in SW Iberia was thought to represent a different basin up to the early 1980s when for the first time some integrated studies on sedimentology, litho and biostratigraphy, petrology and structural geology allowed establishing a coherent correlation and classification of them all into the different types and ages applied herein (Quesada 1983; Oliveira 1983; Quesada and Garrote 1983; Gabaldón et al. 1883, 1985a, b; Wagner 1983; Wallis 1985). Concerning the numerous largely marine Mississippian outcrops, they occur in three main areas: (i) the northernmost OMZ and southern CIZ, (ii) the central OMZ, and (iii) the vast Baixo Alentejo Flysch Group area of the SPZ (dealt with in the next section). The northerly ones were considered for the first time as different parts of a large, single marine basin: so-called Northern Ossa Morena basin at the time (Quesada 1983; Quesada and Garrote 1983; Gabaldón et al. 1985a, b). Subsequent studies have confirmed this interpretation and provided many details on the overall constitution and evolution of the basin (e.g. Quesada et al. 1990; Rodríguez-Martínez et al. 2000; Cózar et al. 2004, 2006; Armendáriz et al. 2005, 2007a, 2008a, b, 2013; Rodríguez-Martínez 2005; Armendáriz 2006, 2008). The name Pedroches basin, which stands for the Pedroches valley, a wide region in northern Córdoba province where the basin fill has its larger exposure, was first published by Gabaldón et al. (2004) and is preferred here. The Mississippian outcrops in the central OMZ lie along a major lineament and form the now disconnected exposures at Los Santos de Maimona, Bienvenida, Casas de Reina and Cerrón del Hornillo (Fig. 11.8).

Most part of the southeasterly escaping OMZ was emerged by the early Mississippian. This is indicated by the removal by erosion of most of the pre-Carboniferous passive margin succession and even parts of the thick Cambrian rift sequence throughout the zone, with the exception of the area occupied by the Terena flysch basin that remained as a trough until the early Visean at least (Fig. 11.9). The cause of this uplift has been interpreted in connection with processes of transpressional uplift during OMZ escape (Quesada and Dallmeyer 1994; Quesada 2006). By late Tournaisian time a period dominated by extensional tectonic conditions affected the entire southern part of the escaping Gondwana margin giving rise to formation of several basins separated by intervening emerged horsts as well as significant bimodal igneous activity (Fig. 11.9). This extensional event lasted until the onset of collision in the late Visean.

Terrestrial syn-extensional sedimentation occurred in fault-bounded, fluviatile and lacustrine basins developed on the emerged landmasses. The Valdeinfierno coal-bearing basin described in the previous section (Figs. 11.8 and 11.9) is the only preserved remain of such type of basins (Wagner 1978; Garrote and Broutin 1979; Gabaldón et al. 1983; Quesada and Garrote 1983; Gabaldón and Quesada 1986). In turn, marine conditions were rapidly established in the subsiding troughs: the Pedroches basin to the north of the OMZ and another depocenter in the central OMZ (COMB in Fig. 11.9), now represented by aligned disconnected exposures at Los Santos de Maimona, Bienvenida, Casas de Reina and Cerrón del Hornillo (Figs. 11.8 and 11.9).

11.3.5.1 Pedroches Basin

The Mississippian Pedroches basin is located in the vicinity of, and oversteps onto the Badajoz-Córdoba shear zone, the sinistrally reactivated suture zone separating the Ossa Morena (OMZ) and Central Iberian (CIZ) zones of the SW Iberian Massif (Figs. 11.8 and 11.9). The southern margin of the Pedroches basin, roughly running WNW-ESE, i.e. parallel to the overall orientation of the basin and the regional structural grain (Fig. 11.8), is characterized by transitional, terrestrial to coastal sedimentary sequences, which unconformably onlap onto exhumed metamorphic OMZ rocks, most commonly onto the Precambrian basement (Garrote and Broutin 1979; Quesada 1983; Quesada and Garrote 1983; Gabaldón et al. 1985a, b). This southern margin lies very close to the Badajoz-Córdoba shear zone. The central and northern parts of the Pedroches basin fill sit through a variably large sedimentary hiatus and/or erosional unconformity onto Late Devonian metasedimentary rocks of the CIZ (Gabaldón et al. 1985a, b; Gabaldón 1989), thus indicating that this southern part of the CIZ was also subjected to uplift prior to basin nucleation but much less than the adjacent OMZ. No evidence of the northern margin of the basin is preserved, although some terrestrial to marine transitional facies occur in an isolated outcrop at the core of the Guadalmez syncline (Fig. 11.8), some tens of kilometres north of the main exposure of Mississippian rocks (Quesada 1983; Lorenzo Álvarez et al. 2005).

Structural Division

The Pedroches Basin is presently compartmentalized into many fault-bounded structural units. This statement is particularly true for the southern part, in which the basin developed within, and was affected by deformation along the Badajoz-Córdoba shear zone. The main structural elements with a significant paleogeographic influence on basin evolution were three roughly syn-sedimentary, sigmoidal shape igneous belts (Fig. 11.9); i.e. from south to north: Villaviciosa de Córdoba-La Coronada, Varas-Guadalbarbo and Pedroches Batholith, along which severe facies, structural and paleoceanograhic changes took place. They allow for a first order division of the basin into several structural/paleogeographic

domains, in turn internally subdivided into second order structural units, especially towards the southern margin (from south to north, Fig. 11.9):

- Benajarafe-Berlanga southern marginal unit
- Villaviciosa de Córdoba-La Coronada igneous belt
- Guadiato unit
- Guadalbarbo (volcanic) unit
- South Pedroches valley unit
- Pedroches batholith
- North Pedroches valley unit
- Guadalmez syncline.

Volcanic rocks occur scattered throughout the basin towards the bottom of the respective stratigraphic sections but are massive and constitute the most part of the stratigraphic record within the three igneous belts, the sigmoidal shape of which is consistent with sinistral movements during and after emplacement. Not all three igneous belts had the same paleogeographic importance. The Villaviciosa de Córdoba-La Coronada igneous belt (Fig. 11.9) is presently formed of both plutonic and volcanic rocks, the latter showing evidence of subaerial eruption locally (Pascual and Pérez Lorente 1975; Pascual 1981, 1985; Sánchez Carretero et al. 1989). It must have formed, therefore, a belt of volcanic islands isolating a marginal lagoon area (Benajarafe-Berlanga unit; Fig. 11.9), partially disconnected from the main part of the basin (Quesada and Garrote 1983; Gabaldón et al. 1985a, b). The Guadalbarbo belt (Fig. 11.9) is exclusively formed of submarine basaltic volcanic rocks, frequently pillowed and interbedded with fine-grained turbiditic metasediments. Their N-MORB composition and highly positive ε_{Nd} values (Armendáriz 2008, Armendáriz et al. 2008a) indicate a depleted mantle source and perhaps incipient oceanization (the so-called Varas-Guadalbarbo ophiolite; Crousilles et al. 1976; Crousilles and Dixsaut 1977), or at least extreme thinning of the CIZ crust in this part of the basin. Whatever the case, the Guadalbarbo belt may have constituted a somewhat deeper trough with respect to the adjacent domains, at least during the first part of the fill (Armendáriz 2008; Armendáriz et al. 2008a, 2013). Finally, the very large Pedroches Batholith (Fig. 11.9), which presently consists almost exclusively of shallow plutonic rocks intruded into the already deformed basin fill, had not been at first glance considered to have had a profound influence on sedimentation. Nevertheless, presence towards their margins or within roof-pendants of some relics of syn-sedimentary volcanic rocks (Quesada 1983; Gabaldón et al. 1985a) and very shallow water quartzarenite interbeds in the tempestite/turbidite succession (Larrea et al. 1992) may indicate that here also a significant paleogeographic boundary may have existed during basin development, currently obscured by subsequent intrusion, uplift and erosion of the presumed syn-sedimentary volcanic belt (Armendáriz 2008).

According to available geochronological data, igneous activity within the two belts in which plutonic rocks are currently exposed (Villaviciosa de Córdoba–La Coronada and Pedroches Batholith) extended well beyond basin development and inversion (up to ca. 300 Ma; Garrote and Sánchez-Carretero 1983; Gabaldón et al. 1985a; Fernández-Ruiz et al. 1990; Alonso-Olazábal et al. 1999; Donaire et al. 1999; Alonso-Olazábal 2001; García de Madinabeitia et al. 2001; García de Madinabeitia 2002). This fact probably implies an alternation of multiple transtension/transpression events as well as persistence of an underlying mantle thermal anomaly responsible for magma generation.

Stratigraphy of the Basin Fill

A major limiting problem for the study of this basin lies in the scarcity of fossil remains. Only near the basin margins, where abundant plant remains exist in terrestrial and transitional sequences (Garrote and Broutin 1979; Quesada 1983; Quesada and Garrote 1983; Wagner 1983, 1999; Pardo and García Alcalde 1984; García Alcalde et al. 1984), and in the sparse carbonate rocks (e.g. Mamet and Martínez-Díaz 1981; Cózar 1998, 2000; Cózar and Rodríguez 1999; Rodríguez-Martínez et al. 2000; Cózar et al. 2004, 2006; Rodríguez-Martínez 2005), which on average do not exceed a few percent of the stratigraphic record, there is some control on the age of the sedimentary fill of the basin. Terrigenous rocks, making up more than 90% of the fill, barely contain any identifiable, stratigraphically valuable fossils. Variably altered palynomorphs appear from time to time but, when identifiable, they show evidence of strong reworking of non-coeval remains, making them extremely difficult to use for stratigraphic purposes. Despite all these limitations, it can be established that the Pedroches basin started to develop not later than the late Tournaisian, and perhaps earlier (Garrote and Broutin 1979; Quesada 1983; Pardo and García Alcalde 1984). Its life as a marine basin extended for most of the remaining Mississippian, for sure up to the early Namurian/Serpukhovian (e.g. Gabaldón et al. 1983; Wagner 1983; Cózar et al. 2004, 2006).

From a lithostratigraphic point of view, when exposed, the basal sequence in all the units starts with a variably thick fluviatile to deltaic polymict conglomerate, which overlies the local basement either unconformably (in the south) or paraconformably. Above the basal conglomerate the lower part of the basin fill succession, which may reach up to several hundred metres in thickness, shows the highest variability in terms of lithology and facies. It is within the lower few hundred metres where most volcanic rocks are located, within and in between the igneous belts, suggesting the important

role of lithosphere-through, extension/transtension-related faulting in the origin and evolution of the basin at this stage. Within the igneous belts, probably located atop major lithospheric lineaments, igneous activity extended throughout the whole life of the basin and even beyond. Sedimentary rocks within this lower part of the successions are represented by deltaic to shallow-marine siliciclastics, including some conglomerates, which interfinger with the volcanic rocks (Gabaldón et al. 1985a, b). On the other hand, the upper part of the successions is very similar throughout the basin and corresponds to flyschoid, greywacke-mudstone alternations (Culm facies); the differences among units residing in their variable thickness (up to several thousand metres), local facies variations and vertical evolution. Conglomeratic debris flows locally occur interbedded within this upper sequence, attesting for syn-sedimentary tectonic activity. This change is interpreted as evidence for a transition from an overall extensional/transtensional regime during basin generation and early evolution to an overall transpressional one, during which the basin was transformed into a sort of peripheral foreland basin (Armendáriz et al. 2008a, 2013). A very peculiar rock unit delineates the transition from the lower to the upper part of the Mississippian succession in central and northern units (from the Guadalbarbo unit northwards; Fig. 11.9). It consists of a few metres thick package of radiolarian-bearing, iron oxide-rich purple shale (Haematite Dust of Pérez-Lorente 1979), which is interpreted as a condensed sequence recording initial flexural subsidence in the newly transformed foreland basin (Armendáriz et al. 2008a, 2013). This evolution may have started from the Late Visean when complete closure of the remaining Rheic Ocean brought the South Portuguese part of Laurussia to collide with the OMZ, outer margin of Gondwana (Ribeiro et al. 1990; Quesada 1991). This collision forced the upthrusting of the OMZ onto the CIZ and the intervening Pedroches basin that had been recently created by extensional/transtensional processes near the boundary between the two. As a result, the southern basin margin became an upthrusting active one but still with a significant strike-slip component throughout its evolution (Gabaldón et al. 2004). Towards the north, the present boundary of the Carboniferous exposure is defined by an extensional fault (Puente Génave-Castelo de Vide shear zone; Martín Parra et al. 2006), locally inverted (Fig. 11.8). We interpret this fault to represent the southern boundary of a syn-sedimentary forebulge, which developed to accommodate the flexural response of the CIZ crust subjected to loading by the upthrusting of the OMZ onto its southern margin.

North of the then active southern margin, sedimentation during this final marine stage took place on an open continental shelf dominated by storm activity (Gabaldón et al. 1985a, b). Apart from local tectonically driven collapse and formation of debris flow deposits, sediment supply and dispersal were mostly controlled by storm surge ebb currents that produced turbiditic sand bodies of a storm sand layer type (tempestites). When deposited above storm wave base, they were reworked to form hummocky cross-bedding and wave ripples as storm activity waned. Locally, mainly towards the southeast, and/or at periods of enhanced subsidence, some layers reached areas below storm wave base, being then indicated by classical Bouma sequence turbidites. Lateral and vertical alternation of both types of facies indicates that in any case deposition took place on a continental shelf during all the basin evolution. This also applies to the Guadalbarbo unit, where MORB-like basalts occur, implying that no real oceanic crust formed there at any time despite the somewhat deeper environment deduced for this unit (see above). Fair-weather deposition is represented everywhere by mud settling and intense bioturbation. In situ carbonate or mixed platforms only developed during the late Visean and early Serpukhovian near the basin margins (Guadalmez syncline and close to the Puente Génave shear zone in the north; Pardo and García Alcalde 1984; and in the Sierra del Castillo and Guadalmellato subunits of the Guadiato unit near the southern margin (Fig. 11.9; Cózar and Rodríguez 1999; Cózar et al. 2006; Armendáriz et al. 2008a, b and references therein). Reworked (tempestitic/turbiditic) carbonate layers occur dispersed within the siliciclastic succession in central parts of the basin, mainly towards the lower strata of this upper sequence. Carbonates also appear as olistoliths (from centimetres to hectometres in size) in late Visean and Serpukhovian chaotic deposits interbedded in the dominantly siliciclastic succession within the units located to the immediate north of the southern carbonate platforms (Fig. 11.21), namely the northern divisions of the Guadiato unit and the Guadalbarbo unit (Fig. 11.9); Cózar and Rodríguez 2004; Cózar et al. 2004; Armendáriz 2008; Armendáriz et al. 2008a, 2013; Rodríguez Martínez et al. 2012; Gutiérrez Marco et al. 2014; Matas et al. 2014). The lack of mélange deposits north of the Guadalbarbo unit suggests that this may have persisted as a relative trough also at this stage, trapping the chaotic deposits that eventually arrived there and preventing their dispersal across it.

Special attention deserves the Guadiato unit. This, which is integrally located within the Badajoz-Córdoba shear zone, is by far the most complex unit in the whole basin. The first peculiar feature is the fact that it sits onto the actual boundary between the OMZ and the CIZ (Fig. 11.9). Internally, it consists of three main second order structural divisions, presently separated by north-verging sinistral thrusts. The intermediate thrust sheet (Central unit of Quesada and Garrote 1983; Sierra del Castillo and San Antonio La Juliana units of Cózar and Rodríguez 1999), whose northern margin is the actual boundary fault between the CIZ and OMZ, contains a very unique stratigraphic record. The main singularity resides in the development of relatively important late Visean to Serpukhovian carbonate platforms (Cózar and

Fig. 11.21 Large olistoliths of late Visean carbonates in Serpukhovian chaotic mélange (Central Guadiato unit)

Rodríguez 2004, Armendáriz et al. 2005, 2007a; Armendáriz 2006; Cózar et al. 2006 and references therein) at the onset of the foreland basin stage. These are succeeded by the "normal" flyschoid successions but in this case they are punctuated by interbedded chaotic mélange deposits, locally very thick, in which up to hectometre-size carbonate platform olistoliths occur in profusion (Fig. 11.21) (Moreno-Eiris et al. 1995; Gutiérrez-Marco and Sarmiento 1999; Cózar et al. 2004; Armendáriz et al. 2005; Armendáriz 2006, 2008). Some of the mélange deposits extend into the adjacent Guadalbarbo unit to the north but, there, no carbonates other than the olistoliths are found. The implication of this unique stratigraphy is that the Central Guadiato unit may have been subjected to transpressional uplift at the time it became incorporated into the deformation wedge, while the rest of units to the north were still undergoing flexural subsidence. Subsequent emergence at the basin floor may have been responsible for the collapse of the uplifted block, and its carbonate cover in particular, triggering the formation of the spectacular chaotic mélanges. Locally, abundant fossil-bearing Lower Paleozoic olistoliths also occur (Gutiérrez Marco et al. 2014; Matas et al. 2014), attesting for eventual unroofing and collapse of deep parts of the unlifting blocks. Also in this unit an upwards transition to molasse type sedimentation (deltaic and eventually fluviatile facies, with some coal measures of early Namurian age; Wagner 1983, 1999; Quesada 1983; Quesada and Garrote 1983; Wagner and Jurado 1988; Cózar and Rodríguez 2004; Armendáriz 2008), is an exception to the general evolution and may indicate the preservation of its final uplift during inversion.

Within this Central Guadiato unit the so-called Valdemilano section in the Guadalmellato subunit shows a unique record. There, a late Visean (Brigantian) carbonate platform (Cózar et al. 2006; Armendáriz 2008) is overlain by an early Serpukhovian (Pendleian) molasse-type cover (deltaic), through a locally abrupt erosional unconformity related to emergence and karstification of the carbonate succession (Armendáriz 2008; Armendáriz et al. 2008b). Emergence of the carbonate platform and consequent karst formation was also probably caused by transpressional uplift but a significant climate-triggered sea level fall may have contributed at this stage (Armendáriz 2008; Armendáriz et al. 2008b). On the basis of oxygen isotope and Mg/Ca composition data recorded in brachiopod (*Gigantoproductidae*) shells collected along the carbonate platform succession, the above authors were able to recognize an overall $\delta^{18}O$ increase of $\sim 1‰$ (relative to the Vienna Pee Dee Belemnite standard) from the oldest to the youngest samples (<4 Ma age difference). This is accompanied by a $\sim 30\%$ decrease in Mg/Ca ratios of the brachiopod calcites, confirming that at least part of this $\delta^{18}O$ shift was related to cooling. A temperature drop of ~ 3.3 °C has been estimated for the stratigraphic period considered (Armendáriz et al. 2008b). Furthermore, the data are consistent with regional seawater cooling accompanied by an increase in continental ice volume, in line with similar positive $\delta^{18}O$ events in other Paleotethyan basins during the Brigantian (Popp et al. 1986; Mii et al. 2001). This synchronous global shift provides evidence for the onset of the Carboniferous glaciation in Gondwana during the Brigantian.

In general terms, the lack of molasse-type sediments in most units may be interpreted as evidence for an underfilled (starved) nature of the basin throughout its evolution; i.e., subsidence equalled or exceeded sediment supply. Apart from the obvious zonation outlined above, facies distribution along the various belts suggests an overall ramping of the basin floor towards the present-day southeast (Cózar et al. 2004; Armendáriz et al. 2008).

Provenance of the Basin Fill

When exposed, the basal conglomerate of the Pedroches basin only includes clasts derived from the local basement. This is an important point to prove an autochthonous relationship of the basin with its underlying basement, despite the significantly large lateral displacements that may have experienced some parts of it with respect to others. In conclusion, each structural division of the basin and its relative basement must have travelled in solidarity. Higher up in the stratigraphy, most metasedimentary rocks are fine or very fine-grained; thus very difficult to use to characterize their sources by means of petrography. Conglomerates and debris flow deposits, though much less common, are far more informative to this purpose. Most conglomerates in the lower sequence and also in the uppermost part of the Central Guadiato unit stratigraphy correspond to fluviatile to deltaic facies. They are thus representative of the adjacent emerged catchment area. Also, many conglomeratic debris flows in the tempestitic/turbiditic upper sequence represent the collapse of similar environments, therefore providing the same type of information. Very significantly and apart from obvious intrabasinal clasts (carbonates, volcanic rocks, slump breccia, etc.), the range of identifiable cobble lithologies in the Guadiato and the Guadalbarbo units (Fig. 11.9) includes protoliths from both the OMZ and the CIZ. On the contrary, in the South and the North Pedroches Valley units (Fig. 11.9) only cobbles derived from the CIZ have been so far identified. This difference allows making a first paleogeographic division into two drainage systems within the basin, with a barrier impeding the transport across it. It may not be fortuitous that the boundary be located at the Guadalbarbo unit, where the typically oceanic-like volcanic rocks occur. The same applies to the dispersal of the carbonate-bearing mélanges that do not trespass northwards beyond the Guadalbarbo unit. Even if the sedimentary structures indicate relative shallow water environments also in this unit, this area may have represented a relative trough (the real basin centre?), at least temporarily.

On the other hand, the combined use of major and trace element geochemical data from both metasedimentary and metaigneous protoliths, together with Sm–Nd systematics, provide a powerful tool to constrain the provenance of old rocks and to identify ancient tectonic settings and their evolution (e.g. Bhatia 1985; Taylor and McLennan 1985; Bhatia and Crook 1986; McLennan 1989; Condie 1993; Hemming et al. 1995). Concerning the metasediments, all the geochemical (major, trace and rare earth elements) characteristics reflect the predominance of upper crustal sources and a high degree of sedimentary recycling (Armendáriz et al. 2008b). Additionally, strongly negative $\varepsilon_{Nd(T)}$ (from −6.4 to −11.1) values and depleted mantle model ages (T_{DM}) varying from 1.44 to 1.74 Ga, with an average value of ca. 1.6 Ga, i.e. much older than the depositional ages, clearly demonstrate that the Pedroches basin metasediments were basically the result of crustal reworking processes. Besides, no significant differences appear to exist among the metasedimentary rocks within the different basin units concerning their geochemical and Nd isotope characteristics.

Concerning the syn-sedimentary volcanic rocks interbedded within the lower metasedimentary sequence, they generally correspond to a bimodal association typical of extensional within-plate environments. An exception is the Guadalbarbo unit where only basalts occur. The N-MORB geochemical signature of the Guadalbarbo basalts (Armendáriz 2008; Armendáriz et al. 2008a) indicates a strongly depleted mantle source. Basaltic rocks in the other intrabasinal volcanic belts show instead the characteristics of an enriched mantle melt close to E-MORB (incompatible and light rare earth element enrichment and HREE fractionation; Armendáriz et al. 2008a), suggesting derivation from an enriched lithospheric mantle source or, alternatively, contamination with crustal melts and rocks. The latter option is supported by the Sm–Nd isotope data. These show markedly negative $\varepsilon_{Nd(T)}$ values and model ages (T_{DM}) ranging between 1.2 and 1.5 Ga, i.e. very much older than the eruption age, for basaltic and intermediate rocks in all the volcanic belts other than the Guadalbarbo. In this latter unit basalts show instead high $^{147}Sm/^{144}Nd$ ratios and strongly positive $\varepsilon_{Nd(T)}$ values (Armendáriz et al. 2008a). Such highly radiogenic Nd isotope signature implies that these basalts were extracted from mantle sources with strong LREE-depletion on a time-integrated basis, and did not suffer any significant interaction with typical continental crust components.

A Model of Basin Development

It is worthwhile reminding that the Pedroches basin formed and evolved within a classical example of transpressional orogen (Ribeiro et al. 1990; Quesada 1991, 2006) and that part of the basin developed atop a major sinistral wrench lineament, the Badajoz-Córdoba shear zone (Burg et al. 1981; Quesada and Dallmeyer 1994). The onset of collision between already amalgamated Laurussia and the so-called Ibero-Aquitanian Indentor, a promontory in northern Gondwana (Brun and Burg 1982; Burg et al. 1987), promoted initiation of southeasterly tectonic escape of the OMZ, which occupied the outer margin of Gondwana, from the zone of collision (Quesada 1991; Sánchez-García et al. 2003). This displacement was accommodated by reactivation under a sinistral strike-slip regime of a preexisting lithospheric weakness: the suture between the OMZ and the Iberian Massif, which thence became the so-called Badajoz-Córdoba shear zone (Quesada 1991, 2006). The escape of the OMZ resulted in southeasterly propagating transpressional uplift, not only of the zone itself but also of the adjacent, more internal passive margin of the CIZ, which by the early Mississippian was entirely emerged and subjected to erosion.

Those were the conditions prior to the formation of the synorogenic Pedroches basin. What changes in this scenario contributed for it to happen? In our view, two interrelated elements were responsible for it (a cross-section sketch of the proposed model is depicted on Fig. 11.22): (i) a change to transtensional conditions, allowing for extension, lithospheric thinning and facilitating magma ascent and emplacement in the upper crust, and (ii) the overriding of a deep mantle thermal anomaly, responsible for the generation of magmas. These two elements find support on, and help explaining the varied stratigraphic record in the first part of the basin history and its compartmentalization into different units separated by volcanic belts (Figs. 11.8 and 11.9).

As outlined above two drainage systems, one in the south (OMZ) and another in the north (CIZ), appear to have been the sources of detrital sediments at that early stage. A physiographic low can be identified at the location of the Guadalbarbo unit, as suggested by the fact that no detrital elements sourced in the OMZ trespass this unit northwards. Geochemical and Nd isotope data confirm that the source of the sediments involved largely recycled old-continental crust, as is the case of the two flanking zones of the Iberian Massif, but cannot discriminate among units. On the other hand, they also tell that the mafic igneous rocks had a source in the asthenospheric mantle, though contamination by continental lithosphere rocks or magmas is indicated in all the igneous belts other than the central, Guadalbarbo unit. The cause of the deep thermal anomaly responsible for basin magmatism remains unexplained but the fact that episodic igneous activity lasted until the waning of the Variscan orogeny implies its persistence at depth until Early Permian times.

The recent recognition of a significant see water temperature drop of c. 4 °C recorded within the in situ carbonate platform preserved in the Central Guadiato unit near Adamuz by means of oxygen isotopic data from brachiopod shells (Armendáriz et al. 2007a, b, 2008a) may provide paleogeographic indications. This severe cooling recorded in nearly equatorial areas (McKerrow and Scotese 1990; Scotese et al. 1994; Witzke 1990; Scotese 2000; Torsvik and Cocks 2004), which may represent the expression of the coeval glaciations in southern Gondwana (e.g., Smith 1963; Charrier 1986; Rocha-Campos et al. 2000; Isbell et al. 2001, 2003; Stone and Thomson 2005; Trosdtorf et al. 2005), implies the existence of a connection of the Pedroches basin with open ocean areas. According to the overall plate configuration in the Mississippian (Scotese 2000; Stampfli and Borel 2004) such a seaway was more likely located towards the present southeast; i.e., in the direction where a Paleotethys MOR was spreading close to the northern margin of Gondwana. In the opposite direction the Variscan collisional mountain belt was then being formed (Matte 1986a, b, 1991, 2001, 2002; Martínez-Catalán 1997). This possibility is given support by the overall ramping of the Pedroches basin towards the SE mentioned above.

A speculative and provocative hypothesis forwarded by Armendáriz et al. (2013) is that during collision between Laurussia and Gondwana the latter as a whole might have been pushed southeastwards to override such Paleotethys spreading ridge or, perhaps, a branch departing from it. In this context, the first part of the evolution of the Pedroches basin could in fact be the consequence of a combination of both transtension and the overriding of a slab window

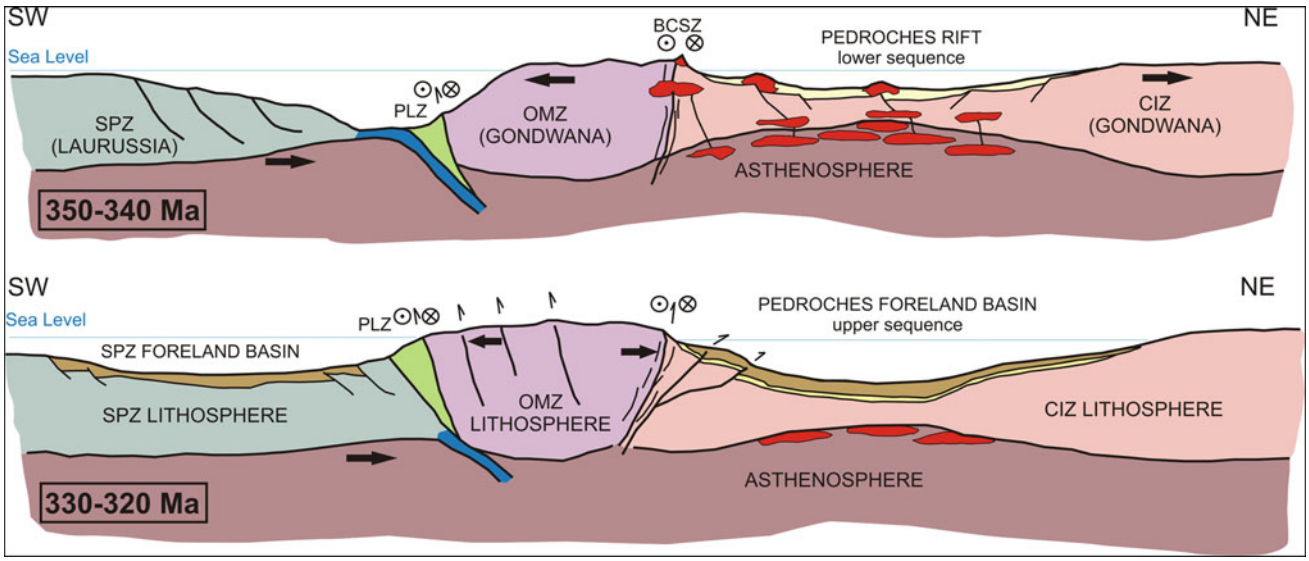

Fig. 11.22 Sketch 2D model of Pedroches basin formation (above) and transformation into a foreland basin (below)

developed atop a subducted oceanic ridge and inducing rifting in the upper (Iberian) plate. Subsequent collision at the southern margin of the OMZ with the South Portuguese Zone, which culminated the closure of this part of the Rheic Ocean, imposed a change to more orthogonal strain conditions that triggered basin inversion and may have also caused abortion of the propagating rift.

Whatever the case, a major recent finding (Armendáriz 2008; Armendáriz et al. 2013) is the recognition of the far more homogeneous character of the upper part of the stratigraphic record across the basin, with only few exceptions. It consists in most cases of tempestite/turbidite sequences of the so-called Culm flysch, which are interpreted as the classical type of synorogenic sedimentation once the basin was transformed into a peripheral foreland basin in the hanging wall plate (Fig. 11.22). This change implied returning to the prevailing regional transpressional conditions that apparently persisted until the complete inversion of the basin, its emergence and the deformation of the basin fill. Explaining this turn back is not a problem since transpression was the permanent strain regime during the whole Variscan orogeny in SW Iberia (Ribeiro et al. 1990; Quesada 1991; Silva and Pereira 2004), the problem lies in understanding the previous switch to a transtensional regime, which could be related to either presence of a releasing bend, to rifting triggered by the overriding of the speculated MOR, or to a combination of both. The final evolution of the basin as a peripheral foredeep from the Late Visean onwards was coeval to, and probably connected with the final closure of the remaining part of the Rheic Ocean that existed between the OMZ (Gondwana) and the South Portuguese Zone (Laurussia) (Quesada 2006 and references therein). This closure resulted in oblique collision between the two continents and pushed the OMZ northwards on top of the adjacent CIZ and the recently created Pedroches basin (Fig. 11.22). The first expression in our basin of the oblique (sinistral) overthrusting of the OMZ onto the leading edge of the CIZ was a sudden deepening, beautifully expressed by the condensed radiolarian purple shale that separates the two sequences in central and northern parts. Strong facies similarities in the stratigraphy from this purple shale upwards suggest that no obvious compartmentalization remained in these parts of the basin at this stage. The subsequent evolution was related to massive detrital sedimentation (the Culm flysch) that dispersed across the basin from the southern active margin subjected to uplift and erosion. According to Gabaldón et al. (1985a, b) and Gabaldón (1989) sediment supply and dispersal from the coastal and transitional areas was mainly controlled by an intense storm activity, something easy to understand given the subequatorial position of this part of the world during the Carboniferous assumed by most researchers (McKerrow and Scotese 1990; Scotese et al. 1994; Witzke 1990; Scotese 2000; Torsvik and Cocks 2004). This fundamental mechanism interoperated with other tectonically driven processes such as slumps, gravitational slides and debris flows as in typical in most synorogenic basins. Petrographic, geochemical and Nd isotope data from rocks belonging to this upper sequence are very similar in all units. They collectively indicate derivation from recycled upper continental crust sources.

Eventual returning to transtensional conditions is demonstrated by post-inversion magma emplacement along the Villaviciosa de Córdoba-La Coronada igneous belt and especially the Pedroches Batholith, whose main phase of magma emplacement took place around 307–300 Ma ago (upper Westphalian-Stephanian) (Fernández-Ruiz et al. 1990; Alonso-Olazábal et al. 1999; Alonso-Olazábal 2001; García de Madinabeitia et al. 2001; García de Madinabeitia 2002). Transtensional conditions also led to formation of the terrestrial, intermontane successor basins; e.g., the Westphalian B Peñarroya-Belmez-Espiel basin and others (Quesada 1983; Gabaldón et al. 2004) dealt with in this chapter.

11.3.5.2 Mississippian Outcrops in the Central Ossa Morena Zone

C. Quesada

A series of narrow and elongated outcrops of Mississippian rocks occur along several major fault zones in the central part of the OMZ (Fig. 11.8), attesting for the existence of another depocenter in this part of the SW Iberian orogen: Central Ossa Morena basin (COMB) in Fig. 11.9. The original extent of this basin and the possible connections to the other better documented coeval basins in the region are unknown, owing to the sparse and discontinuous current esposure. The largest remains occur at Los Santos de Maimona, Bienvenida, Casas de Reina and Cerrón del Hornillo (Fig. 11.8). Generally fault-bounded at least on one of their margins, the Mississippian successions in most of them lie unconformable over variably deformed Cambrian rocks, providing evidence of significant uplift and denudation prior to basin formation. The only exception happens at Cerrón del Hornillo where mid Tournaisian rocks unconformably rest over a tilted lower Paleozoic succession reaching up to the Emsian (Robardet et al. 1986, 1988). The gap involving the Mid Devonian and the early Tournaisian indicates that this area was also subjected to uplift prior to basin formation but much less than in the other outcrops. This difference implies that the uplift event must have been associated, at least in its final stages, to prevailing extensional (or transtensional) tectonic conditions, leading to formation of a horst and graben structure and allowing deep denudation of the horsts and partial preservation of the lower Paleozoic passive margin successions in the grabens (Cerrón del Hornillo). Far away from the continental margin, enhanced extension in Mississippian times led to

formation of regional scale grabens (Pedroches basin, described in the previous section, and COMB; Fig. 11.9).

The sedimentary fill of the COMB shares many characteristics with the lower succession in the Pedroches basin. When exposed, it commences with terrestrial conglomerates or breccia showing features typical of alluvial fans (Odriozola et al. 1883; Quesada 1983; Robardet et al. 1986; Rodríguez et al. 1992); therefore confirming subaerial exposure of the underlying successions. The conglomeratic base is conformably overlain by a sandstone/siltstone/mudstone alternation, locally bearing abundant plant remains and even coal seams at Los Santos de Maimona and Casas de Reina. A transition to persistent marine conditions is recorded in this part of the succession as indicated by intercalations of fossiliferous limestones, progressively increasing upwards; thus documenting a transgressive system tract (Robardet et al. 1986; Rodríguez et al. 1992). Finally, the uppermost strata correspond to a sequence of dark mudstone with interbedded sandstone and conglomerate and eventual limestone olistoliths, being only preserved at Los Santos de Maimona that is by far the most complete exposure (Odriozola et al. 1983; Quesada 1983; Rodríguez et al. 1992). Another common element with the Pedroches basin lower succession is the presence at various levels of the stratigraphic sequence of mafic volcanic and hypabyssal rocks (lava and pyroclastic flows, epiclastic rocks, sills and dikes; Odriozola et al. 1983; Larrondo et al. 2005). Volcanic rocks are absent in the Cerrón del Hornillo syncline and very rare at Casas de Reina. In geochemical terms, these mafic volcanic rocks vary from trachybasalts to trachyandesites and show a moderate alkaline affinity (Larrondo et al. 2005, 2007) suggestive of a within-plate environment.

At Los Santos de Maimona the carbonate rich part of the succession is composed of shales, marls and carbonates with sedimentary structures suggesting deposition in a tidal-influenced shallow platform. Limestone rocks are dominated by bioclastic layers and (patch) reefs (Rodríguez et al. 1992; Rodríguez and Sánchez-Chico 1994; Rodríguez and Falces 1994; Rodríguez 1996, 2014), and contain abundant faunas of rugose and tabulate corals, brachiopods, calcareous algae, echinoderms, bryozoans, molluscs, foraminifers, ostracods, trilobites, etc., which indicate a late Visean age. In turn, carbonates at Cerrón del Hornillo have yielded a rich conodont fauna of mid Tournaisian age (Robardet et al. 1986). This significant age difference implies basin formation and onset of carbonate deposition much earlier in the latter area than in the rest of the COMB, and suggests initial nucleation of a graben at Cerrón del Hornillo, later on propagated and widened towards the other areas to become the COMB.

Also here, as in the case of the Pedroches basin, extension and existence of seaways towards the NW (present coordinates) are hard to reconcile with the fact that continent-continent collision was taken place in this direction at the time. Connection towards the north with the Pedroches basin in very likely owing to the above referred similarities. In addition, connection via other coeval basins (Terena, Cabrela/Toca da Moura; Fig. 11.9) towards the south, where relic Rheic Ocean lithosphere had not been fully subducted yet, is a likely option but the lack of exposure and complex structure of the OMZ prevent recognition of the possible links. Alternatively, and/or complementarily, connection towards the east (Paleotethys) seems also possible (Armendáriz et al. 2013).

Finally, the basin was inverted and deformed during the second deformation event in the OMZ, when closure of the remaining Rheic Ocean brought the OMZ margin to collide with the northern margin of the SPT, starting in the late Visean and subsequently propagating towards both forelands until the waning of Variscan convergence in Early Permian times (Ribeiro et al. 1990; Quesada 1991, 2006).

11.3.6 The Carboniferous Baixo Alentejo Flysch Group: Sedimentary Provenance and Basin Development

P. Fernandes, Raul S. Jorge, B. Rodrigues, J. T. Oliveira

11.3.6.1 Stratigraphy

The Baixo Alentejo Flysch Group (BAFG) represents the development of a foreland basin formed as a result of the collision of the South Portuguese Zone (SPZ) and the Ossa Morena Zone (OMZ), with associated tectonic stacking that propagated from NE to SW (Oliveira 1990; Silva et al. 1990; Pereira 1997, 1999).

The BAFG crops out extensively in the SPZ (Fig. 11.8) and consists essentially of sediments deposited by gravity flow, forming a thick (>5 km) turbiditic sequence. Sedimentological studies and stratigraphic dating have contributed to subdivision of the BAFG into the Mértola, Mira and Brejeira Formations, in decreasing age order (Oliveira et al. 1979; Oliveira 1983; Oliveira and Wagner-Gentis 1983). In Spain, the sequence equivalent to the BAFG, and designated as the Culm Group, is not subdivided into formations, though it shows the same lithologies and sedimentary features as those of the Mértola Fm.

The Mértola Formation, more than 1000 m thick (Oliveira 1983, 1988), consists of greywacke beds of variable thickness (few centimetres to more than a meter) interbedded with shales, siltstones and conglomerates. The greywacke beds show sedimentary structures typical of proximal turbidites, namely: dominance of the Ta-c divisions of the Bouma Sequence, amalgamated beds, fluidisation structures (clastic dykes) and synsedimentary folds (slumps). Conglomerate beds are more frequent close to the contact with Iberian Pyrite Belts lithologies and are made up of cobbles

and boulders of lithologies that are common in the Iberian Pyrite Belt. The turbidites of the Mértola Formation are usually organized in several thinning-upward sequences that resulted from lateral migration and avulsion of depositional lobes of submarine fans (Oliveira 1988). The average modal composition of greywackes from the Mértola Formation is Qt46.2F26.9L26.19, where Qt is the modal abundance of quartz, F is the modal abundance of feldspar and L is the sum of all lithic fragments (Jorge et al. 2013). Thick shaley strata within the Mértola Formation turbiditic lobes contain late Visean ammonoid fauna and miospores (Oliveira et al. 1979; Korn 1997; Pereira et al. 2008). Paleocurrent studies in the Mértola region indicate progradation of the turbidite lobes to S-SW (Oliveira 1983, 1988).

The boundary between the Mértola Formation and the younger Mira Formation is represented by a belt with great lateral continuity, composed of shales and siltstones with ca. 50–100 m in thickness, which may indicate a major transgression and/or basin floundering after propagation of the orogenic wedge. This sequence, where mudstones predominate, has yielded ammonoids indicating late Visean age (Oliveira and Wagner-Gentis 1983; Korn 1997).

The Mira Formation consists of greywackes interbedded with shales and rare conglomerate beds, showing turbidite-type sedimentary structures. Although there are no comprehensive sedimentological studies of this formation, the available data indicate that the turbidites of the Mira Formation are generally thinner-bedded and have fewer sand-rich strata than those from the Mértola Formation (Oliveira et al. 1979; Oliveira 1983). The average modal composition of the Mira Formation greywackes is Qt61.7F7.6L30.7 (Jorge et al. 2013). Ammonoid faunas from the Mira Formation shale beds indicate Serpukhovian to middle Bashkirian age (Oliveira et al. 1979; Oliveira 1983).

The Brejeira Formation is made up of greywackes, shales and quartzwackes, and, similarly to the other two formations of the BAFG, exhibits an overall turbiditic character. The basal part of this formation consists of thick beds of matrix-poor quartzwackes interbedded with shales (Oliveira et al. 1979; Oliveira 1990), forming a 5–10 km-wide, NW-SE trending belt. Another belt comprising thick-bedded matrix-rich greywackes and shales occupies a vast area to the southwest. The average modal composition of greywackes from the Brejeira Formation is Qt83.1F6.7L10.1. Abundant quartz grains are rounded to sub-rounded and well sorted (Jorge et al. 2013). The clastic lithologies in this formation contain abundant clasts of sedimentary rocks and metamorphic quartz, but are poor in volcanic fragments (Jorge et al. 2013). Paleocurrents recorded from the Brejeira Formation show a predominant NNW to SSE flow direction, though it becomes more variable towards the S-SW, probably due to the fact that the turbidite flows were constrained to fill up the submarine topography made by the carbonate platform of the Carrapateira Group. Detailed studies of the palynomorphs and ammonoid fauna of the Brejeira Formation indicate ages ranging from the middle Bashkirian (Miospore Biozone FR), near the contact with the Mira Formation, to the upper Moscovian (Miospore Biozone OT), in the coastal sections to the north of Cabo de São Vicente (Pereira 1999; Pereira et al. 2008).

11.3.6.2 Whole-Rock and Isotope Geochemistry

Paleoweathering Conditions and Implication for Source Area Composition

The values of the Chemical Index of Alteration (CIA = [$Al_2O_3/(Al_2O_3 + CaO^* + Na_2O + K_2O)$] × 100, where CaO* is the amount of CaO incorporated in the silicate; Nesbitt and Young 1982) for the greywackes of the Mértola and Mira formations show small variation (62–74 and 67–72, respectively), and suggest moderate and steady state chemical weathering conditions in the sediment source areas. On the other hand, the greywackes from the Brejeira Formation display CIA values within the 63–83 range, with the highest CIA values for the greywackes at the base of the Brejeira Formation, and the lowest associated with the greywackes from the top of this Formation. The dispersion observed in the CIA values is illustrated in the A-CN-K ($Al_2O_3 - (CaO^* + Na_2O) - K_2O$) diagram, where the values for the Brejeira Formation greywackes are plotted on an ideal weathering trend parallel to the A-CN line (Fig. 11.23; Jorge et al. 2013). Therefore, the considerable variation in the weathering conditions recorded for the Brejeira Formation suggests the occurrence of non-steady state conditions of weathering typical of a source area where active tectonism allows erosion of all zones within weathering profiles developed on source rocks (Nesbitt et al. 1997).

The shales from the Mértola, Mira and Brejeira formations have average CIA values of 72 ± 3.6, 78 ± 1.8 and 79 ± 1, respectively. These values are higher than the CIA values recorded from the associated greywackes, and are consistent with a lengthy history of chemical weathering (McLennan et al. 1990). The CIA values obtained from both fine- and coarse-grained siliciclastic lithologies suggest that during deposition of the BAFG, between the middle Visean to Moscovian times, important variations occurred in the chemical weathering conditions in the sediment source areas. The progressive change from moderate to intense chemical weathering conditions suggests fast tectonic uplift rates of the source area(s) (Fernandes et al. 2008; Jorge et al. 2013).

In the A-CN-K diagram (Fig. 11.23), the ideal regression lines for the Mértola Formation greywackes intercept the plagioclase-alkaline feldspar joint mostly along the composition of granite to granodiorite rocks and, to lesser extent,

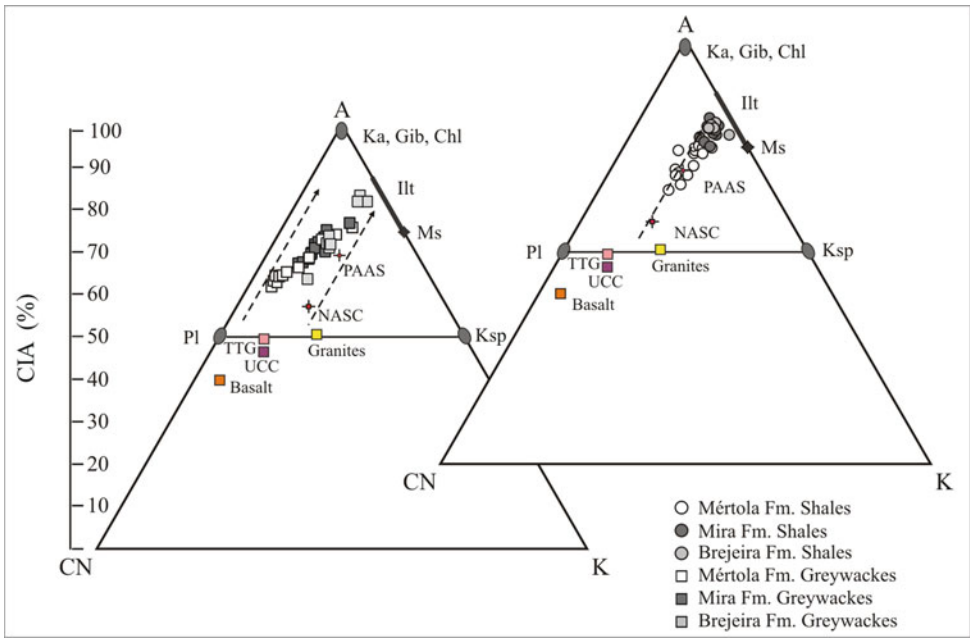

Fig. 11.23 A-CN-K diagrams (after Nesbitt and Young 1982) for the BAFG greywackes (**a**) and shales (**b**). Pl = plagioclase; Ksp = K-feldspar; Ka = kaolinite; Gib = gibbsite; Chl = chlorite; Ms = muscovite; and Ilt = Illite. Dotted lines indicate ideal weathering trends for these protoliths

the basalt-tonalite trend. The greywackes from the Mira and Brejeira formations are plotted along the granite-granodiorite trend only. On other hand, the greywackes from the Mértola, Mira and Brejeira formations plot along the PAAS trend, indicating a sediment source area dominated by igneous rocks of granodiorite composition.

Provenance

The composition of the sediment source area(s) can also be ascertained through trace element geochemistry (e.g. Taylor and McLenann 1985; Wronkiewkz and Condie 1987; McLenann et al. 1990, 1993; Bhatia and Crook 1986; Feng and Kerrich 1990; Cullers 1995; Slack et al. 2004). The chondrite normalized pattern for the shales and greywackes of the three BAFG formations is characterized by a strong LREE enrichment (La/Sm < 4) and by the absence of HREE fractionation (Gb/Yb: 1.5–2; Fig. 11.24). The Eu/Eu* ratios are quite variable: in the greywackes from the Mértola and Mira formations, Eu/Eu* ratios fall within the 1.02–0.65 and 0.95–0.65 ranges, respectively (Table 11.2), whereas the shales of the Mértola and Mira formations present Eu/Eu* ratios of 0.79–0.56 and 0.85–0.66, respectively. The Eu/Eu* ratios obtained for the siliciclastic lithologies of the Mértola and Mira formations suggest a heterogeneous provenance area(s), though markedly dominated by felsic igneous rocks, with subordinated mafic contribution (Jorge et al. 2013).

The greywackes and shales from the Brejeira Formation have less variable Eu/Eu* ratios: 0.70–0.67 and 0.74–0.70, respectively, suggesting marked predominance of felsicigneous rocks and/or mature reworked sedimentary rocks in the provenance area(s) of the Brejeira Formation sediments (Table 11.2).

By plotting Eu/Eu* versus Th/Sc ratios (Slack et al. 2004), it is possible to deduce the relative contribution of the felsic versus mafic rocks for the BAFG sediments. In Fig. 11.25, most siliciclastic rocks of the BAFG fall within the field ascribed to felsic sources. However, a few greywacke and shale samples from the Mértola and Mira formations plot in the field for the mafic sources (Th/Sc < 0.5 and Eu/Eu* > 7) or on the boundary between the fields for mafic and felsic sources. These conclusions are also supported by critical provenance ratios such as La/Sc, La/Co and Cr/Th (Table 11.1). In the Th/Sc versus Zr/Sc diagram (Fig. 11.26), there is a considerable increase of the Zr/Sc ratio in the greywackes of the Mira Formation, and particularly, of the Brejeira Formation. This reflects a significant increase of the sedimentary reworking rates associated to these lithologies.

Bulk geochemistry of the BAFG siliciclastic rocks thus suggests sediment provenance area(s) characterized by compositional heterogeneities. Granitic rocks with minor proportion of mafic lithologies dominated the source areas for the greywackes of the Mértola Formation. The mafic component is residual for the Mira Formation greywackes, whereas the Brejeira Formation greywackes probably had a conspicuous felsic source, which is associated to an increase in sedimentary reworking. Consistently, the shales of the three BAGF formations suggest granodiorite composition for the sediment source area(s) (Fernandes et al. 2008; Jorge et al. 2013).

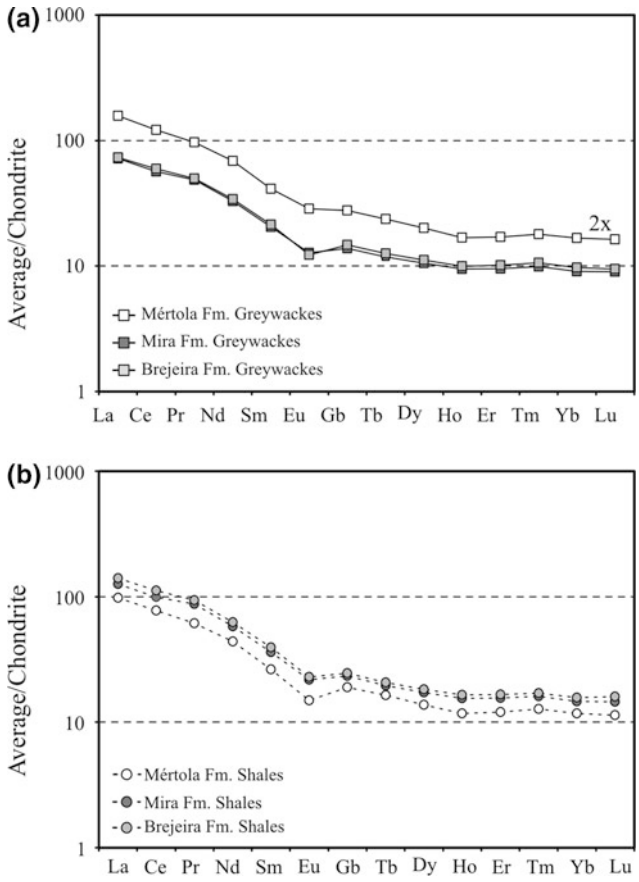

Fig. 11.24 Chondrite-normalized average REE patterns for the BAFG greywackes (**a**) and shales (**b**). Chondrite normalization factors from Taylor and McLennan (1985)

Tectonic Setting

In order to characterize the tectonic setting of the BAFG sedimentary basin, the geochemical composition of the greywackes of the three formations were normalized using the criteria proposed by Floyd et al. (1991). The multi-elemental normalized patterns of the three BAFG formations (Fig. 11.27) are consistent with a geotectonic setting of continental arc/active margin, in spite of the occurrence of positive Hf–Zr–Y anomalies (except for the Mértola Formation) and negative Sr anomalies, which features are typical of passive margins, probably due to the importance of processes associated to sedimentary recycling in these geotectonic settings. Moreover, these anomalies increase in value from the base to the top of the BAFG sedimentary sequence.

The occurrence of both geochemical signatures are, however, common in active margin tectonic setting (forearc, continental arc, back-arc and strike-slip; cf. McLennan et al. 1990, 1993), since in these geodynamic settings sedimentation is marked by "mixtures of young arc-derived material, with variable composition, and old upper crustal rocks". An identical geochemical pattern was recorded for the Devonian synorogenic sediments of the Gramscatho Basin in SW England, Rheno-Hercynian Zone (Floyd and Leveridge 1987; Floyd et al. 1991). On the other hand, the geochemical signatures recorded for the BAFG rocks, especially in the Mértola and Mira formations, may also reflect the cumulative mixture of extra-basinal and intra-basinal sources, corroborating independent palynological, petrographic and paleocurrent evidence that suggests the rocks located at the SW margin of the Ossa Morena Zone and Devonian Phyllite Quartzite Group (PQG) rocks of the Iberian Pyrite Belt acted as source regions for the BAFG (Oliveira 1988; Moreno and Sáez 1989; Moreno 1993; Fernandes et al. 2008; Jorge et al. 2013; Rodrigues et al. 2015). However, for the Brejeira Formation, the average modal component, the geochemical critical ratios of provenance (e.g. CIA, Eu/Eu*, Th/Sc and Zr/Sc) and the normalized multi-elemental pattern (sensu Floyd et al. 1991), are also compatible with the presence of an orogenic external sediment source area with geochemical features typical of old upper continental crust (Jorge et al. 2013).

Rodrigues et al. (2015) made a systematic study of U–Pb ages of detrital zircons from the three BAFG formations. In the Mértola Formation (FM1 sample), 68% of the dated detrital zircons were dated within the 388–326 Ma time interval. This age spectrum can be related to several source areas located both in the South Portuguese Zone and in the Ossa Morena Zone, namely: (i) to Iberian Pyrite Belt volcanic rocks, constrained to the 375–345 Ma time interval (late Frasnian to late Tournaisian; Rosa et al. 2009, Barrie et al. 2002); (ii) to the Campofrio Granite Batholith in the South Portuguese Zone, with estimated crystallization age at 360–349 Ma (de la Rosa et al. 2002; Rosas et al. 2008); (iii) to syn-collisional magmatism and metamorphism occurring in the 355–320 Ma time interval, at the SW limit of the Ossa Morena Zone (Santos et al. 1987; Jesus et al. 2007; Azor et al. 2008), and/or (iv) to the late Tournaisian to Visean volcanism responsible for the Toca da Moura and Cabrela VS complexes of the Ossa PQG Morena Zone (Pereira et al. 2006). From the detrital zircon population in the Mértola Formation sample, only 22% yielded U–Pb ages in the 630–410 Ma range, compatible with an intra-basinal source (Iberian Pyrite Belt, South Portuguese Zone) and/or an extra-basinal source (Ossa Morena Zone), where Ediacaran to Lower Paleozoic zircons are common (Barrie et al. 2002; Braid et al. 2011; Pereira et al. 2012a; Jorge et al. 2013). Ten percentage of the Mértola Formation sample detrital zircons yielded U–Pb ages in the 2193–637 Ma range, very common for detrital zircons in the Phyllite-Quartzite Group of the Iberian Pyrite Belt (Jorge 2009; Jorge et al. 2013).

The age spectra of detrital zircons from the Mira Formation are similar to those from the Mértola Formation (Fig. 11.28). The most numerous populations, making 53% of all detrital zircons, falls within the 369–316 Ma time

Table 11.2 Provenance geochemical data for the Brejeira formation

Elemental ratio	Granites[a]	Andesites	Basalts[a]	UCC[b]	PAAS[b]	Coarse fractions from		Fine fractions from		Greywackes			Shales		
						Silicic sources[c]	Basic sources[c]	Silicic sources[c]	Basic sources[c]	Mértola Fm.	Mira Fm.	Brejeira Fm.	Mértola Fm.	Mira Fm.	Brejeira Fm.
La/Sc	8.00	0.90	0.32	2.73	2.38	2.50–16.30	0.43–0.86	00.7–27.7	00.4–1.1	1.40–2.55	11.34–2.64	2.28–4.63	11.42–2.16	11.49–2.68	11.93–2.68
Th/Sc	3.60	0.22	0.07	0.97	0.91	0.84–20.50	0.05–0.22	00.64–18.1	00.05–0.4	0.47–0.83	0.48–1.05	0.72–1.17	0.47–0.63	0.51–0.74	0.63–0.83
La/Co	3.33	0.90	0.32	3.00	1.65	1.8–13.8	0.14–0.38	10.4–22.2	–	1.24–3.39	0.98–3.00	1.25–25.90	1.25–3.23	1.64–17.5	1.44–7.09
Cr/Th	0.44	9.77	61.25	3.27	7.53	0.5–7.7	22–100	–	–	5.16–9.55	5.55–11.72	5.81–10.09	5.74–8.33	6.96–9.35	7.55–8.64
Eu/Eu*	0.34	0.66	1.09	0.65	0.66	0.40–0.94	0.71–0.95	0.32–0.83	0.7–1.02	0.65–1.02	0.62–0.92	0.67–0.70	0.56–0.74	0.66–0.85	0.70–0.74

[a]Condie (1993); [b]Taylor and McLennan (1985); [c]Cullers (2000)

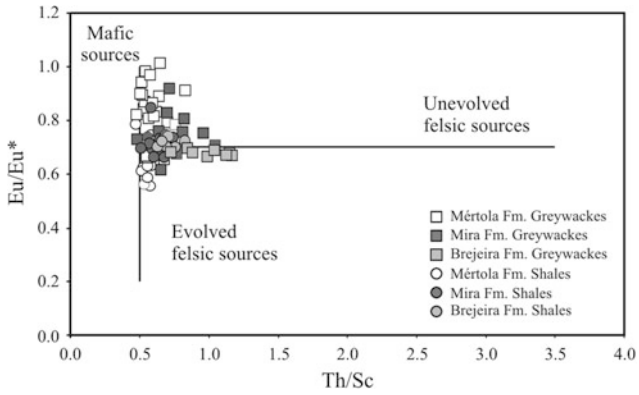

Fig. 11.25 Eu/Eu* versus Th/Sc plot (after McLennan et al. 1990 and Slack et al. 2004) showing the distribution of the BAFG siliciclastic rocks in the fields established for sediments derived from mafic and felsic sources

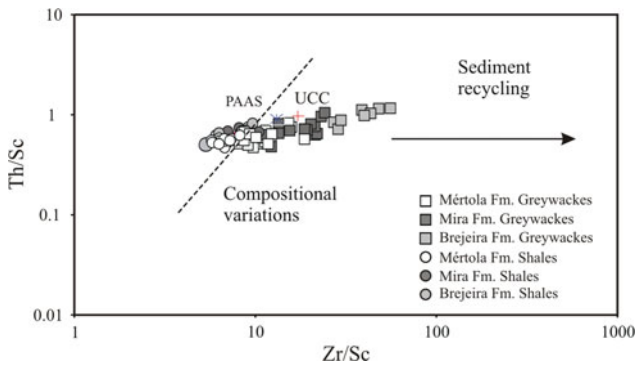

Fig. 11.26 Th/Sc versus Zr/Sc plot (after McLennan et al. 1993). Samples stray from the compositional trend, possibly reflecting the effects of sediment recycling

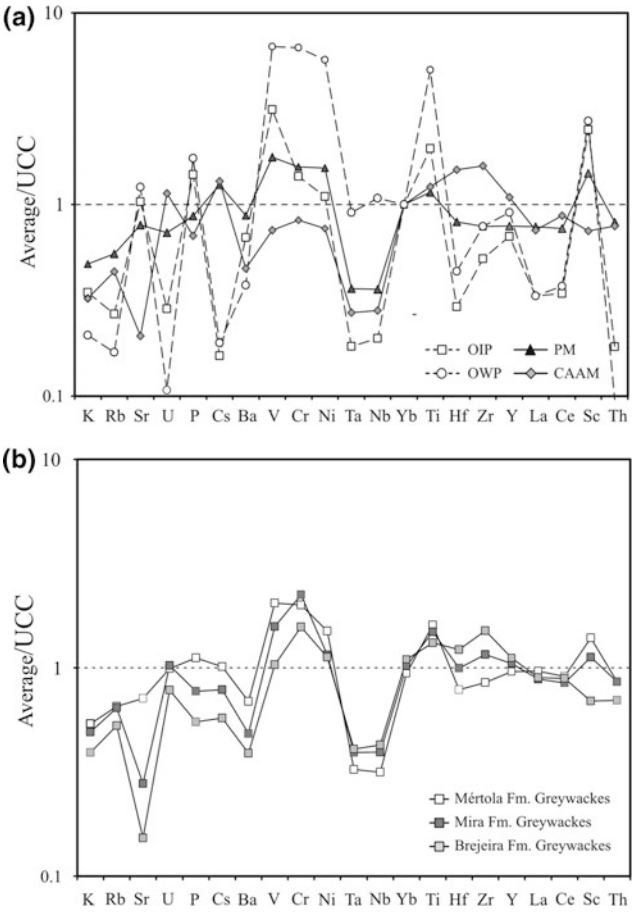

Fig. 11.27 Multi-element plots (after Floyd et al. (1991) of **a**) average greywacke abundance in passive margins (PM), continental arc/active continental margins (CAAM), oceanic island arcs (OIA), oceanic within-plate (OWP); and **b**) average composition of BAFG greywackes

range, showing a conspicuous peak at 323 Ma. The presence of detrital zircons with a U–Pb age close to the depositional age of the Mira Formation (323–315 Ma) suggests the increasing importance of extra-basinal sources, given the absence of zircons of those ages in the South Portuguese Zone (Rodrigues et al. 2015). The source for the detrital zircons of the latter population is most likely related to the multiple Variscan magmatic events that have occurred at the SW border of the Ossa Morena Zone (ca. 355–300 Ma; Santos et al. 1987; Jesus et al. 2007; Azor et al. 2008). The second most abundant detrital zircon subpopulation (30% of all dated zircons) corresponds to the 612–410 Ma time interval, implying source areas probably similar to the areas proposed for the Mértola Formation. Provenance analysis based on the age spectra of the detrital zircons from the Mértola and Mira formations therefore suggests a strong contribution of extra-basinal source areas, located at the SW border of the Ossa Morena Zone, and a minor contribution of intra-basinal rocks (Iberian Pyrite Belt, South Portuguese Zone).

According to Rodrigues et al. (2015), the age spectra of the detrital zircons from the Brejeira Formation are different from the data obtained for the Mértola and Mira formations. Remarkably, the detrital zircons of the Brejeira Formation samples did not yielded U–Pb ages younger than 350 Ma, in clear contrast with the results for the Mértola and Mira formations. In the analysed samples of the Brejeira Formation, 11–16% of dated detrital grains fall within the 467–367 time interval, with peaks at 420, 415 and 366 Ma. The most abundant detrital zircon subpopulation of the Brejeira Formation (ca. 50% of dated zircons), corresponds to the 800–470 Ma time interval and show two main peaks at 680 ma and 623 Ma. This subpopulation was also identified in detrital zircons of the PQG (Jorge 2009; Braid et al. 2011) and in the Tercenas Formation of the SW Portugal Domain (Pereira et al. 2012b), and was related to tectono-magmatic events that occurred in the Cadomian—Avalonian Belt during the Neoproterozoic-Lower Paleozoic period (Jorge 2009; Jorge et al. 2013; Braid et al. 2011). Remarkably, in the Brejeira

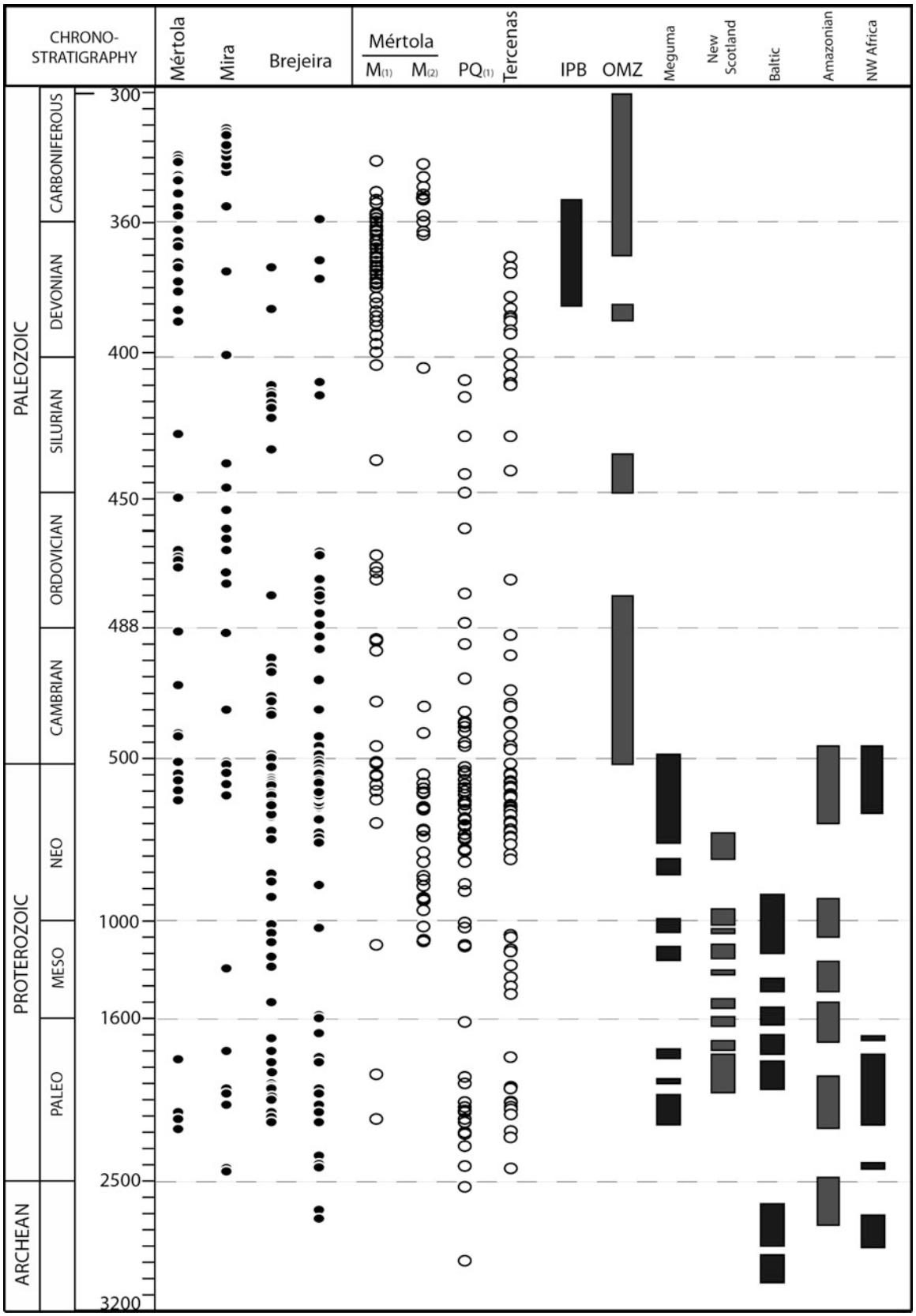
CHRONO-STRATIGRAPHY
Mértola
Mira
Brejeira
Mértola
M(1)
M(2)
PQ(1)
Tercenas
IPB
OMZ
Meguma
New Scotland
Baltic
Amazonian
NW Africa
PALEOZOIC
PROTEROZOIC
ARCHEAN
CARBONIFEROUS
DEVONIAN
SILURIAN
ORDOVICIAN
CAMBRIAN
NEO
MESO
PALEO
300
360
400
450
488
500
1000
1600
2500
3200

Fig. 11.28 Major tectonomagmatic events and zircon ages in the South Portuguese Zone and Ossa–Morena Zone (after Rodrigues et al. 2015). Data sources are as follows. Mértola (Mértola Formation), Mira (Mira Formation), Brejeira (Brejeira Formation): Rodrigues et al. (2015). M1 (Mértola Formation): Pereira et al. (2012a). M2 (Mértola Formation): Jorge (2009). PQG (Jorge 2009), Pereira et al. (2012a). (Tercenas Formation): Pereira et al. (2012a). OMZ (Ossa-Morena Zone): Priem et al. (1970), Munhá et al. (1986), Pinto and Andrade (1987), Santos et al. (1987), Mata and Munhá (1990), Dallmeyer and Quesada (1992), Piçarra and Gutiérrez-Marco (1992), Ribeiro et al. (1992), Mata et al. (1993), Piçarra (2000), Rosas (2003), Carrilho (2004), Salman (2004), Moita et al. (2005a, b), Jesus et al. (2007) and Azor et al. (2008). IPB (Iberian Pyrite Belt): Nesbitt et al. (1999), Barrie et al. (2002), Dunning et al. (2002), Rosa et al. (2009) and Oliveira et al. (2013). Meguma: Krogh and Keppie (1990), Nance et al. (1991), Barr et al. (2003), Collins and Buchan (2004), Murphy et al. (2004a, b, c), Fyffe et al. (2009) and Murphy et al. (2010). Nova Scotia: Keppie et al. (1998). Baltica: Gower et al. (1990), Goodwin (1991), Starmer (1993), Roberts and Siedlecka (2002) and Roberts (2003). Amazonia: Teixeira et al. (1989) and Sadowski and Bettencourt (1996). NW Africa: Rocci et al. (1991)

Formation a subpopulation of detrital zircons with U–Pb ages within the 1100–900 Ma range was also recorded, this time spectrum being usually associated to terranes with an Avalonia-Meguma affinity (Nance et al. 1991; Murphy et al. 2004a, b, c; Fyffe et al. 2009). It is worth noticing that detrital zircons with these U–Pb ages are not represented in the Mértola and Mira formations. Again, these data substantiate other independent data (greywacke petrography and geochemical critical indicators of provenance) that point to a sediment source area external to the Variscan Orogen, with an Avalonian-Meguma affinity, acting as the main provenance area for the Brejeira Formation sediments.

11.3.6.3 Depositional Model

Several reviews on the geological evolution of the SW branch of the European Variscan Orogen were published in the last decades (e.g. Matte 1986a, b, 1991, 2001; Franke 1989; Franke et al. 1990; Oliveira and Quesada 1998; Kroner and Romer 2013; Schumann et al. 2014, among others). The exotic character of the South Portuguese Zone Terrane in relation to the Iberian Terrane is now consensual (e.g. Munhá et al. 1986; Silva et al. 1990; Ribeiro et al. 1990, 2007; Quesada et al. 1991; Onézime et al. 2003; Simancas et al. 2005; Pereira et al. 2012a). Taking this last assertion into account, all sediment provenance indicators investigated in the Mértola and Mira formations lithologies are compatible with sedimentation models that evoke a Variscan collision between the Ossa Morena Zone and the South Portuguese Zone as the main mechanism accountable for the beginning of the turbiditic sedimentation of the BAFG. The provenance indicators suggest that, during the time of deposition of the Mértola and Mira formations (middle Visean to early Bashkirian), both the Ossa Morena Zone and the Iberian Pyrite Belt of the South Portuguese Zone, in different proportions, contributed with sediments to the foreland basin of the BAFG. The fast exhumation and erosion processes that occurred at the SW border of the Ossa Morena Zone (e.g. Rosas et al. 2008), as well as intra-basinal sediment reworking processes, were very important for the development of the SW prograding turbiditic synorogenic sedimentation that characterizes this stage of the evolution of the BAFG sedimentary basin (Schermerhorn 1971; Oliveira 1983, 1990; Oliveira et al. 2013). These conclusions are also supported by the presence of reworked palynomorphs in fine-grained clastic lithologies of the Iberian Pyrite Belt, in the Mértola Formation and in the Toca da Moura and Cabrela Volcano Sedimentary Complexes, located at the SW limit of the Ossa Morena Zone, which indicate that both the Ossa Morena Zone and the Iberian Pyrite Belt were likely provenance areas for the Mértola and Mira formations (Pereira et al. 1999b, 2006, 2008; Lopes et al. 2014).

Detailed mapping of the Mértola Formation, map sheets Mértola and Almodovar, scale 1: 50.000 (Oliveira 1988) identified five main marker bands (B0 to B4) characterized by dark shales and thin-bedded turbidites with variable thicknesses that change from one to several hundred meters thick (Fig. 11.29). These marker bands are dated by ammonoids that belong to the following biozones and corresponding numeric ages (Korn and Klug 2015): Bo-*Goniatites hudsoni* (339–337 Ma) and *Goniatites globostriatus* (338–335 Ma), Brancanes Formation (site 9), stratigraphic equivalent to the Posidonia condensed shales in the Pomarão-Puebla de Guzmán antiform; B1-*Goniatites crenistria* (336–334.5 Ma) and *Goniatites fimbriatus* (334–333 Ma), sites 1, 2, 3 and 4; B2-*Arnsbergensis arnsbergensis* (333–332.116 Ma), site 5; B3-*Paraglyphioceras rotundum* (330.8–330.3 Ma), sites 6, 7 and 8. Well preserved ammonoids were not recovered from Marker band.

The relationship between these marker bands and the allochthonous units of the Pyrite Belt incorporating the Phyllite Quartzite Group (PQG), the Volcanic Sedimentary Complex (VSC) and the Represa Formation, shows that the tectonic load created by SW thrust stacking led to the flexure of the crust generating a depression where the Mértola Formation sediments accumulated (Fig. 11.30). This was the beginning of the foreland basin development, which propagated south-westward in the same manner embracing all the Mértola and the Mira formations sediments.

The continuous southward prograding turbiditic sequence model for the Mértola and Mira formations does not seem compatible with the geochemical provenance indicators and the U–Pb detrital zircon ages from the Brejeira Formation. Rodrigues et al. (2015) proposed a depositional model for the BAFG which tried to conciliate the different phases in

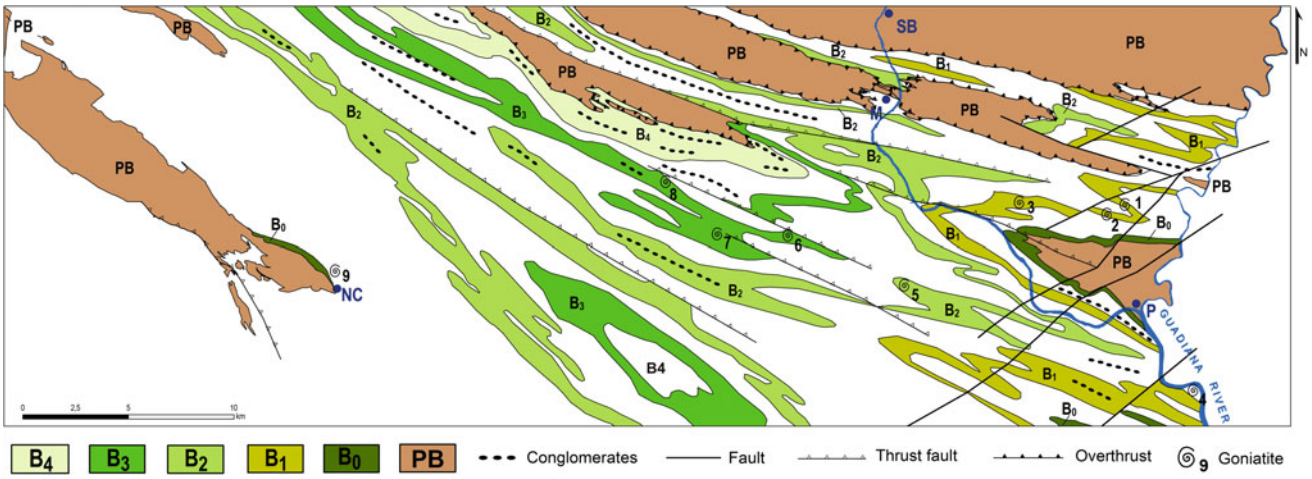

Fig. 11.29 Mértola Formation marker bands, map sheets Mértola and Almodovar, scale 1:50000. Symbols: B0 to B4 marker bands; 1, 2,… 9, sites with identified ammonoids; PB-allochthonous units (PQG-Phyllite Quartzite Group, VSC-Volcanic Sedimentary Complex and Represa Formation, undifferentiated). P-Pomarão; M-Mértola; NC-Neves-Corvo mine

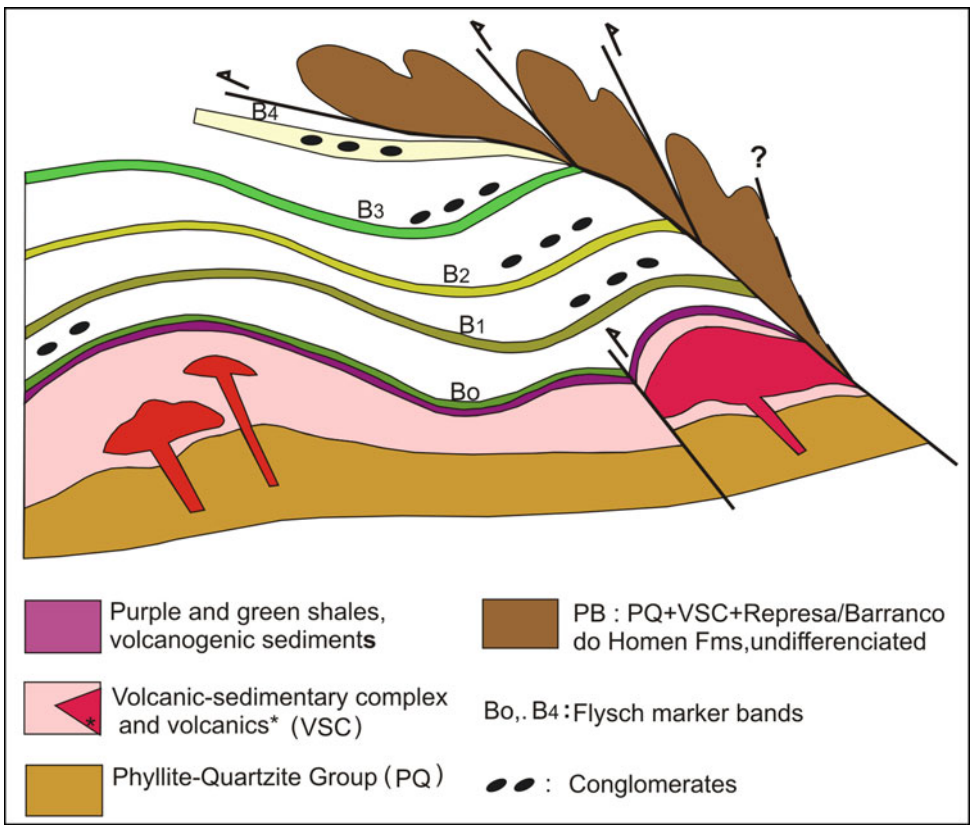

Fig. 11.30 Interpretative sketch for de deposition of the Mértola Formation turbidites. The tectonic load induced by thrusting caused crustal depression where the Mértola Formation turbidites were deposited

the development of BAFG foreland basin and the sediment provenance areas. According to this model, the tectonic load generated the Mértola and Mira formations foreland and an area with positive relief (forebulge) that created a physical barrier separating two sedimentary depocenters. During the time of deposition of the Mértola and Mira formations the forebulge was the site where accumulation of distal marine carbonates and mudstones of the Murração Formation of the Carrapateira Group, South Portugal Domain, took place (Oliveira 1983). From the lower Bashkirian, successive tectonic stacking and sedimentary infill of the foreland basin (Mértola and Mira formations) would have caused uplift of the forebulge area, erosion of the Bordalete and Murração formations, the lower units of the Carrapateira Group and emersion (?) of the Upper Devonian Tercenas Formation sandstones. The forebulge area became a sandy ridge

separating the Mértola and Mira formations from the backbulge basin where the sediments of the Brejeira Formation overlapped the anoxic sediments of the Quebradas Formation. Furthermore, sea-level fall attained a minimum during the lower Bashkirian (Haq and Shutter 2008), and this may also have caused reworking of the uplifted Tercenas Formation and further incorporation of the eroded sediments into the Brejeira Formation, presently represented by a 5–10 km wide band at the lower part of this formation. Palynology data indicate that the sedimentation of the Brejeira Formation prograded to W-SW (today's coordinates) from the lower Bashkirian to late Moscovian (Pereira 1999) implying, therefore, enhanced subsidence in the same direction. Taking into account the provenance indicators and the sedimentological and palynological data from the Brejeira Formation, we suggest that the depocenter of this formation coincided with the backbulge basin. The paths of the sediments arriving to this active subsiding basin were mainly oblique and parallel to today's NW-SE strike of the Brejeira Formation, and were sourced from lateral elevated crustal blocks of the Avalonian-Meguma Terrane, as indicated by paleocurrents.

11.3.7 Late-Orogenic Intermontane Basins in SW Iberia

C. Quesada, V. Gabaldón

Continuous oblique convergence after the onset of collision in this SW part of the Variscan orogen produced a deformation wave that propagated centrifugally from the suture zone towards both forelands, and involved the inversion of the two peripheral foreland basins described in the previous sections (Pedroches and Baixo Alentejo). As a result, the SW Iberia orogen became progressively emerged from Bashkirian through to late Moscovian time. Nevertheless, persistence of the oblique convergent regime induced reactivation of some major lineaments that allowed formation of several terrestrial basins, as well as its subsequent inversion and deformation. Finally, under waning convergence, some other basins formed in Stephanian and Early Permian times, probably in response to gravitational readjustment of the previously thickened lithosphere.

11.3.7.1 Westphalian Successor Basins Associated to Reactivation of Major Lineaments

Reactivation of the two major shear zones bounding the OMZ triggered formation of terrestrial basins, among which the following are currently preserved: Peñarroya-Belmez-Espiel (Westphalian B) at the northern OMZ boundary with the CIZ (Badajoz-Córdoba shear zone; Fig. 11.8); and Villanueva del Río y Minas (late Westphalian A) and Santa Susana (Westphalian D) at the southern limit of the OMZ with the SPZ (South Iberian shear zone; Fig. 11.8). These are to be considered as successor basins as they exploited the same, or associated faults that played a master role in the development of previous basins, i.e. the Pedroches basin in the former case and the Toca da Moura and Cabrela intra-arc basins in the two latter cases. The preserved outcrop of the Villanueva del Río y Minas basin is very small and poorly exposed. In addition, no studies have been performed since the shutdown of coal exploitation in 1972; reason why no further information is provided here (see Mingarro 1962 and Quesada 1983 for details). In turn, the Santa Susana basin is dealt with below, in the section devoted to the Carboniferous intermontane basins of Portugal.

Peñarroya-Belmez-Espiel Coalfield Basin

This is the largest and best known terrestrial basin in SW Iberia, the latter due to important coal exploration and mining operations performed for most of the XXth century. Preserved exposure forms a linear, ca. 50 km long, <2 km wide, continuous WNW-ESE belt and some other disconnected outcrops extending along strike towards both WNW and ESE. Its present structure, acquired during post-depositional inversion, defines a locally complex asymmetrical syncline, with a gently dipping northern limb and a steeply dipping, locally overturned southern flank. The syncline is located in the footwall of an important sinistral thrust, bringing in the hanging wall OMZ Precambrian basement and unconformably overlying Mississippian rocks belonging to the Guadiato division of the Pedroches basin (Wagner et al. 1983; Quesada and Garrote 1983; Gabaldón and Quesada 1986; Wagner 2004).

In general terms, basin fill is constituted by terrestrial deposits characterizing an alluvial fan depositional system (Wagner et al. 1983; Gabaldón and Quesada 1986) in which: (i) proximal facies (debris flows) make most of the preserved record in the eastern part (E of Espiel); (ii) braided river deposits (alluvial plain mudstone with abundant rootlet beds and coal seams and amalgamated sand/conglomerate channels) predominate in intermediate areas (between Espiel and Belmez); and (iii) distal lacustrine facies (laminated mudstone with fresh water fossils and allochthonous coal seams) dominate the western end of the exposure. Paleocurrents indicate predominant longitudinal, ESE towards WNW drainage pattern (Wagner et al. 1983; Gabaldón and Quesada 1986). However, at the preserved northern margin of the Westphalian outcrop the base of the succession consists of debris flow deposits infilling a paleotopography, with an apron-like geometry and showing N to S paleocurrent direction (Andreis and Wagner 1983; Wagner et al. 1983). This change relative to the predominant longitudinal drainage pattern, together with the local derivation of the basal debris flows constituents (Paleozoic passive margin rocks of

the CIZ), suggests proximity to the northern original basin margin, probably a fault (or a series of faults) scarp(s) fringed by an apron of anastomosing debris fans, laterally supplying sediments to the basin (Andreis and Wagner 1983; Gabaldón and Quesada 1986; Wagner 2004). The southern basin margin is not preserved as it was affected by the late sinistral thrust that now makes the southern limit of the exposure. Nevertheless, existence of conglomerates bearing cobbles derived from the adjacent Mississippian strata has been reported from boreholes drilled near the present south margin (Wagner in Gabaldón and Quesada 1986). This may probably indicate lateral supply also at this margin and an overall graben structure of the basin.

On the basis of the paleofloristic content (summarized by Wagner 1999), a W to E migration of depocenters along the strike of the basin has been documented by Wagner (2004), with an early depocenter in the area near Peñarroya during late Langsettian and early Duckmantian (Álvarez-Vázquez 1995), and a second one located eastwards during the late Duckmantian (Álvarez-Vázquez 1995). Wagner (2004) interpreted this migration in connection with sinistral displacements along the southern margin fault, which he considered the Principal Displacement Zone (MDZ), in the sense of Christie-Blick and Biddle (1985). In fact, this important fault zone marks the actual boundary between the OMZ and the CIZ. In this fundamental paper, Wagner (2004) interpreted this basin, and many others in SW Iberia, as a strike-slip basin developed at a releasing bend along the MDZ; its subsequent inversion taking place at a restraining bend along it. Moreover, he envisaged as apparent the overall synclinal structure, just being the result of tightening an original basinal sag structure.

An interesting feature of the basin fill with important paleogeographic significance is provided by the presence of abundant polished and striated pebbles and blocks in debris flows at the eastern part of the exposure (Delgado et al. 1980). These typically glacial-related structures suggest transport of the clasts by glaciers prior to alluvial reworking and incorporation to the debris flow deposits where they occur at present. Bearing in mind the subequatorial position estimated for Iberia in the paleogeographic reconstructions available for the time considered (e.g. Stampfli et al. 2002, 2013; Scotese 2004; Torsvik and Cocks 2004, 2013a, b, 2017; Domeier and Torsvik 2014; Matthews et al. 2016), the glacial features could only form in several thousand meters high mountains, which provide evidence of the generation of an important relief in this part of the Variscan belt (Wagner et al. 1983; Quesada et al. 1990).

11.3.7.2 Stephanian-Early Permian Basins

Puertollano Basin (Late Stephanian B)

This is a very singular basin, located in the southern Central Iberian zone (Fig. 11.8) and currently covered by Miocene to recent sediments. The basin fill is only known by coal and bituminous shale mining and drill cores as no natural outcrops exist. The structure of the preserved part consists of a very gentle E-W striking syncline split by a smooth central anticline (Wagner 1983, 1985; Quesada and Garrote 1983). Unconformably overlying Paleozoic passive margin CIZ successions, the base of the basin fill onlaps over a marked paleotopography, as made evident by borehole data (Wagner 1983, 1985). A majority of the stratigraphic record corresponds to lacustrine deposits with important volcaniclastic intercalations, mainly in the lower part of the succession (Wagner 1985; Wallis 1985). Maximum preserved thickness reaches ca. 470 m in a borehole that drilled into the basement (Wagner 1983). The dominant lithology consists of massive mudstone with a significant volcaniclastic component and abundant fresh-water fauna (fishes, bivalves), in which variably thick interbeds (cm-to-m-scale) of argillitized felsic tuffs (K-bentonites ∼ tonsteins; Králík and Pešek 1985), banded coals and oil shale, frequently occur. The upper part of the succession includes fluvial deposits, progressively more abundant upwards (Wagner 1985; Wallis 1985). In addition, local presence of rootlet beds and fossil standing trees may indicate marshy transitional areas. In fact, Wallis (1985) identified a marginal delta filling up the lake in the western part of the basin, thence becoming a swamp area.

On the basis of the macroflora, Wagner (1985) established a late Stephanian B age for the preserved Carboniferous succession. The source of the felsic volcaniclastic rocks is unknown.

Viar Basin and Other Autunian Outcrops

Autunian rocks occur in various disconnected outcrops with similar characteristics located in the southeastern OMZ, collectively known as Guadalcanal basin (Broutin et al. 1983a). Rocks of this age are also exposed in the Viar basin (Fig. 11.8), also called Valdeviar basin by Wagner (2004), at the easternmost SPZ close (most of the outcrop actually juxtaposed) to its boundary with the OMZ. Both the Guadalcanal (sensu Broutin et al. 1983a) and Viar basins developed under terrestrial, fluviolacustrine conditions (Broutin et al. 1983a; Simancas et al. 1983; Simancas 1985; Sierra and Moreno 1997; Wagner 2004; Wagner and Mayoral 2007), although some discrepancy among authors exists on the interpretation of some deposits within the Viar basin (i.e. relative importance of fluviatile versus lacustrine facies).

All the preserved outcrops of the Guadalcanal basin show a flat-lying fill, locally cut by post-deposition faults and eventually tilted, attesting for its post-orogenic nature. The exposed basin fill consists of: (1) a lower fluviatile succession (Broutin et al. 1983a) filling up a remarkable paleotopography (still obvious near San Nicolás del Puerto). Locally, the top of the fluvial succession is represented by a sandstone horizon with abundant rootlets, which underlies a discontinuous (up to 60 cm thick) coal seam; (2) an intensely bioturbated, fresh-water fauna-bearing, laminated

mudstone succession, interpreted as a lacustrine deposit (Broutin 1981; Broutin et al. 1983a); and (3) a several meters thick sandy horizon, in which wave ripples, flaser and linsen sedimentary structures are very abundant, suggesting deposition in lacustrine nearshore environments under conditions of important wave activity (Broutin et al. 1983a). Locally a second, also discontinuous coal seam separates the top sandstones from the lacustrine mudstones. Also, several cm-thick, altered felsic volcaniclastic layers (tonsteins) occur in places. Fossil paleoflora allowed assigning an Autunian age to the Guadalcanal basin (Broutin 1981, 1986).

On the other hand, the Viar basin represents the largest preserved outcrop of Autunian rocks in SW Iberia, being well exposed along the Viar river valley and those of some tributaries. In contrast with the Guadalcanal basin (usually exhibiting light gray/blueish to yellowish colors), the most salient characteristic of its fill is the predominance of red beds. The only exception occurs in the northern part of the exposure, where a several decameters thick package of felsic (rhyolite-rhyodacite) volcaniclastic and epiclastic rocks show greyish colors (Grey Member; Simancas et al. 1983; Simancas 1983, 1985; later called Los Canchales Fm. by Sierra et al. 2009 and Moreno et al. 2010). The felsic volcaniclastic and epiclastic rocks were originally interpreted as variably silicified siliciclastic rocks derived from a granitic source (Simancas 1983, 1985; Simancas et al. 1983). The presence of fossiliferous (fresh-water) limestone interbeds and several sedimentary structures suggesting wave activity, led these authors to consider the Grey Member as deposited in a lacustrine environment. Also in the northern part of the outcrop, two basaltic packages occur right above and below the Grey Member. Generally considered lava flows (Simancas 1983, 1985; Simancas et al. 1983; Wagner and Mayoral 2007), they have been interpreted as sills by Sierra (2003) and Sierra et al. (2009). Basalts have tholeiitic to alkaline compositions and show affinity to continental rift basalts (Simancas and Rodríguez Gordillo 1980; Sierra 2003). On top of the upper basalts, red beds make all the remaining record in the northern part of the outcrop.

At the southern half of the present exposure only red beds occur. This distribution had been previously interpreted as a result of wedging out of the basaltic and grey felsic units towards the SE (Simancas 1985; Sierra 2003). Alternatively, Wagner and Mayoral (2007) consider depocenter migration and onlap of the top red beds over the previously deposited succession, reaching even the basement in the SW. This interpretation fits with the thickening of the basin fill towards the S shown by an old seismic survey (García Siñeriz 1944). In recent years, the discussion has been centred on whether the red beds, classically considered fluviatile deposits (Simancas et al. 1983; Simancas 1983, 1985), are really mostly fluviatile (Sierra and Moreno 1997, 1998) or mainly lacustrine deposits (Wagner and Mayoral 2007). In our opinion both types coexist.

The structure of the basin defines a very asymmetric syncline, with a shallowly dipping (<10º) western limb and a narrow, steep (locally overturned) eastern limb. The Autunian succession rests unconformably over SPZ rocks in the western limb. In the eastern limb, a late thrust fault, steeply dipping towards the E, brings OMZ rocks onto the basin fill. In fact, this fault is just the frontal one of a system that makes the present boundary between the two Variscan zones (García-Navarro and Sierra 1998). Simancas (1985) interpreted this fault to be active during sedimentation of the Autunian succession, and defined the basin as a half-graben. However, proximal facies such as breccia fans, typical of fault bounded basins, do not exist near the present boundary fault, which can no longer be regarded as the original basin margin. In fact, Wagner and Mayoral (2007) have reported Autunian redbeds overlying OMZ rocks in the hanging wall. It played an important role, though, in the formation of the synclinal structure, subparallel to it, by tilting and dragging the, otherwise undeformed, Autunian rocks in the footwall (Wagner and Mayoral 2007).

Paleofloral remains, mainly recovered from the Grey Member but also present in the red beds, are similar to those at the Guadalcanal basin and of equivalent Autunian age (Broutin 1981, 1986; Wagner and Mayoral 2007). However, the latter authors interpret a somewhat younger age for the Viar basin to account for the contrasting paleoclimatic conditions: more humid at Guadalcanal, arid and stational at Viar, as suggested by the predominance of red beds.

Finally, it is worthwhile mentioning that Broutin (1981, 1982, 1986) described the existence of mix flora at Guadalcanal, composed of exotic Gondwanan, Cathaysian and Angaran-affinity species, both macroflora and palynomorphs, and a predominant Euroamerican flora. This mixed association does not exist in coeval basins on northern Iberia or Western Europe but became widespread in those areas in Late Permian or Triassic times. On this basis, Broutin (1986) considered a connection of the SW Iberian Massif with African areas of Pangea and the existence of a physical barrier, which he interpreted as a high mountain range that impeded migration of the exotic flora towards more northerly areas. This interpretation has been critizised by Wagner and Mayoral (2007) but could find support in the above mentioned evidence of glaciarism in the Westphalian B Peñarroya-Belmez-Espiel basin (Delgado et al. 1980), if the high relief persisted until Autunian times.

11.3.8 Carboniferous Intermontane Basins of Portugal

A. Pinto de Jesus

The Carboniferous intermontane basins of Portugal form small depressions installed unconformably on the present west borders of the Central Iberia and Ossa Morena Zone already

structured during the Variscan orogeny (Fig. 11.31). Three main basins are identified: the Douro Carboniferous Basin, the Buçaco Basin, and the Santa Susana Basin. The basins are aligned along major brittle shear bands and were generated between the Westphalian B and the Stephanian C-Autunian.

Although coal exploitation in the Douro Carboniferous Basin is reported from the beginning of the XVIII century (Cunha et al. 2012), the first coal mining concessions in Portugal are dated of 1850 for the Santa Cristina mine (Buçaco Basin), and 1854 for S. Pedro da Cova mine (Douro Carboniferous Basin). All these basins were studied looking for coal, particularly during the periods of the world wars. The history of these studies is synthetized in Lemos de Sousa and Wagner (1983) deserving special mention the tens of publications carried out by C. Teixeira between 1939 and 1981.

11.3.8.1 Basins Associated to the Douro-Beira Carboniferous Trough

The basins occupy a NW-SE narrow strip extending from Apúlia (NW) to Mioma (SE), which is cut halfway by the granitic massif of Castro Daire (Fig. 11.32). The main structural control is the sinistral shear thrust fault Douro-Beiras Shear Zone (DBSZ) that limits at NE the Douro-Beira Carboniferous Trough. These basins have been studied since the middle of last century in several grounds, mostly with emphasis on their floras (e.g. Teixeira 1944, 1954; Wagner and Lemos de Sousa 1983; Correia 2016) and tectono-stratigraphic development (e.g. Domingos et al. 1983; Ribeiro et al. 1997; Pinto de Jesus 2001, 2003), fauna (e.g. Teixeira 1944, 1954; Eagar 1983; Loureiro et al. 2010) and coal exploration.

The composing outcrops can be grouped in two main distinct basins: Bougado-Ervedosa (1, 2, 3) and Douro Carboniferous (4). Outcrops at Arco and S. Miguel (5) are poorly understood due the bad exposure and because they are strongly deformed and metamorphosed.

11.3.8.1.1 Bougado-Ervedosa Basin (Westphalian D)

The outcrops of this basin are poorly preserved and fractured which prevent a comprehensive sedimentological study. In spite of this limitation it has been possible to identify two stratigraphic units, the Bougado and the Ervedosa formations. The composition of the Bougado Formation is dominated by very coarse breccias at the base and matrix-supported conglomerates, arcosic sandstones, wackes and some interbedded shales at the upper part. Boulders and pebbles of the coarse lithofacies derived mainly from the underlying "Schist-Grewacke Complex" of Lower Cambrian (?) age with a minor contribution from Ordovician quartzites in the NE margin. Taken together these lithologies may represent proximal facies of an alluvial fan. Floras of Linopteris florin, Calamites sp and other megafloristic elements recovered from shales indicates the Westphalian D age (Teixeira 1944, 1954), which matches the interval mid Westphalian—early Stephanian pointed out by Wagner and Lemos de Sousa (1983).

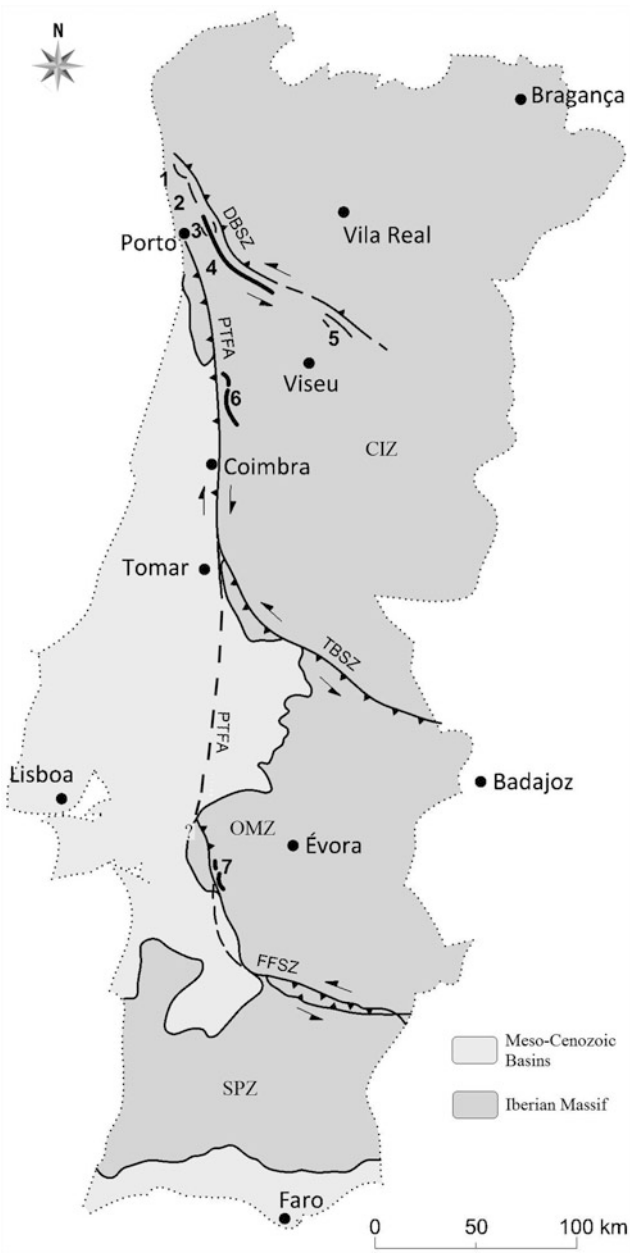

Fig. 11.31 Carboniferous terrestrial outcrops of Portugal. 1. Criaz-Serra de Rates (mid-Westphalian to early Stephanian); 2. Casais-Alvarelhos (Westephalian B to early Westphalian D); 3. Ervedosa (Westphalian D); 4. Douro Carboniferous Basin (lower Stephanian C); 5. Arco and S. Miguel (Westphalian?); 6. Buçaco Basin (uppermost Stephanian C to early Autunian); 7. Santa Susana Basin (uppermost Westephalian D to Cantabrian). CIZ-Central Iberian Zone; OMZ-Ossa Morena Zone; SPZ-South Portuguese Zone; DBSZ-Douro-Beira Shear Zone; PTFA-Porto-Tomar-Ferreira do Alentejo Shear Zone; TBSZ-Tomar-Badajoz Shear Zone; FFSZ-Ferreira-Ficalho Shear Zone (modified from Lemos de Sousa and Wagner 1983)

The Ervedosa Formation consists of thin beds of fine conglomerates and medium to coarse grained sandstones at the lower part and shales at the upper part. The lithofacies

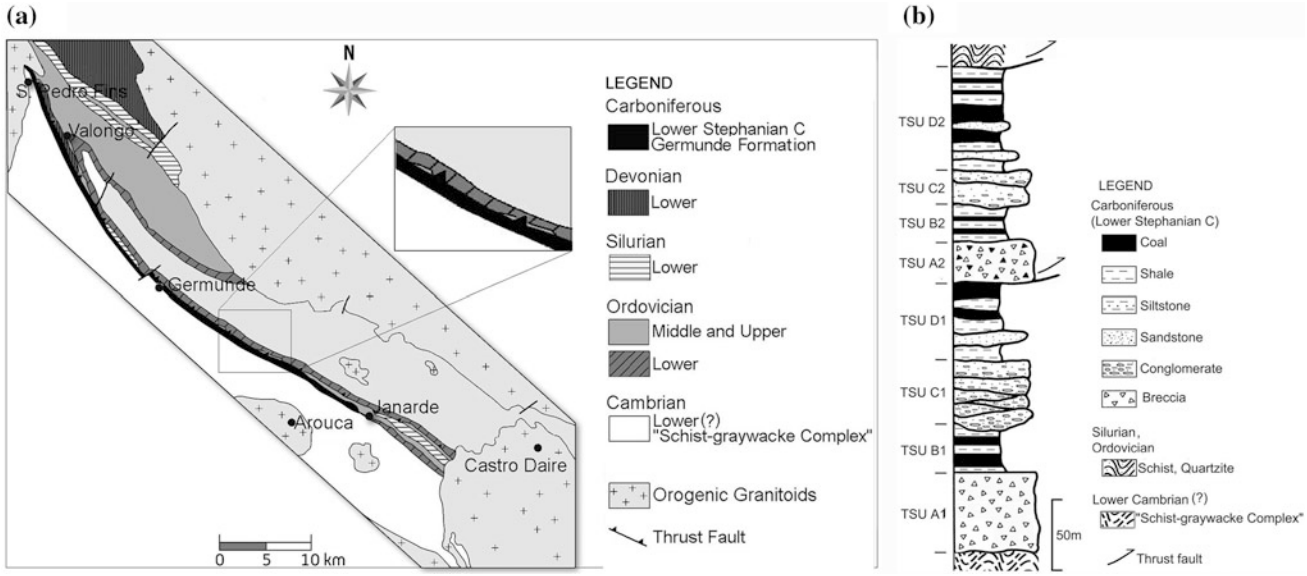

Fig. 11.32 **a** Simplified geological map of the Douro Carboniferous basin (modified from Pinto de Jesus 2003); **b** synthetic lithological succession of the Germunde formation of the Douro Carboniferous basin (Pinto de Jesus 2001, 2003)

of the lower part suggest deposition in the distal area of an alluvial fan fluvial-dominated system with fine alternating layers of shales. The shales which dominate at the upper part are indicative of the floodplain of the same alluvial fan. Megafloristic fossil remains of *Callipteridium jongmansi*, *Alethopteris corsini*, and *Linopteris obliqua* among others indicate a Westphalian D age (Wagner and Lemos de Sousa 1983). A particularity of the Ervedosa Formation is the occurrence of medium scale upright symmetrical folds without associated cleavage which led Pinto de Jesus (2003) to assume that they are contemporaneous of the sedimentation. Regardless the high fossiliferous content of vegetal remains in the beds of this unit coal seam is unknown.

The available data suggest that the Bougado and Ervedosa Formations were laid down in distinct alluvial fans sourced mainly from the uplifted "Schist-Greywacke Complex" in the SW margin, with a minor contribution from the Ordovician of the NE margin.

11.3.8.1.2 Douro Carboniferous Basin (Lower Stephanian C)

The outcrops of Douro Carboniferous Basin are also exposed along strike of a narrow strip between São Pedro de Fins and Janarde. The base of the basin rests unconformably over "Schist-Grewacke Complex" except at Sete Casais outcrop (NW sector) where the basal contact is made by an angular unconformity over the Westphalian D of the Bougado-Ervedosa Basin (Pinto de Jesus and Lemos de Sousa 1998). The strip is thrusted by the reverse limb of the Valongo anticline (Fig. 11.32a). In spite of the strong tectonic deformation it was possible to erect a lithological succession and the composing lithofacies, which are assembled in the Germunde Formation.

The Germunde Formation, after the sequence established by Pinto de Jesus (2001, 2003) is composed of four main tecto-sedimentary units (TSU, in the sense of Megias 1982) with a total thickness of circa 350 m (Fig. 11.32b): TSU A-Alluvial fan debris-flow dominated characterized by matrix-supported breccia; TSU B-Lacustrine/palustrine system marked by fossiliferous shales and coal seams; TSU C-Braided fluvial complex developing multistory/multichannel architecture with predominant SE to NW paleocurrent flow and minor lateral flows from tributaries; TSU D-Lacustrine or palustrine system formed by fossiliferous shale beds and coal seams with intercalations of sandy-conglomeratic beds of deltaic lobes whose main flows had their sources in the NE margin, the rock clasts being mainly composed by quartzite, schist, and lydite (black chert) with provenance from Ordovician and Silurian terranes. The succession is repeated by a thrust fault, the reason by which the symbols of the units in Fig. 11.33 are marked by the numbers 1 and 2.11.

The units bedding has a general strike of N140°, dipping circa 60° to 80° to NE, and the lithological succession is segmented in tectonic slices controlled by thrust faults which form a triplex in S. Pedro da Cova region (NW sector) and a duplex in Germunde region (central sector).

The Douro Carboniferous Basin was the aim of intense coal mining in several underground and open mines. The coal raised to the rank of methanthracite that currently is classified as Anthracite A (Cunha et al. 2012), the incarbonization resulting from the intrusion of granitic rocks in the region, which occurred mainly prior to the basin tectonic deformation (Pinto de Jesus 2001).

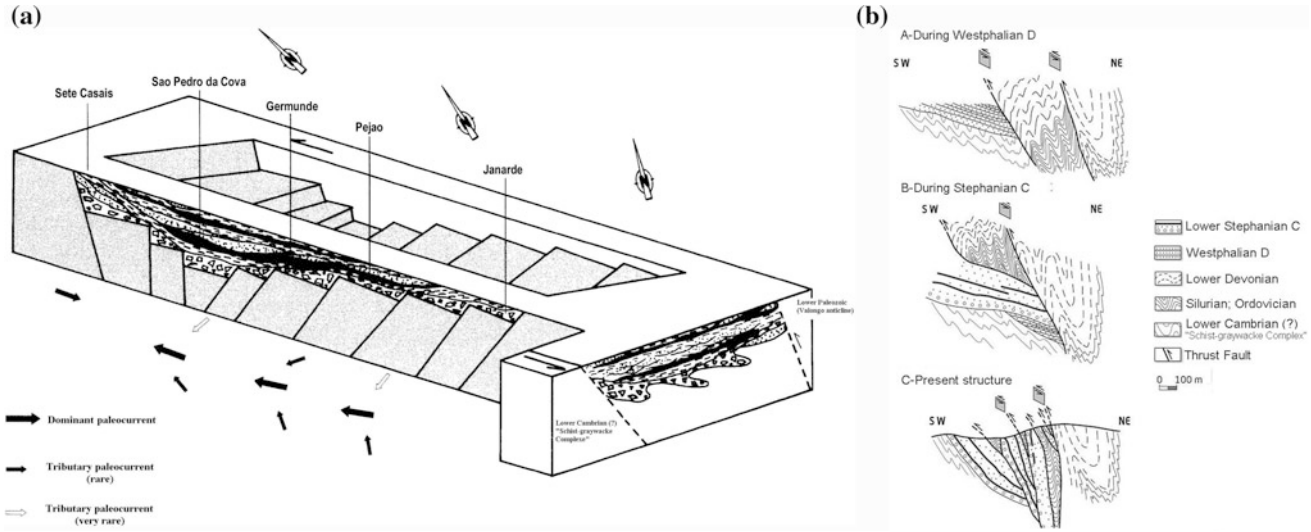

Fig. 11.33 **a** Schematic structure of the genesis and evolution of the Douro Carboniferous basin (Pinto de Jesus 2003); **b** structural evolution of the Douro Carboniferous basin (Domingos et al. 1983)

SE of Germunde (Fig. 11.32a) the upper part of the lithological succession is tectonically eliminated by the thrust fault that places the reverse limb of the Valongo anticline over the Germunde Fm. In this sector only units TSU A1, B1 and rarely C1 occur. The thrust fault is in close relationship with a transpressive regime that was originated during the later phases of the Variscan orogeny.

The Douro-Beira Carboniferous Trough formed as a pull-apart basin related with left lateral transtension tectonics that occurred in two major and similar episodes at different times. The first one took place during the Westphalian in relation with the 3rd phase (D_3) of Variscan Orogeny. The migration of depocenters occurred gradually from NW (Criaz) to SE (Ervedosa) where the most recent outcrops of the Ervedosa Formation are located. At this time the main paleocurrents and the detrital lithologies indicate that the sedimentary filling was coming from the SW margin ("Schist-Grewacke Complex"), with tributary infilling from the NE margin (Ordovician to Lower Devonian) of the Douro-Beira Carboniferous Trough.

The second and stronger episode occurred during the early Stephanian C in relation to the late phase of the Variscan orogeny. The tectonic reactivation of the sinistral transcurrent shear in the Douro-Beira Carboniferous Trough formed another pull-apart with the depocenter gradually migrating from NW to SE until the area of Germunde. In São Pedro da Cova sector (NW part of the Douro Carboniferous Basin), the opening by pull-apart promoted the crustal thinning which led to limited volcanism as indicated by volcanic bombs recognized underground interbedded with coal seams in the São Pedro da Cova mine. The beds lithology and related sedimentary structures indicate fluvial paleocurrents mainly from SE as the migration of the depocenter is evolving in this direction. Sedimentary structures and clasts lithology and mineralogy also indicate provenance of tributary paleocurrents from both margins of the Douro Carboniferous Basin, being more effective from the SW margin.

The structural evolution of the Douro Carboniferous Basin is depicted in Fig. 11.33b (Domingos et al. 1983). According to this interpretation from the Westphalian D to post-Stephanian C the tectonic activity was restricted to successive pulses of thrust faults, usually assumed to be related to the Variscan D_3 tectonic phase.

Pinto de Jesus (2001, 2003) taking mostly into account the tilting of the Douro Carboniferous Basin as well as microfolds in coal seams of this basin and also the intense thrust faulting deformation, suggested the occurrence of a D_4 post-Lower Stephanian C Variscan phase. In fact, Teixeira (1954) had already considered this hypothesis when referring "…if one consider an orogenic phase posterior to the mid-Stephanian and ante-Permian."

11.3.8.2 Buçaco Basin

The Buçaco Basin is located north of Coimbra, on the western border of the Central Iberian Zone. The basin is structurally linked to the Porto-Tomar-Ferreira do Alentejoshear zone (PTFA) an old and major Variscan tectonic structure. The stratigraphic succession is exposed in two main outcrops (Fig. 11.34a): Algeriz to the N, which shows the best exposure and the entire stratigraphic section, and Santa Cristina to the S (Wagner et al. 1983). The basin fill unconformably overlies the "Schist-Grewacke Complex" to the east and contacts the "Crystalophyllic Complex" (Precambrian) through the PTFA to the west.

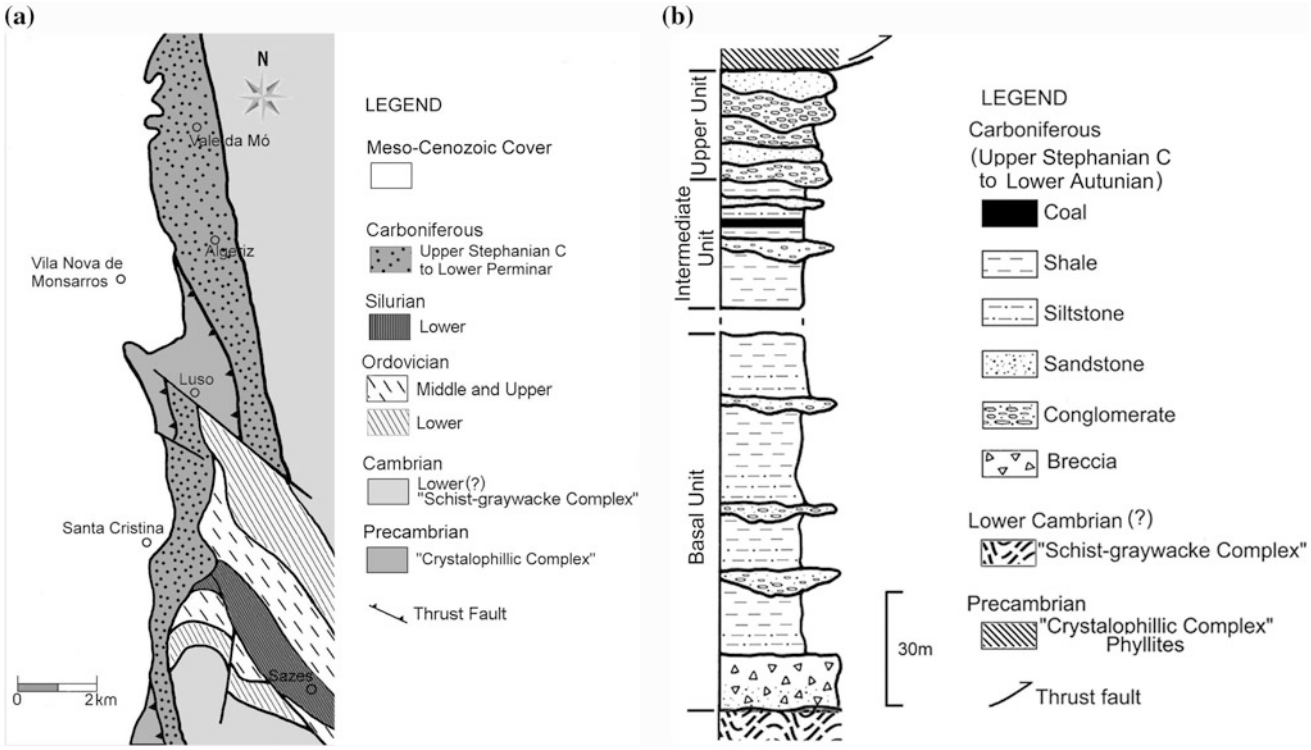

Fig. 11.34 **a** Simplified geological map of the Buçaco basin (after Valle Aguado et al. 2013); **b** synthetic sedimentological and stratigraphic record of the Buçaco Carboniferous formation (adapted from Wagner et al. 1983; Flores et al. 2010; Valle Aguado et al. 2013)

The stratigraphic sequence (Fig. 11.34b) was established by Wagner and Lemos de Sousa (1983) and Wagner et al. (1983), who recognized three formations, from base to top: Algeriz Vale da Mó and Monçarros. More recently Valle Aguado et al. (2013) renamed these formations as: Basal Unit (C1), Intermediate Unit (C2) and Upper Unit (C3). This new stratigraphic nomenclature is adopted in the present work.

The Basal Unit (ca. 600 m thick) is mostly composed of fanglomerates at the base followed by matrix-supported conglomerates, mud flows and layers of siltstones, sandstones and fine conglomerates at the upper part. The clastic content of the basal breccia and conglomerates consists mainly of clasts derived from the uplifted "Schist-Grewacke Complex". The unit was deposited in a debris-flow dominated alluvial fan in subaerial conditions as suggested by red colors in the the entire sequence.

The Intermediate Unit (ca. 40 m thick) comprises siltstones and fossiliferous mudstones with alternating grey and yellow-reddish coloration. Paleosol levels are found throughout the lithological succession. This unit provided most of the flora found in the Buçaco Basin, associated to floating material with some contribution from extrabasinal origin. The studied floras suggest an late Stephanian C to early Autunian age (Teixeira 1944, 1954; Wagner and Lemos de Sousa 1983). Roots in primary position at the upper part of the unit are associated with a thin layer (10–15 cm thick) of coal (bituminous coal C, according to Cunha et al. 2012). This coal was exploited in small open mines. The lithological characteristics and facies are indicative of a lacustrine environment of low depth, subjected to rises and falls of the water level that generated alternating reducing and oxidizing environments. The palustrine environment has a small expression and seems to be restricted to the stratigraphic level in which the coal seam is found (cf. Wagner et al. 1983, p.145 Wagner and Lemos de Sousa 1983).

The Upper Unit (ca. 180 m thick) has an erosive contact with the Intermediate Unit and consists of decametric-thick finning upward cycles formed by conglomerates and coarse to medium and fine sandstones. The conglomerates are composed of well-rounded clasts of quartz, quartzite and black chert arranged in a clastic-supported matrix. They have lenticular geometries and erosive bases and the stratigraphic architecture has a multichannel/multistory fluvial braided signature. Provenance was probably from the south.

The genesis of the basin was interpreted in close relationship with a pull-apart tectonic regime that resulted from right lateral transcurrent shear activity of the Porto-Tomar-Ferreira do Alentejo shear zone (Gama Pereira et al. 2008; Flores et al. 2010). In the field this pull-apart regime is difficult to be recognized. As an alternative interpretation it is suggested that the Buçaco Basin resulted from

the uplift of the east margin ("Schist-Grewacke Complex") caused by a normal fault (Fig. 11.35a).

From the erosion of the uplifted block and consequent downslope sedimentary transport resulted the alluvial fan (Basal Unit) and the palustrine environment (Intermediate Unit) on the alluvial plain. The Upper Unit represents a trunk river whose sedimentary structure indicates sedimentary transport from south to north. Lately, top to the east thrusting associated to the PTFA shear zone placed the Ossa Morena Zone (presently interpreted as the Finisterra Terrane) over the Central Iberian Zone generating open and slight folding (Domingos et al. 1983). The current tectonic interpretation is presented in Fig. 11.35b.

11.3.8.3 Santa Susana Basin

The Santa Susana Basin is located in the south-central zone of Portugal at the boundary between the Ossa Morena (OMZ) and South Portuguese (SPZ) zones (Fig. 11.31). It is controlled by the Ferreira-Ficalho shear zone (FFSZ; western extent of the South Iberian shear zone) and possibly also by the southern extension of the Porto-Tomar-Ferreira do Alentejo shear zone (Chaminé et al. 2003). The geological setting of the Santa Susana Basin is summarized in Fig. 11.36a.

The basin lithologies occur in scattered outcrops with poor exposure which overly magmatic porphyries of the Beja Massif (OMZ) and Toca da Moura Volcano-sedimentary complex, as is the case of the Remeiras and Jongeis outcrops, or are bounded by NW trending faults in Vale Figueira and Moinho da Ordem outcrops. The basin was recently studied by Machado et al. (2012) and Lopes et al. (2014) whose main conclusions are here followed.

Figure 11.36 represents the Vale Figueira section erected by Machado et al. (2012), which is the best although incomplete representative of the basin infilling. Two main stratigraphic units are identified, Basal and Upper units. The Basal unit is represented by very coarse grained conglomerate with abundant felsic "porphyry" boulders, which is overlain by coarse sandstones and polygenic conglomerates. Finer grained rocks and coal seams are rare. The Upper unit is composed of "quartz and quartzite-rich gravel conglomerates, sandstones, shales and coals. The upper shales yielded floristic (Wagner and Lemos de Sousa 1983) and palynological data (Fernandes 1996) that allow dating the unit as Westphalian D and possibly Cantabrian. The unit contained all the coal seams that are now exhausted. The porphyries in the Basal unit indicate provenance from the OMZ and quartzite, quartz and phyllite gravel and clasts suggest a source shift from the SPZ (Horta da Torre Fm). The conglomerates with gravel and boulders of the Basal unit were probably laid down in an alluvial environment. This gave way to a fluvial (meandering?) system as indicated by the positive cyclic sequences where the conglomerates may represent channels and the fine sandstones and shales flooding plains. The upper siltstones and claystones with interbedded coal seams represent lacustrine/palustrine environments.

An alternative interpretation of the sedimentary sequences is here suggested: the positive cycles may correspond to the installation of fluvial-dominated alluvial fans followed by deltaic systems which converge in a lacustrine environment as suggested by delta lobes incised in finer sediments, including coal. The contact at the base of the deltaic lobes is sharp and erosive.

According to Almeida et al. (2006) the basin is closely related to the Santa Susana Shear Zone (SSSZ), along which a right lateral transtensive pull-apart basin was generated. No folding or cleavage has been detected and the tectonic deformation is restricted to the occurrence of some mylonites associated to the present OMZ/SPZ boundary. A former tectonic interpretation by Domingos et al. (1983) places the Toca da Moura Volcanic-Sedimentary Complex and the overlying Santa Susana succession trusted over the Horta da Torre Formation, the upper unit of the Pulo do Lobo Antiform (Fig. 11.36c). A recent study of a local drill found that the Santa Susana Basin sediments are thrusted by the Toca da Moura Complex (Lopes et al. 2014).

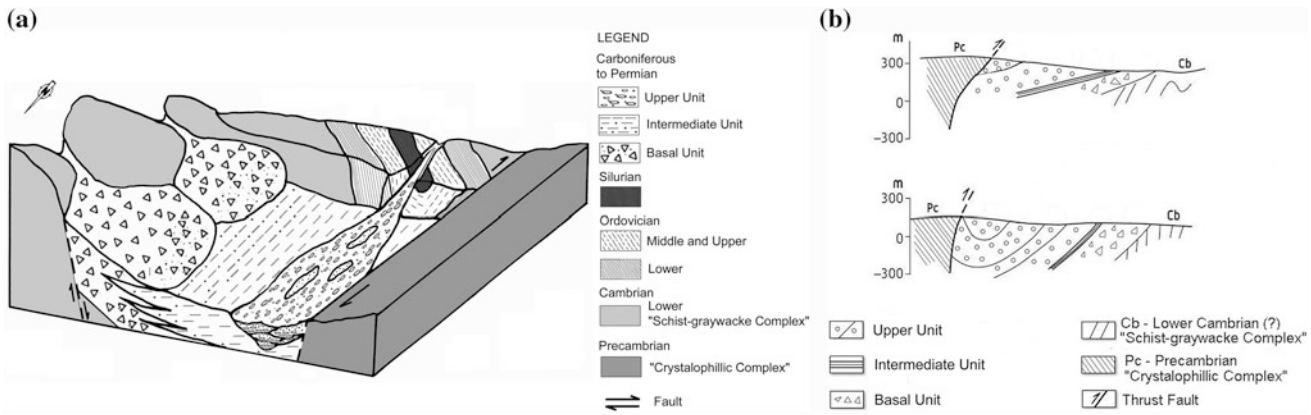

Fig. 11.35 **a** Schematic structure of the genesis of the Buçaco basin; **b** structural evolution of the Buçaco basin (modified from Domingos et al. 1983)

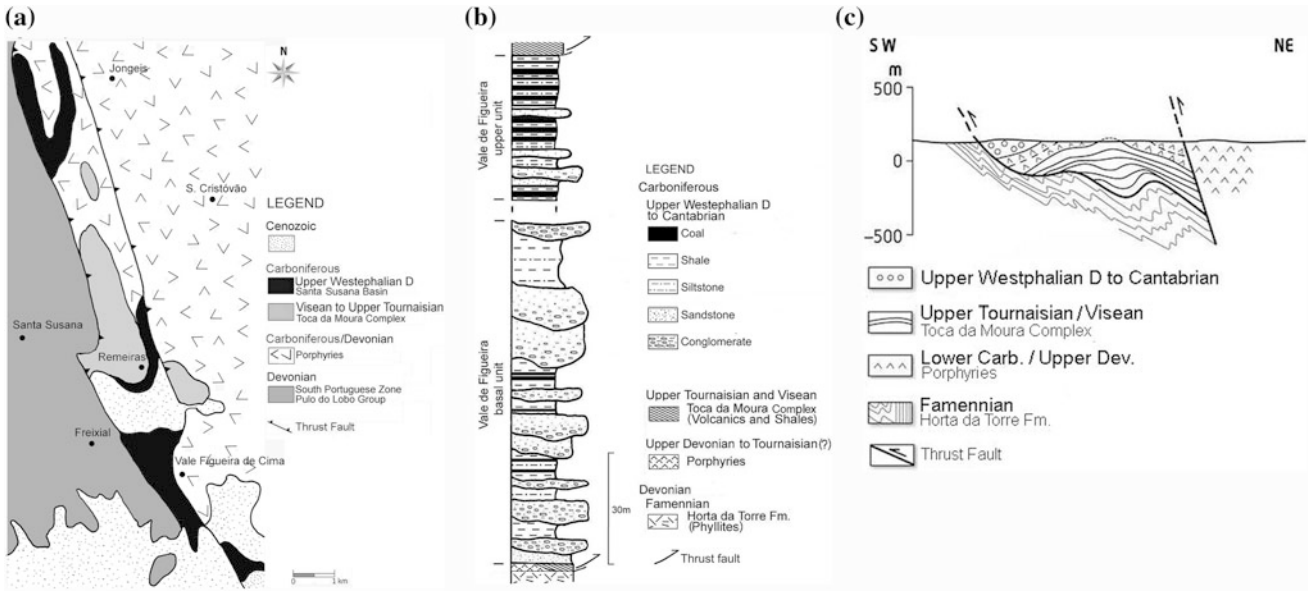

Fig. 11.36 **a** Geological setting of the Santa Susana basin (adapted from Machado et al. 2012); **b** sedimentary record of Santa Susana basin in the Vale de Figueira outcrops (adapted from Machado et al. 2012); **c** structure of Santa Susana basin (adapted from Domingos et al. 1983)

Conclusions

The intermontane basins of Portugal were generated during the Pennsylvanian in clear dependence of shear zones. The basins situated in the Douro-Beira Trough had the following development:

(a) The opening of the Bougado-Ervedosa Basin (Westphalian D) resulted from a pull-apart tectonic regime, probably with two pulses that caused the migration of the depocenters from NW (Bougado) to SE (Ervedosa). The synorogenic sedimentary infilling was structured by a compressive Variscan phase of deformation (D_3?);

(b) The Douro Carboniferous Basin was also generated in connection with a left lateral transtensional pull-apart between the Westphalian D and the early Stephanian C. The depocenters migrate to SE reaching the maximum thickness in Germunde (Pinto de Jesus 2001). A compressive deformation occurred in post-Stephanian time (the late phase (D_4?) of the Variscan Orogeny) causing deformation that resulted from the activity of reverse faults responsible of tectonic slices as well as the week fracture cleavage that affect the sedimentary pile;

(c) The Buçaco Basin is also linked to crustal extension (Valle Aguado et al. 2013) that caused uplifting in the east boundary and an alluvial plain in the down going block. A trunk braided river flowing northwards cut the alluvial plain structuring the Upper Unit. The west part of the basin was probably eliminated by top to the east thrusting in connection with the PTFA shear zone. Slight open folds and fractures may have been caused by the reactivation of the PTFA shear zone.

(d) Concerning the Santa Susana Basin two distinct interpretations have been pointed: the infilling of a subsided area in the eastern side of the OMZ/SPZ thrust boundary (Domingos et al. 1983); in a transtensional pull-apart basin linked to the PTFA shear zone (Dias da Silva et al. 2007).

11.4 Synorogenic Eastern Iberian Peninsula Basins Related to the Paleotethys Margin

J. Sanz-López

Schmidt (1931) introduced the so-called Culm facies, or Culm series, in the geological literature of the Spanish Pyrenees. It usually applied it to designate the upper Paleozoic marine synorogenic siliciclastic flysch-like successions deposited in relation to the Variscan deformation. Indeed, the Culm series is only comparable to the flysch or "Kulmgrauwacken" in the deep water basinal facies of the Kulm sequence filling the German Rhenohercynian basin. In the Alpine chains of the eastern part of the Iberian Peninsula, the Culm series crops out in isolated basement units between Mesozoic–Cenozoic rocks (the so-called Paleozoic massifs in the Pyrenees, Montagne Noire, Catalonian Coastal Ranges, Iberian Ranges and Betic Cordillera; Fig. 11.37). Local stratigraphic units have been defined in each massif and references to the original studies may be found in recent published synthesis, such as Delvolvé et al. (1996), Colmenero et al. (2002) and various chapters included in Vera (2004).

Sedimentation of the Culm series is normally interpreted in a deep sea setting from prevailing transport through gravity flows. The local successions correspond to deposits

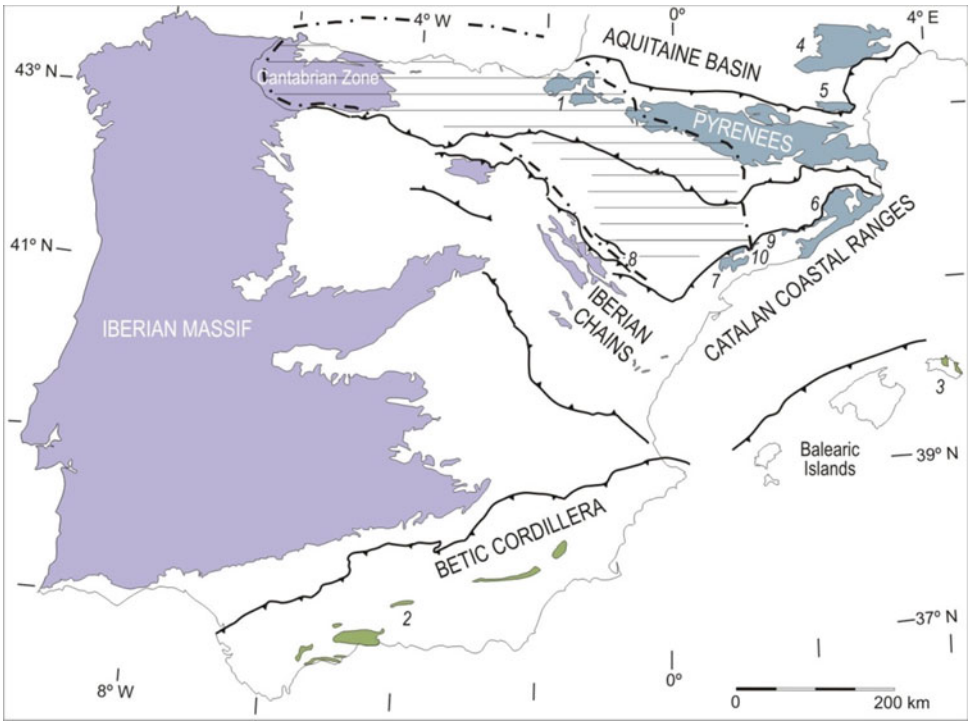

Fig. 11.37 Distribution of Paleozoic rocks in the Iberian Peninsula and Balearic Islands, showing Alpine chains where Carboniferous synorogenic deposits are known. 1. Basque massifs, 2. Malaguide Complex, 3. Minorque, 4. Montagne Noire, 5. Mouthoumet massif, 6. Northern Catalan Coastal Ranges, 7. Priorat and Serra de Prades, 8. Puig Moreno, 9. serra de Miramar, 10. Valls. Dashed-and-point line indicates the boundary between the late Serpukhovian–early Bashkirian carbonate deposits on the Variscan foreland and the siliciclastic Culm series in the foredeep

on slope, canyon fill and deep sea fan systems, whereas a few are rarely recognized as deltaic or shallow-water deposits. Blocks and clasts from the underlying Silurian and Devonian successions are common, whereas older rocks are less abundant, maybe in relation to depth of the erosion in the deformed and exhumed orogen. Polygenic conglomerates may have transported clasts from long distances and they generally show abundant reworked pebbles and cobbles of milky quartz, black jaspers and sandstones, together with metamorphic and igneous lithologies. A rare supply of Carboniferous carbonate clasts and blocks from facies of shallow-water carbonate platform sometimes occur. The location of the carbonate platforms is usually speculative and in relation with denudation of exhumed areas added to the hinterland or unpreserved wedge-top basins (Engel et al. 1981; Delvolvé et al. 1998).

The attempts for reconstructing the sequence of deformation in the Variscan foreland through Culm series analysis face the following problems: (i) the fragmentary nature and scarce extension of the Paleozoic outcrops, (ii) questionable paleogeographic hypotheses, and (iii) the sparsity of reliable age data. Biostratigraphic data are the most abundant, although fossil data from reworked clasts and from the youngest carbonate beds just below siliciclastic sedimentation provide older ages than that of the synorogenic sediments. Recently, radiometric ages obtained from the youngest zircon grain population also resulted to be older than the host rocks (Martínez et al. 2016). Notwithstanding, the changing age of the synorogenic units have supported a model of sedimentation that was migrating along successive wedges or depocenters in the Pyrenees and the Montagne Noire (Mirouse et al. 1983; Engel 1984, Delvolvé et al. 1993, 1998). In this line, the carbonate sedimentation in the foreland shows a progressively younger age cratonwards (Delvolvé and Perret 1989). The sedimentary migration was explained as a response to folding and thrust propagation caused by Variscan compressive shortening. Nevertheless, the spatial relationships between the local tectonic structures and the sedimentary units are only poorly known because they correspond to early structures, subsequently deformed during younger phases.

11.4.1 Carbonate Sedimentation–First Siliciclastic Deposits

The oldest known succession (probably Tournaisian to early Visean in age) is located in the Serra de Miramar (southern Catalan Coastal Ranges; Figs. 11.37 and 11.38), and consists of 50–60 m of carbonate breccias, shales with thin sandstone beds, cherts, volcanic flows and tuffs (Figuerola unit). It is interpreted to be related to extensional tectonics (Melgarejo 1987, 1992) and coeval with the vast siliceous shale and chert condensed sedimentation including radiolarites in the rest of basins (Raymond and Lethiers 1990). Above, late Visean siliciclastics corresponds to about 150 m of sandstone and shales with conglomerate and breccia beds (Miramar unit after Melgarejo 1987) than are thicker southwards in the Priorat and Serra de Prades. There, the

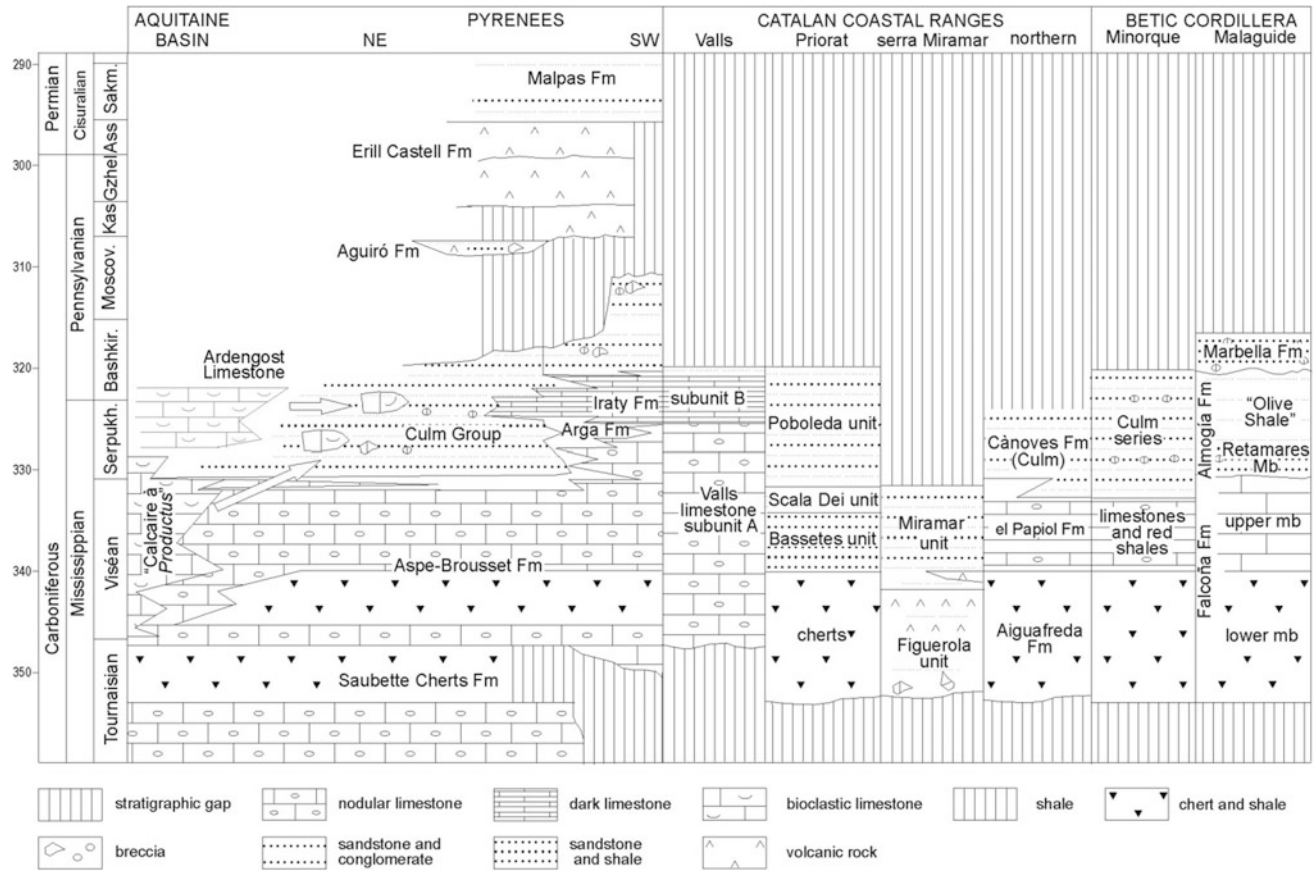

Fig. 11.38 Stratigraphic correlation chart of the Early Mississippian (Carboniferous) to Cisuralian (Permian) stratigraphic units from the Pyrenees, Catalonian Coastal Ranges and Betic Cordillera. Aquitaine basin is indicating the source of reworked Mississippian limestone clasts in the Pyrenean siliciclastic successions

Bassetes and Scala Dei units (780 m thick) were deposited in a slope setting or as a slope-apron system below the outer part of a deep-sea fan, although delta facies were also interpreted (Saéz and Anadón 1989; Maestro-Maideu et al. 1998). A similar sandstone unit described in the Montalbán massif (northeast of the Iberian Ranges; Quarch 1975) could indicate a southern source area. Distal, condensed, siliceous shales and limestones (el Papiol Formation) were deposited in the northern Catalan Coastal Ranges and Minorque Island (the latter interpreted to lay at an extension of the External Betic zones). Both successions have been closely related and yielded similar trilobite faunas, mostly from the *G. bilineatus* Zone (Gandl et al. 2015). Above, deep sea fan systems deposited in Minorque, whereas the condensed siliceous sedimentation locally continued in the latest Visean or the early Serpukhovian in the northern Catalan Coastal Ranges according to the ammonoid occurrences (Kullmann et al. 2001, 2005).

The Aspe-Brousset Formation in the Pyrenees (Perret 1993) consists of condensed sedimentation of nodular limestone bearing deep-water fauna and deposited from the late Tournaisian to the late Serpukhovian. This deep condensed carbonate sedimentation extended from the Cantabrian zone of the Iberian Massif (Alba Formation) to the Montagne Noire (Faugères Formation). It is also recorded in the upper member of the Falcoña Formation of the Malaguide Complex (Internal Betics), where late Visean conodonts occur (*G. bilineatus* to *L. nodosa* zones; Herbig 1983; O'Dogherty et al. 2000). The nodular limestones include carbonate turbidites close to a northern shallow-platform preserved in the Roc de Nitable Variscan nappe (Mouthoumet massif, Fig. 11.37). Platform grew up from the Visean (V1b-V3bγ) to probably the early Serpukhovian (Perret 1976, 1993; Engel et al. 1981; Bessière and Schulze 1984; Poty et al. 2002). Visean breccias and calciturbidites are also interbedded in the nodular limestone succession of the Montagne Noire. There, a shallow-water platform was eroded and deposited as blocks and exotic units ("Calcaire à *Productus*" and "écailles de Cabrières") in the synorogenic siliciclastic basin. They represent a mélange in front of the advancing thrust sheets that moved from the northeast of the Axial Zone of the Montagne Noire (Engel et al. 1978). Carbonate production ended in the early Serpukhovian (Vachard et al. 2016), and may be

contemporaneous with siliciclastic sedimentation in the shallow-water environment (Engel et al. 1981).

Southwards, another shallow-water platform must be located in the Betic-Rifean block, because supplies derived from this area are reworked in the Culm series of the Betic Malaguide Complex and of Minorque (Herbig 1985). Carboniferous shallow-water foraminifer and coral faunas from the Montagne Noire, Pyrenees and the Rif (northern Africa) are closely related geographically and included in the Mediterranean Subprovince of the western Paleotethys Province (Somerville et al. 2013).

11.4.2 Serpukhovian Synorogenic Deposits

The occurrence of siliceous shales at the top of the Aspe-Brousset Limestone was identified as a drowning episode in the foreland basin heralding siliciclastic arrival (Delvolvé et al. 1993). It is diachronous, although at least two events may be recognized: late Visean–early Serpukhovian and late Serpukhovian. The uppermost limestones of the Aspe-Brousset Formation yielded late Visean and occasionally early Serpukhovian conodonts (Boersma 1973; Perret 1993; Sanz-López 1995) whereas shales locally included ammonoids of the Mandette fauna (*Lusitanites subcircularis* among them) in the eastern and northern parts of the Pyrenees (Delépine 1935). This fauna, assigned previously to the latest Visean, is now correlated with the early Serpukhovian. Late Serpukhovian conodonts and ammonoids (Kullmann et al. 2008) occur in the uppermost beds of the Aspe-Brousset Formation in the southwestern–central Pyrenees (Alduides-Mendibelza, Sallent and Baliera domains in Sanz-López (2002, 2004). They consist of 1–2 m of nodular limestones and marls correlated with a drowning event described in the Cantabrian zone (Millaró Beds in Sanz-López 2004, 2007). Siliceous shales in the Alduides-Mendibeltza domain (Arga Formation) contain both drowning horizons (Delépine et al. 1929).

Sedimentation of the Pyrenean Culm series seems to have started in the early Serpukhovian if we consider the ammonoid Mandette fauna, which is also reported in the lowermost part of the Culm series of the Mouthoumet and the Montagne Noire areas (Bessière et al. 1980; Engel et al. 1981; Korn and Feist 2007). The locally preserved succession is more than 1,000 thick and consists of dark shales with intercalated lenses of conglomerates and sandstones filling paleochannels. This facies association was often interpreted as low transport efficiency submarine fans. Paleocurrents indicate sediment supply from the north, but changed probably in relation to basin morphology (Delvolvé et al. 1996). Preservation of proximal siliciclastic facies is rather occasional and is normally associated with an erosive basal unconformity over a paleeotopography and common occurrence of reworked blocks of Silurian–Devonian rocks. These proximal facies form small (40–100 m thick) marginal systems in the Pyrenees (Isòvol, Béixec, Biscarbó, Molières and Merial). Deltaic sandstones and siliceous conglomerates are preserved in a small basin top (Tosa d'Alp; Sanz-López 1992), being laterally replaced by a body of debris flows and olistoliths at the front of the thrust sheet. The buried paleotopography was conditioned by extensional faults. Paleokarst development on the Aspe-Brousset Formation was related to exhumation during thrust sheet emplacement.

The Culm series was mainly deposited during the Serpukhovian according to a few ammonoid and trilobites occurrences (Delvolvé et al. 1996). Late Visean to early Serpukhovian exotic clasts and olistoliths of shallow-water platform limestone are also known in the Arize massif, Pays de Sault, Cadí nappe and the Nogueres units (Vachard et al. 1991; Delvolvé et al. 1994, 1998; Perret 1993; Sanz-López et al. 2005, 2006). These reworked clasts were eroded and transported from shallow-water carbonate platforms located to the north (as those preserved in the Mouthoumet and Montagne Noire massifs; Fig. 11.38).

11.4.3 Late Serpukhovian/Early Bashkirian Synorogenic Deposits

The Iraty Formation corresponds to a southwards retrograding deep carbonate ramp deposited on the foreland (Delvolvé et al. 1993). It consists of black laminated limestone (from a few to up 100 m preserved) along the southwestern Pyrenees that reaches 325 m in thickness in the Basque Alduides-Mendibeltza domain (Perret 1993; Sanz-López and Blanco-Ferrera 2012a). Late Serpukhovian to early Bashkirian age (Kinderscoutian to basal Marsdenian English substages) is supported on the basis of conodonts and ammonoids (Perret 1985; Sanz-López and Blanco-Ferrera 2012b). The lower boundary of the Pennsylvanian is ten meters above the base of the formation. The Culm series shows sometimes a transitional and diachronic interval from the underlying Iraty Formation interpreted in connection with several recurrent tilting episodes of the foreland prior to the burial of the carbonate sedimentation (Sanz-López and Blanco-Ferrera 2012). In other localities, the top of the Iraty formation is marked by intraformational carbonate breccias, slumps, slides and small syn-sedimentary faults (Bichot 1986). At Tantes, one mound (10–20 m thick) grew up just during the drowning of the carbonate platform favoured by seepage fluids (Buggisch and Krumm 2005). Northwards, the Iraty Formation is replaced by the Culm series through an intermediate (150–200 m thick) unit made of shales, limestone and sandstones (Cambasque unit after Mirouse 1966).

The similar age and facies of the Iraty Formation and the Barcaliente Formation (Cantabrian Zone) suggest deposition on the same Variscan foreland, away from the siliciclastic sedimentation and in a restricted and water-stratified basin. The late Serpukhovian–early Bashkirian boundary between the Variscan foredeep and the foreland located in the western Cantabrian Zone may then be continued in the southern Pyrenees and probably along the subsurface of the Ebro basin to the Serra de Miramar (southern Catalonian Coastal Ranges; Fig. 11.37). There, the condensed Valls unit includes a lower part similar to the Aspe-Brousset Formation and an upper part, which consists of black laminated limestones with early Bashkirian conodonts as the Iraty Formation (Sanz-López et al. 2000).

The Iraty Formation was deposited coeval with the upper part of the synorogenic siliciclastic succession in the central and north Pyrenees (Serre de Castets Formation; Delvolvé et al. 1996). It consists of dark shales in which are intercalated muddy supported centimetric to kilometric, reworked limestone blocks and olistolihts derived from the rich shallow-platform called Ardengost Limestone. The olistostrome extends for 15 km with a maximum thickness of 550 m (Bouquet and Stoppel 1995). Current directions from siliciclastic beds show supplies from the north where the carbonate platform should be located before its gravity sliding to the base of the slope (Delvolvé et al. 1996). Foraminifers and corals indicate late Visean to late Serpukhovian age for the platform growth (Perret and Vachard 1977; Perret 1993), whereas brachiopods and trilobites seems to indicate a late Serpukhovian to early Bashkirian age (Legrand-Blain et al. 1983, 1984; Gandl and Delvolvé 1990). Olistrostrome emplacement probably occurred between the late Serpukhovian and the early Bashkirian, since siliciclastic beds above and below yielded late Serpukhovian plant remains, early–middle Bashkirian trilobites, and Baskhirian or Moscovian brachiopods and bivalves (Delvolvé 1981; Babin and Delvolvé 1982, 1989; Legrand-Blain et al. 1983, 1984; Gandl and Delvolvé 1990).

The Culm series reaches 2000 m in thickness in Minorque (Bourrouilh 1983). Icnites from deep sea-fan systems were described by Bourrouilh (1983) and Orr et al. (1996), particularly in interchannel deposits among other concentrated deposits, debris flows and diluted turbidity currents. The succession spans from the late Visean to the early Bashkirian, on the basis of a few ammonoid occurrences (Schindewolf 1934, 1958; Bourrouilh 1983; Rosell and Llompart 2002). A few debris flows include clasts with a reworked Serpukhovian foraminifer association (Bourrouilh and Lys 1977) and were correlated with horizons described in the Malaguide Complex. Deep sea fan sedimentation was also recognized in the Catalonian Coastal Ranges, where the Poboleda unit consists of the progradation of three turbiditc lobes (1,000 m thick all together) along in the central Priorat (Saéz and Anadón 1989). The paleocurrents measured indicate southwards flow. The age of tye Poboleda unit is unknown, but it should span the Serpukhovian to early Bashkirian.

In the Internal Betics, the Retamares Member (Almogía Formation) was interpreted as a braided suprafan deposit at the base of the continental slope (Herbig 1983). It consists of 40–60 m thick, massive greywackes with intercalated conglomerate lenses and allochthonous Devonian limestone blocks slides. The age is probably early Serpukhovian, because late Visean to probably basal Serpukhovian limestone clasts derived from a shallow marine carbonate shelf occur (Herbig 1984). Above, the "Olive Shale" (Almogía Formation, 150 m thick) represents a primarily pelitic slope facies probably Serpukhovian to early Bashkirian in age (Herbig 1983). It may be correlated with the upper part of the Iraty Formation according to the conodonts described by Navas-Parejo et al. (2012) from the Vélez Rubio-Lorca unit.

11.4.4 Bashkirian to Moscovian Synorogenic Deposits

In the Pyrenees, the reworked limestone clasts in the Culm series above the Iraty Formation yielded Bashkirian (Kinderscoutian to Yeadonian English substages) ammonoids, conodonts, foraminifers, algae and corals and late Langsettian macroflora (Delvolvé et al. 1996, and references therein; Sanz-López and Blanco-Ferrera 2012; Wagner and Álvarez-Vázquez 2010). The westernmost Basque Cinco Villas domain is the last basin being filled by marine beds, whereas the rest of the Pyrenean chain may be uplifted at this time. The Culm series yielded rare early Bashkirian ammonoids and reworked early Moscovian shallow water limestone clasts (Delvolvé et al. 1996). The age of the clasts is Moscovian, supported by probably Bolsovian ostracods (Requadt et al. 1977) and Kashirian foraminifers (Delvolvé et al. 1987). The location of the shallow-water platform that provided the Bashkirian and Moscovian clasts is speculative, and the closest outcrops are in the eastern margin of the Cantabrian Zone (Valdeteja and Picos de Europa formations).

In the Malaguide Complex, the conglomerates and debris flows of the Marbella Formation (as much as 100 m thick) were deposited in submarine canyons incised in continental slopes, or in main upper-fan channels (Herbig 1983). The age is younger than that indicated by late Visean to early Bashkirian fossils yielded by blocks eroded from a shallow-water Betic-Rifean platform.

11.4.5 Late and Post-Orogenic Deposits

Unconformable continental and molassic deposits fill isolated small basins in the Pyrenees (total thickness could attain 2,000 m). Rare fills of paleovalleys include late

Asturian, or maybe basal Cantabrian (Moscovian) flora (Aguiró Formation; Talens and Wagner 1995). Unconformable dacitic to rhyolitic calc-alkaline volcanic rocks (Eric Castell Formation) provided radiometric ages from 307 to 296 Ma (Kasimovian to Asselian; Late Pennsylvanian to Permian; Pereira et al. 2014). Consequently, these continental and volcanic beds were contemporaneous with the development of the Asturian arc. Marine beds are only known in some small isolated outcrops of the southern part of the Ebro basin (Puig Moreno). Shales with thin beds of calcarenites, greywackes and quartzites (175 m thick) yielded reworked fauna, among them late Kasimovian to early Gzhelian fusulinids (Villa et al. 1996).

Younger post-orogenic continental units were deposited in relation to a late strike-slip tectonic regime (trastension). In the Pyrenees, fluvio-lacustrine and volcanic deposits (Malpas Formation) yielded Stephanian C (or early Autunian) to mid-late Autunian floras (Wagner and Álvarez-Vázquez 2010). In turn, alluvial fan sediments and meandering river flood-plain deposits (Peranera Formation) contain Autunian flora and Artinskian (Cisuralian) volcanic beds (Gretter et al. 2015). The Permian calc-alkaline magmatism is widely represented in the Iberian Ranges and intruded in, or unconformable on older Paleozoic rocks. Radiometric ages are early Permian, whereas macroflora and microflora are mid to late Autunian (Castro et al. 2002; Wagner and Álvarez-Vázquez 2010). The oldest preserved continental basins in the Catalonian Coastal Ranges and Minorque formed during the late Permian extensional phase (López-Gómez et al. 2005) but they do not belong to the Variscan cycle but to the next, Alpine cycle.

References

Águeda JA, Bahamonde JR, Barba FJ, Barba P, Colmenero JR, Fernández LP, Salvador CI, Vera de la Puente C (1991) Depositional environments in Westphalian coal-bearing successions of the Cantabrian Mountains, northwest Spain. Bulletin de la Société Géologique de France 162:325–337.

Aldaya F, Arribas A, González Lodeiro F, Iglesias Ponce de León M, Martínez Catalán JR, Martínez García E (1973) Presencia de una nueva fase de deformación, probablemente prehercínica, en el NW y centro de la Península Ibérica, Stvd. Geol. Salmant. VI:29–48.

Aldaya F, Carls P, Martínez-García E, Quiroga JL (1976) Nouvelles précisions sur la série de San Vitero (Zamora, nord-ouest de l'Espagne). C. R. Acad. Sci. Paris, Série D 283:881–883.

Almeida P, Dias da Silva I, Oliveira H (2006) Caracterização Tectono-Estratigráfica da Zona de Cisalhamento de Santa Susana (ZCSS) no Bordo SW da Zona de Ossa-Morena (ZOM), (Portugal). VII Congresso Nacional de Geologia,Livro de Resumos volume I: 49–53.

Alonso JL (1987a) Estructura y evolución tectonoestratigráfica de la Región del Manto del Esla (Zona Cantábrica, NW de España). Institución Fray Bernardino de Sahagún-Diputación Provincial de León, 276 p.

Alonso JL, Alvarez-Marrón J, Pulgar FJ (1989) Síntesis cartográfica de la parte suroccidental de la Zona Cantábrica. Trabajos de Geología, Universidad de Oviedo 18:145–153.

Alonso JL, Marcos A, Pulgar FJ (1991) Persistent basement wrenching as controlling mechanism of Variscan thin-skinned thrusting and sedimentation, Cantabrian Mountains, Spain. Comment. Tectonophysics 194:171–182.

Alonso JL, Marcos A, Suárez A (2006) Structure and organization of the Porma mélange: progressive denudation of a submarine nappe toe by gravitational collapse. American Journal of Science 306:32–65.

Alonso JL, Marcos A, Suárez A (2009) Paleogeographic inversion resulting from large out of sequence breaching thrusts: The Leon Fault (Cantabrian Zone, NW Iberia). Anew picture of the external Variscan Thrust Belt in the Ibero-Armorican Arc. Geologica Acta: 7/4:451–473.

Alonso JL, Marcos A, Villa A, Suárez A, Merino-Tomé OA, Fernández LP (2015) Mélanges and other types of block-in-matrix formations in the Cantabrian Zone (Variscan Orogen, northwest Spain): origin and significance. International Geology Reviews 57:563–580.

Alonso-Olazábal A (2001) El plutón de Campanario-La Haba: caracterización petrológica y fábrica magnética. Phd thesisl, Univ País Vasco, 322 p.

Alonso-Olazábal A, Carracedo M, Aranguren A (1999) Petrology, magnetic fabric and emplacement in a strike-slip regime of a zoned peraluminous granite: the Campanario-La Haba pluton, Spain. In: Castro A, Fernández F, Vigneresse JL (eds) Understanding Granites: Integrating New and Classical Techniques. Geological Society, London, Special Publication 168:177–190.

Álvarez-Marrón J, Pérez-Estaun A (1988) Thin skinned tectonics in the Ponga region (Cantabrian Zone, NW Spain). Geologische Rundschau 77:539–550.

Álvarez-Vázquez C (1995) Macroflora del Westfaliense inferior de la cuenca de Peñarroya-Belmez-Espiel (Córdoba). PhD thesis, Univ Oviedo, 393 p.

Andrade AAS (1983) Contribution à l'analyse de la suture hercynienne de Beja (Portugal): perspectives métallogéniques. PhD thesis, Laboratoire de Métallogénie I Nancy, Institut National Polytechnique de Lorraine, 137 p.

Andrade AAS, Pinto A, Conde L (1976) Sur la géologie du Massif de Beja: Observations sur la transversale d`Odivelas. Comun. Serv. Geol. Portugal 60:171–202.

Andreis RR, Wagner RH (1983) Estudio de abanicos aluviales en el borde Norte de la cuenca Westfaliense B de Peñarroya-Belmez (Córdoba). In: MJ Lemos de Sousa (ed.) Contributions to the Carboniferous Geology and Palaeontology of the Iberian Peninsula. Universidade do Porto, Faculdade de Ciencias, Mineralogia e Geologia. Volume dedicated to Wenceslau de Lima: 171-227

Andresen N, Reijmer JJG, Droxler AW (2003) Timing and distribution of calciturbidites around a deeply submerged carbonate platform in a seismically active setting (Pedro Bank, NorthernNicaragua Rise, Caribbean Sea). Int J Earth Sci (Geol Rundsch) 92: 573–592.11https://doi.org/10.1007/s00531-003-0340-0.

Apalategui O, Barranco E, Contreras F, Delgado M, Roldán FJ (1979) Mapa Geológico de España E/1:50,000. Sheet 917: Aracena. Instituto Geológico Minero de España, 78 p.

Apalategui O, Contreras F, Eguiluz L (1990) Mapa Geológico de España E/1:50,000. Sheet 918: Santa Olalla del Cala. Instituto Geológico Minero de España, 65 p.

Araújo A, Fonseca P, Munhá, J, Moita P, Pedro J, Ribeiro A (2005) The Moura Phyllonitic Complex: an Accretionary Complex related with obduction in the Southern Iberia Variscan Suture. Geodinamica Acta, 18:375–388.

Araújo A, Piçarra Almeida J, Borrego J, Pedro J, Oliveira JT (2013) As regiões central e sul da Zona de Ossa-Morena. In: Dias R, Araújo A,

Terrinha P, Kullberg JC (eds) Geologia de Portugal, Escolar Editora, Lisboa, I: 509–549.
Arboleya ML (1978) Estudio estructural del Manto del Esla (Cordillera Cantábrica, León). PhD thesis, Univ Oviedo, 227 p.
Arboleya ML (1981) La estructura del Manto del Esla (Cordillera Cantábrica, León): Boletín Geológico Minero 92/1:19–40.
Arenas R, Sánchez Martínez S, Díez Fernández R, Gerdes A, Abati J, Fernández-Suárez J, Andonaegui, P., González Cuadra, P, López Carmona A, Albert R, Fuenlabrada JM, Rubio Pascual FJ (2016) Allochthonous terranes involved in the Variscan suture of NW Iberia: A review of their origin and tectonothermal evolution. Earth-Science Reviews 161:140–178. https://doi.org/10.1016/j.earscirev.2016.08.010
Armendáriz M (2006) Los depósitos carbonatados de la cuenca carbonífera del Guadiato (Córdoba, SW del Macizo Ibérico). Boletín Geológico Minero 117:513–518.
Armendáriz M (2008) Génesis y evolución tectonosedimentaria de la parte meridional de la cuenca mississippiense de Los Pedroches (SO del Macizo Ibérico): implicaciones paleogeográficas. PhD Thesis, Univ. Complutense Madrid, 452 p.
Armendáriz M, Quesada C, Gabaldón V, Gómez JJ (2005) Destruction and resedimentation processes of carbonate platforms in the Carboniferous Guadiato basin (Córdoba, SW Iberian Massif). In: Freiwald A, Röhling HG, Löffler SB (eds) System Earth - Biosphere Coupling, Regional Geology of Central Europe. International Conference and Annual Meeting Geologische Vereinigung, Erlangen-Nürnberg, abstracts:8–9.
Armendáriz M, Rosales I, Quesada C. (2007a) Estudio diagenético en conchas de braquiópodos de la cuenca del Guadiato (Mississippiense, SO del Macizo Ibérico). Geogaceta 42:103–106.
Armendáriz M, Rosales I, Quesada C (2007b) Oxygen and carbon isotope records of brachiopod shells calcite (Late Visean, SW Spain): evidence of Carboniferous paleoclimatic change. European Geosciences Union, General Assembly 2007, abstract.
Armendáriz M, Rosales I, Quesada C (2008a) Oxygen isotope and Mg/Ca composition of Late Viséan (Mississippian) brachiopod shells from SW Iberia: Palaeoclimatic and palaeogeographic implications in northern Gondwana. Palaeogeography, Palaeoclimatology, Palaeoecology 268:65–79.
Armendáriz M, López-Guijarro R, Quesada C, Pin C, Bellido F (2008b) Genesis and evolution of a syn-orogenic basin in transpression: Insights from petrography, geochemistry and Sm–Nd systematics in the Variscan Pedroches basin (Mississippian, SW Iberia). Tectonophysics 461:395–413. https://doi.org/10.1016/j.tecto.2008.02.
Armendáriz M, Quesada C, Rosales I (2013) The Mississippian Pedroches basin: a failed attempt to propagate a Palaeotethys arm across Southern Iberia? EGU General Assembly 2013, abstract.
Azor A (1994) Evolución tectonometamórfica del límite entre las zonas Centroibérica y de Ossa-Morena (Cordillera Varisca, SO de España). PhD Thesis, University of. Granada, Spain.
Azor A, Rubatto D, Simancas JF, González Lodeiro F, Martínez Poyatos D, Martín Parra LM, Mata, J (2008) Rheic Ocean ophiolitic remnants in southern Iberia questioned by SHRIMP U-Pb zircon ages on the Beja-Acebuches amphibolites. Tectonics 27, TC5006. https://doi.org/10.1029/2008TC002306.
Babin C, Delvolvé JJ (1982) Une faune de mollusques bivalves du Namurien des Pyrénées centrales françaises. Geobios 15:729–753.
Babin C, Delvolvé JJ (1989) Les mollusques bivalves du Namurien des Pyrénées françaises et leur intérêt paléogéographique. Sci Geol Bull 42:117–137.
Bahamonde JR, Colmenero JR (1993) Análisis estratigráfico del Carbonífero medio y superior del Manto de Ponga (Zona Cantábrica). Trabajos Geol, Univ. Oviedo 19:155–193.
Bahamonde JR, Colmenero JR, Vera C (1997a) Growth and demise of Late Carboniferous carbonate platforms in the eastern Cantabrian Zone, Asturias, northwestern Spain. Sedimentary Geology 110:99–122.
Bahamonde JR, Vera C, Colmenero JR (1997b) Geometría y facies del margen progadante de una plataforma carbonatada carbonífera (Unidad de Picos de Europa, Zona Cantábrica). Revista de la Sociedad Geológica de España 1:163–181.
Bahamonde JR, Vera C, Colmenero JR (2000) A steep-fronted Carboniferous carbonate platform: clinoformal geometry and lithofacies (Picos de Europa, NW Spain). Sedimentology 47:645–664.
Bahamonde JR, Kenter JAM, Della Porta G, Keim L, Immenhauser A, Reijmer JJG (2004) Lithofacies and depositional processes on a high, steep-margined Carboniferous (Bashkirian-Moscovian) carbonate platform slope, Sierra del Cuera, NW Spain. Sedimentary Geology 166:145–156.
Bahamonde JR, Merino-Tomé O, Heredia N (2007) A Pennsylvanian microbial boundstone-dominated carbonate shelf in a distal foreland margin (Picos de Europa Province, NW Spain). Sedimentary Geology 198:167–193.
Bahamonde JR, Kenter JAM, Della Porta G, van Hoeflaken F (2008) Facies belts of a Carboniferous carbonate platform (San Antolin-La Huelga section, NE Cantabrian Zone, Northern Spain). Trabajos de Geología, Univ Oviedo 28:69–86.
Bahamonde JR, Martín L, Fernández LP (2014) The Penssylvanian microbial-dominated carbonate platform of the El Sueve Massif: contriburion to the reconstruction of the Variscan foreland basin of the Cantabrian Zone (N Spain). Rev. Soc. Geol. España 27:47–62.
Bahamonde JR, Merino-Tomé O, Della Porta G, Villa E (2015) Pennsylvanian carbonate platforms adjacent to deltaic systems in an active marine foreland basin (Escalada Fm., Cantabrian Zone, NW Spain). Basin Research 27(2):208–229.
Barba P, Colmenero JR (1994) Estratigrafía y Sedimentología de la sucesión Westfaliense del borde sureste de la Cuenca Carbonífera Central (Zona Cantábrica, N de España). Studia Geologica Salmanticensia 30:139–204.
Bard JP (1965) Introduction à la géologie de la chaîne hercynienne da la Sierra Morena occidentale (Espagne). Hypothèses sur les caractères de l'évolution géotectonique de cette chaîne. Rev Géogr Phys 7: 323–337.
Barr SM, Davis DW, Kamo S, White CE (2003) Significance of U–Pb detrital zircon ages in quartzite from peri-Gondwanan terranes, New Brunswick and Nova Scotia, Canada. *Precambrian Research*, **126**, 123–145, https://doi.org/10.1016/S0301-9268(03)00192-X.
Barrie CT, Amelin Y, Pascual E (2002) U–Pb Geochronology of VMS mineralization in the Iberian Pyrite Belt. Mineralium Deposita 37:684–703. https://doi.org/10.1007/s00126-002-0302-7.
Bastida F, Marcos A, Pérez Estaún A, Pulgar JA (1984) Geometría y evolución estructural del Manto de Somiedo (Zona Cantábrica, NO de España). Boletín Geológico Minero 92/6:517–539.
Bea F, Montero P, Talavera C, Anbar MA, Scarrow JH, Molina JF, Moreno JA (2010) The palaeogeographic position of Central Iberia in Gondwana during the Ordovician: evidence from zircon chronology and Nd isotopes. Terra Nova 22:341–346. https://doi.org/10.1111/j.1365-3121.2010.00957.x.
Berkyová S, Frýda J, Koptíková L (2008) Environmental and biotic changes close to the Emsian/ Eifelian boundary in the Prague Basin, Czech Republic: paleontological, geochemical and sedimentological approach. In: Kim AI, Salimova FA, Meshchankina NA (eds) International Conference Global Alignments of Lower Devonian Carbonate and Clastic Sequences, SDS/ IGCP Project 499 joint field meeting, 25.8.-3.9.2008, State Committee of the Republic of Uzbekistan on Geology and Resources & Kitab State Geological Reserve, Contributions, Taskhent-Novosibirsk, 18–19.
Bessière G, Schulze H (1984) Le Massif de Mouthoumet (Aude, France): nouvelle définition des unités structurales et essai d'une reconstruction paléogéographique. Bull Soc géol France 26:885–894.
Bessière G, Mirouse R, Perret MF (1980) Découverte de faunes de la limite Viséen-Namurien sous le « Culm » carbonifère du massif de Mouthoumet (Aude). C R Acad Sci Paris 291:521–524.

Bhatia MR (1985) Rare earth element geochemistry of Australian Paleozoic graywackes and mudrocks: provenance and tectonic control. Sedimentary Geology 45:97–113.
Bhatia MR, Crook KAW (1986) Trace element characteristics of graywackes and tectonic discrimination of sedimentary basin. Contributions to Mineralogy and Petrology 92:181–193.
Bichot F (1986) Les tectoniques superposées hercyniennes de la région du Somport (Pyrénées occidentales). Affinités avec le domaine Basco-Cantabrique. Ann Soc Geol Nord 107:177–185.
Boersma KT (1973) Devonian and Lower Carboniferous biostratigraphy, Spanish Central Pyrénées. Leidse Geol Meded 49:303–377.
Boogaard M van den (1972) Conodont faunas from Portugal and Southwestern Spain. Part 1: A Middle Devonian fauna from near Montemor-o-Novo. Scripta Geologica 13:1–11.
Boogaard M van den (1983) Conodont faunas from Portugal and southwestern Spain. Part 7. A Frasnian conodont fauna near the Estação de Cabrela (Portugal). Scripta Geologica 69:1–17.
Boogaard M van den, Vázquez F (1981) Conodont faunas from Portugal and Southwester Spain. Part 5.Lower Carboniferous conodonts at Santa Olalla de Cala (Spain). Scripta Geologica 61:1–8.
Borrego J (2009) Cartografia Geológico-Estrutural de um sector da Zona de Ossa-Morena (Sector de Estremoz - Barrancos) e sua interpretação Tectónica. PhD Thesis, Dept. Geociências, Universidade de Évora.
Borrego J, Araújo A, Fonseca PE (2005) A geotraverse through the south and central sectors of the Ossa-Morena Zone in Portugal (Iberian Massif). In Carosi R, Dias R, Iacopini D, Rosenbaum G (Ed) The southern Variscan belt, J. Virtual Explorer 19:10. https://doi.org/10.3809/jvirtex.2005.00117.
Bouquet Ch, Stoppel D (1995) L'Olistostrome Paléozoïque de la Serre-de-Castets. Cour Forsch-Inst Senckenberg 188:133–157
Bourrouilh R (1983) Estratigrafía, sedimentología y tectónica de la isla de Menorca y del noreste de Mallorca (Baleares). La terminación nororiental de las Cordilleras béticas en el Mediterráneo occidental. Mem IGME 99, Madrid.
Bourrouilh R, Lys M (1977) Sédimentologie et micropaléontologie d'olistostromes et coulées boueuses du Carbonifère des zones internes bético-kabylo-rifaines (Méditerranée occidentaile). Ann Soc Geol Nord 47:87–94.
Bowman MB (1985) The sedimentology and paleogeographic setting of late Namurian-Westfalian. A basin-fill succession in the San Emiliano and Cármenes areas of NW León, Cantabrian Mountains, NW Spain. In: Lemos de Sousa HJ, Wagner RH (eds) Papers on the Carboniferous of the Iberian Peninsula (Sedimentology, Stratigraphy, Paleontology, Tectonics and Geochemistry). Annales Fac Ciên, Univ Porto, Spec Supplement to Vol 64:117–168.
Braid JA (2011) Dynamics of Allochthonous Terranes in the Pangean Suture Zone of Sothern Iberia. PhD thesis, Dalhousie University.
Braid JA, Murphy JB, Quesada C (2010) Structural analysis of an accretionary prism in a continental collision setting, the Late Paleozoic Pulo do Lobo Zone, Southern Iberia. Gondwana Research 17:422–439. https://doi.org/10.1016/j.gr.2009.09.003.
Braid JA, Murphy JB, Quesada C, Mortensen J (2011) Tectonic escape of a crustal fragment during the closure of the Rheic Ocean: U–Pb detrital zircon data from the Late Palaeozoic Pulo do Lobo and South Portuguese zones, southern Iberia. J Geol Soc London 168:383–392. https://doi.org/10.1144/0016-76492010-104.
Braid JA, Murphy JB, Quesada C, Bickerton L, Mortensen JK (2012) Probing the composition of unexposed basement, South Portuguese Zone, southern Iberia: implications for the connections between the Appalachian and Variscan orogens. Can J Earth Sci 49(4):591–613.
Braid JA, Murphy JB, Quesada C, Gladney ER, Dupuis N (2018) Progressive magmatism and evolution of the Variscan suture in southern Iberia. International Journal of Earth Sciences 107:971-983.
Braun R, Oetken S, Königshof P, Kornder L, Wehrmann A (1994) Development and biofacies of reef-influenced carbonates (Lahn - syncline, Rheinisches Schieferge-birge). Courier Forschungsinstitut Senckenberg 169:351–386.
Broutin J (1981) Étude paleobotanique et palynologique du passage Carbonifère–Permien dans les bassins continentaux du Sud-Est de la Zone d´Ossa-Morena (environs de Guadalcanal, Espagne du Sud). Implications paléogéographiques et stratigraphiques. PhD thesis, Univ Paris VI, 2 vols.
Broutin J (1982) Importance paléobiogéographique de la découverte d'une flore continental mixte dans le p < ermien inférieur du Sud-Ouest de la Péninsule Ibérique. CR Acad Sci Paris, II, 295:419–422.
Broutin J (1986) Étude paléobotanique et palynologique du passage Carbonifère Permien dans le Sud-Ouest de la Péninsule Ibérique. Cahiers de Paléontologie, Éditions du CNRS, 165 p.
Broutin J, Garrote A, Gabaldón V (1983a) The Autunian occurrences around Guadalcanal. In: Quesada C, Garrote A, eds, Carboniferous Geology of the Sierra Morena. Guidebook of Field Trip D, 10th Int Carboniferous Congr, Madrid, 77–85.
Broutin J, Garrote A, Gabaldón V, Wagner RH, Quesada C (1983b) Valdeinfierno Coalfield (late Tournaisian). In: Quesada C, Garrote A, eds, Carboniferous Geology of the Sierra Morena. Guidebook of Field Trip D, 10th Int Caeboniferous Congr, Madrid, 68–76.
Brun JP, Burg JP (1982) Combined thrusting and wrenching in the Ibero-Armorican arc: a corner effect during continental collision. Earth and Planetary Science Letters 61:319–332.
Buggisch W, Krumm S (2005) Paleozoic cold seep carbonates from Europe and North Africa – and integrated isotopic and geochemical approach. Facies 51:566–583.
Bulnes, M., Marcos, A., 1994, Internal structure and kinematics of Variscan thrust sheets in the valley of the Trubia River (Cantabrian Zone, NW Spain): regional tectonic implications: International Journal of Earth Sciences, 90, pp. 287–303.
Burg JP, Iglesias M, Laurent Ph, Matte Ph, Ribeiro A (1981) Variscan intracontinental deformation: the Coimbra-Córdoba Shear Zone (SW Iberian Peninsula). Tectonophysics 78:161–177.
Burg JP, Balé P, Brun JP, Girardeau J (1987) Stretching lineation and transport direction in the Ibero-Armorican arc during the Siluro-Devonian collision. Geodinamica Acta 1:71–87.
Buys J, Spandler C, Holm RJ, Richards SW (2014) Remnants of ancient Australia in Vanuatu: implications for crustal evolution in island arcs and tectonic development of the SW Pacific. Geology 42 (11):939–942.
Cabral J (2012) Neotectonics of mainland Portugal: state of the art and future perspectives. J Iber Geol 38(1):71–84. https://doi.org/10.5209/rev_JIGE.2012.v38.n1.39206.
Carbonell R, Simancas F, Juhlin C, Pous J, Pérez-Estaún A, González Lodeiro F, Muñoz G, Heise W, Ayarza P (2004) Geophysical evidence of a mantle derived intrusion in SW Iberia. Geophysical Research Letters 31:L11601. https://doi.org/10.1029/2004GL019684.
Carrilho L (2004) Petrologia e Geoquímica de Complexos Plutónicos do Nordeste Alentejano (Portugal Central). Província Alcalino e Maciço de Campo Maior. PhD thesis, Universidade de Évora.
Carvalho D, Correia M, Inverno C (1976) Contribuição para o conhecimento geológico do Grupo de Ferreira-Ficalho. Suas relações com a Faixa Piritosa e o Grupo do Pulo do Lobo. Memórias e Noticias, Universidade de Coimbra 82:145–169.
Carvalhosa A (1977) Características geológicas do Maciço de Évora (Nota preliminar). Boletim da Sociedade Geológica de Portugal, Lisboa, 20:283–312.
Castro A, Corretgé LG, De La Rosa J, Enrique P, Martínez FJ, Pascual E, Lago M, Arranz E, Galé C, Fernández C, Donaire T, López S (2002) Palaeozoic Magmatism. In: Gibbons, W., Moreno, T. (eds), The Geology of Spain. Geological Society, London, 117–153.
Chacón J, Delgado Quesada M, Garrote A (1974) Sobre la existencia de dos diferentes dominios de metamorfismo regional en la banda

Elvas-Badajoz-Córdoba (Macizo Hespérico Meridional). Boletín Geológico Minero 85/6:713–717.
Chaminé HI, Gama Pereira LC, Fonseca PE, Moço LP, Fernandes JP, Rocha FT, Flores D, Pinto de Jesus A, Gomes C, Soares de Andrade AA, Araújo A (2003) Tectonostratigraphy of middle and upper Palaeozoic black shales from the Porto-Tomar-Ferreira do Alentejo shear zone (W Portugal): new.
Charrier R (1986) The Gondwana glaciation in Chile: description of alleged glacial deposits and paleogeographic conditions bearing on the extension of the ice cover in southern South America. Palaeogeography, Palaeoclimatology, Palaeoecology 56:151–175.
Chesnel V, Samankassou E, Merino-Tomé Ó, Fernández LP, Villa E (2016a) Facies, geometry and growth phases of the Valdorria carbonate platform (Pennsylvanian, northern Spain). Sedimentology 63(1):60–104.
Chesnel V, Merino-Tomé Ó, Fernández LP, Villa E, Samankassou E (2016b) Isotopic fingerprints of Milankovitch cycles in Pennsylvanian carbonate platform-top deposits: The Valdorria record, Northern Spain. Terra Nova 28:364–373. https://doi.org/10.1111/ter.12229.
Chichorro M (2006) Estrutura do Sudoeste da Zona de Ossa-Morena: Área de Santiago de Escoural — Cabrela (Zona de Cisalhamento de Montemor-o-Novo, Maciço de Évora). PhD thesis (unpublished), Univ.
Chlupáč I, Kukal Z (1986) Reflection of possible global Devonian events in the Barrandian area, C.S.S.R. In: Walliser OH (Ed) Global Bio-events, Lect Notes Earth Sci, Springer-Verlag, Berlin, 8:169–179.
Christie-Blick N, Biddle KT (1985) Deformation and basin formation along strike-slip faults. In: Biddle KT and Christie-Blick N (eds) Strike-slip deformation, basin formation and sedimentation. Society of Economic.
Collins AS, Buchan C (2004) Provenance and age constraints of the South Stack Group, Anglesey, UK: U–Pb SIMS detrital zircon data. Journal of the Geological Society London 161:743–746 https://doi.org/10.1144/0016-764904-036.
Colmenero JR, Prado JG (1993) Coal basins in the Cantabrian Mountains, northwestern Spain. International Journal of Coal Geology 23:215–229.
Colmenero JR, Águeda JA, Fernández LP, Salvador CI, Bahamonde JR, Barba P (1988) Fan-delta system related to the Carboniferous evolution of the Cantabrian Zone, northwestern Spain. In: Nemec W, Steel RJ (eds) Fan Deltas: Sedimentology and Tectonics Settings, Blackie & Son, Glasgow, 267–285.
Colmenero JR, Fernández LP, Moreno C, Bahamonde JR, Barba P, Heredia N, González F (2002) Carboniferous In: Gibbons W, Moreno MT (eds) The Geology of Spain. Geol. Soc. London, 93–116.
Comte P (1959) Recherches sur les terrains anciens de la Cordillère Cantabrique. IGME, Madrid, Colección Memorias 60, 440 p.
Conde LN, Andrade AAS (1974) Sur la faune meso et/ou néodévonienne des calcaires du Monte das Cortes, Odivelas (Massif de Beja). Memórias e Notícias, Univ. Coimbra 78:141–146.
Condie KC (1993) Chemical-composition and evolution of the upper continental-crust contrasting results from surface samples and shales. Chemical Geology 104:1–37.
Corrales I (1971) La sedimentación durante el Estefaniense B-C en Cangas de Narcea, Rengos y Villablino (NW de España). Trabajos de Geología, Univ Oviedo 3:69–73.
Correia P (2016) Contribution to the knowledge of the fossil flora and fauna of the Douro Carboniferous Basin (NW of Portugal). Universidade do Porto (PhD thesis).
Corrochano D, Barba P, Colmenero JR (2012a) Glacioeustatic cyclicity of a Pennsylvanian carbonate platform in a foreland basin setting: an example from the Bachende Formation of the Cantabrian Zone (NW Spain). Sediment Geol 245–246:76–93.
Corrochano D, Barba P, Colmenero JR (2012b) Transgressive-regressive sequence stratigraphy of Pennsylvanian Donezella bioherms in a foreland basin (Lena Group, Cantabrian Zone, NW Spain). Facies 58:457–476.
Costa D, Viana A, Munhá J (1990) Petrologia e geoquímica dos maciços de Veiros e Vale Maceira. In: Abstracts of the VIII Semana de Geoquímica, Lisboa.
Cózar P (1998) Bioestratigrafía con foraminíferos del Carbonífero Inferior en el Sector Norte del Área del Guadiato (Córdoba). PhD thesis Univ Complutense Madrid, 590 p.
Cózar P (2000) Two new Late Viséan (Mississippian) species of the genera Nevillea and Mikhailovella (Foraminiferida) from Guadiato Area (SW Spain). Coloquios de Paleontología 52:3–11.
Cózar P, Rodríguez S (1999) Propuesta de nueva nomenclatura para las unidades del Carbonífero Inferior del sector Norte del área del Guadiato (Córdoba). Boletín Geológico y Minero 110:237–254.
Cózar P, Rodríguez S (2004) Pendleian (early Serpukhovian) marine carbonates from SW Spain: sedimentology, biostratigraphy and depositional model. Geol J 39:25–47.
Cózar P, Rodríguez S, Mas R (2004) Análisis sedimentológico y bioestratigráfico de afloramientos del Serpujoviense inferior (Mississippiense) en las proximidades de Adamuz (Córdoba, SO de España). Coloquios de Paleontología 54:115–130.
Cózar P, Somerville ID, Rodríguez S, Mas R, Medina-Varea P (2006) Development of a late Viséan (Mississippian) mixed carbonate/siliciclastic platform in the Guadalmellato Valley (southwestern Spain), Sedimentary Geology 183:269–295.
Crespo-Blanc A (1989) Evolución geotectónica del contacto entre la Zona de Ossa-Morena y la Zona Surportuguesa en las sierras de Aracena y Aroche (Macizo Ibérico meridional): un contacto mayor en la Cadena Hercínica europea. PhD Thesis, University of Sevilla.
Crespo-Blanc A, Orozco M (1988) The Southern Iberian Shear Zone: a major boundary in the Hercynian folded belt. Tectonophysics 148:221–227.
Crespo-Blanc A, Orozco M (1991) The boundary between the Ossa-Morena and the South-portuguese Zones (southern Iberian Massif): a major suture in the european Hercynian chain. Geologische Rundschau 80:691–702.
Crousilles M, Dixsaut C (1977) L'association ophiolitique varisque du Varas-Guadalbarbo (Cordoue, Espagne). Aspects structural et métallogénique. Thèse 3e cycle. Univ. Paris-Sud. Centre d'Orsay, 289 p.
Crousilles M, Dixsaut C, Lys M, Tamain G (1976) L'alignement basique-ultrabasique du Varas-Guadalbarbo (Cordoue, Espagne). CR'Acad Sci Paris, Série D 283:1141–1143.
Cullers RL (1995) The Controls on the Major-Element and Trace-Element Evolution of Shales, Siltstones and Sandstones of Ordovician to Tertiary Age in the Wet Mountains Region, Colorado, USA. Chemical Geology 123:107–131.
Cullers RL (2000) The geochemistry of shales, siltstones and sandstones of Pennsylvanian-Permian age, Colorado, USA: Implications for provenance and metamorphic studies. Lithos 51 (3):181-203. https://doi.org/10.1016/S0024-4937(99)00063-8
Cunha PP, Lemos de Sousa MJ, Pinto de Jesus A, Rodrigues CF, Telles Antunes M, Tomás CA (2012) O Carvão em Portugal: Geologia, Petrologia e Geoquímica. In: Lemos de Sousa MJ, Rodrigues CF.
Dinis MAP (Eds) O Carvão na Actualidade, Volume I, Petrologia, Métodos Analíticos, Classificação e Avaliação de Recursos e Reservas, Papel no Contexto Energético, Carvão em Portugal, p 309–381. Universidade Fernando Pessoa (Porto), Academia das Ciências de Lisboa.
Da Silva Domingo RM (2004) Contribuição para o conhecimento da fauna do Devónico do Anticlinal de Valongo (Norte de Portugal). Tese de Mestrado em Paleontologia, Univ Évora and Univ Nova de Lisboa, 136 p.
Dahn DRL, Braid JA, Murphy JB, Quesada C, Dupuis N, McFarlane CRM (2014) Geochemistry of the Peramora Mélange and Pulo

do Lobo schist: geochemical investigation and tectonic interpretation of mafic mélange in the Pangean suture zone, Southern Iberia. International Journal of Earth Sciences (Geol Rundsch) 103:1415–1431. https://doi.org/10.1007/s00531-014-1024-7.

Dallmeyer RD, Quesada C (1992) Cadomian vs. Variscan evolution of the Ossa-Morena Zone (SW Iberia): field and $^{40}Ar/^{39}Ar$ mineral age constraints. Tectonophysics 216:339–364.

Dallmeyer RD, Martínez Catalán JR, Arenas R, Gil Ibarguchi JI, Gutiérrez-Alonso G, Farias P, Aller J, Bastida F (1997) Diachronous Variscan tectonothermal activity in the NW Iberian Massif: Evidence from $^{40}Ar/^{39}Ar$ dating of regional fabrics. Tectonophysics 277:307–337. https://doi.org/10.1016/S0040-1951(97)00035-8.

De la Rosa JD, Jenner GA, Castro A (2002) A study of inherited zircons in granitoid rocks from the South Portuguese and Ossa - Morena Zones, Iberian Massif: support for the exotic origin of the South Portuguese Zone: Tectonophysics. 352:245–256.

De Sitter LU (1962) The structure of the southern slope of the Cantabrian Mountains: Leidse Geologische Mededelingen 26:255–264.

DeCelles PG, Giles KA (1996) Foreland basin systems. Basin Res 8:105–123.

Delépine G (1935) Contribution a l'étude de la faune du Dinantien des Pyrénées Deuxième partie: la faune de Mondette. Bull Soc géol Fr (sér 5) 5:171–189.

Delépine G, Dubar G, Laverdiere PW (1929) Observations sur quelques gisements du Carbonifère des.

Delgado F, Jiménez A, Pérez Lorente F (1980) Observaciones acerca del origen fluvioglacial del conglomerado de Espiel (Namuriense-Westphaliense). Sierra Morena, España. Temas Geol Min IGME 4:101–120.

Delgado JFN (1908) Système Silurique du Portugal. Étude de stratigraphie paléontologique. Mem Com Serviços Geol Portugal, Lisboa, 245 p.

Delgado Quesada M (1971) Esquema geológico de la hoja nº 878 de Azuaga (Badajoz). Boletín Geológico Minero 82:277–286.

Delgado Quesada M, Liñán E, Pascual E, Pérez Lorente F (1977) Criterios para la diferenciación de dominios en Sierra Morena central. Stvdia Geológica XII:75–99.

Della Porta G, Kenter JAM, Bahamonde JR (2002a) Microfacies and Paleoenvironment of *Donezella* Accumulations across an Upper Carboniferous High-Rising Carbonate Platform (Asturias, NW Spain). Facies 46:149–168.

Della Porta G, Kenter JAM, Immenhauser A, Bahamonde JR (2002b) Lithofacies Character and Architecture Across a Pennsylvanian Inner-Platform Transect (Sierra del Cuera, Asturias, Spain). Journal of Sedimentary Research 72:898–916.

Della Porta G, Kenter JAM, Bahamonde JR, Immenhauser A, Villa E (2003) Microbial Boundstone Dominated Carbonate Slope (Upper Carboniferous, N Spain): Microfacies, Lithofacies Distribution and Stratal Geometry. Facies 49:175–207.

Della Porta G, Kenter JAM, Bahamonde JR (2004) Depositional facies and stratal geometry of an Upper Carboniferous prograding and aggrading high-relief carbonate platform (Cantabrian Mountains, N Spain). Sedimentology 51:267–295.

Delvolvé JJ (1981) Arguments en faveur de l'âge namurien du Culm des Pyrénées Centrales françaises. C.R. Acad. Sc.Paris, Série II 293:219–222.

Delvolvé JJ, Perret MF, Vachard D (1987) Découverte du Kachirien (Moscovien inférieur) à Fusulines et Algues dans le massif des Cinco Villas (Pyrénées basques). Geobios 20:541–548

Delvolvé JJ, et al (1996) Carbonifère à faciès Culm. In: Barnolas A, Chiron JC (eds) Synthèse géologique et géophysique des Pyrénées vol 1. Editions BRGM-ITGE, Orléans, Madrid, 303–338.

Delvolvé JJ, Perret MF (1989) Variations de l'âge des sédiments calcaires et "Culm" carbonifère dans la chaîne varisque du Sud de la France: migration de l'orogenèse varisque. Geodinamica Acta (Paris) 3:117–126.

Delvolvé JJ, Souquet P, Vachard D, Perret MF, Aguirre P (1993) Caractérisation d'un bassin d'avant-pays dans le Carbonifère des Pyrénées: faciès, chronologie de la tectonique synsédimentaire. C.R. Acad. Sci. Paris Série II 316:959–966.

Delvolvé JJ, Hansotte M, Vachard D (1994) Biostratigraphy by foraminifera and algae of the Carboniferous deposits (Uppermost Viséan-Sepukhovian) of the Arize Massif (Ariège, France). N J Geol Palaontol Abh 19:183–201.

Delvolvé JJ, Vachard D, Souquet P (1998) Stratigraphic record of thrust propagation, Carboniferous foreland basin, Pyrénées, with emphasis on Pays-de-Sault (France/Spain). Geol Rundsch 87:363–372.

Dias da Silva Í, Almeida P, Oliveira H (2007). Tectonic and stratigraphic evolution of the Santa Susana Shear Zone: associated fabrics and sedimentary episodes related to the late Carboniferous dextral transtensional regime in the SW boundary between the Ossa Morena Zone and the South Portuguese Zone -Santa Suzana area (Alcácer do Sal -Portugal). I EGIGUL. Lisboa. 136 p.

Dias da Silva Í, Valverde-Vaquero P, González-Clavijo E, Díez-Montes A, Martínez Catalán JR (2014) Structural and stratigraphical significance of U–Pb ages from the Mora and Saldanha volcanic complexes (NE Portugal, Iberian Variscides). Geological Society, London, Special Publications 405:115–135. https://doi.org/10.1144/sp405.3.

Dias da Silva Í, González Clavijo E, Díez Montes A (2015a) Lateral escape tectonics in the Variscan Orogen: A new approach for the emplacement of the Allochthonous terranes and for the birth of the Central Iberian Orocline. In: Pitra P, Ballèvre M, Martínez Catalán JR (eds) Variscan 15 - The Variscan belt: Correlations and plate dynamics, Rennes, BRGM/SGF, 48–49.

Dias da Silva Í, Linnemann U, Hofmann M, González-Clavijo E, Díez-Montes A, Martínez Catalán JR (2015b) Detrital zircon and tectonostratigraphy of the Parautochthon under the Morais Complex (NE Portugal): implications for the Variscan accretionary history of the Iberian Massif. Journal of the Geological Society 172 (1):45–61. https://doi.org/10.1144/jgs2014-005.

Díez Fernández R, Martínez Catalán JR, Gerdes A, Abati J, Arenas R, Fernández-Suárez J (2010) U-Pb ages of detrital zircons from the basal allochthonous units of NW Iberia: Provenance and paleoposition on the northern margin of Gondwana during the Neoproterozoic and Paleozoic. Gondwana Research 18:385–399.

Domeier M, Torsvik TH (2014) Plate tectonics in the late Paleozoic. Geoscience Frontiers 5:303–350. https://doi.org/10.1016/j.gsf.2014.01.002.

Domingos LCFG, Freire JLS, Silva FG, Gonçalves F, Pereira E, Ribeiro A (1983) The structure of the intermontane Upper Carboniferous basins in Portugal. In: Lemos de Sousa MJ and Oliveira JT (Eds) The Carboniferous of Portugal. Memórias dos Serviços Geológicos de Portugal, Lisboa, 29: 187–194.

Donaire T, Pascual E, Pin Ch, Duthou JL (1999) Two-stage granitoid-forming event from an isotopically homogeneous crustal source: The Pedroches batholith, Iberian Massif, Spain. Geological Society of America Bulletin 111: 1897–1906.

Dunning GR, Díez Montes A, Matas J, Martín Parra LM, Almarza J, Donaire M (2002) Geocronología U/Pb del volcanismo ácido y granitoides de la Faja Pirítica Ibérica (Zona Sudportuguesa). Geogaceta 32: 127-130.

Drost K, Gerdes A, Jeffries T, Linnemann U, Storey C (2011) Provenance of Neoproterozoic and early Paleozoic siliciclastic rocks of the Teplá-Barrandian unit (Bohemian Massif): Evidence from U-Pb detrital zircon ages. Gondwana Research 19:213–231. doi:https://doi.org/10.1016/j.gr.2010.05.003.

Eagar RMC (1983) The non-marine bivalve fauna of the Stephanian C of North Portugal. In: Lemos de SousaMJ and Oliveira JT (Eds) The

Carboniferous of Portugal. Memórias dos Serviços Geológicos de Portugal, Lisboa, 29: 179–185.
Eden CP (1991) Tectonostratigraphic analysis of the northern extent of the oceanic exotic terrane, Northwestern Huelva Province, Spain. PhD thesis, University of Southampton, 293 p.
Eden CP, Andrews JR (1990) Middle to Upper Devonian melanges in SW Spain and their relationship to the Meneage Formation in south Cornwall. Proceedings of the Ussher Society 7:217–222.
Eichmüller K (1985) The Valdeteja Formation: environment and history of an Upper Carboniferous platform (Cantabrian Mountains, northern Spain). Facies 13(1):45–153.
Engel W (1984) Migration of folding and flysch sedimentation on the southern flank of the variscan belt (Montagne Noire, Mouthoumet massif, Pyrenees). Z Dtsch Geol Ges 135:279–292.
Engel W, Feist R, Franke W (1978) Syn-orogenic gravitational transport in the Carboniferous of the Montyagne Noire (S-France). Z dt geol Ges 129:461–472.
Engel W, Feist R, Franke W (1981) Le Carbonifère anté-Stéphanien de la Montagne Noire: rapports entre mise en place des nappes et sédimentation. Bull Bur Rerch Géol Minièr 4:341–389.
Expósito I (2000) Evolución Estructural de la mitad septentrional de la Zona de Ossa-Morena, y su relación con el límite Zona de Ossa-Morena / Zona Centroibérica. PhD Thesis, University of Granada.
Feng R, Kerrich R (1990) Geochemistry of Fine-Grained Clastic Sediments in the Archean Abitibi Greenstone-Belt, Canada - Implications for Provenance and Tectonic Setting: Geochimica et Cosmochimica Acta 54:1061–1081.
Fernandes JPM (1996) Resultados preliminares del estudio palinológico de la Cuenca de Santa Susana (Alcácer do Sal, Portugal). In: Ruiz Zapata B (Ed) Estudios Palinológicos, XI Simposio de Palinología (A.P.L.E.), Alcalá de Henares, 1996, 43–45. Universidad de Alcalá, Servicio de Publicaciones, Alcalá de Henares.
Fernandes P, Jorge RCGS, Pereira Z, Oliveira JT (2008) Caracterização Geoquímica do Grupo do Flysch do Baixo Alentejo (Zona Sul Portuguesa): Resultados Preliminares. In: Silva E, Azevedo M, Santos F, Patinha C, Reis A (coord) IX Congresso de Geoquímica dos Países de Língua Portuguesa. Praia, Santiago, Cabo Verde, 103.
Fernández F (1993) La deformación de los gneisses de chimparra en Punta Tarroiba (Cabo Ortegal, NW de España). Rev Soc Geol España 6,3–4.
Fernández LP, Águeda JA, Colmenero JR, Salvador CI, Barba P (1988) A coal-bearing fan-delta complex in the Westfalian D of the Central Coal Basin, Cantabrian Mountains, northwestern Spain: implications for the recognition of humid-type fan deltas. In: W. Nemec y R.J., Steel (eds) Fan Deltas: Sedimentology and Tectonic Settings. Blackie & Son, Glasgow, 287–302.
Fernández LP, Bahamonde JR, Barba P, Colmenero JR, Heredia N, Rodríguez-Fernández LR, Salvador C, Sánchez de Posada LC, Villa E, Merino-Tomé O, Motis K (2004) Zona Cantábrica. Estratigrafía. Secuencia sinorogénica. In: Vera, J.A. (ed), Geología de España, SGE-IGME, Madrid, 34–42.
Fernández-Ruiz FJ, Cueto LA, Larrea FJ, Quesada C (1990) El plutón de El Guijo: pertrología, geoquímica, edad y relación con otras rocas del batolito de Los Pedroches. Cuadernos Laboratorio Xeolóxico de Laxe 15:89–103.
Fernández-Suárez J, Gutiérrez-Alonso G, Pastor-Galán D, Hofmann M, Murphy JB, Linnemann U (2014) The Ediacaran–Early Cambrian detrital zircon record of NW Iberia: possible sources and paleogeographic constraints. International Journal of Earth Sciences 103:1335–1357. https://doi.org/10.1007/s00531-013-0923-3.
Festa A, Ogata K, Pini GA, Dilek Y, Alonso JL (2016) Origin and significance of olistostromes in the evolution of orogenic belts: A global synthesis. Gondwana Research 39: 180–203.
Flores D, Gama Pereira LC, Ribeiro J, Marques MM, Ribeiro MA, Bobus I, Pinto de Jesus AP (2010) The Buçaco Basin (Portugal): Organic petrology and geochemistry study. In: Suárez-Ruiz I (Ed) ICCP-TSOP 2008. Selected papers from the ICCP-TSOP joint meeting 2008: International conference. International Journal of Coal Geology, 81, 4: 281–286.
Floyd PA, Leveridge BE (1987) Tectonic environment of the Devonian Gramscatho basin, south Cornwall: framework mode and geochemical evidence from turbiditic sandstones. Journal of the Geological Society 144:531–542. https://doi.org/10.1144/gsjgs.144.4.0531.
Floyd PA, Shail R, Leveridge BE, Franke W (1991) Geochemistry and provenance of Rhenohercynian syn-orogenic sandstones: implications for the tectonic environment discrimination. In: Morton AC, Todd SP, Haughton PDW (eds) Developments in sedimentary provenance studies. Geological Society Special Publication 57:173–188.
Franke W (1989) Variscan plate tectonics in Central Europe- current ideas and open questions. Tectonophysics, 169: 221–228.
Franke W, Bortfeld RK, Brix M, Drozdzewski G, Dürbaum HJ, Giese P, Janoth W, Jödicke H, Reichert C, Scherp A, Schmoll J, Thomas R, Thünker M, Weber K, Wiesner MG, Wong HK (1990) Crustal structure of the Rhenish Massif: results of deep seismic reflection lines DEKORP 2-North and 2-North-Q. Geologische Rundschau 79:523–566.
Frets DC (1965) The geology of the southern part of the Pisuerga basin and the adjacent area of Santibañez de Resoba, Palencia, Spain. Leidse Geol Meded 31:113–163.
Fyffe L, Barr S, Johnson S, McLeod M, McNicoll V, Valverde-Vaquero P, Van Staal C, White C (2009) Detrital zircon ages from Neoproterozoic and Early Paleozoic conglomerate and sandstone units of New Brunswick and coastal Maine: implications for the tectonic evolution of Ganderia. Atlantic Geology 45:110–144. https://doi.org/10.4138/atlgeol.2009.006.
Gabaldón V (1989) Plataformas siliciclásticas externas: facies y su distribución areal. (Plataformas dominadas por tormentas). PhD thesis Univ Autónoma de Barcelona, 200 p.
Gabaldón V, Quesada C (1986) Exemples de bassins houillers limniques du sud-ouest de la péninsule Ibérique: évolution sédimentaire et contrôle structural. Mém Soc géol France, NS 149:27–36.
Gabaldón V, Garrote A, Quesada C (1983) Las cuencas de Valdeinfierno y Benajarafe (Tournaisiense-Viseense). Caracterización sedimentológica e implicaciones regionales. Dominio de Sª Albarrana (Zona de Ossa-Morena. Comun Serv Geol Portugal 69/2:209–218.
Gabaldón V, Garrote A, Quesada C (1985a) El Carbonífero Inferior del Norte de la Zona de Ossa-Morena (SW de España. CR 10th Int Carboniferous Congr, Madrid, 3:173–186.
Gabaldón V, Garrote A, Quesada C (1985b) Geología del Carbonífero Inferior del Norte de la Zona de Ossa-Morena. Introducción a la excursión. Temas Geológico-Mineros IGME 5: 101–137.
Gabaldón V, Quesada C, Gómez JJ (2004) Sedimentation within syn-orogenic basins in a transpressional orogen (SW Iberia Variscan Belt). 32th International Geological Congress, Florence. Abstract.
Galle A, Hladil J, Isaacson PE (1995) Middle Devonian biogeography of closing South Laurussia to North Gondwana Variscides; examples from the Bohemian Massif, Czech Republic, with emphasis on Horni Benešov. Palaios 10:221–239. https://doi.org/10.2307/3515254.
Gama Pereira LC, Pina B, Flores D, Ribeiro MA (2008) Tectónica distensiva: O exemplo da Bacia Permo-Carbónica do Buçaco. In: As Geociências no Desenvolvimento das Comunidades Lusófonas, Conferência Internacional, Coimbra 13–14 de Outubro de 2008. Memórias e Notícias, Coimbra, Nova Série. 3: 199–205.
Gandl J, Delvolvé JJ (1990) Une première faune de trilobites du Carbonifère supérieur des Pyrénées centrals françaises. Geobios 23:587–605.
Gandl J, Ferrer E, Magrans J, Sanz-López J (2015) Trilobiten aus dem Unter-Karbon des Katalonischen Küstengebirges (NE-Spanien).

Abh Senckenberg Ges Naturforsch 571, Schweizerbart and Borntraeger Science Publishers, Stuttgart.

García-Alcalde JL, Arbizu M, Pardo Alonso MV, García López S (1984) El límite Devónico-Carbonífero en el área de Guadalmez-Santa Eufemia (Provs. de Ciudad Real y Córdoba, Sierra Morena, España). I Congreso Español de Geología 1:421–430.

García de Madinabeitia S (2002) Implementación y aplicación de los análisis isotópicos de Pb al estudio de las mineralizaciones y la geocronología del área Los Pedroches-Alcudia (Zona Centro-Ibérica). PhD thesis Univ País Vasco, 207 p.

García de Madinabeitia S, Santos-Zalduegui JF, Carracedo-Sánchez M, Gil-Ibarguchi JI (2001) Edades preliminares Pb-Pb y U-Pb de circones y monacitas del batolito de Los Pedroches (España). III Congreso Ibérico de Geoquímica-VIII Congreso de Geoquímica de España (Zaragoza), 603–607.

García Loygorri A, Ortuño G, Caride de Liñán C, Gervilla M, Greber Ch, Feys R (1971) El Carbonífero de la Cuenca Carbonífera Central Asturiana. *Trabajos de Geología*, Univ Oviedo 3:101–150.

García-Navarro E, Sierra S (1998) Evolución tectónica del borde oriental de la cuenca del Viar (ZSP). Rev Soc Geol Esp 11/3–4:223–232.

García Siñériz J (1944) Investigación sísmica en la cuenca del Viar. In: La interpretación geológica de las mediciones geofísicas. Mem IGME III.

Garrote A (1976) Asociaciones minerales del núcleo metamórfico de Sierra Albarrana (Prov. de Córdoba). Sierra Morena Central. Memórias e Noticias Publ Mus Lab Mineral Geol Univ Coimbra 82:17–39.

Garrote A, Broutin J (1979) Le bassin tournaisien de Benajarafe (Province de Cordoue, Espagne). Géologie et prémières données paléobotaniques et palynologiques. Congr Nat Soc Savantes, Bordeaux, 1:175–184.

Garrote A, Sánchez-Carretero R (1983) Materiales volcanoclásticos en el Carbonífero inferior, al S-SW de Villaviciosa de Córdoba (Zona de Ossa Morena). Comunicações dos Serviços Geológicos de Portugal 69:249–257.

Giese U, Rainer H, Hollman G, Walter R (1994) Geology of the southwestern Iberian Meseta. I: The Paleozoic of the Ossa Morena Zone north and south of the Olivenza-Monesterio Anticline (Huelva Province, SW Spain). N Jahrb für Geol Paläont Abh 192:293–331.

Gladney ER, Braid JA, Murphy JB, Quesada C, McFarlane CRM (2014) U-Pb geochronology and petrology of the late Paleozoic Gil Marquez pluton: Magmatism in the Variscan suture zone, southern Iberia, during continental collision and the amalgamation of Pangea. International Journal of the Earth Sciences 103:1433–1451. https://doi.org/10.1007/s00531-014-1034-5.

Gómez Barreiro J, Martínez Catalán JR, Arenas R, Castiñeiras P, Abati J, Díaz García F, Wijbrans JR (2007) Tectonic evolution of the upper allochtonon of the Órdenes complex (Northwestern Iberian Massif): Structural constraints to a poligenic peri-Gondwanan terrane. In: Linnemann U, Nance RD, Kraft P, Zulauf G (eds) The Evolution of the Rheic Ocean: From Avalonian–Cadomian Active Margin to Alleghenian–Variscan Collision, Geologic Society of America - Special paper 423:315–332. https://doi.org/10.1130/2007.2423(15).

González Clavijo E (2006) La geología del sinforme de Alcañices, Oeste de Zamora. Ediciós do Castro, Serie Nova Terra 31, 238 p, A Coruña.

González Clavijo E, Martínez Catalán JR (2002) Stratigraphic record of preorogenic to synorogenic sedimentation, and tectonic evolution of imbricate units in the Alcañices synform (northwestern Iberian Massif). In: Martínez Catalán JR, Hatcher RD Jr, Arenas R, Díaz García F (eds), Variscan-Appalachian dynamics: The building of the late Paleozoic basement: Boulder, Colorado, Geological Society of America Special Paper 364:17–35.

González Clavijo E, Gutiérrez-Marco JC, Jiménez Fuentes E, Moro Benito MC, Storch P (1997) Graptolitos Silúricos del Sinforme de Alcañices (prov. de Zamora, Zonas Centroibérica y Galaico-Trasmontana). In: Grandal D'Anglade A, Gutiérrez-Marco JC, Santos Fidalgo L (eds) Paleozoico Inferior del Noroeste de Gondwana, 71–74.

González Clavijo E, Dias da Silva Í, Gutiérrez-Alonso G, Díez Montes A (2016) U/Pb age of a large dacitic block locked in an early carboniferous synorogenic mélange in the parautochthon of NW Iberia: New insights on the structure/sedimentation variscan interplay. Tectonophysics first online (TECTO-126895):11. https://doi.org/10.1016/j.tecto.2016.01.001.

Goodwin AM (1991) *Precambrian Geology*. Academic Press, London.

Gower CF, Ryan AB, Rivers T (1990) Mid-Proterozoic Laurentia–Baltica: An overview of its geological evolution and a summary of the contributions made by this volume. In: Gower CF, Rivers T, Ryan AB (eds) Mid- Proterozoic Laurentia–Baltica. Geological Association of Canada, Special Papers 38:1–22.

Gretter N, Ronchi A, López-Gómez J, Arche A, De la Horra R, Barrenechea J, Lago M (2015) The Late Paleozoic-Early Mesozoic from the Catalan Pyrenees (Spain): 60 Myr of environmental evolution in the frame of the western peri-Tethyan palaeogeography. Earth-Sci Rev 150:679–708.

Gutiérrez-Alonso G, Fernández-Suárez J, Weil AB (2004) Orocline triggered lithospheric delamination. Geological Society of America, Special Paper 383:121–130.

Gutiérrez-Marco JC, Sarmiento GN (1999) Microfósiles ordovícicos en olistolitos carboníferos de la cuenca del Guadiato, Adamuz (Córdoba). Temas Geológico-Mineros IGME 26:580–584.

Gutiérrez-Alonso G, Fernández-Suárez J, Jeffries TE, Johnston ST, Pastor-Galán D, Murphy BJ, Franco MP, Gonzalo JC (2011a) Diachronous post-orogenic magmatism within a developing orocline in Iberia, European Variscides. Tectonics 30:TC5008. doi: 10.1029/2010TC002845

Gutiérrez-Alonso G, Murphy JB, Fernández-Suárez J, Weil AB, Franco MP, Gonzalo JC (2011b) Lithospheric delamination in the core of Pangea: Sm-Nd insights from the Iberian mantle. Geology 39:155-158.

Gutiérrez-Marco JC, Sarmiento GN, Rábano I (2014) Un olistostroma con cantos y bloques del Paleozoico Inferior en la cuenca carbonífera del Guadalmellato (Córdoba). Parte 2: Bioestratigrafía y afinidades paleogeográficas. Revista de la Sociedad Geológica de España 27:25–43.

Haq BU, Shutter SR (2008) A chronology of Paleozoic sea-level changes. Science 322:64-68. doi: 10.1126/science.1161648.

Helmig HM (1965) The geology of the Valderrueda Tejerina, Ocejo and Sabero coal basins (Cantabrian mountains, Sapin). Leidse Geologische Mededelingen 32:75–149.

Hemming SR, McLennan SM, Hanson GN (1995) Geochemical and Nd/Pb isotopic evidence for the provenance of the Early Proterozoic Virginia Formation, Minnesota. Implications for the tectonic setting of the Animikie basin. Journal of Geology 103:147–168.

Herbig HG (1983) El Carbonífero de las Cordilleras Béticas. In: Díaz M (ed) Carbonífero y Pérmico de España X Congreso Internacional de Estratigrafía y Geología del Carbonífero Madrid 343–356.

Herbig HG (1984) Rekonstruktion eines nicht mehr existenten Sedimentations-Raums: die Kalk-Gerölle im Karbon Flysch der Malagiden (Betische Kordillere, Südspanien). Facies 11:1–108.

Herbig HG (1985) An upper Devonian limestone slide block near Marbella (Betic Cordillera, southern Spain) and the palaeogeographic relations between Malaguides and Menorca. Acta Geológica Hispánica 20:155–178.

Heredia N (1991) Estructura Geológica de la Región del Mampodre y áreas adyacentes (Zona Cantábrica). Spain. PhD thesis, Univ Oviedo, 320 p.

Heward A (1978) Alluvial fan sequence and lacustrine sediments from the Stephanian A and B (La Magadalena, Ciñera and Sabero) coalfields, northern Spain. Sedimentology 25:451–488.

Hirt AM, Lowrie W, Julivert M, Arboleya ML (1992) Paleomagnetic results in support of a model for the origin of the Asturian Arc. Tectonophysics 213:321–339.

Hladil J, Helešicová K, Hrubanová J, Müller P, Ureš M (1994) Devonian island elevations under the scope - Central Europe, basement of the Carpathian Mountains in Moravia. Jahrbuch der Geologischen Bundesanstalt in Wien 136(4):741–750.

Hladil J, Geršl M, Strnad L, Frána J, Langrová A, Spišiak J (2006) Stratigraphic variation of complex impurities in platform limestones and possible significance of atmospheric dust: a study with emphasis on gamma-ray spectrometry and magnetic susceptibility outcrop logging (Eifelian-Frasnian, Moravia, Czech Rep.). Int J Earth Sci, 95 (4):703–723. https://doi.org/10.1007/s00531-005-0052-8.

Horvarth V (1985) Apports de la palynologie a la stratigraphie du Carbonifère moyen de l'Unité structurale de la Sobia-Bodón (Zone Cantabrique – Espagne). Thèse Troisième Cycle, Univ Sci Tech Lille, 137 p.

Isbell JL, Miller MF, Babcock LE, Hasiotis ST (2001) Ice-marginal environment and ecosystem prior to initial advance of the late Palaeozoic ice sheet in the Mount Butters area of the central Transantarctic Mountains, Antarctica. Sedimentology 48:953–970.

Isbell JL, Lenaker PA, Askin RA, Miller MF, Babcock LE (2003) Reevaluation of the timing and extent of late Paleozoic glaciation in Gondwana; role of the Transantarctic Mountains. Geology 31:977–980.

Jaeger H, Robardet M (1979) Le Silurien et le Dévonien basal dans le nord de la province de Séville (Espagne). Geobios 12/5:687–714.

Jesus AP, Munhá J, Mateus A, Tassinari C, Nutman AP (2007) The Beja layered gabbroic sequence (Ossa-Morena Zone, Southern Portugal): geochronology and geodynamic implications. Geodin Acta 20: 139–157.

Jesus AP, Mateus A, Munhá JM, Tassinari CGC, Bento dos Santos TM, Benoit M (2016) Evidence for underplating in the genesis of the Variscan synorogenic Beja Layered Gabbroic Sequence (Portugal) and related mesocratic rocks. Tectonophysics 683 (30): 148–171. https://doi.org/10.1016/j.tecto.2016.06.001.

Johnston ST, Weil AB, Gutiérrez-Alonso G (2013) Oroclines: thick and thin. Geological Society of America Bulletin 125:643–663. https://doi.org/10.1130/B30765.1.

Jongmans WJ (1949) Note préliminaire sur la flore de Valdeinfierno. Notas y Comunicaciones IGME 19:187–190.

Jongmans WJ, Meléndez B (1950) El hullero inferior de Valdeinfierno (Córdoba). Estudios Geológicos 11:191–200.

Jorge RCGS (2009) Caracterização petrográfica, geoquímica e isotópica dos reservatórios metaliferos crustais, dos processos de extracção de metais e dos fluidos hidrotermais envolvidos em sistemas mineralizantes híbridos na Faixa Piritosa Ibérica. PhD thesis Univ Lisboa.

Jorge RCGS, Fernandes P, Rodrigues B, Pereira Z, Oliveira J (2013) Geochemistry and provenance of the Carboniferous Baixo Alentejo Flysch Group, South Portuguese Zone. Sediment Geol 284:133–148, https://doi.org/10.1016/j.sedgeo.2012.12.005.

Julivert M (1971) Décollement tectonics in the Hercinian Cordillera of NW Spain. American Journal of Science 270:1–29.

Julivert M (1978) Hercynian orogeny and Carboniferous paleogeography in NW Spain: a model of deformation-sedimentation relationships. Zeitschrift der Deutschen Geologischen Gesellschaft 129:565–592.

Keller M, Bahlburg H, and Reuther CD (2007) The transition from passive to active margin sedimentation in the Cantabrian Mountains, Northern Spain: Devonian or Carboniferous? Tectonophysics 461: 414–427

Kenter JAM, van Hoeflaken F, Bahamonde JR, Bracco Gartner GL, Keim L, Besems RE (2003) Anatomy and Lithofacies of an Intact and Seismic-Scale Carboniferous Carbonate Platform (Asturias, NW Spain): Analogues of Hydrocarbon Reservoirs in the Pricaspian Basin (Kazakhstan).In: Zempolich WG, Cook HE (eds) Paleozoic Carbonates of the Commonwealth of Independent States (CIS), SEPM Special Publication 77:185–207.

Keppie JD, Davis DW, Krogh TE (1998) U-Pb geochronological constraints on Precambrian stratified units in the Avalon composite terrane of Nova Scotia, Canada: tectonic implications. Canadian Journal of Earth.

Knight JA (1983) The stratigraphy of Stephanian rocks of Sabero Coalfield, León (NW. Spain) and an investigation of the fossil flora. Part I. The stratigraphy and general geology of the Sabero Coalfield. Paleobothanica Abt B 187:1–88.

Knight JA, Wagner RH (2014) Proposal for recognition of a Saberian Substage in the mid-Stephanian (West European chronostratigraphic schem). Freiberger Forschungshefte C548:179–195.

Kollmeier JM, Van der Pluijm BA, Van der Voo R (2000) Analysis of Variscan dynamics; early bending of the Cantabria–Asturias Arc, northern Spain. Earth and Planetary Science Letters 181:203–216. https://doi.org/10.1016/S0012-821X(00)00203-X.

Königshof P, Nesbor HD, Flick H (2010) Volcanism and reef development in the Devonian: a case study from the Rheinisches Schiefergebirge (Lahn Syncline, Germany). Gondwana Res 17(2–3):264–280. https://doi.org/10.1016/j.gr.2009.09.006.

Korn D (1997) The Palaeozoic ammonoids of the South Portuguese Zone. Memórias dos Serviços Geológicos de Portugal 33:1–129.

Korn D, Feist R (2007) Early Carboniferous ammonoid faunas and stratigraphy of the Montagne Noire (France). Fossil Record 10:99–124.

Korn D, Klug C (2015) Paleozoic ammonoid biostratigraphy. In: Klug C, Korn D, de Baefs K, Kruta I (eds) Ammonoid paleobiology. From macroevolution to paleogeography. (Springer) Topics in Geobiology 44, chapter 12:299-328.

Králík J, Pešek J (1985) The volcanic rocks of the Puertollano Basin (Ciudad Real, Spain). In: Lemos de Sousa M.J (ed.) Contributions to the Carboniferous Geology and Palaeontology of the Iberian Peninsula. Universidade do Porto-Faculdade de Ciencias, 245–268.

Krebs W (1974) Devonian carbonate complexes of central Europe. In: Laporte LF (ed) Reefs in time and space. Society Economic Paleontologists Mineralogists Special Publication 18:155–208.

Krogh T, Keppie JD (1990) Age of detrital zircon and titanite in the Meguma Group, southern Nova Scotia, Canada: Clues to the origin of the Meguma terrane. Tectonophysics 177:307–323.

Kroner A, Romer RL (2013) Two plates—many subduction zones: the Variscan orogeny reconsidered. Gondwana Res 24(1):298–329.

Kullmann J (1960) Die Ammonoidea des Devon im Kantabrischen Gebirge (Nordspanien): Abh.Math. Naturwiss. Kl. Akad. Wiss. Lit. Mainz 1960-7:455–559.

Kullmann J, Reuther CD, Schönenberg R (1977) La transición del estado geosinclinal a la orogénesis en la formación varíscica de la Cordillera Cantábrica. Breviora Geologica Astúrica 21:4–11.

Kullmann J, Magrans J, Ferrer E, Abad A (2001) Primer hallazgo del género *Dombarites* (Cephalopoda, Ammonoidea) del Carbonífero inferior en El Papiol (Cataluña, España). Batalleria 10:5–8.

Kullmann J, Llompart C, Bolet A (2005) *Lusitanoceras* sp. (Ammonoidea, Goniatitida) en el Carbonífero de Menorca (Baleares). Batalleria 12:135–140.

Kullmann J, Perret MF, Mirouse R, Delvolvé JJ (2008) Goniatites et conodontes du Viséen/Serpukhovien dans les Pyrénées centrales et occidentales, France. Geobios 41:635–656.

Larrea FJ, Quesada C, Cueto LA, Fernández-Ruiz FJ (1992) Mapa Geológico de España, scale 1:50,000. Sheet nº 883 (Virgen de la Cabeza). Instituto Geológico Minero de España, 86 p.

Larrondo E, Carracedo M, Eguiluz, Gil Ibarguchi JI (2005) Vulcanismo lávico y explosivo en la cuenca carbonífera de Los Santos de Maimona (Zona de Ossa-Morena, Badajoz). Geogaceta 37:47–50.

Larrondo E, Carracedo M, Eguiluz, Gil Ibarguchi JI (2007) Significado del vulcanismo calcoalcalino a alcalino de la cuenca de Los Santos de Maimona (Badaloz, Zona de Ossa-Morena). XV Semana/VI Congresso Ibérico de Geoquímica, Proceedings, 121–124.

Le Menn J, Gourvennec R, Plusquellec Y, Piçarra JM, Pereira Z, Robardet M, Oliveira JT (2002) Lower Devonian benthic faunas from the Barrancos area (Ossa Morena Zone, Portugal) and their paleobiogeographic affinities, Comunicações do Instituto Geológico e Mineiro 89,19–38.

Legrand-Blain M, Delvolvé JJ, Perret MF (1983) Les Brachiopodes carbonifères des Pyrénées centrales françaises. 1 : cadre stratigraphique et sédimentaire; étude des Strophomenida. Géobios 16:285–327.

Legrand-Blain M, Delvolvé JJ, Perret MF (1984) Les Brachiopodes carbonifères des Pyrénées centrales françaises. 2 : Étude des Orthida et des Spiriferida ; biostratigraphie, paléoécologie, paléobiogéographie. Géobios 17:297–325.

Lemos de Sousa MJ, Wagner RH (1983) General description of the terrestrial Carboniferous basins in Portugal and history of investigations. In: Lemos de Sousa MJ and Oliveira JT, (eds) The Carboniferous of Portugal. Memórias dos Serviços Geológicos de Portugal 29:117–126.

Lopes G, Pereira Z, Fernandes P, Wicander R, Matos J, Rosa D, Oliveira JT (2014) The significance of the reworked palynomorphs (Middle Cambrian to Tournaisian) in the Viséan Toca da Moura Complex (South Portugal). Implications for the geodynamic evolution of Ossa Morena Zone. Rev Palaeobot and Palyno 200:1–23. https://doi.org/10.1016/j.revpalbo.2013.07.003.

López-Gómez J, Arche A, Marzo M, Durand M (2005) Stratigraphical and palaeogeographical significance of the continental sedimentary transition across the Permian-Triassic boundary in Spain. Palaeogeography, Palaeoclimatology, Palaeoecology 229:3–23.

Lorenzo Álvarez S, Martín Herrero D, Valverde MF (2005) Mapa Geológico de España, scale 1:50,000. Sheet nº 807 (Chillón). Instituto Geológico y Minero de España, Madrid, 113 p.

Lotze F (1945) Zur Gliederung der Varisziden der Iberischen Meseta. Geotekt Forsch 6:78–92.

Loureiro JP, Correia P, Nel A, Pinto de Jesus A (2010) *Lusitaneura covensis n.* gen, n. sp, first *Caloneurodea* from the Carboniferous of Portugal (*Insecta: Pterygota: Panorthoptera*). Annales de la Société Entomologique de France (N.S.) International Journal of Entomology Volume 46, 2010–Issue 1–2. Paris.

Loydell DK, Frýda J, Gutiérrez-Marco JC (2015) The Aeronian/Telychian (Llandovery, Silurian) boundary, with particular reference to sections around the El Pintado reservoir, Seville Province, Spain. Bulletin of Geosciences 90:743–794.

LNEG (2010) Carta Geológica de Portugal na escala 1:1000000.

Maas K (1974) The geology of Liebana, Cantabrian Mountains, Spain. Deposition and deformation in a flysch area. Leidse Geologische Mededlingen 49:379–465.

Maas K, Ginkel A. van (1983) Variscan olistostrome deposition and sedimentary nappe emplacement, Valdeón area, Cantabrian Mountains, Spain. Leidse Geologische Mededelingen 52(2):341–381.

Machado G, Hladil J (2010) On the age and significance of the limestone localities included in the Toca da Moura volcano-sedimentary Complex: preliminary results. In: Santos A, Mayoral E, Melendez G, Silva CMD, Cachão M (eds) III Congresso Ibérico de Paleontología/XXVI Jornadas de la Sociedad Española de Paleontología, Lisbon, Portugal. Publicaciones del Seminario de Paleontología de Zaragoza (PSPZ) 9:153–156.

Machado G, Hladil J, Koptikova L, Fonseca P, Rocha FT, Galle A (2009) The Odivelas Limestone: Evidence for a Middle Devonian reef system in western Ossa-Morena Zone. Geologica Carpathica 60 (2):121–137.

Machado G, Hladil J, Koptikova L, Slavik L, Moreira N, Fonseca M, Fonseca P (2010) An Emsian-Eifelian Carbonate-Volcaniclastic Sequence and the possible Record of the basal Choteč event in western Ossa-Morena Zone, Portugal (Odivelas Limestone). Geol Belg 13:431–446.

Machado G, Dias da Silva I, Almeida P (2012) Palynology, Stratigraphy and Geometry of the Pennsylvanian continental Santa Susana Basin (SW Portugal). J Iber Geol 38(2):429–448. https://doi.org/10.5209/rev_JIGE.2012.v38.n2.40467.

Maestro-Madieu E, Estrada R, Remacha E (1998) La sección del Carbonífero en el Priorat Central (Prov. de Tarragona). Geogaceta 23:91–94.

Mallada L (1898–1927) Explicación del Mapa Geológico de España. Tomo III: Sistemas Devoniano y Carbonífero. Mem Com Mapa Geol España, 415 p.

Mamet BL, Martínez-Díaz C (1981) Late Visean microfossils of the Las Caleras Bajas limestone (Córdoba, Spain). Revista Española de Micropaleontología 13:105–118.

Marcos A, Pulgar JA (1982) An approach to the tectonostratigraphic evolution of the Cantabrian foreland thrust and fold belt, Hercynian Cordillera of NW Spain. Neues Jahrbuch für Geologie und Paläontologie, Abhandlungen 163:256–260.

Martín-Merino G, Fernández LP, Colmenero JR, Bahamonde JR (2014) Mass-transport deposits in a Variscan wedge-top foreland basin (Pisuerga área, Cantrabrian Zone, NW Spain). Marine Geology 356:71–87 https://doi.org/10.1016/j.margeo.2014.01.012.

Martín Parra LM, González Lodeiro F, Martínez Poyatos D, Matas J (2006) The Puente Génave-Castelo de Vide shear zone (southern Central Iberian Zone, Iberian Massif): geometry, kinematics and regional implications. Bulletin de la Société Géologique de France 177:191–202. https://doi.org/10.2113/gssgfbull.177.4.191.

Martínez FJ, Dietsch C, Aleinikoff J, Cirés J, Arboleya ML, Reche J, Gómez-Gras D (2016) Provenance, age, and tectonic evolution of Varyscan flysch, southeastern France and notheastern Spain, based on zircon geochronology. Geol Soc Am Bull 128:842–859.

Martínez Catalán JR, González Lodeiro F, González Clavijo E, Fernández Rodríguez C, Díez Montes A (2004) Zona Centro Ibérica. Estructura. In: Vera JA (ed) Geología de España. SGE-IGME, Madrid, pp 75–78.

Martínez Catalán JR, Fernández-Suárez J, Meireles C, González Clavijo E, Belousova E, Saeed A (2008) U-Pb detrital zircon ages in sinorogenic deposits of the NW Iberian Massif (Variscan belt): Interplay of Devonian-Carboniferous sedimentation and thrust tectonics. Journal of the Geological Society 165:687–698. https://doi.org/10.1144/0016-76492007-066.

Martínez Catalán JR, González Clavijo E, Meireles C, Díez Fernández R, Bevis J (2016) Relationships between syn-orogenic sedimentation and nappe emplacement in the hinterland of the Variscan belt in NW Iberia deduced from detrital zircons. Geological Magazine 153:38–60, https://doi.org/10.1017/S001675681500028X.

Martínez García E (1972) El Silúrico de San Vitero (Zamora). Comparación con las series vecinas e importancia orogénica. *Acta Geol Hisp* VII (4):104–108.

Mata J, Munhá J (1990) Magmatogénese de Metavulcanito Cambricos do Nordeste Alentejano: os stadios iniciais de rifting continental. Comunicaçoes dos Serviços Geológicos de Portugal 76:61–89.

Mata J, Ribeiro L, Piçarra J (1993) S. Marcos do Campo volcanic complex: Geochemical evidence for a volcanic arc in the Ossa – Morena Zone (Ordovician). Terra Nova, Abstracts Supplement 5: 2.

Matas J, Martín Parra, LM, Rubio Pascual FJ, Roldán FJ, Martín Serrano A (2010) Mapa Geológico de España, scale 1:200,000. Sheet: Sevilla-Puebla de Guzmán. IGME, Madrid, 322 p.

Matas J, Martín Parra LM, Montes Santiago M (2014) Un olistostroma con cantos y bloques del Paleozoico inferior en la cuenca carbonífera del Guadalmellato (Córdoba). Parte I: Estratigrafía y marco geodinámico varisco. Revista de la Sociedad Geológica de España 27(1):11–25.

Mateus A, Munhá J, Ribeiro A, Tassinari CCG, Sato K, Pereira E, Santos JF (2016) U-Pb SHRIMP zircon dating of high-grade rocks from the Upper Allochthonous Terrane of Bragança and Morais Massifs (NE Portugal); geodynamic consequences. Tectonophysics 675:23–49, https://doi.org/10.1016.j.tecto.2016.02.048.

Matte Ph (1986a) Tectonics and plate tectonics model for the Variscan belt of Europe. Tectonophysics 126:329–374.

Matte Ph (1986b) La chaîne varisque parmi les chaînes paléozoïques péri – atlantiques, modèle d'évolution et position des grands blocs continentaux au Permo – Carbonifère. Bulletin Societé géologique de France 8:9–24.

Matte Ph (1991) Accretionary history and crustal evolution of the Variscan belt in Western Europe. Tectonophysics 196:309–337.

Matte Ph (2001) The Variscan collage and orogeny (480-290 Ma) and the tectonic definition of the Armorica microplate: a review. Terra Nova 13:122–128.

Matte Ph (2002) Variscides between the Appalachians and the Urals: Similarities and differences between Paleozoic subduction and collision belts. In: Martínez Catalán JR, Hatcher RD Jr, Arenas R, Díaz García F (eds), Variscan-Appalachian dynamics: The building of the late Paleozoic basement: Boulder, Colorado, Geological Society of America Special Paper 364:239–251.

Matthews KJ, Maloney KT, Zahirovic S, Williams SE, Seton M, Müller RD (2016) Global plate boundary evolution and kinematics since the late Paleozoic. Global and Planetary Change 146:226–250 https://doi.org/10.1016/j.gloplacha.2016.10.002.

May A (1999) Stromatoporen aus dem Ober-Emsium (Unter-Devon der Sierra Morena (Süd-Spanien). Münstersche Forsch. Geol. Paläont. 86: 97–105.

McArthur JM, Howarth RJ, Shields GA (2012) Strontium Isotope Stratigraphy. In: Gradstein FM, Ogg JG, Schmotz MD, Ogg GM (eds) A Geologic Time Scale 2012 (Chapter 7), Elsevier, 127–144.

McKerrow WS, Scotese CR (1990) Revised world maps and introduction. In: McKerrow WS, Scotese CR (eds) Paleozoic Paleogeography and Biogeography. The Geological Society of London, Memoir 12:1–24.

McLennan SM (1989) Rare earth elements in sedimentary rocks: influence of provenance and sedimentary processes. In: Lipin BR, McKay GA (eds) Geochemistry and mineralogy of rare earth elements. Reviews in Mineralogy 21:169–200.

McLennan SM, Taylor SR, McCulloch MT, Maynard JB (1990) Geochemical and Nd-Sr Isotopic Composition of Deep-Sea Turbidites - Crustal Evolution and Plate Tectonic Associations. Geochimica et Cosmochimica Acta 54:2015–2050.

McLennan SM, Hemming S, McDaniel DK, Hanson GN (1993) Geochemical approaches to sedimentation, provenance, and tectonics. In: Basu MJJA (ed) Processes controlling the composition of clastic sediments. The Geological Society of America, 21–40.

Megias AG (1982). Introducción al análisis tectosedimentario: Applicación al estudio dinámico de cuencas. Actas Congresso Latino-americano de Geología, Argentina, Vol.I, p. 385–401.

Meinhold G, Morton AC, Fanning CM, Frei D, Howard JD, Phillips RJ, Strogen D, Whithan AG (2011) Evidence from detrital zircons for recycling of Mesoproterozoic and Neoproterozoic crust recorded in Paleozoic and Mesozoic sandstones of southern Libya. Earth and Planetary Science Letter, 312:164–175. https://doi.org/10.1016/j.epsl.2011.09.056.

Meinhold, G., Morton, A.C. and Avigad, D. (2013). New insights into peri-Gondwana paleogeography and the Gondwana super-fan system from detrital zircon U-Pb ages. *Gondwana Research,* 23, pp. 661–665, https://doi.org/10.1016/j.gr.2012.05.003.

Meireles CAP (2013) Litoestratigrafia do Paleozóico do sector a nordeste de Bragança (Trás-os-Montes), Instituto Universitario de Geología Isidro Parga Pondal, Serie Nova Terra 42, 471 p., A Coruña.

Melgarejo JC (1987) Estudi geològic i metal.logénetic del Paleozoic del Sud de les Serralades Costaneres Catalanes. PhD thesis, Univ Barcelona.

Melgarejo JC (1992) Estudio geológico y metalogenético del Paleozoico del sur de las Cordilleras Costeras Catalanas. Mem ITGE 103:1–605.

Merino-Tomé OA, Villa E, Bahamonde JR, Colmenero JR (2006) Fusulinoidean characterization of the uppermost Moscovian-Gzhelian (upper Pennsylvanian) synorogenicc depositional sequences from northern Picos de Europa Unit (Spain). Facies 52:521–540.

Merino-Tomé OA, Bahamonde JR, Fernández LP, Colmenero JR (2007) Facies architecture and cyclicity of a Upper Carboniferous carbonate ramp developed in a Variscan piggy-back basin (Cantabrian Mountains, NW Spain). In: Nichols G, Williams E, Paola C (eds) Sedimentary Processes, Environments and Basins: a Tribute to Peter Friend. International Association of Sedimentologists Special Publication 38:183–217.

Merino-Tomé OA, Bahamonde JR, Colmenero JR, Heredia N, Villa E, Farias P (2009a) Emplacement of the Cuera and Picos de Europa imbricate system at the core of the Iberian-Armorican arc (Cantabrian zone, north Spain): New precisions concerning the timing of arc closure. Geological Society of America Bulletin 121:729–751.

Merino-Tomé OA, Bahamonde JR, Samankassou E, Villa E (2009b) The influence of terrestrial run off on marine biotic communities. An example from a thrust-top carbonate ramp (Upper Pennsylvanian foreland basin, Picos de Europa, NW Spain). Palaeogeography, Palaeoclimatology, Palaeoecology 278:1–23.

Mii HS, Grossman EL, Yancey TE, Chuvashov B, Egorov A (2001) Isotopic records of brachiopod shells from the Russian Platform — evidence for the onset of mid-Carboniferous glaciation. Chemical Geology 175:133–147.

Mingarro F (1962) Estudio del Carbonífero del norte de la provincia de Sevilla. Boletín Geológico Minero 73:480–599.

Mirouse R (1966) Recherches géologiques dans la partie occidentale de la zone primaire axiale des Pyrénées. Mém Serv Carte géol Fr, Paris.

Mirouse R, Barrouquère G, Bessière G, Delvolvé JJ, Perret MF (1983) Amorce de la sédimentation synorogénique dans les Pyrénées varisques. Données chronologiques; implications paléogéographiques. Geol Rundsch 72:253–281.

Moita P, Munhá J, Fonseca PE, Tassinari C, Araújo A, Palácios T (2005a) Dating orogenic events in Ossa-Morena Zone. In: Actas XIV Semana de Gequimica/VIII Congresso de geoquimica dos Paises de Lingua Portuguesa 2:459–461, Aveiro.

Moita P, Munhá J, Fonseca P, Pedro J, Tassinari CCG, Araújo A, Palácios T (2005b) Phase equilibria and geochronology of Ossa-Morena eclogites. In: Actas XIV Semana de Geoquímica/VIII Congresso do Geoquímica dos Países de Língua Portuguesa 2:471–474, Aveiro.

Moreira N, Machado G, Fonseca PE, Silva JC, Jorge RCGS, Mata J (2010) The Odivelas Palaeozoic volcano-sedimentary sequence: Implications for the geology of the Ossa-Morena Southwestern border. Comunicações Geológicas 97:129–146.

Moreira N, Araújo A, Pedro J, Dias R (2014) Evolução geodinâmica da Zona de Ossa-Morena no contexto do SW Ibérico durante o Ciclo Varisco. Comunicações Geológicas 101 (I):275–278.

Moreira N, Pedro J, Santos JF, Araújo A, Romão J, Dias R, Ribeiro A, Ribeiro S, Mirão J (2016) 87Sr/86Sr ratios discrimination applied to the main Paleozoic carbonate sedimentation in Ossa-Morena Zone. *In*: IX Congreso Geológico de España (special volume). Geo-Temas 16(1):161–164.

Moreno C (1993) Postvolcanic Paleozoic of the Iberian Pyrite Belt: an example of basin morphologic control on sediment in a turbidite basin. Journal of Sedimentary Petrology 63:1118–1128, https://doi.org/10.1306/d4267cbc-2b26-11d7-8648000102c1865d.

Moreno C, Sáez R (1989) Petrología y procedencia de las areniscas del Culm de la parte occidental de la Faja Pirítica Ibérica (Zona Sur-Portuguesa). Boletín Geológicoy Minero 100, 134–147.
Moreno C, Sierra S, González F (2010) Formación Los Canchales (Cuenca Pérmica del Viar, SOde España). Propuesta de definición formal. Revista de la Sociedad Geológica de España 23(1–2):3–8.
Moreno-Eiris E, Perejón A, Rodríguez S, Falces S (1995) Field Trip D: Paleozoic Cnidaria and Porifera from Sierra Morena. In: VIII Internacional Symposium on fossil Cnidaria and Porifera, Madrid, 68 p.
Moro Benito MC (1980) Los yacimientos de Barita asociados al Sinclinorio de Alcañices-Carbajales de Alba y sus métodos de prospección. PhD thesis, Univ. Salamanca.
Munhá J, Oliveira JT, Ribeiro A, Oliveira V, Quesada C, Kerrich R (1986) Beja-Acebuches Ophiolite: characterization and geodynamic significance. Maleo (Bol Soc Geol Portugal) 2:31.
Murphy JB, Fernández-Suárez J, Keppie JD, Jeffries TE (2004a) Contiguous rather than discrete Paleozoic histories forthe Avalon and Meguma terranes based on detrital zircon data. Geology 32:585–588. https://doi.org/10.1130/g20351.1.
Murphy JB, Pisarevsky SA, Nance RD, Keppie JD (2004b) Neoproterozoic-Early Paleozoic evolution of peri-Gondwanan terranes: implications for Laurentia-Gondwana connections. International Journal of Earth Sciences (Geol Rundsch) 93:659–682. https://doi.org/10.1007/s00531-004-0412-9.
Murphy JB, Fernández-Suárez J, Jeffries TE, Strachan RA (2004c) U-Pb (LA-ICP MS) dating of detrital zircons from Cambrian clastic rocks in Avalonia: erosion of a Neoproterozoic arc along the northern Gondwanan margin. Journal of the Geological Society 161:243–254.
Murphy JB, Keppie JD, Nance RD, Dostal J (2010) Comparative evolution of the Iapetus and Rheic oceans: A North America perspective. Gondwana Research 17:482–499. https://doi.org/10.1016/j.gr.2009.08.009.
Murphy JB, Cousens BL, Braid JA, Strachan RA, Dostal J, Keppie JD, Nance RD (2011) Highly depleted oceanic lithosphere in the Rheic Ocean: implications for Paleozoic plate reconstructions. Lithos 123:165–175.
Murphy JB, Waldron JWF, Schofield DI, Barry TL, Band AR (2014) Highly depleted isotopic compositions evident in Iapetus and Rheic Ocean basalts: implications for crustal generation and preservation. Int J Earth Sci 103/5:1212–1232.
Murphy JB, Braid JA, Quesada C, Dahn D, Gladney E, Dupuis NE (2015) An eastern Mediterranean analogue for the Late Paleozoic evolution of the Pangean suture zone. In: Li ZX, Evans DAD, Murphy JB (eds) Supercontinent Cycles Through Earth History. Geological Society of London Special Publication 424: https://doi.org/10.1144/sp424.9.
Nance RD, Murphy JB, Strachan RA (1991) Late Proterozoic tectonostratigraphic evolution of the Avalonian and Cadomian terranes. Precambrian Research 53:41–78. https://doi.org/10.1016/0301-9268(91)90005-U.
Navas-Parejo P, Rodríguez-Cañero R, Martín-Algarra A (2012) Primer registro de un horizonte estratigráfico hemipelágico con conodontos del Carbonífero Superior en el Complejo Maláguide (Cordillera Bética oriental). Geogaceta 52:81–84.
Nesbitt HW, Young GM (1982) Early Proterozoic Climates and Plate Motions Inferred from Major Element Chemistry of Lutites. Nature 299:715-717.
Nesbitt HW, Fedo CM, Young GM (1997) Quartz and feldspar stability, steady and non-steady state weathering, and petrogenesis of siliciclastic sands and muds. Journal of Geology 105:173–191.
Nesbitt R, Pascual E, Fanning MC, Toscano M, Sáez R, Almodóvar G (1999) First zircon U–Pb dating of stockwork zircons from the eastern Iberian Pyrite Belt, Spain. Journal of the Geological Society, London 156:7–10, http://dx.doi.org/10.1144/gsjgs.156.1.0007.
O'Dogherty L, Rodríguez-Cañero R, Gursky HJ, Martín-Algarra A, Caridroit M (2000) New data on Lower Carboniferous stratigraphy and palaeogeography of the Malaguide Complex (Betic Cordillera, southern Spain). Comptes Rendus de l'Académie des Sciences Paris IIa 331:533–541.
Odriozola JM, Peón A, Vargas I, Quesada C, Cueto LA (1983) Mapa Geológico de España, scale 1:50,000. Sheet nª 854: Zafra. Instituto Geológico Minero de España, 56 p.
Ogg JG, Ogg GM, Gradstein FM (2016) A Concise Geological Time Scale 2016. Elsevier.
Okay AI, Topuz G (2017) Variscan orogeny in the Black Sea region. International Journal of Earth Sciences (Geol Rundsch) 106:569–592. https://doi.org/10.1007/s00531-016-1395-z.
Oliveira JT (1983) The marine Carboniferous of South Portugal: a stratigraphic and sedimentological approach. In: Lemos de Sousa MJ, Oliveira JT (eds) The Carboniferous of Portugal, Mem Serv. Geol. Portugal, 29:3–38, Lisboa.
Oliveira JT (1988) Estratigrafia, sedimentologia e estrutura do flysch da formacão de Mértola, na Região de Mértola. Comunicações dos Serviços Geológicos Portugal 74:3–19.
Oliveira JT (1990) The South Portuguese Zone. Stratigraphy and Synsedimentary Tectonism. In: Dallmeyer RD, Martínez García E (eds) Pre-Mesozoic Geology of Iberia. Springer, Berlin, 334–347.
Oliveira JT, Quesada C (1998) A comparison of stratigraphy, structure, and palaeogeography of the South Portuguese Zone and southwest England, European Variscides. Proc Ussher Soc, Geoscience in South-West England 9:141–150.
Oliveira JT, Relvas J, Pereira Z, Munhá J, Matos J, Barriga F, Rosa C (2013) O Complexo Vulcano-Sedimentar de Toca da Moura-Cabrela (Zona de Ossa Morena): evolução tectono-estratigráfica e mineralizações associadas. In: Dias R, Araújo A, Terrinha P, Kullberg JC (Ed), Geologia de Portugal (Vol.I), Escolar Editora, Lisboa, p 621–645.
Oliveira JT, Wagner Genthis C (1983) The Mértola and Mira formations boundary between Doguedo and Almada do Ouro, marine Carboniferous of South Portugal. In: Lemos de Sousa MJ (ed) Contributions to the Carboniferous Geology and Palaeontology of the Iberian Peninsula, Faculdade de Ciências da Universidade do Porto, 1–39.
Oliveira JT, Horn M, Paproth E (1979) Preliminary note on the stratigraphy of the Baixo-Alentejo Flysch Group, Carboniferous of Portugal, and on the palaeogeographic development compared to corresponding units in North-West Germany. Comunicações dos Serviços Geológicos de Portugal 65:151–168.
Oliveira JT, Cunha T, Streel M, Vangestaine M (1986) Dating the Horta da Torre Formation, a new lithostratigraphic unit in the Ferreira-Ficalho Group, South Portuguese Zone: geological consequences. Com Serv. Geol. Portugal 72:129–135.
Oliveira JT, Oliveira V, Piçarra, J (1991) Traços gerais da evolução tectono-estratigráfica da Zona de Ossa-Morena, em Portugal: síntese crítica do estado actual dos conhecimentos. Comun. Serv. Geol. Portugal 77:3–26.
Onézime J, Charvet J, Faure M, Bourdier JL, Chauvet A (2003) A new geodynamic interpretation for the South Portuguese Zone (SW Iberia) and the Iberian Pyrite Belt genesis. Tectonics 22/4:1027. https://doi.org/10.1029/2002tc001387.
Orr PJ, Benton MJ, Trewin NH (1996) Deep marine trace fossil assemblages from theLower Carboniferous of Menorca, Balearic Islands, western Mediterranean. Geol J 31:235–258.
Pardo MV, García Alcalde JL (1984) Bioestratigrafía del Devónico de la región de Almadén (Ciudad Real, España). Trabajos de Geología Univ Oviedo 14:79–120.
Parés JM, Van der Voo R, Stamatakos J, Pérez-Estaún A (1994) Remagnetizations and postfolding oroclinal rotations in the Cantabrian/Asturian arc, northern Spain. Tectonics 13:1461–1471.

Pascual E (1981) Investigaciones Geológicas en el sector Córdoba--Villaviciosa de Córdoba (Sector Central de Sierra Morena). PhD thesis Univ Granada, 521 p.

Pascual E (1985) El complejo anular del S de Villaviciosa de Córdoba (Córdoba, España): datos petrológicos y geoquímicos y relaciones con otras rocas ígneas del área. Temas Geol Min IGME 5: 65–71.

Pascual E, Pérez Lorente F (1975) El magmatismo ácido superficial al sur de Villanueva del Rey-Villaviciosa de Córdoba (Sierra Morena, Córdoba). Cuadernos de Geología Univ Granada 6:15–30.

Pastor-Galán D, Gutiérrez-Alonso G, Weil AB (2011) Orocline timing through joint analysis: Insights from the Ibero-Armorican Arc. Tectonophysics 507 (1–4):31–46. https://doi.org/10.1016/j.tecto.2011.05.005.

Pastor-Galán D, Gutiérrez-Alonso G, Zulauf G, Zanella F (2012) Analogue modeling of lithospheric-scale orocline buckling: Constraints on the evolution of the Iberian-Armorican Arc. Geological Society of America Bulletin 124:1293–1309. https://doi.org/10.1130/b30640.1.

Pastor- Galán D, Gutiérrez-Alonso G, Murphy JB, Fernández-Suárez J, Hofmann M, Linnemann U (2013a) Provenance analysis of the Paleozoic sequences of the northern Gondwana margin in NW Iberia: Passive margin to Variscan collision and orocline development. Gondwana Research 23:1089–1103. https://doi.org/10.1016/j.gr.2012.06.015.

Pastor-Galán D, Gutiérrez-Alonso G, Fernández-Suárez J, Murphy JB, Nieto F (2013b) Tectonic evolution of NW Iberia during the Paleozoic inferred from the geochemical record of detrital rocks in the Cantabrian Zone. Lithos 182–183:211–228. https://doi.org/10.1016/j.lithos.2013.09.007.

Pastor-Galán D, Martín-Merino G, Corrochano D (2014) Timing and structural evolution in the limb of an orocline: The Pisuerga–Carrión Unit (southern limb of the Cantabrian Orocline, NW Spain). Tectonophysics 622:110–121. https://doi.org/10.1016/j.tecto.2014.03.004.

Pedro J, Araújo A, Fonseca P, Munhá J, Ribeiro A, Mateus A (2013) Cinturas Ofiolíticas e Metamorfismo de Alta Pressão no Bordo SW da Zona de Ossa-Morena. In: Dias R, Araújo A, Terrinha P, Kullberg, JC (eds) Geologia de Portugal, Escolar Editora, 1:647–671, Lisboa.

Perdigão JC, Oliveira JT, Ribeiro A (1982) Notícia explicativa da folha 44-B (Barrancos) da Carta Geológica de Portugal à escala 1:50 000, Serviços Geológicos de Portugal, Lisboa.

Pereira E (2006) Unidades Metassedimentares Sub-autóctones. Unidades Metassedimentares. Notícia Explicativa da Folha 2 da Carta Geológica de Portugal de escala 1:200.000. Inst. Nal. Tecn. Innov. (INETI), Lisboa, 25–27.

Pereira E (coord), Ribeiro A, Marques FO, et al. (2000) Carta Geológica de Portugal, escala 1:200.000. Ministério da Economia.

Pereira E, Ribeiro A, Rebelo J (2003) Carta Geológica de Portugal, escala 1:50.000, folha 11-B (Carviçais), Laborátorio Nacional de Energia e Geologia, Lisboa.

Pereira MF, Chichorro M, Johnston ST, Gutiérrez-Alonso G, Silva JB, Linnemann U, Hofmann M, Drost K (2012a) The missing Rheic Ocean magmatic arcs: Provenance analysis of Late Paleozoic sedimentary clastic rocks of SW Iberia. Gondwana Research 22:882–891. https://doi.org/10.1016/j.gr.2012.03.010.

Pereira MF, Chichorro M, Silva JB, Ordóñez-Casado B, Lee JKW, Williams IS (2012b) Early Carboniferous wrenching, exhumation of high-grade metamorphic rocks and basin instability in SW iberia: Constraints derived from structural geology and U-Pb and $^{40}Ar/^{39}Ar$ geochronology. Tectonophysics 558–559:28–44. https://doi.org/10.1016/j.tecto.2012.06.020.

Pereira MF, Ribeiro C, Vilallonga F, Chichorro M, Drost K, Silva JB, Albardeiro L, Hofmann M, Linnemann U (2014) Variability over time in the sources of South Portuguese Zone turbidites: evidence of denudation of different crustal blocks during the assembly of Pangaea. International Journal of Earth Sciences 103 (5):1453–1470. https://doi.org/10.1007/s00531-013-0902-8.

Pereira MF, Castro A, Fernández C (2015) The inception of a Paleotethyan magmatic arc in Iberia. Geoscience Frontiers 6:297–306. https://doi.org/10.1016/j.gsf.2014.02.006.

Pereira Z (1997) Palinologia e petrologia orgânica do Sector Sudoeste da Zona Sul Portuguesa. PhD thesis, Univ Porto.

Pereira Z (1999) Palinoestratigrafia do Sector Sudoeste da Zona Sul Portuguesa. Comunicações dos Serviços Geológicos de Portugal 86:25–57.

Pereira Z, Oliveira JT (2003a) Estudo palinostratigráfico do sinclinal da Estação de Cabrela. Implicações tectonostratigráficas. Cienc. Terra UNL Lisboa 5:118–119.

Pereira Z, Oliveira JT (2003b) Palinomorfos do Viseano do Complexo vulcânico da Toca da Moura, Zona de Ossa Morena. Cienc. Terra UNL Lisboa 5:120–121.

Pereira Z, Meireles C, Pereira E (1999a) Upper Devonian palynomorphs of NE sector of Trás-os-Montes (Central Iberian Zone). XV Reunión Geología del Oeste Peninsular—International Meeting on Cadomians Orogens, Badajoz, España, 201–206.

Pereira Z, Piçarra JM, Oliveira JT (1999b) Lower Devonian Palynomorphs from the Barrancos region, Ossa-Morena Zone, Portugal. Bolletino della Società Paleontologica Italiana 38:239–245.

Pereira Z, Oliveira V, Oliveira JT (2006) Palynostratigraphy of the Toca da Moura and Cabrela Complexes, Ossa Morena Zone, Portugal. Geodynamic implications. Review of Palaeobotany and Palynology 139(1–4): 227–240. https://doi.org/10.1016/j.revpalbo.2005.07.008.

Pereira Z, Matos J, Fernandes P, Oliveira JT (2008) Palynostratigraphy and systematic palynology of the Devonian and Carboniferous successions of the South Portuguese Zone, Portugal. Memórias Geológicas do Instituto Nacional de Engenharia, Tecnologia e Innovaçao 34:129–146.

Pereira Z, Fernandes P, Matos J, Jorge RCGS, Oliveira JT (2018) Stratigraphy of the Northern Pulo do Lobo Domain, SW Iberia Variscides: A palynological contribution. Geobios, 51, 491–506. Elsevier.

Pérez-Cáceres I, Martínez Poyatos D, Simancas JF, Azor A (2016) Detrital zircon populations in the lower formations of the South Portuguese Zone (SW Iberia, Variscan Orogen). Geo-Temas 16 (1):25–28.

Pérez-Cáceres I, Martínez Poyatos D, Simancas JF, Azor A (2017) Testing the Avalonian affinity of the South Portuguese Zone and the Neoproterozoic evolution of SW Iberia through detrital zircon populations. Gondwana Research 42:177–192. https://doi.org/10.1016/j.gr.2016.10.010.

Pérez-Estaún A, Bastida F, Alonso JL, Marquínez J, Aller J, Álvarez-Marrón J, Marcos A, Pulgar JA. (1988) A thin-skinned tectonic model for an arcuate fold and thrust belt: The Cantabrian Zone (Variscan Ibero-Armorican Arc). Tectonics 7:517–537. https://doi.org/10.1029/tc007i003p00517.

Pérez-Lorente F (1979) Geología de la Zona de Ossa-Morena al norte de Córdoba (Pozoblanco-Belmez-Villaviciosa de Córdoba). Tesis Doctorales de la Universidad de Granada 281:1–340.

Perret MF (1976) Une transgression dinantienne dans les Pyrénées occidentales: datation micropaléontologique et analogies. C R somm Soc géol Fr 6:257–259.

Perret MF (1985) La limite Mississipien-Pennsylvanien dans les Pyrénées françaises. In: Escobedo JL, Granados LF, Meléndez B, Pignatelli R, Rey R, Wagner RH (eds) 10th Int Congr Strat Geol Carbon Madrid 1983 vol. 4. Inst. Geol. Miner Esp, Madrid, pp 350–369

Perret MF (1993) Récherches micropaléontologiques et biostratigraphiques (Conodontes –Foraminifères) dans le Carbonifère pyrénéen. Strata 21, Toulouse.

Perret MF, Vachard D (1977) Algues et pseudo-algues des calcaires serpukhoviens d'Ardengost (Hautes-Pyrénées). Ann Paleont Invertébrés Paris 63:85–156.

Piçarra JM (2000) Stratigraphical study of the Estremoz-Barrancos sector, Ossa-Morena Zone, Portugal. Middle Cambrian?-Lower Devonian Lithostratigraphy and Biostratigraphy. PhD thesis, Univ Évora 268p.

Piçarra J, Gutierrez-Marco JC (1992) Estudo dos graptólitos Silúricos do flanco oriental do anticlinal de Moura – Ficalho (Sector de Montemor – Ficalho, Zona de Ossa – Morena, Portugal). Comun dos Servi Geol Portugal 78:23–29.

Piçarra JM and Rebelo J (1997) Novos dados bioestratigráficos para o conhecimento do Silúrico da região de Meirinhos – Lagoaça (Dominio do Douro Inferior, Nordeste de Portugal). XIV Reunião de Geol Oeste Peninsular, Univ Oviedo-UTAD, 189–191.

Piçarra JM and Sarmiento G (2006) Problemas de posicionamento estratigráfico dos Calcários Paleozóicos da Zona de Ossa Morena (Portugal). In: VII Congresso Nacional de Geologia II:657–660.

Piçarra JM, Le Menn J, Pereira Z, Gourvennec R, Oliveira JT, Robardet M (1999b) Novos dados sobre o Devónico inferior de Barrancos (Zona de Ossa Morena, Portugal). Temas Geológico--Mineros ITGE 26:628–631.

Piçarra JM, Gutiérrez-Marco JC, Sá AA, Meireles C, Clavijo E (2006) Silurian graptolite biostratigraphy of the Galicia-Tras-os-Montes Zone (Spain and Portugal). GFF/The Geological Society of Sweden Geologiske Föreningen/The Geological Society of Sweden, 128:185–188.

Pimentel N, Azevedo TM (1994) Etapas e controlo Alpino da Sedimentação na bacia do Sado (SW de Portugal). Cuad Lab Xeol de Laxe 19:229–238.

Pini GA (1999) Tectonosomes and olistostromes in the Argille Scagliose of the Northern Apennines, Italy: Geological Society of America Special Papers 335, 73 p

Pini GA, Lucente CC, Cowan DS, De Libero CM, Dellisanti F, Landuzzi A, Negri A, Tateo F, Del Castello M, Morrone M, and Cantelli L (2004) The role of olistostromes and argille scagliose in the structural evolution of the Northern Apennines. In: *Guerreri L, Rischia I, Serva L, (Eds.), Field Trip Guidebooks*. 32nd IGC Florence 20-28 August 2004. pp. 1-40

Pin C, Fonseca P, Paquette JL, Castro P, Matte Ph (2008) The ca. 350 Ma Beja Igneous Complex: A record of transcurrent slab break-off in the southern Iberia Variscan Belt? Tectonophysics 461:356–377. https://doi.org/10.1016/j.tecto.2008.06.001.

Pinto M, Andrade AAS (1987) Geocronologia dos granitóides da Zona de Ossa-Morena no contexto do Arco Ibero-Armoricano. Geociências 2:95–103.

Pinto de Jesus A (2001) Génese e Evolução da Bacia Carbonífera do Douro (Estefaniano C inferior, NW de Portugal); Um Modelo. 2 Volumes; Texto 232 pp., 4 anexos; Atlas 71 pp. Universidade do Porto. (Tese de Doutoramento).

Pinto de Jesus A (2003) Evolução sedimentar e tectónica da Bacia Carbonífera doDouro (Estefaniano C inferior, NW de Portugal). Cadernos. Laboratório Xeoloxico deLaxe, Coruña, 28: 107–125.

Pinto de Jesus A, Lemos de Sousa MJ (1998) Modelo deposicional da BaciaCarbonífera do Douro na região de Sete Casais (Sector NW do Sulco CarboníferoDúrico-Beirão). In: Actas do V Congresso Nacional de Geologia (Resumos Alargados), Lisboa, 1998. Comunicações do Instituto Geológico Mineiro, Lisboa, 84, 1: A-22-A25.

Popp et al. (1986) Popp BN, Anderson TF, Sandberg, PA (1986) Brachiopods as indicators of original isotopic compositions in some Paleozoic limestones. Geological Society of America Bulletin 97:1262–1269.

Poty E, Aretz M, Barchy L (2002) Stratigraphie et sédimentologie des "Calcaires à *Productus*" du Carbonifère inférieur de la Montagne Noire (Massif Central, France). C R Acad Sc Paris, Geosc 334:843–848.

Priem HNA, Boelrijk NAIM, Verschure RH, Hebeda EH, Verdurmen EAT (1970) Dating events of acid plutonism through the Paleozoic of the western Iberian Peninsula. Eclogae Geologicae Helvetiae 63:255–274.

Quarch H (1975) Stratigraphie und tektonik des Jungpalaozoikums im sattel von Montalban (Ostliche Iberische Kettn, NE-Spanien). Geol Jahrb 16:3–43.

Quesada C (1983) El Carbonífero de Sierra Morena. In: Martínez Díaz C (coord) Carbohífero y Pérmico de España, Instituto Geológico y Minero de España, Madrid, 244–278.

Quesada C (1990) Introduction of the Ossa-Morena Zone (part V). In: Dallmeyer RD, Martínez García E (eds), Pre-Mesozoic geology of Iberia, Springer-Verlag, Berlin, p 249–251.

Quesada C (1991) Geological constraints on the Paleozoic tectonic evolution of tectonostratigraphic terranes in the Iberian Massif. Tectonophysics 185:225–245.

Quesada C (2006) The Ossa-Morena Zone of the Iberian Massif: a tectonostratigraphic approach to its evolution. Z. dt. Ges. Geowiss. 157/4:585–595.

Quesada C, Dallmeyer RD (1994) Tectonothermal evolution of the Badajoz-Córdoba shear zone (SW Iberia): characteristics and 40Ar/39Ar mineral age constrains. Tectonophysics 231:195–213.

Quesada C, Garrote A (1983) Carboniferous Geology of the Sierra Morena. Guidebook of Field Trip D, 10th Int Caeboniferous Congr, Madrid, 104 p.

Quesada C, Robardet M, Gabaldón V (1990) Synorogenic Phase (Upper Devonian-Carboniferous-Lower Permian. In: Dallmeyer RD, Martínez García E (eds) Pre-Mesozoic geology of Iberia, Springer-Verlag, Berlin, 273–279.

Quesada C, Bellido F, Dallmeyer RD, Gil-Ibarguchi I, Oliveira JT, Pérez-Estaún A, Ribeiro A, Robardet M, Silva JB (1991) Terranes within the Iberian Massif: correlations with West African sequences. In: Dallmeyer RD, Lécorché JP (eds) The West African orogens and Circum-Atlantic correlatives, Springer, Berlin, 268–293.

Quesada C, Fonseca PE, Munhá J, Oliveira JT, Ribeiro A (1994) The Beja-Acebuches Ophiolite (Southern Iberia Variscan fold belt): geological characterization and geodynamic significance. Boletín Geológio y Minero 105:3–49.

Quiroga JL (1980) La sucesión silúrica en tierras de Aliste y Carbajales (Zamora). Cuad Lab Xeol Laxe 1:147–155.

Raymond D, Lethiers F (1990) Signification géodynamique de l'evénement radiolaritique dinantien dans les zones externes sud-varisques (Sud de la France et Nord de l'Espagne). C R Acad Sci Paris 310:1263–1269.

Requadt H, Becker G, Bless MJ, Eickoff G, Sanchez de Posada LC (1977) Microfaunen aus dem Westfal der Spanischen West-pyrenaen (Ostracoda, Conodonta, Foraminifera). N Jb Geol Palaont Abh 155:65–107.

Reuther CD (1977) Das Namur im südlichen Kantabrischen Gebirge (Nordspanien). Klustenbewegungen und Faziesdifferenzierung im Übergang Geosynklinale-Orogen. Clausthaler Geologische Abhandlunge, 28:1–122.

Ribeiro A (1974) Contribution à L'étude Tectonique de Trás-os-Montes Oriental. Serv Geol Portugal Memórias (Nova Série) 24:168 p.

Ribeiro A (1983) Relações entre formações do Devónico superior e o Maciço de Évora na região de Cabrela (Vendas Novas). Comun Serv Geol Portugal 69 (2):267–269.

Ribeiro A et al (1979). Introduction a la géologie du Portugal. Serv Geol Portugal. Lisboa.

Ribeiro A, Quesada C, Dallmeyer RD (1990) Geodynamic evolution of the Iberian Massif. In: Dallmeyer RD, Martínez García E (eds) Pre-Mesozoic Geology of Iberia. Berlin-Heidelberg-New York Springer-Verlag: 399–409.

Ribeiro A, Munhá J, Dias R, Mateus A, Pereira E, Ribeiro ML, Fonseca P, Araújo A, Oliveira JT, Romão J, Chaminé H, Coke C, Pedro J (2007) Geodynamic evolution of the SW Europe Variscides. Tectonics 26:TC6009. https://doi.org/10.1029/2006tc002058.

Ribeiro A, Munhá J, Fonseca P, Araújo A, Pedro JC, Mateus A, Tassinari C, Machado G, Jesus A (2010) Variscan ophiolite belts in the Ossa-Morena Zone (Southwest Iberia): Geological

characterization and geodynamic significance. Gondwana Research 17:408–421. https://doi.org/10.1016/j.gr.2009.09.005.
Ribeiro ML and Ribeiro A (1974) Signification paléogéographique et tectonique de la présence de galets de roches métamorphiques dans un flysch d'âge dévonien supérieur du Tras-Os-Montes oriental (Nord-Est du Portugal). C.R. Acad. Sc. Paris, Série D, 278:3161–3163.
Ribeiro ML, Mata J, Munhá J (1992) Magmatismo do Paleozóico Inferior em Portugal. In: Gutiérrez-Marco JC, Saavedra J, Rábano I (eds) Paleozoico Inferior de Ibero-América. Universidad de Extremadura, Cáceres, 377–395.
Riemer W (1963) Entwicklung des Paläozoikums in der Südlichen Provinz Lugo (Spanien). Neues Jarbuch für Geologie und Paläontologie, Abhandlungen 117: 273–85
Riemer W (1966) Datos para el conocimiento de la estratigrafía de Galicia. Notas y Comunicaciones del Instituto Geológico y Minero de España 81: 7–20
Ries AC, Shackleton RM (1971) Catazonal complexes of North-West Spain and North Portugal, renmants of an Hercynian thrust plate. Nature Physical Sciences 234:65–68.
Robardet M, Gutiérrez-Marco JC (1990) Passive margin phase (Ordovician-Silurian-Devonian). In: Dallmeyer RD, Martínez García E (eds) Pre-Mesozoic geology of Iberia, Springer-Verlag, Berlin, 249–251.
Robardet M, Gutiérrez-Marco JC (2002) Silurian. In: Gibbons W, Moreno MT (eds) The Geology of Spain. Geological Society, London, 51–66.
Robardet M, Gutiérrez-Marco JC (2004) The Ordovician, Silurian and Devonian sedimentary rocks of the Ossa-Morena Zone (SW Iberian Peninsula, Spain). J Iber Geol 30:73–92.
Robardet M, Weyant M, Laveine JP, Racheboeuf P (1986) Le Carbonifère inférieur du synclinal du Cerrón del Hornillo (Province de Séville, Espagne). Révue de Paléobiologie 5/1:71–90.
Robardet M, Weyant M, Brice D, Racheboeuf P (1988) Dévonien supérieur et Carbonifère inférieur dans le nord de la province de Séville (Espagne).Âge et importance de la première phase hercynienne dans la zone d'Ossa-Morena. CR Acad Sci Paris, Série II, 307:1091–1095
Roberts D (2003) The Scandinavian Caledonides: Event chronology, palaeo-geographic settings and likely modern analogues. Tectonophysics 365:283–299. https://doi.org/10.1016/S0040-1951(03)00026-X.
Roberts D, Siedlecka A (2002) Timanian orogenic deformation along the northeastern margin of Baltica, northwest Russia and northeast Norway, and Avalonian–Cadomian connections. Tectonophysics 352:169–184. https://doi.org/10.1016/S0040-1951(02)00195-6.
Rocci G, Bronner G, Deschamps M (1991) Crystalline basement of the West African craton. In: Dallmeyer, RD, Lecorché JP (eds) The West African Orogens and Circum-Atlantic Correlatives. Springer, Berlin, 31–61.
Rocha-Campos AC, Canuto JR, dos-Santos PR (2000) Late Paleozoic glaciotectonic structures in northern Parana Basin, Brazil. Sedimentary Geology 130:131–143.
Rodrigues B, Chew DM, Jorge RCGS, Fernandes P, Veiga-Pires C, Oliveira JT (2015) Detrital zircon geochronology of the Carboniferous Baixo Alentejo Flysch Group (South Portugal); Constraints on the provenance and geodynamic evolution of the South Portuguese Zone, J Geol Soc London 172:294–308. https://doi.org/10.1144/jgs2013-084.
Rodríguez S (1996) Development of coral reef-facies during the Visean at Los Santos de Maimona, SW Spain. In: Strogen P, Somerville ID, Jones GLL (eds) Recent Advances in Lower Carboniferous Geology, Geological Society Special Publication 107:145–152.
Rodríguez S (2014) Los Santos de Maimona: un arrecife del Carbonífero. Rev R Soc Esp Hist Nat, 2ª época, 12:73–81.
Rodríguez S, Falces S (1994) Coral distribution patterns in the Los Santos de Maimona Lower Carboniferous Basin (Badajoz, SW Spain). Cour Forsch-Inst Senckenberg 172:193–202.
Rodríguez S, Sánchez-Chico F (1994) Bioconstrucciones de corales rugosos y algas calcáreas de la sección del Torreón (Visean, Badajoz). Coloquios de Paleontología 46:61–76.
Rodríguez S, Arribas ME, Comas-Rengifo MJ, de la Peña JA, Falces S, Gegúndez P, Martínez Chacón ML, Moreno-Eiris E, Perejón A, Sánchez JL, Sánchez Chico F (1992) Estratigrafía. In: Rodríguez S (ed) Análisis Paleontológico y Sedimentológico de la cuenca carbonífera de Los Santos de Maimona (Badajoz), Coloquios de Paleontología 44:23–48.
Rodríguez S, Fernández-Martínez E, Cózar P, Valenzuela-Ríos JI, Liao J-Ch, Pardo MV, May A (2007) Emsian reefal development in Ossa-Morena Zone (SW Spain): Stratigraphic succession, microfacies, fauna and depositional environment. In: Abstracts of the X Internacional Congress on Fossil Cnidaria and Porifera, Saint Petersburg, 76–77.
Rodríguez Fernandez LR (1994) La estratigrafía del Paleozoico y estructura de la Región de Fuentes Carrionas y áreas adyacentes (Cordillera Cantábrica, NO de España): Laboratorio Xeolóxico de Laxe, Ediciós do Castro. Sada. A Coruña, 240 p.
Rodríguez-Martínez M (2005) Las bioconstrucciones viseenses de tipo mudmound del Área del Guadiato (Córdoba, SO de España). PhD thesis, Univ Complutense Madrid, 286 p.
Rodríguez-Martínez M, Moreno González I, Rodríguez S, Mas R (2000) Sedimentación de plataforma interna-externa con desarrollo de montículos en el Viseense del sector central de la Sierra de la Estrella (Carbonífero, Córdoba). Coloquios de Paleontología 51:9–33.
Rodríguez-Martínez M, Moreno-González I, Mas R, Reitner J (2012) Paleoenvironmental reconstruction of microbial mud mound derived boulders from gravity-flow polymictic megabreccias (Visean, SW Spain). Sedimentary Geology 263–264:157–173.
Roldán García FJ (1983) La cuenca Tournaisiense de Valdeinfierno. Interpretación tectónica y paleoambiental (Córdoba, España). In: Lemos de Sousa MJ (ed) Contributions to the Carboniferous geology and paleontology of the Iberian Peninsula. Uni. Porto, 41–50.
Roldán García FJ, Rodríguez Fernández J (1986–1987) La cuenca carbonífera de Valdeinfierno (Dominio de Sierra Albarrana, Zona de Ossa-Morena). Un ejemplo de sedimentación relacionada con accidentes de desgarre. Acta Geológica Hispánica 21–22:321–327.
Romariz, C. (1969) Graptolitos Silúricos do Noroeste Peninsular. Institution of Minig and Metallurgy, The Mineralogical Society. Com Serv Geol Portugal 53:107–156.
Rosa D, Finch A, Andersen T, Inverno C (2009) U-Pb geochronology and Hf isotope ratios of magmatic zircons from the Iberian Pyrite Belt. Mineralogy and Petrology 95/1–2:47–69. https://doi.org/10.1007/s00710-008-0022-5.
Rosas F (2003) Estudo Tectónico do Sector de Viana do Alentejo – Alvito: Evolução Geodinâmica e Modelação Analógica de Estruturas em Afloramentos Chave. PhD thesis, Lisbon Univ, 345p.
Rosas F, Marques FO, Ballèvre M, Tassinari C (2008) Geodynamic evolution of the SW Variscides: Orogenic collapse shown by new tectonometamorphic and isotopic data from western Ossa-Morena Zone, SW Iberia. Tectonics 27:TC6008. https://doi.org/10.1029/2008tc002333.
Rosell J, Llompart C (2002) El naixement d'una illa. Menorca. Guia de geologia pràctica. Dacs, Indústria Gràfica, Moncada i Reixac.
Rubio Pascual FJ, Matas J, Martín Parra LM (2013) High-pressure metamorphism in the Early Variscan subduction complex of the SW Iberian Massif. Tectonophysics 592:187–199. https://doi.org/10.1016/j.tecto.2013.02.022.
Sadowski G, Bettencourt J (1996) Mesoproterozoic tectonic correlations between eastern Laurentia and the western border of the Amazon craton. Precambrian Research 76:213–227. https://doi.org/10.1016/0301-9268(95)00026-7.
Saéz A, Anadón P (1989) El Complejo Turbidítico del Carbonífero del Priorato (Tarragona). Acta Geol Hisp 24:33–47.

Salman K (2004) The timing of the Cadomian and Variscan cycles in the Ossa-Morena Zone, SW Iberia: granitic magmatism from subduction to extension. Journal of Iberian Geology 30:119–132.
Salvador CI (1993) La sedimentación durante el Westfaliense en una cuenca de antepaís (Cuenca Carbonífera Central de Asturias, N de España). Trabajos de Geología, Univ Oviedo 9:195–264.
Sánchez de Posada LC, Martínez Chacón ML, Villa E, Menéndez CA (2002) The Carboniferous succession of the Asturian-Leonese Domain. In: García-López S, Bastida F (eds) Palaeozoic conodonts from northern Spain. Cuadernos del Museo Geominero 1:125–161.
Sánchez-García T, Bellido F, Quesada C (2003) Geodynamic setting and geochemical signatures of Cambrian-Ordovician rift-related igneous rocks (Ossa-Morena Zone, SW Iberia). Tectonophysics 365:233–255.
Sánchez Carretero R, Carracedo M, Gil Ibarguchi JI, Ortega LA, Cuesta A (1989) Unidades y datos geoquímicos del magmatismo hercínico de la Aliceación Villaviciosa de Córdoba-La Coronada (Ossa Morena oriental. Stvdia Geologica Salmanticensia 4: 105–130.
Santos JF, Mata J, Gonçalves F, Munhá J (1987) Contribuição para o conhecimento geológico-petrológico da região de Santa Susana: o Complexo Vulcano-Sedimentar da Toca da Moura. Comun Serv Geol Portugal 73:29–48.
Santos JF, Andrade A, Munhá J (1990) Magmatismo orogénico varisco no limite meridional da Zona de Ossa-Morena. Comun Serv Geol Portugal 76:91–124.
Santos JF, Mata J, Ribeiro S, Fernandes J, Silva J (2013) Sr and Nd isotope data for arc-related (meta) volcanics (SW Iberia). Goldschmidt Conference Abstracts, 2132.
Sanz-López J (1992) Caracterización del límite entre la sedimentación carbonática y los depósitos siliciclásticos del Carbonífero inferior en la Unidad de la Tosa d'Alp (Pirineo Oriental). III Congr Geol Esp/VIII Congr Latinoamer Geol, Salamanca 2:186–195.
Sanz-López J (1995) Estratigrafía y bioestratigrafía (Conodontos) del Silúrico superior–Carbonífero inferior del Pirineo Oriental y Central. PhD thesis, Univ Barcelona.
Sanz-López J (2002) Devonian and Carboniferous pre-Stephanian rocks from the Pyrenees. In: García-López S, Bastida F (eds) Paleozoic conodonts from northern Spain. 8th International Conodont Symposium held in Europe. Cuadernos Museo Geominero 1:367–389.
Sanz-López J (2004) Silúrico, Devónico y Carbonífero pre- y sin-varisco en Geología de los Pirineos. In: Vera JA (ed.) Geología de España. SGE-IGME, Madrid, 250–254.
Sanz-López J, Blanco-Ferrera S (2012a) Lower Bashkirian conodonts from the Iraty Formation in the Alduides-Quinto Real Massif (Pyrenees, Spain). Geobios 45:397–411.
Sanz-López J, Blanco-Ferrera S (2012b) Revisión estratigráfica del Misisipiense al Pensilvaniense más bajo de la zona Cantábrica y la posición de los límites entre los pisos. Geo-Temas 13:90 (annexed CD: 163–166).
Sanz-López J, Blanco-Ferrera S (2013) Early evolution of Declinognathodus close to the Mid-Carboniferous boundary interval in the Barcaliente type section (Spain). Palaeontology 56:927–946.
Sanz-López J, Melgarejo JC, Crimes PT (2000) Stratigraphy of Lower Cambrian and unconformable Lower Carboniferous beds from the Valls unit (Catalonian Coastal Ranges). C R Acad Sci Paris 330:147–153.
Sanz-López J, Vachard D, Perret MF (2005) Foraminifers and algae from the reworked late Viséan limestones of the Bellver Formation, eastern Pyrenees, Spain. Ann Soc Geol Nord 12:47–61.
Sanz-López J, Perret MF, Vachard D (2006) Silurian to Mississipian series of the eastern Catalan Pyrenees (Spain), updated by conodonts, foraminifers and algae. Geobios 39:709–725.
Sanz-López J, Blanco-Ferrera S, Sánchez de Posada LC, García-López S (2007) Serpukhovian conodonts from Northern Spain and their biostratigraphic application. Palaeontology 50:883–904.
Sarmiento GN, Calvo AA, González Clavijo E (1997) Conodontos paleozoicos (Ashgill-Emsiense) del Sinforme de Alcañices (Oeste de Zamora, España). In: Grandal D'Anglade, A, Gutiérrez-Marco JC, Santos Fidalgo L (eds). Paleozoico Inferior del Noroeste de Gondwana, 108–111.
Savage JF (1961) The structural geology of the area round Portilla de la Reina, León, Northwest Spain. PhD thesis, Univ London.
Schermerhorn LJG (1971) An outline stratigraphy of the Iberian Pyrite Belt. Boletín Geológico Minero 82:239–268.
Schermerhorn LJG, Kotsch S (1984) First occurrence of lawsonite in Portugal and tectonic implications. Comunicações do Instituto Geológico e Mineiro 70:23–29.
Schermerhörn LJG, Stanton WI (1969) Folded overthrust at Aljustrel (South Portugal). Geological Magazine 106:130–141.
Schindewolf OH (1934) Über zwei jungpaläozoische Cephalopodenfaunen von Menorca. Abh Ges Wiss Göttingen, Math-Phys K III 10:159–191.
Schindewolf OH (1958) Über eine Namur·Fauna von Menorca. N Jb Geol Palaontol Mh 1:1–8.
Schmidt H (1931) Das Paläozoikum der spanischen Pyrenäen. Abh Ges Wiss K 3 5, Göttingen.
Schumann K, Martinez Catalán J, Lardeaux JM, Janousek V, Oggiano G (2014) The Variscan Orogen: extend, timescale and formation of the European crust. Geol Soc London, Spec Pub 405: 1–6.
Scotese CR (2000) The Paleomap Project. www.scotese.com/late.hmt.
Scotese CR (2004) A continental drift flipbook. Journal of Geology 112:729–741.
Scotese CR, MacKinnon DL, Marlatt JR, Reilly WJ, Smith AG, Stanford BD (1994) Continental Drift, 6th Ed. The PALEOMAP Project, 75 p.
Shaw J, Gutiérrez-Alonso G, Johnston ST, Pastor Galán D (2014) Provenance variability along the Early Ordovician north Gondwana margin: Paleogeographic and tectonic implications of U-Pb detrital zircon ages from the Armorican Quartzite of the Iberian Variscan belt. Geological Society of America Bulletin 126:702–719. https://doi.org/10.1130/b30935.1.
Sierra S (2003) Análisis estratigráfico de la cuenca pérmica del Viar. PhD thesis, Univ Huelva.
Sierra S, Moreno C (1997) La cuenca Pérmica del río Viar, SO de España: análisis petrográfico de las areniscas. Cuad Geol Ibérica 22:447–472.
Sierra S, Moreno C (1998) Arquitectura fluvial de la cuenca Pérmica del Viar (Sevilla, SO de España). Rev Soc Geol España 11/3–4:197-212.
Sierra S, Moreno C, Pascual E (2009) Stratigraphy, petrography and dispersion of the lower Permian syn eruptive deposits in the Viar Basin, Spain. Sedimentary Geology 217:1–29.
Silva JB, Pereira MF (2004) Transcurrent continental tectonics model for the Ossa-Morena Zone Neoproterozoic-Paleozoic evolution, SW Iberian Massif, Portugal. International Journal of Earth Sciences (Geol Rundsch) 93:886–896. https://doi.org/10.1007/s00531-004-0424-5.
Silva JB, Oliveira JT, Ribeiro A (1990) The South Portuguese Zone. Structural Outline. In: Dallmeyer RD, Martínez E (eds) Pre-Mesozoic Geology of Iberia. Springer, Berlin, 334–362.
Silva JC, Mata J, Moreira N, Fonseca PE, Jorge, RCGS, Machado G (2011) Evidence for a Lower Devonian subduction zone in the southeastern boundary of the Ossa-Morena-Zone. In: Absctracts of the VIII Congresso Ibérico de Geoquímica, Castelo Branco, 295–299.
Simancas JF (1983) Geología de la extremidad oriental de la Zona Sudportuguesa. PhD Thesis University of Granada, Spain.
Simancas JF (1985) Estudio estratigráfico de la cuenca del Viar. Temas Geol Min IGME 5:7–17.
Simancas JF, Rodríguez Gordillo JF (1980) Magmatismo basáltico hercínico tardío en el SW de Sevilla. Cuad Geol Univ Granada 11:49–60.
Simancas JF, Broutin J, Gabaldón V (1983) The Autunian of the Viar area. In: Quesada C, Garrote A (eds) Carboniferous Geology of the

Sierra Morena. Guidebook of Field Trip D, 10th Int Carboniferous Congr, Madrid, 86–95.
Simancas JF, Tahiri A, Azor A, González Lodeiro F, Martínez Poyatos D, El Hadi H (2005) The tectonic frame of the Variscan-Alleghanian Orogen in Southern Europe and Northern Africa. Tectonophysics 398:181–198. https://doi.org/10.1016/j.tecto.2005.02.006.
Sjerp N (1967) The geology of the San Isidro-Porma area (Cantabrian Mountains, Spain). Leidse Geologische Mededelingen 39:55–128.
Slack JF, Kelley KD, Anderson VM, Clark JL, Ayuso RA (2004) Multistage hydrothermal silicification made Fe-Tl-As-Sb-Ge-REE enrichment in the Red Dog Zn-Pb-Ag district, northern Alaska: Geochemistry, origin, and exploration applications. Economic Geology 99:1481–1508.
Smith AJ (1963) Evidence for a Talchir (lower Gondwana) glaciation; striated pavement and boulder bed at Irai, central India. Journal of Sedimentary Petrology 33:739–750.
Somerville ID, Cózar P, Said I, Vachard d, Medina-Varea P, Rodríguez S (2013) Palaeobiogeographical constraints on the distribution of foraminifers and rugose corals in the Carboniferous Tindouf Basin, South Morocco. J Palaeogeogr 2:1–18.
Stampfli GM, Borel GD (2004) The TRANSMED Transects in Space and Time: Constraints on the Paleotectonic Evolution of the Mediterranean Domain. In: Cavazza W, Roure F, Spakman W, Stampfli GM, Ziegler P (eds) The TRANSMED Atlas: the Mediterranean Region from Crust to Mantle. Springer Verlag 53–80 (and CD ROM).
Stampfli GM, von Raumer JF, Borel GD (2002) Paleozoic evolution of pre-Variscan terranes: from Gondwana to the Variscan collision. In: Martínez Catalán JR, Hatcher RD, Arenas R, Díaz García F (eds) Variscan-Appalachian dynamics: the building of the Late Paleozoic basement. Geological Society of America, Special Papers 364:263–280.
Stampfli GM, Hochard C, Vérard C, Wilhem C, vonRaumer J (2013) The formation of Pangea. Tectonophysics 593:1–19. https://doi.org/10.1016/j.tecto.2013.02.037.
Starmer IC (1993) The Sveconorwegian orogeny in southern Norway, relative to deep crustal structures and events in the North Atlantic Proterozoic supercontinent. Norsk Geologisk Tidsskrift 73:109–132.
Stewart SA (1995) Paleomagnetic analysis of fold kinematics and implications for geological models of the Cantabrian/Asturian arc, north Spain. Journal of Geophysical Research: Solid Earth 100:20079–20094.
Stone P, Thomson MRA (2005) Archaeocyathan limestone blocks of likely Antarctic origin in Gondwanan tillite from the Falkland Islands. In: Vaughan APM, Leat PT, Pankhurst RJ (eds) Terrane processes at the margins of Gondwana. Geological Society Special Publications 246:347–357.
Talens J, Wagner RH (1995) Stratigraphic implications of late Carboniferous and early Permian megafloras in Lérida, south-central Pyrenees; comparison with the Cantabrian Mountains. Coloquios Paleontol 47:177–192.
Taylor S, McLennan S (1985) The Continental Crust: Its Composition and Evolution. Balckwell, Oxford. 312 p.
Teixeira C (1944). O Antracolítico continental português (Estratigrafia e Tectónica). Porto. (Tese de doutoramento).
Teixeira C (1951) Notas sobre a geologia da região de Barrancos, e em especial sobre a sua flora de Psilofitíneas. Com Serv Geol Portugal 32: 75–84.
Teixeira C (1954) Notas sobre Geologia de Portugal. O Sistema Permo-Carbónico. Lisboa.
Teixeira C, Pais J (1973) Sobre a presença de devónico na região de Bragança (Guadramil e Mofreita) e de Alcañices (Zamora). Bol Soc Geol Port XVIII: 199–200.
Teixeira W, Tassinari CCG, Cordani UG, Kawashita K (1989) A review of the geochronology of the Amazon craton: Tectonic implications. Precambrian Research 42:213–227. https://doi.org/10.1016/0301-9268(89)90012-0.
Torsvik TH, Cocks LRM (2004) Earth geography from 400 to 250 Ma: a paleomagnetic, faunal and facies review. Journal of the Geological Society of London 161:555–572.
Torsvik TH, Cocks LRM (2013a) Gondwana from top to base in space and time. Gondwana Research 24:999–1030. https://doi.org/10.1016/j.gr.2013.06.012.
Torsvik TH, Cocks LRM (2013b) New global palaeogeographical reconstructions for the Early Palaeozoic and their generation. In: Harper DAT, Servais T (eds) Early Palaeozoic Biogeography and Palaeogeography. Geological Society, London, Memoirs 38:5–24.
Torsvik TH, Cocks LRM (2017) Earth History and Palaeogeography, Cambridge University Press, 317 p., Cambridge.
Trosdtorf IJr, Rocha-Campos AC, dos-Santos PR, Tomio A (2005) Origin of late Paleozoic, multiple, glacially striated surfaces in northern Parana Basin (Brazil); some implications for the dynamics of the Parana glacial lobe. Sedimentary Geology 181:59–71.
Truyols-Massoni M, Quiroga JL (1981) Tentaculites dacrioconáridos en el Sinforme de Alcañices (Prov. de Zamora). Cuad Lab Xeol Laxe 2/1:171–173.
Vachard D, Delvolvé JJ, Hansotte M (1991) Foraminifères, algues et pseudo-algues du Serphoukhovien du massif de l'Arize (Carbonifère inférieur des Pyrénées). Geobios 24:251–256.
Vachard D, Cózar P, Aretz M, Izart A (2016) Late Viséan–Serpukhovian foraminifers in the Montagne Noire (France): Biostratigraphic revision and correlation with the Russian substages. Geobios 49:469–498.
Valle Aguado B, Azevedo M, Gonçalves R (2013) A sedimentação carbonífera na Bacia do Buçaco (Centro de Portugal). In: R. Dias, A. Araújo, P. Terrinha, J.C. Kullberg (Eds) Geologia de Portugal, Volume I, Escolar Editora, Lisboa, 259–274.
Van Adrichem Boogaert HA (1967) Devonian and Lower Carboniferous conodonts of the Cantabrian Mountains (Spain) and their stratigraphic application. Leidse Geologische Mededelingen 39:129–192.
Van der Kooij B, Immenhauser A, Steuber T, Hagmaier M, Bahamonde JR, Samankassou E, Merino Tomé O (2007) Marine Red Staining of a Pennsylvanian Carbonate Slope: Environmental and Oceanographic Significance. Journal of Sedimentary Research 77:1026–1045. https://doi.org/10.2110/jsr.2007.092.
Van der Voo R, Stamatakos JA, Parés JM (1997) Kinematic constraints on thrust- belt curvature from syndeformational magnetizations in the Lagos del Valle Syncline in the Cantabrian arc, Spain. Journal of Geophysical Research 102:10105–10120.
Van Ginkel AC (1965) Carboniferous fusulinids from the Cantabrian Mountains (Spain). Leidse Geologische Mededelingen 34:1–225.
Van Veen J (1965) The tectonic and stratigraphic history of the Cardaño area, Cantabrian Mountains, Northwest Spain. Leidse Geologische Mededelingen 35:43–103.
Veizer J, Ala D, Azmy K, Bruckschen P, Buhl D, Bruhn F, Carden GAF, Diener A, Ebneth S, Godderis Y, Jasper T, Korte C, Pawellek F, Podlaha OG, Strauss H (1999) 87Sr/86Sr, δ13C and δ18O evolution of Phanerozoic seawater. Chem Geol 161:59–88. https://doi.org/10.1016/S0009-2541(99)00081-9.
Vera JA (ed) (2004) Geología de España. SGE-IGME, Madrid.
Villa E, Escuder J, van Ginkel AC (1996) Fusulináceos y edad de los afloramientos carboníferos de Puig Moreno (Cordillera Ibérica, Teruel, España). Rev Esp Paleontol 11:207–215.
Wagner RH (1955) Rasgos estratigráfico-tectónicos del Paleozoico Superior de Barruelo (Palencia): Estudios Geol XI/26:145–202.
Wagner RH (1971a) The stratigraphy and structure of the Ciñera-Matallana Coalfield (Prov. León, NW Spain). Trabajos de Geología, Univ Oviedo 4:385–429.
Wagner RH (1971b) Carboniferous nappe structures in northeastern Palencia (Spain). Trabajos de Geología, Univ Oviedo 4:431–459.
Wagner RH (1978) The Valdeinfierno sequence (prov. Córdoba): its tectonic, sedimentary and floral significance. Ann Soc Géol Nord 98:59–66.

Wagner RH (1983) The Stephanian B of Puertollano. In: Quesada C, Garrote A (eds) Carboniferous Geology of the Sierra Morena. Guidebook of Field Trip D, 10th Int Carboniferous Congr, Madrid, 16–22.

Wagner RH (1985) Upper Stephanian stratigraphy and palaeontology of the Puertollano basin, Ciudad Real, Spain. In: Lemos de Sousa MJ (ed) Contributions to the Carboniferous Geology and Palaeontology of the Iberian Peninsula. Universidade do Porto-Faculdade de Ciencias, 51–67.

Wagner RH (1999) Peñarroya, a strike-slip controlled basin of early Westphalian age in Southwest Spain. Bulletin of the Czech Geological Survey 74:87–108.

Wagner RH (2004) The Iberian Massif: a Carboniferous assembly. Journal of Iberian Geology 30:93–108.

Wagner RH, Álvarez-Vázquez C (1991) Floral characterisation and biozones of the Westphalian D Stage in NW Spain. Neues Jahrbuch für Geologie und Palaöntologie, Abhandlungen 183:171–202.

Wagner RH, Álvarez-Vázquez C (1995) Upper Namurian/lower Westphalian of La Camocha, Asturias : Review of floral and faunal data. Coloquios de Paleontologia 47:151–176.

Wagner RH, Álvarez-Vázquez C (2010) The Carboniferous floras of the Iberian Peninsula: a synthesis with geological connotations. Rev Palaeobot Palynol 162:239–324.

Wagner RH, Castro MP (2011) Compositional changes in a mid-Stephanian (Kasimovian) flora in relation to alluvial plain deposits derived from westward-receding mountains and bordered by the paleotethys: La Magdalena Coalfield, northwestern Spain. Palaios 26:33–54.

Wagner RH, Jurado J (1988) Geología de la cuenca Carbonífera de Peñarroya y explotación de antracitas escondidas en un lentejón tectónico. In: VIII Congreso Internacional de Minería y Metalurgia, Instituto del Carbón de Oviedo, Oviedo, 225–241.

Wagner RH, Lemos de Sousa MJ (1983) The Carboniferous Megafloras of Portugal - A revision of identifications and discussion of stratigraphic ages. In: Lemos de Sousa MJ and Oliveira JT (Eds) The Carboniferous of Portugal. Memórias dos Serviços Geológicos de Portugal, Lisboa, 29: 127–152.

Wagner RH, Lemos de Sousa MJ, Gomes da Silva F (1983) Stratigraphy and fossil flora of the Upper Stephanian C of Buçaco, north of Coimbra (Portugal). In: M. J. Lemos de Sousa, Ed., Contributions to the Carboniferous Geology and Palaeontology of the Iberian Peninsula, p. 127–156. Universidade do Porto, Faculdade de Ciências, Mineralogia e Geologia, Porto.

Wagner RH, Mayoral EJ (2007) The Early Permian of Valdeviar in Sevilla province, SW Spain: basin history and climatic/palaeogeographic implications. J Iberian Geol 33:93–124.

Wagner RH, Wagner-Gentis CHT (1963) Summary of the stratigraphy of Upper Paleozoic rocks in NE Palencia, Spain. Proccedings Koninklijke Nederlandse Akademie van Wetenschappen B/66:149–163.

Wagner RH, Winkler Prins CF (1985a) Stratotypes of the lower Stephanian stages, Cantabrian and Barruelian. Compte Rendu X Congrès International de Stratigraphie et de Géologie du Carbonifère, Madrid 1983, 4:473–483.

Wagner RH, Winkler Prins CF, Riding RE (1971) Lithostratigraphic units of the lower part of the Carboniferous in Northern Leon, Spain. Trabajos de Geología, Univ Oviedo 4:603–663.

Wagner RH, Sánchez de Posada LC, Martínez Chacón ML, Fernández LP, Villa E, Winkler Prins CF (2002) The Asturian stage: a preliminary proposal for the definition of a substitute for Westphalian D. In: Hills LV, Henderson CM, Bamber EW (eds) Carbonifeorus and Permian of the World. Canadian Society of Petroleum Geologists 19:832–850.

Wallis R.J (1985) A lacustrine/deltaic/fluvial/swamp succession from the Stepahanian B of Puertollano, Spain. In: Lemos de Sousa M.J (ed) Contributions to the Carboniferous Geology and Palaeontology of the Iberian Peninsula. Universidade do Porto-Faculdade de Ciencias, 51–67.

Weil AB (2006) Kinematics of orocline tightening in the core of an arc: Paleomagnetic analysis of the Ponga Unit, Cantabrian Arc, northern Spain. Tectonics 25, TC3012:1–23. https://doi.org/10.1029/2005tc001861.

Weil AB, Van der Voo, R, van der Pluijm BA, Parés JM (2000) The formation of an orocline by multiphase deformation: a paleomagnetic investigation of the Cantabria-Asturias Arc (northern Spain). Journal of Structural Geology 22:735–756. https://doi.org/10.1016/s0191-8141(99)00188-1.

Weil AB, Van der Voo R, van der Pluijm BA (2001) Oroclinal bending and evidence against the Pangea megashear: The Cantabria-Asturias arc (northern Spain). Geology 29:991–994. https://doi.org/10.1130/0091-7613(2001)029%3c0991:obaeat%3e2.0.co;2.

Weil AB, Gutiérrez-Alonso G, Wicks D (2013a) Investigating the kinematics of local thrust sheet rotation in the limb of an orocline: a paleomagnetic and structural analysis of the Esla tectonic unit, Cantabrian–Asturian Arc, NW Iberia. International Journal of Earth Sciences 102:43–60. https://doi.org/10.1007/s00531-012-0790-3.

Weil AB, Gutiérrez-Alonso G, Johnston ST, Pastor-Galán D (2013b) Kinematic constraints on buckling a lithospheric-scale orocline along the northern margin of Gondwana: A geologic synthesis. Tectonophysics 582:25–49. https://doi.org/10.1016/j.tecto.2012.10.006.

Wendt J and Aigner T (1985) Facies patterns and depositional environments of Paleozoic cephalopod limestones. Sedimentary Geology 44:263–300.

Weyant M, Brice D, Racheboeuf PR, Babin C, Robardet M (1988) Le Dévonien supérieur du synclinal du Valle (province de Séville, Espagne). Revue de Paléobiologie 7/1:233–260.

Witzke BJ (1990) Palaeoclimatic constraints for Palaeozoic palaeolatitudes of Laurentia and Euramerica. In: McKerrow WS, Scotese CR (eds) Palaeozoic Palaeogeography and Biogeography. The Geological Society of London, Memoir 12:57–73.

Wronkiewkz DJ, Condie KC (1987) Geochemistry of Archean Shales from the Witwatersrand Supergroup, South-Africa - Source-Area Weathering and Provenance. Geochimica et Cosmochimica Acta 51:2401–2416.

Variscan Metamorphism

12

M. L. Ribeiro, J. Reche, A. López-Carmona, C. Aguilar, T. Bento dos Santos, M. Chichorro, Í. Dias da Silva, A. Díez-Montes, E. González-Clavijo, G. Gutiérrez-Alonso, N. Leal, M. Liesa, F. J. Martínez, A. Mateus, M. H. Mendes, P. Moita, J. Pedro, C. Quesada, J. F. Santos, A. R. Solá, and P. Valverde-Vaquero

Abstract

Various segments of Variscan crust are currently exposed in Iberia in response to successive tectonic events during the Variscan orogeny itself and subsequent extensional and compressive events during the Alpine cycle, all accompanied by surface erosion, and collectively contributing to their exhumation. We review the main characteristics and geodynamic contexts of the metamorphic complexes developed in Iberia during the Variscan cycle, which include: (i) LP-HT complexes associated to the Cambrian-Early Ordovician rift stage; (ii) HP-LT complexes associated to subduction; and (iii) syn-to-post-collisional, MP and LP/HT complexes from the hinterland to the foreland fold-and thrust belts. All the above contexts are illustrated with case studies. Finally, a review of Variscan metamorphism in the Pyrenees and Catalan Coastal Ranges, located far away from the Rheic suture is also presented.

Coordinators: M. L. Ribeiro, J. Reche, A. López-Carmona, C. Quesada.

M. L. Ribeiro (✉)
Serviços Geológicos de Portugal, Laboratório Nacional de Energia e Geologia (LNEG), Estrada da Portela, Bairro do Zambujal, Apartado 7586 Alfragide, 2610-999 Amadora, Portugal
e-mail: luisacarvalhoduarte@gmail.com

J. Reche · F. J. Martínez
Departament de Geologia, Facultat de Ciències, Universitat Autònoma de Barcelona, c/Vall Moronta s/n, 08193 Bellaterra (Barcelona), Spain
e-mail: joan.reche@uab.cat

F. J. Martínez
e-mail: francisco.martinez@uab.cat

A. López-Carmona · G. Gutiérrez-Alonso
Facultad de Ciencias, Área de Geodinámica Interna, Departamento de Geologia, Universidad de Salamanca, Plaza de la Merced s/n, 37008 Salamanca, Spain
e-mail: alioli@usal.es

G. Gutiérrez-Alonso
e-mail: gabi@usal.es

C. Aguilar
Centre for Lithospheric Research, Czech Geological Survey, Metamorphic Petrology and Geochronology, Klárov 3, 11821 Prague, Czech Republic
e-mail: carmen.gil@geology.cz

T. Bento dos Santos · Í. Dias da Silva · A. Mateus
Departamento de Geologia, Faculdade de Ciências, Instituto Dom Luiz (IDL), Universidade de Lisboa, Ed. C1, Piso 1, Campo Grande, 1749-016 Lisboa, Portugal
e-mail: tmsantos@fc.ul.pt

Í. Dias da Silva
e-mail: ipicaparopo@gmail.com

A. Mateus
e-mail: amateus@fc.ul.pt

M. Chichorro
Department of Earth Sciences, Faculty of Science and Technology, New University of Lisbon, Campus de Caparica, Quinta da Torre, 2829-516 Lisboa, Portugal
e-mail: ma.chichorro@fct.unl.pt

A. Díez-Montes · E. González-Clavijo
Instituto Geológico Minero de España (IGME), Oficina de Salamanca, Plaza de la Constitución, 1 - Planta 3ª, 37001 Salamanca, Spain
e-mail: al.diez@igme.es

E. González-Clavijo
e-mail: e.clavijo@igme.es

N. Leal
GeoBioTec and Departamento de Ciências da Terra, Faculdade de Ciências e Tecnologia, Universidade Nova de Lisboa, Qta da Torre, 2829-516 Costa da Caparica, Portugal
e-mail: n.leal@fct.unl.pt

M. Liesa
Departament de Mineralogia, Petrologia i Geologia Aplicada, Facultat de Ciències de la Terra, Universitat de Barcelona, Carrer Martí i Franquès, s/n, 08028 Barcelona, Spain
e-mail: mliesa@ub.edu

M. H. Mendes · J. F. Santos
Geobiotec, Departamento de Geociências da Universidade de Aveiro, 3810-193 Aveiro, Portugal
e-mail: mmendes@ua.pt

J. F. Santos
e-mail: jfsantos@ua.pt

C. Quesada and J. T. Oliveira (eds.), *The Geology of Iberia: A Geodynamic Approach*, Regional Geology Reviews,
https://doi.org/10.1007/978-3-030-10519-8_12

12.1 Introduction

A. López-Carmona, G. Gutiérrez-Alonso, J. Reche, M. L. Ribeiro, C. Quesada

Understanding global-scale orogenic processes related to the amalgamation (i.e. collision) and breakup (i.e. rifting) of supercontinents, and their relationship to the evolution of the Earth's lithosphere, is largely one of the main challenges for Earth scientists nowadays. Earth's lithosphere is constantly being reconfigured through a cyclical succession (spanning from 300–500 Ma) of tectonic regimes, which broadly involves rift/ocean realms, followed by passive margin environments and finally, subduction-collision settings.

The metamorphic record represents a fundamental source of information to understand the geodynamic evolution of an ancient orogen, as metamorphic rocks record information related to the thermal (variation of temperature -T- with time -t-) and burial/exhumation (variation of pressure -P- with t) evolution of the crust. Thus, metamorphic rocks provide key P–T–t data to parameterize orogenic processes and constrain geodynamic models (e.g. Brown 2014).

During the late Neoproterozoic through the Paleozoic, rocks currently making the basement of the Iberian Peninsula were involved in two important orogenic events: Cadomian and Variscan-Appalachian, separated by the pre-orogenic part of a new (Variscan) Wilson cycle. The Variscan cycle started with and important rifting event (Cambrian-Early Ordovician) that culminated in opening a new oceanic tract interpreted to be a part of the Rheic Ocean (Ribeiro 1987; Ribeiro et al. 1990b; Quesada 1991, 2006; Sánchez-García et al. 2003, 2008, 2010, 2016; Murphy et al. 2006; among others). This was followed by drifting apart of one or several ribbon-terranes, presumed to have later formed parts of the Avalonian terrane assemblage of Williams (1979) and Keppie (1985) or simply Avalonia, as currently used nowadays, whereas the Gondwanan counterpart inaugurated a passive margin stage that lasted until the onset of Variscan convergence in Lower Devonian times. This culminated in the amalgamation of Pangea after consumption of the Rheic and collision of Gondwana with Laurussia (see under Chap. 1 in this volume). Owing to this protracted history, the Iberian Variscan orogen is one of the key geological realms to study the latest Precambrian and Paleozoic evolution of the Earth (e.g. Ribeiro et al. 2007; Martínez Catalán et al. 2008; Romão et al. 2010).

The Cadomian orogeny, involving arc growth at the periphery of Gondwana and accretion to the continent, recorded the latest stages of the amalgamation of this large continent. Exposed evidence of the Cadomian orogen in Iberia is restricted to late, orogenic stages of the corresponding Wilson cycle, which is dealt with in Volume 1 of this publication.

The Iberian segment of the European Variscan fold belt shows a magnificent, almost complete space-temporal cross-section of the Variscan orogen (e.g. Julivert et al. 1980), which includes various exposures of the suture zone between Gondwana and Laurussia in the Iberian Massif. However, as described in Chap. 10 of this volume, two highly contrasting structural segments are to be distinguished within the Iberian Massif: (i) the NW Iberia segment, dominated by large-scale crustal imbrication, including on top a far-travelled, unrooted nappe pile which carries the Variscan suture (e.g. Ribeiro 1981; Iglesias et al. 1983; Martínez Catalán et al. 2009); and (ii) the SW Iberia segment, dominated by tectonic escape and left-lateral transpression processes (Quesada 2006; Ribeiro et al. 2010; Romão et al. 2010). This significant difference accounts for the very different burial/exhumation patterns in each segment and, as a consequence, the different P–T–t paths and apparent thermal gradients retrieved from the distinctive metamorphic rocks that crop out in each area.

Despite the existence of remarkable exhumation of the Variscan crust in response to both extensional (pre-orogenic) and compressional (syn-orogenic) events during the Alpine cycle, mainly in the Pyrenean and Betic orogens and in some intraplate uplifts (e.g. Central System), most of the exhumation of lower and middle crustal segments took place during the Variscan orogeny itself, mostly in the hinterland areas.

The Variscan cycle started with the undocking of Avalonia from the Gondwana margin during the late

P. Moita
HERCULES, Departamento de Geociências, Universidade de Évora, 7000-671 Évora, Portugal
e-mail: pmoita@uevora.pt

J. Pedro
Departamento de Geociências da Universidade de Évora, Instituto de Ciências da Terra, 7000-671 Évora, Portugal
e-mail: jpedro@uevora.pt

C. Quesada
Instituto Geológico Minero de España (IGME), c/ Ríos Rosas 23, 28003 Madrid, Spain
e-mail: quesada.cecilio@gmail.com

C. Quesada
Facultad de Ciencias Geológicas, Universidad Complutense de Madrid, Madrid, Spain

A. R. Solá
Laboratório Nacional de Energia e Geologia (LNEG), Unidade de Geologia, Hidrogeologia e Geologia Costeira, Estrada da Portela, Bairro do Zambujal, Apartado 7586 Alfragide, 2610-999 Amadora, Portugal
e-mail: rita.sola@lneg.pt

P. Valverde-Vaquero
Instituto Geológico Minero de España (IGME), C/ La Calera, 1, 28760 Tres Cantos (Madrid), Madrid, Spain
e-mail: p.valverde@igme.es

Cambrian-early Ordovician together with the aperture of the Rheic Ocean (e.g. Murphy et al. 2006). Extension related magmatism was widespread, although scarce evidences of coeval metamorphic events are recognized during this stage with the exception of the Ossa Morena Zone, where the combination of moderate post-rifting burial and less pervasive structural overprinting during the Variscan orogeny allowed preservation in some units of several migmatite domes, previously interpreted as either Cadomian or Variscan (Quesada and Munhá 1990; Ochsner 1993; Ordóñez Casado 1998; Ordóñez Casado et al. 1997), but recently dated as Cambrian in age, i.e. coeval to the massive rift-related magmatism preserved in this zone (Expósito et al. 2003; Salman 2004; Chichorro 2006; Sánchez-García et al. 2008, 2010, 2016; Azor et al. 2012, 2016).

The subsequent closure of the Rheic Ocean led to progressive amalgamation through the subduction of the oceanic lithosphere, together with the collision of the previously detached Gondwanan and peri-Gondwanan continental terranes and finally, of the Gondwana continental mainland with Laurentia-Baltica northern landmasses (Matte 2001). These processes concluded in the structuring of the Variscan collisional orogenic edifice that comprises a double-thickened crust in NW Iberia, thick crustal granulite roots and upper crustal low-grade units (e.g. Schulmann et al. 2014), like in modern orogens such as the Himalaya, with which many analogies have been found (Maierová et al. 2016).

As progressively younger tectonothermal events superimpose on the ancient ones, unraveling the details of the previous processes become more difficult and its current knowledge is rather discrete. Thus, the most complete metamorphic records recognized in Iberia are related to the latest Variscan cycle events. Each of these show different characteristics according to the location and timing of the different units involved in the Variscan collision during its development: (i) the units involved in the subduction of the Gondwana continental margin, together with the units corresponding to the upper plate (the so called allochthonous units) recorded high-pressure conditions and their subsequent exhumation, whereas (ii) the units that did not undergo subduction were affected by a typical record of orogenic Barrowian metamorphism followed by higher temperature episodes in the authochthonous and parauthochthonous units.

This chapter shows a descriptive synthesis of the most representative metamorphic events recorded in the Iberian Peninsula during the Variscan cycle beginning with the oldest ones, those related to the Cambro-Ordovician rifting stage which gave birth to the Rheic Ocean and the coeval evolution of the "exotic" upper allochthon units of the Galicia-Trás-os-Montes Zone (Sect. 12.2), following with the ones related to the earliest subduction beginning in Devonian times (Sect. 12.3) and the syn-collisional compressive-transpressive/transtensive events (Sect. 12.4) and finally, those related to gravity-driven collapse features that balanced the former tectonic architecture (Sect. 12.5).

For some of these stages case studies are presented in more detail to better illustrate the metamorphic evolution as well as the thermobaric behavior of different levels of the orogenic Variscan crustal section.

12.2 Cambrian-Early Ordovician Metamorphism

A. López-Carmona, C. Quesada, M. L. Ribeiro, A. Mateus

Recognition of the effects of metamorphic events older than the onset of the Variscan convergence is generally difficult and requires detailed metamorphic studies and profuse mineral age dating. In Iberia these conditions only exist in the case of the allochthonous nappes of the Galicia-Trás-os-Montes Zone. In the remaining areas, such recognition is only possible in those areas that were not affected by significant burial during the Paleozoic and/or that were not pervasively deformed during the Variscan orogeny. In this respect, two different geodynamic contexts must be considered: (i) the units forming the upper allochthon of the Galicia-Trás-os-Montes Zone, "exotic" at some extent since they override the ophiolites that make the intermediate allochthon, and (ii) the remaining units in Iberia, which show a Paleozoic evolution clearly linked to that of Gondwana (lower allochthon, parautochthon and autochthon in NW Iberia, the Ossa Morena Zone in SW Iberia and the basement exposed in the Alpine mountain ranges in E Iberia).

12.2.1 The Upper Allochthon of the Galicia-Trás-os-Montes Zone

A. López-Carmona

In the upper allochthon of NW Iberia, the oldest evidence of post-Cadomian geodynamic activity appears to represent an extension of the subduction process previously existing around Gondwana during the Neoproterozoic (Abati et al.

1999). The upper allochthonous units in NW Iberia are considered a single and coherent terrane because of its systematic position above the ophiolites (middle allochthon). Based on their tectonothermal evolution the upper allochthon is divided in two groups, the intermediate-pressure (IP) units and the high-pressure and high-temperature units, located structurally below.

According to Abati et al. (1999) a pre-Variscan orogeny tectonothermal event is recorded in the IP units of the upper allochthon. This metamorphism is related to the activity of a magmatic arc operating at ca. 500 Ma in an active part of the northern margin of Gondwana, and displays greenschist, amphibolite and/or granulite facies assemblages, characterized by an IP gradient. Rapid changes in metamorphic grade occur due to extensional detachments (Díaz García 1990; Abati 2002; Gómez-Barreiro et al. 2006; González-Cuadra 2007). The IP units comprise a thick terrigenous sequence of semipelitic-pelitic schists and paragneisses intruded by Cambro-Ordovician gabbros with island-arc tholeiitic affinity (Andonaegui et al. 2002), orthogneisses of granodioritic to tonalitic composition and calc-akaline granitoids (Díaz García 1990; Abati 2002; Castiñeiras et al. 2002). The highest structural levels consist of turbiditic successions that still preserve primary sedimentary structures (Betanzos, O Pino and Cariño units) affected by chlorite-zone low-grade metamorphism in the greenschists facies. Downward in the structural pile metamorphism reaches medium-grade in the almandine-sillimanite zones in amphibolite facies conditions (Corredoiras, O Pino and Cariño units), with regional development of kyanite pseudomorphs after andalusite that grew in a prograde counter-clockwise P–T path (O Pino unit; Castiñeiras 2005; Fig. 12.1), indicating a pressure increase downwards in the structural pile, together with widespread migmatization.

The lowest structural levels of the IP units (Monte Castelo and Corredoiras units) contain hectometric metapelitic xenoliths affected by high-temperature recrystallization during their assimilation by the gabbro body and were subsequently metamorphosed into IP granulites (ca. 800 °C and 0.95 GPa; Abati et al. 2003; Fig. 12.1) during the lower Ordovician (ca. 480–496 Ma; Abati et al. 2007). Granulite facies assemblage (spinel-garnet-orthopyroxene-cordierite-sillimanite-biotite; Monte Castelo unit) crystallized following a counter-clockwise metamorphic path (Abati et al. 2003; González Cuadra 2007; Fig. 12.1) with a first segment of high-temperature and low-pressure conditions interpreted to be related to magmatic underplating in the continental arc environment (e.g. Will and Schmädicke 2003), followed by a pressure increase linked to fore arc processes during continued subduction of the northern Iapetus Ocean. This is supported by the presence of thick garnet overgrowth rims, surrounding previous core domains, developed at higher temperatures and lower pressure conditions (Abati et al. 2003). The best outcrops are represented in Cabo Ortegal (Cariño unit), Ódenes and Morais complexes (Lagoa unit Figs. 12.1 and 12.2).

12.2.2 The Lower Allochthon of the Galicia-Trás-os-Montes Zone

A. López-Carmona

As for the other Gondwanan affinity units in Iberia, the geodynamic evolution during the Cambrian-lower Ordovician was dominated by a rifting event. In the lower allochthonous units of NW Iberia this is also characterized by a bimodal magmatism recorded by felsic orthogneisses alternating with amphibolites (Díez Fernández and Martínez Catalán 2009; Díez Fernández et al. 2011, 2012a; Ballèvre et al. 2014; Andonaegui et al. 2017), which compositions vary from tholeiite to alkali basalt (Marquínez 1984). Felsic orthogneisses comprise two different igneous associations, a calc-alkaline suite and an alkaline to peralkaline suite derived from mantellic A-type granitoids, possibly genetically linked to alkali basalts (Floor 1966; Ribeiro and Floor 1987; Ribeiro 1987; Pin et al. 1992; Montero 1993). Nonetheless, the most recent studies suggest that the calc-alkaline magmatic suite is ca. 20 Ma older (495–500 Ma) than the alkaline to peralkaline plutonic suite (dated at ca. 470–475 Ma; Santos Zalduegui et al. 1996; Rodríguez et al. 2007; Montero et al. 2009), and thus probably represents a distinct geologic event (Abati et al. 2010; Díez Fernández et al. 2012a). The maximum depositional age and provenance of the metasediments intruded by the magmatic suites suggest a Neoproterozoic/Cambro-Ordovician peripheral Gondwanan subduction/arc setting (Díez Fernández et al. 2010; Fuenlabrada et al. 2012; Puelles et al. 2017). The largest exposures that record this event crop out in the Malpica-Tui Complex (Malpica unit; Figs. 12.1 and 12.2). During the subsequent onset of the Variscan convergence both magmatic series were metamorphosed into the eclogite facies conditions (Rodríguez 2005; Abati et al. 2010; Puelles et al. 2017; see Sect. 12.3).

12.2.3 Rift-Related Metamorphism in the Autochthonous Iberian Massif

C. Quesada, M. L. Ribeiro, A. Mateus, A. López-Carmona, G. Gutiérrez-Alonso

Evidence of Cambro-Ordovician syn-rift metamorphism has been interpreted mainly from assemblages corresponding to

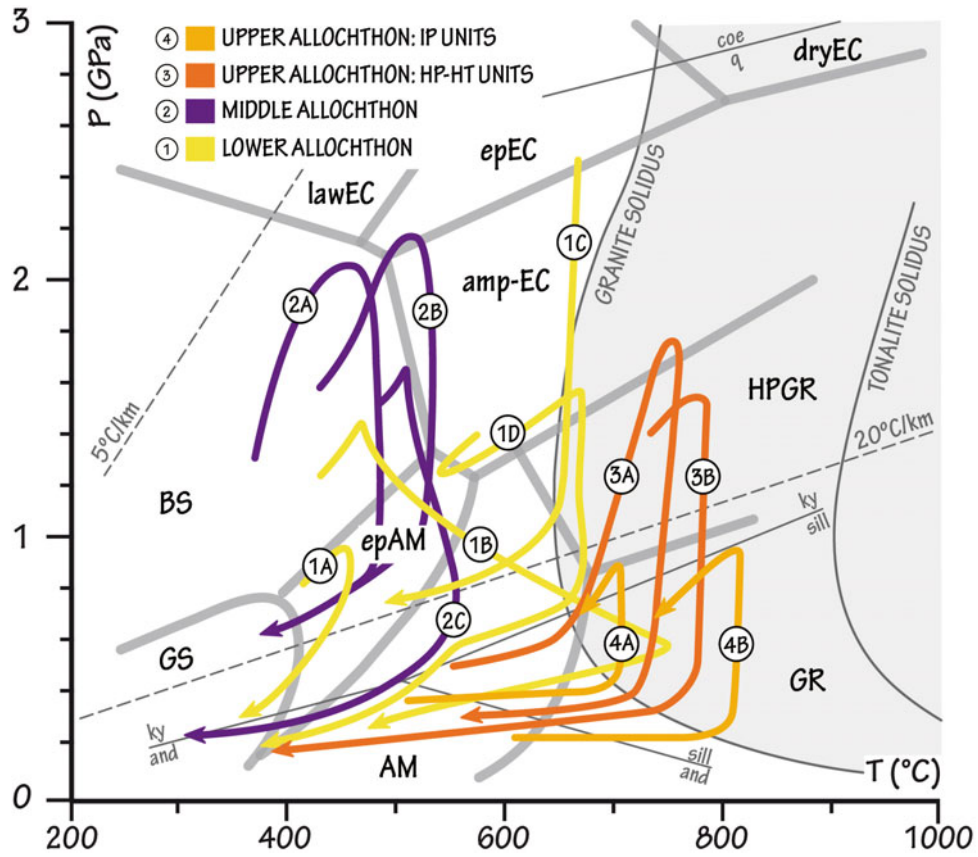

Fig. 12.1 Summary of the P–T paths recorded in the allochthonous units of the Galicia-Trás-os-Montes Zone (NW Spain). The lower and middle allochthons experienced monocyclic P–T paths with strong pressurization followed by an isothermal decompression (1A, Forcarei; 1B Lalín; 1C, Malpica; 1D, Agualada; 2A–B, Ceán and 2C, Lamas de Abad units). The upper allochthon records subduction-type paths in the high-pressure and high-temperature (HP-HT) units (3A, Sobrado and 3B, Fornás units) and anticlockwise paths comprising pressurization after strong heating in the IP (intermediate-pressure) units (4A, O Pino and 4B, Monte Castelo units). Modified from Ballèvre et al. (2014). Thick lines separate facies fields simplified after Spear (1993), Liou et al. (1998, 2009) and Okamoto and Maruyama (1999). Facies fields abbreviations: GS, greenschist facies; epAM, epidote-amphibolite facies; AM, amphibolite facies; BS, blueschist facies; lawEC, lawsonite-eclogite facies; epEC, epidote-eclogite facies; ampEC, amphibole-eclogite facies; dryEC, anhydrous eclogite facies; HPGR, high-pressure granulite facies; GR, granulite facies. Thin dashed lines represent geotherms of 5 and 20 °C/km. Al_2SiO_5 (Bohlen et al. 1991) and the minimum melting of granite and tonalite solidus (Huang and Wyllie 1975) are shown for reference. Modified from Ballèvre et al. (2014)

low-pressure and high-temperature regimes in contact metamorphic aureoles around intrusive bodies in the Central Iberian Zone (Rubio-Ordóñez et al. 2012) or as anchizonal during the Ordovician in the Cantabrian Zone (Keller and Krumm 1992). However, it is in the Ossa Morena Zone (OMZ) where recent dating and geochemical correlation of migmatite neosomes with nearby intrusive and volcanic rocks have demonstrated that several migmatite domes, previously considered as either Cadomian or Variscan, actually developed during the Cambrian-Early Ordovician rifting event (e.g. Montero et al. 1999, 2000; Expósito et al. 2003; Sánchez García et al. 2003, 2008, 2010, 2016; Salman 2004; Azor et al. 2012, 2016; Henriques 2013, Henriques et al. 2015, 2017).

Evidences of polymetamorphism in the OMZ are known since MacPherson (1879), Quesada and Munhá (1990), Ábalos (1990), Quesada (1997) and Eguiluz et al. (2000). Prior to publication of the recent age data referred to above most researchers interpreted the pre-Variscan metamorphism as related to the Cadomian orogeny, and a compilation of evidences for Precambrian metamorphic complexes can be found in Quesada and Munha (1990) and Quesada (1997). Furthermore, presence of two major tectono-metamorphic episodes during the Cadomian cycle was described by Eguiluz and Ábalos (1992). Although Cadomian metamorphism can be proven in some OMZ areas, many of the previously considered as such, especially those recording LP-HT regimes must now be reinterpreted in connection to

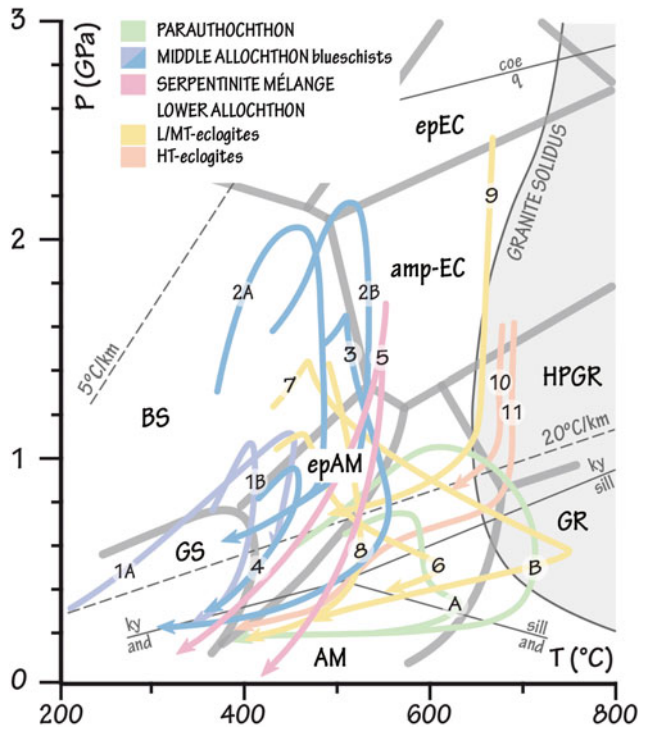

Fig. 12.2 P–T diagram showing the tectonometamorphic evolution recorded by several units from the lower and middle allochthonous terranes, and by the high-pressure blocks of the Somozas Mélange in the NW Iberian Massif. In the middle allochthon: 1A–B, basal unit of the NW Morais Complex from Gil Ibarguchi and Dallmeyer (1991) and Balcázar et al. (2005), respectively; 2A–B, Ceán unit (López-Carmona et al. 2013, 2014); 3, Lamas de Abad unit; 4, Forcarei unit (basal zone); 5, Somozas serpentinite Mélange (Novo-Fernández et al. 2016). In the lower allochthon: 6, Forcarei unit (upper zone); 7, Lalín unit; 8, Santiago unit (Rubio Pascual et al. 1993); 9, Malpica unit (López--Carmona et al. 2013); 10, Espasante unit (Arenas 1988, 1991); 11, Agualada unit (Abati 1994). Based on Martínez Catalán et al. (1996) and López-Carmona (2015). P–T paths for the (A) upper zone and (B) basal migmatitic zone of the parauthocthon in the Malpica-Tui Complex are also indicated (modified from Díez Fernández 2011). Thick lines separate facies fields simplified after Spear (1993), Liou et al. (1998, 2009) and Okamoto and Maruyama (1999). Facies fields abbreviations: GS, greenschist facies; epAM, epidote-amphibolite facies; AM, amphibolite facies; BS, blueschist facies; lawEC, lawsonite-eclogite facies; epEC, epidote-eclogite facies; ampEC, amphibole-eclogite facies; HPGR, high-pressure granulite facies; GR, granulite facies. Thin dashed lines represent geotherms of 5 and 20 °C/km. Al_2SiO_5 (Bohlen et al. 1991) and the minimum melting of granite solidus (Huang and Wyllie 1975) are shown for reference

the Cambrian-Early Ordovician rifting event that inaugurated the Variscan cycle. Proven Cambrian-Ordovician metamorphic complexes are known along three different locations within the OMZ: (1) a series of migmatite domes developed after Neoproterozoic Serie Negra protoliths roughly aligned along the core of the Variscan Monesterio antiform in the central OMZ (Valuengo, Monesterio and Lora del Río); (2) within the inner core of the Badajoz-Córdoba shear zone (Central Unit of Azor 1994): Mina Afortunada migmatite dome, also developed after Serie Negra protoliths, and SE of Abrantes (see below under Sect. 12.2.3.4 for a detailed description); and (3) the Sierra Albarrana metamorphic complex, south of the Badajoz-Córdoba shear zone, and developed after Sierra Albarrana domain protoliths. Probably, other metamorphic complexes with similar characteristics within the OMZ or elsewhere (e.g. Sierra de Guadarrama; Talavera et al. 2012, 2013) may have had a similar origin but the lack of geochronological evidence and/or a severe Variscan tectonothermal overprint prevent proving this possibility.

12.2.3.1 Migmatite Domes After Serie Negra Protoliths Along the Monesterio Antiform

C. Quesada

The Monesterio antiform is one of the major structures in the central OMZ, along the core of which the largest outcrop of Cadomian basement in this zone occurs. The antiform is split along most of its length into two blocks by the south-verging, Variscan Monesterio thrust (see under Chap. 10 in this volume). Two migmatite domes were exhumed in the hangingwall of the Monesterio thrust (Valuengo and Monesterio), being surrounded by much lower grade (biotite or less) Neoproterozoic and/or Terreneuvian and Cambrian Series 2 rocks (Eguiluz 1987; Apraiz and Eguiluz 1996; Expósito et al. 2003; Sánchez García et al. 2003, 2008, 2010). The contact zone is defined by either a narrow (hectometre to metre scale) band of anastomosing ductile to brittle shear zones or by discrete flat-lying brittle faults. On the basis of the age of the migmatites (ca. 530 Ma; Oschner 1993; Montero et al. 1999, 2000; Expósito et al. 2003; Salman 2004; Sánchez García et al. 2008), these domes are interpreted as variably overprinted relics of core-complexes developed in the middle crust of the Ossa-Morena Zone during early rifting stages (Sánchez García et al. 2003, 2008, 2010).

A third anatectic dome occurs near Lora del Río at the southeastern end of the Monesterio antiform but the situation there is far more complex. Evidence of Cambrian LP-HT metamorphism is provided by zircon dating of migmatite leucosomes at ca. 530 Ma (Ordóñez Casado 1998) but this is severely overprinted by a complex history of burial,

compressive deformation and extensional exhumation leading to a second LP-HT metamorphic event during the Variscan orogeny (Apraiz et al. 1993; Apraiz 1998; Apraiz and Eguiluz 2002). This Variscan extensional event produced a second anatectic event in the already migmatitic core of the dome, which was dated at ca. 340 Ma by Ordóñez Casado (1998).

The core of all three domes is composed of migmatites derived from Serie Negra protoliths (metasediments and amphibolites) and variable proportions of metagranitoids, varying in composition between inhomogeneous granodiorite, with abundant restite and country-rock enclaves, and leocogranite. Among the former, the Monesterio granodiorite represents the largest body (several km long and several hundred meters thick). Leucogranite appears as mm-thick in situ leucosomes, cm- to m-thick veins in stromatic migmatites, to tens of meters thick dikes and apophyses. The highest grade zone in the Valuengo and Monesterio domes is characterized by the following association of index minerals in pelitic and quartz-feldspathic rocks: sillimanite + K feldspar + cordierite + reddish-brown biotite ± garnet, wrapped by a thin intermediate zone with sillimanite ± andalusite ± muscovite but without K-feldspar, followed by rocks with brown biotite as the only index mineral. Away from the migmatitic core of the domes, index minerals are scarce in Serie Negra medium/high grade rocks, especially garnet (rare or absent) whereas cordierite is relatively abundant. This implies a strong dependence of metamorphic blastesis on the chemical composition of the protoliths (Arriola et al. 1984; Eguiluz 1987; Apraiz 1998; Expósito et al. 2003). In metabasite protoliths the parageneses evolve from: brown hornblende + plagioclase + quartz ± clinopyroxene ± ilmenite ± biotite ± sphene in the anatectic zone, through green hornblende + plagioclase + quartz + ilmenite ± epidote ± sphene ± biotite, to actinolite + plagioclase + quartz ± chlorite in the most widespread external low-grade zones (Apraiz et al. 1993). These mineral assemblages are typical of LP metamorphic regimes. Thermobaric estimations vary between 650 °C at 250 MPa in the Monesterio migmatites (Eguiluz 1987) and 720 °C at 5 kbar in the Lora del Río dome (Apraiz et al. 1993), although in the latter case, overprinted by Variscan metamorphic events, the estimations cast some doubts. At the Valuengo dome Apraiz and Eguiluz (1996) estimated ca. 1.0–1.2 GPa peak P conditions at 600–650 °C, evolving to ca. 0.8 GPa at 700–750 °C. They based their estimation on the application of the garnet-biotite geothermometer and the garnet-Al silicate-plagioclase (GASP) geobarometer on few samples containing garnet. This apparent higher pressure regime relative to the other domes may represent either presence of relic parageneses developed during the previous Cadomian orogeny or lack of mineral equilibrium in the analysed samples (Expósito et al. 2003).

The age constraints so far obtained by various methods to date this LP-HT rift-related event range between ca. 530–510 Ma for the crystallization of migmatite leucosomes and compositionally correlative plutonic and volcanic rocks (Schäfer 1990; Ochsner 1993; Ordóñez Casado 1998; Montero et al. 1999; Expósito et al. 2003; Sánchez García et al. 2003, 2008, 2010; Romeo et al. 2006), ca. 500 Ma for cooling ($^{40}Ar/^{39}Ar$ amphibole; cf. Dallmeyer and Quesada 1992), and 480 ± 7 Ma for a post-metamorphic intrusive microgranite at Valuengo (Expósito et al. 2003).

12.2.3.2 The Mina Afortunada Gneiss Dome Within the Badajoz-Córdoba Shear Zone

C. Quesada

This migmatite dome, also derived after partial melting of Serie Negra metasediments and located within the inner core of the Badajoz-Córdoba shear zone, was described by Apalategui and Quesada (1987), Ábalos (1990), Ábalos and Eguiluz (1992), Ordóñez Casado et al. (1997) and Sánchez García et al. (2008). Besides various types of migmatites derived from metasediments, an inhomogeneous orthogneiss makes the largest part of the dome. A sharp contact separates the migmatitic core from an overlying lower grade unit (lower amphibolite to greenschist) also composed of Serie Negra rocks and the so-called Cuartel amphibolite (Ábalos 1990; Ábalos and Eguiluz 1992). All the rocks within the dome are affected by strong flat-lying mylonitization parallel to the contact, along which severe retrogression to lower amphibolite conditions took place. Metamorphic phases growing along the mylonitic foliation are restricted to biotite, quartz, muscovite and locally garnet. In the mylonitic orthogneiss and migmatites, several less sheared boudins and frequent large white mica porphyroclasts within the mylonites preserve relics of kyanite overgrown by sillimanite, and garnet in some specific horizons.

In addition to retrogression, the location of this gneiss dome within the highly deformed core of the Badajoz-Córdoba shear zone makes almost impossible proving whether it also formed as an extensional core-complex during rifting or not. We include it here because of the recent publication by Sánchez García et al. (2008) of a 532 ± 4 Ma (TIMS U-Pb zircon) age for igneous crystallization of the anatectic neosome precursor to the orthogneiss, which is indistinguishable from those of other rift-related metaigneous rocks elsewhere in the OMZ (Ochsner 1993; Ordóñez Casado 1998; Romeo et al. 2006; Chichorro 2006; Pereira et al. 2006). Sánchez-García et al. (2008) also obtained U-Pb data from monazite in the Mina Afortunada orthogneiss that yielded a discordia line with a poorly constrained lower intercept at ca. 340 ± 35 Ma,

interpreted to date the Variscan overprint, and an upper intercept age of 515 + 9/−7 Ma interpreted to reflect a Cambrian metamorphic event. In fact, this latter age is coeval to development of the so-called Main Rift-related Igneous Event in the OMZ (Sánchez García et al. 2003, 2008, 2010, 2016; see also Chap. 2 in this volume).

12.2.3.3 The Sierra Albarrana Metamorphic Dome

C. Quesada

This is the most recent surprise that absolute age dating has produced in the OMZ. Previously considered either Cadomian (Delgado Quesada 1971; Garrote 1976; Quesada et al. 1990) or Variscan (Quesada and Munhá 1990; Dallmeyer and Quesada 1992; Azor 1994; Azor and Ballèvre 1997; Azor et al. 2004), recent U-Pb (SHRIMP) zircon dating of a migmatite leucosome yielded two age populations at 497 ± 4 Ma, interpreted as the age of the rift-related metamorphic event, and at 577 ± 8 Ma, interpreted as the age of a Cadomian tectonothermal event recorded in the basement protolith of the migmatites (Azor et al. 2012). These authors also obtained a $^{40}Ar/^{39}Ar$ amphibole plateau cooling age of ca. 481 Ma, which they interpreted to date post-metamorphic cooling after the Cambrian event. The scarce previously available age constraints were provided by Dallmeyer and Quesada (1992) who reported ca. 350 Ma and ca. 390 Ma $^{40}Ar/^{39}Ar$ plateau cooling ages from muscovite and amphibole concentrates, respectively, which they interpreted as evidence for the Variscan age of the metamorphic event. Similar $^{40}Ar/^{39}Ar$ ages have been reported by Azor et al. (2012), which indicate that most of the deeper parts of this unit must have remained at temperatures greater than that of Ar retention in amphibole until its exhumation during the early stages of the Variscan orogeny (i.e. ca. 390 Ma ago).

An additional proof of the Cambro-Ordovician age of the Sierra Albarrana metamorphism is provided by the Cardenchosa pluton, which intruded the Sierra Albarrana sequence after development of its most prominent cleavage. Crystallization of this pluton has been dated at ca. 478–480 Ma (U-Pb SHRIMP on zircon; Azor et al. 2016).

A neat metamorphic zonation was first defined by Garrote (1976) and subsequently refined by González del Tánago and Peinado (1990), González del Tánago and Arenas (1991), González del Tánago (1993), Azor (1994) and Azor end Ballèvre (1997). The metamorphic zones exhibit a NW-SE trending domal structure with a migmatitic inner core, concentrically wrapped by progressively lower grade zones. At odds with the Serie Negra derived metamorphic complexes and owing to the high Al_2O_3 content of the Sierra Albarrana protoliths, mainly the pelites (Albariza schists of Delgado Quesada 1971 and subsequent workers), the amount and size of metamorphic index minerals is outstanding, This allowed definition and detailed mapping of the sillimanite + K-feldspar, sillimanite + muscovite, andalusite, staurolite, garnet and biotite isograds (Garrote 1976 and subsequent workers). The structural thickness between the anatectic core and the biotite isograd is barely 5–6 km, which is indicative of a very high geothermal gradient. Presence of relic kyanite within andalusite porphyroblasts (Garrote 1976; González del Tánago 1993; Azor 1994; Azor and Ballèvre 1997) is consistent with a decompression path (i.e. crustal thinning). Peak thermobarometric estimations were established at 3.5–4 Kbar and 650–700 °C by Azor and Ballèvre (1997).

According to the above authors, metamorphic blastesis overlapped in time the development of the main foliation in the Sierra Albarrana unit; therefore, related to the Cambrian-Early Ordovician rifting event. An outstanding feature in this area is the presence of an important swarm of pegmatite dikes, some of them several km in length and many decametres in thickness. Dikes are generally parallel to the elongation of the dome and mostly concentrated in the highest grade zones (up to the andalusite zone). Interestingly, although generally containing a large variety of mineral phases (Garrote 1976; Garrote et al. 1980; González del Tánago 1993), the pegmatites within the anatectic zone are largely quartz-feldspathic whereas those intruded in lower grade zones are very rich in Al-silicate, mainly andalusite (locally up to 50% of the rock), which has been taken as evidence for a metamorphic (anatectic) origin of the pegmatites (Garrote et al. 1980; Pérez Lorente 1979).

12.2.3.4 Cambro-Ordovician Overprint of Cadomian Remnants at the Ossa-Morena Zone North-Western Border (SE of Abrantes, Portugal)

M. L. Ribeiro, A. Mateus

A relatively continuous exposure of well-preserved Cadomian basement can be observed all over a sizable area located to the SE of Abrantes (surrounding the Castelo do Bode Dam), close to the tectonic contact between the Ossa-Morena and Central-Iberian Zones (Mo in Fig. 12.3). This basement comprises a considerable variety of intensely

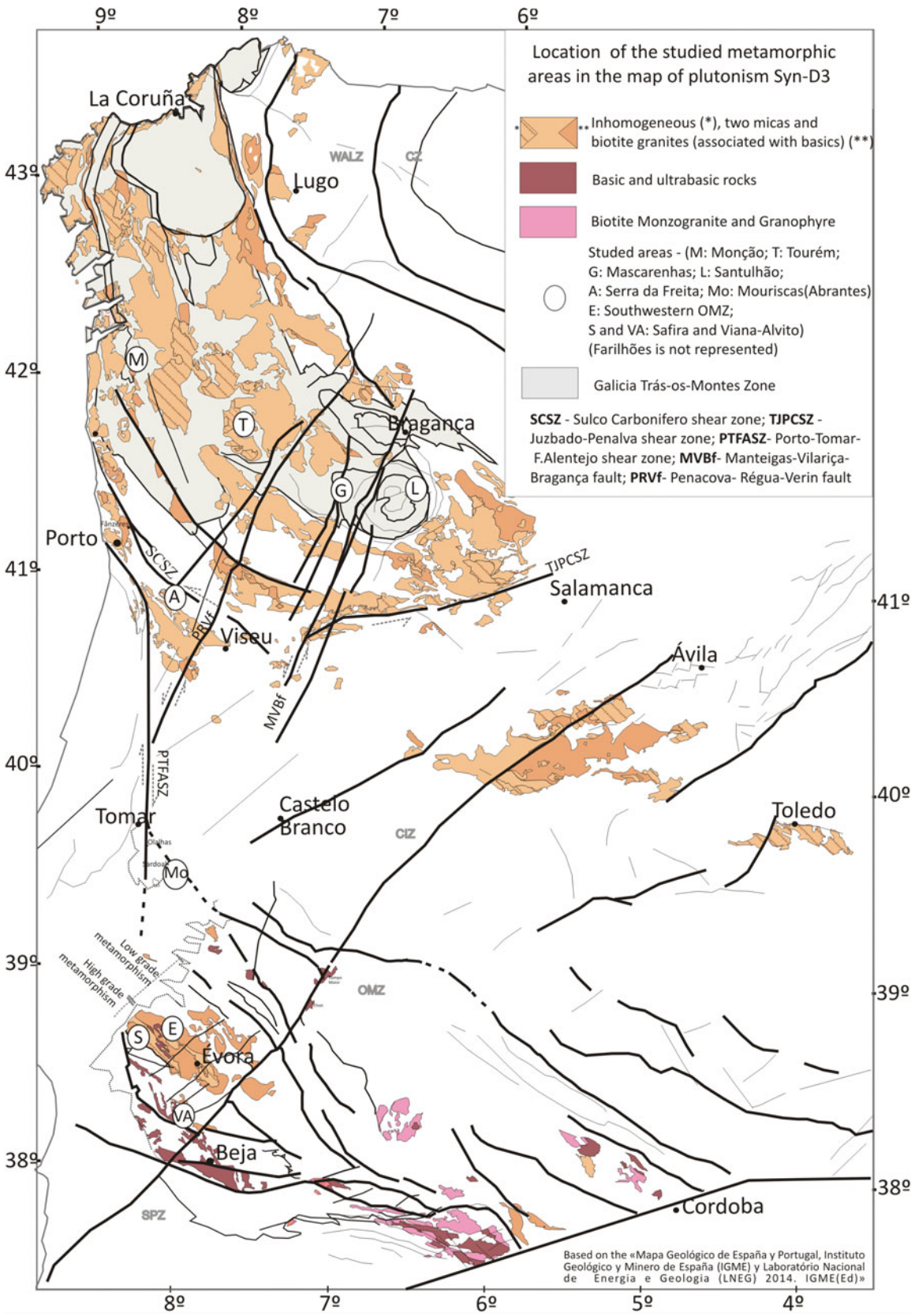

Fig. 12.3 Location of the metamorphic areas studied in Portugal on a reference frame of the Variscan syntectonic granites (D3) and migmatites of the Iberian Massif (Adapted from: "Mapa Geológico de España y Portugal" scale 1/1,000,000, IGME-LNEG 2014)

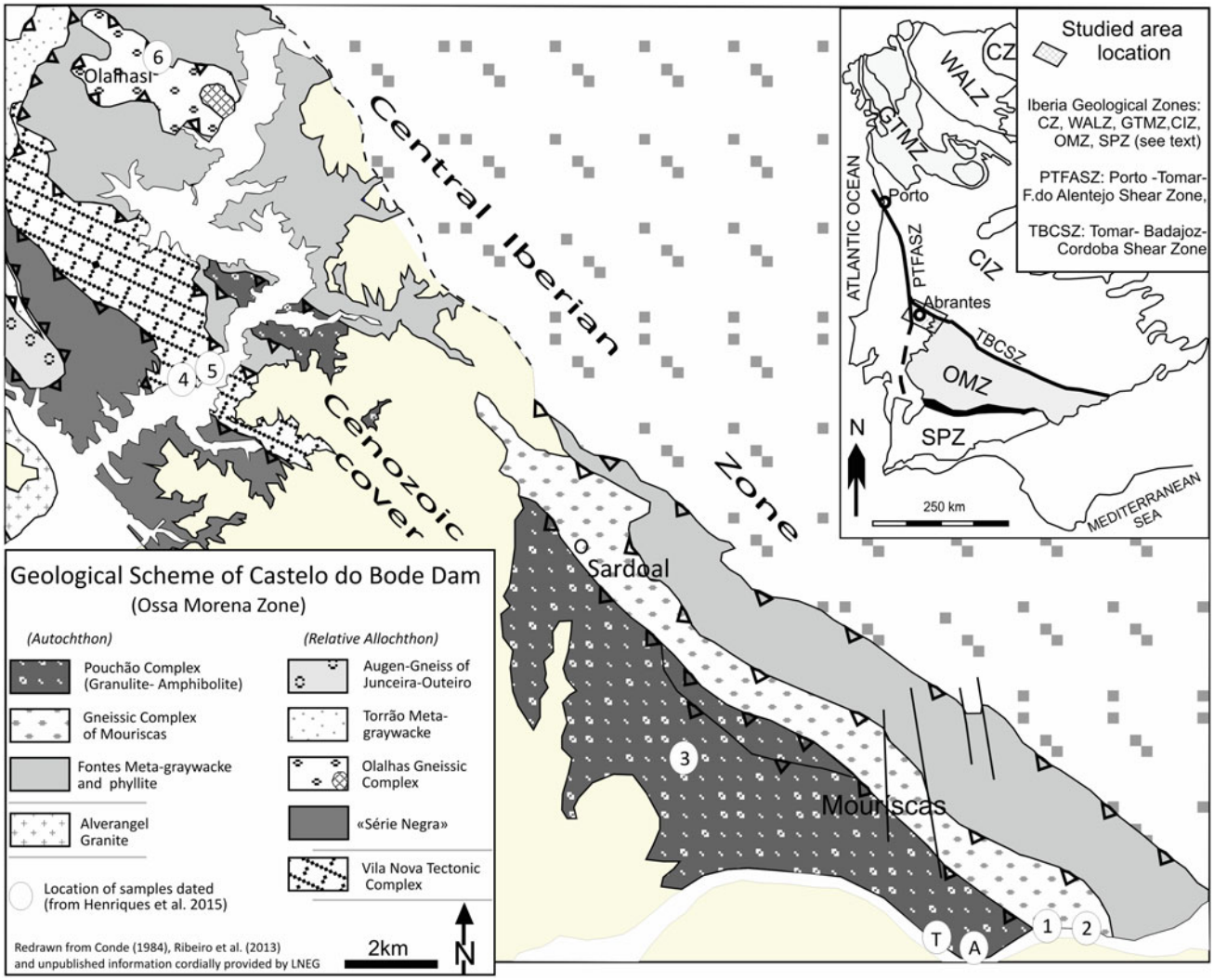

Fig. 12.4 Geological outline of the Castelo do Bode Dam area and setting in relation to the main geological units of the Iberian massif (inset)

deformed and metamorphosed rocks (mostly igneous-derived), representing the remnants of a folded tectonic stacking developed over the Ediacaran autochthon (Ribeiro et al. 2013b). Notwithstanding the different mapping solutions (Conde 1984; Romão and Esperancinha 2000, 2016; Ribeiro et al. 2013b; Henriques et al. 2015) the following three main groups of geological units can be recognized (Fig. 12.4):

(1) Units of prevailing metasedimentary origin ("Phyllites and meta-greywackes of Fontes", "Série Negra" and "Torrão greywackes") whose original siliciclastic sediments, at places interbedded with cherts/flints and volcanic-derived rocks, were intruded by different igneous bodies, and the ensemble later subjected to poly-metamorphic recrystallization under distinct P-T conditions.

(2) Units of prevailing igneous origin, separated into a Felsic-dominated Group and a Mafic Group. The former Group, locally presenting noteworthy mafic components, includes the "Olalhas Gneissic Complex", the "Mouriscas Gneissic Complex" and the "Augen-gneiss of Junceira-Outeiro" (?) assigned to the "Sardoal Complex" in previous works. The Mafic Group, quite homogeneous, comprises the "Granulite-amphibolite Complex of Pouchão", previously named "Mouriscas Complex".

(3) A Unit preserving effects of intense tectonic overprinting and called "Gneiss-amphibolite Tectonic Complex of Vila Nova", once integrated in the "Sardoal

Complex". Even though this Unit encloses elements of the former two, those belonging to the Felsic Group/Sardoal Complex prevail. Although realising the correlations just presented, the classification scheme reported in Henriques et al. (2015) will be used herein.

According to the available geochronological and geochemical information (Henriques 2013; Henriques et al. 2015, 2017): (i) the crystallization timing of protoliths related to the prevalent orthogneisses (Sardoal Complex) is bracketed in the ca. 570–550 Ma time-span; (ii) the crystallization of calc-alkaline mafic protoliths linked to the older amphibolite suite (within the Mouriscas Complex) is clustered at ca. 544 Ma; (iii) evidence of a LP-HT metamorphic event progressed up to amphibolite or amphibolite-granulite transitional facies conditions is consistently dated at ca. 540 Ma in a large range of lithologies belonging to the Sardoal and Mouriscas Complexes; and (iv) the igneous protolith of amphibolites included in Complexes that preserve this metamorphic record should be older than ca. 540 Ma. All these metamorphic rock suites are heterogeneously affected by anatexis processes interpreted as a result of irregular, but significant, decompression-driven crustal melting concomitant with rapid exhumation of basement rocks that conceivably occurred in fini-Proterozoic times. Notably, in the same area, three additional subsets of igneous rocks were identified, all of them postdating the aforementioned sequence of events, therefore tracing geological processes able to affect the Cadomian basement. These younger subsets include trondhjemite bodies and garnet-bearing amphibolites (respectively T and A, in Fig. 12.4), found in the Mouriscas Complex, as well as rhyodacite dykes lately intruded in the Série Negra and Sardoal Complex.

The late emplacement of rhyodacite dykes does not raise any fundamental misgivings (Henriques et al. 2015, 2016): primary monazite grains provided an igneous crystallization age of 308 ± 1 Ma (ID-TIMS U-Pb method); and their calc-alkaline character, as well as their Sm–Nd and $\delta^{18}O$ isotopic fingerprints, indicate melts resulting from a depleted-mantle juvenile source further mixed with components derived from a meta-igneous lower crust containing Meso- (ca. 1054 Ma) to Neoproterozoic (ca. 619 Ma) inherited zircons. Therefore, a strong compositional affinity and chronological agreement can be established between these rhyodacite bodies and the late Variscan granites emplaced during the Upper Carboniferous period.

In turn, trondhjemite bodies, usually displaying protomylonitic textures, intrude the older amphibolite suite in the Mouriscas (Mafic) Complex. Their generation can be envisaged as a result of partial melting of a hydrous mafic crust (comparable to the metagabbros intruded in the older sections of the Sardoal (Felsic) Complex?), followed by melt crystallization (after some displacement) under P-T conditions below ≈6 kbar and around ≈650 °C, respectively, at ca. 483 ± 1.5 Ma (Henriques 2013; Henriques et al. 2015). This $^{206}Pb/^{238}U$ crystallization age, provided by ID-TIMS in zircon prisms, is roughly consistent with the upper intercept age of 484 ± 10 Ma (fit probability of 71, 95% CI) estimated for a Discordia line containing 3–10% discordant monazite data points, anchored at 10 ± 10 Ma and co-linear with the concordant zircon fraction.

The garnet-bearing amphibolites do not show structural and/or mineral/textural arrangements equivalent to those recorded by the (prevailing) older suite of amphibolites included in the Mouriscas Complex (such as tight-folded foliation, mylonitic fabrics, and products of metamorphic segregation processes or of inhomogeneous anatexis). Instead, they display a relatively regular and fine-grained matrix over which almandine develops large porphyroblasts enclosed in quartz–andesine/oligoclase coronas that crisscross the foliation, clearly indicating post-kinematic recrystallization. Furthermore, their geochemical affinity with MORB protoliths affected by significant crustal contamination contrasts with the calc-alkaline nature inferred for the mafic protoliths linked to the older (Cadomian) amphibolite suite (Ribeiro et al. 1995, 2013b; Henriques 2013). Zircon prism fragments extracted from a garnet-bearing amphibolite also yielded a distinct younger ID-TIMS $^{206}Pb/^{238}U$ age, conceivably dating the emplacement/crystallization of the MORB-like protoliths at ca. 477 ± 2 Ma (MSWD = 0.17, 95% CI—Henriques 2013; Henriques et al. 2015). Consequently, the almandine garnet porphyroblasts and their coronas should document a late chemical readjustment progressed under ≤ ≈6.5 kb and 550 °C (Henriques 2013; Henriques et al. 2015); this mineral/textural rearrangement can be tentatively correlated with an Early Ordovician metamorphic overprint, thus integrating the retrogression path recorded by the basement rocks (Série Negra Unit, Sardoal and Mouriscas Complexes).

The ca. 483–477 Ma time-window should sign a particular geodynamic evolving stage during which some magma batches were generated and emplaced in the pre-Variscan tectonostratigraphic basement sequence located to the SE of Abrantes. Trondhjemites can be tentatively correlated with similar occurrences described in other sectors of the Iberian Variscan belt, namely in NE Portugal, tracing the development climax of bimodal (alkaline to subalkaline tholeiitic, and MORB-like) metavolcanic rocks during Ordovician through Lower Devonian times (e.g. Ribeiro et al. 1985; Arenas et al. 1986; Ribeiro 1986; Martínez Catalán et al. 1997, 2014; López-Carmona et al. 2010). The generation of trondhjemites implies, though, that suitable conditions to sustain a robust heating affecting the pre-existent crust were

achieved at ca. 483 Ma, therefore triggering partial melting of its mafic components. The Early Ordovician garnet-bearing amphibolites are isotopically distinct of chronologically equivalent rocks observed in other sectors of the Ossa-Morena Zone and ascribed to intracontinental rifting on the basis of their geochemical features (e.g. Sánchez García et al. 2003, 2008, 2010; Solá et al. 2008; and references therein). However, the protoliths of these garnet-bearing amphibolites may represent products of a rejuvenated mantle melting possibly correlative of early stages of tectonic thinning of lithosphere and asthenosphere upwelling, prior to the major continental break-up in Tremadocian times recorded throughout the European Variscan belt (e.g. Lotout et al. 2017; Pouclet et al. 2017; and references therein). Accepting this interpretation, the trondhjemite bodies and garnet-bearing amphibolites can be viewed as proxies to an early Variscan cycle overprint in the Cadomian basement preserved to the SE of Abrantes. Probably, these rocks may characterize the deep (mantle) expression of the extensional processes that created the conditions for the formation higher up within the crust of the metamorphic domes referred to in the previous sections. Note also that the ca. 483–477 Ma time-window is consistent with the extensively documented Variscan Cycle onset in the occidental and central orogenic belts of Europe; this foremost geodynamic event, proceeded along with a generalised continental rifting event, is dated from ca. 530 to 450 Ma (but peaking at ca. 520–500 Ma), as reported in many works (e.g. Ducrot et al. 1979; Gebauer et al. 1981; García Garzón et al. 1981; Lancelot and Allegret 1982; Pin and Lancelot 1982; Weber 1984; Lancelot et al. 1985; Ribeiro et al. 1985; Ribeiro 1986; Ribeiro and Floor 1987; Franke 1989, 2000; Matte 1991; Crowley et al. 2000; Montero and Floor 2004; Sánchez García et al. 2008, 2010, 2016; Díez Fernández et al. 2015). Culmination of Lower Paleozoic continental break-up is traced by widespread magmatic activity of peralkaline nature, but abundant Cambrian–Ordovician calc-alkaline to peraluminous metagranites and metavolcanic rocks also occur. For some authors (e.g. Gebauer et al. 1993; Valverde-Vaquero and Dunning 2000; von Raumer et al. 2003; Rubio-Ordoñez et al. 2012) the geochemical fingerprint displayed by the latter suite of rocks was taken as evidence of an active margin setting. However, as clearly demonstrated by Bea et al. (2007), the atypical zircon inheritance and calc-alkaline/peraluminous character of these igneous rocks may simply document fast melting rates of lower crust under temperature conditions of at least 900 °C, followed by quick magma transfer to the uppermost crust levels. In these circumstances, the anatexis swiftness is envisaged as a result of anomalously high heat flow supplied by intermittent arrival of batches of hot mantle-derived mafic magmas at the base of the crust, a process that is favoured in a continental rift-related tectonic setting (Bea et al. 2007; and references therein).

12.3 Subduction Related Metamorphism

A. López-Carmona, M. L. Ribeiro, A. Mateus, N. Leal, J. Pedro, P. Moita, J. Reche, C. Quesada

12.3.1 The Unrooted High-Pressure Allochthonous Units of the Galicia-Trás-os-Montes Zone

A. López-Carmona, M. L. Ribeiro

Three subduction events related with the early Variscan convergence are recognized in NW Iberia (cf. Martínez Catalán et al. 2009; Ballèvre et al. 2014; Arenas et al. 2016b). The first is recorded by the lower part of the upper allochthon (HP/HT units) during the early-middle Devonian transition (ca. 400–390 Ma; Fernández-Suárez et al. 2007), and may represent its accretion to a northward terrane (southern margin of Laurussia).

The second subduction event is roughly coeval (ca. 395 Ma) and suggests the development of an intraoceanic supra-subduction zone, located close to the southern margin of Laurussia, that generated the early Devonian oceanic lithosphere of the middle allochthon, subsequently imbricated and accreted during the following 10 Ma. Such subduction would have generated buoyant oceanic lithosphere that would have been readily accreted beneath Laurussia, and eventually obducted over the external margin of Gondwana at the beginning of the Variscan collision (ca. 370 Ma). According to Arenas et al. (2014) a two-stage collisional model affecting a wide Gondwanan platform may explain most of the evidences in NW Iberia. The generation of a long pull-apart basin, where the Devonian ophiolites were formed, probably occurred after the first collision (ca. 400–395 Ma). These ophiolites have been in general described in the context of the Rheic Ocean, but according to the proposed model, they were formed after its closure.

The third continental subduction event involved the most external part of Gondwana´s margin (middle and lower allochthons) during the late Devonian (ca. 370–365 Ma) at the beginning of the Variscan collision, enabling the oceanic closure.

Besides the genesis of the Devonian ophiolites, any model for the Variscan convergence may consider the existence of

the two well-constrained high-pressure metamorphic events (dated at ca. 400–390 and ca. 370 Ma, respectively). Both are described below.

12.3.1.1 The Upper Allochthon

A. López-Carmona

The lower part of the upper allochthon comprises the high-pressure and high-temperature (HP/HT) units. Remnants of the first Cambro-Ordovician arc-related metamorphism have been almost fully overprinted, except for the occurrence of relict monazites in high-grade gneisses which age has been estimated by U-Pb (500–480 Ma; Fernández-Suárez et al. 2002) being equivalent to that recorded in the IP units described above in Sect. 12.2.1. Both ensembles share the same protoliths, but the HP/HT units reached eclogite- (A Capelada unit) and high-pressure granulite-facies conditions (Fornás, Belmil, Melide, Sobrado and Cedeira units). The Devonian metamorphic event (Gil Ibarguchi et al. 1999; Mendía 2000) was followed by decompression and partial melting together with the development of a penetrative mylonitization in the amphibolite facies. The retrograde amphibolite-facies metamorphism has been dated at ca. 390–380 Ma (Dallmeyer et al. 1991, 1997; Valverde Vaquero and Fernández 1996; Gomez Barreiro et al. 2006). Finally, recumbent folding and thrusting occurred under greenschist-facies conditions (Vogel 1967; Marcos et al. 1984; Gil Ibarguchi et al. 1990).

Diamond- and/or coesite-bearing rocks have been reported in equivalent units in different massifs of the European Variscan belt (cf. Nasdala and Massonne 2000; Massone 2001; Lardeaux et al. 2001; Kotková and Janák 2015). However, although peak pressures may be close to ultrahigh-pressure values, evidence of microdiamonds or coesite is absent in the NW Iberian Massif. The most distinctive rocks in the HP/HT units are serpentinized ultramafic rocks, variably migmatised paragneisses, garnet-clinopyroxene-bearing granulites and eclogites retrogressed to the amphibolite-facies (Vogel 1967; Hubregtse 1973). Gil Ibarguchi et al. (1990) and Mendía (2000) described three main eclogitic types: common eclogites, Fe–Ti eclogites after Fe–Ti gabbros and Al–Mg eclogites derived from troctolitic gabbros. Peak pressures have been estimated in kyanite-bearing Al–Mg-rich eclogites in ca. 2.3 GPa at 750–800 °C (A Capelada unit; Mendía 2000). Tholeiitic gabbros show a quite complete textural evolution, from undeformed types with almost pristine igneous textures including clinopyroxene + orthopyroxene + plagioclase ± olivine, through coronitic gabbros and metagabbros, to high-pressure granulites with granonematoblastic textures and without any relict of the previous stages (Arenas and Martínez Catalán 2002). These gabbros define a prograde P–T path related to subduction, peaking at 1.6 GPa and between 725–875 °C (Sobrado unit, Arenas and Martínez Catalán 2002; Cedeira unit; Puelles et al. 2005; Fig. 12.1). Temperature and migmatization increase downwards in the structural pile during exhumation, together with the progressive hydration of these units (Arenas and Martínez Catalán 2002). The gabbros geochemical signature has been compared to MORB (Gil Ibarguchi et al. 1990) and related to continental rifting (Galán and Marcos 1997). On the other hand, geochemistry of the ultramafic rocks indicates that they are probably related to an arc environment (Santos Zalduegui et al. 2002).

12.3.1.2 The Lower and Middle Allochthons

A. López-Carmona

Early Variscan (ca. 370–365 Ma) high-pressure metamorphism, related to continental subduction (Santos Zalduegui et al. 1996; Rodríguez et al. 2003; Abati et al. 2010; López-Carmona et al. 2014), is recorded by blueschists, eclogites and jadeite-bearing orthogneisses, dispersed in different units throughout the lower and middle allochthons of the NW Iberian Massif, and by the metavolcanic rocks preserved within the Somozas Mélange (Ribeiro 1976; van der Wegen 1978; Munhá et al. 1984; Schermerhorn and Kotsch 1984; Gil Ibarguchi and Ortega Gironés 1985; Arenas 1991; Gil Ibarguchi 1995; Arenas et al. 1995; Rubio Pascual et al. 2002; Rodríguez et al. 2003; Rodríguez 2005; López-Carmona et al. 2010; Ballèvre et al. 2014; Li et al. 2017; Novo-Fernández et al. 2016; Puelles et al. 2017). Peak P–T conditions vary from blueschist- to high-temperature eclogite-facies according to their initial location in the subducting slab within the subduction complex (Martínez Catalán et al. 1996; Gómez-Barreiro et al. 2010; López-Carmona et al. 2013; Figs. 12.1 and 12.2).

Blueschist-facies terranes are restricted to scarce and relatively small areas and are usually highly retrogressed. Blueschists were first described in the Trás-os-Montes region in northern Portugal (Ribeiro 1976; Munhá et al. 1984; Gil Ibarguchi and Dallmeyer 1991) and were subsequently reported in the middle allochthon of Galicia (Martínez Catalán et al. 1996; Rodríguez et al. 2003; López-Carmona et al. 2010). Particularly, regarding the blueschists-facies metamorphism, the comprehensive characterization of the westernmost exposure of the middle allochthon of the Variscan belt in Western Europe (Cean unit, Malpica-Tui complex) has turned this terrain into a key element to parameterize the initial stages of Variscan subduction (López-Carmona et al. 2013, 2014). On the other hand, Île de Groix is considered the classical blueschists Variscan outcrop (southern coast of Brittany, France; Barrois 1883). Over the last decade, several correlations between the NW Iberian Massif and equivalent units in the south of the

Armorican Massif have been suggested (cf. Ballévre et al. 2014). From their age and tectonometamorphic evolution, correlations between the Ceán unit and the upper unit of Île de Groix are widely accepted. Both terranes show similar lithologic associations constituted by variable proportions of glaucophane-chloritoid-bearing metapelites and N-MORB metabasic rocks with pseudomorphs after lawsonite. The upper unit of Île de Groix and the Ceán unit share a blueschist-facies event constrained by $^{40}Ar/^{39}Ar$ dating of phengitic muscovite at ca. 370–365 Ma (Bosse et al. 2005; Rodríguez et al. 2003; López-Carmona et al. 2014). Paradoxically, although fresh lawsonite has never been found in the well-preserved blueschists from Île de Groix or in the middle allochthon of Galicia, it has been described in the Morais Complex in northern Portugal (Macedo de Cavaleiros unit; Schermerhorn and Kotsch 1984).

According to their tectonostratigraphy and metamorphism, the lower and middle allochthon form two tectonically juxtaposed sequences. Felsic orthogneisses and terrigenous metasediments predominate in the lower structural levels (Malpica, Agualada, Santiago, Forcarei, Lalín, Espasante and Centro-Transmontane units), whereas the upper part of the structural pile is interpreted as a volcanosedimentary sequence (Ceán, Lamas de Abad, Cercio, Macedo de Cavaleiros and Pombais units). In general, the lower structural levels developed eclogite-facies metamorphism (Gil Ibarguchi and Ortega Gironés 1985; Arenas et al. 1997; Rubio Pascual et al. 2002; Rodríguez et al. 2003; Li et al. 2017; Puelles et al. 2017), while the overlying levels, separated by a major tectonic contact (i.e. the Bembibre-Ceán detachment), reached blueschist-facies conditions (Rodríguez et al. 2003; López-Carmona et al. 2010). Knowing the northwest directed component of subduction in present day coordinates (Alcock et al. 2005; Díez Fernández et al. 2012b), the upper sequence would occupy an oceanward position compared to the lower sequence before the Variscan collision. Although their outcrops in the different allochthonous complexes are separated by relatively large distances, structural reconstructions indicate that both sequences formed a coherent and continuous sheet of associated continental and transitional to oceanic rocks (Martínez Catalán et al. 2007; Díez Fernández et al. 2011).

The occurrence of a pressure gradient along the sheet, where pressure increases from east to west, supports that the subduction had a significant westward component in present coordinates (Martínez Catalán et al. 1996). The original position of the different units in both allochthons during subduction was preserved despite the subsequent post-high-pressure history (Gómez-Barreiro et al. 2010; López-Carmona et al. 2013). In a few places, the blueschist facies units are interlayered between two eclogite facies units (e.g. the Ceán unit is sandwiched between the Malpica and the Agualada unit). The interlayering is interpreted as an original feature of the subducting slab/accretionary wedge, related with the typical geometry of the isotherms in subduction zones (López-Carmona et al. 2013, 2014).

Three main tectonometamorphic episodes have been established in the lower and middle allochthons of NW Iberia (Fig. 12.2). The first event records an eclogite- and blueschist-facies prograde metamorphism related to continental subduction. The maximum peak pressures have been estimated in the Malpica-Tui Complex at 2.2 GPa for the blueschists (López-Carmona et al. 2013, 2014) and between 2.25 and 2.6 GPa for the eclogites (Rodríguez et al. 2003; Li et al. 2017; Puelles et al. 2017).

Subduction zone metamorphism occurred in H_2O-undersaturated conditions induced by the crystallization of a significant modal amount of lawsonite. Then, the transition from eclogite- and lawsonite blueschist-facies to amphibolite-greenschist-facies involved a significant hydration, chiefly because of lawsonite breakdown (López-Carmona et al. 2014). Post-peak metamorphic evolution has been constrained between ca. 360 and 350 Ma (Rodríguez et al. 2003; López-Carmona et al. 2014) whilst decompression was driven by thrust and recumbent folding in the amphibolite-facies. The beginning of post-nappe tectonics is defined by the intrusion of early I-type Variscan granodiorites at ca. 350–340 Ma (Gutiérrez-Alonso et al. 2018). This time interval would include the incipient partial melting related to decompression that took place under amphibolite-facies conditions in the lower allochthon, dated by U–Pb in zircon in the Agualada unit at ca. 346 Ma (Abati and Dunning 2002), and the ultimate emplacement of the lower and middle allochthon nappes by the underthrusting of a new crustal sheet (the Parautochthon; Martínez Catalán et al. 2002, 2007). Subsequently, exhumation was driven by thrusting and recumbent folding from 340 to 317 ± 15 Ma, coeval with widespread magmatism and the late orogenic collapse (Gómez-Barreiro et al. 2007; Martínez Catalán et al. 2009; Díez Fernández et al. 2011). The final exhumation due to late orogenic readjustments during the gravitational extension of the orogenic pile took place under greenschist-facies conditions comprising the out of sequence thrust system, originated during the obduction of the ophiolitic sequences and the upper allochthon (Martínez Catalán et al. 2002). Lastly, the ductile to ductile-brittle extensional shearing and the strike-slip tectonics that buckled all previous fabrics into open to tight upright folds was subsequently cut by transcurrent shear bands (Gómez-Barreiro et al. 2010; Díez Fernández et al. 2012c) that led to the gravitational collapse of the orogen dated at ca. 337 ± 3 Ma (López-Carmona et al. 2014).

In the Malpica-Tui Complex, differences between the high-pressure and low-temperature event (ca. 363 ± 2 Ma) and the beginning of the post-nappe tectonics (ca. 350–340 Ma) suggest that the exhumation of the lower

allochthon lasted ca. 15–20 Ma. Assuming peak pressures of 1.9–2.2 GPa (ca. 65–70 km of subduction depth) and a nearly isothermal decompression from 2.2 to 1.0 GPa, an exhumation rate of ca. 2.5 mm/year from 70 to 30 km can be estimated. Afterwards, during the orogenic collapse, a fast cooling may follow rapid exhumation because of the upward advection of heat (e.g. Ring et al. 1999). Therefore, the last stages of exhumation from 1.0 to 0.5 GPa occurred within a period of ca. 15 Ma (from 350 to 335 Ma) and from temperatures of ca. 480 to 380 °C, suggesting a cooling rate of 7 °C/Ma (or a geothermal gradient of 10 °C/km). These rates agree with well-constrained natural examples and numerical thermal-mechanical models (e.g. Grasemann et al. 1998; Gerya et al. 2002; Warren et al. 2008; Burov et al. 2014), which suggest that decompression occurs in two stages: (i) a fast exhumation stage with little temperature change over a large depth interval and (ii) a phase of fast cooling once the rocks have reached an upper crustal level (López-Carmona et al. 2014).

12.3.1.3 An Anomalous Case (?): Carboniferous HP-LT Metamorphism in the Lower Allochthon of the Morais Complex

M. L. Ribeiro

In the SE part of the Galicia-Trás-os-Montes Zone, the Lower-Allochthonous-Unit (LAU), structurally located between the Parautochthonous Unit (below) and the Ophiolite Complex (above), is regionally affected by Barrowian type metamosphism (Ferreira 1964) showing a zonation with well spaced isograds going from chlorite, through biotite to almandine. Sporadically, however, the metamorphic pattern changes and high-pressure and low-temperature (HP-LT) mineralogical assemblages are preserved (Ribeiro 1976). In the vicinities of the Morais Massif HP-LT mineral assemblages are related to the 2nd Variscan phase of deformation (Ribeiro 1976; Ribeiro et al. 1982; Schermerhorn and Kotsch 1984; Munhá et al. 1984). The spatial distribution of HP-LT outcrops suggests that an important area was affected (G and L in Fig. 12.3), probably the entire LAU.

The Mascarenhas area, on the western side of the Morais Massif (G in Fig. 12.3) lies just above the contact with the Parautochthonous Unit; the Santulhão area, on the eastern border of the same massif, crops out just below the contact with the Ophiolitic Complex (L in Fig. 12.3).

Within the LAU, textural data display characteristic features of helicitic crystallization relative to the first Variscan phase of deformation (Ribeiro 1974). In the Santulhão area, sediments and volcanics (intermediate and basic rocks), including the Siliceous-Volcanic Complex (VSC) of Pereira et al. (1998), were sheared and metamorphosed to the greenschist facies. Biotite, phengite, stilpnomelane are frequent phases along with chloritoid in some phyllites. In the metabasic rocks magnesioriebeckite occasionally replaces actinolite. Lawsonite occurs in intermediate dacitic rocks that overlie the basic metavolcanics. The dacites are sheared tuffs with plagioclase and quartz phenocrysts and millimetre lithic fragments. Lawsonite has developed as tiny unoriented idioblasts, through the destabilization of plagioclase (An4). It developed length-fast tabular crystals, sometimes presenting corroded boundaries due to replacement by albite (Schermerhorn and Kotsch 1984).

The main lithology of the area consists of low-grade pelitic schists, within which greenschist and blueschist bodies occur interlayered in localized areas (namely at the Valbom dos Figos (VBF) village), adjacent to zones of important tectonic dislocation. Petrographic and field relations indicate that sodic amphiboles (glaucophane-crossite) grew synchronously with thrusting during the 2nd phase of Variscan deformation (Ribeiro 1976). Gil-Ibarguchi and Dallmeyer (1991) reported an $^{40}Ar/^{39}Ar$ age of ~330 Ma on white mica from the VBF blueschist; which they interpreted to date the HP recrystallization in the area. Even considering the method used, which suggests that the dating will not correspond to the peak of the HP metamorphic event this interpretation is in contradiction with the abundant age data produced in other blueschists and eclogites within the Lower Allochthonous Unit, which indicate a ca. 370–360 Ma age for the HP-LT event (Rodríguez et al. 2003; López-Carmona et al. 2014; and references therein). A similar 370–360 Ma age was obtained from HP-LT rocks in the Ossa Morena Zone (Moita et al. 2005; Ribeiro et al. 2010). Thus, if the data obtained by Gil Ibarguchi and Dallmeyer (1991) are correct, they represent an anomalous situation within the regional metamorphic framework and the youngest age published so far for HP-LT metamorphism in the entire Variscan belt.

In the pelitic rocks contemporaneous development of biotite and chloritoid in some samples could suggest derivation by a reaction of the type: garnet + chlorite = chloritoid + biotite. Rare intercalations of Mn-rich calc-silicate rocks include equilibrium assemblages composed of quartz + albite + paragonite + phengite + garnet + epidote + calcite. Greenschists are homogeneous, including variable amounts of actinolite, chlorite, epidote, albite, phengite and rare biotite and magnetite; locally, greenschists display porphyroblastic textures where large albite crystals include epidote + hornblende). Blueschists, the minor lithotype component, are coarser grained than greenschists with which they are associated. The typical mineral assemblage includes albite + Na amphibole (crossite and iron-rich glaucophane) + epidote + chlorite + phengite and minor amounts of late talc, hematite, quartz and

carbonates (Munhá et al. 1984). Gil Ibarguchi and Dallmeyer (1991) reported jadeitic clinopyroxene (up to 64% of jadeitic component) in the blueschists of Valbom dos Figos outcrop; a unique discovery among the researchers who studied the area (Ribeiro 1976; Ribeiro et al. 1982; Munhá et al. 1984; Balcázar et al. 2005). According to Gil Ibarguchi and Dallmeyer (1991), albite = jadeite (0.6) + quartz equilibrium indicates that blueschists may have sustained pressures up to 11 kb (~400 °C).

Balcázar et al. (2005) extended the sampling (in the Mascarenhas region) about twenty km to the NE of the VBF blueschist outcrop. In their report, true blueschists were not recorded outside the VBF locality. Garnet/biotite, Si-in phengite and albite- (jadeite poor) aegirine -quartz equilibria allowed Balcázar et al. (2005) to calculate PT conditions of 7.5–8 kb and 400–450 °C for metamorphic recrystallization; however, the authors considered the calculated pressures as minimum values and suggested peak metamorphic conditions of 400–450 °C and 10–12 kb for all the studied area. Both Balcázar et al. (2005) and Gil-Ibarguchi and Dallmeyer (1991) proposed very similar PT-time metamorphic paths for the Mascarenhas HP-LT rocks.

Those PT paths are in contrast with that of Munhá et al. (1984), reflecting different geothermobarometric techniques and the available data at the time of writing. Thus, on the basis of the results reported by Gil-Ibarguchi and Dallmeyer (1991) and Balcázar et al. (2005), it seems that 10–12 kb and 400–450 °C could have been the regional metamorphic peak conditions in the Mascarenhas area. There are, however, several difficulties in order to reconcile the development of greenschists and associated blueschists under the same HP-LT metamorphic conditions (see Balcázar et al. 2005). The PT-pseudosection in Fig. 12.5 is an attempt to illustrate the situation. The observed PT distribution of mineral assemblages (Fig. 12.5) indicates that within the temperature range of 400–450 °C, small pressure variations (ca. ~6 ± 0.5 kb) could indeed allow the coexistence of blueschists and greenschists. Furthermore, as discussed by Munhá et al. (1984), the higher oxidation state of blueschists (assumed at $X(Fe^{3+}) = 0.4$ in Fig. 12.5) expands the stability of Na-amphibole towards lower pressures; thus, oxidation state heterogeneity could make it possible to develop (Fe^{3+} rich) crossite-bearing and actinolite-bearing assemblages under the same PT conditions (Fig. 12.5).

On the other hand, the occurrence of jadeite, reported by Gil-Ibarguchi and Dallmeyer (1991), causes serious incompatibilities. For the bulk rock composition used to elaborate Fig. 12.5 Na-pyroxene becomes stable at 9–10 kb (400–450 °C) and calculated compositions (Xjd ~ 0.44) are poorer in jadeite component than that of the jadeite-rich (X (jd) = 0.64) sampled by Gil-Ibarguchi and Dallmeyer (1991) from VBF blueschist outcrop. Albite + jadeite (Xjd = 0.64) + quartz equilibrium requires pressures of 11–12 kb (400–450 °C; Holland 1980). Application of Thermocalc AvPT method (Holland and Powell 1998) to a typical blueschist (glaucophane, epidote, chlorite, muscovite, albite, quartz and H_2O) provided a (crude) estimate of 8 and 9 kb for the metamorphic recrystallization of blueschists at 400 °C and 420 °C, respectively. The same methodology applied to a greenschist provides better statistics and suggest that at 450 °C (garnet-biotite geothermometry by Balcázar et al. (2005) local greenschists recrystallized at pressures of 6–7 kb. Thus, at the temperatures of interest, geobarometric data suggests a wide range of pressures for different rock types in the area: 12–11 kb for jadeite-rich blueschist, 9–8 kb for glaucophane/crossite blueschists and 8–6 kb (see Balcázar et al. 2005) for greenschists. Furthermore, inclusions of Tschermackite-rich hornblende in albite porphyroblasts of greenschists suggest that these rocks underwent early high-T (epidote-amphibolite facies) metamorphism. In contrast, there is no evidence for high-T metamorphic episodes in blueschists; their main decompression paths are almost isothermal (Gil-Ibarguchi and Dallmeyer 1991; Balcázar et al. 2005). Thus, (despite the fact that all rock types seem to have undergone relatively high-P metamorphism), petrologic evidence requires that blueschists and greenschists should have had distinct tectonic settings during the main metamorphic recrystallization episode.

The rocks affected by HP-LT metamorphism in the Mascarenhas region appear to have originated on the western margin of the Iberian part of Gondwana (Iglesias et al. 1983; Behr et al. 1982; Ribeiro et al. 1983, 1990a; Martínez Catalán et al. 1996). These correspond to the lowermost parts of the regional Lower Allochthon and their protoliths are correlated with a Silurian volcanosedimentary complex, which is thought to represent the stretched continental margin adjacent to a rift zone and associated ocean (Ribeiro and Ribeiro 1982; Ribeiro 1987). The LAU is overlain by the Ophiolitic Unit and the Upper Allocthon, the latter including pre-Variscan high-grade metamorphic rocks (Ribeiro et al. 1990a, 2013a). Variscan reworking within the high-grade upper nappe started at ~400 Ma (Mateus et al. 2016) and was associated with over thickening and HT prograde metamorphism (up to 680 °C, 11 kb; Munhá et al. 2005) of the Morais ophiolite unit at c. 380 Ma (see Munhá et al. 2005). In the LAU, early recrystallization of the greenschist unit under epidote-amphibolite/amphibolite facies conditions (see above) suggest temperatures of c. 450–500 °C at the base of the overriding composite nappe. At this stage, the protoliths of blueschists should have been deeper within the lower parts of the Lower Allochthonous nappe. High permeability (see Munhá et al. 1984) promoted efficient

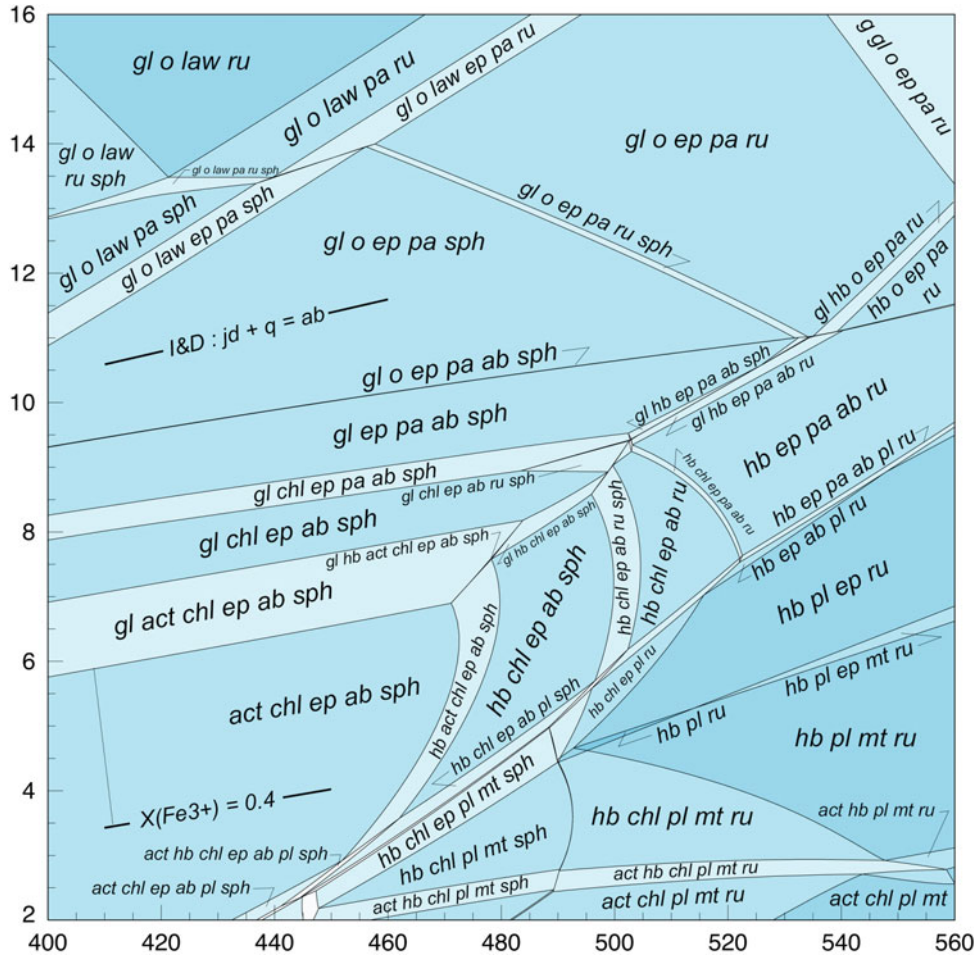

Fig. 12.5 P-T pseudosection in the NCFMHASTO system calculated for the bulk rock composition of Valbom dos Figos 2640 blueschist sample (Balcázar et al. 2005); CaO in the original composition was corrected for carbonates and the oxidation state reduced to $X(Fe^{3+})$ = 0.25. White/light blue fields are divariant and increasing variance is shown with progressively darker shades of blue. The P-T pseudosection has been calculated with the THERMOCALC (v. 3.33) software of Holland and Powell (1998), using the internally consistent thermodynamic data set (tcds55.txt of October 2009), updated from that of Holland and Powell (1998). Solid solution models used in the calculations are as follows: Amphiboles (Diener et al. 2007: act = actinolite, hb = hornblende, gl = glaucophane); Clinopyroxene (Green et al. 2007: o = Na-clinopyroxene); Chlorite (Holland et al. 1998: chl); Epidote (Holland and Powell 1998: ep); Albite-plagioclase (Holland and Powell 2003: ab—albite, pl—plagioclase); Garnet (White et al. 2007: g); Ilmenite-Magnetite (White et al. 2000: mt = magnetite). Quartz is stable in all fields, and H_2O was assumed as in excess phase. Hematite was not considered in the calculations I&D: jd + qz = ab equilibrium calculated from Gil Ibarguchi and Dallmeyer (1991) data at a (jd) = 0.62. $X(Fe^{3+})$ = 0.4 illustrates the effect of increasing oxidation on the act chl ep ab sph (Na-amphibole in) equilibrium. Note that sphene (sph) and rutile (ru) equilibria within the paragonite stability field near the (pa, sph) invariant (upper left corner) should be regarded as qualitative. (**The pseudosection was provided by Professor J. Munhá (who co-authored previous work on the same topic) as well as the correlated interpretation. To refer to it please use: J. Munhá in Ribeiro ML, followed by the reference of this text.*)

advective cooling and development of high-pressure fluid channels may have helped on the exhumation process; these processes preserved low-T blueschist facies assemblages and promoted rapid exhumation.

Late, ductile, intense imbrication at the front of the Lower Allochthonous nappe may have assembled the greenschist and blueschist units; this stage corresponds with generalized greenschist facies retrogressive metamorphism and development of abundant albite porphiroblasts, destabilization of glaucophane => talc + paragonite + hematite and intense carbonation. The LAU around the Morais ophiolite displays a metamorphic regime that is similar to those with the same P-T-path from the units outcropping further to the NW, such as the Forcarei Unit of the Órdenes Complex (Martinez-Catalán et al. 1996) among others. Therefore, considering that: (i) the petrographic data clearly show the crossite-glaucophane is related to the second phase of deformation (Ribeiro 1976), and (ii) the age of 333 ± 4 Ma

interpreted to date the resetting of the K-Ar isotope system during the early stages of D3 (see below Mendes and Santos, Sect. Metamorphism Related to Late-Orogenic Stages in Serra da Freita (CIZ)—Case-Study and Discussion) in the surrounding CIZ (see location in Fig. 12.3), the age of 330 Ma reported by Gil-Ibarguchi and Dallmeyer (1991) can hardly match the episode of high pressure under this study. To date, the age of ca. 370–360 Ma (Rodríguez et al. 2003; López-Carmona et al. 2014; and references therein) seems to correspond better to that of the HP-LT metamorphic event of the lower Allochthon units of GTMZ.

12.3.2 High Pressure Metamorphism Associated to the SW Iberia Variscan Suture

C. Quesada, N. Leal, A. López-Carmona, P. Moita, J. Pedro, J. Reche

The SW branch of the Iberian Massif comprises: (i) a NW Gondwana hinterland terrane accreted to the mainland during upper Proterozoic to lower Paleozoic times (the Ossa Morena zone-OMZ; Quesada 1990a, b, 1991, 1997, 2006; Ábalos 1990; Eguiluz et al. 2000; among others), separated from (ii) a SW exotic terrane thought to pertain to the Avalonian continental plate (the South Portuguese terrane; SPT) that migrated away from Gondwana mainland after opening of the Rheic Ocean in the late Cambrian-early Ordovician (Murphy et al. 2006; and references therein). In between the two zones/terranes, (iii) oceanic affinity rocks and syn-orogenic metasedimentary units characterize the Pulo do Lobo terrane (PLT), thought to materialize the suture zone proper (Quesada 1991). This includes metamafic rocks of ocenic affinity, the so-called "Beja-Acebuches ophiolite complex" (BAO; Bard 1977; Munhá et al. 1986; Crespo-Blanc 1989; Crespo-Blanc and Orozco 1991; Dallmeyer et al. 1993; Quesada et al. 1994; Fonseca 1997; Fonseca et al. 1999; Díaz Azpíroz and Fernández 2003).

The OMZ and the SPZ terranes were accreted to each other after closure of the Rheic Ocean, during the collisional and transpressional stages of the Variscan orogeny, which started in this part of the belt in Late Visean time (ca. 335 Ma), i.e. much later than in the northern branch of the Iberian Massif.

In the OMZ, relict high-pressure assemblages are found in two different locations, both close to its margins: (i) along the Badajoz-Córdoba shear zone inner core (Mata and Munhá 1986; Ábalos 1990; Ábalos et al. 1991; Quesada and Dallmeyer 1994; Azor 1994; Pereira 1999; López Sánchez-Vizcaíno et al. 2003; Abati et al. 2018), and (ii) in the southwestern OMZ, adjacent to the suture with the PLT and SPT terranes, which also show evidence of having undergone HP metamorphism (Bard 1969; De Jong et al. 1991a, b; Pedro et al. 1995a, b; Pedro 1996; Moita 1997; Fonseca et al. 1993, 1999, 2004; Leal 2001; Aráujo et al. 2005; Moita et al. 2005; Booth Rea et al. 2006; Rosas et al. 2008; Ribeiro et al. 2010; Ponce et al. 2012; Rubio Pascual et al. 2013a). Consensus exists on the Variscan age of these HP rocks at the southwestern OMZ, PLT and SPZ, which attest for a process of continental subduction also in this southern Iberia suture zone.

Rocks that recorded high-pressure conditions within the Badajoz-Córdoba shear zone occur within the so-called Central Unit (Azor et al. 1994) and together with presence of serpentinised ultrabasic rocks and MORB metabasic rocks have been taken as evidence for the presence of another suture zone separating the OMZ from the adjacent Central Iberian Zone. However, no consensus has been reached concerning its timing. On one hand, Azor (1994), Azor et al. (1993, 1994, 1995), Simancas et al. (2001), Abati et al. (2018), among others, who consider that all the rocks within the Central Unit were affected by the HP event, interpret a Variscan age on the basis of scarce, imprecise and contradictory geochronological data: a Sm–Nd on garnet age of 427 ± 45 Ma (Schäfer et al. 1991), and a U-Pb SHRIMP on zircon age of 340 ± 15 Ma (Ordóñez Casado 1998). More recently, Abati et al. (2018) have reported two age peaks at ca. 340 Ma and ca. 380 Ma from metamorphic zircons extracted from metabasites in the Central Unit, the older of which they interpret to date the HP event. On the other hand, Mata and Munhá (1986), Ábalos (1990), Quesada (1990a, b, 1991, 1997), Ábalos et al. (1991), Eguiluz et al. (2000), among others, consider that the suture must be Neoproterozoic (Cadomian) in age mainly on the basis of the following geological evidence:

(1) Only a minimal part of the rocks exposed within the Central Unit of Azor (1994) are affected by the HP event: the so-called Eclogitic Unit of Ábalos (1990) or Accretionary Unit of Quesada (1997), previously called Blastomylonitic Formation by Delgado Quesada (1971). They form an intermediate nappe overlying a Parautochthonous Unit (Ábalos 1990) and overlain by another nappe where the Ediacaran Serie Negra succession is exposed. Neither the Parautochthonous nor the Serie Negra units were ever affected by HP metamorphism. The metamorphic regime in the Parautochthonous unit varies between the greenschist to the lower amphibolite facies and is of a Barrowian type (Chacón 1979; Ábalos 1990). In turn, the upper, Serie Negra nappe is generally under greenschist facies conditions except for LP-HP migmatite domes such as the Mina Afortunada dome described in Sect. 12.2.2 and developed during the Cambrian-Ordovician rifting event.

(2) The three tectonic units were intruded by Cambrian-lower Ordovician calcalkaline, subalkaline and peralkaline plutons (Priem et al. 1970; Lancelot and Allegret 1982; García Casquero et al. 1985; Ochsner 1993; Ordóñez Casado 1998; Solá et al. 2008; Sánchez García et al. 2008; Díez-Fernández et al. 2015), themselves never affected by HP metamorphism. Note that rocks (volcanic, subvolcanic and plutonic) with similar age and characteristics are widespread across the OMZ, associated to the rift-stage of the Variscan cycle (see Chap. 2 in this volume).

(3) Anchimetamorphic to very low grade Cambrian successions locally cover unconformably the highly deformed metamorphic rocks described above (Ouguela and Assumar synclines; Gonçalves 1971; Pereira 1999; Pereira and Silva 2002).

For the above and other reasons (see Quesada 1990a, b, 1997; Ábalos 1990; Quesada and Dallmeyer 1994), and despite the lack of compelling geochronological data, the latter point of view is adopted here and no further attention is paid to the HP rocks in the Badajoz-Córdoba shear zone. Instead, they are dealt with in detail in Chap. 6 (volume 1 of this publication), which is devoted to the Cadomian orogeny.

12.3.2.1 HP Metamorphism in the Pulo do Lobo and South Portuguese Terranes

C. Quesada, A. López-Carmona, J. Reche

Evidence for HP metamorphism in the Pulo do Lobo terrane and in the SPT is very meagre. In the SPT, Munhá (1990) described a systematic south to north increase in metamorphic grade, i.e. towards the suture, from the anchizone up to the lower greenschist facies but no evidence of HP relicts was reported. Only recently, Rubio Pascual et al. (2013a) also found evidence of high-pressure conditions within the so-called La Minilla formation (Matas et al. 2010), previously known as Ronquillo Fm (Simancas 1983), at the easternmost end of the SPT. This is a peculiar area profusely intruded by plutonic rocks of the Sierra Norte Batholith, around which thermal aureoles developed. The La Minilla Fm exhibits two fabric generations prior to the intrusion of the plutons, the oldest of which are dated at ca. 350 Ma (Barrie et al. 2002; Dunning et al. 2002; Braid et al. 2011, 2018; Gladney et al. 2014). This is at least 20 Ma older than the age of deformation of the well-established SPT stratigraphy, which started after deposition of the Late Visean Culm succession, i.e. after ca. 335 Ma (Quesada 1998). For this reason, if not an exotic fragment within the suture zone, the La Minilla Fm might represent a relative basement to the SPT. Unfortunately, no age control exists so far on either its deposition age or the age of deformation and metamorphism, other than the above mentioned age of the intrusives that provide a minimum age limit.

Most rocks in La Minilla Fm do not exhibit evidence of HP metamorphism. Only some metagreywacke samples contain the mineral assemblage phengite + albite + quartz + garnet + chlorite ± biotite ± rutile ± ilmenite, but white micas from these rocks have low silica content and do not witness HP conditions, probably due to re-equilibration during decompression (Rubio Pascual et al. 2013a). However, these authors were able to calculate P = 8.7 ± 0.4 GPa and T = 388 ± 16 °C conditions for the studied samples applying TWQ v2.3 (Berman 1991, 2007) multiequilibrium calculations.

On the other hand, the metamorphic mineral assenblages exhibited by the oldest rocks exposed in the Pulo do Lobo terrane (Alfarrobeira metabasalts, Peramora mélange, or Pulo do Lobo and Ribeira de Limas metasedimentary formations; see Chap. 5 in this volume) do not provide significant thermobarometric results, probably due to reequilibration at lower pressure conditions (see below under Sect. 12.5). However, N-MORB amphibolite layers and greenschists within the Peramora mélange (Eden 1991) show a foliation that wraps around some rhomboidal mm-sized epidote aggregates which resemble similar ones found in the lower allochthon of the Galicia-Trás-os-Montes Zone (Martínez Catalán et al. 1996; Rodríguez Aller 2005; López-Carmona et al. 2014). Following this model, Rubio Pascual et al. (2013a) interpreted the romb-shaped aggregates as pseudomorphs after lawsonite, estimating P–T conditions for lawsonite crystallization at around 0.5–0.7 GPa and ca. 200 °C (Fig. 12.6), consistent with a high structural position of the Pulo do Lobo unit in a subduction complex. The Pulo do Lobo schist Fm, which is thought to represent ocean floor sediments originally overlying the N-MORB metabasalts (Eden and Andrews 1990; Eden 1991; Braid et al. 2011, 2012; Dahn et al. 2014), currently appears tectonically imbricated with them in the Peramora mélange and has been recently dated as mid-Frasnian (ca. 375 Ma) on the basis of its palynomorph content (Pereira et al. 2018). This provides a maximum age constraint to the onset of subduction along the SW Iberia suture zone, which may have lasted until the onset on collision in the Late Visean (Quesada 1991, 1998). Nonetheless, the presently exposed rocks in the Pulo do Lobo terrane, especially the Peramora mélange, were already accreted to the margin of the OMZ at the time of intrusion of the oldest, subduction-related rocks of the Gil Márquez pluton ca. 354 Ma ago (Gladney et al. 2014; Braid et al. 2018), thus providing an upper time limit for development of the HP metamorphic event in the Pulo do Lobo terrane.

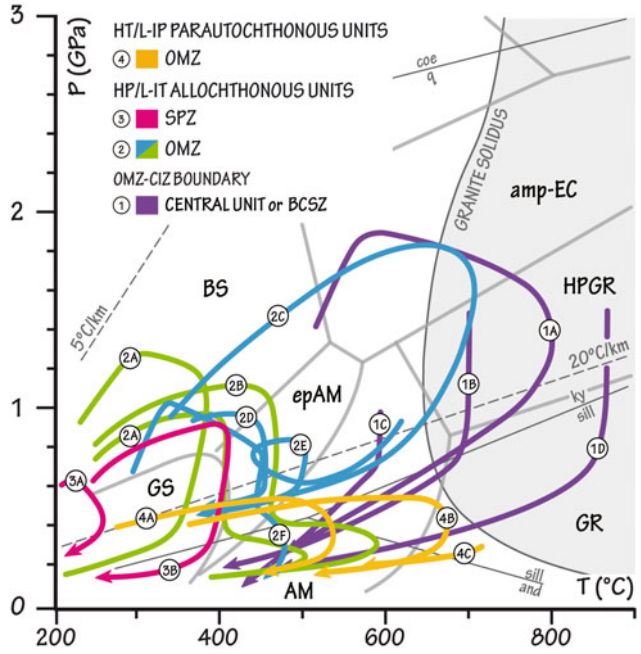

Fig. 12.6 Summary of the P–T paths recorded in the Ossa Morena and South Portuguese Zones. Proposed P–T paths recorded by the Central Unit (Badajoz-Córdoba Shear Zone; BCSZ) are: 1A (López Sánchez--Vizcaino et al. 2003); 1B–C, lower and upper part, respectively (Simancas et al. 2001); 1D (adapted from Pereira 1999). High-pressure and low- to intermediate-temperature (HP/L-IT) allochthonous units include: 2A, Cubito–Moura and 2B, Fuenteheridos Group (Rubio Pascual et al. 2013a); 2C–E (adapted from Leal 2001; see Fig. 12.8 for details) and 2F (Booth-Rea et al. 2006) in the Ossa Morena Zone (OMZ) and 3A, Pulo do Lobo unit and 3B, La Minilla Formation in the South Portuguese Zone (SPZ; Rubio Pascual et al. 2013a). High-temperature and low- to intermediate-pressure (HT/L-IP) para-utochthonous units from the OMZ comprise: 4A–B, Aracena Group and 4C, Beja–Acebuches amphibolite (Rubio Pascual et al. 2013a). Thick lines separate facies fields simplified after Spear (1993), Liou et al. (1998, 2009) and Okamoto and Maruyama (1999). Facies fields abbreviations: GS, greenschist facies; epAM, epidote-amphibolite facies; AM, amphibolite facies; BS, blueschist facies; ampEC, amphibole-eclogite facies; HPGR, high-pressure granulite facies; GR, granulite facies. Thin dashed lines represent geotherms of 5 and 20 °C/km. Stabilities of coesite (Hemingway et al. 1998), Al_2SiO_5 (Bohlen et al. 1991) and the minimum melting of granite solidus (Huang and Wyllie 1975) are shown for reference

12.3.2.2 High Pressure Metamorphism in the Southwestern Ossa-Morena Zone

N. Leal, P. Moita, J. Pedro, J. Reche, A. López-Carmona

Up until the beginning of the 1990s, with exception to the Badajoz-Córdoba shear zone, no occurrences of high-pressure metamorphic rocks were known in the Ossa Morena Zone (OMZ). Although De Jong et al. (1991a, b) described the ocurrence of bluish pleochroic alkaline amphiboles in greenschists from the Pedrógão-Moura region, they were interpreted as the result of protolith composition and not related to high-pressure metamorphism. Later, Fonseca et al. (1993) reported the presence of glaucophane-eclogitic rocks in the Alvito-Viana do Alentejo Region (AVAR in Fig. 12.7), related to a polyphasic eclogite facies prograde metamorphism (550 °C at 12 kb to 650 °C, at >15 kb) followed by amphibolite and greenschist facies retrograde conditions (<450–500 °C at 6–4 kb). These new data led to the discovery of up until then unknowned occurrences of Variscan high-pressure metamorphic rocks (Pedro et al. 1995a, b) in the Safira Region (SR in Fig. 12.7), and several works began being rolled out with special focus on the related metamorphic event in the OMZ (e.g. Pedro 1996; Moita 1997; Fonseca et al. 1999; Leal 2001, Booth-Rea et al. 2006; Rosas et al. 2008; Rubio Pascual et al. 2013a).

In the southwestern domains of the OMZ, where the Variscan high-pressure metamorphism has been recorded, two main tectonostratigraphic units should be considered: the OMZ Relative Autochthonous (OMZRA), represented in Spain by the so-called Fuenteheridos Group (Rubio Pascual et al. 2013a), and the allochthonous Moura Phyllonitic Complex (MPC; Araújo et al. 2005, 2013; Ribeiro et al. 2010), also known in Spain as Cubito-Moura unit (Rubio Pascual et al. 2013a; Pérez Cáceres 2017; Pérez Cáceres et al. 2017). The OMZRA is formed from bottom to top by (1) a Neoproterozoic metasedimentary-metavolcanic sequence with intercalations of metabasic rocks (Serie Negra); (2) a Cambrian (Lower-Middle?) carbonate sequence with interlayered metavolcanic rocks; and (3) a Cambrian/Ordovician to Silurian metasedimentary-metavolcanic sequence with intercalations of marbles and bimodal metavolcanic rocks. The MPC is an allochthonous complex, regarded as a tectonic mélange, that is mainly composed by micaschists showing frequent imbrications of Neoproterozoic-Lower Paleozoic rocks from the OMZRA, as well as klippen of a dismembered ophiolite sequence (Internal Ossa-Morena Zone Ophiolite Sequences; Pedro et al. 2010; see also Chap. 5 in this volume). Although the MPC has an uncertain Lower Paleozoic age, some enclosing imbricated bodies were affected by high-pressure metamorphism during the Late Devonian (Araújo et al. 2005; Booth-Rea et al. 2006; Rosas et al. 2008; Rubio Pascual et al. 2013a).

In the OMZRA, the Variscan high-pressure metamorphic rocks crop out as decimetric to metric eclogite lens-shaped bodies inside Neoproterozoic-Cambrian gneisses, garnet/quartz-feldspar micaschists and marbles. The eclogite parageneses are well-preserved in the core of the lenses, but at the edges they were overprinted by subsequent and widespread amphibolite to greenschist retrogression parageneses. The lenses of eclogites inside OMZRA gneisses and micaschists also occur as imbrications within the MPC. In turn, the main high-pressure feature of the MPC is the

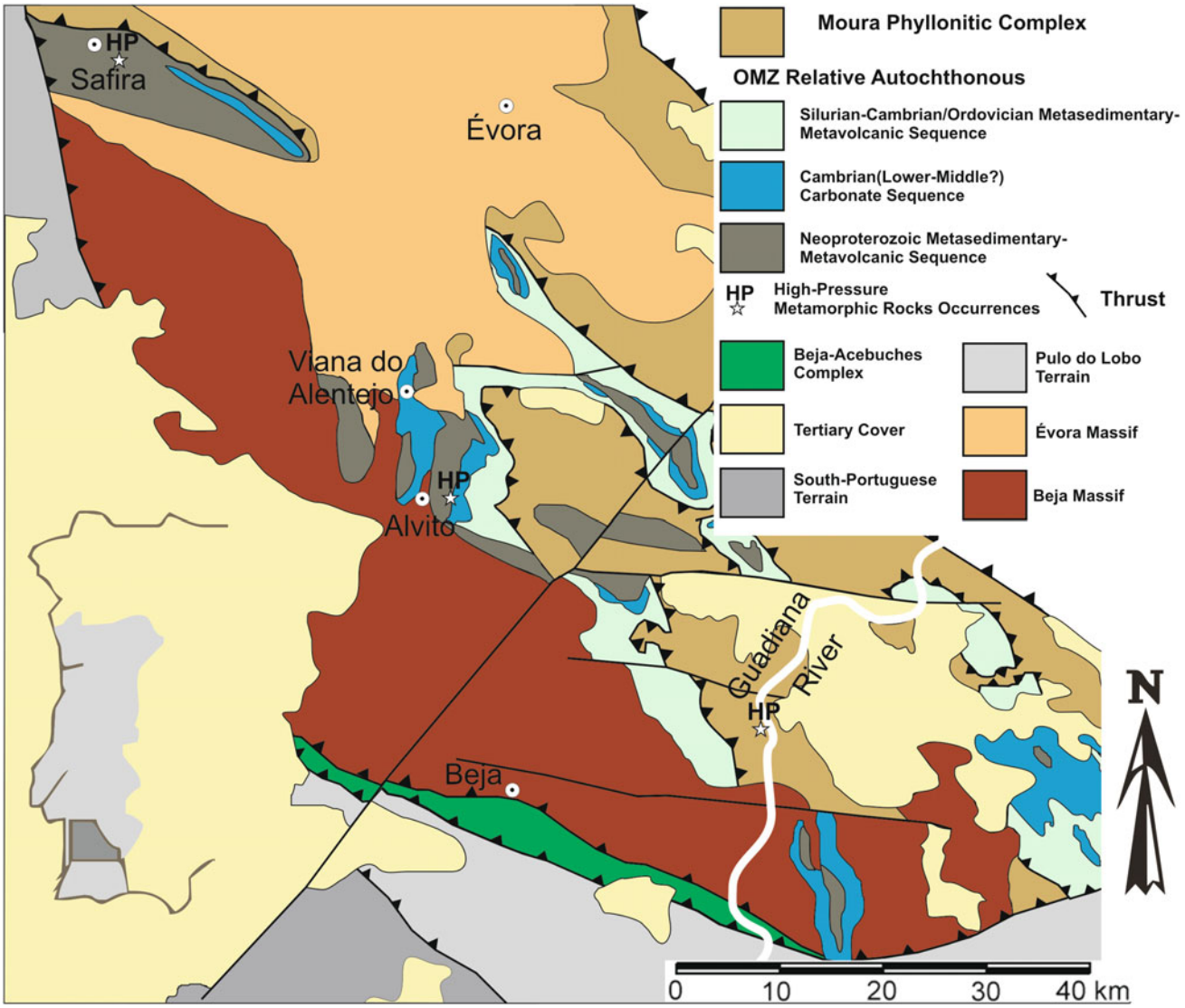

Fig. 12.7 Geological outline of the high-pressure metamorphic area in the Southwestern OMZ

presence of imbricates of Cambrian/Ordovician-Silurian OMZRA metabasic rocks affected by blueschist facies metamorphic recrystallisation. These occurrences were firstly described in the Guadiana Valley by De Jong et al. (1991a, b) and Araújo et al. (2005) and later in the Cubito-Moura Unit (Booth-Rea et al. 2006; Rubio Pascual et al. 2013a).

The eclogites and blueschists and their retrograded parageneses in the OMZRA present subalkaline tholeiitic basaltic/andesitic compositions, with depleted to slightly LREE enriched patterns. Detailed multi-elemental analysis suggests that the metabasics protoliths correspond to anorogenic continental basalts, which magmatic evolution took place by AFC processes, involving crustal material assimilation (Leal 2001), related with intrusion mechanism during a passive margin regime.

According to their metamorphic parageneses, the high-pressure rocks can be divided in two major groups: blueschist facies rocks and eclogite facies rocks. The blueschist facies rocks are composed by porphyroclasts of garnet + glaucophane, wrapped by a late syn-kinematic chlorite + plagioclase + barroisite + clinozoisite + quartz assemblage. Garnets are almandine-rich, sometimes with high spessartine contents (up to 27%, in the crystal cores). These rocks are interpreted as the remnants of a low geothermal gradient regime that underwent strong pervasive deformation. In some cases, however, the original assemblage was not deformed and experienced a period of increasing temperature and slight decrease in pressure, during which barroisite rims developed around the glaucophane crystals, followed by symplectite growth. The eclogite facies rocks are composed by garnet + omphacite + glaucophane,

frequently together with primary paragonite and clinozoisite. Garnet is almandine-rich, and omphacite is typically Jd_{50}. Textures are varied and range from granoblastic to granonematoblastic. The post-eclogite facies metamorphic path (decompression and/or retrogression processes) begins with the development of a bluish green amphibole (barroisite) rim in the contact between garnet and pyroxene (or glaucophane) crystals, not affecting the original textures; later, secondary paragonite partially or totally substitutes pyroxene; finally, symplectite develops, with simultaneous crystallization of plagioclase and amphibole. In some cases, porphyroclastic textures were developed. Locally, some retrograde eclogites developed late post-symplectite glaucophane porphyroblasts, together with green aegirinic pyroxene ($Quad_{70}Jd_{10}$), at the amphibolite/ greenschist facies conditions limit. The process ended with similar late syn- to post-kinematic greenschist facies recrystallization of all these rocks.

When analysed as a whole, the available data define a set of clockwise P-T-t paths that is interpreted as the result of a subduction mechanism (Fig. 12.8): an initial high-pressure low to medium temperature prograde stage, with blueschist and eclogite facies parageneses development, followed by exhumation, during which amphibolite and greenschist facies assemblages recrystallized. On the basis of amphibole $^{40}Ar/^{38}Ar$ and garnet Sm–Nd geochronology data, Moita et al. (2005) reported an age of 370 Ma for the eclogitization peak and 360 Ma for their subsequent exhumation. The above mentioned late baric peak followed by retrogression after the main clockwise P-T-t path defining a "loop" has been interpreted (Moita 1997; Fonseca et al. 1999) as a new burial before final eclogite exhumation and subsequent nappe emplacement on top of the OMZRA. However, invoking the very localised occurrence of these rocks, Leal (2001) suggested changes in the subduction channels sense, rather than to a major regional tectonic process. While recrystallizing during the exhumation process some of the rocks that previously underwent high-pressure conditions could accrete to the footwall descending slab. Later accretion to the hanging wall could restart exhumation. The presence of kyanite inclusions in micaschist garnet, primary aragonite in marbles and high-Si contents in phengites from the Serie Negra graphitic micaschist, recrystallized during the retrograde stage, as well as quartz-feldspar lithologies P-T estimates suggest that other lithologies of the OMZRA may have experienced the same tectonometamorphic event. Mafic rocks may have had an important role in the preservation of some of the high-pressure assemblages during the decompression stage, acting as a buffer envelope, inhibiting major retrogression recrystallization, and acting as lubricants and partially accommodating the deformation involved, thus preventing stronger damaging of the eclogites original textures.

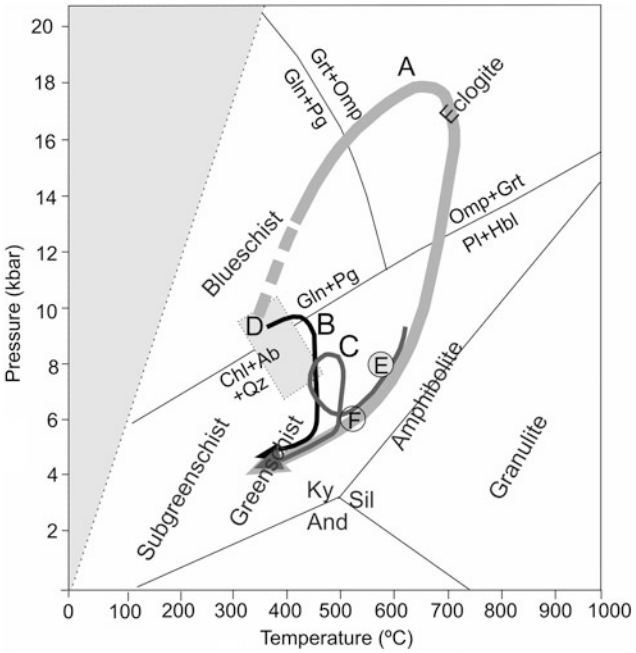

Fig. 12.8 Pressure versus temperature diagram, showing the Pressure-Temperature-time paths for metabasic rocks from OMZRA: A—Omphacitic eclogites; B—Blueschists; C—Porphyroblastic-amphibolite (adapted from Leal 2001) and for MPC: D—Blueschists (Booth-Rea et al. 2006); E—Quartz-feldspatic rock from Safira region (Pedro 1996); F—Quartz-feldspatic rock from Alvito-Viana do Alentejo region (Fonseca et al. 1999). Metamorphic facies, equilibrium equations and stability fields adapted from Bucher and Frey (1994). Mineral abbreviations (Whitney and Evans 2010): Brs—Barroisite; Ep—Epidote; Fsp—Feldspar; Gln—Glaucophane; Grt—Garnet; Omp—Omphacite; Chl—Chlorite; Ab—Albite; Pg—Paragonite; Pl—Plagioclase; Hbl—Hornblende; Qz—Quartz; Ky—Kyanite; Sil—Silimanite; And—Andalusite

As previous mentioned, the MPC is a major unit made up by micaschists and a large diversity of rocks imbrications overprinted by a late widespread recrystallisation in greenschist facies. Nevertheless, in some preserved sectors, like in Guadiana Valley, it is possible to recognise an early blueschist facies metamorphic recrystallisation event (Booth-Rea et al. 2006; Rubio Pascual et al. 2013a) recorded in metabasic rocks imbrications from the Cambrian/Ordovician to Silurian metasedimentary-metavolcanic sequence of the OMZRA. In thin section, amphibole from metabasic exhibit bluish/pale violet colors (glaucophane/crossite, glaucophane-riebeckite to winchite compositions) and green to uncolored rims (actinolitic horneblende to actinolite). This composition evolution is interpreted as the record of an early Variscan high-pressure event (e.g. Araújo et al. 2005), correlated with the overpressure due to nappe emplacement, followed by late widespread greenschist facies recrystallisation.

According to Pérez-Cáceres (2017) the allocthonous complex (Cubito-Moura unit) was emplaced over the OMZ

parauthocton-authocton, becoming part of a set of sub-parallel units (see Sect. 12.5) of which only some of them recorded high-pressure conditions. Blueschist-facies conditions of ca. 0.9–1.0 GPa and 340–370 °C were inferred in the Cubito-Moura unit by Booth-Rea et al. (2006) using multiequilibrium thermobarometry in chloritoid-bearing phyllites (Fig. 12.6). Refined multiequilibrium P–T calculations together with detailed kinematic structural data where presented by Ponce et al. (2012) and provided 0.9–1.2 GPa and 300–400 °C conditions for the high-pressure event. These authors compared the obtained conditions with the eclogitic P–T conditions of ca. 1.5 GPa and 650 °C estimated by Fonseca et al. (1999, 2004) and Araujo et al. (2005) in the amphibolite boudins and proposed that different units of the same complex may have not experienced identical P–T paths within the subduction channel, suggesting a tectonic mélange character for the complex in line with the interpretation by Leal (2001). Conventional thermobarometry calculations yielded P–T conditions of ca. 1.24 GPa and 310 ± 11 °C (lawsonite-blueschist-facies conditions) in the structurally lower imbricates of the Cubito-Moura unit. Similar geothermobarometers applied to samples from upper structural levels yielded 0.92 GPa and 395 ± 45 °C, similar to those obtained by Booth-Rea et al. (2006) (Fig. 12.6).

Recently, on the basis of some similarities between the HP units in the OMZ and the Lower Allocthton (basal units) of the Galicia-Tras-os-Montes Zone, including the age of the metamorphic peak, Díez Fernández and Arenas (2015) have postulated the existence of a huge elongated allocthonous unit subducted during the late Devonian (ca. 370 Ma) and subsequently exhumed and emplaced throughout the lower Carboniferous (350–340 Ma) onto the Gondwana margin. Based on this correlation, Arenas et al. (2016a) proposed the existence of a new zone in the Iberian Massif so called the Galicia-Ossa Morena zone. This hypothesis has been seriously questioned by Simancas et al. (2016) and has not gained wide acceptance so far.

12.4 An Enigma, or Out-of-Place?

12.4.1 Metamorfic Evolution of the Farilhões Anatectic Complex (Berlengas Archipelago): Geodynamic Implications

T. Bento dos Santos, P. Valverde Vaquero, M. L. Ribeiro, A. R. Solá, E. González-Clavijo, A. Díez-Montes, Í. Dias da Silva

The Berlengas Archipelago, located 15 km west of the Portuguese continental shore, constitutes the westernmost exposure of the Iberian Massif (Fig. 12.9) and is composed by the Berlengas Group, the main set of islands that includes the Estelas islets, and the Farilhões-Forcadas Group, a set of islets located 10 km NW (Freire de Andrade 1937). In geological terms, the Berlengas crustal block consists of:

- The Berlengas Granite, a late-Variscan coarse-grained biotitic granite (zircon and monazite ID-TIMS U-Pb age of 305.2 ± 0.5 Ma; Valverde Vaquero et al. 2011), profusely episyenitized. This granite had previously been dated at 280 ± 15 Ma (Whole-rock Rb-Sr age; Priem et al. 1965):
- The Farilhões Anatectic Complex, displaying diatexites, metatexites and small-scale granulite relics (Bento dos Santos et al. 2010).

In the Farilhões Anatectic Complex, the diatexites, previously named Farilhões gneissic granitoid (Bento dos Santos et al. 2010) and Farilhões anatectic granitoid (Valverde Vaquero et al. 2011) occupy the largest portion of the Farilhões islets and are medium to fine-grained. They are composed of quartz, K-feldspar, plagioclase, sillimanite, biotite and retrograde muscovite, presenting pervasive ductile deformation. The diatexite has an ID-TIMS U-Pb monazite and zircon concordia age of 380.0 ± 3.0 (Valverde Vaquero et al. 2011). In addition, LA-ICP-MS U-Pb dating of zircon also revealed the presence of Cadomian (550–650 Ma) inherited grains.

The metatexites also show intense ductile deformation, being frequently folded, and are composed of paleosomes and neosomes that broadly display the same mineral assemblages, although with different mineral proportions: plagioclase + K-feldspar + quartz + biotite ± muscovite ± garnet ± sillimanite ± graphite. Due to their genetic relationship, age constrains for the metatexites are the same as for the diatexites.

Granulite relics occur as decimetric pockets placed near a N-S fault within the metatexites, obfuscating the interpretation of their geological meaning and geodynamic context. These are composed by plagioclase + quartz + biotite + amphibole ± garnet ± clinopyroxene ± ilmenite ± titanite. The granulites present an M1 prograde metamorphic paragenesis composed of plagioclase (XAn = 0.94) + quartz + type-1 grossular-rich garnet (XGross = 0.75–0.76; Fe/Mg = 8.5–16.2) + clinopyroxene (Fe/Mg = 0.55–0.58) that define P-T conditions consistent with the baric peak at P = 8.6 ± 1 kbar and T = 915 ± 50 °C, followed by an M2 paragenesis composed of plagioclase (XAn = 0.90) + quartz + type-1 grossular-rich garnet (XGross = 0.72–0.81; Fe/Mg = 22.9–28.1) + clinopyroxene (Fe/Mg = 1.5–2.0), representative of the establishment of the metamorphic peak temperature at T = 950 ± 50 °C during decompression to P = 6 ± 1 kbar (Bento dos Santos et al. 2010) (Fig. 12.10).

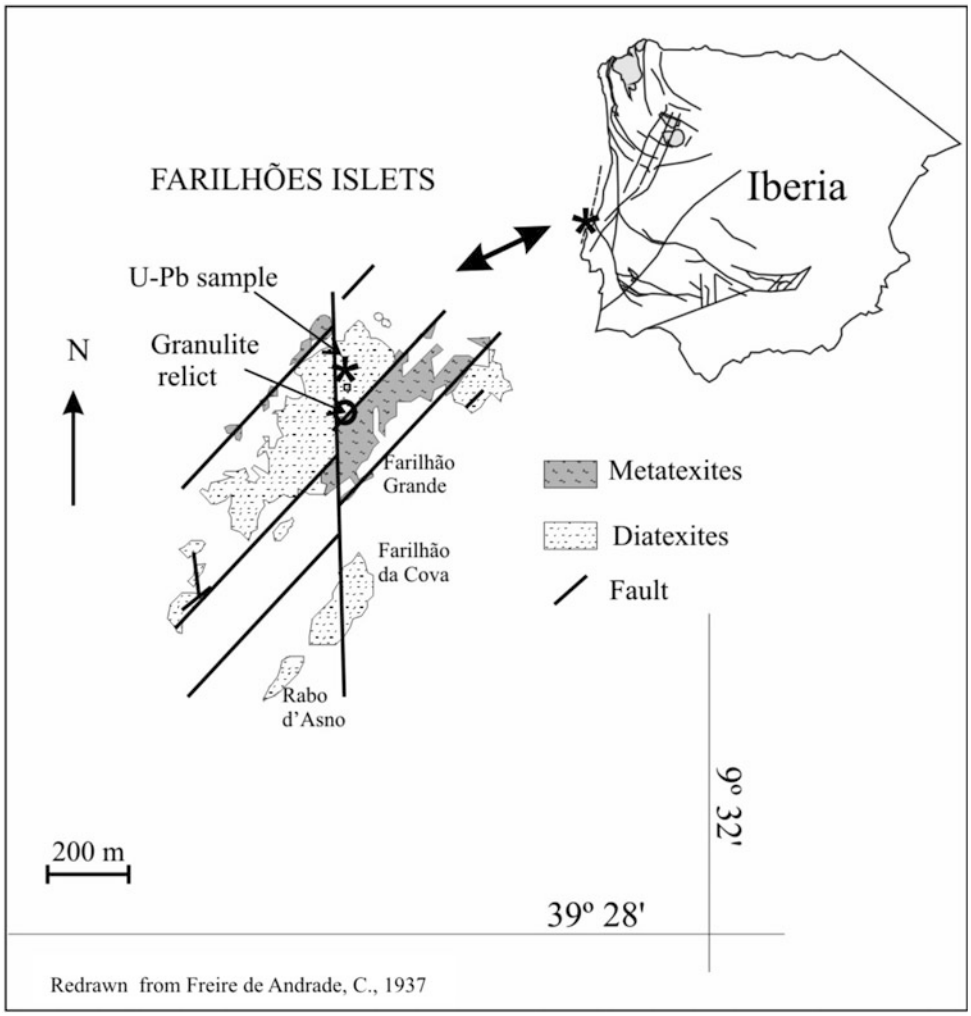

Fig. 12.9 Geological map of the Farilhões Islets (modified from Freire de Andrade 1937) and their location relative to the main structures of the Iberian Peninsula

This prograde metamorphic trajectory reached the amphibole dehydration-melting curve (Patiño Douce and Beard 1995). Asthenospheric upwelling and/or magma underplating was considered to explain this P-T path (Bento dos Santos et al. 2010). Retrogressive stages to lower P and T show an M3 assemblage with plagioclase (XAn = 0.98) + quartz + biotite + type-2 almandine-rich garnet (XGross = 0.23–0.33; XSpss = 0.12–0.15; Fe/Mg = 5.0–7.5) ± amphibole ± ilmenite ± clinopyroxene relics (Fe/Mg = 0.86–0.89), implying T ≈ 720 °C and P ≈ 5 kbar. Continuous exhumation to T ≈ 630 °C and P ≈ 3.5 kbar (P-T estimates on the rims of type-2 almandine-rich garnet and clinopyroxene) are consistent with very high thermal flux at shallow depths. Water influx during retrogression provided late crystallization of plagioclase + biotite + amphibole + ilmenite ± titanite (Bento dos Santos et al. 2010).

The metatexites have a prograde paragenesis composed of plagioclase (XAn = 0.29–0.33) + K-feldspar + quartz + type-3 almandine-rich garnet (XGross = 0.046–0.074; Fe/Mg = 5.4–6.3) + biotite (Fe/Mg = 1.08–1.27) ± sillimanite that defines a metamorphic peak of T ≈ 720 °C and P ≈ 5.5 kbar and a retrogressive stage of T ≈ 600 °C and P ≈ 4.5 kbar (P-T estimates on the rims of type-3 garnet and nearby matrix biotite). This P-T evolution is very similar to the M3 metamorphic stage of the granulites, suggesting juxtaposition of the granulites with the metatexites during the Variscan Orogeny (Bento dos Santos et al. 2010).

However, the granulite facies metamorphism and the late Devonian 380 Ma MP/HT crustal anatexis in the Farilhões Islands (M3 event) are not easily explained. The geographical position of this crustal block leaves open the possibility that it may represent a basement belonging either to:

- The Ossa Morena Zone, where the nearest granulite outcrop close to its northern border (about 100 km east) displayed 540 Ma ages (Henriques et al. 2015) and do not record any younger age. Similar ca. 370–380 Ma ages are recorded in OMZ but they correspond to the

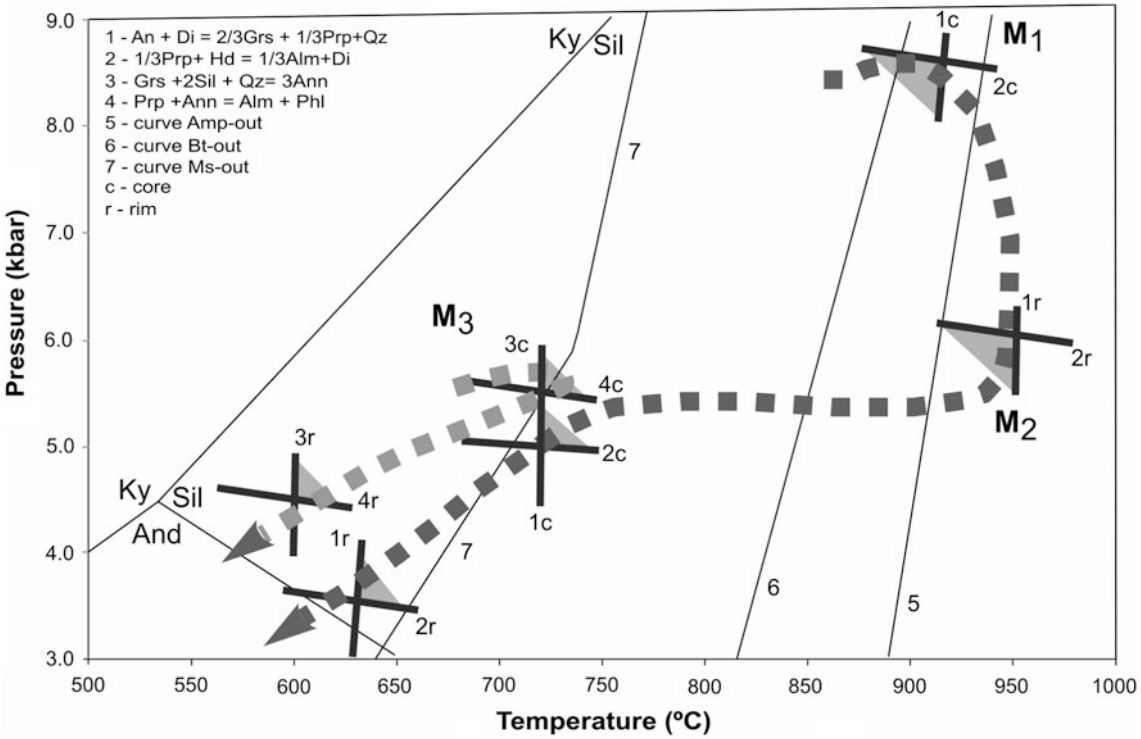

Fig. 12.10 Summary of the P-T-t evolution of the Farilhões Anatectic Complex rocks (Bento dos Santos et al. 2010). The metamorphic stages and P-T evolution (given by arrows) corresponding to the migmatites are shown in grey, whereas black refers to the granulites

high-pressure metamorphic facies described in the previous section (Moita et al. 2005).

- The South Portuguese Terrane (since this domain is considered equivalent to the Meguma terrane of Avalonia (380–370 Ma metamorphism and deformation), located in the opposing Atlantic margin in the Grand Banks of Newfoundland) (Braid et al. 2011; Pereira et al. 2014).
- The SW England Variscan domain, such as the granulite facies event coeval with the formation of the Lizard ophiolite at 392 Ma with plutonism at 376–373 Ma (Shail and Leveridge 2009);
- Another terrane, also belonging to the Variscan orogenic system, whose analogue has not yet been fully featured (e.g. Ribeiro et al. 2007; Ribeiro 2013; Ballèvre et al. 2009). In this respect, the recently proposed Finisterra-Léon-Mid German Cristalline Rise terrane (see Chap. 7 in this volume) appears as a suitable candidate.

12.5 Syn-collisional to Post-collisional MP and HT/LP Metamorphism

C. Aguilar, M. Liesa, F. J. Martínez, M. H. Mendes, C. Quesada, J. Reche, M. L. Ribeiro, J. F. Santos

12.5.1 The Iberian Massif

F. J. Martínez, M. H. Mendes, C. Quesada, J. Reche, M. L. Ribeiro, J. F. Santos

12.5.1.1 The Schistose Domain of the Galicia-Trás-Os-Montes Zone

M. L. Ribeiro

The Galicia-Trás-os-Montes Zone covers an important area from NW Iberia. The geological map of this zone shows a large Parautochthonous Thrust Complex (Ribeiro et al. 1990a), also entitled (Farias and Marcos 2004) Schistose Domain of the Galicia-Trás-os-Montes Zone (SDGTZ). In the southeast of the zone, where the SDGTZ surrounds the allochthonous massifs of Bragança and Morais the regional metasediments display low-grade metamorphic facies usually in the chlorite and biotite zones of greenschist facies (and, occasionally, relics of the blueschist facies: see above under Sect. 12.3.1.3). The textural data show a locally penetrative 2nd deformation phase with synchronous metamorphic mineral recrystallization that does not fully erase the macrostructures of the 1st phase (subduction-related). The 3rd phase of deformation is generally weak, producing NW–SE crenulations with vertical axial plane.

However, when we move away towards the NW from the inner regions of SDGTM, and consequently of the allochthonous massifs, the metamorphic pattern described above may change. Indeed, at Tourém and Monção areas (Fig. 12.3) metamorphism can reach high grades with development of migmatites and the appearance of heterogeneous granites. The Tourém area is located inside the SDGTZ near the northern border of Portugal. In this area two lithostratigraphic units were mapped: the Quartzites and Quartzite Schists, at the base, and the Pelitic Schists and Paragneiss interbedded with black cherts and calk-silicate rocks, at the top (Martins and Ribeiro 1979). These units adscribed to a Silurian age (by stratigraphic correlation) were related with units in their extension to the East (south of Vinhais) and apparently extend to their northern neighbouring region (Farias and Marcos 2004). Migmatites, granites and some small basic dykes intruded these metasediments. Ordovician orthogneiss dated at 468 ± 32 Ma (whole-rock Rb-Sr analyses; Schermerhorn, personal communication 1986) are also recorded nearby Padroso village (Martins and Ribeiro 1979).

All major phases of Variscan deformation were observed in the area: 1st phase displays very tight isoclinal folds, with NW-SE axial-plane foliation and sub-horizontal axes, slightly plunging to the SE; the 2nd phase is responsible for an open synform (west of Padroso village) with subvertical axial plane, gently sloping to the south. On the flanks of this synform smaller antithetic folds formed with axial-plane cleavage (S2) and hinges sub-parallel to that of the macro-structure. S2 tends to erase the foliation S1. Locally, some granitic dykes (thickness <1 m) were bent by the 2nd phase (Martins and Ribeiro 1979); these granitic dykes display a plane-linear fabric concordant with S2. The structural relationships suggest that the high-grade gneiss, the migmatites and the granitic dyke emplacement can be correlated with the 2nd phase of deformation (Moreira and Ribeiro 1991). The 3rd phase of deformation is more penetrative in the SW of the region where it originates vertical kilometric folds of NW-SE orientation. To the south of Tourém the 3rd phase is responsible for the SW tilting of the 1st and 2nd phase structures. Thus, 1st phase folds may have had, originally, subhorizontal axial planes. The sequence of the deformation phases is everywhere comparable to that of Eastern-Trás-os-Montes (Ribeiro 1974). Clearly the Tourém area was also affected by a Variscan polyphase deformation and metamorphism (Ribeiro 1978; Martins and Ribeiro 1979; Ribeiro 1980; Noronha and Ribeiro 1983). Predominant mineral assemblages in calc-silicate rocks are: Cpx + Pl and Cpx + Pl ± Grt. Quartz and plagioclase (73–92% An) are ubiquitous and subordinate mineral assemblages include: Spinel ± apatite ± clinozoisite ± sericite ± amphibole ± calcite ± ilmenite (see Whitney and Evans 2010). The basic dykes occur inside the regional (heterogeneous) granite and were recrystallized to hornblende + plagioclase ± clinopyroxene ± apatite ± ilmenite ± spinel ± biotite ± chlorite ± clinozoisite.

Mineral assemblages of regional metapelites allowed identifying the staurolite-andalusite ± fibrolite and the sillimanite + Kfeldspar zones. Staurolite recrystallization precedes the growth of andalusite; garnet is uncommon although it is somewhat more abundant in the southern part of the region; cordierite is mostly retrograded; fibrolite occurs near granitic bodies and mainly included in quartz, muscovite and biotite. Two main simplified reactions were inferred from mineralogical analyses:

$K_2Fe_5Al(OH)_4Si_5Al_3O_{20} + SiO_2 = 2KAlSi_3O_8 + Al_2SiO_5 + 2H_2O + 5FeO$, explaining the growth of sillimanite from biotite (not excluding the andalusite/sillimanite inversion) and muscovite + quartz = sillimanite + K-feldspar + 2 water related with the quartz- and water-saturated muscovite breakdown.

To explain the discrete presence of cordierite in some mineral assemblages with potassium feldspar + sillimanite ± andalusite and also in the granite of Covelães the following reaction was proposed: 2 biotite + 6 sillimanite + 9 quartz = 3 cordierite + 2 K-feldspar + Liquid + Vapour, explaining the cordierite growth in migmatites as a consequence of the incongruent melting of biotite (Ribeiro and Munhá 1983–1985). However, this is yet an open question, and in fact, the presence of cordierite in the highest metamorphic grades of the Tourém area seems to fit better in the retrograde path of the metamorphic process (Fig. 12.11).

Calc-silicate rock mineral assemblages suggest PT conditions lower than 630 °C and 5kbar. The parageneses found in metapelites grew between the second and third phases of deformation. PT conditions of metamorphism were estimated at 3–4 Kb and 600º–700 °C (Ribeiro 1980). On the other hand, PT conditions estimated for generation of the Parada leucogranite (included in the regional heterogeneous granite) are 4–8 kb and 700–750 °C; furthermore, the normative composition of Parada leucogranite is consistent with the eutectic minimum at 3 kb. The above considerations led to characterize the Tourém regional metamorphic episode as of low-pressure intermediate type.

The Monção area is located about 50 km Northwest of Tourém, and both areas belong to the same tectonic domain. However, Monção and Tourém regions display significant differences in terms of metamorphic patterns. The most conspicuous mineralogical and textural features in each region are: (1) The early growth (1st phase) of staurolite minerals in Tourém where it remains, as a relic in andalusite porphiroblasts; (2) the long-term and widespread occurrence of cordierite (early 2nd phase) in Monção, whereas in Tourém cordierite development only occurs at the metamorphic peak by incongruent melting of biotite; (3) the granoblastic textures visible in Tourém, that do not occur in

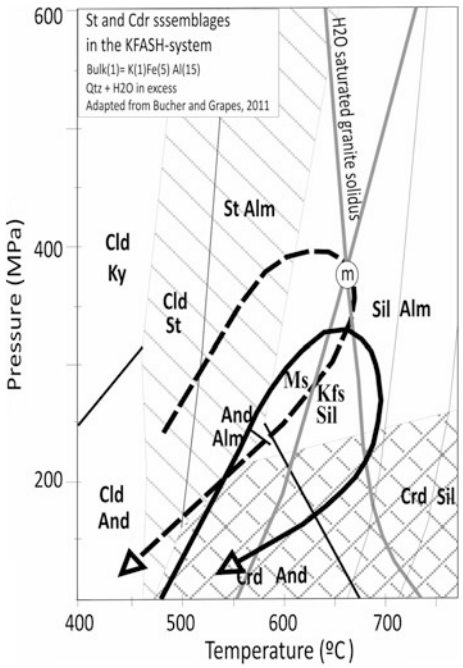

Fig. 12.11 Diagram P-T showing two possible PT-paths for the studied regions of Tourém (dashed line) and Monção (full line)

the Monção area. For both regions, textural data indicate distinct metamorphic evolution patterns; an earlier and rapid heating process at Monção contrasts with slower and also younger isothermal rise in the Tourém region. The thermal peak reached partial melting with the production of migmatites and heterogeneous granites. Figure 12.11 displays the two possible general PTt paths using one appropriate metapelitic composition on their correspondent staurolite and cordierite fields. Tourém (dashed line) and Monção (full line) indicate some different PT in these areas to achieve granitic melt production.

The conspicuous presence of cordierite accompanying the mineral assemblages of metamorphic high degrees of the Monção area suggests that more water was available at the time of the crustal partial melting of this area. This fact, the presence of major faults and the large amount of granitic rocks outcropping in the region contributed to the partial melting being reached at a lower pressure than at Tourém area. Equivalent paths were found in the CIZ (Arenas and Martínez Catalán 2002; Areias 2014).

12.5.1.2 The Central Iberian and West-Asturian Leonese Zones

J. Reche, F. J. Martínez

The metamorphic areas on the Central Iberian (CIZ) and West Asturian-Leonese (WALZ) zones depict elongated metamorphic belts (Martínez and Rolet 1988) subparallel to the main arcuate structural trends of the Variscan chain. From more internal (CIZ) to less internal (WALZ) zones, this belts are: Porto-Viseu, Vila Real-Moncorvo-Vitigudino-Guadarrama, Santa Comba-Santiago-Bande, Finisterre-La Guardia, Puentes de García Rodríguez-Sanabria, Viveiro-Lugo-Sarria, Boal-Los Ancares and Novellana-Pola de Allande-Degaña. Metamorphism reached the high grade granulite facies and is delineated by thermal domes nearly coincidental with structural antiformal-dome like structures (Martínez et al. 1988). Away from the domal-antiformal axes metamorphic grade decreases quickly to greenschist facies in few kilometres.

Following Alcock et al. (2015), who synthesized the time relationships between metamorphism, deformation and magmatic events, the P–T evolution began with a prograde medium-P Barrowian event (M_1) related with a deformational compressional D_1 event at 359–347 Ma (Dallmeyer et al. 1997; Rubio-Pascual et al. 2013b), producing large overturned to recumbent folds and just before the also compressional D2 event that produced the emplacement of the Galicia-Trás-os-Montes Zone (GTMZ) alloctonous nappe stack at 345–335 Ma (Dallmeyer et al. 1997). The compressional event generated an anomalous geotherm that led finally to transient thermal relaxation. The thermal relaxation led to heating and softening of the crust that must have taken place at still increasing pressure or at previously attained medium pressures and isobarically on the parautochthonous/autochthonous units or on units located below reverse limbs of large recumbent folds or nappe stacks. Nevertheless, in the upper thrust units and in normal large fold limbs the heating episode would be at approximate constant and lower pressures according to accepted tectonothermal modelling since the pioneering work of England and Richardson (1977) and England and Thopmson (1984). Heating due to thermal relaxation in both cases directed the P–T paths towards conditions reaching eventually the sillimanite field either from the kyanite field, in the parautochthonous middle-lower crustal units or in the footwall of nappe stacks, or from the andalusite field in the hanging wall of allochthonous nappes or recumbent folds, in the higher crustal units. These events of increasing temperature contributed to the initial segments of the M_2 high-temperature and low-pressure metamorphic episode that woud lead to supra-solidus conditions in the middle-lower crust (therafter the cores of the D_3 domes) and eventually, and much less frequently in the peripheric upper crustal units.

Following Escuder Viruete et al. (1997) and Alcock et al. (2015) heating would finally led to a gravitationally driven extension of the previously thickened crust simultaneous with decompression and melting in the lower crustal units and also to voluminous granitic magmatism intruding this

units. This would contribute to the highest temperature segments of the P–T paths. The thermal relaxation has been dated at 340–327 Ma and the migmatites coeval with extension at 329–316 Ma (Valverde-Vaquero and Dunning 2000; Rubio-Pascual et al. 2013b; López-Moro et al. 2018). The oldest Variscan intrusions range 325–320 Ma, according to Fernández-Suárez et al. (2000b) and Valverde-Vaquero et al. (2007). They are I-type, meta-aluminous granodiorites and tonalites sometimes accompanied with more mafic varieties (quartz-diorites, diorites, gabbros and hornblendites) and derived by melting of the lower crust with some mantle influences (Capdevila 1969; Galán et al. 1996). For Alcock et al. (2015) the emplacement and crystallization of these granitoids was syn-kynematic extensional. Then, the M_2 high-temperature and low-pressure metamorphic event is also syn-kynematic and extensional. Heating from the magma bodies would contribute to the high-temperature, quasi-isothermal decompression during continuing extension in the overthrust lower parautochthonous units and to lower pressure, near-isobaric increase in temperature in the upper units. This is the high-temperature decompressional part of M_2 in the dome cores (Alcock et al. 2015) and would constitute the episode leading to peak temperature conditions of M_2 in peripheral areas. Due to the previous softening of the crust and generation of granitoid-migmatitic areas a new generation of folds with subvertical axial planes (D_3) contributed to the ascent of granitic-granulitic-migmatitic domes. Continued extensional deformation (D_2) took place at the limbs of these D_3 domes, dated between 310–305 Ma (Fernández-Suárez et al. 2000b). The D_3 folds/domes would have developed coeval with intrusion of S-type, per-aluminous two-mica granites and monzogranites between 320–305 Ma with a maximum at 307 Ma (Martínez Catalán et al. 2014). Intrusion would have been simultaneous to M_2 peak temperatures. The retrogression (M_3) from peak temperatures postdated S-type granitoid crystallization and was coeval to D_3 and continued extension in the dome limbs. In the periphery of the M_3 domes the metamorphic evolution corresponds to a simple isobaric cooling or cooling associated to local burial tied to synformal formation (Reche et al. 1998). I-type late to post-kinematic granodiorites to monzogranites continued to intrude at upper Carboniferous—lower Permian times 310–285 Ma (Fernández-Suárez et al. 2000b; Gutiérrez Alonso et al. 2011). They produced local contact-like metamorphic effects, mainly concentrated in the peripheral, lower grade areas.

Selected areas where the metamorphic evolution in the internal parts (CIZ) has been studied in more detail in the last years pertain to the elongated belts: Viveiro-Lugo-Sarria (Reche et al. 1998; Arenas and Martínez Catalán 2003), Vila-Real-Vitigudino at El Tormes dome (Gil Ibarguchi and Martínez 1982; Martínez et al. 1988; Escuder-Viruete et al. 1997, 2000), the Spanish Central System in Guadarrama-Somosierra (Casquet and Navidad 1985; Barbero and Villaseca 2000; Rubio-Pascual et al. 2013b; Rubio-Pascual et al. 2016) and the Toledo Anatectic complex (Barbero 1995). Some of the best constrained P-T paths for the internal parts of the dome-sized areas of the CIZ are summarized in Fig. 12.12.

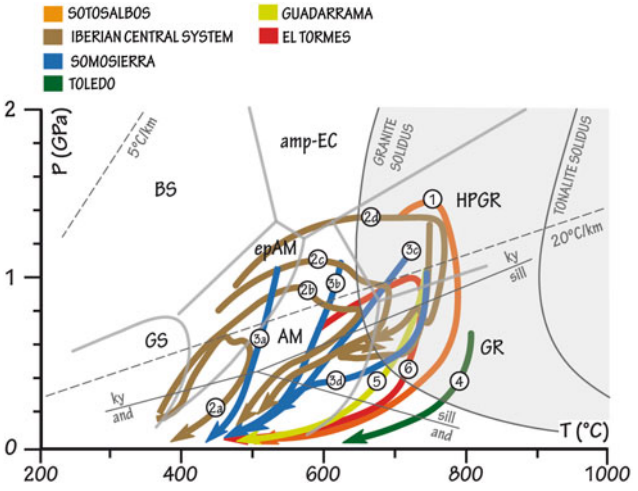

Fig. 12.12 Summary of the P–T paths recorded in the cores of domal areas of the CIZ. 1: P-T path proposed for the Sotosalbos domain by Barbero and Villaseca (2000). 2a, b, c and d: P-T paths deduced for the Iberian Central System (Somosierra) garnet, staurolite, sillimanite and sillimanite + K-feldspar metamorphic zones, respectively by Rubio Pascual et al. (2013b). 3a, b, c and d: P-T paths deduced by pseudosection modelling for Somosierra samples of the garnet, staurolite, sillimanite and sillimanite + K-feldspar zones respectively by Rubio Pascual et al. (2016). 4: P-T path for the Anatetic complex of Toledo (Barbero 1995). 5: Guadarrama P-T path, after Escuder Viruete et al. (1998). 6: P-T path for el Tormes Dome (Escuder Viruete et al. 2000). Thick lines separate facies fields simplified after Spear (1993), Liou et al. (1998, 2009) and Okamoto and Maruyama (1999). Facies fields abbreviations: GS, greenschist facies; epAM, epidote-amphibolite facies; AM, amphibolite facies; BS, blueschist facies; ampEC, amphibole-eclogite facies; HPGR, high-pressure granulite facies; GR, granulite facies. Thin dashed lines represent geotherms of 5 and 20 °C/km. Al_2SiO_5 (Bohlen et al. 1991) and the minimum melting of granite solidus (Huang and Wyllie 1975) are shown for reference

Reche et al. (1998), later complemented by Martínez et al. (2001, 2004), provided a detailed study centered in an extensional D_3 fault zone (the Viveiro fault zone) bounded towards the W by the VPB (Viveiro pelite belt) and further W by the Ollo de Sapo antiformal domain, and to the E by the Lugo dome. This area can be depicted as an example of the metamorphic evolution of non migmatitic domes and their periphery in the CIZ. The P–T paths on the Ordovician-Silurian Al-rich black metapelites of the VPB were studied in detail in Reche et al. (1998) and Martínez et al. (2001) and show the aluminosilicate sequence andalusite-kyanite-andalusite. In the Cantabrian coast, at the northern part of the VPB synformal structure, far from

granite intrusives and from the contact with the Lugo dome (Area I), the authors show the replacement of post S_1, pre-S_2 chiastolitic andalusite (andalusite-I) porphyroblasts by aggregates of kyanite and micas. Matrix assemblage I is: kyanite + chloritoid + chlorite + muscovite. In an area (Area II) near to the Viveiro fault, the Lugo dome and the Murás milonitic, syn-kynematic granitoid an assemblage II is found with: kyanite + staurolite + chlorite + muscovite ± relict cloritoid. The samples are variably affected by an S_3 sub-horizontal cleavage related to collapse of subvertical S_{1+2} due to a transtensional activity of the Viveiro fault zone. Staurolite in these samples is locally syn-S_3 and overgrowths pre-S_3 kyanite and chloritoid. Kyanite—muscovite aggregates similar to those found in Areas I and II appear also bent by the S_3 fault-related cleavage. A third assemblage, found in the same area II is: andalusite II + staurolite + biotite + muscovite ± plagioclase. The hornfels-like samples show andalusite porphyroblasts that are clearly post-S_3. In the matrix, remnants of assemblage II with resorbed kyanite and staurolite relicts are still seen and lens shaped mica-rich aggregates after andalusite I are also visible. Using a pseudosection analysis of the former paragenesis in the VPB the authors deduced a P–T path with two main segments: first a increase in pressure from ca. 0.225 to 0.4–0.45 GPa acting on previously andalusite I bearing assemblages, and then a clockwise segment of increasing T for samples near synkinematic granites in Area II, going from the kyanite + staurolite + chlorite through the andalusite II + staurolite + chlorite to the andalusite II + staurolite + biotite and finally andalusite II + biotite fields.

On the other hand, the assemblages studied in the psamo-pelites from the nearby western Lugo dome area, in the footwall of the Viveiro fault permitted deducing a general decompressive P–T path with some temperature increase in its middle part. There, assemblages with garnet + staurolite + chlorite are replaced during decompression by garnet + staurolite + andalusite (±sillimanite) + biotite, garnet + andalusite + biotite and finally by garnet + andalusite + cordierite + biotite.

Samples with Andalusite I in the VPB imply an anomalous pre-D_2 (42–48 °C/km) geothermal gradient probably linked to the effect of the earlier I-type intrusives. As the VPB constitutes the hanging wall of the Viveiro fault zone this is coherent with the kyanite replacing andalusite I in the VPB and not related to the earlier Barrowian evolution postulated in other areas that, if present, was already overprinted by andalusite I. In the footwall, Lugo dome, the decompressional P–T paths would have been related by the steep-folding D_3 stage that triggered the exhumation of the earlier Barrowian garnet + staurolite assemblages. During the transtensional activity of the Viveiro fault, the injection of S-type syn-kynematic granitoids and of I-type late to post-kynematic granitoids would have been responsible for the genesis of the andalusite II in the VPB and of the 0.5–0.4 GPa bending towards higher temperatures shown by the decompressional Lugo dome P–T path. The relict S1 included in andalusite I can be interpreted as traces of the earlier compressional stages (D_1–D_2 of Alcock et al. 2015). The general pressure conditions, the age of the rocks (Silurian pelites), and the sub-vertical supra-structural attitude of S_{1+2} first foliations also suggest that the VPB domain has not been affected by the early Barrowian gradients, more probably settled only in deeper parts of the crust. Conversely, in the Lugo dome, the initial medium pressure conditions at ca. 0.7 GPa witness for this type of early gradients, which may be related to the overburden caused by the Mondoñedo nappe stack during D_{1+2} compression (Arenas and Martínez Catalán 2002). In conclusion, it must be stated that transtensional activity along the Viveiro fault, with lateral movement towards the N of the VPB block, and the coeval exhumation of the Lugo dome took place under a general compressive regime (Martínez et al. 1996) that after D_{1+2} produced the D_3 folding stage with subvertical axial planes. These conditions can also apply for other domal-peripheral areas in the CIZ and the WALZ where hangingwall units exhibit typical Barrowian type gradients while footwall units depict low-pressure and high-temperature type assemblages. Examples of comparison between two contrasting P-T evolutions between peripheries and adjacent central domal areas are depicted in Fig. 12.13. The examples correspond to (a) the area Wof the Viveiro fault zone versus the Lugo dome and (b) Periphery versus central areas in El Tormes dome.

E and S of the Lugo dome, in the Mondoñedo nappe domain, Arenas and Martínez Catalán (2002) described two contrasting metamorphic zonations. One affects the psamo-pelitic materials of the hangingwall units of the thrust sheet itself with isograds roughly parallel to the eastern limb of the Lugo dome. These are wide zones depicting a typical Barrowian gradient. From east of Foz to near Burela, on the Cantrabrian coast, chlorite, biotite, garnet, staurolite-kyanite, sillimanite and sillimanite-orthoclase zones have been mapped. The other metamorphic regime occurs in a footwall unit that crops out in the so-named Xistral tectonic window near the Lugo dome. There the succession is of the low-pressure and high-temperature type and the authors include the zones: chlorite, biotite, cordierite-staurolite (no andalusite is common)-sillimanite-muscovite and sillimanite-orthoclase with evidences of partial melting. The P–T paths are calculated by the authors following a petrogenetic grid approach (using the KFMASH grid of Powell and Holland 1990) and show either decompression from a range of peak pressures for samples of the Barrowian sequence (ca. 0.11 GPa for migmatitic gneisses of the sillimanite + orthoclase zone at the base of the Mondoñedo

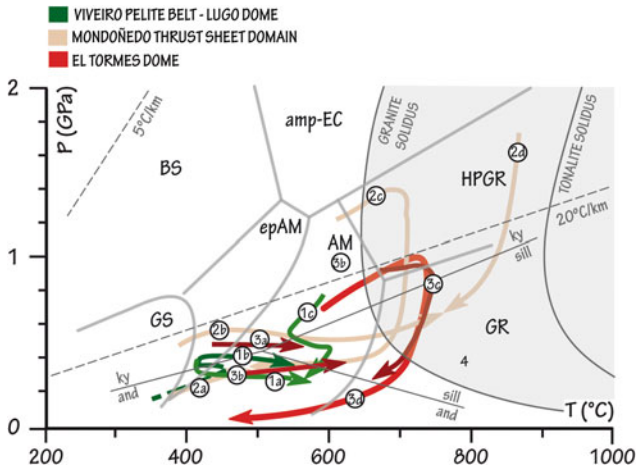

Fig. 12.13 Comparison of the P–T paths recorded in the peripheral areas of some CIZ thermal domes with the adjacent cores of nearby areas. 1a, b: P-T path for the Viveiro pelite belt synformal domain by Martínez et al. 2001 versus 1c: P-T path for the nearby Lugo dome antiform, to the east of the Viveiro fault zone. 2: P-T paths for the Mondoñedo thrust domain, E. and S. of Lugo dome (Arenas and Martínez Catalán 2002). 2a (upper part of footwall unit), b (deeper part of footwall unit), c (basal zone of the nappe) and d (underlying thermal source). 3a, b: P-T paths for the periphery of el Tormes dome (Martínez et al. 1988) versus 3c, d: P-T paths in the core of el Tormes dome (3c from Martínez et al. 1988 and 3d from Escuder Viruete et al. 2000). Thick lines separate facies fields simplified after Spear (1993), Liou et al. (1998; 2009) and Okamoto and Maruyama (1999). Facies fields abbreviations: GS, greenschist facies; epAM, epidote-amphibolite facies; AM, amphibolite facies; BS, blueschist facies; ampEC, amphibole-eclogite facies; HPGR, high-pressure granulite facies; GR, granulite facies. Thin dashed lines represent geotherms of 5 and 20 °C/km. Al_2SiO_5 (Bohlen et al. 1991) and the minimum melting of granite solidus (Huang and Wyllie 1975) are shown as reference

nappe and ca. 0.6 GPa in the upper levels of the Mondoñedo thrust sheet in the core of a late open synform in biotite zone materials) or more or less isobaric heating, also with a range in pressure level and attained peak temperatures (ca. 0.3GPa–500 °C to 0.66 GPa–720 °C). The authors interpret that the upper, middle and lower levels of the Mondoñedo thrust sheet experienced Barrowian conditions during the prograde P–T path in response to recumbent folding at ca. 360–340 Ma Peak P, followed by decompression from variable depth structural levels. The isothermal decompression part of the P–T path is interpreted in connection to the thinning or the crust caused by a upper crustal extensive detachment zone developed during continued thickening (upper extensional shear zone, a precursor of the Viveiro fault zone) at ca. 340–310 Ma. The low-pressure and high-temperature P–T paths are seen as associated to a probable channel of migmatites and magma injection along a deep extensional detachment zone ("lower extensional detachment") of roughly the same age.

In the core of the Tormes gneissic dome (TGD), Gil Ibarguchi and Martínez (1982), Martínez et al. (1988) and Sebastián and Martínez (1989) described garnet + cordierite + sillimanite metapelitic gneisses with garnet, having various stages of resorption to cordierite ± plagioclase ± biotite, and suggested the operative of the discontinuous KFMASH equilibria: biotite + sillimanite + garnet + quartz = cordierite + K-feldspar + water along a P–T path of decreasing pressure due to uplift of the dome core related to the D_3 subvertical folding stage of the Variscan general compressive deformation. Martínez et al. (1988) constrained the P–T conditions to a peak of 0.7–0.8 GPa at ca. 750 °C, followed by 0.5–0.6 GPa and 700–750° during uplift. Escuder-Viruete et al. (1994, 1997) related the steep decompressional P–T path in the lower migmatite units (dome core) to D_2 extensional ductile shearing, due to gravitational collapse after the D_1 overthrusting episode and the subsequent heating due to thermal relaxation. In the upper crustal peripheral units of the El Tormes area pressures attained during D_1 would have been much less than in its core (ca. 0.4 GPa) and would have followed a syn-D_2 (simultaneous to core uplift) low-pressure and high-temperature P–T path, probably related to progressive contact with the uplifting hotter lower units plus emplacement of S-type biotite and two-mica peraluminous granitoids and of I-type biotite meta-aluminous granodiorites and tonalites. Such low-pressure and high-temperature path is recorded in andalusite + biotite + muscovite ± chlorite ± albite assemblages. Whereas the results of Escuder Viruete et al. (1994) relied mainly on considerations using the KFMASH grids of Vielzeuf and Holloway (1988) and Spear and Cheney (1989), those of Escuder Viruete et al. (1997) were based on analyses of garnet zoning and thermobarometric calculations using various single and multiple TWEEQU software (Berman 1988, 1991; updated in 1992) equilibria.

In the Iberian Central System (ICS) Rubio Pascual et al. (2013b) described a sequence showing the imprints of an early M_1 medium-pressure Barrowian metamorphic episode syntectonic with a D_1 event, followed by later M_2 low-pressure and high-temperature gradients during a syn-compressional extension (D_2) parallel to the orogen linear structure (Escuder Viruete et al. 1998) and finally by D_3 upright folding. The authors distinguish three crustal units with distinct tectonic and metamorphic evolution. All are characterized by an early Barrowian event and by two late low-pressure and high-temperature events associated to syntectonic partial melting originating a widespread migmatitic area with abundant syn- to post-tectonic granitoids (Bishoff et al. 1973; Martínez et al. 1988; Arenas et al. 1991; Escuder Viruete et al. 1998). The upper unit of ICS,

probably equivalent to the upper unit of the Tormes dome (Escuder Viruete et al. 1994) is separated from the intermediate and lower units by the Berzosa Shear Zone (BSZ; Capote et al. 1977; Arenas et al. 1982; Escuder Viruete et al. 1998) and is constituted by a thick sequence of early Ordovician to early Devonian metapelites and metapsamites with early Ordovician felsic metavulcanites (Ollo de Sapo) in its lower part (Gebauer et al. 1993; Montero et al. 2007; Valverde-Vaquero and Dunning 2000). In this unit M_1 isograds are found folded by the D_3 upright folds. The M_2 low-pressure and high-temperature event overprints the earlier medium-pressure event only near the contact with the core of the dome containing high grade assemblages and due to the activity of the BSZ during D_2. Most of the unit far from the BSZ develop a well preserved Barrowian sequence (M_1) in which the chlorite, biotite, garnet and staurolite isograds can be traced. The Barrowian isograds are inclined towards the SE, probably due to $D_{2\text{-}3}$ tectonic events, and a new, almost vertical and subparallel to D_3 axial plane, set of isograds with staurolite II—andalusite and sillimanite II of the low-pressure and high-temperature T type intersects the earlier M_1 zones. The middle unit, similar to uppermost lower unit of El Tormes dome, shows the imprints of intense D_2 extensional deformation but still preserve the Barrowian assemblages within the staurolite and kyanite zones, mainly to the east, in the Hiendelaencina area, and to the west, in Santa María area, whereas replacement by sin-D_2 sillimanite is found in the Somosierra central area, indicating some effects of the domal phase related to decompression. The lower unit is in part like the lower unit of the Tormes dome and contains a large body of late Ordovician orthogneisses (Valverde Vaquero and Dunning 2000) intrusive in Neoproterozoic to early Cambrian metapelites and semipelites. This unit attained high temperatures under low to middle pressure conditions. Metapelitic gneisses contain sillimanite + K-feldspar and thus are above the muscovite stability field, except in the upper part of the unit, where coexistence of K-feldspar and muscovite is detected, although some of this muscovite is interpreted as formed during retrograde reactions related to cooling and decompression along the BSZ. Migmatites, restricted to the lowest part of the unit, are diatexitic paragneisses with sillimanite + cordierite + K-feldspar and developed during $D_{2\text{-}3}$ extensional and doming episodes. The authors used a classical thermobarometric approach plus AvPT THERMOCALC methods (Holland and Powell 1985, 1990; Powell and Holland 1985, 1988) and found average conditions of 0.72 ± 0.16 GPa and 494 ± 71 °C from samples in the structurally lower garnet zone. On another set of samples from the staurolite zone the found conditions were 8.1 ± 1.8 GPa and 615 ± 56 °C; and 0.89 ± 0.12 and 658 ± 57 °C from the upper and lower parts of the zone. For the syn-M_2 sillimanite zone equilibration conditions where found to vary from 0.94 ± 0.11 GPa and 687 ± 25 °C (upper part) to 0.84 ± 0.11 and 676 ± 26 °C (lower part). For the sillimanite + K-feldspar lower pressure conditions among 0.59 ± 0.14 GPa and 659 ± 105 °C, and in the highest-grade part of 0.75 ± 0.16 GPa and 746 ± 94 °C. According to $^{40}Ar/^{39}Ar$ (Rubio Pascual et al. 2013b) and U-Pb monazite data (Escuder Viruete et al. 1998) the age of S_1 compressional foliation and hence of the sin-M_1 Barrowian event would be in the range 354–347 Ma, toghether with an associated field gradient of around 23 °C/km. A lower field gradient of ca. 18 °C/km is implied by the 1.4 GPa–750 °C conditions deduced by Barbero and Villaseca (2000) for a retroeclogite boudin found in the lower unit of the ICS. These conditions evolved to 33–36 °C/km (deduced along the BSZ) during syn-D_2 decompressive evolution, thus implying an exhumation with removal of some 12–15 km of material above the garnet zone. The D_2–M_2 events are brakethed by ^{40}Ar-^{39}Ar youngest ages of S_2 (Rubio Pascual et al. 2013b) at ca. 316 Ma and by the oldest age of post-D_2 granitoids at ca. 315 Ma (Bea et al. 2009) and mark the beginning of D_3 and of further decompression along the P–T paths. A D_4 event of shearing is deduced from some retrograde shear zones crosscutting contact aureoles of 300–295 Ma granitoids. Pseudosection modelling using PERPLE_X 6.7.0 (Connolly 1990, 2005) in the MnNCKFMASHT chemical system on metapelitic-metapsamitic samples from Somosierra has been recently performed by Rubio Pascual et al. (2016) yielding conditions of 0.6 GPa and 500–540 °C for the garnet zone, 0.5–0.97 GPa and 580–620 °C for the staurolite zone, above 0.9 GPa and 680 °C for a kyanite bearing sample from the sillimanite zone, and 0.4–0.9 GPa and 750–800 °C for a migmatitic sample. From the petrologic modelling results the authors deduced a D_1 emplacement of an allochthonous nappe, >9 km thick, above the CIZ in early Carboniferous times that would be responsible for the recorded Barrowian event.

Metamorphism Related to Late-Orogenic Stages in Serra da Freita (CIZ)—Case-Study and Discussion

M. H. Mendes, J. F. Santos

The Serra da Freita area lies in north-central Portugal, and is part of the Porto-Viseu metamorphic belt within the CIZ (Martínez et al. 1990). This area is located in the eastern side of the Porto-Tomar-Ferreira do Alentejo dextral shear zone and to the south of the NW-SE Carboniferous Dúrico-Beirão and W-E Traguntia de Juzbado-Penalva do Castelo sinistral shear zones (Ribeiro et al. 1980; Iglesias and Ribeiro 1981; Ribeiro 2013; Martínez Catalán 2011) (Fig. 12.3). The main

lithologies cropping out in Serra da Freita are: (1) pre-Ordovician metasedimentary rocks (metagreywackes and metapelites) of the "Complexo Xisto Grauváquico" (Carrington da Costa 1950), and (2) syn- and late-post D3 Variscan granitoids (Reavy 1987; Reavy et al. 1991; Pinto et al. 1987; Pereira et al. 1980, 2006). Reavy (1987) attributed to the large NW-SE trending granitic pluton (Serra da Freita pluton—SFP) an emplacement age of 324 ± 4 Ma (this age, recalculated with the ^{87}Rb decay constant proposed by Villa et al. (2015) corresponds to 329 ± 4 Ma), based on whole-rock Rb-Sr analyses. This multi-stage synkinematic peraluminous D3 granitic pluton, intrusive into sillimanite zone metasediments, was probably the result of partial melting of metagreywacke and its emplacement was controlled by a NW-SE shear zone (Reavy 1987; Reavy et al. 1991). In the continuity of SFP to other areas, geochronological results different from the one reported by Reavy (1987) have been obtained: a 320 Ma K-Ar muscovite age and a 310 Ma K-Ar biotite age in nodules of Castanheira granite (Pereira et al. 2011); a 315 ± 3 Ma (320 ± 3 Ma, with the new 87Rb decay constant) whole-rock Rb-Sr isochron (Priem et al. 1984) in a porphyritic facies to the southeast of SFP; and a 308 Ma U-Pb monazite age (Aguado et al. 2005) on a sample collected to the southwest of this area. Geochemical data obtained by Reavy (1987) show that the Serra da Freita metasediments have a highly aluminous pelitic protolith, with bulk compositions plotting above the garnet-chlorite tie-line on the AFM projection from Muscovite + Quartz + water, and are strongly depleted in calcium ($\leq$0.6%) and in MnO ($\leq$0.07%). All three Al_2SiO_5 polymorphs can be observed, sometimes coexisting with each other. Kyanite, when present, typically occurs inside syn-D3 andalusite, but the textural relationships have been interpreted, in alternative, either as indicating that Ky is a relic of Barrowian metamorphism contemporaneous of Variscan D1 (Aguado et al. 1993, 2005), or that it is a late-D3 mineral partially replacing andalusite (Reavy 1987; Mendes and Munhá 1993; Mendes 1997). All the three Variscan deformation phases (D1, D2, D3) usually considered in the CIZ have been recognized in Serra da Freita area (Pereira et al. 1980, 2006; Aguado 1992; Mendes 1997). In low-grade metamorphic rocks (slates and phyllites), the most penetrative tectonic structures are S1 and S2 slaty cleavages, which are usually disturbed by D3 folds. In amphibolite facies schists, S2 foliation was always strongly affected by NW-SE subvertical D3 folding, which often transposed the previous tectonic anisotropy and produced a S3 crenulation schistosity (Aguado 1992; Mendes 1997). Late-D3 shear movements affected S1, S2 and S3 planar anisotropies, generating, in both metasediments and SFP, subvertical ductile sinistral S-C structures, striking W-E (Aguado 1992; Mendes 1997). Mapping of the metamorphic zonality, microstructural observations and mineral chemistry data (Mendes 1997; Acciaioli and Munhá 2000) allowed defining: (1) a LP-HT regional prograde metamorphism, and (2) a localized syn to late-D3 metamorphic event, characterized by development of muscovite, chlorite, kyanite and staurolite II, overprinting earlier regional mineral assemblages. A different scenario to the extensional domes described in the previous section.

Variscan regional metamorphism is characterized by (Mendes 1997): (a) a prograde sequence of zones: chlorite-biotite, staurolite- andalusite, sillimanite, marked by dehydration reactions and by mineral isograds that are subparallel to regional S3 structures and SFP limits; (b) an increase of metamorphic grade as approaching SFP; (c) being of the low-pressure/high-temperature type, with parageneses containing andalusite in medium and high-grade metamorphic zones, and attainment of the sillimanite isograd only after passing through the andalusite stability field; (d) a practically isobaric path which passed near the triple point of the Al_2SiO_5 system, defining a facies series similar to the low pressure intermediate group of Miyashiro (1961) and to facies series 2b (3.5–4.5 kbar) of Pattison (1991).

The lowest metamorphic grade is recorded in the northern sector, in phyllites with chlorite, muscovite, and biotite. To the south, the metamorphic grade increases, as testified by the staurolite-andalusite zone, where, according to microtextural analysis (Mendes 1997), the first stages of blastesis of the two index minerals took place simultaneous during D2, as revealed by staurolite and andalusite porphyroblasts that contain folded inclusion trails (Si = S1, folded by D2) and are contoured by S2 external schistosity. The continuous metamorphic evolution is recorded in early-D3 time and its most relevant consequences were the partial breakdown of staurolite (Staurolite + Muscovite + Quartz = Andalusite + Biotite + water), within the stability field of andalusite, and the formation of sillimanite at expenses of andalusite and staurolite, in areas that were submitted to greater temperatures. Therefore, in the staurolite-andalusite zone, the association quartz-muscovite-biotite-staurolite-andalusite (with andalusite containing staurolite and biotite inclusions) is considered the peak metamorphic assemblage (Mendes 1997; Acciaioli and Munhá 2000) and suggests a trajectory crossing the first staurolite consuming reaction at conditions around 530–560 °C and 3–4 kbar, below but close to the Al_2SiO_5 triple point. The first sillimanite growth period is interpreted as having taken place also in early-D3 times. Sillimanite (as either fibrolite or prismatic sillimanite) is mainly associated with biotite oriented in S2 and S3 foliations or defining polygonal arcs mimetic of D3 folds. Sillimanite and biotite are observed surrounding partially resorbed staurolite and andalusite. Elongation of idioblastic sillimanite following crystallographic directions (namely, cleavage planes) of andalusite provides textural evidence pointing to the direct replacement of andalusite by

sillimanite. As such, the assemblage quartz-biotite-sillimanite-muscovite-staurolite -andalusite is interpreted as resulting mainly from two prograde reactions: Staurolite + Muscovite + Quartz = Sillimanite + Biotite + water and Andalusite → Sillimanite, under conditions around 570–600 °C and 3–4 kbar.

Locally, within staurolite-andalusite and sillimanite zones, the regional metamorphic sequence is overprinted by parageneses including idioblastic fascicular kyanite and a second generation of idioblastic staurolite II. This overprinting is observed in areas where S3 and S-C structures are important and intense fluid circulation had taken place. The very significant role of an aqueous phase during blastesis in these domains is testified by the high density of syn-D3 metamorphic quartz veins, the presence of syn- and late-D3 quartz porphyroblasts and the modal importance of hydrous minerals (mainly muscovite). The fluids responsible by the development of the strongly hydrated parageneses probably resulted from metamorphic devolatilization reactions in the sillimanite zone and were probably channelized along the W-E shear zone.

Kyanite occurring in the strongly hydrated metapelites and in quartz veins is not a relic phase, since it replaces syn to late-D3 andalusite and is in textural equilibrium with both muscovite and a second generation of staurolite (resulting from partial breakdown of andalusite and biotite). Furthermore, if kyanite was a relic mineral it would not be expected that its presence was preserved in the domains most strongly affected by late metamorphic episodes, whilst it is absent from the rocks that better preserve the earliest regional metamorphic stages.

In an attempt to constrain the age of the Variscan metamorphic episodes in the two specific domains, biotite and muscovite concentrates from two samples were dated by Ar–Ar method using step-heating technique (Acciaioli et al. 2005). Biotite from a sillimanite bearing micaschist yielded a plateau that corresponds to an age of 333.5 ± 4.4 Ma. In this sample, S2 was crenulated during D3 but without the development of a homogeneous S3 crenulation schistosity. In this sample the growth of biotite occurred essentially during D2, but since the metamorphic peak (with sillimanite blastesis) took place during D3 folding, the 333.5 ± 4.4 Ma age is interpreted as dating the resetting of the K-Ar isotope system in the early stages of D3. In contrast, measurements on muscovite from a kyanite-bearing micaschist sample, collected in a domain strongly affected by the late-D3 hydration events, gave a plateau of 312.8 ± 3.3 Ma. These ages suggest that in Serra da Freita area the third Variscan phase would have operated during a significant period: at 335–330 Ma folding of the previous structures was taking place, whilst at ca. 310 Ma late-D3 shear zone, striking W-E, were active and operating as upward channels of hot aqueous fluids (Acciaioli et al. 2005).

12.5.1.3 Variscan Metamorphism in the Ossa-Morena Zone

C. Quesada, J. Reche

Owing to the predominant sinistral transpressional regime that characterized the tectonic evolution of the OMZ since the onset of collision in Lower Devonian times (Quesada 1991, 2006; Quesada et al. 1991; among others), rather than the stacking of nappes and consequent metamorphic evolution described in previous sections for the NW Iberia segment, the greatest part of the OMZ appears not to have been affected by significant crustal thickening. Instead, uplift (transpressional?; Quesada 1991; Dallmeyer and Quesada 1992) and erosion dominated the escape of the zone since the early Devonian beginning of collision until the Early Carboniferous, accommodated by displacement along the Badajoz-Córdoba shear zone (BCSZ), in the north, and N-directed subduction of a relic of the Rheic Ocean forming a re-entrant SW of an Ibero-Aquitanian indentor (Burg et al. 1981, 1987; Brun and Burg 1982; Quesada 1991; Murphy et al. 2016), in the south. The fact that most of this zone was submitted to uplift and denudation coeval to syn-collisional exhumation of the HP rocks and crustal thickening propagation of the orogenic wedge towards the Cantabrian Zone foreland in NW Iberia, explains the almost generalized lack of exposure of metamorphic rocks higher in grade than the lower greenschist facies (Quesada and Munhá 1990). In fact, most of the OMZ units exhibit anchimetamorphic parageneses. This fact also explains preservation in this zone of the HT-LP metamorphic domes developed during the Cambrian-Early Ordovician rifting event described in Sect. 12.2.3 as well as some units affected by Cadomian metamorphism (Blatrix and Burg 1981; Quesada and Munhá 1990; Dallmeyer and Quesada 1992; see Part 2 in volume 1).

Exceptions to the above generalization occur along two belts adjacent to both the northern and southern limits of the OMZ, where medium and high-grade rocks are exposed. Away from these two flanking belts, only very locally lower amphibolite grade rocks occur (e.g. Villarreal dome close to the Spanish-Portuguese border, where staurolite-andalusite-garnet bearing schists crop out within a lower-middle Ordovician succession in the footwall of the regionally important Juromenha-Hinojales fault; Jorquera et al. 1988). In the remaining areas Variscan recrystallization of biotite barely happened, being the chlorite zone the deeper

zone exposed. Owing to significant thermobaric and age differences, we describe separately the two OMZ belts where Variscan medium and/or high grade rocks crop out.

Variscan Metamorphism Along the Badajoz-Córdoba Shear Zone

C. Quesada, J. Reche

The BCSZ, which separates the OMZ from the CIZ, constitutes a major Variscan intracontinental shear zone (Burg et al. 1981). It is interpreted by some authors as one of the major sutures of the Variscan chain in Iberia (Matte 1986a, b; Azor et al. 1994; Simancas et al. 2001), whereas others interpret the evidence for suturing to date back to the Cadomian orogeny (Ábalos 1990; Quesada 1990a, b, 1991, 1997, 2006; Ábalos et al. 1991; Quesada and Dallmeyer 1994). No matter the interpretation of the age of the subduction event attested by the HP metamorphic relics preserved in some units within the BCSZ, there is general consensus on the major role played by this structure during the Variscan collisional event, during which the former suture zone, either Cadomian or early Variscan in age, acted as a major intracontinental left-lateral shear zone accommodating the displacement (escape) of the OMZ towards the SE.

A complex flower structure characterizes the internal structure of the BCSZ, the inner core of which (Central Unit of Azor et al. 1994) shows evidence of significant exhumation of middle and lower crustal segments (Quesada and Dallmeyer 1994) relative to the adjacent blocks. To the north, the so-called Obejo-Valsequillo domain shows a northerly vergence and is only affected by lower greenschist facies metamorphism, which has allowed preservation of the Cadomian age of the metamorphism that affects the Serie Negra basement (ca. 550 Ma; $^{40}Ar/^{39}Ar$ on amphibole and white mica, Blatrix and Burg 1981; Dallmeyer and Quesada 1992). Therefore, the Variscan metamorphism in the exposed part of this unit never exceeded ca. 400 °C, probably much less. To the south of the Central Unit, the Sierra Albarrana domain verges to the south and shows a somewhat higher Variscan metamorphic grade, locally reaching the transition from the greenschist to the amphibolite facies. Again, $^{40}Ar/^{39}Ar$ thermochronology gives the clues. Above (Sect. 12.2.3.3), we provided evidence proving the Cambro-Ordovician age of the metamorphic dome which makes the most characteristic structure in this domain on the basis of U-Pb zircon dating of migmatite neosomes (ca. 500 Ma; Azor et al. 2012). In the same study a very significant ca. 480 Ma amphibole $^{40}Ar/^{39}Ar$ age was reported, suggesting that at least locally this unit was never buried to amphibolite facies depths after that date. However, Azor et al. (2012) also obtained some Variscan amphibole (ca. 385 Ma) and white mica (ca. 336 Ma) $^{40}Ar/^{39}Ar$ cooling ages, partly corroborating previous data by Dallmeyer and Quesada (1992), and which prove that a part of the Sierra Albarrana unit may have been buried at amphibolite facies depths prior to its exhumation to the surface in early Mississippian time (Gabaldón et al. 1985; Quesada and Dallmeyer 1994). The large age difference (ca. 40 Ma) between the amphibole and white mica $^{40}Ar/^{39}Ar$ cooling ages indicates very slow exhumation rate, which is compatible with its interpretation in connection with transpressional uplift processes (Quesada and Dallmeyer 1994).

The inner core of the BCSZ (Central Unit), 6–20 km wide, exhibits a very complex array of sigmoidal sinistral duplexes (Quesada and Dallmeyer 1994) with contrasting tectonostratigrapic units and degree of exhumation, both in Spain (Burg et al. 1981; Ábalos et al. 1991; Quesada and Dallmeyer 1994) and in Portugal (Pereira 1999; Pereira and Silva 2002; Pereira and Apraiz 2002; Pereira et al. 2008). In the largest horses, three superposed tectonostratigraphic units can be distinguished separated by originally subhorizontal contacts (Ábalos 1990; Ábalos et al. 1991; Quesada and Dallmeyer 1994): (1) The lower unit is composed of highly aluminous micaschist and quartzites affected by greenschist to lower amphibolite facies metamorphism (i.e. Atalaya schist of Chacón 1979, correlated with the Albariza schist (Garrote 1976) of the Sierra Albarrana domain); (2) the intermediate, extremely mylonitized unit (Blastomylonitic Fm of Delgado Quesada 1971, also known as Azuaga gneiss, Apalategui et al. 1985), consists of an alternation of felsic gneisses, migmatitic paragneisses and amphibolites (Las Mesas amphibolites of Delgado Quesada 1971). This intermediate unit represents high-grade lower crustal segments, including the retrogressed eclogites discussed in Sect. 12.3.2 and whose age is still under debate. Towards its structural base, a discontinuous sheet of serpentinites and MORB-like amphibolites separates the intermediate from the lower unit. These rocks were interpreted as dismembered remnants of an ophiolite unit (Quesada 1990a, b, 1997) and together with the HP rocks in the overlying Azuaga gneiss and Las Mesas amphibolites, thought to define a suture zone (Accretionary unit of Quesada 1997; probably a dismembered subduction channel); (3) the upper unit consists of Neoproterozoic Serie Negra rocks generally affected by greenschist facies metamorphism (Ábalos 1990; Ábalos et al. 1991; Quesada and Dallmeyer 1994), except in local areas where Cambrian metamorphic domes are preserved (e.g. Mina Afortunada dome, described in Sect. 12.2.3.2).

Irrespective of the debated age of the HP metamorphic event, peak metamorphism in the intermediate unit (Azuaga gneiss or Blastomylonitic Fm, in Spain; Ouguela, Arronches

Contenda Barragen or Campo Maior units, in Portugal) was attained mainly during shearing and fast exhumation from high-pressure granulite to high-grade amphibolite and finally to greenschist facies conditions (Azor et al. 1994; Pereira and Apraiz 2002; Pereira et al. 2008; Pereira et al. 2010). Thermobarometry was calculated by Pereira et al. (2008) on distinct units of the BCSZ in Portugal yielding average results of 1.00–0.75 GPa and 790–500 °C for the granulite to amphibolite stages recorded in the intermediate unit (See Fig. 12.6). Typical mineral parageneses include: quartz + K-feldspar + plagioclase + muscovite ± biotite ± garnet ± kyanite ± sillimanite in quartzo-feldspatic gneisses, and biotite + kyanite + quartz + K-feldspar + garnet + sillimanite + muscovite ± plagioclase ± andalusite in metapelitic gneisses. In the same study, Pereira et al. (2008) determined 0.4–0.4 GPa and 400–350 °C (greenschist facies) for the Azeiteiros unit (Serie Negra), a part of the upper unit referred to above.

Concerning the metabasic rocks, Gomez-Pugnaire et al. (2003) obtained some geochemical and tectonic constraints for garnet bearing and garnet absent amphibolites of the intermediate unit (Las Mesas amphibolites). The authors found clear oceanic affinities, which suggest the existence at some stage of an oceanic domain between the CIZ and OMZ, later involved in a process of subduction where they reached eclogite facies conditions. The amphibolites where emplaced finally as a rooted ophiolitic unit, either during the Cadomian orogeny or during early Variscan orogeny stages. The serpentinites which crop out at the base of the intermediate unit could well represent mantle sections of this ophiolite nappe. Lopez Sánchez-Vizcaíno et al. (2003) detailed the petrography of these amphibolites. The assemblages in garnet absent amphibolites consist of amphibole + plagioclase + quartz + titanite + ilmenite ± biotite ± epidote, and in the garnet bearing amphibolites, of clinopiroxene + garnet + amphibole + plagioclase + quartz ± biotite ± scapolite ± zoisite ± rutile ± titanite ± ilmenite. The retrieval of metamorphic P–T conditions for these amphibolites using a pseudosection forward modelling approach with PERPLE_X (Connolly and Petrini 2002) confirmed peak P and T values similar to those given in previous works by Mata and Munhá (1986), Ábalos et al. (1991) and Azor (1994) but, in addition, Lopez Sánchez-Vizcaíno et al. (2003) defined the most probable P–T path (see Fig. 12.6). The trajectory records initial eclogite facies with pressure peaking at ca. 1.9 GPa and 550 °C, indicated by grossular-rich garnet and jadeite-rich clinopyroxene probably coexisting with chlorite + glaucophane + paragonite. After, these samples suffered decompression with strong heating up to 1.6 GPa and 725 °C, then nearly isothermal decompression to ca. 1.18 GPa and finally, cooling with decompression to ca. 0.3 GPa and 455 °C.

Pereira et al. (2010) presented a detailed tectonothermal and geochronological analysis of the exhumation of the intermediate unit of the BCSZ focused on amphibolites and felsic gneisses and migmatites of the Campo Maior Unit (Pereira 1999), and deduced cooling along with decompression and melting from 1.45–1.65 GPa and 850–880 °C, through a simplectitization stage at 1.25–1.45 GPa and 725–750 °C (mafic granulites), to 0.95–1.15 GPa and 615–675 °C (high-grade amphibolites). Further retrogression and cooling took place during shearing in amphibolite facies conditions to 0.7–0.9 GPa and 550–700 °C (amphibolites), 0.6–0.8 GPa and 620–640 °C (gneisses) or 0.5–0.65 GPa and 560–610 °C (migmatites). On the basis of U-Th-Pb in situ zircon SHRIMP II geochronology, Pereira et al. (2010) interpreted Ediacaran ages (ca. 590 Ma) for the protoliths, and beginning of exhumation from granulite facies coditions at ca. 340 Ma. However, in a recent paper (Pereira et al. 2012) revisited some protolith ages, dating the migmatite protoliths as middle Ordovician (465 ± 14 Ma). Fast exhumation rates of ca. 10 mm/y where confirmed in this study for the 340–330 Ma interval, as also suggested by unconformable relationship of the metamorphic rocks beneath Mississippian sedimentary rocks (Gabaldón et al. 1985; Quesada and Dallmeyer 1994).

More recently, Abati et al. (2018) also reported Neoproterozoic and Ordovician protolith ages from another locality in Spain but found two populations of metamorphic zircon growth at ca. 380 Ma and ca. 340 Ma, which they interpreted as developed during initial HP conditions and later amphibolite facies recrystallization, respectively. These data confirm the slow exhumation rate between ca. 390 and 340 Ma estimated for the adjacent Sierra Albarrana domain (see above), probably related to a process of transpressional uplift, and a rapid shift to much higher rates between 340 and 330 Ma, probably related to the onset of collision of the southern OMZ margin with the South Portuguese Zone (Quesada and Dallmeyer 1994; Quesada 2006).

Variscan Metamorphism in the Southwestern Ossa Morena Zone

C. Quesada, M. Chichorro, J. Reche, A. R. Solá

The second belt where medium and high-grade metamorphic rocks crop out in the OMZ corresponds to a series of sigmoidal-shape strike-slip duplexes which delineates the southern boundary of the OMZ; from W to E: Évora, Aracena and Almadén de la Plata massifs, progressively smaller in size in the same direction. To the N, all those massifs are in tectonic contact with the allochthonous Cubito-Moura HP

unit described in Sect. 12.3.2.2. To the S, all are bounded by the Beja-Acebuches ophiolite through a shear zone developed under granulite to HT-amphibolite facies conditions. On metamorphic ground, the most conspicuous feature of these massifs is the existence of an important HT-LP (locally ultrahigh temperature) event (Bard 1969; Apalategui et al. 1984; Crespo-Blanc 1989; Quesada and Munhá 1990; Castro et al. 1996a, b; Pereira et al. 2007, 2009). In the Aracena massif two different units exist, separated by another important shear zone (El Repilado fault, Florido and Quesada 1984): to the NE, the already described Fuenteheridos group, affected by HP-LT metamorphism (see under Sect. 12.3.2.2), which escaped the HT-LP event, and, to the SW, the Aguafría-Cortegana unit, showing HT-LP granulite facies conditions. In turn, the overall structure of the Évora massif (see below under Sect. General Structure of the Évora Massif) is defined by a two-layer crustal section separated by mylonitic shear zones: One (footwall) representing an HT-LP metamorphic core (Évora high-grade metamorphic Domain) and other representing the hangingwall blocks with relatively low-to medium metamorphic grade (Évora medium-grade metamorphic Domains and Montemor-o-Novo shear zone). The latter, which includes some HP-LT metamorphic relics (see under Sect. 12.3.2.2) is equivalent to the Fuenteheridos unit but reaching here higher metamorphic grades at this stage.

The stratigraphy affected by the HT-LP event is identical in all the massifs, including the Fuenteheridos unit; and consists of Serie Negra Cadomian basement unconformably overlain by lower Cambrian carbonates followed by a Cambrian-Ordovician bimodal volcanosedimentary succession with important carbonate packages; i.e. a succession characteristic of the rifting stage in the southwestern OMZ (see Chap. 2 in this volume). Another common element of the HT-LP units is the presence of voluminous early Carboniferous intrusives, both mafic and felsic, more abundant in the Évora Massif and progressively rarer towards the east (Pin et al. 2008; Pereira et al. 2009; 2015; Lima et al. 2011, 2012; Moita et al. 2015).

The continental HT-LP sequence includes stromatic to agmatitic pelitic and felsic gneisses, nebulites, diatexites, marbles and calcsilicates, amphibolites and granulites where no relicts of any previous higher-pressure episodes have been found so far. Common parageneses in migmatitic stromatic to agmatitic metapelitic-gneisses contain (Bard 1969) garnet + sillimanite + biotite ± cordierite ± spinel ± orthopyroxene + K-feldspar + plagioclase + quartz + graphite. Near in situ nebulitic migmatites associated to the layered metapelitic gneisses contain similar peak metamorphic mineral assemblages, and both clearly derive from Serie Negra basement protoliths as indicated by abundant black chert restites and significant presence of graphite. These rocks are spatially related to basic to intermediate orthopyroxene + clinopyroxene + hornblende + plagioclase + biotite + quartz + rutile metaplutonic rocks of boninitic affinity, e.g. Los Molares metanorites (Castro et al. 1999). Mafic granulites contain orthopyroxene + clinopyroxene + plagioclase + rutile + spinel + sphene (Bard 1969) and probably derive from the mafic components on the Cambrian-Ordovician volcanosedimentary succession (Apalategui et al. 1984). In turn, the felsic granulites, which probably derive from the felsic components of the same rift-related volcanosedimentary succession, contain non-diagnostic mineral parageneses (quartz + K-feldspar + plagioclase + rutile + spinel) but exhibit a prominent medium-to-coarse-grained granoblastic texture with linear grain boundaries and triple points (Bard 1969; Apalategui et al. 1984). Finally, carbonate rocks, derived from the early Cambrian carbonate succession as well as those interbedded within the Cambrian-Ordovician volcanosedimentary succession, are characterized in the impure varieties by carbonate + garnet + clinopyroxene ± olivine ± phlogopite ± wollastonite ± spinel.

All the above parageneses indicate conditions of 4–6 GPa and 900 °C (Castro et al. 1996a; Díaz Azpíroz 2001; Díaz Azpíroz et al. 2004, 2006). Alternatively, Rubio Pascual et al. (2013a) estimated ca. 5 GPa and 650 °C using multi-equilibrium TWQ v.2.3 (Fig. 12.6). These are conditions cleary above muscovite dehydration melting and compatible with biotite dehydration melting (El-Biad et al. 1999; El-Biad 2000). The existence of plagioclase rich, K-feldspar absent leucosomes of granodioritic to tonalitic composition (Díaz Azpíroz et al. 2006) is compatible with local H_2O-saturated melting conditions (Patiño Douce 1996; Patiño-Douce et al. 1997; Patiño Douce and Harris 1998).

Patiño-Douce et al. (1997) deduced a clockwise P-T path for this domain that reached ultra-high temperature conditions of ca.1000 °C (spinel-cordierite granulites) postdating the main foliation. The metamorphic zonal arrangement is one of increasing metamorphic grade towards the Beja-Acebuches amphibolite (BAO) unit located to the SW. The highest metamorphic grade in the BAO unit is located right at the contact with the continental rocks, which led to propose it as an inverted metamorphic sequence (Quesada et al. 1994; Castro et al. 1996a, b).

Ábalos et al. (1991) also suggested a similar HT-LP P-T path for the easternmost Almadén de la Plata massif. They reported the widespread occurrence of garnet + cordierite + sillimanite + biotite assemblages in the highest grade metapelites but based on thermobarometric and textural constraints (breakdown of garnet and staurolite to andalusite) they suggested an intermediate episode of medium-low pressure metamorphism followed by a final HT-LP event. Classic thermobarometric results yielded conditions of 3.5–4.5 GPa and 560–700 °C.

In the Évora massif, the largest exposure of the HT-LP belt, Pereira et al. (2016, and references therein) described

the existence of a major D2 transtensional event, associated to massive plutonism and coeval to the HT-LP metamorphism, which they held responsible for the exhumation of the high-grade core (footwall). Ductile shear zones, active between ca. 356–322 Ma (Pereira et al. 2012, 2013), separate the core from medium-low grade hangingwall units with the same stratigraphy. This was probably also the case in the Aracena and Almadén de la Plata massifs but so far it has not been documented. Another singularity of the Évora Massif is the fact that the low-to-medium grade hangingwall unit is unconformably overlain by a Carboniferous syn-orogenic sedimentary basin (Cabrela basin, see Chap. 11 in this volume). The Cabrela basin also includes volcanism coeval with the Carboniferous intrusives in the Évora Massif. This coincidence between the age of sedimentation, the age of HT-LP metamorphism and associated intrusive/extrusive magmatism demonstrates the contemporaneity of the exhumation guided by extensional shearing and sedimentary basin formation, reinforcing the models of Variscan intra-orogenic extensional tectonics in the southwestern Ossa-Morena Zone (see below under Sect. General Structure of the Évora Massif).

In the Beja-Acebuches amphibolites oceanic unit, according to Díaz Azpíroz et al. (1997) peak hornblende-plagioclase (Holland and Blundy 1994) temperatures during the HT-LP event would have been up to 200 °C lower than in the continental belt. Peak temperatures found by Rubio Pascual et al. (2013a) are ca. 720 °C using also the hornblende-plagioclase thermometer of Holland and Blundy (1994). These authors also obtained retrograde conditions of 2.3–5.2 GPa and 430–600 °C using TWQ 2.3 calculations in garnet + biotite ± andalusite + muscovite + plagioclase + quartz metapelites tectonically imbricated with the BAO amphibolites. Concerning the amphibolites proper, Castro et al. (1999) described a greenschist facies retrogression event with stabilization of actinolite + chlorite bearing assemblages, which increases towards the south, associated to late transpressional emplacement of the BAO onto the Pulo do Lobo terrane lying to the south along the so-called South Iberian shear zone (Crespo-Blanc and Orozco 1991).

The close relation of this continental belt of HT-LP rocks and the Beja-Acebuches amphibolites together with the marginal basin, oceanic affinity of the latter led Quesada et al. (1994) to propose a mechanism of obduction of the BAO over the outer margin of the OMZ during closure of the BAO marginal basin, but prior to complete closure of the Rheic Ocean. These authors interpreted the HT-LP metamorphism affecting the two domains (continental and BAO) in response to a "thermal doming event", a period dominated by asthenospheric uprisal, which they held responsible for both the extremely high geothermal gradient and the voluminous roughly coeval magmatism (see below). Later, Castro et al. (1996a) and Díaz Azpíroz et al. (2004, 2006) refined the previous model and proposed a process of oblique ridge subduction and ridge-trench interactions to account for the superposition of the HT-LP metamorphism on both the BAO unit and the continental belt. In both models, the metamorphic event predates the final closure of the Rheic Ocean.

Azor et al. (2008) published SHRIMP U-Pb zircon data from two BAO samples and obtained early Carboniferous ages (332 ± 3 and 340 ± 4 Ma), which they interpreted to date the crystallization of the protoliths. Other available geochronology apparently contradicts those results. First, if the ages reported by Pereira et al. (2013) for the exhumation of the high-grade core of the Évora massif are right, then the juxtaposition with the BAO should have been achieved by ca. 350 Ma. The same inference is pointed out by the early Carboniferous magmatism intrusive into the HT-LP metamorphic rocks, the oldest dating back to ca. 353 Ma (Beja gabbro, Pin et al. 2008) and with a peak of granitoid emplacement ca. 340 Ma ago, extending up to ca. 317 Ma (Pereira et al. 2009, 2015; Lima et al. 2011, 2012; Moita et al. 2015). Additionally, $^{40}Ar/^{39}Ar$, Sm–Nd and Rb-Sr data (Dallmeyer et al. 1993; Castro et al. 1999) from samples belonging to both the continental high-grade unit, the BAO and the Beja gabbro, constrain the metamorphic event (at least its cooling below the Ar retention temperature in amphibole) between ca. 342 and 328 Ma. On the basis of their geochronological data, Castro et al. (1999) inferred younging of the metamorphic event from west (ca. 342 Ma) to east (ca. 328 Ma) along the HT-LP belt, which they interpreted as evidence of the eastward migration of a mantle plume related triple junction along the continental margin within their model of oblique ridge-trench collision described above. Finally, Braid et al. (2018) described and dated ca. 354 Ma subduction-related gabbros intrusive into the Pulo do Lobo terrane, which indicate persistence of northerly subduction at that time south of the OMZ.

Intra-orogenic Extension-Related Metamorphism: The Évora Massif Example

M. Chichorro, A. R. Solá

Variscan intra-continental extensional tectonics associated to ductile shear zones and migmatization, and resulting in plutono-metamorphic complexes, have been described on the Spanish side of the Ossa-Morena Zone (e.g. González del Tánago 1993; Apraiz 1998; Apraiz and Eguiluz 1996, 2002). In Portugal, the Évora Massif also attests for an

episode of continental extension (transtension) syn-to-post crustal shortening related with the subduction stage (Pereira et al. 2009, 2012).

General Structure of the Évora Massif

The overall structure of the Évora Massif (Carvalhosa 1983; Quesada and Munhá 1990) is fundamentally defined by a two-layer crustal section, separated by mylonitic shear zones (Fig. 12.14): (i) the footwall unit represents a metamorphic core (Évora high-grade metamorphic Domain), comprising a complex interaction between two series: (a) high-grade gneisses, migmatites, diatexites and leucogranites, and (b) few tonalites, gabbros and diorites; and (ii) hangingwall blocks of relatively low metamorphic grade, mainly composed of medium-grade gneisses, schists and amphibolites (Évora medium-grade metamorphic Domains and Montemor-o-Novo shear zone) (Pereira et al. 2007, 2009, 2012). Those two crustal sections are separated by extensional shear zones, which are responsible for regional telescoping of Variscan metamorphic isograds (Pereira et al. 2009, 2012). Despite the extensional nature of the current tectonic contact between the high-grade domains and the hangingwall sections (Chichorro et al. 2003; Pereira et al. 2009), the presence of high-pressure relics in the hangingwall units (see above and Sect. 12.3.2.2) suggests that those tectonic boundaries were former major D1 thrusts (Díez Fernández et al. 2017).

As in the other SW-OMZ massifs, the protoliths of the high-grade rocks in the Évora massif were Serie Negra Cadomian basement and Cambrian-to-Ordovician rift-to-drift (ca. 590–480 Ma) successions (Carvalhosa 1983; Chichorro et al. 2008). The heterogeneities of high-grade domains depend of the nature of the protolith, as well the type and volume of partially molten rocks and igneous intrusives.

Metamorphism (Prograde/Retrograde evolution)

The highest temperatures were reached within the dome-like high-grade metamorphic domains, made of diatexites, anatetic granitoids and migmatitic ortho and paragneisses with mineral assemblages typical of the high-T amphibolite facies and the transition to the granulite facies. The transtensional deformation controlled the rapid exhumation of deep crust segments and triggered partial melting and magma production, which in turn promoted heat transfer by conduction from the footwall (high grade units) to the hangingwall (low-to-medium grade domains). This is partly sustained by the fact that in several sectors of footwall high-grade domains, prograde reactions and melting occurred within the garnet stability field (developed under HT/MP metamorphism: 6–7 kbar/600º–800 °C).

The mineral assemblages developed in the tectonites related with the extensional shear zones, mainly the Montemor-o-Novo shear zone, consist of quartz + biotite + plagioclase + K-feldspar + sillimanite + cordierite ± andalusite ± garnet (scarce) and were associated with progressive partial melting through dehydration reactions of muscovite and biotite. The subsequent decrease of temperature produced low grade assemblages and destabilization of cordierite, biotite, and feldspar, and growth of chlorite and albite. The intrusion of tonalites and diorites took place while the Variscan migmatization was in progress, enhancing local partial melting and mixing of melts (Moita et al. 2009; Pereira et al. 2015). In these shear zones is remarkable the rapid increase of metamorphic grade from greenschist facies conditions (biotite zone) at the SW, to upper amphibolitic facies conditions (sillimanite—K-feldspar—cordierite zone). The tight spacing of the isograds suggests a strong thermal gradient induced by the exhumation of the high-grade domains (Chichorro 2006). In the transition zones, the observed mineral parageneses in Serie Negra paragneisses allow to describe the prograde sequence attested by the appearance of the andalusite isograd, the frequent association and + crd + bt and the partial replacement of andalusite by cordierite. The biotite dehydration reactions and the peritetic cordierite related with first melting reaction mark the first sillimanite isograd. Fibrous sillimanite that grew parallel to the foliation surrounds eye-shaped restite nodules and occurred as the result of the breakdown of biotite due to the generation of water-saturated melts. These mineral associations reflect a progressive prograde metamorphism with P–T conditions ranging from 550 °C and 3–3.5 kbar to 600–740 °C and 4–5 kbar (Chichorro 2006). The onset of decompression is indicated by the pervasive growth of a second generation of cordierite (Crd II). It is important to underline the close relationship between ductile deformation and regional metamorphism, since most prograde mineral phases (developed under green schist, amphibolite and high amphibolite facies) show a strong preferred orientation parallel to the tectonic stretching lineation. Finally, spots of K-feldspar and plagioclase blastesis and quartz ± feldspar venules/veins in the paragneisses represent the initial stages of partial melting.

The quick variation in metamorphic grade together with the scarcity of garnet in pelitic rocks suggest a prograde evolution under low pressure conditions, reaching temperatures high enough to cause dehydration melting reactions

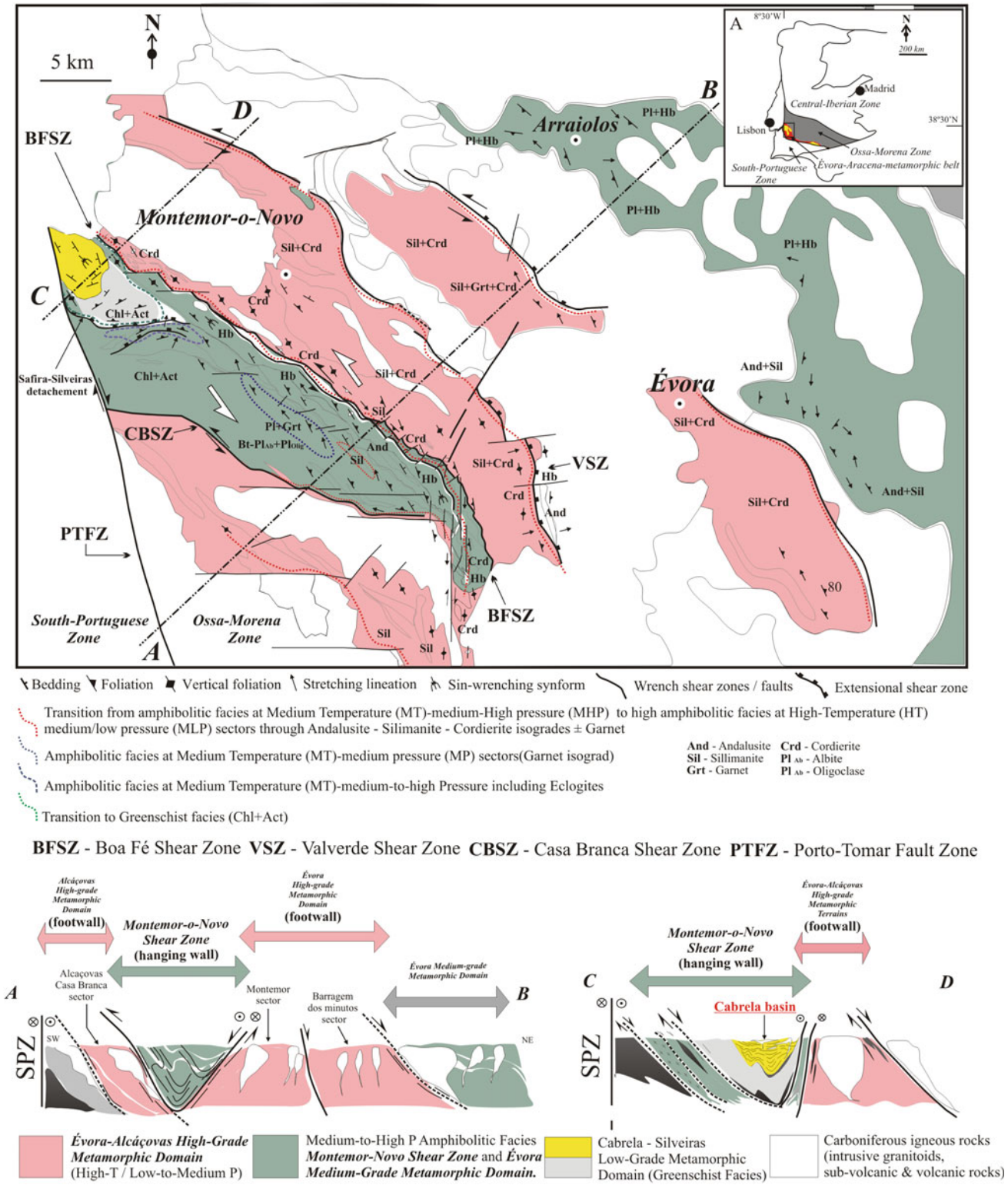

Fig. 12.14 Schematic representation of the overall structure of the Évora Massif showing the two-layer crustal sections separated by mylonitic shear zones (see text for explanation). Cross-sections A–B and C-D show the major structures controlled by extensional tectonics that acted in SW Iberia during the Early Carboniferous (adapted from Pereira et al. 2012, 2013, 2015)

(650–750 °C). This fact means that the tectonic evolution of several boundary sheared sectors was intimately related with a prograde metamorphic event of high-temperature/low-pressure type, which is assumed to be the response of the exhumation of the high-grade domain.

The dehydration melting reactions related with HT-LP metamorphism enhanced the generation of melts which ascended along weakness planes, as pointed by the presence of several granitic, leucogranitic and dacitic veins/dikes not showing solid state deformation (Chichorro 2006; Matias et al. 2015). The injection of that melts took place predominantly along dilatant extensional planes slightly oblique to foliation/compositional layering, highlighting the transtensional character of the major detachment structures (Chichorro 2006; Pereira et al. 2013; Fernández et al. 2016).

Later, the transtensional activity along major shear zones involved a metamorphic P-T evolution with cooling (up to 350–400 °C) and concomitant decompression that attained 2–2.5 kbar (Chichorro 2006). The retrogression is patent by growth of randomly oriented muscovite II replacing biotite, andalusite, sillimanite and cordierite, and by symplectic intergrowths of muscovite + quartz at the expenses of K-feldspar and sillimanite in response to falling temperature. Biotite was replaced by chlorite, feldspar was sericitized and cordierite was strongly pinnitized.

Timing of thermal events in the Évora Massif

SHRIMP U-Th–Pb age determinations on metamorphic zircon overgrowths from the Serie Negra paragneisses and the Valverde, Escoural and Alcáçovas orthogneisses indicate a diachronic and variable spatial distribution of multiple zircon growths and recrystallizations related with an extended high-temperature tectonothermal history concentrated in the Mississipian with a main peak at 342 Ma (Pereira et al. 2009). Valverde amphibolite from the coarse-grained facies yielded a ^{39}Ar–^{40}Ar plateau age of 356 ± 12 Ma developed during deformation under amphibolite-facies conditions. It coincides in time with the age of 358 ± 11 Ma obtained for a Serie Negra micaschist (white mica K–Ar; Rosas et al. 2008) and is slightly older than the crystallization of the Beja Complex tonalite and diorites (ca. 353–350 Ma; zircon U–Pb; Pin et al. 2008). Priem et al. (1986) reported K–Ar ages of 333–339 Ma for biotites of the Alcáçovas orthogneisses, concluding that these ages could date the end of Variscan metamorphism.

The weighted mean U/Pb age of 339.7 ± 5.5 Ma, estimated for the metamorphic imprint on the Alcáçovas orthogneiss, is similar to the weighted mean age of 333 ± 14 Ma obtained on overgrowths on detrital zircons from Serie Negra paragneiss (Pereira et al. 2009). Biotite from the same paragneisses yielded an Ar–Ar age of 337 ± 3 Ma (Visean). These estimates of deformation age overlap with: (1) metamorphic ages in the range 342–336 Ma from the Beja metagabbro, the Ventosa amphibolite, the Alcáçovas gneiss and the São Brissos amphibolite (Dallmeyer et al. 1993; Pereira et al. 2009); (2) cooling ages in the range 339–337 Ma from the Beja Complex gabbros (amphibole Ar–Ar; Dallmeyer et al. 1993) and (3) the crystallization ages of ca. 340–332 Ma for the protoliths of the Beja and Acebuches amphibolites (zircon U–Pb; Azor et al. 2008), and Arraiolos and Reguengos de Monsaraz granitoids at ca. 337 Ma (zircon U–Pb; Antunes et al. 2011; Pereira et al. 2009). Recent work (Pereira et al. 2015), focused on two calcalkaline granitoids intruded in the Évora high-grade domain shows a multistage crystallization of zircon revealed by two main zircon growth stages (ca. 344–342 Ma and ca. 336–335 Ma). However, based on their youngest age clusters it was estimated that crystallization ages for the two calcalkaline granitoids took place at ca. 336–335 Ma. This study allowed reinforcing the concept that Variscan magmatism was spatially and temporally related to high-temperature metamorphism, anatexis, processes of interaction between crustal and mantle-derived magmas, and extensional tectonics that acted in SW Iberia during the Early Carboniferous.

Based on zircon metamorphic overgrowths in Cambrian zircons from Valverde orthogneiss, it is possible to infer a high-grade metamorphic peak in Tournaisian-Visean times (probably related to a long-lived thermal event). However, recent monazite analyses gave a precise slightly younger Carboniferous age (322 ± 6 Ma, Serpukhovian; Pereira et al. 2009) for the high-grade metamorphism which affected these rocks.

In conclusion, mylonitization related with extension and wrenching (D2–D3) was associated with syn-kinematic prograde metamorphism reaching conditions of medium-high temperature and low to medium pressure. Ductile extensional shear zones and wrenching in transtension was responsible for the rapid exhumation of deep crust, metamorphism, partial melting and magma production in the interval ca. 356–321 Ma. U-Pb and ^{40}Ar–^{39}Ar geochronology constrain the Variscan extensional-wrenching and related high-grade metamorphism recorded in Early Paleozoic rocks mostly with Ediacaran and Cambrian protoliths to the interval Tournaisian-Visean. For this reason, the high-grade metamorphism in the Évora massif should be considered as a long-lived thermal event (Tournaisian-Visean) with a main peak at ca. 342 Ma (Visean) (Chichorro 2006; Pereira et al. 2009). It remains unclear if such long-lived heating of the crust reflects a regional thermal steady-state condition and/or the response of short-lived thermal pulses related to a specific local tectonic movement associated with orogenic collapse.

Geodynamic Implications of Metamorphism in the Southwestern Ossa Morena Zone

C. Quesada

Any geodynamic scenario capable of making compatible all the above geocronological data and interpretations should take into consideration the following regional aspects:

(1) According to the geological evidence in the Iberian Massif (both the northern and southern segments), convergence between Gondwana and Laurussia as a consequence of the closure of the Rheic ocean must have been accommodated by subduction beneath the latter; i.e. Gondwana in the lower plate (Martínez Catalán et al. 2009; Braid et al. 2018; and references therein).

(2) In NW Iberia collision started ca. 375 Ma ago with subduction of the outer margin of Gondwana (lower plate) beneath Laurussia, giving rise to the HP-LT metamorphism recorded in the Middle, Lower Allochthon and Parautochthon units of the Galicia-Trás-os-Montes Zone (see Sect. 12.3.1.2). Coeval development of the HP-LT event recorded in the Cubito-Moura and Fuenteheridos units of the southwestern OMZ (see Sect. 12.3.2.2) as well as the emplacement of the "Internal OMZ ophiolite sequences" (IOMZOS) onto the Cubito-Moura unit (see Chap. 5 of this volume) may have taken place during the same process of subduction beneath Laurussia. This is suggested by the NE vergence of the structure associated to such emplacement (Fonseca and Ribeiro 1993; Quesada et al. 1994; Pérez Cáceres et al. 2015, 2017) and by the formation in the southwestern OMZ of the Terena syn-orogenic flysch basin in late Early Devonian time that contains foliated clasts and rutile grains interpreted to have a provenance from quasi contemporaneously emplaced Cubito-Moura, Fuenteheridos HP-LT units and the IOMZOS (Aráujo et al. 2005).

(3) The subsequent evolution in both segments differs significantly. In NW Iberia, the period after ca. 370 Ma recorded the post-collisional eastward propagation of a nappe pile towards the foreland (Cantabrian Zone), which was reached by the orogenic wedge in late Carboniferous time (see Chap. 10 of this volume). In SW Iberia the situation during the late Devonian was as follows: (i) the Laurussian affinity South Portuguese terrane (SPT) was undergoing a passive margin period with deposition of the PQ Group in shallow platform environments (see under Chap. 6 of this volume); (ii) the Pulo do Lobo oceanic terrane (PLT) was being accreted with a northerly polarity coeval to formation of syn-orogenic basins and mélange deposits (such as the Peramora ophiolitic mélange; Eden and Andrews 1990; Eden 1991; Braid et al. 2010, 2011; Dahn et al. 2014; Braid et al. 2018) in trench/forearc environments (Quesada et al. 1994; Braid et al. 2018); (iii) both the PLT and the southwestern OMZ were the locus of subduction-related magmatism, starting in the mid-Devonian and episodically extending until the Tournaisian-early Visean (Santos et al. 1987, 1990; Andrade et al. 1991; Quesada 1991; Quesada et al. 1994; Braid et al. 2018); (iv) the remaining of the OMZ were either subjected to uplift and erosion or the site of platformal sedimentation (in the SE). All these facts indicate that an oceanic re-entrant must have existed SW of the OMZ, separating it from the South Portuguese part of Laurussia (Quesada 1991; Murphy et al. 2015, 2016; Braid et al. 2018). The passive margin conditions on the latter suggest locking of the westerly subduction process responsible for previous continental approximation. In turn, northerly accretion in the PLT, together with arc magmatism in it and in the southwestern OMZ, indicates nucleation of a new subduction zone with opposite polarity (northerly). Quesada (1991, 2006) explained this polarity flip in response to the southeasterly escape of the OMZ, accommodated by sinistral displacement along the Badajoz-Córdoba shear zone and oblique overriding onto the adjacent oceanic re-entrant.

(4) In early Carboniferous time the situation in SW Iberia evolved as follows: (i) the outer margin of the SPT were subjected to an important transtensional event accompanied by massive bimodal volcanism (see under Chap. 6 of this volume); (ii) in the PLT, initial arc-type magmatism was replaced by slab break-off affinity magmas (ca. 345 Ma; Braid et al. 2018); in the southwestern OMZ, the HT-LP metamorphic event developed coeval to significant transtension, magma underplating (Simancas 1983; Pin et al. 2008; Cambeses et al. 2014), mantle and crust-derived magma intrusion (Pereira et al. 2016; and references therein) and formation of the BAO oceanic basin, in the interval ca. 350–335 Ma. In the highly-oblique regime outlined above, the BAO marginal oceanic basin could develop as either a transient and small intra/back-arc basin or a transtensional (pull-apart) basin between the previously formed Pulo do Lobo accretionary prism to the SW and allochthonous HP and ofiolitic domains (Cubito-Moura, Fuenteheridos and IOMZOS) to the NW, in response to the migration of a mantle plume related triple junction along the continental margin (Castro et al. 1999), also responsible for the HT-LP metamorphic event.

(5) The remaining Rheic ocean re-entrant was entirely subducted by late Visean times, giving rise to the onset of continent-continent collision with south vergence, i.e. synthetic to the subduction zone active since the late

Devonian (Quesada 1991, 1998). We believe that it was during this stage when the BAO basin was inverted soon after its formation, and a fragment of which was imbricated with the HT-LP units still under high-grade conditions. The inverted metamorphic gradient in the BAO unit is interpreted as formed during a subsequent event, coeval to the formation of the South Iberian shear zone (Crespo-Blanc and Orozco 1991), along which the high-grade rocks were exhumed and retrogressed at ca. 338 Ma (Pérez-Cáceres et al. 2015, 2017).

12.5.1.4 Metamorphism in the External Thrust and Fold Belt Domains

J. Reche, F. J. Martínez, C. Quesada

Cantabrian Zone

J. Reche, F. J. Martínez

The Cantabrian zone (CZ), constitutes the most external part of the NW Iberia branch of the Variscan orogen and is characterized by the thin-skinned tectonic style that is typical of foreland thrust and fold belts. Rocks exposed in the core of the Cantabrian orocline are either non-metamorphic or show an incipient metamorphic grade in the diagenetic–metamorphic transitional domain. In the CZ Late Devonian to Mississippian and Pennsylvanian syn-orogenic rocks rest unconformably over a Cambrian to upper Devonian passive margin sedimentary pile (Julivert 1978; Marcos and Pulgar 1982). Following García-López et al. (2007) and Bastida et al. (2002), the regional metamorphism related to the Variscan orogeny only slightly affects the western part of the CZ (Gutiérrez-Alonso and Nieto 1996). In its NE sector (Ponga-Cuera and Picos de Europa units), recent studies of organic matter maturation (conodont color alteration index-CAI) in limestones and Kluber index (KI) in pelites have been performed by Blanco-Ferrera et al. (2017) in order to trace the evolution from diagenetic to low-grade metamorphic conditions. According to these authors diagenetic to epizonal conditions are present in the northeastern sector of the CZ, with CAI values ranging from 1 to 5.5 and diagenetic to anchimetamorphic KI values. The Ponga-Cuera unit and the Picos de Europa unit exhibit CAI values lower than 2 along with KI values within the domain of diagenesis with $T < 80$ °C, in part related to burial by Carboniferous sediments. Nevertheless, towards the southern part of the Picos de Europa domain a high thermal gradient is detected, and temperature reached ca. 375 °C (diacaizone/ancaizone) within the Picos de Europa basal trhust), the metamorphic conditions extending into the southern Pisuerga-Carrión unit and ascribed to upper Carboniferous to lower Permian thermal doming and post-orogenic extension.

South Portuguese Terrane

J. Reche, C. Quesada

The South Portuguese terrane (SPT) is a continental unit of Laurussian affinity (see Chap. 6 in this volume), which collided in late Visean times with the southern margin of the OMZ and previously accreted Pulo do Lobo terrane (PLT) oceanic affinity units, after complete closure of the Rheic ocean re-entrant referred to in the previous section (Quesada 1991, 1998, 2006; Murphy et al. 2015, 2016; Braid et al. 2010, 2011, 2012, 2018; among others). As a consequence of collision, a S-verging, S-propagating thin-skinned fold and thrust belt developed, rooted in a mid-crustal décollement located within the late Devonian PQ group, which is the oldest rock unit exposed in the entire SPT (Quesada 1998; see also Chaps. 6 and 10 in this volume). Variscan metamorphism in the SPT was first studied by Munhá (1976, 1979, 1983, 1990) and varies from diagenetic-anchizonal, in the southernmost SW Portugal domain and most of the Baixo Alentejo Flysch domain, to very-low grade and low-grade in the Pyrite Belt domain. This syn-orogenic metamorphism overprints a previous hydrothermal metamorphic event contemporaneous with the volcanic activity in the Pyrite Belt domain, which induced chemical and mineralogical changes (spilitization) in the rocks, leading to neoformation of adularia, chlorite and white mica in the volcanic protoliths (Munhá and Kerrich 1980; Munhá et al. 1980; Munhá 1983, 1990; Leistel et al. 1998).

Munhá (1983, 1990) described a systematic S-to-N metamorphic grade increase and defined four metamorphic zones: Zone 1, corresponding to the afore-mentioned SW Portugal and Baixo Alentejo Flysch domains, with zeolite facies rocks; Zone 2, in most of the Pyrite Belt domain, with prehnite-pumpellyite facies; Zone 3, in the northermost Pyrite Belt, with lower greenschist facies (chlorite zone); and Zone 4, corresponding to the PLT (at the time considered a part of the South Portuguese Zone), with greenschist facies metamorphism (chlorite and biotite zones).

More recently, Abad et al. (2001) completed and refined the picture by application of optical and electron-microscopy (SEM, HRTEM and AEM) and XR diffraction techniques on pelitic lithologies to characterize the textural relationships and chemical evolution of the minerals (mainly the phyllosilicates) and the clay mineralogy and crystal-chemical parameters (IC, the index of "crystallinity", b and $d001$), respectively. Their conclusions can be summarized as

follows: (i) the main mineral parageneses consist of quartz + dioctahedral K-rich mica + feldspars, but Na–K intermediate mica, paragonite, kaolinite and chlorite also occur locally; (ii) crystal thickness increases and defects decrease in the phyllosilicates with increasing metamorphic grade, although chlorite shows a higher density of strain-related defects than mica; (iii) XRD and AEM reveal a tendency for the micas to be more similar to muscovite and less to illite with increasing metamorphic grade, although both compositions coexist in all samples; (iv) muscovite, intermediate Na–K micas and paragonite commonly coexist in samples of anchizone grade; (v) the crystallinity index of illite increases with grade; (vi) the extent of phengitic substitution is extremely low, indicating LP conditions. This study confirmed the metamorphic grade increase from S-to-N found by Munhá (1983, 1990), but Abad et al. (2001) detected that it is not gradual but stepwise, in connection to the superposition of different thrust sheets in the fold and thrust belt.

12.5.2 The Pyrenean-Catalan Coastal Ranges Area

J. Reche, F. J. Martínez, M. Liesa, C. Aguilar

The Variscan basement crops out in the core of the Pyrenees in two E-W elongated areas, the North Pyrenean Zone (NPZ) and the Pyrenean Axial Zone (PAZ), parallel to the Alpine trend of the chain. Both areas are separated by the North Pyrenean Fault (NPF), a fault that was active during the sinistral movement of Iberia during the Early Cretaceous (Choukroune and Mattauer 1978; Debroas 1987, 1990). The Variscan basement also occurs in the Catalan Coastal Ranges (CCR), a set of two smaller ranges elongated in NE-SW direction, parallel to the main Alpine structures and the Mediterranean coast (Fig. 12.15). All these Variscan areas are constituted by several structural-thermal dome-shaped massifs formed by late Neoproterozoic to Ordovician metasediments, separated by pinched synforms constituted by younger rocks (Late Ordovician to Moscovian) (Vitrac-Michard 1975; Zwart 1986; Laumonier et al. 2004; Castiñeiras et al. 2008). Early Ordovician (Delaperrière and Respaud 1995; Deloule et al. 2002; Cocherie et al. 2005; Castiñeiras et al. 2008) and Late Ordovician (Casas et al. 2010) granitic intrusions were emplaced in the sequence. A comprehensive compilation of the Variscan metamorphism of the Pyrenean area is contained in the *Synthèse Géologique et Géophysique des Pyrénées* (Guitard et al. 1996).

According to a number of studies carried out in the Pyrenees (e.g. Zwart 1979; Carreras and Capellà 1994), two structural domains are distinguished. In the upper structural levels corresponding to low-grade metamorphic rocks, the main deformation phase is characterized by folds associated to thrust systems and to a poorly developed cleavage. In the lower structural levels, corresponding to medium- to high-grade metamorphic rocks, isoclinal folds are mostly formed with a pervasive axial plane foliation transposing the previous structures. The main Variscan crustal deformation began with a first D1 episode of N–S compression with S vergent folds and thrust nappes in the upper structural levels (Carreras and Capellà 1994; Gleizes et al. 1998; Vilà et al. 2007; Carreras and Druguet 2014; Denèle et al. 2014; Aguilar et al. 2015) during the Bashkirian to Moscovian (323–308 Ma). In the lower structural levels, this episode was probably coeval to an early Barrovian medium-pressure metamorphism (Martínez and Rolet 1988; Denèle et al. 2014). D2 took place from late Moscovian to Artinskian (308–290 Ma) times. It started before the P–T metamorphic climax, coeval with the widespread development of a pervasive foliation and continued after the metamorphic peak in retrograde conditions (D3 for several authors). D2 represents a thermal event characterized by the migmatization and granulitization of the lower crust coeval the intrusion of smaller mafic bodies. In the upper crust, syn- to late orogenic calc-alkaline granitoids and volcanics were emplaced (Pin and Vielzeuf 1988; Pin and Peucat 1986; Carreras and Capellà 1994; Debon et al. 1996; Gleizes et al. 1998; Vilà et al. 2007; Aguilar et al. 2015, 2016).

More than fifty years of research has led to propose different models for the tectonometamorphic and magmatic evolution of the Pyrenees during the late Variscan (Carboniferous—Permian, c. 325– 280 Ma). For some auhtors, D2 is interpreted as a dextral transpressive phase (Carreras and Capellà 1994; Gleizes et al. 1998; Druguet 2001; Román-Berdiel et al. 2004; Carreras and Druguet 2014; Vilà et al. 2007) associated with doming (Denèle et al. 2014). Other authors suggest that D2 is associated to diapiring doming of hot lower crust that took place coeval with the formation of a pervasive foliation and high temperature metamorphism (e.g. Soula 1982; Soula et al. 1986; Pouget 1991; Aguilar et al. 2015). At odds with these two models, there are other ones implying lithosphere scale extension associated with HT/LP metamorphism (e.g. Wickham 1987; van den Eeckhout and Zwart 1988; Gibson 1991; Vissers 1992).

The Pyrenean Variscan metamorphism has been presented as the type example for a continuous HT/LP metamorphic sequence since the early work of Zwart (1962, 1963) and Guitard (1970). The main characteristic sequence is divided in a series of zones and sequence of assemblages (all containing muscovite, quartz and plagioclase): chlorite-muscovite zone, biotite zone (biotite ± chlorite ± staurolite), andalusite-cordierite zone (andalusite + biotite ± cordierite ± staurolite ± garnet), sillimanite + muscovite zone (sillimanite +

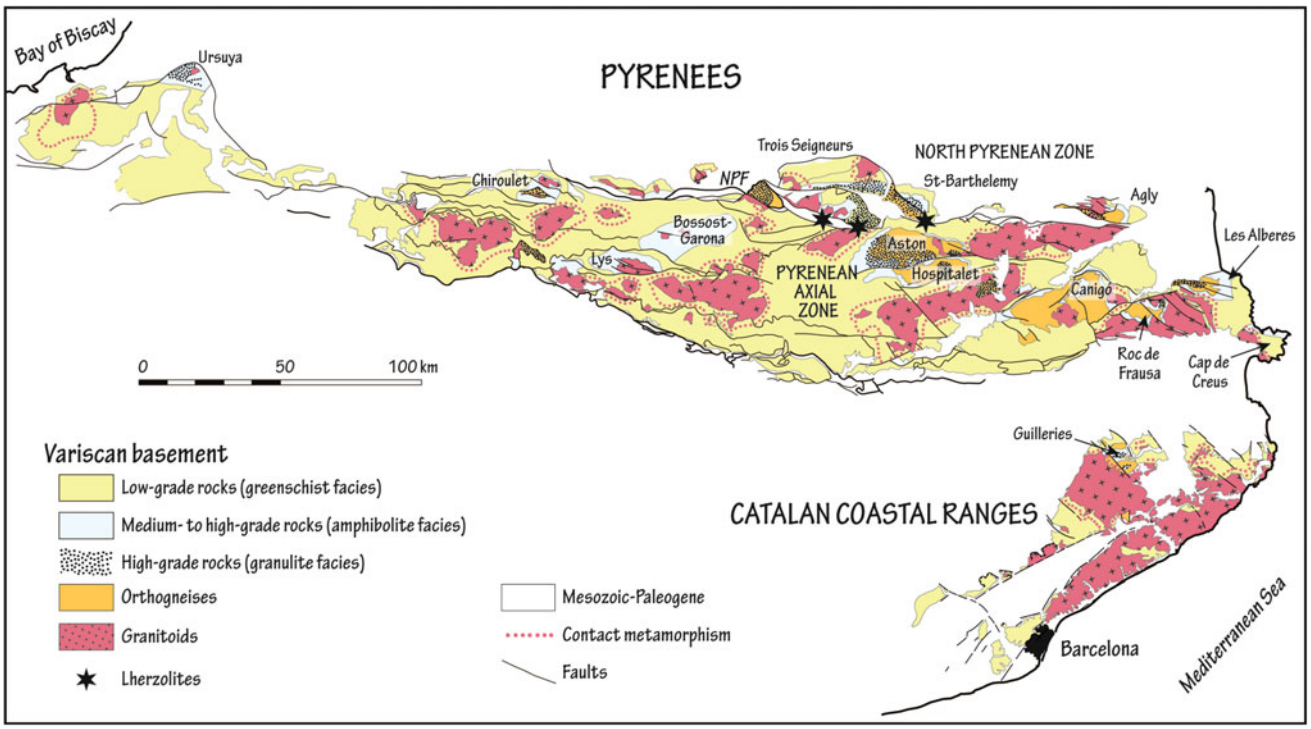

Fig. 12.15 Geological overview map of NE Iberia showing the Variscan basement of the Pyrenees and the Catalan Coastal Ranges (CCR) (modified after Debon and Guitard 1996). The distribution of low- to high-grade regional metamorphic rocks and the contact metamorphic aureoles is shown. NPF, North Pyrenean Fault

biotite ± andalusite ± cordierite ± staurolite ± garnet), and at the highest grade, sillimanite—K-feldspar zone (sillimanite + biotite ± garnet ± cordierite ± muscovite + K-feldspar). The presence of garnet, staurolite, chloritoid and even kyanite bearing assemblages has been signaled either as indicative of a previous and/or of a later medium pressure evolution (Laumonier et al. 2010). Metamorphic sequences are highly condensed and have extremely high apparent metamorphic field gradients with an average of 65–85 °C/km (Guitard et al. 1996).

The location of the NPZ, PAZ and CCR in the main zonal arrangement of the Variscan orogen of the Iberian massif is the object of debate. Whereas there is a general consensus to locate these areas in the southern branch of the Variscan fold belt, correlation with the CIZ or WALZ zones of the Iberian massif (Julivert 1981; Matte 1986a, b; Kroner and Romer 2013) is not clear yet. Álvaro et al. (2018 and references therein) consider that the Pyrenees and CCR have more affinity with the French Montagne Noire and Occitan domains, Sardinia or the Alps. Following plate reconstructions at 330 Ma by von Raumer et al. (2009, 2013), the Pyrenean domain was close to a NE-directed subduction zone of the Paleotethys. This setting or the location of the Pyrenean domain in an intracontinental subduction zone, N of the Armorican Spur proposed by Kroner and Romer (2013) could help to explain the Early Visean granitoid occurrences dated by Mezger and Gerdes (2014).

12.5.2.1 The North Pyrenean Zone (NPZ)

J. Reche, F. J. Martínez, M. Liesa, C. Aguilar

The metamorphic imprint in the NPZ is particularly well exposed on deep levels of the Variscan crust, which were exhumed due to post-Variscan tectonics (Fig. 12.15). The characteristic HT/LP metamorphic zoning was previously described by Fonteilles (1970) in the Agly massif, Guchereau (1975) and Saint-Blanquat (1993) in Saint Barthélemy massif and by Wickham (1984, 1987) and Mercier (1988) in the Trois Seigneurs massif (see Fig. 12.16).

In the basement of the Agly massif, the highest grade granulitic assemblages contain garnet + cordierite + sillimanite + K-feldspar + plagioclase + quartz ± biotite ± spinel in the Al-rich metapelitc paragneisses of the Belesta and Caramany series (Guitard and Raguin 1958) and orthopyroxene and clinopyroxene ± amphibole in the interlayered metabasites (Fonteilles 1970; Guitard et al. 1996). For the Agly gneissic core, peak P-T conditions of 0.6 ± 0.1 GPa and 750 ± 25 °C were estimated by Andrieux (1982a, b) and 0.5 ± 0.05 GPa and 800 ± 100 °C

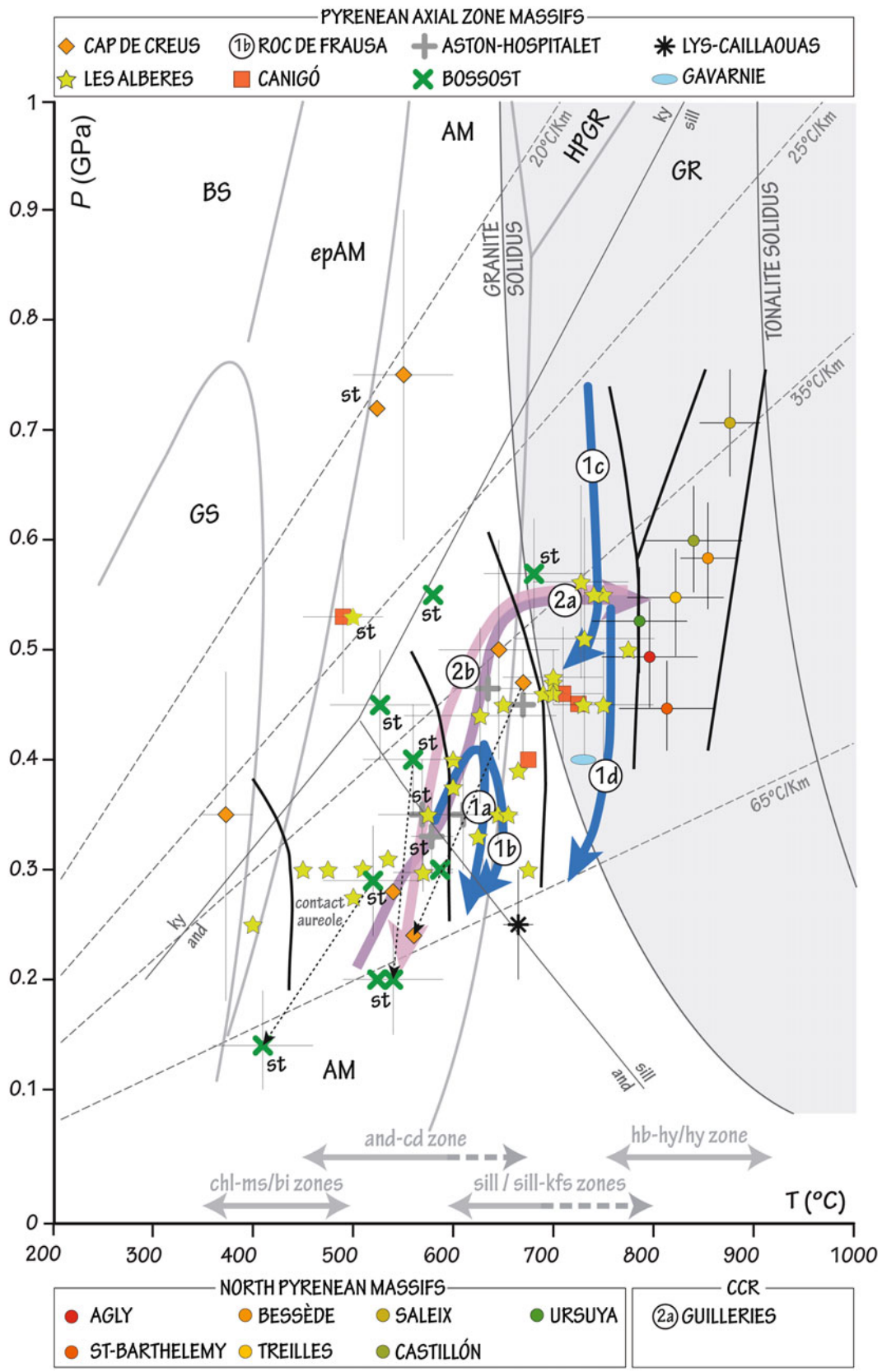
PYRENEAN AXIAL ZONE MASSIFS
CAP DE CREUS
1b ROC DE FRAUSA
ASTON-HOSPITALET
LYS-CAILLAOUAS
LES ALBERES
CANIGÓ
BOSSOST
GAVARNIE
P (GPa)
BS
AM
epAM
GS
HPGR
GR
GRANITE SOLIDUS
TONALITE SOLIDUS
20°C/Km
25°C/Km
35°C/Km
65°C/Km
ky
sill
and
st
1a
1b
1c
1d
2a
2b
contact aureole
and-cd zone
hb-hy/hy zone
chl-ms/bi zones
sill / sill-kfs zones
T (°C)
NORTH PYRENEAN MASSIFS
AGLY
BESSÈDE
SALEIX
URSUYA
ST-BARTHELEMY
TREILLES
CASTILLÓN
CCR
2a GUILLERIES

◀ **Fig. 12.16** Compilation of the P–T data of the Variscan metamorphism recorded in several massifs of the Pyrenees and Catalan Coastal Ranges from various authors. Colour symbols refer to single P-T determinations and arrows to P-T paths. Blue P-T paths calculated for (1a) a low-grade micaschist of the upper crustal level, (1b) a medium-grade g-sill bearing micaschist and (1c) a contact aureole migmatite of the intermediate crustal level, and (1d) a migmatite of Lower crustal level in the Roc de Frausa massif (Eastern Pyrenees) by Aguilar et al. (2015). Prograde (2a) and retrograde (2b) P-T paths deduced from the highest-grade zone in the Guilleries massif (Catalan Coastal Ranges) by Reche and Martínez (2002). Grey lines separate facies fields simplified after Spear (1993), Liou et al. (1998, 2009) and Okamoto and Maruyama (1999). Facies fields abbreviations: GS, greenschist facies; epAM, epidote-amphibolite facies; AM, amphibolite facies; BS, blueschist facies; ampEC, amphibole-eclogite facies; HPGR, high-pressure granulite facies; GR, granulite facies. Thin grey dashed lines represent geotherms of 20, 25, 35 and 65 °C/km. Al_2SiO_5 (Bohlen et al. 1991) and the minimum melting of granite solidus (Huang and Wyllie 1975) are shown for reference. Vertical black lines indicate approximate separation of the mineral zones

by Vielzeuf (1984). The latter author calculated similar P and higher T (0.6 GPa and 830–890 °C) in garnet + biotite + orthopyroxene metapelites from Bessede de Sault. Low-P granulitic assemblages were also found in the migmatitic zone and in the basal mylonitic paragneisses of the Saint Barthélemy Massif (the *gneiss de base* of Zwart 1954) that were stabilized around 0.45 ± 0.5 GPa and 750 ± 50 °C (Vielzeuf 1984). In Lherz-Saleix, the psamopelitic assemblage garnet + biotite + sillimanite + cordierite ± orthopyroxene (with K-feldspar and quartz) is present in Al-rich bulk compositions whereas the Al-poor bulk psamopelitic gneisses contain garnet + biotite + orthopyroxene.

Charnockites from this massif contain plagioclase + orthopyroxene ± clinopyroxene ± garnet ± K-feldspar ± biotite and mafic granulites have the assemblage clinopyroxene + orthopyroxene ± garnet ± amphibole ± biotite. Piriclasites (meta-intermediate rocks) contain garnet + orthopyroxene + clinopyroxene + plagioclase + quartz. Geothermobarometry for these granulites gave conditions of 0.7 ± 0.05 GPa and 750–800 °C (Vielzeuf 1984). West of Trois Seigneurs, in the Castillon massif the assemblage garnet + sillimanite + K-felspar ± biotite ± cordierite ± plagioclase crops out also extensively in felsic granulites (Roux 1977). Cordierite locally forms rims around garnet, as in the sillimanite zone of the Trois Seigneurs massif (Wickham 1984, 1987; Mercier 1988) or in Lherz-Saleix. This assemblage implies a decompressive and slightly cooling P-T path. In the Lherz-Saleix area, Vielzeuf (1980) deduced conditions around 0.5–0.6 GPa and 750 °C for the same assemblage.

The Ansignan charnockite (orthopyroxene ± garnet granodiorite lacolith, Guitard 1960) of the Agly massif was interpreted by Fonteilles (1976) as the product of anatexis, with growth of perithectic phases and partial assimilation of the migmatitic gneisses. The thermal anomaly is attributed to the calc-alkaline mafic diorite-gabbro-hornblendite intrusives. The U-Pb zircon ages of 316 ± 3 Ma obtained by Respaut and Lancelot (1983) in the mafic intrusives and 305 ± 9 Ma for the charnockites are in accordance with this hypothesis. In the Castillon massif, two-pyroxene charnockitic granite and a cordierite bearing anatectic granite were described by Thiebaut (1964) as well as a basic-ultrabasic "stratified complex" composed of peridotites, amphibolites and anorthosites, located inside the metapelitic granulites (Monchoux and Roux 1973; Roux 1977). A similar syn-metamorphic basic-ultrabasic "stratified complex" is found in the Ursuya Massif containing peripheral garnet + biotite bearing quartz-diorites (Boissonnas 1974). P–T conditions in the enclosing granulitic gneisses at Ursuya are estimated to be around 0.53 ± 0.05 GPa and 780 ± 50 °C (Vielzeuf 1984).

A striking feature of the metamorphic terrains in the North Pyrenean Zone is the thickness of the series. In the Bessede de Sault massif, the orthopyroxene-granulites and the biotite bearing greenschist facies zone are around 2 km apart (Vielzeuf 1984). In the Saint Barthélemy massif, Guchereau (1975) and Saint-Blanquat (1993) mapped a metamorphic sequence less than 3 km thick. As P determinations on the granulitic domains are on the range 0.5–0.7 GPa, this implies thinning of the series by tectonic processes along late ductile shear zones such as the Caladroy-Latour in the Agly massif (Bouhallier et al. 1991) or the BMM (Bande mylonitique majeur) responsible for major uplift of the Saint Barthélemy migmatitic-granulitic dome (Passchier 1982b). Saint-Blanquat (1993) considered the BMM as late-Variscan in age and Delaperrière et al. (1994) dated it (U/Pb monazite) at 300 ± 7 Ma. Delaperrière et al. (1994) also dated the granulite facies metamorphism of Saint Barthélemy at 310 ± 25 Ma and the beginning of cooling at 295 ± 5 Ma, data that are consistent with the ages determined by Respaut and Lancelot (1983) in the Agly massif.

12.5.2.2 The Pyrenean Axial Zone Massifs

J. Reche, F. J. Martínez, M. Liesa, C. Aguilar

The PAZ is characterized by large areas of low- to medium metamorphic grade and narrow areas of medium- to high-grade including migmatitic-granulitic domains. Metamorphic isograds tend to be concentric around the metamorphic/structural domes from the low-grade zones in the external envelopes to higher grade zones towards the core of the domes. Metamorphism increases in accordance

with the stratigraphic age. Nevertheless, along the PAZ, from W to E, deeper stratigraphic and structural levels crop out and metamorphism is discordant with the stratigraphy (Zwart 1986) (Fig. 12.15). Thus, in the western Bossost-Garona dome, medium-grade metamorphism affects rocks of Siluro-Devonian age whereas in the eastern Pyrenees medium-grade metamorphism is restricted to the Late Neoproterozoic-Ordovician succession.

The main metamorphic zonal arrangement of the different massifs is largely similar to the one described in Sect. 12.5.2. This is the case in the Cap de Creus (Carreras 1974; Reche et al. 1996; Druguet 2001), L'Albera (Autran et al. 1966; Guitard et al. 1996; Vilà et al. 2007), Canigó-Carançà (Guitard 1970; Zwart 1979; Ayora et al. 1993; Gibson and Bickle 1994; Guitard et al. 1996), Roc de Frausa (Liesa and Carreras 1989; Aguilar et al. 2015, 2016), Aston-Hospitalet (Zwart 1965; Van den Eeckhout 1986; Guitard et al. 1996; Mezger 2005, 2009; Mezger and Régnier 2016) and Bossost (Zwart 1962, 1963; Pouget 1991; Guitard et al. 1996; Pouget et al. 1996; Mezger and Passchier 2003, 2004). Some aspects, as the first appearance of andalusite or cordierite, the coexistence of stable staurolite, or the inclusions of staurolite or garnet in andalusite and/or cordierite in the andalusite-cordierite zone introduce variability into the main dominant HT/LP zoning. These features could be related to bulk compositional effects or to a previous Barrovian event of higher pressure. For example, garnet and staurolite are conspicuous minerals in the andalusite zone of several massifs as the Canigó, Aston and Bossost with the assemblage andalusite + biotite ± garnet ± staurolite ± cordierite (+ muscovite and quartz). Reaction textures indicative of garnet resorption to andalusite + biotite and to micas + plagioclase are present. Some garnets at the base of the Canigó lower sequence contain staurolite inclusions. Matrix staurolite is common, although in the upper part of the andalusite zone, staurolite constitutes an armoured relic in andalusite, and andalusite can be included in cordierite. On this basis, Guitard et al. (1996) defined three sub-zones with increasing grade: andalusite without staurolite, andalusite-staurolite and andalusite with armoured staurolite. Garnet can be present in either of these sub-zones. As stated by Mezger (2005, 2009) from observations in the Aston massif, staurolite and andalusite can form part of a unique equilibrium assemblage.

Kyanite has been found as relict inclusions in the Aston massif (Besson 1996) or as an assemblage with staurolite inside cordierite in the Canigó massif (Guitard et al. 1996; Azambre and Guitard 2001; Laumonier et al. 2010). These findings point to the evolution of the P-T paths from medium- to low pressure and the strong obliteration of the previous event by the main HT/LP event. Other remarkable special cases are related to the presence of medium P assemblages equilibrated in the kyanite field with garnet + chloritoid + staurolite + paragonite + muscovite ± biotite in Al-rich metapelites NW of the Cap de Creus massif. Guitard et al. (1996) related these assemblages to a late retrograde pressure increase in synformal areas during the doming phase, although they can also be formed by isobaric cooling. Retrograde kyanite is also found in L'Albera massif (Autran et al. 1970; Fonteilles and Guitard 1971; Guitard et al. 1996; Vilà et al. 2007).

Representative Variscan metamorphic P-T conditions and P-T paths for the PAZ are depicted in Fig. 12.16. Note that, with the exception of some kyanite-field P-T data in the Canigó and Cap de Creus massifs, the rest of P-T determinations are in accordance with a general andalusite—sillimanite HT/LP field gradient type. Maximum P conditions have been determined for the sillimanite- K-feldspar zone and are around 0.7–0.5 GPa with maximum temperatures from near 800–650 °C. P-T paths are clockwise in most of the massifs and they all depict a marked decrease in pressure to 0.3–0.2 GPa, followed in some cases by cooling. For example, Vilà et al. (2007) drew a P–T path for the migmatitic area of the L'Albera massif that goes from peak super-solidus conditions at 0.45 GPa and 730 °C, through a first segment of decompression down to 0.32 GPa and 625 °C followed by isobaric cooling to 400 °C. In the Cap de Creus massif, Reche et al. (1996) deduced a clockwise cooling segment from 0.5 ± 0.1 GPa and 650° to 0.1 GPa and 400 °C. Gibson and Bickle (1994) found peak conditions for the sillimanite-K-feldspar zone in the Canigó massif of 725 ± 25 °C for 0.45 GPa. MnNCKFMASHTO pseudosection modelling by Aguilar et al. (2015) recorded a decompressive P-T path with a slight cooling from ca. 0.55 GPa and 750 °C to ca. 0.25 GPa and 720 °C for the lower series of the Roc de Frausa massif. In the Hospitalet massif, Mezger and Régnier (2016) based on a MnNCKFMASH model obtained for the andalusite zone 0.35 GPa and 620° to 0.25 GPa and 530 °C and concluded that andalusite, cordierite and staurolite pertained to the same assemblage. In the andalusite-staurolite-cordierite zone of the Bossost dome, Mezger and Passchier (2003) and Mezger et al. (2004) distinguished also two metamorphic episodes: a M1 medium pressure episode with peak at ca. 0.55 GPa and 580 °C and a M2 low-pressure episode at ca. 0.20 GPa and 525 °C, syntectonic with doming and emplacement of granitoids. The work of Triboulet et al. (2005) in the Canigó massif is one of the few studies that deduced anti-clockwise P-T paths, in accordance with late intermediate P conditions. This author established peak conditions of ca. 650 °C–0.6 GPa using amphibole—plagioclase thermobarometry.

In general, authors agree that peak P–T conditions for the HT/LP main episode occurred during a syn-D2 event associated to migmatization and emplacement of deep seated

granitoids (Guitard et al. 1996; Denèle et al. 2014). According to Mezger and Gerdes (2014), migmatization took place at ca. 331 Ma (from zircon metamorphic overgrowths) or 340–320 Ma (monazite ages) and the emplacement of Bossost granitoids associated with the M2 event was at ca. 339–335 Ma. From these data, the authors deduced that a Visean early igneous activity and a related HT/LP gradient could have prevailed in some upper crustal domains and rejected the hypothesis of an early medium pressure event related to thickening. These determinations imply that even the M2 HT/LP episode, at least in this area, can be older than 305–309 Ma, ages generally accepted for M2 peak conditions in the Variscan Pyrenees (e.g. Denèle et al. 2014; Aguilar et al. 2014). Denèle et al. (2014) consider that the Visean ages might reflect zircon inheritance. In contrast, high-grade rocks cropping out in the lower crustal level of the Roc de Frausa massif were migmatized during a thermal episode that occurred in the interval 320–315 Ma coeval with the main Variscan deformation event and a syn-D2 gabbro was dated at 312–307 Ma (Aguilar et al. 2014). In the Cap de Creus massif, a 298 ± 3.8 Ma age for a syn-D2 quartz diorite from a migmatite complex and a 290 ± 2.9 Ma age for a syn-D2 granodiorite from lowest metamorphic grade rocks was obtained by Druguet et al. (2014). In a recent study, López Sánchez et al. (2018) obtained an Early Permian age (295 ± 2 Ma) for the Lys Caillaouas leucogranite and 297 ± 2 Ma for the Bossost massif. All these data also question the Visean age for the HT/LP metamorphism.

Migmatite complexes form metatexitic to diatexitic domains, generally associated to small intrusions of syn-D2 quartz-gabroic, quartz-dioritic and tonalitic lenses, and syn- to late-D2 leucogranitic and pegmatoid bodies. Examples are found in the northern coast of Cap de Creus, L'Albera and Roc de Frausa massifs (Druguet 2001; Druguet and Hutton 1998, Vilà et al. 2005, 2007; Aguilar et al. 2015, 2016) or around the Canigó deep granite (Guitard et al. 1996). In the contact aureole of the Ceret gabbro-diorite, Aguilar et al. (2016) determined peak conditions around 0.7–0.8 GPa and 840 °C. Peak metamorphism was followed by nearly isothermal decompression down to 0.55 GPa and then isobaric cooling to near 690 °C. These data represent the metamorphic climax of the country rocks and constrain the conditions at which the mafic rocks intruded.

12.5.2.3 The Catalan Coastal Ranges

J. Reche, F. J. Martínez

A low to high grade Variscan metamorphic sequence crops out in the Montseny and Guilleries massifs located at the NE end of the (CCR) Catalan Coastal Ranges (Fig. 12.15), developed after a Ediacaran (Martínez et al. 2011) to Devonian age metasedimentary succession. In the Guilleries massif the lower infra-Caradocian metamorphic sequence is divided into a high grade complex (Osor) and a medium to low grade complex (Susqueda). Above, lie a Caradocian low to medium grade volcanosedimentary sequence (Sant Martí Sacalm) and low grade Siluro-Devonian rocks (Durán 1985). These metasedimentary units contain various pre-Variscan intrusive bodies such as: Ordovician orthogneisses located in the Osor high grade complex with ages ranging from 488 ± 3 to 459 ± 3 Ma and Late Ordovician rhyolitic metavulcanites in the Sant Martí Sacalm formation (452 ± 4 Ma), according to Martínez et al. (2011). The zonal arrangement is also of the HT/LP type with chlorite-muscovite, biotite, andalusite-cordierite, sillimanite and migmatitic zones (Durán 1985; Sebastián et al. 1990). The chlorite zone is found in the Siluro-Devonian outcrops and the biotite zone is recognized in pelitic levels of the Sant Martí Sacalm volcanosedimentary sequence. The Susqueda complex is mainly within the cordierite-andalusite zone and the Osor complex contains sillimanite and higher-grade rocks. Contacts between zones are nearly coincidental with NE-SW trending faults whose age is still unclear but that could have already played a role as detachment zones during late Variscan times, thus helping to explain the high degree of condensation of metamorphic isograds, similar to what is also common in most of the Pyrenean massifs. The dominant foliation in high grade rocks is an evolved main D2 schistosity or gneissic foliation with a sub-horizontal attitude (Durán 1985). A D3 event generates a more widely spaced foliation (S3) and has a shear band style.

Variscan intrusives are per-aluminous two mica, pre- to syn-D3 leucogranites and biotite calcalkaline granitoids of similar ages (305.3 ± 1.9 to 299 ± 2.3 for the leucogranites, and 305.9 ± 1.5 for the biotite-granitoids; Martínez et al. 2008). Some syn-D2, syn-anatectic, quartz-diorite (Durán 1985), leucogranitic and garnet ± cordierite quartz-plagioclase bearing granitoide small lenses are found also in the Osor complex (Reche et al. 2015). These lenses depict mineralogical and textural evidence that suggests they could correspond to the earliest anatectic melts (Reche et al. 2016, 2017).

The ca. 323 ± 2 Ma composite hornblendite-gabbro-diorite Susqueda intrusive complex, emplaced in the cordierite-andalusite zone, generated a very irregular metamorphic aureole with ambient pressure conditions of ca. 0.3 GPa (Riesco et al. 2004). Contact anatexis oiriginated by this intrusive gave rise to garnet + cordierite + orthopyroxene bearing metapelitic granulites in its inner part. The ca. 320 Ma age of this intrusive is problematic as it seems more related to the earlier D1 episode. In the context of a study of provenance, age and tectonic evolution of the Variscan flysch in S France and NE Iberia (Martínez et al. 2016), SHRIMP in situ U-Pb monazite (included in garnet and in

the matrix) from sillimanite grade pelitic gneisses of the Osor complex yielded three age groups: ca. 360 Ma, ca. 327 ± 5 Ma and ca. 305 ± 6 Ma. The significance of the old 360–350 Ma (Upper Devonian—earliest Carboniferous) thermal event is still unclear although it can be related with local extensional processes. Significantly, the 327 ± 5 Ma age group is identical to the 327 ± 4 Ma (Visean—Namurian) detrital zircon ages obtained from pebbles of deformed orthogneiss found in a Carboniferous flysch deposit in the near locality of Cànoves (Montseny massif), very similar in appearance to the Guilleries gneiss. This suggests that Guilleries massif Variscan metamorphic rocks could have been exposed to surface erosion already at that time. This can be related to the effects of the D1 phase of deformation producing recumbent folds and/or nappes. Since ages determined for the Variscan syntectonic Susqueda complex (Martinez et al. 2008) are 323.6 ± 2.8 Ma, this would imply at least a local synchronicity of some HT/LP events in the Guilleries massif already during the D1 deformation episode, generally related to Barrowian-like gradients in other massifs from the Pyrenees and the Central Iberian zone. A near complete P-T path for the Osor complex was calculated by Reche and Martínez (2002) and it is one of increasing P and T from ca. 0.2 GPa and 500 °C to ca. 0.5 GPa and 700 °C (see Fig. 12.16). More recent data suggest higher peak values of around 0.6 GPa and at least locally, near 800 °C (Reche et al. 2015, 2016, 2017).

References

Abad I, Mata MP, Nieto F et al. (2001) The phyllosilicates in diagenetic-metamorphic rocks of the South Portuguese Zone, southwestern Portugal. Can Mineral 39:1571–1589.

Ábalos B (1990) Cinemática y mecanismos de la deformación en régimen de transpresión. Evolución estructural y metamórfica de la Zona de Cizalla Dúctil de Badajoz-Córdoba. PhD thesis, Univ País Vasco.

Ábalos B, Eguiluz L (1992) Structural geology of the Mina Afortunada gneiss dome (Badajoz-Córdoba shear zone, SW Spain. Annales Tectonicae VI (1): 95–110.

Ábalos B, Gil Ibarguchi I, Eguiluz L (1991) Evolución tectono-metamórfica del Corredor Blastomilonítico de Badajoz-Córdoba. II: Las unidades alóctonas y evolución PTt. Boletin Geológico y Minero 102: 617–671.

Abati J (1994) Evolución tectonotermal de las eclogitas de la unidad de Agualada (Complejo de Ordenes, NW del Macizo Ibérico). MSc dissertation, Universidad Complutense de Madrid.

Abati J (2002) Petrología metamórfica y geocronología de la unidad culminante del Complejo de Órdenes en la región de Carballo (Galicia, NW del Macizo Ibérico). Nova Terra, A Coruña.

Abati J, Dunning GR (2002) Edad U–Pb en monacitas y rutilos de los paragneisses de la Unidad de Agualada (Complejo de Órdenes, NW del Macizo Ibérico). Geogaceta 32:95–98.

Abati J, Dunning GR, Arenas R et al. (1999) Early Ordovician orogenic event in Galicia (NW Spain): evidence from U–Pb ages in the uppermost unit of the Órdenes Complex. Earth Planet Sci Lett 165:213–228.

Abati J, Arenas R, Martínez Catalán JR et al. (2003) Anticlockwise P–T path of granulites from the Monte Castelo Gabbro (Órdenes Complex, NW Spain). J Petrol 44:305–327.

Abati J, Castiñeiras P, Arenas R et al (2007) Using SHRIMP zircon dating to unravel tectonothermal events in arc environments. The early Palaeozoic arc of NW Iberia revisited. Terra Nova 19: 432–439.

Abati J, Gerdes A, Fernández-Suárez J, et al. (2010) Magmatism and early–Variscan continental subduction in the northern Gondwana margin recorded in zircons from the basal units of Galicia, NW Spain. Geol Soc Am Bull 122:219–235.

Abati J, Arenas R, Díez Fernández, Albert R, Gerdes A (2018) Combined zircon U\Pb and Lu\Hf isotopes study of magmatism and high-P metamorphism of the basal allochthonous units in the SW Iberian Massif (Ossa-Morena complex). Lithos 322: 20–37.

Acciaioli MHM, Munhá J (2000) Metamorphic zonality of the Serra da Freita area, Central-Iberian zone, North-Central Portugal. In: Variscan-Appalachian dynamics: the building of the Upper Paleozoic basement. Tectonics 15, A Coruna, Spain, Programs and abstracts.

Acciaioli MHM, Santos JF, Munhá JM (2005) Ar–Ar dates for two different stages of the Variscan D3 recorded in metapelites of Serra da Freita (North-Central Portugal). Geophysical Research Abstracts 7:10076, 5 p.

Aguado BV (1992) Geología estructural de la zona de cizalla de Porto-Tomar en la región de Oliveira de Azeméis -Serra de Arada (Norte de Portugal). PHD thesis, Universidad de Salamanca, Spain, 254 pp.

Aguado BV, Arenas R, Martínez Catalán JR (1993) Evolución metamórfica hercínica en la región de la Serra de Arada (Norte de Portugal). Comun. Serviços Geolológicos Portugal 79: 41–61.

Aguado BV, Azevedo MR, Schaltegger U, Martínez C, Nolan J (2005) U–Pb zircon and monazite geochronology of Variscan magmatism related to syn-convergence extension in Central Northern Portugal. Lithos 82 (1–2): 169–184.

Aguilar C, Liesa M, Castiñeiras P, Navidad M (2014) Late-Variscan metamorphic and magmatic evolution in the eastern Pyrenees revealed by U-Pb age zircon dating. Journal of the Geological Society, London 171: 181–192.

Aguilar C, Liesa M, Stıpska P, Schulmann K, Muñoz JA, Casas JM (2015) P–T–t–d evolution of orogenic middle crust of the Roc de Frausa Massif (Eastern Pyrenees): a result of horizontal crustal flow and Carboniferous doming? Journal of Metamorphic Geology 33: 273–294.

Aguilar C, Liesa M, Reche J, Powell R (2016) Fluid-fluxed melting and melt loss in a syntectonic contact metamorphic aureole from the Variscan Pyrenees. Journal of Metamorphic Geology 34:379–400.

Albert R, Arenas R, Gerdes A et al (2015) Provenance of the Variscan upper allochthon (Cabo Ortegal Complex, NW Iberian Massif). Gondwana Res 28 (4): 1434–1448. http://dx.doi.org/10.1016/j.gr.2014.10.016.

Alcock J, Arenas R, Martínez Catalán JR (2005) Shear stress in subducting continental margin from high-pressure, moderate-temperature metamorphism in the Órdenes Complex, Galicia, NW Spain. Tectonophysics 397:181–194.

Alcock JE, Martínez Catalán JR, Rubio Pascual F et al (2015) 2-D thermal modeling of HT–LP metamorphism in NW and Central Iberia: Implications for Variscan magmatism, rheology of the lithosphere and orogenic evolution. Tectonophysics 657: 21–37.

Álvaro JJ, Casas JM, Clausen S, Quesada C (2018) Early Palaeozoic Geodynamics in NW Gondwana. Journal of Iberian Geology 44: 551–565.

Andonaegui P, González del Tánago J, Arenas R et al (2002) Tectonic setting of the Monte Castelo gabbro (Órdenes Complex, northwestern Iberian Massif): evidence for an arc-related terrane in the hanging wall to the Variscan suture. In: Martínez Catalán JR et al

(eds). Variscan-Appalachian Dynamics: The Building of the Late Paleozoic Basement. Geol Soc Spec Pap 364:37–56.
Andonaegui P, Abati J and Díez Fernández R (2017) Late Cambrian magmatic arc activity in peri-Gondwana: geochemical evidence from the Basal Allochthonous Units of NW Iberia. Geologica Acta 15: 305–321.
Andrade AAS, Santos JF, Oliveira JT et al (1991) Magmatismo orogénico na transversal de Odivelas-Santa Susana. XI Reun Geol Oeste Peninsular, Huelva, Excursion guide-book, 47–54.
Andrieux P (1982a) La charnockite d'Ansignan (massif de l'Agly-Pyrénées orientales). Mise en place et évolution paragénétique. Introduction a l'étude des equilibres grenat-orthopyroxene. Thèse 3ème cycle, Clermont-Ferrand, 109 p.
Andrieux P (1982b) Conditions de cristallisation et évolution paragénétique d'une charnockite hercynienne: le complexe granulitique d'Ansignan (massif de l'Agly, Pyrénées orientales). Bull Mineral 105: 253–266.
Antunes A, Santos JF, Azevedo MR, Corfu F (2011) New U–Pb zircon age constraints for the emplacement of the Reguengos de Monsaraz Massif (Ossa Morena Zone). Seventh Hutton symposium on granites and related rocks—abstracts book, Ávila, 9–10.
Apalategui O, Quesada C (1987) Transversal geológica de la zona Ossa-Morena. Open-file report, Instituto Geológico Minero de España, 89 p.
Apalategui O, Barranco E, Contreras F et al (1984) Mapa Geológico de España, E. 1:50000, sheet 917: Aracena. Instituto Geológico Minero España, Madrid.
Apalategui O, Borrero JD, Higueras P (1985) Division en grupos de rocas en Ossa-Morena oriental. Temas Geol Min 7: 73–80.
Apraiz A (1998) Geología de los macizos de Lora del Rio y Valuengo (Zona de Ossa-Morena). Evolución tectonometamórfica y significado geodinámico. PhD thesis, Univ País Vasco.
Apraiz A, Eguiluz L (1996) El núcleo metamórfico de Valuengo (Zona de Ossa-Morena, Macizo Ibérico): petrografía, termobarometría y evolución geodinámica. Rev Soc Geol España 9: 29–49.
Apraiz A, Eguiluz L (2002) Hercynian tectono-thermal evolution associated with crustal extension and exhumation of the Lora del Río metamorphic core complex (Ossa-Morena zone, Iberian Massif, SW Spain). Int J Earth Sci (Geol Runds) 91:76–92. https://doi.org/10.1007/s005310100206.
Apraiz A, Eguiluz L, Ábalos B (1993) Evolución metamórfica y anatexia en el Núcleo de Lora del Río (Zona de Ossa-Morena). Rev Soc Geol España 6: 85–103.
Araújo A, Fonseca P, Munhá J, Moita P, Pedro J, Ribeiro A (2005) The Moura Phyllonitic Complex: An Accretionary Complex related with obduction in the Southern Iberia Variscan Suture. Geod Act 18 (5): 375–388.
Araújo A, Piçarra J, Borrego J, Pedro J, Oliveira JT (2013) As regiões central e sul da Zona de Ossa-Morena. In: Dias R, Araújo A, Terrinha P, Kullberg JC (eds), Geologia de Portugal, Vol I – Geologia Pré-mesozóica de Portugal, Escolar Editora.
Areias M (2014) Petrogenesis of a Variscan migmatite complex (NW Portugal): petrography, geochemistry and fluids. PhD thesis, Fac Ciênc Univ Porto.
Arenas R (1988) Evolución petrológica y geoquímica de la unidad alóctona inferior del complejo metamórfico básico-ultrabásico de Cabo Ortegal (Unidad de Moeche) y del Silúrico paraautóctono, Cadena Hercínica Ibérica (NW de España). Corpus Geologicum Gallaeciae, A Coruña.
Arenas R (1991) Opposite P–T–t paths of Hercynian metamorphism between the upper units of the Cabo Ortegal Complex and their substratum (northwest of the Iberian Massif). Tectonophysics 191:347–364.
Arenas R, Martínez Catalán JR (2002) Prograde development of corona textures in metagabbros of the Sobrado window (Ordenes Complex, NW Iberian Massif). In: Martínez Catalán JR et al (eds). Variscan-Appalachian Dynamics: The Building of the Late Paleozoic Basement. Geol Soc Spec Pap 364:73–88.
Arenas R, Martínez Catalán J (2003) Low-P metamorphism following a Barrovian type evolution. Complex tectonic controls for a common transition, as deduced in the Mondonedo thrust sheet (NW Iberian Massif). Tectonophysics 365: 143–164.
Arenas R, González Lodeiro F, Peinado M (1982) La zona de cizalla de Berzosa-Riaza en el sector septentrional. Influencia sobre la configuración de las zonas metamórficas. Cadernos do Laboratorio Xeolóxico de Laxe 3: 123–161.
Arenas R, Gil Ibarguchi JI, González Lodeiro F, et al. (1986) Tectonostratigraphic units in the complexes with mafic and related rocks of the Iberian Massif. Hercynica II (2): 87–110.
Arenas R, Fúster JM, González Lodeiro F et al (1991) Evolución metamórfica hercínica de la región de Segovia (Sierra de Guadarrama). Revista de la Sociedad Geológica de España 4: 195–201.
Arenas R, Rubio Pascual FJ, Díaz García F et al (1995) High pressure micro-inclusions and development of an inverted metamorphic gradient in the Santiago Schists (Ordenes Complex, NW Iberian Massif, Spain): evidence of subduction and syncollisional decompression. J Metamorph Geol 13:141–164.
Arenas R, Abati J, Martínez Catalán JR et al (1997) P–T evolution of eclogites from the Agualada Unit (Órdenes Complex, NW Iberian Massif (Spain): Implications for crustal subduction. Lithos 40:221–242.
Arenas R, Díez Fernández R, Sánchez Martínez S et al (2014) Two-stage collision: Exploring the birth of Pangea in the Variscan terranes. Gondwana Res 25:756–763.
Arenas R, Díez Fernández R, Rubio Pascual, FJ et al (2016a) The Galicia-Ossa-Morena zone: proposal for a new zone of the Iberian Massif. Variscan implications. Tectonophysics 681:135–143.
Arenas R, Sánchez Martínez S, Díez Fernández R et al (2016b) Allochthonous terranes involved in the Variscan suture of NW Iberia: A review of their origin and tectonothermal evolution. Earth-Science Reviews, 161:140–178.
Arenas R, Fernández-Suárez J, Montero P et al (2018) The Calzadilla Ophiolite (SW Iberia) and the Ediacaran fore-arc evolution of the African margin of Gondwana. Gondwana Res 58:71–86.
Arriola A, Eguiluz L, Fernández-Carrasco J et al (1984) Zonación metamórfica en el área Monesterio-Fuente de Cantos: criterios texturales y mineralógicos. Cadernos Laboratorio Xeolóxico Laxe 8: 169–193.
Autran A, Fonteilles M, Guitard G (1966) Discordance du Paléozoïque inférieur métamorphique sur un socle gneissique antéhercynien dans le massif des Alberes (Pyrénées orientales). C R Acad Sci Paris 263:317–320.
Autran A, Fonteilles M, Guitard G (1970) Rélations entre les intrusions de granitoïdes, l'anatexie, et le métamorphisme régional considerées principalment du point de vue de l'eau: cas de la Chaîne hercynienne des Pyrénées Orientales. Bulletin Societé Géologique de France 7: 673–731.
Ayora C, Liesa M, Delgado J (1993) Low-thermal gradient Hercynian metamorphism in the eastern Pyrenees. Journal of Meta- morphic Geology 11, 49–58.
Azambre B, Guitard G (2001) Disthène et staurotide réliques dans les métapelites du Canigou (Pyrénées orientales). Rélations avec les épisodes hercyniens de basse et moyenne pressions. CR Acad Sci Paris, Sciences de la Terre et des planètes/Earth and Planetary Sciences 333: 601–609.
Azor A (1994) Evolución tectonometamórfica del límite entre las zonas Centroibérica y de Ossa-Morena (Cordillera Varisca, SO de España). PhD thesis, Univ Granada.

Azor A, Ballèvre M (1997) Low-pressure metamorphism in the Sierra Albarrana Area (Variscan Belt, Iberian Massif). Journal of Petrology 38 (1): 35–64.

Azor A, González Lodeiro F, Simancas JF (1993) Cadomian subduction/collision and Variscan transpression in the Badajoz-C6rdoba Shear Belt, southwest Spain: a discussion on the age of the main tectonometamorphic events. Tectonophysics 217:343–346.

Azor A, González Lodeiro F, Simancas JF (1994) Tectonic evolution of the boundary between the Central Iberian and Ossa-Morena zones (Variscan belt, southwest Spain). Tectonics 13:45–61.

Azor A, Bea F, González Lodeiro F, Simancas JF (1995) Geochronological constraints on the evolution of a suture: the Ossa-Morena/Central Iberian contact. Geologische Rundschau 84:375–383.

Azor A, Expósito I, González Lodeiro F, Simancas JF, Martínez Poyatos D (2004) Zona de Ossa-Morena. Estructura y metamorfismo. In: Vera JA (ed), Geología de España, SGE-IGME, Madrid, 173–189.

Azor A, Rubatto D, Simancas JF et al (2008) Rheic Ocean ophiolitic remnants in Southern Iberia questioned by SHRIMP U-Pb zircon ages on the Beja-Acebuches amphibolites. Tectonics 27:TC5014. https://doi.org/10.1029/2009tc002527.

Azor A, Simancas JF, Martínez Poyatos DJ, Montero P, Bea F, Gonzalez Lodeiro F, Gabites J (2012) Nuevos datos geocronológicos sobre la evolución tectonometamórfica de la Unidad de Sierra Albarrana (Zona de Ossa-Morena, SO de Iberia). VIII Congreso Geológico de España, Geo-Temas 13.

Azor A, Simancas JF, Martínez Poyatos D, Montero P, González Lodeiro F, Pérez-Cáceres I (2016) U-Pb zircon age and tectonic meaning of the Cardenchosa pluton (Ossa-Morena Zone). IX Congreso Geológico de España, Geo-Temas 16 (2): 23–26.

Balcázar N, Meresch WV, Schertl HP et al. (2005) Petrology of the high-pressure "Basal Unit" Morais Complex, Northeast Portugal. Indian Journal of Geology 75 (2003):9–37.

Ballèvre M, Bosse V, Ducassou C, Pitra P (2009) Palaeozoic history of the Armorican Massif: Models for the tectonic evolution of the suture zones. C. R. Geoscience 341: 174–201.

Ballèvre M, Martínez Catalán JR, López-Carmona A et al (2014) Correlation of the nappe stack in the Ibero-Armorican arc across the Bay of Biscay: a joint French-Spanish project. Geol Soc London Spec Publ 405:77–113.

Barbero L (1995) Granulite-facies metamorphism in the Anatectic Complex of Toledo, Spain: late Hercynian evolution by crustal extension. J Geol Soc Lond 152: 365–383.

Barbero L, Villaseca C (2000) Eclogite facies relics in metabasites from the Sierra de Guadarrama (Spanish Central System): P–T estimations and implications for the hercynian evolution. Mineral Mag 64: 815–836.

Bard JP (1969) Le métamorphisme régional progressif des Sierras d'Aracena en Andalousie occidentale (Espagne). Sa place dans le segment sud-Ibérique. Thèse, Univ Montpellier, 1–398.

Bard JP (1977) Signification tectonique des métatholéites d'affinité abyssale de la ceinture métamorphique de basse pression d'Aracena (Huelva, Espagne). Bull Soc Géol France (7) 19: 385–393.

Barrois C (1883) Mémoire sur les schistes métamorphiques de Île de Groix. Annales de la Société Géologique du Nord XI 9:18–71.

Barrie CT, Amelin Y, Pascual E (2002) U-Pb Geochronology of VMS mineralization in the Iberian Pyrite Belt. Mineralium Deposita 37: 684–703. https://doi.org/10.1007/s00126-002-0302-7.

Bastida F, Brime C, García-López S, Aller J, Valín ML, Sanz-López J (2002) Tectono-thermal evolution of the Cantabrian Zone (NW Spain). Palaeozoic conodonts from northern Spain. IGME, Madrid, 105–124.

Bea F, Montero P, González-Lodeiro F, Talavera C (2007) Zircon inheritance reveals exceptionally fast crustal magma generation processes in Central Iberia during the Cambro-Ordovician. J Petrol 48: 2327–2339.

Bea F, Pesquera A, Montero P, Torres-Ruiz J, Gil-Crespo PP (2009) Tourmaline 40Ar/ 39Ar chronology of tourmaline-rich rocks from Central Iberia dates the main Variscan deformation phases. Geologica Acta 7: 399–412.

Bento-dos-Santos T, Ribeiro ML, González-Clavijo E, Díez-Montes A, Solá AR (2010) Geothermobarometric estimates and P-T paths for migmatites from Farilhões Islands, Berlengas Archipelago, W Portugal. VIII Congresso Nacional de Geologia, Braga, e-Terra 16, 11: 1–4.

Behr HJ, Engel W, Franke W (1982) Variscan wild-flysch and nappe tectonics in the Saxothuringian Zone (northeast Bavaria, West Germany). Am J Sci 282: 1438–1470.

Berman RG (1988) Internally consistent thermodynamic data for minerals in the system Na2 O–K2 O–v CaO–MgO–FeO–Fe2 O3 – Al2 O3 –SiO2 –H2 O–CO2. Journal of Petrology 29: 445–522.

Berman RG (1991) Thermobarometry using multi-equilibrium calculations: a new technique, with petrological applications. Canadian Mineralogist 29: 833–855.

Berman RG (2007) winTWQ (version 2.3): a software package for performing internally-consistent thermobarometric calculations. Geological Survey of Canada, Open File 5462, (ed. 2.32), 41 p.

Besson M (1996) Métamorphisme Hercynien: Le massif Aston-Hospitalet. In : Barnolas A, Chiron JC, Guérangé B (eds), Synthèse Géologique et Géophysique des Pyrénées. BRGM-ITGE, Orleans-Madrid, 550–560.

Bischoff L, Schäfer G, Schmidt K, Walter R (1973) Zur geologie der mittleren Sierra de Guadarrama. Forsch Geol Paläont Münster 28: 27–30.

Blanco-Ferrera S, Sanz-López J, García-López S, Bastida F (2017) Tectonothermal evolution of the northeastern Cantabrian zone (Spain). Int J Earth Sci (Geol Rundsch) 106: 1539–1555.

Blatrix P, Burg JP (1981) $^{40}Ar/^{39}Ar$ dates from Sierra Morena (Southern Spain). Variscan metamorphism and Cadomian Orogeny. Neues Jharbuch für Mineralogie-Monatshefte 10:470–478.

Boissonnas J (1974) Iholdy, carte géologique détaillée à 1/50000. Service Géologique National – BRGM Orleans.

Bohlen SR, Montana A, Kerrick DM (1991) Precise determinations of the equilibria kyanite=sillimanite and kyanite=andalusite and a revised triple point for AI_2SiO_5 polymorphs. Am Mineral 76:677–680.

Booth-Rea G, Simancas JF, Azor A, Azañón JM, González-Lodeiro F, Fonseca P (2006) HP-LT Variscan metamorphism in the Cubito-Moura schists (Ossa-Morena zone, southern Iberia). Compt Rendus Geosci 338: 1260–1267.

Bosse V, Féraud G, Ballèvre M et al (2005) Rb–Sr and $^{40}Ar/^{39}Ar$ ages in blueschists from the Île de Groix (Armorican Massif, France): Implications for closure mechanisms in isotopic systems. Chem Geol 220:21–45.

Bouhallier H, Choukroune P, Ballèvre M (1991) Évolution structurale de la croûte profonde hercynienne: exemple du massif de l'Agly (Pyrénées orientales, France). C R Acad Sci Paris 312: 647–654.

Braid JA, Murphy JB, Quesada C (2010) Structural analysis of an accretionary prism in a continental collision setting, the Late Paleozoic Pulo do Lobo Zone, Southern Iberia. Gondwana Research 17: 422–439. https://doi.org/10.1016/j.gr.2009.09.003.

Braid JA, Murphy JB, Quesada C, Mortensen J (2011) Tectonic escape of a crustal fragment during the closure of the Rheic Ocean: U–Pb detrital zircon data from the Late Palaeozoic Pulo do Lobo and South Portuguese zones, southern Iberia. J Geol Soc London 168: 383–392. https://doi.org/10.1144/0016-76492010-104.

Braid JA, Murphy JB, Quesada C, Bickerton L, Mortensen JK (2012) Probing the composition of unexposed basement, South Portuguese Zone, southern Iberia: implications for the connections between the Appalachian and Variscan orogens. Can J Earth Sci 49(4):591–613.

Braid JA, Murphy JB, Quesada C, Gladney ER, Dupuis N (2018) Progressive magmatism and evolution of the Variscan suture in southern Iberia. Int J Eartn Sci (Geol Runds) 107: 971–983.

Brown M (2014) The contribution of metamorphic petrology to understanding lithosphere evolution and geodynamics. Geoscience Frontiers 5:553–569.

Brun JP, Burg JP (1982) Combined thrusting and wrenching in the Ibero-Armorican arc: a corner effect during continental collision. Earth and Planetary Science Letters 61:319–332.

Bucher K, Frey M (1994) Petrogenesis of metamorphic rocks. 6th Ed, Springer-Verlag (Berlin), 318 pp.

Burg JP, Iglesias M, Laurent Ph, Matte Ph, Ribeiro A (1981) Variscan intracontinental deformation: the Coimbra–Córdoba Shear Zone (SW Iberian Peninsula). Tectonophysics 78: 161–177.

Burg JP, Balé P, Brun JP, Girardeau J (1987) Stretching lineation and transport direction in the Ibero-Armorican arc during the Siluro-Devonian collision. Geodinamica Acta 1:71–87.

Burov E, François T, Yamato P et al (2012) Mechanisms of continental subduction and exhumation of HP and UHP rocks. Gondwana Res 25:464–493.

Cambeses A, Scarrow J, Montero P et al (2014) SHRIMP U–Pb zircon dating of the Valencia del Ventoso plutonic complex, Ossa-Morena Zone, SW Iberia: Early Carboniferous intra-orogenic extension-related 'calc-alkaline' magmatism. Gondwana Res 21 (4): 887–900.

Capdevila R (1969) Le métamorphisme régional progressif et les granites dans le segment hercynien de Galice nord oriental (NW de l'Espagne). PhD thesis, Univ Montpellier, 430 p.

Capote R, Fernández Casals MJ, González Lodeiro F, Iglesias M (1977) El límite entre las zonas Astur Occidental–Leonesa y Galáico-Castelllana en el Sistema Central. Boletín Geológico Minero 88: 517–520.

Carreras J (1974) Petrologia y analisis estructural de las rocas metamorficas de la zona del Cap de Creus (prov. de Gerona). Tesis doctoral, Univ. de Barcelona.

Carreras J, Capellà (1994) Tectonic Levels in the Paleozoic basement of the Pyrenees – A review and a new interpretation. Journal of Structural Geology 16: 1509–1524.

Carreras J, Druguet E (2014) Framing the tectonic regime of the NE Iberian Variscan segment. Geological Society Special Publication 405: 249–264.

Carreras J, Cirés J (1986) The geological significance of the western termination of the Mérens fault at Port Vell (Central Pyrenees). Tectonophysics 129: 99–114.

Carrington-da-Costa M (1950) Noticia sobre uma carta geológica do Buçaco de Nery Delgado. Comunicações dos Serviços Geológicos de Portugal 28.

Carvalhosa A (1983) Esquema Geológico do Maciço de Évora. Comunicações dos Serviços Geológicos de Portugal 69/2, 201–208.

Casas JM, Castiñeiras P, Navidad M, Liesa M, Carreras J (2010) New insights into the Late Ordovician magmatism in the Eastern Pyrenees: U–Pb SHRIMP zircon data from the Canigó massif. Gondwana Research 17 (2–3): 317–324.

Casquet C, Navidad M (1985) El metamorfismo en el Sistema central Español. Comparación entre el sector central y el oriental en base al zonado del granate. Revista de la Real Academia de Ciencias Exactas, Físicas y Naturales de Madrid, LXXIX- 4.

Castiñeiras P (2005) Origen y evolución tectonotermal de las unidades de O Pino y Cariño (Complejos Alóctonos de Galicia). Nova Terra, A Coruña.

Castiñeiras P, Andonaegui P, Arenas R et al (2002) Descripción y resultados preliminares del plutón compuesto de San Xiao, Complejo de Cabo Ortegal (noroeste del Macizo Ibérico). Geogaceta 32:111–114.

Castiñeiras P, Navidad M, Liesa M et al (2008) U-Pb zircon ages (SHRIMP) for Cadomian and Early Ordovician magmatism in the Eastern Pyrenees: New insights into the pre-Variscan evolution of the northern Gondwana margin. Tectonophysics 461: 228–239.

Castro A, Fernández C, de la Rosa JD et al (1996a) Triple-junction migration during Paleozoic plate convergence: the Aracena metamorphic belt, Hercynian massif, Spain. Geol Rundsch 85:180–185.

Castro A, Fernández C, de la Rosa JD, Moreno-Ventas I, Rogers G (1996b) Significance of MORB-derived amphibolites from the Aracena metamorphic belt, Southwest Spain. J Petrol 37: 235–260.

Castro A, Fernández C, El-Hmidi H et al (1999) Age constraints to the relationships between magmatism, metamorphism and tectonism in the Aracena metamorphic belt, southern Spain. Int Journ Earth Sciences 88: 26–37.

Chacón J (1979) Estudio geológico del sector central del anticlinorio Portalegre-Badajoz-Córdoba (Macizo Ibérico Meridional). PhD thesis Univ Granada, 728 p.

Chichorro M (2006) Estrutura do Sudoeste da Zona de Ossa-Morena: Área de Santiago de Escoural—Cabrela (Zona de Cisalhamento de Montemor-o-Novo, Maciço de Évora). PhD thesis, Univ Évora, 502 p.

Chichorro M, Pereira MF, Apraiz A, Silva JB (2003) Syntectonic High-Temperature / Low-Pressure metamorphism in the Boa Fé Fault Zone (Évora Massif, Western Ossa-Morena Zone), Proceedings VI Congresso Nacional de Geologia. Universidade Nova Lisboa.

Chichorro M, Pereira MF, Díaz-Azpíroz M, Williams IS, Fernández C, Pin C, Silva JB (2008) Cambrian ensialic rift-related magmatism in the Ossa-Morena Zone (Évora-Aracena metamorphic belt, SW Iberian Massif): Sm-Nd isotopes and SHRIMP zircon U-Th-Pb geochronology. Tectonophysics 461:91–113.

Choukroune, P & Mattauer, M (1978): Tectonique de plaques et Pyrénées: sur le fonctionement de la faille trasformante Nord-Pyrénnéenne: comparaison avec les modèles actuels. Bull Soc. Géol. France, 7, 20 (5), 689–700.

Cocherie A, Baudin Th, Autran A, Guerra C, Fanning CM, Laumonier B (2005) U–Pb zircon (ID-TIMS and SHRIMP) evidence for the early Ordovician intrusion of metagranites in the late Proterozoic Canaveilles Group of the Pyrenees and the Montagne Noire (France). Bull Soc Géol France 176: 269–282.

Conde LEN (1984) Excursão geológica na região de Ferreira do Zêzere-Abrantes. In: Livro-Guia das excursões da VI Reunião do Grupo Ossa-Morena. Museu e Laboratório Mineralógico e Geológico da Universidade de Coimbra, 8 p.

Connolly JAD (1990) Multivariable phase diagrams; an algorithm based on generalized thermodynamics. Am J Sci 290: 666–718.

Connolly JAD (2005) Computation of phase equilibria by linear programming: a tool for geodynamic modeling and its application to subduction zone decarbonation. Earth Planet Sci Lett 236: 524–541.

Connolly JAD, Petrini K (2002) An automated strategy for calculation of phase diagram sections and retrieval of rock properties as a function of physical conditions. J Metamorph Geol 20: 697–708.

Crespo-Blanc A (1989) Evolución geotectónica del contacto entre la Zona de Ossa-Morena y la Zona Surportuguesa en las sierras de Aracena y Aroche (Macizo Ibérico Meridional): un contacto mayor en la Cadena Hercínica Europea. PhD thesis, Univ Granada, 324 p.

Crespo-Blanc A, Orozco M (1991) The boundary between the Ossa-Morena and South Portuguese zones (Southern Iberian Massif): a major suture in the European Hercynian Chain. Geol Rundsch 80: 691–702.

Crowley QG, Floyd PA, Winchester JA, Franke W, Holland JG (2000) Early Palaeozoic rift-related magmatism in Variscan Europe: fragmentation of the Armorican Terrane Assemblage. Terra Nova 12: 171–180.

Dahn DRL, Braid JA, Murphy JB, Quesada C, Dupuis N, McFarlane CRM (2014) Geochemistry of the Peramora Mélange and Pulo do Lobo schist: geochemical investigation and tectonic interpretation of mafic mélange in the Pangean suture zone, Southern Iberia. Int J Earth Sci (Geol Rundsch) 103: 1415–1431. https://doi.org/10.1007/s00531-014-1024-7.

Dallmeyer RD, Quesada C (1992) Cadomian vs. Variscan evolution of the Ossa-Morena Zone (SW Iberia): field and 40Ar/39Ar mineral age constraints. Tectonophysics 216: 339–364.

Dallmeyer RD, Ribeiro A, Marques F (1991) Polyphase Variscan emplacement of exotic terranes (Morais and Bragança Massifs) onto Iberian successions: Evidence from $^{40}Ar/^{39}Ar$ mineral ages. Lithos 27:133–144.

Dallmeyer RD, Fonseca PE, Quesada C, Ribeiro A (1993) $^{40}Ar/^{39}Ar$ mineral age constraints on the tectonothermal evolution of the Variscan Suture in SW Iberia. Tectonophysics 222: 177–194.

Dallmeyer RD, Martínez Catalán JR, Arenas R et al (1997) Diachronous Variscan tectonothermal activity in the NW Iberian Massif: Evidence from $^{40}Ar/^{39}Ar$ dating of regional fabrics. Tectonophysics 277:307–337.

Debon, F., Enrique, P. & Autran, A.,1996. Magmatisme Hercynian. In: Barnolas, A. & Chiron, J.C (eds) Synthèse gèologique et géophysique des Pyrénées. Vol. 1: Introduction. Géophysique. Cycle Hercynien. Bulletin de la Société Géologique de France and Instituto Geológico y Minero de España, Orléans and Madrid, pp. 303–359.

Debon F, Guitard G (1996) Carte de synthèse métamorphisme et plutonisme hercyniens. In: Barnolas A, Chiron JC (Eds), Synthèse géologique et géophysique des Pyrénées 1: Introduction. Géophysique. Cycle hercynien. BRGM, Orleans, Mag H3.

Delgado Quesada M (1971) Esquema geológico de la hoja nº 878 de Azuaga (Badajoz). Boletín Geológico Minero 82:277–286.

Debroas, EJ (1987) Modéle de bassin triangulaire à l'intersection de décrochements divergents pour le fossé albo-cénomanien de la Ballongue (zone nord-pyrénéenne, France. Bull. Soc. Géol. France, 8, 887–898.

Debroas, EJ (1990) Le Flysch noir albo-cénomanien témoin de la structuration albienne a sénonienne de la zone nord-pyrénéenne en Bigorre (Hautes Pyrénées, France). Bull. Soc. Géol. France, 8, 273–285.

De Jong G, Dalstra H, Boorder H, Savage JF (1991a) Blue amphiboles, Variscan deformation and plate tectonics in the Beja Massif, South Portugal. XI Reunión sobre la Geología del Oeste Peninsular, Huelva, Resúmenes, p 15.

De Jong G, Dalstra H, Boorder H, Savage JF (1991b) Blue amphiboles, Variscan deformation and plate tectonics in the Beja Massif, South Portugal. Comun Serv Geol Portugal 77: 59–64.

Delapièrre E, Respaut JP (1995) Un âge ordovicien de l'orthogneiss de La Preste par le méthode d'évaporation directe du plomb sur monozircon remet en question l'existence d'un soc1e precambrien dans le Massif du Canigou (Pyrénées Orientales, France). CR Acad Sci Paris 320: 1179–1185.

Delapièrre E, Saint-Blanquat M, Brunel M, Lancelot J (1994) Géochronologie U-Pb sur zircons et monazite dans le massif du Saint-Barthélémy (Pyrénées, France); discussion des âges des événements varisques et prevarisques. Bull Soc Géol Fr 165–2: 101–112.

Deloule E, Alexandrov P, Cheilletz A et al. (2002) In-situ U-Pb zircon ages for Early Ordovician magmatism in the eastern Pyrenees, France: the Canigou orthogneisses. Int J Earth Sci 91: 398–405.

Denèle Y, Laumonier B, Paquette JL, Olivier P, Gleizes G, Barbey P (2014) Timing of granite emplacement, crustal flow and gneiss dome formation in the Variscan segment of the Pyrenees. In: Schulmann K, Martínez Catalán JR, Lardeaux JM, Janousek V, Oggiano G (eds), The Variscan Orogeny: Extent, Timescale and the Formation of the European Crust. Geological Society of London Special Publications 405: 265–287.

Díaz Azpíroz M (2001) Evolución tectono-metamórfica del dominio de alto grado de la banda metamorfica de Aracena. PhD thesis, Univ Huelva, 556 p.

Díaz Azpíroz M, Fernández C (2003) Characterization of tectono-metamorphic events using crystal size distribution (CSD) diagrams. A case study from the Acebuches metabasites (SW Spain). Journal Structural Geology, 25, 935–947.

Díaz Azpíroz M, Fernández C, Castro A (1997) Structural and metamorphic characteristics of the Acebuches amphibolites (SW Iberian massif). A model for the preservation of the upper oceanic crust in sutures resulting from triple junction evolution. Terra Nova 9: 384.

Díaz Azpíroz M, Castro A, Fernández C et al (2004) The contact between the Ossa-Morena and the South Portuguese zones. Characteristics and significance of the Aracena metamorphic belt, in its central sector between Aroche and Aracena (Huelva). Journal of Iberian Geology 30: 23–51.

Díaz Azpiroz M, Fernández C, Castro A, El-Biad M (2006) Tectono-metamorphic evolution of the Aracena metamorphic belt (SW Spain) resulting from ridge–trench interaction during Variscan plate convergence. Tectonics 25: TC1001. http://dx.doi.org/10.1029/2004TC001742.

Díaz García F (1990) La geología del sector occidental del Complejo de Ordenes (Cordillera Hercínica, NW de España). Nova Terra, A Coruña.

Diener JFA, Powell R, White RW, Holland TJB (2007) A new thermodynamic model for clino- and orthoamphiboles in Na2O-CaO-FeO-MgO-Al2O3-SiO2-H2O-O. Journal of Metamorphic Geology 25: 631–656.

Díez Fernández R, Martínez Catalán JR, Gerdes A, Abati J, Arenas R and Fernández-Suárez J (2010) U–Pb ages of detrital zircons from the Basal allochthonous units of NW Iberia: Provenance and paleoposition on the northern margin of Gondwana during the Neoproterozoic and Paleozoic. Gondwana Research 18: 385–399.

Díez Fernández R (2011) Evolución estructural y cinemática de una corteza continental subducida: la unidad de Malpica-Tui (NO del Mazico Ibérico). Nova Terra, A Coruña.

Díez Fernández R, Arenas R (2015) The Late Devonian Variscan suture of the Iberian Massif: A correlation of high-pressure belts in NW and SW Iberia". Tectonophysics 654: 96–100.

Díez Fernández R, Arenas R (2016) Reply to Comment on "The Late Devonian Variscan suture of the Iberian Massif: A correlation of high-pressure belts in NW and SW Iberia". Tectonophysics 670:155–160.

Díez Fernández R, Martínez Catalán JR (2009) 3D Analysis of an Ordovician igneous ensemble: A complex magmatic structure hidden in a polydeformed allochthonous Variscan unit. J Struct Geol 31:222–236.

Díez Fernández R, Martínez Catalán JR, Arenas R et al (2011) Tectonic evolution of a continental subduction-exhumation channel: Variscan structure of the basal allochthonous units in NW Spain. Tectonics 30:TC3009.

Díez Fernández R, Castiñeiras P, Gómez Barreiro J (2012a) Age constraints on Lower Paleozoic convection system: Magmatic events in the NW Iberian Gondwana margin. Gondwana Res 21:1066–1079.

Díez Fernández R, Martínez Catalán JR, Arenas R et al (2012b) U–Pb detrital zircon analysis of the lower allochthon of NW Iberia: age

constrains, provenance and links with the Variscan mobile belt and Gondwanan cratons. J Geol Soc London 169:655–665.
Díez Fernández R, Martínez Catalán JR, Gómez Barreiro J et al (2012c) Extensional flow during gravitational collapse: A tool for setting plate convergence (Padrón migmatitic dome, Variscan belt, NW Iberia). J Geol 120:83–103.
Díez Fernández R, Pereira MF and Foster DA (2015) Peralkaline and alkaline magmatism of the Ossa-Morena zone (SW Iberia): Age, source, and implications for the Paleozoic evolution of Gondwanan lithosphere. Lithosphere 7:73–90.
Díez Fernández R, Fuenlabrada JM, Chichorro M et al. (2017) Geochemistry and tectonostratigraphy of the basal allochthonous units of SW Iberia (Évora Massif, Portugal): keys to the reconstruction of pre-Pangean paleogeography in southern Europe. Lithos 268-271: 285–301.
Díez Montes A (2007) La geología del Dominio "Ollo de Sapo" en las comarcas de Sanabria y Terra do Bolo. Nova Terra, A Coruña.
Díez Montes A, Navidad M, González Lodeiro F et al (2004) El Ollo de Sapo. In: Vera JA (ed), Geología de España. Sociedad Geológica Española e Instituto Geológico y Minero de España, Madrid, p 69–72.
Díez Montes A, Martínez Catalán JR, Bellido Mulas F (2010) Role of the Ollo de Sapo massive felsic volcanism of NW Iberia in the Early Ordovician dynamics of northern Gondwana. Gondwana Res 17:363–376.
Druguet H (2001) Development of high thermal gradients by coeval transpression and magmatism during the Variscan orogeny: insights from the Cap de Creus (Eastern Pyrenees). Tectonophysics 332, 1–2: 275–293.
Druguet H, Hutton DHW (1998) Syntectonic anatexis and magmatism in a mid-crustal transpressional shear zone: an example from the Hercynian rocks of the eastern Pyrenees. Journal of Structural Geology 20–7: 905–916.
Druguet H, Castro A, Chichorro, M et al. (2014) Zircon geochronology of intrusive rocks from Cap de Creus, Eastern Pyrenees. Geological Magazine 151–6: 1095–1114.
Ducrot J, Lancelot JR, Reille JL (1979) Datation en Montagne Noire d'un témoin d'une phase majeure d'amincissement crustal caractéristique de l'Europe pré-varisque. Bull Soc Géol Fr 21: 501–505.
Dunning GR, Díez Montes A, Matas J, Martín Parra LM, Almarza J, Donaire M (2002) Geocronología U/Pb del volcanismo ácido y granitoides de la Faja Pirítica Ibérica (Zona Surportuguesa). Geogaceta 32: 127–130.
Durán H (1985) El Paleozoico de Les Guilleries. PhD thesis, Univ Autónoma Barcelona, 243 p.
Eden CP (1991) Tectonostratigraphic analysis of the northern extent of the oceanic exotic terrane, Northwestern Huelva Province, Spain. PhD thesis, Univ Southampton, 293 p.
Eden CP, Andrews JR (1990) Middle to upper Devonian mélanges in SW Spain and their relationship to the Meneage formation in south Cornwall. Proc Ussher Soc 7: 217–222.
Eguiluz L (1987) Petrogénesis de rocas ígneas y metamórficas en el antiforme de Burguillos-Monesterio. Macizo Ibérico Meridional. PhD thesis, Univ Pais Vasco, 649 p.
Eguiluz L, Ábalos B (1992) Tectonic setting of Cadomian low-pressure metamorphism in the central Ossa–Morena Zone (Iberian Massif, SW Spain). Precambrian Research 56: 113–117.
Eguiluz L, Gil Ibarguchi JI, Ábalos B, Apraiz A (2000) Superposed Hercynian and Cadomian orogenic cycles in the Ossa–Morena zone and related areas of the Iberian Massif. Geol Soc Am Bull 112: 1398–1413.
El-Biad M (2000) Generación de granitoides en ambientes geológicamente contrastados del Macizo Ibérico: Limitaciones experimentales entre 2 y 15 kbar. PhD thesis, Univ Huelva, 310 p.
El-Biad M, El-Hmidi H, Castro A (1999) Experimental constraints to igneous rocks petrogenesis in the Aracena Metamorphic Belt, Iberian Massif. XV Reunión de Geología del Oeste Peninsular (International Meeting on Cadomian Orogens), Badajoz, Spain.
England PC, Richardson SW (1977) The influence of erosion upon the mineral facies of rocks from different metamorphic environments. J Geol Soc Lond 134: 201–213.
England PC, Thompson AB (1984) Pressure–temperature–time paths of regional metamorphism. I. Heat transfer during the evolution of regions of thickened continental crust. J Petrol 25: 894–928.
Escuder Viruete J, Arenas R, Martínez Catalán JR (1994) Tectonothermal evolution associated with Variscan crustal extension in the Tormes Gneiss Dome (NW Salamanca, Iberian Massif, Spain). Tectonophysics, 238, 117–138.
Escuder Viruete J, Indares A, Arenas R (1997) P–T path determinations in the Tormes Gneissic Dome, NW Iberian Massif, Spain. J Metamorph Geol 15: 645–663.
Escuder Viruete J, Hernáiz Huerta PP, Valverde-Vaquero P et al (1998) Variscan extension in the Iberian Massif: structural, metamorphic and geochronological evidence from the Somosierra sector of the Sierra de Guadarrama (Central Iberian Zone, Spain). Tectonophysics 290: 87–109.
Escuder Viruete J, Indares A, Arenas R (2000) P–T paths derived from garnet growth zoning in an extensional setting: an example from the Tormes Gneissic Dome (Iberian Massif, Spain). J Petrol 41: 1488–1518.
Esteban JJ, Aranguren A, Cuevas J et al (2015) Is there a time lag between the metamorphism and emplacement of plutons in the Axial Zone of the Pyrenees? Geol Mag 152 (5): 935–941.
Evans NG (1993) Deformation during the emplacement of the Maladeta granodiorite, Spanish Pyrenees. PhD thesis, Univ Leeds.
Expósito I, Simancas JF, González Lodeiro F et al (2003) Metamorphic and deformational imprint of Cambrian-Lower Ordovician rifting in the Ossa-Morena Zone (Iberian Massif, Spain). J Struct Geol 25: 2077–2087.
Farias P, Marcos A (2004) Domínio Esquistoso de Galícia-Trás-os--Montes. In: Vera JA (ed), Geología de España. Instituto Geológico y Minero de España/Sociedad Geológica de España, pp. 135–138. Madrid.
Fernández C, Becchio R, Castro A et al (2008) Massive generation of atypical ferrosilicic magmas along the Gondwana active margin: implications for cold plumes and back-arc magma generation. Gondwana Res 14:451–473.
Fernández-Suárez J, Gutiérrez-Alonso G, Jenner GA et al (2000a) New ideas on the Proterozoic-Early Palaeozoic evolution of NW Iberia: insights from U–Pb detrital zircon ages. Precambr Res 102:185–206.
Fernández C, Díaz-Azpiroz M, Pereira MF, Chichorro M, Czeck D (2016). Kinematic model of triclinic transtension zones: The case of the Boa Fé shear zone (Ossa-Morena Zone, Iberian Variscan Massif). IX Congresso Geológico de España, Huelva.
Fernández-Suárez J, Dunning GR, Jenner GA et al (2000b) Variscan collisional magmatism and deformation in NW Iberia: constraints from U-Pb geochronology of granitoids. J Geol Soc London 157:565–576.
Fernández-Suárez J, Corfu F, Arenas R et al (2002) U-Pb evidence for a polyorogenic evolution of the HP–HT units of the NW Iberian Massif. Mineral Petrol 143:236–253.
Fernández-Suárez J, Arenas R, Abati, J et al (2007) U–Pb Chronometry of polymetamorphic high–pressure granulites: An example from the allochthonous terranes of the NW Iberian Variscan belt. In: Hatcher RDJ et al (eds), 4-D framework of continental crust, Geol Soc Am Memoir 200: 469–488.
Ferreira M (1964) Geologia e petrologia da região de Rebordelo – Vinhais. Memórias e Notícias Museu e Laboratório Mineralógico e Geológico da Universidade de Coimbra 58: 282 p.
Florido P, Quesada C (1984) Estado actual de conocimientos sobre el Macizo de Aracena. Cadernos Lab Xeolóxico de Laxe 8: 257–277.

Floor P (1966) Petrology of an aegirine-riebeckite gneiss-bearing part of the Hesperian Massif: The Galiñeiro and surrounding areas, Vigo, Spain. Leidse Geol Meded 36:1–20.

Fonseca PE (1997) Dominios meridionais da Zona de Ossa-Morena e limites com a Zona Sul Portuguesa: metamorfismo de alta pressão relacionado com a sutura varisca ibérica. In: Aráujo AA, Pereira MF (eds), Estudos sobre a Geologia da Zona de Ossa-Morena (Maciço Ibérico), Univ. Évora, 133–168.

Fonseca P, Ribeiro A (1993) Tectonics of the Beja-Acebuches Ophiolite: a major suture in the Iberian Variscan Fold-belt. Geol Rundsch 82: 440–447.

Fonseca PE, Araújo A, Leal N, Munhá J (1993) Variscan glaucophane eclogites in the Ossa Morena Zone. XII Reunião de Geologia do Oeste Peninsular. Évora, Terra Abstracts, supplement nº 6 to Terra Nova 5: 11–12.

Fonseca PE, Munhá J, Pedro J, Rosas F, Moita P, Araújo A, Leal N (1999) Variscan ophiolites and high-pressure metamorphism in Southern Iberia. Ofioliti 24 (2): 259–268.

Fonseca PE, Fonseca MM, Munhá JM (2004) Ocorrência de aragonite em mármores da região de Alvito-Viana do Alentejo (zona de Ossa-Morena): significado geodinâmico. Cadernos Laboratorio Xeolóxico Laxe 29: 79–96.

Fonteilles M (1970) Géologie des terrains métamorphiques et granitiques du massif hercynien de l'Agly (Pyrénées orientales). Bull BRGM (2) IV: 21–72.

Fonteilles M (1976) Éssai d'interpretation des compositions chimiques des roches d'origine métamorphique et magmatique du massif hercynien de l'Agly (Pyrénées orientales). Thèse d'Etat, Paris VI, 684 p.

Fonteilles M, Guitard G (1971) Disthène relique et disthène hystérogène dans les terrains métamorphiques hercyniens des Pyrénées orientales franco-espagnoles. C R Acad Sci Paris 272: 361–363.

Franke W (1989) Tectonostratigraphic units in the Variscan belt of central Europe. In: Dallmeyer RD (Ed), Terranes in the Circum-Atlantic Palaeozoic Orogens. Geol Soc America Spec Paper 230: 67–90.

Franke W (2000) The mid-European segment of the Variscides: tectonostratigraphic units, terrane boundaries and plate tectonic evolution. In: Franke W, Haak V, Oncken O, Tanner D (eds), Orogenic Processes: Quantification and Modelling, Variscan Belt. Geol Soc London Spec Publ 179: 35–64.

Freire-de-Andrade C (1937) Os Vales Submarinos Portugueses e o Diastrofismo das Berlengas e da Estremadura. Memórias dos Serviços Geológicos de Portugal 5:35 p.

Fuenlabrada JM, Arenas R, Díez Fernández R, Sánchez Martínez S, Abati J, López-Carmona A (2012) Sm–Nd isotope geochemistry and tectonic setting of the metasedimentary rocks from the basal allochthonous units of NW Iberia (Variscan suture, Galicia). Lithos 148: 196–208.

Gabaldón V, Garrote A, Quesada C (1985) El Carbonífero Inferior del Norte de la Zona de Ossa-Morena (SW de España. CR 10th Int Carboniferous Congr, Madrid, 3:173–186.

Galán G (1987) Las rocas graníticas del Macizo de Vivero en el sector Norte (Lugo, NO de España). Corpus Geol Gallaeciae, 2nd Ser, 3, 376 p.

Galán G, Marcos A (1997) Geochemical evolution of high-pressure mafic granulites from the Bacariza formation (Cabo Ortegal complex, NW Spain): an example of a heterogeneous lower crust. Geol Rundsch 86:539–555.

Galán G, Pin C, Duthou JL (1996) Sr–Nd isotopic record of multi-stage interactions between mantle-derived magmas and crustal components in a collision context: the ultramafic–granitoid association from Vivero (Hercynian belt, NW Spain). Chem Geol 131: 67–91.

García-Arias M, Díez-Montes A, Villaseca C et al (2018) The Cambro-Ordovician Ollo de Sapo magmatism in the Iberian Massif and its Variscan evolution: A review. Earth Sci Rev176:345–372.

García Casquero JL, Boelrijk NAIM, Chacón J, Priem HNA (1985) Rb-Sr evidence for the presence of Ordovician granites in the deformed basement of the Badajoz-Córdoba belt, SW Spain. Geol Rundschau 74: 379–384.

García Garzón J, De Pablo Maciá JG, Llamas Borrajo JF (1981) Edades absolutas obtenidas mediante el método Rb/Sr de los cuerpos de ortogneises en Galicia Occidental. Bol Geol Min 92: 463–466.

García-López S, Brime C, Valín ML et al (2007) Tectonothermal evolution of a foreland fold and thrust belt: the Cantabrian Zone (Iberian Variscan belt, NW Spain) Terra Nova 19: 469–475.

García-Sansegundo J, Poblet J, Evans NG, Gleizes G et al (1999) Discussion on syntectonic emplacement of the Maladeta granite (Pyrenees) deduced from relationships between Hercynian deformation and contact metamorphism. J Geol Soc Lond 156: 651–652.

Garrote A (1976) Asociaciones minerales del núcleo metamórfico de Sierra Albarrana (Prov. de Córdoba). Sierra Morena Central. Memórias e Noticias Publ Mus Lab Mineral Geol Univ Coimbra 82: 17–39.

Garrote A, Ortega Huertas M, Romero J (1980) Los yacimientos de pegmatitas de Sierra Albarrana (Provincia de Córdoba, Sierra Morena). 1ª Reunión Grupo Ossa-Morena. Temas Geológico Mineros, 5: 145–168.

Gebauer D, Bernard-Griffiths J, Grünenfelder M (1981) U–Pb zircon and monazite dating of a mafic-ultramafic complex and its country rocks. Example: Sauviat-sur-Vige, French Central Massif. Contrib Mineral Petrol 76: 292–300.

Gebauer D, Martínez-García E, Hepburn JC (1993) Geodynamic significance, age and origin of the Ollo de Sapo augengneiss (NW Iberian Massif, Spain). Geological Society of America, 1993 Annual Meeting, Boston, Abstracts with programs p 342.

Gerya TV, Stöckhert B, Perchuk AL (2002) Exhumation of high–pressure metamorphic rocks in a subduction channel-a numerical simulation. Tectonics 21:TC001406.

Gibson RL (1991) Hercynian low-pressure–high-temperature regional metamorphism in the Canigou massif, Pyrenees, France. Evidence for crustal extension. Geology 19: 380–383.

Gibson RL, Bickle MJ (1994) Thermobarometric constraints on the conditions of metamorphism in Canigou Massif (Pyrenees): implications for Hercynian gradients. J Geol Soc London 151: 987–997.

Gil Ibarguchi JI (1995). Petrology of jadeite–metagranite and associated orthogneiss from the Malpica–Tuy allochthon (Northwest Spain). Eur J Mineral 7:403–415.

Gil Ibarguchi JI, Dallmeyer RD (1991) Hercynian blueschist metamorphism in North Portugal: tectonotherrnal implications. J Metamorph Geol 9:539–549.

Gil Ibarguchi JI, Martínez FJ (1982) Petrology of garnet-cordierite-sillimanite gneises from the El Tormes termal dome, Iberian Hercynian fold-belt (W Spain). Contributions to Mineralogy and Petrology 80: 14–24.

Gil Ibarguchi JI, Ortega Gironés E (1985) Petrology, structure and geotectonic implications of glaucophane-bearing eclogites and related rocks from the Malpica–Tuy unit, Galicia, northwest Spain. Chem Geol 50:145–162.

Gil Ibarguchi JI, Mendia M, Girardeau J et al (1990) Petrology of eclogites and clinopyroxene–garnet metabasites from the Cabo Ortegal Complex (northwestern Spain). Lithos 25:133–162.

Gil Ibarguchi JI, Abalos B, Azcárraga J et al (1999) Deformation, high-pressure metamorphism and exhumation of ultramafic rocks in a deep subduction/collision setting (Cabo Ortegal, NW Spain). J Metamorph Geol 17:747–764.

Gladney ER, Braid JA, Murphy JB, Quesada C, McFarlane CRM (2014) U-Pb geochronology and petrology of the late Paleozoic Gil

Márquez pluton: Magmatism in the Variscan suture zone, southern Iberia, during continental collision and the amalgamation of Pangea. Int J Earth Sci (Geol Runds) 103:1433–1451. https://doi.org/10.1007/s00531-014-1034-5.

Gleizes, G., Leblanc, D. & Bouchez, JL. (1998) The main phase of the Hercynian orogeny in the Pyrenees is a dextral transpression. En: Holdsworth, RE., Strachan, RA. & Dewey, JF. eds: Continental transpressional and transtensional tectonics. Geological Society of London, Special Publications, 135, 267–273.

Gómez-Barreiro J, Wijbrans JR, Castiñeiras P et al (2006) $^{40}Ar/^{39}Ar$ laser probe dating of mylonitic fabrics in a polyorogenic terrane of the NW Iberia. J Geol Soc London 163:61–73.

Gómez-Barreiro J, Martínez Catalán JR, Arenas R et al (2007) Tectonic evolution of the upper allochthon of the Órdenes Complex (northwestern Iberian Massif): structural constraints to a polyorogenic peri–Gondwanan terrane. In: Linnemann U et al (eds), The Evolution of the Rheic Ocean: from Avalonian-Cadomian Active Margin to Alleghenian-Variscan Collision. Geol Soc, London, Spec Pap 423:315–332.

Gómez-Barreiro J, Martínez Catalán JR, Díez Fernández R et al (2010) Upper crust reworking during gravitational collapse: the Bembibre-Pico Sacro detachment system (NW Iberia). J Geol Soc London 167:769–784.

Gómez-Pugnaire MT, Azor A, Fernández-Soler JM, López Sánchez--Vizcaíno V (2003) The amphibolites from the Ossa–Morena/Central Iberian Variscan suture (Southwestern Iberian Massif): geochemistry and tectonic interpretation. Lithos 68: 23– 42.

Gonçalves F (1971) Subsidios para 0 conhecimento geologico do Nordeste alentejano. Mem Serv Geol Port (Nova serie) 18: 1–62.

González-Cuadra P (2007) La Unidad de Corredoiras (Complejo de Órdenes, Galicia): Evolución estructural y metamórfica. Nova Terra, A Coruña.

González del Tánago J (1993) El núcleo metamórfico de Sierra Albarrana y su campo de pegmatitas asociado, Macizo Ibérico, Córdoba, España. PhD thesis, Univ Complutense Madrid, 885 p.

González del Tánago J, Arenas R (1991) Anfibolitas granatíferas de Sierra Albarrana Córdoba). Termobarometría e implicaciones para el desarrollo del metamorfismo regional. Rev Soc Geol España 4:251–269.

González del Tánago J, Peinado M (1990) Contribución al estudio del metamorfismo de Sierra Albarrana (ZOM, Córdoba, España. Bol Geol Min 101: 678–700.

Grasemann B, Ratschbacher L, Hacker BR (1998) Exhumation of ultrahigh-pressure rocks: Thermal boundary conditions and cooling history. In: Hacker BR and Liou JG (eds), When Continents Collide: Geodynamics and Geochemistry of Ultrahigh-Pressure Rocks. Springer, New York, p 117–139.

Green ECR, Holland TJB, Powell R (2007) An order-disorder model for omphacitic pyroxenes in the system jadeite-diopside-hedenbergite-acmite, with applications to eclogite rocks. American Mineralogist 92: 1181–1189.

Guerrot C, Peucat, JJ, Capdevilla R (1989) Archean protoliths within Early Proterozoic granulitic crust of the West European Hercynian belts: Possible relics of the West African craton, Geology 17:241–244.

Guchereau JY (1975) Le Saint-Barthélemy métamorphique (Pyrénées ariégeoises). Pétrographie et structure. Thèse 3ème cycle, Toulouse, 172 p.

Guitard G (1960) Sur la présence et l'âge d'un granite à hypersrthène d'affinité charnockitique dans le massif de l'Agly (Pyrénées orientales). C R Acad Sci Paris, 251: 2554–2555.

Guitard G (1970) Le métamorphisme hercynien mésozonal et les gneiss oeillés du massif du Canigou (Pyrénées-Orientales). Mémoire Bureau Recherches Géologiques et Minières 63.

Guitard G, Raguin E (1958) Sur la présence de gneiss à grenat et hypersthène dans le massif de l'Agly (Pyrénées Orientales). C R Acad Sci Paris 247: 2385–2388.

Guitard G, Vielzeuf D, Martínez FJ (coord) et al. (1996). Métamorphisme Hercynien. In: Barnolas A, Chiron JC (eds), Synthèse géologique et géophysique des Pyrénées 1, Cycle Hercynien. Ed BRGM – ITGE (Orléans – Madrid).

Gutiérrez-Alonso G, and Nieto F (1996). White-mica 'crystallinity', finite strain and cleavage development across a large Variscan structure, NW Spain. Journal of the Geological Society, 153(2), 287–299 Gutiérrez-Alonso G, Nieto F (1996) White-mica 'crystallinity', finite strain and cleavage development across a large Variscan structure, NW Spain. J Geol Soc London 153(2): 287–299.

Gutiérrez-Alonso G, Fernández-Suárez J, Jeffries TE et al (2011) Diachronous post-orogenic magmatism within a developing orocline in Iberia, European Variscides. Tectonics 30: 1–17. http://dx.doi.org/10.1029/2010TC002845 (TC5008).

Gutiérrez-Alonso G, Gutiérrez-Marco JC, Fernández-Suárez J et al (2016) Was there a super-eruption on the Gondwanan coast 477 Ma ago?. Tectonophysics 681:85–94.

Gutiérrez-Alonso G, Fernández-Suárez J, López-Carmona A et al (2018) Exhuming a cold case: The early granodiorites of the northwest Iberian Variscan belt-A Visean magmatic flare-up? Lithosphere 10:194–216.

Hemingway BS, Bohlen SR, Hankins WB et al (1998) Heat capacity and thermodynamic properties for coesite and jadeite, re-examination of the quartz-coesite equilibrium boundary. Am Mineral 83: 409–418.

Henriques SBA (2013) Magmatitos e metamorfitos de alto grau no contacto entre as zonas de Ossa Morena e Centro Ibérica: significado geodinâmico. PhD thesis, Univ Coimbra, Portugal, 249 pp.

Henriques SBA, Neiva AMR, Ribeiro ML, Dunning GR, Tajčmanová L (2015) Evolution of a Neoproterozoic suture in the Iberian Massif, Central Portugal: New U-Pb ages of igneous and metamorphic events at the contact between the Ossa Morena Zone and Central Iberian Zone. Lithos 220–223: 43–59. http://dx.doi.org/10.1016/j.lithos.2015.02.001.

Henriques SBA, Neiva AMR, Dunning GR (2016) Petrogenesis of a late-Variscan rhyodacite at the Ossa Morena-Central Iberian zones boundary, Iberian Massif, Central Portugal: Evidence for the involvement of lithospheric mantle and meta-igneous lower crust. Chemie der Erde – Geochemistry 76: 429–439.

Henriques SBA, Neiva AMR, Tajčmanová L, Dunning GR (2017) Cadomian magmatism and metamorphism at the Ossa Morena/Central Iberian zone boundary, Iberian Massif, Central Portugal: Geochemistry and P-T constraints of the Sardoal Complex. Lithos 268–272: 131–148. https://doi.org/10.1016/j.lithos.2016.11.002.

Holland TJB (1980) The reaction albite=jadeite+quartz determined experimentally in the range of 600–1200 °C. American Mineralogist 65: 129–134.

Holland TJB, Blundy J (1994) Non-ideal interactions in calcic amphiboles and their bearing on amphibole–plagioclase thermometry. Contributions to Mineralogy and Petrology 116: 443–447.

Holland TJB, Powell R (1985) An internally consistent thermodynamic dataset with uncertainties and correlations. 2-Data and results. Journal of Metamorphic Geology 3: 343–370.

Holland TJB, Powell R (1990) An enlarged and updated internally consistent thermodynamic dataset with uncertainties and correlations: the system K_2O–Na_2O–CaO–MgO–MnO–FeO–Fe_2O_3–Al_2O_3–TiO_2–SiO_2–C–H_2–O_2. Journal of Metamorphic Geology 8: 89–124.

Holland TJB, Powell R (1992) Plagioclase feldspars: activity-composition relations based upon Darken's Quadratic Formalism and Landau theory. American Mineralogist 77: 53–61.
Holland TJB, Powell R (1998) An internally consistent thermodynamic dataset for phases of petrological interest. Journal of Metamorphic Geology 16 (3): 309–343.
Holland TJB, Powell R (2003) Activity-composition relations for phases in petrological calculations: an asymmetric multicomponent formulation. Contributions to Mineralogy and Petrology 145: 492–501.
Holland TJB, Baker JM, Powell R (1998) Mixing properties and activity-composition relationships of chlorites in the system MgO–FeO–Al_2O_3–SiO_2–H_2O. European Journal of Mineralogy 10: 395–406.
Huang WL, Wyllie PJ (1975) Melting reactions in the system to 35 kilobars, dry and with excess water. J Geol 83: 737–748.
Hubregtse JJMV (1973) High-grade metamorphic rocks of the Mellid área, Galicia, NW Spain. Leidse Geol Meded 49:9–31.
Iglesias M, Ribeiro A (1981) La zone de cisaillement ductile Juzbado (Salamanca) – Penalva do Castelo (Viseu): un linéament réactivé pendant l'orogénèse hercynienne? Comunicações dos Serviços Geológicos de Portugal 67(1): 89–93.
Iglesias M, Ribeiro ML, Ribeiro A (1983) La interpretación aloctonista de la estructura del noroeste peninsular. In: Libro Jubilar JM. Ríos, Geología de España, Tomo I, Instituto Geológico Minero España, 459–467.
Jorquera A, Apalategui O, Villalobos M (1988) Mapa Geológico de España, E 1:50.000, Sheet 800: Villarreal. Instituto Geológico Minero España, Madrid.
Julivert M (1978) Hercynian orogeny and Carboniferous paleogeography in Northwestern Spain: a model of deformation-sedimentation relationships. Z Dtsch Geol Ges 129: 565–592.
Julivert M, Martínez FJ, Ribeiro A (1980) The Iberian segment of the European Hercinian foldbelt. In: Proceedings of the 26th International Geologic Congress, Colloque C6, Geology of Europe from Precambrian to the post Hercynian sedimentary basins, IUGS, Paris, 108: 122–158.
Julivert M (1981) Guide to the Field Trips in the Eastern Pyrenees and Catalonian Coastal Ranges (Introduction). IGCP Project no 5. Correlation of Pre-Variscan and Variscan Events of the Alpine – Mediterranean Mountain Belt.
Keller M, Krumm S (1992) Evidence of an Upper Ordovician thermo-metamorphic event in the SW-corner of the Cantabrian Mountains (N-Spain). Estudios Geológicos 48:289–296.
Keppie JD (1985) The Appalachian Collage. In: Gee DG, Sturt B (eds), The Caledonide orogen, Scandinavia, and related areas. Wiley, New York, 1217–1226.
Kerrick DM (1987) Fibrolite in contact aureoles of Donegal, Ireland. American Mineralogist 72: 240–254.
Kerrick DM, Woodsworth GJ (1989) Aluminum silicates in the Mount Raleigh pendant, British Columbia. Journal of Metamorphic Geology 7: 547–563.
Kotková J, Janák M (2015) UHP kyanite eclogite associated with garnet peridotite and diamond-bearing granulite, northern Bohemian Massif. Lithos 226: 255–264.
Kroner U, Romer RL (2013) Two plates – Many subduction zones. The Variscan orogeny reconsidered. Gondwana Research 24: 298–329.
Lancelot JR, Allegret A (1982) Radiochronologie U-Pb de l'orthogneiss alcalin de Pedroso (Alto Alentejo, Portugal) et évolution antéhercynienne de l'Europe Occidental. N J Mineral Mth 9: 385–394.
Lancelot JR, Allegret A, Iglesias M (1985) Outline of Upper Precambrian and Lower Palaeozoic evolution of the Iberian Peninsula according to U–Pb dating of zircons. Earth Planet Sci Lett 74: 325–337.
Lardeaux JM, Ledru P, Daniel I et al (2001) The Variscan French Massif Central - A new addition to the ultra-high pressure metamorphic 'club': Exhumation processes and geodynamic consequences. Tectonophysics 332:143–167.
Laumonier B, Autran A, Barbey P et al. (2004) On the non-existence of a Cadomian basement in Southern France (Pyrenees, Montagne Noire): implications for the significance of the pre-Variscan (pre-Upper Ordovician) series. Bull Soc Géol France 175–6: 643–655.
Laumonier B, Marignac C, Kister P (2010) Polymetamorphism and crustal evolution of the eastern Pyrenees during the Late Carboniferous Variscan orogenesis. Bull Soc Geol France 181–5: 411–428.
Leal N (2001) Estudo Petrológico e Geoquímico de Rochas Metamórficas Máficas de Alta Pressão das Regiões de Alvito – Viana do Alentejo e de Safira (Zona de Ossa – Morena, Maciço Ibérico). PhD thesis, Univ Lisboa, Portugal.
Leistel JM, Marcoux E, Thiéblemont D, Quesada C, Sánchez, A, Almodóvar GR, Pascual E, Sáez R (1998) The volcanic-hosted massive sulphide deposits of the IPB. Miner Depos 33: 2–30.
Li B, Massonne HJ, Opitz J (2017) Clockwise and Anticlockwise P–T Paths of High-pressure Rocks from the 'La Pioza' Eclogite Body of the Malpica–Tuy Complex, NW Spain. J Petrol 58:1363–1392.
Liesa M, Carreras J (1989) On the structure and metamorphism of the Roc de Frausa Massif (Eastern Pyrenees). Geodinamica Acta 3: 149–161.
Lima SM, Corfu F, Neiva AMR, Ramos JMF (2011) Source and age constraints of a Variscan plutonic suite from the Ossa-Morena Zone (SW Portugal): from U-Pb and δ18O systematics in zircon. 7th Hutton Symposium on Granites and related Rocks, Ávila, Spain.
Lima SM, Corfu F, Neiva AMR, Ramos MF (2012) Dissecting complex magmatic processes: an in-depth U–Pb study of the Pavia pluton, Ossa-Morena Zone, Portugal. Journal of Petrology 53 (9): 1887–1911.
Liou JG, Zhang RY, Ernst WG et al (1998) High-pressure minerals from deeply subducted metamorphic rocks. Rev Mineral 37:33–96.
Liou JG, Ernst WG, Zhang RY et al (2009) Ultrahigh-pressure minerals and metamorphic terranes–the view from China. J Asian Earth Sci 35:199–231.
López-Carmona A (2015) Blueschist-facies rocks from the Malpica-Tui Complex (NW Iberian Massif). Nova Terra, A Coruña.
López-Carmona A, Abati J, Reche J (2010) Petrologic modeling of chloritoid–glaucophane schists from the NW Iberian Massif. Gondwana Res 17 (2): 377–391.
López-Carmona A, Pitra P, Abati J (2013) Blueschist-facies metapelites from the Malpica–Tui Unit (NW Iberian Massif): phase equilibria modelling and H_2O and Fe_2O_3 influence in high-pressure assemblages. J Metamorph Geol 31:263–280.
López-Carmona A, Abati J, Pitra P et al (2014) Retrogressed lawsonite blueschists from the NW Iberian Massif: P–T–t constraints from thermodynamic modelling and $^{40}Ar/^{39}Ar$ geochronology. Contrib Mineral Petrol 167: 987.
López-Moro FJ, López-Plaza M, Gutiérrez-Alonso G, Fernández--Suárez J, López-Carmona A, Hofmann M, Romer RL (2018) Crustal melting and recycling: geochronology and sources of Variscan syn-kinematic anatectic granitoids of the Tormes Dome (Central Iberian Zone). A U–Pb LA-ICP-MS study. Int J Earth Sci (Geol Rundsch) 107: 985–1004.
López-Sánchez MA, García-Sansegundo J, Martínez FJ (2018) The significance of Early Permian and Early Carboniferous ages in the Bossòst and Lys-Caillaouas granitoids (Pyrenean Axial Zone). Geological Journal 2018 : 1–16. https://doi.org/10.1002/gj.3283.
López Sánchez-Vizcaíno V, Gómez-Pugnaire MT, Azor A et al (2003) Phase diagram sections applied to amphibolites: a case study from the Ossa-Morena/Central Iberian Variscan suture (Southwestern Iberian Massif). Lithos 68:1–21.

Lotout C, Pitra P, Poujol M, Van Den Driessche J (2017) Ordovician magmatism in the Lévézou massif (French Massif Central): tectonic and geodynamic implications. International Journal of Earth Sciences (Geologisches Rundschau), 106 (2): 501–515. https://doi.org/10.1007/s00531-016-1387-z.

Macpherson J (1879) Estudio geológico y petrográfico del norte de la provincia de Sevilla. Bol Com Mapa Geol España 6: 97–268.

Maierová P, Schulmann K, Lexa O, Guillot S, Stípská P, Janousek V, Cadek O (2016) European Variscan orogenic evolution as an analogue of Tibetan-Himalayan orogen: Insights from petrology and numerical modeling. AGU Publications. Tectonics 35. https://doi.org/10.1002/2015TC004098.

Marcos A, Pulgar JA (1982) An approach to the tectonostratigraphic evolution of the Cantabrian foreland thrust and fold belt, Hercynian Cordillera of NW Spain. N Jahrb Geol Paläontol Abh 163: 256–26.

Marcos A, Marquínez J, Pérez-Estaún A et al (1984) Nuevas aportaciones al conocimiento de la evolución tectono-metamórfica del complejo de Cabo Ortegal". Cuadernos Laboratorio Xeolóxico de Laxe 7:125–137.

Marquínez J (1984) La geología del área esquistosa de Galicia Central (Cordillera Herciniana, NW de España). Memorias del Instituto Geológico y Minero de España 100: 237 p.

Martínez FJ, Rolet J (1988) Late Palaeozoic metamorphism in the northwestern Iberian Peninsula, Brittany and related áreas in SW Europe. In: Harris AL, Fettes DJ (eds), The Caledonian-Appalachian Orogen. Geol Soc Lond Spec Publ 38: 611–620.

Martínez FJ, Julivert M, Sebastián A, Arboleya ML, Gil Ibarguchi JI (1988) Structural and thermal evolution of high-grade areas in the Northwestern parts of the Iberian massif. Am J Sci 288: 969–996.

Martínez FJ, Corretgé LG, Suárez O (1990) Characteristics and evolution of metamorphism. In: Dallmeyer RD, Martínez-Garcia E (eds), Pre-Mesozoic Geology of Iberia. Springer, Berlin, 207–211.

Martínez FJ, Carreras J, Arboleya ML, Dietsch C (1996) Structural and metamorphic evidence of local extension along the Vivero fault coeval with bulk crustal shortening in the Variscan chain (NW Spain). J Struct Geol 18: 61–73.

Martínez FJ, Reche, Arboleya ML (2001) P-T modelling of the andalusite±kyanite±andalusite sequence and related assemblages in high-Al graphitic pelites. Prograde and retrograde paths in a late kyanite belt in the Variscan Iberia. J Metamorphic Geol 19: 661–677.

Martínez FJ, Reche, Arboleya ML, Julivert M (2004) Retrograde replacement of andalusite by Ca–Na mica in chloritoid-bearing metapelites. PTX modelling of rocks with different Al content in the MnNCKFMASH system. J Metamorphic Geol 22: 777–792.

Martínez FJ, Reche J, Iriondo A (2008) U-Pb SHRIMP-RG zircon ages of Variscan igneous rocks from the Guilleries massif (NE Iberia pre-Mesozoic basement): Geological implications: Comptes Rendus Geoscience 340: 223–232. https://doi.org/10.1016/j.crte.2007.12.006.

Martínez FJ, Iriondo A, Dietsch C et al (2011) U-Pb SHRIMP-RG zircon ages and Nd signature of lower Paleozoic rifting-related magmatism in the Variscan basement of the Eastern Pyrenees. Lithos 127: 10–23.

Martínez FJ, Dietsch C, Aleinikoff J et al (2016) Provenance, age, and tectonic evolution of Variscan flysch, southeastern France and northeastern Spain, based on zircon geochronology. Geol Soc Am Bull 128 (5–6): 842–859. https://doi.org/10.1130/b31316.1.

Martínez Catalán JR (2011) Are the oroclines of the Variscan belt related to late Variscan strike–slip tectonics? Terra Nova 23 (4): 241–247.

Martínez Catalán JR, Hacar MP, Villar P et al (1992) Lower Paleozoic extensional tectonics in the limit between the West Asturian-Leonese and Central Iberian zones of the Variscan fold-belt in NW Spain. Geol Rundsch 81:545–560.

Martínez Catalán JR, Arenas R, Díaz-García F, Rubio-Pascual FJ, Abati J, Marquínez J (1996) Variscan exhumation of the subducted Palaeozoic continental margin: Basal Unit of the Ordenes Complex (Galicia, NW Spain). Tectonics 15: 106–121.

Martínez Catalán JR, Arenas R, Díaz García F, Abati J (1997) Variscan accrecionary complex of northwest Iberia: terrane correlation and succession of tectonothermal events. Geology 25: 1103–1106.

Martínez Catalán JR, Díaz García F, Arenas R et al (2002) Thrust and detachment systems in the Órdenes Complex (northwestern Spain): Implications for the Variscan-Appalachian geodynamics. In: Martínez Catalán JR et al (eds), Variscan-Appalachian Dynamics: The Building of the Late Paleozoic Basement. Geol Soc Am Spec Pap 364:163–182.

Martínez Catalán JR, Arenas R, Díaz García F et al (2007) Space and time in the tectonic evolution of the northwestern Iberian Massif: implications for the Variscan belt. In: Hatcher RD, Carlson MP, McBride JH, Martínez Catalán JR (eds), 4-D Framework of Continental crust. Geol Soc Am Mem 200:403–423.

Martínez Catalán JR, Aller J, Alonso JL, Bastida F (2008) The Iberian Variscan orogen. In: García Cortés A (ed), Contextos geológicos españoles. Instituto Geológico y Minero de España, Madrid, p 13–30.

Martínez Catalán JR, Arenas R, Abati J, Sánchez Martínez S et al (2009) A rootless suture and the loss of the roots of a mountain chain: the Variscan belt of NW Iberia. Comptes Rendus Geoscience 341:114–126.

Martínez Catalán JR, Rubio Pascual F, Díez Montes A, Díez Fernández R, Gómez Barreiro J, Dias da Silva Í, González Clavijo E, Ayarza Arribas P, Alcock JE (2014) The late Variscan HT/LP metamorphic event in NW and central Iberia: relationships with crustal thickening, extension, orocline development, and crustal evolution. In: Schulmann K, Oggiano G, Lardeaux JM, Janousek V, Martínez Catalán JR, Scrivener R (eds), The Variscan Orogeny: Extent, Timescale and the Formation of the European Crust. Geological Society, London, Special Publications 405: 225–247.

Martins JA, Ribeiro ML (1979) Notícia Explicativa da Folha 2-C (Tourém) – Carta Geológica de Portugal à escala 1/50000. Dir Geral de Minas e Serviços Geológicos. Lisboa.

Massonne HJ (2001) First find of coesite in the ultrahigh-pressure metamorphic area of the central Erzgebirge, Germany. Eur J Mineral 13:565–570.

Massonne HJ, Schreyer R (1987) Phengite geobarometry based on the limiting assemblage with K-feldspar, phlogopite, and quartz. Contributions to Mineralogy and Petrology 96: 212–224.

Mata J, Munhá J (1986) Geodynamic significance of high grade metamorphic rocks from Degolados–Campo Maior (Tomar–Badajoz–Córdoba shear zone). Maleo-Bol Soc Geol Portugal 2: 28.

Matas J, Martín Parra LM, Rubio Pascual F et al (2010) Mapa Geológico de España 1:200.000, sheet 75/74: Sevilla-Puebla de Guzmán. Instituto Geológico Minero España, Madrid.

Matte P (1986a) Tectonics and plate tectonic model for the Variscan Belt of Europe. Tectonophysics 126: 331–334.

Matte P (1986b) La chaîne varisque parmi les chaînes paléozoïques péri-atlantiques, modèle d'évolution et position des grands blocs continentaux au Permo-Carbonifère. Bull Soc Géol Fr 8: 9–24.

Matte P (1991) Accretionary history of the Variscan belt in western Europe. Tectonophysics 196: 309–337.

Matte P (2001) The Variscan collage and orogeny (480–290 Ma) and the tectonic definition of the Armorica microplate: a review. Terra Nova 13(2):122–128.

Mateus A, Munhá J, Ribeiro A, Tassinari CCG, Sato K, Pereira E, Santos JF (2016) U–Pb SHRIMP zircon dating of high-grade rocks from the Upper Allochthonous Terrane of Bragança and Morais Massifs (NE Portugal); geodynamic consequences. Tectonophysics 675: 23–49.

Matias FV, Almeida JA, Chichorro M (2015) A Multistep Methodology for Building a Stochastic Model of Gold Grades in the Disseminated and Complex Deposit of Casas Novas in Alentejo, Southern Portugal. Resource Geology, Vol. 65, No. 4: 361–374.

Mendes MHA (1997) Processos metamórficos variscos na Serra da Freita (Zona Centro Ibérica-Portugal). PhD thesis Univ Aveiro, Portugal, 288 p.

Mendes MHA, Munhá JM (1993) Ocorrência de distena hercínica na Serra da Freita (Zona Centro Ibérica, Portugal). IX Semana de Geoquímica e II Congr. Geoquímica dos Países de Língua Portuguesa. Museu Laboratório Mineralógico Geológico Faculdade Ciências, Universidade do Porto, Mem 3: 119–120.

Mendía M (2000) Petrología de la unidad eclogítica del Complejo de Cabo Ortegal (NW de España). Nova Terra, A Coruña.

Mercier A (1988) Illustration du métamorphisme hercynien dans les Pyrénées. Le massif nord-pyrénéen des Trois Seigneurs (Ariège), modalités, implications géodynamiques. Thèse, Université Toulouse, 388 p.

Mezger JE (2005) Comparison of the western Aston-Hospitalet and the Bossòst domes: Evidence for polymetamorphism and its implications for the Variscan tectonic evolution of the Axial Zone of the Pyrenees. In: Carosi R, Dias R, Iacopini D, Rosenbaum G (eds), The southern Variscan belt. Journal of the Virtual Explorer, Electronic Edition, ISSN 1441–8142, Volume 19, 6 p.

Mezger JE (2009) Transpressional tectonic setting during the main Variscan deformation: evidence from fourstructural levels in the Bossòst and Aston-Hospitalet mantled gneiss domes, central Axial Zone, Pyrenees. Bull Soc Géol France 180: 199–207.

Mezger JE, Gerdes A (2014) Early Variscan (Visean) granites in the core of central Pyrenean gneiss domes: Implications from laser ablation U-Pb and Th-Pb studies. Gondwana Research 29(1): 181–198.

Mezger JE, Passchier CW (2003) Polymetamorphism and ductile deformation of staurolite-cordierite schist of the Bossòst dome: indication for Variscan extension in the Axial Zone of the central Pyrenees. Geological Magazine 140: 595–612.

Mezger JE, Passchier CW, Régnier JL (2004) Metastable staurolite-cordierite assemblage of the Bossòst dome: Late Variscan decompression and polyphase metamorphism in the Axial Zone of the central Pyrenees. Comptes Rendus Geoscience 336: 827–837.

Mezger JE, Régnier JL (2014) Isobaric evolution of staurolite-andalusite-cordierite-sillimanite schist in the Central Pyrenees: Early Variscan metamorphism of the Aston-Hospitalet domes.

Mezger JE, Régnier JL (2016) Stable staurolite-cordierite assemblages in K-poor metapelitic schists in Aston and Hospitalet gneiss domes of the central Pyrenees (France, Andorra). Journal of Metamorphic Geology 34(2): 167–190.

Mezger JE, Gerdes A (2016) Early Variscan (Visean) granites in the core of central Pyrenean gneiss domes: Implications from laser ablation U-Pb and Th-Pb studies. Gondwana Research 29(1): 181–198.

Miyashiro A (1961) Evolution of metamorphic belts. Journal of Petrology 2 (3): 277–311.

Moita P (1997) Caracterização petrográfica e geoquímica do metamorfismo de alta pressão no sector de Viana do Alentejo – Alvito (Zona de Ossa – Morena). Master Diss, Univ Lisboa.

Moita P, Munhá J, Fonseca P, Pedro J, Tassinari C, Araújo A, Palacios T (2005) Phase equilibria and geochronology of Ossa Morena eclogites. Actas da XIV Semana de Geoquímica (VIII Congresso de Geoquímica dos Países de Língua Portuguesa) 2: 471–474.

Moita P, Santos JF, Pereira MF (2009) Layered granitoids: interaction between continental crust recycling processes and mantle-derived magmatism. Examples from the Évora Massif (Ossa-Morena Zone, southwest Iberia, Portugal). Lithos 111(3–4):125–141.

Moita P, Santos JF, Pereira MF, CostaMM, Corfu F (2015) The quartz-dioritic Hospitais intrusion (SW Iberian Massif) and its mafic microgranular enclaves — Evidence for mineral clustering. Lithos 224–225: 78–100.

Monchoux P, Roux L (1973) Péridotites et amphibolites à sapphirine du massif de Castillon (Pyrénées ariégeoises). C R Acad Sci Paris 276: 449–451.

Montero P (1993) Geoquímica y petrogénesis del complejo peralcalino de la Sierra del Galiñeiro (Pontevedra, Españ a). PhD thesis, Univ Oviedo.

Montero P, Floor P (2004) Los complejos alcalinos prevariscos (magmatismo del Palezoico Inferior en las unidades basales). In: Vera JA (Ed), Geología de España. SGE-IGME, Madrid, Spain, 149–150.

Montero P, Salman K, Zinger T, Bea F (1999) Rb-Sr and single - zircon grain ^{207}Pbf/^{206}Pb chronology of the Monesterio granodiorite and related migmatites. Evidence of a late Cambrian melting event in the Ossa-Morena Zone, Iberian Massif. Estudios Geol 55: 3–8.

Montero P, Salman K, Bea F et al (2000) New data on the geochronology of the Ossa-Morena Zone, Iberian Massif. In: Variscan-Appalachian dynamics: the building of the Upper Paleozoic basement. Tectonics 15: 136–138, A Coruña.

Montero P, Bea F, Zinger TF, Scarrow JH, Molina JF, Whitehouse M (2004) 55 million years of continuous anatexis in Central Iberia: single-zircon dating of the Peña Negra Complex. Journal of the Geological Society 161: 255–263.

Montero P, Bea F, González-Lodeiro F et al (2007) Zircon crystallization age and protolith history of the metavolcanic rocks and metagranites of the Ollo de Sapo Domain in central Spain. Implications for the Neoproterozoic to Early-Paleozoic evolution of Iberia. Geol Mag 144: 963–976.

Montero P, Talavera C, Bea F et al (2009) Zircon geochronology and the age of the Cambro-Ordovician rifting in Iberia. J Geol 117:174–191.

Moreira A, Ribeiro ML (1991) Carta Geológica do Parque Nacional da Peneda Gerês à escala 1/50000 (Notícia Explicativa). Serviço Nacional de Parques, Reservas e Conservação da Natureza/Parque Nacional da Peneda–Gerês. ISBN: 972-9034-75-3.

Munhá J (1976) Nota preliminar sobre o metamorfismo na Faixa Piritosa Portuguesa. Comun Serv Geol Port 60: 151–161.

Munhá J (1979) Blue Amphiboles, Metamorphic Regime and Plate Tectonic Modelling in the Iberian Pyrite Belt. Contrib Mineral Petrol 69:279–289.

Munhá J (1983) Low-grade regional metamorphism in the Iberian Pyrite Belt. Comun Serv Geol Port 69: 3–35.

Munhá J (1990) Metamorphic Evolution of the South Portuguese/Pulo do Lobo Zone. In: Dallmeyer RD, Martínez García E (eds), Pre-Mesozoic Geology of Iberia. Springer, Berlin, 361–367.

Munhá J, Kerrich R (1980) Sea water basalt interaction in spilites from the Iberian Pyrite Belt. Contrib Mineral Petrol 73: 191–200.

Munhá J, Fyfe WS, Kerrich R (1980) Adularia, the characteristic mineral of felsic spilites. Contrib Mineral Petrol 75: 15–19.

Munhá J, Ribeiro A, Ribeiro ML (1984) Blueschists in the Iberian Variscan Chain (Trás-os-Montes: NE Portugal). Comunicações dos Serviços Geológicos Portugal 70 (1): 31–53.

Munhá J, Oliveira JT, Ribeiro A, Oliveira V, Quesada C, Kerrich R (1986) Beja-Acebuches Ophiolite: characterization and geodynamic significance. Maleo-Bol Soc Geol Portugal 2: 31.

Munhá J, Moita P, Tassinari CCG, Araújo A, Palácios T (2005) U/Pb, Sm/Nd and Ar/Ar geochronology of the Morais ophiolite. XIV Semana de Geoquímica/VIII Congresso de Geoquímica dos Países de Língua Portuguesa. Universidade de Aveiro, Portugal.

Murphy JB, Gutierrez-Alonso G, Nance RD et al (2006) Origin of the Rheic Ocean: rifting along a Neoproterozoic suture? Geology 34:325–328.

Murphy JB, Braid JA, Quesada C, Dahn D, Gladney E, Dupuis NE (2015) An eastern Mediterranean analogue for the Late Paleozoic evolution of the Pangean suture zone. In: Li ZX, Evans DAD, Murphy JB (eds), Supercontinent Cycles Through Earth History. Geol Soc London Spec Publ 424: 241–264. https://doi.org/10.1144/sp424.9.

Murphy JB, Quesada C, Gutiérrez-Alonso G, Johnston, ST, Weil A (2016) Reconciling competing models for the tectono-stratigraphic zonation of the Variscan orogen in western Europe. Tectonophysics 681:209–219. https://doi.org/10.1016/j.tecto.2016.01.006.

Nasdala L and Massonne HJ (2000) Microdiamonds from the Saxonian Erzgebirge, Germany: in situ micro-Raman characterisation. Eur J Mineral 12:495–498.

Noronha F, Ribeiro ML (1983) Notícia Explicativa da Folha 6-A (Montalegre). Carta Geológica de Portugal, esc. 1/ 50000. Serviços Geológicos de Portugal. Lisboa.

Novo-Fernández I, García-Casco A, Arenas R et al (2016) The metahyaloclastitic matrix of a unique metavolcanic block reveals subduction in the Somozas Mélange (Cabo Ortegal Complex, NW Iberia): tectonic implications for the assembly of Pangea. J Metamorph Geol 34:963–985.

Ochsner A (1993) U–Pb Geochronology of the Upper Proterozoic–Lower Paleozoic geodynamic evolution in the Ossa-Morena Zone (SW Iberia): constraints on the timing of the Cadomian Orogeny. PhD Thesis, ETH Zurich, 249 p.

Okamoto K, Maruyama S (1999) The high-pressure synthesis of lawsonite in the MORB + H_2O system. Am Mineral 84:362–373.

Olivier Ph, Druguet E, Castaño ML, Gleizes G (2016) Granitoid emplacement by multiple sheeting during Variscan dextral transpression: The Saint-Laurent e La Jonquera pluton (Eastern Pyrenees). Journal of Structural Geology 82: 80.92.

Ordóñez Casado B (1998) Geochronological studies of the Pre-Mesozoic basement of the Iberian Massif: the Ossa Morena zone and the Allochthonous Complexes within the Central Iberian zone. PhD Thesis, ETH Zurich, No. 12940, 235 p.

Ordóñez Casado B, Gebauer D, Eguiluz L (1997) Late Cadomian formation of two anatectic gneiss domes in the Ossa-Morena Zone: Monesterio and Mina Afortunada. XIV Reunión Geología Oeste Peninsular, Abstracts and Programme, 161–163.

Orejana D, Villaseca C, Armstrong RA et al (2011) Geochronology and trace element chemistry of zircon and garnet from granulite xenoliths: Constraints on the tectonothermal evolution of the lower crust under central Spain. Lithos 124:103–116.

Parga-Pondal I, Matte P, Capdevila R (1964) Introduction à la géologie de 'l'Ollo de Sapo', Formation porphyroide antésilurienne du nord ouest de l'Espagne. Notas y Comunicaciones del Instituto Geológico y Minero de España 76:119–153.

Passchier CW (1982a) Mylonitic deformation in che Saint-Barthélémy Massif, French Pyrenees, with emphasis on the genetic relationship between ultramylonite and pseudotachylite. G UA, Pap Geol 16:1–173.

Passchier CW (1982b) Pseudotachylyte and the development of ultramylonite bands in the Saint Barthélémy massif, French Pyrénées. Struc Geol 4: 69–79.

Patiño-Douce A, Beard J (1995) Dehydration-melting of biotite gneiss and quartz amphibolite from 3 to 15 kbar. Journal of Petrology 36 (3): 707–738.

Patiño Douce AE (1996) Effects of pressure and H2O content on the compositions of primary crustal melts. Trans R Soc Edinburgh Earth Sci 87: 11–21.

Patiño-Douce AE, Castro A, El-Biad M (1997) Thermal evolution and tectonic implications of spinel–cordierite granulites from the Aracena metamorphic belt, Southwest Spain. In: GAC/MAC Annual Meeting, Ottawa, vol 22: A113.

Pattison DRM (1991) Instability of Al2SiO5 "triple-point" assemblages in muscovite+biotite+quartzbearing metapelites, with implications. American Mineralogist, V. 86: 1414–1422, 2001.

Pattinson DRM (2001) Instability of Al_2SiO_5 "triple-point" assemblages in muscovite+biotite+quartz -bearing metapelites, with implications. American Mineralogist 86: 1414–1422.

Pedro J (1996) Estudo do Metamorfismo de Alta Pressão na Área de Safira (Montemor-o-Novo) Zona de Ossa – Morena. Master Diss, Universidade de Lisboa.

Pedro J, Fonseca P, Leal N, Munhá J (1995a) Estudo petrológico e estrutural do evento tectono-metamórfico varisco de alta pressão no Sector de Safira – Santiago do Escoural (SW da Zona de Ossa – Morena). Universidade do Porto – Faculdade de Ciências, Museu e Laboratório Mineralógico e Geológico, Memória 4: 781–786.

Pedro J, Leal, N, Munhá J, Fonseca P (1995b) Metamorfismo de alta pressão no sector de Safira (Montemor-o-Novo), Zona de Ossa – Morena. In: Rodríguez-Alonso MD, Gonzalo-Corral JC (eds), XIII Reunión de Geología del Oeste Peninsular, Annual IGCP Project-319 Meeting. Comunicaciones, p. 129.

Pedro J, Araújo A, Fonseca P, Tassinari C, Ribeiro A (2010) Geochemistry and U-Pb zircon age of the Internal Ossa-Morena Zone Ophiolite Sequences: a remnant of Rheic Ocean in SW Iberia. Ofioliti 35 (2): 117–130.

Pereira E, Gonçalves L, Moreira A (1980) Notícia explicativa da Carta Geológica de Oliveira de Azeméis -folha 13D. Serviços Geológicos de Portugal, 68 p.

Pereira E, Gonçalves S, Moreira A, Medeiros A, Cramez P, Silva N, Monteiro J, Lopes JT, Ribeiro I, Silva A, Arruda L, Fernandes I (1981) Folha 13-D Oliveira de Azemeis, Carta Geológica de Portugal à esc. 1/50000. Serviços Geológicos de Portugal, Lisboa.

Pereira E, Ribeiro A, Silva N (1998) Folha 7D-Macedo de Cavaleiros, Carta Geológica de Portugal à esc. 1/50000. Instituto Geológico e Mineiro, Lisboa, Portugal.

Pereira E, Rodrigues J, Gonçalves L, Moreira A, Silva AF (2006) Notícia explicativa da Carta Geológica de Oliveira de Azeméis--folha 13D. Serviços Geológicos de Portugal, 55 p.

Pereira MF (1999) Caracterização da estrutura dos domínios setentrionais da Zona de Ossa-Morena e seu limite com a Zona Centro-Ibérica, no Nordeste Alentejano. PhD thesis, Univ Évora, 115 p.

Pereira MF, Apraiz A (2002) Preliminary thermobarometric data from the Ouguela and Contenda Barragem do Caia Units: Coimbra–Córdoba shear zone (Northeast Alentejo, Portugal). Geogaceta 31: 73–76.

Pereira MF, Silva JB (2002) Neoproterozoic-Paleozoic tectonic evolution of the Coimbra-Cordoba shear zone and related areas of the Ossa-Morena and Central-Iberian zones (Northeast Alentejo, Portugal). Comunicações Instituto Geológico e Mineiro 89: 47–62.

Pereira MF, Chichorro M, Linnemann U, Eguiluz L, Silva JB (2006) Inherited arc signature in Ediacaran and Early Cambrian basin of the Ossa-Morena Zone (Iberian Massif Portugal): paleogeographic link with European and North African Cadomian correlatives. Precambrian Research 144: 297–315.

Pereira MF, Apraiz A, Silva JB, Chichorro M (2008) Tectonothermal analysis of high-temperature mylonitization in the Coimbra–Córdoba shear zone (SW Iberian Massif, Ouguela tectonic unit, Portugal): Evidence of intra-continental transcurrent transport during the amalgamation of Pangea. Tectonophysics 461: 378–394.

Pereira MF, Chichorro M, Williams IS, Silva JB, Fernández C, Dias-Azpíroz M, Apraiz A, Castro A (2009) Variscan intra-orogenic extensional tectonics in the Ossa–Morena Zone (Évora–Aracena–Lora del Río metamorphic belt, SW Iberian Massif): SHRIMP zircon U–Th–Pb geochronology. In: Murphy JB, Keppie JD,

Hynes AJ, Ancient orogens and modern analogues. Geol Soc London Spec Publ 327: 215–237.
Pereira MF, Apraiz A, Chichorro M, Silva JB, Armstrong RA (2010) Exhumation of high-pressure rocks in northern Gondwana during the Early Carboniferours (Coimbra–Córdoba shear zone, SW Iberian Massif): Tectonothermal analysis and U–Th–Pb SHRIMP in-situ zircon geochronology. Gondwana Res 17: 440–460.
Pereira MF, Chichorro M, Silva JB, Ordóñez-Casado B, Lee JKW, Williams IS (2012) Early Carboniferous wrenching, exhumation of high-grade metamorphic rocks and basin instability in SW Iberia: constraints derived from structural geology and U–Pb and 40Ar–39Ar geochronology. Tectonophysics 558–559: 28–44.
Pereira MF, Chichorro M, Fernández C, Silva JB, Matias FV (2013) The role of strain localization in magma injection into a transtensional shear zone (Variscan belt, SW Iberia). J Geol Soc London 170: 93–105.
Pereira MF, Ribeiro C, Vilallonga F, Chichorro M, Drost K, Silva JB, Albardeiro L, Hofmann M, Linnemann U (2014) Variability over time in the sources of South Portuguese Zone turbidites: evidence of denudation of different crustal blocks during the assembly of Pangaea. International Journal of Earth Sciences 103 (5):1453–1470. https://doi.org/10.1007/s00531-013-0902-8.
Pereira MF, Chichorro M, Moita P et al (2015) The multistage crystallization of zircon in calc-alkaline granitoids: U–Pb age constraints on the timing of Variscan tectonic activity in SW Iberia. Int J Earth Sci (Geol Rundsch) 104 (5): 1167–1183.
Pereira MF, Chichorro M, Solá AR, Silva JB, Sanchez-Garcia T, Bellido F (2011) Tracing the Cadomian magmatism with detrital/inherited zircon ages by in-situ U-Pb SHRIMP geochronology (Ossa Morena Zone, SW Iberian Massif), Lithos, v. 123, p. 204–217.
Pereira MF, Castro A, Dias da Silva Í, Fernández C (2016) Granitic rocks of the European Variscan Belt: the case study of the Évora Massif (Alentejo, Portugal). 7 Congr Geol España, Geo-Guías 10: 89–107.
Pereira Z, Matos J, Fernandes P, Oliveira JT (2007) Devonian and Carboniferous palynostratigraphy of the South Portuguese Zone, Portugal – An overview. Comun Geol 94: 53–79.
Pereira Z, Fernandes P, Matos J, Jorge RCGS, Oliveira JT (2018) Stratigraphy of the Northern Pulo do Lobo Domain, SW Iberia Variscides: A palynological contribution. Geobios (in press). https://doi.org/10.1016/j.geobios.2018.04.001.
Pérez-Cáceres I, Martínez-Poyatos DJ, Simancas JF et al (2015) The elusive nature of the Rheic Ocean suture in SW Iberia. Tectonics 34:2429–2450.
Pérez-Cáceres I (2017) Terranes affinity and Variscan transpressional evolution of Rheic-related units in SW Iberia. PhD thesis, Univ Granada.
Pérez-Cáceres I, Martínez Poyatos D, Simancas JF, Azor A (2017) Testing the Avalonian affinity of the South Portuguese Zone and the Neoproterozoic evolution of SW Iberia through detrital zircon populations. Gondwana Research 42: 177–192. https://doi.org/10.1016/j.gr.2016.10.010.
Pérez-Estaún A, Martínez Catalán JR, Bastida F (1991) Crustal thickening and deformation sequence in the footwall to the suture of the Variscan belt of northwest Spain. Tectonophysics 191: 243–253.
Pérez-Lorente F (1979) Geología de la Zona de Ossa-Morena al norte de Córdoba (Pozoblanco-Belmez-Villaviciosa de Córdoba), Tesis Doctorales de la Universidad de Granada 281: 1–340.
Pin C, Lancelot JR (1982) U–Pb dating of an early Palaeozoic bimodal magmatism in the French Massif Central and of its further metamorphic evolution. Contrib Mineral Petrol 79: 1–12.
Pin C, Ortega Cuesta LA, Gil Ibarguchi JI (1992) Mantle–derived, early Paleozoic A–type metagranitoids from the NW Iberian massif: Nd isotope and trace–element constraints. Bull Soc Géol France 163:483–494.
Pin C, Fonseca PE, Paquette JL, Castro P, Matte Ph (2008) The ca. 350 Ma Beja Igneous Complex: A record of transcurrent slab break-off in the Southern Iberia Variscan Belt? Tectonophysics 461 (1–4): 356–377.
Pin, C & Peucat, JJ (1986) Ages des episodes de métamorphisme paléozoique dans le Massif central et le Massif Armoricain. Bull. Sóc. Géol. France 8, II, 3: 461–46.
Pin, C. & Vielzeulf, D (1988): Les granulites de haute pression d'Europe moyenne témoins d'une subuction éo-hercynienne. Implications sur l'orgine des groupes leptyno–amphiboliques. Bull. Soc. Géol. Fr., 1, 1: 13–2.
Pinto CS, Casquet C, Ibarrola E, Corretgé LG, Ferreira MP (1987) Síntese geocronologica dos granitoides do Maciço Hespérico. In: Bea F, Carnicero A, Gonzalo JC, López-Plaza M, Rodríguez-Alonso MD (eds), Geología de los granitoides y rocas asociadas del macizo Hespérico- Editorial Rueda, Madrid, 69–86.
Pitra P, Martínez FJ, Van Den Driessche J, Reche J (2016) Staurolite +Kyanite-bearing pseudomorphs after andalusite (Cap de Creus, Spain). In: Carmina B, Pasero M (eds), Second European Mineralogical Conference, Abstracts, 301. Rimini, Italia.
Ponce C, Simancas JF, Azor A et al (2012) Metamorphism and kinematics of the early deformation in the Variscan suture of SW Iberia. J Metamorphic Geol 30(7): 625–638.
Pouclet A, Álvaro JJ, Bardintzeff JM, Gil Imaz A, Monceret E, Vizcaïno E (2017) Cambrian-early Ordovician volcanism across the South Armorican and Occitan domains of the Variscan Belt in France: Continental breakup and rifting of the northern Gondwana margin. Geoscience Frontiers 8 (1): 25–64. http://dx.doi.org/10.1016/j.gsf.2016.03.002.
Pouget P (1991) Hercynian tectonometamorphic evolution of the Bossost dome (French-Spanish Central Pyrenees). J Geol Soc London 148: 299–314.
Pouget P, Lamouroux C, Debat P (1988) Le Dome de Bossost (Pyrénées centrales): reinterpretation majeure de sa forme et de son évolution tectono-métamorphique. CR Acad Sci Paris 307 (II): 949–955.
Pouget P, Liesa M, Alias G, Vaquer R (1996) Metamorphisme Hercynien (6. Le Massif de Bossost). In: Barnolas, A. & Chiron, J.C (eds) Synthèse gèologique et géophysique des Pyrénées. Vol. 1: Introduction. Géophysique. Cycle Hercynien. Bulletin de la Société Géologique de France and Instituto Geológico y Minero de España, Orléans and Madrid, pp. 561–564.
Powell R, Holland TJB (1985) An internally consistent dataset with uncertainties and correlations. 1: methods and a worked example. J Metamorphic Geol 3: 327–342.
Powell R, Holland TJB (1988) An internally consistent dataset with uncertainties and correlations. 3: applications to geobarometry, worked examples and a computer program. J Metamorphic Geol 6: 173–204.
Powell R, Holland TJB (1990) Calculated mineral equilibria in the pelite system, KFMASH (K2O-FeO-MgO-Al2O3-SiO2-H2O). Am Mineral 75: 367– 380.
Priem HNA, Boelrijk NAIM, Verschure RH, Hebeda EH (1965) Isotopic ages of two granites on the Iberian continental margin: The Traba Granite (Spain) and the Berlenga Granite (Portugal). Geologie en Mijnbouw 44e: 353–354.
Priem H, Boelrijk N, Verschure RH, Hebeda EH, Verdurmen EAT (1970) Dating events of acid plutonism through the Paleozoic of the western Iberian Peninsula. Eclogae Geologicae Helvetiae 63: 255–274.
Priem HNA, Schermerhorn LJC, Boelrijk NAIM, Hebeda EH (1984) Rb-Sr geochronology of Variscan granitoids in the tin-tungsteen province of Northern Portugal: a progress report. Terra Cognita 4: 212–213.

Priem HNA, Boelrijk NAIM, Hebeda EH, Schermerhorn LJG (1986) Isotopic ages of the Alcáçovas orthogneiss and the Beja porphyries, South Portugal. Comunicações Serviços Geológicos Portugal 72: 3–7.

Puelles P, Ábalos B, Gil Ibarguchi JI (2005) Metamorphic evolution and thermobaric structure of the subduction-related Bacariza high-pressure granulite formation (Cabo Ortegal Complex, NW Spain). Lithos 84:125–149.

Puelles P, Beranoaguirre A, Ábalos B et al (2017) Eclogite inclusions from subducted metaigneous continental crust (Malpica-Tui Allochthonous Complex, NW Spain): petrofabric, geochronology and calculated seismic properties. Tectonics 36 (7): 1376–1406. https://doi.org/10.1002/2016tc004367.

Quesada C (1990a) Precambrian successions in SW Iberia: their relationships to Cadomian orogenic events. In: D'Lemos RS, Strachan RA, Topley CG (Eds), The Cadomian Orogeny. Geol Soc London Spec Publ 51: 353–362.

Quesada C (1990b) Precambrian terranes in the Iberian Variscan Foldbelt. In: Strachan RA, Taylor GK (Eds), Avalonian and Cadomian Geology of the North Atlantic, Blackie, Glasgow, 109–133.

Quesada C (1991) Geological constraints on the Paleozoic tectonic evolution of tectonostratigraphic terranes in the Iberian Massif. Tectonophysics 185: 225–245.

Quesada C (1997) Evolución geodinámica de la Zona Ossa Morena durante el ciclo Cadomiense. In: Araújo AA, Pereira MF (Eds), Estudo sobre a geología da zona de Ossa Morena (Maciço Ibérico). Livro homenagem Prof. Francisco Gonçalves, University of Évora, 205–230.

Quesada C (1998) A reappraisal of the structure of the Spanish segment of the Iberian Pyrite Belt. Mineralium Deposita 33: 31–44.

Quesada C (2006) The Ossa-Morena Zone of the Iberian Massif: a tectonostratigraphic approach to its evolution. Z dt Ges Geowiss 157 (4): 585–595.

Quesada C, Dallmeyer RD (1994) Tectonothermal evolution of the Badajoz-Córdoba shear zone (SW Iberia): characteristics and 40Ar/39Ar mineral age constraints. Tectonophysics 231: 195–213.

Quesada C, Munhá J (1990) Metamorphism in the Ossa-Morena Zone. In: Dallmeyer RD, Martínez García E (Eds), Pre-Mesozoic geology of Iberia. Springer-Verlag, Heidelberg, 314–320.

Quesada C, Apalategui O, Eguiluz L, Liñán E, Palacios T (1990) Precambrian stratigraphy of the Ossa morena zone. In: Dallmeyer RD, Martínez García E (eds), Pre-Mesozoic geology of Iberia. Springer, Heidelberg, 252–258.

Quesada C, Bellido F, Dallmeyer RD, Gil-Ibarguchi I, Oliveira JT, Pérez-Estaún A, Ribeiro A, Robardet M, Silva JB (1991) Terranes within the Iberian Massif: correlations with West African sequences. In: Dallmeyer RD, Lecorché JP (eds), The West African orogens and Circum-Atlantic correlatives, Springer, Berlin, 268–293.

Quesada C, Fonseca PE, Munhá J, Oliveira JT, Ribeiro A (1994) The Beja–Acebuches Ophiolite (Southern Iberia Variscan Foldbelt): geological characterization and geodynamic significance. Boletín Geológico Minero 105: 3–49.

Reavy RJ (1987) An investigation into the controls of granite plutonism in the Serra da Freita region, northern Portugal. PhD Thesis, Univ of St Andrews.

Reavy RJ, Stephens WE, Fallick AE, Hallidar AN, Godinho MM (1991) Geochemical and isotopic constraints on petrogenesis: the Serra da Freita pluton, a typical granite body from the Portuguese Hercynian collision belt. Geological Society of America Bulletin 103: 392–401.

Reche J, Martinez FJ (2002) Evolution of bulk composition, mineralogy, strain style and fluid flow during an HT–LP metamorphic event: sillimanite zone of the Catalan Coastal Ranges Variscan basement, NE Iberia. Tectonophysics 348: 111–134.

Reche J, Martinez FJ (2013) Relations between fluid flow, igneous intrusion, metamorphic and metasomatic events and deformation during low P, hight T regional thermal metamorphism. An example from the Osor high grade Complex (Catalan Coastal Ranges, NE Iberia). Godschmidt Conference 2013, Firenze (Italy).

Reche J, Carreras J, Druguet H (1996) Le massif du Cap de Creus. In: Guitard G, Vielzeuf D, Martínez FJ (coord): Métamorphisme Hercynien. Synthèse géologique et géophysique des Pyrénées. Edition BRGM – ITGE 1: 524–531.

Reche J, Martínez FJ, Arboleya ML, Dietsch C, Briggs WD (1998) Evolution of a kyanite-bearing belt within a HT–LP orogen: the case of NE Variscan Iberia. J Metamorph Geol 16: 379–394.

Reche J, Martinez FJ, Leoz G (2015) Prograde PT path, prograde fluid flow, metasomatism and hydrous melting in the Osor high-grade complex (Catalan Coastal Ranges, CCR, NE Iberia). EGU general Assembly 2015, Vienna.

Reche J, Martinez FJ, Travería M (2016) Coupled Thermo-Chemo-Mechanical phenomena including genesis of COR from low-K psammopelites during syn-D2, HT-LP Variscan metamorphism and hidrous melting (Osor complex, CCR, NE Iberia). In: Carmina B, Pasero M (eds), Second European Mineralogical Conference, Abstracts book, 166. Rimini, Italia.

Reche J, Martinez FJ, Cirés J, Aleinikoff J (2017) Two Variscan magmatic events in a HT/LP g-bt-sil semipelitic gneisses (Guilleries massif, Catalan Coastal Ranges, NE Iberia). Geophysical Research Abstracts 19, EGU2017-17725-5, Vienna.

Respaut JP, Lancelot JR (1983) Datation de la mise en place synmétamorphe de la charnockite d'Ansignan (massif de l'Agly) par la méthode U-Pb sur zircons et monazites. N Jhb Miner Abh 147: 24–34.

Ribeiro A (1974) Contribution à l'étude tectonique de Trás-os-Montes Oriental. Memórias dos Serviços Geológicos de Portugal 24, Lisboa.

Ribeiro A (1981) Geotraverse through the variscan fold belt in Portugal. Geology Mijnbouw, 16, pp. 41–44.

Ribeiro A (2013) Evolução Geodinâmica de Portugal: os ciclos ante-mesozóicos. In: Dias R, Araújo A, Terrinha P, Kullberg JC (eds), Geologia de Portugal I: 15–57, Escolar Editora.

Ribeiro A, Pereira E, Severo L (1980a) Análise da deformação na zona de cisalhamento Porto-Tomar na transversal de Oliveira de Azeméis. Comunicações dos Serviços Geológicos Portugal 66: 33–48.

Ribeiro A, Iglésias M, Ribeiro ML, Pereira E (1983) Modèle geodynamique des Hercynides Ibériques. Comunicações dos Serviços Geológicos Portugal 69 (2): 291–293.

Ribeiro A, Pereira E, Dias R (1990a) Structure in the Northwest of the Iberian Peninsula. In: Dallmeyer RD, Martínez-García E (eds), Pre-Mesozoic Geology of Iberia. Springer-Verlag, Berlin, 220–236.

Ribeiro A, Quesada C, Dallmeyer RD (1990b) Geodynamic evolution of the Iberian Massif. In: Dallmeyer RD, Martínez-García E (eds), Pre-Mesozoic Geology of Iberia. Springer-Verlag, Berlin, 399–409.

Ribeiro ML, Ribeiro A (1982) Nouvelles donnés sur le volcanisme bimodal de l'unité Centro-Transmontane dans la région de Macedo de Cavaleiros (Trás-os-Montes Oriental). Terra Cognita, 3, 202 (abstract).

Ribeiro A, Munhá J, Dias R, Mateus A, Pereira E, Ribeiro ML, Fonseca P, Araújo A, Oliveira JT, Coke C, Pedro JC (2007) Geodynamic Evolution of the SW Europe Variscides. Tectonics 26: TC6009, https://doi.org/10.1029/2006tc002058, 24 p.

Ribeiro A, Munhá J, Fonseca P, Araújo A, Pedro J, Mateus A, Tassinari C, Machado G, Jesus A (2010) Variscan Ophiolite Belt in the Ossa-Morena Zone (Southwest Iberia): Geological caracterization and geodynamic significance. Gondwana Res 17: 408–421.

Ribeiro A, Pereira E, Ribeiro ML, Castro P (2013a) Unidades Alóctones da região de Morais (Trás-os-Montes oriental). In:

Dias R, Araújo A, Terrinha P, Kullberg JC (eds), Geologia de Portugal, 1, Escolar Editora.
Ribeiro A, Romão J, Munhá J, Rodrigues JF, Pereira E, Mateus A, Araújo A, Dias R (2013b) Relações tectono-estratigráficas e fronteiras entre as Zonas Centro-Ibérica e Ossa-Morena do Terreno Ibérico e o Terreno Finisterra. In: Dias R, Araújo A, Terrinha P, Kullberg JC (eds), Geologia de Portugal, 1: pp 439–481, Escolar Editora.
Ribeiro ML (1976) Considerações sobre uma ocorrência de crossite em Trás-os-Montes oriental. Memórias e Notícias, Museu e Laboratório Mineralógico e Geológico da Universidade de Coimbra 82: 1–16.
Ribeiro ML (1978) Algumas observações sobre o metamorfismo da região de Tourém (Norte de Portugal). Comunicações dos Serviços Geológicos de Portugal XXI: 151–169.
Ribeiro ML (1980) Algumas observações sobre a petrologia e o quimismo da região de Tourém - Montalegre (Norte de Portugal). Comunicações dos Serviços Geológicos de Portugal 66: 33–48.
Ribeiro ML (1986) Geologia e petrologia da região a SW de Macedo de Cavaleiros (Trás-os-Montes). PhD. Thesis, Univ Lisboa, 202 p.
Ribeiro ML (1987) Petrogenesis of early Paleozoic peralkaline rhyolites from Macedo de Cavaleiros region (NE Portugal). Geologische Rundschau 76 (1): 147–168
Ribeiro ML (1991) Contribução para o conhecimento estratigráfico e petrológico da região a SW de Macedo de Cavaleiros (Trás-os--Montes Oriental). Mem Serv Geol Portugal 30, Lisboa.
Ribeiro ML, Floor P (1987) Magmatismo peralcalino no Maciço Hespérico: sua distribuição e significado geodinâmico. In: Bea F, Carnicero A, Gonzalo JC, López Plaza M, Rodríguez Alonso MD (Eds), Geología de los granitoides y rocas associadas del Macizo Hespérico. Rueda, Madrid, p. 211–221.
Ribeiro ML, Munhá J (1983–85) Estudo comparativo do metamorfismo nas regiões de Monção e Tourém (Zona Centro Ibérica). Resumo, Comunicações I Congresso Nacional de Geologia, Aveiro.
Ribeiro ML, Barnett RL, Munhá J, Ribeiro A (1982) Blueschist in Eastern Trás-os-Montes (NE Portugal): evidence for overthrusting. Comunicações V Semana de Geoquímica, Aveiro (1983), abstracts, Terra Cognita 3.
Ribeiro A, Pereira E, Severo L (1980) Análise da deformação na zona de cisalhamento Porto-Tomar na transversal de Oliveira de Azeméis. Comunicações dos Serviços Geológicos Portugal 66: 33–48.
Ribeiro ML, Priem HA, Boelrijk NM, Schermerhorn L J (1985) Rb-Sr whole rock age of peralkaline acidic volcanics in the Macedo de Cavaleiros área, Trás-os-Montes (NE Portugal). Comunicações dos Serviços Geológicos Portugal 71 (2): 171–174.
Ribeiro ML, Palácios T, Munhá J (1995) Aspectos petrológicos-geoquímicos do Complexo eruptivo de Mouriscas (Abrantes). Resumo alargado. IV Congresso Nacional de Geologia. Memórias do Museu do Laboratório Mineralógico e Geológico da Faculdade de Ciências da Universidade do Porto 4: 805–807.
Riesco M, Stüwe K, Reche J, Martínez FJ (2004) Silica depleted melting of pelites. A petrogenetic grid with application to the Susqueda Aureole, Spain. J Metamorphic Geol 22: 475–494.
Ring U, Brandon MT, Willett SD et al (1999) Exhumation processes. In: Ring U et al (eds), Exhumation Processes: normal faulting, ductile flow and erosion. Geol Soc London Spec Publ 154: 1–27.
Rodríguez J (2005) Recristalización y deformación de litologías supracorticales sometidas a metamorfismo de alta presión (Complejo de Malpica–Tui, NO del Macizo Ibérico). Nova Terra, A Coruña.
Rodríguez J, Cosca MA, Gil Ibarguchi JI et al (2003) Strain partitioning and preservation of $^{40}Ar/^{39}Ar$ ages during Variscan exhumation of a subducted crust (Malpica–Tui complex, NW Spain). Lithos 70:111–139.
Rodríguez J, Paquette JL and Gil Ibarguchi JI (2007) U–Pb dating of Coger Ordovician alkaline magmatism in the Gondwana margin (Malpica–Tui Complex, Iberian Massif): Latest continental events before oceanic spreading. In: Arenas R et al (eds), The rootless Variscan suture of NW Iberia (Galicia, Spain): Field trip guide and conference abstracts: International Geological Correlation Programme 497, The Rheic Ocean: Its origin, evolution and correlatives. Publicaciones del Instituto Geológico y Minero de España (IGME), Madrid, 163–164.
Romão J, Esperancinha A. 2000 Carta Geológica à escala 1/50000, Folha 28A-Mação. IGM, Lisboa.
Romão J, Ribeiro A, Pereira E, Fonseca P, Rodrigues J, Mateus A, Noronha F, Dias R (2010) Interplate versus intraplate strike-slip deformed belts: examples from SW Iberia Variscides. Trabajos de Geología, Universidad de Oviedo 30, 176–172.
Román-Berdiel T, Casas AM, Oliva-Urcia B, Pueyo E, Rillo C, 2004, The main Variscan deformation event in the Pyrenees: new data from the structural study of the Bielsa granite. Journal of Structural Geology 26 (4), 659–677.
Romão J, Esperancinha A, Ribeiro A, Pereira E, Manuppella G, Rocha R, Barbosa B, Barra A, Ribeiro J (2016) Folha 27B-Tomar. Carta Geológica de Portugal à escala 1/ 50 000, LNEG.
Romeo I, Lunar R, Capote R, Quesada C, Piña R, Dunning GR, Ortega L (2006) U/Pb age constraints on Variscan magmatism and Ni-Cu-PGE metallogeny in the Ossa-Morena zone (SW Iberia). J Geol Soc London 163: 1–9.
Rosas FM, Marques F, Ballèvre M, Tassinari C (2008) Geodynamic evolution of the SW Variscides: Orogenic collapse shown by new tectonometamorphic and isotopic data from western Ossa-Morena Zone, SW Iberia. Tectonics 27: TC6008. https://doi.org/10.1029/2008tc002333.
Roux L (1977) L'évolution des roches du faciès granulite et le problème des ultramafites dans le massif de Castillon (Ariège). These d'Etat, Univ Toulouse, 487 p.
Rubio-Ordóñez A, Valverde-Vaquero P, Corretgé LG, Cuesta-Fernández A, Gallastegui G, Fernández-González M, Gerdes A (2012) An Early Ordovician tonalitic–granodioritic belt along the Schistose-Greywacke Domain of the Central Iberian Zone (Iberian Massif, Variscan Belt). Geol Mag 149: 927–939.
Rubio Pascual FJ (2013) Evolución tectonotermal varisca del Sistema Central en Somosierra-Honrubia. Nova Terra, A Coruña.
Rubio Pascual FJ, Arenas R, Díaz García F et al (1993) Metamorfismo eo-hercínico de alta presión y desarrollo de un gradiente metamórfico invertido en los esquistos de la Unidad de Santiago (Complejo de Ordenes, NW del Macizo Ibérico). Cadernos Lab Xeolóxico de Laxe 18:37–45.
Rubio Pascual FJ, Arenas A, Díaz García F et al (2002) Eclogites and eclogite-amphibolites from the Santiago Unit (Ordenes Complex, NW Iberian Massif, Spain): a case study of contrasting high-pressure metabasites in a context of crustal subduction. In: Martínez Catalán JR et al (eds). Variscan-Appalachian Dynamics: The Building of the Late Paleozoic Basement. Geol Soc Am Spec Pap 364:105–124.
Rubio Pascual FJ, Matas J, Martín Parra LM (2013a). High-pressure metamorphism in the Early Variscan subduction complex of the SW Iberian Massif. Tectonophysics 592:187–199.
Rubio Pascual FJ, Arenas R, Martínez Catalán JR et al (2013b) Thickening and exhumation of the Variscan roots in the Iberian Central System: tectonothermal processes and $^{40}Ar/^{39}Ar$ ages. Tectonophysics 587:207–221.
Rubio Pascual FJ, López-Carmona A, Arenas R (2016) Thickening vs. extension in the Variscan belt: P–T modelling in the Central Iberian Autochthon. Tectonophysics 681:144–158.
Saint-Blanquat M (1993) La faille normale ductile du massif du Saint-Barthélémy. Evolution hercynienne des massifs nord- pyrénéens catazonaux considérée du point de vue de leur histoire thermique. Geodynamica Acta 6 (1): 59–77.

Salman K (2004) The timing of the Cadomian and Variscan cycles in the Ossa Morena Zone, SW Iberia: granitic magmatism from subduction to extension. Journal Iberian Geology 30: 119–132.

Sánchez-García T, Bellido F, Quesada C (2003) Geodynamic setting and geochemical signatures of Cambrian-Ordovician rift-related igneous rocks (Ossa-Morena Zone, SW Iberia). Tectonophysics 365:233–255.

Sánchez-García T, Quesada C, Bellido F, Dunning G, González de Tánago J (2008) Two-step magma flooding of the upper crust during rifting: The Early Paleozoic of the Ossa-Morena Zone (SW Iberia). Tectonophysics 461: 72–90.

Sánchez-García T, Bellido F, Pereira MF, Chichorro M, Quesada C, Pin Ch, Silva JB. (2010) Rift-related volcanism predating the birth of the Rheic Ocean (Ossa-Morena zone, SW Iberia). Gondwana Research 17:392–407.

Sánchez-García T, Quesada C, Bellido F, Dunning GR., Pin Ch, Moreno-Eiris E, Perejón A (2016) Age and characteristics of the Loma delAire unit (SW Iberia): Implications for the regional correlation of the Ossa-Morena Zone. Tectonophysics 681: 58–72.

Santos JF, Mata J, Gonçalves F, Munhá J (1987) Contribuição para o conhecimento geológico-petrológico da região de Santa Susana: O complexo vulcano-sedimentar da Toca da Moura. Comunicações Serviços Geológicos de Portugal 73: 29–48.

Santos, JF., Andrade, AS., Munhá, JM. (1990). Magmatismo Orogénico Varisco no limite meridional da Zona de Ossa-Morena. Comunicações Serviços Geológicos de Portugal 76: 91–124.

Santos Zalduegui JF, Schärer U, Gil Ibarguchi JI (1996) Origin and evolution of the Paleozoic Cabo Ortegal ultramafic-mafic complex (NW Spain): U-Pb, Rb-Sr, and Pb-Pb isotope data. Chem Geol 129: 281–304.

Santos Zalduegui FJ, Schärer U, Gil Ibarguchi JI et al (2002) Genesis of pyroxenite-rich peridotite at Cabo Ortegal (NW Spain): geochemical and Pb-Sr-Nd isotope data. J Petrol 43:17–43.

Sawyer EW (2008) Atlas of Migmatites. The Canadian Mineralogist, Spe Publ 9, NRC Research Press, Ottawa, 371.

Schäfer HJ (1990) Geochronological investigations in the Ossa Morena Zone, SW Spain. PhD thesis, ETH Zurich, 153 p.

Schäfer HJ, Gebauer D, Nägler TF (1991) Evidernce for Silurian eclogite and granulite facies metamorphism in the Badajoz-Córdoba shear belt (SW Spain). Terra Abst Terra Nova 3 (6): 11.

Schermerhorn LJG (1971) An outline stratigraphy of the Iberian Pyrite Belt. Boletín Geológico Minero 82: 239–268.

Schermerhorn LJG, Kotsch S (1984) First occurrence of lawsonite in Portugal and tectonic implications. Comunicações dos Serviços Geológicos Portugal 70 (1): 23–30.

Schulmann K, Lexa O, Janousek V et al (2006) Anatomy of a diffuse cryptic suture zone: An example from the Bohemian massif, European Variscides. Geology 42:275–278.

Schulmann K, Oggiano G, Lardeaux JM, Janousek V, Martínez Catalán JR, Scrivener R (eds) (2014), The Variscan Orogeny: Extent, Timescale and the Formation of the European Crust. Geological Society, London, Special Publications 405: 400 p.

Sebastián A, Martínez FJ (1989) Equilibrios minerales y zonacion de granates en el núcleo del domo del Tormes (provincia de Salamanca y Zamora). Acta Geologica Hispanica 24 (2): 103–113.

Sebastián A, Reche J, Durán H (1990) Hercynian metamorphism in the Catalonian coastal ranges. Acta Geologica Hispanica 25: 31–38.

Shail R, Leveridge B (2009) The Rhenohercnian passive margin of SW England: development, inversion and extensional reactivation. Comptes Rendus Geoscience 341: 140–155.

Silva JB, Oliveira JT, Ribeiro A (1990) Structural outline of the South Portuguese Zone. In: Dallmeyer RD, Martínez García E (eds), Pre-Mesozoic geology of Iberia, Springer, Heidelberg, 348–361.

Simancas JF (1983) Geología de la Extremidad Oriental de la Zona Sudportuguesa. PhD thesis, Univ Granada, 439 p.

Simancas JF, Martínez-Poyatos DJ, Expósito I et al (2001) The structure of a major suture zone in the SW Iberian Massif: the Ossa-Morena/Central Iberian contact. Tectonophysics 332:295–308.

Simancas JF, Azor A, Martínez Poyatos DJ et al (2016) Comment on "The Late Devonian Variscan suture of the Iberian Massif: A correlation of high-pressure belts in NW and SW Iberia. Tectonophysics 654, 96–100" by R. Fernández and R. Arenas. Tectonophysics 666:281–284.

Solá AR, Montero P, Neiva AMR et al (2005) Pb/Pb age of the Carrascal Massif, central Portugal. Geochim Cosmochim Acta 69:856–856.

Solá AR, Pereira MF, Ribeiro ML et al (2006) The Urra Formation: Age and Precambrian inherited record. In: Libro dos Resumos VII Congresso Nacional de Geologia, Universidade de Évora, Évora, 5–7 July 2006.

Solá AR, Pereira MF, Ribeiro ML, Neiva AMR, Williams IS, Montero P, Bea F, Zinger T (2008) New insights from zircon ages on the Lower Ordovician magmatism of the northern Gondwana margin: the Urra Formation (SW Iberian Massif, Portugal). Tectonophysics 461: 114–129.

Soula JC (1982): Characteristics and mode of emplacement of gneiss domes and plutonic domes in central-eastern Pyrenees. J. Struct. Geol., 3: 313–342.

Soula JC, Debat J, Deramond J & Pouget O (1986) A dynamic model of the structural evolution of the Variscan Pyrenees. Tectonophysics, 129, 29–51.

Spear FS (1993) Metamorphic phase equilibria and pressure-temperature-time paths. Mineralogical Society of America, Washington DC.

Spear F, Cheney JT (1989) A petrogenetic grid for pelitic schists in the system SiO_2–Al_2O_3–FeO–MgO–K_2O–H_2O. Contributions to Mineralogy and Petrology 101: 149–164.

Talavera C, Montero P, Martínez Poyatos D, Williams IS (2012) Ediacaran to Lower Ordovician age for rocks ascribed to the Schist–Graywacke Complex (Iberian Massif, Spain): Evidence from detrital zircon SHRIMP U–Pb geochronology. Gondwana Research 22: 928–942.

Talavera C, Montero P, Bea F, González-Lodeiro F, Whitehouse M (2013) U–Pb Zircon geochronology of the Cambrian-Ordovician metagranites and metavolcanic rocks of central and NW Iberia. Int J Earth Sci (Geol Rundsch) 102:1–23.

Thiebaut J (1964) Etude géologique du massif de la forêt de Castillon. Bull Soc Hist Nat Toulouse 99 (3–4): 363–389.

Triboulet C, Guitard G, Katona I, Navidad M (2005) Évolution pression–température des amphibolites de la zone axiale au cours du métamorphisme hercynien des Pyrénées orientales. CR Geoscience 337: 1244–1249.

Valverde-Vaquero P, Dunning GR (2000) New U–Pb ages for Early Ordovician magmatism in Central Spain. J Geol Soc London 157: 15–26.

Valverde Vaquero P, Fernández FJ (1996) Edad de enfriamiento U/Pb en rutilos del Gneis de Chímparra (Cabo Ortegal, NO de España). Geogaceta 20:475–478.

Valverde-Vaquero P, Díez Balda MA, Díez Montes A et al (2007) The "hot orogen": two separate Variscan low-pressure metamorphic events in the Central Iberian Zone. In: SGF, BRGM (Eds), Mechanics of Variscan Orogeny: A Modern View on Orogenic Research. Géologie de la France 2: 168.

Valverde-Vaquero P, Bento-dos-Santos T, González-Clavijo E, Díez--Montes A, Ribeiro ML, Solá AR, Dias-da-Silva Í (2011) The Berlengas Archipelago granitoids within the frame of the Variscan

Orogeny, W Portugal: new data and insights. 7th Hutton Symposium on Granites and Related Rocks, Ávila, 153.
van den Eeckhout B (1986) A case study of a mantled gneiss antiform, the Hospitalet massif, Pyrenees (Andorra, France). GeolUltraiect 45, Univ. Utrecht, 193 p.
van den Eeckhout B, & Zwart HJ, (1988) Hercynian crustal-scale extensional shear zone in the Pyrenees Geology, 16(2) 135–138.
van der Wegen G (1978) Garnet–bearing metabasites from the Blastomylonitic Graben, Western Galicia, Spain. Scripta Geologica 45:1–95.
Vielzeuf D (1980) Orthopyroxene and cordierite secondary assemblages in rhe granulitic paragneisses from Lherz and Saleix (French Pyrenees). Bull. Minéral., 103, pp. 66–78.
Vielzeuf D (1984) Relations de phases dans le faciès granulite et implications géodynamiques. L'exemple des granulites des Pyrénées. PhD thesis, Clermont-Ferrand University.
Vielzeuf D, Holloway JR (1988) Experimental determination of fluid absent melting relations in the pelitic system. Consequences for crustal differentiation. Contributions Mineralogy Petrology 98: 257–276.
Vilà M, Pin C, Enrique P, Liesa M, (2005). Telescoping of three distinct magmatic suites in an orogenic setting: Generation of Hercynian igneous rocks of the Albera Massif (Eastern Pyrenees). Lithos, 83, 97–127.
Vilà M, Pin C, Liesa M, Enrique P (2007) LPHT metamorphism in a late orogenic transpressional setting, Albera Massif, NE Iberia: implications for the geodynamic evolution of the Variscan Pyrenees. Journal of Metamorphic Geology 25 (3): 321–347.
Villa IM, De-Bièvre P, Holden NE, Renne PR (2015) IUPAC/IUGS recommendation on the half-life of 87Rb. Geochim Cosmochim Acta 164: 382–385.
Villaseca C, Castiñeiras P, Orejana D (2015) Early Ordovician metabasites from the Spanish Central System: A remnant of intraplate HP rocks in the Central Iberian Zone. Gondwana Res 27: 392–409.
Vissers, RLM (1992) Variscan extension in the Pyrenees. Tectonics, 11, 6, 1369–1384.
Vitrac-Michard A (1975) Chronologie er développement d'une orogenèse. Exemple des Pyrénées orientales. Thèse d'Etat, Univ Paris VII, 142 p.
Vogel DE (1967) Petrology of an eclogite-and pyrigarnite-bearing polymetamorphic rock complex at Cabo Ortegal. NW Spain. Leidse Geol Meded 40:121–213.
von Raumer JF, Stampfli GM, Bussy F (2003) Gondwana derived microcontinents—the constituents of the Variscan and Alpine collisional orogens. Tectonophysics 365: 7–22.
von Raumer JF, Bussy F, Stampfly GM (2009) The Variscan evolution in the external massifs of the Alps and place in their Variscan framework. CR Geoscience 341: 239–252.
von Raumer JF, Bussy F, Schaltegger U et al. (2013) Pre-Mesozoic Alpine basements – their place in the European Paleozoic framework. GSA Bulletin 125: 89–108.
Warren CJ, Beaumont C, Jamieson RA (2008) Modelling tectonic styles and ultrahigh pressure (UHP) rock exhumation during the transition from oceanic subduction to continental collision. Earth Planet Sci Lett 267:129–145.
Weber K (1984) Variscan events: Early Palaeozoic continental rift magmatism and Late Palaeozoic crustal shortening. In: Hutton DHW, Sanderson DJ (Eds), Variscan Tectonics in the North Atlantic Region. Geol Soc, London, Spec Publ 14: 3–22.
Wickham SM (1984) Crustal anatexis in the Trois Seigneurs massif, Pyrénées, France. Thesis, Cambridge, 194 p.
Wickham SM (1987) Crustal anatexis and granite petrogenesis during low-pressure regional metamorphism: the Trois Seigneurs massif, Pyrenees, France. Petrology 28: 127–169.
White RW, Powell R, Holland TJB, Worley BA (2000) The effect of TiO2 and Fe2O3 on metapelitic assemblages at greenschist and amphibolite facies conditions: mineral equilibria calculations in the system K_2O–FeO–MgO–Al_2O_3–SiO_2–H_2O–TiO_2–Fe_2O_3. Journal of Metamorphic Geology 18: 497–511.
White RW, Powell R, Holland TJB (2007) Progress relating to calculation of partial melting equilibria for metapelites. Journal of Metamorphic Geology 25: 511–527.
Whitney D, Evans B (2010) Abbreviations for names of rock-forming minerals. American Mineralogist 95: 185–187. https://doi.org/10.2138/am.2010.3371 185.
Will TM, Schmädicke E (2003) Isobaric cooling and anti-clockwise P–T paths in the Variscan Odenwald Crystalline Complex, Germany. J Metamorph Geol 21:469–480.
Williams H (1979) Appalachian orogen in Canada. Can J Earth Sci 16: 792–807.
Zwart HJ (1959) Metamorphic history of the central Pyrenees, part 1. Arize, Trois Seigneurs and Saint-Barthélémy massifs (sheet 3). Leidse Geol Meded 22: 419–490.
Zwart HJ (1962) On the determination of polymetamorphic mineral associations and its application to the Bosost area (central Pyrenees). Geol Rundschau 52: 38–65.
Zwart HJ (1963) Metamorphic history of the Central Pyrenees II. Leidse Geol Meded 28: 321–376.
Zwart HJ (1965) Geological map of the Paleozoic of the Central Pyrenees, sheet 6, Aston, France, Andorra, Spain 1/50000. Leidse Geol Meded 33: 191–254.
Zwart HJ (1979) The geology of the central Pyrenees. Leidse Geol Meded 50: 1–74.
Zwart HJ (1986) The Variscan geology of the Pyrenees. Tectonophysics, 129, 9–27.

Variscan Magmatism

13

M. L. Ribeiro, A. Castro, A. Almeida, L. González Menéndez, A. Jesus, J. A. Lains, J. C. Lopes, H. C. B. Martins, J. Mata, A. Mateus, P. Moita, A. M. R. Neiva, M. A. Ribeiro, J. F. Santos, and A. R. Solá

Abstract

This chapter aims to identify, characterize and locate the main facts/events related to orogenesis in the Iberian Peninsula. Its succession in space and time determines the geodynamic environment of the broader geological phenomenon corresponding to the Variscan cycle. In this sense, this section comprises two parts: *I—The Iberian orogenic magmatism seen through a space-time approach of its westernmost region*—focus on the enormous complexity of the inherited basement, its nature, age and distribution in space. Establishes a space-time sequence of geodynamic environments correlated with the obtained data and tries to identify the agents responsible for its genesis. Some case studies are presented to illustrated significant regional aspects of the magmatic process and *II—An overview of the petrogenesis of the great batholiths and of the basic, intermediate and mantle-related rocks*—identify and analyze a great amount of these rocks intruding and extruded from 400 to 280 Ma and to better understanding

Coordinators: M. L. Ribeiro and A. Castro.

M. L. Ribeiro (✉)
Laboratório Nacional de Energia e Geologia (LNEG), Estrada da Portela, Bairro do Zambujal, Apartado 7586 Alfragide, 2610-999 Amadora, Portugal
e-mail: luisacarvalhoduarte@gmail.com

A. Castro
Institute of Geosciences (IGEO), CSIC-UCM, Ciudad Universitaria, 28040 Madrid, Spain
e-mail: antonio.castro@csic.es

A. Almeida · H. C. B. Martins · M. A. Ribeiro
Departamento de Ciências do Ambiente e Ordenamento do Território, Instituto de Ciências da Terra, FCUP, Rua do Campo Alegre, Porto 1021/1055, 4169-007 Porto, Portugal
e-mail: aalmeida@fc.up.pt

H. C. B. Martins
e-mail: hbrites@fc.up.pt

M. A. Ribeiro
e-mail: maribeir@fc.up.pt

L. G. Menéndez
Instituto Geológico y Minero de España Parque Científico de León, Avda. Real 1. Edificio 1, 24006 León, Spain
e-mail: l.gonzalez@igme.es

A. Jesus
Departamento de Geologia, Faculdade de Ciências, Universidade de Lisboa, 1749-016 Lisbon, Portugal
e-mail: ana.jesus@fc.ul.pt

J. C. Lopes
Departamento de Geociências, Universidade de Évora, 7000-671 Évora, Portugal
e-mail: carrilho@uevora.pt

J. A. Lains · J. Mata · A. Mateus
Departamento de Geologia, Faculdade de Ciências, Instituto Dom Luiz (IDL), Universidade de Lisboa, Ed. C6, Piso 4, Campo Grande, 1749-016 Lisbon, Portugal
e-mail: Joao.Lains.Amaral@gmail.com

J. Mata
e-mail: jmata@fc.ul.pt

A. Mateus
e-mail: amateus@fc.ul.pt

J. A. Lains · J. Mata · A. Mateus
Instituto Dom Luiz (IDL), Ed. C1, Piso 1, Campo Grande, 1749-016 Lisbon, Portugal

A. M. R. Neiva
Departamento de Ciências da Terra, Universidade de Coimbra, 3030-790 Coimbra, Portugal
e-mail: neiva@dct.uc.pt

A. M. R. Neiva · J. F. Santos
Geobiotec, Departamento de Geociências, Universidade de Aveiro, 3810-193 Aveiro, Portugal
e-mail: jfsantos@ua.pt

A. R. Solá
Laboratório Nacional de Energia e Geologia (LNEG), Unidade de Geologia, Hidrogeologia e Geologia Costeira, 2610-999 Amadora, Portugal
e-mail: rita.sola@lneg.pt

P. Moita
HERCULES, Departamento de Geociências, Universidade de Évora, 7000-671 Évora, Portugal
e-mail: pmoita@uevora.pt

C. Quesada and J. T. Oliveira (eds.), *The Geology of Iberia: A Geodynamic Approach*, Regional Geology Reviews,
https://doi.org/10.1007/978-3-030-10519-8_13

the large-scale process involving the whole lithosphere during Variscan cycle.

13.1 General Introduction

M. L. Ribeiro, A. Castro

This section aims to identify and characterize the main facts/events related to orogenesis and their location in the Iberian area. Its succession in space and time determines the geodynamic environment of the wider geological phenomenon that encircles the Variscan cycle. In this sense, this section comprises two parts:

I—The Iberian orogenic magmatism seen through a space-time approach of its westernmost region

This part shows: (i) The enormous complexity of the inherited basement and the diversity of lithotypes associated with the Variscan Iberian orogenesis, its nature, age and distribution in space; (ii)—Establishes a space-time sequence of geodynamic environments correlated with the obtained data and tries to identify the agents responsible for its genesis.

II—An overview of the petrogenesis of the great batholiths and of the basic, intermediate and mantle-related rocks

It tries to establish cogenetic relationships between the mantle liquids that originated outcropping rocks in several points of the Iberian Peninsula, rocks of intermediate compositions and some granitic types and discusses the possible implications.

13.2 The Iberian Orogenic Magmatism Seen Through a Space-Time Approach of Its Westernmost Region

13.2.1 Introduction

M. L. Ribeiro

If orogenesis is the last major event of any geological cycle, orogenic magmatism is one of its most conspicuous expressions. In many ways, all the processes and products of each geological cycle are implicated in their respective orogenic magmatism, as well as their own basement. In the case of the Variscan cycle the specificities of orogenic magmatism are so evident, specially the great extension and volume of granites and similar rocks, which for decades have attracted the attention of many generations of geologists (e.g. Schermerhorn 1956, 1987; Soen 1970; Capdevilla et al. 1973; Beckinsale 1979; Pitcher 1979; Ribeiro 1993; Bea 2004, 2007; Castro et al. 2010).

Granitic rocks occupy more than one third of the outcropping basement in the Iberian massif. In the Central Iberian Zone the areal proportion of granitic rocks represents more than 50%, on average, of the basement. Minor intermediate and mafic rocks, ranging in composition from gabbro to quartz-diorite, monzonite and tonalite, are also widespread forming small plutons and complexes. The large production of granitic rocks is a key fingerprint of magmatism throughout the Variscan cycle in Iberia, especially in its northern and central domains (Galicia-Trás-os-Montes Zone, Central Iberian Zone and West Asturian-Leonese Zone) (Fig. 13.1). To the South of Iberia, especially at the border of Ossa Morena, adjoining the contact with the South Portuguese Zone, the mafic and intermediate rocks are much more abundant (Bard and Fabries 1970; Ribeiro et al. 1997; Moita et al. 2009; Pereira et al. 2013). Here, the magmatism displays peculiarities typical of an orogenic boundary setting (Jesus et al. 2016, and references therein) (Fig. 13.2). Despite of this particular feature, granites are also abundant in OMZ, in particular in its northern and central belts (LNEG 2010; IGME and LNEG 2014) (Fig. 13.2). In addition, quite diverse magmatic products, sometimes including rocks of granitic composition, were also produced all through the classically considered as Variscan extensional period, especially in Cambrian and Ordovician times.

The remarkable production of granites, exceeding the standards usually observed in other orogenic chains, is a recognised Variscan specificity that deserves particular attention. In a first approach, the huge heterogeneity of the inherited basement, mainly due to the location of Iberian Peninsula (IP) in a mobile zone at a global scale, should be considered (see Miyashiro et al. 1982). This crust was subjected to strong and multiphase reactivation throughout the geological time, as recorded by the geochronological data so far gathered for various populations of inherited zircons (Bea et al. 2006; Solá et al. 2007, 2008; Villaseca et al. 2011). Rocks generated during the Cadomian cycle still remain preserved in some extensive outcrops containing pelitic, quartz-pelitic and quartz-feldspatic metasediments, amphibolite and granitic/gneiss (occasionally including zircons retaining inherited ages of several events of the same cycle).

Various structural and lithological heterogeneities developed during the extensional periods of the Variscan cycle played also significant roles in subsequent evolving stages. These include listric fault zones, later reactivated as important shear zones (Iglesias and Choukroune 1980; Ribeiro et al. 1983; Pereira et al. 2013), and several types of magmatism (intense in this time-span) crossing the basement and the sedimentary pile meanwhile deposited. Magmatic rocks formed throughout this considerable time window, mafic to felsic in nature, were emplaced as lava flows, dykes, domes and plutons (Ribeiro 1986; Ribeiro et al. 1992; Solá et al. 2007; Ribeiro et al. 2010).

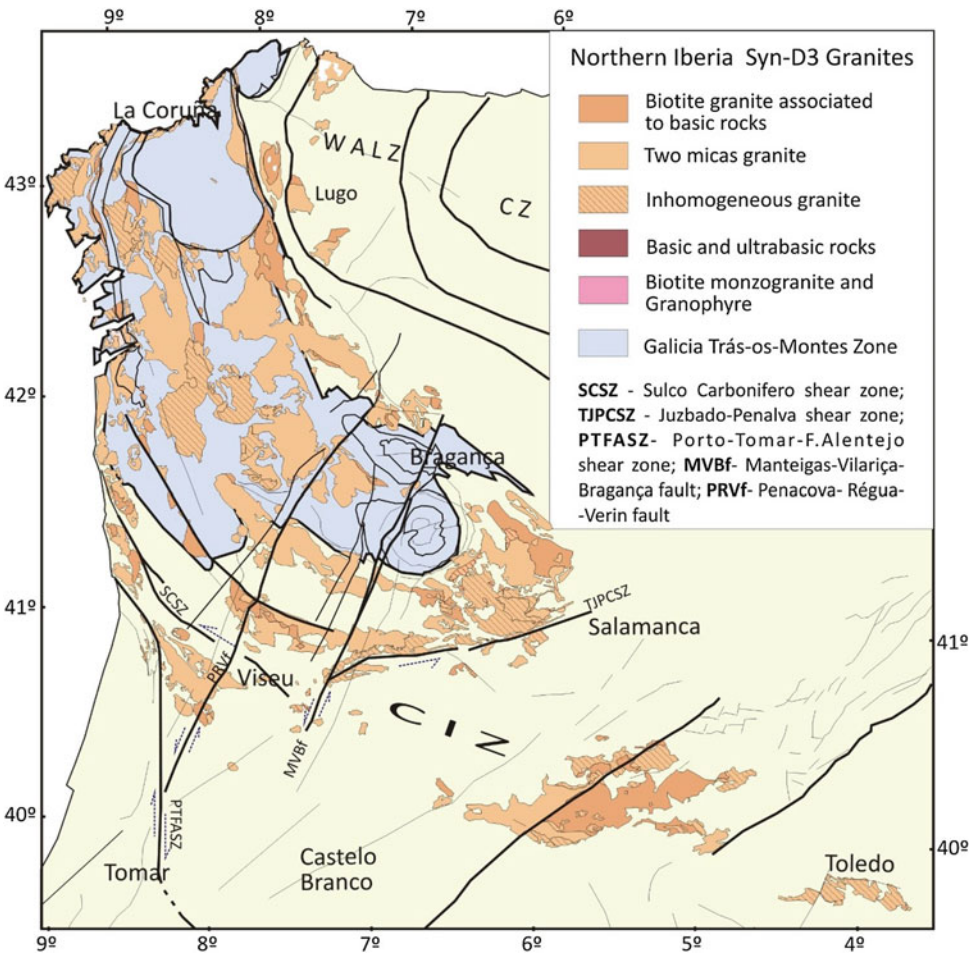

Fig. 13.1 Sketch map displaying the distribution of Syn-D3 granites of Northern part of Iberia (adapted from Mapa Geológico de España y Portugal, escala 1:1 000 000 IGME and LNEG 2014)

In addition, the Neoproterozoic-Cambrian flysch sequence (named Complexo Xisto Grauváquico), resulting of the Cadomian Chain erosion, cannot be considered "monotonous" and "homogeneous" as until now because several sequences are distinctly enriched in limestone (in the lower Douro) and/or calc-silicate rocks (in Trás-os-Montes and Beiras regions, some of them exploited for tungsten as scheelite) and comprise abundant (metamorphosed) mafic dykes (see Portugal Ferreira 1982). These heterogeneities were never suitably pondered in petrogenetic models, but they might make all the difference.

All these different lithologies, their geochemical and geophysical nature, and relative location, along with variations in time of the geothermal regime, led to a wide diversity of systems able to respond differently in what concerns strain accommodation and melt production, in general and at local scales. Considering as well the modern tendency of metamorphic petrology, that emphasizes the importance of water-fluxed melting in relation to the progressive dehydration of mineral phases during metamorphism, the importance of all these physical heterogeneities in time and space gain renewed meaning (Weinberg and Hasalová 2015).

The granites (sensu lato) are generally associated with regional tectono-thermal processes that favour the conditions of partial melting and magma production in the crust and mantle; their typology and composition are closely related to the respective sources, allowing the identification of the places and physical-chemical conditions under which their development and further evolution took place. In addition, granites generally contain either primary or inherited zircon crystals, which provide essential information for deciphering the history of previous regional processes, offering also the factual basis to sustain their correlation (e.g. Bea et al. 2007). Inherited ages found in Iberian zircons range from Archean times (3.2–3.3 Ga) to Visean times (312–286 Ma), passing from Paleo-Neoproterozoic, (e.g. 2228 ± 15, 1765, 698 Ma) and Cambrian-Ordovician (585, 506 and 494–488 Ma) (e.g. Solá et al. 2007, 2008). Such long and complex history evidenced by the Iberian zircons is at least a serious warning to those wishing to establish simple fractional crystallization correlations from liquids generated by partial melting of the mantle or the crust during the Variscan orogenic process.

Several types of granite, classified according to IUGS (Le Bas and Streckeisen 1991), were identified in the Iberic

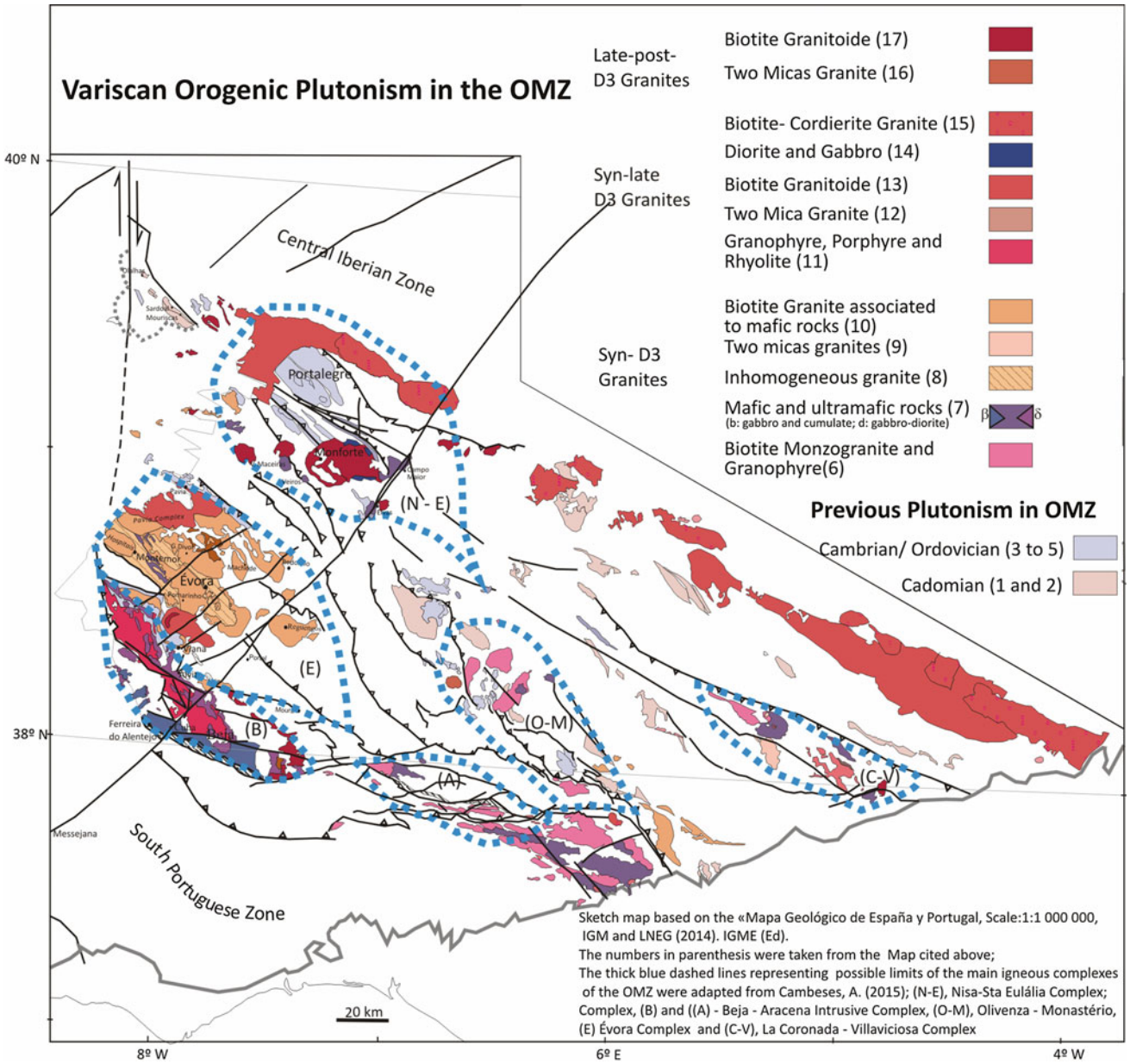

Fig. 13.2 Sketch map displaying the distribution of plutonic rocks of the OMZ. The thick blue dash (from Cambeses 2015) constitutes one of the possible delimitations of the various regional igneous complexes

Peninsula (LNEG 2010, IGME and LNEG 2014). Some of these granites have petrologic and geochemical attributes that suggest genetic links with mafic and intermediate rocks. However, the vast majority of granitoids outcropping in Iberia, and certainly almost all peraluminous, result from the heterogeneous development of the crustal melting process.

Comparing the Variscan magmatism of WALZ, GTMZ and North and Central CIZ from one side and the OMZ by the other), some contrasting features can be found (Figs. 13.1 and 13.2), namely the presence of numerous granitic plutons, mostly small-sized, intruded between ca. 335 and 290 Ma (e.g. Mendes 1967/68; Pinto 1983; Corretgé 1983; Dias et al. 2010) in the first group versus the abundance of mafic rocks (e.g. Bard and Fabries 1970) either associated with felsic intrusions or as isolated bodies (360–318 Ma) in the OMZ (Moita et al. 2011; Jesus et al. 2007; Pin et al. 2008), including also minor calc-alkaline volcanism,[1] interbedded in Carboniferous Sediments (e.g. Toca da Moura and Cabrela

[1]The word calc-alkaline appears in this text with two not exactly coincident meanings: (i) for the subalkaline magmatic evolving series characterized by low levels of iron in the intermediate terms; (ii) for the granitoids plotting in the respective field of the Frost et al. (2001) diagram.

volcanism (Santos et al. 1990). The OMZ plutonic rocks constitute several typologically diversified Complexes (Fig. 13.2) (e.g. Cambeses 2014).

Section 13.2 comprises five articles (13.2.2–13.2.6) that focus on the most significant (structural, petrological, geochemical and geochronological) events of orogenic magmatism in western Iberia. The first four articles focus on regional aspects of orogenic magmatism of ZOM. Its chaining allows a complementary view of the magmatic process correlated with the orogenesis in this Zone. The last article gives an overview of the same magmatism in the areas immediately to the north, especially ZCI and ZGTM.

13.2.2. Identify and describe the large magmatic sequences identified in the Beja Igneous Complex (BIC): the Sequence of Banded Gabbros (LGS) with gabbro and anortosites, the Cuba-Alvito Complex (CAC) including mainly massive gabbros for quartzodiorites and the Baleizão Porphyries Complex (BPC), involving a large variety of porphyritic quartz-feldspathic rocks.

The numerical modeling of the data shows the details of the very significante petrogenetic process that led to the installation of the current matrix of the BIC and the interpretation of its geodynamic meaning.

The results obtained allow concluding that the BIC is an example of the lytic expression of the synogenic magmatism that installed in the northern border of the contact between OMZ and SPZ during the Visean times.

13.2.3. Display the great variety of variscan plutonism of the Maciço de Évora (ZOM) at the north of the BIC described above. Such lithologies (from gabbro to leucogranites) were implaced during the Visean (360–318 Ma) associated to the extensive crustal migmatization. The isotopic data allowed to establish petrogenetic relationships with a source derived from the mantle messomatized with contamination of lower and upper crust in an orogenic environment. The migmatization of the continental crust of this region produced the spatially associated peraluminous granites.

13.2.4. Describes and discuss the late-Devonian basic to intermediate shoshonitic magmatism occurring in the NE of the OMZ. Its source is considered to be metasomatized supra-subduction mantle domain. These shoshonitic occurrences, considered in conjunction with Devonian tholeiitic and calc-alkaline subduction-related magmatism, allow the proposal of the operation of northward dipping subduction beneath the OMZ, reinforcing geodynamic models put forward by Ribeiro et al. (2007, 2010) for the closure of the Rheic Ocean, once existed at south of OMZ.

13.2.5. Focus on two of the large late batholiths (307–290 Ma) outcropping on each side of the ZOM/ZCI contact region. Both have very diverse typologies and chemistry (from acidic, most abundant, to basic). The petrological, geochemical and isotopic data suggest origins from equally diverse, be it in the mantle or in crust and subsequent evolutions through variable proportions of mixing of the magmatic liquids. The data show greater involvement of mafic and intermediary liquids and higher production of type I granites, for that outcropping in ZOM. This fact suggests that these batholiths will have crosscut different basement composition and nature in each of the two zones, ZCI and ZOM.

13.2.6. The vast area corresponding to the Center-West part of the Central-Iberian Zone (CIZ) exhibits intense orogenic variscan magmatism. This magmatism perfectly framed in the tectonic structure, imposes the joint appreciation of the two orogenic events. In contrast to that described for ZOM, granitoid masses occur in close association with migmatites and other metamorphic rocks, underlining the axes of D3 antiforms. During orogenic rebalancing, some posterior intrusions were installed. The time interval in which the intrusion of the regional granitic rocks occurred mainly between 321 Ma and 290 Ma

Several sources were identified mainly in the mid-low crust from the partial melting of several protoliths: metapelites, metagreywackes, immature sediments and granulites. The few vaugnerites found in some CIZ sites indicate the presence of liquids resulting from the partial melting of not depleted mantle under this zone of Iberia during the orogenic event.

These articles show that one (or two) intense tectonothermal event produced extensive partial melting of the midle-lower crust with the involvement of the underlying (metassomatized) mantle of Iberia between Uper Devonian to Visean times. Correspondent liquids and their hybridization producted the several lithotypes now outcropping. Shoshonitic compositions are also referred to in two periods distant in time. The Upper Devonian shoshonites (ZOM) are related to a source in the metassomatized supra-subduction mantle domain; The Visean vaugnerites (ZCI) origin is related with by mantle input followed by mantle crust interaction.

A better detail these occurrences of shoshonitic rocks could be the key to understanding if underplating of basaltic magmas at the lower crust base gave rise to a durable deep-crustal hot-zone responsable for a single, long-lived magmatic event accountable for the progressive geochemical and lithological diversification due to the involvement of distinct crustal components.

13.2.2 Synorogenic Variscan Magmatism at the Ossa-Morena Zone Southern Border; the Beja Igneous Complex

A. Mateus, A. Jesus

The Beja Igneous Complex (BIC) spreads for ≈100 km, exposing different and relatively continuous internal sections

all over a quite large area (Fig. 13.2). According to field, petrographic, geochemical (including isotopic) and geochronological criteria, three main units are usually recognized (Silva et al. 1970; Andrade 1983; Santos et al. 1990; Pin et al. 1999, 2008; Jesus 2010; Jesus et al. 2007, 2014, 2016): (i) the Layered Gabbroic Sequence (LGS), comprising well-banded series chiefly composed of gabbros and anorthosites; (ii) the Cuba-Alvito Complex (CAC), including mostly massive gabbros, diorites and quartz-diorites; and (iii) the Baleizão Porphyry Complex (BPC), involving a wide array of compositionally evolved quartz-feldspar rocks with (micro)porphyric texture that are still poorly characterized. The available ID-TIMS and SHRIMP U–Pb zircon dating indicates a rather homogenous crystallization/emplacement age of *ca.* 350 Ma for rocks forming the early LGS and diorites included in CAC (Pin et al. 1999, 2008). The evolved late-stage hydrous derivatives crisscrossing different groups and series of LGS, such as amphibole-albite pegmatites and felsic dykes, show overlapping SHRIMP U-Pb zircon (Jesus et al. 2007; Pin et al. 2008) and $^{40}Ar/^{39}Ar$ amphibole (Ruffet 1990; Dallmmeyer et al. 1993) ages, suggesting that cooling and the admixture of crustal and magmatic fluids took place at 340 ± 5 Ma, coeval with regional crustal uplift (Jesus et al. 2007; Ribeiro et al. 2010). Compiled evidence for the Évora-Beja-Aracena Domain allow to correlate the following stages of BIC development with the two main magmatic events occurred in the time-window from *ca.* 335–330 Ma to *ca*. 320 Ma and clustering at *ca.* 300 Ma, respectively (Jesus 2010).

The Messejana-Plasencia strike-slip fault zone separates the LGS into two major segments: to the west, from W Torrão to Beringel, grouping four sectors that, from NW to SE, were labelled as Soberanas (SB I and II), Odivelas (ODV I and II), Ventoso (ODV III) and Ferreira-Beringel, the Border Group (BRG I and II); and to the east, from Beringel to Serpa. In general, primary features displayed by rock suites forming these two segments are well preserved from post-crystallization metamorphic and deformation events. Therefore, variations in layering (type, orientation and associated mineral lineation) and other structural features should reflect the prevailing stress field at the time each series was emplaced/consolidated. Early structural features are subparallel to layering (from NW–SE to WNW–ESE, dipping 30° ± 6° to the SW) and develop C/S fabrics with top-to-the-N shear (Jesus et al. 2016); these structural features are compatible with those typifying D2 in Allochthon Complexes and D2a in the OMZ Autochthon (Ribeiro et al. 2010). Subsequent deformation is accommodated in ductile shear zones, mainly striking WNW–ESE and dipping steeply (N65°) to SW. Kinematical criteria, when preserved, indicate a dominant left-lateral component of movement, coupled with thrusting to NNE; these early shear zones are commonly reactivated under (semi-) brittle conditions, the respective movement planes being subparallel but dipping to the NNE (Mateus et al. 1999).

At the LGS eastern segment, magmatic layering is only observed at small scales and amphibole-rich rocks are quite abundant (Pin et al. 2008). The much wider LGS western segment comprises six Series of layered gabbroic rocks representing successive magma replenishments (Jesus et al. 2005a, b, 2006a, b, 2014, 2016; Pin et al. 2008; Jesus 2010). The six gabbroic Series include various groups that comprise dominant (leuco) gabbros/anorthosites along with melanocratic rocks (troctolite, olivine melagabbro or olivine norite) and scarce ultramafics [wehrlite (SB I and ODV I Lower Group), clinopyroxenite (BRG I Lower Group) and centimetre-rhythms of olivine websterite or clinopyroxenite (BRG II Series)]. These series come along with an assortment of rocks forming the Border Group which include cognate xenoliths of variably metasomatized gabbroic rocks and of primitive troctolites. Mesocratic to felsic rock suites found in close spatial and temporal association to LGS were categorized into: (i) marginal diorites and associated amphibolitic gabbros; (ii) the ATT suite, developing a large-scale dyke-swarm (often controlled by NW-SE (semi-) ductile shear zones) that includes the Border Group, being mostly composed of deformed anorthosites, tonalites and (quartz-rich) trondhjemites; (iii) pegmatoid dykes; and (iv) felsic (quartz-feldspar) dykes and sills.

Multi-element whole-rock geochemical data obtained for LGS rocks and their systematic mineral chemistry variation, complemented by equilibrium crystallization modelling with COMAGMAT (Jesus et al. 2014, 2016) show that: (i) SB I troctolites and their equivalents within Border Group developed from parental magmas alike to high-alumina, low-K, primitive (#Mg0.63) basalts; (ii) SB II Series represents a chilled margin made of fine-grained gabbronorites derived from SB I parental magmas after some differentiation (#Mg0.59); (iii) ODV I Series results from fractional crystallization of SB II residual magma; and (iv) the SB I–SB II—ODV I sequence covers the full compositional range so far documented within LGS, being followed by the monotonous ODV II, III—BRG I, II gabbroic Series. The large range of Nd-Sr isotopic compositions available for LGS rocks provide additional firm evidence for lower and upper crustal contamination of magmas involved in the generation of LGS and CAC rocks (Pin et al. 1999, 2008; Jesus 2010; Jesus et al. 2014, 2016).

Further numerical modelling (Jesus et al. 2014, 2016) strongly suggest that the SB I—SB II—ODV I sequence should have formed during a first prolonged fractionation event occurred mostly at the final stage of a mid-crustal magma emplacement at *ca*. 5–6 kbar. Therefore, the formation of primitive end-members for post-ODV I Series implies significant crystallization at depth, possibly within deep-seated transient chambers from which recurrent

extractions of magma batches took place, feeding the magmatic chamber(s) sited at mid-crustal levels. This inference is consistent with barometric estimates performed for the ODV II, III—BRG I, II sequence, peaking at *ca*. 9 kbar within BRG II. Therefore, the later emplaced magmas experienced longer residence time at lower crustal levels, followed by a narrower period of low-pressure re-equilibrium. The limited degree of fractionation shown by post-ODV I Series (Fo78–66) suggests that magma upwelling from deep chambers became more frequent; so, magma batches should arrive at the mid-crustal chamber(s) with composition approximately equivalent to the primitive pole for each Series (Fo78). Subsequent mixing of variable proportions of resident magma and LP-fractionation melts allowed reaching the most evolved compositions observed within each Series. Magma extraction from depth to mid-crustal magma chamber(s) was likely facilitated by concurrent tectonic activity and fractionation of the melts, thus overcoming the lack of density contrasts with surrounding lower crustal rocks.

The geobarometric constrains indicate an intricate evolution for LGS rocks, at least partly shared with CAC diorite suites, spanning through a significant portion of the crust, from *ca*. 27–12 km depth. Since the maximum barometric estimates for LGS (*ca*. 9 kbar) correspond to preserved prymocrysts affected by some degree of subsolidus re-equilibrium, it is conceivable that the primary locus of magma emplacement was at Moho. This means that a magma underplating scenario, with staling and ponding of LGS magmas at deep crustal levels, should be favoured, which is consistent with the rheological and mechanical decoupling that characterizes OMZ (Simancas et al. 2003; Pous et al. 2004; Almeida et al. 2005; Vieira da Silva et al. 2007; Muñoz et al. 2008). Nonetheless, a significant part of the BIC evolving stages should involve magma chamber(s) sited at a mid-crustal levels, i.e. at depths of 12–15 km if the minimum barometric estimates of 4–5 kbar are considered, being as well in agreement with the regional amphibolite facies metamorphism affecting the OMZ autochthonous rocks at *ca*. 340–350 Ma; emplacement and cooling temperatures well above the regional thermal peak explains the lack of regional metamorphic imprint in LGS and CAC rocks. Further evolving stages, traced by the Border Group and ODV I amphibolite-gabbros adjoining diorites, record distinct tectono-thermal paths related to local (tectono-) magmatic/hydrothermal induced anomalies.

Following the deep crustal hot zone (DCHZ) concept (Annen et al. 2006), the origin of diorite-prevalent and higher crustal-contaminated suites may be envisaged as products of a dynamic system triggered by the underplating of LGS basaltic magmas at the OMZ lower crust; the BIC-DCHZ would thus include LGS deep magmatic chamber(s), as well as the surrounding and overlying lower to mid-crustal domains (Jesus et al. 2016). The isotopic homogeneity of the melts produced at BIC-DCHZ prior to the emplacement of the ATT suite reflects mainly the composition of the basaltic underplated melt, with minor lower crustal assimilation followed by mild upper crustal contamination at final stages of emplacement. Consequently, the considerable volumetric expression of the ATT suite can interpreted as a result of an increasing productivity and geochemical/isotopic diversification of BIC-DCHZ through time. Actually, the border facies anorthosites and ATT suite dykes are increasingly felsic in nature (in comparison to previous events) and record decreasing contributions from LGS residual melt and partial melts from mid-crustal rocks (Jesus et al. 2016).

13.2.3 The Évora Massif: The Variscan Plutonism at the Western—Border of the Ossa Morena Zone

P. Moita, J. F. Santos

As is common throughout the OMZ, the Évora Massif is characterized by a significant compositional diversity of intrusive igneous rocks. Mainly along an area characterized by extensive migmatization (high-grade metamorphic unit, Pereira et al. 2009), there are numerous plutonic bodies (Fig. 13.2) ranging from gabbros to leucogranites, with a very extensive cartographic representation of quartz-diorites, tonalites and granodiorites. The geochronological data (Gomes 2000; Rosas 2003; Moita et al. 2005a; Antunes 2006; Chichorro 2006; Silva and Pinto 2006) show that the intrusive processes took place mostly in the Carboniferous (360–318 Ma), and especially during Visean times.

Most of the intrusions show structures parallel to the main Variscan direction displayed by the regional metamorphic country rocks. Both the cartographic elongated shape of the plutons and the mesoscopic anisotropy (observed in some granitoids) conferred by the alignment of mafic minerals (Carvalhosa and Zbyszewski 1994) suggest that they were conditioned by the most conspicuous tectonic deformation phase, as can be seen in the intrusions of Évora-São Manços, Divor, Hospitais, São Miguel de Machede and Redondo, which are essentially of quartz dioritic/tonalitic composition, occasionally associated with granodiorites (e.g. Pomarinho, Moita et al. 2011) and gabbro-diorites. Differently, the intrusion of Reguengos de Monsaraz (east of Évora Massif), predominantly tonalitic to granodioritic, as well as those of Pavia and Pedrógão-Pias (north of Évora Massif), both granitic, would represent late-tectonic magmatic events (Lima et al. 2012) since they do not present, at any studied scale, structures concordant with the main Variscan orientation. However, it should be noted that it cannot be ruled

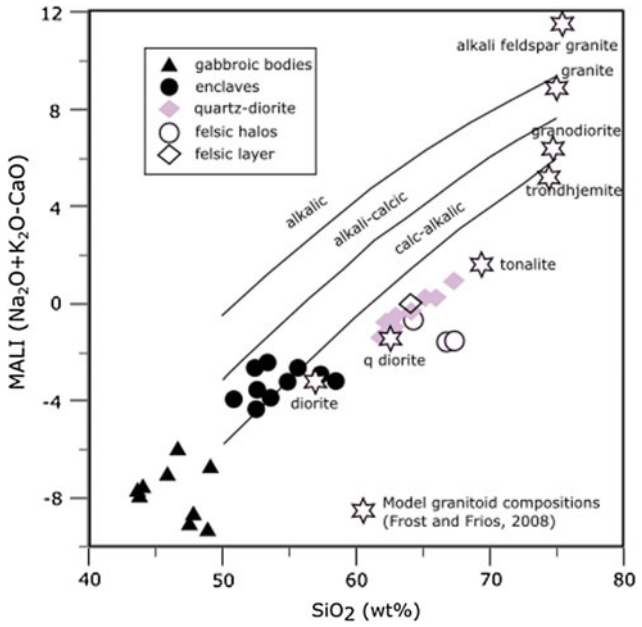

Fig. 13.3 Major elements geochemical classification from Frost et al. (2001) applied to Hospitais intrusion lithologies and gabbroic bodies from Évora Massif (Moita et al. 2015)

out that some intrusions devoid of structures and textures with preferred orientation may, in fact, be approximately contemporaneous with those that are obviously syn-tectonic. An example is given by U–Pb magmatic zircon ages between 337 and 339 Ma obtained in samples of the Reguengos de Monsaraz intrusion (Antunes et al. 2011).

One of the most relevant plutons that crop out in the Évora Massif, near the town of Montemor-o-Novo, is the intrusion of Hospitais, whose main structural features agree with a syn-tectonic emplacement, which has been recently dated at 337 Ma (Moita et al. 2015). It corresponds essentially to a quartz dioritic body, enclosing mafic microgranular enclaves. The mineralogical composition of the quartz diorite is dominated by the presence of plagioclase (usually andesine), quartz, hornblende, cummingtonite-grunerite and biotite, whereas the most common accessory phases are apatite, oxides, zircon and allanite. The elemental geochemistry indicates that the various gabbroic bodies of the neighbouring areas and the metaluminous quartz diorite of the Hospitais intrusion may belong to a magmatic suite related by fractional crystallization (Moita et al. 2005b; Moita 2008; Moita et al. 2015). These lithologies display a geochemical calc-alkaline signature (Fig. 13.3), as typical of magmas generated in a continental magmatic arc setting. The similarity between isotopic ratios of some gabbros and of the quartz-diorite [gabbros: $\varepsilon Nd_{337} = -1.62$ and -1.98; $(^{87}Sr/^{86}Sr)_{337} = 0.705431$ and 0.705529; quartz diorite: $\varepsilon Nd_{337} = -3.22$ to -1.87; $(^{87}Sr/^{86}Sr)_{337} = 0.706147$–$0.706491$; Moita et al. 2015] suggests the possible existence of genetic bonds, and the former may correspond to the parental magma that evolved to quartz-dioritic compositions. Isotopic geochemistry data for these two occurrences are similarly consistent with the continental magmatic arc environment, in which the most primitive magmas would have as source peridotites from a mantle wedge modified by ascending fluids and/or melts originated in a subduction zone (Moita 2008).

Nevertheless, Moita et al. (2015) also defend the hypothesis that the genesis of the intrusion of the Hospitals results from a mechanism of mixing (Fig. 13.4) between a mantle-derived basic magma, with a Sr–Nd isotopic composition ($\varepsilon Nd_{337} = 3.63$; $[^{87}Sr/^{86}Sr]_{337} = 0.703569$) represented by an olivine gabbro from the surroundings of Évora, and a felsic component derived from a meta-igneous source that could be represented by the Lower Cambrian Alcáçovas orthognaisse.

For the genesis of the slightly peraluminous to metaluminous granitoids (tonalite, granodiorite and porphyritic granite) that occur near Évora (at Alto de São Bento), elemental geochemistry data are compatible with a mechanism of differentiation by fractional crystallization (Moita 2008; Moita et al. 2009). Although the modes of occurrence are very different, the various lithologies show calc-alkaline signature and exhibit trace element patterns very similar to each other. They also show resemblances with the patterns displayed by the lithologies of the Hospitais intrusions and gabbroic bodies. However, the isotopic signatures of the Alto de São Bento granodiorite [$\varepsilon Nd_{337} = -5.26$; $(^{87}Sr/^{86}Sr)_{337} = 0.705940$] and tonalite [$\varepsilon Nd_{337} = -4.71$; $(^{87}Sr/^{86}Sr)_{337} = 0.706350$], require a model that combines fractional crystallization and magma mixing (Moita 2008; Moita et al. 2009) involving a crustal felsic component (in proportions of 40% and 30%, respectively for the granodiorite and the tonalite) and melts of mantle origin. When considering the role of hybridization, the crustal pole that best fits the mixing curve drawn by the intrusive rocks of the Alto de São Bento area seem to correspond to diatexites derived from the Ediacaran metasediments of the Série Negra (Moita et al. 2009).

Similarly, Casquet and Galindo (2004), Antunes (2006) and Silva and Pinto (2006) invoke mixing mechanisms to explain the isotopic composition of metaluminous to weakly peraluminous granitoids along the ZOM. The isotopic data (Sr and Nd) obtained by Antunes (2006) for several intrusive bodies from Évora Massif (tonalites and granodiorites from the Redondo intrusion, Graça do Divor) show a certain overlap with those of the intrusive rocks mentioned above. However, the results presented by Antunes (2006) suggested the possibility of participation of a felsic component with an infracrustal origin (with strongly negative values of εNd).

Thus, considering the whole set of evidence, it cannot be ruled out that there may have been contributions from

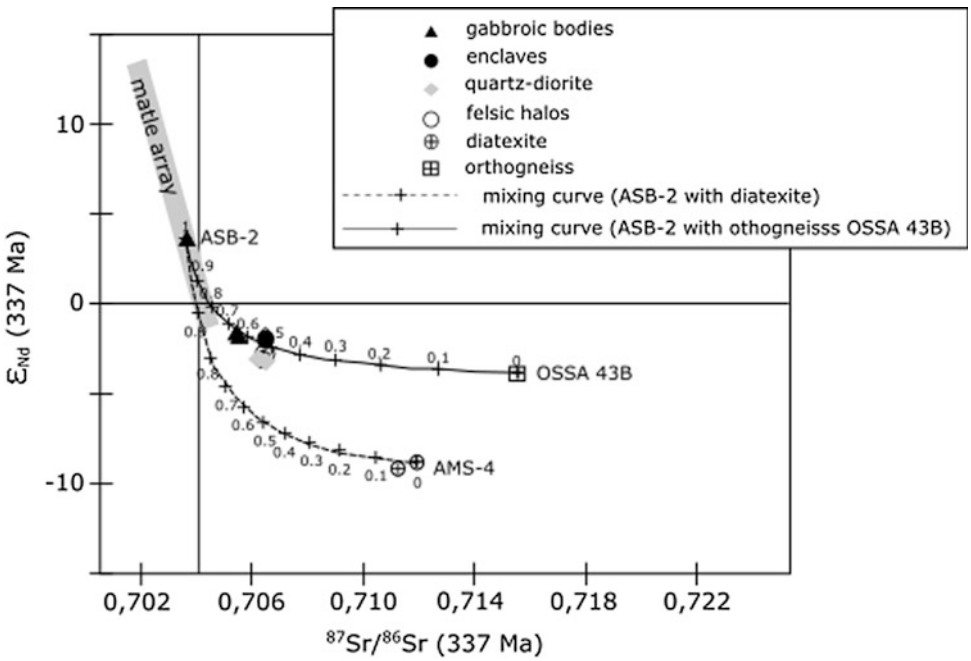

Fig. 13.4 The $(^{87}Sr/^{86}Sr)_I$ ratio versus εNd_i diagram for gabbros, qtz–diorites and enclaves from Hospitais intrusion (Moita et al. 2015). Isotope compositions were calculated for 337 Ma. Mixing curve model from Faure (1986). Crustal end members are from Cordani et al. (2006) and Moita et al. (2009)

different types of crustal components (metasedimentary source vs. meta-igneous source; shallow crust vs. deep crust), whose importance has varied according to local conditions.

When the metaluminous to weakly peraluminous granitoids from the Montemor-o-Novo-Évora area are compared with the metaluminous association defined by Casquet and Galindo (2004) in the Spanish part of the OMZ, in terms of Sr-Nd compositions there is again overlapping, but it is also noteworthy that some of the signatures obtained in Spain are clearly more enriched in radiogenic Sr, which suggests a larger supracrustal contribution in several metaluminous granitoids of the Spanish sector than in their Évora Massif analogues.

In addition to the aforementioned lithologies, in the Alto de São Bento (Évora) it was also recorded the occurrence of a peraluminous two-mica leucogranite, thus revealing to have an origin very different from the other lithologies outcropping in the same area. Its high peraluminous (A/CNK = 1.18; 1.19) and high radiogenic Sr isotopic signatures suggest that it might have been generated by anatexis of Ediacaran or Cambrian metassediments (Moita et al. 2009). The low levels of incompatible elements and a generally horizontal normalized REE pattern with a significant negative anomaly of Eu may be related either to low degree of partial melting in the presence of refractory plagioclase and accessory phases with high partition coefficients for hygromagmatophile trace elements, or by extreme differentiation of the anatectic melts. Considering the age of 337 Ma (Pereira et al. 2015b) for the porphyritic granite that outcrops at Alto de São Bento and was installed over the leucogranite (Moita et al. 2009), anatexis should not be chronologically far displaced from the calc-alkaline magmatism in the region.

Therefore, and accordingly with Moita et al. (2015) the Évora Massif is a repository of a significant diversity of magmatic processes during the Visean: mafic magmas coming from subduction enriched mantle were emplaced, underwent differentiation and gave origin to calc-alkaline suites. Concomitantly (and probably induced in part by the heating caused by the ascent of mafic magmas), continental crustal rocks (metasedimentary and orthogneiss) locally attained conditions for partial melting to occur. These anatectic melts, although in part directly producing peraluminous granites, interacted significantly with the mafic magmas and their differentiation products (Moita et al. 2015). This interaction between mantle-derived magmas and anatectic melts is conspicuously testified by layered granitoids recording mingling/mixing processes, as can be observed at Almansor (Moita et al. 2009). Mixing between two types of contrasting melts may also have been very effective and responsible for the several granitoid intrusions (e.g. Hospitais quartz–diorite, and Alto de São Bento tonalite, granodiorite and porphyritic granite) of Évora Massif.

13.2.4 Late-Devonian Shoshonitic Magmatism at the Ossa-Morena Zone

J. A. Lains, P. Moita, J. C. Lopes, J. Mata

Two small intrusive bodies (Ve: Veiros, 5 km^2; VM: Vale de Maceira, 22 km^2) occur at the NE of the Ossa Morena

Zone (OMZ) close to the contact between the Elvas-Alter do Chão and Estremoz-Barrancos sectors (Oliveira et al. 1991; LNEG 2010) (Fig. 13.2). They intrude Cambrian to Silurian meta-sediments, producing narrow metamorphic aureoles, and being crossed by tardi-Variscan (?) NE-SW dykes (Gonçalves et al. 1975). Based on previous petrological, geochemical and geochronological data (Pinto Coelho et al. 1974; Canilho 1977; Costa et al. 1990; Moita et al. 2005a), as well as on new whole-rock and mineral-chemistry data (see Lains 2015), we will characterize the chemical affinities of these massifs and discuss their implications to the interpretation of the Variscan orogeny in the Iberia. For comparative purposes we also address the Campo Maior massif (CM), a neighbouring (≈ 40 km to ENE) Late-Devonian calc-alkaline igneous intrusion located inside Faixa Blastomilonítica (Lopes 2004; Lopes et al. 2005).

The studied plutons are granular (Ve: often fine-grained; VM: often medium-grained) presenting a compositional range from gabbros to syenites, with predominance of monzonites and monzogabros. They are characterized by mineral assemblages composed by different proportions of olivine ($Fo_{56–77}$), augite and hypersthene, plagioclase ($An_{40–85}$; commonly labradorite), alkali feldspar ($Or_{70–90}$), phlogopite, and in some rocks brown hornblende (kaersutite and pargasite) or quartz. As accessory minerals Fe–Ti oxides, apatite, sphene and zircon has been described (e.g. Canilho 1977). Hydrous minerals have distinctly high Ti and K contents (phlogopite: $Ti_{0.42–0.94}$ and $K_{1.78–2.20}$ apfu; brown amphibole: $Ti_{0.35–0.56}$ and $K_{0.24–0.34}$; apfu).

The Campo Maior massif is readily distinguished by the absence of olivine and by the lower K and Ti contents in the hydrous minerals (phlogopite: $Ti_{0.36–0.64}$ and $K_{1.61–1.93}$ apfu; brown amphibole: $Ti_{0.25–0.45}$ and $K_{0.15–0.32}$; apfu).

Ve and VM massifs present a K-rich signature (Fig. 13.5a, b) with typical attributes of a shoshonite association as defined by Morrison (1980): (1) high total alkali content, leading the rocks of these massifs to plot along the compositional divider between alkaline and sub-alkaline fields (Irvine and Baragar 1971), i.e. indicating a higher total alkali content than the typical calc-alkaline trends; (2) high K_2O/Na_2O ratios (Fig. 13.5a), with most of the VE samples having $K_2O/Na_2O > 2$ (e.g. Costa et al. 1990), emphasizing their ultrapotassic signature according the criteria of Foley et al. (1987); (3) high contents of LILE (e.g. Ba: 127–1705 ppm) and high LILE/HFSE ratios (Fig. 13.5b) (4) near-saturated modal and normative compositions.

In contrast, CM has the typical geochemical attributes of a calc-alkaline series: (1) lower total alkali content (sub-alkaline on TAS diagram); (2) moderate LILE enrichment (e.g. Ba: 49.1–639.1 ppm) (3) low iron enrichment. εNd_i values are highly variable ranging from −6.0 to +4.8 reflecting the variability of his mantle source and/or variable degree of crustal assimilation processes (Lopes et al. 2005)

Gabbroic samples of Vale de Maceira igneous body were dated by Moita et al. (2005a) using Rb–Sr and K–Ar methods. The date of 362 ± 13 Ma was interpreted as representing the mean age of the cooling below 500 °C, i.e. below feldspar and amphibole closure temperatures in Rb–Sr and K–Ar isotopic systems, respectively. These authors also calculated an internal isochron (whole rock—biotite) obtaining an age of 315 ± 3 Ma. This was interpreted as representing the later reopening of the biotite Rb–Sr isotopic

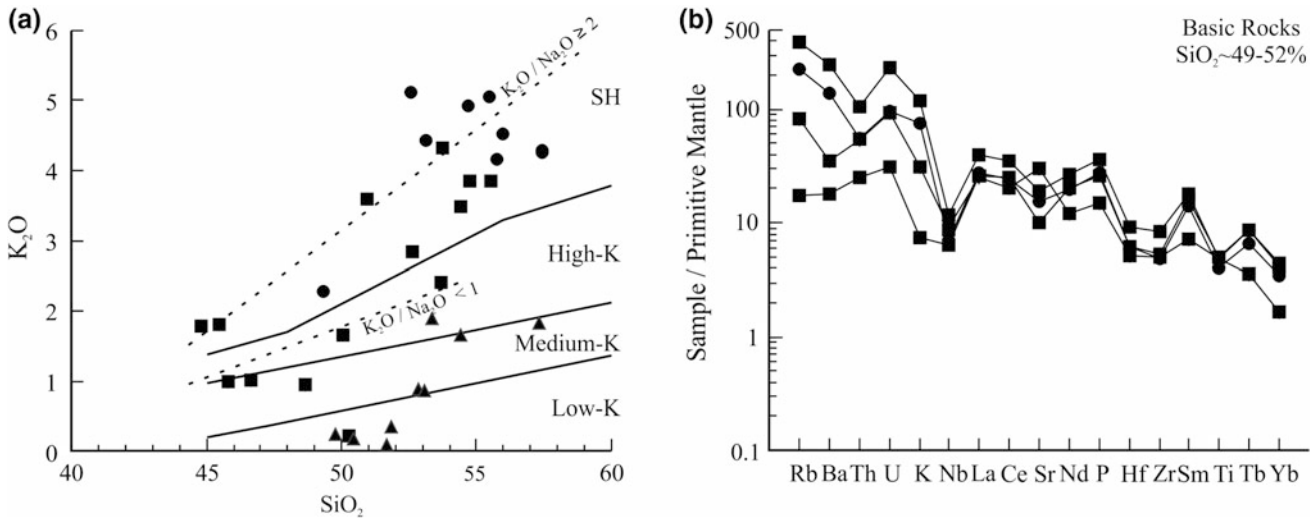

Fig. 13.5 **a** K_2O versus SiO_2 diagram. Boundary lines from Rickwood (1989) (upper limits). Note that all CM samples have $K_2O/Na_2O < 1$. **b** Trace elements normalized to mantle compositions (Sun and McDonough 1989) for selected basic rocks substituir por Ve: circles; VM: squares; CM: triangles

system above 300 °C and below 500 °C associated to a metamorphic event, which subjected the region to conditions transitional between those of the greenschist and amphibolite facies.

Sm–Nd isotopic data on selected samples indicate that the Campo Maior Massif was emplaced at 376 ± 22 Ma (Lopes et al. 2005).

It has been widely accepted that shoshonitic associations are derived from enriched metasomatized sources and generated during the late stages of subduction processes or at collisional to post-collisional times (Morrison 1980; Wenzel et al. 1997; Nomade et al. 2004; Leslie et al. 2009; Peccerillo and Frezzotti 2015). In this perspective, the close age and spatial association of the shoshonitic rocks of Ve and VM with the calc-alkaline massif of Campo Maior is a clear evidence for the existence of a subduction slab beneath the northwestern part of the OMZ during the Late-Devonian. Subduction-related magmatism has been reported further South in the OMZ, where tholeiitic to calc-alkaline rocks were generated during the Lower to Middle Devonian times (see Santos et al. 1990; Silva et al. 2011). The presence of these older tholeiite to calc-alkaline magmatism at SW of the Ossa-Morena (Lower Devonian tholeiite volcanic rocks of Mt. Covas Ruivas, Silva et al. 2011; Middle Devonian tholeiite and calc-alkaline volcanic rocks of Mt. Cortes, Santos et al. 1990), and younger calc-alkaline to shoshonite magmatism at NE of Ossa-Morena (Upper Devonian intrusions of CM, Ve and VM), indicates a northwards dipping subduction zone beneath the Ossa-Morena Zone since the Lower Devonian.

Considering the geodynamic models for the evolution of the Southwestern Iberia Variscides (e.g. Ribeiro et al. 2007, 2010 and references therein) the existence of two Paleozoic subduction zones operating South of the OMZ can be envisaged. One related with the subduction of the Rheic Ocean and another linked to the closing of the back-arc basin now represented by the Beja-Acebuches Ophiolitic Complex. For these basins Ribeiro et al. (2007) consider a simultaneous final closure, which means that two subduction zones may have operated partially in simultaneous.

At the southern domains of the OMZ, the only relicts of rocks affected by metamorphism under low geothermal gradient conditions (blueschists and eclogites) were found in the IOMOZOS ophiolite sequence, which has been considered a remnant of the Rheic ocean (e.g. Pedro et al. 2010; Ribeiro et al. 2010). Considering this, the presumable small dimension and ephemeral character of the Beja-Acebuches basin (Ribeiro et al. 2007) and that the closure of this basin must have occurred between ca. 370 and 350 Ma (Ribeiro et al. 2007), the N-dipping subduction-related magmatism occurred in the OMZ, between circa 395 Ma and 360 Ma, is here assigned to the Rheic subduction.

Sm/Nd and $^{40}Ar/^{39}Ar$ dating placed the generation of eclogites imbricated into the IOMOZOS at 371 ± 17 Ma, which was followed shortly after by exhumation (Moita et al. 2005c). The age of Vale de Maceira massif (362 ± 13 Ma; Moita et al. 2005a; see also above) suggests that the shoshonitic magmatism may have occurred closely after the subduction cessation. This would explain the composition highly enriched in incompatible elements of the Vale de Maceira and, principally, Veiros rocks (Lains 2015). Indeed such enrichment suggests the magmatic generation by adicionar very low degrees of partial melting in absence of water, while the high LILE/HFSE ratios (e.g. Ba/Nb: 27–292) suggest the genesis on a mantle domain previously metasomatized by H_2O-rich fluids issued from a dehydrating subducting slab.

13.2.5 The Variscan Plutonism at the Northwester Border of Ossa Morena Zone: The Nisa-Albuquerque and Santa Eulália Massifs

A. R. Solá, L. González Menéndez, M. L. Ribeiro, A. M. R. Neiva

The contact of OMZ with CIZ to the north is marked by the Coimbra-Córdoba Shear zone or Badajoz-Córdoba Shear zone (Burg et al. 1981; Ábalos et al. 1991, respectively), also called the Central Unit (Azor 2004). To the north of this major shear zone the Nisa-Albuquerque-Los Pedroches batholiths forms part of an important alignment of granitoids, which also has been used as a criterion for separating OMZ and CIZ (e.g. Julivert et al. 1974).

It is important to underline, that in this particular region (northern OMZ, including the transition to CIZ of OMZ) the Variscan intrusions crosscuts the former pre-Variscan ones, that forms parallel NW-SE elongated and elliptical-shape intrusions bounded by transcurrent faults (e.g. Pereira and Silva 2001). Also, late-orogenic bodies are larger and predominant over syn-orogenic small intrusions, in opposition to Évora massif and Beja–Aracena intrusive complex (Fig. 13.2).

Overall, like in all OMZ the geochemical composition can be included in two series: metaluminous (I-type) "calc-alkaline" granitoids, gabbros and diorites, and peraluminous (S-type).

The syn-orogenic plutonism of the northern OMZ is represented by several intrusive bodies with compositions ranging from gabbros to monzogranites described in detail in the previous point 13.2.4.

The late-orogenic granitoids are characterized by a smaller abundance of basic lithologies and a predominance of acid rock types. These granitoids range from metaluminous (I-type) to peraluminous (S-type) and can be exemplified by the two well studied granitoid batholiths that are of

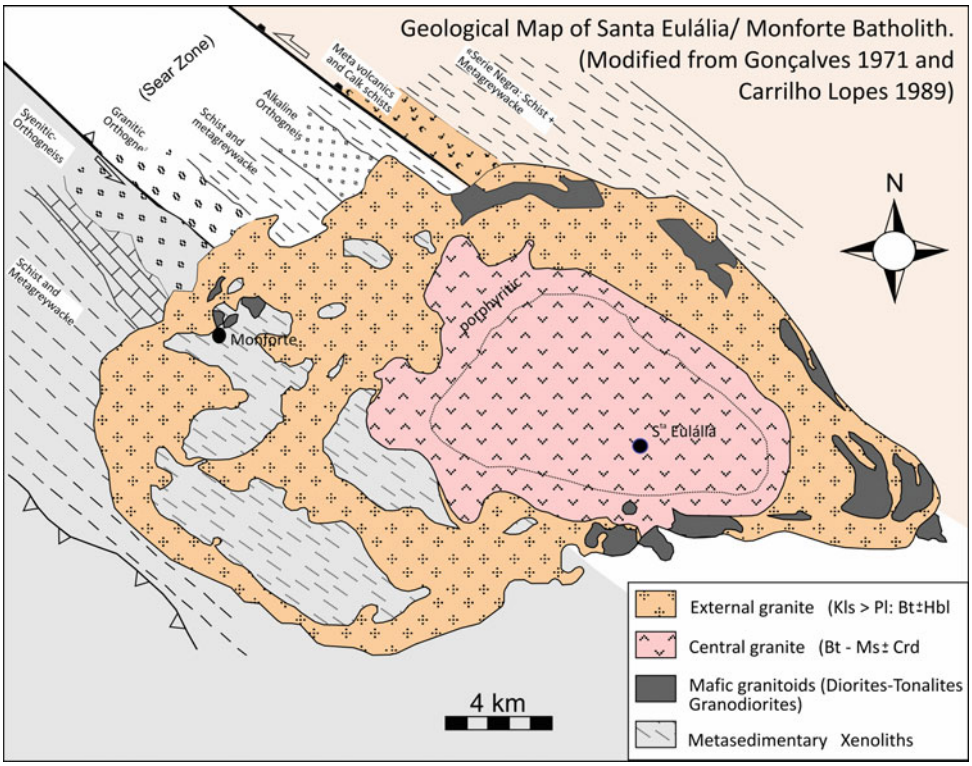

Fig. 13.6 Geologic map of Santa Eulalia-Monforte plutonic complex

similar age and located close to each other but separated by the Coimbra-Cordoba Shear Zone: Nisa-Alburquerque batholith, in the contact with the CIZ, and the Santa Eulalia-Monforte complex in the northern OMZ (Fig. 13.6).

S.ta Eulalia-Monforte Plutonic Complex

The Santa Eulália pluton has been dated by Pinto (1984) who obtained an Rb–Sr isochron age of 290 ± 5 Ma. Recently, Lopes et al. (2016) obtained 306–301 Ma (U-Pb, SHRIMP). The pluton is formed of granitoids, mainly of I-type nature, that can be grouped into two units: (i) the external granite, formed by granites showing equigranular texture, dominant K-feldspar and biotite as the main mafic mineral, (ii) the central granite, has equigranular texture and a biotite ± muscovite association. Several gabbro-diorite and granodiorite tonalite igneous bodies also occur. The external granite shows a ring-type outcrop pattern, and includes most of the gabbro-diorite and tonalite-granodiorite rocks as well as large metasedimentary country rocks. The central granite forms a circular outcrop and is totally surrounded by the external granite (Fig. 13.6).

The mafic rocks of this pluton, $SiO_2 \approx 47$–68 wt%, have variable Mg# (32–61) and ASI values (0.61–1.09), and most have negative anomalies of Ba, Nb, Sr and Ti relative to primitive mantle values. Despite these similar features some variation trends Zr versus SiO_2 and element ratios Nb/La indicate a different petrogenesis for the gabbro-diorites and the tonalite-granodiorites. Regarding the granites, the external ones have low ASI values (0.99–1.05) and low contents in CaO (0.48–1.43 wt%), P_2O_5 (0.02–0.09 wt%) and Sr (2–90 ppm). On the other hand, the central granites have higher ASI values (1–1.18) and higher contents in CaO (1.6–2.15 wt%), P_2O_5 (0.13–0.23 wt%) and Sr (170–220 ppm) (Fig. 13.7).

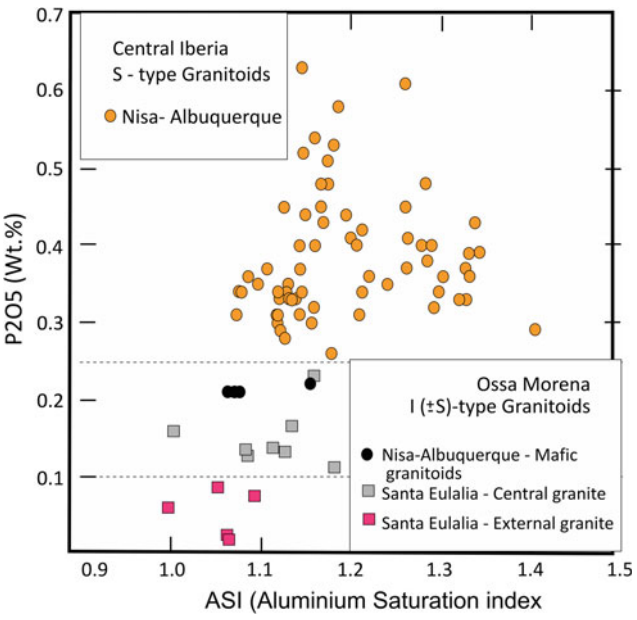

Fig. 13.7 P_2O_5 versus ASI for the Nisa- Alberquerque and Santa Eulália rocks (from González Menéndez and Solá 2011)

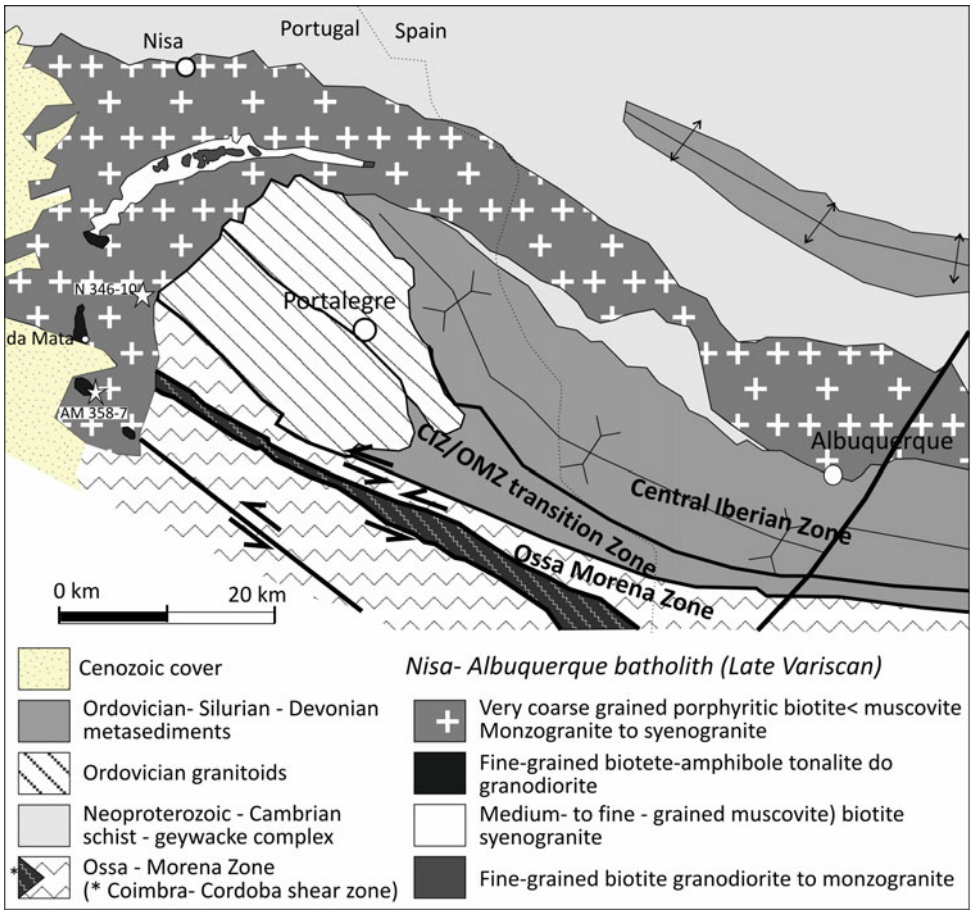

Fig. 13.8 Simplified geological map of the Nisa-Albuquerque batholith (Solá et al. 2009 and references therein)

The data available suggest that all of the igneous units forming this batholith are coeval although petrogenetically independent. Gabbro-diorite rocks derive from an enriched mantle source. These rocks show no or little crustal contamination. Partial melting in the low-middle crust of mafic/gneissic lithologies and intermediate igneous/metasedimentary lithologies generated the tonalite-granodiorite rocks and the granite rocks of the pluton respectively. The emplacement in the upper crust probably started with the gabbro-diorite and tonalite-granodiorite igneous magmas, being followed almost simultaneously by the external granite. The central granite might have intruded shortly after the external granite, pushing aside all of the previous units and thus generating the annular outcrop pattern.

The petrology and geochemistry of the different igneous units of the Santa Eulália plutonic complex suggest that were coeval but with independent petrogenesis (González Menéndez et al. 2006). The more mafic rocks, gabbros-diorites, were probably derived from an enriched mantle affected by previous subduction processes. The intermediate mafic rocks, tonalites and granodiorites, have a very variable geochemistry and are thought to be the result of partial melting processes of a lower mafic crust. The Kfs granites of the External unit were probably generated by partial melting of intermediate gneissic rocks in the mid-lower crust, whereas the grey Bt-granites of the Central unit probably have a mixed source of metasediments, S-component, and intermediate to acid igneous.

Nisa-Alburquerque Batholith

The Nisa-Albuquerque batholith is a composite intrusion of late Variscan age formed by different granitoid units, mostly with sharp contacts or transitional within a few meters that can be grouped into dominant S-type granites and minor I-type granitoids (Fig. 13.8).

It has been dated by various authors in the past decades. The most recent data are from González Menéndez (1998) a Rb–Sr isochron age of 294 ± 13 Ma (MSWD = 1.12), and Solá et al. (2009) who obtained SHRIMP U-Pb ages of 309 ± 4.6 Ma, mean age of the youngest zircon cores, and 307.4 ± 4.0 Ma, mean age of zircon overgrowths, for the main porphyritic S-type granite unit.

S-type granites include: i. porphyritic monzogranites and leucogranites that usually define Kfs + Pl magmatic orientations which are especially intense towards the western zones of the batholith. ii. central leucogranites, Gafete

granites, with Ms > Bt. In some locations some are present, possibly related to interaction with the porphyritic granites. I-type granitoids are composed of tonalite-granodiorite, Bt + Amp + Tnt, and monzogranites, Bt, or Bt > Ms, that form small to intermediate size bodies within the S-type granites, porphyritic and Central leucogranite. Contacts are sharp but in some locations there is evidence of mixing with the S-type granites.

The S-type granites and leucogranites of the batholith are characterized by a strong peraluminous nature, ASI ≈ 1.05–1.35, high K_2O contents (3–6 wt%), P_2O_5 (0.25–0.6) wt% and low CaO (0.1–0.6 wt%), Sr ≤ 100 ppm and Zr 100 ppm (Fig. 13.7). Isotopic signatures are $^{87}Sr/^{86}Sr_i$ 0.7105–0.7176.

The I-type tonalites-granodiorite-monzogranites, have lower ASI values (0.97–1.15) and lower P_2O_5 contents (0.2–0.25 wt%), but higher contents in CaO (1.3–2 wt%), Sr (160–200 ppm) and Zr (150–180 ppm) (Fig. 13.7). The isotopic signature of $^{87}Sr/^{86}Sr_i$ (0.7053–0.7068) are lower than S-type granites. The zircon in the Nisa-Albuquerque granite records a history of a magma genesis involving mixing between (1) a metaluminous magma progressively contaminated by a small sedimentary component, and (2) a more voluminous peraluminous magma originated from a large sedimentary source. The zircon in tonalite records nothing of the age of the magma's source rocks, but the moderately high $\delta^{18}O_{zir}$ (ca. 7.4‰) does preclude derivation of the magma directly from the mantle. Both the chemical and isotopic compositions of the tonalite zircon make it highly unlikely that the tonalite magma was a component in the main granite magma mixture (Solá et al. 2009).

Both intrusions (Nisa-Albuquerque and Sta Eulália) are concentric zoned and consistent with melting and recycling of the continental crust as well as magma mixing processes. The magmatism of the Santa Eulália complex involved important amounts of mafic-intermediate melts and the granitic melts produced were I-type with relatively minor S-type component. This suggests an important involvement of mantle-derived components in the source of Ossa-Morena Variscan granitoids. On the other hand, the Nisa-Albuquerque batholith that was emplaced along the contact with Central-Iberian zone, involved less mafic-intermediate melts and S-type granitoids predominant, indicating important melting-recycling processes in the continental crust. This comparison suggests substantial differences in basement composition and/or melting processes between Ossa-Morena and Central Iberian zones.

During the Variscan regional heating event, partial melting of heterogeneous source rocks probably occurred at different lower to mid-crustal levels. Magmas from two contrasting sources were emplaced into an upper crust magma chamber with some local mixing.

13.2.6 Variscan Magmatism at the Central Iberian Zone, the Central and Northern Border

H. C. B. Martins, M. A. Ribeiro, A. Almeida

The West-Central sector of the Central Iberian Zone (CIZ) display intense Variscan orogenic magmatism where the similarity of the NW-SE tectonic-structuring of the igneous bodies and the surrounding metasedimentary is particularly obvious (Fig. 13.2).

The geological expression of this magmatic—metamorphic and structural set is expressed by: (i) The presence of large antiformal alignments such as the magmatic-metamorphic belts of Porto-Viseu; Cabeceiras de Basto-Vila Real-Torre de Moncorvo and Meda-Penedono-Lumbrales where the two-mica granites prevail; (ii) The development of first-order crustal ductile shear zones—Vigo-Régua and Juzbado-Penalva do Castelo—to which are spatially associated predominantly biotitic granites, generally integrating complexes with acid-base associations; (iii) The last intrusion of a less voluminous magmatism (Peneda-Gerês and Vila Pouca de Aguiar—Águas Frias-Chaves massifs and Lavadores massif) associated with late-variscan fragile deformation phase (Gerês-Loivos and Penacova-Régua-Verin and Porto-Tomar Régua faults).

In ZCI the post-collisional period records the successive generation of granitic magmas, which exhibit different chemical and isotopic signatures and are related in a distinctive way, with the aforementioned structures. As a consequence of these relationships, the typology of CIZ granite plutonism is established on the basis of the chronology of the last variscan ductile phase (D3), corroborated by geochronologic data: granitoids sin-D3, 321–312 Ma (two-mica granites, biotite granites and leucogranites); Late-to post-D3 granitoids, 312–300 Ma (biotite or dominant-biotite granites, sometimes associated with basic rocks, and some leucogranites); Granitoids post-D3, 290–299 Ma (mainly biotite to biotite-muscovite granites) (Dias et al. 1998; Ferreira et al. 1987) (Table 13.1).

The geochronological data reveal that in the CIZ successive granite intrusions were emplaced during a short time interval of about 30 Ma, without any significant geochronological gap, corresponding to the latest stages of the Variscan orogeny. The data further suggests that the D_3 and the late variscan fragil deformation will had active in the

Table 13.1 Synthesis of geological, structural and isotopic data from the granitoids in the central and northern border of the Central Iberian Zone

Structural context	Plutonic zone/dominant rock type	Structural relations/classification	Age (zircon age, pref.)/ reference	Isotopic data	ASI	Observations
D3 antiform	Porto-Viseu belt/two-mica granites	S type/syn-kinematic	Junqueira granite 308 (mz)/(Valle Aguado et al. 2005)	εNd: −3.5 to −5.7	1.15–1.50	Leucogranites and two mica granites associated with migmatites
			Porto Granite 306 ± 7 (Rb–Sr)/(Almeida et al. 2014)	εNd: −1.9 to −3.6	1.2–1.5	
			Pedregal Granite 311 ± 5 (zr)/(Ferreira et al. 2014, 2015)	εNd: −5.8 to −7.16	0.18–1.62	
			Diatexite—Mindelo 309–319(zr)/(Areias et al. 2014)	εNd: −2.1 to −5.4	1.3–1.7	
D3 antiform	Cabeceiras-Vila Real—Torre de Moncorvo complex/Two-mica granites	S type/syn-kinematic	Cabeceiras de Basto Complex 311 ± 1 Ma (zr + mz)/(Almeida et al. 1998)	εNd: –8.66 to –10.60	1.2–1.4	Leucogranites and two mica granites
			Carrazeda Ansiães Complex: 318–329 (zr + mz)/(Teixeira et al. 2012)	εNd: −6.3 to −8.8	1.21–1.45	
D3 antiform	Mêda-Penedono—Lumbrales Complex/Two-mica granites	Type/syn-kinematic	Granito de Lumbrales: 300 ± 8 (Rb–Sr)/ (Garcia Garzon and Locutura 1981)			Leucogranites and two mica granites with associated migmatites
Regional shear zone Vigo-Régua	Refoios do Lima, Sameiro, Felgueiras, Lamego, Ucanha-Vilar/Biotite monzogranites	I/S type/syn kynematic	Refoios do Lima to Ucanha-Vilar 321-314/ (Dias et al. 2002)	εNd: −4.39 to −6.28	1.18–1.31	Small plutons along the shear zone
	Braga—Celeirós—Vieira do Minho—Guimarães/Granodiorite, Monzogranites	I/S type/late-kynematic	Braga—Vieira do Minho—308-313/(Dias et al, 1998; Dias et al. 2002; Martins et al. 2013)	εNd: −5.16 to −6.20	1.04–1.22	Small plutons along the shear zone
Regional shear zone Juzbado-Penalva do Castelo	Maceira and Casal Vasco/Granodiorite/monzgranite	I-S transitional/syn kinematic	Maceira 314 Casal Vasco 313/(Valle Aguado et al. 2005)	εNd: −3.4 to −6.9	1.0–1.37	Biotite gneiss granites
	Cota-Viseu/Monzogranite	I-type/late kinematic	Cota-Viseu 306/ (Azevedo et al. 2005)	εNd: +0.11 to −3.51	0.9–1.12	Acid-basic association
	Aguiar da Beira/Monzogranite	I-S transitional/late to post-kinematic	Aguiar da Beira 302/ (Costa 2011)	εNd: −2.23 to −3.39	1.11–1.20	Composite massif
	Castro Daire/Monzogranite	Post-kinematic	Castro Daire 294/ (Azevedo et al. 2005)			
Plutons associated with late-variscan faults	Peneda-Gerês/biotite monzogranites	I-type/post-kynematic	Gerês -296/(Mendes and Dias 2004)	εNd: −1.04 to −2.6	0.99–1.13	Zoned plutons
	Vila Pouca de Aguiar/biotite monzogranites		V. Pouca de Aguiar—299/(Martins et al. 2009)			
	Lavadores/biotite monzogranites		Lavadores -295/ (Martins et al. 2013, 2014)			Affected by a pos-D3 shear zone

timespans of 321–300 Ma and 290–299 Ma, respectively (Table 13.1).

Integrating the results of isotopic geochemistry, the geochronology the petrographic and the typological characteristics of the different granitic associations, the following aspects stand out:

(1) A successive emplacement of leucogranitic magmas is verified in the range 321–300 Ma, represented by two-mica granites and leucogranites (Table 13.1). These are granite rocks with S-type affinity, with high alumina index (AIS = 1.17–1.52), alkali-calcic magnesian-ferroan (Frost el al. 2001) and strongly enriched isotopic compositions ($Sr_i > 0.713$, $\varepsilon Nd < -7.7$). These peraluminous magmas were generated from aluminous metasedimentary middle/lower-crustal sources with a major pelitic contribution (Almeida et al. 1998, 2014; Areias et al. 2014; Dias et al. 2002 and references there in, Ferreira et al. 2014, 2015; Garcia Garzon and Locutura 1981; Teixeira et al. 2012; Valle Aguado et al. 2005).

(2) In the range 321–305 Ma, and simultaneously with the leucogranitic plutonism, occurred the emplacement of granite complexes. They associate: (i) essentially biotitic monzogranites moderately peraluminous (AIS = 1.18–1.31) magnesian and alkali-calcic affinity, with rare and absent mafic microgranular enclaves and less enriched isotopic signature compared to (1) (Sr_i = 0.7084–0.7106, $\varepsilon Nd = -5.2$ to -6.8). They are also S-type and their composition suggest a major involvement of metaigneous protoliths or imature metasedimentary sources. An origin by partial melting of metagraywackes and/or felsic metaigneous lower crust materials in the granulitic facies, is proposed (Avezedo and Valle Aguado 2013; Costa 2011; Dias et al. 1998, Dias 2001; Dias et al. 2002, 2010; Martins et al. 2013; Simões 2000; Valle Aguado et al. 2005. (ii) biotitic monzogranites/granodiorites with abundant mafic microgranular enclaves, weak to moderate peraluminous character (AIS = 1.04–1.22) with alkali-calcic magnesian signature (granitoids syn-D_3) or alkali-calcic magnesian-ferroan (granitoids late—D_3) and more depleted isotopic signature (Sr_i = 0.7064–0.7085, $\varepsilon Nd = -4.4$ to -6.2). These granitic units are associated with very scarce vaugnerites (Andrade and Noronha 1981) and hectometric to kilometric gabbroic to granodiorite bodies (gabbronorites, quartz-diorites, monzodiorites, quartz-monzodiorites and granodiorites) defining continuous evolutionary (chemical and isotopic) trends of metaluminous to peraluminous rocks (AIS = 0.80–1.06) with isotopic composition in the following range of values: Sr_i = 0.7049–0.7106, $\varepsilon Nd = -2.1$ to -6.8. To the gabbronorites correspond the less enriched isotopic composition (Sr_i = 0.7049–0.7053, $\varepsilon Nd = -2.1$ to -2.5). They do not reveal a depleted mantle isotopic signature, in addition their primitive mantle-derived character [(Mg/(Fe + Mg) = 0.68–0.72 and Cr = 439–626 ppm] is incompatible with an extensive process of crustal contamination of a depleted mantle magma. The shoshonite affinity and the isotopic composition of these rocks suggest the existence of sub-Iberian enriched mantle domain during the Variscan event (Dias and Leterrier 1994; Dias et al. 2002, 2010).

It is noteworthy that the chemical and isotopic compositions of the grabbroic rocks associated to the different plutons are similar, revealing compositional homogeneity of the mantle component involved in their genesis.

The genesis of these acid-basic associations can be explained by a complex petrogenetic process combining factional crystallization and magma mixing between a mantle-derived magma (represented by the gabbros) and felsic crustal melts (represented by the biotitic monzogranites). The differences in the isotopic composition of the different hybrid rocks can be related to the compositional heterogeneity of the crustal source region in lower crust and also to variable degree of crustal contamination (Azevedo et al. 2005; Azevedo and Valle Aguado 2013; Dias et al. 2002, 2010; Martins et al. 2013; Simões 2000; Valle Aguado et al. 2005).

(3) The last emplacement of granitic magmatism occurred in the range 299–290 Ma (post-D_3), in a geodynamic context of extensional processes, being represented in the studied region by the composite and zoned massifs of Vila Pouca de Aguiar—Águas Frias-Chaves and Peneda-Gerês and Lavadores massif (Fig. 13.9).

They include weakly metaluminous to peraluminous (AIS = 0.99–1.13) granites with calc-alkaline-K and ferroan affinity and depleted isotopic composition compared to the remaining granitoid groups (Sr_i = 0.7033–0.7079, $\varepsilon Nd = -1.04$ to -2.6). This mantle like isotopic signature is a distinctive feature of the post-D_3 plutonism.

The nature of possible sources reservoirs for this type of plutonism are still a matter of debate, however an origin by mantle input followed by mantle crust interaction is suggested, implying the contribution of a less enriched mantle component than that involved in the genesis of synorogenic hybrid granitoids (Dias et al. 2010; Mendes and Dias 2004; Martins et al. 2009; Silva 2010).

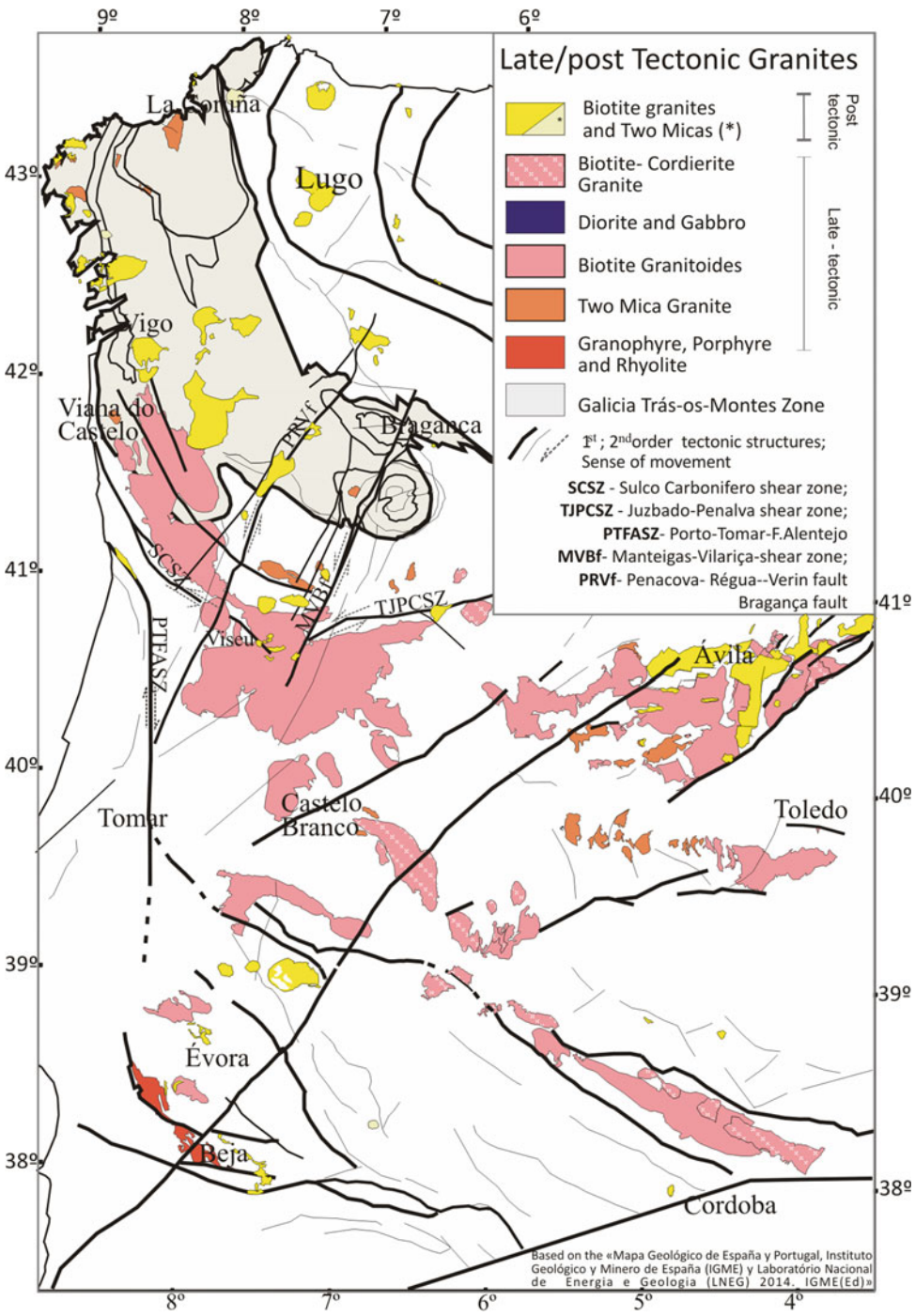

Fig. 13.9 Location of the Variscan late/post D3 granites of the Ibéria. (Adapted from Mapa Geológico de España y Portugal", scale 1/1000000, IGME (Ed)

13.3 An Overview on the Petrogenesis of the Large Batholiths and the Mantle-Related, Basic and Intermediate Rocks

A. Castro

13.3.1 Introduction

Several granite types and different magmatic trends linking basic and intermediate rocks are identified. These are analysed here separately to facilitate comprehension. The genetic relations between granite types and magmatic series are of interest for a better understanding of large-scale geodynamic processes involving the whole lithosphere during the Variscan cycle.

Variscan magmatism includes all magmatic rocks intruded and extruded in the period of the Variscan orogeny. That is, from Devonian to Lower Permian (400–280 Ma), covering a time span of about 100 Ma. The production of magmatic rocks along this time period is not continuous. Large batholiths and anatectic complexes, which were formed in a short time interval of about 40 Ma, from 340–300 Ma, represent most of the volume of magmatic rocks of the Variscan belt of Iberia. Although this short review is focussed to the granitic rocks forming large batholiths, attention is also given to the mantle-related, basic and intermediate rocks that are closely associated in space and time, and possibly in origin, with the large calc-alkaline batholiths. The origin of these batholiths remains controversial in the Variscan belt. Current petrologenetic models are unable to explain the geochemical features in terms of source composition and petrological constraints imposed by thermodynamic models and phase equilibrium experiments. However, important advances have been made in the last years on the petrogenesis and tectonic implications of large calc-alkaline batholiths (Castro 2013, 2014).

13.3.1.1 The Meaning and Implications of Granite Magmatism During the Variscan Cycle

A major problem is about the tectonic meaning of magmatism, which is not exclusive of the Variscan belt of Iberia. To find a correlation between the chemistry of magmatic rocks and a particular plate tectonic scenario, has been the central endeavour of geology from the inception of plate tectonics more than 50 years ago. Granites (sensu lato) are particularly interesting on this concern for several reasons. First, many granites represent crustal melts and, hence, their origin is related to tectono-thermal processes within the continental crust. Second, granites contain abundant zircons and can be used to get accurate age determinations. And third, granites record in their structure the history of emplacement allowing us to establish a timing relationship between intrusion and tectonic structures.

That granites are witness of crustal recycling is strongly supported by their isotopic signatures. For instance, a crustal residence time can be approached by means of Nd model ages, being this age systematically older than the age of magma generation (Hawkesworth and Kemp 2006; Windley 1995). Recycling of old crustal material is the rule emerging from the measured Nd model ages along the evolution of the continental crust. However, inputs of juvenile material are also identified with variable relative weight over recycling depending on the type of granites. Juvenile material, which are mantle-derived components that are extracted for the first time form the mantle at the time of granite magma generation, are identified by Sr initial ratios in granites, and by a correlation between Nd and Sr initial isotopic ratios. However, the way by which juvenile or recycled materials are incorporated to granite magma is a matter of controversy. More than a single mechanism is, in principle, possible. For instance, contrasted processes such as assimilation of terrigenous sediments, magma mixing or melting form a crust-mantle mixed source, may lead to identical isotopic relationships. Additional constraints imposed by phase equilibrium relations are necessary to reject impossible processes. Experimental petrology tells us which is possible and which is impossible in generating granitic magmas (Patiño Douce 1999; Wyllie et al. 1976). Fortunately, petrological constraints are being incorporated step by step into the limbo of possible scenarios for granitic magma generation. However, additional efforts are still needed to introduce new conceptions and new paradigms in granite petrology.

The second point of interest of granite studies, mentioned above, is zircon. The study of zircons in granites, and in any other metamorphic or igneous rocks, has revealed as a powerful tool to constrain age, source materials and history.

13.3.1.2 Zircon Ages

Zircon (U–Th–Pb) geochronology, using in situ isotopic determinations with secondary-ion mass spectrometry (SIMS), has revealed as a powerful technique in granite studies in general and in particular in the Iberian massif. Granite magmatism, with their thermal and geodynamic implications for magma generation, can be related in time with relative accuracy to regional tectonic accidents and deformational events. In most cases, zircon ages confirm previous estimates on the relative sequence of granite intrusions that were based on cutting relations from outcrops or maps. However, in spite of the great advance of zircon studies in granitic rocks, in situ zircon geochronology still entails uncertainties in terms of geological interpretations.

Uncertainties are of two types. One is related to the frequently observed short-range age groups in a single sample. The other is about the meaning of zircon ages that are much older (long-range) than the magma crystallization age (the average age). Large-scale geological processes are often based on interpretations to zircon ages. The above-mentioned uncertainties tell us that these interpretations must be taken with care. Short-range variations are poorly understood. The range of time is longer than the residence time of magma bodies in the middle-upper crust. The time span can be on the order of several Ma, while the time for complete crystallization of discrete magma pulses of granite composition in the upper crust is on the order of less than 1 Ma. Moreover, short-range age variations are clustered in two or more groups with differences of few Ma between them. A typical case is found in the Gredos layered intrusions of granodiorites forming part of the large Central System batholith. In this case groups of ages can correspond with thermal events produced by arrival of new magma pulses, or new layers, to the emplacement level of the whole batholith (Díaz-Alvarado et al. 2013). The meaning of an average age is only an estimate of the age of emplacement. The case of the long-range age variations may have important implications on petrological and geodynamic interpretations. Older-than-normal zircons are frequently, but not always, observed in zircon age populations, either as cores of new zircon crystals or as euhedral crystals. Two antagonist interpretations are possible: (1) Old zircons are *relict crystals* from the source where granitic magma was generated by anatexis. (2) Old zircons are xenocrysts; that is, they represent crystals from the country rocks that were captured by the granitic magma by assimilation.

13.3.2 Granite (Sensu Lato) Types of the Variscan Cycle in Iberia

Granite studies in the Iberian massif were pioneered by R. Capdevila, J. P. Bard and G. Corretgé in the sixteen and seventies (Bard, et al. 1970; Capdevila 1969; Capdevila et al. 1973; Capdevila and Floor 1970; Corretgé 1969, 1971; Corretgé, et al. 1977) and followed by other Spanish teams till present days. The abundance of granite intrusions, the diversity of types and tectonic relations, as well as the quality of exposures, made the Iberian massif a world-class granitic area, where relevant contributions to the old and unsolved "granite problem" (Read 1957) have been provided along the years. Interestingly, the basis of the modern classification of granites, and the key problems relating orogenic processes and granite magma generation, do not departs considerably from the early ideas introduced by Capdevila and co-workers, which predated the classical S-I granite type classification introduced by the Australian School (Chappell and White 1974). Each granite type has a particular origin. To assess the tectonic implication of granite magmatism it is necessary to constrain the mechanisms that gave rise to granite magmas. Although this short outline on Variscan magmatism tends to simplify the number of magmatic groups in few large categories, it is a fact that types and ages are significantly different in the northern and southern domains of the Iberian massif (Fig. 13.10), being the boundary between Ossa-Morena and Central Iberian zones a boundary for magmatic associations.

13.3.2.1 Granitic and Intermediate Magmatism of the Northern Domain

Two main groups of granites (sensu lato) are clearly distinguished (Capdevila et al. 1973; Castro et al. 2002) in the northern domain of the Iberian massif. These broadly correspond with the features of S-type (sedimentary source) and I-type (igneous source) according to the Chappell-White classification (Chappell and White 1974). (1) The first is formed by anatectic, S-type leucogranites, with colour index $M < 10$ (<10 vol.% of dark, mafic minerals) and characterized by a peraluminous chemistry with alumina saturation index, $ASI > 1$ [$ASI = \text{mol } Al_2O_3/(Na_2O + K_2O + CaO)$]. (2) A second group is formed by granodiorites and monzogranites (I-type), showing characteristic affinities to calc-alkaline batholith associations of active continental margins. They may evolve from metaluminous ($ASI < 1$) to slightly peraluminous ($ASI > 1$). Biotite is the dominant mafic mineral. Some local variations may contain amphibole, displaying less silicic and less potassic compositions and plotting in the field of tonalites and Qz-diorites. Mafic microgranular enclaves are common. Contamination with the local metasedimentary host may produce locally a subtype of granites that, though retaining typical features of calc-alkaline granites of the second group, may have peraluminous chemistry and contain metamorphic minerals, mainly cordierite. This subgroup is referred to here as calc-alkaline contaminated. A compositional space has been designed to distinguish these two main groups (Fig. 13.11).

13.3.2.2 Anatectic Granites (S-Type)

Anatectic granites of the Variscan cycle are typically peraluminous leucogranites with varieties depending on the presence of biotite and/or muscovite. Names as two-mica granites, biotite granites, etc. are common in the regional literature. The may appear in two distinct kind of massifs depending on the degree of uprooting from the migmatitic source (Corretgé et al. 1977). These are referred to as (1) autochthonous granites when they are linked directly in the field with migmatitic complexes, and (2) allochthonous granites for those that were uprooted from the migmatitic source and are emplaced in lower grade metamorphic

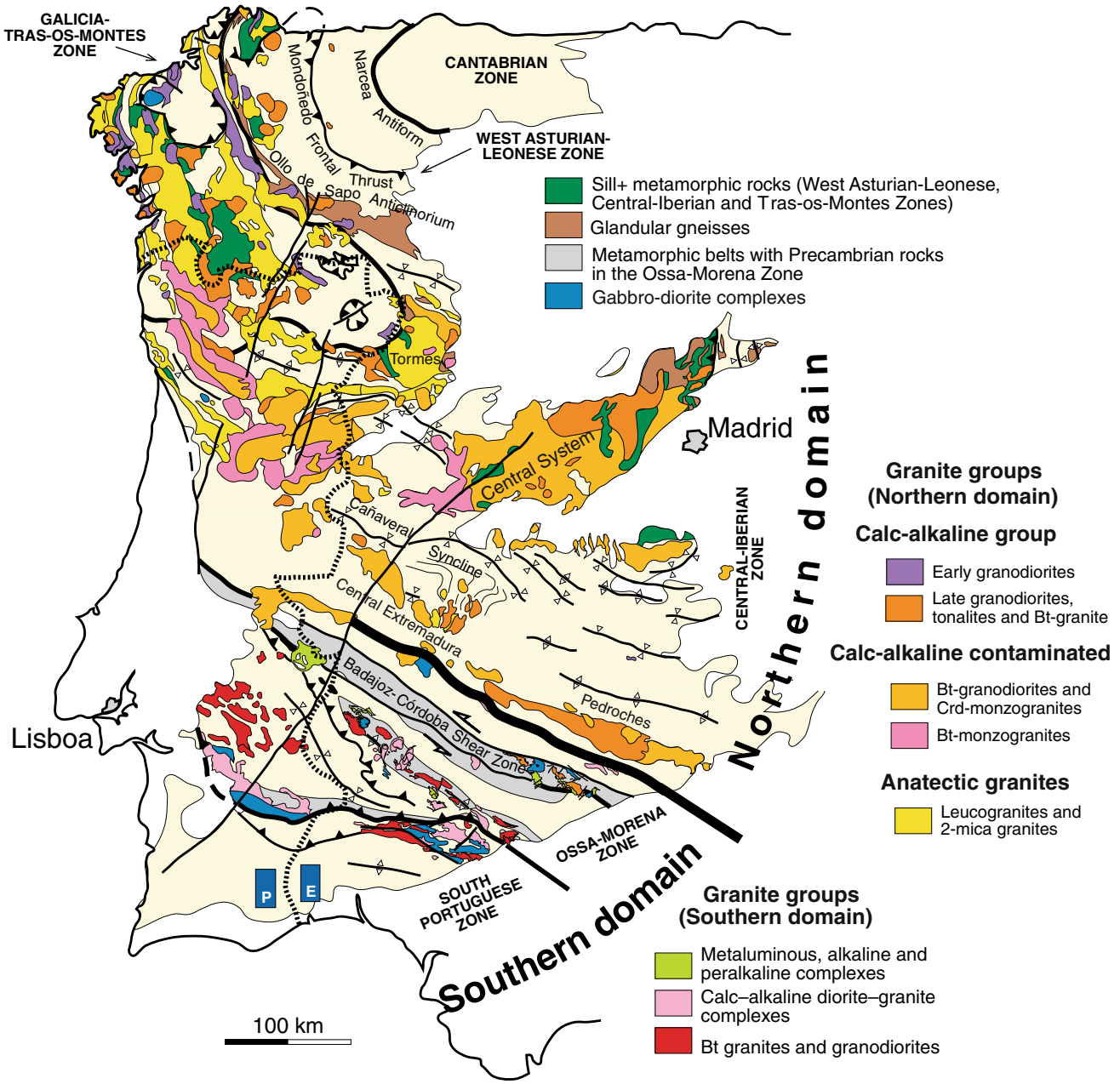

Fig. 13.10 Distribution of granite (sensu lato) intrusions in the Iberian massif. Most of these intrusions belong to the Variscan cycle (≈350–290 Ma). Some Older intrusions are not distinguished in this general sketch. The relative abundance and ages of granitic intrusions are markedly different each side of the boundary between the Ossa-Morena and Central Iberian zones. This boundary separates two magmatic domains (northern and southern) in the Iberian massif. Modified after Castro et al. (2002)

domains. Some anatectic granites are slightly uprooted and emplaced into migmatitic rocks showing locally cutting relations. These are called sub-authocthonous granites. In the Variscan massif of Iberia the three groups of anatectic granites were profusely developed in the Central Iberian zone (CIZ), in close association with the thick sequences of Neoproterozoic greywackes. These rocks, together with the Cambro-Ordovician volcanoclastic, and greywacke-like in composition, Ollo de Sapo formation, constitute a fertile source for leucogranite generation. Independent approaches from geochemistry, experimental petrology (Castro et al. 2000; García-Arias et al. 2012) field and metamorphic studies (Escuder Viruete 1998; Escuder Viruete et al. 1997; Gil Ibarguchi and Martínez 1982; López-Moro et al. 2012; Escuder Viruete et al. 2000) and zircon studies (Montero et al. 2009) confirm the magma-source linkage for this

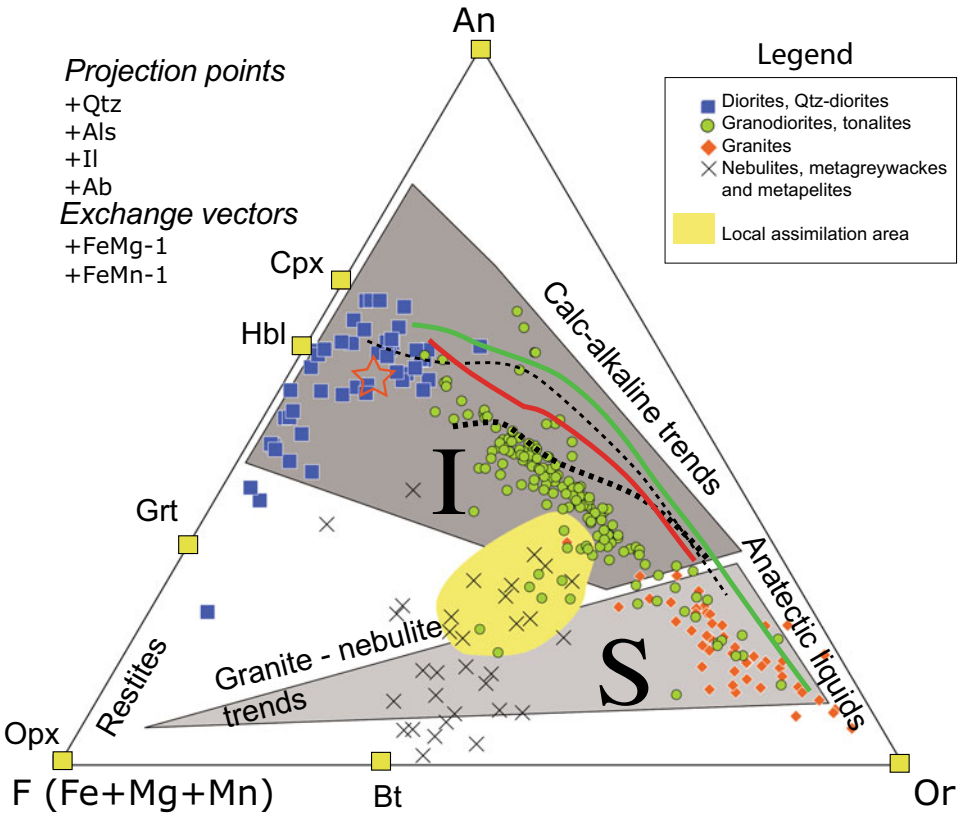

Fig. 13.11 Compositional space diagram using the three main components that define the granitic (sensu lato) compositional spectrum, from tonalites to alkali-feldspar granites and the intermediate diorites and Qz diorites that are linked by cotectic patterns forming the I-type series. The division line between S- and I-type is traced empirically. Detailed explanations on the diagram and its implications are given in (Castro 2013)

granitic group in the Tormes dome (Salamanca and Zamora), one of the best studied anatectic domains of the Iberian massif. The large production of anatectic (S-type) granites is anomalous compared with other sectors of the European Variscan belt. The reason for this anomaly is the confluence of thick fertile greywacke and volcanoclastic successions of Neorpoterozoic (CXG complex) and Cambro-Ordovician (Ollo de Sapo) ages.

13.3.2.3 Calc-Alkaline Group (I-Type) and Related Types

The group of I-type granites, volumetrically dominated by granodiorites and monzogranites with subordinated tonalites and Qz-diorites, is the most relevant in the Variscan massif of Iberia and has been the focus of debate on tectonic implications. Granitic rocks of this group form large batholiths (e.g. the Central System batholith extending from Portugal to Guadarrama in Madrid) that intruded at the middle-upper crust into either anatectic deep-seated domains or shallow level of low-grade metamorphic rocks. In some locations, granodiorites intruded along extensional detachments, at the contact between high and low grade metamorphic domains. Three important facts must be taken into account into any petrogenetic and/or tectonic model of the Variscan belt: (1) In the Northern Domain of the massif (North of the Ossa Morena–Central Iberian boundary) I-type granite intruded mostly at the late stages of the Variscan orogeny, at Upper Carboniferous to Lower Permian times. (2) When they are in contact with high-grade, anatectic domains, they display apparently transitions to local migmatites. (3) Compositions are totally incompatible with an anatectic origin from metasediments, and very unlikely from any other crustal source either sedimentary or igneous. By contrast, they form cotectic trends that support differentiation from a common intermediate magma of broadly andesitic composition (Castro 2013).

In the early classification of granite types in the Iberian massif (Capdevila et al. 1973), calc-alkaline granitic rocks (that they called hybrid series) are separate in two groups, "*early granodiorites*" and "*late granodiorites*", on the basis of the relative age of emplacement with respect to the main Variscan deformation phases. Early granodiorites were described in Galicia as synkinematic with the second deformation phase, and late granodiorites as postkinematic with respect to the third deformation phase. Zircon ages have been profusely supplied along the last decades, providing a well-defined time framework of granite magma emplacement. Extensive references to ages are given in other sections of his monograph. Most granodiorites, and calc-alkaline batholiths in general, belong to the late

group. They were emplaced in a narrow time period from 315 to 300 Ma, postdating the main tectonic episodes, and even the late extensional structures, of the Variscan cycle. Consequently, they are referred to as post-tectonic in many regional studies; a categorization that contrasts with the typical orogenic calc-alkaline features of these batholiths.

13.3.2.4 Transitional (Contaminated) Granites

A third series of granites, showing intermediate features between anatectic (S-type) and calc-alkaline (I-type), was identified in early classifications of granite types from the Iberian massif (Corretgé et al. 1977). They are referred to here as *transitional* or *contaminated granites* and, thus, considered as a subgroup of the calc-alkaline granites with whom they show continuous transitions at the scale of km. The most distinctive features of these granites are: (1) Presence of cordierite in large euhedral crystals. (2) Porphyritic appearance with large Kfsp megacrysts, (3) A marked peraluminous chemistry. (4) Presence of mafic microgranular enclaves as autoliths. These transitional granites can appear in two different settings. One is in the marginal, and more mafic, areas of zoned, epizonal plutons. A representative example is the Cabeza de Araya intrusion in Extremadura (Corretgé 1971; Corretgé et al. 1985). The other setting is represented by transitions from granodiorite batholiths at the contact with pelitic migmatites in deep-seated regions. A representative example is the Gredos massif in the vicinity of a large high-grade metamorphic (anatectic) complex (the Barco-Béjar complex). The generation of these deep-seated, cordierite-bearing granites as the product of local bulk assimilation is supported by all kind of geochemical, petrological and experimental studies (Díaz-Alvarado et al. 2013; Ugidos and Recio 1993; Ugidos et al. 2008). In the case of zoned plutons (e.g., Cabeza de Araya), assimilation took place in ascent conduits and at the level of final emplacement.

The peculiar composition of the middle-upper crust in the Central Iberian zone, characterized by several km thick sequences of pelites and greywackes, is the cause of profuse local assimilation and contamination of calc-alkaline granites in the course of ascent and emplacement. Transitional granites with S-I intermediate features are described in many areas of the Central System (Villaseca et al. 2012). Interestingly, the age of these contaminated granites is almost coincident with the age of the calc-alkaline batholiths (mostly in the range 310–300 Ma).

13.3.2.5 Basic and Intermediate Magmatic Associations

In spite of the scarcity in relative volume, compared with the large granodiorite batholiths, mafic (gabbroic) and intermediate (dioritic and monzonitic) rocks are widespread along the Variscan belt of Iberia. They may appear in a diversity of small outcrops such as (1) isolated enclaves inside granodioritic rocks and (2) more complex bodies, from few meters to nearly one km, showing a marked heterogeneity in textures, grain-size and compositions. Some intermediate rocks may form small plutons of few km in diameter. Most of these mafic and intermediate complexes are intimately associated in space and time with the intrusion of calc-alkaline (granodioritic) batholiths. Three main series can be distinguished on the basis of compositional trends displayed in major-element diagrams. Each one of these series may have common origins from different parts of a metasomatized mantle source. The distinction of three series is a simplification due to the large heterogeneity displayed in these complexes. The three series are: (1) A gabbro-diorite association that can be included in the so-called appinitic association (Murphy 2013; Pitcher 1997). (2) A high-K, high-Mg series of broadly shoshonitic affiliation. (3) An intermediate series of monzonitic composition. The three series are intimately related between then and also with the granodiorite batholiths. They may appear altogether in complex mafic massifs (e.g., Sanabria; Castro et al. 2003). As they are co-magmatic with granodiorites, hybridization by local mixing and mingling are common processes in appinitic massifs (Galán et al. 1996; Moreno-Ventas et al. 1995). When they are intrusive into migmatites, hybridization is restricted to aureoles of fluid exsolution and local reaction with pelitic migmatites, giving rise to intermediate hybrid magmas (Castro et al. 2003). The three mafic series have in common a marked potassic character and subalkaline chemistry. The high contents in K_2O for low silica values displayed by shoshonitic and monzonitic series is a general feature. However, they commonly evolve to silica saturated residual liquids of broadly granitic composition. Some mafic syenites (shonkinites) are described in mafic-potassic massifs (López-Moro and López-Plaza 2004).

13.3.2.6 Calc-Alkaline Batholiths of the Southern Domain

All the above-mentioned time relationships of the K-rich, calc-alkaline (I-type granites and associated basic and intermediate rocks) magmatism is in general terms applicable to the batholiths outcropping in the northern domain (Fig. 13.10) of the Iberian massif. However, in the southern domain of the Iberian massif calc-alkaline intrusions are older and lack of significant contamination with the local host. New U-Pb zircon data yield ages within the range of 334–320 Ma for calc-alkaline plutons of the Olivenza-Monesterio alignment (Cambeses et al. 2015) and of about 350–335 Ma for similar calc-alkaline intrusions of the Evora massif in Portugal (Pereira et al. 2015b). These ages are on average 20 Ma older than I-type calc-alkaline batholiths of the northern domain.

13.3.3 The Origin of Granite (s.l.) Magmas. Problems and Perspectives

13.3.3.1 Anatectic Granites

The generation of these anatectic granites is linked to ultrametamorphism and anatexis, normally in the absence of a free vapour phase, of metasedimentary fertile sources through two main peritectic reactions. These are (13.1) the breakdown reaction of muscovite:

$$\mathrm{Ms} + \mathrm{Qz} + \mathrm{Pl} \rightarrow \mathrm{Kfsp} + \mathrm{Al\text{-}silicate} + \mathrm{Melt} \qquad (13.1)$$

and (13.2) the breakdown reaction of Bt in presence of Al-silicate:

$$\mathrm{Bt} + \mathrm{Qz} + \mathrm{Pl} + \mathrm{Al\text{-}silicate} \rightarrow \mathrm{Kfsp} + \mathrm{Cord}(+\mathrm{Grt}) + \mathrm{Melt} \qquad (13.2)$$

Both reactions are the responsible for leucogranite magma generation in many areas of the Variscan belt. The compositions of melts from these reactions are almost identical in terms of major elements. The Ms breakdown melts are richer in water (about 4 wt% H_2O) compared with the higher temperature melts of the Bt breakdown reaction (about 2 wt% H_2O). Whatever the melting reaction, anatectic melts cannot be more calcic than the source. Only in the case of water-assisted melting, Ca-rich melts can be produced as the consequence of the activation of the Pl-Qz eutectic at relatively low temperatures (about 650 °C at middle crust pressures). Some leucosomes in migmatites are of this type, showing a trondhjemitic (leucotonalitic) composition. Plutons of this composition are absent in the anatectic domains of the Variscan belt. Thus, melting occurred in a water-free environment by peritectic breakdown of Ms at low T and Bt in presence of Als at higher T.

Melting relations were determined experimentally for the particular case of the Variscan metasedimentary sources (Castro et al. 2000). The positive Clapeyron slope (∂P/∂T) of these reactions, and the relative positions with respect to the PT paths determined by metamorphic mineral equilibria (Escuder-Viruete et al. 1997), lead to confirm that anatexis occurred in the middle crust during the Variscan orogeny in relation to decompression of a previously thickened continental crust. This is in agreement with geological and structural relations that support a synkinematic melting and leucogranite (S-type) magmatism in relation with the second deformation phase of the Variscan cycle, which is characterized by subhorizontal extensional shear zones in large areas of the CIZ. The generation of leucogranites by extensional melting spans over a time period from 340 to 320 Ma (e.g. 330–317 Ma in Toledo, Castiñeiras et al. 2008; 320 Ma in the Tormes Dome, López-Moro et al. 2012; 320–310 Ma in the Lugo Dome, Fernández-Suárez et al. 2000).

A second generation of peraluminous leucogranites was formed lately during the period 310–290 Ma. This is broadly represented in small plutons in many parts of the northern domain, in some places these granites are sub-autochthonous bodies, which are associated to second-generation migmatites that form at the contact aureoles of the large calc-alkaline batholiths (e.g., The 305 Ma leucogranite of Refugio del Rey in Gredos, Díaz-Alvarado et al. 2013). These usually form allochthonous intrusions and are closely related in space and time with the emplacement of the large granodiorite batholiths. They form as a consequence of local heating around large batholiths. Cordierite is the characteristic peritectic mineral associated to these leucogranites. The existence of two groups of anatectic granites was recognized since the first classification of granite series in the Iberian massif (Capdevila et al. 1973; Corretgé et al. 1977) and lately confirmed by detailed geochronological studies (Fernández-Suárez et al. 2000).

13.3.3.2 The Origin of Calc-Alkaline Granitic and Intermediate Rocks. Evidence for Subduction and Slab Detachment?

In contrast with the simple petrogenetic framework of S-type granites, granodiorites and related rocks (I-type) of the calc-alkaline group have a more enigmatic and controversial origin. In the northern domain, they form large batholiths that are emplaced into low- and high-grade (anatectic) domains of the crust postdating the main deformation events (D1 and D2). They are late with respect to the peak of tectonic activity in more than 20 Ma. This is a fundamental observation and entails a prima facie paradox of the Variscan massif in Western Europe: Upon being of calc-alkaline affinity and having a subduction-related origin, they postdate in more than 40 Ma the age of ocean closures that preceded continental collision. For this reason, these batholiths have been related to the inception of Tethyan subduction, a process that possibly started with the selfsubduction of Pangea associated to the Iberian orocline (Gutiérrez-Alonso et al. 2008). Post-tectonic batholiths are also considered as a case of "within plate" magmatism" (Scarrow et al. 2009).

The relation with anatectic domains has been a point of debate. Transitions from granodiorites to pelitic migmatites were studied in detail in the area of Gredos (Díaz-Alvarado et al. 2013), being a process of local assimilation the cause of the observed transitions. This is consubstantial to the fact that Ca-rich liquids (granodioritic) cannot be derived by anatexis of peraluminous metasediments (schists and greywackes). However, the interactions between calc-alkaline magmas and migmatites may be very complex and effective in producing hybrid magmas of broadly monzogranite composition and characterized by the presence of cordierite. They form a new series that is called here the "I-type

contaminated", in accordance with previous works that identified a group of "mixed features" in the Iberian massif (Corretgé et al. 1977).

An interesting observation, that must be considered substantial in petrogenetic interpretations, is that rocks of this calc-alkaline group, including massif granodiorites, Qz-diorites and diorites, plot on major-element geochemical diagrams following cotectic trends (Fig. 13.11) that are totally comparable with experimental cotectic liquids formed by equilibrium crystallization (batch) and melt extraction from a parental intermediate (dioritic) magma. Because dioritic (= andesitic) liquids require a particular mafic source and temperatures of the order of 1300 °C and higher (Castro et al. 2010), and both source layer and high temperature cannot be found in the lower continental crust, the origin of these magmas and their potential tectonic implications are still under debate.

The high volume proportion of fractionated granodiorites in relation to the reduced volume of parental diorites is simply the consequence of the high crustal level (middle-upper crust) of observation. Batholiths outcropping at deeper levels (e.g., the Newer Caledonian plutons, Halliday et al. 1980) or those outcropping in a tilted crust section (e.g., the Famatinian Valle Fértil batholith in South America, Castro et al. 2012; Otamendi et al. 2009a, b) or the Kohistan arc section (Garrido et al. 2006), show a large profusion of mafic magmatic rocks increasing in volume proportion with respect to granodiorites with depth.

The calc-alkaline character, which is totally comparable with active margin batholiths, remains unexplained. The problem is similar to other collisional orogens in which, the closure of oceans by subduction preceded continent-continent collision. In the southern domain, the age of calc-alkaline magmatism, which is represented by granitic and intermediate intrusions of the Evora complex and the Olivenza-Monesterio batholith in the Ossa-Morena zone (see above), is compatible with a northward subduction of the Laurussia lithosphere below the Gondwana margin at the time of Variscan collision (Ribeiro et al. 2010). New zircon ages from these calc-alkaline intrusions (Cambeses et al. 2015; Pereira et al. 2015b), are compatible with a northwards subduction below the Ossa-Morena lithosphere. The calc-alkaline signature of magmatism is reinforcing this interpretation. In the case of the Olivenza-Monesterio batholith, the age of calc-alkaline magmatism (334–320 Ma) is almost coincident with the age of metamorphism of oceanic remnants located at the suture between Ossa-Morena and South Portuguese zones. With independence that these ophiolite-like remnants (The Beja-Acebuches ophiolite) represent a local proto-ocean domain (Pérez-Cáceres et al. 2015) or, by contrast, they represent the Rheic ocean, the age of metamorphism and deformation within the range 345–330 Ma (Azor et al. 2008; Castro et al. 1999; Pérez-Cáceres et al. 2015), which may represent the end of subduction and final collision, is almost coincident with the age of calc-alkaline magmatism in the Ossa-Morena zone (334–320 Ma in Olivenza-Monesterio and 350–335 Ma in Evora). Accurate time relations between subduction and magma extraction form fertile zones of the lithosphere, can be very complex in detail, as processes of coupling and decoupling are followed each other in time periods of tens million years (Vogt et al. 2012). Because magma generation and extraction is favoured during periods of decompression (decoupling), it is expected that the last magmatic episodes can postdate by several million years the last coupling period, ending with plate assembly, continent-continent collision and slab detachment (Duretz et al. 2010). Slab detachment may have been favoured by subduction of continental crust of Avalonia below the Ossa-Morena after the closure of the Rheic Ocean (Ribeiro et al. 2010); a process that is predicted by numerical thermomechanical models (Duretz et al. 2010). The calc-alkaline magmatism of the southern domain may have been generated in periods of decoupling during subduction at discrete distances from the trench, represented by the Beja-Acebuches suture at the south. Subduction of Avalonia crust, or fragments from it, may have fertilized the Central Iberian lithosphere. Several millions years after collision, slab detachement below the Central Iberia lithosphere may have produce the large volume of calc-alkaline magmatism from varied sources, including the metasomatized mantle and subducted crust (oceanic and continental). A delay of about 24 Ma, from the time of ocean closure to the time of final slab detachment, is predicted by thermomechanical models of continental collision (Duretz et al. 2010). In the Central Iberian zone, this delay of 24 Ma is almost coincident with the time lapse from peak metamorphism and deformation at ca. 330 Ma and emplacement of the late granodiorite batholiths at ca. 305 Ma. Slab detachment, following subduction and collision is also compatible with the orocline model of the Iberian arc, entailing the selfsubduction of Pangea (Gutiérrez-Alonso et al. 2008, 2011a) and, hence, contributing to an extra refertilization of the lithosphere mantle (Gutiérrez-Alonso et al. 2011b) prior to slab-detachment and batholith generation. This model is also compatible with the beginning of Paleotethys closure, a tectonic scenario that has been proposed to account for the production of calc-alkaline batholiths during post-Variscan times (Pereira et al. 2015b).

It is noteworthy that the generation of mafic and intermediate magmas at the end of the Variscan cycle means that a mantle source was activated during post-collision extension. The chemistry of these mafic-potassic rocks is compatible with a mantle-metasomatized source, being pargasite a key phase in the generation of magmas. As these mafic rocks are coeval with granodiorite batholiths, the possibility of a cause-effect relation has been suggested. It is also

interesting to note the marked calc-alkaline affinity of I-type batholiths of the Variscan cycle. This magmatic affinity is well preserved in cotectic relations of granodiorites and related rocks, even if locally they may have been partially obscured by local assimilation with pelitic migmatites in the middle-upper crust. Nevertheless, a hypothetical crustal source for such an intermediate parental magma (andesitic) of the calc-alkaline batholiths, and associated intermediate potassic series, is totally incompatible with thermal models and composition of the crust, even in the most favourable conditions of large proportions of basalt input to the lower crust (Annen et al. 2006).

References

Ábalos B, Gil Ibarguchi JI, Eguiluz L (1991) Cadomian subduction/collision and variscan transpression in the Badajoz-Cordoba shear Belt (SW Spain), Tectonophysics, 199, 51–72.

Aghazadeh M, Castro A, Omran NR, Emami MH, Moinvaziri H, Badrzadeh Z (2010) The gabbro (shoshonitic)-monzonite-granodiorite association of Khankandi pluton, Alborz Mountains, NW Iran. Journal of Asian Earth Sciences 38(5): 199–219.

Almeida A, Leterrier J, Noronha F, Bertrand JM (1998)—U-Pb zircon and monazite geochronology of the Hercynian two-mica granite composite pluton of Cabeceiras de Basto (Northern Portugal). C. R. Acad. Sci. Paris, 326, pp. 779–785.

Almeida A, Santos JF, Noronha F (2014) Contribuição dos sistemas isotópicos Sm-Nd e Rb-Sr para o estudo petrogenético do maciço granítico peraluminoso de duas micas da cidade do Porto (NW Portugal). Comunicações Geológicas 101 (I): 27–30.

Almeida E, Santos FM, Mateus A, Heise W, Pous J (2005) Magnetotelluric measurements in SW Iberia: new data for the Variscan crustal structures. Geophys. Res. Lett. 32, L08312.

Andrade AS (1983) Contribuition à la analyse d la suture Hercynièn ne de Beja (Portugal), perspectives metallogéniques (Nancy: PhD Thesis) University of Nancy.

Andrade M, Noronha F (1981) Sobre a ocorrência de “vaugneritos” e de rochas gabróicas na região de Fafe. In: II Congresso Nacional de Geociências. Livro de resumos. Universidade de Coimbra.

Annen C, Blundy JD, Sparks RSJ (2006) The genesis of intermediate and silicic magmas in deep crustal hot zones. J. Petrol. 47, 505–539.

Antunes I (2006) Mineralogia, Petrologia e Geoquímica de Rochas Granitóides da área de Castelo Branco—Idanha-a-Nova. PhD dissertation, University of Coimbra.

Antunes A, Santos JF, Azevedo MR, Corfu F (2011) New U–Pb zircon age constraints for the emplacement of the Reguengos de Monsaraz Massif (Ossa Morena Zone). In: Abstracts of the Seventh Hutton Symposium on Granites and Related Rocks, University of Ávila.

Areias M, Ribeiro MA, Santos JF, Dória A (2014) LP-HT anatectic processes and lithological heterogeneity in Mindelo Migmatite Complex (NW Portugal). Estudios Geológicos 70(2), e017. http://dx.doi.org/10.3989/egeol.41730.323.

Azevedo MR, Valle Aguado B, Nolan J, Martins M, Medina J (2005) Origin and emplacement of syn-orogenic Variscan granitoids in Iberia the Beiras massif. In: Carosi R, Dias R, Lacopini D, Rosenbaum G (eds). The Southern Vriscn belt, Jounal of the Virtual Explorer, Electronic Edition, ISSN 1441–8142, (19) Paper 7.

Azevedo, MR, Valle Aguado B (2013) Origem e instalação de granitóides variscos na Zona Centro Ibérica. In: Dias R, Araújo A, Terrinha P, Kullberg C, Geologia de Portugal. Escolar Editora, pp 377–401.

Azor A (2004) El Macizo Ibérico durante el Paleozoico inferior. In: Vera JA (ed), Geología de España, SGEIGME, Madrid, 223–224.

Azor A, Rubatto D, Simancas JF, González Lodeiro F, Martínez Poyatos D, Martin Parra LM, Matas J (2008) Rheic Ocean ophiolitic remnants in southern Iberia questioned by SHRIMP U-Pb zircon ages on the Beja-Acebuches amphibolites. Tectonics 27(5).https://doi.org/10.1029/2008TC002306.

Bard JP and Fabries J (1970) Aperçu pétrographique et structural sur les granitoïdes de la Sierra Morena occidentale (Espagne). Bol. Geol. Min. España, T. LXXXI-II-III, pp. 226–241.

Bard JP, Capdevila R, Matte P (1970) Les grands traits stratigraphiques, tectoniques, métamorphiques et plutoniques des Sierra de Gredos et de Guadarrama (Espagne Centrale). Comptes Rendus —Academie des Sciences de Paris 270 (2630–2633)

Bea F (2004) La naturaleza del magmatismo de la Zona Centroibérica: consideraciones generales y ensayo de correlación. Libro de Geología de España (SGE-IGME), Ed J-A Vera, pp. 128–132.

Bea F, Montero P, Montero P, Talavera C, Zinger, T (2006) A revisited Ordovician age for the Miranda do Douro orthogneiss, Portugal. Zircon U-Pb ion-microprobe and LA-ICPMS dating. Geologica Acta, 4 (3), 395–401.

Bea F, Montero P, Gonzalez-Lodeiro F, Talavera C (2007) Zircon Inheritance Reveals Exceptionally Fast Crustal Magma Generation Processes in Central Iberia during the Cambro-Ordovician. Journal of Petrology. 48 (12), 2327–2339.

Beckinsale RD (1979) Granite magmatism in the tin belt of the South-East Asia. Origin of granite batholiths-geochemical evidence » . Shiva Publ. Ltd., Atherton and Tarney (eds), pp. 34–44.

Burg JP, Iglesias M, Laurent P, Matte Ph, Ribeiro A (1981) Variscan intracontinental deformation: the Coimbra–Cordoba shear zone (SW Iberian Peninsula). Tectonophysics (78) 161–177.

Cambeses A (2015) Ossa-morena zone variscan’calc-alkaline’hybrid rocks: interaction of mantle-and crustal-derived magmas as a result of intra-orogenic extension-related intraplating. Ph.d Universidad de Granada, España.

Cambeses A, Scarrow JH, Montero P, Molina JF, Moreno JA (2015) SHRIMP U-Pb zircon dating of the Valencia del Ventoso plutonic complex, Ossa-Morena Zone, SW Iberia: Early Carboniferous intra-orogenic extension-related 'calc-alkaline' magmatism. Gondwana Research 28(2): 735–756. https://doi.org/10.1016/j.gr.2014.05.013.

Canilho, MH (1977). Estudo dos maciços eruptivos de Veiros e Vale de Maceira (Alto Alentejo). Boletim da Sociedade Geológica de Portugal (20) 233–245.

Capdevila R (1969) Le métamorphisme régional progressive et les granites dans le segment Hercyniene de Galice Nord Oriental (NW de l’Espagne). Thèse d’etat Université de Montpellier:430.

Capdevila R, Floor P (1970) Les différents types de granites hercyniens et leur distribution dans le nord ouest de l´Espagne. Bol Geol Min 81: 215–225.

Capdevilla R, Corretgé LG, Floor P (1973) Les granitoïdes varisques de la Meseta ibérique. Bulletin de la Societé Géologique de France 15 (3-4): 209–228.

Carvalhosa A, Zbyszewski G (1994) Carta Geológica de Portugal 1:50.000—Notícia explicativa da folha 35-D, Montemor-o-Novo. Instituto Geológico e Mineiro pp 86.

Casquet C, Galindo C (2004) Magmatismo varisco y postvarisco en la Zona de Ossa-Morena. In: Vera, J.A. (ed.) Geología de España. Soc. Geol. España; IGME, Madrid, pp 194–198.

Castiñeiras P, Villaseca C, Barbero L, Romera MC (2008) SHRIMP U-Pb zircon dating of anatexis in high-grade migmatite complexes of Central Spain: Implications in the Hercynian evolution of Central Iberia. International Journal of Earth Sciences 97(1): 35–50.

Castro A (2013) Tonalite-granodiorite suites as cotectic systems: A review of experimental studies with applications to granitoid petrogenesis. Earth-Science Reviews 124: 68–95. https://doi.org/10.1016/j.earscirev.2013.05.006.

Castro A (2014) Erratum to 'Tonalite-granodiorite suites as cotectic systems: A review of experimental studies with apllications to granitoid petrogenesis' (Earth Sci. Rev. 124, 2013, 68–95). Earth Science Reviwes 129:178.

Castro A, Corretgé LG, El-Biad M, Fernández C, Patiño-Douce AE (2000) Experimental Constraints on Hercynian Anatexis in the Iberian Massif, Spain. Journal of Petrology 41(10): 1471–1488

Castro A, Corretgé LG, De la Rosa J, Enrique P, Martínez FJ, Pascual E, Lago M, Arranz E, Galé C, Fernández C, Donaire T, López S (2002) Paleozoic Magmatism. In: Gibbons W, Moreno MT (eds) The Geology of Spain, vol. Geological Society, London, London, pp 117–153.

Castro A, Corretgé LG, De la Rosa JD, Fernández C, López S, Chacón H (2003) The appinite–migmatite complex of Sanabria, NW Iberian massif, Spain. Journal of Petrology 44: 1309–1334.

Castro A, Diaz-Alvarado J, Fernandez C (2012) Fractionation and incipient self-granulitization during deep-crust emplacement of Lower Ordovician Valle Fértil batholith at the Gondwana active margin of South America. Gondwana Research (in press): https://doi.org/10.1016/j.gr.2012.1008.1011.

Castro A, Fernández C, El-Hmidi H, El-Biad M, Díaz M, De La Rosa J, Stuart F (1999) Age constraints to the relationships between magmatism, metamorphism and tectonism in the Aracena metamorphic belt, southern Spain. International Journal of Earth Sciences 88(1): 26–37.

Castro A, Gerya T, García-Casco A, Fernández C, Díaz-Alvarado J, Moreno-Ventas I, Löw I (2010) Melting Relations of MORB–Sediment Mélanges in Underplated Mantle Wedge Plumes; Implications for the Origin of Cordilleran-type Batholiths. Journal of Petrology 51, 1267–1295.

Castro A, Vogt K, Gerya TV (2013) Generation of new continental crust by sublithospheric silicic-magma relamination in arcs: A test of Taylor's andesite model. Gondwana Research 23: 68–95

Chappell BW, White AJR (1974) Two contrasting granite types. Pacific Geology 8: 173–174.

Chichorro M (2006) A evolução tectónica da Zona de Cisalhamento de Montemor-o-Novo (Sudoeste da Zona de Ossa Morena—área de Santiago do Escoural—Cabrela). PhD dissertation, Universidade de Évora.

Cordani U, Nutman A, Andrade A, Santos J, Azevedo M, Mendes M, Pinto M (2006) New U–Pb SHRIMP zircon ages for pre-variscan orthogneisses from Portugal and their bearing on the evolution of the Ossa—Morena Tectonic Zone. An. Acad. Bras. Cienc. 78 (1): 133–149.

Corretgé LG (1969) Las diferencias aplíticas cupuliformes en la tonalita de Zarza la Mayor-Ceclavín (Cáceres) y su interpretación petrogenética. Acta Geológica Hispánica Iv 5: 119–123

Corretgé LG (1971) Estudio petrológico del batolito de Cabeza de Araya (Cáceres). Tesis Doctoral Univ de Salamanca P453

Corretgé LG (1983) Rocas graníticas y granitóides del Macizo Ibérico. Libro Jubilar JM Rios. Inst. Geológico y Minero de España 1, pp 569–592.

Corretgé LG, Bea F, Suarez O (1985) Las características geoquímicas del Batolito de Cabeza de Araya (Cáceres, España): implicaciones petrogenéticas. Trabajos de Geología 15: 219–238.

Corretgé LG, Ugidos JM, Martínez FJ (1977) Les series granitiques du secteur Centre-Occidental Espagnol. La chaine varisque d´Europe moyenne et occidentale. Coll intern Cnrs, Rennes 243: 453–461.

Costa, M (2011) Geoquímica dos granitóides de Aguiar da Beira, Norte de Portugal. PhD Thesis (unpubl) Universidade de Aveiro, 316 pp.

Costa D, Viana A, Munhá J (1990) Petrologia e geoquímica dos maciços de Veiros e Vale Maceira. In: VII Semana Geoquímica. Universidade de Lisboa.

Dallmmeyer RD, Fonseca PE, Quesada C, Ribeiro A (1993) 40Ar/39Ar mineral age constraints for the tectonothermal evolution of a Variscan suture in SW Iberia. Tectonophysics (222): 177–194.

Dias G (2001) -Fontes de Granitóides Hercínicos da Zona Centro-Ibérica (Norte de Portugal): evidências isotópicas (Sr, Nd). Memórias Acad. Ciências Lisboa, tomo XXXIX, pp. 121–143.

Dias G, Leterrier J (1994) The genesis of felsic-mafic plutonic associations: a Sr and Nd isotopic study of the Hercynian Braga Granitoid Massif (Northern Portugal). Lithos, 32: 207–223.

Dias G, Leterrier J, Mendes A, Simões PP, Bertrand JM (1998) U-Pb zircon and monazite geochronology of post-collisional Hercynian granitoids from the Central Iberian Zone (Northern Portugal). Lithos 45: 349–369.

Dias G, Simões PP, Ferreira N, Leterrier J (2002) Mantle and crustal sources in the genesis of late-hercynian granitoids (NW Portugal): geochemical and Sr-Nd isotopic constraints. Gondwana Research 5 (2): 287–305.

Dias D, Noronha F, Simões PP, Almeida A, Martins HCB, Ferreira N (2010) Geocronologia e Petrogénese do Plutonismo Tardi-Varisco (NW de Portugal): Síntese e Inferências sobre os Processos de Acreção e Reciclagem Crustal na Zona Centro-Ibérica- In: Cotelo Neiva JM, Ribeiro A, Mendes Victor, Noronha F, Magalhães Ramalho (Eds), Ciências Geológicas—Ensino e Investigação e sua História (1): 143–160.

Díaz-Alvarado J, Castro A, Fernández C, Moreno-Ventas I (2011) Assessing bulk assimilation in cordierite-bearing granitoids from the central system batholith, Spain; experimental, geochemical and geochronological constraints. Journal of Petrology 52(2): 223–256

Díaz-Alvarado J, Fernandez C, Castro A, Moreno-Ventas I (2013) SHRIMP U-Pb zircon geochronology and thermal modeling of multilayer granitoid intrusions. Implications for the building and thermal evolution of the Central System batholith, Iberian Massif, Spain. Lithos 175-176:104–123.

Duretz T, Gerya TV, May DA (2010) Numerical modelling of spontaneous slab breakoff and subsequent topographic response. Tectonophysics

Escuder Viruete J (1998) Relationships between structural units in the Tormes gneiss dome (NW Iberian Massif, Spain): geometry, structure and kinematics of contractional and extensional Variscan deformation. Geologische Rundschau 87(2): 165–179. https://doi.org/10.1007/s005310050199.

Escuder Viruete J, Indares A, Arenas R (1997) P-T path determinations in the Tormes Gneissic Dome, NW Iberian Massif, Spain. Journal of Metamorphic Geology 15(5): 645–663.

Escuder Viruete J, Indares A, Arenas R, (2000). P-T paths derived from garnet growth zoning in an extensional setting: an example from the Tormes Gneiss Dome (Iberian Massif, Spain). Journal of Petrology 41 (10): 1489–1515

Faure G (1986) Principles of Isotope Geology. Wiley & Sons, New York.

Fernández Suárez J, Dunning GR, Jenner GA, Gutiérrez Alonso G (2000) Variscan collisional magmatism and deformation in NW Iberia: constraints from U-Pb geochronology of granitoids. Journal of the Geological Society, London 157: 565–576.

Ferreira N, Iglesias M, Noronha F, Pereira E, Ribeiro A, Ribeiro ML (1987) -Granitóides da Zona Centro Ibérica e seu enquadramento geodinâmico. In: Bea F, Carnicero A, Gonzalo JC, López Plaza M, Rodriguez Alonso MD (eds) Geologia de los granitoides y rocas asociadas del Macizo Hespérico. Rueda (ed), Madrid, pp 37–51.

Ferreira J, Martins HCB, Ribeiro MA (2014) Geocronologia (U-Pb) e Geoquímica do granito do Pedregal. Comunicações Geológicas, Tomo 101 (I): 89–92.
Ferreira J, Martins H, Santos JF, Ribeiro MA (2015) Características isotópicas (Sr-Nd) do Granito do Pedregal e rochas migmatíticas associadas Comunicações Geológicas (102)1: 147–151.
Foley SF, Venturelli G, Green DH, Toscani L (1987) The ultrapotassic rocks: Characteristics, classification, and constraints for petrogenetic models. Earth Science Reviews (24): 81–134 https://doi.org/10.1016/0012-8252(87)90001-8.
Frost BR, Barnes CG, Collins WJ, Arculus RJ, Ellis DJ, Frost CD (2001) A geochemical classification for granitic rocks. J Petrol (42): 2033–2048.
Galán G, Pin C, Duthou JL (1996) Sr-Nd isotopic record of multi-stage interactions between mantle-derived magmas and crustal components in a collision context - The ultramafic-granitoid association from Vivero (Hercynian belt, NW Spain). Chemical Geology 131(1-4): 67–91.
Garcia Garzon J, Locutura j (1981) Datación por el método Rb-Sr de los granitos de Lumbrales-Sobradillo y Villar de Ciervos-Puerto Seguro. Boletin Geológico y Minero XCII (1): 68–72.
García-Arias M, Corretgé LG, Castro A (2012) Trace element behavior during partial melting of Iberian orthogneisses: An experimental study. Chemical Geology 292-293:1–17. https://doi.org/10.1016/j.chemgeo.2011.10.024.
Garrido CJ, Bodinier J-L, Burg J-P, Zeilinger G, Hussani SS, Dawood H, Chaudhry MN, Gervilla F (2006) Petrogenesis of mafic garnet granulite in the lower crust of the Kohistan paleo-arc complex (Northern Pakistan): Implications for intra-crustal differentiation of Island arcs and generation of continental crust. Journal of Petrology 47: 1873–1914.
Gil Ibarguchi JI, Martinez FJ (1982) Petrology of garnet - cordierite - sillimanite gneisses from the El Tormes thermal dome, Iberian Hercynian foldbelt (W Spain). Contributions to Mineralogy and Petrology 80(1): 14–24. https://doi.org/10.1007/BF00376731.
Gomes E (2000) Metamorfismo de rochas carbonatadas siliciosas da região de Alvito (Alentejo, Sul de Portugal). PhD Dissertation, Universidade de Coimbra.
Gonçalves F (1971) Subsídios para o conhecimento geológico do Nordeste alentejano. Mem. Serv. Geol. Port. Ns 18: 62 p.
Gonçalves F, Zbyszewski G, Pinto Coelho AV (1975) Carta Geológica de Portugal 1:50 000. Notícia Explicativa da Folha 32-D (Sousel). Serviços Geológicos de Portugal.
Gonzalez Menendez L (1998) Petrología y geoquímica del batolito granítico de Nisa-Alburquerque. PhD thesis, University of Granada, Spain, 221.
González Menéndez L, Azor A, Pereira MD, Acosta A, (2006) Petrogénesis del plutón de Santa Eulalia (Alto Alentejo, Portugal). Revista de la Sociedad Geológica de España (19): 69–86.
González Menéndez L, Solá AR (2011) Late Variscan Santa Eulalia Complex and the Nisa-Alburquerque Batholith. In: Scarrow JH (ed) VII Hutton Symposium on Granites and Related Rocks, Pre-meeting field trip-Southern Iberia Transverse, 49–61.
Gutiérrez-Alonso G, Fernández-Suárez J, Weil AB, Brendan Murphy J, Damian Nance R, Corf F, Johnston ST (2008) Self-subduction of the Pangaean global plate. Nature Geoscience 1(8): 549–553. https://doi.org/10.1038/ngeo250.
Gutiérrez-Alonso G, Fernández-Suárez J, Jeffries TE, Johnston ST, Pastor-Galán D, Murphy JB, Franco MP, Gonzalo JC (2011a) Diachronous post-orogenic magmatism within a developing orocline in Iberia, European Variscides. Tectonics 30(5). https://doi.org/10.1029/2010TC002845.
Gutiérrez-Alonso G, Murphy JB, Fernández-Suárez J, Weil AB, Franco MP, Gonzalo JC (2011b) Lithospheric delamination in the core of Pangea: Sm-Nd insights from the Iberian mantle. Geology 39(2): 155–158. https://doi.org/10.1130/G31468.1.
Halliday AN, Stephens WE, Harmon RS (1980) Rb-Sr and O isotopic relationships in 3 zoned Caledonian granitic plutons, Southern Uplands, Scotland: evidence for varied sources and hybridization of magmas. Journal of the Geological Society London 137: 329–348.
Hawkesworth CJ, Kemp AIS (2006) Evolution of the continental crust. Nature 443: 811–817.
Iglesias M, Choukroune P (1980) Shear zones in the Iberian arc. Journal Strctural Geology, 2 (1–2), pp 63–68.
IGME and LNEG (2014) Mapa Geológico de España y Portugal, Escala 1:1.000.000. Instituto Geológico y Minero de España, Madrid (Ed).
Irvine TN, Baragar WRA (1971). A Guide to the Chemical Classification of the Common Volcanic Rocks. Canadian Journal of Earth Sciences (8): 523–548. https://doi.org/10.1139/e71-055.
Jesus AP (2010) Ore forming systems in the western compartment of the Beja Layered Gabbroic sequence (Ossa Morena Zone Portugal). Universidade Lisboa (PhD Thesis).
Jesus A, Mateus A, Munhá J, Branco JMC, Araújo VH (2006a) Magmatic, Ni-Cu sulphide mineralization in the western compartment of the Beja Layered Gabbroic Sequence. VII Congresso Nacional de Geologia, Estremoz (Portugal), pp. 1019–1022.
Jesus A, Mateus A, Munhá J, Pinto A (2005a) Intercummulus massive Ni–Cu–Co, PGE-bearing sulphides in pyroxenite: a new mineralization type in the Layered Gabbroic Sequence of the Beja Igneous Complex (Portugal). In: Mao J, Bierlein FP (Eds), SGA Meeting? Mineral Deposit Research: Meeting the Global Change, Beijing (China). Springer Verlag, pp. 405–407.
Jesus AP, Mateus A, Munhá JM, Tassinari C (2014) Internal architecture and Fe–Ti–V oxide ore genesis in a Variscan synorogenic layered mafic intrusion, the Beja Layered Gabbroic Sequence (Portugal). Lithos (190): 111–136.
Jesus AP, Mateus A, Munhá J, Tassinari CCG, Bento dos Santos TM, Benoit M (2016) Evidence for underplating in the genesis of the Variscan synorogenic Beja Layered Gabbroic Sequence (Portugal) and related mesocratic rocks. Tectonophysics (683): 148–171.
Jesus A, Munhá J, Mateus A (2005b) Critical features controlling the evolution of the Beja Layered Gabbroic Sequence; implications to ore-forming processes. VIII Congresso de Geoquímica dos Países de Língua Portuguesa? XIV Semana de Geoquímica, Aveiro (Portugal), pp. 305–310.
Jesus A, Munhá J, Mateus A (2006b) The western compartment of the Beja Layered Gabbroic Sequence: internal architecture and main petrogenetic features. VII Congresso Nacional de Geologia, Estremoz (Portugal), pp. 171–174.
Jesus AP, Munhá J, Mateus A, Tassirari C, Nutman AP (2007) The Beja layered gabbroic sequence (Ossa Morena Zone),Southern Portugal): geochronology and geodynamic implications. Geodynamic Acta, 20/3, 139–157.
Julivert M, Fonbote JM, Ribeiro A, Conde L (1974) Mapa tectónico de la península Ibérica y Baleares, escala 1: 1000 000. Instituto Geológico y Minero de España, Madrid.
Le Bas MJ, Streckeisen AL (1991) The IUGS systematics of igneous rocks Journ of Geological Society, London (148): 825–833.
Lains JA (2015) Notas sobre os Complexos Ígneos de Veiros e Vale de Maceira. Livro de Resumos do X Congresso Ibérico de Geoquímica/XVIII Semana de Geoquímica. Lisboa, 27–30.
Leslie RAJ, Danyushevsky LV, Crawford AJ, Verbeeten AC (2009) Primitive shoshonites from Fiji: Geochemistry and source components. Geochemistry, Geophysics, Geosystems 10. https://doi.org/10.1029/2008GC002326
Lima SM, Corfu F, Neiva AMR, Ramos MF (2012) Dissecting complex magmatic processes: an in-depth U–Pb study of the Pavia pluton, Ossa-Morena Zone, Portugal. J Petrol 53 (9): 1887–1911.
LNEG (ed) (2010) Carta Geológica de Portugal, Escala 1: 1 000 000. Laboratório Nacional de Energia e Geologia, Lisboa (Ed).

Lopes JC (1989) Geoquímica de Granitóides Hercínicos na Zona de Ossa-Morena: o Maciço de St.ª Eulália. Dissertação apresentada em Provas de Aptidão Pedagógica e Capacidade Científica (Estatuto da Carreira Docente Universitária), Universidade de Évora, 138 pp.

Lopes JC (2004) Petrologia e Geoquímica de Complexos Plutónicos do Nordeste Alentejano (Portugal Central). Província Alcalino e Maciço de Campo Maior. Unpl. PhD thesis, Universidadde de Évora, 505 pp.

Lopes JC, Munhá J, Tassinari C, Pin C (2005) Petrologia e geocronologia, Sm-Nd, do maciço de Campo Maior, Alentejo, Portugal central. Comunicações Geológicas (92): 5–30.

Lopes JC, Munhá J, Wu CT, Oliveira V (1998) O Complexo Plutónico de Monforte-Santa Eulália (Alentejo-NE, Portugal Central): caracterização geoquímica e considerações petrogenéticas. Comunicações do Instituto Geológico e Mineiro, Tomo 83: 127–142.

Lopes JC, Sant'Ovaia H, Martins HCB, Nogueira P, Lopes L (2016) U-Pb geochronology and Nd isotope contributions to the interpretation of a peculiar ring massif: the Santa Eulália plutonic complex (SW Iberia, Portugal). Abstracts of the 35th International Geological Congress, Cape Town, South Africa. https://www.americangeosciences.org/sites/default/files/igc/2503.pdf.

López-Moro F-J, López-Plaza M (2004) Monzonitic series from the Variscan Tormes Dome (Central Iberian Zone): petrogenetic evolution from monzogabbro to granite magmas. Lithos 72(1–2): 19–44.

López-Moro FJ, López-Plaza M, Romer RL (2012) Generation and emplacement of shear-related highly mobile crustal melts: The synkinematic leucogranites from the Variscan Tormes Dome, Western Spain. International Journal of Earth Sciences 101(5): 1273–1298. https://doi.org/10.1007/s00531-011-0728-1.

Martins HCB, Sant'Ovaia H, Noronha F (2009) Genesis and emplacement of felsic Variscan plutons within a deep crustal lineation, the Penacova-Régua-Verín fault: an integrated geophysics and geochemical study (NW Iberian Peninsula). Lithos (111): 142–155.

Martins HCB, Sant'Ovaia H, Abreu J, Oliveira M, Noronha F (2011) Emplacement of the Lavadores granite (NW Portugal): U-Pb and AMS results. Comptes Rendus Geosciences 343 (6): 387–396.

Martins HCB, Sant'Ovaia H, Noronha F (2013) Late-Variscan emplacement and genesis of the Vieira do Minho composite pluton, Central Iberian Zone: Constraints from U-Pb zircon geochronology, AMS data and Sr-Nd-O isotope geochemistry. Lithos: (162/163): 221–235.

Martins HCB, Ribeiro MA, Sant'Ovaia H, Abreu J, Garcia de Madinabeitia S (2014) SHRIMP and LA-ICPMS U–Pb zircon geochronology of post-tectonic granitoid intrusions in NW of Central Iberian Zone. Comunicações Geológicas Tomo 101 (I): 147–150.

Mateus A, Figueiras J, Gonçalves MA, Fonseca P (1999) Evolving fluid circulation within the Variscan Beja-Acebuches Ophiolite Complex (SE, Portugal). Ofioliti (24): 269–282.

Mendes A, Dias G (2004) Mantle-like Sr-Nd isotope composition of Fe-K subalkaline granites: the Peneda-Gerês Variscan massif (NW Iberian Peninsula). Terra Nova, vol. 16 (3): 109–115.

Mendes F (1967/68) Contribution l'étude géochronologique, par la méthode au strontium, des formations cristallines du Portugal. Bol. Mus. Lab. Geol. Fac. Ciências (11)1: 156 pp.

Miyashiro A, Aki K, Sengor AMC (1982) Orogeny. John Wiley, Chichester.

Moita P (2008) Granitóides no SW da Zona de Ossa-Morena (Montemor-o-Novo—Évora): Petrogénese e Processos Geodinâmicos. PhD Dissertation, Universidade de Évora.

Moita P, Munhá J, Fonseca P, Tassinari C, Araújo A, Palácios T (2005a) Dating orogenic events in Ossa-Morena Zone. Actas do XIV Semana de Geoquímica/VIII Congresso de Geoquímica dos Países de Língua Portuguesa (2): 459–462.

Moita P, Santos J, Pereira MF (2005b) Dados geocronológicos de rochas intrusivas sintectónicas no Maciço dos Hospitais (Montemor-o-Novo, ZOM). Actas do XIV Semana de Geoquímica/VIII Congresso de Geoquímica dos Países de Língua Portuguesa (2): 471–474.

Moita P, Munhá J, Fonseca P, Tassinari C, Araújo A, Palácios T (2005c) Phase equilibria and geochronology of Ossa-Morena eclogites. In: XIV Semana de Geoquímica/VIII Congresso de Geoquímica dos Países de Língua Portuguesa. pp 463–466.

Moita P, Santos JF, Pereira MF (2009) Layered granitoids: interaction between continental crust recycling processes and mantle-derived magmatism. Examples from the Évora Massif (Ossa-Morena Zone, southwest Iberia, Portugal). Lithos 111, (3–4): 125–141.

Moita P, Santos JF, Silva P, Pardal E, (2011) Geochemical signature of the Pomarinho enclave swarm (Ossa-Morena Zone, Portugal). In: Abstracts of Seventh Hutton Symposium on Granites and Related Rocks. University of Ávila (Spain).

Moita P, Santos JF, Pereira MF, Costa M, Corfu, F, (2015) The quartz-dioritic Hospitais intrusion (SW Iberian Massif) and its mafic microgranular enclaves—evidence for mineral clustering. Lithos 224–225: 78–100.

Montero P, Talavera C, Bea F, Lodeiro FG, Whitehouse MJ (2009) Zircon geochronology of the Ollo de Sapo Formation and the age of the Cambro-Ordovician rifting in Iberia. Journal of Geology 117(2): 174–191.

Moreno-Ventas I, Rogers G, Castro A (1995) The role of hybridization in the genesis of Hercynian granitoids in the Gredos massif, Spain: inferences from Sr-Nd isotopes. Contributions to Mineralogy and Petrology 120(2): 137–149.

Morrison CW (1980) Characteristics and tectonic settings of shoshonite rock association. Lithos (13): 97–108. https://doi.org/10.1016/0024-4937(80)90067-5.

Muñoz G, Mateus A, Pous J, Heise W, Monteiro-Santos F, Almeida E (2008) Unravelling middle crust conductive layers in Paleozoic Orogens through 3D modelling of magnetotelluric data: the Ossa-Morena Zone case study (SW Iberian Variscides). J. Geophys. Res. (113): B06106.

Murphy JB (2013) Appinite suites: A record of the role of water in the genesis, Transport, Emplacement and crystallization of magma. Earth Science Reviews 119: 35–59.

Nomade S, Renne PR, Mo X, Zhao Z, Zhou S (2004).Miocene volcanism in the Lhasa block Tibet: Spatial trends and geodynamic implications. Earth and Planetary Science Letters 227–243. https://doi.org/10.1016/s0012-821x(04)00072-x.

Oliveira JT, Oliveira V, Piçarra JM (1991) Traços gerais da evolução tectono-estratigráfica da Zona de Ossa-Morena, em Portugal. Cuadernos do Laboratorio Xeolóxico de Laxe (16): 221–250.

Otamendi JE, Ducea MN, Tibaldi AM, Bergantz GW, de la Rosa JD, Vujovich GI (2009a) Generation of tonalitic and dioritic magmas by coupled partial melting of gabbroic and metasedimentary rocks within the deep crust of the Famatinian magmatic arc, Argentina. Journal of Petrology 50(5): 841–873.

Otamendi JE, Vujovich GI, de la Rosa JD, Tibaldi AM, Castro A, Martino RD, Pinotti LP (2009b) Geology and petrology of a deep crustal zone from the Famatinian paleo-arc, Sierras de Valle Fértil and La Huerta, San Juan, Argentina. Journal of South American Earth Sciences 27(4): 258–279.

Patiño Douce AE (1999) What do experiments tell us about the relative contributions of crust and mantle to the origin of granitic magmas? In: Castro A, Fernández C, Vigneresse JL (eds) Understanding granites Integrating new and classical techniques, vol 168. The Geological Society, London, pp 55–75.

Peccerillo A, Frezzotti ML(2015). Magmatism, mantle evolution and geodynamics at the converging plate margins of Italy. Journal of the

Geological Society (172): 407–427. https://doi.org/10.1144/jgs2014-085.
Pedro JC, Araújo A, Fonseca P. Tassinari C, Ribeiro A (2010). Geochemistry and U-Pb zircon age of the Internal Ossa-Morena Zone Ophiolite Sequences: a remnant of rheic ocean in SW Iberia. Ofioliti (35): 117–130. https://doi.org/10.4454/ofioliti.v35i2.390.
Pereira MF, Chichorro M, Williams IA, Silva JB, Fernández C, Díaz-azpíroz M, Apraiz A, Castro A (2009) Variscan intra-orogenic extensional tectonics in the Ossa-Morena Zone (Évora-Aracena--Lora del Río metamorphic belt, SW Iberian Massif): SHRIMP zircon U-Th-Pb geochronology. Geol Soc London Spec Publ (327): 215–237.
Pereira M, Chichorro M, Fernández C, Silva JB, Matias FV (2013) The role of strain localization in magma injection into a transtensional shear zone (Variscan belt, SW Iberia). Journal of the Geological Society, London (170): 93–105.
Pereira MF, Castro A, Fernández C (2015a) The inception of a Paleotethyan magmatic arc in Iberia. Geoscience Frontiers. 6 (2):297–306. https://doi.org/10.1016/j.gsf.2014.02.006.
Pereira MF, Chichorro M, Moita P, Santos J F, Solá AMR, Williams IS, Silva JBR, Armstrong A (2015b) The multistage crystallization of zircon in calc alkaline granitoids: U–Pb age constraints on the timing of Variscan tectonic activity in SW IberiaInt J Earth Sci (Geol Rundsch), https://doi.org/10.1007/s00531-015-1149-3.
Pereira MF, Silva JBS (2001) The Portalegre-Esperança shear zone: sinistral transcurrent transpression along the Ossa-Morena/Central-Iberian zones boundary (Northeast Alentejo, Portugal). Comunicações do Instituto Geológico e Mineiro (88): 19–32.
Pérez-Cáceres I, Martínez Poyatos D, Simancas JF, Azor A (2015) The elusive nature of the Rheic Ocean suture in SW Iberia. Tectonics 34 (12): 2429–2450. https://doi.org/10.1002/2015TC003947.
Pin C, Paquette J-L, Fonseca PE (1999) 350 Ma (U-Pb zircon) igneous emplacement age and Sr-Nd isotopic study of the Beja gabbroic complex (S. Portugal). In: Gámez JA, Eguiluz L, Palácios T (Eds.), Proceedings on the XV Reunión de Geología del Oeste Peninsular, Badajoz, pp 190–194.
Pin C, Fonseca PE, Paquette J-L, Castro P, Matte P (2008) The ca. 350 Ma Beja Igneous Complex: a record of transcurrent slab break-off in the Southern Iberia Variscan Belt? Tectonophysics (461): 356–377.
Pinto Coelho, A. V., Gonçalves, F. & Torquato, J. R. (1974). Rochas hipersténicas do Alto-Alentejo. Boletín Geológico y Minero (15): 601–603.
Pinto MS (1983) Geochronology of portuguese granitoids: a contribution. Stvd. Geol. Salmant., XVIII, pp. 277–306.
Pinto MS (1984) Granitóides Caledónicos e Hercínicos na Zona de Ossa-Morena (Portugal). Memórias e Noticias Publicações do Museu e Laboratório Mineralógico e Geológico da Universidade de Coimbra, Portugal (97): 81–94.
Pitcher WS (1979) Origin of granite batholiths, geochemical evidence. Atherton and Tarney (ed).
Pitcher WS (1997) The nature and origin of Granite. Chapman & Hall, Glasgow
Portugal Ferreira M (1982) A magmatic arc in the iberian segment of the Hercynian chain: I- The Nortwest-Southeast lineament between Oporto (Portugal) and Zarza la Mayor (Spain). Memórias e Notícias Museu Mineralógico e Geológico Universidade de Coimbra (94): 31–50.
Pous J, Muñoz G, Heise W, Melgarejo JC, Quesada C (2004) Electromagnetic imaging of Variscan crustal structures in SWIberia: the role of interconnected graphite. Earth Planet. Sci. Lett. (217): 435–450.
Read HH (1957) The granite controversy. Thomas Murby & Co., London.
Ribeiro A, Iglésias M, Ribeiro ML, Pereira E (1983) Modèle geodynamique des Hercynides Ibériques. Com. Serv. Geol. Portugal, Lisboa, (69)2: 291–293.
Ribeiro, A., Munhá, J., Dias, R., Mateus, A., Pereira, E., Ribeiro, L., Fonseca, P., Araújo, A., Oliveira T, Romão JC, Chaminé H, Coke C, Pedro J (2007)—Geodynamic evolution of SW Europe Variscides. Tectonics (26), TC6009. https://doi.org/10.1029/2006tc002058.
Ribeiro A, Munhá J, Fonseca PE, Araújo A, Pedro JC, Mateus A, Tassinari C, Machado G, Jesus, AP (2010) Variscan ophiolite belts in the Ossa-Morena Zone (Southwest Iberia): geological characterization and geodynamic significance. Gondwana Res (17): 408–421. https://doi.org/10.1016/j.gr.2009.09.005.
Ribeiro ML (1986) Geologia e Petrologia da região a SW de Macedo de Cavaleiros (Trás-os-Montes). Tese de doutoramento, Universidade de Lisboa.
Ribeiro ML, Mata J, Munhá J (1992)—Magmatismo do Paleozóico inferior em Portugal. 1ª Conf. Intern. da Ibero-América, pp 378–394. Gutiérrez Marco, J.G. Saavedra, J. & Rábano, I. (Eds) Universidade Extremadura, Espanha.
Ribeiro ML (1993) Granitos do Ocidente ibérico: contribuição para a sua interpretação geodinâmica. Cuaderno do Laboratório Xeolóxico de Laxe: (18): 7–26. La Coruña.
Ribeiro ML, Munhá J, Mata J, Palácios T (1997) Vulcanismo na Zona de Ossa Morena e seu enquadramento geodinâmico. Estudo sobre a Geologia da Zona de Ossa-Morena (Maciço Ibérico), Homenagem ao Prof. Francisco Gonçalves, pp. 37–55. A Alexandre Araújo, MF Pereira (Eds). Évora.
Rickwood PC (1989) Boundary lines within petrologic diagrams which use oxides of major and minor elements. Lithos (22): 247–263.
Rosas F (2003) Estudo tectónico do sector de Viana do Alentejo-Alvito. PhD dissertation, University of Lisbon.
Ruffet G (1990) 40Ar/39Ar dating of the Beja gabbro: timing of the accretion of southern Portugal. Geophys. Res. Lett. (17): 2121–2124.
Sant'Ovaia H, Nogueira P, Lopes JC, Gomes C, Ribeiro MA, Martins HCB, Dória A, Cruz C, Lopes L, Sardinha R, Rocha A, Noronha F (2015) Building up of a nested granite intrusion: magnetic fabric, gravity modelling and fluid inclusion planes studies in Santa Eulália Plutonic Complex (Ossa-Morena Zone, Portugal). Geological Magazine, 152, 4: 648–667. https://doi.org/10.1017/S0016756814000569.
Santos J F, Andrade A S and Munhá J (1990) Magmatismo Orogénico Varisco no limite meridional da Zona de Ossa-Morena. Comunicações dos Serviços Geológicos de Portugal. (76): 91–124.
Scarrow JH, Molina JF, Bea F, Montero P (2009) Within-plate calc-alkaline rocks: Insights from alkaline mafic magma–peraluminous crustal melt hybrid appinites of the Central Iberian Variscan continental collision. Lithos 110: 50–64.
Schermerhorn LJG (1956) Igneous metamorphic and ore geology of Castro-Daire-S. Pedro do Sul-Satão region (northern Portugal). Comun. Serv. Geol. Portugal, Lisboa. (37): 617.
Schermerhorn LJG (1987) The Hercynian gabbro-tonalite-leucogranite suite of Iberia: geochemistry and fractionation. Geol. Rundschau (76) 1: 137–145.
Silva JC, Mata J, Moreira N, Fonseca PE, Jorge RCGS, Machado G (2011). Evidência para o funcionamento, desde o Devónico Inferior, de subducção no bordo meridional da Zona de Ossa-Morena. Livro de Resumos do VIII Congresso Ibérico de Geoquímica/XVII Semana de Geoquímica. Castelo Branco, 295–299.
Silva LC, Quadrado R, Ribeiro L (1970) Nota prévia sobre a existência de uma estrutura zonada e de anortositos no maciço gabro-diorítico de Beja. Bol. Mus. Lab. Mineral. Geol. Univ. Lisboa (11): 223–232.
Silva MMVG (2010) O granito de Lavadores e seus encraves. In: Cotelo Neiva JM, Ribeiro A, Mendes Victor, Noronha F,

Magalhães Ramalho (Eds), Ciências Geológicas—Ensino e Investigação e sua História (1): 269–279.

Silva M, Pinto M (2006) Geoquímica das rochas ígneas do plutão de Reguengos de Monsaraz (Alto Alentejo). In: Abstracts of VII Congresso Nacional de Geologia, Centro de Geofísica de Évora.

Simancas JF, Carbonell R, Gonzalez-Lodeiro F, Perez-Estaun A, Juhlin C, Ayarza P, Kashubin A, Azor A, Martínez-Poyatos D, Ruiz-Almodovar G, Pascual E, Saez R, Expósito I (2003) Crustal structure of the transpressional Variscan orogen of SW Iberia: SW Iberia deep seismic reflection profile (IBERSEIS). Tectonics (22): 1962–1974.

Simões PP (2000) Instalação, geocronologia e petrogénese de granitóides biotíticos sintectónicos associados ao cisalhamento Vigo-Régua (ZCI, Norte de Portugal). PhD Thesis (unpubl) Universidade do Minho, Braga, 351 pp.

Soen OI (1970) Granite intrusion, folding and metamorphism in central northern Portugal » . Bol. Geol. Min. España. (LXXXI)-II-III: 271–298.

Solá AR, Williams IS, Neiva AMR, Ribeiro ML (2007) The Nisa granitic massif: SRIMP zircon U-Pb age and source constrains. Geochimica et Cosmochimica Acta, A953, Goldschmidt, Conference Abstracts.

Solá AR, Pereira MF, Williams IS, Ribeiro ML, Neiva AMR, Montero P, Bea F, Zinger T (2008) New insights from U–Pb zircon dating of Early Ordovician magmatism on the northern Gondwana margin: The Urra Formation (SW Iberian Massif, Portugal). Tectonophysics (461): 114–129.

Solá AR, Williams IS, Neiva AMR, Ribeiro ML (2009) U-Th-Pb SHRIMP ages and oxygen isotope composition of zircon from two contrasting late Variscan granitoids, Nisa-Albuquerque batholith, SW Iberian Massif: Petrologic and regional implications. Essevier BV, Lithos (111): 156–167.

Sun S, McDonough WF (1989) Chemical and isotopic systematics of oceanic basalts: implications for mantle composition and processes. Geological Society, London (42): 313–345.

Teixeira RJS, Neiva AMR, Gomes MEP, Corfu F, Cuesta A, Croudace IW (2012) The role of fractional crystallization in the genesis of early syn-D3, tin-mineralized Variscan two-mica granites from the Carrazeda de Ansiães area, northern Portugal. Lithos (153): 177–191.

Ugidos JM, Recio C (1993) Origin of cordierite-bearing granites by assimilation in the Central Iberian Massif (CIM), Spain. Chemical Geology 103(1–4): 27–43.

Ugidos JM, Stephens WE, Carnicero A, Ellam RM (2008) A reactive assimilation model for regional-scale cordierite-bearing granitoids: geochemical evidence from the Late Variscan granites of the Central Iberian Zone, Spain. Earth and Environmental Science Transactions of the Royal Society of Edinburgh 99: 225–250.

Valle Aguado B, Azevedo MR, Schaltegger U, Martínez Catalán JR, Nolan J (2005) U-Pb zircon and monazite geocrhronology of Variscan magmatism related to syn-convergence extension in Central Northern Potugal. Lithos (82): 169–184.

Vieira-da-Silva N, Mateus A, Monteiro-Santos FA, Almeida EP, Pous J (2007) 3-D electromagnetic imaging of a Palaeozoic plate-tectonic boundary segment in SW Iberian Variscides (S Alentejo, Portugal). Tectonophysics (445): 98–115.

Villaseca C, Belousova E, Orejana D, Castiñeiras P, Pérez-Soba C (2011) Presence of Palaeoproterozoic and Archean components in the granulite-facies rocks of central Iberia: The Hf isotopic evidence. Precambrian Research (187): 143–154.

Villaseca C, Orejana D, Belousova EA (2012) Recycled metaigneous crustal sources for S- and I-type Variscan granitoids from the Spanish Central System batholith: Constraints from Hf isotope zircon composition. Lithos 153: 84–93. https://doi.org/10.1016/j.lithos.2012.03.024.

Viruete JE, Indares A, Arenas R (2000) P-T paths derived from garnet growth zoning in an extensional setting: An example from the Tormes Gneiss Dome (Iberian Massif, Spain). Journal of Petrology 41(10): 1489–1515.

Vogt K, Gerya TV, Castro A (2012) Crustal growth at active continental margins: Numerical modeling. Physics of the Earth and Planetary Interiors 192–193: 1–20.

Weinberg RF, Hasalová P (2015) Water-fluxed melting of the continental crust: A review. Lithos (212–215): 158–188.

Wenzel T, Mertz DF, Oberhänsli R, Becker T, Renne PR (1997) Age, geodynamic setting, and mantle enrichment processes of a K-rich intrusion from the Meissen massif (northern Bohemian massif) and implications for related occurrences from the mid-European Hercynian. International Journal of Earth Sciences (Geologische Rundschau) (86): 556–570. https://doi.org/10.1007/s005310050163.

Windley BF (1995) The Evolving Continents. John Wiley & Sons Ltd., Chichester.

Wyllie PJ, Huang WL, Stern CR, Maaloe S (1976) Granitic magmas: possible and impossible sources, water contens, and crystallization sequences. Canadian Journal of Earth Sciences 13: 1007–1019.

Late/Post Variscan Orocline Formation and Widespread Magmatism

14

Arlo Weil, D. Pastor-Galán, S. T. Johnston, and G. Gutiérrez-Alonso

Abstract

The Paleozoic geology of Iberia is dominated by the tectonics of the Variscan orogeny and its aftermath. This defining geologic event was the result of large-scale collision that involved amalgamation of multiple continents and micro-continents, the closure of oceanic basins and eventual orogenic collapse, and finally modification and oroclinal bending during the waning stages of Pangea amalgamation. Existing data from the western Variscan orogen, suggests oroclinal bending of an originally near-linear convergent margin during the last stages of Variscan deformation occurred in the late Paleozoic. Earlier closure of the Rheic Ocean resulted in E-W shortening (in present-day coordinates) in the Carboniferous, producing a N-S trending, east verging belt. Subsequent deformation near the Carboniferous-Permian boundary resulted in oroclinal bending. This late-stage orogenic event remains an enigmatic part of Iberia's Paleozoic history.

Coordinator: Arlo Weil.

A. Weil (✉)
Department of Geology, Bryn Mawr College, Bryn Mawr, PA, USA
e-mail: aweil@brynmawr.edu

D. Pastor-Galán
Center for Northeast Asian Studies, Tohoku University, Sendai, Japan
e-mail: dpastorgalan@gmail.com

S. T. Johnston
Earth and Atmospheric Sciences, University of Alberta, Edmonton, AB, Canada
e-mail: stjohnst@ualberta.ca

G. Gutiérrez-Alonso
Departamento de Geología, Universidad de Salamanca, Salamanca, Spain
e-mail: gabi@usal.es

G. Gutiérrez-Alonso
Geology and Geography Department, Tomsk State University, Lenin Street 36, Tomsk, 634050, Russian Federation

14.1 Introduction

The formation of the supercontinent Pangea, one of the cornerstones of geology and plate tectonics, has a complex history that is preserved in the geologic record of the Paleozoic Era. Although, the kinematics and mechanisms responsible for its amalgamation are not fully understood and still debated (e.g. Domeier et al. 2012; Stampfli et al. 2013; Domeier and Torsvik 2014; Gallo et al. 2017), the general consensus is that the final amalgamation of Pangea occurred during the late Paleozoic. At the supercontinents center was the sinuous Variscan–Alleghanian orogeny, which formed from the oblique collision between Gondwana, Laurussia, and several microplates, and the closure of at least two and probably four oceans (Fig. 14.1) (Winchester et al. 2002; Martínez-Catalán et al. 1997, 2007; Matte 2001; Franke et al. 2017). This collisional belt is a complex continental-scale orogen (1000 km wide and 8000 km long) that formed through a series of protracted tectonic episodes from initial convergence at about 420 Ma to final collision at about 310 Ma (e.g., Franke et al. 2005; Martínez-Catalán et al. 2007; Diez-Fernández et al. 2016).

Though not the focus of this section, a brief review of the Variscan system in Iberia is given to establish the existing geologic framework of the region prior to the late-Variscan modification that produced oroclinal rotations, and resulted in coeval widespread magmatism. The European Variscan autochthon is generally thought to be of Gondwanan affinity and consists of an early Paleozoic passive margin sequence constructed unconformably on Proterozoic crust that itself was deformed during Cadomian (late Ediacaran) orogenesis (e.g. Abati et al. 2010; Pastor-Galán et al. 2013a; Shaw et al. 2014; Gutiérrez-Alonso et al. 2015). The allochthonous terranes of the Variscan orogen include continental terranes of peri-Gondwanan affinity and oceanic terranes containing ophiolites, arc rocks and associated accretionary complexes. The Rheic Ocean is the paleogeographic realm that opened during the early Paleozoic drift of peri-Gondwanan terranes

C. Quesada and J. T. Oliveira (eds.), *The Geology of Iberia: A Geodynamic Approach*, Regional Geology Reviews,
https://doi.org/10.1007/978-3-030-10519-8_14

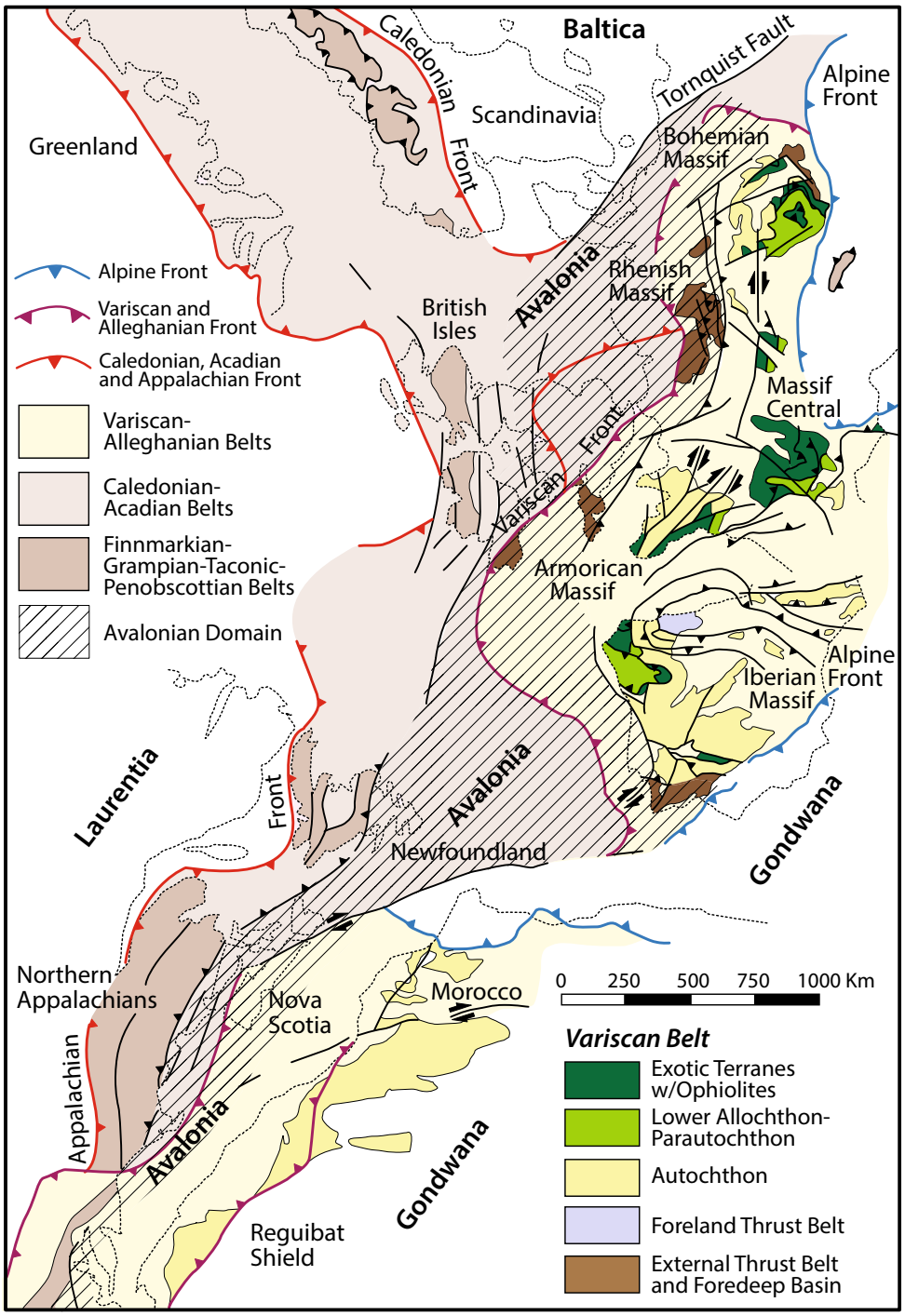

Fig. 14.1 Tectonostratigraphic and paleogeographic map of the Caledonide-Appalachian-Variscan orogenic system (modified after Martínez-Catalán et al. 2009)

(e.g., Avalonia-Meguma) from the northern margin of West Gondwana. Opening of the Rheic Ocean produced passive margin sedimentation along the north-facing Variscan margin of Gondwana. The boundary between the Variscan autochthon and peri-Gondwanan allochthon marks the suture of the Rheic Ocean (e.g., Murphy et al. 2006; Nance and Linnemann 2008; Nance et al. 2010, 2012). Though consensus exists on the importance of the Rheic Ocean in the tectonic evolution of the Variscan orogeny, there remains debate on the existence of additional basins that may have been involved in generating the tectonostratigraphic framework observed today (e.g., Lardeaux 2014; von Raumer

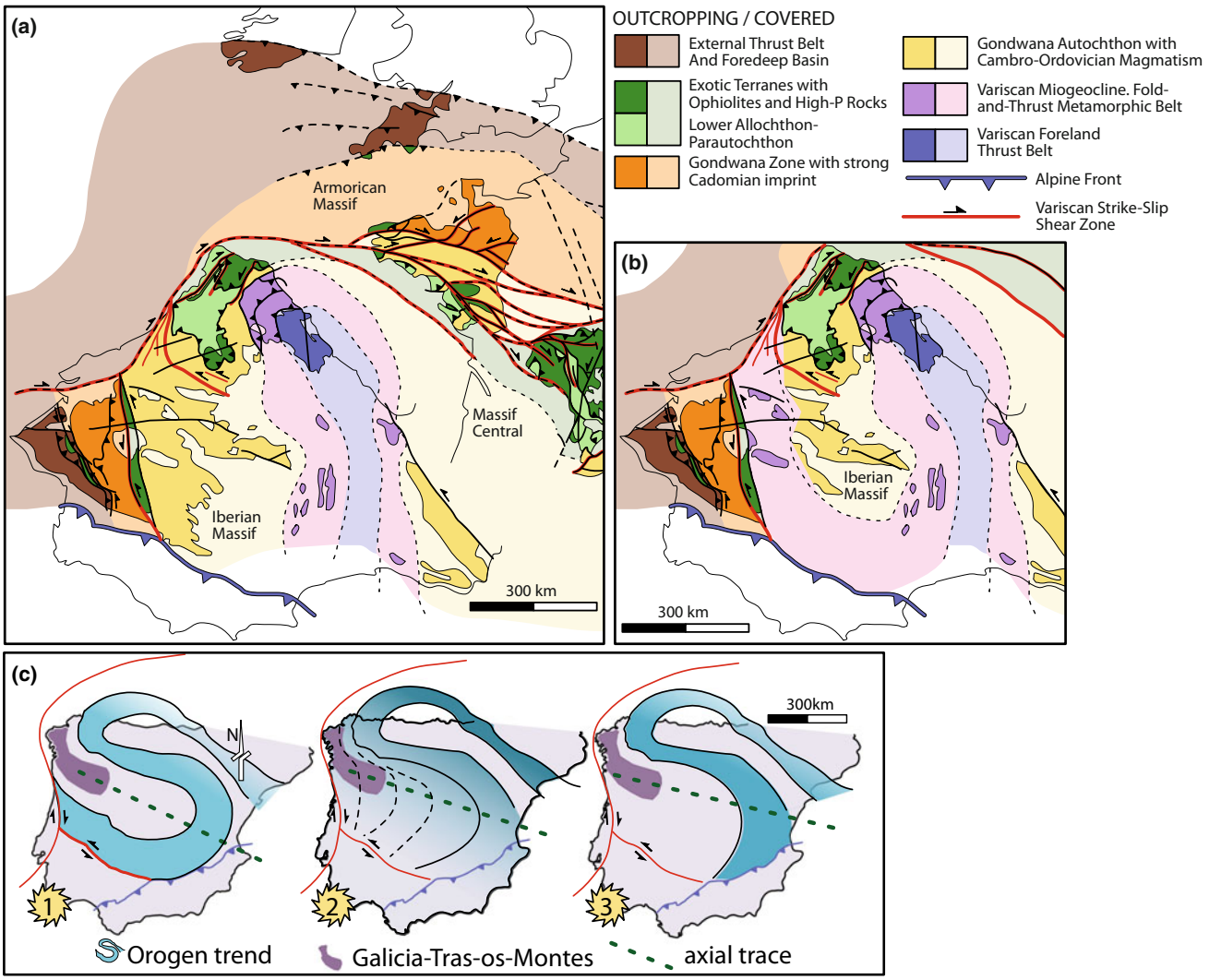

Fig. 14.2 **a** A classic interpretation of the tectonostratigraphic zonation of the Variscan orogen in southwestern Europe (modified from Franke 1989; Martínez-Catalán et al. 2007). **b** Alternative interpretation with Iberian oroclines after Shaw et al. (2015). **c** Alternative geometries of the proposed double orocline of Iberia

et al. 2009, 2013; Stampfli et al. 2002; Franke et al. 2000, 2017; Tait et al. 2000; Matte 1986, 1991, 2001).

The Iberian Massif preserves the most complete exposure of the Variscan autochthon (Fig. 14.2) (e.g., Du Toit 1937; Dvorak 1983; Martínez Catalán 2011). The autochthon has historically been divided into a series of tectonostratigraphic domains based on their pre-Variscan stratigraphy and Variscan deformational style. From east to west, in present-day coordinates, is a thin-skinned foreland fold and thrust belt, and external and internal hinterland domains that become progressively more deformed and metamorphosed toward the shallowly emplaced ophiolites to the west (Fig. 14.2) (e.g., Martínez-Catalán et al. 2007). Sedimentological, geochemical, and paleontological constraints indicate that during the early Paleozoic, the foreland and hinterland autochthonous domains were positioned as a north-facing passive margin off the north margin of West Gondwana (e.g., Shaw and Johnston 2016a).

Late, to post-orogenic modification of the Europe Variscan Belt was ultimately responsible for its characteristic sinuous shape that today traces at least one, and possibly four complete arcs (arc is used throughout this section as a geometric description of a curved orogenic system, with no implications on genesis of the curvature or magmatism) from Poland to Brittany, and then across the Bay of Biscay (Cantabrian Sea) into Iberia, where the belt is truncated by the Betic Alpine front in southern Spain (Fig. 14.2). Today the Variscan of Iberia is interpreted to define a sinuous "S" shape trend that has stimulated debate for more than a century (Fig. 14.2; e.g. Suess 1885; Staub 1926). The Cantabrian Orocline (orocline is used throughout this paper as a kinematic term that describes the secondary rotation of

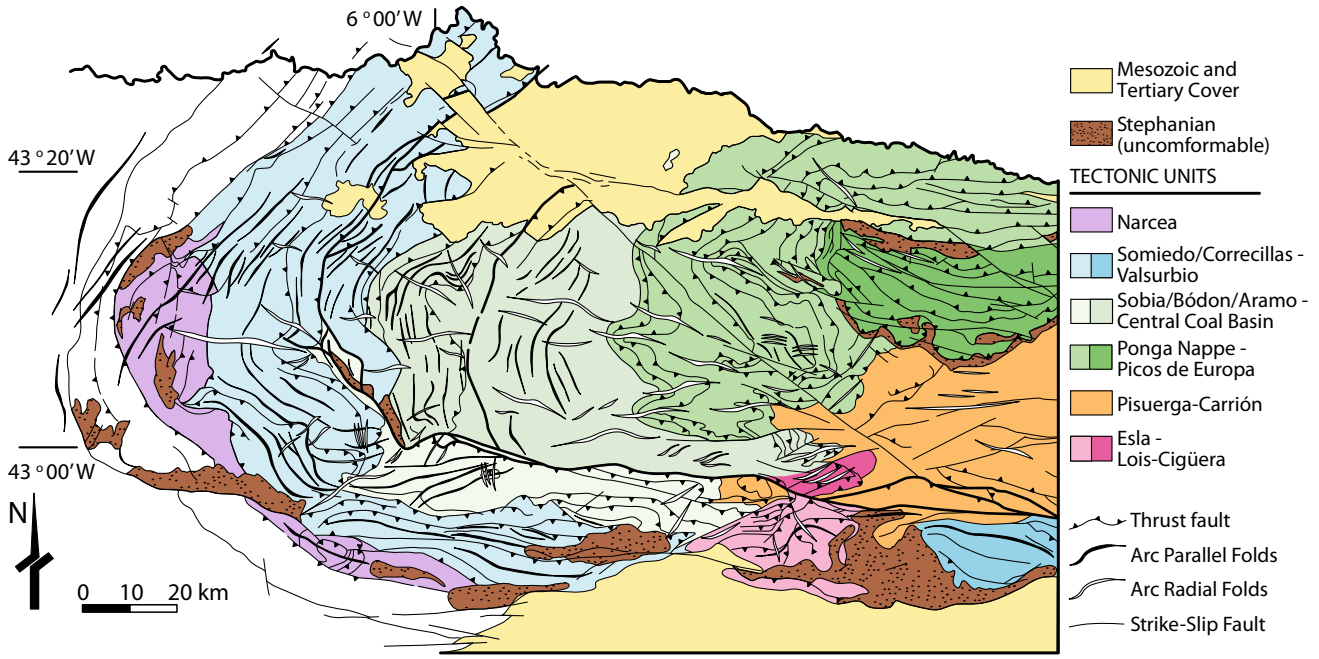

Fig. 14.3 Simplified structure/tectonic map of the Cantabrian Orocline, highlighting the geometry of major thrusts and the orientation of arc-parallel and arc-perpendicular folds. Tectonic unit divisions modified from Alonso et al. (2009)

an originally linear orogenic system—as originally defined by Carey 1955) is the name used herein to describe the concave to the east (forelandward) curvature located in northwest Spain and northern Portugal (Fig. 14.3) (a.k.a. Cantabrian Arc and Cantabria-Asturias Arc). The Central Iberian Arc, which is less conspicuous, is located in central Spain and is characterized by a convex to the west curvature (Fig. 14.2) (a.k.a. Central Iberian Curve, Central Iberian Orocline). Whereas the kinematics of the Cantabrian Orocline is well established, the shape, kinematic and tectonic implications of the Central Iberian Arc are debated (Fig. 14.2c).

14.2 The Cantabrian Orocline: Geometry and Kinematics

The Cantabrian Orocline is one of the first curved orogens ever described in the literature. Referred to as the "Asturian knee" (Suess 1885), the tectonic bend was recognized by the change in structural trend of thrusts and fold axes that when mapped, trace an arc curvature of up to 180° that opens towards the foreland (Fig. 14.3). At its full extent, the Cantabrian Orocline is a first order vertical axis fold that refolds pre-existing Variscan structures. In the core of the orocline are an assortment of structures that record non-coaxial strain, which produced complex interference folds and rotated thrust sheets (e.g. Julivert and Marcos 1973; Aller and Gallastegui 1995; Weil 2006; Pastor-Galán et al. 2012; Shaw et al. 2016; Del Greco et al. 2016).

Many authors have studied the Cantabrian Orocline over the past few decades, especially within its core, the Cantabrian Zone (Fig. 14.3). This body of work resulted in a variety of hypotheses for how, when, and why the orocline formed. The Cantabrian Zone, representing the Gondwanan foreland fold-and-thrust belt of the Variscan Orogen, is characterized by tectonic transport towards the core of the orocline, i.e., the orocline has a contractional core, where low finite strain values and locally developed cleavage occur (Pérez-Estaún et al. 1988; Gutiérrez-Alonso 1996; Pastor-Galán et al. 2009). Illite crystallinity and conodont color alteration indexes are consistent with diagenetic conditions to very low-grade metamorphism in this region (e.g. Gutiérrez-Alonso and Nieto 1996; Abad et al. 2003; Colmenero et al. 2008, Pastor-Galán et al. 2013b, Garcia-Lopez et al. 2013).

A wealth of paleomagnetic (e.g. Hirt et al. 1992; Parés et al. 1994; Stewart 1995; van der Voo et al. 1997; Weil 2006; Weil et al. 2000, 2001, 2010), structural (e.g. Julivert and Marcos 1973; Pérez-Estaún 1988; Gutiérrez-Alonso 1992; Kollmeier et al. 2000; Pastor-Galán et al. 2011, 2012, 2014; Shaw et al. 2016) and geochronological data (e.g., Gutiérrez-Alonso et al. 2015) support the hypothesis that the Cantabrian Orocline formed due to secondary vertical axis rotation subsequent to the main collisional phases of the Variscan orogen (meaning younger than ca. 310 Ma).

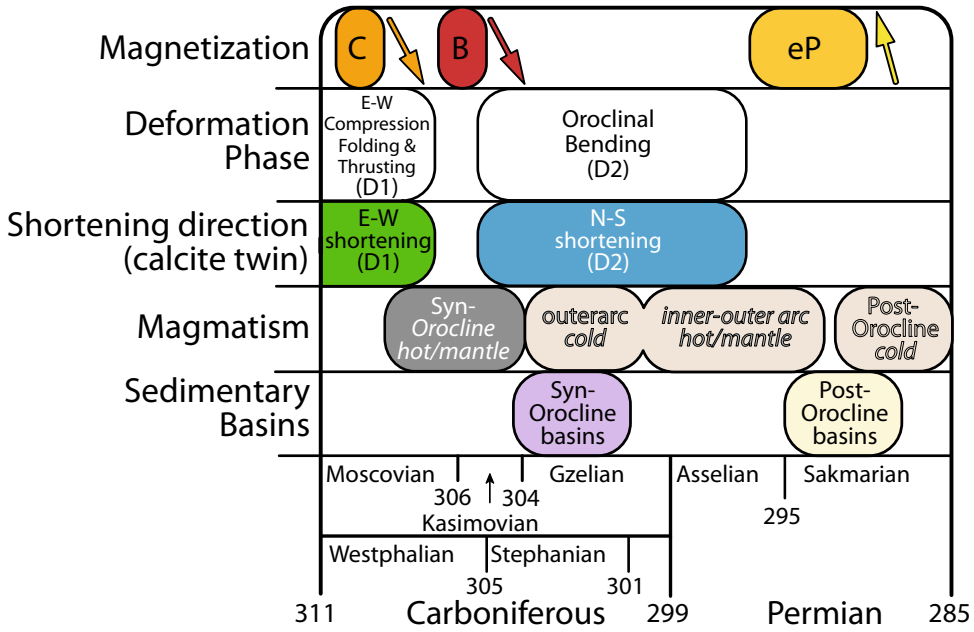

Fig. 14.4 Proposed timeline for the temporal relationship between the successive magnetizations recorded in the Cantabrian Orocline and their relationship to the two main phases of oroclinal formation, the acquisition of twin strains (and associated stresses) during deformation, the age of various magmatic pulses, and the age of sedimentary basins. Modified from the review article of Weil et al. (2013a, b)

Importantly, the documented rotations, which are recorded in rock units throughout the foreland and hinterland of the Iberian Variscan system, occurred over a relatively short interval of time from 310 to 295 Ma (Fig. 14.4) (see summary at Gutiérrez-Alonso et al. 2012; Weil et al. 2013a, b), and thus are truly secondary and post-orogenic with respect to Variscan deformation.

14.2.1 A Forgotten Curvature: Geometry and Kinematics of the Central Iberia Arc

Although described as early as 1926 by Staub (see Martínez-Catalán et al. (2015) for a historical perspective), the shape, kinematic and tectonic implications of the Central Iberian Arc remained overlooked for decades; thus, many models of orocline development for the Cantabrian Orocline completely ignored the influence on and of its potential southern counterpart (Fig. 14.2b). Based on his observations of the structural trend of folds and inclusions in garnets around the putative hinge of the Central Iberian Arc, Aerden (2004) reignited the hypothesis of their being an additional Central Iberian Arc and suggested that it was secondary in nature. Since then, multiple authors have tried to unravel its geometry and kinematics with conflicting results. The observations used in support of the Central Iberian curved geometry are: (i) paleocurrents recorded in Ordovician quartzites (Shaw et al. 2012); (ii) structural trend of folds and inclusions in garnets (Aerden 2004) and (iii) aeromagnetic anomalies and fold trends (Martínez-Catalán 2012). Based on these arguments, three geometries have been proposed (Fig. 14.2c) that have two features in common: (1) the curvature runs parallel to the Central Iberian Zone, located in the center-west of Iberia and (2) the Galicia-Tras-os-Montes Zone occurs in the core of the curve.

Paleomagnetic results from the Central Iberian Arc published by Pastor-Galán et al. (2015a, 2016, 2018), suggest a lack of secondary rotation on the southern limb of the arc that were penecontemporaneous with rotations recorded in the limbs of the Cantabrian Orocline (Fig. 14.5). However, the timing constraints provided by these results only established that no relative rotation occurred younger than ca. 318 Ma. Consequently, the available paleomagnetic data from the Central Iberian Arc neither definitively supports or refute a secondary nature for the arc, but does require that if it is secondary, and thus an orocline, it had to have occurred prior to 318 Ma, and is thus diachronous with the Cantabrian Orocline (Fig. 14.5). This ambiguity makes the kinematic nature of the Central Iberian Arc one of the most important outstanding questions in terms of the Variscan of Iberia, and the broader tectonics and paleogeography of Western Europe during the late-stages of Pangea amalgamation.

Coupled oroclines, like the Cantabrian and Central Iberian oroclines, are not uncommon, and have been documented in Mesozoic, Paleozoic and Precambrian orogens. Examples include the coupled North Alaskan and Kulukbuk Hills oroclines of the Cordilleran orogen of Alaska, the Carpathian and Balkan oroclines of the Eastern Alpine belt, and the Bothnian oroclines of the Svecofennian orogen of Baltica (Shaw and Johnston 2016a, b; Lahtinen et al. 2014). A model of coupled orocline development as a result of concentric buckling of a pre-existing linear orogen (Johnston et al. 2013) involves the development of an initial concentric buckle whose axial surface is perpendicular to the strike of

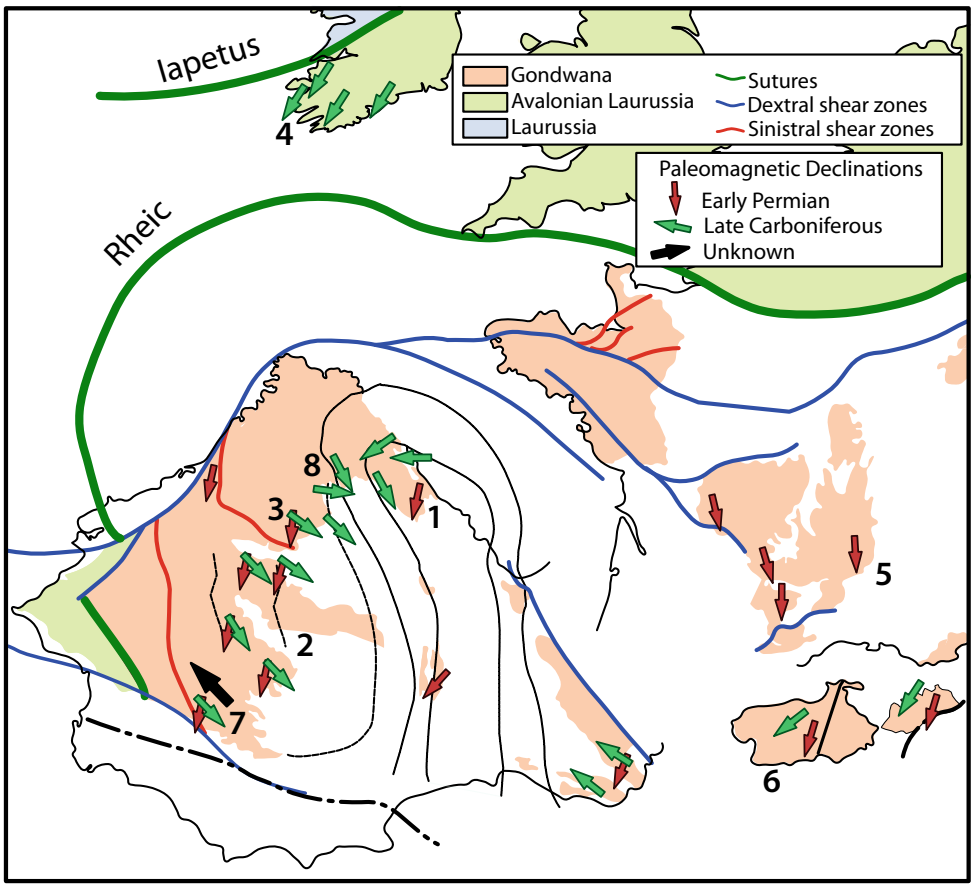

Fig. 14.5 Compilation of Pensylvannian and Early Permian paleomagnetic declinations in Iberia, France and Ireland (see Weil et al. 2013a, b [1]; Pastor-Galán et al. 2015a [2]; 2016 [3]; 2015b [4]; Edel et al. 2014 [5] and 2015 [6]; Parés and van der Voo 1992 [7]; Fernández-Lozano et al. 2016 [8]). Note the absence of Pensylvannian clock-wise rotations around the Central Iberian curve, however a declination of unknown age might indicate an earlier formation of the Central Iberian orocline (arrow in black [7])

the deforming orogen. Continued orogen-parallel shortening is then taken up by continued rotation of the initial buckle. A 90° rotation of the initial buckle gives rise to two coupled oroclines whose axial surfaces strike parallel to the regional strike of the orogen. Diachroneity of the two coupled oroclines is a prediction of this model. The paleomagnetic data provided by Pastor-Galán et al. (2015a, 2016) indicates that the Central Iberian arc predates the Cantabrian arc. If correct, the implication of the concentric buckling model is that the Central Iberian arc developed first by concentric buckling of the Variscan orogen to the south (present-day coordinates) and that continued orogen-parallel shortening was subsequently taken up by counter-clockwise rotation of the Central Iberian orocline, giving rise to the Cantabrian orocline. Further paleomagnetic and structural data are required to test this two-stage coupled orocline model.

14.3 Magmatism

Iberia preserves an impressive record of magmatic pulses that flared up during the Late Paleozoic, including 350–330 Ma (orogen building); 325–315 Ma (orogen collapse) and 310–285 (Late orogenic) (Fig. 14.6) (Fernández-Suárez et al. 2000). Late-orogenic magmatism comprises intrusive and volcanic rocks emplaced from 310 to 285 Ma, which are penecontemporaneous with, and slightly post-date formation of the Cantabrian Orocline. The late-orogenic magmatic record consists of mantle and crustal derived melts that show systematic changes in their age, spatial distribution, petrology, and geochemistry, and include foreland magmatism (a rarity in classic foreland systems) in the core of the Cantabrian Orocline (Gutiérrez-Alonso et al. 2011a, b).

Available geochronological data indicate that late orogenic magmatism (310–285 Ma) progressively youngs towards the core of the Cantabrian Orocline (Fig. 14.7) (Fernández-Suárez et al. 2000; Gutiérrez-Alonso et al. 2011a, b). In the outer regions of the Cantabrian Orocline, scarce but significant mantle and lower crustal derived mafic melts intruded from 310 to 305 Ma, which were followed by intrusion of felsic, crustal derived magmas between 305 and 295 Ma. Within the inner orocline (the Cantabrian Zone), magmatism did not begin until 300 Ma and did not end until 285 Ma (Fig. 14.7b). Similar to the outer orocline, magmatism began with the intrusion of mantle and lower crust-derived mafic rocks and granitoids, and widespread volcanism that continued until 292 Ma (Gutiérrez-Alonso et al. 2011b). Subsequently, felsic, crustal-derived

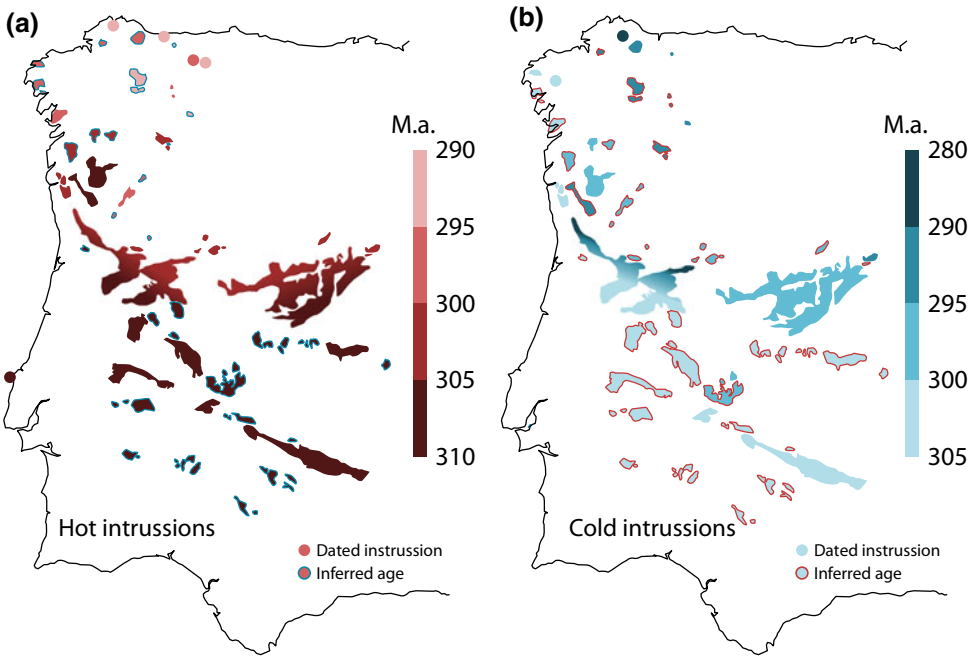

Fig. 14.6 Map of western Iberia showing spatial distribution of Late Variscan magmatism. **a** Distribution and time of emplacement of mafic rocks, granodiorites and monzogranites ("hot"). **b** Distribution and time of emplacement of leucogranites ("cold"). After Gutierrez-Alonso et al. (2011a, b); Orejana et al. (2012)

leucogranite magmatism continued for another 7 m.y. (Gutiérrez-Alonso et al. 2011b).

Sm/Nd isotopes from mantle-derived rocks revealed that the mantle lithosphere in NW Iberia was emplaced, or strongly metasomatized, at ca. 1.0 Ga, while post-Variscan mantle-derived magmatic rocks yield neodymium model ages (TDM) of ca. 300 Ma (Fig. 14.7c) (Gutiérrez-Alonso et al. 2011b). The newer model age is roughly coeval with the formation of the Cantabrian Orocline and the late Variscan magmatic pulse and implies a lithospheric-scale readjustment and replacement during oroclinal development.

14.4 Late Variscan Tectonic Models

The large amount of work over the past two decades on the kinematics of the Cantabrian (see reviews of Weil et al. 2013a, b; Johnston et al. 2013) and Central Iberian arcs (e.g. Martínez-Catalán, et al. 2015; Shaw and Johnston 2016a, b; Pastor-Galán et al. 2016; 2017; da Silva et al. 2017) inspired a revitalization of published tectonic models for the mechanisms that formed these first-order geologic structures. The kinematic restrictions imposed by paleomagnetism and structural geology established that formation of the Cantabrian Orocline occurred within 15–20 million year time window from late Carboniferous to the earliest Permian (Fig. 14.4) (e.g., Merino-Tomé et al. 2009; Weil et al. 2010; Pastor-Galán et al. 2011, 2014; Gutiérrez-Alonso et al. 2015; Shaw et al. 2016). Consequently, any viable tectonic model must conform to the kinematic framework of secondary rotation of the northern and southern limbs of the Cantabrian Orocline during a period of less than 20 m.y. around the Carboniferous-Permian boundary. However, the still ambiguous nature on the geometry and kinematics of the Central Iberian arc limits any proposed tectonic scenario and therefore adds uncertainty to all the proposed current models.

Like many events in ancient Earth history, authors working on the Late Variscan have proposed a number of competing non-unique explanations that are based on, and limited by, a particular set of published observations (Fig. 14.8). Based on our current understanding of late Variscan kinematics (see Weil et al. 2013a, b; Dias et al. 2016 for recent reviews), the most common hypotheses for the Variscan orocline(s) in Iberia involve: (1) a collision between irregular coastlines including promontory–salient pairs, in which indentation of blocks and/or deformation of embayments initiated the observed curvature(s) (e.g., Lefort 1979; Dias and Ribeiro 1995; Simancas et al. 2005); (2) the buckling of a ribbon-like continent that requires at least one side of the ancient landmass to be bound by oceanic lithosphere (e.g., Johnston et al. 2013; Shaw and Johnston 2016b); (3) a stress-field change due to paleogeographic position of Iberia in the core of the Pangea supercontinent and at the apex of the Tethyan realm (e.g., Gutiérrez-Alonso et al. 2008); (4) regional rotation of existing tectonostratigraphic zones due to continental-scale shear faulting associated with oblique shortening and/or transpression (e.g. Brun and Burg 1982; Martínez-Catalán 2011); and (5) a change in the regional stress field by 90°, which causes non-coaxial deformation and vertical-axis rotation of initially linear features, generally interpreted as lithospheric-scale buckling.

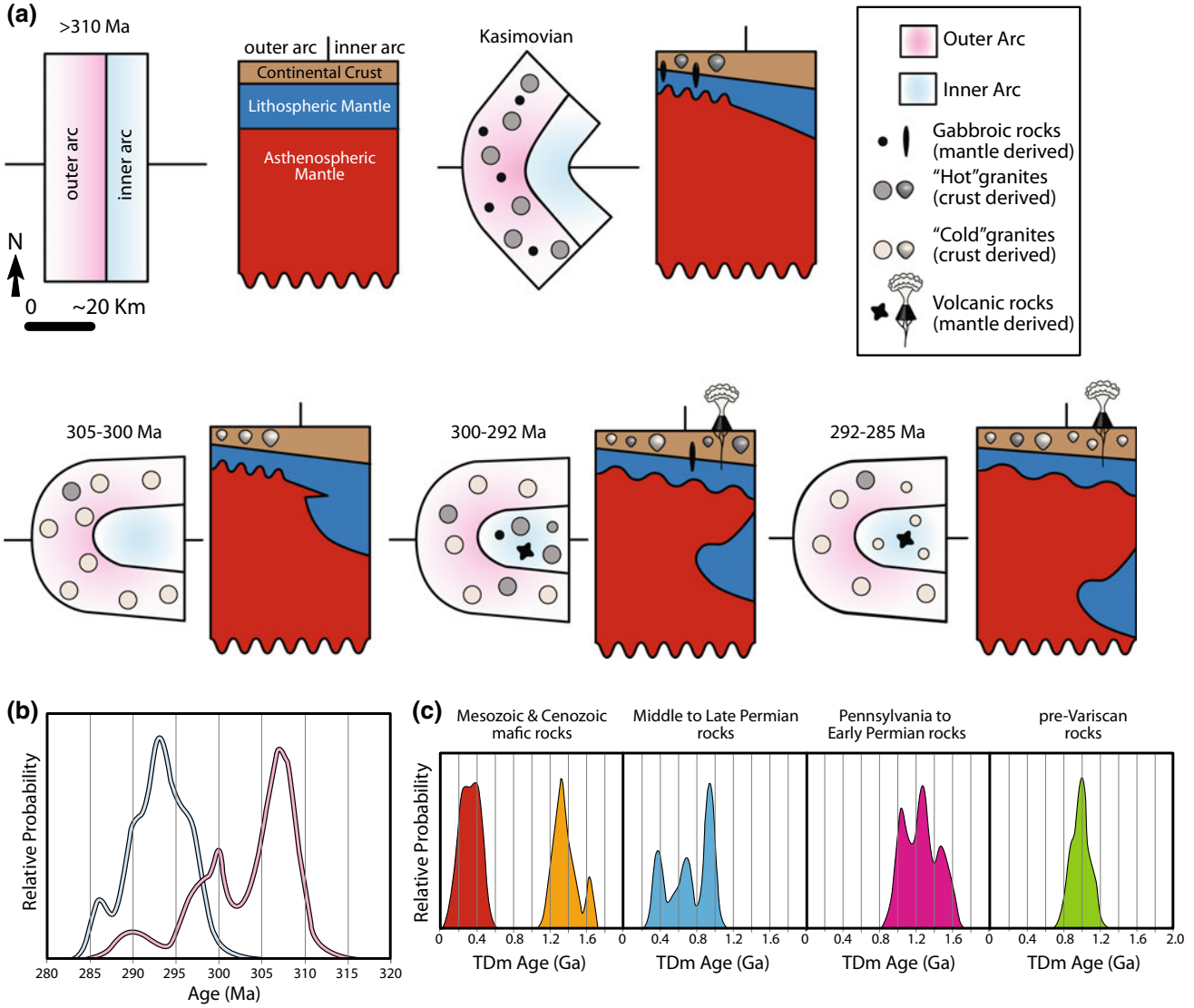

Fig. 14.7 Cartoon sketches summarizing the episodes of magmatism during formation of the Cantabrian Orocline. Outer (inner) arc region highlighted in pink (blue). **a** Plan view and profile view models for lithospheric structure of inner and outer arc during oroclinal development. **b** Probability age distributions for magmatic rocks from the inner (blue) and outer (pink) arc regions. Note the general younging trend of magmatic ages from outer to inner arc during oroclinal buckling and related lithospheric delamination. **c** Model εNd age probability plots grouped as: Mesozoic and Cenozoic mafic rocks, Middle to Late Permian rocks, Pennsylvanian to Early Permian samples, and pre-Variscan samples. Data and schematic cartoons taken and modified Gutiérrez-Alonso (2011a, b)

None of these models are necessarily mutually exclusive, and the truth may lie at the intersection of two or more of these scenarios. These models are discussed below with an emphasis on recent publications. This discussion is followed by a review of the nature and number of Variscan aged oroclines in Iberia.

Models that call upon the modification of a linear Variscan margin by the impingement of a rigid block began with the promontory hypothesis of Lorenz (1976) and Lorenz and Nicholls (1984). These models focused on the final collision of Pangea and the collapsing of the recently deformed and weakened European Variscan realm between the irregular margins of the stronger Laurussia and Gondwana plates (Fig. 14.8a). Thus, the strong rheological contrast within the colliding collage caused progressive rotation and formation of the Iberian orocline(s). An alternative model was later proposed by Matte and Burg (1981) and modified by Matte (1991), in which a rigid block migrated from the east (in present-day coordinates) and indented into the European Variscan belt causing opposite shear sense on either arm of the centripetal vergent bend (Fig. 14.8b). The more recent iteration for this model, which has indentation occurring in two stages, comes from Dias and Ribeiro (1995) (Fig. 14.8 c). Invariably, the hypothesized indentor has a Gondwana

affinity basement, and was likely a promontory off the northern margin of Gondwana (e.g., Lefort and Van der Voo 1981; Lefort 1989; Quesada et al. 1991) (Fig. 14.8d). Şengör (2013) brought back a modified version of Matte's westward indentor, linking deformation in the distal Pyrenean realm of the Variscan to the development of the Cantabrian Orocline. In his model, oroclinal bending is related to a westward moving strut, which caused thin-skinned deformation and associated shear faulting, and is explicitly not lithospheric-scale in nature. Simancas et al. (2013) expands on earlier indentor models to include the formation of the Central Iberian arc, which they argue nucleated around an Avalonian salient that was subsequently modified by shear faulting (Fig. 14.8e). In addition, models related with roll-back curvature caused by a post-Variscan subduction zone located to the south of the Cantabrian orocline have been proposed (Pereira et al. 2015).

The indentor model faces several challenges including the absence of an identified indentor, the difficulty in reconciling the extreme tightening observed in the inner Cantabrian Orocline with the expected radial deformation (e.g. Weil 2006; Merino-Tomé et al. 2009; Reiter et al. 2011); and importantly, the fact that vertical-axis rotations happened after larger-scale regional tectonic convergence (e.g. Dallmeyer et al. 1997; Ribeiro et al. 2007; Weil et al. 2000, 2010, 2013a, b). Consequently, the most recent models have

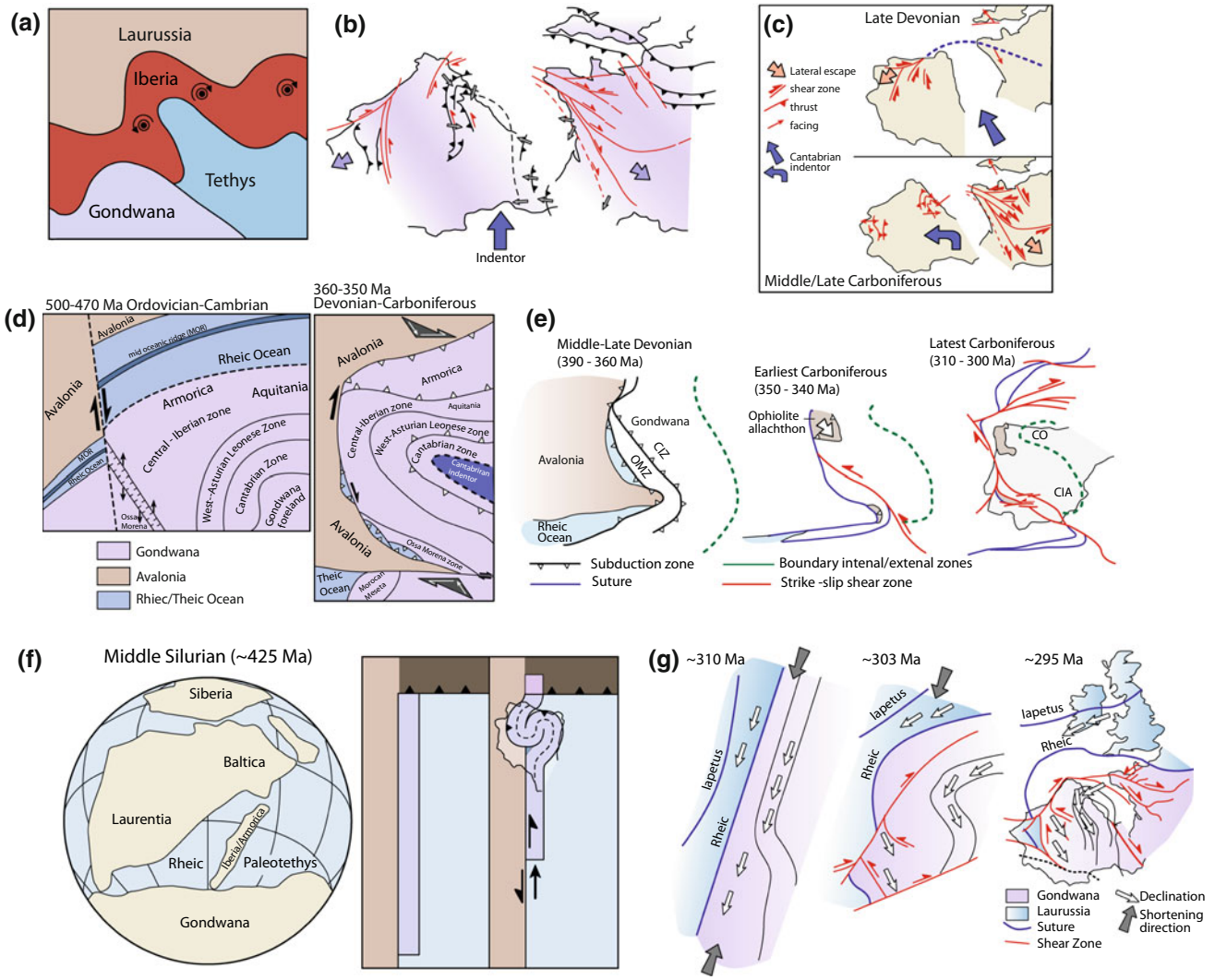

Fig. 14.8 Various models of oroclinal formation. **a** Indentor model after Lorenz and Nicholls (1984). **b** Indentor mode with fault kinematics from Matte and Ribeiro (1975) and Matte (1991). **c** Two-stage indentor model after Dias and Ribeiro (1995). **d** Gondwana promontory indentor model after Ribeiro (2007). **e** Kinematic model with indentation and left-lateral shearing after Simancas et al. (2013). **f** Simplified ribbon continent model after Johnston et al. (2013) and Shaw and Johnston (2016a, b). **g** Stress-Field rotation and shear zone kinematic model of Pastor-Galán et al. (2015b). **h** Pangea self-subduction model from Gutiérrez-Alonso et al. (2008). **i** Dextral mega-shear model from Martínez-Catalán (2014). **j** North Iberian mega-shear model after Martínez-García (2013). **k** Oroclinal induced lithospheric delamination model after Gutiérrez-Alonso et al. (2004, 2012)

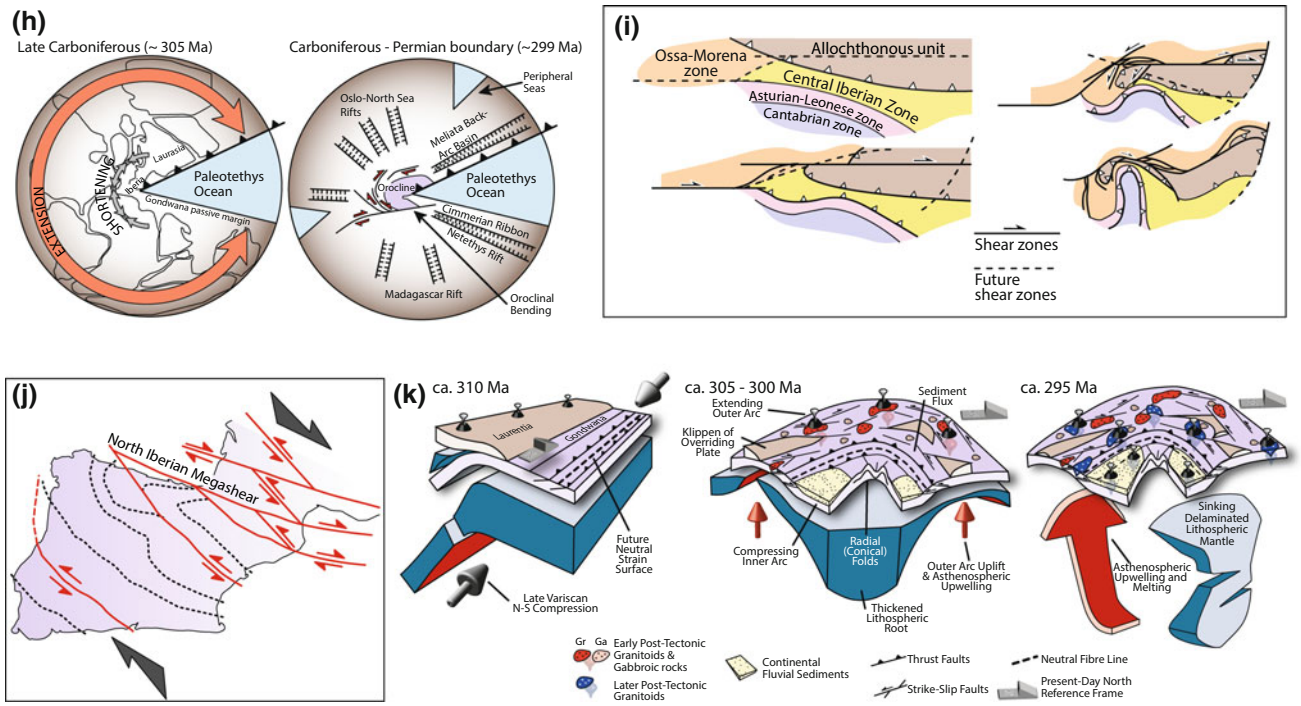

Fig. 14.8 (continued)

been formulated with an effort in reconciling the indentor model with late-stage oroclinal formation by integrating an early phase of indentation with later oroclinal bending and arc tightening. To this end, Dias et al. (2016) argues that the irregular shape of the Laurussian margin induced rotation in Iberia by translating the Cantabrian basement to the east, forming a tight fold in the hinge area of the arc, while the more external limbs of the belt in Central Iberia and north into Brittany underwent only minor rotation. These more distal regions of the arc are therefore not part of the established oroclinal system, but instead represent the trends of two mostly independent tectonic zones that were at a high angle to one another at the end of Variscan tectonics. However, recent paleomagnetic data from Ireland does not support the proposed trend for the northern arm of this system in the Late Paleozoic (Pastor-Galán et al. 2015b). Murphy et al. (2016) further hypothesized a two-stage tectonic model in which the first phase initiated with the collision of a large promontory into Iberia in the Devonian. This collision resulted in a relatively straight inner Cantabrian zone and an outer zone that accommodated indentation by sinistral and dextral motion along shear zones on either side of an impinging promontory. The main tectonostratigraphic zones were subsequently bent due to a change in the stress field associated with regional heterogeneities in small ocean tracks preserved in the reentrants and promontories produced during the earlier collision.

Although indentor/promontory models vary in their details, they inevitably place the Variscan of Iberia in the continental interior of an amalgamating Pangea. An alternative set of models argue that the Variscan of Iberia was initially a ribbon continent that rifted away from the northern margin of Gondwana leaving a new tract of oceanic lithosphere on its eastern flank (Fig. 14.8f) (Johnston et al. 2013; Shaw et al. 2014, 2015; Shaw and Johnston 2016a, b). In this scenario both the Cantabrian Orocline and the Central Iberian Arc are secondary curves that result in the buckling of an initially ~2100 km long linear orogen. In order to account for the present-day arc curvature of the coupled bends, roughly 1100 km of shortening is required. This massive shortening is argued to have been accommodated by a subduction-related driving mechanism that produced orogen-parallel shortening (Johnston et al. 2013). This model results in a 90° change in the shortening field from an early east-west (in present-day coordinates) event that resulted in establishment of the early longitudinal folds and faults that define the main structural grain of Variscan deformation in Iberia, to north-south, causing the ribbon continent to buckle between Gondwana and Laurussia. Recently Fernández-Lozano et al. (2016) published new paleomagnetic data from the hinterland of the Cantabrian Orocline, which they argue supports such a 90° change in the stress field and therefore a purely secondary cause for the observed arc. Such a model of purely secondary rotations is

at odds with a more progressive model in which rotations are acquired during deformation due to an indentor. The work of Del Greco et al. (2016) in the innermost core of the Cantabrian Orocline further supports two discrete phases of shortening and a nearly orthogonal change in the stress field in order to produce the observed interference folds that are documented throughout the hinge-zone of the orocline. Similarly, Pastor-Galán et al. (2015b) proposed a kinematic model for Cantabrian Orocline formation that was facilitated by a regional 90° change in the stress-field at ca. 310 Ma, which led to along strike buckling of the Variscan orogen accommodated by large-scale shear zones (Fig. 14.8g).

Though not specifically advocating a ribbon continent model, Pereira et al. (2014) published new geochronologic and petrologic work from Variscan basement found in the Pyrenees, which they argue supports the existence of oceanic lithosphere involvement in late Variscan magmatism. Like the ribbon continent model of Johnston et al. (2013), their model requires oceanic lithosphere to exist east of the present-day Iberian Massif. Pereira et al. (2015) argued that forces related to roll-back caused by a north-dipping subduction zone near the western corner of the newly developing Paleotethys Ocean would have subsequently driven the formation of the Cantabrian Orocline. This model is a modification of the Gutiérrez-Alonso et al. (2008) Pangea self-subduction model (Fig. 14.8h). In the self-subduction model, Iberia was paleogeographically positioned close to the center of the Pangea supercontinent during orocline formation. The east margin of the supercontinent was characterized by a westward-tapering Tethyan oceanic embayment that pinched out near Iberia. The Tethys was inferred to have had an E-W trending mid-ocean ridge; a north-dipping subduction zone along its northern margin in which Laurussia was the overriding plate; and a passive southern margin developed along the Gondwanan portion of Pangea. This unique paleogeography of the Tethyan realm would have resulted in the subduction of the Tethyan mid-ocean ridge to the north, resulting in Pangean oceanic lithosphere being subducted beneath the Pangean continental crust of Laurasia, a process referred to as 'self-subduction'. Because of the continuity of the oceanic lithosphere with the Pangean continental lithosphere across the northern Gondwanan passive margin, subduction related slab pull forces would have transmitted into continental Pangea. The result would have been a profound change in the Pangean strain regime, with shortening and contraction within the inner region of Pangea that surrounded the western end of the Tethys, and extension around the supercontinents periphery. Ultimately, contraction within the inner tract of the Pangean superplate would have given rise to the Iberian Orocline(s). Slab pull forces subsequently resulted in failure of the continental lithosphere along what was the northern Gondwanan margin, creating a rift basin south of and parallel to the southern Tethys margin. Self-subduction ended with the formation of the Neotethys mid-ocean ridge, which separated continental Pangea from the subducting slab.

To account for the large-scale rotations associated with orocline development, many authors have advocated for orocline formation models that rely on a combination of shear faulting, oblique convergence and transpression as a means of inducing secondary rotation. Martínez-Catalán (2011) developed a model that involves dextral transpression that he links to an intercontinental transform that formed between Gondwana and Laurussia after final closure of the Rheic Ocean (Fig. 14.8i). A rigid strut trapped within this large shear system would have subsequently initiated regional rotation and arc formation (Martínez-Catalán et al. 2015), similar to some of the previously discussed indentor models. In the model presented by Martínez-García (2013), the shear system is referred to as the North Iberian Megashear and is characterized by a series of near-vertical strike-slip faults that help to accommodate rotation around a vertical-axis—similar to a flexural slip model for fold formation (Fig. 14.8j). In this scenario the belt started out with a roughly linear NW-SE orientation and was subsequently folded due to drag along the megashear. This shear caused CW rotation in the north and CCW rotation in the south. More recently, Arenas et al. (2014) presented data from the Rheic suture of northern Iberia, which they argue records two discrete phases of high pressure activity that they relate to successive collision events between Gondwana and Laurussia. They argue that these collision events were oblique in nature and were separated by a minor phase of extension and the formation of pull-apart basins. Oroclinal bending would have occurred during the second phase of oblique convergence in the latest Carboniferous. Chopin et al. (2014) link oroclinal bending in Iberia to deformation in the Rehamma Massif in Morocco and the Alleghenian thrust system of North America. They argue for the collision of Gondwana with a previously assembled European Variscan belt in the late Carboniferous, while penecontemporaneously dextral deformation is dominating the Alleghenian of North America. This phase was followed by a change in the stress field, likely due to the counterclockwise rotation of Gondwana, which resulted in a more head-on collision between Gondwana and Laurentia and a final phase of dextral shear in the Variscan of Iberia as the plate-scale kinematics changed. Edel et al. (2015) present new paleomagnetic data from the Catalan Coast Ranges that they argue supports a secondary rotation model for the Cantabrian Orocline that they also link to late-stage north-south shortening due to larger continent-scale transpression and dextral shearing within the European plate during final Pangea amalgamation. In a recent review article on the tectonic evolution of the Variscan of Iberia, Diez-Fernández et al. (2016) present a similar model in which the bending of the

Cantabrian Orocline is due to late Variscan strike-slip tectonics that ultimately segmented the Variscan hinterland of Iberia into the complex network of lithotectonic domains seen today.

A pure lithospheric buckling model for oroclinal development was first proposed by Gutiérrez-Alonso et al. (2004) who argued for thick-skinned deformation of the entire lithosphere (Fig. 14.8k). Such a kinematic model involves lithospheric-scale rotation of the orogen limbs, with extension and thinning in the outer arc, and coeval shortening and thickening in the inner arc (Julivert and Marcos 1973; Julivert and Arboleya 1986; Alvarez-Marron and Perez-Estaún 1988; Gutiérrez-Alonso et al. 2015; Pastor-Galán et al. 2012). If buckling occurred at the lithosphere scale, thickening beneath the inner arc would have resulted in gravitational instability causing detachment and removal of the mantle lithosphere (and perhaps even the lower crust), in turn resulting in upwelling of the asthenosphere. This upwelling is recorded in the voluminous Late Carboniferous–Permian magmatism found throughout the Variscan fold-and-thrust belt (Fernández-Suárez et al. 2000, 2011; Gutiérrez-Alonso et al. 2004, 2011a, b). This hypothesis explains many unusual geologic phenomena found in the core of the Cantabrian orocline, including uncommon high coal ranks in the uppermost Carboniferous continental basins (Colmenero and Prado 1993; Colmenero et al. 2008); gold mineralization in the foreland fold and thrust belt (Martín-Izard et al. 2000); remagnetization recorded in Late Carboniferous–Permian strata (Weil and Van der Voo 2002); dolomitization along late breaching and out-of-sequence thrusts (Gasparrini et al. 2006; Lapponi et al. 2014; Blanco-Ferrera 2017); the tectonothermal evolution of the Cantabrian Oroclines core as recorded by cleavage development (Valín et al. 2016) and the thermal history of xenoliths found in Mesozoic diatreme samples (Puelles et al. 2017); post-orogenic topographic elevation (Muñoz-Quijano and Gutiérrez-Alonso 2007); and the late onset of foreland magmatism in the Cantabrian Zone foreland (Gutiérrez-Alonso et al. 2004, 2011a, b; Cuesta and Gallastegui 2007). Delayed onset of magmatism within the foreland is interpreted to reflect initial thickening of the lithospheric mantle in the core of the orocline, forming an orogenic root that subsequently became gravitationally unstable (Fig. 14.8). Subsequent felsic melts are attributed to melting of the fertile (pelite- and greywacke-rich) middle crust upon upward migration of the thermal anomaly above a high-standing asthenosphere.

These mafic rocks and their accompanying granitoids are interpreted as a byproduct of decompressive mantle and lower crustal melting, caused by lithospheric extension around the outer orocline arc during buckling (Fig. 14.8). Thinning of the lithosphere in the outer arc, a concomitant rise of the asthenosphere, and coupled intrusion of gabbro resulted in a regionally elevated geothermal gradient across the arc. This increase in thermal energy resulted in melting of middle-upper crustal rocks still hot from Variscan orogenesis, which led to intrusion of felsic, crustal derived magmas into the outer arc of the orocline between 305 and 295 Ma.

Each of the above models is biased in their consideration of the nature and number of secondary oroclines inferred to have formed during the final stages of Variscan tectonics in Iberia. All of the previously discussed models consider the northern Cantabrian Orocline as a secondary featured that underwent some amount of vertical axis rotation subsequent to main Variscan collisional event; whereas few of the models argue explicitly for a second orocline in central Iberia—the so-called Central Iberian Arc (e.g., Aerden 2004; Martínez-Catalán 2011; Shaw et al. 2012; Johnston et al. 2013). As highlighted by Johnston et al. (2013), if the Central Iberian Arc is truly a secondary feature, any viable tectonic model must start with an Iberian Variscan belt that is greater than 2000 km long, which is paleogeographically absent in nearly all of the existing tectonic models for the Variscan. Consequently, it is vitally important to continue to test whether the Central Iberian Arc is in fact a secondary feature, or alternatively a primary structure of the Iberian Massif (e.g. Pastor-Galán et al. 2015a; in press; Shaw et al. 2016; Dias et al. 2016).

14.5 Existing Constraints on Current and Future Models of Arc/Orocline Formation in Iberia

- The Cantabrian Zone represents a secondary orocline that resulted from bending or buckling of a roughly linear orogenic belt, that had major thrusts and faults oriented north-south in present-day coordinates.
- The vertical axis rotations that led to oroclinal bending/buckling are constrained to a time span of c.a. 15 m.y., and likely no longer than 20 m.y., between 315 and 295 Ma.
- Paleomagnetic, structural and sedimentological patterns/geometries around the Cantabrian Orocline match predictions of a secondary oroclinal model.
- Penecontemporaneous with the formation of the Cantabrian Orocline, was widespread magmatism emplaced throughout Iberia, and which youngs progressively towards the core of the Cantabrian Orocline.
- The Central Iberian arc, if caused by vertical axis rotations, formed prior to the Cantabrian Orocline and likely before 318 Ma, without any other kinematic constraints up to date.

14.5.1 Outstanding Questions

- What is the geometry and geographic extent of the Central Iberia Arc? More specifically, what is the orientation of the axial trace of the arc and where is its hinge zone?
- What is the kinematic nature of the Central Iberian Arc in terms of possible secondary rotations?
- How extensive are the rotations associated with the northern and southern limbs of the Cantabrian Orocline? Does rotation extend out and incorporate all of the major Variscan tectonostratigraphic belts, or is it restricted to only the inner most zones?
- What are the amounts of displacement, timing and kinematics of the major shear zones across the Variscan of Iberia, are their motions coupled, and are they involved in oroclinal bending?
- With respect to present-day coordinates, what was the orientation of maximum shortening during formation of the Cantabrian Orocline? Such information will help determine if orocline formation was due to a bending mechanism with loading perpendicular to the trend of the initial belt, or a buckling mechanism with loading parallel to the trend of the initial belt.
- How do the tectonostratigraphic zones of northern and southern Iberia correlate given the possibility that the Central Iberian arc may be a secondary feature.
- How do we better constrain the paleogeography of Gondwana, Laurussia and the various blocks that make up Variscan Europe in the time from the Devonian, through the Carboniferous, and into the Permian.
- What was the nature of the lithosphere to the east of the Iberian Massif during the Carboniferous and Permian. Was it positioned in an intercontinental setting, or was it bound by oceanic lithosphere that would have accommodated ribbon continental buckling.
- How do we better constrain the nature of the basement below and to the east of the Variscan foreland.
- What tests can be applied to the indentor models that would show whether indentation contributed to bending one or more of the Iberian oroclines.

References

Abad I, Nieto F, Gutiérrez-Alonso G (2003) Textural, chemical changes in slate-forming phyllosilicates across the external-internal zones transition in the low-grade metamorphic belt of the NW Iberian Variscan Chain. Swiss Bulletin of Mineralogy, Petrology, 83(1), 63–80.

Abati J, Gerdes A, Suárez JF, Arenas R, Whitehouse MJ, Fernández RD, 2010. Magmatism, early-Variscan continental subduction in the northern Gondwana margin recorded in zircons from the basal units of Galicia, NW Spain. Geological Society of America Bulletin, 122 (1–2), 219–235.

Aerden DG (2004) Correlating deformation in Variscan NW-Iberia using porphyroblasts; implications for the Ibero-Armorican Arc. Journal of Structural Geology, 26(1), 177–196.

Aller J, Gallastegui J (1995) Analysis of kilometric-scale superposed folding in the Central Coal Basin (Cantabrian zone, NW Spain). Journal of Structural Geology, 17(7), 961–969.

Alonso, JL, Marcos, A, Suarez, A (2009) Paleogeographic inversion resulting from large out of sequence breaching thrusts: The Leon Fault (Cantabrian Zone, NW Iberia). A new picture of the external Variscan Thrust Belt in the Ibero-Armorican Arc. *Geologica Acta*, 7, 451–473.

Alvarez-Marron J, Perez-Estaun A (1988) Thin skinned tectonics in the Ponga region (Cantabrian Zone, NW Spain). Geologische Rundschau, 77(2), 539–550.

Arenas R, Fernández RD, Martínez SS, Gerdes A, Fernández-Suarez, J, Albert R(2014) Two-stage collision: exploring the birth of Pangea in the Variscan terranes. *Gondwana Research*, *25*(2), 756–763.

Blanco-Ferrera S, Sanz-López J, García-López S, Bastida F (2017) Tectonothermal evolution of the northeastern Cantabrian zone (Spain). International Journal of Earth Sciences, 106(5), 1539–1555.

Brun JP, Burg JP (1982) Combined thrusting and wrenching in the Ibero-armorican arc - a corner effect during continental collision. *Earth and Planetary Science Letters*, 61, 319–332.

Carey SW (1955). The orocline concept in geotectonics-Part I. In Papers, proceedings of the Royal Society of Tasmania, Vol. 89, 255–288.

Chopin F, Corsini M, Schulmann K, El Houicha M, Ghienne JF, Edel JB (2014) Tectonic evolution of the Rehamna metamorphic dome (Morocco) in the context of the Alleghanian-Variscan orogeny. *Tectonics*, *33*(6), 1154–1177.

Colmenero JR, Prado JG (1993) Coal basins in the Cantabrian Mountains, northwestern Spain. International Journal of Coal Geology, 23(1–4), 215–229.

Colmenero JR, Suárez-Ruiz I, Fernández-Suárez J, Barba P, Llorens T (2008) Genesis, rank distribution of Upper Carboniferous coal basins in the Cantabrian Mountains, Northern Spain. International Journal of Coal Geology, 76(3), 187–204.

Cuesta A, Gallastegui G (2007) El magmatismo varisco postcinemático en zonas externas del NO del Macizo Ibérico. In: XV Semana-VI Congreso Ibérico de Geoquímica, Vila Real, Portugal, DVD-ROM (pp. 11–16).

Dallmeyer RD, Catalán JM, Arenas R, Ibarguchi JG, Gutiérrez G, Farias P, Bastida F, Aller J (1997) Diachronous Variscan tectonothermal activity in the NW Iberian Massif: evidence from 40 Ar/39 Ar dating of regional fabrics. Tectonophysics, 277(4), 307–337.

da Silva ÍD, Gómez-Barreiro J, Catalán JRM, Ayarza P, Pohl J, Martínez E (2017) Structural, microstructural analysis of the Retortillo Syncline (Variscan belt, Central Iberia). Implications for the Central Iberian Orocline. *Tectonophysics*.

Del Greco K, Johnston ST, Gutiérrez-Alonso G, Shaw J, Lozano JF (2016) Interference folding, orocline implications: A structural study of the Ponga Unit, Cantabrian orocline, northern Spain. *Lithosphere*, *8*(6), 757–768.

Dias R, Ribeiro A (1995) The Ibero-Armorican Arc: A collision effect against an irregular continent? Tectonophysics, 246(1–3), 113–128.

Dias R, Ribeiro A, Romão J, Coke C, Moreira N (2016) A review of the arcuate structures in the Iberian Variscides; constraints, genetic models. *Tectonophysics*, *681*, 170–194.

Diez-Fernández RD, Arenas R, Pereira MF, Sánchez-Martínez S, Albert R, Parra LMM, Pascual FJR, Matas J (2016) Tectonic evolution of Variscan Iberia: Gondwana–Laurussia collision revisited. *Earth-Science Reviews*, *162*, 269–292.

Domeier M, Van der Voo R, Torsvik TH (2012) Paleomagnetism, Pangea: the road to reconciliation. Tectonophysics, 514, 14–43.
Domeier M, Torsvik TH (2014) Plate tectonics in the late Paleozoic. Geoscience Frontiers, 5(3), 303–350.
Du Toit AL (1937) Our wering continents: an hypothesis of continental drifting. Oliver, Boyd.
Dvorak J (1983) The development of Variscan Orogeny in Europe. Compte Rendu: Dixième Congrès International de Stratigraphie et de Géologie Du Carbonifère, 3, 549–551.
Edel JB, Schulmann K, Lexa O, Diraison M, Géraud Y (2015) Permian clockwise rotations of the Ebro, Corso-Sardinian blocks during Iberian–Armorican oroclinal bending: preliminary paleomagnetic data from the Catalan Coastal Range (NE Spain). *Tectonophysics*, *657*, 172–186.
Edel JB, Casini L, Oggiano G, Rossi P, Schulmann K (2014). Early Permian 90 clockwise rotation of the Maures–Esterel–Corsica–Sardinia block confirmed by new palaeomagnetic data, followed by a Triassic 60 clockwise rotation. Geological Society, London, Special Publications, 405(1), 333–361.
Fernández-Lozano J, Pastor-Galán D, Gutiérrez-Alonso G, Franco P (2016) New kinematic constraints on the Cantabrian orocline: A paleomagnetic study from the Peñalba, Truchas synclines, NW Spain. *Tectonophysics*, *681*, 195–208.
Fernández-Suárez J, Gutiérrez-Alonso G, Jenner GA, Tubrett MN (2000) New ideas on the Proterozoic-Early Palaeozoic evolution of NW Iberia: insights from U–Pb detrital zircon ages. Precambrian Research, 102(3), 185–206.
Fernández-Suárez J, Gutierrez-Alonso G, Johnston ST, Jeffries TE, Pastor-Galán D, Jenner GA, Murphy JB 2011 Iberian late-Variscan granitoids: some considerations on crustal sources, the significance of "mantle extraction ages". Lithos, 123(1), 121–132.
Franke, W (1989) Variscan plate tectonics in Central Europe – current ideas and open questions. *Tectonophysics*, 169, 221–228.
Franke W, Haak V, Oncken O, Tanner D (2000). Orogenic processes: quantification, modelling in the Variscan belt. Geological Society, London, Special Publications, 179(1), 1–3.
Franke W, Matte P, Tait J (2005) Europe: Variscan Orogeny. In: Encyclopedia of Geology, Volume 2. Elsevier, Oxford, 75–85.
Franke W, Cocks LRM, Torsvik TH (2017). The Palaeozoic Variscan oceans revisited. Gondwana Research, 48, 257–284.
Gallo L C, Tomezzoli RN, Cristallini EO (2017) A pure dipole analysis of the Gondwana apparent polar wander path: Paleogeographic implications in the evolution of Pangea, Geochemistry, Geophysics, Geosystems, 18, 1499–1519, https://doi.org/10.1002/2016gc006692.
Garcia-Lopez S, Bastida F, Aller J, Sanz-Lopez J, Marin JA, Blanco-Ferrera S (2013). Tectonothermal evolution of a major thrust system: the Esla–Valsurbio unit (Cantabrian Zone, NW Spain). Geological Magazine, 150(6), 1047–1061.
Gasparrini M, Bechstädt T, Boni M (2006) Massive hydrothermal dolomites in the southwestern Cantabrian Zone (Spain), their relation to the Late Variscan evolution. Marine, Petroleum Geology, 23(5), 543–568.
Gutiérrez Alonso G (1992) El Antiforme del Narcea y su relación con los mantos occidentales de la Zona Cantábrica.
Gutiérrez-Alonso G (1996) Strain partitioning in the footwall of the Somiedo Nappe: structural evolution of the Narcea Tectonic Window, NW Spain. Journal of Structural Geology, 18(10), 1217–1229.
Gutiérrez-Alonso G, Nieto F (1996) White-mica 'crystallinity', finite strain, cleavage development across a large Variscan structure, NW Spain. Journal of the Geological Society, 153(2), 287–299.
Gutiérrez-Alonso G, Fernández-Suárez J, Weil AB (2004) Orocline triggered lithospheric delamination. Geological Society of America Special Papers, 383, 121–130.
Gutiérrez-Alonso G, Fernández-Suárez J, Weil AB, Murphy JB, Nance RD, Corfu F, Johnston ST(2008) Self-subduction of the Pangaean global plate. Nature Geoscience, 1, 549–553.
Gutiérrez-Alonso G, Fernández-Suárez J, Jeffries TE, Johnston ST, Pastor-Galán D, Murphy JB, Franco MP, Gonzalo JC (2011a) Diachronous post-orogenic magmatism within a developing orocline in Iberia, European Variscides. Tectonics, 30(5).
Gutiérrez-Alonso G, Murphy JB, Fernández-Suárez J, Weil AB, Franco MP, Gonzalo JC (2011b) Lithospheric delamination in the core of Pangea: Sm-Nd insights from the Iberian mantle. Geology, 39(2), 155–158.
Gutiérrez-Alonso G, Johnston ST, Weil AB, Pastor-Galán D, Fernández-Suárez J (2012) Buckling an orogen: the Cantabrian Orocline. GSA Today, 22(7), 4–9.
Gutiérrez-Alonso G, Collins AS, Fernández-Suárez J, Pastor-Galán D, González-Clavijo E, Jourdan F, Weil AB, Johnston ST, 2015 Dating of lithospheric buckling: 40 Ar/39 Ar ages of syn-orocline strike–slip shear zones in northwestern Iberia. *Tectonophysics*, *643*, 44–54.
Hirt AM, Lowrie W, Julivert M, Arboleya ML (1992) Paleomagnetic results in support of a model for the origin of the Asturian Arc. Tectonophysics, 213(3–4), 321–339.
Johnston ST, Weil AB, Gutiérrez-Alonso G (2013) Oroclines: Thick, thin. *Geological Society of America Bulletin*, *125*(5–6), 643–663.
Julivert M, Marcos A (1973) Superimposed folding under flexural conditions in the Cantabrian Zone (Hercynian Cordillera, northwest Spain). American Journal of Science, 273(5), 353–375.
Julivert M, Arboleya ML (1986) Areal balancing and estimate of areal reduction in a thin-skinned foldand-thrust belt (Cantabrian Zone, NW Spain): constraints on its emplacement mechanism. *Journal of Structural Geology*, 8(3–4), 407–414.
Kollmeier JM, Van der Pluijm BA, Van der Voo R (2000) Analysis of Variscan dynamics; early bending of the Cantabria–Asturias Arc, northern Spain. Earth, Planetary Science Letters, 181(1), 203–216.
Lahtinen R, Johnston ST, Nironen M (2014) The Bothnian coupled oroclines of the Svecofennian Orogen: a Palaeoproterozoic terrane wreck. Terra Nova, 26(4), 330–335.
Lapponi F, Bechstädt T, Boni M, Banks DA, Schneider J (2014) Hydrothermal dolomitization in a complex geodynamic setting (Lower Palaeozoic, northern Spain). *Sedimentology*, 61, 411–443.
Lardeaux JM (2014) Deciphering orogeny: a metamorphic perspective Examples from European Alpine, Variscan belts. Bulletin de la Société Géologique de France, 185(5), 281–310.
Lefort JP (1979) Iberian-Armorican arc, Hercynian orogeny in Western Europe. Geology, 7(8), 384–388.
Lefort JP (1989). The Avalon Spur; Former Southern Margin of the Iapetus Ocean, Northern Border of the Theic Ocean. In Basement Correlation Across the North Atlantic (pp. 28–51). Springer Berlin Heidelberg.
Lefort JP, Van der Voo R (1981) A kinematic model for the collision, complete suturing between Gondwanal, Laurussia in the Carboniferous. The Journal of Geology, 89(5), 537–550.
Lorenz, V., 1976. Formation of Hercynian subplates, possible causes, consequences. Nature, 262(5567), 374–377.
Lorenz V, Nicholls IA (1984) Plate, intraplate processes of Hercynian Europe during the Late Paleozoic. Tectonophysics, 107(1–2), 25–56.
Martínez-Catalán JR, Arenas R, Díaz-García F, Abati J (1997) Variscan accretionary complex of NW Iberia: Terrane correlation, succession of tectonothermal events. Geology 25, 1103–1106.
Martínez-Catalán JR et al (2007) Space, time in the tectonic evolution of the northwestern Iberian Massif. Implications for the comprehension of the Variscan belt. In: R.D. Hatcher Jr, M.P. Carlson, J.H. McBride, J.R. Martínez Catalán (Editors), 4-D framework of continental crust. Memoir. Geological Society of America, Boulder.

Martínez-Catalán JR (2011). Are the oroclines of the Variscan belt related to late Variscan strike-slip tectonics? Terra nova, 23(4), 241–247.

Martínez-Catalán, JR (2012) The Central Iberian arc, an orocline centered in the Iberian Massif and some implications for the Variscan belt. *International Journal of Earth Sciences*, 101, 1299–1314.

Martínez-Catalán JR, Pascual FJR, Montes AD, Fernández RD, Barreiro JG, Da Silva ÍD, Clavijo EG, Ayarza P, Alcock JE (2014) The late Variscan HT/LP metamorphic event in NW, Central Iberia: relationships to crustal thickening, extension, orocline development, crustal evolution. Geological Society, London, Special Publications, 405(1), 225–247.

Martínez-Catalán JR, Aerden DG, Carreras J (2015) The "Castilian bend" of Rudolf Staub (1926): historical perspective of a forgotten orocline in Central Iberia. *Swiss Journal of Geosciences*, *108*(2–3), 289–303.

Martínez-García E (2013) An Alleghenian orocline: the Asturian Arc, northwestern Spain. International Geology Review, 55(3), 367–381.

Martín-Izard A, Fuertes-Fuente M, Cepedal A, Moreiras D, Nieto JG, Maldonado C, Pevida LR (2000) The Rio Narcea gold belt intrusions: geology, petrology, geochemistry, timing. Journal of Geochemical Exploration, 71(2), 103–117.

Matte P (1986) Tectonics, plate tectonics model for the Variscan belt of Europe. Tectonophysics, 126(2–4), 329335347–332344374.

Matte P (1991) Accretionary history, crustal evolution of the Variscan belt in Western Europe. Tectonophysics, 196(3–4), 309–337.

Matte P (2001) The Variscan collage, orogeny (480 ± 290 Ma), the tectonic definition of the Armorica microplate: a review. Terra Nova 13, 122–128.

Matte P, Burg JP (1981) Sutures, thrusts, nappes in the Variscan Arc of Western Europe: plate tectonic implications. Geological Society, London, Special Publications, 9(1), 353–358.

Matte, P, Ribeiro, A (1975) Forme et orientation de l'ellipsoide de deformation dans la vibration Hercynienne de Galicia: relation avec le plissement et hypotheses sur la genese de l'arc Iberio-Armoricain. *Comptes Rendus de l'Academie des Sciences*, 280, 2825–2828.

Merino-Tomé OA, Bahamonde JR, Colmenero JR, Heredia N, Villa E, Farias P (2009). Emplacement of the Cuera, Picos de Europa imbricate system at the core of the Iberian-Armorican arc (Cantabrian zone, north Spain): New precisions concerning the timing of arc closure. Geological Society of America Bulletin, 121 (5–6), 729–751.

Muñoz-Quijano IN, Gutiérrez Alonso G (2007) Modelo de evolución topográfica en el NO de la Península Ibérica durante la delaminación litosférica al final de la Orogenia Varisca.

Murphy JB, Gutierrez-Alonso G, Nance RD, Fernandéz-Suarez J, Keppie JD, Quesada C, Strachan RA, Dostal J (2006) Origin of the Rheic Ocean: Rifting along a Neoproterozoic suture? Geology, 34 (5), 325–328.

Murphy JB, Quesada C, Gutiérrez-Alonso G, Johnston ST, Weil A (2016. Reconciling competing models for the tectono-stratigraphic zonation of the Variscan orogen in Western Europe. *Tectonophysics*, *681*, 209–219.

Nance RD, Linnemann U (2008) The Rheic Ocean: origin, evolution, significance. GSA Today, 18(12), 4–12.

Nance RD, Gutiérrez-Alonso G, Keppie JD, Linnemann U, Murphy JB, Quesada C, Strachan RA, Woodcock, NH (2010) Evolution of the Rheic ocean. Gondwana Research, 17(2), 194–222.

Nance RD, Gutiérrez-Alonso G, Keppie JD, Linnemann U, Murphy JB, Quesada C, Strachan RA, Woodcock, NH 2012. A brief history of the Rheic Ocean. Geoscience Frontiers, 3(2), 125–135.

Orejana D, Villaseca C, Valverde-Vaquero P, Belousova EA, Armstrong RA (2012) U–Pb geochronology, zircon composition of late Variscan S, I-type granitoids from the Spanish Central System batholith. International Journal of Earth Sciences, 101(7), 1789–1815.

Parés JM, Van der Voo R, Stamatakos J, Pérez-Estaún A (1994) Remagnetizations, postfolding oroclinal rotations in the Cantabrian/Asturian arc, northern Spain. Tectonics, 13(6), 1461–1471.

Parés JM, Van der Voo R (1992) Paleozoic paleomagnetism of Almaden, Spain: A cautionary note. Journal of Geophysical Research: Solid Earth, 97(B6), 9353–9356.

Pastor-Galán D, (2009) Gutiérrez-Alonso G, Meere PA, Mulchrone KF (2009) Factors affecting finite strain estimation in low-grade, low-strain clastic rocks. Journal of Structural Geology, 31(12), 1586–1596.

Pastor-Galán D, Gutiérrez-Alonso G, Weil AB (2011) Orocline timing through joint analysis: Insights from the Ibero-Armorican Arc. Tectonophysics, 507(1), 31–46.

Pastor-Galán D, Gutiérrez-Alonso G, Zulauf G, Zanella F (2012) Analogue modeling of lithospheric-scale orocline buckling: Constraints on the evolution of the Iberian-Armorican Arc. Geological Society of America Bulletin, 124(7–8), 1293–1309.

Pastor-Galán D, Gutiérrez-Alonso G, Murphy JB, Fernández-Suárez J, Hofmann M, Linnemann U (2013a) Provenance analysis of the Paleozoic sequences of the northern Gondwana margin in NW Iberia: passive margin to Variscan collision, orocline development. *Gondwana Research*, *23*(3), 1089–1103.

Pastor-Galán D, Gutiérrez-Alonso G., Fernández-Suárez J, Murphy JB, Nieto F (2013b) Tectonic evolution of NW Iberia during the Paleozoic inferred from the geochemical record of detrital rocks in the Cantabrian Zone. Lithos, 182, 211–228.

Pastor-Galán D, Martín-Merino G, Corrochano D (2014) Timing, structural evolution in the limb of an orocline: the Pisuerga–Carrión Unit (southern limb of the Cantabrian Orocline, NW Spain). *Tectonophysics*, *622*, 110–121.

Pastor-Galán D, Groenewegen T, Brouwer D, Krijgsman W, Dekkers MJ (2015a) One or two oroclines in the Variscan orogen of Iberia? Implications for Pangea amalgamation. *Geology*, *43*(6), 527–530.

Pastor-Galán D, Ursem B, Meere PA, Langereis C (2015b) Extending the Cantabrian orocline to two continents (from Gondwana to Laurussia) paleomagnetism from South Ireland. *Earth, Planetary Science Letters*, *432*, 223–231.

Pastor-Galán D, Dekkers MJ, Gutiérrez-Alonso G, Brouwer D, Groenewegen T, Krijgsman W, Fernández-Lozano J, Yenes M, Álvarez-Lobato F (2016) Paleomagnetism of the Central Iberian curve's putative hinge: Too many oroclines in the Iberian Variscides. *Gondwana Research*, *39*, 96–113.

Pastor-Galán D, Gutiérrez-Alonso G, Dekkers MJ, Langereis CG (2017) Paleomagnetism in Extremadura (Central Iberian Zone, Spain) Paleozoic rocks: extensive remagnetizations, further constraints on the extent of the Cantabrian orocline, Journal of Iberian Geology, 43, 583–600.

Pastor-Galán, D, Pueyo EL, Diederen M, García-Lasanta C, Langereis CG, (2018) Late Paleozoic Iberian Orocline (s) and the Missing Shortening in the Core of Pangea. Paleomagnetism From the Iberian Range. *Tectonics*, 37(10), 3877–3892.

Pereira MF, Castro A, Chichorro M, Fernandéz C, Diaz-Alvarado J, Marti J, Rodriguez C (2014). Chronological link between deep-seated processes in magma chambers, eruptions: Permo-Carboniferous magmatism in the core of Pangaea (Southern Pyrenees). Gondwana Research, 25(1), 290–308.

Pereira MF, Castro A, Fernandéz C (2015) The inception of a Paleotethyan magmatic arc in Iberia. Geoscience Frontiers, 6(2), 297–306.

Pérez-Estaún A, Bastida F, Alonso JL, Marquínez J, Aller J, Alvarez-Marrón J, Marcos A, Pulgar JA (1988) A thin-skinned

tectonics model for an arcuate fold, thrust belt: the Cantabrian Zone (Variscan Ibero-Armorican Arc). Tectonics, 7(3), 517–537.

Puelles P, Agirrezabala LM, Sarrionia F, Ábalos B, Carracedo-Sánchez M, Gil-Ibarguchi JI (2017). Discerning Permian orogenic metamorphism from other tectonothermal events (Mesoproterozoic to Alpine, contact to orogenic or extensional) in the concealed basement of the Basque-Cantabrian Basin (northern Spain). *Lithosphere*, *9*(3), 441–452.

Quesada C, Bellido F, Dallmeyer RD, Gil Ibarguchi JI, Oliveira JT, Pérez Estaún A, Ribeiro A, Robardet M, Silva JB (1991) Terranes within the Iberian Massif: correlations with West African sequences. In: Dallmeyer R.D. & Lecorché, J.P. (eds) The West African Orogens and Circum–Atlantic Correlations, Springer-Verlag, Berlin, 267–294.

Reiter K, Kukowski N, Ratschbacher L (2011) The interaction of two indenters in analogue experiments, implications for curved fold-thrust belts. Earth, Planetary Science Letters, 302(1), 132–146.

Ribeiro A, Munhá J, Dias R, Mateus A, Pereira E, Ribeiro L, Fonseca P, Araújo A, Oliveira JT, Romão J, Chaminé H (2007). Geodynamic evolution of the SW Europe Variscides. Tectonics, 26(6).

Şengör AC (2013) The Pyrenean Hercynian Keirogen, the Cantabrian Orocline as genetically coupled structures. *Journal of Geodynamics*, *65*, 3–21.

Shaw J, Johnston ST, Gutiérrez-Alonso G, Weil AB (2012) Oroclines of the Variscan orogen of Iberia: Paleocurrent analysis, paleogeographic implications. Earth, Planetary Science Letters, 329, 60–70.

Shaw J, Gutiérrez-Alonso G, Johnston ST, Galán DP (2014) Provenance variability along the Early Ordovician north Gondwana margin: Paleogeographic, tectonic implications of U-Pb detrital zircon ages from the Armorican Quartzite of the Iberian Variscan belt. *Geological Society of America Bulletin*, *126*(5–6), 702–719.

Shaw J, Johnston ST, Gutiérrez-Alonso G (2015) Orocline formation at the core of Pangea: A structural study of the Cantabrian orocline, NW Iberian Massif. *Lithosphere*, *7*(6), 653–661.

Shaw J, Johnston ST (2016a) Oroclinal buckling of the Armorican ribbon continent: An alternative tectonic model for Pangean amalgamation, Variscan orogenesis. *Lithosphere*, *8*(6), 769–777.

Shaw J, Johnston, ST (2016b). Terrane wrecks (coupled oroclines), paleomagnetic inclination anomalies. *Earth-Science Reviews*, *154*, 191–209.

Shaw J, Johnston ST, Gutiérrez-Alonso G (2016c) Orocline formation at the core of Pangea: A structural study of the Cantabrian orocline, NW Iberian Massif. *Lithosphere*, *8*(1), 97–97.

Simancas JF, Tahiri A, Azor A, Lodeiro FG, Poyatos DJM, El Hadi H (2005) The tectonic frame of the Variscan–Alleghanian orogen in Southern Europe, Northern Africa. Tectonophysics, 398(3), 181–198.

Simancas JF, Ayarza P, Azor A, Carbonell R, Martínez Poyatos D, Pérez-Estaún A, González Lodeiro F (2013) A seismic geotraverse across the Iberian Variscides: orogenic shortening, collisional magmatism,, orocline development. *Tectonics*, *32*(3), 417–432.

Stampfli GM, von Raumer JF, Borel GD (2002) Paleozoic evolution of pre-Variscan terranes: from Gondwana to the Variscan collision. Special Papers-Geological Society of America, 263–280.

Stampfli GM, Hochard C, Vérard C, Wilhem C (2013) The formation of Pangea. Tectonophysics, 593, 1–19.

Staub R (1926) Gedanken zur Tektonik Spaniens. Vierteljahrsschrift der Naturforschenden Gesellschaft, Zürich, 71, 196–260.

Stewart SA (1995) Paleomagnetic analysis of fold kinematics, implications for geological models of the Cantabrian/Asturian arc, north Spain. Journal of Geophysical Research: Solid Earth, 100(B10), 20079–20094.

Suess E (1885) Das antlitz der Erde: Volume 3: Wien, F. Tempsky.

Tait J, Schätz M, Bachtadse V, Soffel H (2000). Palaeomagnetism, Palaeozoic palaeogeography of Gondwana, European terranes. Geological Society, London, Special Publications, 179(1), 21–34.

Valín ML, García-López S, Brime C, Bastida F, Aller J (2016) Tectonothermal evolution in the core of an arcuate fold, thrust belt: the south-eastern sector of the Cantabrian Zone (Variscan belt, north-western Spain). Solid Earth, 7(4), 1003–1022.

von Raumer JF, Bussy F, Stampfli GM (2009) The Variscan evolution in the External massifs of the Alps, place in their Variscan framework. Comptes Rendus Geoscience, 341(2), 239–252.

Von Raumer JF, Bussy F, Schaltegger U, Schulz B, Stampfli GM (2013) Pre-Mesozoic Alpine basements—their place in the European Paleozoic framework. Geological Society of America Bulletin, 125(1–2), 89–108.

Van der Voo R, Stamatakos JA, Parés JM (1997) Kinematic constraints on thrust-belt curvature from syndeformational magnetizations in the Lagos del Valle Syncline in the Cantabrian arc, Spain. *Journal of Geophysical Research*, 102, 10105–10120.

Weil AB, Van der Voo R, van der Pluijm B, Parés JM (2000). The formation of an orocline by multiphased deformation: A paleomagnetic investigation of the Cantabria-Asturias arc hinge-zone (northern Spain). Journal of Structural Geology, 22, 735–756.

Weil AB, Van der Voo R, van der Pluijm BA (2001) Oroclinal bending, evidence against the Pangea megashear: The Cantabria-Asturias arc (northern Spain). Geology, 29(11), 991–994.

Weil AB, Van der Voo R (2002) Insights into the mechanism for orogen-related carbonate remagnetization from growth of authigenic Fe-oxide: A scanning electron microscopy, rock magnetic study of Devonian carbonates from northern Spain. Journal of Geophysical Research: Solid Earth, 107(B4).

Weil AB (2006) Kinematics of orocline tightening in the core of an arc: Paleomagnetic analysis of the Ponga Unit, Cantabrian Arc, northern Spain. Tectonics, 25(3).

Weil AB, Gutierrez-Alonso G, Conan J (2010) New time constraints on lithospheric-scale oroclinal bending of the Ibero-Armorican Arc: a palaeomagnetic study of earliest Permian rocks from Iberia. Journal of the Geological Society, 167(1), 127–143.

Weil AB, Gutiérrez-Alonso G, Wicks D (2013a) Investigating the kinematics of local thrust sheet rotation in the limb of an orocline: a paleomagnetic, structural analysis of the Esla tectonic unit, Cantabrian–Asturian Arc, NW Iberia. *International Journal of Earth Sciences*, *102*(1), 43–60.

Weil AB, Gutiérrez-Alonso G, Johnston ST, Pastor-Galán D (2013b). Kinematic constraints on buckling a lithospheric-scale orocline along the northern margin of Gondwana: A geologic synthesis. *Tectonophysics*, *582*, 25–49.

Winchester JA, Pharaoh TC, Verniers J (2002). Palaeozoic amalgamation of Central Europe: an introduction, synthesis of new results from recent geological, geophysical investigations. In: Winchester JA, Pharaoh TC, Verniers J (Eds.) Palaeozoic Amalgamation of Central Europe. Geological Society Special Publication 201, 1–18.

The Geology of Iberia: A Geodynamic Approach

Cecilio Quesada and José Tomás Oliveira

Table of Contents

C. Quesada and J. T. Oliveira (eds.), *The Geology of Iberia: A Geodynamic Approach*, Regional Geology Reviews,
https://doi.org/10.1007/978-3-030-10519-8

Volume 5: Active Processes: Seismicity, Active Faulting and Relief